

TECHNICAL VOLUME

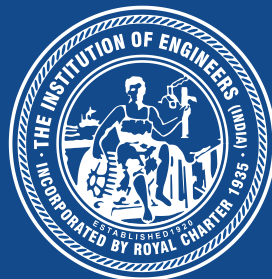


33rd Indian Engineering Congress

Udaipur, December 21-23, 2018

Theme

Integration of Technologies:
Emerging Engineering Paradigm



The Institution of Engineers (India)

8 Gokhale Road, Kolkata 700020



R&D Grant-in-Aid Scheme

The Institution of Engineers (India), the apex body of the engineers of India provides Grant-in-Aid support to its Corporate Members, Student Members and Institutional Members to pursue research and development in the field of engineering and technology.

Salient Points of IEI R&D Grant-in-Aid

Project Category	Institutional Membership	Guide	Student/ Applicant Membership	Quantum of Grant	Project Duration
Diploma	Not Mandatory	Should be Corporate Member(s)	Not Mandatory	Not exceeding Rs 20,000/- for a single project	Not exceeding six (06) months
Under Graduate (UG)	Institutional Member will be preferred	Should be Corporate Member(s)	Not Mandatory (Preferably an SMIE)	Not exceeding Rs 50,000/- for a single project	Not exceeding six (09) months
Post Graduate (PG)	Institutional Member will be preferred	Should be Corporate Member(s)	Should be Corporate Member(s)*	Not exceeding Rs 1,00,000/- for a single project	Not exceeding twelve (12) months
Doctoral (Ph. D)	Institutional Member will be preferred	Should be Corporate Member(s)	Should be Corporate Member(s)*	Not exceeding Rs 1,50,000/- for a single project	Not exceeding Twenty-four (24) months
*At the time of application they may not have membership, but before release of grant they must obtain membership of IEI					

The soft copy of the duly filled-up applications (in editable format), as per the given proforma available in our website, should be sent through email to research@ieindia.org and two hard copies of the same should reach the following address:

Director (Technical)

The Institution of Engineers (India), 8 Gokhale Road, Kolkata 700 020

Applications received in format other than that available on our website will not be accepted. Application should be forwarded through the Guide, Head of the Department or Head of the Institution. Please note that preference will be given to project proposals received from Institutions who are members of The Institution of Engineers (India). Kindly go through the guidelines (visit link https://www.ieindia.org/PDF_IMAGES/R&D/General%20Guidelines.pdf) carefully before filling up the application. The grant is not intended for the faculty members who have access to other avenues of research funding. Proposals received are scrutinized on a fortnightly basis and the recipients of R&D Grants are informed accordingly. Sanctioned projects are uploaded in IEI Website periodically.

TECHNICAL VOLUME

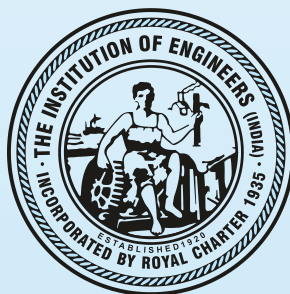


33rd Indian Engineering Congress

Udaipur, December 21-23, 2018

theme

Integration of Technologies :
Emerging Engineering Paradigm



The Institution of Engineers (India)

8 Gokhale Road, Kolkata 700020

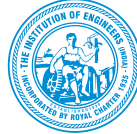
Composed by
Technical Department
The Institution of Engineers (India)
8 Gokhale Road, Kolkata 700020

Published by
The Institution of Engineers (India)
8 Gokhale Road, Kolkata 700020

Printed by
M/s Bharat Lithographing Co. (P) Ltd
98/4, S N Banerjee Road, Kolkata 700014

The Institution of Engineers (India)

AN ISO 9001 : 2008 CERTIFIED ORGANISATION
(ESTABLISHED 1920, INCORPORATED BY ROYAL CHARTER 1935)
8 GOKHALE ROAD, KOLKATA 700 020



“99 Years of Relentless Journey towards Engineering Advancement for Nation-building”

Mr Sisir Kumar Banerjee, FIE
President
The Institution of Engineers (India)



Message

I am glad to know that The Institution of Engineers (India) is organising the 33rd Indian Engineering Congress on the theme “Integration of Technologies: Emerging Engineering Paradigm” hosted by the Udaipur Local Centre during December 21-23, 2018 at Udaipur.

The Indian Engineering Congress is the apex activity of the Institution. The Institution of Engineers (India) organizes the Indian Engineering Congress every year to cater to the needs of entire engineering professional community of India. It is intended to broaden the scope of interaction and transfusion of knowledge amongst engineers from the country as well as from the prominent parts of the globe.

I take this opportunity to briefly acquaint you with some of the initiatives taken by IEI to address the professional needs of engineers in the country. We have launched 'Ideathon' to engage the engineering students by way of digital learning; 'ENGGTALKS' -- online professional networks for engineers; and Cloud Based E-Learning Solution for the students of AMIE. For improving the quality of IEI Journals, 'IEI-Springer Journals' Editors Meet' was organised. In addition, 'Industry-Academia Interface' is being organized in various parts of the country to ascertain employability of the engineering professionals.

Effective integration of technology is achieved when students are able to select technology tools to help them in obtaining information in a timely manner, analyze and synthesize the information, and present it professionally. Technology integration has always been important, but in the last decade it has become much more important and challenging too.

I believe that eminent speakers will enlighten us about various aspects of integration of technology and the participants from the country and abroad will be benefited through these deliberations and sharing of knowledge. I also congratulate the Technical Committee of the 33rd Indian Engineering Congress for bringing out such an important document in the form of Technical Volume.



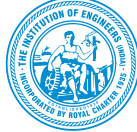
Sisir Kumar Banerjee

The Institution of Engineers (India)

AN ISO 9001 : 2008 CERTIFIED ORGANISATION

(ESTABLISHED 1920, INCORPORATED BY ROYAL CHARTER 1935)

8 GOKHALE ROAD, KOLKATA 700 020



*“99 Years of Relentless Journey towards
Engineering Advancement for Nation-building”*

Mr T M Gunaraja, FIE
President-Elect
The Institution of Engineers (India)



Message

I extend my sincere thanks and gratitude to all members of Technical Committee and the IEI Secretariat whose untiring effort and relentless contribution have made this 'Technical Volume' a reality.

The Indian Engineering Congress, which is the apex activity of the Institution, has become very popular among the engineering fraternity. The professionals and engineers belonging to all engineering disciplines from the country and abroad converge at this common platform to deliberate on the theme of the Congress and to share their knowledge and experience on contemporary technical issues.

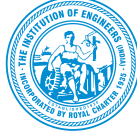
This Technical Volume comprises of 115 articles by engineering professionals from both academia and industry, with rich experience in their respective discipline. I am sure that the presentations and discussions on these scholarly articles will strengthen the industry-academia interaction.

A handwritten signature in black ink, appearing to read 'T M Gunaraja'.

T M Gunaraja

The Institution of Engineers (India)

AN ISO 9001 : 2008 CERTIFIED ORGANISATION
(ESTABLISHED 1920, INCORPORATED BY ROYAL CHARTER 1935)
8 GOKHALE ROAD, KOLKATA 700 020



*"99 Years of Relentless Journey towards
Engineering Advancement for Nation-building"*



Er. Sohan Singh Rathore
Chairman, Organizing Committee
33rd Indian Engineering Congress, 2018

Message

I am pleased to know that Technical Committee has done a praiseworthy work for publication of Proceedings of "33rd Indian Engineering Congress" which will be hosted by The Institution of Engineers (India) Udaipur Local Centre.

33rd Indian Engineering Congress will be a Mega and Flagship Event of The Institution of Engineers (India). The Congress will help and assist participants, Educational institutions, Engineering Faculty members, Students, Research Scholars, Industrialists etc. for which an appropriate and important theme of "Integration of Technologies : Emerging Engineering Paradigm" has been kept for the Congress. The Theme reflects present day requirement of world including research for solving various technological problems, Improving environment and enhancement of newer technological developments in various engineering disciplines.

I am thankful to Technical Committee, Writers of various articles and others engaged for this work. I hope that proceedings will be very useful to all.

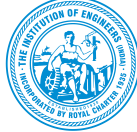
I convey my best wishes for the grand success of the 33rd Indian Engineering Congress-2018.

A handwritten signature in black ink, appearing to read 'Sohan Singh Rathore'.

Sohan Singh Rathore

The Institution of Engineers (India)

AN ISO 9001 : 2008 CERTIFIED ORGANISATION
(ESTABLISHED 1920, INCORPORATED BY ROYAL CHARTER 1935)
8 GOKHALE ROAD, KOLKATA 700 020



*“99 Years of Relentless Journey towards
Engineering Advancement for Nation-building”*

Er. Anirudh Singh Choondawat
Chairman, Technical Committee
33rd Indian Engineering Congress, 2018



Message

It is matter of proud and pleasure that The Institution of Engineers (India), Local Centre, Udaipur is hosting 33rd Indian Engineering Congress at Udaipur from December 21-23, 2018 on theme "Integration of Technologies; Emerging Engineering Paradigm".

21st Century world is witnessing great changes in development of Science & Technology in terms of research, innovation with development in newer and other engineering disciplines like Nanotechnology, Artificial intelligence, Virtual and Augmented realities, Robotics, Automation, Manufacturing, Modelling and Simulation, Bio-technology, Agriculture, Communication engineering, Space Science and Medical technology etc. Besides, now-a-days lot of stress is placed on environment protection, use of non-conventional energy sources with augmenting process and cost efficiency. Integration of various emerging technologies is going to affect and change the future.

I hope 33rd Indian Engineering Congress will benefit in all respects to participants, industries leaders, stack holders, educational institutions, research scholars, students and engineering fraternity.

I convey my best wishes to the writers of various technical articles and all associated with the publication for proceedings of 33rd Indian Engineering Congress. I presume it will be very beneficial to all participants, engineers, students, industrialists and engineering faculties.

I wish for the great success of the Event of 33rd Indian Engineering Congress-2018.

A handwritten signature in black ink, appearing to read 'Anirudh Singh Choondawat'.

Anirudh Singh Choondawat

Technical Volume of 33rd Indian Engineering Congress, 2018

President, IEI

Mr Sisir Kumar Banerjee

President-Elect, IEI

Mr T M Gunaraja

Secretary & Director General, IEI

Maj Gen (Dr) S Bhattacharya, VSM (Retd)

Organising Committee

Chairman : ER. SOHAN SINGH RATHORE, Former Chairman, ULC, IEI

*Co-Chairman & Convenor : ER. ANURODH PRASHANT SHARMA, Chairman,
ULC, IEI*

*Organising Secretary : ER. YAWANTI KUMAR BOLIA, Honorary Secretary,
ULC, IEI*

*Joint Organising Secretary: ER. M.K. MATHUR, Immediate Past Chairman,
ULC, IEI*

Technical Committee

Chairman **MR. A. S. CHOONDAWAT**

Co-Chairman **DR. B.P. NANDWANA**

Members **DR. R.C. PUROHIT**
DR. SUDHAKAR JINDAL
DR. NAVNEET KUMAR AGARWAL

Convenor **MR. NILANJAN SENGUPTA,**
Director (Technical), IEI

Editorial Team

*Mr N. Sengupta, Mr. S. Chaudhury, Dr. S. Ghosh, Mr. K. Sen, Mr. T. Chakraborty,
Ms. A. Dutta, Mr P. Chakraborty, Ms P. Nath, Mr Prasenjit Mukhopadhyay,
Mr. S. Bagchi, Ms H Roy*

Copyright Information

For Authors

As soon as an article is accepted for publication, authors will be requested to assign copyright of the article (or to grant exclusive publication and dissemination rights) to the organizer. This will ensure the widest possible protection and dissemination of information under copyright laws. More information about copyright regulations for this Technical volume is available at: www.ieindia.org

For Readers

While the advice and information in this Technical Volume is believed to be true and accurate at the date of its publications, neither the authors, the editors nor the publisher can accept any legal responsibility for any errors or omissions that may have been made. The publisher/ organizer make no warranty, express or implied, with respect to the material contained herein.

All articles published in this Technical Volume are protected by copyright, which covers the exclusive rights to reproduce and distribute the article (e.g., as offprint), as well as all translation rights. No material published in this Technical Volume may be reproduced photographically or stored on microfilm, in electronic data bases, on video disks, etc., without first obtaining written permission from the organizer (respective the copyright owner). The use of general description names, trade names, trademarks, etc., in this publication, even if not specifically identified, does not imply that these names are not protected by the relevant laws and regulations. For permission to reuse our content please send request addressed to: The Director (Technical), The Institution of Engineers (India), 8 Gokhale Road, Kolkata 700020 (Tel.: 033-40106213 or Email: technical@ieindia.org)

Copyright

As per By-Law 118, Copyright of each paper published in the Institution journals or proceedings in full or in abstract at its Centres shall lie with the Institution.

©The Institution of Engineers (India) 2018

The Institution of Engineers (India) has exclusive rights and license to publish and distribute the print as well as online edition of proceeding worldwide. The views expressed in this publication do not necessarily reflect those of the Institution. All rights reserved. No part of this publication may be reproduced, stored in a retrieval system or transmitted in any form or by any means, without prior written permission of The Institution of Engineers (India).

CONTENTS

Agricultural Engineering

AG/061/03	Upgrading Agricultural Industry through Drone Premal Amin, Bhargav Bhoi, Devang Chavda, Vivek Chattbar, Mehul Gor	1-6
AG/071/04	Power Operated Mulch Laying Machine with Punching Arrangement for Agricultural Operation P.S. Joshi, S.V. Pathak	7-9
AG/111/06	Effect of Mulch Paper Thickness and Speed on Performance of Manual Mulching cum Punching Machine A. V. Rangbhal, S. V. Pathak	10-13
AG/171/08	Self Optimizing Drip Irrigation System to reduce the Wastage of Water R. Raj Kumar, K. Sriram, I. Surya Narayanan	14-17
AG/196/11	Economic Evaluation of Solar Tunnel Dryer for Drying of Moringa Oleifera Leaves Divyesh R. Vaghela, Maulik L. Ramani, Satish S. Vaghasiya, S.H. Sengar	18-22

Aerospace Engineering

AS/142/02	Improvements in Functional Surfaces of the Engineering Parts using Microwave Cladding (MWC): A Detail Discussion Amit Kumar, Harpreet Singh, Neeraj Bhoi	23-27
AS/248/03	Effect of Merman Band Separation System on Payload Fairing Separation Rivets Ramashankar Sahu, S Balakrishnan, G Ayyappan	28-33

Chemical Engineering

CH/064/03	Improvement in Blast Furnace Grade Coke Mean Size by Altering the Fissure Formation during Coal Carbonisation Process S K Kushwaha, A Kumar, P K Pankaj, K K Manjhi, S K Das	34-38
CH/065/04	Smart Manufacturing Framework and its Challenges in Present-day Hydrocarbon Industries Vaibhav Ahuja, K Ramesh, Chitranjan Mehta	39-43
CH/118/07	Development of Economical Colour Measuring Instrument for Solid Food S. R. Kumbhar, A.K. Sahoo, G.V. Mote, I. S. Udachan	44-48
CH/121/08	Genetic Diversity Analysis of <i>Staphylococcus aureus</i> of Various Samples Collected from Bay of Bengal using Restriction Fragment Length Polymorphism (RFLP) K.Saranya, V.Manivasagan, S.Kavitha, D. Kubendran	49-52
CH/127/09	Mitigation Pathways for CO ₂ Emission in Chemical Industries by Integration of Technologies S. C. Nimkar, Deepa P, Cissy Shaji	53-58
CH/157/10	Fortification of Fenugreek Seeds Powder in Soya Sticks Gurunath Mote, Supriya Khade, I. S. Udachan, Akshaykumar Sahoo	59-62
CH/158/11	Design and Development of a Trapping System for Tritium (³ H) Aaditya Shah, Chetan Kothalkar, S. Chemte, K. M. Mathew, D. Kalgutkar, N. Jayachandran, A. C. Dey, Amit Chindarkar, D. K. Sawant	63-65
CH/161/12	Technological Advancements in Processing of I-131 Radio-isotope at Radio-Pharmaceuticals Laboratory Rohit Kamble, Chetan Kothalkar, A.S Gundekar, Pradip Bagde, S.B Panchal, Nitin Jadhav, Niteesh Kumar Tukuna Muni, Ravi Seshan, A.C. Dey, D.K. Sawant	66-69
CH/235/16	Extraction of Essential oil of Frankincense (<i>Boswellia serrata</i>) using Microwave-Assisted Hydrodistillation Swati Yadav . S. K. Gupta	70-74

Computer Engineering

CP/007/01	Pancreatic Cancer Stage Detection using Hybrid Neuro-fuzzy System T M N Vamsi, N V Ramana Murty	75-77
CP/023/04	Enhancing Safety at Construction Sites using Digital Technologies Krishna Nirmalya Sen, A Vinoth, Vimal Raj	78-80
CP/046/06	A Knowledge based Approach to Personify Ocean Data in RDF Format by the Exploitation of Semantic Technology Anitha V, T Menakadevi	81-85
CP/067/07	A Taxonomic Classification of Load Balancing Metrics : A Systematic Review Shahbaz Afzal, G Kavitha	86-91
CP/106/10	Digitization of Product Development Processes Manas Kr. Mishra, Vivek Barhanpurkar, Arnab Dasgupta, Souvik Karmakar	92-95
CP/138/11	Integrated VR Platform for IoT Learning Environment to Improve Skill Development A Raksha Thammaiah, Rahul Singh, Sooraj K Babu	96-101
CP/150/12	A Framework for Selecting Effective Learning Technologies in Indian Higher Education Asawari Shiposkar, Manohar Desai	102-106
CP/173/13	A Survey on Automation and Monitoring of Hydroponically Growing Crops Using IoT Vishnu T, Karthiga D, Meenu D Nair	107-110
CP/211/17	Implementation of Radius Security with Two-factor Authentication Eashan Singh Gill, Balakrishnan P, Patrick Kasiama	111-115

Civil Engineering

CV/001/01	RCC Deck with Steel Truss Composite Bridge Abhishek Sharma, Pramod K Singh, Krishna K Pathak	116-119
-----------	---	---------

CV/012/02	Robust Box Type Minor Bridge Pramod K Singh, Abhishek Sharma, Krishna K Pathak	120-123
CV/020/05	Strategic Plan for the Development of NH Network in Kerala: A Case Study of Kozhikode Division in Kerala V S Sanjay Kumar	124-129
CV/026/07	Load-Settlement Behavior of Geogrid-Reinforced Sand Bed over Granular Piles Sateesh Kumar Pisini, Swetha Priya Darshini, Sanjay Kumar Shukla	130-135
CV/037/08	Comparative Study of Characteristic Properties of Basalt Composite Rebars Ashish S. Srivastava, Rajendra B. Magar, Afroz N. Khan	136-140
CV/053/10	Stepped Cascade as an Energy Dissipator : A Survey and Perspective Sumit Gandhi, Anukrati Joshi, Sapana Jaiswal, Santosh Sharma	141-145
CV/076/14	Protection Measures for Alluvial River: Integrated Approach V G Bhawe, H S Sandhu, Rakesh Dhapola	146-150
CV/084/18	Some Major Properties of High Strength Self-Compacting Concrete Aijaz Zende, R B Khadiranaikar	151-158
CV/088/20	Enhancing Reuse and Recycling in Construction Industry through Modern Technologies Krishna Nirmalya Sen, A. K Poddar, G Muralidhar, Vimal Raj	159-162
CV/093/21	Response of Multi-Storied Building on Raft and Pile Foundation under Soil-Structure Interaction Sayanti Banerjee, Kamal Bhattacharya	163-168
CV/104/24	Analysis of Buckling Strength of Circular Plates with Discrete Stiffeners V Lakshmi Shireen Banu, V Vasudeva Rao	169-173
CV/125/25	Innovative use of Rubberized Concrete in Construction Technology Nisha Kumawat, Vishnu Kumar Kumawat	174-180
CV/133/26	Elastic properties of High Performance Concrete Beam under Flexure A.A. Momin, R. B. Khadiranaikar	181-185
CV/136/28	Diagnosing Characteristics of Fibers in Concrete Mix Design for Rigid Pavements Nikunj Patel, C. B. Mishra, Shaaqib Mansuri	186-190
CV/143/30	Development and Properties of Self-compacting Aluminosilicate Composites with Diverse Consequences of Alkaline Activator Ratio and Molarity V K Nagaraj, D. L. Venkatesh Babu	191-198
CV/145/31	Estimation of Storm Water Drainage: A Case Study Arun S Bagi, S P Wathar	199-203
CV/147/32	Challenges and Opportunities in Recycling of Construction and Demolition Waste: A Case of Jaipur in India G K Attari, R C Gupta, Sandeep Shrivastava	204-209
CV/176/37	Flood Response to Catchment Characteristics in West Flowing Rivers of Kerala Drissia T K, V Jothiprakash, A B Anitha	210-214
CV/182/38	Revisiting the Indian Road Congress Code Guidelines for Conduction of Road Safety Audit at Detailed Design Stage Shawon Aziz, Pradeep Kumar Sarkar	215-222
CV/185/40	Sedimentation: It's Impact and Management Kumar Abhishek Kishore, Prashant Kumar	223-227
CV/191/44	Improved Cement Quality and Grindability by using Grinding Aids Devendra Kumar Patel	228-231
CV/194/46	Linear Earthquake Analysis of Multi-storey Building on Raft Foundation including Soil Structure Interaction S Mondal, K Bhattacharya	232-237
CV/204/48	Assessment of Lattice Towers through Web Integrated Technologies Srinivas Tanuku, Ganesh Kolli, Sayi Raghu Ram Achanta	238-241
CV/217/49	Experimental Studies on the Performance of Hybrid Fiber (Areca Nut + Plastic) Reinforced Concrete Sumukh M N, Manjunath Itagi, B.P. Annapurna	242-247
CV/247/54	Mix Design Methodology for Concrete Paving Blocks in India B.C.Panda, P. K. Parhi	248-253

Electrical Engineering

EL/005/01	Use of Emerging Technologies for Rural India Amitabh Kumar Sinha	254-259
EL/068/04	Performance Analysis of PV Panel under Dusty Condition Abhishek Kumar Tripathi, Mangalpady Aruna, Ch S N Murthy	260-264
EL/069/05	An efficient Static Rotor: Resistance Control for the Motors of Preparatory Devices of a Sugar Factory Vinay Kumar, Sanjiv Kumar	265-269
EL/095/07	Evaluation of the Performances of Biomass Briquettes Produced with Sugarcane Bagasse and Cow Dung for Domestic and Small Scale Industries Anupriya Gupta, Deepak Sharma, N. L. Panwar	270-272
EL/100/08	Solar Net Metering : Perspective and Challenges Shreya Karmakar, Joy Chakraborty	273-276
EL/116/09	Transformation of Electrical System in Commercial Vehicles Manas Kumar Mishra, Anuj Kapoor, Sushant Mishra, Kumar Satyam	277-282
EL/131/10	Integration of Solar Photovoltaic (SPV) Module with Direct Ethanol Fuel Cell (DEFC) Technology: A Review R. G. Bodkhe, R. L. Shrivastava, R. B. Chadge, Vinodkumar Soni	283-286
EL/141/13	Advanced Distribution Management System: State-of-Art Integration of Technologies in Power Distribution P. Devanand, Tarun Batra, Md Shadab Ahmad, Tarun Bhardwaj	287-291
EL/178/14	Integrated DC Micro Grid, Renewable Energy and AC Grid with Energy Efficient Hybrid Appliances Pilot Study at NLCIL, Neyveli, Tamilnadu, India M.Coumarane, V.Manoharan	292-296

EL/212/16	Design and Control of Power Quality Improved 250 kW PV- based Grid-tied with Low Voltage Ride Through B Murali Krishna, Suhashini Shinde, Gireesha.B, BVVN Manikanta	297-300
EL/224/18	An Investigate Study on Electric Generators for Isolated Operation B Murali Krishna V, V. Sandeep	301-306

Environmental Engineering

EN/014/01	Rain Water Harvesting on Roads and Highways : An Innovative Approach to Conserve Water and to Prevent Waterlogging on Roads and Highways Raghu Pillai	307-310
EN/021/02	Climate Change Impact on Indian Agriculture and Food Security Parminder Singh Bhogal	311-314
EN/074/05	Comparative Evaluation and Efficacy of using Different Heating Techniques for Effective Management of e-Waste H. Mishra, A. S. Pente, R. Mishra, S. K. Mishra, B. P. Patidar, G. K. Mallik, A. Sharma, C. P. Kaushik, A. P. Tiwari	315-320
EN/122/08	Battery-run and Traditional Fuel Vehicle Mix: Perspectives of Road Traffic Environment and Operations Sabyasachi Mondal, Pritam Saha	321-325
EN/164/12	Exceptional Effects on Life and it's Remedies of Environmental Pollution in Earth Samrin Sheikh, Anil K Mathur	326-328
EN/230/16	Network Biology Approach to Identify Key Components Triggered during Exposure to Fluoride for Therapeutics in Human Shubham Pant, Rajesh Kumar Pathak, Mamta Baunthiyal	329-334
EN/233/17	Artificial Neural Network for Air Quality Index Prediction in Kota City Shikha Saxena, Anil K Mathur, A.K Dwivedi	335-338
EN/249/20	Treatment Process Development for Iron Removal from Underground Water Rajendrakumar V Saraf	339-345

Electronics & Telecommunication Engineering

ET/034/02	IoT based Aqua Q Sense for Indian Railways M.Gunasekaran	346-351
ET/054/04	Hardware Programming to Improve Embedded System Performance T Harinath, K Lal Kishore	352-358
ET/057/05	Exploring Mechatronics System and Investigation of Hydraulic and Pneumatic System Maneuver for Archetypal Engineering Applications G.S. Mundada, Rupesh C. Jaiswal, Zakee Ahmed	359-364
ET/096/07	Circular Patch Partial and Slotted Ground with Rectangular CSRR Metamaterial Antenna for Wireless Application Dheeraj Pandey, Paras, Mitesh Upreti	365-368
ET/097/08	A Metamaterial based Micro-strip Triangular Patch Antenna having Angular Steep with Triangular SRR and Defective Ground for Dual-Band Applications Mitesh Upreti, Paras, Dheeraj Pandey	369-373
ET/098/09	LPWAN Technology Enabling Industrial IoT Applications for Energy Intensive Industries Surendra Kumar Dogra	374-379
ET/192/17	Field based Observations of ECG Analysis in Night-Workmen using Time Series Analysis for Ascertaining of Circadian Rhythm M.Srinagesh, J.V.Anand	380-384
ET/202/18	Design of Hybrid Style Full Adder for Low Power and High Speed Applications Shivam Adhikari, Vijay Joshi, Jyoti Kandpal, Abhishek Tomar	385-389
ET/239/20	Integration Technology using Information and Communication Technology for Problem based Learning and Teaching Learning Process Araddhana Deshmukh, Girish Mundada, Aakanksha Girish Mundada	390-394

Mechanical Engineering

MC/016/03	Reliability Evaluation of NBC Protection Shelter using the Fault Tree Analysis Nitinkumar Pol, Sushil Kumar Parida	395-399
MC/027/05	Improving the Fuel Efficiency of a Diesel Truck by Blending Online-Onboard Produced Hydrogen Gas with Diesel Parth Jain, Sivarajan S	400-403
MC/029/06	Application of Technology Integration: Mechanical a Core Sector Anurodh Prashant	404-407
MC/048/09	Feasibility Study of Solar Vapour Absorption Cogeneration Plant for Space Cooling or Heating and Electrification of Residential Buildings Pereddy Nageswara Reddy	408-416
MC/056/12	Investigate the Effect of Multi-Stage and Single-Stage Forming on Sheet Metal Part, Brake Plate Gajendra Kumar Nhaichaniya, Chandra Pal Singh	417-421
MC/073/15	Parametric Analysis and Optimization of Production of Karanja Methyl Ester using Taguchi Design of Experiment Pramod Kumar, Shailendra Sinha, Praveen Tyagi	422-426
MC/102/18	Material Selection in Product Design: An Extension of Pugh Chart D. Das, S. Bhattacharya, B. Sarkar	427-431
MC/105/19	From Logistic to Racing: Innovation in Trucks Manas Mishra, Rajesh Pandey, Naveen Mishra , Kunal Gaurav	432-435
MC/110/21	Value Engineering and Value Analysis Methodology Manas Kr. Mishra, Bhushan Vaidhya, Rajeev Mishra, Peeyush Anshu	436-441
MC/117/23	Remote Operation of Fuel Handling Systems of Prototype Fast Breeder Reactors H.Nalini, S.Narasimhan	442-446

MC/123/24	Integration of Various Active and Passive Cooling Techniques on MJT Solar Cell Yogesh Nandurkar, R.L.Shrivastava, Vinod Kumar Soni	447-451
MC/144/26	Factors Affecting Mixing and Fabrication of Polymer-Ceramics Granules Prakhar Khemka, Harpreet Singh, Tanuja Sheorey	452-456
MC/151/28	A Computational Fluid Dynamics Study on Various Methods for Enhancement of Bio-oil Recovery by using a Shell and Tube Condenser B.L. Salvi, T. Soni, S. Jindal, M.A. Saloda	457-461
MC/195/36	Integration of Analytical Software and 3D Platform in Plant Design and Engineering: A Paradigm Shift for the Upcoming and Revamped Process Plants Anirban Datta, Gautam Gangopadhyay	462-468
MC/201/37	Development of Glass Reinforced Metal Matrix Composite and Study of its Properties Ajay Biswas, Moutoshi Singha Roy, Akshar S. Vasekar	469-472
MC/206/38	Blending of Lignite: Impacts and Challenges S. Raghuthaman	473-476
MC/213/40	Formulation of Optimisation Methodology for Prevention of any Emergency Scenario while Permitting Cost-Effective Design Safety Margin Rajesh Kumar Mishra, Vinay Karanam	477-479
MC/216/42	Elimination of Gear Grinding Operation of Gears by Finish Hobbing Manufacturing of Gears Arup Mukherjee, Sanjiv Ranjan, Abhijit Kar	480-483
MC/242/43	Investigation of Thermofluid Properties of Open Cell Copper Metal Foam for Cooling of Power Electronics Devices Kishor Borakhade, Ashish Mahalle	484-489
MC/245/44	Trends in Brake System for Mass Rapid Transport System in Metro Cars Gautam Dua, M. Sudhrashan, Sunil Kumar, Manjunath S	490-494

Metallurgical and Materials Engineering

MM/002/01	Sixty Years of Hot Metal Production in SAIL Bishnu Kumar Das, Ajay Arora, Anand Kumar	495-503
MM/043/03	Effect of Operational Logistics on Steel Ladle Life in a Steel Plant Rakesh Kumar Singh, Rajeev Kumar Singh	504-507
MM/050/05	Thermo-Mechanical Processing of High Strength Low Carbon Microalloyed Steel for Automotive Sector at Bokaro Steel Plant Santosh Kumar, N Mondal, B Sunita Minz, R Dodrea, B Mishra, D Kumar, S Kumar	508-511
MM/129/11	Slow Strain Rate Testing Behavior of Tailor Welded Blank (TWB) of Al 5052 H32-6061 T6 Alloy Arpit R Patil, S T Vagge	512-516
MM/153/14	Material Selection for Wear Control in Industries Pradip Sahana, K K Singh	517-522
MM/214/15	Creep Studies of Nuclear-Grade Aluminium-Silicon Alloy Vinay Karanam, Rajesh Kumar Mishra	523-525
MM/218/16	Sustainable use of Natural Resources: Integrating Technologies for Iron Making from Low Grade Ores A. Ghosh, B. Sensarma	526-530
MM/231/18	Use of Goethitic Ore Fines in Sintering and Measures to Improve Sinter Plant Performance Mahadeo Roy, S. Dhara, M. K. Singh, Sudip Acharyya, S.A. Balaji, S.K. Pan	531-536

Mining Engineering

MN/022/01	A Critical Study of Environmental Impact of Responsible Mining Practice for Kotah Stone within Framework of Initiative Responsible Mining Assurance (IRMA) Standards-16 S. C. Agarwal	537-541
MN/160/05	An Overview of Modified Foreign Technology for Indian Mining Conditions P.Venkatesan	542-546

Marine Engineering

MR/119/02	Challenges in the Restoration of Inland Waterways for Navigation: A Case Study of Parvathy Puthanar in Kerala N.M. Sabitha, B G Sreedevi	547-552
-----------	---	---------

Production Engineering

PR/019/02	Preparing Organizations for Digital Manufacturing K V Santhosh	553-558
PR/107/12	Simultaneous Engineering for New Product Implementation Manas Kr. Mishra, Arnab Dasgupta, Bivas Bhattacharyya, Ankit Mehta	559-562
PR/126/07	Integrated Casting of Steel and Cast Iron by Full Mold Process Sunil Sahu, A. N. Dutta	563-565
PR/203/08	Calibration of Core Temperature Measurement Channels of Prototype Fast Breeder Reactor R. Pandiarajamani, S. Narasimhan	566-570
PR/221/10	Technology Integration: the Mantra for Progress Satheeschandra. P, Shaji Jose	571-574

Textile Engineering

TX/004/01	A Study on High Efficiency Particulate Air (HEPA) Filtration Process E Dey, U Choudhary, R Bhattacharyya, S K Ghosh	575-578
TX/047/02	Automatic Electronic Fibre Bundle Strength Tester for Multiple Fibres G Roy, S C Saha, G Sardar, A Sarkar	579-582



Upgrading Agricultural Industry through Drone

Premal Amin^{*1}, Bhargav Bhoi¹, Devang Chavda¹, Vivek Chattbar¹, Mehul Gor¹
G H Patel Institute of Technology, V V Nagar, panthu110@gmail.com*

ABSTRACT

Use of technology in farming will transform the agriculture industry. This work discusses technological aspects of prominently used unmanned aerial vehicles or drone and their applications in agriculture. Agriculture is facing lack of labor, and hence drones can be served as a savior and can bring revolution in agriculture sector. Here, working principle of drone is discussed first and then entire process of development is discussed in detail. To make it useful for agricultural application separate mechanism is introduced. Proposed concept can be used for effective pesticide spraying and seed sowing. Pesticide spraying and Seed sowing can be done alternatively using portable attachment. Proposed drone consists of six rotors each connected to rotary wings with propellers. This will be controlled using flight controller (micro controller) and remote controller (RC). The work discussed in this paper recommends the use of drones for spraying pesticide to save crops and for seed sowing of crops like wheat, rice and millet extensively. Over and above distressed and healthy plant can be identified by the use of camera mounted on drone. Thus, this work will help the reader in interpreting the scope of drones in the agriculture sector, entire procedure of development and challenges in the development and operation of drone.

KEYWORDS Unmanned Aerial Vehicle, Seed sowing mechanism, Pesticide spraying mechanism

INTRODUCTION

Agriculture industry gives the food which is basic amenity for human survival. Also, it is the backbone of any country's economy. It provides approximately 52% of the employment in India and contributes around 18% of GDP every year. The agriculture industry in India occupies around 43% of India's geographical area [1]. In a study by Federation of Indian Chambers of Commerce and Industry (FICCI) the challenge of shortage of labour in agriculture came forth. It is estimated that percentage of people employment in agriculture will be around 41% till 2019-20 [2]. Also the health of labourers working is at risk due to the harmful pesticides and fertilizers to be used. So automation is a solution to both the problems. Using drones labourer can be far away from harmful fluids and the requirement of labour also reduces.

The first pilotless aircraft was developed after World War I in 1916, which was a failure. Later, the Hewitt-Sperry's Automatic Airplane (the flying bomb) made its maiden flight, demonstrating the concept of unmanned aircraft. Most UAVs were utilized by the military; the technology was commissioned by the Central Intelligence Agency (CIA) after the September 11, 2001 terrorist attacks. Recently, UAVs are becoming increasingly popular in the commercial and private market. Amazon.com, the largest online retailer, said in December 2013 that it was developing drone technology to one day deliver the consignment or order autonomously [3].

Drones are used in agricultural industry currently as follows [4]:

- Soil and field analysis: Images using drones can be used to produce precise 3-D maps for early soil analysis, useful in planning seed planting patterns.
- Planting: Start-ups have created drone-planting systems that achieve an uptake rate of 75% and decrease planting costs by 85%.
- Crop spraying: Experts estimate that aerial spraying can be completed up to five times faster with drones than with traditional machinery.
- Irrigation: Drones with hyper spectral, multispectral, or thermal sensors can identify which parts of a field are dry or need improvements.



DEVELOPMENT OF DRONE

Drone uses aerodynamic drag, thrust and lift to fly. Drag opposes the motion of any object using air. Thrust is the upward force generated when the propellers spin. Lift is the force that acts against the weight of the drone. Hexacopter consists of six rotor arms, and every alternate motor rotates in opposite direction to each other. This balances the forces and gives stable lift to the hexacopter. Propellers are the main source to generate thrust. They are shaped using principle of aerofoil. Coanda effect is responsible for the generation of lift. The tendency of fluid jet approaching a curved surface to remain attached to a surface [5].

As shown in **Figure 1**, air gets divided into low pressure air, above the propeller and high pressure air, below the propeller. This gives lift to the drone.

The primary components for a drone are: Frame/Body, Actuators, Electronics Speed Controller, Flight Controller, Power Distribution Board, Receiver Transmitter System, Battery, Propellers and Camera.

Frame

Frame is the main structure in drone that holds and supports the electronics. Feasible materials for frame are plastic, aluminium, wood, carbon fiber and G10. Each material has its own pros and cons. Plastic lacks strength and is comparatively heavy. Aluminium is durable but it might block RC signals. Wood is easily available but thin wood lacks strength and thick wood increases the weight. Carbon fiber is lighter, durable and can bare the heavy load. Carbon fiber can be CNC cut and custom designs can be made. G10 is another material that beats every other material since it is cheaper than carbon fiber.

Selection of frame size depends on the application that is to be performed by a drone and the overall weight. Drone type for specific load/application is shown in **Table 1**.

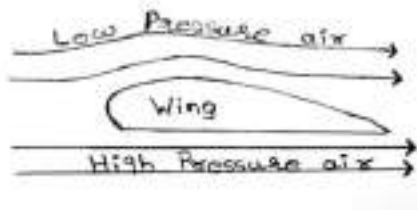


Table 1 Type of drone for specific load/application

Load/Application	Drone type
< 2kg / Less fatigue application	Quadcopter
2kg < load < 6kg / fatigue application	Hexacopter
> 6kg/ Heavy duty application	Octacopter

Figure 1 Aerofoil shape of propeller

Tekit's[18] HJ450 frame is one of the most popular Quadcopter frame, because it is inexpensive. The centre plate doubles as a power distribution board which tidies things up quite a bit and allows to get rid of ugly Do-It-Yourself (DIY) wiring harness [6]. Frames can also be built at home using aluminium or balsa sheet (balsa wood). But results will vary from manufactured frames, both aesthetically and in terms of flight attributes [6]. Octocopter results in increase in deadweight of the drone and further adding external equipment results in more weight so octocopter is not feasible for agriculture because of variable loading of pesticide for spraying and seeds for seed sowing [7].

In this work, Hexacopter is chosen for agriculture application, because spraying mechanism and seed sowing mechanism requires carrying the weight of around 6.22 kg which can be justified as shown in **Table 2**.

Actuators

Actuator selection is important because it decides how much thrust can be generated and hence helps to decide the maximum allowable load (weight of drone inclusive). Generally, brushless dc motors are used in drones. Motor selection depends on the total weight of the drone. Motors are specified in kV rating. Here kV refers to constant velocity of motor (please do not misinterpret with kilovolt kV). It is given in rpm per volt (rpm/V). Higher the kV, higher is the speed of rotation of motors. But for more thrust, that is, to lift heavy load, lesser kV motors are required.

Equation for calculating total thrust required is [8],

$$\text{Thrust} = (2T + 0.40T) / 6,$$

where, T = weight of hexacopter + weight of mechanism.



For chosen application, total load is 6.22 kg, so each motor for hexacopter should generate minimum of 1.5 kg thrust at 50% throttle (**Figure 2**).

Table 2 Weight of various parts of drone

Parts	Weight
Frame, motors, ESC, Flight controller, GPS module	1850 g
Battery	1189 g
Mechanism (spraying and seed sowing)	3181 g

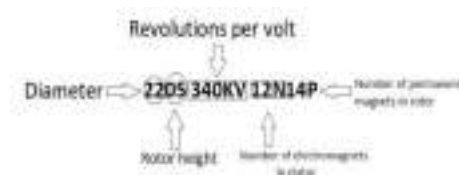


Figure 2 Motor designated form

High kV motor gives high RPM and hence increases the speed of drone. Such motors are preferred for first person view (FPV) drone racing. Because for racing, high power to thrust ratio is required [9].

For commercial application, stability is an important factor and, fertilizer spraying and seed sowing will have variable loading during flight of the drone, so motor from sunny sky [10] fits best for our application. It has following specifications:

- Model: X4110S 340 kV [10]
- kV: 340 kV
- Weight: 148g(with cable)
- Maximum battery cell: 6S
- Recommended propeller: DJI15 × 5.5 1750 carbon fiber propeller.

Electronic Speed Controller

The brushless motors are multi-phased, normally 3 phases, so direct supply of DC power will not turn the motors on. That is where the Electronic Speed Controllers (ESC) comes into play. The ESC generating three high frequency signals with different but controllable phases continually to keep the motor turning [11]. ESC selection is done on the basis of maximum current rating of motor. For example, if a motor has a current rating of 14.6A, an ESC with current rating greater than 14.6A can be used.

Two types of ESC's are available, combined ESC and separate ESC. Combined ESC is available in 4 in1 ESC board, which saves space, easy installation and are light in weight, but, if any one ESC gets damaged, whole ESC board gets shot [12]. So use of separate ESC's is preferred. For hexacopter, we will use 40A ESC keeping the motor specifications in mind.

Flight Controller

Flight controller is the brain of drone. It senses and controls the orientation of a drone using onboard sensors. Accelerometer, gyroscope, barometer, magnetometer are the basic sensors that comes inbuilt in the flight controller. For agriculture application, flight controllers that are able to connect with external sensors and components are used. Such type of flight controllers are Ardupilot[18], Pixhawk[18], Top gun[18].

Looking at the physical constraints of hexacopter and task to be performed, pixhawk[13] flight controller suits best.

Power Distribution Board

Power distribution board (PDB) distributes battery power to all the motors. Positive and Negative from each ESC is connected to PDB's positive and negative.

Receiver Transmitter System

Receiver Transmitter system is the communication system, where transmitter sends radio signal to receiver which is attached with the drone. Transmitter is the remote control which sends signal to receiver wirelessly.

Generally, six channel transmitter is used because four channels are required to control the drone, that is, throttle, yaw, pitch and roll. Rest two channels can be used to control external mechanism or servo motor.

In hexacopter for agriculture application, four channels are used to control the drone and rest two for controlling the actuation of servo motors for spraying and seed sowing. For proposed hexacopter, Taranis transmitter will be used, since it is adaptable to different flight modes [14]. Following terms are used.



Throttle: Upward thrust

Yaw: Left/Right turn

Pitch: Forward/Backward movement

Roll: Rotation on it's own axis.

Battery

Lithium polymer or LIPO batteries are used in drones. They are powerful, compact in size and are rechargeable. Lipos are designated according to number of cells, Discharge rate and Ampere rating. Lipos are available in wide variety.

75C: $75 \times 1.3 = 97.5\text{A}$ (max current draw)

4S: 4×3.7 (voltage per cell) = 14.8 V

1300 mAh: shows maximum capacity

1300 mAh can give maximum of 1.3 A discharge per hour, so it can also be noted that 1300mAh = 1.3Ah (Ampere hour)

Generally, higher C rate, 4S battery is used for FPV racing because of more discharge rate [9]. For hexacopter, less C rate, 6S battery is preferred since it is lucrative to get more flight time. The basic diagram of ESC, PDB and Lipo Battery shown in **Figure 3**.

Propellers

Propellers convert rotational motion into thrust. A pressure difference is produced between the forward and rear surfaces of the air foil-shaped blade, and a fluid (such as air or water) is accelerated behind the blade. Higher pitch means slower rotation, but will increase your vehicle speed which also uses more power [15].

There are three different tip propellers are available, they are: pointy nose, bull nose (BN) and hybrid bull nose (HBN). Most efficient is pointy nose but it pulls least thrust[9].

Generally for hexacopter, propeller size ranges from 10 inches to 16 inches. As per the motor selection, DJI15*5.5 1750 fits best to the hexacopter.

Camera

Camera plays important role in drone. In case if it happens that drone gets out of control due to unavoidable reason, we can keep an eye on the monitor screen and activate Return-to-Home (RTL) mode. RTL mode brings drone to the co-ordinates where take-off was done.

First person view (FPV) camera can be attached to the drone so that we can check the crop growth and keep a track of field.

Multispectral imaging helps to identify pests, diseases and weeds. It also monitors livestock especially at night, using thermal camera. Aerial footage can also detect fungal infestations that are not visible to naked eye; the combination of multispectral images, infrared or visible, can create an image of crop that emphasizes healthy plants and those in need; by monitoring the crop at regular intervals, animations can be created, images that show changes over time, revealing problem areas or opportunities to better crop management [16].

Non-dispersive Infra-red (NDIR) detectors can be used to measure the carbon dioxide content in crops so that measures can be taken to improve the yield of crops [17].

Also, Camera can help in counting plants, observe crop yield [18].

CHALLENGES IN THE DEVELOPMENT AND OPERATION

During development of a drone, one has to pass through various barriers. One of the biggest barrier is “where to order parts from?”. Currently in India, drone parts can be imported only if a person has legal permission from DGCA (Directorate General of Civil Aviation). Also, we are supposed to get drone registered with UIN (Unique Identification Number) issued from DGCA [19]. Designing the drone is not a hefty work but getting the frame cut with accuracy is a tough job. Once the drone is developed, testing is a risky job since we never know how will a drone behave in it's first flight.

PESTICIDE SPRAYING AND SEED SOWING MECHANISM

For spraying and seed sowing mechanism, the basic signal flow is as shown in the **Figure 4**.

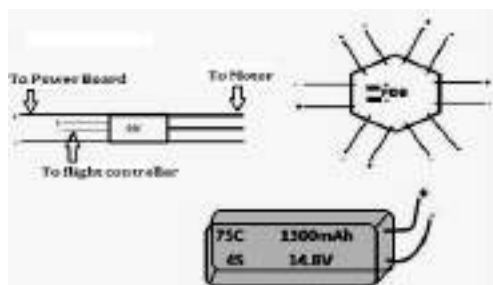


Figure 3 Basic diagram of ESC, PDB and Battery

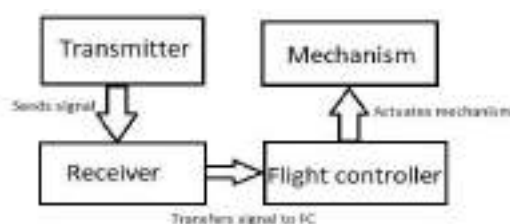


Figure 4 Signal flow for mechanism

Signals first will get feed in receiver with the help of transmitter, and the receiver will further send the signal to the flight controller so flight controller actuates the mechanism as per the feed given by the receiver.

Seeds of crops like wheat, millet and rice are sprinkled randomly over a row in a field. This can be done using a drone with less time consumption.

A plastic cylinder will be attached using spiral knob, and seeds will be filled inside the cylinder. Cylinder has a small diameter door that is servo controlled. So when drone reaches the destination, input from transmitter will actuate the servo and the door will open accordingly. Cylinder dimension are as follow:

Outer diameter: 120 mm

Overall length: 150 mm

Volume of cylinder: $1.696 \times 10^6 \text{ mm}^3$

Servo dimension: $38 \times 11.5 \times 24 \text{ mm}$ [20]

As shown in **Figure 5**, cylindrical box will have a servo controlled door on the bottom side which actuates using servo control switch and according to the opening of door, corresponding amount of seeds will start falling on the ground

This cylinder will have threads for smooth assembling and disassembling with drone. Pesticide spray mechanism for our drone is shown in **Figure 6**.

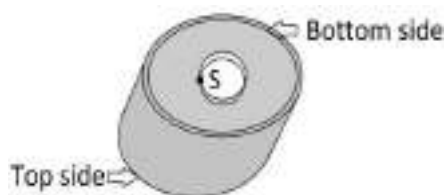


Figure 5 Servo controlled door(S) on a cylinder

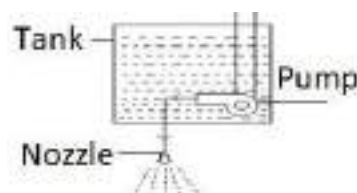


Figure 6 Spray mechanism

Basically the pesticide spray mechanism consist of three major components, submersible direct current (dc) pump, tank and nozzle. As per the proposed design the tank dimensions will be 15 cm diameter and 15 cm length. The tank will be made from plastic material with provision of cap at top to fill the liquid. The tank capacity is 2270 ml. 12 V DC pump will be submerged in the filled tank of pesticide solution as shown in **Figure 5**. Outlet of DC pump is connected to the sprayer nozzle. For the multiple spray more than one nozzle can be provided by T split connections. The pump connection is to be done with controller and one channel is assigned to operate pump. The specifications of pump (as per proposed design):

Lift: 1-2m

Flow rate:- 300 L/H

Dimensions of pump:- $5 \times 5 \times 7.5 \text{ cm}$

Dimensions of inlet and outlet:- 15 mm and 5 mm

Weight:-150gms [21].



The specifications of nozzle (as per proposed design):

Spray range: 1m to 4 m

Connecting port:- 6 mm outer diameter, inner diameter 3 mm

Material:- Brass

Weight:-5g

CONCLUSIONS

Spraying and seed sowing mechanism, both using single drone revamp the use of drones in agriculture. Farmers will no longer be dependent on the labor. Advanced technology in automation and drones can bring revolutionary benefits. The mechanism proposed here will help to reduce the cost because two applications can be performed on single drone, so indirectly, two applications at the cost of one drone. Farm yield will increase, and resources utilization will be optimized. So conclusively, productivity of the farm will increase and this will prove to be lucrative to farmers as well the country.

REFERENCES

1. International Journal of Agriculture and Food Science Technology, ISSN 2249-3050, Volume 4, Number 4 (2013), pp. 343-346
2. www.ficci.com
3. <https://www.redorbit.com>
4. <https://www.technologyreview.com/s/601935/six-ways-drones-are-revolutionizing-agriculture/>
5. Michele Trancossi, an overview of scientific and technical literature on coanda effect applied to nozzles, DOI: 10.4271/2011-01-2591
6. David riches emmanuel, Sava Jaswanth, Jogendra Mani Kumar, Design and implementation of quadcopter drone with KK 2.1.5 Flight controller, DOI: 10.13140/RG.2.1.1684.3762
7. Oscar oscarson, Design, Modeling and control of an Octocopter, Stockholm, Sweden 2015
8. www.tomsguide.com
9. www.oscarliang.com
10. www.hobby-wing.com/sunnysky-x4110s-motor.html
11. S.Selvaganapathy, A.Ilangumaran, Design of Quadcopter for Aerial View and Organ Transportation Using Drone Technology, Volume 1, Issue 3, Pages 311-315, April 2017
12. www.rcgroups.com
13. www.pixhawk.org
14. www.getfpv.com
15. www.topdronesforsale.org/drone-propellers/
16. George IPATE, Gheorghe VOICU, Ion DINU, U.P.B. Sci. Bull., Series D, Vol. 77, Iss. 4, 2015
17. www.cambustion.com
18. www.dronezon.com
19. www.qz.com
20. www.electroniccomp.com
21. www.aliexpress.com



Power Operated Mulch Laying Machine with Punching Arrangement for Agricultural Operation

P.S. Joshi¹, S.V. Pathak²

Department of Farm Machinery and Power Engineering, College of Agricultural Engineering and Technology,
Dapoli^{1,2}, 123priyankajoshi@gmail.com

ABSTRACT

A power operated mulch laying machine with punching arrangement machine was developed in order to mechanize the conventional method of mulch laying. The machine was able to perform functions such as bund shaping, laying of mulch film, pressing of mulch film, covering of film with soil along with making punch holes on the mulch film, which reduces the drudgery of labour in all these operations. Power operated mulch laying machine proved to be more economically beneficial in terms of cost of operation, than the conventional method of mulch laying. Power is supplied through the engine to the ground wheel. Handle arrangement was given to provide the direction as well as pulling force to the machine.

KEYWORDS Plastic mulch, Mulch laying unit, Soil covering unit, Pressing wheel unit, Punching holes assembly.

INTRODUCTION

Field faces some problems such as how to maximize the profit, how to increase productivity and how to reduce the cost. Farmers and horticulturists use mulching as method of improving the condition of agricultural soils by covering the soil surface with different kind of material. Improvement of the soil physical environment contributes to better plant production. Covering the ground with mulch add organic matter to the soil, reduce weed growth, and reduce or eliminate erosion. Mulching is the process of covering soil around the plant root area with a view to insulate the plant and its roots from the effects of extreme temperature fluctuations. The use of plastic mulches results in higher yields, improvement of yields quality, decreased need of irrigation and pesticides, reduced leach of fertilizers to water systems.

In India, two types of agricultural equipment are used, manual method (conventional method) and mechanized type. Mechanization involves the use of a hybrid device between the power source and the work. Mechanized agriculture is a process of using agricultural machinery to mechanize the work of agriculture, greatly increasing farm worker productivity. In modern agriculture, powered machinery has replaced many farm jobs formerly carried out by manual labour or by working animals such as oxen, horses, and mules. The biggest profit of automation is that it saves the labour. However, it also saves energy and materials and to improve the quality, accuracy, and precision.

Hence, powered machineries have become the integral part of mechanized agriculture. Plastic mulching by conventional method requires more human labour, more time and more cost of operation. Keeping the above facts in view, present study has been undertaken to develop power operated plastic mulch laying with punching arrangement. The scope of the project extends to building a small size portable machine which integrates all the above mentioned tasks like laying paper as well as drilling holes performs them efficiently. Such a machine reduces the efforts and saves time taken from ploughing to seeding.

METHODOLOGY

Theoretical considerations:

- Soil moisture content should be in range of 17-22% at field capacity.
- It will be capable of performing various functions such as shaping of bunds, laying plastic mulch, making punching holes in single pass and soil covering from both side of plastic mulch.
- The size and weight of the machine will be such that the implement will be stable on prepared land surface.
- The time, energy required and the cost of operation for mulch laying machine will be lower than existing conventional systems.
- The spacing of punching holes must be equidistant and uniform.
- The developed mulching machine will be simple to operate, easy to manufacture and low cost.



Fabrication of Power operated Plastic Mulch Laying Machine with Punching Arrangement:

The power operated plastic mulch laying equipment consists of one plastic mulch laying unit having a working width of 900 to 1200 mm. The tractor operated plastic mulch laying equipment gets power for motion from drawbar of the tractor.

Mulch Laying Unit: Mulch laying unit consisting of main frame, handle arrangement, drive wheels, bund shaping unit, mulch laying arrangement, press wheel, soil covering devices and punching arrangement.

Main Frame and Handle Arrangement: All components of the machine were supported on the main frame. A handle arrangement was provided for easy pulling. Mulch laying and punching unit were detachable and could be use separately as per requirement.

Bed Shaping Unit: For preparation of beds, the bed shaper shovels will be use. The shovels will be attached to the front of main frame.

Soil Covering Unit: Soil covering unit was used for cutting, lifting, turning and throwing the soil over the plastic mulch. The M.B. plough bottom was attached to the soil covering to cut, lift and throw the soil on the plastic mulch.

Press Wheel Assembly: Press wheels need to run at the bottom of the trench and not on the side to stretch the plastic properly. Tilt the front of the press wheel on an inward angle to stretch the plastic. The press wheel height and distance can be adjusted as needed.

Punching Holes Unit: Arrangement of the punching cups was mounted on backward side of frame for punching the holes in the plastic mulch film. The cups were made in such a way that, when it goes into the ground it punches the hole. The adjustments will be made for changing the distance of periphery hole.

Power Transmission Unit: Power supply from engine were taken and supplied to the ground wheel. Gear system will be used for speed reduction mechanism. Then the trials were carried out at different speeds ranging between 0.8-1.8 km/h.

CONCLUSION

In this work, a power operated mulch laying machine with punching arrangement has been developed for agricultural application which is going to laying mulch film on ground as well as punching holes on mulch film with reducing effort, drudgery of labour. Mulch film had various advantages and mechanical application reduces the working time as compared to the conventional method of mulch laying.

REFERENCES

1. H. D. Jadhav, J. J. Kadam, A. D. Karche, H. P. Kharat, W. Monish, Review Paper on Automatic Mulch Laying and Hole Generation in Farm. International Journal of Engineering Science and Computing., Volume 7, Number 4, 2017.
2. S. Marihonnappanavara and M. Veerangouda. Development and evaluation of tractor operated plastic mulch laying equipment. Internat. J. Agric. Engg., Volume 10, Number 2, 2017, 374-378, DOI: 10.15740/HAS/IJAE/10.2/374-378.
3. N. Mishra, K. Kumar., S. Shashwat, M. Singh. Multi-Purpose Agriculture Machine, International Journal of Advances in Science Engineering and Technology, 2017, ISSN:2321-900.
4. M. S. Salunke, A. Tipayle, Samadhan Thete U., Sandip Thete B., Tushar Thete S., Advance Mulching Paper Laying Machine. International Journal for Scientific Research & Development. Volume 5, Number 3, pp 2321-0613, 2017
5. Veer, V. P and P. R. Thete., Mulching Paper and Drip Laying Machine. International Journal of Science Technology Management and Research, Volume 2, Number 3, pp 2456-0006, 2017.



Effect of Mulch Paper Thickness and Speed on Performance of Manual Mulching cum Punching Machine

A. V. Rangbhal^{*1}, S. V. Pathak²

Department of Farm Machinery and Power, College of Agricultural Engineering and Technology, Dapoli^{1,2},
rangbhalajinkya8@gmail.com*

ABSTRACT

Mulching is the process or practice of covering the soil/ground to make more favorable conditions for plant growth, development and efficient crop production. The scope of the project extends to building a small size portable machine which integrates all the above mentioned tasks like laying paper as well as drilling holes performs them efficiently. Such a machine reduces the efforts and saves time taken from ploughing to seeding. The main objective is to reduce or eliminate to some extent the manual labor and time required for mulching paper laying process. The performance of developed mulch laying cum punching machine was evaluated in field. The performance was evaluated at three mulch paper thicknesses (15, 20 and 25 micron) and three forward speeds (1.3, 1.5 and 1.7 km/h) to study their effect on effective field capacity, field efficiency and punching efficiency. The effect of both parameter was shows the significant effects on dependent parameters. The result was found as the effective field capacity and field efficiency was observed as 0.148 ha/h and 79.40% and the mean punching efficiency were observed as 82.46%.

KEYWORDS Mulch paper thickness, Speed of operation, Mulching machine, RSM, ANOVA

INTRODUCTION

Since, ancient time, mulching has been considered as the better water conservation techniques to grow crops in water scarcity areas. Mulching is nothing but process of covering soil around the plant root area with a view to insulate the plant and its root from the effect of extreme temperature fluctuation. The advantages of mulching are to reduce deterioration of soil by controlling the rate of movement of water and its runoff, restrict the rain water flow rate, soil water runoff and avoiding the direct entry of solar radiation. It maintains the optimum soil temperature, improves the soil organic carbon content in the soil, and all the physical, chemical and biological properties of soil.

Vast research has been carried out on suitability of different materials to be used for mulching but plastic mulch paper is one of the better options. The popularity of using mulch paper for growing vegetables and fruit crops is increasing day by day in India but the application of the mulch paper in the field with manual method limits its effective use. Considering all these points it is necessary to develop manual operated mulch laying machine. Based on the literature reviewed for the study, effects of planting method, duration of plastic mulch, water use efficiency, soil moisture, growth yield and soil temperature on plastic mulch were reported. Some literature reported the study on different parameters, 7 to 30 micron thickness of mulch paper was used for the mulching operation (Dutta 2008). The width of mulch paper ranging between 70 to 120 cm was used. It was also stated that black plastic mulch significantly affected the crop yield. The yield increased with use of black plastic mulch from 20.7 to 29.8% as compared to bare soil. Different plastic mulch laying techniques and machines were developed for different soil conditions by many researchers. Some of the developed machines were capable of carrying multiple operations i.e. mulch laying, making punch holes, drip laying, fertilizer placement and retrieving mulch paper. The outcomes of their research concluded that the speed of operation and plant spacing affected the performance of machine. From some of the other reviews it was also suggested that, forward speed of 0.8, 1.0 and 1.2 km/h were recommended for punch spacing of 300, 600 and 1200 mm, respectively (Avtade 2015, Job 2016). The study related with the effect of operational speed of machine and thickness of mulch paper on machine performance.

MATERIAL AND METHODS

Development and Theoretical Consideration of Mulching cum Punching Machine

To suit the requirement of small farmers, partial mechanization of some operations like laying of mulch paper and making holes for planting was envisaged by developing a manual mulch laying machine with making punching holes. This machine was simple in design and easy to operate. The developed machine should be easy to operate,



simple in construction and should have minimum cost. The development requirements were envisaged for the proposed development of mulching machine. It should be capable of performing various functions like forming of bunds, laying plastic mulch, covering soil from both sides of plastic mulch and making punching holes in single pass. The implement should be capable of operating in lateritic soil conditions. The size and weight of the implement was such that the implement will be stable on prepared land surface. The time, energy required and the cost of operation for mulch laying machine should be lower than existing conventional systems. The spacing of punching holes must be equidistant and uniform. The implement should not cause compaction of the soil which could inhibit plant growth. Considering these considerations, a mulch laying machine was developed. The manually operated mulch laying machine was essentially consisted of two main sections, mulch laying section and punching section.

Mulch Laying Section

Mulch laying section consists of main frame with handle arrangement, bed shaping shovels, mulch laying arrangement, press wheel, soil covering devices and punching arrangement. For laying the mulch paper on the prepared bed, an arrangement of roller pipe carrying mulch paper was fitted at 200 mm height behind the bund forming shovels. Two stoppers were mounted on the mulch roller so that mulch paper remains in position and also it can be effectively used for different mulch sizes. During the operation one person holds the mulch paper on the bund behind the machine before the operation started. Two persons were pulled by the handle to move the machine forward, the roller automatically starts rotating and the mulch paper is laid on the bed.

Punching Section

To achieve desired punch spacing as per the crop requirement. The adjustments were provided for making holes. The punching unit was made by using MS flats and square pipes of different sizes. The punching wheels were attached to the main frame with attachment link for making holes at uniform distance. The variation in the plant spacing was achieved by varying the number of punching cups mounted on the punching wheels. The process was repeated for several times. During mulching operation on the field, plant spacing generally varies from 250 to 1000 mm. For this experiment, three plant spacings viz., 250, 500 and 1000 mm were selected. The variation in plant spacing was achieved by varying the number of punching cups mounted on the punching wheel.

Performance Evaluation of Developed Mulching cum Punching Machine

The performance of developed mulching cum punching machine was evaluated in field. The performance was evaluated at different levels of thickness of mulch paper and speed of operation to study their effect on effective field capacity, field efficiency and punching efficiency. Each experiment was replicated three times for better accuracy of results.

Measurement of Forward Speed

Two poles were fixed at 20 m distance. By using stopwatch, time required to cover 20 m distance was measured, respectively. The average speed was calculated. Then the experiment was carried out at three different speeds i.e. 1.3 km/h, 1.5 km/h and 1.7 km/h. The operators were trained to maintain the required steps distance to achieve the selected speed of operation.

RESULT AND DISCUSSIONS

The mulching machine with making punch holes was developed as per considerations. Performance of the machine was evaluated at three thicknesses of mulch paper (15, 20 and 25 micron) and speed of operation (1.3, 1.5 and 1.7 km/h) to study their effect on effective field capacity, field efficiency and punching efficiency.

Individual effect of mulch paper thickness on effective field capacity, field efficiency and punching efficiency:

The effect of mulch paper thickness, namely, 15, 20 and 25 micron on effective field capacity, field efficiency and punching efficiency was studied. It was observed that effective field capacity was increasing with increased mulch thickness. The field efficiency was also seen to increase as the thickness of mulch paper increases. The punching efficiency was found to decrease with increase in thickness of mulch paper. The results were seen that for the 15 micron thickness of mulch paper the effective field capacity was 0.142 ha/h which has been increased to 0.149 for the 25 micron mulch paper thickness. The field efficiency was seen that for the 15 micron thickness of mulch paper was 77.43% which has been increased to 80.73% for the 25 micron mulch paper thickness. It may be because

thickness of mulch paper were reduced the length and weight of the paper were increased which implies the extra additional load on machine frame. The 25 micron mulch paper was easily unrolled on prepared bed with operating speed of machine. As such a slight variation has been observed with field capacity of machine but it was considered as a negligible effect. The punching efficiency for the 15 micron mulch paper was observed as 88.20% which has been decreased to 78.55% for 25 micron mulch paper. It may be because of punching cups were easily penetrate on the minimum thickness mulch paper. Past study (Avtade 2015) observed that the field capacity and field efficiency was 0.122 ha/h and 92.42% for tractor operated mulch laying machine. (Job 2016) reported that field capacity and field efficiency was 0.320 ha/h and 74.18% was observed using 20 to 35 micron thickness of mulch paper for mulch laying machine. It against that we observed the field capacity and field efficiency for 15 to 25 micron mulch paper as 0.149 ha/h and 80.73%. It was found nearer to the previous results.

Individual Effect of Speed on Effective Field Capacity, Field Efficiency and Punching Efficiency

The effect of speed of operation, namely, 1.3, 1.5 and 1.7 km/h on effective field capacity, field efficiency and punching efficiency was studied. It was observed that effective field capacity was increased with increases speed of operation. The field efficiency was also seen to be increased as the speed of operation increases but the punching efficiency was decreased with increase operating speed. The result was obtained for the 1.3 km/h speed of operation the effective field capacity was observed as 0.11 ha/h which has been increased to 0.19 ha/h at 1.7 km/h speed of operation. The field efficiency was observed as 72.04% at 1.3 km/h speed of operation which has been increased to 89.61 per cent at 1.7 km/h speed of operation. The punching efficiency at 1.3 km/h speed was observed as 85.18% which has been decreased to 84.40% at 1.7 km/h speed of operation. It may be because of when machine operated at maximum speed then maximum area was covered per unit time. Past study (Avtade, 2015; Minto Job, 2016) reported that the field capacity and field efficiency was observed as 0.122 ha/h and 94.83%, respectively. The mean operating speed was taken 1.2 km/h for tractor operated mulch laying machine and 2.6 km/h for manually operated machine.

Effect of thickness of mulch paper and speed of operation on field capacity, field efficiency and punching efficiency:

The effect of thickness of mulch and speed of operation on field capacity shows in **Figure 2**. It was observed that the field capacity was increasing with increasing speed of operation from 1.3 to 1.7 km/h. The maximum field capacity was found as 0.185 ha/h at 1.7 km/h operating speed of machine.

Figure 3 presents the effect of thickness of mulch and speed of operation on field efficiency. It was observed that the field efficiency was increasing with increasing speed of operation from 1.3 to 1.7 km/h. The maximum field efficiency was found as 90% at 1.7 km/h operating speed of machine.

Figure 4 represents the effect of thickness of mulch paper and speed of operation on punching efficiency. It was perceived that the punching efficiency was decreasing with increased speed of operation from 1.3 to 1.7 km/h. The maximum punching efficiency was observed above 89% at 1.3 km/h speed of operation. Similarly, it was decreasing with increased thickness of mulch paper from 15 to 25 micron.



Figure 1 Developed mulching machine

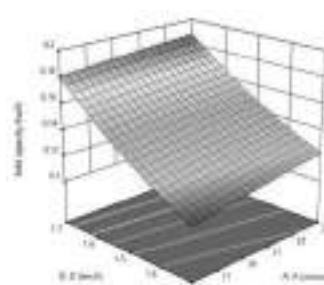


Figure 2 Effect of thickness of mulch and speed of operation on field capacity

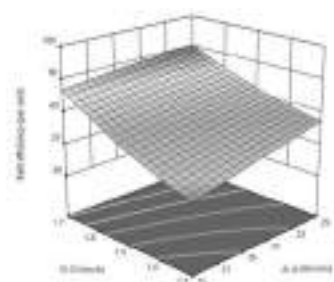


Figure 3 Effect of thickness of mulch and speed of operation on field efficiency

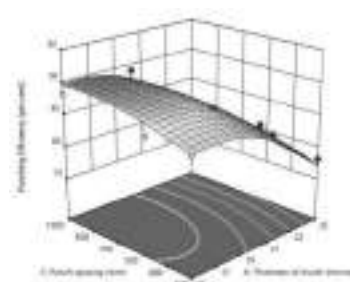


Figure 4 Effect of thickness of mulch and speed of operation on punching efficiency

Table 1 Mean value table for effect of thickness of mulch and speed of operation on field capacity, field efficiency and punching efficiency

Thickness of mulch paper, micron	Field capacity, ha/h			Field efficiency, %			Punching efficiency, %		
	Speed of operation, km/h			Speed of operation, km/h			Speed of operation, km/h		
	1.3	1.5	1.7	1.3	1.5	1.7	1.3	1.5	1.7
15	0.11	0.15	0.19	71.99	79.43	89.55	88.61	87.81	88.18
20	0.11	0.15	0.19	72.17	79.87	89.45	87.53	85.56	87.45
25	0.11	0.15	0.19	71.96	80.70	89.54	79.40	78.67	77.58

CONCLUSION

Intended operations have been achieved by the machine such as bed forming, laying of mulch, covering of mulch from both sides and punching holes on mulch paper.

Thickness of mulch paper has shown the significant effect on performance of machine. As the thickness of mulch paper increases the effective field capacity shows the slight variation and field efficiency increases with increased mulch paper thickness. The punching efficiency was decreased with increased mulch paper thickness.

The speed of operation shows the highly significant effect, as the speed of operation increases the effective field capacity and field efficiency also increases as against of that the punching efficiency decreases effectively.

REFERENCES

1. AS 1289 B1.1. Standards association of Australia, Determination of moisture content of a soil: Oven drying method (Standard method), 1977.
2. Avtade, (2015). Development of tractor operated mulch laying machine, submitted post Graduation Thesis, Department of Farm Machinery and Power Engineering, CTAE, Udaipur, Chapter 4, 31-39.
3. Dutta, D. (2006). Studies on effect of planting method and mulch on summer groundnut (*Arachis hypogaea* L.), International Journal of Agricultural Science 2 (2) 441-443.
4. Lawrence, M.J., D. R. Buckmaster and W.J. Lamont (2007). A Pneumatic Dibbling Machine for Plastic Mulch. Applied Engineering in Agriculture, 23: 419-424.
5. Job, (2016). Evaluation of Plastic Mulch for Mechanical Installation, Degradation and Moisture Distribution Pattern under Onion Cultivation. Submitted Doctor of Philosophy thesis, Department of Soil and Water Conservation Engineering, CTAE, Udaipur Chapter 4. 64-81.
6. Singh, A. K. and S. Kamal (2012). Effect of black plastic mulch on soil temperature and tomato yield in mid hills of Garhwal Himalayas, Journal of Horticulture and Forestry 4(4), pp. 78-80.
7. Timothy, C. (2010). Performance of Paper Mulches using a Mechanical Plastic Layer and Water Wheel Transplanter for the Production of Summer Squash. Horticulture Technology, 20:319-324.

Self Optimizing Drip Irrigation System to reduce the Wastage of Water

R. Raj Kumar¹, K. Sriram*¹, I. Surya Narayanan¹

Department of Electronics and Instrumentation Engineering, Kongu Engineering College, Erode¹, sriramk146@gmail.com*

ABSTRACT

The water scarcity is one of the major issues that makes the farmers to spend more for the efficient irrigation for their farmlands. The government needs to pay compensation cost in millions to the farmers during droughts. Utmost care should be taken for the effective utilization of the available water source in present situation. The effective way of irrigation that had been introduced in near past is the Drip Irrigation System (DIS). The wastage of water to irrigate crops and plants in the agricultural fields are reduced to 60% to 70% at the maximum but, there is approximately 30 to 40% of water being not properly utilized. Further, an idea is needed to maximize the utilization and to reduce the wastage of water in drip irrigation. The Actual water flow through drip irrigation is 4GPH. The proposed idea aims to reduce the water wastage which is approximately 2GPH while irrigating plants in existing drip irrigation system. So, the optimization made in this proposal will help the farmers in water conservation and effective utilization of water.

KEYWORDS Arduino, Drip irrigation, Earth resistance, Water conservation

INTRODUCTION

The Infrastructure development to conserve the water resources has been a common agenda in many developing countries like India. India has both arid and semiarid tropical condition. The water demand will increase 50% in 2025 in India according to the survey of International Water Management Institute (IWMI) done recently [1]. The average consumption of water per citizen in India is 100 to 150 l/day [2]. This 'high demand low supply' state of water has to be considered seriously and effective water conservation techniques are needed to meet the water demand. The one among the major water consumptions is the irrigation of crops in agricultural land by farmers in India. The rising global challenge of water includes irrigation for crops. The farmers need to spend more money to irrigate their crops despite of water demand [3]. The effective Irrigation Method introduced in the recent decade is Drip Irrigation System (DIS) [4]. The DIS produces 4 GPH water flow to the Agricultural Fields [5]. The water flow produced by the DIS is not utilized at maximum [6]. Based on the literature survey, DIS has a drawback that it is not utilizing the water for irrigation. The optimization is required in the existing DIS. Even though the DIS is more effective than other irrigation techniques, there is still a part of water is underutilized and therefore, water conservation is affected. As a result, Government has to pay compensation in millions at the time of water scarcity to farmers [7]. The other water irrigation systems which are practiced before the DIS and introduced after the DIS are not proved as better practices [8,9]. The observations from existing irrigation systems are: (i) Reduction in wastage of water, (ii) Installation should be easy and (iii) Proper water distribution. The outcomes of the proposed system are: (i) Reduction in wastage of water, (ii) Enhanced water utilization and (iii) optimized efficient irrigation system. Water conservation is agricultural field and the irrigation systems are needed to be upgraded.

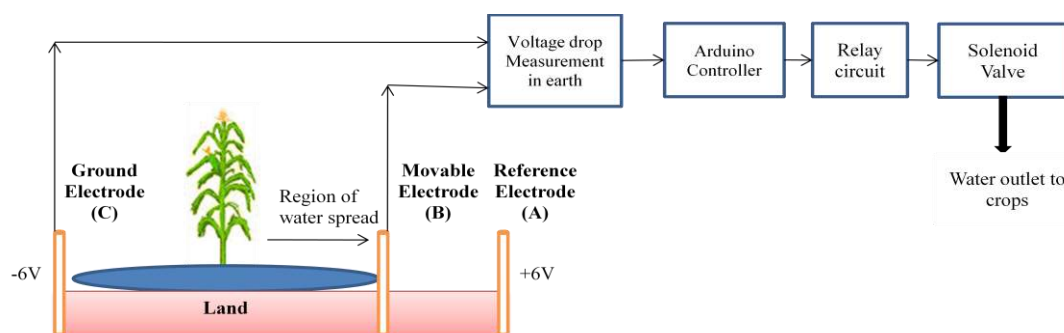


Figure 1 Block diagram

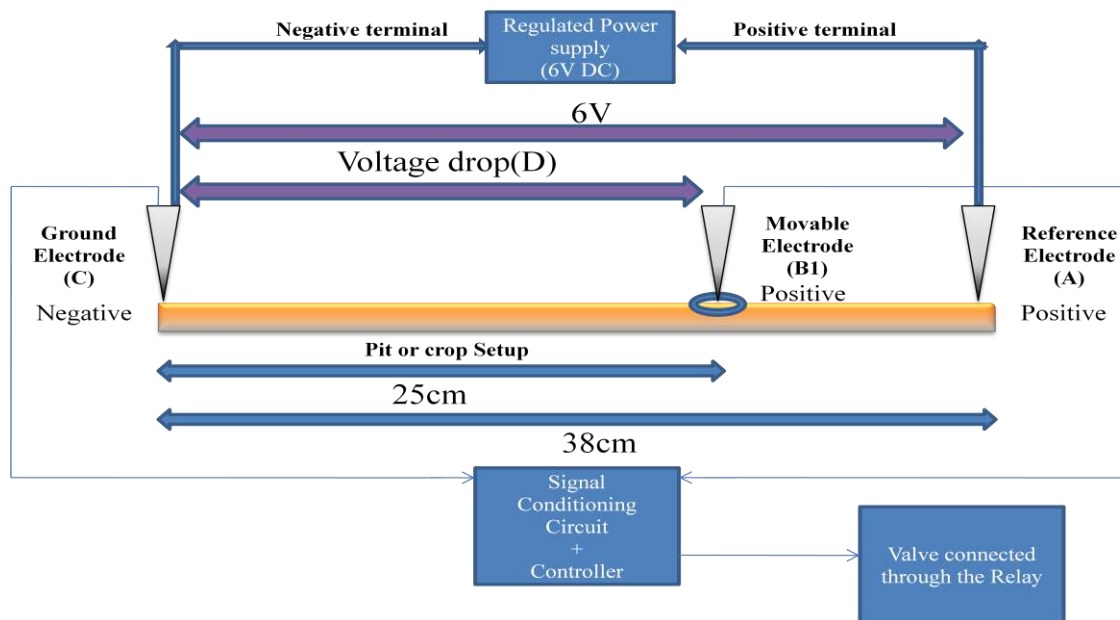


Figure 2 Prototype layout

SYSTEM DESCRIPTION

The major functional blocks of the proposed system is shown in **Figure 1** which includes 6V DC supply, earth electrodes, Arduino controller, signal conditioning unit, flow control valve setup and relay circuit. The voltage supply is given to the earth electrodes and the terminals of the electrodes acts as the terminals of a resistor (earth resistance). Therefore, when the voltage is given, there will be a voltage drop across electrodes due to the earth resistance. The voltage drop obtained is fed into the signal conditioning circuits and according to the changes in the voltage drop due to the change in the state of wetness in the soil the flow valve control will be actuated by the control pulse generated through Arduino controller. According to the control signal the relay circuit will and controller actuate the control valve in order to control the flow of the water towards the plants. Once the water reaches the plant root's maximum absorbance point the control valve should get closed.

DESIGN AND METHODOLOGY OF THE PROTOTYPE

The prototype is designed as shown in the **Figure 2**. The 6V DC supply is given to the Electrodes A and C. The electrodes are placed in such a manner that the crop or pit is located Electrode B1 and C as shown in Fig.2. The movable electrode is placed at a particular distance from the specific plant at the maximum absorbance point of the crop. Every crop variety has different maximum water absorbance point (e.g. Turmeric plant 15cm).

The absorbance point can be calculated by field surveying the particular crop used for drip irrigation. The distance to place the movable electrode (B1) for different crops is found, based on the water absorbance point of the particular crop or pit. The voltage drop (D) is observed between the B1 and C in both wet and dry conditions of the soil.

It is inferred that the soil exhibits conductivity properties. The conductivity varies according to the type of the soil and the various soil types contain different ion contents naturally. This prototype is tested in the red soil and the voltage drop (D) readings are tabulated in Table 1 which shows the conductivity in soil at wet and dry conditions.

The conductivity of the soil is decreased due to the resistance created by the water when soil is irrigated. The decrease in conductivity happens due to the resistance created for flow of ions in the soil when soil gets wet. This phenomenon is sensed in terms of change in voltage drop (D). To achieve the required outcome, conductivity phenomenon is used for controlling action.

Table 1 Voltage drop in dry and wet soil



Distance between the Reference and Ground electrode	38cm	
Distance between the Movable and Ground electrode	25cm	
Supply given to the Reference and Ground electrode	6V	
Voltage drop between the Movable and Ground electrode in normal(dry) condition	2.78V	Difference in Voltage Drops=0.53V
Voltage drop between the Movable and Ground electrode in wet condition	2.25V	

SIGNAL CONDITIONING CIRCUIT

The Arduino board is used for the controlling action with respect to the voltage signal from the voltage sensor circuit. The voltage sensory circuit comprises a 10k Ω and a 100k Ω resistor which is actually a voltage divider circuit. The input voltage acquired from the electrodes varies due to the soil conditions. The sensed voltage from the electrodes is not compatible with the Arduino processor. Therefore, voltage sensory circuit is used to stabilize the above mentioned incompatible voltage drop signal and then passed to the Arduino processor. The maximum acceptable voltage is 5V. The prototype set up is shown in Fig. 3. This is because the analog input port of the Arduino controller can access signals only up to 5V. Further, the voltage signal received from the voltage sensory circuit is converted to byte-wise values by byte-wise mapping process, where 0V to 5V signal is directly converted 0 byte to 1023 bytes through Arduino programming [10].

RESULTS OBTAINED

It is inferred from the **Table 1** that the voltage drop (D) occurred during the change in state of the soil wetness can be used to control the flow valve of the DIS in the agricultural fields. The prototype was tested for the Turmeric plant which has maximum absorbance point of 10cm. The outlet flow rate of the drip tube is absorbed 0.5GPH the valve shuts down when the water spreading reaches to maximum water absorbance point and the irrigation is controlled. All these occurred within the time period of 90 to 100 minutes which shorter than the time period practiced by the farmers (150 to 180 min). As per the field survey conducted for the turmeric plant, it is observed that the maximum absorbance point turmeric root is 15 cm and any quantity of water irrigated beyond this distance will not be absorbed by it. This fact can be explained in **Figure 4**.

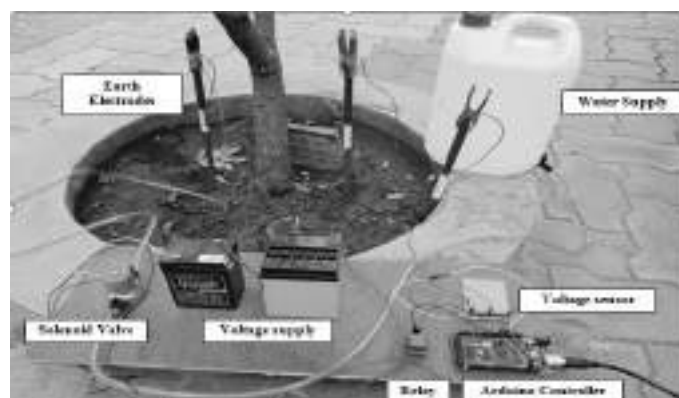


Figure 3 Prototype setup

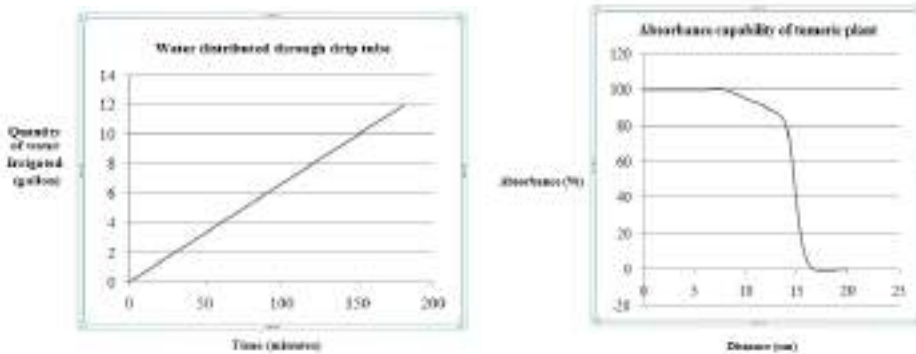


Figure 4 Absorbance capability of turmeric plant **Figure 5** Water distribution from drip tube to soil

The analysis of the obtained results on the quantity of water and time saved is described in **Figure 5**. It is observed from **Figure 5** that the actual time taken for the optimized irrigation is 90 to 120 min where as in the conventional irrigation practice it is 150 to 180 minutes. Therefore, the implementation of the proposed idea in the agricultural fields results in the conservation of 4 to 8 gallons of water per irrigation.

CONCLUSION

To entrust the awareness about the water wastage in the drip irrigation among the farmers of this generation and the future generations is the sole purpose of this whole attempt. As from all that has been discussed in this proposed system, it is inferred that with a controller and the change in voltage from electrodes, the wastage of water in the drip irrigation system being reduced completely. In the upcoming days, the essentiality of water will grow humongous and every drop of water matters. Hence this prototype ensures that the water wastage will be drastically abridged and there is a high possibility that the unutilized 30-40% of irrigation water get retained completely.

REFERENCES

1. Meredith Giordano, Hugh Turrall, Susanne M. Scheierling, David O. Tréguer, Peter G. McCornick, Beyond More Crop per Drop: Evolving Agricultural Water Productivity, IWMI Research Report 2016-16.
2. S.Viswanath, how much water an urban need?, The Hindu-Feb 15,2013.
3. International Water Management Institute (IWMI), IWMI Annual Report, 2017.
4. D.Suresh Kumar, K.Palanisamy, Impact of Drip Irrigation system on Farming system: Evidence from South India, Management, Performance and Applications of Micro Irrigation Systems-chapter 2, 2016.
5. Tamil Nadu Agricultural University, Drip irrigation methodology and statistical data on water consumption, TNAU <http://www.tnau.ac.in/agritech> portal.
6. Information gathered from interviewing Mr.Iyappan.N , a farmer in Mulanur and his subordinate farmers about "Drip Irrigation".
7. Tamil Nadu State Government, TNAU drought survey 2016, TNAU portal.
8. Karagiannis,G.,Tzouvelekas,V., & Xepapadeas,A. Measuring irrigation water efficiency with a stochastic production. Frontier Environmental and resource economics, 26(1), 57-72, 2003.
9. Dawalibi FP, Ma J, Southey RD, Behaviour of grounding systems in multilayer soils: a parameter analysis. IEEE Trans Power Deliv 9(1):334-342, 1994.
10. Er.Sukhjot Singh, Er.Neha Sharma, Research Paper on Drip Irrigation Management using wireless sensors. IRACST – International Journal of Computer Networks and Wireless Communications (IJCNCW), ISSN: 2250-3501 Vol.2, No4, August 2012.



Economic Evaluation of Solar Tunnel Dryer for Drying of Moringa Oleifera Leaves

Divyesh R. Vaghela^{1*}, Maulik L. Ramani¹, Satish S. Vaghasiya¹, S.H. Sengar²

Department of Renewable Energy Engineering, CTAE, MPUAT, Udaipur¹, vagheladivyesh08@gmail.com*

Department of Renewable Energy Engineering, CAET, NAU, Dediapada²

ABSTRACT

Moringa leaves are outstanding as a source of vitamin A, B group, all amino acids, rich in iron and are among the best plant sources of minerals. Moringa leaves are highly perishable and they require processing treatment to prevent post-harvest losses. Drying could be a good way of protective moringa leaves and to scale back them into powder, creating it easier to store and use at any time. Traditionally, the moringa leaves are dried by spreading in open sun in a thin layer. In comparison to sun drying, minimum spoilage and microbial infestation, improved and more consistent product quality are obtained in solar tunnel drying. In open sun drying the losses of valuable nutritional properties of moringa leaves take place, so to retain that nutritional property solar tunnel drying is preferred. The performance of solar tunnel dryer for Sargava leaves (“Moringa Oleifera”) drying and also its techno-economic analysis were carried out by different indicators such as Net Present Worth (NPW), Benefit-Cost ratio (B:C) and Payback Period for one-fourth loading capacity of solar tunnel dryer. Net Present Value for the first year and Benefit-Cost Ratio for moringa leaves drying under solar tunnel dryer were found as 39545, and 1.9 respectively.

KEYWORDS Moringa Oleifera leaves, Drying, Solar tunnel dryer, Economics

INTRODUCTION

Moringa Oleifera is a miracle tree. All parts of the tree are useful because they possess pharmacologic and nutritional properties [1]. Some common features of the moringa species are high nutritional values, presence of antioxidant and glucosinolates. However, the nutritional values can be changed by 1.5 to 3 times during the leaf stages and harvesting season especially for β -carotene and iron [2]. They are among the best nutritional sources from plants and their leaves are outstanding sources of vitamin A, B group and C (when raw). They contain more from than kantonmire, 7 times higher source of vitamin C than an orange, higher in protein and calcium content than milk and vitamin A in carrot by 4 times and higher potassium than bananas by 3 times [3]. Moringa leaves can cure disease along with 100 of other health benefit. It has more than 90 nutrients, 40 powerful antioxidant and 8 essential amino acids [4]. Morniga leaves have been used in its dried state or powdered form as a supplement in diets to make delicious meals, porridge for pregnant and nursing mothers, infants, and young children, as well as adults of all age groups [5]. It can be calculated that solely 20 to 40% of fat-soluble vitamins are preserved if leaves are dried underneath direct daylight, but that 50 to 70% will be retained if leaves are dried in the shade [6].

Enoh-Arthur and Damme [7] stated that using moringa leaves powder is a way of preserving nutrients as the powder can be added to food after cooking. Makkar and Becker [8] reported that moringa powder can be added to almost any food as a nutrient supplement. The nutritive values of pap, cereals, and drinks can be improved using dried moringa powder [9] and cookies can also be fortified with moringa leaf powder [10]. Gaman and Shenngton [11] stated that moringa leaves can be stored and consumed in different ways such as eating fresh, cooked or stored as dried in powder form without refrigeration for many months. Moringa Oleifera leaves are mostly available and consumed in dried form to preserve and facilitate transportation, packaging, and distribution.

Moringa leaves are highly perishable and they require processing treatment to prevent post-harvest losses. This implied that treatment such as drying preserves them from fast deterioration. To preserve the leaves and make them easier to store and use any times, drying is a great way to achieve this. The dried leaves still constitute a very rich nutrition value concentrated in them even if a large number of water-soluble vitamin are lost during the operation [12]. The leaves are traditionally dried by spreading in the open sun in thin layers. However, this method has several disadvantages like the rate of drying cannot be controlled, non-uniform drying, deterioration due to exposure of leaves against rain, dirt, storm, insect, pest which goes poor quality of the dried moringa leaves [13-14]. In open sun drying the losses of valuable properties of moringa leaves take place, so to retain those valuable property solar tunnel drying is preferred [15].



Mohod et al. [16] conducted the economic analysis of peeled prawns by comparing solar tunnel dryer and open sun drying methods. The financial assessment of the solar tunnel dryer was introduced in term of Net Present Worth, Benefit-Cost Ratio, Payback Period. The Payback Period for solar tunnel dryer was found to be 2.84 years. Badgujar et al. [17] evaluated a solar tunnel dryer installed at Ramakrishna Agro. Vegetables & Food Product Kodoli. And its techno-monetary investigation was conveyed by various variables, such as Net Present Worth, Benefit-Cost proportion and Payback Period. The Net Present Worth, Cost-benefit Ratio and Payback period for solar tunnel dryer were ₹ 62,894/, 1.11 and 7 months 2 days, respectively.

METHODOLOGY

The solar tunnel dryer mainly consists of a cover of U.V. stabilized polyethylene sheet of 200 µm fixed on the angle iron frame with the help of the zig-zag C-locking device. The dryer is large enough that one can enter inside to load and unload the green leaves to be dried. The floor of the solar tunnel dryer is developed with bond concrete and painted dull black for retaining more solar radiation to increase the temperature inside the dryer. The supports for the chimney, door were welded. The isometric view of the solar tunnel dryer (100 kg per batch) is shown in **Figure 1**.

Performance of Solar Tunnel Dryer

Solar tunnel dryer was evaluated in terms of mass reduction of moringa leaves with respect to time and other parameters like, (i) moisture content variation, and (ii) temperature inside and outside of the tunnel dryer.

The variation in solar radiation intensity, inside-outside temperature, humidity, moisture loss etc were observed in the month of April during the experiment. The experiment was conducted under one-fourth load condition of tunnel dryer for drying of Moringa leaves.

Techno-Economic Analysis

The economics of drying operation changes as per the dryer used as well as other factors. The economics was calculated separately for drying of Moringa leaves by solar tunnel dryer. Drying was proceeded till the moisture content of the leaves reached the safe moisture content (i.e. 6 % on w.b.). The different economic indicators for the economic analysis of the dried green leaves powder business for drying of Moringa leaves in the solar tunnel dryer are described in subsequent sections.

Economic Indicators

To assess the financial practicality of solar tunnel dryer, three different economic indicators namely net present worth, the benefit-cost ratio, and payback period have been used [18,19].

Net Present Worth

The present value of the future returns was calculated by subtracting gross benefit or the investment cost from the net benefit.

The net present worth of drying system for moringa leaves was calculated by given formula,

$$NPW = \sum_{t=1}^{t=n} \frac{B_t - C_t}{(1+i)^t} \quad (1)$$

where, C_t = cost in each year (₹), B_t = benefit in each year (₹), $t = 1, 2, 3, \dots, n$ (years), and i = discount rate, %.

Benefit-Cost Ratio

Benefit-cost ratio was calculated by comparing the present worth of costs with a present worth of benefit. The mathematically cost-benefit ratio was computed as follow:

$$B/C \text{ ratio} = \frac{\text{total benefit received per year}}{\text{capital cost of solar tunnel dryer}} = \frac{\sum_{t=1}^{t=n} B_t}{\sum_{t=1}^{t=n} C_t} \quad (2)$$

Payback Period

The payback period was calculated to describe the length of time between cumulative net cash outflow recovered in the form of yearly net cash inflows. The payback period (PP) of the solar tunnel dryer was calculated by the given formula,

$$\text{Payback period} = \frac{\text{Total investment}}{\text{Net profit}} \quad (3)$$

RESULTS AND DISCUSSION

Experimental results for drying of moringa leaves in solar tunnel dryer showed that 25 kg Moringa Oleifera leaves were required 12 h (1.5 days drying) to yield 6 kg dried moringa leaves. 1st day of drying was done from 10 AM to 5 PM, 2nd day of drying start at 10 PM to obtain a safe moisture content of Moringa Oleifera leaves which was obtained up to 1 PM.

Figures 2 and 3 show the variation in a mass reduction of moringa leaves during the drying process under the solar tunnel dryer. From these figures, it can be seen that initially mass reduction of moringa leaves recorded very fast and it was depleted as drying time passed. Due to the higher intensity of solar radiation between 1 to 2 PM, higher mass reduction was observed.

The financial investigation of the solar tunnel dryer for the drying of Moringa leaves was calculated by considering the initial investment of the dryer, average repair, and maintenance cost, cost of raw material, gathering and selling price of the material after drying. The parameter was calculated for economic analysis depicted in **Table 1**.

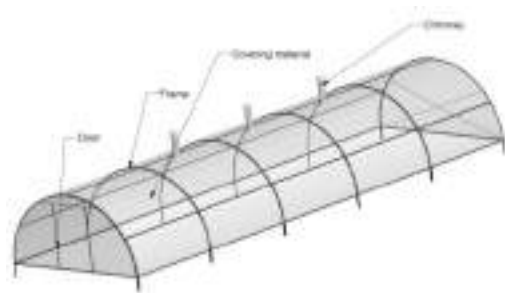


Figure 1 Isometric view of the solar tunnel dryer

Table 1 Cost incurred in economic analysis

Parameter	Cost, INR
Cost of raw material and collection	36000
Cost of dryer	15500
Selling price of dried leaves (per kg)	120
Cost of operation After every year	500
and maintenance After every 5 year	2500

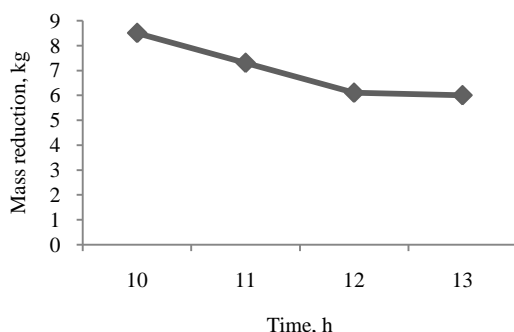


Figure 2 Mass reduction with respect to time (Day 1)

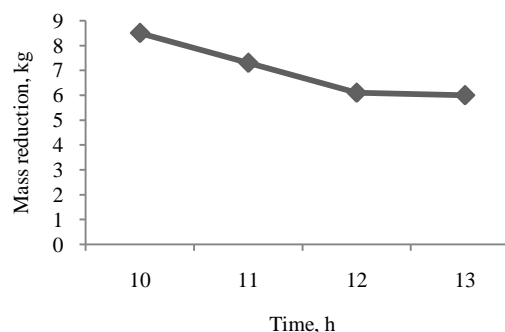


Figure 3 Mass reduction with respect to time (Day 2)

The economic evaluation was carried out for one-fourth loading capacity of solar tunnel dryer. If sarvaga is dried under solar tunnel dryer for a month total dried powder could be storing up to 126 kg and if this process is continued in a whole year (that is, 186 days) it can be prepared up to 744 kg. In the market, the selling price of dried moringa powder is ₹ 120 per kg. If a farmer can install solar tunnel dryer on his own farm, so he earn ₹ 89,280 yearly by drying of moringa leaves. Net Present Value for the first year, Payback period and Benefit-Cost Ratio for Moringa drying under solar tunnel dryer were found as ₹ 39,535, 8 months 9 days and 1.9 respectively. Economic indicators for drying of sargava leaves are described in **Table 2**.

Table 2 Economic indicators

Indicators	Details
Initially investment	₹ 55000
NPW @ 12% interest	₹ 39535



Benefit-Cost ratio	1.9
Payback period	8 month 9 days

The finding for economic analysis of solar tunnel dryer and detail cost for construction of solar tunnel dryer having 100 kg capacity are described in **Tables 3** and **4**, respectively.

Table 3 Present worth of total cash inflow and out flow for solar tunnel dryer

Year	Cash outflow, ₹	PW of Cash outflow (@ 12% interest)	Cash inflow	PW of Cash inflow (@ 12% interest)	NPW, ₹
0	55000	55000	0	0	-55000
1	45000	40178.6	89280	79714.3	39535.7
2	45000	35873.7	89280	71173.5	35299.7
3	45000	32030.1	89280	63547.7	31517.6
4	45000	28598.3	89280	56739.1	28140.7
5	47500	26952.8	89280	50659.9	23707.1
6	45000	22798.4	89280	45232.0	22433.6
7	45000	20355.7	89280	40385.7	20030.0
8	45000	18174.7	89280	36058.7	17883.9
9	45000	16227.5	89280	32195.3	15967.8
10	47500	15293.7	89280	28745.8	13452.0
11	45000	12936.4	89280	25665.9	12729.4
12	45000	11550.4	89280	22916.0	11365.6
13	45000	10312.8	89280	20460.7	10147.8
14	45000	9207.9	89280	18268.5	9060.6
15	47500	8678.1	89280	16311.1	7633.0
16	45000	7340.5	89280	14563.5	7223.0
17	45000	6554.0	89280	13003.1	6449.1
18	45000	5851.8	89280	11609.9	5758.2
19	45000	5224.8	89280	10366.0	5141.2
20	0.0	0.0	89280	9255.4	9255.4
TOTAL		334140.2		666871.9	332731.7

Table 4 Construction cost details of solar tunnel dryer

Item	Specification	Quantity required	Rate of item	Total cost, ₹
M. S. angle (low-grade angle)	35 mm diameter	84 kg	38 Rs/ kg	3192/-
	40 mm diameter	14 kg	50 Rs/ kg	700/-
Polythene film	Gauge	30 m ²	78 Rs/m ²	2340/-
Flat iron strips	-	88 kg	38 Rs/ kg	3344/-
GI sheet	24 Gauge	9 kg	65 Rs/ kg	585/-
Black color		2 liter	150 Rs/l	300/-
Welding rod	Long length	49 rods	12/rod	588/-
Locking mechanism	-	36 m	10 Rs/m	360
Nut – bolts	-	4 kg	50 Rs/ kg	200/-
Cement	53 Grade	49 kg	6/ kg	294/-
Labour charge (per day)	3 Labour	4 days	Rs.300	3600/-
TOTAL				15500/-

CONCLUSION

The cost economics of solar tunnel dryer for sargva leaves are proved that farmer can earn ₹ 89, 280 by adopting solar tunnel drying technology with installation on its own farm. According to beneficial characteristics and market value of dried sargava leaf powder farmer can earn side income by this technology. A farmer can recover the cost of solar tunnel dryer within 8 months and 9 days time period.



REFERENCES

1. Daba, Mekonnen. Miracle tree: A review on multi-purposes of *Moringa oleifera* and its implication for climate change mitigation. *J. Earth Sci. Clim. Change* 7, no. 4 (2016).
2. Yang, Ray-Yu, Lien-Chung Chang, Jenn-Chung Hsu, Brian BC Weng, Manuel C. Palada, M. L. Chadha, and Virginie Levasseur. Nutritional and functional properties of *Moringa* leaves–From germplasm, to plant, to food, to health. *Moringa leaves: Strategies, standards and markets for a better impact on nutrition in Africa*. Moringanews, CDE, CTA, GFU. Paris (2006).
3. Sengev, Abraham I., Joseph O. Abu, and Dick I. Gernah. Effect of *Moringa oleifera* leaf powder supplementation on some quality characteristics of wheat bread. *Food and nutrition sciences* 4, no. 3 (2013): 270.
4. www.fhc-ng.com/pdf/healthbenefits.pdf
5. Alakali, J. S., C. T. Kucha, and I. A. Rabi. "Effect of drying temperature on the nutritional quality of *Moringa oleifera* leaves." *African Journal of Food Science* 9, no. 7 (2015): 395-399.
6. Mishra, Satya Prakash, Pankaj Singh, and Sanjay Singh. "Processing of *Moringa oleifera* leaves for human consumption." *Bulletin of Environment, Pharmacology and life sciences* 2, no. 1 (2012): 28-31.
7. Enoh-Arthur S and Damme P.V, household analysis on local knowledge, domestication and use of *moringa oleifera* in the volta region of ghana. *Proceedings of the 5th International Symposium on New Crops and Uses: Their Role in a Rapidly Changing World*, Southampton, UK, 3-4th September, 2007, 456457. (2008).
8. Makkar H.P.S and Becker K Nutritional value and anti-nutritional components of whole and ethanol extracted *Moringa oleifera* leaves. *Animal Feed Science and Technology*, 63, 211–228 (1996).
9. Gardener and Ellen, *Moringa Tree has Many Uses, From Food to Firewood*. Yumasun. Portal Market, *Moringa Tree Powder*. (2002).
10. Emelike N.J.T, Uwa F.O, Ebere C.O and Kiin-Kabari D.B, Effect of drying methods on the physico-chemical and sensory properties of cookies fortified with *Moringa (Moringa oleifera)* leaves. *Asian Journal of Agriculture and Food Sciences*, 3(4), 361-367 (2015)
11. Gaman D and Shenngton R, The vegetable garden in the tropics. *Journal of Tropical Agriculture and Food Science*, 24-27(1996)
12. Oluwalana, S. A., W. Bankole, G. A. Bolaji, O. Martins, and O. Alegbeleye. "Domestic water purification using *Moringa oleifera* Lam." *nigerian Journal of forestry* 29, no. 1/2 (1999): 28-32.
13. N. S. Rathore, & N. L. Panwar, design and development of energy efficient solar tunnel dryer for industrial drying. *Clean Technologies and Environmental Policy*, 13(1), 125-132. (2011)
14. Assefa, S. Ayyappan, K. Mayilsamy, solar tunnel drier with thermal storage for drying of copra", *Proceedings of the 37th National and 4th International Conference on Fluid Mechanics and Fluid Power* Dec 16-18, 2010, IIT Madras, Chennai, India. (2010)
15. Pravin M. Gupta Roshan G. Pandav Raviprakash V. Singh Sagar K. Khuje, Review of Solar Dryer for Drying Agricultural Products *International Journal for Scientific Research & Development* 4(11), 524-528 (2017)
16. A.G. Mohod, S.H. Sengar, Y.P. Khandetod, Solar tunnel dryer as an income generation unit for fisherman. *BIOINFO Renewable & Sustainable Energy* 1(1), 01-04 (2011)
17. C.M. Badgujar, O.S. Karpe, S.R. Kalbande, Techno-economic evaluation of solar tunnel dryer for drying of basil (*Ocimum sanctum*). *Int. J. Curr. Microbiol. App. Sci* 7(7), 332-339 (2018)
18. S Kothari, NS Rathore, NL Panwar Techno economics of greenhouse for cultivation of aswagandha under composite climate of Udaipur. *Agric Eng Today* 25(3–4), 36–40 (2001)
19. Panwar, N.L., Kothari, S. and Kaushik, S.C., 2014. Cost-benefit and systems analysis of passively ventilated solar greenhouses for food production in arid and semi-arid regions. *Environment Systems and Decisions*, 34(1), pp.160-167.



Improvements in Functional Surfaces of the Engineering Parts using Microwave Cladding (MWC): A Detail Discussion

Amit Kumar^{*1}, Harpreet Singh¹, Neeraj Bhoi¹

Mechanical Engineering Department, IITDM Jabalpur, India¹, amit.sah1204@gmail.com*

ABSTRACT

Designing for improved performance in surface chemistry is a key concern in the mechanical and tribological industry. High wear and corrosion resistant material draw larger interest to the various sectors in automobile, aerospace, naval and spacecraft industries. The requirement of higher specific energy, larger processing time and numerous process variables need to control for better functional application. Owing to various disadvantages in conventional cladding process demands new and faster processing techniques which overcome such problems. Microwave cladding (MWC) is an alternative and developed method for the surface modification of various metallic and non-metallic components. The paper describes the various fundamental aspect of MWC process and their importance in the material processing. The paper describes the various literature which is available in the field of MWC in the timeline of material development. The different approaches for the MWC and affecting process variables are described to understand the capabilities of the microwave for the various functional applications. The article provides comprehensive knowledge about recent development in MWC process and their future application area.

KEYWORDS Microwave cladding, Hardness, Wear, Surface morphology

INTRODUCTION

Modification of surface as per the desired intention is major breakthrough in material processing technology. Cladding and coating are widely in use in the tribological and surface application where high resistance, better hardness, reduce porosity, improved smoothness is of prime requirement [1]. A number of cladding methods are available in the process industries such as laser cladding, chemical vapour deposition (CVD), electro chemical deposition, plasma assisted cladding, physical vapour deposition (PVD), thermally sprayed, magnetron sputtering and high velocity oxygen fuel coating (HVOF). However, the processing time, development and setup cost, process parameters are difficult to control. Recently, a new and developed method which is Microwave cladding comes into picture due to its unique feature in material processing [2–4]. Microwave material processing (MWP) inhibit several advantageous such as shorter processing time, improved densification factor, reduced porosity, better mechanical and tribological properties, enhanced diffusion capabilities etc., which separates form other conventional techniques [5,6]. By the use of microwave techniques numerous material processing applications such as sintering, joining, drilling, casting and coating operations are executed successfully. For tribological application surface modification is major works which are carried for the higher and better functional applications. Microwave cladding is a relatively new technique for the use in material synthesis for enhanced productivity with shorter processing time [7].

This paper aims to review the various experimental approaches which were done for cladding with the use of microwave. The main objective of this paper is to highlight the importance of the microwave cladding for different work material. The paper is categorizing in following phases: (a) working principle of microwave cladding, (b) historical development (c) effect of processing parameters on the output response of the clad surface (d) summary of the past research work on the microwave cladding.

WORKING PRINCIPLE OF MICROWAVE CLADDING

Microwave is the combination of electric and magnetic wave both is orthogonal to each other. The frequency range lies between 0.3 GHz to 300 GHz and wavelength in the range of 1mm to 1000mm. Most of the frequency is restricted by the international telecommunication union (ITU). However, a very few frequencies are available for industrial and commercial uses. For MWP mostly used frequencies are in the range of 915 MHz to 2.45 GHz and their corresponding wave lengths are 12.2 cm and 13.5 cm [7]. Microwave absorption capacities depends on material properties. For non-metal microwave absorption capacity of material depends on depth of penetration capacity of material.

$$D_p = \frac{1}{\omega \sqrt{0.5 \mu_0 \epsilon_0 \epsilon_r \left\{ \left(\sqrt{1 + \left(\frac{\mu_r}{\epsilon_r} \right)^2} - 1 \right) \right\}}}$$

Where, D_p = Depth of penetration, μ_0 = Magnetic permeability of air (Hm^{-1}), μ_r =magnetic constant (Hm^{-1}), ϵ_0 =Permittivity in air (Fm^{-1}), ϵ_r =Dielectric constant (Fm^{-1}), ω =Angular frequency (S^{-1}).

Microwave cladding mainly dependent upon the skin depth of the depositing material and substrate. In the case of microwave cladding the mixture of monolithic powder or compound of alloy is used to enhance the surface properties of the functional material. The cladding imparts higher hardness, toughness, wear and corrosion resistance over base material [3,4,8,9].

The powder material which is used in cladding process is pre heated in conventional furnace process with temperature range of 100-180°C for 24 h to remove possible moisture content. The substrate materials were cleaned through alcohol and acetone in ultrasonic prior to removal of impurities and dust particles. Further the clad powder is manually placed over the substrate for the deposition purpose. In the case of Microwave cladding generally hybrid heating is employed for the enhanced bonding with the substrate material. Generally, graphite or alumina plate is placed over the clad and susceptor material. The susceptor is used for the hybrid heating phenomenon and to increase the heat transfer rate to the clad material [3,4]. For cladding charcoal and silicon carbide is used as susceptor material. Susceptor is materials which absorb the microwave radiation and convert into heat which further transfer to the functional surface [1,10]. A basic schematic representation of the microwave cladding process is shown in the **Figure 1**.

MICROWAVE CLADDING: HISTORICAL BACKGROUND

Demands in rapid and better process leads to development of numerous new and advanced technology after second world war. Microwave was invented in the year 1945 for simple heating application. Later the microwave was applied for the curing and melting of low density plastic material. Later the use of microwave energy was applied for sintering of hard ceramic material. First successful sintering of powder metal body was done in the year 1999 [11]. After the successful experimentation of sintering of hard material various material processing operation was tested with the use of microwave energy. Later the processing of composite material using microwave energy was successfully implemented from large variety of material [12]. The main problem associated with the processing of bulk material using microwave is the formation of plasma which harm the magnetron and functioning of microwave. The processing of bulk material can be done by the proper insulation of microwave transparent material. The cladding using microwave was started in the year 2005 for brazing application. Later in the year 2008-2009 the cladding of bulk material in the different functional surface was applied. This was the breakthrough processing technique which require short processing time, easily available with strong metallurgical bonding between the clad and substrate material. The chronological development in the microwave material processing is depicted in the **Figure 2**.

EXPERIMENTAL STUDY ON MICROWAVE CLADDING

Present section highlight the various observations made by the researchers in the time span for the development of different types of cladding in the substrate material by the use of microwave energy. A general list of input process parameter is given in **Table 1** which was given by the various investigators for the microwave cladding process.

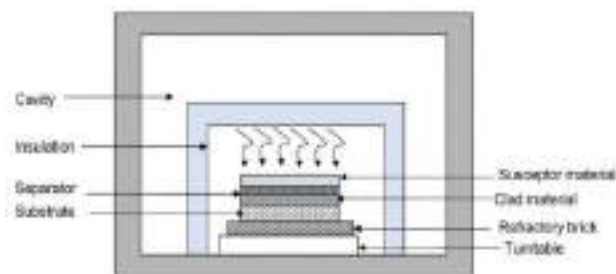


Figure 1 Schematic representation of microwave cladding process



Figure 2 Historical development in microwave material processing [12]



Gupta and Sharma in the year 2011 marvelously coated copper on the austenitic stainless steel (SS-316) with the use of microwave energy at normal operating frequency and power. They found that the hardness and wear resistance of the developed coating were significantly improved by 270 HV. A uniform and dense microstructure of the clad surface supports the improved mechanical and tribological performance of the material [3]. Subsequently the corrosion and wear resistance of the SS-316 was successfully improved by the use of nickel (EWAC) as clad material. For the uniform and improved heating charcoal as susceptor medium was applied over the clad material. Similarly the wear resisting property of the material significantly improved by the use of WC10Co2Ni clad material. The clad material exhibits 84 times higher wear resistance than parent material although the thickness of the clad surface is only 2 mm. The formation of hard inter-metallic substance on the substrate material leads to the higher wear resisting property in the material [9].

Table 1 Reported input process condition during microwave cladding

Parameter	Level/Range	Ref.
Operating frequency	2.45 GHz	[1,4,6-22]
Exposure time	5 to 25 min.	[6-22]
Exposure power	0.6-1.445 kW	[6-22]
Separator material	Pure alumina, graphite	[6-22]
Susceptor material	Charcoal, Graphite, silicon carbide	[6-22]

Nickel considered as potential material for the improvement in the hardness, corrosion resistance and wear resistance. The cladding of nickel on the substrate significantly enhance the material response at normal and elevated temperature. The concept of composite cladding utilizes the different material properties and response of different material to increase the output response (that is, mechanical and tribological properties). The EWAC and WC10Co2Ni were coated in the SS316 material by the use of microwave radiation. The three-point bending test of the clad material shows improved load deformation characteristics compare to substrate material. The average bending strength of the clad material found to be 629N with much higher hardness value as 416Hv. The volumetric heating process in microwave leads to the development of valley and cellar structure in the clad surface [13]. **Figures 3 and 4** shows the typical XRD pattern after microwave cladding and the micrographs of the clad sample in 3-point bending test a) fracture surface topography, (b) crack propagation inside the clad depth, and (c) secondary cracking. The presence of inter-metallic compound in the substrate material and crack propagation in the clad surface can be clearly visible from the micrographs.

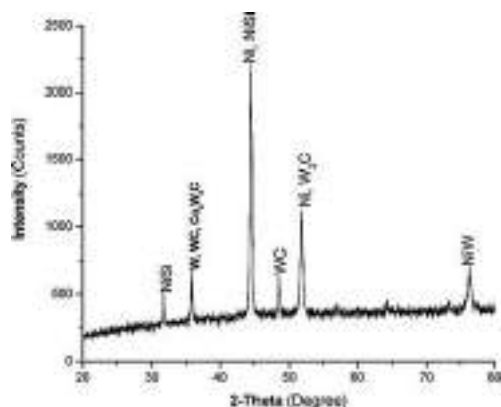


Figure 3 Typical XRD spectrum of composite cladding developed through MHH adapted from Sharma and Gupta, 2012

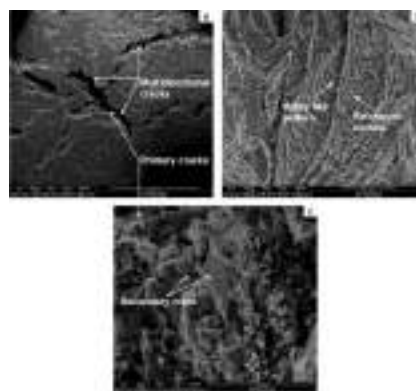


Figure 4 Scanning electron micrographs of fractured clad samples in 3-point bend test: (a) fracture surface topography, (b) crack propagation inside the clad depth, and (c) secondary cracking adapted from Sharma and Gupta, 2012

Similar report published in which WC–12Co cermet cladding of very less thickness (i.e. 1 mm) on the stainless steel material exhibits 3.5 times higher hardness value which can be used for wear resistant application without affecting the parent material [14]. In the same year Gupta and Sharma reported the formation of hard material during microwave cladding improves the surface properties significantly [1]. Similar results were experienced for the wear

resistant of the material by the use of EWAC and 20% WC10Co2Ni improves the hardness and wear resistant by 128 times compared to parent material [15]. Subsequently Bansal et al., reported the excellent wear resistant property in the substrate material by the cladding of WC and Ni in the mild steel. Fig. 5 depicts the wear rate of the substrate material with and without cladding. It can be noted that the wear resisting capacity with clad surface improves by approximately 70% [16].

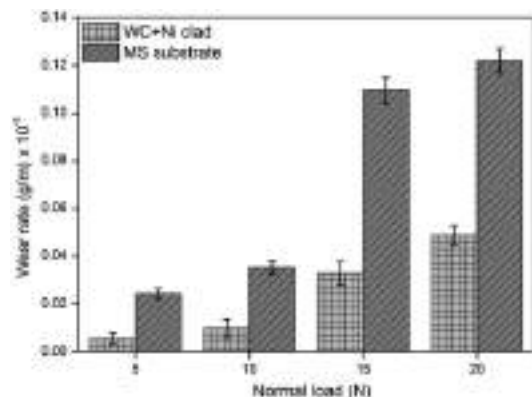


Figure 5 Wear rate of the Ni-WC microwave clad and MS substrate as a function of normal load adapted from Bansal et al., 2015

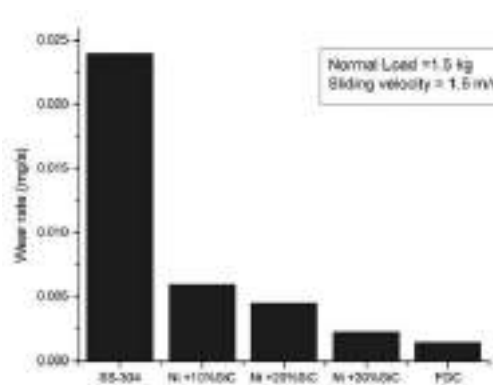


Figure 6 Wear rate comparison of FGC, single layer clads and SS-304 substrate adapted from Kaushal et al., 2017

Similar results were given by the use of WC-12Co clad material the friction co-efficient reduced by 56% compared to substrate material under different operating environment [17]. The use of composite cladding in the substrate material enhances the hardness and wear resistance under different operating and loading environment significantly [15,18–22]. Development of different kinds of harder ceramics and metallic material improves the hardness and wear resistance exceptionally. The stated concept can be related to the report given by Kaushal et al., 2017 where the wear resistance of the SS304 is largely improved by the addition of Ni and SiC in the clad surface. Fig. 6 illustrate the wear rate comparison of the clad surface and substrate material [21].

CONCLUSION AND FUTURE PROSPECTS

Microwave cladding is relatively new and effective method for the surface modification and enhance the surface properties of the substrate material. Various type of composite cladding is applied by the use of microwave processing. However, there are few challenges which required additional research for the effective utilization of the microwave energy for functional surface modification. Some challenges in the field of microwave cladding is given as:

- Microwave cladding (MWC) process parameters influences on the process performance characteristics are not completely investigated for corrosion resistance materials.
- Complete information on surface morphology aspects and characteristics of MW clad parts is not available.
- Clad surface wear aspects (rotational and translational) of MWC process have not been evaluated effectively.
- Process effects on work surface residual stress are not known.
- No efforts seem to have been made towards process modeling. Development of mathematical model which count the various input process conditions and output parameters required more research.

REFERENCES

1. D. Gupta, A.K. Sharma, Microwave cladding: A new approach in surface engineering, J. Manuf. Process. Volume 16, pp 176–182, 2014.
2. R. Che, L.M. Peng, X. Duan, Q. Chen, X. Liang, Microwave absorption enhancement and complex permittivity and permeability of Fe encapsulated within carbon nanotubes, Adv. Mater. Volume 16, pp 401–405, 2004.
3. D. Gupta, A.K. Sharma, Development and microstructural characterization of microwave cladding on austenitic stainless steel, Surf. Coatings Technol. Volume 205, pp 5147–5155, 2011.
4. D. Gupta, A.K. Sharma, Development of copper coating on austenitic stainless steel through microwave hybrid heating, Suppl. Proc. Gen. Pap. Sel. Volume 3, pp 263–270, 2011.
5. H. Singh, P.K. Jain, N. Bhoi, S. Pratap, Experimental study pertaining to microwave sintering (MWS) of Al-Metal Matrix Composite - A review, 3rd Int. Conf. Compos. Mater. Mater. Eng. Volume 928, pp 150–155, 2018.



6. S. Singh, D. Gupta, V. Jain, Recent applications of microwaves in materials joining and surface coatings, *Proc. Inst. Mech. Eng. Part B J. Eng. Manuf.* Volume 230, pp 603–617, 2016.
7. R. R. Mishra, A. K. Sharma, Microwave-material interaction phenomena: heating mechanisms, challenges and opportunities in material processing, *Compos. Part A Appl. Sci. Manuf.* Volume 81, pp 78–97, 2016.
8. A. Gaonkar, A. M. Hebbale, M. S. Srinath, Microwave cladding and characterization of WC-12Co on Nickel Based Super Alloy, pp 1–8, 2017.
9. D. Gupta, A. K. Sharma, Investigation on sliding wear performance of WC10Co2Ni cladding developed through microwave irradiation, *Wear.* Volume 271, pp 1642–1650, 2011.
10. D. Gupta, A. K. Sharma, Microstructural characterization of cermet cladding developed through microwave irradiation, *J. Mater. Eng. Perform.* Volume 21, pp 2165–2172, 2012.
11. R. Roy, D. Agrawal, J. Cheng, S. Gedevanishvili, Full sintering of powdered-metal bodies in a microwave field, *Nature.* Volume 399, pp 668–670, 1999.
12. R. R. Mishra, A. K. Sharma, A review of research trends in microwave processing of metal-based materials and opportunities in microwave metal casting, *Crit. Rev. Solid State Mater. Sci.* Volume 41, pp 217–255, 2016.
13. A.K. Sharma, D. Gupta, On microstructure and flexural strength of metal-ceramic composite cladding developed through microwave heating, *Appl. Surf. Sci.* Volume 258, pp 5583–5592, 2012.
14. S. Zafar, A. K. Sharma, Development and characterisations of WC-12Co microwave clad, *Mater. Charact.* Volume 96, pp 241–248, 2014.
15. A. Pathania, S. Singh, D. Gupta, V. Jain, Development and analysis of tribological behavior of microwave processed EWAC + 20% WC10Co2Ni composite cladding on mild steel substrate, *J. Manuf. Process.* Volume 20, pp 79–87, 2015.
16. A. Bansal, S. Zafar, A. K. Sharma, Microstructure and abrasive wear performance of Ni-Wc composite microwave clad, *J. Mater. Eng. Perform.* Volume 24, pp 3708–3716, 2015.
17. S. Zafar, A. K. Sharma, On friction and wear behavior of WC-12Co microwave clad, *Tribol. Trans.* Volume 58, pp 584–591, 2015.
18. S. Zafar, A. K. Sharma, Investigations on flexural performance and residual stresses in nanometric WC-12Co microwave clads, *Surf. Coatings Technol.* Volume 291, pp 413–422, 2016.
19. S. Zafar, A.K. Sharma, Abrasive and erosive wear behaviour of nanometric WC-12Co microwave clads, *Wear.* 346–347, 29–45 (2016).
20. S. Zafar, A.K. Sharma, Microstructure and wear performance of heat treated WC-12Co microwave clad, *Vacuum.* 131, 213–222 (2016).
21. S. Kaushal, D. Gupta, H. Bhowmick, An approach for functionally graded cladding of composite material on austenitic stainless steel substrate through microwave heating, *J. Compos. Mater.* 52, 301–312 (2018).
22. S. Kaushal, D. Gupta, H. Bhowmick, On surface modification of austenitic stainless steel using microwave processed Ni/Cr3C2 composite cladding, *Surf. Eng.* 34, 809–817 (2018).



Effect of Merman Band Separation System on Payload Fairing Separation Rivet

Ramashankar Sahu^{*1}, S. Balakrishnan¹, G. Ayyappan¹

Space Transportation Systems, Vikram Sarabhai Space Centre, Indian Space Research Organisation, Thiruvananthapuram, India¹, rssahu@gmail.com*

ABSTRACT

Payload fairing of a launch vehicle protects the payload from aerodynamic and thermal loads in ground as well as during the atmospheric phase of flight. A typical launch vehicle's payload fairing (PLF) has to separate horizontally and vertically from the thrusting vehicle. For horizontal separation a merman band separation system is used and for vertical separation system linear bellow system housed inside of piston and cylinder assembly is used. Expansion of the bellow results in the shearing of the rivets connecting the piston and the cylinder assembly which separates the both halves of PLF. PLF is attached to the launch vehicle with the preloading of merman band system. While preloading the merman band, nearby separation rivet also get loaded.

To find out the separation rivets forces due to tightening of the merman band assembly in addition to the flight loads (external loads) non linear contact analysis is carried out. Shear force distribution for the separation rivets are plotted for different load cases. Resultant shear force for the last rivet reaches near to rivet capacity, hence effect of introduction of shim is studied which reduces the rivet forces and increase the margin.

KEYWORDS Merman band, separation rivets, shear force, band tension, PLF

INTRODUCTION

For any launch vehicle payload fairing protects the payload from thermal effect on ground as well as during the atmospheric phase of flight. Once the launch vehicle clears the dense atmospheric regime, the payload fairing is jettisoned from the launch vehicle [1].

A typical launch vehicle payload fairing structure consists of four portions, spherical nose cap, nose cone, cylinder and the boat tail. These are connected by interface rings. Each of these are made in two halves joined by piston–cylinder jettisoning system through separation rivet except in the nose-cap region, where the interface is such that the two halves can freely slide against each other during separation (**Figures 1A and 1B**). The interface joint is thermally sealed and does not provide any interference during separation. Cutouts of required sizes are provided in cylindrical portion and boat tail region of payload fairing for payload cooling, RF transparency requirements, vent holes and access to various systems and optical alignment.

The nose cap is made of Aluminum alloy, which consists of hemispherical shell split into two halves made out of sheet with rings at separation plane and base. The edges at the separation plane are so interfaced that each half can slide freely against each other due to deformation caused during flight.

Nose cone is a conical shell structure stiffened with circumferential rings (bulk heads) to resist the external pressure and to prevent overall buckling of the shell. The skin thickness of the shell, number of rings and the spacing between rings are so adjusted that the margin of safety of the skin segments are maintained.

The largest part of the payload fairing is the cylindrical region having iso-grid construction. Loads coming on the components are mainly the axial load and bending moment. Considering the fabrication feasibility, cylindrical region is made in different panels of equal and covering 180° in circumference. Isogrid Cylinder is proposed to be made of Aluminum alloy material. Each isogrid panel has been designed for the expected flight loads at its aft end. Various parameters of iso-grid like rib width (b), rib depth (d), skin thickness (t) and triangle height (h) are decided based on design iterations to arrive at the final sizing. The boat tail portion is a conical frustum, skin stiffened construction with longitudinal hat stiffeners.

PLF aft end ring and PLA ring are held together circumferentially through discrete wedge blocks which are held by merman band. Merman band is held at the separation plane through bolt cutters. All the components of PLF, Wedge block and PLA are made of aluminum alloy (AA2014) whereas merman band is made of Maraging steel.

When the charge is initiated, the bolt cutters cut the bolt and the merman band gets released thus initiating the circumferential separation. In the preloading of merman band nearby piston cylinder separation rivet also get loaded.

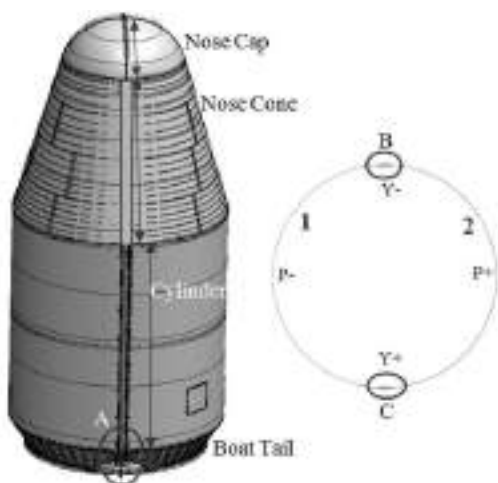


Figure 1A A typical PLF

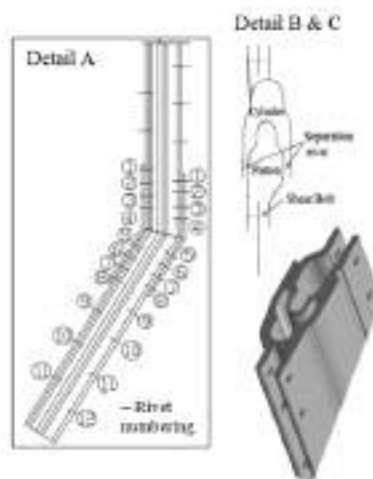


Figure 1B Piston cylinder assembly

If excessive loads (band tension and flight loads) cause these rivets to fail, this results early separation of PLF and hence total mission failure. Hence it is mandatory to find out rivet forces due to merman band and due to flight separately. This is why analysis is carried out in two load steps. PLF aft end ring is in two halves with 2 mm of gap. In first load steps with preloading of merman band these ring halves move closer which loads the separation rivets. In second load step flight load in addition to merman band load, is simulated. Objective of this study is to find out the separation rivets forces due to tightening of the merman band assembly in addition to the flight loads (external loads).

MERMAN BAND SYSTEM

Many separation systems are being used in a launch vehicle but the advantage of merman band system is that it does not use the mechanical fasteners or adhesives on either of the assembled component. Merman band system uses pyrotechnic devices to release the system and that makes this system useful for remote separation of components. Merman band system is used in other separation systems like spacecraft separation also [2].

The merman band system consists of three components - the payload fairing aft end ring flange, the PLA ring flange and the band system. The payload fairing aft end ring flange is made in two halves and the PLA ring is a continuous ring. The band clamp consists of 44 numbers of wedge blocks and an exterior merman band. The wedge block wedge together the flanges of the PLF aft end ring and the PLA ring flange. The merman band wraps around the wedge blocks and is preloaded by tightening a pair of bolts. As a result merman band transfer this preload to the wedge block which forces the wedge blocks up the inclined surface of the flanges generating contact forces between the both the flanges. During PLF separation the bolts are cut and wedge block and merman band become free to move which result into separation of PLF from the thrusting vehicle [3].

Merman band system is interface element between the PLF and the rest part of the launch vehicle. All the aerodynamic loads on the PLF is transferred to the adjacent structure through merman band system, which makes it, a critical element of launch vehicle. Wedge block converts the radial force of band to the axial compressive forces of flanges through wedging action. Coefficient of friction between the mating parts, wedge angle of the blocks and merman band tension are the important controlling parameters for the compressive forces. **Figure 1A** shows a typical launch vehicle payload fairing (diameter 3.4 m) and adjacent figure shows the two halves of the PLF which are joined by piston cylinder assembly. Piston of 1st half is connected to cylinder of 2nd half through separation rivets. **Figure 1B** shows detail A, detail B and detail C of **Figure 1A**. Detail A shows the boat tail to isogrid cylinder separation rivet scheme and its id number. Rivet number 1 to 8 are inside and outside transition separation rivets (dia. 5.6 mm). Rivet number 9 to 12 are boat tail outside and inside separation rivets (dia. 4 mm). Detail B and detail C show the piston cylinder assembly cross section and its component. The merman band configuration is shown in **Figure 2**. Part 1 is PLF aft end ring, part 2 is PLA ring, part 3 is wedge block and part 4 is merman band. Linear Bellow system is housed inside of piston and cylinder assembly. Expansion of the bellow results in the shearing of

the rivets connecting the piston and the cylinder assembly which separates both halves of PLF. Piston cylinder runs throughout the length of PLF (except at the nose cap).

FE Model

FE model is developed in ABAQUS software. FE model of a section of PLF structure is shown in **Figure 3**. PLF aft end ring, PLA ring, wedge blocks and merman band are modelled using solid elements as shown in **Figure 4**. Other portion of PLF like isogrid, boat tail and adjacent structures are modelled with shell and beam elements. Elements are assigned proper section properties and material properties. Material properties [4] are given in **Table 1**.

Table 1 Materials used and properties

	Materials	Ultimate strength, N/mm ²	Yield strength, N/mm ²	Shear strength, N/mm ²
Skin	AA2014-T6 clad sheet	420	360	205
Isogrid	AA7075-T7351	469	400	228
Piston and cylinder	AA2014-T6 extrusions	415	375	213
Merman band	Maraging steel	1765	1725	980
Rivets	V65	-	-	245

Separation rivet scheme of piston cylinder assembly at boat tail and isogrid cylinder transition is shown in **Figure 1B**. FE model contains 510705 nos. of total nodes and 415661 numbers of total elements.

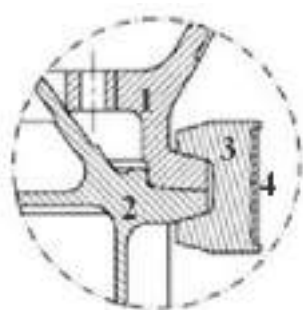


Figure 2 Merman band configuration



Figure 3 FE model of PLF with loads and BC

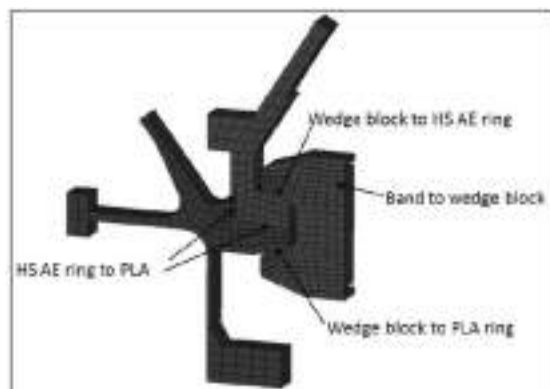


Figure 4 PLF aft end interface details

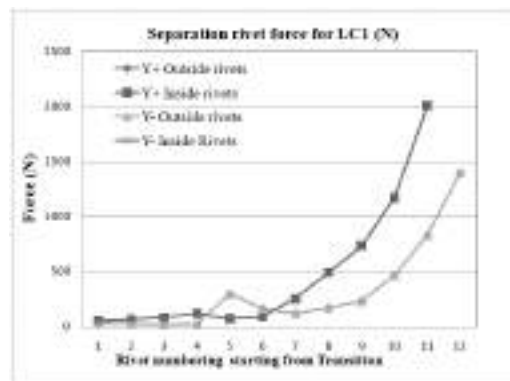


Figure 5 Separation rivet force for LC1

Contact need to be defined in all the interface surfaces in merman band systems this in turn adds more numbers of contact degree of freedom in the analysis. Contact are defined between the merman band to wedge block, wedge block to aft end ring, wedge block to PLA ring and aft end ring to the PLA ring as shown in **Figure 4**.



Coefficient of friction between the mating parts plays a very important role in the contact definition. Usually lubricants are applied between the band and wedge blocks, hence band to wedge blocks coefficient of friction is used as 0.1. Other contact surfaces coefficient of friction is used as 0.17. At the aft end of the FE model, all the translations are arrested.

When the launch vehicle is in launch pad only merman band tension exist in the PLF interface. After the lift off aerodynamic forces starts acting on the PLF. Hence analysis is carried out in two load steps. In 1st load step only launch pad loads condition i.e. merman band pretension is simulated and in second load step flight load is simulated in addition to merman band load. In 1st load step (LC1), 80 kN band tension is applied and in the 2nd load step (LC2) in addition to band tension, flight loads are applied in terms of axial load and bending moments. Bending moment is simulated through variable axial load. Loads and boundary conditions are shown in **Figure 3**.

Contact problems come under boundary nonlinearity problems. Standard equilibrium relation is given by $Ku = F$ but for contact problems, K is nonlinear function of u . These equations are solved by Newton-Raphson (N-R) method [5].

Nonlinear equation is written as $[K_T]\{\Delta u\} = \{F\} - \{F_{nr}\}$, here $[K_T]$ = tangent stiffness matrix, $\{\Delta u\}$ = displacement increment, $\{F\}$ = external load vector, and $\{F_{nr}\}$ = internal force vector.

RESULTS AND DISCUSSION

Nonlinear FE analysis has been carried out for PLF with merman band separation systems. For load case-1, where only band tension is applied, load verification and model validation are done through hoop stress distribution in the band and aft end rings. Separation rivets shear forces for isogrid to boat tail transition and boat tail are plotted (Y+ and Y-) for LC1 as shown in **Figure 5**. Since Y+ outside rivet forces are same as Y- outside rivet forces hence both graphs are overlapping and the same is true for inside rivets also.

Boat tail aft end separation rivets, which are near to the merman band joints get load shared due to tensioning of the band. This is the reason, the shear force distribution gradually increases from transition to boat tail aft end. Within the transition, rivet number 5 as a first rivet in boat tail transition shares maximum load, which reflects as a kink in the graphs.

Rivets shear forces at both Y- and Y+ sides show the same behaviour as expected. The deformation pattern of boat tail aft end ring in hoop direction for LC1 is shown in **Figure 6**. Figure shows the gap closure of boat tail aft end ring due to band tension is 0.68 mm ($0.34 + 0.34 = 0.68$ mm). Before loading ring end gap is 2 mm which reduces to ($2 - 0.68 = 1.32$ mm) 1.32 mm after loading.

In LC2 flight load is applied in terms of axial load and bending moment. Axial compression load is applied uniformly at the FE side, bending moment is applied with respect to P+ and P- axis. Due to the LC1 in both the ends of boat tail is in compression but when flight loads acts, in tension side boat tail aft end ring gap try to open it out and compression side it will try to close it further, which result in tension side less gap closure and compression side more gap closure. This is shown schematically in **Figure 6**. Hence higher rivet shear forces is observed in compression side as shown in **Figure 7**.

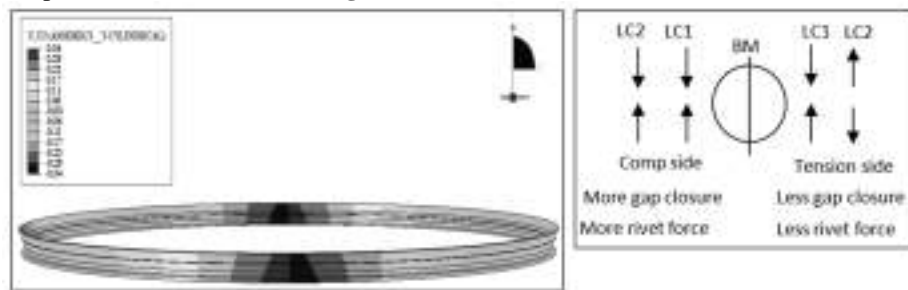


Figure 6 Deformation pattern of boat tail aft end ring in hoop direction for LC1 and gap closure scheme

Figure 7 (Y+ curves) shows that maximum shear force is coming on the transition rivet, then force is gradually decreasing but being a last rivet and band tension effect, last rivet again shares high forces. In tension side (**Figure 7**, Y- curves) because of compression force get relieved, force gradually decreases from aft end to transition. In transition inside rivet 4 and 5 is in higher distance than outside rivet 4 and 5 (**Figure 1B**) so inside rivet shares maximum load. In transition slightly higher size rivets are used as compared to boat tail and isogrid portion. Boat tail last rivets resultant shear force comes out to be very close to its capacity. Gap closure of the boat tail aft end ring

due to LC2 in tension side and in compression side is 0.5 mm (0.25+0.25) and 1.54 mm (0.78+0.76 =1.54 mm) respectively, as shown in **Figure 8**.

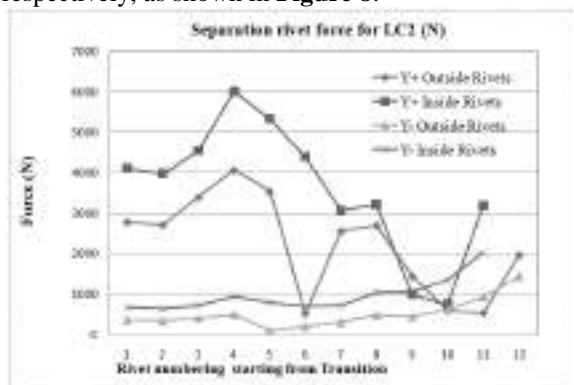


Figure 7 Separation rivet force for LC2

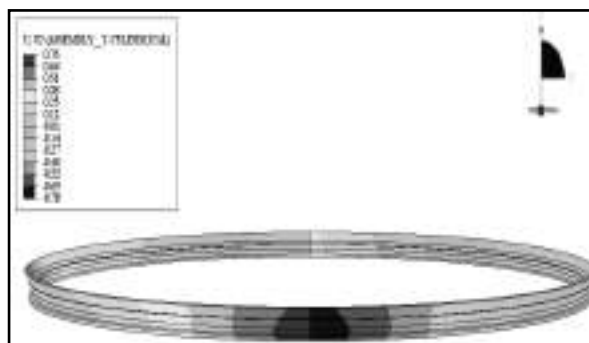


Figure 8 Deformation pattern of boat tail aft end ring in hoop direction for LC2

The resultant gap between the ring ends is 0.46 mm ($2 - 1.54 = 0.46$ mm) in compression side and 1.5 mm gap in tension side.

With Shim

Resultant shear force at boat tail 1st rivet from aft end is very close to its shear capacity. This is because it shares the load due to band tension. To reduce the load, a shim is introduced at P+ boat tail aft end ring in both Y- and Y+ sides. Shim is a metallic piece having the same cross section as aft end ring and thickness equal to the gap between both half of rings. With the shim, aft end ring gap closes with band tension application and subsequently transfer the load direct through butting hence very less rivet force is observed at boat tail last separation rivet. This results in less shear force due to band tension. Last rivet shear force LC1, (**Figure 9**) observed is 538N as compared to 2012 N without shim, which is 73.3% less. Hence with introduction of shim merman band load sharing to separation rivet is very less. Resultant shear force distribution for LC2 is also plotted as shown in **Figure 10**.

With shim and without shim shear force distribution graph is similar in nature but a large gap is observed in force magnitude. Maximum shear force observed for boat tail last rivet is 684 N as compared to the 3202 N without shim.

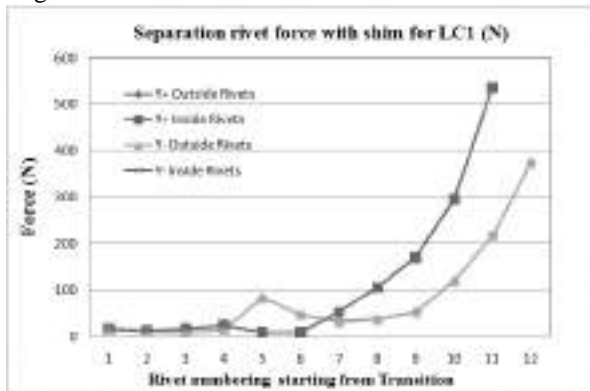


Figure 9 Separation rivet force with shim for LC1

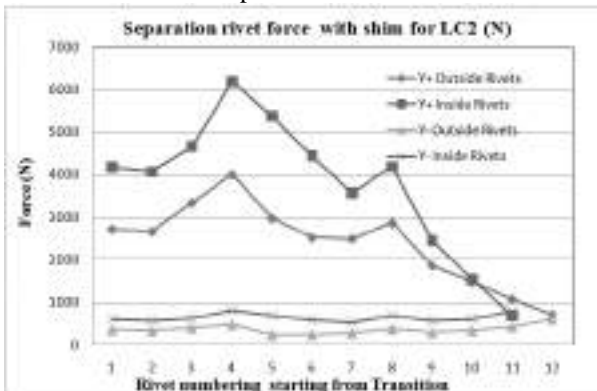


Figure 10 Separation rivet force with shim LC2

CONCLUSION

This paper presents the effect of tightening of merman band assembly in addition to flight loads on the separation rivets. For LC1 and LC2 shear force distribution are plotted and results are discussed.

- Non linear analysis is carried out in two load steps, in LC1 only band tension of 80 kN is applied and in LC2 band tension as well as flight load is applied.



- For LC2 shear force distribution for the separation rivets at Y+ graph shows that the transition rivet share the maximum load and afterward load is gradually decreasing but for last rivet because of merman band load share, it increases again.
- For LC1, shear load on aft end (last) rivet is 50% of its capacity. With LC2 (flight load also), this increases to near its capacity.
- With shim, boat tail aft end ring halves butt with each other when band tension is applied, this butting reduces shear load on separation rivets and increases margin of safety in these rivets.

ACKNOWLEDGEMENT

The authors wish to acknowledge Director VSSC who permitted us to pursue this study and publish the findings.

REFERENCES

1. ESA activities related to launch vehicle. Retrieved from https://www.esa.int/Our_Activities/Space_Transportation/Launch_vehicles/Fairing, March 27, 2018.
2. A. Thampi, A. R. Anwar Khan, Joint characteristic study of a typical merman band joint used for launch vehicles using non-linear FE analysis, International Journal of Engineering Research and Technology (IJERT), Volume 3 Issue 7, July 2014.
3. J. I. Rome, V. K. Goyal, N. E. Martino, Techniques for finite element analysis of clamp band systems, The Aerospace Corporation, El Segundo, CA 90245.
4. E.F. Bruhn, Analysis and design of flight vehicle structures, 2008.
5. ANSYS & ABAQUS User Manuals.



Improvement in Blast Furnace Grade Coke Mean Size by Altering the Fissure Formation during Coal Carbonisation Process

*S K Kushwaha^{*1}, A Kumar¹, P K Pankaj¹, K K Manjhi¹, S K Das¹*

*R & D Centre for Iron and Steel, SAIL, Ranchi, Jharkhand, India¹, skkushwaha@sail-rdcis.com**

ABSTRACT

To enhance the productivity of blast furnace grade coke, alterations in coking parameters is the most feasible option, if change in blend composition is restricted. The mean coke size significantly affects the blast furnace operation and statics, especially in India; where, about 80 % of coking coals are imported from abroad. In coke making, one of the most significant challenge is, how to maintain consistent mean coke size against the variations. Good amount of efforts are still going on in the research area to provide suitable boundary conditions for the parameters which influence the coke shape and size. The present work is the results of the outcome of the exercise done in SAIL, RDCIS laboratory to improve the coke size by altering the heating parameters, that is, coking period and centre coke mass temperature, firstly in laboratory and then validated in commercial ovens. For this study total eight numbers of coals from different origin and maturity were evaluated in pilot ovens and results were analyzed using statistical tools. The mechanism of coke size development during coking of a conventional coal blend was investigated to find the preferred heating and fissuring patterns, for the production of coke of homogeneous quality. Relations of some coke properties with centre coke mass temperature and heating rate were examined. Drum strength indices of the coke increased with increasing centre coke mass temperature but decreased with increasing heating rate. The coke mean size, which was found to be independent of centre coke mass temperature, varied widely with the heating rate and the oven width. With alteration in various parameters in the working range of coke making, the variation in BF coke mean size and hence BF coke productivity was observed to be more than 10 %.

KEYWORDS Coke, Coke mean size, Heating rate, Coke fissures, Coke mass temperature swelling; plasticity

INTRODUCTION

India depends heavily on imports of desired quality coking coals. Accordingly, it is an important task for coke experts to use imported coals most effectively in the production of metallurgical coke. Figure 1 shows the imports of coking coal in India in the month of June '18. As seen from this figure, India imports coals from various countries in the world. Therefore, the study for the judicious usage of precious coals for blending and coke making has always been of importance in coke research. For the future production of coke, development of techniques as described later on, is strongly desired to meet the technological and economic requirements for coke as a major energy source for pig iron production. Almost all the new blast furnaces being built these days are with high volume and productivity resulting more stress on the coke quality in terms of higher strength and bigger coke size. With limited available coal resources very little option are left which covers mainly shifting from coke making technology in longer terms and, judicious blending and coking practices in shorter terms.

Primarily, efforts should be directed toward the development of techniques to meet the diversification of coking coal resources, techniques for the utilization of low-grade coal, techniques for energy saving, and techniques to satisfy stringent quality requirements from blast furnace operators. It should be noted that in the development of such techniques, the relationships of factors is always changing and varies from coal to coal.

It can be summarized the factors relating to coke production into three groups: coal blending (B), pre-treatment (P) and carbonization (C), the coke quality can be expressed as follows:

$$\text{Coke quality} = f(B, P, C) \quad (1)$$

In the above relationship, B may be called internal factor and P and C external factors, when viewed from the coke side.

In the days of rapid economic growth, the emphasis of study to be placed simultaneously on both the internal factor, that is, coal blending, as well as external factors (P and C), and top priority being given to the acquisition of the required quantity of coke. However, the ratio of contribution of external factors to coke quality is becoming more important with changes in the conditions of pretreatment and carbonization (for example, operation at low productivity, and adoption of the coking process for blending the briquette and preheating process) and, with the development of new production processes, such as formed coke process. On the other hand, non or slightly caking coal, caking additives, etc, with new properties have found gradual application in coke production. When deciding



coal blending, therefore, the combined effects of these factors must be taken into consideration. For this reason, the role of all the three factors together have become increasingly important. For the preparation of various plans in connection with the development of coking coal resources, purchase and allocation of coal, coke production, construction and operation of blast furnaces, etc, the estimation of coke quality on the basis of coal blending plans as well as coking process are required. Against the background and needs described above, Research and Development Centre for Iron and Steel, SAIL has been conducting research on new production processes, such as pilot scale preheating, stamp charging pilot stage blend coking and binder addition, as well as on coal blending for the improvement of hot properties of coke on the basis of the results of many years of research undertaken by RDCIS in connection with coal blending. This paper summarizes the results of a series of these studies in a systematic manner, reviewing them from the standpoint of improvement in blast furnace grade coke mean size by altering the fissure formation during coal carbonisation process. The objective of this exercise was to improve the coke size by altering the heating parameters, that is, coking period and centre coke mass temperature, firstly in laboratory and thereafter in commercial ovens for validation. For this study total eight numbers of coals from different origin and maturity were evaluated in pilot ovens and results were analyzed using statistical tools. The mechanism of coke size development during coking of a conventional coal blend was investigated to find the preferred heating and fissuring patterns, for the production of coke of homogeneous quality. Relations of some coke properties with centre coke mass temperature and heating rate were examined.

EXPERIMENTAL

Two experimental approaches were adopted. In the first, attention was given to the development of coke strength as carbonisation proceeded. Since coke is a porous material, this involved an evaluation of coke strength in terms of its porous structure. In the second, coals were carbonised under conditions which simulated those in a commercial coke oven so that the fissure pattern in the coke could be examined. Data from both approaches were used in an attempt to develop a mathematical model which quantitatively explained the observed fissuring.

Many sets of experiments have been conducted to make clear the basic phenomenon of coal caking property; the influence of rapid heating. Emphasis was given to understand the relationship between the caking property of coal particle and its heating characteristic. Basic heating characteristics in a rapid heating process were estimated by the analysis of the result obtained by pilot-plant tests and calculations by simulation model. Electrical heating was assumed as a heating system. As a result, the heating-up performance of the coal rapid heating process was controlled and monitored accurately. On the one hand, it is undesirable for coal particles to break into fine powder in rapid heating process so that the effect of rapid heating conditions on the heat crack of coal particles was studied. And it was indicated that heating rate influences coke size significantly.

The influence of centre coke mass temperature on coke quality was also investigated from the aspect of post coking conditions. That the swelling and agglomeration behaviour of coal particles increased with the rise of heating rate.

Some investigations considering coal and coke quality improvement by rapid heating had been carried out. In order to make clear the effect of rapid heating on thermoplastic behaviour, experiments using a 10 kg pilot oven were conducted. It was found that the thermoplasticity of coal was enhanced when the coal was rapidly heated to 330–380°C, with change in the normal heating rate (3°C/min). The effect of rapid heating on coke quality was ascertained in experiments on small-scale pilot scale facilities. It was shown that the rapid heating of charge coal nearly up to softening temperature raised drum index and a optimum effect of rapid heating on the caking properties of coals. In order to obtain fundamental data for rapid preheating process, the swelling and agglomerating behaviour of coal particles and the thermoplastic behaviours of coal under various heating conditions were investigated. Based on the obtained knowledge regarding the coke strength, fissuring phenomena are discussed on the basis of the measured degree of fissuring in cokes produced using the large scale furnace and the mathematical model of temperature, stress and strength development during carbonisation.

All coals selected for this experiment are mentioned in the **Table 1**. Data are generated using 250 kg pilot oven and 10 kg box type semi pilot oven and commercial oven and stored digitally and corrected to match with commercial ovens. Data generated had a span of 1 year. For carbonization test, the authors have used commercial oven of 4.7 m tall, 250 kg capacity. Pilot coke oven and 10 kg time box charging semi pilot coke oven data generated has been shown in **Tables 2 and 3**.



Table 1 Properties of the coal used in the experiment

Coal Type	Proximate analysis		CSN	Giseler fluidity				Ro	Total reactives
	Ash	VM		ST	MFT	RT	LogMF		
Coal A	9.2	22.4	7.5	425	468	500	2.628	1.18	62
Coal B	8.9	23.6	8	404	447	484	3.079	1.2	76
Coal C	9.5	28	5.5	414	439	472	2.39	0.88	58
Coal D	4.9	27.6	3.5	413	456	483	1.7	1.29	90
Coal E	8.5	32	6	393	443	483	2.17	0.84	64
Coal F	9.4	23	9	399	361	504	3.14	1.19	72
Coal G	21.5	19.2	2.5	409	446	481	2.37	1.15	52
Coal H	26.4	25.4	1.5	419	441	475	0.845	0.72	48

Table 2 Coke quality against heating rate

Heating rate	1 °C /min	2 °C /min	3 °C /min	4 °C /min	5 °C /min
Mean Size	63.4	62.0	55.2	52.3	50.1
M10	7.1	8.5	11.4	11.9	11.9
M40	81.8	80.2	76.2	74.8	74.2

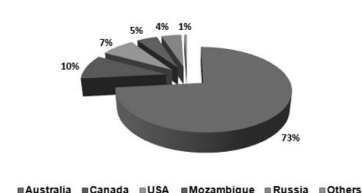


Figure 1 Coal quality against heating rate

Table 3 Micum indices against varying heating rate

CMT	850 °C	900 °C	950 °C	1000 °C	1040 °C
M10	12.5	12.2	10.6	8.2	7.2
M40	74.7	75.2	75.5	80.0	81.7
Mean Size	58.9	60.5	59.6	61.6	61.3

BLEND PREPARATION

Coal blend was selected in such way that the coal blend ash should remain in a narrow range half 11.5 to 12.0%. The focus was to establish the coke quality against the variation heating rate and centre coke mass temperature (CMT)

PREPARATION AND TESTING OF COAL BLENDS

The individual coals constituting each blend were weighed and mixed thoroughly as per the specified blend composition against the coal quality presented in **Table 1**. Blend thus prepared was subjected to crushing in hammer



mill wherever necessary.

The crushing index of each top coal charge was maintained at $81 \pm 1\%$ of $< - 3.2$ mm size fraction. Working moisture was adjusted to $8 \pm 1\%$ just before charging the respective top charge coal blend into the pilot oven. Each prepared top charge coal blend was tested for Proximate analysis, Gieseler's Plastic Properties, Petrography, CSN and LTGK Coke type.

PILOT OVEN CARBONIZATION TESTS

Carbonization tests were carried-out in the electrically heated movable wall pilot coke oven (250 kg capacity) . The following carbonization conditions were maintained during the test campaign: Coking Period: 18 h for top charging and End Centre Coke Mass Temperature : $1000 \pm 10^\circ\text{C}$. Coking pressure during each carbonization test was monitored.

TESTING OF COKE SAMPLES

Coke obtained from the respective carbonization tests after wet quenching was allowed to dry to a moisture level below 3% in coke dryer. The gross dried coke was subjected to screen analysis before and after stabilization. Coke stabilization was carried out by allowing run-of-oven coke to fall twice from a standard height of 1.83 m followed by 100 revolutions in the Micum drum.

The respective coke samples were subjected to following tests: (i) Screen analysis before and after stabilization, and (ii) Micum Indices (M10 & M40).

RESULTS AND DISCUSSION

One of the major goal of the study was to find effect of heating rate on coke quality. **Table 2** summarizes the coke strength indicators, for example, Micum indices against the varying heating rate it also depicts the mean coke size against the changing heating rate. It is obvious from the graph that heating rate affects all the three parameters significantly, all the three parameters were showing their positive biasness towards slow heating rate and thus depicts that coking period increase, affects the coke quality in supportive manners, however **Figure 1** shows that there is not a very steep changes with increase in heating rate. **Table 3** depicts results of effects of centre coke mass temperature (CMT) on coke quality. It can be observed from **Figure 2**, that while coke strength indices were showing there improvement with increase in the CMT but the same time no clear cut trend has been observed for mean coke size. Therefore, a balance is required between coke quality and coke productivity in terms of heating rate and coking period.

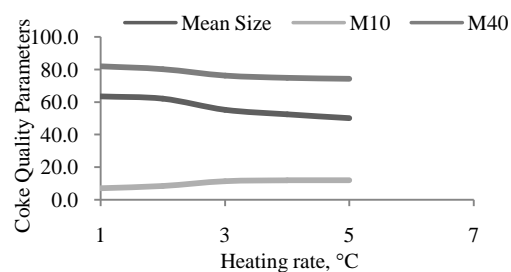


Figure 1 Coke quality against heating rate

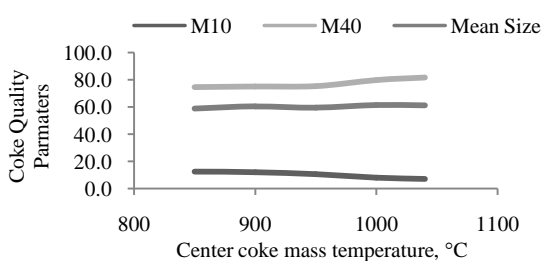


Figure 2 Coke quality against coke mass temperature

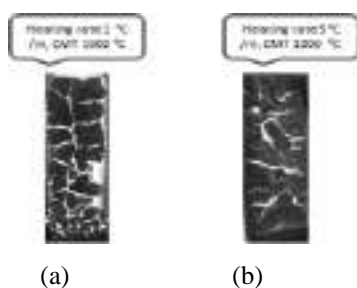




Figure 3 Fissure formations at different heating rate

Figure 3 is showing two representative pictures of the fissures formed. Picture (a) is the ready to push coke formed from 1°C/min heating rate, while picture (b) is coke from 5°C /min. It can be observed that the existence of the distinct difference between the fissuring phenomenon of two heating rate. While first picture is showing the shape having clearly gas flown formed fissure at the centre, the second does not possess the same, resulting the tinny fissures formation in the lump coke and hence breakage of coke during pushing and stabilization.

CONCLUSION

Study was made to examine the effect of coking condition on the coke quality in the wake of fissuring. For this study total eight numbers of coals from different origin and maturity were evaluated in pilot ovens and results were analyzed using statistical tools. The mechanism of coke size development during coking of a conventional coal blend was investigated to find the preferred heating and fissuring patterns, for the production of coke of homogeneous quality. Relations of some coke properties with centre coke mass temperature and heating rate were examined.

Drum strength indices of the coke increased with increasing centre coke mass temperature but decreased with increasing heating rate. The coke mean size, which was found to be independent of centre coke mass temperature, varied widely with the heating rate and the oven width.

ACKNOWLEDGEMENT

The authors wish to thank the management of RDCIS and Bhilai Steel Plant, Bhilai for granting permission for publishing this paper.



Smart Manufacturing Framework and its Challenges in Present-day Hydrocarbon Industries

Vaibhav Ahuja^{*1}, K Ramesh¹, Chittranjan Mehta¹
Reliance Industries Limited, Vadodara, India¹, vaibhav.ahuja@ril.com*

ABSTRACT

With evolution of Industry 4.0, the world sees the emergence of various Cyber physical systems leading to seamless integration of data, in contrast to which the hydrocarbon industries are still laggard in their proper integration of information around the cross functional domains. The reasons being obsolete data collection practices with frequent manual interventions, unavailability of required information at a single place, and most importantly asynchrony amongst the operational, business and maintenance objectives. In an industry as dynamic as Hydrocarbon, implementation of a Smart Manufacturing Model is essentially instrumental in the elimination of these gaps, thereby facilitating a swift progression from the traditional automation to a fully flexible and completely connected system, that uses a constant stream of data from connected operations and production systems so as to learn and adapt to new demands. This paper explores the scope of deploying a Smart Manufacturing Model driven by IIoT, Big data and Data Cloud in a hydrocarbon industry with connected sensors and systems to integrate the diverse technologies across all the downstream plants and their supply chain management system. The transparent nature of the model overcomes the fear of data manipulation, minimizes manual intervention and smoothen data availability across all the cross functional domains. Additionally, the paper also discloses the challenges faced by our team in installing Smart Wireless Sensors in field and subsequently integrating them with the existing sensors and devices on the same network. The complications in deployment run the gamut from being entirely behavioral, with reluctance in adapting to newer methods to the inevitable field obstructions posed by the existing piping and equipment. The systematic adoption of Smart Manufacturing in Hydrocarbon industries promises the enhancement of present-day technologies alongside a proper alignment of the maintenance, operational and business intents. A future research in its easy deployment could thus help make quick and advance decisions, leading to minimum downtime and consequently achieving the common goal of Manufacturing Excellence.

KEYWORDS Smart manufacturing, Industry 4.0, IIoT, Big data

SMART MANUFACTURING: DEFINITION AND FEATURE

Many people use automation and Smart manufacturing as synonym but in reality it is not the case. Automation term suggests the performance of single, discrete task or process. Process automation is commonly used in all hydrocarbon based industries for the purpose of safe and reliable operation based on defined set of rules. On other hand, Smart Manufacturing represents integration of shop floor decisions and insights with the rest of the supply chain and broader enterprise through an interconnected IT/OT landscape. This means Smart Manufacturing does not cover only Process Control but it is more holistic view that affect business at enterprise level.

The key feature of any Smart Plant are: **Connected** information, data and systems; **Adaptive and Responsive** to the changing need of market, customer and other supply chain related demands; and **Transparent** in data availability for quick decision making.

CURRENT APPROACH AGAINST SMART MANUFACTURING

Presently in a hydrocarbon industry both technical and business analytics are performed on steady state model due to lack of interconnection between different systems. The experience shows that steady state model approach does not yield the desired result. In current scenario, many industries adopt approach shown in **Figure 1**, in which one side is plant management team whose focus is primarily on maintaining process variables within specified limits and achieving health, safety and environment compliance. On other side there is business team which give direction to plant operation by updating them with constantly changing market demands.

Today, due to this model of approach many opportunities are not fully exploited and some are even missed as this model lacks integration of data and information. In current scenario, running an industry by maintaining process variables is not enough.

This fuels the requirement of a Smart Manufacturing which integrates Operation Technology (OT) with Information Technology (IT) to facilitate real time analytics. In a 'Smart Plant', each asset — from the smallest sensor, to a



single process unit and to collections of processes — not only executes its basic process function, but also provides feedback and predictive information, through real-time communication networks, on the current and expected performance of that asset to the plant management system. This, in turn, will allow the plant management system, together with human decision-making, to maximize, based on the current and future collective performance of all assets, the use (thus, the value) of each asset as business conditions change and warrant. Smart manufacturing aims to integrate data from system-wide physical, operational, and human assets to drive manufacturing, maintenance, inventory tracking, digitization of operations through activities like predictive modelling, advance process control and other similar activities across the entire manufacturing network.

APPROACH ADOPTED BY THE TEAM

In this paper, the authors explore the possibility of deploying smart manufacturing model based of IIoT, Big Data and Data Cloud in hydrocarbon based industry. Presently a lot of applications has been developed in industries like supply chain management for tracking of material, inventory across the globe but deploying similar model in hydrocarbon based is challenging. The decisions made in typical hydrocarbon industry are not only inventory dependent as hydrocarbon based organization tends to keep minimum inventory due to its hazardous nature. Also by global factors like international crude price, geopolitical relations between countries affect the same directly or indirectly.

Typical model based of Industrial Internet of Things (IIoT), Big Data and Data Cloud can be divided into three layers of data and information network: (i) Physical Layer, (ii) Networking/Transport/Data Link Layer and (iii) Application layer.

Physical Layer

This layer is responsible for gathering valuable raw data from sensors in field either digitally or manually. Manual reading taken by area operators, condition monitoring check sheets filled by maintenance crew in various cyber physical systems are also part of this layer. The main task of the physical layer is to perceive the real time data of hydrocarbon inventory, condition monitoring data of maintenance equipment and the environment around it and convert it into digital form. Several sensing technologies are used in this layer (for example, GPS, IR, RFID, Wireless HART, Bluetooth, Zig bee).

This layer in hydrocarbon based industries is the least digitized and involves lot of manual intervention, paper based approach. Hence, this layer needs to be connected more via digital sensors, Machine to Machine communication protocols and Device to Device communication protocols.

Data Link Layer

This layer is also called as networking/transport layer. As the name suggests, this layer is responsible to connect all the smart sensors, gateways, network devices, and servers together and facilitate the processing of the perceived data from the physical layer. This layer act as middleware between physical and application layer. It defines the rangeability of your application. The type protocol, data and network security used in this layer defines whether application is limited to local based access, server based access or global by using cloud computing

Application Layer

This layer helps to draw meaningful insights out of raw data obtained. All predictive models, user based alerts and linking with portable devices like mobile phones are catered in this layer.

At present most of the vendor companies, IoT developers are working in application layers and developing tools, user based alerts on this layer only. But team's experience shows that to extract best of these tools and application, we need to input correct raw data from physical layer. Lot of manual activities are being done at physical layer at present.

So team proposed to deploy this architecture shown in **Figure 2** in one of hydrocarbon based plant by interlinking existing different manual practices and tools. The key feature of the model is that its transparency and smooth data availability through a single dashboard.

By adopting this model, we were able to achieve all the key features of a smart factory, that is, Connected, Adaptive and Transparent.

To realize the smart manufacturing in one of its plants, the team used following building blocks at different layers:



Physical Layer

At physical layer, the key challenge was first to reduce number of manual activities and second ensuring digitization of the manual work done by the team. This was ensured by usage of

Smart sensors: Smart sensors are the primary requirement for deploying Smart Manufacturing. Team used Wireless Smart Sensors help to eliminate manual processes and fear of data manipulation. Wireless sensor were chosen as they can be easily integrated to data cloud using wireless gateways.

Cyber physical system: Team used Intrinsically Safe (IS) handheld devices for activities condition monitoring related check sheet filling. This ensured digitization of all check and test records.

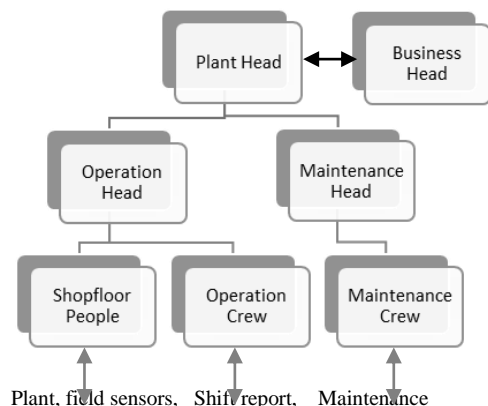


Figure 1 Plant management team



Figure 2 Architecture proposed in present work

Network Layer

As team chose to deploy wireless sensors at physical layer, data communication protocol selection was also required. The team preferred to use Wireless HART based sensors in case of pressure, flow, temperature and acoustic measurement. The Wireless HART was preferred as it is open source not proprietary protocol. For some vibration related measurement team used Bluetooth, 4G LTE based sensors also. The main challenges in Wireless HART is data transmission up to limited distance with only clear Line of Sight (LOS).

Data handling using big data and cloud computing: With deployment of wireless smart sensor, next challenge was to handle three against of dataset namely: variety, velocity and volume. The easiest approach in this case could have been using third party services like Microsoft Azure. In our case, we took cautious approach of storing most data in local server and used encrypting algorithms to share it via data clouds. To avoid any possibility of leakage of confidential data, we tried to limit the data mostly in organization network and made sure same can be accessed through devices with proper authentication certificates only.

Application Layer

At application layer team developed algorithms to calculate real time value of Key Performance Indicators (KPIs) of any hydrocarbon based plant like energy index, production planning against raw material availability, percentage of on grade product. All algorithms were developed using open source software like Python and R studio and front end web interface Dashboard was developed for the same with username and password authentication.

IMMEDIATE BENEFITS

Immediate benefit after deploying this model were visible in following fields:

Proactive Maintenance

All manufacturers have widely accepted the concept of proactive maintenance, which advocates early diagnostics and part replacement based on the prediction and monitoring of machine degradation, in order to reduce costly, unscheduled downtime and unexpected breakdowns. The team was able to realize the same using lower cost sensors, wireless connectivity and in-house developed data analysis tools to model historical and real-time data. The data was



correlated, analyzed and visualized to make machine degradation predictable and visible evaluate machine's status and performance.

Improvement in Energy Index

Manufacturing accounts for approximately one third of global energy demand, along with increasing energy prices, making energy management a non-trivial issue. Team addressed the issue of unaccounted hydrocarbon loss and steam loss through wireless acoustic sensors and identified bad actors in energy optimization. Usage smart wireless sensors and acoustic sensors helped the team to identify and then rectify bad actors of plant.

CHALLENGES FACED IN DEPLOYMENT

While deploying the whole architecture in one of plant team faced lot of challenges. The challenges faced at various fronts can be classified into following categories: (a) Administrative challenges, (b) Technical challenges, and (c) Competent workforce challenges.

Administrative Challenges

Lack of vision, strategy and commitment : To stay competitive in today's market one has to utilize opportunities provided by technology of Industry 4.0, Smart Manufacturing and IIOT to increase their efficiency, productivity and to serve their customer in better way. The difficult task faced by organizations today are its implementation. Few are performing well and mass number of companies are lagging. They don't have digital roadmap and proper governance mechanism to look after its implementation and accountability. To reap the benefit of Smart Manufacturing not only technological investment is required but a clear strategy and vision for how it will be used.

Awareness with respect to Industry 4.0, smart manufacturing or IIOT is required : Acceptability or trustworthiness of Advanced Data Analytics by shop floor level people is required. This can only be achieved by creating more awareness about Industry 4.0, Smart Manufacturing or IIOT. People still think of Advanced Data Analytics as magic. This too has limitation and needs to be understood. On the other hand, people see Smart Manufacturing as a threat to their job. However, it is not a threat, but a way of making life easier. Everything requires to evolve to stay competitive, otherwise, it may perish.

Technical Challenges

Reliability and availability of IoT based system : The reliability of any sensor based control system is defined by its fault tolerant capability. The current wired based conventional closed loop system is made fault tolerant by introducing redundancy at various hardware while in case of wireless sensor there are lot of question marks over reliability, robustness, network failure and data packet loss. Most of the hydrocarbon plants are surrounded by equipment like piping, drum, vessel which act as potential source of attenuating signal from the source/sensor. This requires installation of more and more data repeaters installation in plant, which slows down data communication process and adds extra cost burden.

Huge financial investment for resource availability/infrastructure setup for handling big data: Currently, in hydrocarbon industries, we lack meaningful data especially in QC parameters. In most hydrocarbon plants there is practice of taking manual sample every 2 to 3 h. This data may not be sufficient for any predictive model development. With adoption of Smart Manufacturing, we can install IoT based online analyzer there is a challenge for handling huge without loading plant controller. With online analyzer, robust data management system is required for handling both structured data and unstructured data.

Power consumption : The next challenge in case of wireless sensor is the power consumption. With evolution of smart sensors in every field, the next challenge lies in their power consumption optimization. Power consumption becomes more critical area of concern in hydrocarbon industries due to probability of continuous hazardous environment in vicinity. So every smart IoT based sensor may not be appropriate for its usage in hazardous environment created in hydrocarbon industries

Cyber security and integration with existing OT network : The major challenge is addressing cyber security issue in Smart Plants. The typical Smart plant model based on wireless sensor poses concern over data security, privacy and trust. Presently there is no dedicated and widely accepted model/architecture for addressing cyber security concern. Improper cyber security may lead to stealing critical information and hence this prevent its usage in highly critical systems. The other challenge faced is related to integration with existing system. Most of the manufacturing units are driven by connected automation systems like PLC, condition monitoring etc. for maintaining efficiency. With adoption and implementation of Smart Manufacturing followed by IIOT connected production and connected



application has become a need. However, the conventional manufacturing automation systems are not designed for wireless network. These isolated system poses mobility, adaptability and security issues and are made connected to open network like cloud/wireless network. As IIOT is more focused on wireless network and data storage in cloud system, it has become more vulnerable for hacking. Data breach can lead to physical damage and even loss of human life due to catastrophic event triggered by hackers. The foremost task of any organization implementing Industry 4.0/Smart Manufacturing/IIOT is to recognize the vulnerable sections which can be hacked and prioritize risk associated with IT and OT convergence.

Competent Workforce Challenges

Skilled workforce requirement with competency in knowledge of both domains : With adoption of new technologies at faster pace, there is a gap between industries requirement and research done by the Data Scientist. This can have a pivotal role in enabling the success and adoption of smart manufacturing while ensuring the safety, well-being and optimum user experience of those involved in a smart manufacturing environment.

There is a lack of training program which can cater the needs of the workforce as very few people are there who are well versed with OT and IT. Employer has to spend additional fund and time to bridge this knowledge gap. The training program has to be effective and a mix of both OT and IT. With advancement in technology, the implementation and competitiveness of the training program needs to be revamped for the workforce. It's not just the responsibility of employer to provide training but self-training is also required at the end of the workforce to remain competitive. Workforce also need to evolve with changing time.

CONCLUSION

The current approach in most of the hydrocarbon industries does not allow integration of operational and business objectives. Smart manufacturing technology backed by high speed internet promises to eradicate the gaps to achieve excellence in manufacturing. It is widely accepted as novel paradigm that can radically transform current practices. The team has achieved good success in deploying wireless sensor. Still, there is scope of future improvement in cyber security of data especially related to cloud sharing. This opens up new area for future research especially in the field of designing sensor, cyber physical systems for physical layer of hydrocarbon industry. So it can be concluded that deployment of Smart Manufacturing in hydrocarbon industry is more challenging than other manufacturing sector.

REFERENCES

1. The Smart Factory, article in Deloitte Insights by Rick Burke, Adam Mussomeli, Stephen Laaper, Martin Hartigan and Brenna Sniderman
2. P. Wright, Cyber-physical product manufacturing, Manufacturing Letters, Volume 2, Number 2, pp 49-53, 2014.
3. Smart Plant Operations: Vision, Progress and Challenges by Panagiotis D. Christofides, James F. Davis, Nael H. El-Farra, Don Clark, Kevin R. D. Harris, Jerry N. Gipson in AIChE General
4. Identifying performance assurance challenges for Smart Manufacturing by Mooner Helu, Katherine Morris, Kiwook Jung, Kevin Lyons, and Swee Leong in Science Direct General
5. The Smart Factory: Exploring Adaptive and Flexible Manufacturing Solutions by Agnieszka Radziwona, Arne Bilberga, Marcel Bogersa, Erik Skov Madsenb in Science Direct General
6. India's Readiness for Industry 4.0: Survey done by Confederation of Indian industry



Development of Economical Colour Measuring Instrument for Solid Food

S. R. Kumbhar¹, A.K. Sahoo¹, G.V. Mote¹, I. S. Udachan^{*1}

*Food Technology Programme, Department of Technology, Shivaji University, Kolhapur, Maharashtra State, India¹,
isu_tech@unishivaji.ac.in**

ABSTRACT

Colour is an crucial feature property in the food industries and it impacts buyer's decision and inclinations. The perception of color thus results in the detection of certain defects that food items may present. The instrument was developed with camera, computer, and illumination system for colour measurement of solid foods. The determination of colour can be carried out by visual (human) inspection or by using a colour measuring instrument. With the advances in computer technology, signal processing techniques were applied to food colour measurement and food safety applications. It is often necessary to analyze the surface colour of food samples both qualitatively and quantitatively. The developed low cost instrument for colour measurement, measures colour in L*, a*, b* and RGB values with graphs of each pixel results. Jaggery sample were taken for the experimental purpose to get L*, a*, b* and RGB values. The results obtained were in comparable with high costing colour measuring instrument. Proximate analysis and colour analysis of jaggery samples were carried out to find out the relation between colour and nutritional composition. Jaggery colour changed due to change in moisture content, reducing sugars and ash content.

KEYWORDS Colour measuring instrument, Jaggery, Camera, Computer, illumination

INTRODUCTION

Colour is the primary feature for the acknowledgement and selection of food product, even before the consumption by the consumer. A shade of the surface is the primary vibe that purchaser perceives and utilizes as a device to acknowledge or dismiss the food product. The perception of colour in this way permits the revealing of specific imperfections that may exhibit in the food product. By means of visual (human) inspection or colour measuring instrument colour analysis can be carried out [1]. But there is great degree variable from eyewitness to spectator during visual (human) inspection of colour. With the end goal to do a more target color estimation, shading guidelines are regularly utilized as reference material, but regrettably, it implies a slower assessment and needs more exercise of the observers [2].

With the advances in computer technology, signal processing techniques are applied to many food colour measurement and food safety applications. It is often necessary to analyze the surface colour of food samples both qualitatively and quantitatively. The qualitative measurement may involve visual inspection and comparison of the food samples. The quantitative measurement may involve obtaining colour distribution and averages. It may also be made to correlate colour distribution with other data such as temperature, moisture, shelf life and spoilage content distributions.

Human eye recognizes hues as indicated by the fluctuating affectability of various cone cells in the retina to light of various wavelengths. There are three types of colour photoreceptor cells (cones) for the human with sensitivity peaks in short (bluish, 420 to 440 nm), middle (greenish, 530 to 540 nm), and long (reddish, 60 to 580 nm) wavelengths. Colour can be rapidly analyzed by computerized image analysis techniques, also known as computer vision systems (CVS) [3]. These systems not only offer a methodology for measurement of uneven coloration but it can also be applied to the measurement of other things of total appearance like moisture chemical constituents etc. Dedicated commercial vision systems are currently available for a variety of industrial applications, and they are especially recommended for colour assessments in samples with curved and irregular shapes. The knowledge of these effects, such as the variations of L*, a*, b* for a particular shape of the sample, Red Green Blue (RGB) values could be useful for developing image processing. It will helpful in a measurement of the colour of agricultural produce like fruits, vegetables, cereal grains etc also in processed food products like dairy products, bakery products, meat and meat products industry etc.



There are some instruments for solid food colour measurement like Colour Meter, Hunterlab solutions, CIE lab Solutions. Colour meters are used for the colour measurement of solid food, liquid food. This colour meter can read the difference in colour in $L^*a^*b^*$, $L^*C^*H^*$ and ΔE^*ab . Hunterlab solutions, CIE lab Solutions works on a measurement of $L^*a^*b^*$ values and comparison with another products $L^*a^*b^*$ values [4]. These instruments are well designed and can be operated easily but some instruments do not store data and results. By using computer vision, store data can be resulted batch wise which will be helpful for traceability also. Main objectives of present work were to develop low-cost colour measurement instrument with a camera, illumination system and computer system and colour measurement of food products (jaggery) in $L^*a^*b^*$, RGB values.

Jaggery is sugarcane based natural sweetener made by the concentration of sugarcane juice without any use of chemicals [5]. It is available in the form of solid blocks and in semi-liquid form. It contains the natural sources of minerals and vitamins inherently present in sugarcane juice and it is one of the most wholesome and healthy sugars in the world. Of the total world production, more than 70% of the jaggery is produced in India but most of the jaggery business suffers from losses. The development of different value added products from jaggery and their commercial availability becomes needs of the hour to sustain future profitability in the jaggery trade. Due to high moisture content and humidity, jaggery colour may changes that substantiates the need of colour analysis of jaggery. Jaggery colour also changes due to change in nutrients, structure, atmosphere. Sometimes jaggery cubes become rubbery which leads to change in colour indirectly which also effects on cost. Jaggery colour also depends on varieties of raw cane used for manufacturing of jaggery.

METHODOLOGY

Development of Colour Measurement Instrument

The colour measurement instrument was developed by 2 ft. (breadth) \times 2.5 ft. (length) \times 1.75 ft. (height) steel frame covered with 8mm plywood. The illuminating bulbs and the camera were placed in a box, the interior walls of which were painted black to eliminate background light. Below the camera jaggery sample was placed.

Camera captures photo of sample placed, send signals to computer. While capturing photo illumination light helps to maintain proper lighting condition. Photo was taken in Adobe Photoshop CS4 which displays RGB, $L^*a^*b^*$ values and graphs. Quantum color digital camera with 25 Mega Pixels of resolution, was placed vertically at a distance of 30 cm from the samples. The angle between the axis of the lens and the sources of illumination was approximately 45° . Illumination was achieved with 4 Syska LED, Natural Daylight 3W fluorescent lights, with a color temperature of 6500 K. Material required for instrument is presented in **Table 1**.

Sampling

Various samples were collected from local market Kolhapur for colour measurement and proximate analysis. Sample codes are presented in **Table 2**. The samples used in the experiment along with codes are given in **Figure 1**.

Table1 Material required for development of instrument

Material	Description	Quantity
Steel pipe	1.5 inch	35 ft
Illumination	3 watt Syska LED bulbs	4
Holders	Pipe holders	4
Plywood	8 mm	1.5 piece

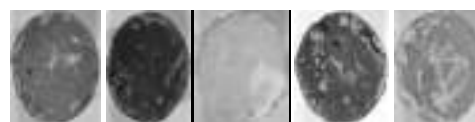
Table 2 Codes of samples

Sample code	Sample name
JI	Fresh jaggery
JII	Organic jaggery fresh
JIII	Chemically processed jaggery
JIV	Organic jaggery old



Colour	Asian paints mat finishing black colour	200 ml
Camera	Web cam 25 megapixel	1
Computer	Photoshop cs 4	1

JV	Kesari jaggery
----	----------------



(JI) (JII) (JIII) (JIV) (JV)

Figure 1 Samples used in experiment

Proximate Analysis of Jaggery

Determination of Moisture Content

About 5.0 g of sample was weighed and transferred into a previously weighed crucible. The crucible was then placed in the drying oven at 105°C for 5 h. After this, the sample was removed and placed in a desiccator to cool. The cooled crucibles were reweighed. This was done in triplicate. The loss in weight after drying was then calculated as the percentage moisture [6].

Determination of Ash Content

About 5.0 g of sample was weighed into a previously weighed crucible and placed in the muffle furnace (600°C) for 4 h. The crucibles were cooled and reweighed. The loss in weight was then calculated as the percentage as or ash content of the sample [6].

Determination of Fat Content

The dry sample was transferred to a paper thimble. Sample was added to a previously dried 250 ml round bottom flask and weighed. 150 ml of petroleum ether was added to the flask and the apparatus was assembled. Condenser was connected to the Soxhlet extractor and kept for 6 h on low heat. The flask was removed and evaporated on a steam bath. The flask with the fat was heated for 30 min in an oven at 103°C. The flask and its contents were cooled to room temperature in a desiccator after which it was weighed and percentage fat calculated [6].

Determination of Reducing Sugar Content by DNSA Method

About 5.0 g of sample dissolved in 50ml water, filtered by Whitman paper no 42. 5.0 ml of the sample taken in conical flask 2.0 ml DNSA reagent added. Solution kept in boiling water for 5 minutes then cooled under tap water. Measured optical density at 530 nm by making 150 times dilution. Plotted the standard curve and calculated the amount in the sample from the standard curve [6].

Sensory Evaluation

The jaggery sensory attributes were evaluated using a 9-point hedonic scale, where a score of 1 is 'dislike extremely' and a score of 9 is 'like extremely'. A panel of judges comprising ten participants were randomly selected from the students of the Department of Technology. Taste, aroma, colour, flavor, texture and general acceptability of the jaggery were determined.

Statistical Analysis

Results were expressed as mean \pm SD values were the average of triplicate experiments. Significant differences between the results were calculated by analysis of variance (ANOVA) with the help of Microsoft Excel 2010 [7].

RESULTS AND DISCUSSION

In this study for comparisons colour measurement (**Table 3**) was done at MPKV Rahuri (Department of Agricultural Process Engineering) on a standard colour measurement instrument (Premier Colour Scanning Machine, Thane).



Two samples, namely, fresh jaggery, organic jaggery were taken in experiment. For standardization piece of tile was used. Developed instrument was calibrated on the basis of standard colour measurement instrument values. L^* , a^* , b^* and RGB values obtained in developed colour measurement instrument of each pixel of image. Comparison between developed colour measurement instrument and Premier colour scanning instrument is presented in **Table 3**.

Table 3 Comparison between developed colour measurement instrument and Premier colour scanning instrument

Parameter	Standard colour measurement instrument		Developed colour measurement instrument	
	Tile	Jaggery	Tile	Jaggery
R	-	-	224	152
G	-	-	225	134
B	-	-	225	52
L^*	87.95	45.327	89	57
a^*	0.017	3.08	-1	6
b^*	8.02	27.63	5.33	30

Measurement of Jaggery Colour in Developed Colour Measurement Instrument

Samples were placed in image acquisition zone where camera captured the image of sample.

Images were analysed by using Adobe Photoshop CS4. L^* , a^* , b^* and RGB values were obtained by taking mean of three values. RGB values stands for percentage of Red, Green, Blue, colour present in sample. Colour values were used for finding the relation between chemical components in jaggery. Basically JIII was lighter and JIV was dark. Values shown in **Table 4** were obtained in measurement of colour of various jaggery samples in developed color measurement instrument. The low value of L^* (lightness) denoted darkness. JIII sample had higher L^* value than JII and JIV samples. JI sample had average L^* , a^* , b^* and RGB values. R and G value of JIII and JV samples were same but slightly changed in L^* value.

Table 4 L^* , a^* , b^* and RGB values from developed colour measurement instrument

Parameter	R	G	B	L^*	a^*	b^*
JI	147.66 \pm 1.0	120 \pm 1.2	43.3 \pm 0.8	47 \pm 1.0	8.66 \pm 0.5	26.33 \pm 0.5
JII	109 \pm 1.5	64.33 \pm 1.3	22.67 \pm 1.0	37.66 \pm 0.8	15.33 \pm 0.6	22.66 \pm 0.8
JIII	178.66 \pm 1.5	135.3 \pm 1.0	47 \pm 0.9	70 \pm 1.0	-2.33 \pm 0.5	21.55 \pm 1.0
JIV	134.3 \pm 1.0	72.33 \pm 1.5	29 \pm 1.4	38.33 \pm 0.7	20.66 \pm 0.8	27.66 \pm 0.5
JV	161.66 \pm 1.2	135.5 \pm 1.2	79 \pm 0.7	58 \pm 1.0	5.33 \pm 0.5	30 \pm 0.5



Proximate Analysis of Jaggery and Relation between Colour and Nutrients

Analysis of proximate composition provides information on the basic chemical composition of jaggery. Sample JII had L* value 37.66 which was in dark in colour with moisture content 15.23%, where as sample JIII had L* value 70 which resulted in lighter in color and moisture content 6.23%. Due to high moisture content colour changed from lighter to darker (Brown) [5]. As presented in **Table 5**, L* values increased with decrease in moisture content and ash content respectively in samples JII, JIV, JI, JV, JIII. There was the little change in fat content and protein content of both the samples. There was small difference in reducing sugars in chemically treated jaggery and organic jaggery. Values of proximate are presented in **Table 5**.

Table 5 Values of proximate analysis of jaggery in percentage

Components	JI	JII	JIII	JIV	JV
Moisture	9.10 ±0.10	15.23 ±0.15	7.25 ±0.15	16.00 ±0.10	12.30 ±0.15
Ash	1.7 ±0.05	2.5 ±0.05	1.25 ±0.05	2.4 ±0.05	2.1 ±0.05
Fat	0.14 ±0.12	0.18 ±0.16	0.13 ±0.12	0.17 ±0.10	0.15 ±0.10
Protein	0.58 ±0.20	0.60 ±0.12	0.55 ±0.12	0.63 ±0.15	0.59 ±0.12
Reducing sugar	17.05 ±0.68	21.19 ±0.76	15.20 ±0.50	22.13 ±0.60	17.8 ±0.45

CONCLUSION

Developed colour measurement instrument was able to measure colour in L*a*b* and RGB units and simultaneously measure the colour of each pixel on the target surface. Colour change occurred due to variation in nutrients of jaggery. With the help of this colour measurement instrument, the relation between colour and nutritional composition can be determined. This instrument can be used for colour analysis other solid food products.

REFERENCES

1. M. Abdullah, L. Guan, K. Lim, A. Karim, The applications of computer vision system and tomographic radar imaging for assessing physical properties of food", Journal of Food Engineering, Volume 61, Number 1, pp. 125-135, 2004.
2. K. León, D. Mery, F. Pedreschi, J. León, Color measurement in L*a*b* units from RGB digital images, Food Research International, Volume 39, Number 10, pp. 1084-1091, 2006.
3. F. Mendoza, P. Dejmek and J. Aguilera, Calibrated color measurements of agricultural foods using image analysis, Postharvest Biology and Technology, Volume 41, Number 3, pp. 285-295, 2006.
4. H. Good, Solving Color Measurement Challenges of the Food Industry, www.HunterLab.com, 2011. [Online]. available: <http://Hal Good, HunterLab, Reston, VA, Solving Color Measurement Challenges of the Food Industry, 2017>.
5. Dilip Kumar, Jarnail Singh, D.R. Rai, S. Bhatia, A.K. Singhand, Mahesh Kumar, Colour Changes in Jaggery Cubes under Modified Atmosphere Packaging in Plastic Film Packages, 2013.
6. W. Horwitz, Official methods of analysis of AOAC International, 1st ed. Gaithersburg: AOAC International, 2000
7. Mohammad Daneshil, Effect of refrigerated storage on the probiotic survival and sensory properties of milk/carrot juice mix drink" Electronic Journal of Biotechnology, 2013.



Genetic Diversity Analysis of *Staphylococcus aureus* of Various Samples Collected from Bay of Bengal using Restriction Fragment Length Polymorphism (RFLP)

K.Saranya^{*1}, V.Manivasagan¹, S.Kavitha¹, D. Kubendran¹

Department of Biotechnology, Adhiyamaan College of Engineering, Hosur, India¹, ksaranya31@gmail.com*

ABSTRACT

Staphylococcus is a recognized genus of bacteria it is a common pathogen causes boils, acne, wound infections, food poison. Staphylococcal resistance to Penicillin is mediated by Penicillinase (a form of Beta-lactamase) which is an enzyme which breaks down the β -lactam ring of the penicillin molecule. The main objective of the present study is to analyze the genetic diversity of *Staphylococcus aureus* using RFLP. The samples Nethili, Sankara, Sudumbu were collected from different areas of Bay of Bengal sea shores. The samples were serially diluted and spread plate technique was done to isolate the microorganism. Identification of microbes were done. Determination of methicillin and vancomycin sensitivity was performed using agar disc diffusion method. Genomic DNA was extracted using genomic DNA extraction kit. Quantification of *Staphylococcus aureus* genome was done using PCR. Genetic diversity were analysed using RFLP. The isolated genomic DNA was allowed for polymerase chain reaction amplification and gene was found to be Mec A with 810 bp. The DNA bands were visualized under UV-transilluminator. RFLP was performed by using 20 μ l of reaction mixture, containing template DNA, restriction enzyme (AluI, HaeIII) and distilled water. The results of the RFLP patterns clearly show that all strains produced more than one bands with different restriction fragments and it was compared with standard DNA ladder. *S.aureus* was digested was AluI, HaeIII and results show different banding pattern, Some bands showed single band and some showed double bands and triple bands. Thus the result was predicted for the genetic relation between the organisms. Nethili were found to be related with two bands similarity. It was concluded that not all the *S.aureus* were closely related.

KEYWORDS PCR, Electrophoresis, DNA isolation, Biochemical test, RFLP.

INTRODUCTION

Staphylococcus is a familiar genus of bacteria. On sheep blood agar solid media colonies are 'gold', or yellow, the golden appearance is the etymology root of the bacteria's name: *aureus* means 'golden' in Latin. *S.aureus* exactly the 'golden cluster seed' or 'the seed gold' and also known as golden Staphi which is a common pathogen, boils, acne, wound infections, food poisoning are among a host of conditions caused by this organism. The organism is a pathogenic and invasive. *S aureus* produces leukotoxin which can kill white blood cells and a wide variety of other toxins. It is moderately pyogenic and in decades past was named *Staphylococcus pyogenes*. Increasingly, and especially in hospital, strains of both *S.aureus* and *S.epidermidis* have become resistant to the antibiotic, methicillin. There are many species in staphylococcus such as *S.aureus*, *S.epidermidis* etc. But the significant species for the production of Penicillinase enzyme was found to be the methicillin resistant *Staphylococcus aureus* (Sutherland and Rolinson, 1964), as it produces higher amount of the enzyme compared to the other species.

Staphylococcal resistance to Penicillin is mediated by Penicillinase (a form of Beta-lactamase) production: an enzyme which breaks down the β -lactam ring of the penicillin molecule. Methicillin, Nafcillin, Oxacillin, Cloxacillin, Dicloxacillin, and Flucloxacillin are penicillinase-resistant penicillins, able to resist degradation by staphylococcal penicillinase. The Methicillin resistance in *Staphylococcus aureus* is mediated by the presence of Mec A gene that is found on a characteristic piece of flanking DNA, the chromosomal cassette Mec. The Mec A gene encoding penicillin binding protein 2a (PBP 2a) confers methicillin resistance, an enzyme which has decreased affinity for beta-lactam antimicrobials. PBP 2a and native PBP 2 work in concert to allow cell wall synthesis despite the presence of beta-lactam antibiotics thus effectively conferring resistance to penicillin's, cephalosporin's and carbapenems (Esteves A, 2007).

The main objective of the present study is to • Identification of microbes from various contaminated fish samples, • Extraction of Genomic DNA from the samples, and • Comparative study of Genomic DNA using RFLP.

MATERIALS AND METHODS

Materials

Fish samples Nethili, Sankara, Sudumbu were collected from different areas of Bay of Bengal sea shores.

Extraction of Microorganism : The samples were serially diluted using sterile saline and spread plate technique was done to isolate the microorganism. (Saranya, 2016) 0.1 ml of samples were spread on Mannitol Salt Agar medium and incubated at 37°C for 24 hours. The colonies appeared on MSA medium were purified by sub culturing.

Extraction of Genomic DNA: Using the Insta Gene™ Matrix genomic DNA isolation kit bacterial genomic DNA was isolated by centrifuged for 1min at 10,000 rpm, supernatant were discarded. To the pellet 20 µL of Insta Gene Matrix were added and incubated at 56°C for 15 min. It has been followed by vortexing for 10 s and tubes are kept into boiling water bath for 8 min. Finally, the tubes were vortexed for 10 s, centrifuged at 10,000 rpm for 2 min. 20 µL of the supernatant was collected and used to perform gel electrophoresis.

Agarose Gel Electrophoresis (AGE) : 1% agarose was prepared and dissolved in 1 × TBE buffer. After cooling 2 µl Ethidium bromide was added in dissolved agarose. Prepared agarose was poured on to gel boat, wells can made by using the comb. 20 µl of digested DNA was loaded along with 3 µl of gel loading buffer and Electrophoresis was performed.

Polymerase Chain Reaction (PCR) : To 20 µL of PCR reaction solution 1 µL of template DNA were added and primers particulars were listed in the **Table 1**. DNA fragments were amplified about 1,400 bp with a positive control (*E.coli* genomic DNA) amplified 16S rRNA gene. Using montage PCR clean up kit (Millipore) the PCR products were purified and sequenced using the 518F/800R primers as given in the **Table 2** sequencing reaction were performed using AB1 Prism BigDye terminator sequencing kit with Ampli Taq DNA polymerase (FS enzyme) and in Applied Biosystem 373a DNA Sequencer. The sequencing parameter details are given in the **Tables 2 and 3**.

Table 1 Sequence detail

Primer name	Sequence detail	Number of base
27F	AGAGTTTGATCMTGGCTCAG	20
1492R	TACGGTTACCTTGTTACGACTT	22

Table 2 Sequence detail of primer

Primer name	Sequence detail	Number of base
518F	CCAGCAGCCGCGGTAATACG	20
800R	TACCAGGGTATCTAATCC	18

Table 3 Sequencing parameters

Parameters	Temperature	Time
Initial denaturation	94 °C	2 min
35 amplification cycles	94 °C	45 S
	55 °C	60 S
	72 °C	60 S
Final extension	72 °C	10 min

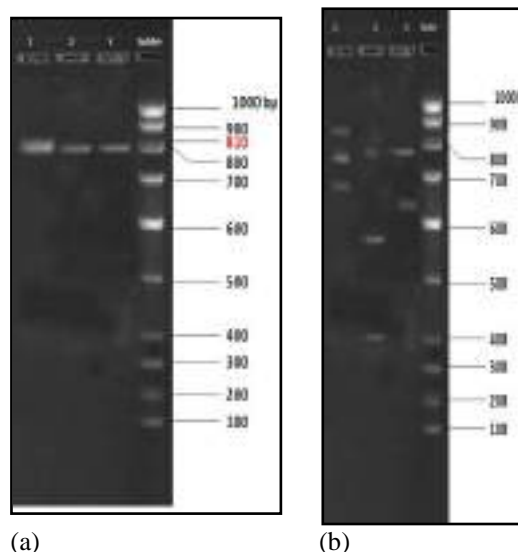


Figure 1 (a) AGE (b) RFLP (lader1,2,3- Nethili, Sankara, Sudumbu)

BIOINFORMATICS TOOLS

The 16S rRNA sequence were analysed by BLAST using NCBI search tool, the phylogeny analysis of the sequence were performed by the program MUSCLE 3.7 was used for multiple sequence alignment (Edwards, 2004).



RFLP Analysis

The restriction materials from the freezer (27°C) were brought to the room temperature. The following materials were added into 0.5 ml microfuge tube. Sample DNA – 2 µl. Restriction enzyme (EcoRI, AluI and HaeIII) – 2 µl. Restriction enzyme buffer – 2 µl. Distilled water - 14µl. The reagents were pooled and tapped to collect the fluids at the bottom. The reaction mixtures were kept for 1 h at 37°C in water bath. After incubation 4µl of gel loading dye was added to the 20µl digested sample. The samples were mixed well and loaded on agarose gel (Coles, N, W, 1967). The power card terminals were connected at respective position and the gel were run at 50 V or 100 V till the gel loading dye migrates more than half the length of the gel. The units were switched off and the gel was transferred to UV Transilluminator to visualize the RFLP pattern (Clauditz, A, 2006).

RESULTS AND DISCUSSION

RFLP analysis were used to find the heterogeneity. Among three samples, two of the samples were found to be positive for the presence of *Staphylococcus aureus* were shown in the table 4. These were confirmed using the biochemical tests.

PCR Analysis to Confirm the Presence of Mec A Gene

The isolated genomic DNA was allowed for polymerase chain reaction to amplify the Mec A gene. The result was found to contain the gene at 810 bp. Wisal et al., 2009 performed PCR using 29 isolates from human and animal environment. Out of 29 amplified product, 21 produced single band and 8 isolates produce two bands. The length of amplicon ranged from 430 and 100 bp. Amplicons of 21 isolates were categorized as 670,930,950,1000bp. Similarly, in present study three isolates got amplified and bands were observed in 810 bp. This confirms the presence of Mec A gene in *S.aureus* shown in the **Figure 1(a)** (Hennekinne, JA, 2009).

RFLP Analysis

The extracted genomic DNA of *Staphylococcus aureus* were run on agarose gel electrophoresis. The DNA bands were visualized under UV-transilluminator. RFLP was performed by using 20µl of reaction mixture, containing template DNA, restriction enzyme (AluI, HaeIII) and distilled water (Didier guillemot et al, 2004). The results of the RFLP patterns clearly show that all strains produced more than one bands with different restriction fragments and it was compared with standard DNA ladder (Hu, DL, 2003). *S.aureus* was digested with AluI, HaeIII and results show different banding pattern (Chiou, CS, 2000). Some bands showed single band and some showed double bands and triple bands. Thus the result was predicted for the genetic relation between the organisms. In present study out of three samples isolated, AluI and HaeIII enzyme produce two to three bands between 600 to 800 bp and 400 to 800 bp, respectively. It was concluded that not all the *S.aureus* were closely related.

CONCLUSION

The present work reveals that the food poison causing microorganism *S.aureus* of same species were not closely related. *S.aureus* is reasonably pyogenic and it secretes leukotoxin which can kill white blood cells and a wide variety of other toxins. The future work of this research deals with analysis of genes of various food poisoning microorganisms.

ACKNOWLEDGEMENT

The authors would like to articulate their sincere thanks to Department of Biotechnology, Adhiyamaan College of Engineering for providing all the facilities to develop the project successfully.

REFERENCES

1. A Esteves, L Patarata, T Aymerich, M Garriga, C Martins, Multiple correspondence analysis and random amplified polymorphic DNA molecular typing to access the sources of *S.aureus* contamination in Alheira production lined, Journal of Food Protection, pp. 685-691, 2007.
2. Didier Guillemot et al., Amoxicillin-clavulanate therapy increases childhood nasal colonization by methicillin-susceptible *Staphylococcus aureus* strains producing high levels of penicillinase, Antimicrobial Agents and Chemotherapy, Volume 48, Number 12, pp. 4618-4623, 2004.
3. N. W Coles, R. Gross, Liberation of surface-located penicillinase from *Staphylococcus aureus*, Commonwealth serum laboratory, Parkville, Victoria, Australia, Biochem. J., Volume 102, pp. 742-747, 1967.
4. A Clauditz, A Resch, K P Wieland, A Peschel, Staphyloxanthin plays a role in the fitness of *staphylococcus aureus* and its ability to cope with oxidative stress, Infection and immunity, Volume 74, Number 8, pp. 4950-4953, 2006.



5. C S Chiou, H L Wei, L C Yang, Comparison of pulsed-field gel electrophoresis and coagulase gene restriction profile analysis techniques in the molecular typing of *Staphylococcus aureus*, *J Clin Microbiol*, Volume 38, pp. 2186–2190, 2000.
6. J A Hennekinne, V Brun, M L De Buyser, A Dupuis, A Ostyn, S Dragacci, Innovative contribution of mass spectrometry to characterise staphylococcal enterotoxins involved in food outbreaks, *Appl Environ Microbiol*, Volume 75, pp.882-884, 2009.
7. D L Hu, K Omoe, Y Shimoda, A Nakane, K Shinagawa, Induction of emetic response to staphylococcal enterotoxins in the House Musk Shrew (*Suncus murinus*), *Infect Immun*, Volume 71, pp.567- 570, 2003.
8. K Saranya, M Thirumarimurugan, V Manivasagan, Biosorption of hexavalent chromium from paint industrial effluent by *Saraca indica* leaves using with and without gel entrapment method, *Int. J. Environment and Sustainable Development*, Volume 15, Number 3, pp.219-226, 2016.
9. Sutherland and Rolinson, Characteristics of methicillin-resistant staphylococci, *Journal of Bacteriology*, Volume 87, pp.887-99, 1964.
10. Wisal Baiker et al., Evaluation of a new commercial taqman PCR assay for direct detection of the *clostridium difficile* toxin B gene in clinical stool specimens, *Journal of clinical microbiology*, Volume 47, pp.3846-3850, 2009.



Mitigation Pathways for CO₂ Emission in Chemical Industries by Integration of Technologies

S. C. Nimkar^{*1}, Deepa P¹, Cissy Shaji¹

Department of Chemical Engineering, Bharati Vidyapeeth Institute of Technology, Navi Mumbai, India¹, scnimkar@yahoo.com*

ABSTRACT

Increasing carbon dioxide emission in world is leading to global warming. Out of total emission, 36% emission is attributable to manufacturing industries including chemical industry. Chemical industries contribute emission in the form of energy and non-energy use. Energy conservation practices will reduce CO₂ emission caused by energy use. For reduction from non energy use, selection of alternative technology, improvement in catalyst selectivity, waste heat recovery plays very important role. In the present paper an attempt has been made to integrate various technologies in existing processes of Nitric Acid and Ethylene Oxide-Ethylene Glycol for reduction in CO₂. Exergy analysis is used as tool for analysis. It has been found that modification in compressor and heat recovery by ORC from cooler condenser in Nitric Acid plant will reduce CO₂ emission. Improvement in catalyst selectivity and adoption of new technology developed helps in mitigation of emission in Ethylene Oxide-Ethylene Glycol process.

KEYWORD Carbon dioxide, Nitric acid, Ethylene oxide, Exergy analysis, Heat recovery

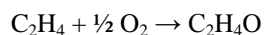
INTRODUCTION

Carbon dioxide (CO₂) emission is a major concern globally. Today development comes with emission. Infrastructure development and Industrial development leaves unavoidable environmental impact. In past two centuries, more than 2.3 trillion tonne of CO₂ is released into atmosphere [1]. Total CO₂ emissions from industry were 9.7 giga tonne (Gt) in 2004 and accounted for 36% of total global CO₂ emissions [2]. Iron, steel and non-metallic industries contribute 27% each followed by chemical industry which contributes to 16 % direct CO₂ emission. Industries are focusing more on energy conservation activities due to increasing fuel prices. Rapid change in climate has forced industries to shift their focus on the reduction of GHG emission. Paris agreement is an important step in this direction.

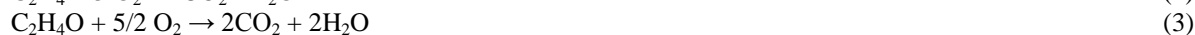
Chemical industry is a significant contributor in CO₂ emission due to energy and non-energy uses of fossil fuels. It is called as 'combustion related emission' and 'process related emission' [3]. A loss due to catalyst selectivity is one of the major concerns in chemical industry. Various studies have been carried out to reduce CO₂ emission in chemical manufacturing processes [2,4,5]. Ethylene oxide manufacture is one of the processes where CO₂ emission is due to lower selectivity of catalyst. Environmental impact of CO₂ can be reduced in two ways : (i) Utilisation of CO₂ for the production of various chemicals, and (ii) Reduction of CO₂ emission at source. In the present paper, an attempt has been made to reduce CO₂ emission for the process having both combustion related and process related emission. Ethylene Oxide-Ethylene Glycol and Nitric Acid manufacturing processes are selected for the study. Exergy analysis is used as tool the for evaluation purpose.

ETHYLENE OXIDE-ETHYLENE GLYCOL PROCESS AND CO₂ EMISSION

Ethylene Glycol is one of the important raw materials used in the manufacture of polyester, fiberglass, polyethylene terephthalate. It is also used as a coolant and antifreeze. Ethylene Glycol is produced by reacting ethylene oxide with water. Manufacturing of ethylene oxide is exothermic while manufacturing of Ethylene Glycol is endothermic. Ethylene is reacted with oxygen in the tubular packed bed reactor to produce Ethylene Oxide in the presence of silver catalyst [6]. Along with main reaction (no.1) two side reactions (no.2 and 3) are also taking place. Conversion per pass is kept low in the reactor to reduce production of CO₂. The catalyst must maximise primary and minimise side reactions. In this process, high activity catalyst with 81% initial selectivity and three-year life is used. Product gases from reactor are send to Ethylene Oxide absorber unit for separation of Ethylene Oxide and then to CO₂ absorber unit for separation of CO₂ as shown in **Figure 1**. Unabsorbed gas is recycled back to the reactor. Small amount of gas is purged to maintain concentration of inert in the recycle stream. Purged stream is used in boiler or furnace as a fuel. Ethylene Glycol is produced by reacting Ethylene Oxide with excess water (reaction no.4). Water present in Ethylene Glycol is separated in series of evaporators and separators.



(1)



During initial period, catalyst activity is higher and CO₂ production is 478.69 kg/ton of EO. Catalyst is replaced at 77.9% selectivity. CO₂ production is 564 kg/ton of EO at the time of replacement (**Figure 2**).

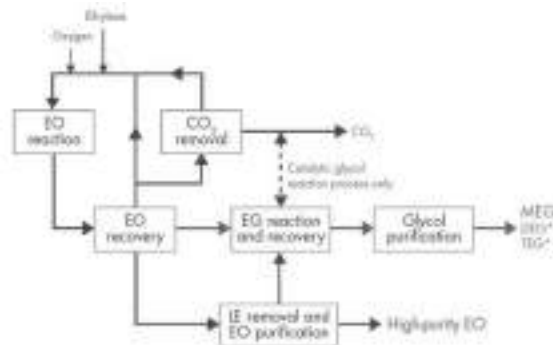


Figure 1 Process flow diagram for production of Ethylene Oxide-Ethylene Glycol [7]

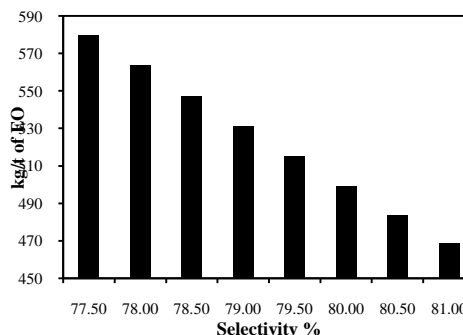


Figure 2 CO₂ production at different catalyst selectivity values

CO₂ MITIGATION IN ETHYLENE OXIDE-ETHYLENE GLYCOL PROCESS

Catalyst Selection

CO₂ reduction is possible in Ethylene Oxide-Ethylene Glycol process either by using high selectivity catalyst or reduction in required energy for the process. Traditional silver catalysts are replaced after three to four years of service. High selectivity catalyst provides higher selectivity (about 90%) during initial period but activity is lower compared to traditional catalyst. Its life is 1.5 to 2 years. CRI Catalyst Company developed Higher Performance catalyst with higher initial selectivity but with a significantly slower performance decline [7]. The average selectivity is significantly higher, currently averaging about 87%, and catalyst life is much longer than high selectivity catalyst.

Ethylene Recovery from Purge Gas

Purging of recycled gas is necessary in Ethylene Oxide-Ethylene Glycol process to maintain the concentration of ethane and argon in the process. Purge gas contain ethylene which may be converted into Ethylene Oxide otherwise. Commercial value of ethylene is lost and only heating value remains due to purging. A semipermeable membrane made up of silicone rubber can be used to recover ethylene (**Figure 3**). Ethylene rich permeate is recycled and argon rich residue streams are separated [8]. Almost 75% ethylene is recovered from purge which will be otherwise burned in boiler as a fuel. 28 kg of CO₂ /tone of Ethylene Oxide can be saved due to recovery of ethylene.

CEBC Process

The CEBC (Centre for Environmentally Beneficial Catalysis) process uses hydrogen peroxide as oxidant and methyl trioxorhenium as a catalyst [9]. Ethylene is introduced into liquid phase mixture of oxidant, catalyst and methanol (as co solvent). Product Ethylene Oxide is completely dissolved into oxidant with decomposition of oxidant. This process does not produce flammable gas mixture hence safer than conventional process. There is no burning of ethylene, hence carbon dioxide production from process is totally eliminated. But production of hydrogen peroxide is energy intensive and CO₂ emission for this process offsets the gain obtained by CEBC process. Improvement in hydrogen peroxide technology can reduce net CO₂ emission from alternate process.

RTI C3-PEO Process

Mobely et. al of RTI international has developed a new process for production of ethylene oxide using carbon dioxide [10]. Oxygen atom in carbon dioxide is used for the reaction using metal oxides. The reactions are



Like conventional process undesirable side reaction take place in this process also.

$$6\text{CO}_2 + 6\text{M}^0 \rightarrow 6\text{CO} + 6\text{MO} \quad (8)$$

$$\text{C}_2\text{H}_4 + 6\text{MO} \rightarrow 2\text{CO}_2 + 2\text{H}_2\text{O} + 6\text{M}^0 \quad (9)$$

$$\text{C}_2\text{H}_4 + 4\text{CO}_2 \rightarrow 6\text{CO} + 2\text{H}_2\text{O} \quad (10)$$

These side reactions must be kept at a minimum to keep the techno-economics of the process favourable. Schematic arrangement of process is shown in **Figure 4**.

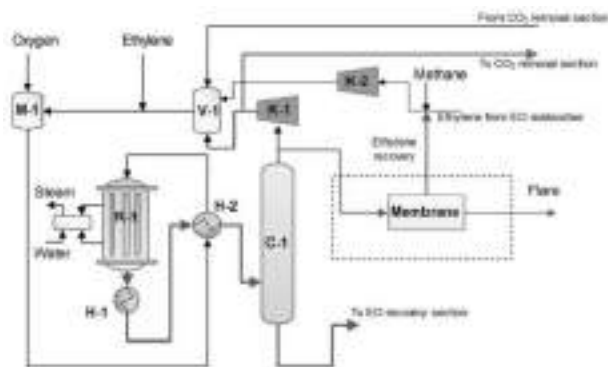


Figure 3 Recovery of ethylene from purge gas

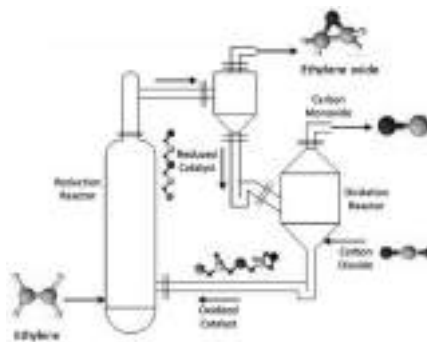


Figure 4 RTI C3-PEO process for the production of Ethylene Oxide[10]

Carbon dioxide and ethylene are compressed and send to the reactor where catalyst is placed. Product gas containing carbon dioxide, carbon monoxide, ethylene oxide and unreacted ethylene is send for separation. Ethylene Oxide and Carbon monoxide are two valuable products obtained in this process. CO₂ separated in this process is again recycled to the reactor. Life cycle analysis shows that overall reduction in CO₂ emission is 2.82 ton/ton of Ethylene Oxide compared to conventional process.

OMEGA Process

OMEGA process is developed by Mitsubishi Chemical Corporation and Shell Chemicals. Mono Ethylene Glycol is produced in two steps using phosphonium salt as the catalyst [11]. Detailed information about the process parameters is not available in the literature because the technology is new and exclusively licensed. Initially Ethylene Oxide reacts with carbon dioxide and water. Simultaneous production of ethylene carbonate and its conversion into mono ethylene glycol takes place in the reactor. Maximum EO will be converted into Ethylene Carbonate (reaction 11). The heat of reaction is recovered in the exothermic Ethylene Carbonate process. Unreacted CO₂ is compressed and recycled back to the reactor after purging a small amount.



Water used for the reaction is sufficient to complete the reaction unlike excess water required in the conventional process. Alkali metal salts are also used along with phosphonium salt to accelerate the reaction. A by-product of higher glycol (Bi, Tri) formation is very limited due to higher selectivity (99%) of the process. Excess water present in glycol is removed by using very less heat compared to conventional process. About 20% less steam is required in OMEGA process which results into saving of 342 kg of CO₂ / ton of Ethylene Oxide [12].

Exergy Analysis

The energy balance of the system shows input energy is a sum of output energy and accumulation. The case is not true for exergy balance because some part of exergy is lost in the process.

Exergy is the availability of energy in provided resource and its value depends upon reference environment. Physical exergy is the work obtained when the system is brought from its original state to environmental state. Exergy (E) of a closed system is the combination of physical, kinetic, potential and chemical Exergy and can be expressed as [13]

$$E_{\text{sys}} = E_{\text{sys}}^{\text{PH}} + E^{\text{KN}} + E^{\text{PT}} + E^{\text{CH}} \quad (13)$$

The exergy of flowing stream is written as [14]



$$E = (H - H_0) - T_0(S - S_0) + E^{KN} + E^{PT} + E^{CH} \quad (14)$$

Where H is enthalpy, S is entropy and 0 indicate environmental state

The quality of hot stream (Q) depends upon the work obtained from it. According to the second law of thermodynamics, it is not possible to convert all heat into work though it contains lots of energy. Exergy of thermal energy is denoted by

$$E^Q = \left(1 - \frac{T_0}{T}\right) Q = \tau Q \quad (15)$$

Chemical exergy can be defined as maximum work that can be obtained when a substance is brought to reference state from its present state. The standard chemical exergy [15] of any chemical compound can be calculated by

$$E_n^{CH} = \Delta G_f + \sum n_e E_e^{CH} \quad (16)$$

Where ΔG_f is the Gibbs energy of formation, n_e is the molar amount element e, and E_e^{CH} is the standard chemical exergy of element e.

Exergy analysis is useful mainly to pinpoint the energy losses in the process under study. Energy balances will not show the true picture of energy quality. Heat losses in cooling tower are higher in many processes, but its usefulness is zero. Exothermic reactions in reactor show perfect energy balance but quality of energy available due to exothermic reaction will be lower due to exergy destruction in reactor as shown in Figure 5. CO₂ emission is indirectly related to exergy quality of the process. It can be reduced by converting available heat into higher exergy applications like work or production of superheated steam. In Ethylene Oxide-Ethylene Glycol process, CO₂ production increases as selectivity of catalyst decreases. Catalyst cost plays an important role while considering its replacement, hence CO₂ production due to decrease in selectivity can not be eliminated. Exergy analysis with economic analysis of the process will help to decide catalyst life. Nimkar and Mewada [8] proposed a new parameter EGRebased upon reduction in exergy destruction potential and income cycle of the processes. As exergy destruction is reduced, it helps in the reduction of CO₂ emission.

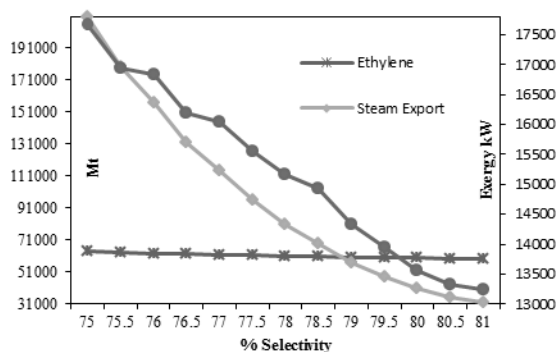


Figure 5 Ethylene requirement and steam export (150 kt/yr of Ethylene Oxide production)

CO₂ Reduction in Nitric Acid Processes

Nitric acid plant is called as mini power house due to use of exothermic heat produced in the process to run turbo compressor and produce excess steam. Ammonia is oxidised with air in ammonia oxidation reactor to produce nitrous gases. These gases are further oxidised and absorbed in absorber. Unabsorbed gas (tail gas) is vented to the atmosphere. Heat generated in the reactor is used to produce superheated steam. Hot gases coming out from reactor are used to heat tail gas coming out from absorber. Both steam and tail gas is used to run turbocompressor which is used to compress air and maintain pressure in the plant. It consumes around 24% of input energy. Nitrous gases are cooled in cooler condenser by using cooling tower water before sending into absorber. Plants energy efficiency is 31% and exergy efficiency is 20.83%. Heat energy discarded through cooling tower water is 67.86% of the total energy[16].

Like Ethylene Oxide-Ethylene Glycol plant, there is no direct emission of CO₂ from the process. If heat lost in cooler condenser and turbocompressor is recovered, CO₂ emission can be reduced. Energy is lost in the form of heat during compression of air. It can be reduced by lowering inlet air temperature up to 17°C. A net energy saving of 31.07 MJ/ton of acid can be achieved by providing 53.53 MJ/ton of acid of compressor energy for refrigeration cycle to bring down air temperature from 35°C to 17°C. Almost 14% reduction in the compressor exergy destruction



takes place when inlet air temperature is reduced to 17°C. Reduction in compressor power saves 51.2 kg/t of steam from steam turbine.

Organic Rankine Cycle (ORC) plant is proposed for heat recovery in cooler condenser of 300 TPD nitric acid process. The working fluid is chosen as pentane to maintain cycle pressure above atmospheric pressure to avoid leakage of air inside the cycle. Heat is available considerably when gases start condensing. The proposed ORC plant gives 205.24 MJ/ton of acid of net output making total plant exergy output 1473.98 MJ/ton of acid. Heat recovery in both the equipment can reduce CO₂ emission by 57.56 kg/ton of acid. Exergy balance of Nitric Acid Plant after installation of new systems is shown in **Table 1**.

Table 1 Exergy balance after installation of new systems

Input	MJ/t	%	Output	MJ/t	%
Air	2.58	0.04	Nitric Acid (PH)	16.49	0.27
Process Water	3.96	0.06	Nitric Acid (CH)	715.34	11.58
NH ₃ (PH)	159.44	2.58	Tail Gas (PH)	2.67	0.04
NH ₃ (CH)	5586.69	90.45	Tail Gas (CH)	112.95	1.83
Electricity	126.72	2.05	Steam Export	585.92	9.49
Make Up Water	212.56	3.44	Electricity (ORC)	205.24	3.32
NH ₃ Heating	84.71	1.37	Heat to Cooling Tower	210.84	3.41
Total	6176.66	100.00	Total	1849.46	29.94
			Exergy Destruction	4324.34	70.06

Table 2 Different measure for mitigation of CO₂ emission in Ethylene Oxide-Ethylene Glycol and Nitric Acid Plant

CO ₂ emission type	Technology integrated to reduce CO ₂ emission	Impact of change
Catalyst selectivity	Use of HP catalyst in EO reactor	Reduction in CO ₂ emission due to increased selectivity and consistent activity. Quantity of CO ₂ reduction is based upon value of selectivity
Combustion emission	Recovery of ethylene from purge gas	Reduction of 28 kg of CO ₂ /ton of EO
Catalyst selectivity	Use of CEBC process	Net CO ₂ reduction is possible if alternate process of H ₂ O ₂ production is developed. Quantity of CO ₂ reduction is depending upon energy requirement of H ₂ O ₂ process
Catalyst selectivity and combustion emission	RTI C3-PEO process	56% reduction of CO ₂ emission compared to conventional process.
Catalyst selectivity and combustion emission	OMEGA process	Saving of 342 kg of CO ₂ / ton of EO
Combustion emission	Reduction in exergy destruction of process	CO ₂ reduction potential depends upon energy saving due to reduction in Exergy destruction
Combustion emission	Reduction in inlet air temperature of compressor	Reduction of 5.3 kg of CO ₂ /tone of acid
Combustion emission	Use of ORC for heat recovery in cooler condenser	Reduction of 52.26 kg of CO ₂ /tone of acid

CONCLUSION

New technologies are essential to reduce CO₂ emission along with improvement in existing plant. In this study both measures are analysed and found that CO₂ mitigation is possible in existing facilities if we integrate different technologies with existing as shown in **Table 2**. Continuous improvement in catalyst selectivity is helping to get more yield of EO and reduction of unwanted side reaction. Development of new processes like CEBC process and RTI C3-PEO process completely eliminate production of CO₂ during reaction. Commercialisation of these processes will bring bigger relief from processes emission. Combustion emission can be reduced by exploring renewable



energy sources. Existing technology based plants will be continued till commercialisation of new technologies. Improvement in the existing process is need of the hour. Minimisation of purge, recovery of hydrocarbons from waste, conservation of energy, heat recovery in the process can reduce CO₂ emission. Conversion of heat into work and electricity is possible in the nitric acid plant. Continuous efforts in this direction can lead to sustainable development without impacting environment.

REFERENCES

1. K. A. Baumert, T. Herzog, J. Pershing, Navigating the Numbers Greenhouse Gas Data and International Climate Policy. World Resources Institute, 2005.
2. Tracking Industrial Energy Efficiency and CO₂ Emissions. International Energy Agency, available at https://www.iea.org/publications/freepublications/publication/tracking_emissions.pdf, 2007.
3. B. Zhu, W. Zhou, S. Hua, Q. Li, C. Griffy-Brown, Y. Jin, CO₂ emissions and reduction potential in China's chemical industry. Energy Volume 35, pp 4663-4670, 2010.
4. W. Zhou, B. Zhu, Q. Li, T. Ma, S. Hu, C. Griffy-Brown, CO₂ emissions and mitigation potential in China's ammonia industry. Energy Policy, Volume 38, pp 3701-3709, 2010.
5. Z. Liu, National carbon emissions from the industry process: Production of glass, soda ash, ammonia, calcium carbide and alumina. Appl. Energy, Volume 166, pp 239-244, 2016.
6. Ullmann's Encyclopedia of Industrial Chemistry. 6th, completely revised edition. Weinheim, Germany: Wiley-VCH, pp. 547-572, 2003
7. H. V. Milligen, B. VanderWilp, G. J. Wells, Enhancements in ethylene oxide/ethylene glycol manufacturing technology, available at www.shell.com/globalsolutions, 2016
8. S.C. Nimkar, R.K. Mewada, An overview of exergy analysis for chemical process industries. Int. J Exergy, Volume 15, Number 4, pp 468-507, 2014.
9. M. Ghanta, T. Ruddy, D. Fahey, D. Busch, B. Subramaniam, Is the liquid-phase H₂O₂-based ethylene oxide process more economical and greener than the gas-phase O₂-based silver-catalyzed process? Ind. Eng. Chem. Res. Volume 52, pp 18-29, 2013.
10. P. D. Mobley, J. E. Peters, N. Akunuri, J. Hlebak, V. Gupta, Q. Zheng, S. J. Zhoua, M. Lai, Utilization of CO₂ for Ethylene Oxide. Energy Procedia. Volume 114, pp 7154 -7161, 2017.
11. K. Kawabe, Development of highly selective process for mono-ethylene glycol production from ethylene oxide via ethylene carbonate using phosphonium salt catalyst. Catal. Surv. Asia, Volume 14, pp 111-115, 2010.
12. Factsheet about OMEGA and ethylene oxide/ethylene glycol technology, available at <https://www.shell.com/business-customers/chemicals/factsheets-speeches-and-articles/factsheets/omega.html>, 2010
13. G. Tsatsaronis, Definitions and nomenclature in exergy analysis and exergoeconomics. Energy, Volume 32, pp 249-253 pp 2007.
14. I. Dincer, M.A. Rosen, Exergy: Energy, Environment and Sustainable Development. 1st ed., Elsevier, Oxford, 2007.
15. J. Szargut, A. Valero, W. Stanek, A. Valero, A. Towards an international reference environment of chemical exergy. ECOS 2005: Proceedings of the 18th International Conference on Efficiency, Cost, Optimization, Simulation and Environmental Impact of Energy Systems, Trondheim, Norway, pp.409-417
16. R.K. Mewada, S.C. Nimkar, Minimisation of exergy losses in mono high pressure nitric acid process. Int J Exergy. Volume 17, Number 2, 192-218, 2015.



Fortification of Fenugreek Seeds Powder in Soya Sticks

Gurunath Mote¹, Supriya Khade¹, I. S. Udachan¹, Akshaykumar Sahoo¹

¹Shivaji University, Department of Technology, Kolhapur 416004, Maharashtra, India¹, guru.mote@gmail.com*

ABSTRACT

The aim of present work was to develop nutritional soya sticks by incorporation of fenugreek seeds. Fenugreek seeds were incorporated in soya sticks in the powder form. As a fenugreek seed was bitter in taste, therefore seeds were debittered by processing like soaking and germination. Fenugreek seeds were soaked for 12hr and then germinated for 48 hr. The germinated seeds were dried and grind into powder form. Chemical properties of raw fenugreek seeds and germinated fenugreek seeds such as moisture, ash content, fat and protein on % dry basis were found to be 4.58%, 3.84%, 6.63%, and 23.56% and 6.36%, 3.25%, 5.70% and 23.20% respectively. The fenugreek seed powder was incorporated at 1%, 2%, 3% and 4% in soya sticks. On the basis of overall analysis, from all samples, sample contains 2% fenugreek seed powder was most acceptable. Sensory attributes like appearance, taste, flavour and overall acceptability were the quality control parameters used for soya sticks evaluation.

KEYWORD Fenugreek seed, soaking, germination, oil frying, oven baking and soya sticks.

INTRODUCTION

There is an increasing customer attention towards ready-to-eat snack foods mostly due to their expediency, large availability, appearance, taste and feel. Customer-based studies have exposed improved food utilization related to the habit [1].

Extruded foods such as snacks have become part of the dietary behaviour of a large element of the population. They can be prepared with ingredients or components that give them specific functional properties [2].

Several extruded products are typically prepared from cereals such as corn, rice and wheat. These cereals are rich in carbohydrates and fibers but comparatively low in protein, therefore, they require enhancing the protein in the extruded food product. Due to customer requirement for healthy extruded snack foods, a lot of industries have increased focus in research and food product development to manufacture products that are nutrient-dense [3].

Various studies have been carried out on the fortification of snacks with diverse ingredients, such as soy flour, soy protein isolate, carrot, vitamins, tomato powder and basil powder, yam flour, with supplementary ingredients, such as oats and fibers [4].

Soybean contains a high level of protein than other legumes and is known to contain isoflavones which are supposed to have anti carcinogenic property. The protein quality of soybean is also equivalent to animal protein sources such as eggs, meat and poultry as soy protein contains necessary amino acids partial in other plant protein sources.

Soybean protein reduces range of cholesterol in blood plasma in individuals with high cholesterol range, decreasing the risk of cardiac diseases. As well as it acts to decrease the risk of breast and prostate cancers and increasing bone density, due to the occurrence of isoflavones and another phytochemicals [4].

Fenugreek is a yearly plant belongs to the family Leguminosae. It is a well-known spice amongst food. The seeds and leaves of fenugreek are utilized in food and additionally in medicinal application that is the old routine with regards to mankind's history.

It has been used to increase the flavoring and colour, and also modifies the texture of food materials. Seeds of fenugreek spice have medicinal properties such as hypocholesterolemic, lactation aid, antibacterial, gastric stimulant, foranorexia, antidiabetic agent, hepatoprotective effect and anti carcinogenic. It is famous for its fiber, other chemical compounds and volatile contents. 25% of dietary fiber present in fenugreek changes the texture of food [5].

In fenugreek seeds contain 45.4% dietary fiber (13.3% solvent and 32% insoluble) and the gum is made out of galactose and mannose. The last compounds are connected with decreased glycemic impact. The hypoglycemic impact of fenugreek has been particularly archived in people and creatures with sort 1 and type 2 diabetes mellitus [6].



It was discovered that all parts of the fenugreek plant indicated antifungal potential and the greatness of impact changes with plant parts and types of mold. It could be proposed that fenugreek is an imperative wellspring of organically dynamic mixes helpful for growing better and novel antifungal medications [7].

The viability of concentrates extract from fenugreek against *Helicobacter pylori* has been accounted by some studies [8-10]. In a study, honey tests with most astounding antibacterial movement against *Staphylococcus aureus*, *Pseudomonas aeruginosa* and *Escherichia coli* demonstrate greatest pollens from fenugreek than different plants [11].

METHODOLOGY

Raw Material : Raw materials such as fenugreek seeds, rice flour and defatted soya flour where purchased from the local market of Kolhapur, Maharashtra.

Physical Characteristics : The following physical characteristics of fenugreek seeds were analyzed.

Length, Width and Thickness : The length, width and thickness of fenugreek seeds are measured by a vernier calliper with an accuracy of 0.01 mm.

Thousand Kernel Weight : To calculate the mass of seed, 1000 seed weight were calculated by an electronic balance to an accuracy of 0.001 g.

Bulk Density : Bulk density was calculated by the ratio of the mass of seed to its total volume.

Proximate Analysis : Fenugreek seeds, rice flour and soy flour were analyzed for their proximate analysis such as moisture, crude fat, ash, crude fiber and crude protein, etc. contents following standard methods.

Preparation of Fenugreek Seed Powder : Fenugreek seeds were first cleaned and then soaked in normal water for 12 h at room temperature. The seed to water ratio of 1:5 (W/V) was used. After soaking seeds are germinated then dried at 55°C for 10 h. The dried seeds were grind to obtain fine powder and stored in air tight containers for further use. The process involved is explained in **Figure 1**.

Preparation of Soya Sticks : The soya sticks were prepared by the following method as shown in **Figure 2**.

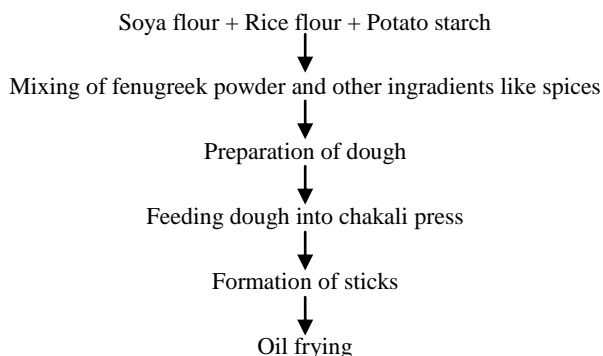
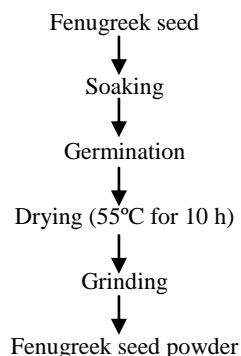


Figure 1 Flow chart of fenugreek seed powder from fenugreek seed

Figure 2 Flow chart of Preparation of soya sticks

RESULT AND DISCUSSION

Physical Characteristics of Fenugreek Seed : The physical characteristics of fenugreek seed is presented in **Table 1**. The seeds have length ranging from 3.42 mm to 5.13 mm. The normal length of fenugreek seeds was 4.35 mm. The seeds have width range from 2.64 mm to 3.79 mm. The common width of fenugreek seeds was 3.14 mm. The seeds have thickness ranging from 1.77 mm to 2.34 mm. The average thickness of fenugreek seeds was 1.93 mm. The kernel weight of thousand fenugreek seeds was ranging from 18.86 g to 19.78 g. The average weight of thousand seeds was 19.28 g. The bulk density of fenugreek seeds ranged from 0.76 gm/ml to 0.93 gm/ml. The average bulk density of seeds was 0.86 g/ml.

Chemical Analysis of Raw Fenugreek Seeds : The chemical analysis of raw fenugreek seeds is presented in **Table 2**.

Proximate Composition of Rice Flour and Soya Flour : **Table 3** shows the proximate composition of rice flour and soya flour. It shows that, soya flour has more protein, fat and mineral contains than rice flour. Rice flour contains more crude fiber than soya flour.



Soaking of Fenugreek Seed : Fenugreek seeds were first cleaned and then soaked in water at room temperature. The seed to water proportion of 1:5 (W/V) was utilized.

Table 1 Physical characteristics of fenugreek seed

Parameter	Observations
Length, mm	4.35±0.58
Width, mm	3.14±0.37
Thickness, mm	1.93±0.18
Thousand kernel weight, g	19.28±0.25
Bulk density, g/ml	0.86±0.30

Data are expressed as mean \pm standard deviation of ten experiments.

Table 2 Chemical composition of raw fenugreek seed

Parameter	fenugreek seed
Moisture, %	4.58±0.21
Ash, %	3.84±0.32
Protein, %	23.56±0.39
Fat, %	6.63±1.0
Crude fiber, %	7.30±0.74
Vitamin C, mg/100 gm	36.46±0.77
Iron, mg/100 gm	10.89±0.24
Calcium, mg/100 gm	71.58±0.47

Data are expressed as mean \pm standard deviation of triplicate experiments.

Water Uptake of Fenugreek Seeds : **Figure 3** illustrates the water uptake of fenugreek seeds. The maximum water was absorbed by seeds during 24 h. After 24 h the rate of water absorption by seeds reduced. The water uptake by seeds after 24 h and after 48 h was almost equal. Therefore, the seeds soaked for 12 h and 24 h were taken for further analysis.

Table 3 Proximate composition of rice flour and soya flour

Parameter	Rice flour	Soya flour
Moisture, %	13.51±0.57	10.18±0.43
Ash, %	1.12±0.14	3.23±0.29
Protein, %	7.3±0.30	37.58±0.20
Fat, %	2.34±0.40	12.51±0.35
Crude fiber, %	3.78±0.20	31.52±0.47

Data are expressed as mean \pm standard deviation of triplicate experiments.

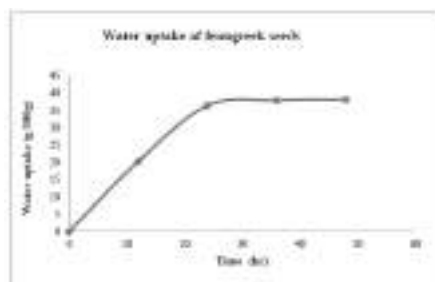


Figure 3 Graphical representation of water uptake of fenugreek seed

Sprouting of Fenugreek Seed : After soaking for 24 h and 48 h, the soaked seeds were washed with water and germinated in sprout maker at room temperature with frequent watering. The seeds soaked for 24 h before germination shows rapid growth of sprouts. It was observed that during germination, seeds soaked for 24 h showed generation of foliage leaves at 72 h. Hence, nutrient content of such sprouts is decreased and as a result these groups of sprouted seeds were not further considered for study. Therefore, seeds soaked for 12 h were preferred for further evolution.

Proximate Analysis of Germinated Fenugreek Seeds (12 h soaking) : **Table 4** shows the proximate analysis of germinated fenugreek seeds after germination. The protein content increased during germination but it slightly reduced after 48hr of germination. The best improvement in protein was observed during 48hr germination period. The fat content gets reduced during germination process. The crude fiber increased during germination. The total mineral content also shows slight changes during germination. On the basis of organoleptic characteristics and proximate analysis of germinated seeds during different time period, the seeds germinated for 24 h were selected for incorporation in the soya sticks.

Preparation of Soya Sticks : Soya sticks were prepared by using chakli press. To prepare soya sticks, all raw ingredients are mixed together to form dough. After formation of dough, it was passed through the chakli press to make sticks. Sticks are then fried in oil as well as baked using oven. The fenugreek seeds powder was incorporated in soya sticks at different concentrations. Fenugreek seed powder was incorporated in soya sticks at 1%, 2%, 3% and 4% concentrations. The concentrations of fenugreek seed powder was kept same for oil fried as well as oven baked soya sticks. On the basis of sensorial analysis from all samples, sample contains 2% fenugreek seed powder was most acceptable. The sensory evolution was carried out using 9 point hedonic scale from semi-trained panel members.



Proximate Analysis of Soya Sticks : **Table 5** shows the proximate analysis of oil fried and oven baked soya sticks. There is no major difference in moisture, crude fiber and mineral content of both oil fried and oven baked soya sticks. The protein content was slightly higher in the oil fried soya sticks. The major difference was the fat content. Oven bake soya sticks contain very less amount of fat as compared to the oil fried soya sticks.

Table 4 Proximate analysis of germinated fenugreek seeds

Parameter	Germination for 24 h	Germination for 48 h	Germination for 72 h
Moisture, %	3.8±0.15	4.78±0.18	4.81±0.08
Protein, %	20.15±0.25	28.22±0.20	25.60±0.20
Fat, %	6.03±0.21	5.90±0.25	5.94±0.26
Crude fiber, %	7.43±0.55	8.16±0.22	10.12±0.30
Ash, %	3.15±0.35	2.96±0.25	2.57±0.45
Carbohydrates, %	62.87±0.21	58.14±0.20	59.56±0.12

Data are expressed as mean ± standard deviation of triplicate experiments.

CONCLUSIONS

The present study shows that, soaking and germination process helps to reduce the bitterness of fenugreek seed as well as increases the nutritive value. The fenugreek seeds germinated for 48 hrs having good nutritive value. On the basis of sensory evolution, soya sticks containing 2% fenugreek seed powder had higher preference. Soya sticks fortified with fenugreek seeds powder, could be a good source of various nutrients like protein, fat, crude fiber, minerals (esp. iron and calcium) which could address many physiological deficiencies like anemia, osteoporosis, obesity ect.

REFERENCES

1. T. A. Nicklas, S. J. Yang, T. Baranowski, I. Zakeri, G. Berenson, Eating patterns and obesity in children: The Bogalusa Heart Study. American journal of preventive medicine, Volume 25, Number 1, pp 9-16, 2003. [https://doi.org/10.1016/S0749-3797\(03\)00098-9](https://doi.org/10.1016/S0749-3797(03)00098-9)
2. R. C. Huang, J. Peng, F. J. Lu, W. B. Lui, J. Lin. The study of optimum operating conditions of extruded snack food with tomato powder. Journal of food process engineering, Volume 29, Number 1, pp 1-21, 2006.
3. M. Omwamba, S. M. Mahungu. Development of a protein-rich ready-to-eat extruded snack from a composite blend of rice, sorghum and soybean flour. Food and Nutrition Sciences, Volume 5, Number 14, pp 1309, 2014. <http://dx.doi.org/10.4236/fns.2014.514142>
4. P. F. P. D. Costa, M. B. M. Ferraz, V. Ros-Polski, E. Quast, F. P. Collares Queiroz, C. J. Steel. Functional extruded snacks with lycopene and soy protein. Food Science and Technology (Campinas), Volume 30, Number 1, pp 143-151, 2010. <http://dx.doi.org/10.1590/S0101-20612010005000017>
5. K. Srinivasan, Fenugreek (Trigonella foenum-graecum): A review of health beneficial physiological effects. Food reviews international, Volume 22, Number 2, pp 203-224, 2006. <http://dx.doi.org/10.1080/87559120600586315>
6. K. T. Roberts. The potential of fenugreek (Trigonella foenum-graecum) as a functional food and nutraceutical and its effects on glycemia and lipidemia. Journal of medicinal food, Volume 14, Number 12, pp 1485-1489, 2011. <https://doi.org/10.1089/jmf.2011.0002>
7. R. Haouala, S. Hawala, A. El-Ayeb, R. Khanfir, N. Boughanmi, Aqueous and organic extracts of Trigonella foenum-graecum L. inhibit the mycelia growth of fungi. Journal of Environmental Sciences, Volume 20, Number 12, pp 1453-1457, 2008. [https://doi.org/10.1016/S1001-0742\(08\)62548-6](https://doi.org/10.1016/S1001-0742(08)62548-6)
8. R.O'Mahony, H. Al-Khtheeri, D. Weerasekera, N. Fernando, D. Vaira, J. Holton, C. Basset. Bactericidal and anti-adhesive properties of culinary and medicinal plants against Helicobacter pylori. World journal of gastroenterology, Volume 11, Number 47, pp 7499, 2005.
9. R. Randhir, Y. T. Lin, K. Shetty. Phenolics, their antioxidant and antimicrobial activity in dark germinated fenugreek sprouts in response to peptide and phytochemical elicitors. Asia Pacific journal of clinical nutrition, Volume 13, Number 3, 2004.
10. R. Randhir, K. Shetty. Improved α-amylase and Helicobacter pylori inhibition by fenugreek extracts derived via solid-state bioconversion using Rhizopus oligosporus. Asia Pacific journal of clinical nutrition, Volume 16, Number 3, pp 382-392, 2007.
11. N. Mercan, A. Guvensen, A. Celik, H. Katircioglu, Antimicrobial activity and pollen composition of honey samples collected from different provinces in Turkey. Natural Product Research, Volume 21, Number 3, pp 187-195, 2007. <http://dx.doi.org/10.1080/14786410600906277>

Table 5 Proximate composition of soya sticks

Parameter	Oil frying	Oven baking
Moisture, %	5.20±0.40	5.60±0.39
Ash, %	4.38±0.26	4.07±0.22
Protein, %	18.21±0.23	14.38±0.11
Fat, %	21.65±0.12	2.56±0.25
Crude fiber, %	2.16±0.11	1.90±0.22
Carbohydrates, %	50.56±0.12	73.39±0.13
Iron, mg/100 g	4.70±0.58	2.60±0.42
Calcium, mg/100g	136.48±0.74	138.80±0.48

Data are expressed as mean ± standard deviation of triplicate experiments



Design and Development of a Trapping System for Tritium (^3H)

Aaditya Shah¹, Chetan Kothalkar^{*1}, S. Chemte¹, K. M. Mathew¹, D. Kalgutkar, N. Jayachandran¹, A.C. Dey¹, Amit Chindarkar², D. K. Sawant²

Technology Development Group and Labelled Compound Laboratory, Board of Radiation and Isotope Technology (BRIT),
Department of Atomic Energy, Sector-20, Vashi, Navi Mumbai¹, chetan@britatom.gov.in*

H.P. Unit, RSSD, BARC, Mumbai²

ABSTRACT

BRIT, produce and supply Tritium Filled Light Sources (TFLS). These sources are used in various industrial applications including defense sector. Production system for TFLS comprise of the components such as glass manifold unit. Under ALARA principle, to reduce discharge of Tritium gas in atmosphere during the TFLS production cycle a Tritium Trapping System was conceptualized. The Tritium Trapping System is a He-leak tested system consisting of a Tritium Trapping Vessel, Getter Cartridge Assembly with in-built heater and thermocouple, metal bellows re-circulation pump, plastic scintillator-based Tritium monitor and a vacuum bourdon gauge. The system uses SS316 tubing and manually operated SS316 bellows sealed valves for flow control. The leftover Tritium gas in the TFLS production facility is flushed using Argon into the previously evacuated Tritium Trapping Vessel. The Tritium-Argon gaseous mixture is further forced through a Getter Cartridge using the metal bellows re-circulation pump. The plastic scintillator-based Tritium monitor is used to record the level of Tritium activity present in the Tritium-Argon gaseous mixture. The tritium concentration in the Tritium-Argon mixture was found to have been reduced by up to 90% within 20 min of running the system.

KEYWORDS Tritium, Getter, Bellows sealed valve, Tritium monitor, Tritium trapping

INTRODUCTION

Production unit of Tritium Filled Light Sources (TFLS) at BRIT mainly consist of a Uranium Tritide bed and glass vacuum manifold units to fill Tritium gas into the phosphor coated glass gadgets. Tritium gas is released into the previously evacuated glass manifold units on heating the Uranium Tritide bed.

When the production cycle is completed and the excess tritium gas is absorbed back on to the Uranium bed, still traces of Tritium gas remains in the glass vacuum manifold units. This residual Tritium gas makes it's way into the environment through the lab ducts and stack when the glass manifold unit is evacuated before the next production cycle. This release into atmosphere is regulated by the regulators Atomic Energy Regulatory Board (AERB). Based on the suggestions from the regulating authority, a Tritium Trapping System (TTS) was designed and fabricated to positively and quantitatively trap this residual Tritium gas using Fe-V-Zr Getters.

The Fe-V-Zr Getter (74, 24, 2) are metallic getters that preferentially trap hydrogen and it's isotopes at temperatures range of 150 to 250°C. These getters experience loss of active hydrogen adsorption sites in presence of oxygen (O_2) or moisture (H_2O) and therefore are to be used in an inert atmosphere devoid of both oxygen (O_2) or moisture (H_2O) for hydrogen (**Figure 1**) trapping applications. Tritium trapping system is explained in brief in subsequent sections of this paper.

COMPONENTS OF TRITIUM TRAPPING SYSTEM (TTS)

The Tritium Trapping System for trapping of residual Tritium consists of the following major components (**Figure 2**):

- (i) An hermetically sealed Stainless Steel Vessel (Capacity : 3L)
- (ii) Metal bellows re-circulation pump.
- (iii) A plastic scintillator-based Tritium monitor.
- (iv) Two getter cartridge assemblies with getter housing and in-built heater.
- (v) A getter housing containing 21 Nos of Fe-V-Zr getters stacked in 03 layers.
- (vi) SS316 bellows sealed valves for flow control.

The system is constructed using AISI 316 tubing and is He-leak tested.

Design of the TTS is shown in **Figure 1** and actual TTS installed at Labelled Compounds Laboratory (LCL), BRIT. Developed TTS was first subjected to its leak tightness test and subsequently on commissioning of the same, clearance for handling tracer level H-3 activity was obtained from the local safety committee and AERB.

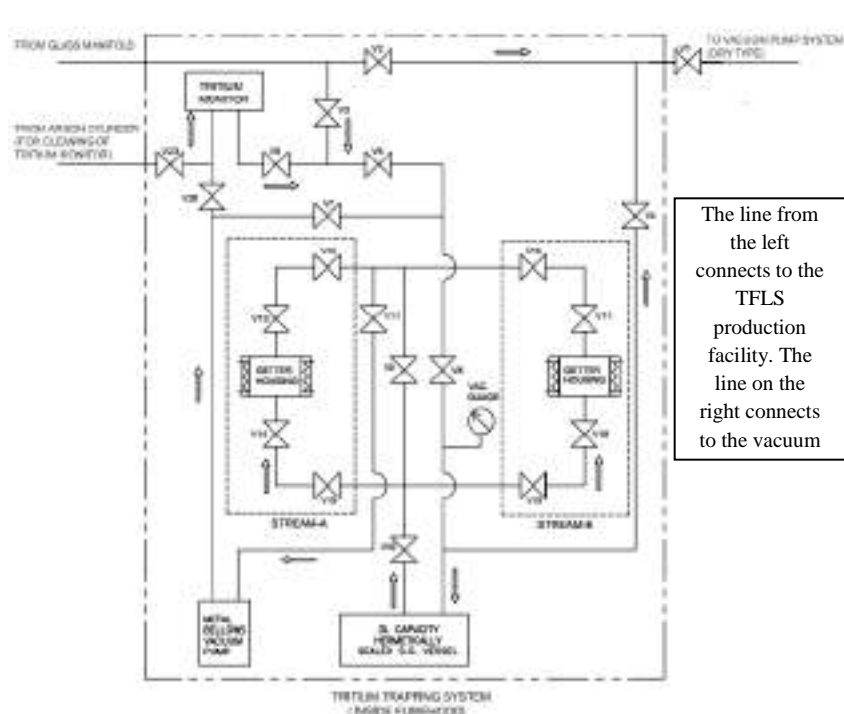


Figure 1 Design drawing of the Tritium Trapping System



Figure 2 The Tritium Trapping System (TTS) installed at Tritium Filled Light Source (TFLS) production unit at Labelled Compounds Laboratory (LCL), BRIT

OPERATING PROCEDURE

The Tritium Trapping System is evacuated to 10^{-6} mbar using a vacuum pump system. The heater of the getter Cartridge assembly is also switched on to maintain a Getter temperature of 200°C .

During production of TFLS the glass manifold is kept isolated from the TTS using a series of valves. After completion of production, glass vacuum manifold unit and the 3L capacity SS vessel is brought inline. Residual tritium gas in the glass manifold is flushed in to the 3L capacity SS vessel by purging with Argon gas. As the pressure inside the 3L SS Vessel reaches 1 bar, it is again isolated from the glass vacuum manifold for the rest of the operations.

At this point all the other valves of the TTS are closed and are sequentially opened to allow the Tritium-Argon gaseous mixture to flow through Getter Cartridge Assembly (pre-heated to 200°C) At this point all the other valves of the TTS are closed and are sequentially opened to allow the Tritium-Argon gas mixture to flow through Getter Cartridge Assembly (pre-heated to 200°C) from the bottom. The Metal bellows re-circulation pump is switched on to enable continuous flow of the Tritium-Argon gas mixture through the Getters.

The magnitude of decrease of Tritium content is measured by taking periodic (every 10 min) samples. This is done by switching on the internal pump of the plastic scintillator-based Tritium Monitor and closing a bypass valve to direct the complete flow of the Tritium-Argon gaseous mixture through the Tritium Monitor and this is maintained till a steady reading is obtained at the display of the Tritium Monitor.

When the Tritium content of the gaseous mixture is reduced to acceptable limits, the Getter Cartridge Assembly is isolated from the rest of the TTS and circulation is stopped. TTS is again evacuated using vacuum pump system in preparation for the next production cycle.



TEST RUN

Primary test run was conducted using 400 mCi of Tritium gas for functional testing of the Tritium Trapping System. The plastic scintillation based Tritium monitor of the system provided Tritium activity in DAC values. Cold finger samples were collected from various spots inside the lab housing the TFS Production setup and the Tritium Trapping System both before and after the test run. The cold finger samples were analyzed in the Hidex 300SL Liquid scintillation counter for Tritium activity. The Tritium activity was recorded in DAC values.

The stack air was also monitored for tritium activity release during the entire experiment and was compared with the activity release data for before and after the trial run.

OBSERVATIONS

Initial DAC value of Tritium Argon gas mixture was indicated by the Tritium monitor. After continuous circulation for 30 min with sampling being done every 10 min, a decreasing trend in the DAC values is observed. The DAC values settle around 1% of the initial values at the end of 30 minutes after which the cycle is concluded and the residual gaseous mixture was pumped out through the stack.

Analysis of the cold finger samples collected from various spots inside the lab housing the TFS Production setup and the Tritium Trapping System show steady DAC values before and during the test run. This indicates the system in use is sufficiently leak proof. The Tritium activity release from the stack during the test run was found to be within the acceptable safe range of Tritium activity release and was similar to the Tritium activity release before and after the test run. This indicates significant trapping of Tritium in the Getter Cartridges of the Tritium Trapping System.

CONCLUSION

Reduction of DAC values of Tritium Argon gas mixture after circulation through the Tritium Trapping System indicates successful trapping of Tritium into the Getter Cartridges. The DAC values derived from the cold finger samples in the laboratory confirm the safe and leak proof nature of the system. Further, the stack release records also confirm Tritium Trapping System minimizes the Tritium activity release along the lines of ALARA concept. Thus, technology for trapping of the H-3 has been developed. This unit is satisfying the requirement of the regulators to minimize H-3 from releasing into atmosphere during TFLS production.

ACKNOWLEDGMENT

Authors are expressing their sincere gratitude for the contributions of LCL & RPL workshop staff particularly Mr. Gundekar, Mr. Chaudhari, Mr Rohit Kamble. Without encouragement from Mr. G. Ganesh, Chief executive, BRIT and guidance from Mr. S.S. Sachdev, Sr. Gen. Manager, RPh, BRIT this set-up to enhance safety of radiation workers was not possible. Thanks to all those who have contributed directly/indirectly towards development of this system.

REFERENCES

1. AERB, Radiological Safety In The Design And Manufacture Of Consumer Products Containing Radioactive Substances, Mumbai, India. AERB-SS-4, 1991.
2. Battelle Memorial Institute, Assessment of End of Life Disposal, Tritium Recovery and Purification Strategies for Radioluminescent Lights, Washington, U.S.A.PNL-7857.
3. IAEA Tecdoc, Safe Handling of Tritium: Review of Data and Experience, Vienna, Austria. ISBN 92-0-125391-5, 1991.
4. U.S. Dept. of Energy (2008), Tritium Handling and Safe Storage, Washington, U.S.A. DOE-HDBK-1129-2008.
5. Canadian Nuclear Safety Commission, H-3 Radiation Safety Data Sheet.



Technological Advancements in Processing of I-131 Radio-isotope at Radio-Pharmaceuticals Laboratory

Rohit Kamble¹, Chetan Kothalkar^{*1}, A.S Gundekar¹, Pradip Bagde¹, S.B Panchal¹, Nitin Jadhav¹, Niteesh Kumar¹, Tukuna Muni¹, Ravi Seshan¹, A.C. Dey¹, D.K. Sawant²

Technology Development Group and RPh Group, Board of Radiation and Isotope Technology (BRIT), Department of Atomic Energy, Sector-20, Vashi, Navi Mumbai¹, chetan@britatom.gov.in^{*}

H.P. Unit, RSSD, BARC, Mumbai²

ABSTRACT

BRIT processes shortlived radioisotope ¹³¹I and ⁹⁹Mo for batch production of various radiopharmaceutical products to be supplied to hospitals and nuclear medicine (NM) centers all over the country. Of the two major isotopes, current demand of I-131 is ~50 Ci per week which is supplied to the hospital/NM centers in various forms such as (i) NaI solution, (ii) capsule (therapeutic and diagnostic application) and (iii) labelled compound (I-131 mIBG injection). Over the decade, market of the product based on I-131 has increased while the processing plants/hot cells are 30-years old. With existing technology, radiation dose received by the radiation worker involved in production of radio-pharmaceuticals is high. Accordingly, to implement Atomic energy Regulatory Board's (AERB) ALARA principle, efforts were made using engineering to develop simple and easy to operate gadgets/devises to improve the radiation safety. Engineering developments, specifically for handling the radioisotope inside as well as outside the lead shielded plant, were taken up for dose reduction while maintaining smooth production of radiopharmaceutical consignments. Efforts resulted in design and development of the following gadgets: (i) trolley mounted device for unlocking the hook toggle clamp of the lead pot LP-30 used for transportation of I-131 sodium iodide solution, (ii) Remotely operated set-up for dose calibrator carrier for activity measurement of I-131 consignment vials, (iii) Remotely operated suspended type vial sealing and unsealing devices. Gadgets were developed, deployed in the lead shielded facilities handling I-131 radio-isotope and have been deployed successfully in other facilities with similar purpose. Using the above-mentioned user-friendly gadgets, even though there is an increase in I-131 activity handing, manRem expenditure for the operator has reduced drastically.

KEYWORDS Radiopharmaceuticals, Gadget, Radiation dose, Lead shielded facility.

INTRODUCTION

In the Radiopharmaceutical (RPh) laboratory, Radioactive I-131 is processed the form of NaI solution and stored during transportation in a sealed glass vial. I-131 decay by emitting Beta and Gamma radiation and therefore is used for both therapeutic as well diagnostic application in nuclear medicine fraternity. I-131 is supplied to the hospitals/NM centers in various forms such as (i) NaI solution, (ii) capsule (therapeutic and diagnostic application) and (iii) labelled compound (I-131 mIBG injection). With three major I-131 products produced, the number of consignments to be handled at RPh lab is also more and so the dose received by the operators. I-131 is handled in physical radiation protection in the form of lead (Pb) shielding during processing inside the hot cell and in lead pots during transportation to reduce the dose receivable by the radiation worker involved in operation. Over the decade, market of the product based on I-131 has increased while the processing plants are 30-years old. With existing technology, radiation dose received by the radiation worker involved in production of radio-pharmaceuticals is also high. Accordingly, to implement Atomic Energy Regulatory Board's (AERB) ALARA principle, efforts were made using engineering to develop simple and easy to operate gadgets/devises to improve the radiation safety. Engineering developments, specifically for handling the radioisotope inside as well as outside the lead shielded plant, were taken up for dose reduction while maintaining smooth production of radiopharmaceutical consignments. Efforts resulted in design and development of the following gadgets:



- (i) trolley mounted device for unlocking the hook toggle clamp of the lead pot LP-30 used for transportation of I-131 sodium iodide solution,
- (ii) Remotely operated set-up for dose calibrator carrier for activity measurement of I-131 consignment vials, and
- (iii) Remotely operated suspended type vial sealing and unsealing devices.

Gadgets were developed, deployed in the lead shielded facilities handling I-131 radio-isotope. Using the above mentioned user-friendly gadgets, even though there is an increase in I-131 activity handling, manRem expenditure for the operator has reduced drastically. Following sections of the paper discuss in brief about the developed gadgets.

Trolley Mounted Device for Unlocking the Hook Toggle Clamp of the Lead Pot LP-30 used for Transportation of I-131 Sodium Iodide Solution

Refer **Figure 1**, this indigenously developed unit is a marvelous example of a dedicated production team who thrive to solve their own problem by getting involved in development process with the designers. Developed system is used for un-clamping lead lid of the lead pot which carries the sealed vial containing I-131 solution. Before development of this unit, the production staff was following the practice of manually unclamping the lid and thus due to proximity with the lead pot carrying the consignment vial was subjected to avoidable dose due to gamma radiation. Operation of unclamping was thus targeted with the objective to be performed from a safe distance (to reduce the dose) for development of a manually operated gadget or system. Developed system is made from SS structural members and uses 02 un-clamping rods of size: Ø12 mm with special attachment to get engaged with the clamps of the Lead pot and unlocking the lead pot clamps using rotary motion. The design allowed the operator to unlock the lid of the lead-pot LP-30 from a distance of 650mm thus reducing the dose due to distance shielding. This unit is also used for manual transferring of lead pot LP-30 to remotely operated dose calibrator set up installed outside the production box for activity measurement of I-131 consignments, thus making it versatile. This unit is now used in performing operation at other facilities as well.

Remotely Operated Set-up for Dose Calibrator Carrier to Measure Activity of I-131 Consignment Vials

Refer **Figure 2** for the remotely operated set-up for dose calibrator carrier to measure activity of I-131 consignment vials. This device allows remote operation (from behind the lead shielding) of movement of the carrier of the dose calibrator during activity measurement. Before development of this unit, radiation workers involved in dose measurement operation used to perform the task without lead shielding and using a long length special tong for transfer of the consignment vial containing I-131 from the trolley carrying the vial to the dose calibrator, thus getting exposed to the avoidable radiation dose. Developed system has a overall size of 570 mm (length) × 1750 mm (height) × 500 mm (width). The structural frame is built using 50 mm × 50 mm × 3 mm thick MS equal angles. The unit is fixed with pneumatic actuator of 300 mm stroke and the shielded with 2" thick lead bricks on front side. There is 145 mm × 145 mm × 50.8 mm lead glass or radiation shielding window installed in the viewing port and tong port with tong length 580 mm with jaws. The dose calibrator is installed on this structure and encased with 2" thick cylindrical lead blocks at the height of 420 mm. This unit requires 6 bar pressure to operate the actuator. The actuator cylinder is clamped with the acrylic holder of the dose calibrator for up and down movement of the vial while measuring the activity of the 131-radioactive consignments. The display monitor is fixed on the set up to view the dose measurement values during the operation.

Remotely Operated Suspended Type Vial Sealing and Unsealing Devices

Before development of this gadget, sealing and unsealing of vials carrying I-131 was carried out using manually operated crimper and de-crimper respectively. This operation was possible only at transfer port of the production box. This manual operation exposed to high dose to the operator from the vial filled with I-131 solution. In process of development for remote operation, some remotely operated gadgets which were mounted on the tong manipulator were developed. However tong mounted gadgets found to have engaged a useful tong manipulator which otherwise



could have been used for material movement. Thus prompting the designer to think about using free roof space of the containment box of the hot cell. Thus Remotely operated suspended type vial sealing and unsealing devices were developed which use pneumatic actuator to power the vial sealing or unsealing adapter and the main set-up suspended to the roof of the hot cell using a spring balancer. Now, using manually operated tong manipulator, the sealing and unsealing device can be taken close to the vial and vial can be easily capped / decapped. Refer picture in **Figure 3**.

RESULTS AND DISCUSSIONS

The technological developments carried out in Radiopharmaceutical Laboratory, BRIT has significantly reduced the cumulative dose to the operator. Record of the **Cumulative annual group dose (mSv) received by the radiation workers involved** shows that even though there is an increase in quantity of I-131 handled, dose received by radiation workers in the group has reduced over a period of time. Refer **Table 1** and graph in **Figure 4**. Development of simple and easy to operate gadgets/devise to improve the radiation safety proved useful and therefore are used by other production groups to derive the benefit of reducing the dose due to radiation.



Figure 1 Device for unlocking the hook toggle clamp of the lead pot LP-30 used for transportation of I-131 sodium iodide solution



Figure 2 Remotely operated set-up for dose calibrator carrier for activity measurement of I-131 consignment vials



Sealed vial unsealing device Vial sealing device

Figure 3 Remotely operated suspended type vial sealing and unsealing devices



Table 1 Activity of ^{131}I handled and the Cumulative annual group dose (mSv) received by the radiation workers involved.

Calendar year	I-131 activity handled in Ci	Cumulative annual group dose (mSv)
2013	1395	41
2014	1675	50.65
2015	1750	38.6
2016	1750	26.7
2017	1850	14.5

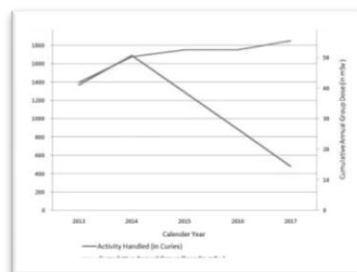


Figure 4 Graph showing I-131 activity handled from the year 2013-17 and cumulative annual group dose (mSv) received the operators

ACKNOWLEDGMENT

Author thankfully acknowledge valuable contribution of RPL Workshop for the fabrication of entire facility, I-131 production team for valuable contribution, inputs and support. Special thanks due to Chief Executive, BRIT for encouragement.

REFERENCES

1. Chetan Kothalkar, A.C. Dey, Developing a remotely operated cap unscrewing machine for screwed cap type vial carrying radioactive liquid for safety and lesslabour dependence, International Conference on Computer Aided Engineering (CAE 2007), IIT Madras, Chennai, pp. 359-365, 2007.
2. Chetan Kothalkar, Design and development of simple gripping cum lifting gadgets for transfer of radioactivity containing vials into processing station, NAARRI annual conference, Mumbai, pp. 16, April 2004.
3. Chetan Kothalkar, Ergonomic considerations in design of gadgets for handling radioactive material (RAM) in the Radiopharmaceutical laboratory (RPL)", EIP2009, AMU, Aligarh, pp. 183-190, November 2009.
4. Chetan Kothalkar, A.C. Dey, A Gadget For Safe Transfer of the Radioactive Liquid (Sodium Molybdate Solution) From A Sealed Vial to a Storage Vessel in the Processing Station, Proceedings of 27th National conference of Indian Association For Radiation Protection, Mumbai, pp. 378-380, November 2005.
5. Chetan Kothalkar, A.C. Dey, A reliable technique for transfer of radioactivity filled vial from transport container to the processing station, Proceedings of 27th National conference of Indian Association For Radiation Protection, Mumbai, pp. 381-384, November 2005.



Extraction of Essential Oil of Frankincense (*Boswellia serrata*) using Microwave-Assisted Hydrodistillation

Swati Yadav^{*1}, S. K. Gupta¹

Department of Chemical Engineering, Harcourt Butler Technical University, Kanpur, Uttar Pradesh, India¹,
swatiyadav887@gmail.com*

ABSTRACT

Frankincense belonging to genus *Boswellia* of Burseraceae family is an aromatic gum resin used in aromatherapy and traditionally all over the world. Frankincense consists of multiple varieties, but this research work is done on the array produced in India called *Boswellia serrata*. *Boswellia serrata* also known as Indian Frankincense, or Olibanum have balsamic and terpenic flavor with woody and spicy fragrance. It appears as colorless pale yellow liquid and has been used for several years to treat health-related conditions in Indian and Chinese medicines. This gum resin has been known for so long for its anti-bacterial, anti-inflammatory, anti-microbial and therapeutic properties. The current work aims to study the effect of the different parameter on yield and composition of volatiles of Frankincense using Microwave-Assisted Hydrodistillation (MAHD). In this procedure, the gum resin of *Boswellia serrata* for raw material was divided into two categories: whole resin (granules) and ground resin (powder, 100 mesh). The microwave was operated at 300 W, 400 W, and 500 W power levels and the setup was made to run for 120 min for 1:2 and 1:4 (g/ml). As per the results, the highest yield (3.4%) was obtained at 500 W (1:2) from whole resin. The chemical composition of the volatiles obtained was analyzed using GC-MS which identified almost 44 chemical compounds. α -Thujene, α -Pinene, Sabinene, α -Phellandrene, Limonene, and Methyl Chavicol were the major components identified in the essential oil. The results concluded that highest yield is obtained at the highest power level from the resin with a small surface area in comparison to that with a large surface area.

KEYWORDS Frankincense, B. Serrata, Olibanum, Volatiles, Extraction.

INTRODUCTION

Frankincense is a resinous extract obtained from the *Boswellia* tree of Burseraceae family popularly known as olibanum, luban, salai guggal, and kundur. The trees of *Boswellia* species are flowering plants having a papery brown, pale bark with a thick brownish inner gummy layer [1]. The oleo-gum resins are obtained by making scrapes in the trunk of *Boswellia* trees which are tropical and deciduous and later, the dried gum resins are collected from the trees [2]. These gum resins then harden slowly into a tear-shaped and amorphous lump with aromatic smell. It has been used as a fumigant by ancient Egyptians in the embalming process and as a traditional agent for treating various inflammatory diseases [3,4].

In Ayurveda, these gum resins of frankincense are used as an anti-arthritic, analgesic and anti-proliferative agent to treat several diseases [5]. These gum resins are burned in daily rituals and spiritual ceremonies to distant evil spirits from ones souls [6,7]. It is also diuretic, diaphoretic, astringent and acts as a stimulant both internally and externally. Traditionally, sesame oil or water-soaked olibanum gum was used as a topical analgesic [8].

The genus *Boswellia* consists of about 25 different species, out of which the most known species are *Boswellia serrata*, *Boswellia papyrifera*, *Boswellia carterii*, *Boswellia frereana*, and *Boswellia sacra* [9]. The Indian Frankincense (*Boswellia serrata*) generally resides in dry and hilly parts of Gujarat, Rajasthan, Andhra Pradesh, Madhya Pradesh, Bihar and Jharkhand [10]. The essential oil of *Boswellia serrata* have spicy, woody and balsamic odour and its chemical composition depend on the changes in climate, harvesting and geographical conditions [11]. The use of olibanum from last few decades has become popular in European countries for the treatment of various inflammatory diseases such as asthma, arthritis, peritumoral brain edema, etc [12].

The boswellic acids which are the active ingredients of Frankincense are responsible for the mechanism of their anti-inflammatory activities. A study reported Frankincense (*Boswellia serrata*) to contain 6-30% gums (mixture of polysaccharides), 60 to 85% resins (mixture of terpenes), and 5 to 9% essential oil (mixture of terpenes). The resin portion is composed of the active functional group-boswellic acid, gum portion is composed of hexose and pentose with few digestive and oxidizing enzymes [13].

There are many extraction techniques to isolate essential oils from plants out of which hydrodistillation (HD) is the most commonly used technique [14]. Standard methods of hydrodistillation (HD) possess several drawbacks such as long duration, high energy consumption and loss of volatiles [15]. Therefore, to reduce the duration of extraction,



increase the yield, decrease the operating cost and upgrade the quality of the essential oil, the researcher pursued microwave-assisted extraction (MAE) [16].

In the current study, microwave-assisted hydrodistillation (MAHD) is chosen and used for extraction of Frankincense oil to withdraw the benefit of microwave heating along with conventional hydrodistillation. However, it is difficult to find the literature for the utilization of the MAHD technique for extracting Frankincense oil and the information available on different power levels and energy consumed in MAHD is limited [17]. Thus, this study aims to compare the effect of extraction parameters on the yield and chemical composition of the essential oil obtained.

MATERIAL AND METHODS

Raw Material

The oleo-gum resins of Indian Frankincense (*Boswellia serrata*) were purchased from local market of Madhya Pradesh, India. The gum resins were separated into two parts, the first part was used as the whole resin (granules) and the second part was used as the ground resin (powder). The ground resin was prepared by grinding the gum resin to a particle size of 100 mesh (0.218 mm) using a mixer grinder.

Extraction of Essential Oil using MAHD

A modified microwave oven with a maximum power output of 800W was used for the microwave-assisted hydrodistillation (MAHD) procedure. The microwave was operated at 300 W, 400 W, and 500 W power levels and the experimental setup was made to run for 120 min at the sample/solvent ratio of 1:2 and 1:4 (g/ml) for both whole and ground resin separately. 100g of both gum resin samples was first placed with 200ml of distilled water and then, with 400 ml of distilled water in a round bottom flask with a capacity of 1000 ml and the setup was made to run for 120 min at 300 W. The microwave was connected with a Clevenger apparatus to collect the extracted essential oil as shown in **Figure 1**. Every experiment was started with an initial temperature of 80°C and atmospheric pressure. Similarly, the experiment was carried out for other portions of the sample at 400 W and 500 W. The essential oil was separated from condensate and to remove traces of water, it was dried over magnesium sulfate and then stored in amber vials at 4°C.

Gas Chromatography-Mass Spectrometry (GC-MS) Analysis

The extracted essential oil was analyzed using Gas Chromatography-Mass Spectrometry (GC-MS) to determine its chemical composition. GC was performed by Nucon 5700 Model, fitted with a fused silica capillary column with a non-polar stationary phase. The condition followed was: injector temperature of 390°C in 10°C steps, an oven temperature of 399°C in 1°C steps. Temperature programming was set by a Microprocessor based programmer with rates from 0.1°C to 29.9°C per min. with initial time holds up to 45 min. 0.10 µL of sample was injected; also an FID detector was used.

MS was performed using Agilent 5977 E Model using a fused silica capillary column with a non-polar stationary phase. 0.05 µL of each sample was injected in a splitting ratio of 1:10 at temperature 250°C; helium was used as a carrier gas. Mass spectra were operated in electron impact mode with ionization energy of 70eV. The compounds of oil were identified by recorded mass spectra in the MS library.

RESULTS AND DISCUSSIONS

Effect of Extraction Time on Yield

Extraction time required to obtain oil was taken 120 min maximum, after which no increment was observed in the yield. As shown in **Figures 2 and 3**, the first droplet was obtained at 10 min. for both whole resin and ground resin. The highest essential oil yield obtained from *Boswellia serrata* was 3.4% at 500 W (1:2) from whole resin. This means whole resin yields more oil in comparison to the ground resin at the highest power level. The yield of essential oil obtained was calculated by:

$$\text{Yield (\%)} = \frac{\text{Quantity of essential oil extracted (g)}}{\text{Quantity of raw material used (g)}} \times 100 \quad (1)$$

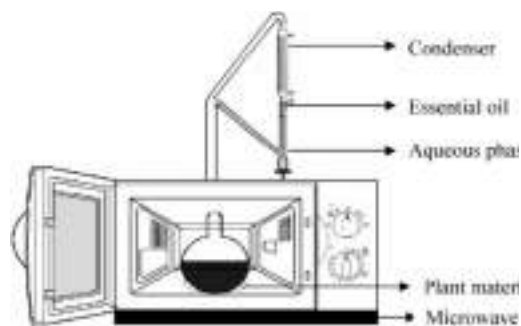


Figure 1 Experimental setup for Microwave-Assisted Hydrodistillation (MAHD)

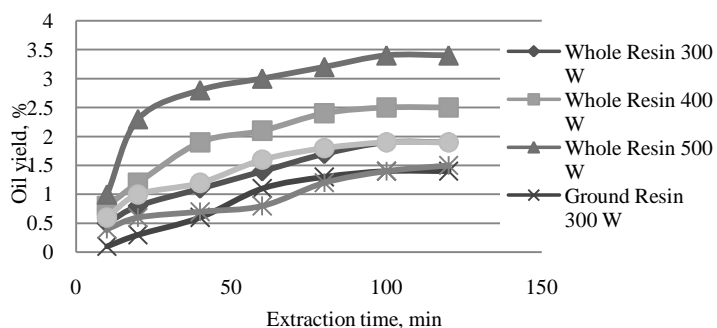


Figure 2 Effect of extraction time on oil yield (MAHD) at 1:2

Chemical Composition Analysis

After the extraction of Frankincense oil, the chemical composition of all essential oil samples was analyzed by GC-MS. The GC-MS analysis identified total 53 compounds in oil obtained by MAHD, out of which 44 compounds were utterly identified as shown in **Table 1**. α -Thujene, α -Pinene, Sabinene, α -Phellandrene, Limonene, and Methyl Chavicol were the main identified components, all reported in Indian olibanum (*Boswellia serrata*) obtained by microwave-assisted hydrodistillation [18].

Comparison of Main Components

Figure 4 shows the comparison of main components present in the essential oil of *Boswellia serrata* obtained by Microwave-Assisted Hydrodistillation.

Among all the major components identified, α -Thujene, which is the principal component of the Frankincense oil, was present in almost all samples in high amount.

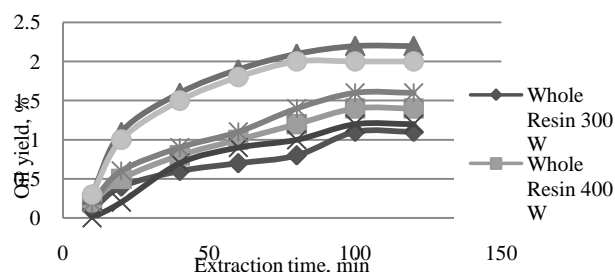


Figure 3 Effect of extraction time on oil yield (MAHD) at 1:4

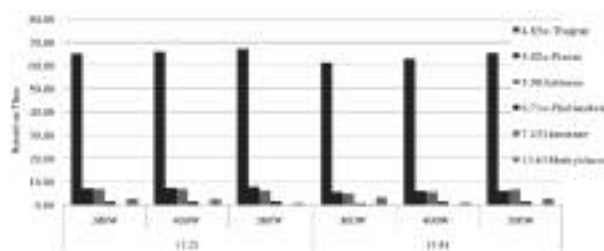


Figure 4 Comparison of main components identified in Frankincense oil by MAHD

Table 1 Chemical composition analysis of extracted essential oil of *Boswellia serrata*

Compound	RT, min	Percentage of composition (MAHD)					
		(1:2)			(1:4)		
		300 W	400 W	500 W	300 W	400 W	500 W
Tricyclene	4.66	0.13	0.12	0.11	0.06	0.10	0.10
α -Thujene	4.85	65.14	65.77	67.17	61.22	62.92	65.32
α -Pinene	5.02	7.07	7.31	7.67	5.77	6.31	6.22
Thuja-2,4(10)diene	5.19	0.48	0.50	0.63	0.81	0.67	0.54
Camphene	5.32	0.15	0.16	0.20	0.09	0.11	0.14
Sabinene	5.90	6.89	6.85	6.34	5.09	5.65	6.76
β -Pinene	5.99	2.96	2.94	2.22	2.46	2.85	2.95
β -Myrcene	6.28	3.66	3.62	3.07	4.73	3.45	3.65
α -Phellandrene	6.71	1.46	1.46	1.64	0.87	1.52	1.46
δ -3-Carene	6.89	0.33	0.32	2.37	0.63	0.53	0.39
α -Terpinene	7.06	1.67	1.61	0.36	2.33	2.15	1.68
m-Cymene	7.21	2.53	2.49	0.2	2.79	2.82	2.52



p-Cymene	7.30	0.36	0.35	0.67	0.52	0.44	0.36
Thujol	7.37	0.04	0.04	0.22	0.04	0.05	0.03
Limonene	7.43	0.22	0.21	0.17	0.26	0.25	0.21
E- β -Ocimene	7.66	0.65	0.63	0.06	1.34	1.10	0.75
Z- β -Ocimene	8.00	0.02	0.02	0.02	0.02	0.02	0.02
γ -Terpinene	8.38	0.22	0.21	0.55	0.46	0.37	0.26
cis-Sabinene hydrate	8.67	0.13	0.13	0.09	0.13	0.08	0.02
α -Terpinolene	9.39	0.18	0.18	0.01	0.16	0.14	0.01
Linalool	9.77	0.06	0.06	0.04	0.28	0.26	0.05
Thujone	10.43	0.02	0.02	0.01	0.02	0.01	0.02
3-Ethoxyaniline	10.55	0.05	0.05	2.08	0.06	0.09	0.06
trans-Sabinol	11.29	0.01	0.01	0.02	0.17	0.01	0.01
cis-Sabinol	12.41	0.05	0.01	0.01	0.01	0.04	0.01
4-Terpineol	12.77	0.52	0.48	0.03	1.65	0.10	0.56
α -Terpineol	13.30	0.05	0.05	0.05	0.10	0.01	0.06
Methylchavicol	13.63	2.65	2.47	1.08	3.17	1.26	2.70
Linalyl Acetate	15.96	0.08	0.07	0.36	0.05	0.08	0.05
α -Copaene	20.90	0.47	0.41	1.08	0.83	2.65	0.52
β -Bourbonene	21.27	0.03	0.02	0.02	0.02	0.03	0.01
allo-Aromadendrene	21.85	0.16	0.13	0.11	0.11	0.13	0.17
Methyleugenol	22.10	0.05	0.04	0.04	0.24	0.71	0.02
β -Ylangene	22.64	0.05	0.04	0.03	0.10	0.07	0.41
β -Cubebene	23.33	0.03	0.02	0.02	0.09	0.22	0.01
γ -Murolene	23.67	0.03	0.03	0.02	0.10	0.09	0.01
α -Cadinene	24.97	0.02	0.02	0.01	0.06	0.07	0.01
Germacrene D	25.13	0.36	0.31	0.01	0.36	0.05	0.03
δ -Cadinene	26.81	0.02	0.02	0.20	0.34	0.31	0.12
5-Methylcyclopent-1-ene-1-carboxylic acid	26.96	0.10	0.08	0.01	0.40	0.23	0.03
β -Santalol	32.56	0.02	0.07	0.06	0.14	0.30	0.05
α -Santalol	34.05	0.07	0.01	0.02	0.02	0.10	0.02
p-Mentha-1,5-diene	36.70	0.02	0.02	0.01	0.02	0.02	0.04
cis-Salvene	48.09	0.03	0.04	0.02	0.07	0.06	0.01

CONCLUSION

The results showed that the whole resin with 200 ml of solvent extracted highest yield (3.4%) of good quality *Boswellia serrata* oil at 500W. It can be concluded that large sized particles with the small surface area will yield more oil operated at the highest power level. In this study, a total of 44 components were identified in Frankincense oil out of which, α -Thujene, α -Pinene, Sabinene, α -Phellandrene, Limonene, and Methyl Chavicol are the main components.

REFERENCES

1. M. Thulin, A.M. Warfa, The frankincense trees (*Boswellia* spp., Burseraceae) of northern Somalia and southern Arabia. Kew Bulletin. Volume 42, Number 3, pp 487–500, 1987.
2. C.A. Michie, E. Cooper, Frankincense and myrrh as remedies in children. J. R. Soc. Med. Volume 84, Number 10, pp 602–605, 1991.
3. MZ Siddiqui, *Boswellia serrata*, a potential anti-inflammatory agent: an overview. Indian J. Pharm. Sci. Volume 73, Number 3, pp 255–261, 2011.
4. S. Afsharypuor, M. Rahmany, Essential oil constituents of two African olibanums available in Isfahan Commercial Market. Iranian J. Pharm. Sci. Volume 1, Number 3, pp 167–170, 2005.
5. M.K. Nusier, H.N. Bataineh, Z.M. Bataineh, H.M. Daradka, Effect of frankincense (*Boswellia thurifera*) on reproductive system in adult male rat. J. Health Sci. Volume 53, Number 4, pp 365–370, 2007.
6. T. Krishnamurthy, M.P. Shiva, Salai guggal (from *Boswellia serrata* Roxb.): Its exploitation and utilization. Indian Forester. Volume 103, Number 7, pp 466–474, 1977.



7. P. Holmes, Frankincense oil: The rainbow bridge. *Int. J. Aromatherapy*. Volume 9, Number 4, pp 156-161, 1999.
8. Z. Du, Z. Liu, Z. Ning, Y. Liu, Z. Song, C. Wang, A. Lu, Prospects of boswellic acids as potential pharmaceuticals. *Planta Medica*. Volume 81, Number 4, pp 259-271, 2015.
9. C.L. Woolley, M.M. Suhail, B.L. Smith, K.E. Boren, L.C. Taylor, M.F. Schreuder, J.K. Chai, H. Casabianca, S. Haq, H.K. Lin, A.A. Al-Shahri, S. Al-Hatmi, D.G. Young, Chemical differentiation of *Boswellia sacra* and *Boswellia carterii* essential oils by gas chromatography and chiral gas chromatography-mass spectrometry. *J. Chromatogr. A*. Volume 1261, pp 158-163, 2012.
10. B.K. Chhetri, N.A. Ali, W.N. Setzer, A survey of chemical compositions and biological activities of Yemeni aromatic medicinal plants. *Medicines*. Volume 2, Number 2, pp 67-92, 2015.
11. S. Hamm, J. Bleton, J. Connan, V. Tchaplal, A chemical investigation by headspace SPME and GC-MS of volatile and semi-volatile terpenes in various olibanum samples. *Phytochemistry*. Volume 66, 12, pp 1499-1514, 2005.
12. H.P. Ammon, Boswellic acids in chronic inflammatory diseases. *Planta Medica*. Volume 72, Number 12, pp 1100-1116.
13. T. Rijkers, W. Ogbazghi, M. Wessel, F. Bongers, The effect of tapping for Frankincense on sexual reproduction in *Boswellia papyrifera*, *J. App. Eco.* Volume 43, Number 6, pp 1188-1195, 2006.
14. E. Stahl-Biskup, F. Saez, R. Hardman, *Thyme: The Genus Thymus*, CRC Press, London, 2002.
15. H.W. Wang, Y.Q. Liu, S.L. Wei, Z.J. Yan, K. Lu, Comparison of Microwave-Assisted and Conventional Hydrodistillation in the Extraction of Essential oils from Mango (*Mangifera indica* L.) Flowers. *Molecules*. Volume 15, Number 11, pp 7715-7723, 2010.
16. B. Kaufmann, P. Christen, Recent extraction techniques for natural products: microwave-assisted extraction and pressurized solvent extraction. *Phytochem. Anal.* Volume 13, Number 2, pp 105-113, 2002.
17. P. Pongmalai, S. Devahastin, N. Chiewchan, S. Soponronnarit, Enhancement of microwave-assisted extraction of bioactive compounds from cabbage outer leaves via the application of ultrasonic pretreatment. *Separation and Purification Technology*. Volume 144, pp 37-45, 2015.
18. A. Dekebo, M. Zewdu, E. Dagne, Volatile oils of frankincense from *Boswellia papyrifera*, *Bulletin of the Chemical Society of Ethiopia*. Volume 13, pp 93-96, 1999.



Pancreatic Cancer Stage Detection using Hybrid Neuro-fuzzy System

T. M. N. Vamsi^{*1}, N. V. Ramana Murty¹

Department of Computer Science and Engineering, School of Engineering, G. V. P. College for Degree and PG Courses, Visakhapatnam, Andhra Pradesh, India¹, bioprativamsi@gmail.com^{*}

ABSTRACT

Cancer in the pancreas is generally caused by uncontrolled growth of cells in the area of pancreas.. If it is malignant and not detected in the early stages, most of the times it may cause death. To detect the pancreatic cancer at an early stage and to increase the mortality, a neural network based fuzzy logic system is developed. This system is a fuzzy based system trained by a back propagation algorithm derived from neural network theory. The heuristic learning methodology is also employed in the design of the fuzzy system. The major purpose of developing this research work is to apply artificial neural network and fuzzy logic techniques on the dataset of pancreatic cancer patients and to find the disease diagnosis. Here a set of symptoms related to this cancer are observed for detection. The actual procedure of pancreatic cancer medical diagnosis suggested by physicians was analysed and it is converted into a format compatible with a machine.

KEYWORDS Artificial neural networks, Neuro-fuzzy hybrid approach, Pancreatic cancer, Fuzzy logic, Heuristic learning

INTRODUCTION

Lung infection is the irregular improvement of cells in one or both lungs, and usually happens in cells that are impeding air exchange. Cells which won't make tough conventional tissues will segment rapidly and as a result of it tumors are structured. If this is detected at an early stage, it can cause the cancer treatment early to help the patient for his survival. The risk of lung cancer for smoking people is significantly more compared to others. Most of the patients of the lung sickness are normally detected at 60 years of age.

Pancreatic cancer normally causes due to malignant type neoplasm originates from transformed cells arising in tissues form the pancreas. The major symptoms of pancreatic cancer may include abdominal pain, weight loss, diarrhea, and jaundice. Treatments include surgery, chemotherapy, and radiation. In this research work these symptoms are used to analyze the cancer detection and diagnosis.

METHODOLOGY

Existing System

Many researchers are working to develop a software system for the identification of pancreatic cancer and its detection and diagnosis. But implementation of such system is still in working stage only.

Proposed Research Work

In the proposed system an attempt is made to develop a neural network and fuzzy logic based approach for pancreatic cancer detection and diagnosis. Here neural networks are used to train the symptoms related to pancreatic cancer. This training process will be continued till an accuracy level is constructed. The design approach used in this research work contains a set of fuzzy values incorporated into neural network which are more precise than the normal Boolean values. The neurons in the output layer are further processed by using activation function to improve the accuracy as compared to existing conventional systems.

The training process using a neural network back propagation algorithm is as shown in the **Figure 1**. According to this algorithm as the number of epochs of training increases the Mean Square Error (MSE) automatically decreases.

This paper is mainly aimed at describing the practical application of artificial intelligence in the health sector. The pancreatic cancer detection and diagnosis using a back propagation algorithm of a multilayer neural network results in a self-learning intelligent system which is capable of handling uncertainties in the process of cancer diagnosis. The result of this research work provides the decision whether a patient with related symptoms is affected with pancreatic cancer or not. The dataset of the patients is collected from their previous medical records and with the help of an expert these symptoms are analyzed. This dataset is applied to a neural network to detect pancreatic cancer. The fuzzy logic approach helps to make the diagnosis more accurate and specific.

RESULTS

A web system is developed for the cancer patients for the detection of pancreatic cancer and the following results are observed. The pancreatic cancer symptoms are applied to the developed web software. Then the step wise result screens are depicted in the **Figures 2 to 6**. Fuzzy techniques are used to implement the stage and risk level of the cancer disease.

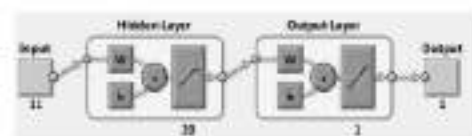


Figure 1 Training phase of the neural network



Figure 2 Pancreatic cancer detection home screen



Figure 3 Registration form



Figure 4 Registered patient login phase and training data set for pancreatic cancer patient



Figure 5 Operations and symptoms entry form



Figure 6 Execution and results evaluation

Fuzzy membership functions are used on the dataset to convert the crisp values of the symptoms (0 or 1) into fuzzified set of symptoms. A linear membership function was applied on each symptom. Here four linguistic variables (low, medium, high and very high) were assigned to each symptom and the classification tests were repeated. The experimental results of implementing the new Hybrid Fuzzy-NN methodology to differentiate between the pancreatic cancer affected and non-affected patients based upon specified symptoms. The efficiency of the neural network system for the cancer detection depends on the effective training patterns corresponding to symptoms of the cancer patients. The observed results are found good and the results optimized by using back propagation algorithm. The accuracy levels are 90% when compared to the results given by the doctor. The Fuzzy system is as shown in Figure 7



Figure 7 FIS editor



CONCLUSION

A neural network based approach for pancreatic cancer diagnosis is able to detect the cancer in 90% of the cases as analyzed by an expert doctor. The automatic diagnosis of pancreatic cancer is very important to decrease the death rate of cancer disease.

REFERENCES

1. V. Prasath, N. Lakshmi, M. Nathiya, N. Bharathan, N. P. Neetha. A Survey on the Applications of Fuzzy Logic in Medical Diagnosis Support Systems Systems Decision, International Journal of Scientific and Engineering Research, ISSN 2229-5518 , Volume 4, Number 4, pp. 1199-1203, 2013.
2. X. Y. Djam, Y. H. Kimbi, A Decision Support System for Tuberculosis Diagnosis,” The Pacific Journal of Science and Technology, Volume 12, Number 2, pp. 410-425, 2011.
3. S. P. Singh, P. Johri, A Review of Estimating Development Time and Efforts of Software Projects by Using Neural Network and Fuzzy Logic in MATLAB, International Journal of Advanced Research in Computer Science and Software Engineering, Volume 2, Number 10, pp. 306-310, 2012.
4. P. D. C. R. Jayarathna, J. V Wijayakulasooriya, S. R. Kodituwakku, Fuzzy Logic and Neural Network Control Systems for Backing up a Truck and a Trailer, Int. J Latest Trends Computing, ISSN: 2045-5364, Number 3, pp. 370-377, 2011.
5. R. Malhotra, N. Singh, Y. Singh, Genetic Algorithms: Concepts, Design for Optimization of Process Controllers, Canadian Center of Science and Education, Volume 4, Number 2, pp. 39-54, 2011.
6. O. Taylan, Computers and Industrial Engineering An adaptive neuro-fuzzy model for prediction of student 's academic performance, Computers and Industrial Engineering, Elsevier, doi:10.1016/j.cie.2009.01.019, Volume 57, pp. 732-741, 2009.
7. K. Adlassnig, Fuzzy Set Theory in Medical Diagnosis,” IEEE Transactions on Systems, Man, and Cybernetics, pp. 260-265, 1986. International Journal of Bio-Science and Bio-Technology Volume 7, Number 6, 2015, 96 Copyright © 2015 SERSC
8. N. Walia, S. K. Tiwari and R. Malhotra, Design and Identification of Tuberculosis using Fuzzy Based Decision Support System, Advances in Computer Science and Information Technology, ISSN: 2393-9915, Volume 2, Number 8, pp. 57-62, 2015.
9. M. A. S. Durai, N. C. S. N. Iyengar, A. Kannan, Enhanced Fuzzy Rule Based Diagnostic Model for Lung Cancer using Priority Values, International Journal of Computer science and information technologies, Volume 2, Number 2, pp. 707-710, 2011.
10. N. Annals, O. F. Natural, Decision Support System fot the Identification of Tuberculosis using Neuro Fuzzy Logic, Nigerian Annals of Natural Sciences, Volume 12, Number 1, pp. 12-20, 2012.
11. T. Uc, A. Karahoca and D. Karahoca, Tuberculosis disease diagnosis by using adaptive neuro fuzzy inference system and rough sets, Neural Comput & Applic, DOI 10.1007/s00521-012-0942-1, pp. 471-483, 2013.
12. K. P. Adlassnig, G. Kolarz, W. Scheithauer, Present State of the Medical Expert System CADIAG-2, 1985
13. Michael Schuerz, Klaus-peter Adlassnig, Charles Lagor, Barbara Scheider, Georg Grabner, Definition of Fuzzy Sets Representing Medical Concepts and Acquisition of Fuzzy Relationships Between Them by Semi-Automatic Procedures
14. J. G. Vaskor, S. M. Dickinson, J. S. Bradley, Effect of sampling on the statistical descriptors of traffic noise, Appl. Acoust., vol.12, pp.111-124, 1979. IJCSNS International Journal of Computer Science and Network Security, Volume 11, Number 4, April 2011.



Enhancing Safety at Construction Sites using Digital Technologies

Krishna Nirmalya Sen^{*1}, A Vinoth¹, Vimal Raj¹

Larsen and Toubro Metallurgical and Material Handling, Kolkata, India¹, knsen@lntecc.com*

ABSTRACT

Ensuring safety of the workmen is a major responsibility of the employing organization. Construction being one of the most hazardous industries, management has more reasons to provide safe systems of work. While improvement in safety culture is a major focus globally, still large number of working population get affected due to work, leading to high incidences of morbidity and mortality. Achieving satisfactory level in safe work environment and work practices still require significant efforts due to multitude of factors which keep on influencing the work-organization. For example, simultaneous management of multiple things and parameters in a transient job poses several big challenges. Because of the complexity and diverse activities mixed with great level of uncertainty, construction presents high level of risk and probable adverse outcomes. Fortunately, in the recent years, technological development has enhanced the capability of enhancing supervisory control and administrative overseeing over the activities, on a continual basis. Fortunately, recent technological advancements have made available various solution to aid the management of complex construction sites. Smartphones and mobile apps have made communication and collaboration on projects simpler. For example, Building Information Modeling (BIM) improves project visualization, efficient scheduling and reduces waste and rework. Today digital drive includes big data, technical innovation and construction come together to facilitate culmination of safer working environment for construction workers.

Some of the applications of digitization in construction industry are mentioned below:

- (i) Tracking the workmen,
- (ii) Location of workmen,
- (iii) Illumination level of the construction site,
- (iv) Health data,
- (v) Training data/training matrix,
- (vi) Access control,
- (vii) Overtime monitoring,
- (viii) Tracking and monitoring the site through the use of drones,
- (ix) Virtual reality, and
- (x) Protective 'Wearables'.

Going forward, utilization of various available and emerging technological solutions, such as wearable products, responsive clothing, GPS enabled safety vests, smart sensors, RFID based monitoring etc. would become part of our workspace. These applications and gadgets can sharpen the management of system, which was not otherwise possible earlier. In this paper an effort has been made to showcase few selected practical applications of these recent technological solutions and highlight their benefits for ensuring safer execution of projects.

KEY WORDS Digital solutions, Gadgets, Monitoring work integration.

INTRODUCTION

Construction industry displays a typical pattern, globally. Various studies have shown in the past, that even in industrialized countries, construction is consistently ranked among the most dangerous occupations. Some of the reasons are common across the globe, as highlighted, such as dynamic nature of the activities, inherent risk associated with the activities, casual nature of employment, migration, exposure to open weather condition etc. Ensuring safety of the workmen is a major responsibility of the employing organization. Achieving satisfactory level in safe work environment and work practices still require significant efforts due to multitude of factors which keep on influencing the work-organization. For example, simultaneous management of multiple things and parameters in a transient job poses several big challenges. Because of the complexity and diverse activities mixed with great level of uncertainty, construction presents high level of risk and probable adverse outcomes. Fortunately, in the recent years, technological development has enhanced the capability of enhancing supervisory control and administrative overseeing over the activities, on a continual basis. Fortunately, recent technological advancements have made available various solution to aid the management of complex construction sites.



APPLICATION OF DIGITAL TECHNOLOGIES IN SAFETY

Building Information Modeling (BIM) is an intelligent 3D model-based process that brings together architecture, engineering, and construction professionals the insight and tools to more effectively and efficiently plan, design, do construction delivery as well as manage buildings and infrastructure. This technology can go a long way to conduct pre-construction risk assessments and safe execution of the job at various work locations. This helps the team to make best use of onsite prefabrication, preassembly and other prevention through design approaches. These methods also help in removing potentially dangerous trips on lifts and ladders during construction, and save thousands of work hours.

VR + AR: Both AR and VR can help in scanning physical buildings with respect to designs. They usually create a virtual image that, for example, workers can use to see where pipes run, or construction professionals can monitor the progress of the work. These 3D scans will then be overlaid against the BIM design, and then the original and current build are compared. Virtual reality (VR) is adding a new dimension to health and safety training. VR creates simulations of real workplaces and hazards thereby give teams the skills to reduce accidents at work locations. Hence this allows users to familiarize themselves with dangerous situations without the risk of being harmed. Augmented Reality (AR) helps in real time collaboration of planners and architects with clients and contractors, for adapting plans and processes at the design stage itself. Data and images from AR can then be overlaid onto physical spaces which allow build information to be shared, leading to reduction of risks. It's especially useful for highlighting hazards in complicated processes. With AR-generated information, line managers can identify and concentrate on pinch points in the construction schedule also.

Smart sensors can be mounted throughout construction sites which can help in detecting and monitoring unseen risks such as temperature, humidity, dust particulates, pressure, noise vibration and the volatile organic compounds that arise from an overload of varnish or paint. The collected data hence obtained is then fed to backend systems that will generate real-time alerts and analysis of longer-term risk level.

Drones which can be fitted with inspection software improves health and safety at work place drastically by highlighting dangers and hazards. Inspection drones have led to an increase in security, monitoring for intruders, theft, vandalism etc.

Wearables GPS-enabled safety vests are example of the wearables, which give some sort of alert to workers when they try to enter a hazardous area, and smart helmets fitted with virtual visors do display job related information, and warn wearers about any adverse changes in the working environment.

Smartphone apps The available smartphone apps in construction sector have wide range. This may include, project management, quality, safety, integrated construction cost, accounting, construction site operations, computer aided design, 2D and 3D designs and drawings, estimating, and building information modelling (BIM) etc. These apps help in increasing productivity and efficiency of job and for managing workflow. These could also be used for health monitoring, monitoring and closure of unsafe practices and initiate corrective measures etc.

Drones are progressively becoming more popular in different professional sectors and construction is, of course, no exception. Drones provide users with an excellent overview of everything that takes place on site. Most importantly, they allow the building team to acquire information from every corner of the working field even in spaces where there is no accessibility.



Project Monitoring

Monitoring a construction project is always one of the biggest challenge for construction managers. This is where drones can be extremely useful. First and foremost, they have the ability to observe the whole site and report back to the office much faster and more efficiently than the on-site personnel. Drones can fly over the whole site, even in corners where there is no access from the ground, very quickly and without putting any worker in danger. Drones can also be

equipped with radar, thermal cameras and laser-based sensors which can substantially improve the surveillance of the site and detect any abnormal activity. Video footage can be used to create a 3D picture of the site that could



subsequently be compared to the computerized architectural design. Contractors can constantly monitor the development of the project and correct any mistake in time.

On-Site Inspection

Aerial videography and photography can prove as powerful ways of monitoring the building site than depending only on the site engineers or supervisors. Drones or UAVs (unmanned aerial vehicles) can easily identify risky situations, problematic materials and hazardous structures which could eventually put construction workers in danger. Being able to detect such troubling situations without engaging people in danger is vital. The use of drones during the inspection process can be cheaper and faster than the current inspection methods, as it allows more frequent inspections and extend a safer construction site. These are particularly helpful for remote inspections. For example inspection of awkward or unapproachable locations of the construction site, eliminating the possibility of exposing workers to high risk. The picture and video footage collected by the inspection process can be used for the precise identification of the building process and for the creation of future safety guides.

Building Maintenance

Drones can be of substantial help during the maintenance process, combining the above two powerful advantages. On one hand, they provide ability to reach in locations and places where it is extremely dangerous for construction workers to go. For instance, the maintenance of skyscrapers or tall building structures, in general, can now be done with the help of UAVs. This applies both to reactive and unplanned maintenance inspections and it eradicates the risk of injury for workers due to falling. On the other hand, the use of drones can accelerate the maintenance inspection process. With the risk of injury to workers minimized, the necessary tasks can be completed faster and in a more automated manner. This could eventually lead to an improved maintenance cycle and to a building structure which would be safer both for its residents and the people who work around it.

Task Completion

Another essential aspect of the construction process where drones can truly help is the completion of repetitive and/or risky building tasks. More analytically, drones can be used for the following tasks on the field: transporting tools, equipment and materials; spray paint; waterproof structural building components; and capture unique image footage that could be used for the promotion of the building. All these tasks take time and a lot of effort to be completed, while some of them can also be quite dangerous for those in charge of them. The use of drones can simplify those to a significant extent and protect the on-site personnel from unpredicted risk.

Extra Security Layer

Drones can be a powerful tool in the hands of the team which is responsible for the safety of the site when the construction work stops. At night, construction sites can be extremely vulnerable to theft of expensive equipment and materials. It is extremely important to monitor the entire location effectively. But it is no secret that in every working site there are some parts where the security level is lower. This is where drones can help significantly as they can provide the security team with information in regard to any unusual movements in real time. Drones can take safety on site to a whole new level. The ability to monitor and maintain the construction site from distance is a big step forward to a safer and more efficient building process.

CONCLUSION

Disruption by digital technologies is the order of the day. Since it has immense capabilities to support and enhance efficacy of traditional activities, we need to embrace it while trying to improve effectiveness and efficiency, leading towards operational excellence. In the present context, application of digital technologies in the domain of safety management is proving to be highly beneficial and helpful. This can be further integrated and adopted across the industry.

REFERENCES

1. W. Zhou, J. Whyte, R. Sacks. Construction safety and digital design: A review. *Automation in Construction*, Volume 22, pp 102-111, 2012.
2. S. Azhar, A. Jackson, A. Sattineni, Construction Apps: a critical review and analysis. In ISARC. Proceedings of the International Symposium on Automation and Robotics in Construction. Vilnius Gediminas Technical University, Department of Construction Economics and Property, Volume 32, p. 1, January 2015.
3. Opportunities and challenges of digitalization for occupational safety and health. available: <https://www.kan.de/en/publications/kanbrief/digitalization-and-industry-40/opportunities-and-challenges-of-digitalization-for-occupational-safety-and-health>



A Knowledge based Approach to Personify Ocean Data in RDF Format by the Exploitation of Semantic Technology

Anitha. V^{*1}, T. Menakadevi¹

Department of Electronics and Communication Engineering, Adhiyamaan College of Engineering, Hosur, India¹,
aniveluece@gmail.com*

ABSTRACT

Semantic web is gaining consequence day by day. One main aim of the semantic web is to make it work like a database. Ontology plays a vital role in semantic web which acts as a solution for finding semantic correspondence. Many government and public administrations recently started to publish the large amount of open data on the web. The provided datasets are available as tabular data such as CSV (Comma Separated Values, *.csv), Excel (*.xls), NetCDF (Network Common Data Format, *.nc) and so on. These heterogeneous formats will not preserve domain semantics. The offered data are semantically quite heterogeneous and leaves many ambiguities open which makes interpreting, integrating and visualizing the data difficult. This initiated a set of researchers to offer a new representation of data, which makes them usable and understandable by web agents. In order to support the utilization of tabular data, it is required to transform the data into a standardised format facilitating the semantic description, linking and integrating such as RDF (Resource Description Framework) format. The RDF description allows the computers to understand the information available in human readable format. The proposed method provides a knowledge based approach by the deployment of semantic technology to represent the ocean data in the standardised RDF format. The data has been collected from the various Research and Development centres where the implementation of proposed method has been reported. This method implies the development of java code in Thredds Data Server (TDS) environment with Linux operating system. In this paper, the authors have transformed and enriched almost 65,000 data sets of about 1 GB of heterogeneous data files in to the reduced RDF file format of about 500 KB in memory storage capacity.

KEYWORDS Semantic Web Technology, Ontology, Heterogeneous files, Resource Description Framework (RDF), Thredds Data Server (TDS).

INTRODUCTION

World Wide Web (WWW) is an information space which provides the user to access and share the information via internet. It consists of three standard representations namely Uniform Resource Locator (URL), Hyper Text Transfer Protocol (HTTP) and Hyper Text Mark-up Language (HTML). The information that is available over the web is in various formats like audio, video, text and image are presented in HTML. These formats presented are said to be individualistic in defining and forming the denotation of the context. Generally the information accessible are said to be unstructured and hence it is very risky to extort and validate the information. Although some hunt engines and display scrapers have been developed, they are not said to be resourceful and require extreme physical pre-processing like crafting a schematic concept, clearing uncooked data, by classifying the credentials physically into catalog and post processing.

‘Web Service’ concept was introduced in web technology to amplify the incorporation and interoperability to access the information. Web services become extremely trending in production in a small span because of its dynamic nature but some authorization problems were identified [1] because of the heavy raise in numeral services with the passage of time. To solve some existing web based problems like information filtering, confidentiality, security and exaggeration of the context that is available in arrangement above the web, a solution “Semantic Web” base on semantic concept was designed by Tim Berners Lee [2]. Semantic web is a shared exertion by the W3C and it can be used to encourage the universal format for data. It cancels vagueness from available data format which has been constituted on the World Wide Web.

Semantic Web has proposed the idea of ‘Ontology’ which is used to structure the information into machine processable format [3]. The three basic categories in which the ontology concept is subdivided are Ontology Instance (OI), Natural Language Ontology (NLO) and Domain Ontology (DO). Produced linguistic token which are acquired from natural language proclamation, can be related by NLO language [4]. Where, the knowledge of a particular domain can be represented by using Domain Ontology and Ontology Instance are used for generating automatic object based web pages.



Constructing ontology for any relevance is an exceedingly challenging research work since it relays on withdrawal of information from the system and processes it to the machine readable format. RDF, OWL are some of the supporting languages used to construct ontology. This has been done in order to convey semantic stuffing visible and organize their margins. The developed ontologies are connected to each other in a manner such that it extorts the available corporal information. Due to the improvement of complex handing of apparatus and large lexical property, ontology plays a vital contribution in the present scenario. Some concepts of ontology based resolution that are projected and urbanized are named as Semantic Desktop [5], Semantic Security Web Services (SSWS) and Cultural Heritage [6].

The concept of “ontology” in general terminology can be referred for developers who need to allocate information in that particular field/area. It encompasses some concepts in domain of machine interoperability and relations between them. The reasons for choosing ontology development concept can be attributed to the assistance it provides:

- To allocate regular accepting of the formation of information among public and software perspective.
- To allow reuse of particular domain familiarity.
- To construct the domain supposition unambiguous.
- To divide domain awareness from the equipped awareness.
- To investigate domain familiarity.

This paper is structured as follows; first it discusses about the conventional method and origin of the research continued by description about the proposed method and its advantages. Later it describes about the materials and methods for the conversion of heterogeneous files in to RDF format. Finally results and discussions are presented in the last section followed by conclusions along with the future enhancement of the research.

Motivation of the Research

Nowadays the concept of Open Government Data is gaining momentum, where the datasets collected through the satellite are made available in web at free of cost for research and public access. Most of these web portals provide the unstructured data as a tabular record or spread sheets. The offered information is semantically quite heterogeneous and are said to be unstructured or linked data. Some of the basic heterogeneous file formats are CSV (Comma Separated Values, *.csv), Excel (*.xls), NetCDF (Network Common Data Form, *.nc), HDF5 (Hierarchical Data Format 5, *.h5), TUV (Tutorial file, *.tuv) TSV (Tab Separated Values, *.tsv) and so on. Also, the afford data can be machine readable but not machine understandable, thereby creating a drawback in data integration which is said to be the developer’s responsibility. This makes difficult for any end user to access the data for further research and any application areas. The present work deals with the study of south eastern coastal areas of India where the ocean data are collected and used for the further research.

PROPOSED METHOD

The proposed algorithm defines the conversion of heterogeneous files using the satellite data of the south-eastern coastal areas of India collected form various Research and Development centres. The ocean data are in the file formats like CSV, Excel and NetCDF, which has been converted in to RDF file format by implementing the algorithm depicted further in this paper. By using RDF format for any beginner the data becomes semantic, which makes it flexible for data integration and addressing interoperability [7]. Furthermore, the resources that are available in RDF are said to be flexible which makes modification easier on part of the developer by adding or removing the RDF triplets. The algorithm for conversion of CSV/Excel and NetCDF to RDF is described further.

Excel file generally refers to a grid of cells containing numbered rows and columns in which the data is stored under each specific vocabulary, representing a row and its corresponding column. CSV is a simple and common standard of tabular data which consist of fields/columns separated by the comma character and records/rows terminated by newlines. The first record is the header, which contains column names in each of the fields. The conversion of Excel and CSV to RDF is simple and most common. The conversion process includes the four basic steps as shown in **Figure 1**.

The Excel and CSV file containing the ocean data is accessed as an input which has defined vocabularies with them. For each Excel and CSV file, the property table and its resources are generated for the model created in the above step. Additionally, the name prefix for each row in the input file is specified. The standard namespace tells any machine reader that the enclosing document is an RDF document, and that the rdf:RDF tag resides in this namespace. The RDF file is written in the language called as Turtle, which can be used inside the query language like SPARQL. Thus the conversion of CSV and Excel file to RDF format can be processed easily.



Many research works have been carried out in collecting the data species and presenting it in NetCDF or HDF5 [8] and [9] but very few concentrate on conversion of heterogeneous data in to RDF format. The proposed work mainly focuses on the NetCDF to RDF conversion algorithm. In this paper the collected NetCDF ocean data from the web portal is considered for the conversion to represent it in RDF format because, querying information from RDF format is simple and efficient than any other tabular or heterogeneous file formats.

The collected datasets in NetCDF file format (*.nc) is of multi dimensions comprises of about 65,000 datasets and occupies memory capacity of about 900 MB. The algorithm for the conversion of NetCDF file to RDF file format is depicted further in this paper. First access the NetCDF file (*.nc) which has to be converted in to RDF (*.rdf) file format. The file can be opened using nc_open() and the header is read which consists of 'n' number of non-record variables of the entire file. Then the Subject, Predicate and Object from the NetCDF file that has to be declared in the converted RDF file. Get the information like dimension ids, name and length and find the group names and their ids.

A number of groups will be present in the input file each consisting of different names, variables and data types in which the values are stored. Then find all the global attributes declared in the input NetCDF file. For each group identified, query for the variable and its ids. After finding the number of variables associated with the identified groups, for each variable query the name of the variable, type of the variable, variable's dimensions and dimension ids. Then all the attributes associated with the variable in the input NetCDF file are found. Query the attribute name and its value and generate the namespace declarative to provide the identifiers like types, functions, variables and so on followed by generate the dimension property of the input NetCDF file. Then the RDF properties and resources to be initialized in the output file for the identified NetCDF variables are generated. With all the information found build the RDF document. Finally write RDF in turtle format. As described in the last step of Excel/CSV to RDF conversion the final output has to be written in the turtle (*.ttl) format.

The flow of the conversion algorithm of NetCDF file to RDF file format has been represented as shown in **Figure 2**. Hence the converted RDF file format is said to be reduced in the memory capacity of about 500 KB. As per the above discussion querying an RDF can be made easier due to its advantages over the other file formats. This converted RDF file will be used in the future for the SPARQL user queries in order to provide efficient information from the database record in the required time. The implemented algorithm uses the ocean data thus it can be applied for the oceanography applications and also used to access data for researchers, academicians, managers and so on in the human readable format like XML/JSON (Java Script Object Notation).



Figure 1 Flow of conversion of CSV/EXCEL file to RDF

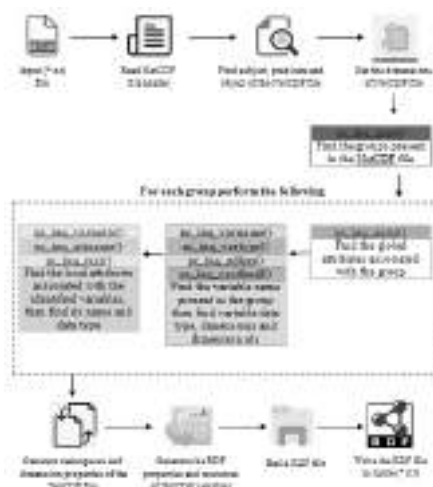


Figure 2 Algorithm for conversion of NetCDF file to RDF

RESULTS AND DISCUSSION

The study area covers south-eastern coastal areas (Bay of Bengal) of India. The field area is monitored by the sensors like Agro Floats, Buoys, Coastal Radars, Gliders and so on hence through the INSAT-3D satellite the

observed datasets from ocean areas are stored in various file formats. The NetCDF input file has been considered for conversion where it occupies memory space of about 880 MB. As per general format of the NetCDF file first it includes NetCDF header which consists of dimensions, variables and then followed by global attributes. This input NetCDF file is said to be a multi dimensional file and its dimensions are noted that XT_OCEAN621_800, YT_OCEAN103_290, bnds, ZT_OCEAN and TIME as shown in the **Figure 3**.

Further, it is followed by variables of the input file which contains information like name, data type and so on. Finally the global attributes are described in the NetCDF header part. The proposed algorithm is carried out such that this input NetCDF file has been converted in to RDF. The converted RDF output file is as shown in **Figure 4**. It is noted that the RDF file consists of prefixes at first and then followed by the dimensions and dimension properties finally it contains global attributes. Under each variable it describes the variable name, data type of the variable, local attributes associated with the variable and the data stored in it.

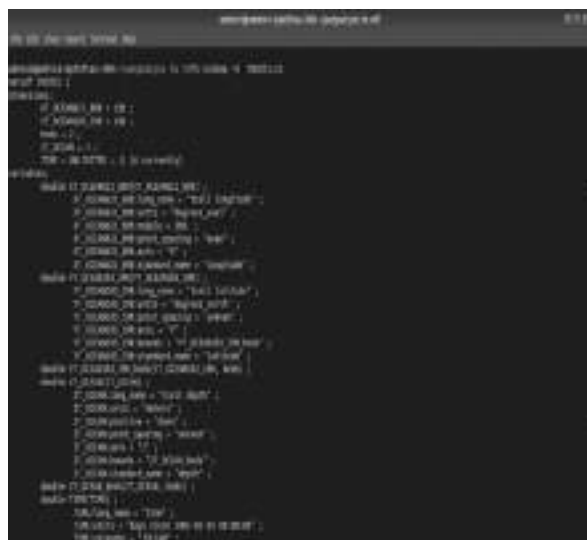


Figure 3 Input NetCDF (*.nc) file containing ocean data **Figure 4** NetCDF to RDF converted output file

The output file is written in turtle (*.ttl) format as explained in the above materials and methods. The converted RDF file format has been reduced in its memory capacity of about 300 KB which is the main advantage of the proposed conversion algorithm.

This conversion method is said to be more efficient for any end users that makes them easy for any SPARQL queries. Compared to the conventional method of directly accessing a large database which consists of tabulated values, the proposed conversion method makes it easier to access the data. Once these heterogeneous files are converted into machine understandable format like RDF it acquires very less time to access the data and present it to the user hence it is said to be time efficient. Also the converted file supports very less storage space hence it is considered to be memory efficient. The complexity of accessing the ocean data can be reduced by implementing the proposed method. **Table 1** illustrates about the advantage parameters of proposed file conversion algorithm over the conventional method.

Table 1 Comparison of the proposed algorithm over the existing method.

Parametric measures/ characteristics	Existing direct access method	Proposed conversion algorithm
Accessibility	Difficult for system to search entire database	Easy since RDF is a machine understandable file format
Complexity of the file	High, approximately of about 74%	Less, approximately of about 58%
Memory space	Need large storage space of about 900 MB	Need very less storage space of about 300 kB
Efficiency of the algorithm	Low	High
Time to access the data	More	Less



CONCLUSION

This work has focused on a novel knowledge based approach to present the available heterogeneous satellite data into a standard RDF file format. The proposed method is concluded to be flexible for multi dimensional array of large database of nearly 900 MB in memory and also addresses the satellite data interoperability. The converted RDF file format is reduced to memory space of about 400 KB. From the results obtained the proposed algorithm is said to be feasible and effective since, it has been experimented with nearly 65,000 datasets. The future work of this research includes the construction and mapping of Ontology to access the SPARQL query posed by user and provide the required data in human readable format like XML and JSON. This framework enables the user to easily access the data in an effective manner, where it is quite useful for individuals like researchers, students, end users and so on.

ACKNOWLEDGEMENT

This work is the partial outcome of a sponsored research project funded by Ministry of Earth Science (MoES), Government of India. This project has been developed in the Research and Development laboratory of Adhiyamaan College of Engineering, where the authors are currently working. The authors would like to express their sincere thanks to MoES for their financial support and Adhiyamaan College of Engineering for providing all the facilities to develop the project.

REFERENCES

1. Grit, N Son, T Andrew, OWL-S Semantics of Security Web Services: a Case Study, Springer-Verlag J. Davies et al. (Eds.): ESWS, LNCS 3053, Berlin Heidelberg Germany, pp. 240–253, 2004.
2. B. Lee Tim, H James, L Ora, The Semantic Web, A new form of Web content that is meaningful to computers will unleash a revolution of new possibilities, Retrieved data from the available website: http://www.geodise.org/useful_links/link_semantic.htm, June 30, 2007.
3. S Heiner, Approximate Information Filtering on the Semantic Web, Springer Verlag M. Jarke et al. (Eds.): KI, LNAI 2479, Berlin Heidelberg Germany, pp. 114–128, 2002.
4. V. Anitha, T. Menakadevi, A Survey Paper on Ontology Concepts in Semantic Web Technology and it's Applications, International Journal of Innovative Science and Research Technology, Volume 3, Issue 6, pp. 181-185, June 2018.
5. S Mark, S Pierre, S Leo, D Andreas, Increasing Search Quality with the Semantic Desktop in Proposal Development, In the proceedings of Practical Aspects of Knowledge Management 6th International Conference. (PAKM), Vienna Austria, 2006.
6. V R Benjamins, J Contreras, M Blázquez, J M Doderó, A Garcia, E Navas, F Hernandez, C Wert, Cultural Heritage and the Semantic Web, Springer Verlag J. Davies et al. (Eds.): ESWS LNCS 3053, Heidelberg Germany, 2004, pp. 433-444.
7. Nitant Dube, Ravindranath Nayak Miyar, Sunitha Abburu, Suresh Babu Golla, An Ontology Based Methodology for Satellite Data Semantic Interoperability, Advances in Electrical and Computer Engineering, Volume 15, Number 3, pp. 105-110, 2015.
8. Dongh young Han, Yoon-Min Nam, Min-Soo Kim, Kyongseok Park, Sunggeun Han SciDFS: An In-situ Processing System for Scientific Array Data based on Distributed File System, IEEE International Conference on Big Data and Smart Computing, 2018.
9. R. Jenkyns, S. Perkins, B. Biffard, M. Jeffries, M. Heesemann, C. Rosa, Extending Possibilities by Leveraging OPeNDAP for Remotely Exchanging Complex Oceanographic Data, IEEE Transactions, 2014.



A Taxonomic Classification of Load Balancing Metrics: A Systematic Review

Shahbaz Afzal^{*1}, G. Kavitha¹

Department of Information Technology, B S Abdur Rahman Crescent Institute of Science and Technology, Chennai, India¹,
shabazafzal@gmail.com*

ABSTRACT

Load unbalancing situation is a serious concern faced by cloud infrastructure providers in delivering the promised Quality of Service (QoS) to the intended users by degrading certain performance and economic parameters that pose a threat to Service Level Agreement (SLA) violation as agreed between the two parties namely Cloud Service Provider (CSP) and Cloud Service Consumer (CSC). Load balancing as a solution tries to overcome this issue by preserving the integrity and stability of the QoS parameters with the further reinforcement of SLA along different dimensions. Load balancing is a multi-constrained optimization problem with the objectives of maximization and minimization of certain metrics with the nature of being either single objective or multi-objective. The work identifies different QoS metrics being used in the existing literature and classifies them in a taxonomical hierarchy in classification by placing metrics under distinct category, they are affiliated with. Further some new metrics were introduced in this work that will give future insights to the researchers in load balancing. To the best of our knowledge, the work presents an in-depth and detailed survey of first of its type in load balancing to classify the metrics based on certain criteria.

KEYWORDS

Load Unbalancing, SLA, CSP, CSC, Load balancing, QoS metrics, Taxonomy

INTRODUCTION

The cloud computing is an on-demand network enabled computing model that shares resources as services billed on pay-as-you-go (PAYG) plan [1]. Nowadays every small and large scale enterprise is moving to cloud due to its versatile characteristics which enables the customers to have global access to the hired resources and services anywhere, anytime on the go. Some of the giant players in the given technology are Amazon, Microsoft, Google, SAP, Oracle, VMware, Sales force, IBM and others [2, 3]. Majority of these cloud providers are high-tech IT organizations. From the statistical data gathered through different research articles, publication and various authentic internet sources for last few years starting from 2010, it is generalized that cloud users showed a trend of rising exponential curve while the computing resources at Cloud Service Provider (CSP) side showed a rising linear curve leaving behind a gap to be filled between the two. This compelled the CSPs to put more compute into action to satisfy the user jobs within the agreed completion bounds. However, at the same time the cloud workload is highly unpredictable and the traffic flow is not uniform every time ensuing at times a very small inflow to the CSP consequently resulting improper resource utilization and its associated negative impacts. This in the course of time ultimately give birth to two unpleasing phenomena commonly known as overloading and under-loading problems and jointly referred as load unbalancing situation.

Cloud technology is in its developmental phase and is covered with a lot of issues may it be data security concern, cloud management, performance issues, transparency, resource management, load balancing or energy efficiency etc [4]. Of these, load unbalancing is viewed as the most crucial concern faced by infrastructure cloud providers. So the major focus of research in cloud is on the load balancing as a proposed solution to avoid the load unbalancing problem. Load unbalancing in cloud computing is an undesirable phenomenon that arises due to the non-uniform distribution of cloud workload among the virtual machines that ultimately diminish the performance and other quality of service parameters in terms of both provider and consumer side. Load balancing in cloud computing is a reaction to load unbalancing situation and is defined as a process of uniform distribution of workload among virtual machines by virtue of which the ideal speed, performance, throughput and other qualitative and quantitative metrics are preserved and stabilized, ensuring no computing machine is overloaded, under-loaded or idle [5, 6]. Load balancing tries to speed up the different constrained parameters like response time, execution time, system stability etc thereby improve performance of cloud [2, 3, 7, 8]. Load balancing is performed by employing an efficient load balancing algorithm that is usually a scheduling algorithm which aims to optimize some key parameters known as metrics. The optimization of metrics may be either single objective or multi-objective. A large number of heuristics and meta-heuristic algorithms have been proposed for load balancing process but still the bottlenecks are there which put an impetus on researchers to search for new advanced methods. The study of load balancing metrics is an



important aspect while designing a load balancing algorithm. The nature of the metric depicts whether to minimize it or maximize it making load unbalancing as an optimization problem and load balancing as an optimization solution. So, a proper classification is needed to group the metrics in a hierarchical taxonomy that will depict the position of a given metric in the taxonomy. In this paper, the key load balancing metrics were identified during the review process and were classified into relevant categories under which they fall. This is first of its kind so far in the literature where systematic survey regarding load balancing metrics is conducted so as to arrive at a well defined well ordered systematized classification. This is also first time in the literature where load balancing is considered as a solution and not a problem. A number of load balancing algorithms, approaches and methods were scrutinized to find the metrics that were used in these approaches. In general, the objectives of the paper are as under:

- (a) To identify the key load balancing metrics used in the existing works.
- (b) Propose novel load balancing metrics that may be used in future by the researchers.
- (c) Classify the metrics according to the category in which they fall.
- (d) Identify the relationship among the different metrics.
- (e) Study the impact of load balancing metrics on QoS.

LITERATURE SURVEY

Majority of the work done in cloud load balancing has been done in presenting an accurate and systematized taxonomy of load balancing algorithms with respect to the classification procedure. However, before going to load balancing classification, it is essential to have a prior knowledge about the load balancing metric classification so as to come out with a novel algorithm that should hold tight relationship with the metrics. However, till date to the best of our knowledge there is no literature work available that depicts the classification of load balancing metrics in a hierarchical order. This is the first of its type where the load balancing metrics are presented in a systematic classification so as to find the roots of that particular metric. The advantage of the classification is to identify the nature of metric and study its impact and find its linkage with the load balancing process.

Bardsiri et al. [9] proposed the evaluation of QoS metrics for cloud computing services as a broad classification and is the only literature available in cloud computing where metrics are classified. Accordingly, the cloud service metrics were classified into four groups, performance metrics, economic metrics, general cloud metrics and security metrics combined at the three service levels of the cloud namely, PaaS, SaaS and IaaS. The advantage of the paper is that classification process of cloud metrics has been initiated and importance of the classification is described for the first time paving a way for researchers to know when and where to evaluate a QoS metric. The limitation of the paper is that a single level classification is proposed instead of a hierarchical classification system which could have been more effective. Also, the classification refers to generalization of cloud metrics rather specialization to load balancing process. Further, the metrics impacting the environment like carbon emission and energy consumption as a step to green computing is missing in the work. Mishra et al. [2] presented a review paper on load balancing in cloud computing with a primary focus on comparing the different load balancing algorithms. The authors presented solely the load balancing performance metrics for evaluation purpose in the work and in the approaches being used. The advantage of the paper is that it outlines an in-depth review regarding the existing approaches. However, the paper has some pitfalls in the sense that it considers some non-performance metrics with the performance metrics e.g. the associated cost has been taken as performance metrics that actually is an economic metric. It is transparent from this survey paper that the comparison of economic metrics is missing from the paper because of lack of taxonomy of load balancing metrics eventually rendering the survey paper as insufficient for further studies. Shah et al. [10] presented a methodological survey in load balancing on different types of load balancing algorithms. The paper presented a review on comparison of different load balancing algorithms based on the nature, state, environment used, metrics used and challenges faced. However, like previous study it also considers only the performance metrics for comparison making it unfit for full survey paper. Hung et al. [11] studied the impact of metrics to load balancing in cloud with respect to the performance change that occur with the change in the values of these metrics. The impact on performance metrics was considered under this study proving the evidence of no systematic classification of load balancing metrics. Milani et al. [12] conducted the comparative analysis of different load balancing metrics in response to the performance gain in static, dynamic and hybrid load balancing algorithms. Like other studies, the same performance metrics were analyzed for comparison in the paper supporting our argument. Manvi et al. [13] surveyed resource management for IaaS cloud by comparing the resource management techniques against different resource provisioning, mapping and allocation performance metrics without considering other kinds of metrics.

While going through the literature survey, the authors arrived at the conclusion that the existing classification lack the systematic classification and are inadequate in the classification process. So, this paper presents the detail view of the taxonomy of load balancing metrics.

LOAD BALANCING METRICS

Load balancing refers to the process of cloud workload distribution among Virtual Machines (VMS) uniformly in an economical manner. The stability of the VMs in a cloud infrastructure depends upon the degree of load distribution across the available resources. A good scheduler results in a better load balancing approach [2]. Bardsiri et al and Li, Zhang, et al. [9,20] classified the cloud computing metrics with respect to the cloud service options along three terms, namely, performance, economics and security. However, we are not concerned with security issue in this paper, so it can be ruled out from the list. Literature in the load balancing proposes [2, 13 - 20] the metrics mentioned in the following sub-sections. The performance and economic metrics considered in the load balancing approaches are grouped into two broad categories; Qualitative metrics and Quantitative metrics. Also the metrics may be either dependent or independent in nature. Taxonomy of the load balancing metrics is shown in the **Figure 1**.

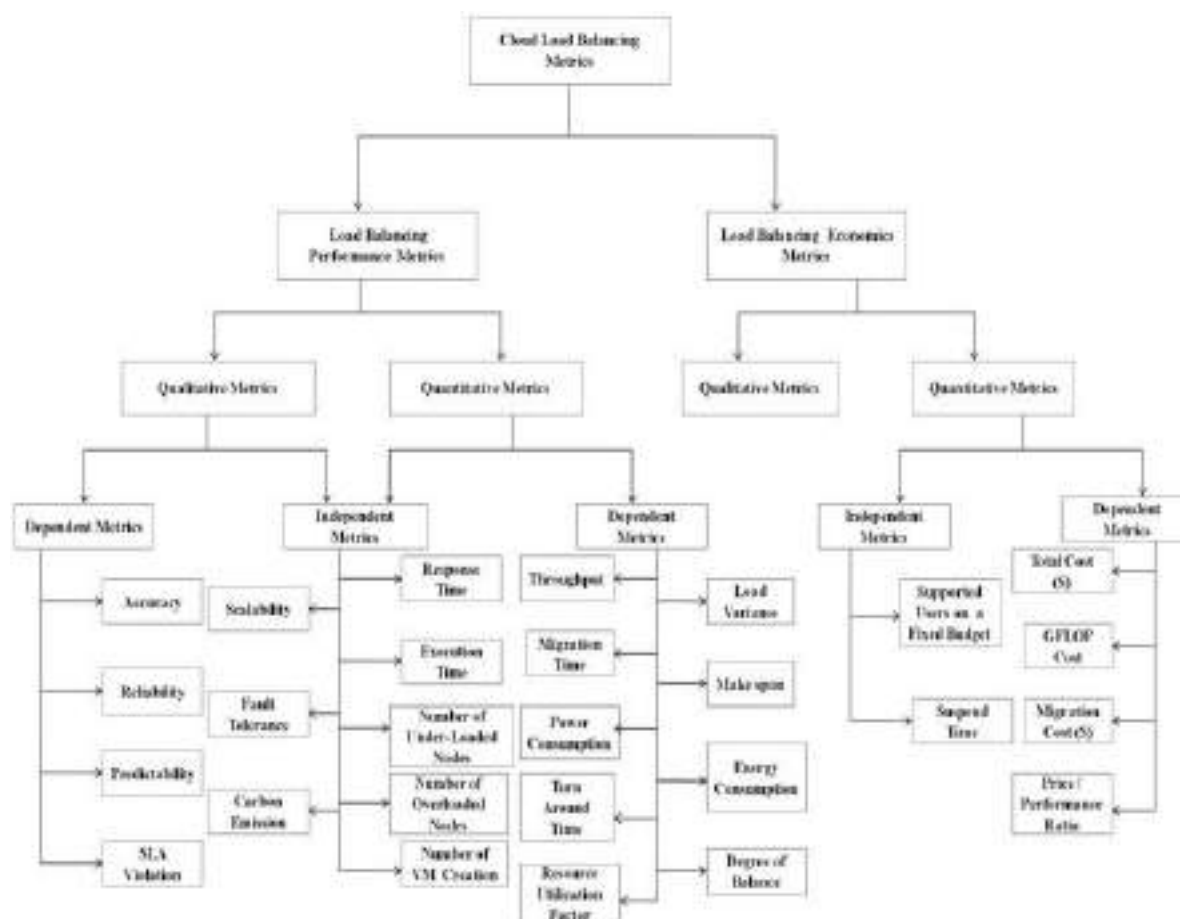


Figure 1 Taxonomy of load balancing metrics

Apart from the existing load balancing metrics some new performance and economics metrics are introduced in this work. Further in future, if new metrics are discovered they can be placed in the taxonomy according to their attributes.

The cloud load balancing metrics in the taxonomy are classified into seven distinct categories.

- Load balancing performance metrics with qualitative attributes and dependent nature.
- Load balancing performance metrics with qualitative attributes and independent nature.
- Load balancing performance metrics with quantitative attributes and dependent nature.
- Load balancing performance metrics with quantitative attributes and independent nature.
- Load balancing economics metrics with qualitative attributes.



- (f) Load balancing economics metrics with quantitative attributes and dependent nature.
- (g) Load balancing economics metrics with quantitative attributes and independent nature.

The above mentioned metrics are grouped under a common category called as Quality of Service (QoS) metrics.

(a) Load balancing performance metrics with qualitative attributes and dependent nature

The following metrics of this type are used in load balancing process.

- Accuracy : It is one of the important performances metric that determines the ability of a VM to execute the user tasks according to the guaranteed SLA. Accuracy is the measurement of deviation of actual value of task execution to the measured value. Load unbalancing results in decreased accuracy of the system while an efficient load balancing algorithm increases the accuracy of the system. A higher accuracy yields a good quality of service delivery with the preservation of SLA.
- Reliability: It assures that the system performs accordingly with the specifications provided in the SLA between CSP and CSC. Reliability goes parallel with other two performance metrics namely availability and serviceability. The reliability of a load balancing algorithm should be high to assure that no task in execution suffers non-availability and non-serviceability during a system failure.
- Predictability: It measures the degree to predict the characteristics and requirements of future user tasks based on the current and previous state of the system. The load balancing algorithm should ensure to provide a good stochastic analysis to make it possible to determine the next state from the current one.
- SLA Violation: It determines the number of user tasks that cannot be serviced because of non-availability of computing resources. Such a phenomenon occurs in a starvation problem when the system resources are highly overloaded and results the rejection of additional incoming user tasks. In case of VM based load balancing, it means the VM cannot fetch enough resources from the physical machine to support user tasks. A smart load balancing algorithm results in less SLA violations.

(b) Load balancing performance metrics with qualitative attributes and independent nature

The load balancing metrics of this type are discussed as follows.

- Scalability : It is the ability of a system to perform under dynamic traffic flow of user tasks. The load balancing algorithm should be able to scale up the resources during peak times and scale-down during off peak times, respectively.
- Fault Tolerance : The ability of a system to perform uninterruptedly during some point of failure in the system which eventually lead to better serviceability and availability. A fault tolerant load balancing algorithm should ensure minimum system failures due to system overload or by other means.
- Carbon Emission: It is the amount of oxides of carbon produced in VMs during their uptime. A load balancing algorithm should reduce the carbon emissions, so as to have eco-friendly and green data centers.

(c) Load balancing performance metrics with quantitative attributes and dependent nature

The performance metrics which can be quantified and are dependent on some factors in one way or the other are discussed as follows.

- Throughput: The metric calculates the number of tasks completed in a unit time after performing load balancing. It defines the rate of doing computational work by a load balancing algorithm. The objective of the load balancing algorithm is to achieve higher throughput.
- Migration Time: The time required to migrate the tasks across the unbalanced machines constitute the migration time. It may also be the time required to move the overloaded VMs from one Physical Machine (PM) to another PM as in VM migration load balancing.
- Power Consumption and Energy Consumption: The metric determines the amount of power and energy consumed by the VM after performing the load balancing process. An efficient load balancing algorithm reduces the power and energy consumption in a VM.
- Turn Around Time: The metric calculates the total time taken by a task from the point of its submission to its completion. A good load balancer allows a shorter turn-around time.
- Load Variance: The metric computes the average utilization of all hosts in data centre.
- Make Span: It is defined as largest processing time taken on all hosts and is one of the solid criteria for evaluating the performance of scheduling algorithm further reinforced by load balancing algorithm.



- Degree of Balance: It is the amount of uniformity achieved in the workload distribution across the VMs after performing the load balancing. Conversely, degree of imbalance is also considered as a metric which measures the imbalance among VMs.
- Resource Utilization Factor: It is the percentage use of currently available resources to the total available resources. It determines the degree at which the resources are being utilized in a VM. When a VM gets overloaded, the tasks consume majority of the resources but that is an undesirable event as the tasks will not execute fast. Higher resource utilization means higher resource consumption which means exhausted resources which in turn mean less free resources. Thus, a desirable load balancing algorithm gives desired resource utilization.

(d) Load balancing performance metrics with quantitative attributes and independent nature

These types of metrics are listed below.

- Response Time: It is the total amount of time a system takes to respond a user task and is numerically equal to the sum of service time and queue waiting time ignoring the transmission time preserving the timeliness property.
- Execution Time: The metric calculates the time taken by a system to execute a given user task. The load balancing algorithm ought to reduce the execution time while performing the migration process keeping in view the tasks that are partially executed on overloaded machines.
- Number of Over-Loaded Machines : The metric identifies the number of overloaded VMs and overloaded PMs in an infrastructure cloud meant for load balancing process.
- Number of under-Loaded Machines: The metric identifies the number of under-loaded VMs and PMs in an infrastructure cloud meant for load balancing process.
- Number of VM Creations : The metric determines the maximum instances of VMs to be delivered from the PMs, so as to support huge number of user tasks with the requirements taken into consideration.

(e) Load balancing economics metrics with qualitative attributes

In the existing literature, no metric of this type was identified related to load balancing. However, in future if any economic metric of this type is proposed, that can be put under this category.

(f) Load balancing economics metrics with quantitative attributes and dependent nature

The following metrics are listed in this category.

- Total Cost: The metric accounts the total cost in dollars charged to a CSC by a CSP for providing the service to the user tasks. An efficient load balancing algorithm reduces the cost of service and increases the profit of CSP.
- GFLOP Cost: It represents the cost in dollars charged per GFLOPS during its execution.
- Migration Cost: The cost in dollars required for migration of tasks or VMs in a migration process during load balancing constitute the migration cost. The load balancing algorithm should reduce the migration cost.

(g) Load balancing economics metrics with quantitative attributes and independent nature

The metrics of this type are as under.

- Supported Users on a Fixed Budget : It refers to the number of users that can be supported within a fixed budget.
- Suspend Time : It refers to the time during which the task is actually being not executed during load balancing process.

CONCLUSION AND FUTURE WORK

The work presents on in-depth classification of load balancing algorithms in the cloud computing domain that is first of its kind in the literature, which analyzes them into seven major distinct groups. In future, if a new load balancing metric is discovered, it can be suitably placed in any one of the class in which it falls. Further, it will be a great aid for researchers to identify the metric during development of a load balancing algorithm. It will also provide statistical insights in the domain area where research is lagging and leading accounting to these metrics. As discussed earlier, no metrics of this type was identified in the literature and can pave a way to discover them. The taxonomical framework presented in this work will form a standard map to be followed by future researchers in context with the load balancing metrics.



REFERENCES

1. R. B. Bohn, J. Messina, F. Liu, J. Tong, J. Mao, NIST Cloud Computing Reference Architecture, IEEE World Congress on Services, Washington, DC, pp. 594–596, 2011.
2. Sambit Kumar Mishra, Bibhudatta Sahoo, Priti Paramita Parida, Load Balancing in Cloud Computing: A Big Picture, Journal of King Saud University, Computer and Information Sciences, 2018.
3. P. Pradhan, P. K. Behera, B. N. B. Ray, Modified Round Robin Algorithm for Resource Allocation in Cloud Computing. Procedia Computer Science, Volume 85, pp 878-890, 2016.
4. V. K. Reddy, B. T. Rao, L. S. S. Reddy, Research issues in cloud computing. Global Journal of Computer Science and Technology, 2011.
5. R Achar, P S Thilagam, N Soans, P V Vikyath, S Rao, A M Vijeth. Load Balancing In Cloud Based On Live Migration Of Virtual Machines. Annual IEEE India Conference, Indicon, pp 1-5, December 13 2013.
6. S Dam, G Mandal, K Dasgupta, P. Dutta, Genetic Algorithm And Gravitational Emulation Based Hybrid Load Balancing Strategy In Cloud Computing. Computer, Communication, Control and Information Technology (C3it), 2015 Third International Conference, IEEE, pp. 1-7, February 7 2015.
7. A. Dave, B. Patel, G. Bhatt, Load balancing in cloud computing using optimization techniques: A study. In Communication and Electronics Systems (ICCES), IEEE International Conference, pp. 1-6, October 2016.
8. A. K. Bardsiri, S. M. Hashemi. QoS metrics for cloud computing services evaluation. International Journal of Intelligent Systems and Applications, Volume 6, Number 12, pp 27, 2014.
9. J. M. Shah, K. Kotecha, S. Pandya, D. B. Choksi, N. Joshi, Load balancing in cloud computing: Methodological survey on different types of algorithm. In Trends in Electronics and Informatics (ICEI), IEEE International Conference, pp. 100-107, May 2017.
10. T. C. Hung, N. X. Phi, Study the effect of parameters to load balancing in cloud computing. Ratio, Volume 45, pp 82-29, 2016.
11. A. S. Milani, N. J. Navimipour, Load balancing mechanisms and techniques in the cloud environments: Systematic literature review and future trends. Journal of Network and Computer Applications, Volume 71, pp 86-98, 2016.
12. S. S. Manvi, G. K. Shyam, Resource management for Infrastructure as a Service (IaaS) in cloud computing: A survey. Journal of Network and Computer Applications, Volume 41, pp 424-440, 2014.
13. E. J. Ghomi, A. M. Rahmani, N. N. Qader, Load-balancing algorithms in cloud computing: a survey. Journal of Network and Computer Applications, Volume 88, pp 50-71, 2017.
14. M. Kalra, S. Singh, A review of metaheuristic scheduling techniques in cloud computing. Egyptian informatics Journal, Volume 16, Number 3, pp 275-295, 2015.
15. M. Katyal, A. Mishra, A comparative study of load balancing algorithms in cloud computing environment. arXiv preprint arXiv:1403.6918, 2014.
16. M. Mesbahi, A. M. Rahmani, Load balancing in cloud computing: a state of the art survey. International Journal of Modern Education and Computer Science, Volume 8, Number 3, pp 64, 2016.
17. V. R. Kanakala, V. K. Reddy, K. Karthik, Performance analysis of load balancing techniques in cloud computing environment. In Electrical, Computer and Communication Technologies (ICECCT), IEEE International Conference, pp. 1-6, March 2015.
18. M. N. Arab, M. Sharifi, A model for communication between resource discovery and load balancing units in computing environments. J. Supercomput. Volume 68, Number 3, pp 1538–1555, 2014.
19. Z. Li, L. O'Brien, H. Zhang, R. Cai, On a catalogue of metrics for evaluating commercial cloud services. In Proceedings of the 2012 ACM/IEEE 13th International Conference on Grid Computing. IEEE Computer Society, pp. 164-173, September 2012.



Digitization of Product Development Processes

*Manas Kr. Mishra¹, Vivek Barhanpurkar², Arnab Dasgupta¹, Souvik Karmakar^{*1}
Tata Motors Ltd., Jamshedpur, India¹, souvik.karmakar@tatatechnologies.com*
Tata Motors Ltd, Pune, India²*

ABSTRACT

Digitization is the process of converting information into a digital format. As a part of digitization, Product Development Team has done digitization of existing offline processes, that is, ProNext, e-Approval of Design Release (DR) flawless launch of new product by digital validation/checking (Design /Process/ Electrical) of vehicle using Simultaneous Engineering (mySE), Maintaining Vehicle dropping pre and post activities, tracking of issues using Vehicle Productionisation Dashboard (VPD), Executive reports for escalations and support require from higher authority was maintain from Digital War Room(DiWAR) applications.

KEYWORDS ProNext, eApproval , mySE , VPD, DiWAR

INTRODUCTION

As per new product introduction workload, it was very difficult for Program Managers, PMO's to maintain proper scheduling of all gateway review. It is a challenging task to maintain all the project closure reports, QA audit docs, vehicle Productionisation status, Critical issue monitoring, project health, agreeing time plan, proper documentation, plan against actual status, hard copy gateway note approval by top-level management. Motto is to develop seamless digital process for CV, which will focus on front loading of activities to enable robust target definition in early phase and handholding post SOP(Start of Production) of the program along with robust projects/issues monitoring and closure mechanism.

As-Is Process

- Existing process of managing all new/upcoming projects was MS Office tools.
- Project information/repository kept with respective stakeholders. No central repository was maintained.
- Project time planning was maintained in excel. Many of the agencies involved might not be aware of the current status of the project. Like at which gateway it was pending or what are the deliverables to be done.
- Every program manager needs to prepare approval notes and take manual approvals on hard copy for PLC, PC, PRC reviews.

Challenges in As-Is Condition

- Managing multiple projects having multiple milestones and deliverables for each project.
- Critical issues tracking, monitoring and closure.
- QA and Veh launch related document access and management to concerned members.
- Projects documentation.
- Plan against Actual multiple reports.
- Monthly PMO report.
- Gateway plan of the year.
- Proper scheduling of all projects.
- Health of all projects.
- Gateway note approval on hard copy.
- Periodic gateways completion report.

To-Be Process

Focuses on addressing the mentioned challenges by developing access based digital systems to eliminate manual errors, paper work, time reduction, robust process monitoring mechanism and central repository creation. Digital systems has been developed as below.

(A) ProNext is all about maintaining the new product plan as per concept of New Product Introduction



(NPI), from the very beginning of kick off stage to Starts of sales, including several milestone and multiple departments. It contains agreed time plan within all the stakeholders, proper documentation of the entire Design Release (DR) Gateway with deliverables status, viewing of project health, customized report and role based access for data security and management.

Key Benefits :

- Proper project management, scheduling and tracking of project health at any time
- Live report of project time plan, gateway and deliverables status.
- Common dashboard given to view the status for concerned stakeholders.
- System will trigger reminder to each stakeholders for updating deliverables within timeline.
- Role based access for data security and management.

(B) E-Approval process also helps in getting the approval without paper. This e-approval process drastically reduce the DR gateway approval cycle time and it also save the paper cost of the organization. Approvers can approve or reject any DR gateway request from any time from system or email.

Key Benefits :

- Paperless and seamless approval process.
- System generated mail authentication and approval.
- Time saving and digital repository of data.

(C) Simultaneous Engineering (mySE) It is a mandatory Design Release Gateway before official release of any new product. Any new product is digitally validated with corrective agreement/sign off from concerned stakeholders before product release to maintain zero defect by eliminating rework at Initial stages. It is a seamless vehicle release tracking and monitoring interface with access-based control among respective departments. A notification mail and reminder mail always trigger for intimation of respective person.

Key Benefits :

- Critical design and BOM issues validation and closure at early stage to avoid rework at later stage.
- Digital library creation and database for commonisation/complexity reduction of parts.
- Zero defect approach and front loading of activities for expediting new product launch.
- Less likelihood of a need to modify the product later due to unforeseen problems.
- A greater sense of involvement across business functions.
- Easiness in planning: Change Matrix, All issues and BOM Compliance documented.

(D) Vehicle Productionisation Dashboard (VPD) : It is mainly used for capturing all the activities of prerequisite vehicle dropping and post vehicle dropping. Before any vehicle dropping, there are multiple no of checklists, which is to be done before Vehicle Drop on the line. After vehicle dropping another multiple no of checklists are to be closed. All the quality and audit checks should be closed for VC dropping with proper documents as attachment and remarks. All request for validation / checking goes for Signoff and signoff copies are available in system for further quality improvement. In this process of prerequisite or VC dropping if any issues faces by the Launch Managers that is also tracked here with escalation to senior management as per criticality.

Key Benefits :

- All information available in the system and updated by all CFT members.
- Micro level tracking of projects until all issues gets closed.
- All agreed and committed time plan in the system.
- All Documents and liveStatus of all projects on single click.



- Live report of project time plan, gateway and deliverables status, issue summary, executive reports.

CONCLUSION

In order to Ready to Market (R2M) to changing technology and demands of customer and with the increase in vehicle variants/volumes it has become an increasingly important to come up with Digital Processes to assist in project monitoring, tracking and digital documentation at every stage. Systems like PMM, eApproval, CE, PTD, DWR assist in project management, monitoring and reporting up to micro level at each phase (Design/ Proto/ Launch/ Production).

REFERENCES

1. GEN 3 Guidelines. Tata Motors Ltd



Integrated VR Platform for IoT Learning Environment to Improve Skill Development

A Raksha Thammaiah^{*1}, Rahul Singh², Sooraj K Babu³
Dheema Labs, Mysore, Karnataka¹, rakshaallumada@gmail.com^{*}
Uddip Consultancy Services, Mysore, Karnataka²
Ammachi Labs, Amritapuri, Kerala, India³

ABSTRACT

The recent increase in the number of smart devices connected to the internet and the Indian government's vision of smart cities have created a need for increased technicians in the Internet of Things (IoT) field. Present methods of education regarding IoT are limited to formal classroom learning methodology or short workshop-based programs. Both these methods have their own challenges. Virtual Reality is emerging as a very prominent tool to teach, experiment new technology at a rapid rate while requiring few physical devices, unlike traditional methods. In this paper, we propose the usage of Virtual Reality systems to teach IoT. The paper discusses a conceptual architectural framework, which details the environmental setup needed to create such a system and the possible advantages of such a system over the traditional method of IoT education.

KEYWORDS Virtual reality, IoT education, Virtual Reality environment, Skill development, Learning pedagogy

INTRODUCTION

Internet of Things, a term first coined by Kevin Ashton, in 1999, has become a buzzword rallying the fourth industrial revolution and a future of interconnected and communicative smart devices. An IoT system can be defined as a system of physical devices which; have some form of intelligence and functions, which gather useful information from their surrounding people, devices and communicate the same to other systems to derive insights and operable knowledge of the environment they operate in, for efficient operation, better decision making and improved system productivity [1].

With the cost of internet data being reduced to a negligible amount, the increased number of Wi-Fi enabled devices, the wide spread usage of smartphones and smart devices across the population and the shrinking sizes of computational devices has led to the onset of IoT era upon us.

This digital era has brought in significant changes to how information is created, curated and processed by everyone across all spectrums of operations. With the Internet of Things being a key enabler in the digital transformation of manufacturing units & processes; data center operations & management; healthcare and personal care; governance & citizen services and personal consumer and household space, with the prospects of new business avenues being found every single day. The global market of the IoT space in 2017 was about \$235 billion, expected to grow to over \$520 billion in 2021 [2].

IoT is expected to create a wave of digital transformation which will not only change the way people perceive and consume technology but will also completely transforms societies. It will create new norms, value chains, and constructs on how people and machines interact. A new challenging frontier requiring new sets of policies and protocols, all interlinked with IoT system is constantly increasing the interconnectivity of all human processes.

RELEVANCE OF IoT IN INDIA

For the past few years, the Indian economy has been transforming towards becoming a digital economy. There are currently 7.6 billion people on Earth[3]; 4.2 billion connected to the Internet; almost 50% of that connected population lives in Asia, 22% reside in India[4]. It is the result of immense investment in infrastructure development towards digitalization, along with the change in the regulatory policies supporting such effort is crucial in this socio-economic development witnessed.



The market potential of all things IoT in India alone is predicted to be \$9 billion by 2020[5]. NASSCOM predicts this would be around \$15 billion by 2020[6]. With the large-scale implementation of projects envisioned in the domain of IoT, it shall not only define the standards for others to take a point but also create acceptance of this technology to pivot humanity's pursuits.

Initiatives by the Indian Government to establish Smart cities and Digital Governance are prime examples of the efforts by the government heavily relying on IoT technology and platforms. For the success of such initiatives, it is of paramount importance for the people to be aware of IoT and people who have expertise in IoT technologies. This is especially true considering the smart city initiatives. **Figure 1** illustrates the various stakeholders involved in such initiatives as well as their involvement based on exposure to this technology

A two-pronged approach is required to set the foundation for such initiatives, i.e., one, create awareness among people on the effective use of IoT, Big Data and cloud technologies, and, second, technicians who can operate, maintain and upgrade the IoT systems and smart city applications. The educators and trainers facilitate all stakeholders.

The dynamic participation of these two stakeholder will result in improved data and information gathering and analytics, driving performance improvement efforts[7]. The efficiency and accuracy of the collected data results in better decision making, driven by Big Data analytics[8]

Challenges in IoT Education

The rollout of IoT systems to the populous would require awareness of the importance of IoT Systems and the intricate working of the components to transform their cities into Smart City. Media, early adopters and government department drive the task. However, the key consideration, which must be given, is towards preparing the IoT technicians, who shall expand, maintain and operate these IoT systems.

There are several challenges, which are faced in providing IoT education to students, and professionals who are seeking a career in the IoT industry.

1. **Technological diversity:** An IoT system has multiple levels of operations and programming language dependency. An IoT Developer must be well versed with Embedded Programming, Computer Hardware, Networking & Communication, and Distributed Computing. For developing newer systems, the developer may also be required to know mobile application development, web applets/application develop, Database programming and server-side programming.
2. **Lack of interoperability:** There are numerous smart IoT technologies; varied sensors and hardware, which have different protocols and interfacing requirements; and completely different means to operate. These varied components and subsystems do have well-defined standards and lack interoperability with each other.
3. **Implementation costs:** The initial cost of the requisite development systems, hardware components and sensors and software licenses are very high. Also, the chances of the hardware and sensors being damaged during the learning and experimenta are extremely high, resulting in high recurring maintenance cost.
4. **Time intensive nature:** The complex nature of the systems, hardware and software makes the time required for mastering even basic systems also long. In addition, the time it would require for students to experiment and develop prototype systems would create resource starvation.
5. **Infrastructure dependency:** As the IoT training infrastructure is fixed and operational in the classroom/lab environment only, the learning process is fixed and stagnated with high fixation to the single facility for the training.



PRESENT IoT EDUCATION PEDAGOGY

In the traditional classroom/lab-oriented approach, a traditional twofold approach is widely used like in most of the engineering studies. The first part presents theoretical knowledge and fundamentals, followed by practical learning sessions, which introduce the actual real-world systems and their applications.

Based on the proficiency of the students or course requirements, they are given some degree of freedom to experiment with the real-world systems to better familiarize themselves with the overall operations, but all this happens in a time-bound and structured environment only. This methodology though time-tested and fruitful, does not cater to any of the challenges of IoT education.

Many enterprising organizations and IoT trainers have opted for a short workshop-based approach to IoT education. These trainers present the students with ready to use IoT kits, which have the configured hardware and ready to use programming snippets which the students can just plug and play [9]. The students are made aware of the functionality of the hardware & the programming snippets and using the same develop simple IoT applications with limited functionality and scope. The kits are handed over to the students for self-exploration if desired. The students can seek further assistance in the form of online training modules or opt for advance workshops later.

There are also vendors who are providing self-paced online training modules which are prerequisite for IoT systems development. Followed by either self-procuring of components and systems or to buy the components from the vendor.

There have been considerations of providing training in IoT based on simulated environments [9] where the rendering of the systems was used to teach the students of the operations of the components and functionality. We are exploring to utilize an extension to this idea, via usage of Virtual Reality (VR).

USING VR FOR SKILL EDUCATION

Virtual Reality (VR) refers to technological platforms that utilize computer-generated simulation of a three-dimensional image or environment that is interacted within a seemingly real or physical way by a person using special electronic equipment, such as a head mounted display or gloves fitted with sensors [10]. VR, which was earlier used exclusively in the entertainment industry, has now become very popular in the gaming industry as well.

VR enables the developers to create environments and gameplay mechanics, which provide complete gaming immersion for the users. The environments provide the players complete immersion into the game. The intricacies of the environment can vary from simple polymorphic designs to finely textured graphics with dynamic lighting and feedbacks.

The advances in VR technology are positioning it to be a very powerful and effective tool to be leveraged to provide training to students. With the capabilities of the VR systems, a virtual workspace can be created for students where they can interact with objects, tools, and environments targeted towards specific learning objectives.

VR can create an environment where experiential learning is promoted, and students are intrigued, motivated and stimulated towards interacting with their virtual environment. Students can visit environments and systems, which could not be reached, via normal means, for example, one could visit the International space station or explore ancient Rome [11].

The key advantages of using VR as a training aid have been well documented [12].

- Increased motivation: the VR scenarios enable the students to be the protagonists of a story, an adventure. This increases the motivation and engagement of the students towards the learning outcome.
- Constructive learning approach: In a VR environment the student can interact with the varied component as desired provided the hardware like HTC Vive and Oculus Go are used. If not, the basic VR devices like Google cardboard allow the student to explore in and around a 3D model of the desired



environment giving a sense of immersion and more control over the processes even though the interaction is passive.

- Accessibility: With smartphone-based VR devices being launched in the market, the cost and accessibility to VR technology in general population have increased.
- Collective experience: Students irrespective of location can collectively share a single experience interacting in the environment.

Based on these advantages, VR is being used to teach across multiple fields such as Geography [13], Nanoscience [14], Business Management [15], Medicine and Healthcare [15] and many more.

Hence the usage of VR as a means to IoT education seems like an apt option in our considerations.

DEVELOPMENT METHODOLOGY

For developing a VR system, which can be utilized to train students in all facets of an IoT system, a conceptual framework has been designed. The framework creates an architecture, which defines the functionality, interactions and dependencies of the requisite system with the input, and output parameters defined.

The architecture has been designed based on high-level qualitative analysis of the available literature on the functionality of the VR and IoT applications, coupled with authors' existing expertise on the domain as an insight. The conceptual framework is intended to act as a blueprint to develop the final system under consideration.

A top-down approach is utilized to break down the constituents of IoT and VR systems, to understand its operational hierarchy and interaction between the constituents. **Figure 2** illustrates the high-level organization of the various key components. The consolidation of this learning has resulted in a conceptual framework proposed in this paper as architecture.

PROPOSED ARCHITECTURE MODEL

The proposed conceptual framework for the architecture is built upon the understanding of the various functionalities corresponding to the aforementioned technologies.

Figure 3 illustrates the proposed conceptual architecture, which primarily consists of the Physical Controller level, VR Computation layer, IoT Application Interface, Programming Interfaces and Hardware emulators.

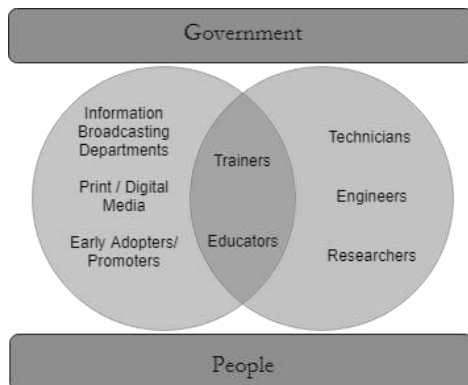


Figure 1 IoT initiatives stakeholders

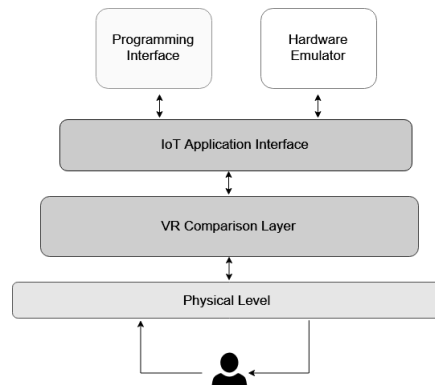


Figure 2 The high-level conceptual framework

The primary interface level operates via Smartphones / VR Headsets and gesture controllers. This interface controls the actions and feedback which are needed for the system operations.

The VR Computation layer utilizes the user inputs and renders required displays and action triggers. The VR Core engine, controlling the Graphic engines and modeling system, provides the responsive output.

The IoT Application Interface designed is the most critical component in the designed architecture. The IoT Application Interface links and simulates the entirety of the IoT Platform operations and interlinks the varied other components which constitute an IoT system. The environment of the system can be configured via this interface, i.e., hardware parameters, communication protocols, and application operation parameters can be configured as per requirement.

An IoT system is a component exhaustive system, with the interaction and interconnectivity of the varied components driving the operability of the system. This task is managed by the IoT Application interface which operates to seamlessly integrate the data flow across the components configured.

The interplay of these hardware components and communication interfaces is very important to be learned and understood by students as in real life scenarios, the cost of these components and communication interfaces constitute most of the project cost.

The IoT management platform runs the applications or core programs which the system operates upon. The management platform performs this by invoking the requisite compilers and run-time engines which are needed. The system must work in a manner such that multiple programming interfaces can work in parallel to stimulate different operational devices, i.e. microcontroller, controller devices (smartphones/web interfaces), etc.

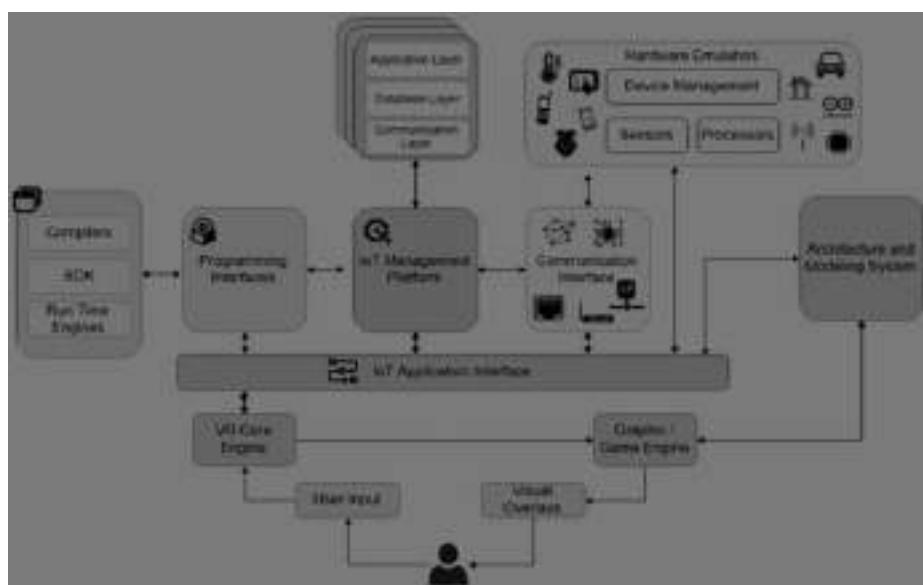


Figure 3 Proposed architecture framework

ADVANTAGES OF THE PROPOSED SYSTEM

The system is intended to remove the shortcomings of the existing methodologies available. The key advantages of a system developed based on this architecture are:

- With the hardware requirements limited to only the head mounted display and controller, the cost of initial investment of the institutions is drastically reduced.
- Implementation of a cloud-based simulated system enables multiple students to work within an environment.
- The students can utilize a plug and play code snippet for the device operations and tweak the code in the run-time based on the operation.
- As each component of the IoT system is being emulated, it becomes easier for students to understand the operational and data flows, crucial in debugging the developed system.



- However, the devices and components have interoperability issues in the real world. The system can create a common interface protocol which manages the output in a uniform manner to enable the system operation.

CONCLUSION

The conceptual framework proposed in this paper can be built upon to create a platform which the students can leverage to run experiments and develop IoT system. This system can be easily deployed to a remote location. The shortcoming of the traditional training methodologies discussed in this paper have been attempted to be eliminated with the usage of this architectural framework.

The ability of the proposed system to create a controlled environment without additional cost for replication and components makes the system an effective means to deliver skill development activities needed for IoT technicians and engineers.

This conceptual architecture is the first step in the series of development activities which are being conducted to facilitate IoT and VR education. Though the core objective of this framework is IoT, it can be used for skill development and training individuals in any of the associated engineering fields.

REFERENCES

1. R. Ramaswamy, S. Tripathi, S. Madakam, Internet of Things (IoT): A Literature Review., Journal of Computer and Communications, vol. 3., pp. pp. 164-173, 2015.
2. A. Bosche, D. Crawford, D. Jackson, M. Schallehn, Unlocking Opportunities in the Internet of Things, Bain & Company, 2018.
3. WorldOMeters, Current World Population, available:<http://www.worldometers.info/world-population/>. [Accessed November 2018].
4. Internet World Stats, Internet usage statistics, available: <http://www.internetworldstats.com/stats.htm>. [Accessed November 2018].
5. Deloitte, Internet of Things (IoT) to be the next big thing for operators—TMT India Predictions, February 2017.
6. NASSCOM, Indian IoT market set to grow upto USD 15 billion by 2020, October 2016.
7. E. Al-Nuaimi, H. Al-Neyadi, N. Mohamed and J. Al-Jaroodi, Applications of big data to smart cities," Journal of Internet Services and Applications,, Volume 6, Number 25, pp.1–15, 2015.
8. P. Krishna, Role of Internet of Things (IoT) In Entrepreneurship, International Journal of Innovations & Advancement in Computer Science, Volume 6, Issue 11, November 2017.
9. Z. Bogdanović, K. Simić, M. Milutinović and B. R. a. M. Despotović-Zrakić, A platform for learning internet of things, International Conference e-Learning, pp. 259-266, 2014.
10. E. Yilmaz, Education set design for smart home applications," Computer Applications in Engineering Education, Volume 19, Number 4, pp. 631–638, 2011.
11. Oxford Dictionaries, Virtual Reality, available: https://en.oxforddictionaries.com/definition/virtual_reality. [accessed November 2018].
12. J. Martín-Gutiérrez, C. E.Mora, B. Añorbe-Díaz and A. González-Marrero, Virtual technologies trends in education, EURASIA Journal of Mathematics Science and Technology Education, Volume 13, Number 2, doi: 10.12973/eurasia.2017.00626a, pp. 469-486, 2017.
13. I. Stojšić, A. I. Džigurski, O. Maričić, L. I. Bibić and S. Đ. Vučković, Possible Application of Virtual Reality in Geography Teaching, Journal of Subject Didactics, Volume 1, Number 2, pp. 83-96, 2016.
14. A. Klick, S. Kim, M. Kim, Using Virtual Reality (VR) for Education in Nanoscience, Microsc. Microanal., Volume 23, Suppl 1, pp. 2302-2303, 2017.
15. H. M.-C. Lee, Jia-Jin, Preliminary Study of VR and AR Applications in Medical and Healthcare Education," Journal of Nursing and Health Studies, Volume 3, Number 1.1, 2017.



A Framework for Selecting Effective Learning Technologies in Indian Higher Education

Asawari Shiposkar^{*1}, Manohar Desai¹

L&T Institute of Technology, Navi Mumbai, Maharashtra, India¹, asawari.shiposkar@larsentoubro.com*

ABSTRACT

With the help of technological resource, teaching in higher education is shifted from classroom to online. Technology plays an important role in enriching student's learning experience. Using technology, the educators can create appropriate learning activities that help the students advance their skills. It has been observed that students like learning with technology. But all students would not be able to grasp the concept. Still, some students would memorize the methods without understanding it. So it is important to use a methodology which helps us know our students and attend to their learning needs. According to Stenberg (June 1990), Students perform better on activities that match their learning styles. According to John Holt (1992), students do not perform well if educators do not question themselves to see which thing they do help learning and which things prevent it. Single tool was not benefitting all students, we have to use Differentiated Instruction method to satisfy learning needs. As technology developing a rapid speed, educators and administrators are constantly faced with challenge of finding or coming up with suitable technological tool for teaching. This paper throws some light on framework for selecting technology tools to have positive impact on students learning outcome.

KEYWORDS Impact of technology, Learning outcome, Conceptual framework, Higher education

INTRODUCTION

We are getting ready to move from a predominantly classroom teaching to a digital learning environment. Technology provides educators with tools that enrich the student's learning experience. It opens the gate to learning anytime anywhere for the students.

Using technology, the educators generate playlist of appropriate learning activities that help the students advance their skills.

As per IGI global, in teaching learning process an educator assesses learner, establishes specific learning activities as per learning needs, develops teaching and learning strategies, implements plan of work and evaluates the outcome of the instruction.

Role of educator has also changed as education system is transforming to learner centre mode. So focus is more on learning side. Now learning can happen anywhere, most important is learning style of students, teaching methodology and teaching mode.

The rapid technological changes, the rapid expansion of available information and the diverse demands of people and condition, have created new opportunities and challenges to provide non-traditional learning delivery system.

DEFINITION OF BLENDED LEARNING.

There are many definitions of blended or hybrid learning. Graham [3] defined blended learning systems as a combination of face-to-face with computer-mediated instruction. Ross and Gage [4] differentiated between web and technology-enhanced courses that incorporate online supplementary components within traditional courses without reducing face-to-face time and hybrid courses where in-class time is replaced by online course.

The most important benefits of blended learning are : Flexibility, Effectiveness, Cost-effectiveness, Personalization, Extended reach, and Covers all learning styles.

LITERATURE REVIEW

Before going into the details of the proposed framework for selecting an effective learning tool, a review of some of the existing system has been carried out.

Blended learning is combination of online learning and classroom learning. While preparing framework, teaching methodology for online and classroom is needed to be mapped for 21st century learner.



A. Students' requirements on blended learning demand :

- Practical and real time application oriented
- Clarify the concept
- Linkage among the content
- Linking fundamentals with industry application
- Individual Attention

B. Teacher's challenges involve :

- Selection of Learning Technology
- Selection of Models for media selection
- Insufficient Technology skills and difficulty to use
- Time constraint and restriction.

Reiser and Gagne (1983) identified a number of common characteristics by comparing ten different theoretical models. [1]

21st century learning framework was designed by considering inputs from all stakeholders like educators, academic consultant, industry experts etc. The skills, knowledge, expertise, and support systems that students need to succeed in work, life, and citizenship is mentioned in P21 framework. [2]

Higher education is posed with lot of challenges like:

- to increase the intake capacity
- More no of droppers in first and second year,
- Quality of education
- Skill acquisition

Blended learning has been found to be a viable and effective approach to deliver high-quality and skill based learning

This paper focuses on a framework for selecting technology tools that will have a positive impact on students learning outcome in this new approach.

METHODOLOGY

In this research, quantitative methodology was used to collect and analyse the data obtained from all the respondents. The researchers developed the questionnaire and finalized it before being distributed to the targeted group of respondents. The questionnaire were designed specifically to address the effectiveness of online learning. Then second questionnaire was designed to find the effect of learning with technology.

Also a case study qualitative analysis method was used in this research. A qualitative focus group study was conducted in the L&T Institute of Technology. As per the learning styles of the students, different activities were carried out with technology and at the end their final examination result of subject was analysed.

FINDINGS

The first survey about online learning took place at L&T Institute of Technology in Navi Mumbai, which was set up in 1983 by LARSEN and TOUBRO Staff and Workmen Welfare Trust to impart need based and application oriented technical education. It is primarily meant for the benefit of the wards of the employees of Larsen and Toubro and its subsidiary companies all over the country.

A good number of students were brought under the survey. The survey finding is as shown in **Table 1**.

The Second survey about learning with technology was conducted using Survey Monkey. Link was shared with different educators and students. 100 Responses were received and finding is as shown in **Table 2**.

The importance of the following technology-enhanced activities for your teaching/learning and result is as shown in **Table 3**.

The second method of research of case study conducted at L&T Institute of Technology, involves final year students of two different batch were taught with different methods and their test result was analysed as shown in **Table 4**.



A FRAMEWORK FOR SELECTING EFFECTIVE LEARNING TECHNOLOGIES FOR BLENDED LEARNING

In such a fast-changing environment and with a plethora of learning technological tool out there educators need a framework or definite set of criteria to guide them in making the right choice. The framework was build based on theory, above findings, practice and by exploring the relationship among student differences, subject requirements, desired approaches to teaching and learning, choice and use of technology, and the availability of resources and institutional support. All these factors should be taken into consideration while designing learning technological tool.

Table 1 First survey finding

Questions	Yes / always	May be / most of time	No
Do you find online learning useful for your education?	93.34%	6.67%	0%
Is your interaction with Online learning Platforms clear and understandable?	80%	13.34%	6.67%
Does it help you Learn things quickly?	66.67%	66.67%	26.67%
Is online learning fun?	26.67%	6.67%	26.67%
Does it increase your knowledge?	73.34%	20%	6.67%
Do you understand all the topics explained online?	20%	46.67%	33.34%
Does your mentors recommend online learning?	73.34%	6.67%	20%
How often do you use online learning platforms?	26.67%	46.67%	26.67%
Do you intend to use online learning in future?	86.67%	6.67%	6.67%
Do you have knowledge to use online learning platform?	93.34%	0%	6.67%
Do you have resources for online learning	80%	0%	20%

Table 2 Second survey finding

Questions	Absolutely	Somewhat	Not at all
Does the technology tool help you to focus on the learning goals (content) with less distraction(s)?	61.00%	36.00%	3.00%
To begin with learning new concept does the technology tool plays major role?	84.85%	5.05%	10.10%
Does the technology cause a shift in the behaviour, where you move from passive to active social learners (co-use)?	46.00%	52.00%	2.00%
Does the technology create scaffolds to make it easier to understand concepts or ideas?	67.00%	33.00%	0.00%
Technology helps students to demonstrate their ideas in a better way than traditional method	85.00%	6.00%	9.00%
The technology tool allows students able to develop a Conceptual understanding in learning goals and content	69.00%	30.00%	1.00%
Does the technology create opportunities for students to learn outside of their typical school day?	88.00%	12.00%	0.00%
Does the technology create a bridge between school/college learning and their everyday life experiences?	53.54%	44.44%	2.02%
Does the technology allow students to build skills that they can use in their everyday lives?	70.00%	30.00%	0.00%

Table3 Activity wise weightage

Activity	Weighted average
Providing revision exercise	4.32
Creation of collaborative documents (e.g. using wikis, shared file space)	4.22
Online submission of coursework	4.24
Distributing learning materials (e.g. copies of lecture notes, reading lists, links to websites)	4.31
Synchronous (in real time): student to teacher (e.g. Twitter, instant messaging)	4.06
Plagiarism detection	4.1
Interactive learning materials (e.g. animations, simulations)	4.38
Online assessment	4.38
Student collaboration or group activities	4.1
Delivering multimedia (e.g. audio, video)	4.46



Table 4 Result analysis

Subject	Batch 1 Single instruction, that is, with single tool	Batch 2 Differentiated instruction, that is, with blended
Management	Average =31.8	Average=32.33
Operating system	Average =54.59	Average =55.24
Management	Passing % =100	Passing % =100
Operating system	Passing % =88	Passing % =95

In 1998 first Bates developed and later refined (Bates, 1995) the ACTION model for distance educators. This model helps in making decisions about investment in technology and also guide how to select specific media and technology applications for a course.

The SECTIONS Model was developed (Haque and Garibay, 2001) for campus-based teaching with technology.

The authors plan to build on both of these models for blended learning. MONASTIC model is as follows:

- M** Mentor, Personalized Industry mentors work with student groups and give the participants valuable insights. The mentor not only clears doubts related to assignment or coursework, but also provides actionable career advice. Timely and relevant guidance by expert mentors.
- O** Organizational Issues: What are the organizational requirements? What are the barriers to be removed before this technology can be used successfully? What changes in organization need to be made?
- N** Novelty: Is this an emerging technology?
- A** Access: Is a particular technology accessible for learners and how? Is it flexible for a particular target group?
- S** Speed: How fast can we shift courses to this new technology? How quickly can materials be changed?
- T** Teaching and learning: what are the different learning needed? Which teaching methodology will best meet these needs? What are the best technologies for supporting this teaching and learning? Is the technology helping students to enhance and extend the learning goal? How to measure *students intended learning outcomes*?
- I** Interactivity: what kind of interaction is seen between learner and technology? Which are the various management techniques to create safe and ethical blended learning environments that includes social collaboration.
- C** Costs: what is the infrastructure cost of technology? What is the unit cost per learner?

The schematic of the MONASTIC model is shown in **Figure 1**.

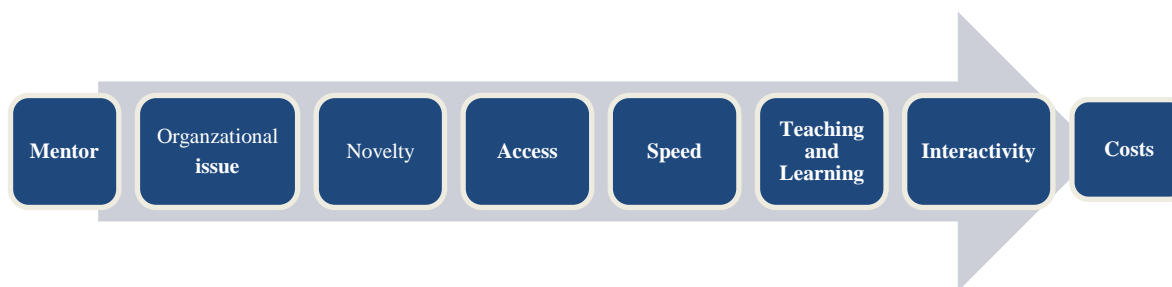


Figure 1 Framework for selecting effective learning technologies for blended learning

CONCLUSION

The framework for selecting effective technology is designed to enhance the teaching methodology for 21st century learners who are entitled for blending learning.

By keeping different factors in consideration, framework helps educators to decide technology to do the justice for the context.

To handle the complexity main factors are identified and each factors are analysed by answering a set of relevant questions.



Finalization of technology and mix of media for their respective subject can be done by collecting, reviewing and assessment of resources likely to be available, in specific time and skills of the educator

REFERENCES

1. A.W. Tony, Bates and Bates, A.W. Teaching in a Digital Age
2. www.p21.org
3. C. Graham, Blended Learning Systems: Definition, Current Trends, and Future Directions. C. Bonk, and C. Graham (Eds.), The Handbook of Blended Learning: Global Perspectives, Local Designs, San Francisco, CA: John Wiley & Sons, Inc., pp 3-21, 2006.
4. B. Ross, K.Gage, Global Perspectives on Blending Learning: Insight from WebCT and Our Customers in Higher Education. In: Bonk, C., and Graham, C. (Eds.), The Handbook of Blended Learning : Global Perspectives, Local Designs, San Francisco, CA: John Wiley & Sons, Inc., pp 155- 168, 2006



A Survey on Automation and Monitoring of Hydroponically Growing Crops using IoT

Vishnu T¹, Karthiga D¹, Meenu D Nair*¹

Department of EEE, Karpagam College of Engineering, Coimbatore, Tamilnadu, India¹, meenudnair@gmail.com*

ABSTRACT

Agriculture is a vital piece of life, most of the Indian families are agro dependent, though it is very important yet our conventional methodologies has lot of disadvantages. Our farmers utilize huge space, and plenty of water for cultivation. Nowadays water scarcity is a major threat to our society, in the name of development, depletion of water increases. The developing technologies had decreased the wealth of the soil. Advancement in agriculture brought artificial fertilizers to eradicate diseases, it turns the soil infertile. This could be overcome by an efficient method called 'Hydroponics'.

This plantation had brought smartness in agriculture. By this, we could achieve lesser space, less man power and 10% of water consumption compared to conventional method. The monitoring and control techniques could be implemented using Internet of Things (IoT) for proper and advance maintenance. The major parameters to be handled in Hydroponics are monitoring temperature, humidity, PH of water, water flow, nutrition level, pump motor speed and efficiency. The collected data are uploaded into cloud using IoT module. The data can be processed in cloud or local server. Remote user can also control the system through Android/Web Application.

KEYWORDS Cloud, Hydroponics, Internet of Things, pH, Web application

INTRODUCTION

The development of technologies had decreased the practice of agriculture in India. The urban population is on the rise resulting in most of the agricultural lands are being converted to urban areas. This fact is well corroborated by statistics provided in Table 1. Water scarcity is also gradually increasing. Considering the above factors agriculture decrease is going to be a major problem in the future. These problems could be overcome by a new technology called Hydroponics. It is a method of growing plants without soil using nutrient solution in water, where the roots of the plants are dipped in the solution. This method could be done in many ways such as in bucket, pipe shallow stream etc. Growing plants without soil was introduced by Francis Bacon in earlier 1672 and he published a book *Sylva Sylvarum*, Later it became popular in 1699. In 1960, 'Allen Cooper' of England developed Nutrient Film Technique (NFT). Shallow stream of water with dissolved nutrients flow past the bare roots of plants in a watertight gully channels. This technique has constant flow of nutrient solution, hence adequate amount of water, oxygen, nutrients which are required for plant growth are available in abundant. NFT also termed as 'Productive Technique'.

URBAN CONVERSION STATISTICS

The above statistics shows the gradual increase of the urban population [1]. Due to the population increase most of the agriculture lands are converted into urban areas.

HYDROPONICS

The term Hydroponics is derived from greek word 'Hydro' means water and 'Ponous' means work. It is a method of growing plants without soil, using nutrient solution in the water solvent. The roots of the plants are exposed directly to the nutrient solution with a holding medium such as rock wool, coco coir, pebbles etc. This system supplies required amount of nutrient to all the plants individually. The plants grows healthier and faster compared to conventional method. This method could be implemented in a greenhouse which requires very smaller space could be constructed in the terrace of the houses, buildings of the urban areas. More plants could be cultivated in a smaller space. The plant grows without soil borne diseases such as Fusarium, Pythium and Rhizoctonia.

There are various types of plantation: Wick Systems, Deep Water Culture (DWC), Nutrient Film Technique (NFT) and Aeroponics.

Wick Systems: This is a basic method of hydroponics and it is also called as dutch bucket system as shown in **Figure 1**, where the plant is cultivated over the top of the bucket cover with a cap and the nutrient solution is poured



inside as shown in the **Figure1**. The solvent in the bucket is sufficient for the plant to grow and no external nutrient supply is needed. Air could be supplied to the bucket using air pump if necessary.

Table 1 Urban conversion statistics

Year	Total population, billion	Urban percentage, %
1980	0.69	23.10
1985	0.77	24.35
1990	0.86	25.55
1995	0.95	26.59
2000	1.05	27.66
2005	1.13	28.70
2010	1.22	30.07
2015	1.30	31.91



Figure 1 Wick system (dutch bucket system)

Deep Water Culture: This method is similar to wick systems. The plant is grown in a bucket or a reservoir that could hold some water with nutrient solution.

Nutrient Film Technique: It is quite popular technique used in most of the hydroponics farm. It could be implemented in two ways circulating and non-circulating method as shown in the **Figures 2** and **3**. In this method the plants are cultivated over a PVC pipe or channel inside which water flows as shallow stream. The roots of the plants are submerged to the level of water so that it could absorb the nutrients required.



Figure 2 NFT (circulating method)



Figure 3 NFT (Non-circulating method)

Circulating Method: Here the channel has to be constructed with a proper slope, with a defined rate of flow of nutrients to plants. Since the water flows continuously the algae formation in the pipes could be avoided. Growth rate of the plant gets affected by channel length, by depletion of 'nitrogen' throughout the length of the gully, So the length of the channel should not exceed 10 m to 15 m.

Non Circulating Method: The water stays stagnant in the channel where the roots are dipped in it. The water is refilled using a water pump as it evaporates or absorbed by the plants.

Aeroponics: The nutrients are directly sprayed as a mist to the roots of the plants. The roots (**Figure 4**) get more oxygen and plants grow rapidly. This system generally use less water compared to other type of hydroponics.

Of above methods implementation of NFT is easier and prescribed for the urban farming. The automation could be implemented for NFT method easily compared to other methods.

NEEDS OF HYDROPONICS

- pH of the water should be maintained between 5.8-6.5.
- Temperature must be between 20- 30 degree Celsius.



- EC of the water must be maintained between 1.5-2.5 ds/m.

The above parameters can be controlled or automated using Internet of Things (IoT) [3]. The parameters depicted in **Table 2** are measured using respective sensors. pH of the water is monitored continuously and if it is not in the range it can be brought down by adding some water and same as if the EC is not at the prescribed range.

INTERNET OF THINGS (IoT)

The concept of IoT is evolving over the last few years, it means anything in this world could be hosted through the Internet [4]. It involves several amount of devices connected together. The devices such as sensors, mobile phones, computers, smart watches, house, buildings, and every IoT enabled devices. These are connected through a network and the data is stored in the server which is popularly called as Cloud. Cloud Computing is also an evolving technology which is used for storing and analyzing the data. This concept has been implemented in many fields. Encryption and decryption of data are done to avoid the data loss while transmission. IoT is used to link the hydroponic farm through mobile/web application where we can control the basic parameters of hydroponics and monitor the plant growth.

AUTOMATION OF HYDROPONICS

The arrangement of sensor network is made to collect the data from the hydroponic system. The sensors such as pH, EC, temperature, humidity, and water level are used. The sensor networks are shown in **Figure 5**.

- pH Sensor: Used to measure the pH of the water and the nutrient solution . It must not exceed the range 5.8 to 6.5. If the pH is not at prescribed range the arrangement of adding water automatically is made.
- EC Sensor: The nutrient in the solution is measured in terms of Electrical conductivity. It measures the salt content in the solution and finds the amount of nutrients.
- Water Level Sensor: The amount of water in the reservoir must be monitored and should be refilled automatically if the water level decreases.
- Temperature Sensor: The temperature of the farm must be in the range 20 to 30°C. A cooling set up of fan or mist fogger can be made if the temperature goes above the range.
- Humidity Sensor: The humidity must also be monitored along with the temperature and similar cooling set up is to be made.
- ‘Raspberry Pi 3’ module can be used for IoT implementation and it is preferable.

The programming of Raspberry Pi can be made using Python language.

- From the **Figure 6**, the NFT method is used for the Hydroponics system.
- The data of the above sensor parameters are collected. These collected data is transmitted to the cloud using IoT module or Raspberry Pi.
- The data gets updated for each interval of time.
- A temporary storage is set up in the system to store the data which avoids the data loss while transmission.
- The data is analyzed and transmitted through the network to the user as shown in **Figure 7**.
- End to end encryption and decryption is done to protect the data.
- The user could be able to monitor the details through the mobile/web application.

User Interface

Mobile applications are popular for IoT in android device. Several applications are available for the automation.

- The farmer or user will have individual account in which they could be able to monitor their farm details.
- User will have login credentials for protection.
- Notification will be sent through SMS or through the application if any error occurs in the system.
- User can also control the electrical appliances through the app.

Advantages of Hydroponics

- Healthier crops could be cultivated without any soil borne diseases.

- pH and EC are maintained automatically in this system.
- Farmer has less complexity of work, he need not go to the farm and check the pH and EC.
- More crops could be cultivated in a lesser space compared to conventional method.
- Plants could be cultivated in all the climate conditions in the greenhouse.
- Notified to the farmer through SMS or through Mobile app immediately if anything in the farm goes wrong.
- It is suitable for urban farming.
- Crops grow faster than it grows in the conventional method.



Figure 4 Aeroponics plant roots

Table 2 Needs of hydroponics

pH	5.8 to 6.5
Temperature	20 to 30°C
EC	1.5 to 2.5 ds/m
Light	14 to 16 h/ day

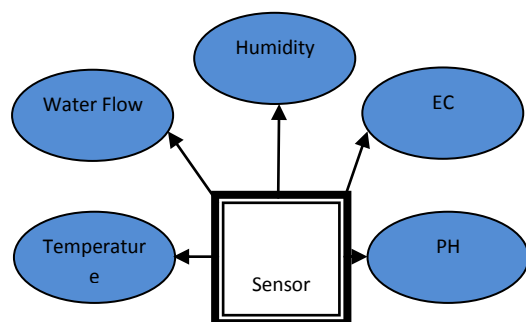


Figure 5 Sensor network

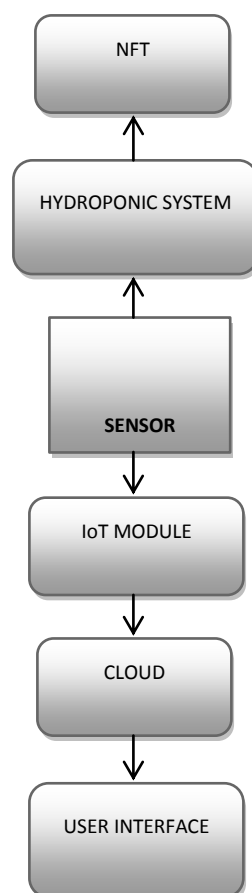


Figure 6 Automation using IoT



Figure 7 Data analysis

CONCLUSION

Hydroponics farming automation is new wave of technology which takes the agriculture to the future in a new way. This technology can be implemented anywhere needed. The hydroponics plant grows effectively and produces healthy food. The implementation of this system is easier and cost efficient as it needs some initial cost.

REFERENCES

1. S.S.Kalamkar, Urbanisation and Agricultural Growth in India, Indian Journal of Agri. Econ. Volume 64, Number 3, July-September 2009.
2. Rahul Nalwade, Tushar Mote, Hydroponics Farming, International Conference on Trends in Electronics and Informatics ICEI, pp 647, 2017.
3. Rahul Nalwade, Tushar Mote, Hydroponics Farming, International Conference on Trends in Electronics and Informatics ICEI, pp 648, 2017.
4. Abdur Rahim Biswas, Raffaele Giaffreda, IoT and Cloud Convergence: Opportunities and Challenges, IEEE World Forum on Internet of Things (WF-IoT), 2014.



Implementation of Radius Security with Two-Factor Authentication

Eashan Singh Gill^{*1}, Balakrishnan P¹, Patrick Kasiana²

School of Computer Science and Engineering, Vellore Institute of Technology, Vellore, India¹,

eashansingh.gill2016@vitsstudent.ac.in^{*}

Manager-System Engineering, SILNAM IT Solutions, Windhoek, Namibia²

ABSTRACT

AAA servers are designed for provisioning of authentication, authorization, and accounting (AAA) services to enterprises and organisations. These servers provide users access to various services and applications based on their authorisations stored in an authorisation database. Latest standard being used for communication of devices with an AAA server is the Remote Authentication Dial-In User Service (RADIUS). However, RADIUS has certain vulnerabilities. This paper proposes implementation of two-factor authentication to improve RADIUS security. This paper also reviews earlier research work on implementation of AAA servers, RADIUS and two factor authentication, which can be used to further develop the RADIUS standard and implementation of AAA services.

KEYWORDS AAA, RADIUS, Security, Two-factor authentication

INTRODUCTION

Nowadays in firms, companies and offices people have various clients accessed by a user. The managers and departmental heads want to restrict access for users to particular files, applications and clients. They also want a single username and password for a user instead of having to remember different passwords for different applications. Also, while modifying a user credentials or creating a new user for the company they don't need to create different credentials for different applications. They can just make one username and password for all applications and grant access as per requirements. This can be done by setting up an AAA server. Different applications like SQL database, Squid, OpenVPN, Wi-Fi portal can be made clients to this server. Scripts can be made to create credentials for a new user as he joins the company and grant access to him or to delete a user as he leaves the company or to modify the credentials of a particular user if required. The Administrator can run these scripts on the server-side [1]

AAA SERVER OVERVIEW

AAA involves access control to networks, resources, applications, policy enforcement, carrying out audit of policies and also provide billing information. First authentication takes place which identifies a user, by the user entering valid credentials before granting access. The authorisations granted by an AAA server are based on a username-password combination which the server matches with an authorisation database and grants access as per the profile of the user. Final step of AAA is accounting. It checks the amount of resources like time, data etc. This information can then be used for billing purposes, planning of network capacities, analysing utilisation trends etc. These services are normally provided by a server program. Devices with an AAA server use Remote Authentication Dial-In User Service (RADIUS) for communication [2].

RADIUS OVERVIEW

RADIUS is a protocol used in networks. It, helps in AAA services. The protocol works on the basis of a common secret shared between the server and the clients. It is used for authentication between the RADIUS server and Network Access Server (NAS) and to hide the credentials. NAS is a RADIUS server client. The RADIUS server has a user database with passwords which it uses to grant access. The user is prompted for the credentials. These credentials are encrypted and sent to the server[3]. Port 1812 is default port for listening for requests. RADIUS server uses User Datagram Protocol (UDP) for communication. The authentication process begins when the request is sent to the NAS which then forwards the packet to the server. The NAS sets information required by the RADIUS server, related to the user credentials and the service requested by the user, in this packet. Once the RADIUS server receives the request it checks the database and verifies if a valid user has sent the request, else, the request is not handled at all. If valid, the password is decrypted and checked if the password matches the one in the database. If not valid or if the password does not match, then RADIUS server sends Access-Reject packet to the user. If valid and the password matches plus no challenge/response required, Access-Accept packet is sent to the user. The packet



is then forwarded to the NAS[4][1]. RADIUS also has a challenge/response authentication method. The RADIUS server verifies the user credentials from the database and sends an Access-Challenge packet to the user, which is displayed to the user by the NAS. The user's response along with the original Access-Request packet and a new identifier is sent back to the RADIUS server. The RADIUS server checks the correctness of the response and accordingly sends Access-Accept or Access-Reject packet. The challenge method strengthens the authentication process. The authentication process is depicted in **Figure 1**. RADIUS Server accounts over port 1813. NAS sends RADIUS Server a packet with Accounting-Request code in it and having the status 'start' for Acct-Status-Type attribute. This request also stores the user details and the details of the services being used by the user. When the user logs out and the NAS has to stop accounting, it sends a packet to the RADIUS Server having the status 'stop' for Acct-Status-Type. The RADIUS Server after receiving this request logs the data and sends an Accounting-Response packet to the Network Access Server. In case of failure of logging, no Accounting-Response packet is sent to the NAS. After timeout, the NAS resends a request to the RADIUS server [5].

LITERATURE REVIEW

This section reviews all earlier research work on implementation of AAA servers, RADIUS protocol and two-factor authentication.

Issues in RADIUS Protocol Implementation

This paper discusses the various protocol dependent issues and implementation dependent issues while implementing RADIUS protocol. It also provides various solutions to the issues mentioned in the paper [4]. RADIUS is open to User-password based attack as it opens a packet while authenticating the access-request. It only uses MD-5 hash on the password stored in the packets, this makes user-password based attacks easy. The password in access-request packet is encrypted whereas in other packets it is in the form of Clear-text and hence can easily be captured by an attacker. RADIUS server does not deal with replay attacks, old packets can easily be used and hence Denial of Services (DoS) attack can be an issue. The server runs on UDP, hence there is no acknowledgment of the messages and there is no accounting of records. Therefore, the cause of failure is unknown to the Network access server. One spoofed packet by the attacker is enough to intervene in the authentication process. Cryptographically strong authenticators are needed. PAP must be avoided and instead CHAP can be used. Two-factor authentication is supported by RADIUS and can be implemented to add another layer of security. The NAS should be configured to send RADIUS Accounting-Update. Accounting information can be kept up to point. The conclusion is that RADIUS is simple and efficient. Its security can be improved by simple changes which can be made without changing the protocol [4].

Usability Study of Two-Factor Authentication

This paper discusses the various technologies used for Two-factor authentication, and in which situations each one of them is used. It focuses on three main two-factor solutions, these are security tokens, OTP received by SMS, and smartphone apps. Differences between all the three technologies are given. OTP on SMS is convenient but maybe time consuming. Security tokens require a device to be bought and configured, can be complicated to use by a user. Dedicated apps are easier if the user has access to a smartphone [6]. The paper focusses on the three key aspects defining 2F usability namely ease of use, trustworthiness, and required cognitive effort. The research done in this paper is based on 219 MTurk users and hence can be biased as they can be more computer savvy [6].

RADIUS Server as Centralized Authentication

This paper proposes the use of a RADIUS Server for centralized authentication of wireless connected users and grant of access to resources based on specific authorization of users. The authentication server was created using a third party software, which connects via a router and a switch to the network of wireless access points. All clients of



the network are authenticated as per the authentication database stored on the server. The system was successfully implemented and tested. However, it does not employ two factor authentication for higher security [7].

Two-Factor Authentication System Design

This paper proposes the design of a two factor authentication system using both alphanumeric and graphical passwords. The system consists of a server and client end software. Client end can be a PC or a smartphone. The system has a software token generated using crypto algorithms and delivered to the client smartphone. The client can also generate his own OTP which is validated by the crypto algorithm to grant access [8]. The OTP generation is done as follows:

- Username, password and DOB is concatenated with current date and time stamp and given as input to the SHA-1 hash function.
- The result is a 160-bit hash digest. This is then converted to 5 bytes or 40 bits by doing XOR of groups of 4 bytes namely bytes 1,4,8,12; 2,5,9,13; 3,6,10,14; 4,7,11,15; 5,8,12,16; 17,18,19,20.
- These 5 bytes are shifted by 4 digits to the right.
- These 5 shifted bytes are changed to their hexadecimal values.
- The final step is changing the ASCII values to a character string, which is then forwarded as OTP to the user.

The advantages of the system include higher security, defense in depth since two levels of authentication required, easy to implement and the disadvantages are space complexity, two gateways required, more time for authentication and remembering two passwords/OTP [8].

RADIUS Vulnerabilities

This paper deals with the properties of RADIUS protocol and of User-Password attribute. It tells about the various vulnerabilities in the protocol.

The various implementation and design issues have been discussed with the suggested solutions. The design and policy are the main reasons for the vulnerability.

User-password is encrypted using a stream cipher, which should not be used also MD5 should not be used. Response authenticator is a good idea but it is not being implemented properly. Shared secret key space is artificially limited [9].

A good cipher block must be selected for the protection of the user-password. The cipher can be keyed from a value derived of the shared secret and request authenticator. The SHA-1-HMAC attribute should be included in the Access-Request packet generated by the user, in the Access-Accept/Access-Reject packet and this attribute should be verified by the server once this request is received. These changes can even be made without changing the RADIUS protocol and can secure the system better [9].

Analysis and Extensions of RADIUS Protocol

This paper focuses on the security analysis of RADIUS protocol and provides extensions as security solutions for the vulnerabilities. A system with two servers for billing is better for accounting RADIUS messages on two servers simultaneously. The ISP can then check if the records in both the servers match each other and if not an attack can be identified. A stream cipher with MD5 hash should not be used. Instead a better cipher block can be found and used to encrypt the packets [10]. Response Authenticator = MD5(Code + Identifier + Length + Request Authenticator + Attributes + Shared Secret) A message can be added to the traditional RADIUS protocol for communication between client and server. It can be started by the server or by the client. The message will be used when RADIUS server restarts. This paper suggests various solutions which can be implemented in the RADIUS protocol without having to change basic principles and can make the server more secure [10].



(d) The RADIUS server then checks the time based OTP and the password stored in the database. If verified, then access is granted to the client. The same is depicted in **Figure 5**.

The two factor authentication provides an extra layer of security other than a simple username and password. It prevents sniffer attacks, DoS attacks and man-in-the-middle attacks. However, there is a time penalty as it takes some additional time for authentication as the user has to input the username, password and also an OTP, which is then verified by the RADIUS server. Another benefit of the above implementation is that it can be done on the existing hardware of any organization at no additional cost assuming the employees of the company have smartphones.



Figure 3 Google-authenticator for test user on RADIUS

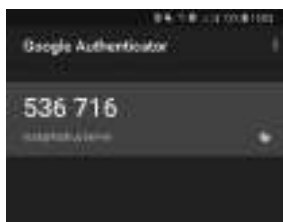


Figure 4 OTP on google authenticator app on phone



Figure 5 User connected after entering credentials with OTP

CONCLUSION

This paper reviews previous work done related to AAA server, RADIUS and two-factor authentication. The single factor authentication of the RADIUS server is vulnerable against replay attacks, DoS attacks and man-in-the-middle attacks. The implemented RADIUS Server with two factor authentication can improve the security of the server and provide security against replay attacks, DoS attacks and man-in-the-middle attacks. 2FA technologies are easy to use, are cheap and are flexible when it comes to implementing depending upon the requirement. This along with the RADIUS protocol which is inbuilt in most network devices can be used to implement a completely secured and centralized AAA server for a single sign-on for users to multiple network applications.

REFERENCES

1. S. Prakash, A. Jyotsana, Network Security, International Journal of Scientific Research Engineering & Technology (IJSRET), Volume 1, Number 1, 2012.
2. S. Y. Phang, H. J. Lee and H. Lim, Secure Deployment Framework of NEMO (Network Mobility), International Conference on Convergence Information Technology, 2007.
3. J. Zhang, Y. Guo, Y. Chen and J. Ma, AAA Based on 802.1x Authentication, Joint International Mechanical, Electronic and Information Technology Conference, Zhengzhou, 2015.
4. M. H. Rehman, D. A. Govardhan, T. V. N. Rao, Design and Implementation of RADIUS – an Network Security Protocol, Global Journal of Computer Science and Technology, 2010.
5. D. Szilagyi, A. Sood, T. Singh, Radius: a remote authentication dial-in user service, Rivier Academic Journal, Volume 5, 2009.



6. E. D. Cristofaro, H. Du, J. Freudiger, G. Norcie, A Comparative Usability Study of Two-Factor Authentication, arXiv:1309.5344v2 [cs.CR], 2014.
7. O. Dmitry, RADIUS server as centralized authentication, Mikkeli University of Applied Sciences, Mikkeli, 2015.
8. A. Amin, I. U. Haq, M. Nazir, Two Factor Authentication, International Journal of Computer Science and Mobile Computing, Volume 6, Number 7, 2017.
9. P. Zhao, X. Cao, P. Luo, Attack on RADIUS Authentication Protocol, ICCT, 2003.
10. J. Feng, Analysis, Implementation and Extensions of RADIUS Protocol, International Conference on Networking and Digital Society, 2009.



RCC Deck and Steel Truss Composite Bridge

Abhishek Sharma^{1*}, Pramod K Singh¹, Krishna K Pathak¹

Department of Civil Engineering, IIT BHU, Varanasi, India¹, 19riken@gmail.com*

ABSTRACT

The most common cause of structural failure in steel bridges is buckling of a compression member. Buckling failure is a sudden failure and offers no warning before collapse. Recently, in the year 2012, a 190m span steel truss bridge over river Alaknanda, in Uttarakhand, India, suddenly collapsed during casting of the deck slab due to buckling of one of its top chord compression members. Its failure during construction stage raised doubts on current design practices where, the factor of safety provided in the codes do not guarantee performance of the bridge in overload condition. In the case of composite under slung steel bridges, premature buckling of a top chord compression member is prevented by the RCC deck connected to the steel truss with the help of shear studs. This allows the top chord steel truss members to take stress up to their ultimate strength. A 30 m span underslung steel truss bridge is analyzed with composite action of RCC deck for service and overload conditions. The maximum flexural strain due to live load alone in the RCC deck slab is found to be 0.00019. Shrinkage strain for M40 concrete deck slab is taken as 0.0003. Hence, even during service condition, composite action between the steel girder and RCC deck slab does not take place. For the analyzed deck type bridge, total load on the bridge in terms of uniformly distributed load in service condition for (DL+LL) case is 131.7kN/m, and in overload condition for $1.5 \times (DL+LL)$ case it is 197.5kN/m. As per analysis, at plastic stage the bridge can carry an equivalent udl of 674.1kN/m. Thus, for the plastic collapse, apart from warning due to excessive deflection, there is a factor of safety of 5.1 in comparison to the service load. For prestressed concrete bridges, load combination at ultimate strength for severe condition (Cl. 12 of IRC: 18-2000) is prescribed as $1.5G+2SG+2.5Q$. IRC codes have not stipulated any specific provision for overload condition and ultimate strength of steel truss bridges. Therefore, a parallel clause for overload condition and ultimate strength of steel truss bridges may also be added in the IRC codes.

KEYWORDS Buckling, Sudden failure, Composite bridge, Under slung truss, Shrinkage strain

INTRODUCTION

Steel-concrete composites are commonly used in building construction. In composite plate girder bridges, the composite construction comprises RCC deck slab connected with steel plate girders with the help of shear studs. Many new ideas on composite truss bridge construction have emerged [1,2], but without design guidelines. Steel truss bridges have higher failure percentage [3] among various types of bridges. In the year 2012, an open web steel girder non composite deck type bridge connecting two cities of Uttarakhand state namely, Srinagar on the left bank and Chauras on the right bank of river Alaknanda, collapsed during casting of the deck slab claiming lives of six people [4]. The failure was due to buckling of one of the top chord compression members of the truss. Failure of the bridge could have been more disastrous, had it failed after completion in overload condition. Another Garudhatti bridge [5], built on the same design was successfully completed, but due to excessive vibrations, it was strengthened before commissioning. As reported earlier, buckling of a compression member in open web steel girder bridges is the most common mode of structural failure [6,7].

Experimental studies on steel concrete composite joists concluded that, not only the composite sections were stronger and stiffer, but the amount of steel used can be considerably reduced [8]. Composite deck type steel truss bridges are one of the most efficient and aesthetically attractive design solution in bridge engineering [9]. One common and efficient solution for this is an under slung truss. When the deck slab is connected with the top chord of the truss using shear studs, deck slab acts in composite action with the compression chord (**Figure 1**). In a deck type composite truss bridge, RCC deck slab provides lateral support to the top chord compression members of the truss and prevents their buckling and premature failure, which permits these to stress up to their ultimate strength. In the Czech Republic twelve simply supported composite underslung steel truss bridges having spans ranging between 21 m to 63 m were completed during last decade [10].

PREVENTION OF BUCKLING

The top chord and web compression members of a simply supported steel truss bridge may buckle much before the tension members reach their ultimate strength (**Figure 2**). Composite action of the RCC deck slab with the top chord compression members prevents their buckling. Shear transfer in composite steel truss bridges between the steel truss and concrete deck slab is mobilised using shear studs.

Due to shrinkage strain in the deck slab, composite action between the steel truss and the deck slab starts only when the shrinkage strain in the deck slab is overcome by the flexural stress due to live load. Therefore, the steel truss may be designed for service condition with fatigue for full dead load and live load, and advantage of the composite section may be derived during overload of the bridge and in its plastic collapse condition.

ANALYSIS FOR SHRINKAGE IN DECK SLAB CONCRETE

In the deck type composite bridge construction, steel truss is first launched and then deck slab and SIDL are cast. After hardening of the deck slab and SIDL, the bridge is opened to traffic. Shrinkage strain in M40 grade deck slab concrete may be taken as 0.0003 [11]. Therefore, composite action between RCC deck and steel truss will not take place until strain in the deck slab concrete exceeds 0.0003.

Geometric details of the analyzed 30m span bridge (**Figure 3**) : Height of truss (c/c distance between top chord and bottom chord members) = 6m, c/c distance between two trusses = 8 m and panel length = 3.0m.

The deck slab is modeled using plate elements, which are connected over the two trusses at every 0.5m interval with the help of rigid studs in rows. STAAD.Pro V8i [12] software has been used for modeling and analysis. As per STAAD analysis result, maximum stress in the deck slab concrete at mid span for live load is found to be 6.06 N/mm² (**Figure 4**). The strain corresponding to 6.06 N/mm² stress (**Figure 4**) is 0.00019, which is less than 0.0003 deck slab shrinkage strain. Therefore, composite action in the bridge will not take place even under full service load condition.

Although, composite action between deck slab and truss is not possible in the service condition, top chord compression members of the truss are laterally supported by the shear connectors and their lateral buckling is prevented. Thereby, higher compressive stress than the buckling stress, up to the ultimate compressive strength, may take place in these members, provided web members are designed to remain safe [13].

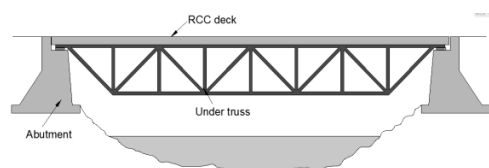


Figure 1 Under slung open web steel girder bridge

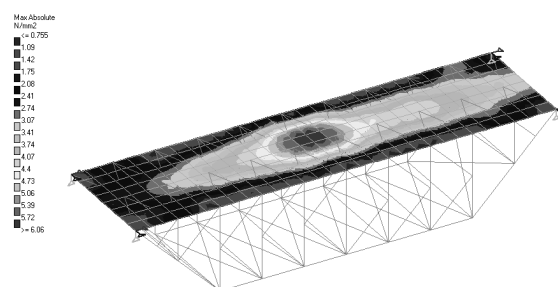


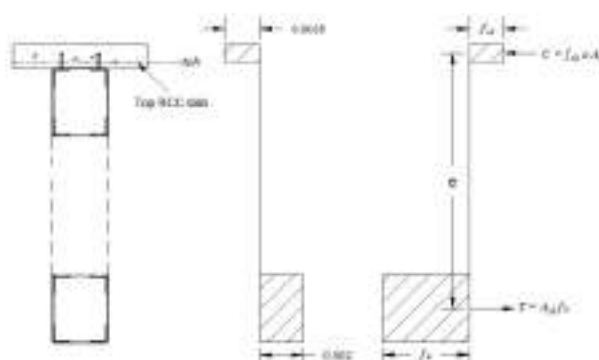
Figure 4 Desk slab stress under LL alone



Figure 2 Stress-strain curves for E-250 structural steel



Figure 3 Elevation of 30 m span bridge



a. Cross section b. Strain diagram c. Stress diagram at mid span

Figure 5 Force equilibrium at plastic collapse



TYPICAL DESIGN OF A 30.0M SPAN COMPOSITE TRUSS BRIDGE

Design of a 30.0m span deck type truss bridge is carried out for serviceability condition as per IRC: 24-2010 [14]. Interactive steel design facility in STAAD Pro.v8i is used, which directly gives interaction ratios under combined axial force and biaxial bending moments. Optimum design of the truss members is carried out using interaction ratio. In the design for overload condition at $1.5 \times (DL+LL)$ load, interaction ratio is limited to 1.0 in all tension members and laterally restrained top chord compression members. For laterally unsupported web compression members it is limited to 0.66.

Live Load during Overload Condition

Ratio of maximum possible live load without impact in the overload condition, and service condition live load with impact, can exceed 2.0.

Ever increasing vehicle load and corrosion of the bridge with time will require even higher load factor at the limit state of strength. Therefore, as applicable in the case of prestressed concrete bridge code (CI-12: IRC :18-2000), composite steel truss bridges may also be checked at failure at an ultimate load of $(1.25G+2SG+2.5Q)$ for moderate exposure condition.

Plastic Collapse Condition

There is no direct literature available for capacity calculation of the composite steel truss bridges in plastic stage [10]. Therefore, design of the bridge at collapse in plastic condition is carried out as per provisions given for composite truss and OWSJ for buildings in CISC 2003 [15] and ASCE Task Committee on Design Criteria for Composite Structures in Steel and Concrete [16]. The design provisions have been modified in accordance with IRC: 24-2010 [14]. For the capacity calculation it has been assumed that the web compression members are sufficiently strong and will not fail before failure of other members.

Details of the composite bridge model for plastic condition are given in **Figure 3**.

The section for plastic design is considered adjacent to the center of the bridge. Hence, only bottom chord and composite top chord carry axial forces. Force equilibrium diagram at the mid span section of the bridge is given in **Figure 5**. As given by Cran [17] and Bouchair, et al [18], area of the top chord truss members below the neutral axis is neglected in calculating the moment of resistance.

a = depth of neutral axis from top of the deck slab; A_{st} = cross-sectional area of steel top chord; A_{sb} = cross-sectional area of steel bottom chord; e = lever arm; b_f = effective width of slab, and f_u = specified ultimate strength of steel.

Equating compression and tension forces: $f_c k a b_f = A_{st} f_u$ or $40 \times a \times (8.0)/2 = 15212 \times 410$

Therefore, $a = 38.98$ mm, eccentricity, $e = 6000 + (200 - 38.98)/2 = 6080.51$ mm.

The plastic moment of resistance (M_p) of the composite section is computed as:

$$M_p = A_{st} \times f_u \times e = 0.030424 \times 410 \times 1000 \times 6.08 = 75840.95 \text{ kNm}$$

Corresponding equivalent UDL on the bridge at plastic collapse ' w_p ' is given by:

$$(w_p \times l^2)/8 = 75840.95 \text{ kNm, or } w_p = 674.14 \text{ kN/m.}$$

Comparisons of Plastic Collapse Load with Service Load and the Overload

Total applied load in service condition, $(DL+LL) = 3951.09$ kN

Equivalent udl = $3951.09 / 30.0 = 131.7$ kN/m

Factor of safety at plastic collapse with respect to service load = $674.14 / 131.7 = 5.1$

Factor of safety at plastic collapse with respect to the overload condition, = $674.14 / (1.5 \times 131.7) = 3.4$

Thus, in the composite steel truss bridge, there is a factor of safety against plastic collapse of **5.1** in comparison to service condition, and **3.4** in comparison to the overload condition.

CONCLUSIONS

Sudden failure of Chauras Bridge, due to buckling of one of its top chord members during casting of the deck slab, has triggered the idea for suitable revision of the design load at the limit state of strength, and construction of composite steel girder bridges. From the presented analytical study on composite steel truss bridges, the following conclusions are drawn.



- ♦ Shrinkage strain in M40 grade deck slab concrete is of the order of 0.0003. Maximum flexural strain due to live load in service condition, in the analyzed 30.0m deck type truss bridge is found to be 0.00019. Therefore, it may be concluded that, there is no composite action of the deck slab even in service condition.
- ♦ Before shrinkage strain in the deck slab concrete is overcome by loading on the bridge, the deck slab provides effective lateral support to the top chord compression members, preventing their buckling, and permitting these to take stress beyond yield stress up to their ultimate compressive strength. Thus, in the overload condition the bridge can excessively deflect but cannot suddenly collapse, provided the web compression members are strong enough.
- ♦ IRC 6:2010 provides for minimum gap between two trains of vehicles, and in the remaining area a load of 5 kN/m^2 is prescribed. Accordingly, maximum possible live load to normal live load ratio works out to 1.7. Ever increasing vehicle load and corrosion of the bridge with time will require even higher load factor.
- ♦ For the analyzed 30.0m span deck type composite steel truss bridge, where it is assumed that premature web failure is prevented, load in terms of UDL in service condition for (DL+LL) case is 131.7 kN/m , and at the plastic stage it is 674.14 kN/m . Therefore, for the plastic stage there is a factor of safety of 5.1 in comparison to service condition and 3.4 for overload condition.
- ♦ As applicable in the case of prestressed concrete bridges (CI-12: IRC: 18-2000), composite steel truss bridges may also be checked at failure at an ultimate load of $(1.25G + 2SG + 2.5Q)$ for moderate exposure condition.

Composite under slung steel truss bridge helps in preventing premature buckling of the top chord compression members, and economically enhances the collapse load in plastic condition to approximately 5.1 times the load in service condition.

REFERENCES

1. A. Reis, J.O. Pedro, Composite truss bridges: New trends, Design and Research, Steel Construction, Volume 4, Number 3, 2011.
2. A. Reis, J.O. Pedro, Composite truss bridges: New trends, Design and Research, Eurosteel Conference, Aug-31st –Sep 2nd, Budapest Hungary, 2011.
3. K. Wardhana, and F. C. Hadipriono, Analysis of Recent Bridge Failures in the United States, Journal of Performance of Constructed Facilities, ASCE, Volume 17, pp. 144-150, 2003.
4. H. S. Birajdar, P. R. Maiti and P. K. Singh. Failure of Chaurasbridge. Engineering Failure Analysis, Elsevier, Volume 45, pp. 339-346, 2014.
5. H. S. Birajdar, P. R. Maiti, and P. K. Singh. Strengthening of Garudhattibridge after failure of Charus Bridge, Engineering Failure Analysis, Elsevier, Volume 62, pp. 339-346, 2015.
6. B. M. Imam and M. K. Chryssanthopoulos, A review of metallic bridge failure statistics, Proc. 5th International conference on bridge maintenance, safety and management, Philadelphia, USA, IABMAS, pp. 635-636, 2010.
7. Z. Šavor, M. Šavor, J. Gao, and M. Franetović, Failures of Arch Bridges Causes, Lessons Learned and Prevention, 3rd Chinese - Croatian Joint Colloquium on Sustainable Arch Bridges, Zagreb, Croatia, 2011, pp. 225-236.
8. H. G. Lembeck, Composite Design of Open Web Steel Joists, Master of Science Thesis, Washington University, St. Louis, MO., 1965.
9. A. J. Reis, Bridge decks: composite systems for improved aesthetics and environmental impact. Proc. 3rd Int. Meeting on Composite Bridges, Madrid, pp. 645, 2001.
10. J. Machacek, M. Charvat. Design of Shear Connection between Steel Truss and Concrete Slab, 11th International Conference on Modern Building Materials, Structures and Techniques, MBMST 2013, Procedia Engineering, Elsevier, Volume 57, pp. 722-729, 2013.
11. IS: 1343-1980, Code of Practice for Prestressed Concrete, India, 1999.
12. User Manual, STAAD.Pro V8i, Bentley Software, 2017.
13. M. H. Azmi, Composite Open-Web Trusses with metal Cellular Floor, Master of Engineering thesis, McMaster University, Hamilton, Ontario, 1972.
14. IRC: 24-2010, Standard specifications and code of practice for road bridges, Section V, Steel road bridges, India, 2010.
15. Canadian Institute of Steel Construction (CISC), Handbook of Steel Construction, CAN/CSA S16.1 94, Section 16, Open-Web Steel Joists, 7th Edition, Willowdale, Ontario, 2003.
16. ASCE Task Committee on Design Criteria for Composite Structures in Steel and Concrete, Proposed Specification and Commentary for Composite Joists and Composite Trusses, ASCE, Journal of Structural Engineering, Volume 122, Number 4, 1996.
17. J.A. Cran. Design and Testing Composite Open Web Steel Joists, Technical Bulletin Volume 11, Stelco, January, p. 28, 1972.
18. A. Bouchair, J. Bujnak, P. Duratna., Connection in Steel-Concrete Composite Truss, Procedia Engineering, Steel Structures and Bridges, Volume 40, pp. 96-101, 2012.



Robust Box Type Minor Bridge

*Pramod K Singh^{*1}, Abhishek Sharma¹, Krishna K Pathak¹
Department of Civil Engineering, IIT BHU, Varanasi, India¹, prof_pks@yahoo.co.in*

ABSTRACT

Corner chamfers in reinforced cement concrete structures are used at numerous locations, but without accounting these as structural elements. Some prominent chamfer uses may be found in box type tunnels and minor bridges. Reinforcement detailing at corner and size of the chamfer are two important issues in accounting for the chamfer as structural element. Whereas, without proper detailing joint efficiency may fall up to one third, chamfer facilitates axial flow of forces through it, and in a box type minor bridge, having say 1.5 times chamfer to its framing arm size, causes framing slab and wall moments to reduce to approximately half.

Design example of a twin box type minor bridge of total span 33.77m is presented. Reduction in moments in the walls and slabs due to axial flow of forces at chamfers is not directly taken in the design, and it is considered to make the structure robust. With proper reinforcement detailing, the chamfer is accounted for in depth of the framing members near corner, and thus, at the chamfer end lower design negative moment and shear are taken for the framing slab and wall.

The estimated cost at Rs 4.0 lacs/m span for the robust bridge, and completion time of less than a year using local technical skill, are very competitive for low scour sites in comparison to the traditional bridges founded in alluvial soil on wells or piles.

KEYWORDS Robust design, Corner chamfer, Box type minor bridge, Tunnel, Reinforcement detailing, Joint efficiency.

INTRODUCTION

Box type minor bridges at low scour sites, due to their simplicity, robustness and cost effectiveness, have gained popularity in recent time. Whereas, continuous boxes can be very economical for rocky foundation, twin boxes having nearly square vents arranged side by side are suitable for stream beds having low bearing capacity and chances of differential settlement (**Figure 1**).

Due to continuous wide base of boxes, the base pressure in box type minor bridges is very low ($\approx 8.0 \text{ N/mm}^2$), and therefore, these can be safely founded on stream beds having low allowable bearing capacity. Also, the monolithic top slab of the box prevents abutment action of the earth retaining vertical wall, and therefore, higher vent size boxes ($\approx 9.0 \text{ m}$ high) can be safely designed.

Unlike bridges founded on deep well or pile foundations, which take long time to construct and need special equipments, it can be constructed swiftly using local technical skill. However, due to shallow foundation, it is suitable only for low stream current velocity ($\approx 2.0 \text{ m/s}$) with U/S and D/S bed protection against scour.

REINFORCEMENT DETAILING AT CORNERS

Corners of the boxes are subjected to corner opening and corner closing moments. Out of the two, corner opening moments need more careful reinforcement detailing [1,2]. A poorly detailed corner joint (**Figure 2**), may have reduced joint efficiency of the order of $1/3^{\text{rd}}$.

Thus, reinforcement detailing at the corners is highly important. It shall consist of loops binding the outer corner, and diagonal bars at the inner corner, of same diameter and spacing as the main reinforcement (**Figure 2**).

CHAMFER AT INNER CORNERS

As per practice, chamfer at inner corner is provided to avoid concentration of stresses and for ease in construction, without considering it as structural member. Harshad [3], using Finite Element Analysis of a plain cement concrete box, has shown that chamfer reduces moments in the box. This is due to part of the load transfer taking place axially through the chamfer, rather than full slab load being transferred to the supports by way of flexure. In the case of chamfer size of 1.5 times the framing slab size, positive B.M. in the deck slab at bottom in the mid-span, and negative B.M. at top at the support reduce to about half in comparison to the bending moments for the no chamfer



case. In addition to this, negative B.M. near support becomes governing at the chamfer end, where it is quite less in comparison to the corner moment for no chamfer case. In fact, slab depth is no longer governed by the negative moment at the support, and it is now governed by the positive slab moment at the mid-span.

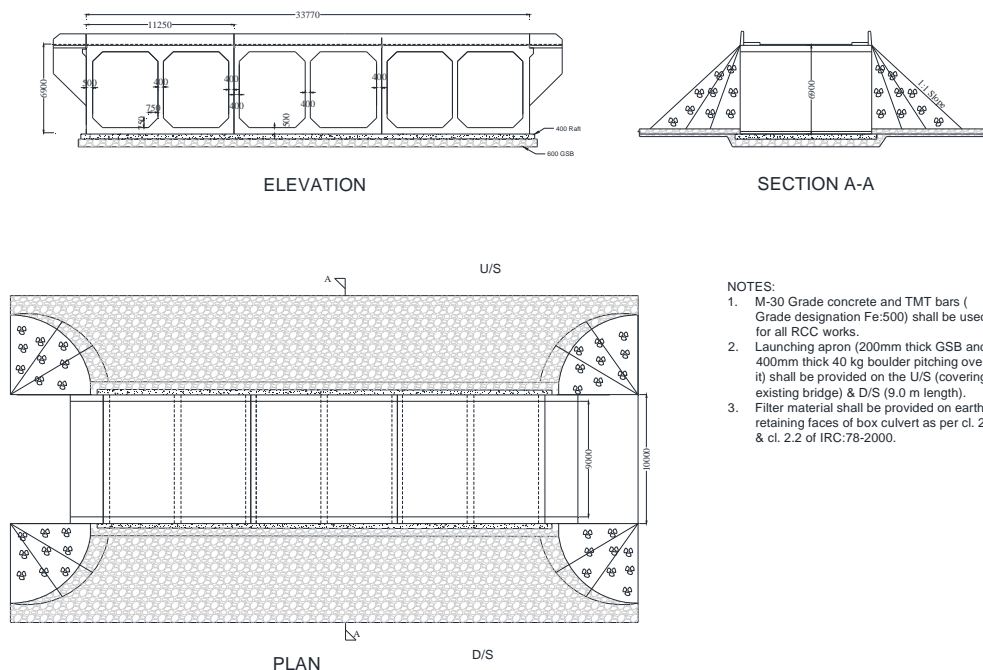


Figure 1 Typical GAD

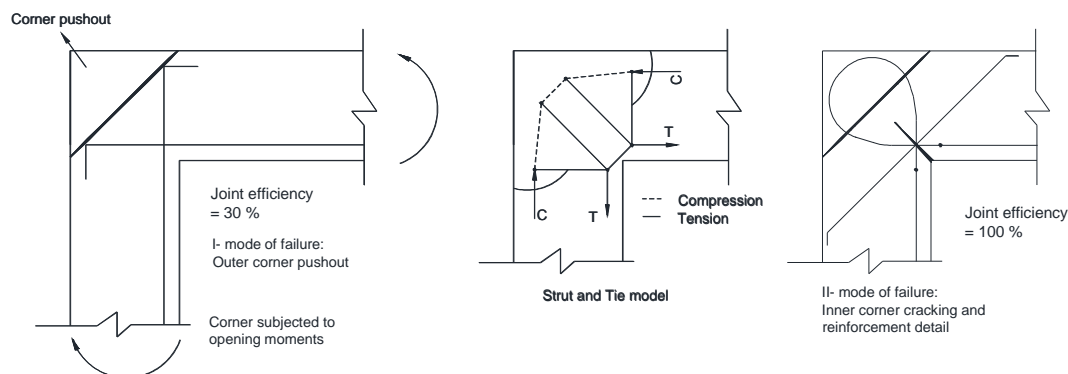


Figure 2 Corner cracking, STM and reinforcement detail

TYPICAL DESIGN EXAMPLE

Analysis and design of a typical box type minor bridge of 33.77m total span, comprising three twin boxes of 11.25 m \times 6.9 m \times 10.0 m each, is presented..It is designed for two lanes Class-A IRC loading.

Analysis is carried out for the following basic loads.

- Dead load including wearing coat (DL),
- Earth pressure with surcharge (EP), and
- Live load including impact (LL).

The following critical load combinations are used to compute the absolute maximum BM and SF envelopes.

- DL + EP
- DL + EP + LL



ANALYSIS

STAAD center line diagram for the side twin box is shown in **Figure 3**. It may be noted that the chamfer effect is not accounted for in the analysis.

Moving load STAAD analysis is performed for LL, and the bridge is designed as per provisions of IRC-21:2000. Net allowable bearing capacity at the foundation level for the soil is taken to be 80.0 kN/m^2 .

ENVELOPS OF BM AND SF

The envelop of BM showing design moments at chamfer ends is given in **Figure 4** and the envelop for SF is given in **Figure 5**.

DESIGN

BMs obtained from STAAD analysis at the chamfer ends (**Figure 5**) are used for the design purpose. Slab is generally safe in shear, but still it is checked for safety at $d/2$ distance from the chamfer ends. The resulting sections and reinforcement diagram are shown in **Figure 6**.

COST ESTIMATE

The abstract of cost for the bridge is given in **Table 1**.

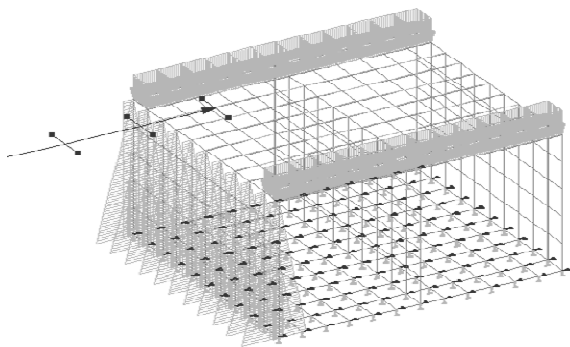


Figure 3 STAAD model with loading

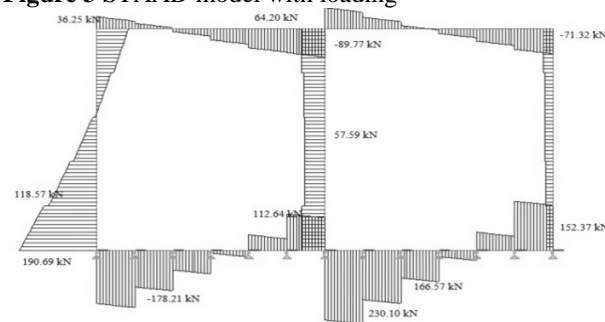


Figure 5 Envelop of shear force at $d/2$ from chamfer ends

Table 1 Abstract of cost

Item	Quantity	Unit rate	Cost, lac Rs
M-30 concrete	719.2 m^3	Rs10,000/ m^3	71.9
Fe-500 bars	474.9 q	Rs 6,000/q	28.5
Add miscellaneous @ 30 %			30.1
Grand Total			130.5

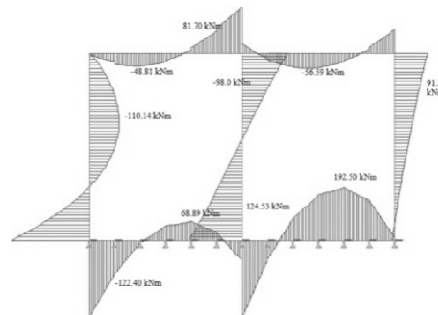


Figure 4 Envelop of BM showing design moments at corner ends

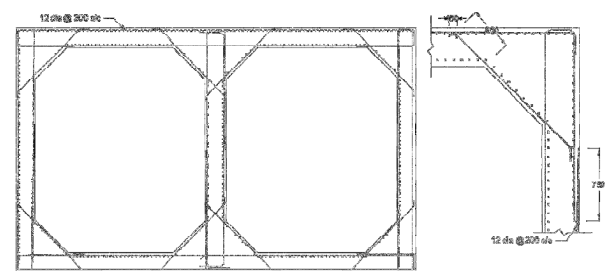


Figure 6 Reinforcement detail for central twin box

Notes:

1. All exterior walls and slabs are 500 mm thick, and all interior walls are 400 mm thick.
2. All main steel and corner bars consist of 16mm dia. bars @ 200 mm c/c, except exterior side longitudinal steel in compression zone which is 12 dia. @ 200 mm c/c.
3. All transverse steel consist of 12 mm dia. bars @ 200 mm c/c.
4. Due to earth pressure, the end twin boxes have additional unsymmetrical reinforcement.



Cost per meter run of the bridge = $130.5/33.77 \approx \text{Rs. 4.0 Lacs / m span}$.

Total cost of the minor bridge is estimated at Rs 4.0 lacs /m run. Completion time for the bridge is estimated to be less than one year.

CONCLUSION

Due to axial transfer of forces through chamfers, chamfers of the recommended size of 1.5 times the framing arm thickness, reduce the negative and positive bending moments in the framing slabs and walls to approximately half. However, in the presented design case this effect is assumed only to result in a robust design.

A very competitive cost of the minor bridge at Rs 4.0 lacs/m span is estimated, with a short completion period of less than a year.

In comparison to traditional bridges founded on wells and piles, box type minor bridges with corner chamfer are presented to be robust and highly competitive for streams having low scour tendency. Structural use of corner chamfers with proper reinforcement detailing is also recommended in other similar situations.

REFERENCES

1. P. K. Singh and H. S. Chaturvedi, Joint Reinforcement: Strut-and-Tie Model, Concrete International, ACI, Jan. 1998.
2. V. N. Dhar and P. K. Singh, Chamfering and Reinforcement Detailing in Reinforced Concrete Corner Subjected to Opening Moment, J of Institution of Engineers (India), Volume 84, 2004.
3. S. B. Harshad, Finite Element Analysis of Box Culverts with and without Haunches, M.Tech. Dissertation, Department of Civil Engineering, IIT (BHU), Varanasi, India, 2012.



Strategic Plan for the Development of NH Network in Kerala: A Case Study of Kozhikode Division in Kerala

V S Sanjay Kumar

National Transportation Planning and Research Centre, Kerala, India, sanjayvs@gmail.com

Abstract

National Highways (NH) forms the economic backbone of a country and has facilitated development along their routes. NH constitutes 1.7% of Indian roads and carries 40% of the traffic. Road network in Kerala carry fast and slow vehicles and pass through built-up areas. The growing mismatch between vehicle population and road infrastructure has resulted in heavy traffic densities and reduced level of service. Entire Kerala region can be considered as a metropolis consisting of a large number of closely situated townships, which obstruct the free flow of traffic. The deficiencies in the road network cause delay in movement of freight and passengers. The transport infrastructure deficiency is one of the major obstacles in the development of tourism, and other industries including information technology. The national highway network will have to be improved to meet the growing passenger and freight traffic. In this context, a perspective plan has been envisioned for the NH network in Kozhikode division, of Kerala state, on a demonstration mode. The corridors include NH 66 from Idimoozhikkal to Poozhithala (75.30 km) including the bypass section from Nisary junction to Vengalam and NH 766 from West Hill to Wayanad District border (53.30 km). The study was undertaken with a detailed methodology, which included reconnaissance survey, demarcation of study stretches and homogeneous sections, collection of data from secondary sources, design and conduct of primary surveys including road inventory and traffic surveys, compilation, analysis and interpretation of the collected data, formulation of development options and economic analysis. It could be seen that the Volume-Capacity ratio (V/C) of the links even at the base year itself, was upto to 2.29. This necessitates improvement of the road for catering to the easy flow of the current traffic. As far as intersections are concerned, the maximum peak hour traffic flow was upto 6300 PCU. Different development options have been identified to ensure a free and safe traffic movement which included construction of paved shoulders, construction of grade separators at major intersections, four/six laning of NH sections etc. Economic analysis was carried out using Benefit-Cost method (B-C). The benefits included the savings in travel time, savings in fuel and reduction in pollution, all of which were converted into monetary values. The costs accounted were the cost for upgradation to four lane carriageway with flyovers in the major intersections including the maintenance cost for 15 years. For both the study corridors, it is observed that the B-C ratio is above one, which proves that the suggested development options are economically feasible.

KEYWORDS National Highway, Traffic, Economic Analysis, Benefit - Cost

INTRODUCTION

India has the second largest road network in the world. National Highways (NH) form the economic backbone of the country and have often facilitated development along their routes. National highways constitute 1.7% of Indian roads and carry 40% of the traffic. Road network in Kerala carry fast and slow vehicles and pass through built-up areas. The growing mismatch between vehicle population and availability of road infrastructure has resulted in heavy traffic densities and reduced level of service. Entire Kerala region can be considered as a metropolis consisting of a large number of closely situated townships, which obstruct the free flow of traffic. The deficiencies in the road network cause delay in movement of freight and passengers. The transport infrastructure deficiency is one of the major obstacles in the development of Tourism, and other industries including information technology. The national highway network will have to be improved to meet the growing passenger and freight traffic. A large section has insufficient road pavement thickness. Other deficiencies are poor riding quality, weak and distressed bridges/culverts, congested city sections, lack of wayside amenities and weak road safety measures.

Kerala has a NH network of 1747 km comprising of 11 NHs. Of these NH 66 and NH 544 are the major carriers of traffic that plies along the North-South and East-West directions. The present paper discusses a perspective plan for the NH network in Kozhikode division, one of the divisions in the state.

OBJECTIVE

The objective of the study was to develop a perspective plan for NH sections in Kozhikode division on a demonstration mode. The corridors included NH 66 from Idimoozhikkal to Poozhithala (75.30 km) including the bypass section from Nisary junction to Vengalam and NH 766 from West Hill to Wayanad District border (53.30 km). The following tasks were undertaken to accomplish the targeted objective.

- Inventory of the corridors



- Traffic volume studies and estimation of link volume, intersection volume and anticipated traffic
- Speed and delay studies to identify the stream speed and average delay
- Pedestrian movement survey
- Identification of specific interventions in the form of intersection improvements, necessity of grade separators, bypasses, pedestrian grade separators etc
- Quantification of benefits accrued with the various suggested interventions
- Economic analysis of the suggested interventions

METHODOLOGY ADOPTED

The study was undertaken with a detailed methodology, which is depicted in **Figure 1**.

STUDY AREA

Kozhikode district is bounded by Kannur, Wayanad and Malappuram Districts in the North, East and South respectively. The road network under consideration is a part of National Highway 66 and 766. The study stretch on NH 66 starts from Poozhithala and passes through Vadakara, Koyilandi, Vengalam, Thondayad, Ramanattukara and terminates at Idimoozhikkal. The network includes 28.12km Kozhikode bypass, forming a part of the NH 66 that stretches from Vengalam to Idimoozhikkal. Right of Way (RoW) of 45m is available for the bypass. NH 766 passes mainly through junctions such as Eraniel, Kunnamangalam, Thamarasseri and Adivaram.

The RoW and carriageway width of the sections varies from 10.5m to 45m and 7m to 8m respectively for the two NHs. Based on the land use, traffic and topography, both highways are divided into 12 and nine homogeneous sections respectively (**Table 1**).

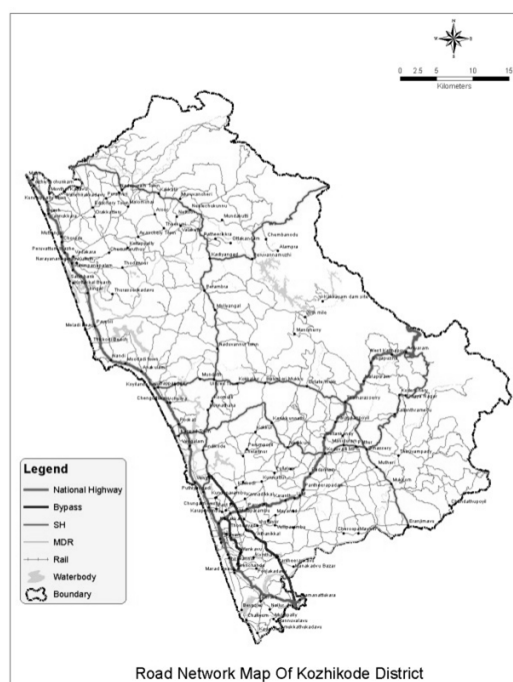
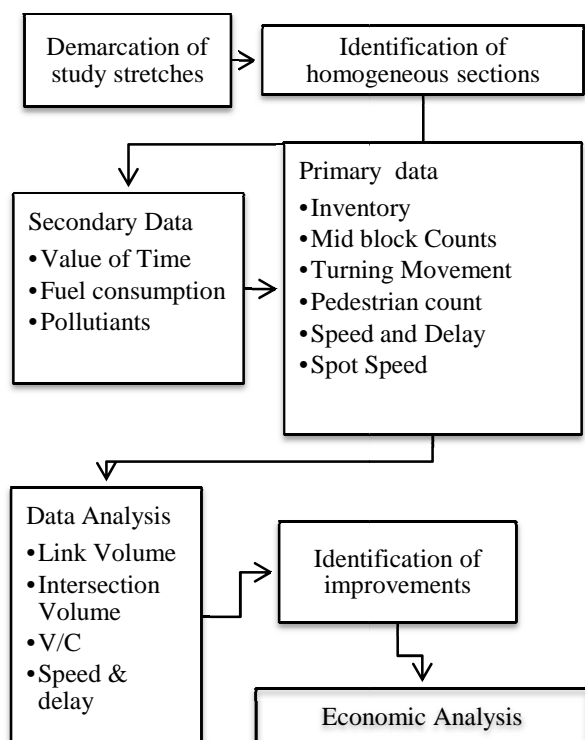


Figure 2 Study area map

Figure 1 Methodology adopted



TRAFFIC SURVEYS AND ANALYSIS

Link Volume and Volume-Capacity Values

Traffic volume data was collected for all the demarcated links. On NH 66 the daily traffic volume has been found to be the maximum for the Koyilandy-Payyoli link with 40000 PCUs followed by Payyoli-Vadakara link with 37,200 PCUs. For NH 766, Karanthoor-Kunnamangalam link possessed the maximum daily traffic with PCU value 34000 followed by Eranhipalam-Malaparamba link with 29000 PCU.

The traffic volume in the two NHs was compared with the capacity of road sections to calculate the Volume-Capacity ratio (V/C). It could be seen that the V/C of the links on NH 66, even at the base year itself, varies from 1.00 to 2.29. Similarly V/C ratio on NH 766 varies from 0.78 to 2.23. This necessitates improvement of the road for catering to the easy flow of the current traffic.

Table 2 summarises the traffic scenario in the study network.

Table 1 Homogeneous Sections

ID	Section	Length, km
L-01	Idimoozhikal - Nisari	0.8
L-02	Nisari-Ramanattukara	0.72
L-03	Ramanattukara-Thondayad	13.1
L-04	Thondayad-Malaparamba	2.7
L-05	Malaparamba-Vengeri	1.9
L-06	Vengeri-Pooladikunnu	5.2
L-07	Pooladikunnu - Vengalam	4.7
L-08	Vengalam-Thiruvangoor	1.3
L-09	Thiruvangoor-Koylandi	9.01
L-10	Koylandi-Payyoli	12.6
L-11	Payyoli-Vadakara	12
L-12	Vadakara-Poozhithala	13.1
L-13	West hill -Karaparamba	0.9
L-14	Karaparamba - Eranjipalam	1.7
L-15	Eranjipalam - Malaparamba	9.5
L-16	Malaparamba - Karanthoor	2.5
L-17	Karanthoor - Kunnamangalam	10.3
L-18	Kunnamangalam - Koduvalli	8.6
L-19	Koduvalli-Thamarassery	14
L-20	Thamarassery-Adivaram	7.8
L-21	Adivaram - District Border	11.9

Table 2 Traffic scenario in the network

Link	Capacity, PCU/ day	Volume, PCU/ day	V/C
L-01	15000	30771	2.05
L-02	17250	37200	2.16
L-03	17250	39477	2.29
L-04	17250	34961	2.03
L-05	17250	27877	1.62
L-06	17250	17282	1.00
L-07	17250	24368	1.41
L-08	15000	30856	2.06
L-09	15000	27462	1.83
L-10	15000	23412	1.56
L-11	15000	22143	1.48
L-12	15000	32893	2.19
L-13	14000	10916	0.78
L-14	14000	28220	2.02
L-15	14000	28942	2.07
L-16	15000	25928	1.73
L-17	15000	33519	2.23
L-18	11000	20849	1.90
L-19	11000	20823	1.89
L-20	7000	14132	2.02
L-21	7000	12916	1.85

INTERSECTION VOLUME

Turning movement surveys at major intersections were conducted to ascertain the peak hour demands. Thondayad had the maximum peak hour traffic flow of 6300 PCU, while Malaparamba had a peak hour flow of 4800 PCU. The traffic details of intersections are shown in **Table 3**.

ESTIMATION OF TRAVEL TIME DELAYS

The entire network has been found to experience traffic delays. Moving car observer survey was carried out to determine the average delay. The data was cumulated for the whole traffic by multiplying with the total traffic in a link-wise manner to obtain the total delay along the network.

**Table 3** Peak hour volume at major intersections

Intersection	Peak hour	Peak traffic, PCU
Nisari	4:45pm to 5:45pm	2555
Ramanattukara	8:15am to 9:15am	3223
Thondayad	5:30pm to 6:30pm	6299
Malaparamba	9:15am to 10:15am	4818
Vengeri	5:45pm to 6:45pm	3338
Pooladikunnu	8:00am to 9:00am	2465
Vengalam	8:45am to 9:45am	1723
Thiruvangoor	4:00pm to 5:00pm	2154
Koyilandy	10:00am to 11:00am	3910
Payyoli	4:15pm to 5:15pm	2703
Vadakara	11:00am to 12:00pm	4446
Westhill	3:30pm to 4:30pm	2542
Karaparamba	5:30pm to 6:30pm	3607
Eranhipalam	9:15am to 10:15am	5558
Malaparamba	9:15am to 10:15am	4818
Karanthoor	3:00pm to 4:00pm	2154
Kunnamangalam	9:00am to 10:00am	3599
Koduvally	5:30pm to 6:30pm	2469

DEVELOPMENT STRATEGY

Taking into consideration of the traffic characteristics as well as the infrastructure options, a development plan is prepared for the NH network in Kozhikode. The plan takes into account the existing traffic scenario and is based on an evaluation of the future traffic on the base year network. Some of the possible interventions/improvements that can be considered are: Construction of paved shoulders, Intersection improvements, Construction of grade separators at major intersections, Four/Six laning of NH, Segregation of pedestrian movement and Provision of two wheeler tracks etc.

Based on the warrants of traffic, a strategy has been worked out to be implemented in a phase wise manner.

Phasing

The identified development options have been proposed to be implemented in phases. Phase I is in the base year itself viz 2017 and Phase II is by the year 2022 which is five years from the base year. The suggested phasing is as follows:

Phase I: Construction of paved shoulders and Improvement of Intersections.

Phase II : Four laning of NH 66 and Construction of grade separators.

Economic Feasibility

An economic analysis was carried out for assessing the feasibility of the suggested plans. Benefit- Cost analysis was carried out considering the benefits that can be achieved once the development plans are implemented. While computing the costs due to delays, environment cost is also accounted.

Benefits due to Developments

The envisaged development options will result in overall improvement of the traffic scenario in the NH, decreased travel time being the most prominent. The delays in travel time greatly contribute to the total travel cost. The total cost due to traffic delay is comprised of different costs, primarily of travel time delay, costs of fuel loss and pollution costs. The reduction of the delay can be assigned as the total benefits.

Travel Time Cost

The Travel Time Cost (TTC) is the total cost incurred due to the additional time spent on travel and is a function of the occupancy of vehicles and the Value of Travel Time (VOT). VOT is the monetary value that a person will be ready to pay for a unit travel time reduction

$$TTC_i = \sum_i (TTD \times VOT \times O \times N) \quad (1)$$

Where, i = Mode, TTD = Travel time delay, VOT = Value of travel time, O = Occupancy and N = Number of vehicle type i .



The VOT for different mode users was taken after Bivina et al [2] as Rs 31.02, Rs 172.5 and Rs111.42 for users of bus, car and two-wheelers respectively. Passenger occupancy for bus, car and two-wheeler were obtained as 42, 2.11 and 1.42 for bus, car and two-wheeler respectively.

Fuel Loss Cost

The Fuel Loss Cost (FLC) is the cost attributed towards fuel spent due to additional travel time.

$$FLC = IFC \times TTD \times FR \times N \quad (2)$$

where IFC= Idling Fuel Consumption, FR = Fuel Rate and N = Number of vehicles of type i.

To assess the average delays to the vehicles, speed and delay survey was conducted using floating car method. The idling fuel consumption in ml/h of different type of vehicles is taken as per Pal and Sarkar, 2012 [5]. The economic loss of fuel for each vehicle was calculated by multiplying fuel loss with the prevailing cost of fuel. The idling fuel consumption for different types of vehicles is shown in **Table 4**.

Pollution Cost

Due to additional travel time, more pollution will be resulted and the corresponding cost, Pollution Cost (PC) is determined by multiplying emission factors of each pollutant with the traffic volume and the delay estimated for each type of vehicle along with the cost of pollutant. When the vehicle is in idle, the amount of pollutant emitted is considerably higher. Each pollutant is converted to CO₂ equivalent and then converted into monetary values.

$$C = N \times E \quad (3)$$

$$PC = C \times D \times P \quad (4)$$

Where, C = Concentration of pollutant, N= Vehicle population, E = Emission factor of the vehicle, PC = Pollution cost, C= Concentration, D= Delay and P= Cost per kg of pollutant.

COST BENEFIT ANALYSIS

Cost for Development

The improvements suggested were mainly the widening of carriageway, construction of grade separators, shoulders etc. The cost for flyover construction, widening, routine and periodic maintenance was worked out considering a discount rate of 10 %.

Benefits

The total cost due to Travel time delay, which is the sum of travel time cost, fuel loss cost and pollution cost will be the benefits of the project.

Cost-Benefit Ratio

Table 5 depicts the total costs, benefits envisioned and the B/C of links in the network. It can be seen that most of the sections have B/C more than 1. The overall B/C is found to be more than 1 for the network. The Internal Rate of Return (IRR) method was also carried out for these sections and it is found to be higher than the interest rate that is prevailing in the present.

Table 4 Idling fuel consumption of modes

Vehicle	Fuel used	Fuel consumption, ml/min
Two wheeler	Petrol	2.975
Car	Petrol	9.55
Car	Diesel	11.75
Bus	Diesel	15.5

Source: Pal &Sarkar, 2012



Table 5 Benefit cost analysis

Section	Length, km	Delay/Day, min	VOT per day, lakhs Rs	FLC per day, lakhs Rs	PC per day, lakhs Rs	Benefits per day, lakhs Rs	Capital cost, croresRs	Discounted benefit, croresRs	B/C
Pooladikunnu-Malaparamba	7.1	11113.64	0.34	10.35	52.7	63.39	263	1145.84	4.36
Malaparamba-Thondayad	2.8	10255.74	0.22	9.24	1.44	10.90	184	194.18	1.06
Thondayad-Pantheeramkavu	6.4	11932.54	0.50	14.37	2.2	17.07	242	300.35	1.24
Pantheeramkavu - Ramanattukara	6.9	15714.92	0.48	11.68	2.44	14.60	257	256.00	1.00
Ramanattukara-Idimoozhikkal	1.1	30026.4	0.70	23.18	3.79	27.67	83	490.28	5.91
Vengalam-Koilandi	10	4410.445	0.10	3.44	0.51	4.05	350	71.77	0.21
Koilandy-Payyoli	13	10326.9	0.31	8.05	1.12	9.48	490	166.39	0.34
Payyoli-Vadakara	9.6	51805.97	1.55	3.67	6.02	11.24	388	774.33	2.00
Vadakara -Mahe	15	18481.55	0.39	9.54	1.63	11.56	500	203.30	0.41
West Hill-Malaparamba	5.3	27874.47	1.08	40.13	3.28	44.49	259	786.70	3.04
Malaparamba-Kunnamangalam	9.9	3946.8	0.14	4.32	4.55	9.02	297	87.17	0.29

CONCLUSION

Based on detailed studies, base line data pertaining to vehicular traffic flow in the National Highway network in Kozhikode has been prepared. It has been found that the vehicular traffic is higher than the capacity in all the links. Based on a conservative growth rate, the traffic has been projected and it has been found that the volume-capacity ratio in all the links will be very high in a do-nothing scenario.

Proposals have been arrived at to be implemented on a phase-wise manner which includes provision of paved shoulders, intersection improvements, widening of roads, grade separators at major intersections etc.

A Cost-benefit analysis was carried out in all the homogenous sections selected. The benefits accounted were the cost saving as Fuel, Time and Pollution. The Cost accounted were the cost for upgradation to a four lane carriageway with the flyovers in the major junctions including the maintenance cost for 15 years. The cost and benefits was converted to the base year's rate. In both NH 66 and NH 766 it is observed that the B/C is above 1. Thus the economic feasibility of the development options is also established.

ACKNOWLEDGEMENT

The author expresses sincere gratitude to the Kerala State Council for Science, Technology and Environment (KSCSTE), Government of Kerala for providing necessary financial assistance for the project. Acknowledgements are due to Dr A Veeraragavan, Chairman, Research Council of NATPAC and Dr B G Sreedevi, (former Director, NATPAC) for the overall guidance. Thanks are also due to project engineers in NATPAC including Mr Vishnu Mohan, MsSuby Charles and MsVishnumaya K V for the general assistance during field data collection and analysis.

REFERENCES

1. Aditi Singh, P. S. (2009). Determination of Congestion cost in Central Business District of New Delhi - A Case Study, Journal of Indian Road Congress, pp.129-141.
2. Bivina G R, VishrutLandge and Sanjay Kumar V S, Socio Economic Valuation of Traffic Delays, TransportationResearchProcedia Volume 17, pp 513 – 520, 2016.
3. Pal &Sarkar (2012), Delay, fuel loss and noise pollution during idling of vehicles at signalized intersection in Agartala city, India- Civil and Environmental Research, Volume 2, Number 6, ISSN 2222-1719.
4. Ravindra Kumar, PurnimaParida, DeveshTiwari, and S. Gangopadhyay, Idling Emission at Intersection and Exploring Suitable Mitigation Measures, Journal of Traffic and Logistics Engineering, Volume 1, Number 2, pp.184-190, 2013.
5. IRC:64-1990, Guidelines for Capacity of Roads in RuralAreas, Indian Roads Congress, New Delhi
6. Strategic Plan for the Development of National Highway Network in Kerala, Study Report, NATPAC, India, 2017.



Load-Settlement Behavior of Geogrid-Reinforced Sand Bed over Granular Piles

Sateesh Kumar Pisini¹, Swetha Priya Darshini¹, Sanjay Kumar Shukla²

School of Building and Civil Engineering, Fiji National University, Fiji¹, sateesh.pisini@fnu.ac.fj*

Discipline of Civil and Environmental Engineering, Edith Cowan University, Australia²

ABSTRACT

Granular piles are a popular ground improvement technique in soft cohesive soils as well as for loose non-cohesive soils. The experimental study was conducted on granular piles in medium dense and loose sands of 60% and 30% relative densities, respectively. The sand beds have geogrid reinforcements over the granular piles. Group piles of up to 5 numbers were placed at spacing, $S = 2d, 3d, 4d$, with d denoting diameter for the piles (diameter = 50 mm) and a length of 0.4 m. The piles were consistent through the series of experiments performed. The load carrying capabilities of the sands and different granular piles modifications observed by applying calculated pressure on square footings, provided evidence that the reinforcements effect increases proportionally to the load bearing capacity of the piles. In addition, an increase in spacing between the piles reduced settlement and compactness for both the medium dense and loose structured soils. It is observed that the load shared by the pile group is relatively small in unreinforced case compared with the reinforced case. Also, the settlement reduction is higher in reinforced case compared with an unreinforced case, especially in the case of loose sand.

KEYWORDS Granular pile structures, load-bearing capacity, settlement and compactness, geogrid reinforcement, sand types.

INTRODUCTION

Generally, construction engineers, architects and geotechnical engineers face daunting tasks of designing safe structures economically on difficult soil conditions. The unfavorable soil conditions include loose soils, poorly graded soils and clays with soft saturation levels of considerable depths. Also, soils with varying densities and non-uniform subsoil patterns of hard crust with limited depth create problems. All these situations require special attention by the project engineers. Presence of thin layered lenses in sand beds or soft clay deposits also need proper handling. Granular piles which are also called stone columns are increasingly getting more common as techniques of ground bearing enhancement in not only soft cohesive soils but also in non-cohesive soil types as reported by Ranjan, et al. [1]. In non-cohesive soil types where there are probable chances for liquefaction because of dynamic tectonic processes, soils with vibro-replacement properties help prevent the process of liquefaction from occurring. The stone column enhances the ground bearing strength due to the higher compactness of the structural columns in comparison to the soil surface thus bearing a significant proportion of the weight. The pressure is distributed evenly among the piles in non-cohesive soil, thus protecting the soil from liquefaction under seismic pressure. The study conducted by Chandrasekaran, et al. [2] and Latha and Murthy [3] proved that reinforced sands with geogrids had better engineering properties than unreinforced. Experimental results achieved by Jagannatha et al. [4] and Sharma et al. [5] concluded that the granular pile properties enhancement is because of reinforcing the sand beds. Alwaji [6] discussed the potential benefits of geogrid-reinforced sands over collapsible soil to control wet-induced collapse settlements. Shenthnan [7] reported that during earthquakes, saturated loose soils and plastic sand with silt deposits are subject to liquefaction. Experimental studies conducted by Elgamal [8] reported that sand deposits densified by vibro-replacement stone column techniques are more resistant to liquefaction during tectonic processes. Stone columns are essential in cohesionless soil types with high chances of liquefaction. Malarvizhi and Ilamparuthi [9] conducted a number of experiments on stone columns encased with geogrid on soft marine clay. Sharma et al. [5] conducted experiments to observe the resulting effects of reinforcements on granular piles in soft clay. They found decrease of bulging effect in granular piles and increase of load bearing capabilities of soil. Laman and Yildiz [10] highlighted the figurative forecasts of final bearing capacities of foundations inclined on sand beds with and without structural reinforcements in place. Deb et al. [11] developed a model operating mechanically to evaluate behaviors of geosynthetic-reinforced granular soils improved with granular piles. Koushik, et al. [12] studied the behavior of many layered geosynthetic-reinforced granular fills over stone columns-reinforced soft soils by use of mechanical models. Phanikumar, et al. [13] performed a series of tests on coarse sands compacted to medium densities of 50% and studied methods of enhancing bearing capabilities. Senthilkumar and Muthukkumaran [14] performed lateral load experiments in double piles of group driven configurations in various soil types, specifically sand types of poor, medium and high relative densities of 30%, 45% and 70%. Ayadat, et al. [15] conducted a series of experiments

where sand columns reinforcement was by plastic, steel and aluminium materials. Samadhiya, et al. [16] observed the behavior of single unit of erected stone column reinforced by horizontal geogrid layers in soft clay soil. Gneil and Bouazza [17] conducted series of small-scale model tests to observe effect of encasement length variations in reducing bulging effects. Deb, et al. [18] conducted a series of experiments to find the effect on sand bed reinforced by geogrid on stone columns. Murugesan and Rajagopal[19] performed laboratory tests on geosynthetic encased stone columns to determine geogrid reinforcements on single units and group piles of granular column piles. Koushik, et al.[20] performed a series of tests for enhancing the qualities of soft clay with and without technical structural reinforcements and bed on top of a stone column. As reported above, it is evident that most of the tests are on reinforced sand beds over granular piles within the weak clay soils. Researchers conducted experimental studies on geogrid reinforced sand bed over stone columns strategically placed in loose to medium dense sands to study the load-carrying behavior. Granular piles and use of geosynthetics are most cost-effective ground improvement techniques for improving soft/weak soils for any region. They can be applied to both shallow and deep weak soils especially for road, railway and earthen embankments. In the present study, a number of tests were conducted on unreinforced and geogrid-reinforced sand beds on a group of stone columns.

STUDY FINDINGS

A series of practical models were conducted on square footing on sand bed over stone columns that are geogrid-reinforced.

MATERIALS USED

The type of soil in this investigational experiment was dry Ranipur sand. The grain-size particle distribution of the soil is shown in **Figure 1**. According to Unified Soil Classification Systems, the soil is classified as poorly graded sand (SP). The other mechanical qualities of soil composition were determined in the laboratory tests as per the relevant Indian standards are in **Table 1**. The angles of internal friction of sands at relative densities of 60% and 30% were determined. The values of angle of internal friction were found as 29.5° and 37° for relative densities of 30% and 60%, respectively.

Table 1 Properties of Ranipur sand

Property	Value
Soil type	Poorly graded
Particle size, D_{10} , mm	0.16
Coefficient of uniformity, C_u	1.84
Coefficient of curvature, C_c	0.93
Specific gravity, G	2.60
Maximum dry weight, γ_{dmax} , kN/m ³	17.4
Minimum dry weight, γ_{dmin} , kN/m ³	14.1
Unit weight of sand at $D_r = 30\%$, kN/m ³	15.3
Unit weight of sand $D_r = 60\%$, kN/m ³	16.0
Angle of friction internally at $D_r = 30\%$	29.5°
Angle of friction internally at $D_r = 60\%$	37°
Cohesion at $D_r = 30\%$, kPa	2.8
Cohesion at $D_r = 60\%$, kPa	3.45

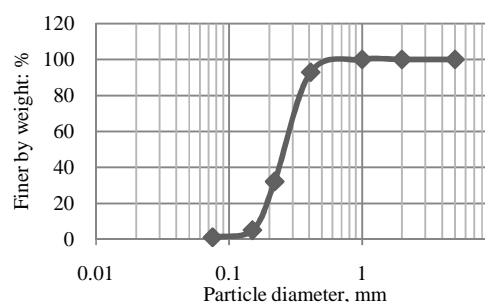


Figure 1 Particle-size distribution of Ranipur sand

The substance constituting the granular pile is an artificial crushed stone material of size 0.1 cm to 0.8 cm. After assortment of stone column material, sieving through 6 mm and 2 mm sieve. The fraction that passed through the 0.6 cm sieve but retained on the 0.2 cm sieve makes up the granular pile materials. Grain size distribution of stone column material is in **Figure 2**, and its properties are in **Table 2**.

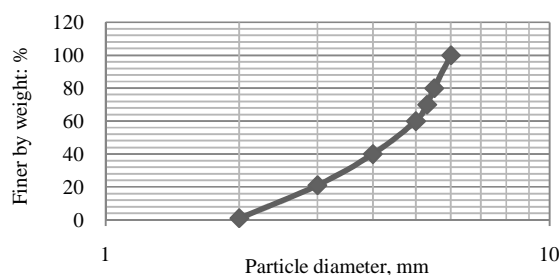


Figure 2 Particle-size distribution for stone column

Table 2 Properties of stone column aggregate

Parameters	Value
Classification	GP
Specific gravity	2.7
Maximum dry unit weight, γ_{dmax} , kN/m ³	17.2
Minimum dry density, γ_{dmin} , kN/m ³	15.1
Cohesion at $D_r = 70\%$, kPa	2
Angle of internal friction at $D_r = 70\%$	47°
Unit weight at $D_r = 70\%$, kN/m ³	16.5
Coefficient of uniformity, C_u	2.3



material

Coefficient of curvature, C_c

0.931

Geogrid material needed for geogrid reinforcements of the sand bed over granular piles is from Netlon Company, India. Random experiments were conducted on the geogrid to understand its features, qualities and advantages. Pull out experiments were performed on geogrid embedded in the sand to know the internal friction between sand and geogrid. The properties of geogrid are given in **Table 3**.

EXPERIMENTAL SETUP

Experimental investigation done on the group of stone columns with and without geogrid reinforcement at different relative densities to test consistency. A testing tank cuboids shaped with a square base of 1.4 m and 1 m length was made for this study. Five steel pipes with radius 25cm and length 40 cm is for filling up the granular material. A 30 cm square footing was used for this study.

Table 3 Properties of Geogrid

Parameters	Value
Netlon identification	Square mesh
Aperture size	4 mm × 4 mm
Thickness	3.0 mm
Mass per unit area, g/m ²	525
Interface friction angle with sand at $D_r = 30\%$	19.7°
Interface friction angle with sand at $D_r = 60\%$	24.7°
Pick tensile strength (uniaxial), MPa	30
Tensile modulus, GPa	4

Table 4 Summary of the experimental cycle

No.	Footing size	Diameter of stone column	Sand the bed thickness	D_r	s/d ratio	Experiments conducted
1	0.3 m	50 mm	0.4 m	30%	2	Unreinforced
2	×0.3 m					Reinforced with 1GL
3						Reinforced with 2GL
4				60%		Unreinforced
5						Reinforced with 1GL
6						Reinforced with 2GL
7				30%	3	Unreinforced
8						Reinforced with 1GL
9						Reinforced with 2GL
10				60%		Unreinforced
11						Reinforced with 1GL
12						Reinforced with 2GL
13				30%	4	Unreinforced
14						Reinforced with 1GL
15						Reinforced with 2GL
16				60%		Unreinforced
17						Reinforced with 1GL
18						Reinforced with 2GL

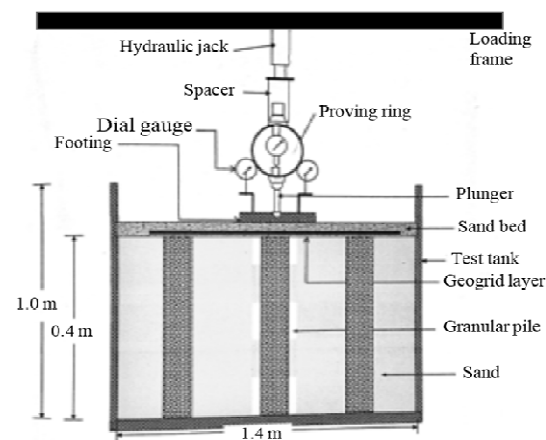


Figure 3 Experimental setup (not to scale)

To obtain the desired density of the aggregate materials (stone and sand), compactors of varying sizes and weight were used. Four dial gauges were attached with footing for measuring the settlement of the footing during loading. For an application of load on soil stratum through footing, a mechanical jack and frame arrangement has been used. The load has been applied through a plunger with proving ring capacity of 50 kN. The thickness of the sand bed on granular pile was 80 mm in case of unreinforced sand bed. In reinforced case with one geogrid layer, 25 mm thick sand bed was provided on granular piles and 55 mm thick sand bed was provided above the geogrid layer. In case of two geogrid layers, 25 mm thick sand bed was provided on granular piles, 25 mm thick sand bed was provided on first geogrid layer and 30 mm thick sand bed was provided on second geogrid layer. A total number of 18 tests was conducted in this experimental study. The test results are summarized in **Table 4**. The details of the experimental arrangement are shown in **Figure 3**.

TEST PROCEDURE

Two steel beams were placed on the steel tank on which four dial gauges were fixed. The needles of dial gauges were placed to touch the vertical Perspex plate which was attached to the footing. Proving ring measurement was recorded for resistance offered by granular piles at an applied load. The initial readings of dial gauges at zero loads were taken and then the load was placed slowly without any impact and readings were taken only after there adding of dial gauges were stabilized. Loads were continuously increased in small steps until the failure took place when the dial gauges showed an increased rate of strain without any further application of loads. Load-settlement curves were plotted. The details of test measurement arrangement are shown in **Figure 4**. After completion of each test, the tank was emptied. The above process was repeated with changed parameters as $s/d = 2, 3, 4$ at relative densities 30% and 60%, in only on the sand bed, unreinforced case, reinforcement with one geogrid layer and reinforcement with two geogrid layers.

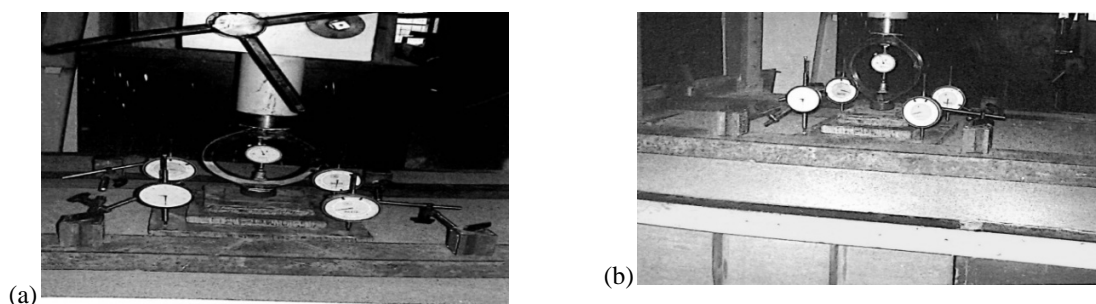


Figure 4 Loading arrangement

RESULTS AND DISCUSSION

Figures 5 to 10 present the load-settlement behavior of granular piles for unreinforced and reinforced cases. The length and diameter (0.4 m and 50 mm) of the piles were kept the same in all the cases by taking spacing as a variable. The increase in settlement has been observed in the range of 5 to 15 % for $D_r = 30\%$ (at $s/d = 2, 3, 4$). For $D_r = 60\%$, the increase in settlement has been observed in the range of 14 to 31 %. Decrease in settlement at 250 kN load has been found to be in the range of 3.5 to 6.5 mm and for 300 kN load it is the range of 4 to 9 mm for $D_r = 30\%$ (at $s/d = 2, 3, 4$). For $D_r = 60\%$, decrease in settlement at 250 kN load has been found to be in the range of 7.5 to 10 mm and for 300 kN load it is the range of 7 to 12 mm (at $s/d = 2, 3, 4$). From the literature, it is clear that stone columns are generally used in soft cohesive soils but it is uncommon in loose cohesion less soils. Although there have been case studies on use of stone columns in loose to medium dense sand, the present study highlights the scope for use of stone columns in weak cohesion less soils. On the other hand, Geosynthetics are available in a wide range of compositions appropriate to different applications and environments. They are noted to offer solutions which are efficient, cost-effective, environment-friendly and/or energy efficient. Geosynthetics are being extensively used for soil reinforcement, Filtration behind hydraulic structures, and Erosion control blanket to prevent soil erosion. Hence, the installation of geogrid-reinforced stone columns in weak cohesion less soils at greater depths is highly effective in increasing the load bearing capacity of foundation soil.

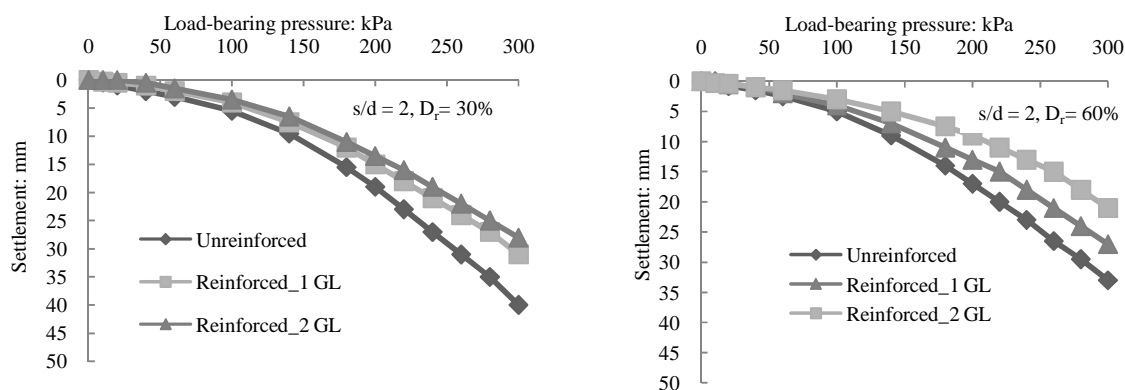


Figure 5 Load-bearing pressure against settlement at



$s/d=2, D_r=30\%$

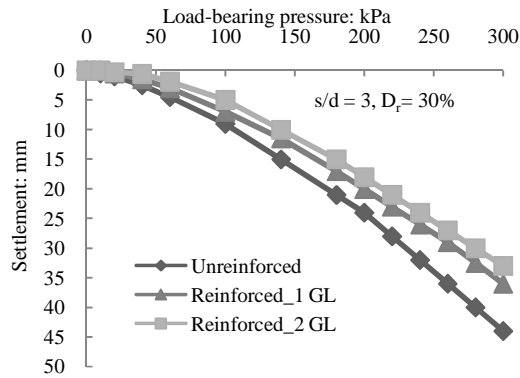


Figure 7 Load-bearing pressure against settlement at $s/d = 3, D_r = 30\%$

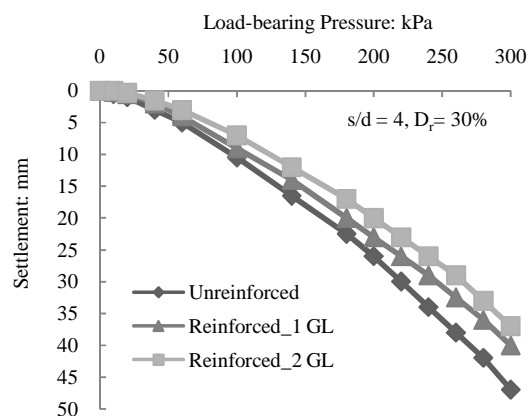


Figure 9 Load-bearing pressure against settlement at $s/d = 4, D_r = 30\%$

Figure 6 Load-bearing pressure against settlement at $s/d=2, D_r=60\%$

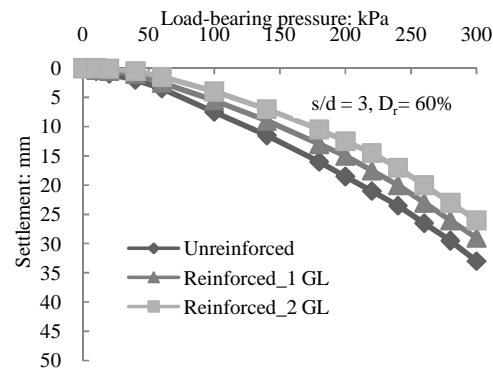


Figure 8 Load-bearing pressure against settlement at $s/d = 3, D_r = 60\%$

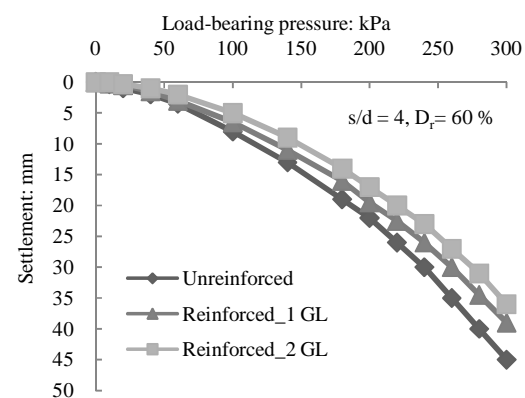


Figure 10 Load-bearing pressure against settlement at $s/d = 4, D_r = 60\%$

CONCLUSIONS

Based on the details presented earlier, the following conclusions can be drawn:

- The improvement in load-carrying capacity is significantly observed in medium dense sand compared to loose sand. For example, the increase in load-carrying capacity at 15 mm settlement has been observed in the range of 14 to 31 % for $D_r = 60\%$ while 5 to 15 % for $D_r = 30\%$ for different spacing of the stone columns.
- Compared with unreinforced case, the geogrid reinforcement within the sand bed over the group of piles is more effective in settlement reduction and increase in load-carrying capacity.
- For both loose and medium dense sands, with an increase of spacing between piles, there is an increase in settlement of the footing while its load-carrying capacity decreases.

REFERENCES

1. G.Ranjan, B. G. Rao, R.K. Bhandari, Reinforcing of non-cohesive soils by granular piles, 6th ARC on SM and FE, Singapore, pp175 – 178, 1979.
2. B.Chandrasekaran, B. Broms Bengt, S. Wong Kai, Strength of fabric reinforced sand under axisymmetric loading, Geotextiles and Geomembranes, pp293-310, 1989.
3. G. M. Latha, V. S.Murthy, Effects of reinforcement form on the behaviour of geosynthetic reinforced sand, Geotextiles and



- geomembranes, Volume 25, Number 1, pp23-32, 2007.
4. P.JagannathaRao, S.Kumar and Bindumadhava, Experimental studies on stone columns, Central Road Research Institute, 1991.
 5. R. S. Sharma, B. R.Phanikumar, and G.Nagendra., Compressive load response of granular piles reinforced with geogrids, Canadian Geotechnical Journal, Volume 41, Number 1, pp 187-192, 2004.
 6. Alwaji H. A., Settlement and bearing capacity of geogrid-reinforced sand over collapsible soil, Geotextiles and Geomembranes, Volume 19, Number 2, pp 75-88, 2001.
 7. T.Shenthana, Factors affecting liquefaction mitigation in silty soils using stone columns, MS Thesis, University at Buffalo, NY, p. 220, 2001.
 8. K. Adalier, A.Elgamal, Mitigation of liquefaction and associated ground deformation by stone columns, Engineering Geology, Volume 72, pp 275-291, 2004.
 9. S. N.Malarvizhi, K.Ilamparuthi, Load versus settlement of clay bed stabilized with stone and reinforced stone column, in: 3rd Asian Regional Conference on Geosynthetics, Seoul, pp. 322-329, 2004.
 10. M.Laman, A.Yildiz, Numerical studies of ring foundations on geogrid reinforced sand, Geosynthetics International, Volume 14, Number 2, pp52-64, 2007.
 11. K.Deb, N. K.Samadhiya, J. B.Namdeo, Laboratory model studies on unreinforced and geogrid-reinforced sand bed over stone column-improved soft clay, Geotextiles and Geomembranes, pp1- 7, 2010.
 12. Kousik Deb, N Sivakugan, S Chandra, PK Basudhar, Numerical analysis of multi-layer geosynthetic-reinforced granular bed over soft fill, Geotechnical and Geological engineering, Volume 25, Number 6, pp639-646, 2007.
 13. Phanikumar, B. R. Ram Prasad and Abhishek Singh, Effect of geogrid reinforcement on load carrying capacity of coarse sand, IGC, pp341-343, 2008.
 14. C.Senthilkumar, K.Muthukkumaran, Effect of soil relative density on pile group lateral load capacity, IGC, pp133-136, 2008.
 15. T.Ayadat, A. M. Hanna, A.Hamitouche, , Soil improvement by internally reinforced stone column. Ground Improvement, Volume 161, Number 2, pp 55-63, 2008.
 16. Samadhiya N., Priti Maheshwari, Attila Zsaki, ParthaBasu, AyanKundu Strengthening of clay by geogrid reinforced granular pile, International Journal of Geotechnical Engineering, Volume 3, pp377-386, 2009.
 17. J.Gniel, A.Bouazza, Improvement of soft soils using geogrid encased stone columns. Geotextiles and Geomembranes, Volume 27, Number 3, pp167-175, 2009.
 18. K. Deb, P. K.Basudhar, S.Chandra, Generalized model for geosynthetic reinforced granular fill-soft soil with stone columns, International Journal of Geomechanics (ASCE), Volume 7, pp 266 – 276, 2007.
 19. S.Murugesan, K.Rajagopal, Studies on the behavior of single and group of geosynthetic encased stone columns, Journal of Geotechnical Geo-environment, Volume 136, Number 1, pp129-139, 2010.
 20. Kousik Deb, Narendra Kumar Samadhiya, Jagtap Babasaheb Namdeo Laboratory model studies on unreinforced and geogrid-reinforced sand bed over stone column-improved soft clay, Geotextiles and Geomembranes, Volume 29, pp190-196, 2011.



Comparative Study of Characteristic Properties of Basalt Composite Rebars

Ashish S. Srivastava^{*1}, Rajendra B. Magar², Afroz N. Khan²
Structech Consulting Engineers India Pvt. Ltd., Navi Mumbai¹, ash@structechindia.com*
Civil Engineering Department, Kalsekar Technical Campus, Panvel²

ABSTRACT

Sustainability has a major role for arresting the impact on environment at the time of construction of building, use of operation and day to day maintenance of the building and demolition of the building in addition to the use of recyclable contents. Thereby, reducing the overall impact on environment due to reduction of carbon footprints by adopting various features like sustainable architecture and design to reduce the consumption of energy by adopting methods of natural lights and ventilation along with minimizing solar irradiation, which are responsible for heat gain increase in the building along with loss of cooled air in an air-conditioned building. Site selection and planning to reduce the overall impact of construction on the natural habitat, preserve natural landscape and water bodies, mitigate the effect of heat and heat island effect in roof and non-roof areas and also reduce the effect of construction by implementing erosion and sedimentation plan. Water conservation to reduce and recycle the water consumed while construction, operation and maintenance of building by use of low consumption fixers and fittings, water metering at various consumer related points in the campus, recycling of waste water and use of waste water for artificial wetlands. Energy efficiency to reduce the overall consumption of energy consumed by building during construction, operation and maintenance of building by using low consumption electrical fitting and an energy efficient, air conditioning system, the overall energy efficiency can also be achieved if proper sustainable and architecture design has been addressed in the planning stage. Indoor environmental quality to deliver a positive environment to the occupiers of the building so as to increase their productivity and keep them healthy. Building materials and resources to reduce overall carbon footprints and reduction of depletion of ozone layer thereby, negating the climate change and its effect on the natural habitat. Building materials and resources consumed nearly 40% of the total energy required for any building. Thereby, use of sustainable materials is a most prioritized in building construction.

A study is conducted to show and prove the successful use of basalt fibre composite bar in lieu of reinforcement steel bar, the study of chemical and mechanical properties has been carried out in addition to concrete bonding properties, alkali corrosion resistance and coefficient of thermal expansion. Basalt fibre reinforced bar prove to have higher tensile strength, same modulus of elasticity as of concrete, hard to corrosion and does not need welding, it is easy to use in transportation and construction due to light weight and thus proves to have promising economic advantages.

KEYWORDS Basalt composite rebars; Reinforcement steel bar; Sustainability; Green building

INTRODUCTION

A variety of synthetic fibres, with a broad spectrum of mechanical properties, have been developed for concrete reinforcing applications. The fibres are generally categorized by their modulus of elasticity with respect to that of the matrix: if it is higher, they are called high modulus fibres and if it is lower, they are called low modulus fibres. The key difference being that high modulus fibres can increase the first-crack strength of the composite, whereas low modulus fibres cannot [1]. The majority of research in this area has focused on aramid (Kevlar) and carbon fibres. FRC made with these fibres exhibits comparable mechanical behavior to steel FRC, but the primary benefits of using these fibres are an increase in first-crack strength and good durability [2,3]. However, widespread application has been prohibited due to their high cost. One method to get cost-effective benefit from the fibres is by using a hybrid reinforcing system.

In general areas of improvement in FRC over PC are increase in tensile and compressive strength along with crack resistance and increase in elasticity modulus. Thereby, resulting in crack control, shrinkage abrasion, durability and resistance to impact in addition to fire resistance and adaptability in characteristics of thermal resistance [4]. The physical and mechanical properties of the fibres are not the only aspects that should be considered when evaluating their potential use in FRC. Factors such as the chemical durability of the fibres in the alkaline environment of concrete, and the increased difficulty of working with the fresh FRC also require careful consideration when selecting the most suitable type of fibre for a specific application. However, these factors are not as straightforward to quantify as those presented in **Table 1**. For example, the influence of fibres on fresh concrete properties (e.g.



workability) will change when using different concrete mixes or production methods. Moreover, due to the uncertainty of accelerated testing, it can take many years of in-situ observation to evaluate the durability of the fibres, or that of the FRC composite as a whole. Therefore, it can be difficult to assess if the benefits of adding fibres are justified in the long-term. The following sub-sections will discuss the basic mechanics of FRC and some typical applications of some commonly used fibres, before delving into more detail on basalt fibre.

Yao et al. [5] found that a combination of steel and carbon fibres was very effective in increasing both strength and toughness. In that case, the smaller, well distributed carbon micro-fibres increased the first-crack strength by preventing the propagation of micro-cracks, and the steel fibres increased the toughness due to their high ultimate strain capacity. Current application of these fibres is limited to specialty structures where light-weight and stiffness is desirable, such as single and double curvature membrane structures and scaffold boards [4]. Commonly used low modulus synthetic fibres include: polypropylene, polyethylene, and nylon. The main draw of the fibres is their good alkaline resistance and low cost. However, they suffer from a lack of fire resistance, and a poor bond with the cement matrix [1]. For these reasons, the most typical use of low modulus synthetic fibres has been for crack control. Low dosages of polypropylene fibres (< 0.3% by volume) have been shown to eliminate cracking due to plastic shrinkage [6]. However, Song et al. [7] found that nylon fibres outperform polypropylene fibres in the reduction shrinkage cracking and attributed it to their higher tensile strength. The use of nylon fibres may be limited to low dosages for crack control, since they are hydrophilic and absorb mix water, which can be problematic at the higher dosages necessary to enhance mechanical behaviour [1]. In regards to mechanical properties, polyethylene fibres were shown to outperform polypropylene fibres in terms of flexural strength and impact resistance, likely due to a higher elastic modulus [8]. It is believed that a lot of research in regards to enhancing the properties of these fibres is done in the private sector and not available in open literature. However, one obvious method that has been adopted is the use of fibrillations in the fibre to enhance the mechanical bond with the matrix. In general, research into the use of natural fibres has been undertaken to develop an economical and environmentally friendly alternative to manufactured fibres and traditional rebar. A lot of research is inspired by the idea of taking advantage of abundant, low-cost, locally available materials to enhance construction in the developing world. There are many types of natural fibres, and thus, discussion in this sub-section only provides a broad overview. Natural fibre reinforced concrete follows the same type of behaviour as discussed in the previous sub-sections. Mechanical properties, such as the modulus of rupture, and toughness, are further enhanced with higher fibre dosages [4]. However, workability and proper consolidation puts an upper limit on the dosage. Fibres with a comparatively high Fig. 1.2. Classification of natural fibres [9] tensile strength and elastic modulus, such as flax, jute, and hemp, are typically best for increasing flexural strength and elastic modulus. On the other hand, coarser fibres, such as sisal and coir, are better in terms of increasing toughness [9].

In regards to durability, flax, sisal, coconut, and cellulose fibres have been shown to prevent early age cracking due to shrinkage [10, 11]. In general, the greatest drawbacks of natural fibres are their lack of durability in concrete due to alkalinity and biological attacks, and inconsistency in mechanical properties [1]. Since, plain concrete (PC) is weak in tension and good in compression which categorizes it as a material which can be easily cracked, even due to minor tensile stresses. The properties of PC can be modified by randomly distributing fibres (glass, steel and polypropylene etc.) in the concrete at the time of mixing which further helps in arresting the surface cracks in concrete and a minor increase in the mechanical properties. Out of glass, steel and polypropylene etc. fibres, steel fibre are the most preferred material due to increase in tensile strength, compressive strength, impact and abrasion properties, the steel fibres have been replaced by steel rebars in some of application like industrial flooring and roads etc[4]. The use of steel fibres reduces the workability and major issue of corrosion is experienced due to direct contact of pavement with moist sub-base. Apart from steel fibre, glass fibre are also used which reduces the issue of corrosion and workability in concrete but due to higher cost and durability concerns, they are used for making glass fibre reinforced concrete (GFRC) architectural grills. However, the GFRC is also not recommended in alkaline conditions. However, other organic and inorganic fibres also modify the properties of concrete, but these fibres are usually not used in practice due to various difficulties. Glass, polypropylene and glass fibres are used commonly in practice due to easy availability and serviceability. In recent times basalt fibre has been preferred the industries due to its mechanical properties and in particular higher tensile strength along with being a natural product and light weight, which helps in maneuverability of rebars at site [1].

The purpose of the experimental work presented in this study is to compare the mechanical properties of basalt reinforced rebars with steel and copper rebars. Comparative performance is evaluated by Tensile strength, yield strength, elastic modulus and density. The basalt fibre composite rebar is in very light weight due to lesser density which also make them easy to handle in transportation and placement. The aim of the study is to perform a comparative study of basalt fibre composite rebars (BFCR) with steel rebars of grade Fe500D and Fe600 is carried



out for its performance comparison in addition to characteristics of basalt fibres composite rebars as compared to steel reinforcement rebars.

The objective of the study are as follows:

- To assess tensile strength, yield strength, elastic modulus and density of basalt fibre composite rebars.
- To assess tensile strength, yield strength, elastic modulus and density of steel and copper rebars.
- To assess the mechanical properties of basalt fibre composite rebars.

Materials and Methodology

An experimental work was undertaken to find the characteristics of basalt fibre composite rebar. This study was carried out to find the probable replacement of steel reinforcement rebars used in reinforced cement concrete (RCC) works. The experimental work

involved testing of three samples of basalt fibre composite rebars marked A, B, C with varying diameters for RCC members shown in **Table 1**.

The above **Table 1** shows type of rebar with varying diameters (D) such as Type A had a diameter of 8mm rebar, Type B had a diameter of 12 mm rebar and Type C had 16 mm rebar. Further, the properties of basalt rebar were compared using experimental procedures with steel rebars of 8 mm, 12 mm and 16 mm tor steel and copper rebars of 8 mm, 12 mm and 16 mm solid bars.

RESULTS AND DISCUSSIONS

The properties like tensile strength (TS), yield strength (YS), elastic modulus (EM) and density was found and are shown in Table 2.

From **Table 2**, it has been observed that, the basalt fibre composite rebar has an upper hand in high strength, light weight and non-corrosive properties.

The coefficient of thermal expansion of weft and warp is different, which depends on the kind of fiber, resin and fiber volume shown in **Table 3**. The coefficient of thermal expansion of warp is affected by fiber property and the weft is affected by kind of resin, here as following as the comparison for different kinds fiber rebar.

The mechanical properties are found as an average of 8mm, 12mm and 16mm diameter bars as shown in Table 4.

From **Table 4**, the basic mechanical properties of the basalt fiber composite bars are as an average of three samples.

Table 1 Experimental data

Item	Type	D, mm
Basalt Rebar	A	8
	B	12
	C	16
Steel Rebar	A	8
	B	12
	C	16
Copper Rebar	A	8
	B	12
	C	16

Table 2 Mechanical properties of rebars

Item	Type	D, mm	TS, MPa	YS, MPa	EM, GPa	Density, g/cm ³
Basalt Rebar	A	8	1005	610	50	1.955
	B	12	1020	625	50	2.05
	C	16	1010	620	55	2
Steel Rebar	A	8	510	305	220	7.9
	B	12	500	315	210	7.9
	C	16	505	310	200	7.9
Copper Rebar	A	8	435	350	110	8.9
	B	12	430	355	130	8.9
	C	16	435	355	135	8.9

Table 3 Coefficient of thermal expansion (CTE)

Direction	CTE. $\times 10^{-6} / ^\circ\text{C}$				
	Steel	Glass fiber	Basalt fiber	Carbon fiber	Aramid Fiber
Weft	11.7	3.3-5.6	9-12	(-4.0)-0	(-3.3) -(-1.1)
Warp	11.7	11.7-12.8	21-22	41-58	33.3-44.4



Table 4 Mechanical properties of basalt fiber composite bars (GB/T 23265-2009)

Item		BFRP
Density, g/cm ³		1.9~2.1
Tensile strength, MPa		≥1000
Bending strength, MPa		≥800
Compressive strength, MPa		≥500
Tensile elastic modulus, GPa		≥50
Elongation rate, %		≥2
Adhesive strength of the concrete, MPa		≥35
Thermal expansion coefficient of $\times 10^{-6}/^{\circ}\text{C}$	Longitudinal	9-12
	Transverse	21-22
Alkali resistance, %		≥85
Magnetic susceptibility (1×10^{-5} CGSM)		$\leq 5 \times 10^{-7}$

Remarks:

- Alkali resist means filament strength retention rate after 4 h in saturated Ca(OH)₂ solution at 100°C
- Standard of magnetic-stability: 4TT $\times 10^{-8}$ SI (1×10^{-5} CGSM)
- Hardness: ≥ 60
- Working life: ≥ 60 years (mini value) tested in 13 PH alkaline environment
- Creeping: the creeping and broken will not happen when lasting loading less than 60% of short period loading
- Bending strength: the strength of bending condition is still 40% of ultimate strength.
- Barcol hardness: ≥ 65
- Life: ≥ 60 years (min) measured in the alkaline environment of 13PH
- Forming and bending: Bending strength after the molding is able to meet 40% of the ultimate strength.

As shown in **Figure 1**, the tensile strength of BFCR is nearly doubled to steel rebar and 2.2 times the tensile strength of copper rebars which signifies a better tensile strength parameter as compared with steel and copper rebar respectively. As shown in **Figure 2**, shows the values of yield strength of BFCR which is nearly double to yield strength of steel rebar and approximately 1.8 times the yield strength of the copper rebar, which clearly signifies that, the BFCR deformation takes place on application of nearly double stress applied on the bar along its axis. Also, **Figure 3**, shows the value of elastic modulus are $1/4^{\text{th}}$ of steel rebar and nearly $1/2$ of copper rebar which signifies that BFCR is a less brittle material as compared to steel and copper, in case of non-permanent elastic property of the material. **Figure 4**, shows that the density of basalt rebar is very low in comparison to steel rebar and copper rebar which indicates that, the BFCR is lighter in weight and is having lesser mass in the per unit volume. The main characteristics of basalt fibre composite rebars are having good combination with cement concrete, good electrical insulation properties, non-magnetic, acid and alkali corrosion resistance, high strength, light weight, less density, thus easy to transport and handle, and can be continuously reinforced without welding. Pultrusion process is used to manufacture basalt composite rebars by using resins to the pulled basalt fiber like natural resins or synthetic resins.

Also, compared with steel rebar, basalt fiber reinforced bars are having higher tensile strength, similar modulus to concrete, hard to corrosion, easy to construction and transportation with considerable economic advantages.

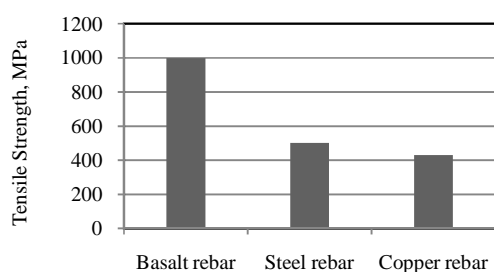


Figure 1 Tensile strength, MPa

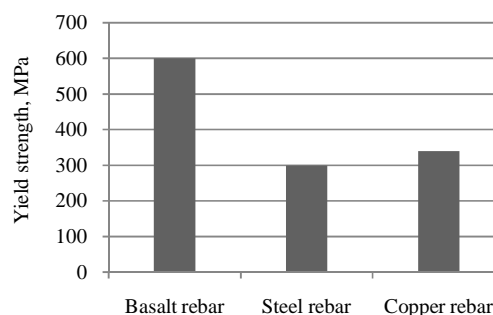


Figure 2 Yield strength, MPa

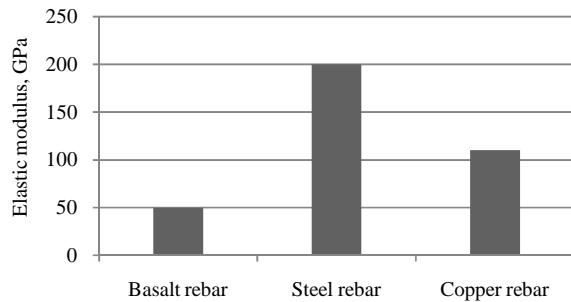


Figure 3 Elastic modulus, GPa

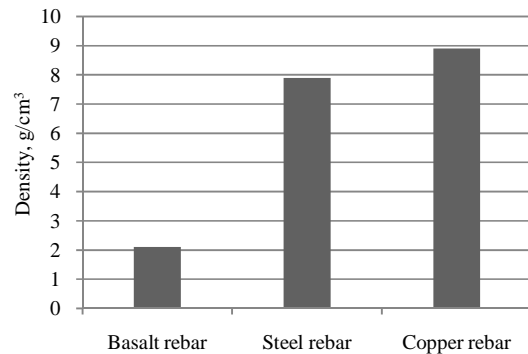


Figure 4 Density, g/cm³

SUMMARY AND CONCLUSIONS

The above experiments signify that, the BFCR have a better mechanical property, high alkali-corrosion resistance and are lighter in weight which makes them the ultimate choice in comparison to conventional steel reinforcement bars and has a better economic benefit as compared to steel bar of around 28% lesser cost in comparison with the weight required which is in addition to indirect benefits like shorter construction period, reduction in overlap joints and increase of durability by 3 times. These benefits thereby help in reduction of carbon footprints in production of reinforcement bars used in construction of green building.

- Higher tensile strength which signifies better load carrying capacity and higher resistance of BFCR to breaking under tension which is required for better load carrying capacity of an RCC structural member.
- Higher yield strength as compared to reinforcement steel which helps in producing better economical design of RCC structural member.
- Lesser elastic modulus is the only disadvantage of BFRC in comparison steel rebars which makes them less ductile and are not recommended for higher lateral forces.
- Density of BFRC is less as compared to steel rebars which has an advantage on the handling placing and fixing of BFRC for any RCC members and also, reduces the lap joints since, longer lengths can be handled easily.
- The coefficient of thermal expansion is similar to that of concrete.

REFERENCES

1. A. Bentur, S. Mindess. Fibre reinforced cementitious composites: CRC Press, 2006.
2. A. Briggs. Carbon fibre-reinforced cement. Journal of Materials Science. Volume 12, 2, pp 384-404, 1977
3. A. Nanni. Properties of aramid-fiber reinforced concrete and SIFCON. Journal of Materials in Civil Engineering. Volume 4, Number 1, pp 1-15, 1992.
4. ACI Committee 544. 544.1R-96: Report on fiber reinforced concrete (Reapproved 2009). Technical Documents. 1996.
5. W. Yao, J. Li, K. Wu. Mechanical properties of hybrid fiber-reinforced concrete at low fiber volume fraction. Cement and Concrete Research. Volume 33, 1, pp 27-30, 2003.
6. N. Banthia, R.Gupta Influence of polypropylene fiber geometry on plastic shrinkage cracking in concrete. Cement and Concrete Research. Volume 36, Number 7, pp 1263-7, 2006.
7. P Song, S Hwang, B Sheu. Strength properties of nylon-and polypropylene-fiber reinforced concretes. Cement and Concrete Research. Volume 35, Number 8, pp1546-50, 2005.
8. P Soroushian, A Khan, J-W Hsu. Mechanical properties of concrete material reinforced with polypropylene or polyethylene fibers. ACI Materials Journal. Volume 89, Number 6, 1992.
9. J Biagiotti, D Puglia, J M Kenny. A review on natural fibre-based composites-part I: structure, processing and properties of vegetable fibres. Journal of Natural Fibers. Volume 1, Number 2, pp 37-68, 2004.
10. E Boghossian, L. D. Wegner. Use of flax fibres to reduce plastic shrinkage cracking in concrete. Cement and Concrete Composites. Volume 30, Number 10, pp 929-37, 2008.
11. P Soroushian, S Ravanbakhsh. Control of plastic shrinkage cracking with specialty cellulose fibers. ACI Materials Journal. Volume 95, Number 4, 1998.



Stepped Cascade as an Energy Dissipator: A Survey and Perspective

Sumit Gandhi^{*1}, Anukrati Joshi¹, Sapana Jaiswal¹, Santosh Sharma¹

Department of Civil Engineering, Jaypee University of Engineering and Technology, Guna, India¹,
sumitgandhi1@rediffmail.com*

ABSTRACT

A technical review about the empirical and numerical models for hydraulic jump characteristics specially the energy loss proposed by different authors in open channel stepped cascade has been reported in the present work. Excessive turbulence induced by the steps leads to jet breaking in air and geometry effects leads water to skim over the edges of steps with energy dissipation. Discussion covers the difference between skimming and nappe flow; efficiency of energy loss under rough and smooth step surfaces; number of steps significant in curved and straight part of stepped spillway; significance of quarter circle shape as step edge under varying flow condition; step height and coefficient of drag with varying range of Froude and Reynolds number, and numerical model to solve turbulence Navier-Stokes equations under such conditions. It has been observed that critical depth and spillway geometry are significant for efficient and safe energy disposal at the toe; and survey results are in agreement among different authors.

KEYWORDS Stepped spillway, Skimming and nappe flow, Rough and smooth steps, End sill, step height, Coefficient of drag

NOTATIONS

B	channel width
C_D	drag coefficient
D	depth of flow over the steps
E_1	energy before the jump
E_2	energy after the jump
E_L	energy loss
E_t	total energy of flow upstream of the fall
F_{r1}	approach Froude number
g	acceleration due to gravity
H_d	spillway height
H_{Dam}	total head of the weir ($N \times S_H$)
L	length of channel
N	number of steps
Q	discharge
Re	Reynolds number
R_s	radius of step
S_s	spillway slope
S_M	model spillway slope
S_H	step height
S_L	step length
V	mean velocity of flow
Y_1	flow depth before jump
Y_2	flow depth after jump
Y_C	critical flow depth
Y_O	depth normal to the flow direction
α	S_H/S_L
ρ	density of water
μ	dynamic viscosity



INTRODUCTION

Estimation of energy loss using stepped spillways for the jet-flow regime is one of the practical applications in dissipating energy downstream when the Froude number ' F_{r1} ' of the incoming discharge is more than 1 and it is of considerable importance in many practical problems to control high energy turbulent flow at downstream of spillways, weir, etc.

It is considered to be advantageous to use stepped spillway where a series of drops are provided from the crest up to the toe instead of the traditional smooth ogee spillway. Stepped spillway is expected to generate correspondingly more energy losses on the spillway structure under wide range of operating conditions, moreover with appurtenances. Excessive turbulence induced by the steps helps in the development of a boundary layer and entrainment of air lead to either nappe flow or skimming flow; moreover when height of the dam is high or head of water above the crest is more, stepped spillway is only solution for safe and efficient disposal of water. In nappe flows energy dissipation takes place by jet breaking in air, water from each step hits the below step as a falling jet with/without the formation of a partial hydraulic jump. Rajaratnam [1] suggested that nappe flow occurs for higher discharges but with very flat slope or when $Y_c/S_H < 0.8$.

Skimming flow occurs at medium to high discharges when water flows down the step as a coherent stream. Water skimming over the steps and is cushioned by the recirculating fluid trapped between the lower nappe and steps surface. As per review carried out by Sorensen [2], the energy dissipation in spillways depends on: discharge; spillway slope; steps geometry and number of steps. Investigation under different stepped spillway and spillway conditions shows that the energy dissipation of flow with end sill and inclined stepped spillways are more than the plain one. It is increased by increasing the thickness of end sill or the reverse slope. Geometry effects of stepped spillways were also studied using physical models to evaluate the impact of additional end sills that have a quarter circle shapes at step edges. Models were also tested for combination of two different ratios by Christodoulou [3] of width to height of steps to improve the effectiveness of energy dissipation.

Literature shows that when discharge increases, there is decrease in dissipation of energy and when the number of steps increases (i.e. height decreases) energy dissipation decreases. Due to number of complexities involved like turbulence, air entrainment, roughness, etc. along with geometrical parameters; simulation of flow, the analysis is difficult. It is also because of existence of non-linear correlation and other factors which are not accurately measurable. Interpolation/extrapolation of design curves in computational model leads to physically incorrect and incomplete solutions. However, many researchers are continuously trying to overcome related limitations through different modeling approach, which are briefly discussed here.

THEORY AND DISCUSSION

Christodoulou [3] experimentally studied the phenomenon for discharge ranging between $0.01 \text{ m}^3/\text{s}$ to $0.45 \text{ m}^3/\text{s}$ considering spillway slope of $1:0.7$ (55° angle to the horizontal). There are seven steps on the curved part of the spillway face with variable height to width ratio, and eight steps on the straight part with constant width $S_L = 1.75 \text{ cm}$ and height $S_H = 2.5 \text{ cm}$. Relative energy loss E_L can be represented using dimensional analysis as:

$$\frac{E_L}{Y_1} = f\left(N, \frac{Y_c}{S_H}, \frac{S_L}{S_H}\right) \quad (1)$$

Importance of parameter Y_c/S_H was suggested by Rajaratnam [1] as above. The ratio of Y_c/S_H is 0.7, which is close to 0.78 by Sorensen [2], 0.60-0.62 by Holingworth and Druyts [4], and 0.75 by Bouyge et al. [5]. Rajaratnam [1] proposed the effective roughness coefficient C_f of stepped surface between 0.11 to 0.20 by assuming uniform skimming flow, as it is not simple and accelerates down the slope with boundary layer formation.

$$C_f = \frac{2Y_0^3 g \sin \theta}{\left(\frac{Q}{B}\right)^3} \quad (2)$$

According to Rajaratnam [1] and Sorenson [2], about 88% and 84% of energy respectively get dissipated for identical steps and for high Froude number discharge at the toe of spillway. It is evident from their graphical results that the energy dissipation is more effective when Y_c/NS_H is small or when the discharge is small in stepped spillway.

Mousavi and Rostami [6] conducted experimental studies on two different models of slope (15° and 25°) for calculation of energy dissipation with respect to dimensionless parameters. Skimming and nappe flows are established over stepped spillways having several falls. In the skimming flow, steps act as a large roughness against



the flow whereas in nappe flow, the flow hits the horizontal part of each step of the spillway. Energy loss between upstream and downstream of the hydraulic jump can be calculated by:

$$\frac{E_L}{S_H} = 1 + 1.5 \left(\frac{Y_C}{S_H} \right) - \frac{Y_1}{S_H} - 0.5 \left(\frac{Y_C}{S_H} \right)^3 \left(\frac{Y_1}{S_H} \right)^{-2} = f_1 \left(\frac{Y_C}{S_H}, \frac{Y_1}{S_H} \right) \quad (3)$$

In the skimming flow over steps a pseudo-bottom which connects the end of steps to each other is established by Ohtsu et al [7]. Chanson [8] has proposed equation for energy dissipation in steeped spillway as:

$$\frac{E_L}{E_t} = \frac{E_t - E_1}{E_t} = 1 - \frac{\frac{Y_C}{Y_1} - \frac{1}{2} \left(\frac{Y_C}{Y_1} \right)}{\frac{3}{2} + \frac{H_{Dam}}{Y_C}} \quad (4)$$

Chanson [8] proposed Eq. (1) can be rewritten as function of (Y_C/S_H) as follows:

$$\frac{E_L}{E_t} = 1 - \frac{0.54 \left(\frac{Y_C}{S_H} \right)^{0.275} + 1.715 \left(\frac{Y_C}{S_H} \right)^{-0.55}}{\frac{3}{2} + \frac{H_{Dam}}{Y_C}} \quad (5)$$

Chanson [8] has compared Eq. (5) with findings of Stephenson [9]. It has been shown that there is good agreement between results of Eq. (5) and the experimental results. The relative head loss equation expressed by Chamani and Rajaratnam [10] as:

$$\frac{E_L}{E_t} = 1 - \frac{\left[(1-\alpha)^N \left\{ 1 + 1.5 \left(\frac{Y_C}{S_H} \right) \right\} + \sum_{i=1}^{N-1} (1-\alpha)^i \right]}{N + 1.5 \left(\frac{Y_C}{S_H} \right)} \quad (6)$$

α depends upon S_H/S_L ratio, α decreases with increase in S_H/S_L .

Barani et al [11] experimentally investigated the energy dissipation over stepped spillways of varying step shapes. Wooden model with 41.41° slope has 84 cm height with 21 steps were taken under varying flow conditions. Experiments have been conducted for plain steps, end sill steps and adverse slope. Result shows that the energy dissipation of flow with end sill and inclined stepped are more than the plain one and it increases with the width of sill or with reverse slope. Their empirical study shows, energy dissipation on a stepped spillway depends upon head of water above the spillway crest (H), depth of flow over the steps (D), step height (S_H), mean velocity (V), density of water (ρ), slope of the spillway (S_s), dynamic viscosity of flow (μ) and gravity (g):

$$f(E_1, E_2, E_L, H, D, S_H, V, \rho, S_s, \mu, g) = 0 \quad (7)$$

Yazdani [12] proposed energy dissipation using dimensional analysis based on experimental results as:

$$E_L = 104.33 \left(\frac{H}{S_H} \right)^{-0.015} C_D^{0.054} \quad (8)$$

$$\text{where } C_D = 3.285 R_e^{-0.013} F_{r1}^{-2.021} \left(\frac{D}{S_H} \right)^{0.015} (S_M)^{0.547}.$$

Udai et. al [13] investigated experimentally the stepped spillway with four different physical models used to evaluate the impact of end sills with a quarter circle shape at step edges. Same behaviour were mentioned by other researchers also for trend of energy dissipation and about the boundaries formation between flow regimes. It can be concluded that nappe flow shows higher efficiency than transition and skimming flows because for low value of Froude number water flows following the profile of steps whereas in transition and in skimming flow water flows through the edges of each steps with large air entrapment. The results for model having greater step length show improved energy dissipation, especially for a nappe flow. The changes in step shape to quarter circle lead to positive impacts for stepped spillway, compared with other models. Also, step number has a greater effect than step height for low discharges. Significant and effective parameters are important to investigate the energy dissipation and aeration in spillway using following correlation:

$$\frac{H_i}{Y_1} = f \left(\frac{H_d}{Y_C}, \frac{L}{Y_C}, \frac{S_w}{Y_C}, \frac{R_s}{Y_C}, \frac{S_L}{Y_C}, R_e, F_{r1}, N \right) \quad (9)$$

According to Chanson [8] entrained air is an important design parameter in spillway flow. Air entrainment increases the bulk of the flow which is a design parameter that determines the height of spillway sidewalls. Also the presence of air in the boundary layer reduces the shear stress between the flow layers and hence the flow resistance. It appears



in the form of air bubble at each step of spillway and very common in nappe flow. The air entrainment characteristics of hydraulic jumps were analyzed by a number of researchers (e.g. Rajaratnam [14] and Resch, et. al [15]. Extensive studies of plunging jet entrainment were performed by Van and Smith [16], Ervine and Elsawy [17], Wood [18] and Chanson and Cummings [19] and concluded that it occurs at the intersection of nappe with the receiving pool.

Saman and Kamanbedast [20] presented a numerical model to solve the turbulence Navier-Stokes equations finite volume discretization method (flow 3D software) to estimates various parameters like; number of steps, step height and horizontal step length and discharge. It is observed that flows are divided in three different regime, nappe, transitional and skimming flow and when number of step increase than dissipating efficiency decreases. Numerical simulations of water flow over stepped spillways with different step configurations are presented by Mazen, et al [21]. The finite element computational fluid dynamics model was used to predict the water surface profile, development of skimming flow over corner vortices and the determination of energy dissipation. K-E flow model was used as flow is turbulent under such conditions. It is equally important to have knowledge of the residual kinetic energy at the toe of a spillway to fix the stability of stilling basin. The computed values for relative energy loss obtained were: 51.6%, 52.5%, 51.9% and 49.8% for different cases considered were as these values are 21.1%, 22.6%, 21.7% and 18.2% for smooth spillway. Similar results were coated by Chatila and Jurdi [22] for energy dissipation and are comparable with the above authors.

Numerical simulations of water flow over stepped spillways with different step configurations were done by Mazen et. al [21] to predict the main characteristics of the flow. Although the results of this study are adopted to model various stepped spillway configurations operating at different flow heads but at the same time for experimental simulation and measurements it is still difficult to refer the data. Mousavi et. al [6] employed ANSYS to simulate hydraulics over stepped spillways for energy loss in nappe flow. Experiments were also conducted for two models with slope angle of 15° and 25° with high discharge ($NS_H/Y_c < 15$), the equations presented by Chamani and Rajaratnam [10] are in good agreement with these results. It is concluded that ANSYS gives comparatively more accurate results with less than 6% error.

CONCLUSION

Christodoulou [3] experimentally explained the importance of relative energy loss through varying number of curved steps and straight part of stepped spillway. Rajaratnam [1] proposed the effective roughness coefficient ' C_f ' with boundary layer formation. However, Rajaratnam [1] and Sorenson [2] given due weightage to flow depth and spillway dimension for identical steps; at high Froude number approximately 85% of energy get dissipated and it becomes more effective when Y_c/NS_H is small. Non-dimensional approach has been followed by Mousavi and Rostami [6] for calculation of energy dissipation for skimming and nappe flows. Chanson [8] compared his result with Stephenson [9] for relative energy loss and found good agreement between the two. Chamani and Rajaratnam [10] introduces the term ' α ' for energy loss which depends upon spillway dimension. Barani et. al [11] experimentally explains the phenomenon for plain steps, with end sill steps and with adverse slope. Results show that the energy dissipation of flow on end sill and inclined stepped spillways are more than the plain one. Yazdani [12] proposed energy dissipation using dimensional analysis by introducing drag coefficient C_D , Reynolds number ' Re ' and Froude numbers ' F_{r1} '. It is observed that when number of step increase than dissipating efficiency decreases as per numerical model by Saman and Kamanbedast [14].

Flow are divided in three different regime nappe, transitional and skimming flow on the basis of various parameters like number of steps, step height and horizontal step length and discharge. Numerical simulations of flow over stepped spillways with different step configurations are presented by Mazen et. al [8]. The finite element computational fluid dynamics model was used to predict the surface profile. It has been found that energy loss is less in smooth steps in comparisons with rough steps. Udai et. al [17] investigated experimentally the stepped spillway with four different physical models to evaluate the impact of adding end sills that have a quarter circle shape at step edges.

Computational and numerical analysis were also done for water surface profile, development of skimming flow, formation of corner vortices and the determination of energy dissipation but it has been observed that in some cases it defines the whole phenomenon significantly but in some cases it is partly explainable the energy loss and hence the structural stability aspect of stilling basin. Empirically many important parameters like roughness, spillway geometry, end sill approach, adverse slope, quarter circle shape of step and non-dimensional approach were considered and satisfactory results were obtained; but few of them found to be non-scalable to real field problem.



REFERENCES

1. N Rajaratnam, Skimming flow in stepped spillways, Journal of Hydraulic Engineering, ASCE, Volume 116, Number 4, pp 587-591, 1990.
2. R. M. Sorensen, Stepped spillway hydraulic model investigation, Journal of hydraulic Engineering, A.S.C.E., Volume 113, Number 12, pp 1461-1472, 1985.
3. C. Christodoulou, Energy dissipation on stepped spillways, Journal of Hydraulic Engineering, Volume 119, Number 5, pp 644-650, 1993.
4. F. Hollingworth, F. H. W. M. Druyts, Rollcrete: some applications to dams in south Africa, Water Power and Dam Construction, Volume 38, 1, pp 13-16, 1986.
5. B. Bouyge, G. Garnier, A. Jensen, J. P. Martin, J. Sterenberg, Construction et controle d'un barrage en beton compacte au rouleau (BCR), Untravail d'equipe, Proceeding of 16^{eme} Congres des Grands Barrages, Commission International des Grands Barrages, pp 588-612, 1988.
6. J. H. Mousavi, R. A. Rostami, Geometrical optimization of stepped spillway models, Agroecology Journal, Journal of New Agricultural Science, Volume 4, Number 12, pp 27-38, 2008.
7. I. Ohtsu, Y. Yasyda, M. Takahshi, Characteristics of skimming flow over stepped spillways, Discussion-Journal of Hydraulic Engineering, ASCE, Volume 126, Number 11, pp 583-588, 2008.
8. H. Chanson, Comparison of energy dissipation between nappe and skimming flow regimes on stepped chutes, Journal of Hydraulic Research, Volume 32, Number 2, pp 213-218, 1994a.
9. D. Stephenson, Energy dissipation down stepped spillways, International Water Power and Dam Construction, Volume 43, Number 9, pp 27-30, 1991.
10. M. R. Chamani, N. Rajaratnam, Jet flow on stepped spillways. Journal of Hydraulic Engineering, Volume 120, Number 2, pp 254-259, 1994.
11. G. A. Barani, M. B. Rahnama, N. Sohrabipoor, Investigation of flow energy dissipation over different stepped spillways, American Journal of Applied Sciences, ISSN 1546-9239, Volume 2, Number 6, pp 1101- 1105, 2005.
12. A. Yazdani, Investigation of slope effect on flow energy dissipation over stepped spillway, International Journal of Science Engineering, Volume 9, pp 1-13, 1998.
13. Udai A. Jahad, Riyadh Al-Amery, Lloyd H. C. Chua, D Subrat, Energy Dissipation and Geometry Effects Over Stepped Spillways, International Journal of Civil Engineering and Technology, Volume 7, Number 4, pp 188-198, 2016.
14. N Rajaratnam, Hydraulic jumps. advances in hydrosiences, Ed. V.T. Chow, Academic Press, New York, USA, Volume 4, pp 197-280, 1967.
15. F. J. Resch, H. J. Leuthesser, S. Alemu, Bubbly two-phase flow in Hydraulic Jump, Journal of hydraulic division, ASCE, Volume 100, HY1, pp 137-149, 1974.
16. S. Van De, J. M Smith, Surface entrainment of air by high velocity water jets, Chemical Engineering Science, Volume 28, pp 1161-1168, 1973.
17. D. A. Ervine, E. M. Elsayy, The effect of falling nappe on river aeration, Proceeding of the 16th IAHR congress, Sao Paulo, Brazil, Volume 3, pp 390, 1975.
18. I. R Wood, Air Entrainment in Free Surface Flows, IAHR Hydraulic Structures Design Manual No. 4, Hydraulic design considerations, Balkema Publications, Rotterdam, Netherlands, Volume 149, pp 1991.
19. H. Chanson, P. Cummings. Aeration of the ocean due to plunging breaking waves, Research Report No. CE142, Department of Civil Engineering, University of Queensland, Australia, Volume 42 pp 1992.
20. A. Saman, A. A. Kamanbedast, Investigation of Effect of Changes in Dimension and Hydraulic of Stepped Spillways for Maximization Energy Dissipation, World Applied Sciences Journal, ISSN 1818-4952, Volume 18, Number 2, pp 261-267, 2012.
21. T. Mazen, C. Jean, A. Rita. Computational simulation of flow over stepped spillways, Computers and Structures, Elsevier, Volume 83, pp. 2215-2224, 2005.
22. J. G Chatila, B. R. Jurdi, Stepped spillway as an energy dissipater, Canadian Water Resources Journal, Volume 29, Number 3, pp 147-158, 2004.



Protection Measures for Alluvial River: Integrated Approach

V G Bhawe^{*1}, H S Sandhu², Rakesh Dhapola²
WAPCOS, Pune¹, vgbhave@yahoo.com^{*}
WAPCOS, Gurgaon, Haryana²

ABSTRACT

Majority of the alluvial rivers rise in Himalaya, continue their journey through sub-mountain and plains to outfall into sea or other river. During the course of travel, these rivers undergo changes in their characteristics related to geometry and morphology. Changes depend on material forming bank and bed as well as sequence and duration of flows. These include scouring, deposition or change in alignment and pattern of river channel. All these aspects require detailed study of each of the component using the appropriate method. Developments in technology yield large number of options for a given situation. Selection of a method to complete each task can be done using intelligence and expertise in a judicious manner. In order to get efficient and long duration solution, it is utmost essential to integrate selected methods. The authors could apply the logic discussed above in the work carried out for development of erosion free zone over a length of about 83km of river Ganga in the state of Jharkhand. Integration of the following components was carried out.

- Estimation of design flood
- Deriving hydraulic design parameters
- Identification of erosion areas
- Confirmation of results by field visits
- Derivation of protection measures
- Construction Programme

KEYWORDS Design flood, Protection measures, Field visit, Sequencing of works, Integration

INTRODUCTION

Ganga River Basin covers over 10,86,000 sq.km² area and ranks among the largest in the world for catchment area and length. River has two main headwaters in the Himalaya, as Bhagirathi and Alaknanda. Bhagirathi flows from Gangotri glacier at Gomukh and the latter from a glacier near Alkapuri.

River Ganga is braiding in the plateau leading to change in course of river resulting in damages to valuable human lives and properties, loss of agricultural lands with crops and livestock.

Government of India has taken an initiative to rejuvenate river Ganga through different measures. The effectual corrective actions could be evolved through an integrated approach that involves series of steps; each taking care of related aspect. The measures are required for identifying the area of erosion and suggesting protection measures.

Government of Jharkhand has proposed to evolve measures for the right bank of River Ganga within state territory in order to develop erosion free area along the length of 83km. The work was carried out by authors, as team of WAPCOS. Different work components are integrated to derive protection measures for length of about 23 km.

STUDY AREA

River Ganga, initially known as Bhagirathi, rises at an elevation of about 7010m from Gangotri glacier in the state of Uttarakhand. River is flowing in meandering manner up to Alaknanda out fall near Devprayag and the combined stream is known as Ganga. The length of River Ganga measured along Hoogly up to Bay of Bengal is 2525 km. Number of tributaries join River Ganga along the length. Important tributaries from right bank are Yamuna and Sone; whereas Ramganga, Ghaghra, Gandak, Kosi and Mahananda meet from left bank.

River Ganga forms northern boundary of the state of Jharkhand in Sahibganj District. Length of River Ganga in the state of Jharkhand is about 83km. An average width in the Sahibganj block is about 4.5 km. River Gumani and River Mural take south-eastern turn and join River Ganga beyond the district boundary. In this study, the reach of River Ganga from LalBathanupto West Bengal border was included.

Water Resources Department (WRD), Govt. of Jharkhand has identified 12 reaches where erosion is active. These 12 reaches are situated in four blocks viz Sahibganj, Taljhari, Udhwa and Rajmahal. Reaches 1 to 3 are in Sahibganj block; 4 to 6 are in Rajmahal block, reach 7 lies in Taljhari block whereas reaches 8 to 12 are situated in Udhwa block. Details of all reaches are given in **Table 1**.



Table 1 Details of erosion reaches

Reach No	Chainage, km	Length, km	Remarks
1	15.65 to 16.56	0.91	Near Gopalpur
2	16.63 to 16.78	0.15	
3	27.50 to 28.80	1.30	Between Ambadiha and Baskola
4	31.00 to 33.00	2.00	Near Maharajpur
5	38.50 to 39.70	1.20	Near Balapokhar
6	41.00 to 46.20	5.20	Budhwaria to KanahiyaAsthan
7	57.60 to 58.10	0.50	Near Launch Ghat
8	58.60 to 61.15	2.55	Near Narayanpur
9	63.60 to 64.60	1.00	Near Felutola
10	65.10 to 68.00	2.90	RaffaTola to KhattiTola
11	70.10 to 75.60	5.50	BanoTola to East Pranpur
12	78.50 to 82.10	3.60	KhatiaKanu to Shreeghar

Scope of Work

The scope of work included following components

- Cross sectional survey with establishment of GTS Bench marks as per the specifications.
- Geological and geotechnical investigation
- Hydrological studies, estimation of peak discharges at various reach of Ganga.
- Identification of reachwise protective measures and formulating erosion proofing proposals as per site conditions.
- Design of protective measures.
- Cost estimate of protection works and calculation of B.C. ratio as per norms/guide lines of GOI/GFCC/WRD.
- Preparation of DPR as per norms/guide lines of WRD/CWC/GFCC for Administrative and Financial sanction.
- To obtain clearance from erstwhile Ministry of Water Resources, Government of India.

Out of the above components, components relevant to integration process are included in this paper.

DATA USED AND METHODOLOGY

The work for derivation of the protection measures to the right bank of River Ganga was carried out using the following data:

- L-Section and Cross Section of River Ganga within the study reach.
- Gauge discharge data of River Ganga at Farakka.
- Engineering properties of soils prevailing in bank of River Ganga within the study reach.

The work for derivation and protection measures was carried out through the following steps:

- Review of L-section and cross section obtained from the topographic survey and satellite data.
- Review of discharge data at Farakka and derive floods with 25, 50 and 100 year return period and lean flow.
- Setting up 1D Hydraulic model viz. HEC-RAS using survey data, cross sections and gauge discharge curve to derive water surface profile for the above discharges and derive hydraulic design parameters.
- Review of soil properties and prevailing conditions at site and carry out slope stability analysis for the range of slope from 1:2 to 1:4 with and without provision of berm(s).
- Identification of erosion area showing changes in bank line and channel width.
- Derive bank protection measures for the erosion reaches.
- Determine the cost of protection work using the prevailing schedule of rates as proposed by Government of Jharkhand.

RESULTS AND DISCUSSIONS

Hydrologic Analysis of Discharge Data

Available discharge data of River Ganga at Farakka Site from 1979 to 2010 [1,2] year was reviewed. These data were tested for homogeneity using t and F tests. The results were positive and confirmed homogeneity of the data.

The data were further analysed using Gumbel Extreme Value (GEV) distribution and above cited floods were derived. Results are given in **Table 2**.



Identification of Erosion Area

Satellite data from 2007 to 2014 showing bank line and channel positions in Ganga river stretch within the state of Jharkhand were collected. These data were digitized and Geo-coded using reference points like Farakka Barrage.

A review of data showed that out of total reaches, erosion at three locations, namely, Rajmahal, Jamnagar and Patra was active. Accordingly bank line vectors were extracted from the satellite data for the above period. These vectors were superimposed to identify bank line changes. A sample comparison is shown in **Figure 1**.

It could be seen that the change in Bank line is varying between 85 m to 383 m.

Channel Width Changes

Nine locations were identified as erosion appeared to be active at these locations. Mark was placed on the first year of the satellite data and also on the last year of the satellite data. Coordinates of channel width were derived using right bank location of first year as the origin. The difference in coordinates yielded change in channel width. Sample results are presented in **Table 3**.

Detailed discussion of the procedure and results are presented by Bhawe[5].

1D Model

The reach of River Ganga in Jharkhand was considered for setting up HEC-RAS model. The geometry of river was defined using cross sections at an interval of 0.5 km in erosion reaches and 3 km in other reaches.

Steady state simulations were carried out using the discharges in **Table 2** for the upstream boundary and gauge discharge curve was used for defining the downstream boundary. Manning's n value of 0.02 for river channel and 0.025 for the flood plain was specified to define the friction in the model.

Simulation runs with flood plain were taken that yielded water level of 30.68 m near Sahibganj, which is close to observed water level of 30.9 m. The model was thus taken as calibrated for estimation of hydraulic design parameters. Reach wise parameters are presented in **Table 4**.

Derivation of Protection Measures

A review of commonly adopted projection measures were taken from the following list [3]:

- Spurs/groins
- Pitching with stone/bricks/concrete blocks
- Vetivers
- Submerged vanes
- RCC Kelleners
- Jetties
- Geocells/Geobags/Geomats

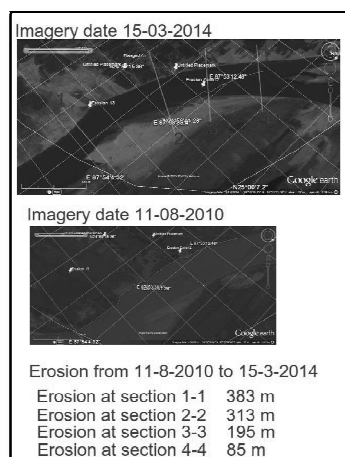


Figure 1 Typical erosion reach

Each of the measure is applicable under certain scenarios prevailing at the site. In the present situation, the following aspects were considered: (i) Location, (ii) Availability of resources and (iii) Ease of application.

Table 2 Floods in river Ganga at Farakka

Return period, year	25	50	100
Flood, cumec	75374.54	82843.19	90258.72

Table 3 Channel width changes

Location		E1		E2	
Year		2000	2013	2003	2013
Bank	Left	580	658	1220	624
	Right	0	130	0	0
Bank width		580	528	1220	624
Shift of Bank	Left		78		- 596
	Right		130		0
Positive value means shift in left side					
Negative value means shift in right side					



In addition, the discussions were held with WRD Officers and local citizens during the site inspection in 2015. Accordingly, it was decided to provide combination of : • Protection of bed/ slope using stone in crates, • Edge crating between ISMB girders, and • Permeable spurs.

During the site inspection carried out in 2015, it was noticed that bank slope of River Ganga in the erosion reaches is varying from nearly vertical to slope flatter than 1:5. The soil properties derived from the samples collected during the site visit indicated that angle of repose is between 17.6° and 18.2° and angle of internal friction shows a variation from 14.9° to 16.4°. Average angle of friction about 16°, which is close to slope of 1:4, was proposed. After consultation with Project Authorities the slope of 1:2 is retained at on going protection measures.

Slope stability analysis using engineering soil properties and different combinations of slope 1:2 to 1:4 was carried out for with and without berm scenarios. Analysis included bank height between 5 m and 12 m and 30 cm thick stone pitching. Factor of safety (FoS) obtained during the analysis under different scenario are presented in **Table 5**.

It can thus be seen that slope of 1:2 is stable for height up to 6 m only.

Crates for Slope Protection

Using the hydraulic design parameters and bank slope of 1:2, the size of crates required for protection of the slope was derived [4]. It is proposed that crates of size 3 m × 1 m × 0.6 m be laid in 2 layers of 300 mm thick.

Toe Wall and Apron

Toe wall for protection of toe against high flow velocity prevailing in flood is proposed. The same crates used for protection of slope are proposed for construction of toe wall (**Figure 2**).

Launching apron, with width varying from 20 m to 30 m in different reaches, for protection of bed is proposed. The apron is to be constructed with stone in crates of sizes 3 m × 1 m × 1.2 m using 3/4 layers of 300 mm thickness[4].

A 300 mm thick layer of good draining soils on dressed bank slope and another layer 300 mm thick of same soil on geotextile filter is proposed for safety of filter against rupture. Geobags of size 1 m × 0.7 m × 0.30 m in adequate layers are to be replaced for both soil layers at locations below LWL.

Permeable Spurs Made from RCC Porcupines

In addition to the pitching, RCC porcupines are proposed at 21 different locations, to provide protection against swirls/eddies experienced during passage of high flood and due to curved alignment of river channel. Details of proposed porcupines are given in **Table 6**.

Construction Program

Mechanized construction has been planned for almost all types of construction jobs so as to achieve consistent quality at a faster rate and also to minimize the requirement of skilled manpower [6].

Table 4 Hydraulic design parameters

Reach no	q, cu.m/s/m	HFL, m	Crate top RL, m
1 ^a	29	30.62	12.08
2	25	30.59	10.23
3	30	30.24	12.88
4	33	30.09	14.34
5	37	29.74	16.36
6	34	29.57	15.23
7	37	28.65	17.39
8	29	28.28	14.23
9	27	28.00	13.57
10	35	27.85	17.31
11	40	27.09	20.16

^a Reach 1 and 2 in **Table 1** are clubbed as Reach 1

Table 5 Factor of safety scenarios

Slope	Height, m	Factor of safety	
		With berm	Without berm
1 : 2	12	0.988	\$
1 : 3	5	1.761	\$
1 : 3	12	1.114	0.771
1 : 4	12	1.184	0.988
1 : 2	6 [@]	1.638	

\$-as Berms are proposed at 4 m height, these cases do not arise.
 @ - FoSis determined with 30cm pitching



Table 6 Details of porcupines

Ch, km	L, m	Ch, km	L, m
38.00	100	63.00	200
38.25	100	63.25	200
38.50	100	63.50	100
38.80	50	64.50	100
40.60	50	66.75	50
59.15	200	75.50	60
59.35	150	75.60	80
59.45	154	76.40	115
62.35	100	79.00	100
62.50	200	79.50	100
62.80	200		

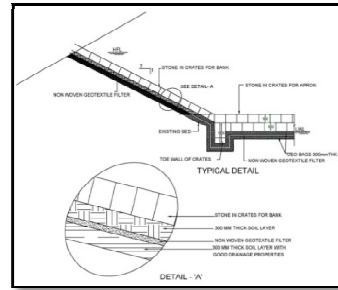


Figure 2 Details of crates for bank, toe and bed

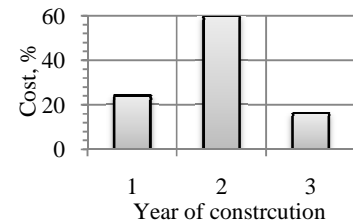


Figure 3 Year-wise cost allocation

Sequencing of construction activities, wherever possible, has been attempted in such a way that equipment from one activity, on its completion can be moved to the other. Thus, the total requirement of equipment at a time would be reduced and proper utilization of equipment on the project site would be ensured.

Locations of different borrow areas and quarries for construction material with respect to the site location; suitable material for construction of stone pitching work and steel girder for deeply eroded locations and for construction of porcupines, good quality of quarries have been identified near the vicinity of river bank.

The general purpose equipment for infrastructure works and inspection and transport vehicles which are required to be procured, were suggested.

The phasing of the cost has been done according to the requirement, based on most vulnerable, vulnerable and less vulnerable erosion areas reach wise. Accordingly the construction schedule has been planned as shown in **Figure 3**.

CONCLUSIONS

Right bank of river Ganga in Jharkhand state is erosion prone. Protection measures are derived to convert this stretch into erosion free zone. Integration of methods related to flood estimation, morphological analysis with satellite data deriving hydraulic parameters from simulation model results and construction program has been carried out to decide combination of protection measures. Important findings of the studies are given below:

- The floods for return period of 25, 50 and 100 years return period were derived. These are given in **Table 2**.
- Protection measures, based on the hydraulic parameters (Table 4) derived from HEC RAS model, for slope, toe and bed in the form of stone in crates are recommended for 11 reaches. In addition, permeable spurs in the form of porcupines constructed using RCC member are suggested at 21 locations. Details are presented in **Table 6**.
- Stability and analysis of bank slope of River Ganga was carried out under a variety of scenarios of bank slopes, berm and stone pitching. It was noticed that slope of 1:2 is stable for bank height up to 6 m.
- The construction programme for the reducing completion time and efficient utilisation of equipment is suggested in phased manner.

ACKNOWLEDGEMENT

The work for development to erosion free zone on River Ganga in Jharkhand State was awarded by Water Resources Department, Government of Jharkhand. Authors express their gratitude to CMD, WAPCOS for kind permission accorded for publishing the paper.

REFERENCES

1. Central Water Commission (CWC), Farakka H.E. Project Report, 1990
2. National Hydro-electric Power Corporation (NHPC) Farakka H.E. Project Report, 2001.
3. Central Water Commission, Handbook for Flood Protection, Anti- erosion and River Training Works, New Delhi, 2012.
4. Bureau of Indian Standards, IS 10751 on Planning and Design of Guide Banks for Alluvial Rivers- Guidelines, ManakBhavan, 9 Bahadur Shah Zafar Marg, New Delhi-110002, India, 1984.
5. V G Bhawe and H S Sandhu Identifying Erosion Areas and Bank Line Changes Using Satellite Data in National Conference on Water Resources & Flood Management with Special Reference to Flood Modelling, SVNIT Surat, pp WRM-12-1 to WRM-12-9, 2016.
6. Preparation of DPR to make the Entire Right Bank of River Ganga lying in Government of Jharkhand Erosion Free as per Guidelines of CWC and GFCC- DPR, 2015



Some Major Properties of High Strength Self-Compacting Concrete

Aijaz Zende^{*1}, R B Khadiranaikar²

Department of Civil Engineering, BLDEA College of Engineering and Technology, Vijayapura, Karnataka¹

Department of Civil Engineering, Basaveshwar Engineering College, Bagalkot²

ABSTRACT

An attempt is made to understand the behaviour of High Strength Self-Compacting Concrete in its fresh and hardened state incorporating mineral admixtures with different percentages of silica fume and fly ash. Experiments were carried out using 12 mixes with different w/c ratios. Four replacements of OPC with fly ash and silica fume of 5%, 10%, 15% and 20% were cast cured for 28 days. The experimental program is carried out in three stages. First, for each mix, fresh properties (slump flow, T-500, V-funnel test and L-box test) are checked. In the second stage, cubes and cylinders were cast and kept in fresh water for curing. Then in the third stage, these samples were used for testing mechanical properties (compressive strength, split tensile strength and modulus of elasticity). The results obtained indicate a direct impact of percentage content of fly-ash and silica fume on the properties of fresh and hardened SCC.

KEYWORDS Self-Compacting Concrete(SCC); Fly ash; Silica fume; Slump flow; V-funnel test; L-box test

INTRODUCTION

Rapidly increasing use of chemical and mineral admixtures, developments in the area of construction technology and the better understanding of the behaviour of fresh and hardened concrete have contributed to our ability and confidence in using concrete in more and more challenging conditions. It has led to the development of special concretes, special construction methods and improvement in concrete properties. Given the dense reinforcement around which concrete is required to move, or the complicated geometry of the formwork, and the distances over which concrete needs to be pumped, makes a high demand on the workability of the concrete, and practically 'flowing' concrete is required. Needless to say, in order that the concrete does not segregate, this workability and flowability strains the ability of the fluid phase to carry with it the denser aggregate fraction to the limit.

Self-Compacting Concrete (SCC) provides a solution by overcoming this problem as it can flow, compact by itself without any need of vibration or another mean of compaction and fills completely on to the formwork with no segregation [1-4]. SCC can reduce the considerable number of the skilled work force and need of good quality control; thereby it reduces the time of construction. It was also reported that Self-Compacting concrete is more economical than conventional concrete [5]. However, because of its requirement of 'highly flowing nature', proper care should be taken so as to achieve filling and passing ability without any segregation [6]. High Strength SCC (HSSCC) requires a lower water to binder ratio with higher cement content and limiting the size of coarse aggregates [7,8]. The production of HSSCC also requires suitable chemical admixture to reduce water content by decreasing interparticle friction but maintaining required workability and also supplementary cementitious materials so as to fill the voids to make the concrete denser increasing its compressive strength [1, 9-11]. In the present work, the procedure followed to produce a cost-effective and high strength SCC is briefly discussed. The objectives of the present work in this experimental investigation is to produce controlled HSSCC and compare its relative performance with HSSCC incorporating fly ash and silica fume with different percentages, that is, 5%, 10%, 15% and 20% at the different water to binder ratios.

MATERIALS

The production of HSSCC requires materials of proper quality. Selection of materials for HSSCC is of paramount importance. In addition to cement water and aggregate, constituents like mineral and chemical admixtures are a must for the production. Chemical admixtures are usually used to control the properties like slump whereas mineral admixtures are used for enhancing the concrete strength. Selection of cement is of utmost importance in HSSCC production as the chemical and physical characteristics of cement affects the compressive strength of concrete more than any other single material. In the present experimental work, Ordinary Portland Cement (Ultra-Tech cement) conforming to IS: 12269-1987 has been used. Fly ash and silica fume were incorporated as supplementary cementitious material. They together act as a binder in the concrete. Silica fume was collected from Shri Sai Durga Enterprises, Bangalore having a specific gravity of 2.15 and the fly ash was obtained from Thermal Power Station, Raichur. The chemical and physical properties of OPC, fly ash and silica fume are given in **Table 1**. The fineness of mineral admixtures was checked by wet sieving over a 45- μ m sieve at every 2 h as per ASTM C430-08 (2009a). After 20 h, it was observed that passing was more than 90%, better than the amount of OPC passing 45- μ m sieve.



Graded crushed aggregates with a maximum particle size of 12 mm with fineness modulus of 6.78, and natural river sand with fineness modulus of 3.43 was used to produce HSSCC. The specific gravity of sand and Coarse Aggregates (CA) was 2.62 and 2.70, respectively. Major tests were carried out on the sand and CA to check specific gravity, water absorption and fineness modulus and are presented in **Table 2**.

Master Glenium Sky 8233, a high range water reducing superplasticizer was used to increase the workability and reduce water content in the concrete. In this experimental work, superplasticizer was obtained from BASF chemicals, Bangalore. Physical and chemical properties of Master Glenium Sky 8233 are tabulated in **Table 3**. The viscosity modifying agent Master matrix 2, which is used to make the concrete more viscous and prevent segregation was provided by the BASF Company, Bangalore. The dosages of viscosity modifying agent for various applications typically range from 0.1 to 1.5% by weight of cement. If the dosage of VMA is higher than the requirement, it will affect the setting time and stability of entrained air.

Table 1 Major physical properties of constituent materials used in concrete

Chemical composition	OPC	Fly ash	Silica fume
SiO ₂ , %	19.3	62.63	91.9
Al ₂ O ₃ , %	5.2	23.34	0.7
Fe ₂ O ₃ , %	2.4	3.93	0.3
CaO, %	61.2	2.04	-
MgO, %	1.25	1.3	0.1
SO ₃ , %	3.2	0.6	0.1
Na ₂ O, %	0.069	0.63	0.06
K ₂ O, %	0.62	2.09	0.65
Loss on ignition, %	4.8	2.8	0.9
Density, kg/m ³	3089	2270	2260
Specific surface area BET, 10 ³ /kg	0.55	2.14	26.43
Fineness % retain on 90 μ sieve	3%	-	-
Initial setting time, min	62	-	-
Final setting time, min	370	-	-
Specific gravity	2.96	2.2	2.15
Compressive Strength, MPa		-	-
7 Days	45		
28 days	65		

Table 2 Physical properties of fine aggregates and coarse aggregate

Properties	Fine Aggregate	Coarse aggregate
Specific gravity	2.62	2.70
Water absorption	0.8 %	0.4%
Fineness modulus	3.43	6.78

Table 3 Physical and chemical properties of Master Glenium Sky 8233

Parameter	Result
Colour	Light brown
Change in Boiling point	>100° c
physical state Melting point	Not applicable
Flash point	Not applicable
Auto-ignition temperature	Not applicable
Viscosity (25°C)	=50-150 cps
Specific gravity (25°C)	=1.2
Thermal decomposition	Not determined
Soluble in water	Soluble
pH	> = 6
Chloride ion content	< 0.2%

Mix Proportions and Casting

A series of trial mixes (**Table 4**) were prepared in order to achieve a target strength of 70 MPa by varying superplasticizer at 2%, 2.5 % and 3% to obtain optimum dosage and water to binder ratio in the range of 0.34 to 0.4. For all the mixes, fresh properties were checked as per EFNARC guidelines to satisfy the conditions of SCC. After obtaining the results, a final mix proportion (TT3 in **Table 4**) was finalized and variations were done by replacing cement with fly ash and silica fume at 5%, 10%, 15% and 20%. These contents were finalized based on the available literature so as to achieve a compressive strength of 70 MPa. A total of 12 HSSCCs were produced to study the performance of SCC and compare their properties as given in **Table 5**.

A Revolving pan concrete mixer was used to prepare cubes and cylinders for the mixes. The batch quantities of coarse aggregates and fine aggregates were first dry mixed in the mixer and then 33.33 % of water was added and mixed for one minute. The binder and another 33.33% of water were then added to this wet mix and mixing process was carried out for 2 min. After this, the remaining 33.33% of water with superplasticizer and VMA was added and mixed for another 3 min. The same process was used to produce all the mixes.

Table 4 Trial mix design



Trial	Designation	Cement, kg/m ³	Sand, kg/m ³	C.A., kg/m ³	Water, l	W/C	Slump flow, mm	V-funnel test, s	L-box test, H2/H1
1 st trial	FT1	575	700	833	196	0.34	-	-	-
SP-2%	FT2	575	700	833	196	0.36	-	-	-
	FT3	575	700	833	196	0.38	-	-	-
	FT4	575	700	833	196	0.40	520	-	-
2 nd trial	ST1	575	700	833	196	0.34	-	-	-
SP-2.5%	ST2	575	700	833	196	0.36	538	46	-
	ST3	575	700	833	196	0.38	554	40	-
	ST4	575	700	833	196	0.40	574	35	-
3 rd trial	TT1	575	700	833	196	0.30	590	28	0.98
SP-3%	TT2	575	700	833	196	0.32	640	19	0.92
	TT3	575	700	833	196	0.34	690	10	0.86
	TT4	575	700	833	196	0.36	750	8	0.80

Table 5 Final mix proportion

Mix proportion ^a	Cement, kg/m ³	Silica fume, kg/m ³	Fly ash, kg/m ³	RCP, kg/m ³	Coarse agg, kg/m ³	Water, kg/m ³	Super plasticizer kg/m ³	3%,	w/c ratio
I0	575	-	-	700	833	196	-		0.34
IF1	546.25	-	28.75	700	833	196	17.25		0.34
IF2	517.5	-	57.5	700	833	196	17.25		0.34
IF3	488.75	-	86.25	700	833	196	17.25		0.34
IF4	460	-	115	700	833	196	17.25		0.34
IS1	546.25	28.75	-	700	833	196	17.25		0.34
IS2	57.5	57.5	-	700	833	196	17.25		0.34
IS3	488.75	86.25	-	700	833	196	17.25		0.34
IS4	460	115	-	700	833	196	17.25		0.34
IC1	546.25	14.38	14.38	700	833	196	17.25		0.34
IC2	517.5	28.75	28.75	700	833	196	17.25		0.34
IC3	488.75	43.13	43.13	700	833	196	17.25		0.34
IC4	460	57.5	57.5	700	833	196	17.25		0.34

^a I0- Conventional concrete, IF1- 5% Fly Ash, IF2-10% Fly Ash, IF3-15% Fly Ash, IF4-20% Fly Ash, IS1-5% S.F, IS2-10% S.F, IS3-15% S.F, IS4-20% S.F, IC1- 2.5%S.F+2.5% Fly ash, IC2-5% S.F+5% Fly ash, IC3-5%S.F+7.5% Fly ash, IC4-10% SF+10% Fly ash

TESTING AND DISCUSSION

Testing of all the mixes was done in both fresh states and hardened states. For Fresh state properties, EFNARC (2002) guidelines were followed. Flow-Ability, Filling-ability and Passing-Ability are the major characteristics of SCC in the fresh state. After mixing, all the mixes were tested for these 3 key parameters. A number of cubes and cylinders were also cast for testing compressive, split tensile strength and elastic properties.

Flow-Ability: The flowing ability of all the mixes was examined with respect to slump flow test and T 500 test as per EFNARC specifications. For slump flow test, the procedure is same as that of normal concrete except there is no need for compaction. After lifting the cone, the concrete spreads out and the diameter is measured (**Figure 1**). **Table 6** shows the slump flow values of conventional SCC concrete and SCC with different mineral admixtures. According to European guidelines the slump flow values are in between 600 mm to 800 mm to be classified as SCC.

From **Table 6** and **Figure 2**, it can be seen that the presence of silica fume in SCC makes the concrete mix more homogenous and stiffer as compared to the SCC with fly ash because of its reactive nature. The slump flow value decreases in a small amount for SCC with fly ash (IF1, IF2, IF3, IF4) and values of slump flow vary from 702 mm to 685 mm, that is, 2.42% decrement in slump values. The slump flow values for SCC with silica fume (IS1, IS2, IS3, IS4) decreases significantly as the amount of silica fume increases from 5% to 20%. The reason behind the reduction of slump values is the highly reactive nature of silica fume. The value of slump flow varies from 684 mm to 650 mm, that is, 4.98% reduction in slump flow values. The reduction of slump values for SCC with silica fume is doubled as compared to SCC with fly ash. For every 5% of addition of silica fume as a cement replacing material, the slump flow values are reduced by 2.11%. The SCC with a combination of both fly ash and silica fume (IC1, IC2, IC3, IC4), the slump flow values are reduced from 692mm to 670mm, i.e. 3.17% reduction in slump flow values. Hence, from above observation, it is clear that in presence of silica fume the slump flow values are rapidly reduced as compared to the fly ash.

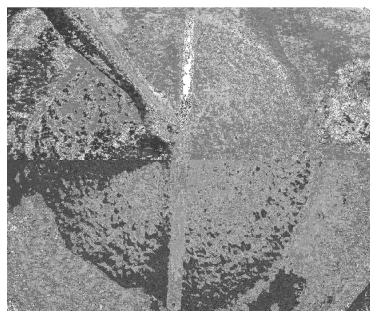


Figure 1 Measuring diameter for slump flow test

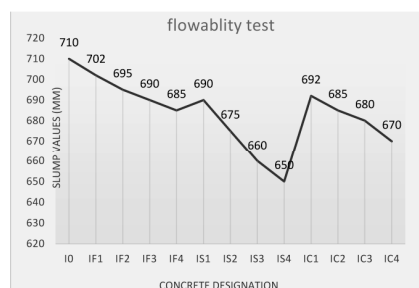


Figure 2 Test results for slump flow tests

Table 6 Slump flow test results

Sl No	1	2	3	4	5	6	7	8	9	10	11	12	13
Concrete designation	I0	IF1	IF2	IF3	IF4	IS1	IS2	IS3	IS4	IC1	IC2	IC3	IC4
Slump flow test, diameter, mm	710	702	695	690	685	690	675	660	650	692	685	680	670

The T50 slump flow time is a time required for concrete for the 50 cm slump flow. The lower value of time indicates the greater flow ability. According to European guidelines the T500 time has minimum 2 s and a maximum of 5 s. The T500 time test results are tabulated for various mix proportion in **Table 7**.

From **Table 7** and **Figure 3**, it can be seen that for SCC with fly ash (IF1, IF2, IF3, and IF4), T500 time did not vary significantly because the fly ash is chemically inactive at an early age of concrete. SCC with silica fume (IS1, IS2, IS3, IS4) gives higher value (4.06 s to 5.00 s) as compared to the SCC with fly ash (3.52 s to 4.20 s). The test results for SCC with a combination of silica fume and fly ash (IC1, IC2, IC3, and IC4) are nearly equal to the SCC with fly ash (IF1, IF2, IF3, IF4). The results showed that the concrete spreads uniformly and set quickly because of the higher dosages of superplasticizer and lower w/c ratio. All the mixes satisfied the requirement as specified by EFNARC.

Filling Ability

To check the filling ability of all the mixes of SCC, V-Funnel test was carried out as per the guidelines. The lower the flow time, better is the ability to fill. EFNARC guidelines give the range of 6 s to 12 s for SCC criteria. All the mixes tested were in this range satisfying the guidelines and the results were similar to T500 tests. The results are tabulated in **Table 8**.

From **Table 8** and **Figure 4** it can be seen that for SCC with fly ash (IF1, IF2, IF3, and IF4), the V-funnel test time did not differ much, values in between 9.50 s to 10.40 s have been found. SCC with silica fume (IS1, IS2, IS3, IS4) gives higher value (10 s, 10.5 s, 11.32 s, 12 s) as compared to the SCC with fly ash (9.50 s, 9.56 s, 10.12 s, 10.40 s). The V-funnel test time results for the SCC with silica fume (IS1, IS2, IS3, IS4) are higher because the silica fume increases the viscosity and homogeneity of concrete. IS4 with silica fume 20% gives 12 s time indicating viscous concrete but near to the boundary limit of satisfying SCC criteria as per EFNARC guidelines.

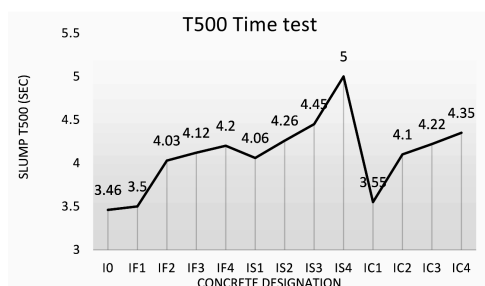


Figure 3 Test results for T-500 test

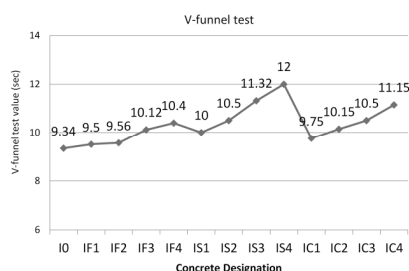


Figure 4 Test results for V-Funnel test



Table 7 T-500 test results

Sl No	1	2	3	4	5	6	7	8	9	10	11	12	13
Concrete designation	I0	IF1	IF2	IF3	IF4	IS1	IS2	IS3	IS4	IC1	IC2	IC3	IC4
T500 time, s	3.50	3.52	4.06	4.15	4.20	4.06	4.26	4.45	5.00	3.55	4.10	4.22	4.35

Table 8 V-Funnel test results

Sl No	1	2	3	4	5	6	7	8	9	10	11	12	13
Concrete designation	I0	IF1	IF2	IF3	IF4	IS1	IS2	IS3	IS4	IC1	IC2	IC3	IC4
V-funnel test value, s	9.34	9.5	9.56	10.12	10.4	10	10.5	11.32	12	9.75	10.15	10.5	11.15

Passing Ability

The passing ability of all the mixes was conducted with respect to L-Box test which gives the measurement of the passing ability of HSSCC with regard to blocking ratio H_2/H_1 . The higher value indicates the greater passing ability of SCC. The higher dosage of superplasticizer helped in achieving the results for passing ability. **Table 9** gives results for passing ability tests.

From **Table 9** and **Figure 5** it can be seen that SCC with fly ash (IF1, IF2, IF3, and IF4), SCC with silica fume (IS1, IS2, IS3, IS4) and SCC with combination (IC1, IC2, IC3, IC4) gives good results for L-box test mainly due to superplasticizer and VMA. The values vary between 0.8 to 1. The L-box test results for the SCC with silica fume (IS1, IS2, IS3, and IS4) gives very less value as the quantity or dosage of silica fume increases, the value varies in between 0.81 to 0.90. The L-box test results for the SCC with fly ash and SCC with the combination of both gives a nearly same value of (H_2/H_1). The L-box test results for the SCC with silica fume (IS1, IS2, IS3, IS4) are lower than other SCC mixes because the silica fume increases the viscosity and homogeneity of concrete similar to that of filling ability tests.

Effect of Water to Binder Ratio

Water to binder ratio is considered as one of the important factor influencing overall properties of all type of concretes. In SCC, here too, it plays a vital role in achieving strength as well as workability. It was seen from the experimental investigation that as the water to binder ratio decreases and binder quantity increases, the workability of HSSCC increases significantly because of superplasticizer and VMA content. This is mainly due to increased paste content and lesser aggregate contents which results in increased binder surface area due to the presence of porous, fine particles of fly ash and silica fume. Thus, the increased paste volume and higher wettable surface area of the binder induces better resistance to SCC flow.

Table 9 Test Results for L-box test

Sl No	1	2	3	4	5	6	7	8	9	10	11	12	13
Concrete designation	I0	IF1	IF2	IF3	IF4	IS1	IS2	IS3	IS4	IC1	IC2	IC3	IC4
H1, cm	10.3	10.2	10.1	10	9.8	10	9.7	9.4	9.0	10.1	9.9	9.7	9.2
H2, cm	9.8	9.4	9.2	8.9	8.5	9.0	8.4	7.9	7.3	9.2	8.8	8.5	7.8
L-box test value, H_2/H_1	0.95	0.92	0.91	0.89	0.87	0.90	0.87	0.84	0.81	0.91	0.89	0.87	0.85

Compressive Strength

The average 7 days and 28-days compressive strength of cube specimens for all mixes are shown in **Figures 6 to 8**. It was found that strength development in concrete specimens containing only silica fume was faster as compared to other specimens. This rate of initial strength gain can be due to using micro silica as the mineral admixture. As the water to binder ratio decreased, increase in compressive strength was observed as the binder content increased which resulted in the higher amount of calcium silicate hydrate (C-S-H) gel improving the physical packing of aggregates. This resulted in higher compressive strengths. It was observed that SCC with 15% silica fume (IS3) gives nearly 4% more compressive strength as compared to conventional SCC, and 5% to 10% more compressive strength as compared to SCC with fly ash. The increase in strength is due to the addition of mineral admixtures having the micro filling ability and pozzolana activity. With the presence of silica fume and fly ash, the concrete becomes dense and voids are reduced by decreasing the pores. Moreover, pozzolana reaction of mineral admixtures influenced the compressive strength of concrete by refining the microstructure of increased binder-paste and



improving interfacial bond between binder-paste and aggregates [12]. At 15% replacement by silica fume, a good amount of CaOH_2 liberated from hydration of cement increasing C-S-H gel by pozzolanic reaction with a high percentage of SiO_2 content in mineral admixture.

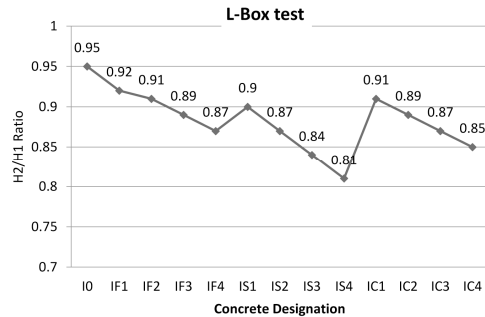


Figure 5 Test results for L-Box test

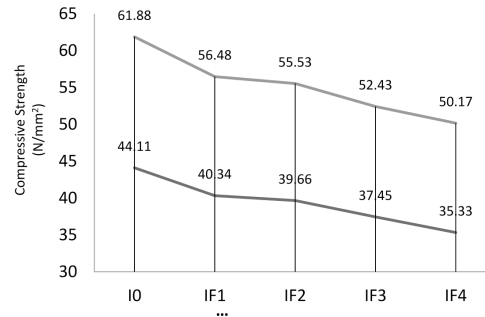


Figure 6 Compressive test results of SCC with fly ash

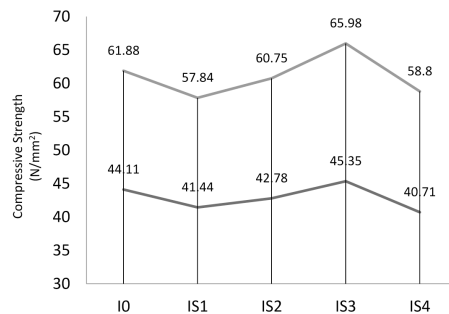


Figure 7 Compressive test results with SF

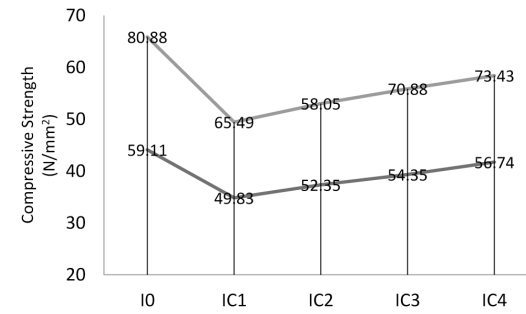


Figure 8 Compressive test results of SCC with SA and FA

It was also observed that CaOH_2 content in fly ash systems reached a maximum value after 7-14 days and was decreasing later as a result of its consumption in pozzolanic reaction. This decrease of CaOH_2 content followed the augmentation of strength due to use of fly ash. **Figure 9** shows a cube specimen after failure.

Split Tensile Test (SPT)

SPT of M70 grade SCC with mineral admixture (silica fume, fly ash), and normal self-compacted concrete were done on cylinders. The split tensile strength of concrete of standard cylinder size 150 mm diameter and 300mm long cylinder specimen is calculated for different curing periods of 7 and 28 days. SCC with fly ash gives higher split tensile strength results and increase in quantity of fly ash in concrete mix results in increased split tensile strength. For SCC with silica fume gives 17% more split tensile strength as compared to SCC with fly ash. The SCC with a combination of both silica fume and fly ash mixes (IC1, IC2, IC3, and IC4) gives nearly 15% more split tensile strength as compared to the SCC with fly ash. From above experimental work, SCC with 15% silica fume (IS3) gives 19.95% more split tensile strength as compared to SCC with fly ash and SCC with a combination of both silica fume and fly ash. **Table 10** gives the split tensile results for all the mixes and **Figure 10** shows a specimen of the cylinder failure.

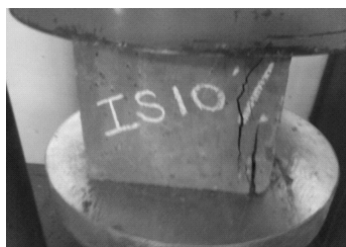


Figure 9 Cube specimen after failure



Figure 10 Cylinder specimen after failure

Table 10 Split tensile results

Concrete designation	Split tensile strength, N/mm ²	
	7 days	28days
I0	2.80	4.25
IF1	2.50	3.67
IF2	2.60	3.80
IF3	2.90	3.96
IF4	3.10	4.11
IS1	2.70	4.39
IS2	2.95	4.67
IS3	3.39	4.95
IS4	2.90	4.52
IC1	2.60	4.11
IC2	2.90	4.39
IC3	3.00	4.55
IC4	3.10	4.70

Modulus of Elasticity (MOE)

Self-Compacting Concrete and conventional concrete shows a similar modulus of elasticity. If the grade of concrete is higher than the modulus of elasticity of that concrete is also higher. For this test, a standard cylinder of 300mm length and 150 mm diameter are used and load applied in uniaxial compression. The MOE of SCC was determined from the stress and strain values of SCC concrete. To obtain the modulus of elasticity, the 80% of ultimate strength load was considered. **Figure 11** shows the test set up of cylinder specimen and **Figure 12** shows modulus of elasticity in N/mm² for different specimens along with the average curve. In **Figure 12**, horizontal axes can be read as follows I0-1, IF1-2, IF2-3, IF3-4, IF4-5, IS1-6, IS2-7, IS3-8, IS4-9, IC1-10, IC2-11, IC3-12 and IC4-13.



Figure 11 Test Setup for MOE

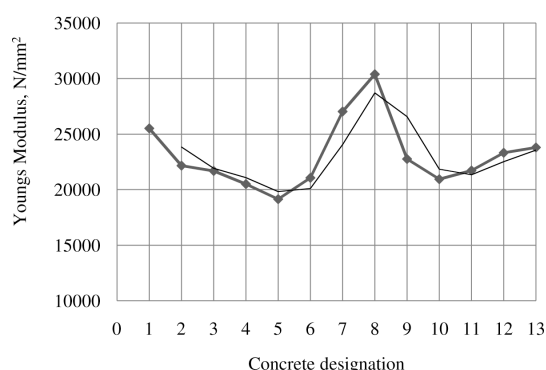


Figure 12 MOE of HSSCC

It was observed that HSSCC shows higher deformability as compared to conventional concrete. This high deformability observed was mainly due to the higher amount of paste content present in HSSCC as compared to conventional concretes. The reason behind this is due to the fact that aggregates are less deformable than hardened paste and high deformability can be observed in higher paste content in a hardened composition.

CONCLUSIONS

Water to binder ratio, SF and FA content and superplasticizer dosage significantly affected the fresh and hardened properties of HSSCC. Following conclusions can be drawn based on the results of this research:

- The results of slump flow test, V-funnel test and L-box test for SCC with silica fume and SCC with fly ash are less than SCC with a combination of both silica fume and fly ash.
- Presence of silica fume and fly ash require more dosages of superplasticizer because of its extremely high surface area for constant w/c ratio and the same was also observed in the previous literature of low strength SCC.



- The results of this study suggest that the SCC with a combination of both mineral admixtures improve the workability of concrete.
- Maximum compressive strength is obtained from SCC with 15% silica fume (IS3). The increases in strength can be attributed to the improved aggregate –matrix bond. For maximum compressive strength, optimum silica fume replacement with cement in percentage is in between 5% to 15%. The compressive strength reduces when silica fume replacement was above 15% of cement and vice versa.
- Maximum split tensile strength was also obtained from SCC with 15% silica fume (IS3). The durability of SCC is better than other normal concrete because SCC is less porous than normal concrete due to the addition of mineral admixtures.
- The value Modulus of elasticity of SCC with mineral admixture is nearly the same as that of conventional concrete.

REFERENCES

- H. El Chabib, A. Syed, Properties of self-consolidating concrete made with high volumes of supplementary cementitious materials. *J. Mater. Civ. Eng.*, Volume 10.1061/(ASCE)MT.1943-5533.0000733, 2012.
- E. Güneyisi, M. Gesoglu, E. Özbay, Permeation properties of self-consolidating concretes with mineral admixtures, *ACI Mater. J.*, Volume 108, Number 2, pp 150–158, 2011.
- A. A. A. Hassan, M. Lachemi, K. M. A. Hossain, Effect of metakaolin and silica fume on rheology of self-consolidating concrete, *ACI Mater. J.*, Volume 109, Number 6, pp 657–664, 2012.
- A. A. A. Hassan, M. Lachemi, K. M. A. Hossain, Effect of metakaolin and silica fume on rheology of self-consolidating concrete, *ACI Mater. J.*, Volume 109, Number 6, pp 657–664, 2012
- C. F. Ferraris, C. Lobo, Processing of HPC, *Concrete International* Volume 20, pp 61-64, 1998.
- M. Sonebi, S. Grunewald, J. Walraven, Filling ability and passing ability of self-consolidating concrete, *ACI Mater. J.*, Volume 104, Number 2, pp 162–170, 2007.
- M. Safiuddin, Development of self-consolidating high performance concrete incorporating rice husk ash, PhD thesis, Dept. of Civil and Environmental Engineering, Univ. of Waterloo, Waterloo, ON, Canada, 2008.
- M. Safiuddin, J. S. West, K. A. Soudki. Self-Consolidating high performance concrete with rice husk ash: Components, properties, and mixture design, 1st Ed., VDM Publishing House, Saabroecken, Germany, 2009.
- K. M. A. Hossain, M. Lachemi. Fresh, mechanical, and durability characteristics of self-consolidating concrete incorporating volcanic ash, *J. Mater. Civ. Eng.*, Volume 22, Number 7, pp 651–657, 2010.
- A. A. Ramezani-pour, A. Kazemian, M. Sarvari, B. Ahmadi. Use of natural zeolite to produce self-consolidating concrete with low Portland cement content and high durability, *J. Mater. Civ. Eng.*, 10.1061/(ASCE) MT.1943-5533.0000621, pp 589–596, 2012.
- V. W. Y. Tam, C. M. Tam. Assessment of durability of recycled aggregate concrete produced by two-stage mixing approach, *J. Mater. Sci.*, Volume 42, Number 10, pp 3592–3602, 2007.
- V. Sata, C. Jaturapitakkul, K. Kiattikomol. Utilization of palm oil fuel ash in high-strength concrete, *J. Mater. Civ. Eng.*, 10.1061/(ASCE)0899-1561(2004)16:6(623), 623–628, (2004).
- ASTM, Standard test method for fineness of hydraulic cement by the 45- μ m (Number 325) sieve, West Conshohocken, PA, pp C430-08, 2009a.
- European Federation of National Associations Representing Concrete (EFNARC). Specifications and guidelines for self-consolidating concrete, Surrey, UK, pp 1–32, 2002.



Enhancing Reuse and Recycling in Construction Industry through Modern Technologies

Krishna Nirmalya Sen^{*1}, A. K Poddar², G Muralidhar¹, Vimal Raj¹
Larsen and Toubro Metallurgical and Material Handling, Kolkata, India¹, knsen@Intecc.com^{*}
Larsen and Toubro Metallurgical and Material Handling, Dariba, India²

ABSTRACT

The construction industry has witnessed rapid growth in recent decades due to various factors, including increase in population, industrialization and urbanization. This in turn enhances usage of construction materials, drawn from natural resources and industrial products, leading to generation of substantial quantity of construction waste in project. Many a times, these construction wastes are not properly handled and get parked in landfills. Planned segregation and treatment could help to recycle or reuse a large portion of the waste thereby unlocking the economic value and environmental sustainability. Diverse range of waste get generated from construction industries, among those wood (2% to 15%), reinforcement bars (2 to 4%), and PCC (1% to 10%) hold the major chunk. For efficient and sustainable management of waste smart regulatory framework and strict enforcement of legislation system are essential aspects. Reduction, recycling, and reuse of wastes are essential for sustainable management of resources and waste. Useful products like reinforcement steel, doors and windows, bricks and other metal items can be taken out easily and can be reused without much processing. Materials those can generally be recycled from construction sites include:

- Metal waste
- Concrete waste
- Wood/Timber waste
- Grinding/cutting wheels waste
- Plastic/paint drums
- Welding rod residuals

There is an urgent need to understand the reuse and recycle potential of construction waste which on one hand will generate potential business opportunity, employment generation and above all environmental sustainability. In this present study various options and opportunities for reuse and recycling of construction waste are listed.

KEY WORDS Construction waste, Sustainability, Reuse and Recycling

INTRODUCTION

Construction industry is a major consumer of natural resources and one of the largest polluters [1]. Construction sector accounts for significant amount of natural resources and virgin material consumption. Construction waste is inert and heavy and is mostly unsuitable for disposal by incineration or composting. Research indicates that construction waste makes up 45% to 65% of waste dumped in landfills [2] and a major contributor of environmental pollutants. Waste is generated at different stages of construction process. Construction waste is generated throughout the different stages of construction process such as site clearance, material use, material damage, material non-use, excess procurement and human error [3]. With short period of duration and dynamic nature of construction industry makes it difficult quantity the waste generation. Different types and composition of waste generated in different stages of construction. Ineffective planning and waste management systems practiced at construction sites exacerbates the generation of construction waste. In recent times sustainability and environmental performance have become extremely popular and decisive in growth of construction industries. Ensuring effective construction management systems will result in better environmental performance/sustainable development of construction industries. It benefits organizations by minimising waste, cost savings and to avoid negative impacts on the environment and use of reclaimed and recycled materials. To achieve this waste hierarchy (The 'three Rs' principle – reduce, reuse, recycle) is the widely adopted system. If the waste is not generated at first, then there won't be any adverse human / environmental impacts. Recycling and re-using materials will make less waste and reduce the use of virgin material. Improving construction management, improved design equipment and practices such as better house-keeping, improved material handling, and equipment maintenance. Even though waste cannot be completely avoided, instead if not contaminated heavily major portion of it can be recovered, reused, and recycled.



CONSTRUCTION WASTE RECYCLING AND REUSE METHODOLOGIES

Various studies indicate that major constituents of construction waste which can be reused / recycled are concrete / aggregate, metal, wood, gypsum / plaster board etc. In this present study, viable technologies / methods which can be used for construction waste recycle / reuse are detailed.

CONCRETE WASTE

At construction site concrete waste mainly originates during pouring of concrete using static pump or hydraulic boom placer system as well as some leftover concrete from each pour. It can be assumed that approximately 1.55 to 5% of the concrete produced might end up as waste [4]. At the end of each day, during cleaning, noticeable amount of concrete waste can be identified. At this time due to various practical constraint and multiple grade of concrete mixture, it is generally not attempted for regular construction work. Such concrete waste is great loss and environmental burden as it won't get decomposed in the landfill because of its inert properties.

Hence recycling and reuse are the best options to deal with concrete waste. Left over concrete collected from pumps can be used for various utility purposes including at temporary facilities. Such as making of concrete blocks for use as secure footings for temporary barricading and hoarding posts across the site. This can also be used as concrete entry pads/slabs for workshops/welfare facilities and concrete planter/pots for plants etc. Dry concrete waste sorted out from the other wastes and can be recycled at recycling plant to form aggregates for road sub-base or underground stabilization [5].

Dry concrete crushed at recycling plants and segregated from other components like paper, steel etc.

Crushed aggregate can be refined by different methods like "Gravity Concentration Method", "Heating and Rubbing", "Mechanical Grinding" and "Screw Grinding". Refined aggregate could be used for producing reclaimed concrete and cement after mixed with rubble and lime.

METAL WASTE

Metal waste originates from construction industry in various phases. Cutting and bending of steel reinforcement to specific requirements for construction of main frames often results in metal waste. For example, one of the source of metal waste generation is internal partition works, which are constructed of a metal stud and plasterboard system. For making necessary openings, they are cut to size on-site to fit the required dimensions. By ensuring proper waste minimisation and reuse plan aligning with design criteria, this waste can be reduced. Recovered metal and concrete waste panels can be used for site fencing and hoarding purposes.

Segregated steel waste can be recycled at existing nearby plants to recover metal. When sorting metals from a mixed stream of recyclable material, paper is removed first leaving only plastics and metals. Eddy current separation by inducing electrical currents used to separate plastic. Modern recycling technologies can effectively identify many different kinds of metals. During the sorting process ferrous metals separated from non-ferrous metals by magnets and pulled out of the mixed waste stream. In scrap yards, cranes fitted with an electromagnet can remove larger pieces of ferrous scrap. Recovering precious metals such as palladium, platinum, gold and other valuable metals such as copper, lead, and silver from electronic waste can be done by using technologically advanced and sophisticated recycling equipment.

WOOD/TIMBER WASTE

Wooden materials are essential to the construction project and timber waste was generated consistently throughout the project. Significant proportion was produced during the construction of the false work and formwork for main concrete structural frames. All wooden materials used on site should be kept separate from other wastes.

By adopting slip-form system at site, amount of wood waste generated can be reduced. On completion of construction phase, remaining reusable wooden material shall be sorted and used at other construction sites by the same contractor. Wooden boards can also be reused on site several times until the quality of the boards is no longer suitable for use.

Timber which cannot be reused again should be sorted and stored separately from all inert waste and kept free from contaminants like nails, glass, plastics, surface coatings etc. **Segregated waste can be recycled to make useful items like** pathways, coverings, compost, garden amendments like landscaping/mulch, storage boxes etc.

Wood/timber waste material at recycling facility initially sorted by heavy equipment such as front-end loaders or excavators depending upon the material type, before being fed to an in-feed system. For large pieces of wood debris,



bulk reduction equipment such as a compactor or hydraulic shears may be required to reduce material sizes so that it can be inducted into the wood grinding system.

Conveyor systems also encompass features that allow for further sortation of foreign materials, including ferrous metal, before entering the grinding equipment.

GYPSUM/PLASTER BOARD WASTE

Gypsum waste mainly consisted of plasterboard off-cuts. Plasterboard sheets were ordered and delivered in standard sizes and then cut to size on site to suit design openings and services requirements. In addition, improper storage resulted in damaged materials that could not be used for their original intended purpose.

By appropriate stacking and weather protection and facilitating effective source segregation more recovery can be done at site. All of the segregated gypsum waste from work elements can be recycled. The recycled gypsum materials useful in cement production process and the paper was shredded and recycled. By consulting with manufactures segregate/discarded plaster board can be sent back to them as a part of take back recycling.

Plaster recycling activity is carried out through a series of highly efficient technological procedures. These processes are based on the separation of plaster from the cardboard and on the complete recycling of both materials. Process consists of a series of phases, in which the waste volume reduction, mechanical separation of plaster and paper. The recycled plaster dust is a high quality powder, almost totally free from cardboard and ready to be reused in a new cycle to produce plasterboard sheets or it can be used to level off pavement as an alternative to hydrated lime, or still, it can be used in the agricultural field as the material for soil conditioning, amending and fertilizing, according to real necessity. Cardboard can be reused in any productive process concerning paper.

CEMENT BAGS SCRAP

Concrete/cement usage occupies top spot when it comes construction industry. In the recent times, by introduction of bulkers and silos the amount of used cement bags reduced to some extent. Still there are some areas where the usage of cement bags is unavoidable. Cement bags can be reused in many ways including as carry bags, curtains, floor mat etc. Alternatively, some recycling agencies accept cement bags for various recycling purposes. The most predominant use is that these recycled polymers are used for making cheaper plastic products such as mugs, buckets and slippers.

GRINDING/CUTTING WHEELS WASTE

Grinding/cutting wheels are typically made up of metal alloys and should be treated as special waste and to be disposed of by a certified disposal company. Several grinding wheel manufacturers take back used grinding wheels back, and then dispose of them correctly as a part of take back recycling. Based on manufacturer and chemical makeup of grinding wheels, gather grinding wheels together and store them separately for easy handling during shipping out to manufacturer/recycler.

At recycling facilities, depending on the base material, these grinding wheels gets compacted. Upon processing grinding wheels can be used for other applications to process re-making wheels, blasting grit and abrasive/polishing materials.

PLASTIC/PAINT DRUMS

Whether the drums/containers used for hazardous or non - hazardous materials handling of used drums to be done with care. Used drums/containers often contains remaining traces of flammable materials and vapours from previously stored material. If handled without care, remaining flammables could result in fire hazards or explosion.

Hence to deal with empty drums and containers, expertise is required and safe handling methods to be followed. Whether drums of hazardous/non-hazardous nature, store drums separately in isolated areas and transport to the recycling facility. There drums will be treated and rinsed off the residuals for re - use or further recycling into other applications. Before recycling, most plastics are sorted according to their resin type. Some plastic products are also separated by colour before they are recycled. Appropriate sort systems can identify the resin, ranging from manual sorting and picking of plastic materials to mechanized automation processes that involve shredding, sieving, separation by rates of density i.e. air, liquid, or magnetic, and complex spectrophotometric distribution technologies [6]. The plastic recyclables are then shredded. These shredded fragments then undergo processes to eliminate impurities like paper labels. This material is melted and often extruded into the form of pellets which are then used to manufacture other products.



WELDING ROD RESIDUALS

In construction industry welding rod residuals originates consistently from structural fabrication and erection works throughout the project. Collection and storage of residual rods need firm and proper planning. Otherwise, these residual welding rods end up as waste and also create nuisance and slip hazard across the site. At one of our construction sites, with 70 to 80% collection efficiency we have recovered 10% of total welding rod weightage used. Further while improving awareness, collection and storage methods, the amount of residual rods quantity can be increased to 15 to 20 % and which can be recycled as same as metal scrap for other applications.

CONCLUSIONS AND RECOMMENDATIONS

Several studies highlighted that the amount of waste generated in construction projects and could have direconsequences on natural resources and environment. Major amounts of waste generation due to planning failures, poor site conditions, poor material storage and inadequate waste management systems etc. This present study highlighted some of the viable methods and technologies for construction waste reuse and recycling. Reuse and recycle of materials have positive impact through various avenues which enables and enhances sustainability of construction industry through cost control, reduction in natural resources usage and protection of environment.

REFERENCES

1. A. Horvath. Construction for Sustainable Development – A Research and Educational Agenda. Department of Civil and Environmental Engineering, University of California, Berkeley, USA. 1999, retrieved from <http://www.ce.berkeley.edu/~tommelein/CEMworkshop/Horvath.pdf> retrieved December 16, 2014
2. Q. Shi, X. Xie. A fuzzy-QFD approach to the assessment of green construction alternatives based on value engineering. In 2009. *International Conference on Management and Service Science (MASS 2009)*, IEEE, pp. 1–6, 2009.
3. D. S. Macozoma, International report - construction site waste management and minimisation. International Council for Research and Innovation in Building and Construction (CIB): South Africa, 2002.
4. C Ugochukwu Stanley, I Agugoesi Samuel, C Mbakwe Chinwendu, C Abazuonu, Lynda, An on-site Quantification of Building Material Wastage on Construction Projects in Anambra State, Nigeria: a comparison with the Literature. *Quest Journals Journal of Architecture and Civil Engineering*, Volume 05, Number 09, pp. 12–23, 2017.
5. A. Bansal, G. Mishra, S. Bishnoi. Recycling and Reuse of Construction and Demolition waste: sustainable approach, 2016.
6. Plastics Europe: Association of Plastics Manufacturers. Waste Pre-Treatment and Sorting. retrieved 8 July 2015.



Response of Multi-Storied Building on Raft and Pile Foundation under Soil-Structure Interaction

Sayanti Banerjee^{*1}, Kamal Bhattacharya¹

Civil Engineering Department, NIT Durgapur, India¹, sayanti06.05@gmail.com^{*}

ABSTRACT

The post-earthquake study of the structure discloses that the interaction between soil and foundation plays an important role in the damage of structure. So it is necessary to study the soil structure interaction effects while determining the behavior of the structures. In this paper, a comparison study of seismic response behavior with the inclusion of SSI effect of asymmetric 3D 28-storied building frame with the shear wall under Pile foundation and raft foundation is done in finite element software LUSAS 15.2. Time History (TARSCETHS) code is used to obtain synthetic time history of ground acceleration. This synthetic time history data is used in DEEPSOIL 6.14 to de-convolute the motion at a 60m soil base for different soil medium, depending upon shear velocities. This bedrock motion (at depth 60 m) is convoluted to get target response spectra at the ground. For the various type of soil, the natural frequency is obtained and it is found there is a small variation of frequency with the variation of soil type. In case of Raft foundation soft soil gives the highest storey shear values than medium and hard soil, but in case of Pile foundation model medium soil gives the highest storey shear values than soft and hard soil, as the model with Pile foundation is a bit stiffer than model with Raft foundation.

KEYWORDS 3D high rise building, Effect of the shear wall, SSI, Simulation of earthquake data, Convolution.

INTRODUCTION

Over the last few decades, various types of high-rise structures have been developed to be efficient in resisting both gravity and lateral loading. One of the most common of these is the wall-frame structure, comprising sets of shear walls and moment resisting frames. An understanding of the interaction in a wall-frame structure is given by the deflected patterns of a shear wall and a frame subjected severally to horizontal loading. With maximum slope at the top, the wall deflects in a flexural mode. While with the maximum slope at the base, the frame deflects in shear mode. The wall restrains or holds back the frame in the lower stories, while the frame restrains the wall in the upper stories. The notably different top slopes of the openly deflecting separate wall and moment resisting frame cause them, when combined in a wall-frame structure, to push on each other with a concentrated interaction force at the top, so that they adopt the same slope.

Soil Structure Interaction is a process in which response of soil influences the motion of structure and vice versa. In case of high rise structures, SSI plays a predominant role in the relative distribution of forces in various structural members. So it is inevitable to SSI during the design of such high rise structures resting on soft soil or a structure with relatively deep foundation. During earthquake, the response of a structure is affected by interactions between the structure, the foundation and the soil underlying and the surrounding the foundation. Soil-Structure Interaction (SSI) and Soil-Foundation-Structure Interaction (SFSI) are both used to evaluate the overall response of the structure. Kinematic interaction and inertial interaction are the two phenomena of soil-structure interaction analyses. All the modification of free field motion at the base of the structure is termed as kinematic interaction. Inertial interaction is the introduction of the deformation in the soil due to inertial force which transmits from the mass of the structure. The present study shows that the response of both the foundation and soil can greatly affect the overall structural response. SSI was found to be one of the strong reasons behind Yashinsky cities damage in the number of pile-supported bridge structures in Loma Prieta earthquake in San Francisco in 1989.

Using finite element approach, Belkar and Ladhane[10] has shown that, soil has significant contribution in structure response during dynamic analysis such as earthquake. Comparing with fixed base analysis, it is observed that a displacement of a structure for same loads increases around 16% for analysis with soil structure interaction as for example for maximum load = 3000 kN, displacement at each level increases around 18% for the analysis with SSI.

Kuladeepu, et.al. [7] have studied the effect of soil flexibility on the seismic response of building frames resting on



raft foundation using FEM software SAP2000, Ver14. It is observed that due to soil flexibility natural period increased and that is due to the overall reduction in lateral stiffness.

Chore et al (2010) [4] studied the SSI analysis of framed structures including pile foundations, and they highlighted the necessity of interactive analysis to build frames resting on pile foundations. They also studied the effect of SSI on a single storey, two bay space frames resting on a pile group embedded in the clayey soil with flexible cap.

In this paper a comparative study on multi-storey building with Pile foundation and Raft foundation is studied. Moreover different parameters such as fundamental frequency variation with different soil stiffness, storey shear and bending moment variation with soil flexibility are also studied. For earthquake analysis deconvoluted earthquake data is used as within motion.

GEOMETRIC MODELLING

A symmetric 3D G + 27 storied RC building is considered in the present study [3]. Plan view of the building is shown in **Figure 1**. In finite element software LUSAS 15.2 this modelling is done and analysed. The floor framing consists of 0.15 m × 0.5 m deep skip joist framing between haunch girders which span the distance of 10.67 m between the shear walls and the exterior frame of the building. The girders are 1.07 m × 0.5 m deep for the exterior part of 8.53 m length, with a haunch in the interior tapering from a pan depth of 0.5 m to 0.84 m. Four shear walls of dimensions 0.45 m × 5.96 m rise for the full height from 1.5 m pile cap. Diameter and length of 168 numbers of the piles are 1m and 12 m, respectively and thickness of 4 piles are 0.85 m, which are below the shear walls. The exterior columns are 0.965 m × 0.864 m. A slab of 0.15 m thick is provided in all the floors. Height of each floor is 3 m. Thickness of the raft foundation is 1.5 m.

Two different models are analysed, that is, building with pile foundation and building with raft foundation. Beams, piles and columns in the structure are modeled as a line using 3D thick Beam element (BMI21). Shear Wall and Pile Cap and Raft Foundation are modeled as a surface with Quadrilateral (QTS4) Thick Shell element. Slab is modeled as a surface with Triangular (TTS3) and Quadrilateral (QTS4) thick shell elements.

The total volume of the soil is $187.3 \times 443.7 \times 60 \text{ m}^3$. For modelling of soil, three times of building plan in two lateral directions are considered and depth of soil is taken as two times (60 m) of the least plan dimension of structural model. Soil is modeled as a volume using 3D Solid Continuum Element (HX8M).

MATERIAL PROPERTIES

Mainly two materials are modeled in this study, that is, reinforced concrete material and soil mass.

To model the soil for different stiffness the elastic modulus [2] is varied between $1\text{e}7 \text{ N/m}^2$ to $2.56\text{e}9 \text{ N/m}^2$ (that is, soft to very hard soil). Soil mass density (1600 kg/m^3) is kept constant for this wide range of variation of soil stiffness.

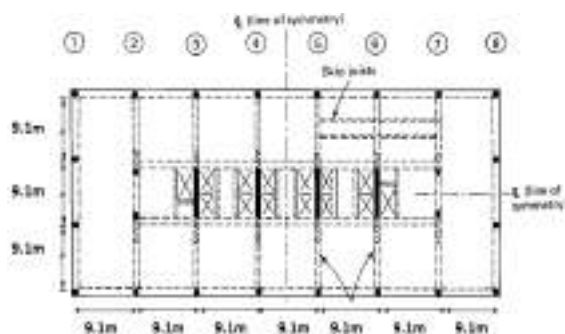


Figure 1 Plan of the structure

Table 1 Material properties of concrete.

Grade of concrete	M30
Young modulus (E)	$2.74 \times 10^{10} \text{ N/m}^2$
Mass density (ρ)	2548.42 kg/m^3

Table 2 Material properties of soil.

Soil type	Shear wave velocity, m/s	Poisson's ratio, μ
Hard	600	0.3
Medium	300	0.35
Soft	150	0.4



VARIATION IN NATURAL FREQUENCY FOR PILE AND RAFT FOUNDATION

In this study, the variation on fundamental natural frequency of the model with Pile Foundation is compared with the model with Raft Foundation. It is seen that the natural frequency for the model with pile for hard soil is lesser than the model with raft. But in medium and soft soil natural frequency comes to be larger than that of the model with raft foundation.

It is seen that, due to pile foundation, with respect to fixed base condition there's a 9.98% decrease in natural frequency, whereas for hard soil a decrease of 7.14% is observed. With increased soil flexibility namely for medium and soft soil, there is merely 3.31% and 0.84% increment is noted.

CHARACTERIZATION AND SIMULATION OF EARTHQUAKE DATA

More often than not when dealing a SSI problem in Finite Element Analysis the ground motion is to be applied at the base of the model. The Response Spectra available in standard seismic codes are generally for free field ground motion. It is not advisable to apply this free field motion directly at the bottom of finite element model because the ground motion changes beneath the foundation due to interaction. Mejia and Dawson (2006)[8] in their study of, "Earthquake de-convolution for FLAC", used de-convolution analysis using a 1-D wave propagation code, such as the program SHAKE, is performed to obtain the appropriate input motion at depth. Frequency domain (FD) equivalent linear (EQL) and time domain (TD) nonlinear (NL) analyses are the most common approaches used for performing 1D seismic site response analysis. However Deconvolution cannot be performed in the time domain analysis. Finding the motion at the bottom of the soil profile for a given motion at the ground surface is an inverse phenomenon which is generally performed in linear elastic one dimensional analysis. In this study frequency approach is followed by 1D wave propagation. The code DEEPSOIL (Hashash et al., 2012), which is capable of performing Frequency domain (FD) equivalent linear (EQL) analyses, is adopted for performing 1D site response analysis. The ground response spectra of IS:1893-2002, **Figure 2** is converted into simulated time history data, by using TARSCSTH code. This synthetic time history response is given as an input to DEEPSOIL V 6.1 (soil column depth 60m) as an 'Outcrop' motion and depending upon shear velocities (**Table 2**) and damping property of soil column (assumed very small) the output is obtained as a 'Within' motion (at the bed rock).

As per, IS 1893-2002, **Figure 3** the response spectra is given in terms of spectral acceleration. In this case for the ease of our calculation this spectral acceleration is converted into factored acceleration by multiplying $\frac{Z_I}{2R}$. The 28-storied building model considered in the study is assumed to be situated in Zone III with zone factor = 0.16. It is considered that building has a ductile shear wall with special moment resisting frame (SMRF), so response reduction factor, $R = 5$. Since it is a high rise structure importance factor associated with the building model is considered as $I = 1.5$.

For other soil conditions, same procedure is done and it can be seen that the reconvolution process is giving almost same response spectra at the ground similar to IS code target spectra and from that it is inferred that the de-convolution at 60 m depth is correct. This study shows that Deconvolution of earthquake motion is required to characterize the response when the soil and structure act together and the motion is given beneath the soil body.

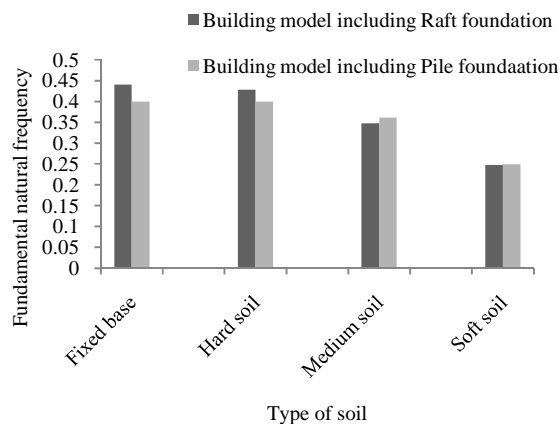


Figure 2 Variation in natural frequency for pile and raft foundation

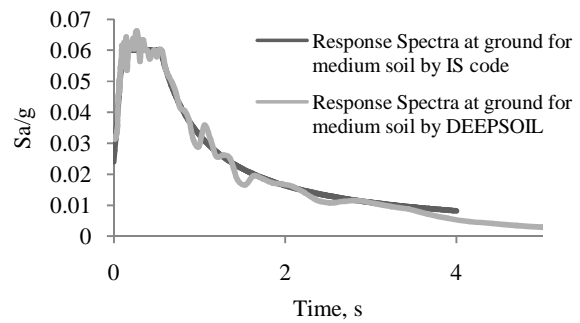


Figure 3 Comparison between target response spectra and re-convoluted response spectra at ground level for medium soil

RESULTS AND DISCUSSION

To understand the effect of Soil Structure Interaction

(SSI) on different types of foundation 'Response Spectrum Analysis' is carried out on building model with pile foundation and Raft foundation resting on soil surface for different soils condition (Hard, Medium, and Soft).

Comparison between Building with Raft Foundation and Pile Foundation under Same Earthquake Loading

In this study, the variation of displacement values of the model with Pile Foundation is compared with the model with Raft Foundation. The effect of pile foundation on the same building model on the displacements under earthquake loading is studied and the results are represented in the **Table 3** and **4**. All these studies have been done on the model of 60 m soil depth.

Table 3 Comparison of displacements for pile and raft foundation for hard and medium soil condition

Floor level	Building with pile foundation		Building with raft foundation	
	Hard soil	Medium soil	Hard soil	Medium soil
28	0.0186	0.0629	0.0187	0.0616
20	0.1444	0.0472	0.0143	0.0458
12	0.0084	0.0274	0.0086	0.0266
1	0.0004	0.0135	0.0010	0.0153

Table 4 Comparison of displacements for pile and raft foundation for soft soil condition

Floor level	Building with pile foundation Soft soil	Building with raft foundation Soft soil
28	0.0914	0.1101
20	0.0737	0.0865
12	0.0523	0.0586
1	0.0223	0.0195

From **Table 5** and **6**, it is seen that, for hard soil both the models are giving almost same displacement behaviour but in case of medium soil condition it is seen that up to 12th floor pile foundation gives higher displacements than raft. Whereas the trend is reverse in soft soil where it is seen that the raft foundation yields greater storey displacements than pile foundation at almost all floors except at the bottom five floors where it is almost equal. Now for further confirmation of this study, storey wise shear values for both the models are computed and results are compared for different soil conditions.



Table 5 Comparison of storey shear distribution for medium soil for pile and raft foundation.

Floor Level	Building with pile foundation Storey shear, kN (medium soil)	Building with raft foundation Storey shear, kN (medium soil)
28	6858.3317	6789.4414
21	8989.9104	8462.3732
16	10948.4269	10240.7066
11	11737.9290	10941.7736
6	10961.0555	10067.7862
1	17721.2602	16275.7004

Table 6 Comparison of storey shear distribution for soft soil for pile and raft foundation.

Floor level	Building with pile foundation Storey shear, kN (soft soil)	Building with raft foundation Storey shear, kN (soft soil)
28	7154.64	9546.19
21	7420.85	9327.19
16	9039.68	11167.04
11	10052.81	12291.06
6	9580.15	11740.74
1	14815	17642.82

Maximum difference of storey shear between the models in hard soil is found at 7th floor where the shear for model upon raft is @ 38% more than over the pile foundation. The same is observed in soft soil where maximum difference in storey shear is observed at 1st floor which is @ 19% higher for raft than pile foundation. However in case of medium soil the pile foundation yields higher shear than raft which is @ 12.65% more at 2nd floor. Thus it is stated that only in medium soil, model on pile yields different result than the other two soils.

The Bending Moment Distribution (BMD) for different stories is also studied as shown in **Figure 5** and **Table 7** and **8**.

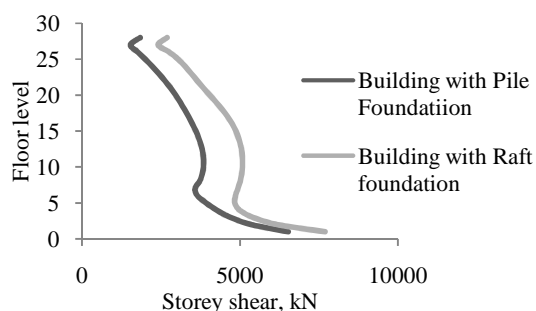


Figure 4 Storey shear distribution for hard soil for Pile and Raft foundation

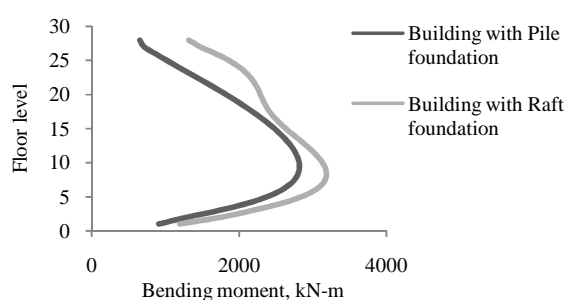


Figure 5 Bending moment distribution for hard soil for pile and raft foundation

Table 7 Comparison of bending moment distribution for medium soil for pile and raft foundation

Floor level	Building with pile foundation Bending moment, kN-m (medium soil)	Building with raft foundation Bending moment, kN-m (medium soil)
28	1674.4960	1398.4098
21	4707.1852	4140.6566
16	6554.7090	5770.8978
11	7460.0120	6554.3266
6	6624.9190	5860.4268
1	2361.5177	2408.5474



Table 8 Comparison of bending moment distribution for soft soil for pile and raft foundation

Floor level	Building with pile foundation Bending moment, kN-m (soft soil)	Building with raft foundation Bending moment, kN-m (soft soil)
28	842.2976	1068.9342
21	2533.5335	2747.1644
16	3928.0843	4320.3746
11	4893.4732	5374.9696
6	4752.2979	5177.3105
1	2122.4566	2527.7158

Maximum difference of bending moment between the models in hard soil is found at 25th floor where the bending moment for model upon raft is @ 81% more than over the pile foundation. The same is observed in soft soil where maximum difference in bending moment is observed at 10th floor which is @ 9.7% higher for raft than pile foundation. However in case of medium soil the pile foundation yields higher bending moment than raft which is @ 12% more at 10th floor. Thus it is stated that only in medium soil, model on pile yields different result than the other two soils.

CONCLUSIONS

In this study a comparison of responses of model with Pile foundation and the model with Raft foundation is done. Following conclusions can be drawn from this study-

- Natural frequency is varying for various types of soil, like for hard soil frequency is highest than medium and soft soil. For soft soil, natural frequency is least.
- In earthquake loading, storey displacement on soft soil is largest than medium soil and hard soil.
- In case of raft foundation model soft soil gives the higher storey shear values than medium and hard soil, but in case of pile foundation model medium soil gives the higher storey shear values than soft and hard soil. For that building model, in medium soil condition, pile foundation is more effective and efficient than raft foundation.
- In medium soil for Pile foundation model the Bending Moment is maximum than other soil conditions, as the model with Pile foundation is a bit stiffer than model with Raft foundation.

REFERENCES

1. A.Papageorgiou, TARSCTHS-User's Manual, Version 1.0.
2. APPC-Soil Properties | SK Kong-Academia.edu.(https://www.academia.edu/8149496/APPC-Soil_Properties)
3. B. S. Taranath, Structural Analysis and Design of Tall Buildings, McGraw-Hill Book Company, 1988.
4. H. Chore, R. Ingle, Interactive analysis of building frame supported on pile group using a simplified F.E. model, J. Struct. Eng. SERC, Volume 34, 6, pp 460-464, 2008.
5. Y.M.A. Hashash, et al. DEEPSOIL 6.1, User Manual, 2016.
6. IS Code-1893 (Part-I), Criteria for earthquake resistant design of structures, 2002.
7. M. N. Kuladeepu, G Narayana, B K Narendra, Soil structure interaction effect on dynamic behaviour of 3D buildings frames with raft footing, IJRET, Volume 4, Issue 7, July 2015.
8. L. H Mejia, E.M. Dawson, Earthquake deconvolution for FLAC, 4th International FLAC Symposium on Numerical Modelling in Geomechanics, Hart & Varona (eds.), pp 04-10, 2006.
9. LUSAS 15.2 Documentation and Application.
10. S. Belkar, K. Ladhane, Dynamic Analysis of Soil Structure Interaction of Pile Supported Frame Structure, International Journal of Scientific and Engineering Research, ISSN 2229-5518, Volume 6, Issue 10, October 2015.



Analysis of Buckling Strength of Circular Plates with Discrete Stiffeners

V. Lakshmi Shireen Banu^{*1}, V Vasudeva Rao²

Department of Civil Engineering, Malla Reddy Engineering College (Autonomous), Dhulapally, Secunderabad, Telangana, India¹, vlsbanu@yahoo.co.in^{*}

Department of Mechanical and Industrial Engineering, CSET, University of South Africa, Florida 1710, South Africa²

ABSTRACT

In the present investigation, numerical simulation and analysis of buckling of stiffened thin circular plates subjected to in-plane loading has been carried out. For the analysis a circular plate with radius 0.5 m and thickness 0.005 m is considered for all the cases that are included in this study. The circular plate under study is reinforced with T, I and H shaped ring stiffeners that are placed at different radial locations of circular plate to investigate their effectiveness. The boundary conditions considered are such that the plate is fixed but released in radial direction. The effect of T, I and H shaped stiffeners placed at various radial locations on circular plates subjected to in-plane radial loads was numerically studied using ABAQUS. In the present investigation, four models of circular plates with different shapes and thickness of stiffeners and cross sections are considered. The deformation shapes and buckling loads are presented pictorially along with the results in tabular form.

KEYWORDS Buckling, Circular plates, Stiffeners, Thin shells

INTRODUCTION

Circular plates are said to be structural members generated by a combination of two flat surfaces and a circumferential edge which is perpendicular to the flat surface. Thickness of the plate is the perpendicular distance between the two parallel faces. Size of a plate is represented by its characteristic dimensions such as thickness, length, width or diameter. For a plate, the thickness is considerably far less than the other characteristic dimensions

Flat or slightly curved plates are frequently used in the construction of space-vehicle structure. Buckling of structural members under dynamic loads is one of the important areas of research and continues to receive increased attention due to applications in space research.

Most of the previous research studies focused attention on simple structures including columns, plates and shells. However, research with focus on the effect of stiffeners attached to circular plates with wide range of applications and boundary conditions is limited. From the applications point of view, plates will have either straight or curved geometry. In general, plates are exposed to loads (static or dynamic) that are normal to flat surfaces with few exceptions.

The system of forces acting on a plate and the resistance offered by the plate to external forces is very similar to beams or cables. Hence, an approximation can be made that the plate acts like a grid work of numerous beams or a grid work of cables. However, the plate being a two-dimensional structural member, the resistance to deformation is much higher and plate structural members offer several advantages including light weight and low cost. Plates are assumed to be initially flat and develop resistance to bending and twisting moments when subjected to external forces. Due to the two-dimensional action, the twisting rigidity of a plate is significantly higher than an equivalent beam with comparable thickness and span. Therefore, thin plates with stiffeners attached at suitable locations offer several advantages in terms of efficiency, capacity to resist loads coupled with economy.

Ma and Wang[1], Brubak and Hellesland [2], Ding and Yu [3], Yu and Wang [4] Luo and Pozrikidis[5] have studied bending and buckling behaviour of thin circular plates subjected to a variety of loads and different boundary conditions. Their work includes functionally graded materials. Li and Batra [6], Jain [7], Rao and Rao [8] have studied the vibration of thin circular plates and their mode shapes. Mandal [9], Lancaster, Calladine and Palmer [10], Mandal and Calladine [11] have investigated the buckling of thin cylindrical shells under axial compression.

In this paper it is proposed to investigate the buckling of stiffened circular plates using the protocols specified in the user manual of ABAQUS [12].

ANALYTICAL SOLUTIONS

Thin circular diaphragm plates are used as sensing elements in pressure measuring devices. These diaphragm plates are subjected to in-plane radial compressive forces from the supporting structure when there is a change in the working temperature of the medium or the device. In the following section governing differential equations for plates subjected to buckling loads are presented.



Circular Plate subjected to Uniformly Distributed In-plane Compressive Radial Forces

As shown in **Figure 1**, in the present analysis, a circular plate is considered that is subjected to in-plane radial compressive forces (q_r). In the buckling analysis of we include only axisymmetric geometries such a circular plates. Thus, we can use polar coordinate system represented by r and θ . Equation (1) that represents buckling of a rectangular plate can be transformed to a circular plate for convenience of analysis.

$$\frac{\partial^4 w}{\partial x^4} + 2 \frac{\partial^4 w}{\partial x^2 \partial y^2} + \frac{\partial^4 w}{\partial y^4} = \frac{1}{D} \left(N_x \frac{\partial^2 w}{\partial x^2} + 2 N_{xy} \frac{\partial^2 w}{\partial x \partial y} + N_y \frac{\partial^2 w}{\partial y^2} \right) \quad (1)$$

In a specific case of equilibrium in an axi-symmetric loading,

$$N_x = N_y = N_r = -q_r, N_{xy} = 0 \quad (2)$$

Denoting, $\mu^2 = \frac{q_r}{D}$ (3)

and using the relations between the polar and Cartesian coordinates, we can derive an equation for axi-symmetric circular plate subjected to circumferential compressive force as shown in **Figure 1**, is given below.

$$\frac{d^4 w}{dr^4} + \frac{2}{r} \frac{d^3 w}{dr^3} - \frac{1}{r^2} \frac{d^2 w}{dr^2} + \frac{1}{r^3} \frac{dw}{dr} + \mu^2 \left[\frac{d^2 w}{dr^2} + \frac{1}{r} \frac{dw}{dr} \right] = 0 \quad (4)$$

Let us introduce the following new variable:

$$\rho = \mu r \quad (5)$$

that denotes a non-dimensional polar radius. By means of new variable ρ , it is possible to rewrite the above Eq. (4), in to the form of Eq. (6) given below.

$$\frac{d^4 w}{d\rho^4} + \frac{2}{\rho} \frac{d^3 w}{d\rho^3} + \left(1 - \frac{1}{\rho^2} \right) \frac{d^2 w}{d\rho^2} + \frac{1}{\rho} \left(1 + \frac{1}{\rho^2} \right) \frac{dw}{d\rho} = 0 \quad (6)$$

Eq. (6) is a linear 4th order, homogeneous differential equation. The general solution for Eq.(6) is given below.

$$w(\rho) = C_1 + C_2 \ln \rho + C_3 J_0(\rho) + C_4 Y_0(\rho) \quad (7)$$

Where $J_0(\rho)$ is Bessel's function of first kind and $Y_0(\rho)$ is Bessel's function of second kind both for zeroth order. In Eq. (7), above, C_1, C_2, C_3 and C_4 are constants of integration. Since $w(\rho)$ must be finite quantify for all values of ρ , including $\rho = 0$, then the two terms with ρ and $Y_0(\rho)$, having singularities at $\rho = 0$, must be dropped for the solid plate because they approach an infinity when $\rho = 0$. Thus, for the solid circular plate, Eq. (7) must be taken in the form,

$$w(\rho) = C_1 + C_3 J_0(\rho) \quad (8)$$

to determine the critical buckling loads q_r . These loads are assumed to be acting at the mid plane of the circular plate.

FE MODELLING AND ANALYSIS

All FEM modeling was completed using ABAQUS software package. The four-node, doubly curved, linear shell element selected for the models can be found in the ABAQUS element library. Shell elements were chosen over three dimensional elements in order to maintain acceptable element aspect ratios with a reasonable mesh density.

Circular plate with stiffeners is subjected to axial compressive load of 20kN. The plate is considered to be fixed but released in radial direction. Circular Plate with three different stiffeners T, I and H-Shape is chosen for stiffening. Material for circular plate and stiffeners chosen is mild steel. The FEM analysis is carried-out with ABAQUS.

The radius of circular plate is 0.5m and thickness is 0.005m. The axial compressive load applied is 20kN. The analysis was done for four different models of circular plate. In first model, circular plate with T-shape and $N=1, N=2, N=3$. Thickness of stiffener is taken in the range from 0.01m to 0.02m with an increment of 0.0025m.

In second model, circular plate with I-shape stiffener is considered for $N=1, N=2, N=3$.

In third model, circular plate with HAT-shape stiffener is considered for $N=1, N=2, N=3$.

Material Properties

Mild steel: Young's modulus $E=200\text{GPa}$, Poisson's ratio $=0.3$.

RESULTS AND DISCUSSION

The results of the numerical analysis are presented in tabular form in **Table.1** and **Table.2**. **Figure 2** and **Figure 3** show the geometric model and the boundary conditions imposed on the plate with stiffeners. **Figure 4** shows schematically the circular plate with ring stiffeners. Typical deformation pattern of circular plates with T, I and H stiffeners subjected to radial in-plane compressive loads is presented in Figure5, Figure6 and Figure7 respectively. It is found from Table-1, that the H-shaped stiffener exhibited highest buckling strength and T-shaped stiffener the lowest strength. It is shown in **Table 2** and **Figure 8** to **Figure 12** that the buckling strength increases with stiffener thickness for all cases considered.

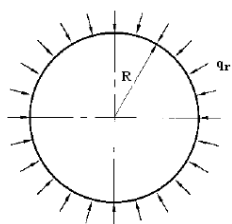


Figure 1 Circular plate subjected to uniformly distributed in-plane compressive radial forces

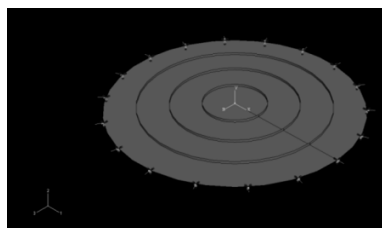


Figure 3 Loading and boundary conditions for stiffened circular plate (T-Shape stiffener)

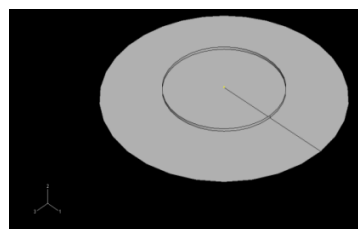


Figure 2 Circular plate with ONE stiffener (T-SHAPE)

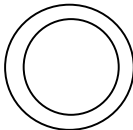
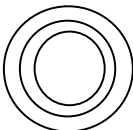
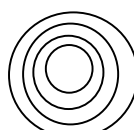
N=1	N=2	N=3
		

Figure 4 Circular plate with stiffeners

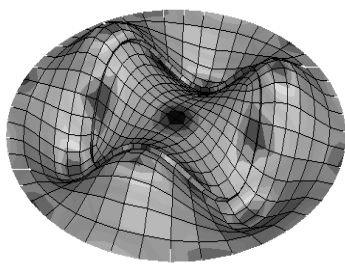


Figure 5 Deformed shape of circular plate with T-Shape stiffener

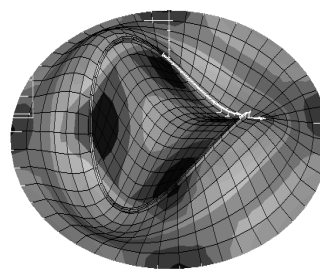


Figure 6 Deformed shape of circular plate with I-shape stiffener

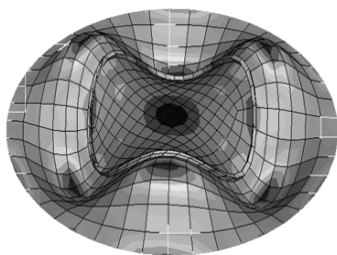


Figure 7 Deformed shape of circular plate with HAT-

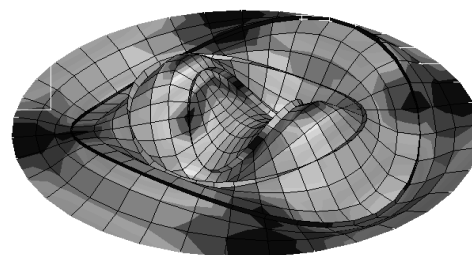


Figure 8 Deformed shape of circular plate with



shape stiffener

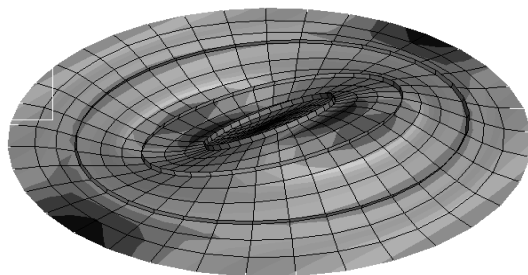


Figure 9 Deformed shape of circular plate with three T-Shape stiffener of thickness 0.0125 m

three T-Shape Stiffener of thickness 0.01m

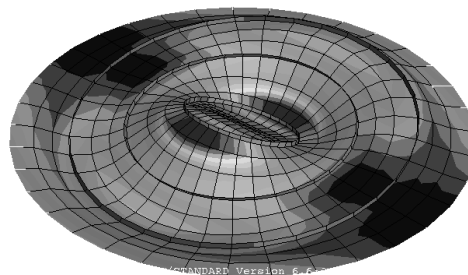


Figure 10 Deformed shape of circular plate with three T-Shape stiffener of thickness 0.015m

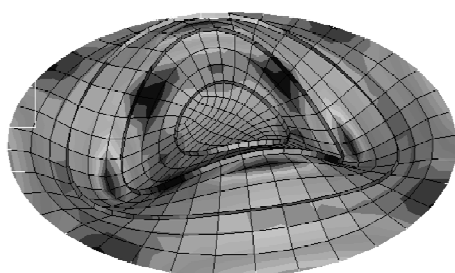


Figure 11 Deformed shape of circular plate with three T-Shape stiffener of thickness 0.0175m

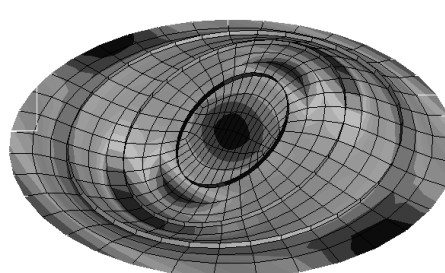


Figure 12 Deformed shape of circular plate with three T-Shape stiffener of thickness 0.02 m

Table 1 Comparison of plate buckling load with different stiffener shape

Shape of stiffener	Buckling Load, kN											
	Mode-1		Mode-2		Mode-3		Mode-4		Mode-5		Mode-6	
	5mm	10mm	5mm	10mm	5mm	10mm	5mm	10mm	5mm	10mm	5mm	10mm
T-shape	138.36	170.16	249.3	281.7	249.4	281.78	388.08	457.32	390.66	458.34	469.12	478.12
I-shape	202.98	250.96	302.96	342.54	303.14	342.82	481.68	494.96	523.28	595.48	524.12	597.16
HAT-shape	218.5	271.64	329.38	371.9	330.12	372.68	497.32	521.26	549.7	631.46	550.28	632.14

Table 2 Buckling strength of circular plate as a function stiffener thickness (t-shaped stiffener)

Thickness of T shape stiffeners, m	Buckling load, kN																	
	Mode-1			Mode-2			Mode-3			Mode-4			Mode-5			Mode-6		
	N=1	N=2	N=3	N=1	N=2	N=3	N=1	N=2	N=3	N=1	N=2	N=3	N=1	N=2	N=3	N=1	N=2	N=3
0.01	170.16	192.3	213	281.7	303.66	326.16	281.78	303.72	326.3	457.32	527.44	581.34	458.34	530.4	581.6	478.12	567.44	613.36
0.0125	178.12	205.22	230.9	291.02	321.5	345.34	291.18	321.7	352.68	471.48	567.66	639.28	472.36	570.84	639.6	480.64	589.46	644.54
0.015	185.54	217.34	247.84	299.56	339.54	379.98	291.18	340	380.04	483.04	605.98	673.34	483.64	609.42	698	484.5	609.84	698.54
0.0175	192.5	228.72	263.92	307.26	357.38	407.8	307.8	358.2	407.88	485.4	628.48	700.38	494.24	641.44	756.02	495.16	645.2	756.68
0.02	199	239.48	279.22	314.16	374.74	435.52	314.9	376	435.72	487.68	645.72	725.84	503.66	673.48	812.2	504.66	677.5	813.02

CONCLUSIONS

- In the present study the buckling strength of stiffened circular plates subjected to in-plane radial compressive loads is determined successfully through FE based numerical simulations.
- It is concluded from the present study that the buckling strength of the circular plate increases with mode of deformation and buckling.



- It is concluded that the geometric shape of stiffener used to reinforce the plate has a great significance in improving the buckling strength of circular plate. The effect of stiffeners configuration is very important since it can affect the overall behavior of the plate buckling considerably.
- It is observed that all stiffer geometric shapes such as T, I and H showed enhancements in buckling strength. While H shaped stiffener showed highest enhancement, T shaped stiffener has relatively lower enhancement in buckling strength of circular plates.
- It is also concluded that the thickness of the stiffener has an effect on the buckling strength. It is observed that, as the thickness of stiffener increases, there is a corresponding improvement in the buckling strength.

SCOPE FOR FUTURE WORK

It is understood that the predictive capabilities of the numerical models and software tools greatly depends on the proper definition of the problem and well-defined boundary conditions specific to a problem. It is possible to explore a variety of problem specifications and boundary conditions with the help of software tools. Estimation of critical buckling loads with number of variations in the geometric parameters is also under way.

Experimental data generated through controlled experiments is always valuable to validate numerical simulations. In these endeavors it is planned to build an experimental test facility with data acquisition and recording systems as an extension the present work.

It is also possible to investigate the role of geometric and material nonlinearities on the critical buckling loads of stiffened circular plates. Relatively there are a very few investigations in the area of buckling of thin plates, made of functionally graded materials, subjected to internal/ external loads.

REFERENCES

1. L. S. Ma, T. J. Wang. Nonlinear bending and post-buckling of a functionally graded circular plate under mechanical and thermal loadings, *Int. J. Solids & Structures*, Volume 40, pp. 3311–3330, 2003.
2. Lars Brubak, and JosteinHellesland. Approximate buckling strength analysis of plates with arbitrarily oriented stiffeners, *University of Oslo.*, Volume 72, pp.1163-1168, 2004.
3. Ding Hao-Jiang., Lee Xiang-Yu. Analytical solutions for a uniformly loaded circular plate with clamped edges, *Journal of Zhejiang University Science*, Volume 72, pp.1163-1168, 2005.
4. L. H. Yu, C. Y. Wang. Buckling mosaic of a circular plate on a partial elastic foundation, *National Chung Cheng University*, Volume 34, pp.135-138, 2010.
5. H. Luo., C. Pozrikidis. Buckling of a circular plate resting over an elastic foundation in simple shear flow, *Journal of Applied Mechanics*, Volume 75, 2008
6. Shi-Rong Li, R. C. Batra, and Lian-Sheng Ma. Vibration of thermally post-buckled orthotropic circular plates, *Journal of Thermal Stresses.*, Volume 30, pp.43-57, 2007.
7. R. K. Jain., Axisymmetric vibrations of ring stiffened circular plates. *Journal of Mechanical Engineering Science*, Volume15, pp. 218-221, 1973.
8. C. K. Rao., L. B. Rao. Vibrations of Elastically Restrained Circular Plates Resting on Partial Winkler Foundation. *The Open Acoustics Journal.*, Volume 2, pp. 68-74, 2009.
9. P. Mandal. Buckling of thin cylindrical shells under axial compression. Ph.D. thesis, University of Cambridge, Department of Engineering. (1997)
10. E. R. Lancaster, C. R. Calladine, S. C. Palmer. Paradoxical buckling behaviour of a thin cylindrical shell under axial compression, Volume 42, pp. 843-865, 2000.
11. P. Mandal, C.R. Calladine. Buckling of thin cylindrical shells under axial compression. *International Journal of Solids and Structures*, Volume 37, pp 4509- 4525, 2000.
12. Hibbit, Karlsson and Sorenson, Inc, ABAQUS User's Manual.
13. J. Shen, Y. L. Wu , Y.H. Liu. Buckling analysis of tank roof with construction defect based on finite element method, 14th international conference on pressure vessel technology. *Procedia engineering* Volume 130, pp 390-399, 2015.



Innovative use of Rubberized Concrete in Construction Technology

Nisha Kumawat^{*1}, Vishnu Kumar Kumawat²
Public Works Department, Rajasthan¹, kumawatnisha90@gmail.com*
North Western Railway²

ABSTRACT

In the present scenario, entire world is facing a serious peril to the environment, and this threat is disposal of used and waste tyres. This problem is triggering many risks to the environment like soothing surface for breeding for mosquitos, causing unrestrained fire and contamination to the earth and vegetation; hence, it is a high time to identify alternative outlets for the used and waste tyres, e.g., recycling the discarded tyres. Concrete, being the most demanded structural material, is considered as essential for the modern civilization and human society. This study reviews the feasibility of using waste tyres in the form of fibers in concrete in terms of the strength as well as protecting the environment. It reviews the effect of sulphuric acid (H_2SO_4) and sodium chloride (NaCl) acidic environment on rubberized concrete (RC) as well.

The study was carried out to develop information about the mechanical and durability properties of RC. The results of this study revealed that compressive strength of concrete decreases with increase of rubber aggregate content. Similarly, compressive strength and weight decreases with increase of rubber content in H_2SO_4 and NaCl acidic environment even though the w/c ratio is kept constant. Reduced compressive strength of concrete due to the inclusion of rubber aggregates do limit its use in some structural applications, but it has few desirable characteristics such as lower density, higher impact and toughness resistance, enhanced ductility, and better sound insulation etc. These properties are advantageous to some construction applications.

KEYWORDS Rubberized concrete; Waste tyre; Crumbed rubber; Silica fume; Fine aggregates

INTRODUCTION

Background of the Study

The goal of sustainability is that life on the planet can be sustained for the foreseeable future and there are three components of sustainability: environment, economy, and society. At the moment, the environment is probably the most important component and an engineer or architect uses sustainability to mean having no net negative impact on the environment.

Among the many threats that affect the environment are the wastes which are generated in the production process or discarded after a specific material ends its lifetime or the intended use. Studies to dispose some solid wastes such as waste tyres in the most beneficial ways are not yet fully exhausted.

Concrete strength is greatly affected by the mix design parameter and the properties of its constituents. Aggregates represent the major constituent of the bulk of a concrete mixture.

In this study mechanical and durability properties of RC in three cases (a) without adding silica fume (SF) (b) with 5% SF and (c) with 10% SF has been evaluated. Fine Aggregates (FA) were partially replaced by 0%, 5%, 10%, 15%, 20% and 25% waste rubber fibres. Concrete cubes of these mixes were tested for compressive strength, visual observation, weight loss and compressive strength after attack by NaCl and H_2SO_4 acids by submerging cubes in these acids for 7 days, 28 days and 56 days.

Environmental Problem Associated with Waste Tyre

Tyres are bulky, and 75% of the space occupied by a tyre is void, hence, the landfilling of scrap tyres has several difficulties and hazards:

- Whole tyre land filling requires a large amount of space.
- Tyres tend to float or rise in a landfill and come to the surface.
- The void space provides potential sites for the harboring of rodents.
- Shredding the tyre eliminates the above problems but requires high processing costs.
- Health Hazards: Tyre piles are excellent breeding grounds for mosquitoes. Because of the shape and impermeability of tyres, they may hold water for long periods of time providing sites for mosquito larvae development.



• **Fire Hazards:** Waste tyres and waste tyre stockpiles (Figure 1) are difficult to ignite. However, once ignited, tyres burn very hot and are very difficult to extinguish. Combustion of tyres produces toxic gases which causes air pollution and results in environment impairment. (Figure 2).



Figure 1 Stockpiles of waste tyres



Figure 2 Fire hazard

Methods of Recycling Tyres

Methods of recycling tyres are shredding and Chipping: This is mechanical shredding of the tyres first in to bigger sizes and then into particles of 20 to 30 mm in size. Crumbing: is the processing of the tyre into fine granular or powdered particles. Mechanical or cryogenic processes: the steel and fabric component of the tyres are also removed during this process. Devulcanization: is the treatment of tyre with heat and chemicals to reverse the vulcanization process in the original tyre production. Pyrolysis and Gasification: are two thermal decomposition processes carried out under different conditions. The processes produce gas, oil, steel, and carbon black (char). Energy Recovery: is the incineration of tyres to generate energy.

Use of Crumbed Rubber

- Crumbed Rubber used in Asphalt
- Moulded and Extruded Products
- Crumbed Rubber used in Athletic Facilities Amendment
- Crumbed Rubber used in Compost

Objectives of the Study

1. To investigate the behavior of RC in H_2SO_4 .
2. To investigate the behavior of RC in NaCl.
3. To investigate the behavior of RC with SF in H_2SO_4 .
4. To investigate the behavior of RC with SF in NaCl.
5. To make use of rubber tyres in some form which would otherwise go as a waste material and add to the existing stockpile of waste rubber tyres.
6. To open up new opportunities in concrete technology and waste management.

Rubber Concrete

RC is defined as concrete mixed with waste rubber added in different volume proportions. Partially replacing the coarse or fine aggregate of concrete with some quantity of small waste tyre cubes can improve qualities such as low unit weight, high resistance to abrasion, absorbing the shocks and vibrations, high ductility and brittleness of concrete. Moreover the inclusion of rubber into concrete results in higher resilience, durability and elasticity. For the constructions that are related to impact effects the use of RC will be beneficial due to the altered state of its properties.

Economic's and Potential Applications

Upon comparing with conventional concrete, it is found that RC bears more impact, temperature and pressure, moreover it draws less cost; hence, is affordable in comparison to conventional concrete.

Rubber Modified Concrete (RMC) have better water & acid resistance and great impact resistance property. It has low shrinkage and superb insulation property to the sound and heat.



In comparison to conventional concrete, the crumb rubber concrete (CRC) remains intact and don't break into pieces after failure; hence, shows good impact resistance properties. The unique qualities of RC are seen in landscaping projects and in architectural works and quake resistance members in buildings.

Identification of Gap Area

Researchers have reported that when cement mortar with rubber tyre waste were used, chloride ion penetration resistance found to be improved but in concrete work it is yet to be evaluated. In previous study mixture of rubber tyre waste with fly ash and metakaoline is recommended for the resistance of H_2SO_4 attack but further work is yet to be completed.

Depths of penetration of H_2SO_4 and NaCl in RC after different time of curing are not yet covered in previous studies. Systematic study for different w/c ratio for RC has not been evaluated. In previous research SFs are considered as a remedy to enhance the chloride penetration resistance of the RC but RC with different percentage of SF are not evaluated.

MATERIAL AND METHODOLOGY

Material

Cement

In this study Ordinary Portland cement (OPC) of grade 43 of Binani was used. The compressive strength at 28 days was found 45 N/mm^2 .

Coarse Aggregates

In this study coarse aggregates of 20mm and 10mm are used. The specific gravity of 10mm aggregates was 2.72 and that of 20 mm was 2.67. They shall be hard, strong, and free from alkalies, impurities and other deleterious substances.

Silica Fumes

SF/micro-silica is "very fine non-crystalline silica produced in electric arc furnaces as a by-product of the production of elemental silicon or alloys containing silicon".

Fine Aggregates

Sand is a naturally occurring granular material composed of finely divided rock and mineral particles. Sand particles range in diameter from 0.0625 mm (or 1/16 mm) to 5 mm. Sand used was locally available sand, which had 3 mm maximum size and specific gravity 2.63.

Admixture

Admixture used is BASF Glenium Sky 777 is the super plasticizer based on second generation poly carboxylic ether polymers, developed using nano-technology. The product has been primarily developed for applications in high performance concrete to facilitate Total Performance Control. It is free of chloride and low alkali. It is compatible with all types of cements.

Table 1 Physical and chemical properties of SF

Particle size	< 1 μm
Bulk –density	
As produced	130 to 430 kg/m^3
Densified	480 to 720 kg/m^3
Specific gravity	2.2

Table 2 Typical properties of Admixture

Aspect	Light brown liquid
Relative densities	1.11 \pm 0.01 at 25 $^{\circ}c$
PH	≥ 6
Chloride ion content	< 2 %



Specific surface	15,000 to 30,000 m ² /kg
Silicon dioxide	>85 %
Amorphous	
Trace elements depending upon type of fume	

Rubber Fibre

In a simple method, particles are made with a high irregularity in the range of 0.425 to 4.75 mm. The rubber fibre used in the study were passed through 2.36 mm and retained on 1.18 mm. Rubber fibers of size 2 to 4 mm wide and 20 mm length (aspect ratio 4 to 10) was used as shown in **Figure 3** in this study. Specific gravity of rubber fibre (1.068) was determined by pycnometer method.

MIX PROPORTIONS

- Three series were cast in this study. In the first series, three w/c ratios 0.35, 0.45 and 0.55 with varied percentage of rubber fibers from 0, 5, 10, 15, 20 and 25 % were used.
- In the next series 5% SF was used in addition to above parameters.
- In the third series 10% SF was used with 0.35 w/c ratio.

METHODOLOGY

Casting of Concrete

Materials used were weighted in weigh pan as per mix proportion. The mixes were prepared in pan type mixer. According to our calculations based on mix design required quantity of materials, water and superplasticizer were added in the mixer. Doses of superplasticizer ranges from 0.5 % to 2% of the quantity of cement. The mix was carried out properly in a pan mixer for about ten minutes. Two batches were cast everyday for each mix proportion. Then three specimens was used for determination of concrete compressive strength after 28 days of water curing then other specimens of same casting was cured in 5 % of NaCl and 5 % of H₂SO₄ solution then weight loss, visual observation and compressive strength of specimens after 7, 28 and 56 days were carried out carefully .

Compaction

Compaction of concrete was done so that concrete was free from segregation. The concrete was filled in the respective moulds in layers and each layer was compacted by vibration. After the compaction was done the top layer surface of concrete was levelled with the help of trowel.

Curing

After compaction test specimens were kept in moist air and at a room temperature for 24 hours \pm ½ hour from the time of addition of water to the dry ingredients. After 24 hours, specimens were removed from their respective moulds and cubes were kept into the curing tank until the date of testing has come. Water was renewed in every seven days and room temperature was maintained.

TESTING

After 28 days water curing compression test was performed for three specimens of each casting then weight of other specimens were taken as initial weight for weigh loss test after that these specimens were sub merged for 7, 28 and 56 days' time period in 5% NaCl and 5% H₂SO₄ then three specimens were used from each solution for each time interval for each test i.e. compression strength test, visual observation and weight loss test were carried out. This solution 5% NaCl and 5% H₂SO₄ was changed in every 30 days in curing tanks.

Visual Observation



After 24 hours of casting, the specimens were cured in to water. Visual observation was done by eye and photo figures are taken after 28 days of curing. Then these specimens were submerged for 7, 28, 56 days in 5% NaCl and 5% H_2SO_4 then condition of specimens were observed again by visual observation, as shown in **Figure 4**.

Weight Loss

For finding weight loss of concrete, Weight of three specimens was taken by electronic weight pan after 28 days of water curing i.e. initial weight. Then these specimens were submerged in 5% NaCl and 5% H_2SO_4 then again weight of specimen taken i.e. final weight after each time period, i.e. 7, 28, 56 days. Now percentage weight loss is determined by initial and final weights.

Compressive Strength of Concrete

The compressive strength was calculated from the failure load divided by the cross-sectional area resisting the load and reported in units of Mega Pascals (MPa). Compressive strength of concrete was tested after 28 days of curing. Then other specimens of same casting were submerged for interval 7, 28, 56 days in 5% NaCl and 5% H_2SO_4 then compression strength test performed again for each interval.



Figure 3 Rubber fibre

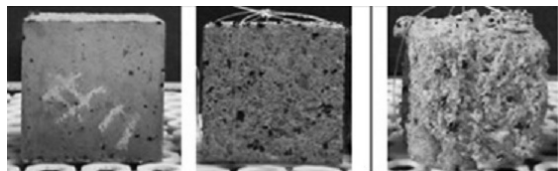


Figure 4 Visual observation in H_2SO_4 (5% H_2SO_4) after 7, 28, 56 days

RESULTS AND DISCUSSION

Compressive Strength of Rubber Concrete after 28 Days Curing in Water

Results show that compressive strength of RC without SF, with 5% SF and 10% SF after 28 days curing in water decreases as the percentage of rubber fibre increases. These results also show that compressive strength of RC decreases with increase of w/c from 0.35 to 0.55.

Rubber fibre is nearly two and half times lighter than the conventional FA; hence, it can be seen that the mass density of the mix is relatively lower. Although the strength of modified concrete is reduced with an increase in the rubber content, its lower unit weight meets the criteria of light weight concrete that fulfill the strength requirements. With the addition of the rubber fibres, the reduction in strength cannot be overruled. The reason for the strength reduction could be attributed both to a reduction of quantity of the solid load carrying material and lack of adhesion at the boundaries of the rubber aggregate, soft rubber particles behave as voids in the concrete matrix. Therefore, rubber aggregate tends to behave like weak inclusions or voids in the concrete resulting in a reduction in compressive strength.

Weight Reduction of Rubber Concrete when Submerged in NaCl/ H_2SO_4 for 7 days, 28 days and 56 days

Reduction in weight of RC is more for the specimen of concrete with higher water cement ratio whereas lesser for concrete with lower water cement ratio. Moreover, results reveal that reduction in weight of RC increases as percentage of rubber fibres in concrete increases. Similarly, reduction in weight of RC increases with increase in days for which RC is submerged in NaCl/ H_2SO_4 .

Compressive Strength of Rubber Concrete when Submerged in NaCl/ H_2SO_4 for 7 days, 28 days and 56 days

Compressive strength of RC is more for the specimen of concrete with lesser water cement ratio whereas it is lesser for the specimen of concrete with higher water cement ratio. Moreover, results reveal that compressive strength of



RC decreases as percentage of rubber fibres in concrete increases. Similarly, compressive strength of RC decreases with increase in days for which RC is submerged in NaCl/H₂SO₄ but compressive strength of RC increases with increase in percentage of SFs in concrete.

Visual Observations of Rubber Concrete when Submerged in NaCl/H₂SO₄ Solution for 7 days, 28 days and 56 days

In visual observation it was observed that specimens of RC had regular and smooth surface after 28 days water curing but its surface got deteriorated after submerging specimens in NaCl/H₂SO₄ solution for 7 days. Specimens had irregular shape consisting cavities, spherical/needle like voids and surface cracks. The irregularity in shape of specimens increases as days for which specimens are submerged in NaCl/H₂SO₄ solution increases. Deterioration decreases as SF increases which cause increased resistance of concrete to NaCl/H₂SO₄ attack through reduced permeability and reduced content of calcium hydroxide.

CONCLUSION

The utilization of waste rubber tyres as FA in concrete addresses sustainability of environment and the concrete. Experiments were performed to check the suitability of waste rubber tyre as FA in concrete. Concrete mix with three w/c ratio (0.35, 0.45 and 0.55) and different replacement level of rubber aggregates (0%, 5%, 10%, 15%, 20% and 25%) were prepared. Cement was also partially replaced by SF (5% and 10%) in two series. The influence of rubber aggregates on mechanical strength after 28 days was evaluated. Visual observation, reduction in weight and compressive strength in NaCl and H₂SO₄ environment after 7 days, 28 days and 56 days were also evaluated.

Following conclusions can be drawn from this experimental study carried out on durability of RC using SF:

- In normal environment, compressive strength of concrete decreases with the increase of replacement level of rubber aggregate (5% to 25%) for all selected w/c ratios however compressive strength is increased with addition of SF. As SF increased resistance of concrete through reduced permeability and reduced content of calcium hydroxide.
- Compressive strength of concrete without SF or with SF (5% and 10%) decreases with increase of replacement level of rubber aggregate in H₂SO₄ and NaClacidic environment.
- Reduction in weight of RC without SF or with SF (5% and 10%) increases with increase of replacement level of rubber aggregate in H₂SO₄ and NaClacidic environment.
- Deterioration of RC is more in H₂SO₄ environment as compared to NaClacidic environment.
- Visual inspection is efficient method to study the behavior of concrete in acidic environment. Visual inspection can be co-related to material deterioration, workmanship and structure serviceability in acidic environment.

The use of rubber aggregates from recycled tyres demonstrates the reduction in environment pollution and provides innovative material for sustainable construction. In addition to this, introduction of an alternative source to natural aggregates in concrete is also proposed. In addition to meeting recycling and sustainability objectives, this study reflects the products with enhanced properties in specific applications with conservation of natural resources.

The proposed benefits of using waste tyres in construction are in three ways as this can offer distinct engineering benefits over traditional aggregates, this can be used as an alternative to primary materials thereby reducing an environmental burden on extraction and their use can help to reduce burden of waste disposal (including illegal stockpiling and disposal, such as fly-tipping, with their associated risks) and the impacts on the environment associated with some other.

A wide range of potential sectors which can benefit from using rubber from waste tyres are identified. The areas were grouped into five classes as Civil engineering (non-road), Civil engineering (road and infrastructure), Sports, safety and outdoor surfaces, Consumer and industrial products and Energy.

Presently, the usage of RC are seen in precast concrete walkway slabs, precast RCC roof slabs in green buildings and for small thickness walls in residential buildings. It can be used in landscaping works like recreational ground & walkways, ramps and road intersections. By virtue of its modified properties, RC has its extensive application in architectural works as well such as nailing concrete, low weight wall panels, non-load bearing walls, facades and in other constructions parts where either strength is not the criteria or which are subject to impact only. Thus it is shown that RC has innovative use in construction technology and is an excellent substitute to the normal weight conventional concrete.



REFERENCES

1. C. Albano, N. Camacho, J. Reyes, J. L. Feliu, and M. Hernandez. Influence of scrap rubber addition to Portland I concrete composites: Destructive and non-destructive testing. *Compos Structures*, Volume 71, Number 3, pp 439-446, 2005.
2. A. K. Al-Tamimi and M. Sonebi. Assessment of Self-Compacting Concrete Immersed in Acidic Solutions. *J. Mater. Civ. Eng.*, Volume 15, Number 4, pp 354-357, 2003.
3. A. R. Bagheri, and H. Zanganeh. Comparison of rapid tests for evaluation of chloride resistance of concretes with supplementary cementitious materials. *J. Mater. Civ. Eng.*, Volume 24, Number 9, pp 1175-1182, 2012.
4. B. B. Das, D. N. Singh, and S. P. Pandey. Rapid chloride ion permeability of opc-and ppc-based carbonated concrete. *J. Mater. Civ. Eng.*, Volume 24, Number 5, pp 606-611, 2011.
5. N. N. Eldin, and A.B. Senouci. Rubber-tyre particles as concrete aggregate. *J. Mater. Civ. Eng.*, Volume 5, Number 2, pp 478-496, 1993.
6. N. N. Eldin, and A. B. Senouci. Observations on rubberised concrete behavior. *Cement, Concrete and Aggregates*, Volume 15, Number 1, 1993.
7. F. Hernandez-Olivares, G. Barluenga, M. Bollati, B. and Witoszek. Static and dynamic behaviour of recycled tyre rubber-filled concrete. *Cement and concrete research.*, Volume 32, Number 10, pp 1587-1596, 2002.
8. E. Hewayde, M. Nehdi, E. Allouche, and G. Nakhla. Effect of Mixture Design Parameters and Wetting-Drying Cycles on Resistance of Concrete to H₂SO₄ Attack. *J. Mater. Civ. Eng.*, Volume 19, Number 2, pp 155-163, 2007.
9. B. Huang, G. Li, S. S. Pang, and J. Eggers. Investigation into waste tyre rubber-filled concrete. *J. Mater. Civ. Eng.*, Volume 16, pp 187-194, 2004.
10. H. Huynh, D. Raghavan, and C. Ferraris. Rubber particles from recycled tyres in cementitious composite materials. *NISTIR*, 5850, Volume 23, 1996.
11. K. E. Kaloush, G. B. Way, and H. Zhu. Properties of crumb rubber concrete. *Transportation Research Record, Journal of the Transportation Research Board.*, Volume 1914, Number 1, pp 8-14, 2005.
12. Z. K. Khatib, and F. M. Bayomy. Rubberized Portland cement concrete. *J. Mater. Civ. Eng.*, Volume 11, Number 3, pp 206-213, 1999.
13. G. S. Kumaran, N. Mushule, and M. Lakshmi pathy. A Review on Construction Technologies that Enables Environmental Protection: Rubberized Concrete. *American J. of Engineering and Applied Sciences.*, Volume 1, Number 1, p 40, 2008.
14. K. B. Najim, and M. R. Hall. A review of the fresh/hardened properties and applications for plain-(PRC) and self-compacting rubberised concrete. *Construction and Building Material.*, Volume 24, Number 11, pp 2043-2051, 2010.
15. E.O. Nnadi and J. LizarazoMarriaga. Acid corrosion of plain and reinforced concrete sewage systems. *J. Mater. Civ. Eng.*, Volume 25, Number 9, pp 1353-1356, 2012.
16. M. M. RedaTata, A. S. EL-Dieb, M. A. Abd EL-Wahab, and M. E. Abdel-Hameed. Mechanical, fracture and microstructural investigation of rubber concrete. *J. Mater. Civ. Eng.*, Volume 20, Number 10, pp 640-649, 2008.
17. H. Rostami, J. Lepore, T. Silverstraim, and I. Zundi. Use of recycled rubber tyres in concrete. *Proc of the international conference on concrete*, London, United Kingdom, Thomas Telford Services Ltd, Vol. 399, 2000.
18. R. R. Schimizza, J. K. Nelson, S. N. Amirkhanian, and J.A. Murden. Use of waste rubber in light-duty concrete pavements. *Infrastructure: New Mat. and Methods of Repair.*, pp 367-374, 1994.
19. N. Serge, and I. Joeke. Use of tyre rubber particles as addition to cement paste. *Cement and Concrete Research.*, 30(9), pp 1421-1425, 2000.
20. I. B. Topcu, and A. Demir. Durability of Rubberized Mortar and Concrete. *J. Mater. Civ. Eng.*, 19(2), pp 173-178, 2007.
21. W. M. Zhang, and H. J. Ba. Accelerated life test of concrete in chloride environment. *J. Mater. Civ. Eng.*, Volume 23, Number 3, pp 330-334, 2010.
22. L. Zheng, X. S. Huo, and Y. Yuan. Strength modulus of elasticity and brittle index of rubberized concrete. *J. Mater. Civ. Eng.*, Volume 20, Number 11, pp 692-699, 2008



Elastic Properties of High Performance Concrete Beam under Flexure

A. A. Momin¹, R. B. Khadiranaikar²

Department of Civil Engineering, BLDEA's V.P. Dr. P.G. Halakatti College of Engineering and Technology, Vijayapur, Karnataka, India¹, asifarzanmomin@gmail.com*

Department of Civil Engineering, Basaveshwar Engineering College, Bagalkot²

ABSTRACT

Due to High-Performance Characteristics of High-Performance Concrete (HPC), its applicability is found to be greater, which is deficient in conventional concrete. The use of elastic properties of HPC in the design of structural members of HPC like beams etc., may not be suitable, since the total cross-sectional area of the section is considered in the design, neglecting the effect of reinforcing steel and confining steel bars. Hence it is essential to evaluate the elastic properties of HPC structures. This study aims at determining the modulus of elasticity of HPC beam under flexure. The beam models of size 150 mm × 300 mm × 2000 mm with varying percentage of tension reinforcement for M₆₀, M₈₀ and M₁₀₀ grade HPC beam are studied using ANSYS software. The experimental investigation is also carried out for the same size models, and the results are compared. Finally, the equation for elastic modulus is derived by regression investigation. The modulus of elasticity of reinforced HPC beam under flexure increased with the increase in longitudinal tension reinforcement ratio of the concrete section. The modulus of elasticity of reinforced HPC beam can be determined for different longitudinal tension reinforcement ratio and grade of HPC by the proposed equation. The maximum variation obtained was 9.61 percent from the three different methods of evaluation of modulus of elasticity of HPC beam.

KEYWORDS Elastic properties, Young's Modulus, High performance concrete beam, Finite element method

INTRODUCTION

The elastic property of concrete, that is, the modulus of elasticity measures its rigidity. This property of concrete is defined as the ratio between the stress applied and the strain obtained within the defined limit of proportionality.

Modulus of elasticity is generally related to compressive strength of concrete; it increases with increase in compressive strength. It depends upon many parameters like aggregate type, the mix proportions, curing conditions, rate of loading etc. The larger the amount of coarse aggregate with a high elastic modulus, the higher would be the modulus of elasticity of concrete. Concrete specimens tested in wet conditions show about 15% higher elastic modulus than tested in dry conditions. [1]. This property is evaluated by drawing slope for the stress strain curve. As most of the part of stress strain curve is non-linear, different methods exist for computing modulus of elasticity. The secant modulus is the commonly used method for evaluating this property by different codes and researchers [2-5]. Now the modulus of elasticity of reinforced concrete member is very indifferent from the modulus of elasticity of concrete alone [6-7], hence the use modulus of elasticity of concrete overestimates the design values in the design of structural members. Also in the design of structural members total cross sectional area of the section is considered neglecting the effect of confining steel reinforcements.

The HSC and the HPC differs largely with the conventional cement concrete because of use of the cementitious material like silica fume, fly ash etc; and hence because of which the mechanical properties of HSC/ HPC also differs [8] and the proposed equation for modulus of elasticity of concrete or reinforced concrete may not be applicable neither for HPC nor for reinforced HPC. The objective of this present research work is to evaluate secant modulus of elasticity of HPC beams for varying concrete grades and longitudinal reinforcement ratio.

METHODOLOGY

In this study a total of 12-beam specimens were casted under experimental study with varying concrete grade 60, 80 and 100 MPa and longitudinal tension reinforcement with details as shown in **Table 1**. The mix-proportioning is carried out by using method proposed by Aitcin [9]. The similar beam specimens are analyzed using ANSYS 10.0 software. The secant modulus of elasticity of HPC beams are evaluated three methods, namely, using experimental stress-strain Curves, using ANSYS results and by using bending equation from the experimental data. Regression test is performed and equation for secant modulus of elasticity is proposed.

Evaluation of Stress-Strain Parameters

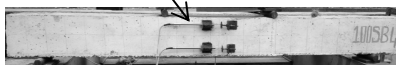


The stress-strain parameters required for the evaluation of modulus of elasticity is determined by working on the values of experimental data and through the ANSYS results. Under the experimental pure flexure test for HPC beams subjected to monotonic two-point loading, the load and the corresponding deformations were recorded by using LVDTs at extreme tensile and compression fiber at center of the span as shown in **Figure 1**. The LVDT at the tensile fiber was kept closed so that it was allowed to open during expansion, while the LVDT at the extreme compression fiber was opened and allowed to close during compression. Later, the tensile and the compressive strains were calculated from the deformations.

Table 1 Details of beam specimens

Beam specimen	Longitudinal reinforcement	%Reinforcement	Balanced reinforcement ρ_b	ρ/ρ_b
60SB1	2 # 12	0.78	4.76	0.16
60SB2	2 # 10 + 1# 12	0.93	4.85	0.19
60SB3	2 # 16 + 1# 10	1.69	4.80	0.35
60SB4	2 # 16 + 2# 10	1.97	4.84	0.40
80SB1	2 # 12 + 1# 10	0.77	5.10	0.15
80SB2	3 # 12	0.86	4.98	0.17
80SB3	2 # 10 + 1# 16	0.91	5.06	0.18
80SB4	2 # 12 + 1# 16	1.09	5.05	0.21
100SB1	2 # 12	0.78	5.99	0.13
100SB2	2 # 10 + 1# 12	0.93	6.08	0.15
100SB3	2 # 16 + 1# 10	1.69	6.13	0.27
100SB4	2 # 16 + 2# 10	1.97	5.92	0.33

LVDT-extreme compression fibre



LVDT-extreme tensile fibre

Figure 1 Beam specimen with LVDT to measure strain under pure flexure

The HPC beam specimens are also analyzed under static analysis type using ANSYS-10.0 software for which three different materials were selected namely HPC, reinforcement bars and steel plates. Solid-65 element was selected for HPC, Link-8 for reinforcement bars and stirrups and Solid-45 for steel plates. The material properties from the laboratory tests are assigned for these ANSYS elements. Loads are applied under two point loading. The beam model is set to the boundary conditions with one end hinged and other end on roller. The maximum compressive and tensile stresses are evaluated and stress-strain curves are plotted. The stress-strain curves obtained for 60 MPa HPC beam specimens by experimental and ANSYS results are shown in **Figures 2 and 3**, respectively.

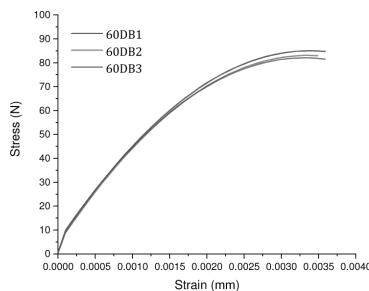


Figure 2 Experimental stress-strain curves for 60 MPa HPC beam specimens

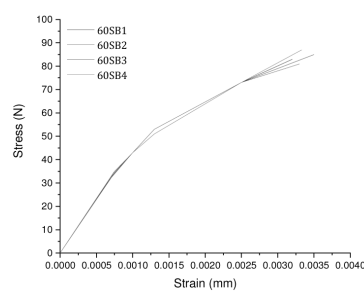


Figure 3 ANSYS stress-strain curves for 60 MPa HPC beam specimens



EVALUATION OF MODULUS OF ELASTICITY OF HPC BEAM

Using Stress-Strain Parameters

The commonly used method secant modulus is employed for evaluating modulus of elasticity of HPC beam from the experimental and ANSYS stress-strain curves determined in the previous section. The modulus of elasticity is determined from the slope of the line joining origin and a point on the curve representing 40% stress at failure. The modulus of elasticity thus evaluated for different grade of HPC and varying longitudinal reinforcement ratio using experimental and ANSYS stress-strain parameters are shown in **Table 2**.

Table 2 Modulus of elasticity from experimental and ANSYS stress-strain parameters for HPC beam specimens

Beam Specimens	ρ / ρ_b	Modulus of elasticity, MPa	
		Using experimental stress strain curves	Using analytical ANSYS stress strain curves
60SB1	0.166	46188.00	46047.16
60SB2	0.193	45662.60	45827.44
60SB3	0.353	46296.70	46448.09
60SB4	0.407	46486.88	46774.19
80SB1	0.152	48849.50	48571.43
80SB2	0.174	49031.82	49855.07
80SB3	0.180	49366.58	49647.39
80SB4	0.216	49672.86	49930.65
100SB1	0.132	52959.17	53146.85
100SB2	0.154	52612.30	52794.29
100SB3	0.276	52061.04	52237.00
100SB4	0.333	52496.29	52670.81

Using bending equation from the experimental data

Experimental evaluation of secant modulus of elasticity is also done for the same beam specimens by using bending equation. The HPC beam being subjected to two point loads, the maximum deflection due to the applied load 'W' is given by equation.

$$\delta_l = \frac{23WL^3}{648E_c I}$$

The deflection due to the self-weight of the HPC beam is given by equation.

$$\delta_s = \frac{5wl^4}{384E_c I}$$

Where L is the effective length of the beam, I is the moment of Inertia and E_c is the secant modulus of elasticity.

And the total deflection considering the self-weight of the HPC beam is given by equation.

$$\delta = \delta_s + \delta_l$$

The applied load 'W' is taken as half the load at first visible crack and the corresponding deflection as ' δ '. The values of load at first visible crack and its corresponding deflection for different beam specimens tested with varying strength of the HPC and longitudinal reinforcement ratio are shown in **Table 3**. By substituting these values, the static modulus of elasticity for single span HPC beam specimens is determined using equation.

$$E_c = \frac{1}{\delta I} \left[\frac{5wl^4}{384} + \frac{23WL^3}{648} \right]$$

Regression Analysis

The static modulus of elasticity of HPC beam specimens determined using experimental stress strain curves, ANSYS results and bending equation from experimental data are compared in **Table 4** and the graphical representation of variation is presented in **Figure 4**. The average static modulus of elasticity is also presented in the **Table 4** for different longitudinal reinforcement ratio.



The stiffness of the HPC beam increases with increase in longitudinal reinforcement ratio as such, the trend line of the average variation of Modulus of Elasticity from different methods shows that it increases with increase in the grade of HPC and longitudinal reinforcement ratio as depicted in **Figure 5**. The values obtained from different methods are almost same for the same longitudinal reinforcement ratio with variation of 9.61%. Taking the data of Modulus of Elasticity from bending equation, regression test is performed and following generalized equation is derived.

$$E_{\text{Ref, HPC}} = 5000\sqrt{1.075f_{ck}} + (300\sqrt{1.36f_{ck}})\rho$$

Table 3 Modulus of elasticity from experimental data using bending equation for HPC beam specimens

Beam Specimens	ρ/ρ_b	Load at first visible crack, kN	Deflection at first visible crack, mm	Modulus of Elasticity, MPa
60SB1	0.166	66.75	5.00	50160.65
60SB2	0.193	71.45	4.75	53090.57
60SB3	0.353	109.05	5.70	51739.64
60SB4	0.407	117.52	5.60	52546.43
80SB1	0.152	105.00	3.16	51867.06
80SB2	0.174	117.00	3.30	53461.88
80SB3	0.180	95.32	2.50	53781.80
80SB4	0.216	122.30	3.10	54236.83
100SB1	0.132	70.35	5.00	57748.24
100SB2	0.154	94.05	6.22	58875.64
100SB3	0.276	124.00	6.60	59289.27
100SB4	0.333	128.32	6.23	59326.57

Table 4 Comparison of modulus of elasticity of HPC beam specimens from different methods

Beam Specimens	Modulus of elasticity, MPa			Average modulus of elasticity, MPa
	Using experimental stress strain curves	Using analytical ANSYS stress strain curves	Using bending equation from the experimental data	
60SB1	46188	46047	50160	47465
60SB2	45662	45827	53090	48193
60SB3	46296	46448	51739	48161
60SB4	46486	46774	52546	48602
80SB1	48849	48571	51867	49762
80SB2	49031	49855	53461	50782
80SB3	49366	49647	53781	50931
80SB4	49672	49930	54236.	51280
100SB1	52959	53146	57748	54618
100SB2	52612	52794	58875	54760.
100SB3	52061	52237	59289.	54529
100SB4	52496	52670	59326.	54831

The generalized equation derived from the regression analysis predicts the value of Modulus of Elasticity for varying grade of HPC and percentage of tension reinforcement. The first part of these equation represents stiffness due to HPC element, while the second part represents stiffness due to reinforcement. The second part of the equation is itself the additional stiffness because of the reinforcement.

To validate the generalized equation predicted for reinforced HPC, the predicted values of modulus of elasticity from the proposed equation are compared with all the three methods of evaluation as shown in **Table 5**. The results shows that the ratio of predicted modulus of elasticity to the values obtained from different methods are in the range of 0.959 to 1.168. Hence the proposed equation from the regression analysis can be used as the generalized equation for determination of modulus of elasticity of reinforced HPC beam specimens, which takes into account the stiffness due to the reinforcing steel.

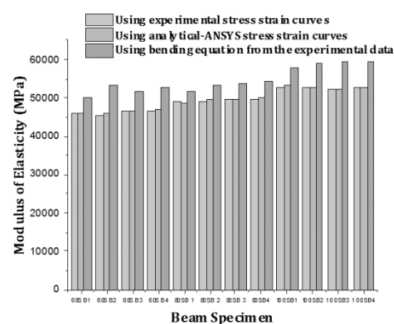


Figure 4 Comparison of modulus of elasticity of HPC beam specimens from different methods

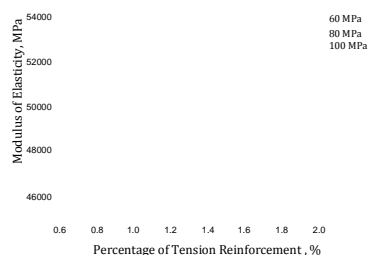


Figure 5 Average variation of modulus of elasticity of HPC beams with longitudinal tension reinforcement

Table 5 Comparison of predicted modulus of elasticity

Beam specimen	Predicted modulus of elasticity, MPa	$E_{c, \text{pred}} / E_{c, \text{bend}}$	$E_{c, \text{pred}} / E_{c, \text{exp}}$	$E_{c, \text{pred}} / E_{c, \text{ANSYS}}$
60SB1	50011	0.99	1.08	1.08
60SB2	50951	0.96	1.11	1.11
60SB3	53124	1.02	1.14	1.14
60SB4	54293	1.03	1.16	1.16
80SB1	51743	0.99	1.05	1.06
80SB2	51769	0.96	1.05	1.03
80SB3	51551	0.95	1.04	1.03
80SB4	52599	0.97	1.05	1.05
100SB1	56124	0.97	1.06	1.05
100SB2	57085	0.97	1.08	1.08
100SB3	60071	1.01	1.15	1.15
100SB4	60001	1.01	1.14	1.13

CONCLUSIONS

The stiffness of the HPC beam increases with increase in longitudinal reinforcement ratio as such, the trend line of the variation of Modulus of Elasticity from experimental and ANSYS results (Fig 4) shows that it increases with increase in longitudinal reinforcement ratio. The modulus of elasticity of reinforced HPC beam specimens so evaluated by using experimental stress-strain curves, ANSYS results and bending equation using experimental data closely matches each other with $\pm 11\%$ variations. Using the experimental data from bending equation, the equation for modulus of elasticity of reinforced HPC beam is proposed in terms of grade of HPC and percentage of tension reinforcement, which provides satisfactory estimate for the analysis of structures with reinforced HPC beams.

REFERENCES

1. Paul Zia, Shuaib Ahmad, and Michael Leming, High-Performance Concretes A State-of-Art Report, Federal Highway Administration Research and Technology, FHWA Publications, 1989-1994.
2. EN 1992-1-1, Eurocode 2: Design of concrete structures - Part 1-1: General rules and rules for buildings, Dec-2004.
3. ACI 318-14, Building Code Requirements for Structural Concrete, American Concrete Institute, 2014.
4. L. Domagała A Study on the Influence of Concrete Type and Strength on the Relationship between Initial and Stabilized Secant Moduli of Elasticity, Solid State Phenomena, Vol. 258, pp. 566-569, 2017.
5. C K. Kankam, Bismark K. Meisuh, GnidaSossou, Thomas K. Buabin, Stress-strain characteristics of concrete containing quarry rock dust as partial replacement of sand, Case Studies in Construction Materials, Volume 7, Pages 66-72, ISSN 2214-5095, 2017. <https://doi.org/10.1016/j.cscm.2017.06.004>.
6. Kulkarni, S., Shiyekar, M.R. &Shiyekar, Confinement Effect on Material Properties of RC Beams Under Flexure, S.M. J. Inst. Eng. India Ser. 98: 413, 2017 <https://doi.org/10.1007/s40030-017-0221-3>
7. Kulkarni, S.K., Shiyekar, M.R., Shiyekar, S.M. et al., Elastic properties of RCC under flexural loading-experimental and analytical approach, Sadhana, vol-39, pp-677-697, Indian Academy of Sciences, June-2014. <https://doi.org/10.1007/s12046-014-0245-6>
8. Iravani, S, Mechanical properties of high-performance concrete, ACI Materials Journal, 93(5), 416-426, 1996.Mehta, P. K., and Aitcin, P. C., Principles Underlying the Production of High-Performance Concrete, Cement, Concrete, and Aggregates, STM, Vol. 12, No. 2, , pp. 70-78, 1990.



Diagnosing Characteristics of Fibers in Concrete Mix Design for Rigid Pavements

Nikunj Patel^{*1}, C. B. Mishra², Shaaqib Mansuri²
Gujarat Energy Transmission Corporation Limited, Junagadh, India¹, mr.shaaqib@gmail.com^{*}
BVM Engineering College, Vallabh Vidyanagar, Anand, India²

ABSTRACT

Advancements of Highways are the establishment of framework change upgrading the essential central purpose to achieve quick and supported financial development in the changing technological advancement. Be that as it may, it is outstanding that asphalts are maturing and breaking down; 33% of the road system on the planet is in poor condition or all the more dreadful. What is required is another approach, the usage of extremely feasible pavement arrangements for enhanced societal advantage, while keeping up the system in a high condition of service for constancy which is an essential progress toward a more economical foundation. The Ministry of Road Transport and Highways in India saw that best in class society can't work sufficiently without durable concrete roads to bring down generation and natural cost of development materials. Although concrete is strong in itself; however, in its cracks are caused by volumetric changes because of dampness and temperature and the use of service loads after the concrete has concreteified. Cracks prompt negative view of value, durability and serviceability; anyway, as a rule they turn out to be just aesthetic problems. Hence this call for the addition of a little amount of discontinuous fibers to an ordinary concrete matrix as a potential solution by controlling cracks and giving acceptable strength qualities. A vital focal point of engineer's vision should now be on increasing the strength and life span of pavement. In this study, M40 concrete with and without added substance Brass Coated Micro Steel Fibers having length 6 mm and width of fiber as 0.18 mm is utilized in three unique doses 0.5 %, 1.0 % and 1.5 % as a partial volumetric substitution of the concrete mix to improve its quality characteristics. The mix course of action utilized as a part of this study was PQC M40 grade concrete by using IS 10262: 2009 and IS 456: 2000. The samples were casted, cured and checked following 28 days to inquire about out the compressive quality and flexural nature of cubes and beams. The most phenomenal compressive and flexural quality is accomplished at 1.0 % of Brass Coated Micro Steel Fibers with substitution by volume of concrete adding to diminish in thickness of road without trade off with quality which can be helpful to highway strategy makers and contractors too.

KEYWORDS Compressive strength, Flexural Strength, M40 Grade Concrete, Brass Coated Micro Steel Fibers, Pavement.

INTRODUCTION

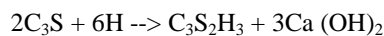
In a developing nation like India, road systems frame the supply routes of the country. The rigid pavements which are worked by plain concrete has some unfavorable basic qualities, for example, low post breaking limit, weakness and low malleability, restricted fatigue life, unequipped for accommodating deformations, low impact quality, low rigidity being only one tenth of its compressive quality., and so forth. As development is getting advance well-ordered due to commercialization, new revelations are being made to explore the probability for expanding the compressive nature of the concrete inside a financial range. FRC is a generally new composite development material which comprised short, thin, and moderately tractable fiber broadly utilized in rigid pavement and additionally Transportation Infrastructure. The presentation of Brass Coated Micro Steel Fibers was brought into thought which is another type of fastener that could be used with Portland concrete in holding with bond frameworks which builds its structural integrity. In this present paper PQC M40 concrete cubes and beams at the exploration office are completed to know compressive quality and flexural nature of plain security concrete with fiber reinforced concrete having brass coated micro steel fibers in different rates like 0.5 %, 1.0 % and 1.5% as an incomplete volumetric substitution of the concrete mix to enhance its quality attributes. The productive outcome is gotten at 1.0 % of brass coated micro steel fibers with substitution by volume of concrete adding to lessen in thickness of road without trade off with quality.

LABORATORY INVESTIGATION FOR MATERIAL USED

Ordinary Portland cement of 53 grades was utilized in this experimentation. Cement is a fastener, a substance utilized for road development that sets, concreteifies and sticks to different materials, restricting them together. It gets its quality from chemical responses between the concrete and water. The procedure is known as hydration.



Mixes like C3S and C2S present in bond respond in nearness of dampness and completely hydrated response can be communicated as



C₂S impacts gain of quality for the most part following two weeks. The hydration of C₃S produces higher heat contrasted with the hydration of C₂S. Fineness of concrete additionally influences the rate of heat advancement. The essential properties of bond are assessed in the research facility to find out the quality of concrete fulfilling important codal rehearse. Checking of materials is a basic part as the life of structure is reliant on the nature of material utilized. All the lab material tests were accomplished according to the Seems to be: 4031 – 1988. The Specific Gravity of Cement acquired is 3.15, Standard Consistency of concrete as 30.5%, Initial Setting Time as 117 minutes, Final setting Time as 230 minutes, Fineness of Cement as 2.48%, Soundness of cement as 2.3 mm and Compressive Strength of Cement (28 Days) as 60.09 N/mm². Aggregates are by and large idea of as dormant filler inside a concrete blend. Be that as it may, a more intensive look uncovers the real job and influence aggregate plays in the properties of both fresh and hardened concrete. Changes in degree, most extreme size, unit weight, and dampness substance would all be able to modify the character and execution of your concrete mix. Fine aggregate found from waterway (particular gravity 2.61) free from characteristic polluting influences alter from IS: 2386 – 1963 and IS: 383 - 1970 were used. Coarse aggregate size of 20 mm and 10 mm, pulverized, free from natural debasements accommodate from IS: 2386 – 1963 were utilized. Brass Coated Micro Steel Fibers having particular gravity 7.86, elasticity >285 MPa, length 6 mm and width of fiber as 0.18 mm is used in the present investigation. A water diminishing admixture, Rheobuild 821 (EJ) was used as the plasticizer in concrete whose appearance is yellow, PH 6 min, dose 0.8% by volume and specific gravity as 1.22. Water utilized in the exploratory work is adjusted to IS: 456-2000 for blending and also restoring of Concrete examples. The combined gradation can be utilized to all the more likely workability, pump ability, shrinkage, and other properties of concrete. The advantages of a combined aggregate analysis are with constant cement content and consistent consistency, there is an ideal for each combination of aggregates that will create the best water to cement proportion and most noteworthy quality. The gradation of all in one combined aggregate is as shown in **Figure 1**.

PQC CONCRETE MIX DESIGN M-40 GRADE WITH AND WITHOUT FIBERS

Concrete blend setup was finished by IRC: 44. In first stage concrete mix design was done by then reasonable concrete extent was found for the different portions by deficient substitution of brass coated micro steel fibers as fibers in different rates like 0.5 %, 1.0 % and 1.5% as an incomplete volumetric substitution of the concrete blend to enhance its quality attributes. After carefully considering all arrangement parameters for concrete blend setup is according to the IRC 58 – 2015 and MORTH (fifth Revision), concrete mix of PQC M40 grade are organized with BMSF as shown in **Table 1**.

Table 1 PQC concrete mixed design

Mass of all materials for 1 m ³ of concrete				
Material	NC	BMSF		
Percentage by volume	0.00%	0.50%	1.00%	1.50%
BMSF	0	39.3	78.6	117.9
Cement	410	407.93	405.41	403.52
Water	139.5	138.8	138.1	137.4
20 mm aggregate	850	845.63	841.54	837.16
10 mm aggregate	539	535.76	533.1	530.43
Fine aggregate	667	661.37	658.24	654.85
Admixture (0.8 %)	3.28	3.29	3.29	3.29
Density, kg/m ³	2608.78	2632.09	2658.28	2684.55
Mixed proportion	1: 1.62: 3.39	1:1.62 : 3.39	1:1.62 : 3.39	1:1.62 : 3.39



Experimental results

Slump Test

It causes us to know the consistency of concrete blend by estimating it after disfigured as a frustum cone in the site or lab to ensure that the concrete blend sections extents are correct. It is time regarded custom in concrete advancement and is dependent on aggregate dampness content, concrete temperature and mixing. One can choose the mix's weakness to isolation when put amid development work from batch to batch. Slump test fulfills the criteria's set down in MoRTH cl. 602.3.4.2. The aftereffect of the slump test is given in **Figure 2**. It is seen that fibers cause hindrance to the free flow of concrete.

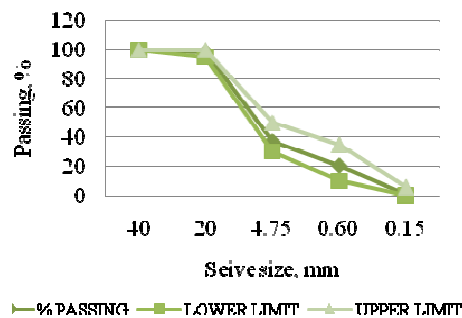


Figure 1 Gradation curve of all in one combined aggregate

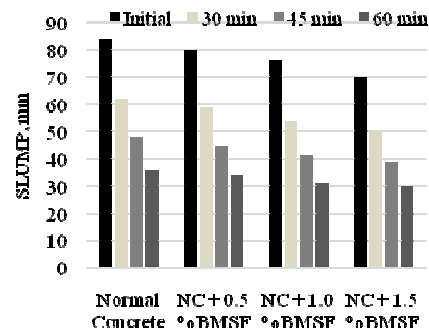


Figure 2 Slump of fresh concrete (mm)

Compressive Strength

For compressive quality test, solid shape cases of measurement $150 \times 150 \times 150$ mm were used for M-40 evaluation of concrete mixed. Super plasticizer (0.8% by volume) was added to this. In this way the concrete mixes can be proposed to meet the mechanical and solid properties for the road by the development of brass coated micro steel fibers in estimations of 0.5%, 1.0 % and 1.5 % by as an incomplete volumetric substitution of the concrete mix. Specimens are endeavored at the ages of 3, 7 and 28 days. To express the compressive quality, make common of attributes of three specimens. It is watched that the compressive idea of concrete is developing with the expansion in fiber substance emerged from standard strong at 3, 7 and 28 days. Aftereffect of Variation of Compressive Strength as for % of fibers is as appeared in **Figure 3**.

Flexural Strength

The flexural quality is directed by the fundamental issue framework. Concrete beam of size $150 \text{ mm} \times 150 \text{ mm} \times 700 \text{ mm}$ were casted to get the Flexural Strength of the concrete mix. A table vibrator was used for compaction of hand filled concrete beams. The samples were demolded taking following 24 hours of casting and were exchanged to restoring tank wherein they were permitted to cure for 28 days. For each age three samples were endeavored under two point stacking as demonstrated by I.S. 516-1959, over a persuading length regarding 400 mm on flexural testing machine used for the assurance of normal flexural quality. The test was performed on Universal Testing Machine (UTM) having breaking point of 50 BT. Load and differentiating contrasting diversions were noted up with disappointment. In each class three beams were attempted and their normal worth is represented to as showed up in the table. Result indicates variety of flexural quality regarding % of fibers is as appeared in **Figure 4**.

Tensile Strength

Splitting tensile strength is a backhanded strategy utilized for deciding the rigidity of concrete. Split Tensile quality was estimated utilizing a pressure testing machine with greatest limit of 2000 KN. The concrete is extremely frail in tension because of its weak nature and isn't relied upon to oppose the immediate pressure. The concrete creates splits when exposed to tensile forces. Accordingly, it is important to decide the tensile strength of concrete to decide the heap at which the concrete individuals may break. Concrete cylinder, diameter across of 150 mm and 300 mm long were casted fitting in with IS 5816: 1976 to get the Tensile Strength of the concrete blended. splitting tensile test is completed by putting the relieved concrete cylinders with its pivot flat, between plates of the testing machine, and the load is increased until the point when the disappointment happened by splitting in the plane containing the



vertical diameter of the specimen. magnitudes of the tensile stress are given by $2P/\pi DL$, where P is the connected load applied load and D, L, are the diameter, length of the cylinder respectively. The cylinders were casted, restored and tried utilizing compression testing machine. Tensile strength was inspected following 7 and 28 days of restoring. Result demonstrates variety of tensile strength regarding % of fibers as appeared in **Figure 5**.

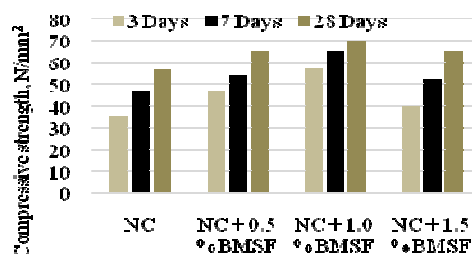


Figure 3 Variation of compressive strength with respect to % of fibers

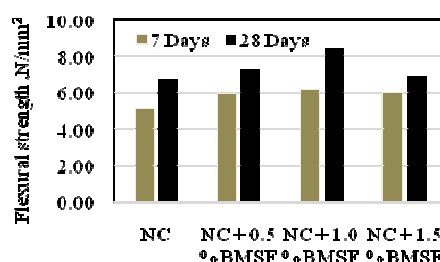


Figure 4 Variation of flexural strength with respect to % of fibers

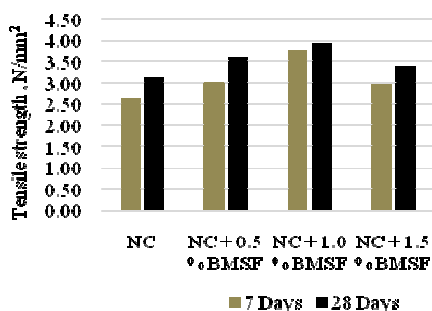


Figure 5 Variation of tensile strength with respect to % of fibers

PAVEMENT THICKNESS DESIGN

Plan of rigid pavement slab utilizing distinctive concrete was done according to the IRC: 58 and IRC SP 46 for the typical plain and fiber strengthen concrete. The flexural quality is straightforwardly taken from the beam flexural test for the structure of concrete mix for pavement. Thickness of slab is as appeared in **Table 2**.

Table 2 Pavement thickness with respect to % of fibers

	Normal Concrete	0.5 % BMSF	1.0 % BMSF	1.5 % BMSF
Flexure strength, N/mm ²	6.73	7.27	8.41	6.92
Design slab thickness, cm	21 cm	18 cm	16 cm	18 cm
Fatigue damage from single axles =	0.191	0	0	0
Fatigue damage from tandem axles =	0	0	0	0
Total bottom-up fatigue damage = Single axle + Tandem axles	0.191	0	0	0
DESIGN IS SAFE < 1	Yes	Yes	Yes	Yes

Plain concrete pavement asphalt has low rigidity and strain constrain, at any rate these auxiliary characteristics are improved by fiber expansion as mechanical properties are upgraded, allowing decline of the concrete layer thickness to help the traffic load. The most basic effect of fiber support is to postpone and control the tensile cracking of concrete. The execution of thinner pavement having 1% BMSF in concrete mix is discovered comparable to thicker plain concrete slab and is seen that the concrete with 1% BMSF is 5cm lower than ordinary concrete mix.

CONCLUSION



The maximum compressive strength (3, 7 and 28 days) of concrete with BMSF is increased significantly. When 1% of BMSF is added by weight of cement, strength increases after 28 days of curing, from 56.75 N/mm² to 70.24 N/mm² which is about 23.77 % increase. The maximum tensile strength (7 and 28 days) of concrete with BMSF is also increased and achieved at the dosage of 1% BMSF by weight of cement and after 28 days of curing, tensile strength increases from 3.12 N/mm² to 3.95 N/mm² which is about 26.60 % increase. The maximum flexural strength (7 and 28 days) of concrete with BMSF is also increased and achieved at the dosage of 1% BMSF by weight of cement and after 28 days of curing, flexural strength increases from 6.73 N/mm² to 8.41 N/mm² which is about 24.96 % increase. Henceforth, it is inferred that the optimum dosage is 1% BMSF by weight of cement, the reason being the highest strength achieved among all other dosages. Utilization of BMSF in concrete also reduces the thickness of the pavement. When optimum dosage 1% is added to the concrete it reduces the thickness by 5 cm when compared to normal concrete. Hence, it considerably reduces the amount of material to be used. Concrete with BMSF has higher strength when compared to normal concrete and it also offers more resistance to the formation of micro cracks in the concrete. So, usage of BMSF not only provides micro crack resisting concrete but also requires less maintenance hence, reducing the maintenance cost proving itself economical in longer run.

REFERENCES

1. IRC: 44 concrete mix designs for rigid pavement.
2. IRC:46-2013 Design and construction of fibre reinforced concrete pavements
3. IRC: 58-2011, Guide line for the design of plain jointed rigid pavement for highways, third edition.
4. IS 1199-1959, Methods of sampling and analysis of Concrete, slump test of concrete.
5. IS: 2386 (Part 4): 1963, Tests on Aggregate
6. IS: 10262:2009 Guidelines for concrete mix design, New Delhi, India.
7. IS: 2386 (Part 1): 1963, Shape test of aggregate
8. IS: 2386 (Part 3): 1963, Specific Gravity and Water absorption test of Aggregate
9. IS: 383:1970 Specification for coarse and fine aggregate from natural source for concrete
10. IS: 4031 (Part 1): 1996, Fineness test of cement
11. IS: 4031 (Part 3): 1988, Soundness of cement by Le-Chatelier test
12. IS: 4031 (Part 4): 1988 Standard consistency test of cement
13. IS: 4031 (Part 5): 1988, Initial and Final setting time test of cement
14. IS: 456:2000 plain and reinforced concrete-code of practice.
15. MORTH 2005- Ministry of road transport and highways.
16. A.M. Shende, A.M. Pande, M. GulfamPathan. Experimental Study on Steel Fiber Reinforced Concrete for M-40 Grade, International Refereed Journal of Engineering and Science (IRJES), ISSN (Online) 2319-183X, (Print) 2319-1821 Volume 1, Issue 1, 043-048(2012).
17. Abdul Ahad, Zishan Raza Khan, Shumank Deep Srivastava., Application of Steel Fiber in Increasing the Strength, Life-Period and Reducing Overall Cost of Road Construction(by Minimizing the Thickness of Pavement). 2015, science research publishing, World Journal of Engineering and Technology. Vol.3 No.4, (2015)
18. K. Vamshi Krishna, J. Venkateswara Rao, Experimental study on behavior of fiber reinforced concrete for rigid pavement, IOSR Journal of Mechanical and Civil Engineering (IOSR-JMCE) Volume 11. ISSN (online): 2319-8753 pp 2972-2987. (2014)
19. Raczkiewicz, Wioletta, The effect of micro-reinforcement steel fibers addition on the size of the shrinkage of concrete and corrosion process of the main reinforcement bars, Elsevier, Procedia Engineering. Volume 195, 2017, pp155-162,(2017)
20. S. A. Mahadik, S. K. Kamane, A. C. Lande Effect of Steel Fibers on Compressive and Flexural Strength of Concrete, October 2014, International Journal of Advanced Structures and Geotechnical Engineering. ISSN 2919- 5347, Vol. 03, No. 04, (2014)
21. Shahid Iqbal, Ahsan Ali, Klaus Holschemacher, Thomas A. Bier, Effect of change in micro steel fiber content on properties of High strength Steel fiber reinforced Lightweight Self-Compacting Concrete (HSLSCC), 2015, Elsevier, Procedia Engineering 122 (2015), Volume 122, 88-94 (2015)
22. Andıç, & Yardımcı, Mert & Ramyar, Kambiz. Performance of carbon, polyvinylalcohol and steel-based microfibers on alkali-silica reaction expansion. Construction and Building Materials - CONSTR BUILD MATER. 22. 1527-1531, (2008).



Development and Properties of Self-compacting Aluminosilicate Composites with Diverse Consequences of Alkaline Activator Ratio and Molarity

V K Nagaraj^{*1}, D L Venkatesh Babu¹

ACS College of Engineering, Bengaluru, Karnataka, India¹, nagaraj.vk18@gmail.com*

ABSTRACT

Globally the interest in lowering the carbon footprint of concrete is growing progressively. Alkaline activated binder, nowadays customarily known as geopolymer binder can be an enduring remedy for absolute replacement of Portland cement. In the present study, mix proportions for self-compacting aluminosilicate composites also known as self-compacting geopolymer concrete was proposed in order to sustain a high compressive strength along with better workability properties and superior durability properties. Class F fly ash, ground granulated blast furnace slag, sodium hydroxide and sodium silicates were nominated as source materials and alkaline activators, respectively. Current study access the behaviour of diverse consequences of substitution of fly ash by ground granulated blast furnace slag (50% and 75%) alkaline activator ratio (2, 4 and 6) and molarity (5M, 10M and 15M). The test results concluded that increasing alkaline activator ratio increased the workability and increase in molarity improved the compressive strength of concrete. Fresh property tests and compressive strength measurements have been employed to scrutinize and optimize the grades of self-compacting geopolymer concrete. Two optimum grades of self-compacting geopolymer concrete i.e., M40 and M50 were proposed, these grades were then tested for durability and volume stability. Durability tests such as water permeability test, sorptivity test, acid attack and sulphate attack tests were carried on optimum grades of self-compacting geopolymer concrete specimens to check the resistance against aggressive environment. The percentage replacement of fly ash by ground granulated blast furnace slag not only eradicated the demand for accelerated curing regime besides the replacement synchronously enhanced the compressive strength and volume stability.

KEYWORDS Low calcium fly ash, Ground granulated blast furnace slag, Optimum grades, Durability, Volume stability.

INTRODUCTION

The cement industries countenance various complications due to ineffectiveness to satisfy the Portland cement demand and also global warming mainly due to CO₂ emissions. The production process of a tonne of cement involves discharge of approximately a tonne of CO₂ into the atmosphere, which makes a consequential increase in global greenhouse gas emission. Consequently, it becomes obligatory to develop alternative binders employing the industrial by-products to diminish the carbon footprint of the construction industries. Thus, aluminosilicate composites/ alkali activated concrete/ geopolymer concrete was developed as an emanate alternative to traditional hydraulic binders [1]. This special concrete requires source material(s) such as blast furnace slag [4], fly ash [1,2], metakaolin [3], silica fume (F.N. Okoye) and rice husk ash [5] which rich in Aluminum (Al) and Silicon (Si) and along with alkaline activators such as the combination of hydroxides of sodium or potassium and silicates of potassium or sodium. The alkaline activators leaches out the Al and Si from the source materials this reaction is known as geopolymeric reaction and the product of this reaction is an inorganic polymer which predominantly binds the aggregates together to produce geopolymer concrete.

This scrutiny aims to investigate the properties of Self-compacting aluminosilicate composites commonly known as Self-compacting Geopolymer Concrete (SCGC), which is an innovative concrete where the concrete does not require any external compaction. This virtually flows to a uniform level under the influence of gravity without segregation. SCGC ameliorates ease of filling of slender and narrow sections, it has better consolidation with and around the reinforcement, it has an improved pumpability, it renders uniform surface finish and it also minimizes labor cost and errors. In the present investigation source materials such as Class F fly ash and ground granulated blast furnace slag (GGBS) was utilized along with sodium silicate (Na₂SiO₃) and sodium hydroxide (NaOH) as alkaline activators.

The vital role of water-reducing chemical admixture in self-compacting concrete (SCC) is to disseminate negative charge on the particles of binder by adsorption process, which then repulse each and ever particles and get promulgated and deflocculated [6], this ameliorate the SCC performance in its fresh and hardened state [7]. But SCGC has no momentous improvement with of water-reducing chemical admixture and it also lowers the setting



time and early strength gain when SCGC specimens were cured under ambient temperature. Therefore, in order to overcome the drawback of water-reducing chemical admixture slightly greater water to geopolymer solids ratio (W/GPS) of 0.53 was opted in present study. This appraisal gauge the consequential impact of partial replacement of fly ash by GGBS by 50% and 75% with a molarity of 5M, 10M and 15M and alkaline activator ratio of 2, 4 and 6 along with a constant alkaline activator to cementitious binder ratio of 0.5. SCGC are evaluated by minimal authors as a solution for 'green' concrete, with only few studies on fresh and hardened properties. But, this current work makes an attempt to scrutinize fresh properties and hardened properties. Two grades of SCGC, that is, M40 and M50 were proposed depending on optimum fresh properties and compressive strength of various series of SCGC mixes. Also, a fair amount of research on volume stability and durability performance were deliberately investigated and then compared with literatures as this green concrete technology has no standard code of practice. SCGC would be beneficial to future applications of the materials and construction industry.

EXPERIMENTAL DETAILS

The coal fired power plants produces substantial quantity of fly ash and the steel manufacturing industries generates significant amount of GGBS as a by-products. Fly ash was obtained from KPTCL, Karnataka and GGBS was procured from JSW, Karnataka. The physical and chemical properties of fly ash are described in **Table 1** and **Table 2** and physical and chemical properties GGBS are described in **Table 3** and **Table 4**. Sodium silicate with 56% water content and sodium hydroxide with 92% purity available commercially were productively utilized as alkaline activators. The coarse aggregate and fine aggregate were analyzed and chosen as per IS 383:2016 [9]. M sand as fine aggregate confirming to zone II of IS 383:2016 with water absorption of 4.10% and a specific gravity of 2.62 was utilized along with 12.5 mm graded coarse aggregate with a water absorption of 0.41% and a specific gravity of 2.68. Water free form foreign matter was utilized. Absolute volume method [10] was employed to estimate the required quantity of materials to produce SCGC. The SCGC has a density quite lower than 2400 kg/m³. Henceforth, SCGC behave as a semi-light weight green concrete which lowers the dead load of structures. The required materials for various series of partial replacement of fly ash by GGBS by 50% (SCGC₁) and 75% (SCGC₂) are described in **Table 5** and **Table 6**, respectively.

Table 1 physical property fly ash

Chemical properties	Content
Loss on Ignition	0.16
Silicon dioxide	65.58
Insoluble residue	96.78
Iron oxide (Fe ₂ O ₃)	4.95
Chloride content	0.010
Alumina (Al ₂ O ₃)	20.83
Magnesia (MgO)	0.57
Reactive silica	36.33
Reactive alumina	10.05
SO ₃	0.08
Titanium dioxide (TiO ₂)	0.11
Phosphorus pentoxide (P ₂ O ₅)	0.17
Alkalis	
Na ₂ O	0.24
K ₂ O	0.78

Table 2 Chemical properties fly ash

Physical properties	Content
Specific gravity	2.34
Average particle size exposed for hydration	1.50μ
Soundness, by autoclave, %	0.08
Fineness, m ² /kg	388.0
Material retained on 45μ Sieve (% by mass)	0.62
Lime reactivity, MPa	7.86
Comparative compressive strength, % 672 ± 4 hour	105

Table 3 Physical properties GGBS

Chemical properties	Content
Gain on Ignition	0.24
Insoluble residue	0.61
Iron oxide (Fe ₂ O ₃)	0.83
Silicon dioxide (SiO ₂)	36.26
Chloride content	0.010
Alumina (Al ₂ O ₃)	18.65
Magnesia (MgO)	6.85
Reactive silica	40.07
Sulphide sulphur	0.08
Manganese oxide (MnO)	0.13
Phosphorus pentoxide (P ₂ O ₅)	0.17
Alkalis	
K ₂ O	0.83
Na ₂ O	0.23

Table 4 Chemical properties of GGBS

Physical properties	Content
Specific gravity	2.88
Bulk density, kg/m ³	1195
Surface area, gm/ cm ²	12,010
Particle shape	Irregular
Comparative compressive strength %	
168±2 hour	66
672±4 hour	86
Material retained on 45μ sieve (% by mass)	Nil
Average particle size	
d ₁₀	< 1 μ
d ₅₀	< 1 μ
d ₉₀	< 1 μ



PROCEDURE FOR MIXING, CASTING AND CURING OF SPECIMENS

The formulation of alkaline activator solution involved dilution of sodium hydroxide flakes in potable water to required molarity and then it was mixed with the required amount of sodium silicate, this alkaline mixture was kept for a day at ambient room conditions. LCFA, GGBS, coarse and fine aggregates were uniformly mixed in a 1×10^3 litres pan mixture for 2-3 minutes, then the alkaline activator mixture along with the calculated quantity of free water was added to dry SCGC mix and this mix was further mixed for another 2 to 3 minutes until a free flow homogenous fluid mix is achieved. This homogeneous SCGC mix was examined for its various fresh property tests and then the mix was shifted to standard moulds. These casted specimens were cured at ambient temperature until the day of testing.

EXPERIMENTAL WORK

Workability Test

The fresh property of various series of SCGC was evaluated as per EFNARC guidelines [8]. The predominant fresh property characteristics for SCC are resistance to segregation, passing ability and filling ability. Hence, SCGC should assure the characteristics of SCC. The EFNARC guidelines are given in **Table 7**.

Compressive Strength Test

The compressive strength test on SCGC was investigated on 0.15 m cube specimens in a 2000 kN CTM as per IS 516:1959 [9]. This test specifies the capability of concrete to resist the compressive pressure. This is an important entity and quite commonly followed test for testing the hardened concrete.

Table 5 Required material for 1 m³ of SCGC₁ mix

Mix no.	AA/CB	AAR	Molarity	50% GGBS, kg/m ³	50% fly ash, kg/m ³	NaOH, kg/m ³	Water ^a , kg/m ³	Na ₂ SiO ₃ , kg/m ³	FA, kg/m ³	CA, kg/m ³	Free water, kg/m ³
SG ₇₃	0.5	2	5M	240.00	240.00	14.40	65.60	160.00	781.56	533.02	144.144
SG ₇₄			10M	240.00	240.00	24.69	55.31	160.00	762.42	519.97	159.88
SG ₇₅			15M	240.00	240.00	32.40	47.60	160.00	748.07	510.18	171.68
SG ₇₆		4	5M	240.00	240.00	8.64	39.36	192.00	778.46	530.90	156.87
SG ₇₇			10M	240.00	240.00	14.81	33.19	192.00	766.98	523.07	166.32
SG ₇₈			15M	240.00	240.00	19.44	28.56	192.00	758.37	517.20	173.40
SG ₇₉		6	5M	240.00	240.00	6.17	28.11	205.71	777.13	530.00	162.33
SG ₈₀			10M	240.00	240.00	10.58	23.71	205.71	768.93	524.41	169.07
SG ₈₁			15M	240.00	240.00	13.89	20.40	205.71	762.78	520.21	174.13

Table 6 Required material for 1 m³ of SCGC₂ mix

Mix no.	AA/CB	AAR	Molarity	75% GGBS, kg/m ³	25% fly ash, kg/m ³	NaOH, kg/m ³	Water ^a , kg/m ³	Na ₂ SiO ₃ , kg/m ³	FA, kg/m ³	CA, kg/m ³	Free water, kg/m ³
SG ₄₆		2	5M	360.00	120.00	14.40	65.60	160.00	795.71	542.67	144.144
SG ₄₇			10M	360.00	120.00	24.69	55.31	160.00	776.57	529.62	159.88
SG ₄₈			15M	360.00	120.00	32.40	47.60	160.00	762.22	519.83	171.68
SG ₄₉		4	5M	360.00	120.00	8.64	39.36	192.00	792.61	540.55	156.87
SG ₅₀	0.5		10M	360.00	120.00	14.81	33.19	192.00	781.13	532.72	166.32
SG ₅₁			15M	360.00	120.00	19.44	28.56	192.00	772.52	526.85	173.40
SG ₅₂		6	5M	360.00	120.00	6.17	28.11	205.71	791.28	539.65	162.33
SG ₅₃			10M	360.00	120.00	10.58	23.71	205.71	783.08	534.06	169.07
SG ₅₄			15M	360.00	120.00	13.89	20.40	205.71	776.93	529.86	174.13



Table 7 Test method and acceptance values as per EFNARC guideline

Test	Properties	Typical ranges of values	
		Minimum	Maximum
Slump flow	Filling ability	650mm	800mm
t ₅₀ cms slump flow	Flow ability	2 s	5 s
V funnel	Filling ability	8 s	12 s
J ring	Passing ability	0mm	10mm
L box	Passing ability	0.8	1.0

Volume Stability

The volume stability (drying shrinkage) of SCGC was conducted on $0.05 \times 0.05 \times 0.15\text{m}$ prisms as per IS 1199-1959 [ACS 31]. This test determines the change in SCGC volume due to moisture.

Durability Test

The resistance of SCGC to aggressive environment attributes was scrutinized by various durability tests. The water permeability tests was conducted on 0.15m SCGC cube specimens as per DIN 1048:1991 [10] to check the rate of water flow in SCGC specimens under pressure. Sorptivity test was conducted on 0.1m diameter and 0.05m thick SCGC specimens as ASTM C 1585-13 [11]. The resistance to acid and sulphate was investigated on 0.1m SCGC cube specimens by acid attack test and sulphate attack test respectively.

TEST RESULTS AND DISCUSSIONS

Workability Test Results

The influence of replacement proportions of GGBS, alkaline activator ratio and molarity are illustrated in **Figure 1** to **Figure 10**. From the experimental tests results it can be concluded that the workability of fresh SCGC ameliorated with the increase in alkaline activator ratio and decrease in molarity. The SCGC series with 50% fly ash content exhibited better workability properties compared to SCGC series with 25% fly ash. The greater GGBS percentages had a negative impact on workability because GGBS expedite the degree of geopolymerization which in turn reduces the setting time of SCGC and aids in expeditious hardening of fresh SCGC. The various SCGC mixtures which qualified the requirements as per EFNARC were SG4, SG5, SG6, SG7, SG8, SG9, SG13, SG14 and SG16.

Compressive Strength Test Results

The compressive strength test results of various SCGC mix at 7 days, 28 days, 56 days and 90 days are illustrated in **Figure 11** and **Figure 12**. The test results of experimental investigation concluded that increase in molarity enhanced the compressive strength and whereas increase in alkaline activator ratio lowered the compressive strength of SCGC. It was discerned that the SCGC series with 75% GGBS had superior compressive strength compare to SCGC series with 50% GGBS this was principally due to greater degree of geopolymerization made the SCGC with superior binding property and with a compact microstructure.

Optimization of SCGC

The various series of SCGC were optimized into two grades, that is, M40 (SG₇₈) and M50 (SG₅₀). The SCGC were optimized depending on better workability, preferable compressive strength and economy. These two optimum grades of SCGC were tested for its volume stability and durability performance.

Volume Stability Test Results

The drying shrinkage test results are illustrated in **Figure 13**. The test results of drying shrinkage stipulated that M50 grade of SCGC had better volume stability compared to M40 grade of SCGC, this was chiefly because M50 grade of SCGC constituted high proportion of GGBS which resulted in rigid zeolitic structure. This particular experimental investigation was conducted at the age of 28 days, 56 days, 90 days and 180 days.



Durability Test

Water permeability test results

The depth of water penetration by water permeability test is illustrated in **Figure 14**. The M40 grade of SCGC exhibited greater depth of water penetration this was mainly due to inferior microstructure compared to more impermeable M50 grade of SCGC. This particular experimental investigation was conducted at the age of 28 days, 56 days, 90 days and 180 days.

Sorptivity test results

The sorptivity test results of M40 and M50 grades of SCGC are illustrated in **Figure 15**. It was observed that the sorptivity coefficient of M50 grade of SCGC was low this was chiefly due to low void fraction compared to M40 grade of SCGC.

Acid Attack Test Results

The mass loss and compressive strength loss of SCGC by acid attack are illustrated in **Figure 17** and **Figure 18**. The experimental test results of M40 and M50 grades of SCGC when immersed in 3% sulfuric acid concluded that M50 grade of SCGC had inferior resistance to mass loss and compressive strength loss this was typically due to greater proportion of GGBS which contain high calcium oxide and it is extensively assaulted by sulfuric acid. This particular experimental investigation was conducted in 13 cycles. Each cycle was divided into 7 days of wetting and 7 days of drying.

Sulphate Attack Test Results

The mass loss and compressive strength loss of SCGC by sulphate attack are illustrated in **Figure 19** and **Figure 20**. The experimental test results concluded that M40 and M50 grades of SCGC when immersed in 5% magnesium sulphate, M40 grade of SCGC exhibited more mass loss and compressive strength loss compared to M50 grade of SCGC this was customarily due to high fly ash content, which was generally attacked when exposed to sulphate environment. This particular experimental investigation was conducted in 13 cycles. Each cycle was divided into 7 days of wetting and 7 days of drying.

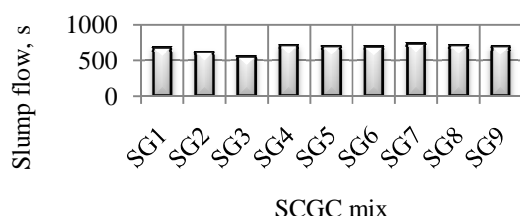


Figure 1 Slump flow test results of 50% GGBS and 50% fly ash SCGC

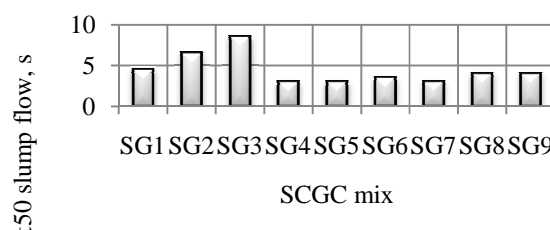


Figure 2 t50cms slump flow test results of 50% GGBS and 50% fly ash SCGC

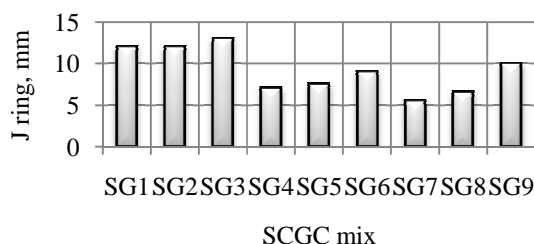


Figure 3 J ring test results of 50% GGBS and 50% fly

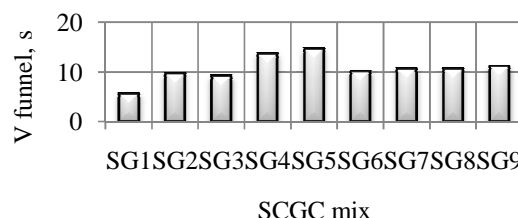


Figure 4 V funnel test results of 50% GGBS and 50% fly



ash SCGC

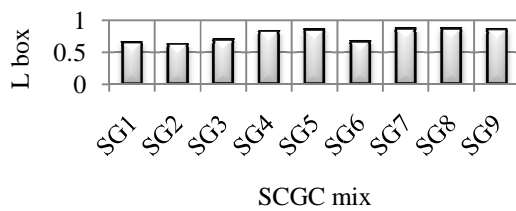


Figure 5 L box test results of 50% GGBS and 50% fly ash SCGC

ash SCGC

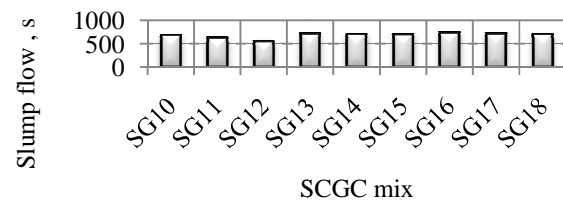


Figure 6 Slump flow test results of 75% GGBS and 25% fly ash SCGC

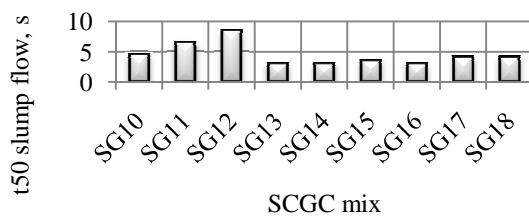


Figure 7 t50 cms slump flow test results of 75% GGBS and 25% fly ash SCGC

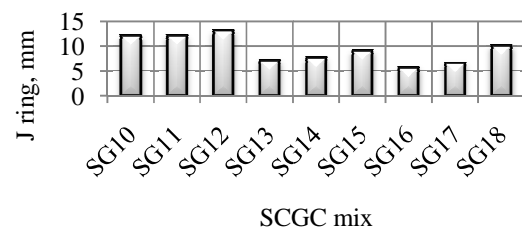


Figure 8 J ring test results of 75% GGBS and 25% fly ash SCGC

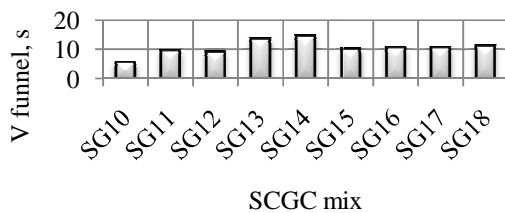


Figure 9 J V funnel test results of 75% GGBS and 25% fly ash SCGC

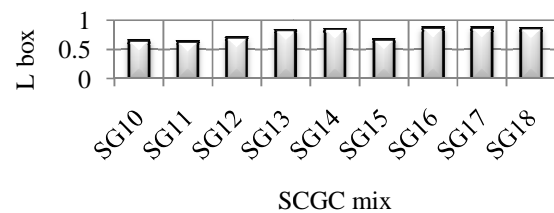


Figure 10 L box test results of 75% GGBS and 25% fly ash SCGC

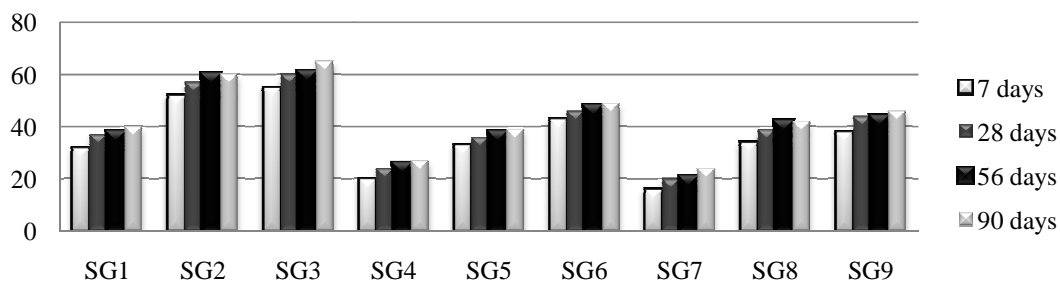


Figure 11 Compressive strength test results of SCGC₁ mix

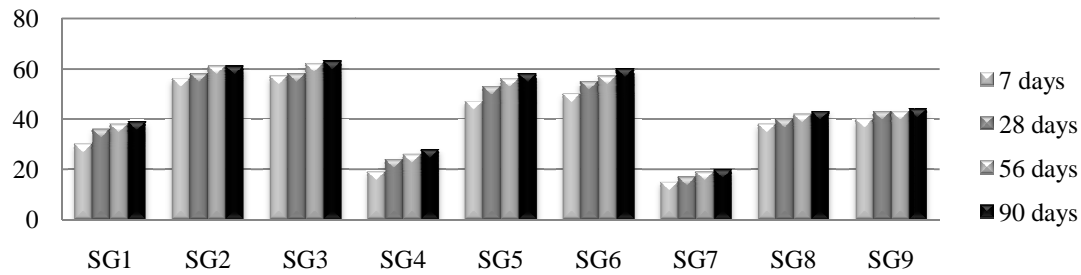


Figure 12 Compressive strength test results of SCGC₂ mix

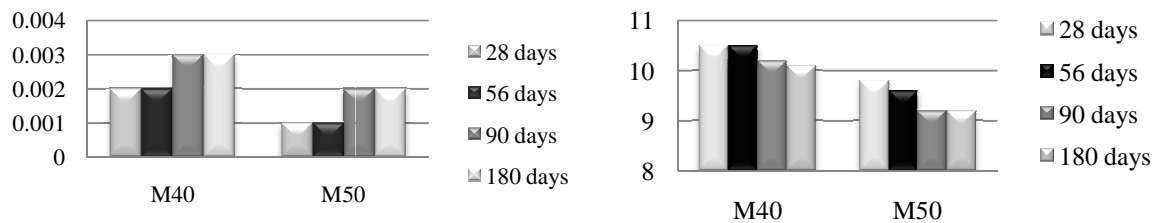


Figure 13 Drying shrinkage test results

Figure 14 Water permeability test results

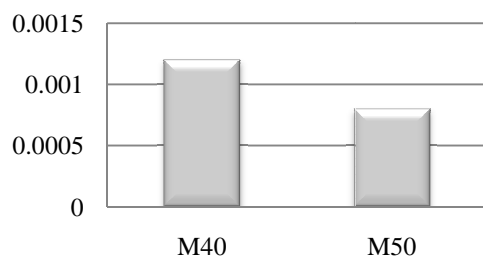


Figure 15 Sorptivity test results

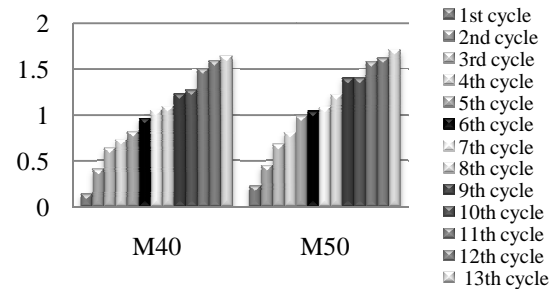


Figure 16 Weight loss test results due to acid attack

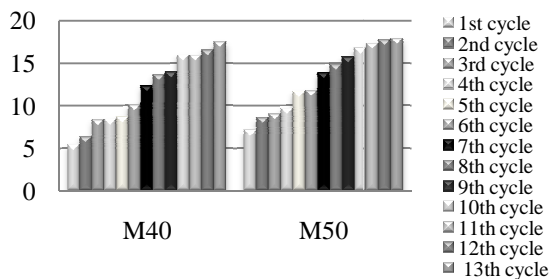


Figure 17 Compressive strength loss test results due to acid attack

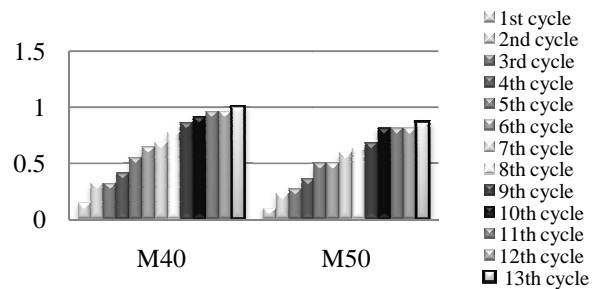


Figure 18 Weight loss test results due to sulphate attack

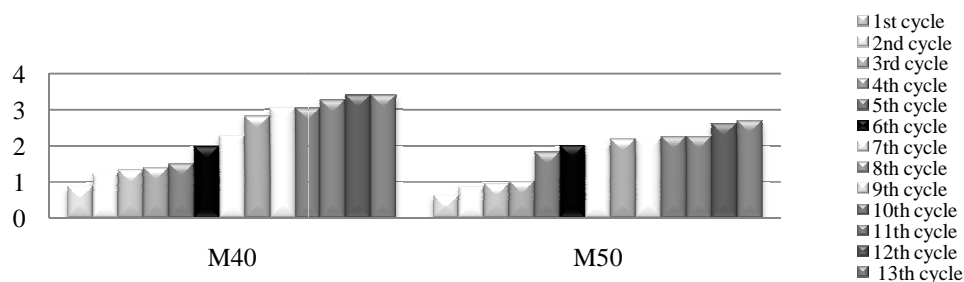


Figure 19 Compressive strength loss test results due to sulphate attack

CONCLUSIONS

The aluminosilicate based industrial source materials like Class F fly ash and GGBS were effectively employed to fabricate SCGC which concluded in lowering the ill effects caused by PC manufacturing industries. From the achieved experimental test results of laboratory evaluation for various series of SCGC mix, the following conclusions can be drawn:

- Increase in fly ash proportion and alkaline activator ratio meliorated the workability of fresh SCGC mix.
- The accelerated curing regime was eradicated with incorporation of GGBS in the mix and it stimulated ambient curing conditions, which made the SCGC applicable for in situ construction.
- The compressive strength of SCGC improved with increase in GGBS content and molarity.
- The M50 grade of SCGC had better volume stability compared to M40 grade of SCGC.
- The depth of water penetration and sorptivity coefficient of M50 grade of SCGC was low compared to M40 grade of SCGC.
- The M50 grade of SCGC had greater mass and compressive strength loss when submerged in 3% H₂SO₄ solution.
- Higher percentage of GGBS exhibited low resistance to mass and compressive strength loss when immersed 5% MgSO₄ solution

REFERENCE

1. B. Singh, G. Ishwarya, M. Gupta, S. K. Bhattacharyya, Geopolymer concrete: a review of some recent developments, Constr. Build. Mater. Volume 85, pp 78–90, 2015.
2. M.Y.J. Liu, U.J. Alengaram, M.Z. Jumaat, K.H. Mo, Evaluation of thermal conductivity, mechanical and transport properties of lightweight aggregate foamed geopolymer concrete, Energy Build. Volume 72, pp 238–245, 2014.
3. D. Hardjito, S.E. Wallah, D.M.J. Sumajouw, B.V. Rangan, Factors influencing the compressive strength of fly ash-based geopolymer concrete, Civil Eng. Dimension, Volume 6, pp 88–93, 2004.
4. X. Zhaohui, X. Yunping, Hardening mechanisms of an alkaline activated class F fly ash, Cem. Concr. Res. 31 (2001) 1245–1249.
5. J.G.S. Jaarsveld, J.S.J. Deventer, Effect of the alkali metal activator on the properties of fly ash based geopolymers, Indian Eng. Chem. Res. 38, pp 3932–3941, 1999.
6. F.E.F.P. Group. The European guidelines for self-compacting concrete specification, production and use, European guidelines 2005, p. 63.
7. M. F. Nuruddin, S. Quazi, N. Shafiq, A. Kusbiantoro. Compressive strength and microstructure of polymeric concrete incorporating fly ash and silica fume. Canadian Journal of Civil Engineering. Volume 1, Number 1, pp 15–8, 2010.
8. IS 383 : 2016, Indian Standard. Coarse and Fine Aggregate for Concrete – Specification.
9. IS 516:1959, Indian Standard. Methods of tests for strength of concrete. [10] IS 1199-1959, Indian standard, Method of Sampling and Analysis of Concrete.
10. DIN 1048:1991, Testing Concrete, Testing of Hardened Concrete (specimens prepared in mould).
11. ASTM: C 1585-13, Standard test method for measurement of rate of absorption of water by hydraulic-cement concretes.



Estimation of Storm Water Drainage: A Case Study

Arun S Bagi^{*1}, S P Wathar¹

Department of Civil Engineering, BLDEA's V.P. Dr. P.G. Halakatti College of Engineering and Technology, Vijayapur, Karnataka, India¹, arunsbagi@gmail.com*

ABSTRACT

Around the world, urban landscape is disturbed by many sources of problems. Storm water and floods in urban cities is one of significant problems faced in India. This work describes the design and estimation of storm water drainage facility for the Vijayapur city, for that the study area considered is Meenakshi Chowk. The problems that are likely to occur on road that may degrade the life span of pavement is, when there is no provision of proper storm water drainage facility. The problems include formation of potholes, rutting of road surface, etc. The study involved in identifying major flooded areas and problems occurring in those areas are identified and most likely an attempt is made to provide solution. The methodology integrated the applications of GIS and STORM CAD. The paper explains delineation of watershed areas using GIS software, extraction of contours from DEM, and lay out of drain pattern. Feasible location of catch basins was provided to divert the surface runoff in to conduits with minimum time of outstanding water. The model was validated and computed in storm cad. The data required for analysis were taken from IRC code books. The discharge at out full is predicted from developed model. It is also proposed to design a reservoir to collect storm water for peak duration of precipitation

KEYWORDS DEM, GIS, Storm Cad, Drainage pattern, Modeling and IRC

INTRODUCTION

Most of Indian cities are affected by several urbanization problem, one the primary and significant problems that arise during monsoon period is flooding up of street. Flooding has severe impacts from health of population to economic losses. Hence it becomes essential to develop an efficient drainage network for the cities. Flash floods seems unpredictable because of their intensity and nature of appearance. Eliminating or controlling of floods is neither practically advisable nor economically viable. Hence, flood management aims at providing a considerable degree protection against flood damage at economic costs and preserves the environment. Flood management consists of predicting possible worst flood discharge and developing an efficient network to dispose of the discharge. To understand the flood discharge, the natural drainage pattern, topography, nature of land use and land cover studies are to be carried out. The geographical area is classified based on watershed and land cover. And it is great significance to include the study of flood forecasting, which accounts the efficiency of existing network the future urban development. Flood plain, zoning, flood proofing, disaster preparedness etc are other measures to be considered while developing the drainage network. In areas with natural, unaltered ground water, about 20% of the precipitation becomes runoff and about 50% infiltrates into the soil to form or replenish ground water and flows into streams [1-2]. Evaporation and uptake by plants accounts to the remaining 40%. When natural conditions change due to development, land use and other activities, this water cycle becomes altered. As the land becomes more covered with impervious surfaces, more precipitation converts as runoff [3]. This runoff carries the dust, other loads, and pollutants. When the development is more as much as 55% may become runoff.

A good and efficient storm water management is badly required at the moment all over the universe especially in developing countries like India. The idea of efficient storm water management is based on the requirement to protect the health of the public, welfare and safety of the public, conservation of water, need to strive for sustainable environment etc [4]. Storm-water management facilities are important elements of civil infrastructure and sensitive to extreme weather events, which generate peak runoff flows. The runoff component of storm water management operates on a collection of sub catchment areas that receive precipitation and generate runoff and pollutant loads [5-6]. The routing portion of storm water management transports this runoff through a system of pipes, channels, storage/treatment devices, pumps, and regulators.

METHODOLOGY

Figure 1 shows the flowchart shows the methodology adopted for case study.

Delineation of catchment area: In order to design a storm water drainage pattern the catchment area and stream line flow is delineated. Catchment area and stream line is delineated using Q-GIS. With the geographical boundary of district, a sub-catchment area is selected, the details are Meenakshi chowk at 16°49'39.92" N, 75°42'44.02" E, coordinates in the Vijayapur city which is of 3.2 km² in area.



Determination of stream line pattern for catchment area: stream line pattern is drawn from catchment area by using QGIS software. Blue line in **Figure 2** depicts stream line pattern.

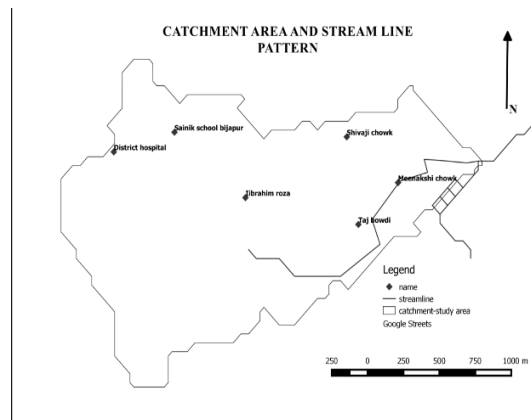
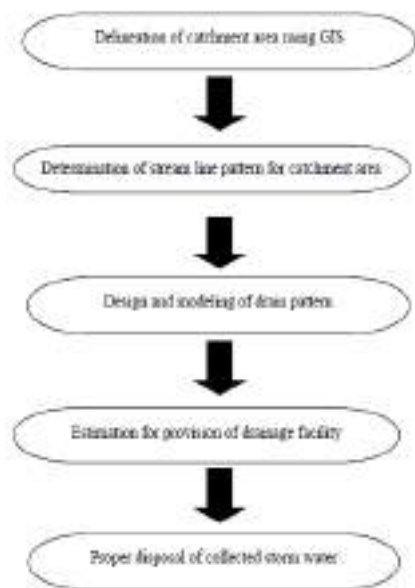


Figure 2 Stream line pattern

Figure 1 Flowchart showing methodology

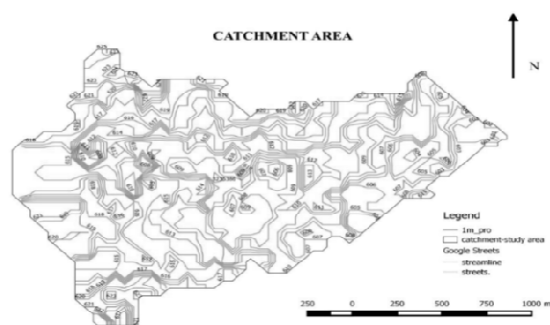


Figure 3 Extracted contours

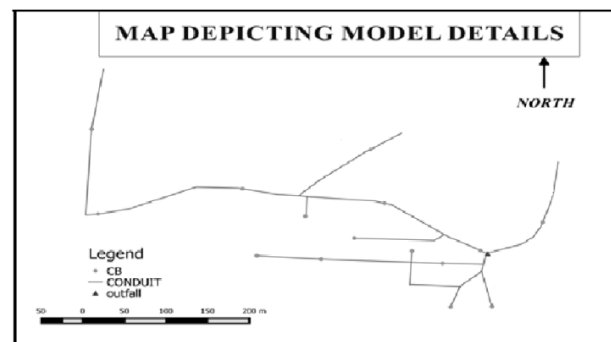


Figure 4 Model details

Drain pipes were mapped in GIS and catch basin were located. The elevation of these conduits were found using profile from line tool. These elevations were later used in storm cad. The map below depicts the drain lines and catch basin locations.

Design and Modeling

In order to understand the topography of the study area, contours are developed using GIS tools. **Figure 3** shows the contours extracted.

The shape files of the drain pipes and catch basin were incorporated in to storm cad using modal builder tool. **Figure 4** shows the details of model. The details of all catchment areas such as area in hectare, is determined by GIS, Run-off coefficient and time of concentration are as follows. The coefficient of runoff adopted for design is 0.8, it is taken from IRC-SP-50 code book for based on pavement conditions. Time of concentration is the time taken by precipitated water in the catchment area to reach catch basin from farthest point. Catch basin is designed to collect precipitated water from catchment area.

The necessary user defined data given for calculation are elevation of ground and invert elevation which are determined from GIS at locations. on grade or in sag, grate length, longitudinal slope of minimum desirable gradient



which is taken from IRC i.e 1 in 250. Manning's constant of 0.013, clogging factor of 20% is assumed and standard head loss coefficient of 0.5. Conduit data such as ground elevation, invert elevation, diameter of pipe and the type of pipe. The type of pipe material used is concrete pipe of 600 mm diameter. The pipe used is of circular cross sections. These concrete pipes are of precast. The circular sections provide self -cleansing velocity. Out fall selected is at lowest elevation, based on the discharge generated at out fall the disposal tank is designed.

The model is validated and the errors were eliminated. Then the modal is computed. The results in the form of discharge at different conduits, catch basin, Velocity at different conduits are obtained, capacity in percentage at each conduit were also obtained. Capture efficiency and spread or top width at each catch basin are observed from the results of model.

The profile depicting total energy line (TEL), hydraulic gradient line (HGL) and flow in pipe were extracted. Total energy line is sum of pressure head, velocity head and datum head. Hydraulic grade line is the sum of pressure head and datum head. The difference between TEL and HGL line is the pressure head. The following figure shows a nature of HGL and TEL for one of conduit.

DATA COLLECTION AND MODELLING

Rainfall Data

The daily rainfall data of 9 rain gauge stations were collected from district statistical office for the period of 10 years, that is, from 2007-2017. The rain gauge stations are located at Mamadapur, Babaleshwar, Hitnali, Kannur, Kumatagi, Nagthan, Tikota, Bhutnal, Vijayapur city. The data pertaining to rain gauge located at Vijayapur city was considered for the study. The rain gauge station of Vijayapur city is located at 602 m above the mean sea level and at Lat: 16°49'00" and Long: 75°43'00". The maximum daily rainfall observed was in the year 2007 on 23 day of June month .the rain fall observed was about 86.2 mm.

The annual rain fall data for the rain gauge station located at Vijayapur city for last 10 years are as shown in **Figure 5**.

Flex Table of Catchment Areas

The total catchment area is divided in to different catchment areas based on the road network and contours.

Totally there are 15 catchment areas being divided. Runoff coefficient is assumed to be 0.8 as the study area is densely built up area and the pavements are of either cc pavements or bitumen pavements. The coefficient of runoff of 0.8 signifies that 80% precipitated water flows as runoff and 20% of precipitated water intercepts in to ground. The time of concentration is assumed as 0.25 h, that is, 15 minutes. The time of concentration for all the areas are assumed same as the area are steep in gradient and shorter length of flow of water from farthest point to sink point (catch basin).The discharge flows for different catchment areas are shown in below flex table. The catchment area containing larger area generates larger flow for example area of 4.53 hectare generates flow of 214.35 L/s and the catchment area of 0.55 hectare generates the flow of 26.02 L/s.

Flex Table of Catch Basin

The catch basins are provided at different locations to divert flow into conduits from catchment area. Totally 15 catch basins are provided for 15 catchment areas. The elevations of these catch basin are taken from GIS. Invert elevation are provided based on trial and error basis to provide continuous flow. Manning's constant for RCC pipes is taken as 0.013 from IRC-SP-50. Inlet location of catch basins are given as on grade except for the catch basin which is located before outfall. For the catch basin located before out fall the, location is given as In sag. The longitudinal slope is assumed as minimum desirable based on IRC criteria. As the roads are provided with bitumen pavements and CC pavements. The clogging factor is assumed as 20%. Head loss coefficient is taken as 0.5. The flow, diameter of catch basin, hydraulic grade line and capture efficiency are obtained as results.

Flex Table of Manhole

Manholes are mainly provided for access in to it for inspection purpose. Totally there are 13 catch basins. The elevations of these manholes are taken from GIS. Invert elevation are provided based on trial and error basis to provide continuous flow. The flow, diameter of man hole, hydraulic grade line and capture efficiency are obtained as results.

Conduit Flex Table

Conduits are provided to convey storm water from different catch basin to out fall. The conduits are linked between two catch basins or two manholes or between catch basin and man hole. The length of each conduit is scaled based



on model generated. Based on the length and invert elevation of two linking point, the slope of conduits is found. For example, conduit 12(CO-12) of length 69.3 m which is linked between manhole-5 and manhole-7 having elevation of 603.00 and 602.44 respectively has the slope of 0.008 m/m (0.8%). As the slope is fixed for the conduits, the feasibility of flow is checked by varying the diameter of pipes. For 300mm diameter pipes, the flow exceeded the capacity of the conduits, at junctions like MH and CB velocity head is converted to pressure head, which resulted in rise of water and it is observed to be flooded. Therefore, a suitable diameter of pipe is selected so that every possible flooding is avoided. For 600 mm pipes the results yielded are feasible. The flow follows the continuity equation i.e. sum of flow coming in to the catch basin or manhole is equal to the flow moving away from it. As some amount of water is held in catch basin, the flow moving out may not be to full extent. For example, sum of discharge of water coming in to man hole-7 from the conduits co-12, co-30 and co-52 which are 245 L/s, 300 L/s and 400 L/s respectively to be equal to the discharge in conduit co-67. But as some amount of water stays in man hole therefore flow in to conduit co-67 reduced

Outfall Flex Table

Out fall is located at lowest elevation to collect water from all conduits. The ground elevation of out fall is taken from GIS. The discharge at out fall obtained is 717.47 L/s.

Profile

The profiles extracted from the results are given below:

After the computation of model, the profiles of each conduit are extracted. Each profile of conduit represents the natural ground level (represented by green line), total energy gradient line (represented by red line), hydraulic gradient line (represented by blue line) and also the flow in the conduits. The profile also shows the flow in to catch basin or manhole. By these profiles it can be easily interpret the flow and variation in velocity head and pressure head. The BBL to MC represents the profile from Babaleshwar Naka to Meenakshi Chowk. The profile graph of elevation with respect to distance. In conduit co-12, there is very less difference between total energy gradient line and hydraulic energy gradient line this is because the flow in the conduit is very slow. The velocity head suddenly increases when the flow enters the man hole. The flow over this conduit is very slow because the water is flowing from three different directions to common man hole at a time therefore it takes time to clear of the water from man hole to conduits carrying water to downstream.

RESULTS

Determination of Efficient Storm Water Drainage Network for Study Area

Hydrologic Analysis

After computation of results discharge estimated at out fall in 717.47 l/s. the discharges at different conduits, catch basin and man hole are given in corresponding flex tables. Hydraulic analysis: Hydraulic analysis results in design of cross section and longitudinal slope of drain. The cross section of drain pipes and slopes is given in the flex table of conduits. The model is created with flow variation in the conduits. Variation in the flow is shown with different colors in **Figure 6**.

The flow variation is classified as shown in **Figure 7**.

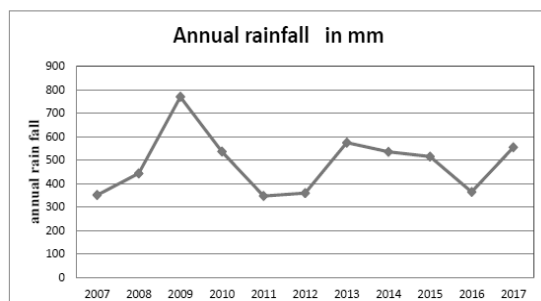


Figure 5 Annual rainfall

	Value <= (L/s)	Color
0	138.23	128, 128,...
1	254.70	192, 0, 192
2	371.18	0, 128, 128
3	487.65	192, 192, 0
4	604.13	192, 255,...
5	720.60	255, 0, 0

Figure 7 Color classification of discharge

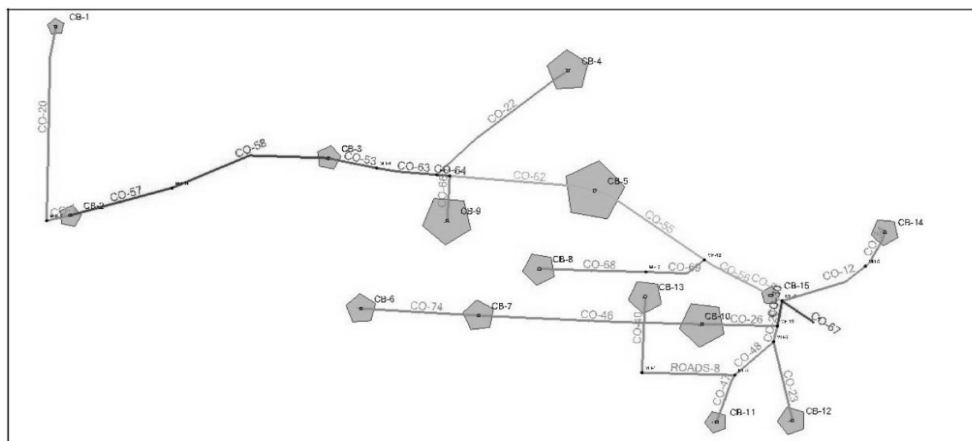


Figure 6 Variation in the flow in conduits

Estimation

Estimated cost for patching of pot hole in the study area approximately Rs 5,60,000. The estimated cost for provision of drainage facility which include earth work, laying of conduits man hole, catch basin and gratings is approximately Rs 50,50,000.

Disposal of Collected Storm Water

It is proposed, 50% of collected storm water at outfall is stored in tank and the rest is left to already existing manhole from where the water flows to Gagan mahal. The size of the tank to store water is $110 \times 55 \times 2$ m.

CONCLUSIONS

- As per the topographical analysis the total catchment area considered for the study is about 3.28 km^2 and it was determined that the storm water was collected at Meenakshi Chowk which acts as a valley point.
- As per the hydrological analysis, the total discharge at the out fall was found to be 717.47 l/s .
- As per hydraulic analysis, catch basins were provided at feasible locations to divert the runoff in to conduits with minimal time of outstanding water. After several trail and errors, it was determined that conduits received storm discharge effectively. The total catch basins in the study area are 15, manholes are 14 in numbers and these are linked by conduits.
- Estimated cost for providing the drainage facility was found to be Rs 50, 50,000 and estimated cost for patching of the pot holes in the study area was found to be Rs 5,60,000.
- As per the study conducted, the Problems occurring at different areas due to lack of drainage facility were identified and the areas where the drainage facility is provided such drainages were found to be clogged.
- As per the study, the cambers provided at many locations are inefficient to facilitate the flow of water and cambers at many locations do not match the prescribed limit of IRC specifications

REFERENCES

1. Sundara Kumar Pitta ,T Santhi, P Manoj, Srivatsa. Storm Water Drainage Design (Case Study Vijayawada), International Journal of Earth Sciences and Engineering Volume 8, Number 2, April 2015.
2. S. Rokade, P.K. Agarwal and R. Shrivastava, Study on drainage related performance of flexible highway pavements, International Journal of Advanced Engineering Technology (IJAET),Volume 3, Issue 1, pp 334-337, 2012.
3. C. Pagotto, M. Legret, Le Cloirec P. Comparison of the hydraulic behavior and quality of highway runoff water according to the type of pavement. Water Res 34, 2000, 4446–4454. doi: 10.1016/s0043-1354(00)00221-9
4. V. K. Bansal, Use of GIS and Topology in the Identification and Resolution of Space Conflicts. Journal of Computing in Civil Engineering, Volume 25, pp 159-171, 2011.
5. Dieter H. Lindner, Surface water drainage design considerations practices, Canadian Water Resources Journal, Volume 12, Number 3, pp 67-78, 2013.
6. Harshil. H. Gajjar, M. B. Dholakia, Storm water Network Design of Jodhpur Tekra area of city of Ahmedabad, IJEDR, volume 2, ISSN:2321-9939, 2014.



Challenges and Opportunities in Recycling of Construction and Demolition Waste: A Case of Jaipur in India

G K Attri¹, R C Gupta¹, Sandeep Shrivastava^{*1}

Department of Civil Engineering, Malaviya National Institute of Engineering, Jaipur, India¹, sshrivastava.ce@mnit.ac.in*

ABSTRACT

The effective management of the construction and demolition waste (C&DW) is a big challenge for the cities in India where rapid urbanisation, industrialization and economic development brings so much of waste. Supreme Court ordered ban on river sand and illegal mining of the stone. Recycled aggregates from the C&DW can be boon in the field of construction, which can replace a significant amount of natural aggregates as per the various research studies. In this study, collection of data takes place based on literature review, demolition sites visit and personal interviews of the demolition contractors. List Challenges and opportunities of recycling C&DW in Jaipur and present suggestions after analysis of the data.

KEYWORDS Construction, Demolition, Jaipur, Recycle, Waste

INTRODUCTION

Indian construction industry is the main contributor towards the economy and is supposed to grow, as there are opportunities in residential, commercial and other infrastructure sectors of the construction industry. This construction industry is going to surge from US\$428.1 billion in 2015 to US\$563.4 billion in 2020. According to the Statista Company, **Figure 1** shows the market value of the Indian construction Industry from 2012 to 2016, it observe 2.4 % average growth in the market value from 2012 to 2016. Infrastructure sector contribute 23% of the total value that is US\$140.1 billion and residential contribute 30.6% that is US\$172.4 in 2020.

The projected investment in the construction sector will grow in a drastic way due to various initiatives of the Indian government that is Make in India, AMRUT, 100 Smart Cities and Swachh Bharat Mission. The management of the construction and demolition waste (C&DW) is the most important for the planners and the civil engineers because of the increasing portion of demolition waste, limited land for dumping waste, transportation and disposal cost increment and the pollution and environmental degradation caused by Construction and demolition waste.

The construction activities are consuming natural resources in a very fast way which may lead to depletion of the conventional sources so we need to have strategy that is reduce/reuse and recycling of the C&DW. (Yuan and Associate, 2017) Recycling of the demolition waste takes place in Germany after the Second World War to manage the large amount of demolition waste generated due to the war, confront the problem of disposal, and use in reconstruction.

RECYCLING OF C&DW

There is a live proof of using C&DW as a raw material in construction in many countries like U.S.A., Netherland, Ireland, Estonia, Germany, Denmark and China etc. (Huang, Wang, Kua, Geng and Bleischwitz, 2018) as demonstrated by different scientific studies carried out by researchers in their respective countries. European Union has decided to increase the recycling capacity to 70% by 2020 (Ulubeyli, Kazaz and Arslan, 2017).

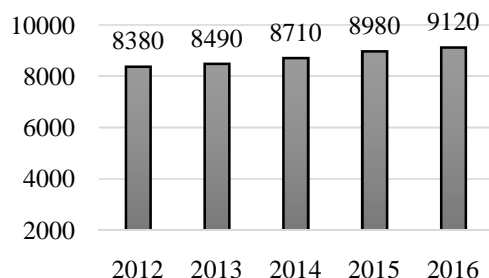


Figure 1 Market value from 2012 to 2016

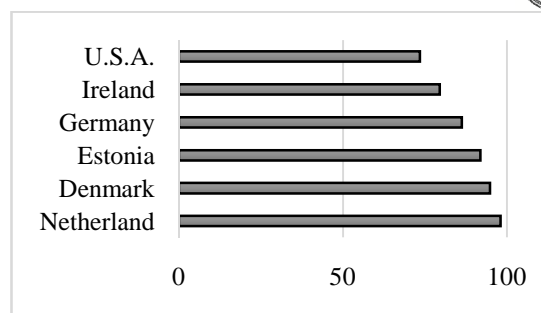


Figure 2 Recycling of C&DW in different countries

1) RECYCLING IN INDIA

In India, any legal formality take a long time to be formed and implemented so without waiting for some proposals of the government, Architects have taken some steps for utilising C&DW in innovative building materials. The example is a school, designed and built by an architect (Mr. Surya Kakani) in Rajkot. He used the debris from the earthquake-effected building from Bhuj in Rajkot (Gujarat), which is an excellent example of steps towards sustainability. Another example is Institute of Rural Research and Development (IRRDI), which recycled its own construction waste and used within its premises. There may be so many other examples, which motivates us towards sustainability development. These steps should be encouraged by the government, which ultimately enhance the collection and utilisation of C&DW.

The most famous initiative taken by Delhi government was Burari Plant, which recycle C&DW into recycled aggregates and pavement blocks etc. (Ponnada and Kameswari, 2015). The government agencies like Delhi Common Wealth Games (CWG) do not accept the products from this plant, as there is no standardisation of this product from any recognised institute. CDE celebrates the Prime Minister Flagship drive, that is, 'Clean India' by initiating process for setting another Recycling Plant in Delhi by the efforts of IL&FS.

The environment ministry rolls out the rules and regulations for construction & demolition waste management in 2016, according to which each state is instructed to make local rules for the management of the C&D. Many smart cities that is Ludhiana, Amritsar, Mumbai, Bangalore, Gurugram and Jaipur starts preparing (Detail Project Report) DPR for setting of recycling plant for processing C&DW. These efforts tell us that the government and different agencies have realised the importance of the processing of C&DW into recycled aggregates.

If India want to change the mentality of the people, then there is an urgent need for preparation of the standards and specifications for acceptance. We should learn from the World where these recycled aggregates are being used extensively due to its proven strength and ultimately saves lot of natural virgin material is to be extracted from the earth crust. The natural sand extraction is banned in different cities of India which slowdown the construction activities, so further delaying the policy regarding recycled aggregates will delay the development of the India.

GENERATION OF C&DW

The C&DW generates from the construction, renovation, repair and maintenance and demolition of the buildings, Roads, bridges and other infrastructure projects (Villoria et al., 2013). The C&DW represent the major proportion of the total municipal solid waste generated in any city of India, which is around 25-30% (TIFAC, 2001).

The Building Materials and Technology Promotion Council (BMTPC) and Centre for Fly-Ash Research and Management and Research (C-FARM) estimate generation of the C&DW in India which is around 165-175 million ton in 2016. Quantum of C&DW comprised of 5000 ton in Delhi, 3000 tonnes in Mumbai, Kolkata generates 2000 ton, 1500 ton is generated in Chennai and Hyderabad, Gurugram, Pune, Lucknow and Jaipur generates in the range of 500 to 1000 ton. **Figure 3** shows the generation of C&DW in major cities of India.

Centre for Science and Engineering calculates the generation of C&DW based on the built-up area, which is 4 times higher than the estimation of other agencies.

As per the literature study and reports there is no correct data available regarding the generation of C&DW (Huang, Wang, Kua, Geng and Bleischwitz, 2018). Jaipur city generates 200 tonnes of C&DW per day as per the data of (TIFAC, 2001) which is under-estimated as per the recent calculation based on type of work per square metre of built-up area. **Figure 4** shows average percentage of different constituents of construction and demolition waste per



square metre of built-up area of eight building projects in Pune and Mumbai area, which was conducted from 1990 to 1994.

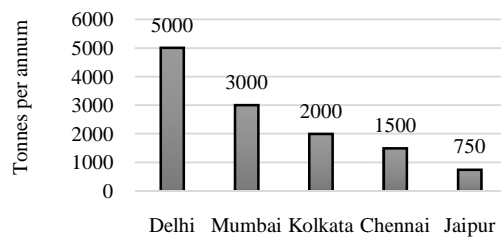


Figure 3 Generation of C&DW in India

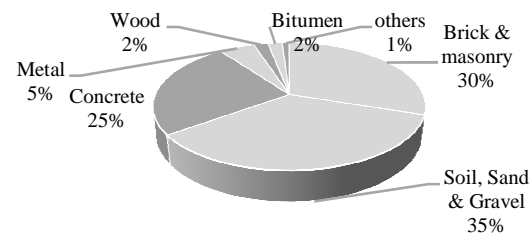


Figure 4 Constituents of C&DW in India

The C&DW is very much bulky and difficult to handle due to its shape and size and hard to dispose through incineration and composting (Medina, Alegre and Asensio, 2015). The growing population need a lot of land for their residential and commercial purposes for their livelihood and C&DW use large portion of the land for the disposal.

There characteristics of C&DW varies a lot according to the location and type of construction (Zheng et al., 2017). There are different kinds of waste generated from C&DW, that is, Sand and Gravel, Soil, Concrete, Mortar, Bricks, Stone, Wood, Metal, Bituminous material, Glass, Plastics, Tiles and other materials. The nature of the C&DW is inert and non-hazardous so there is no such necessary steps taken for its management, and if not managed and control in an effective way it may pollute environment as well as land. Therefore, the quantification of C&DW is very important so that we may prepared for the effective and efficient management of the same (Huang, Wang, Kua, Geng, Bleischwitz, et al., 2018). So recycling is the only way forward for the effective management of the C&DW, which ultimately have so many advantages, that is, saving lot of natural resources and stop environmental degradation.

Research Scope and Methodology

This scope of the study is to provide a better option for the natural aggregates as natural resources are very much limited in the earth crust and various government agencies are banning the extraction of natural aggregates. So for continue the developmental activities which are generally depend on the construction of the various infrastructure, we need to have some alternative of the natural aggregates and the recycled concrete aggregates are better option as demonstrated by various research studies carried out in various countries.

The research methodology consists of three steps that is visiting the demolition sites, interaction with demolition contractors through personal interviews and questionnaire, and finally collection and interpreting the data. Observation of the demolition process and characterization of the C&DW is done personally. Based on interpretation of the collected data, suggested some best practices that should be followed for the effective and efficient utilization of C&DW. **Figure 4** shows the graphical representation of the steps followed in the study.

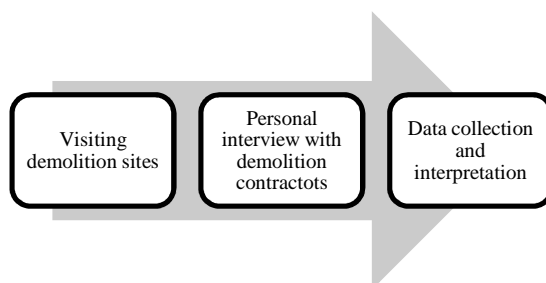


Figure 5 Methodology followed in the study

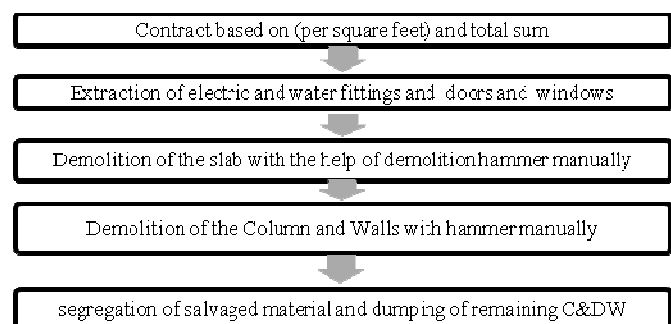


Figure 6 Process of demolition in Jaipur



RESULT AND DISCUSSION

Data is collected by visiting demolition site in person and interviewing the demolition contractors. During the sites visits, observe the process for demolition, present in Figure 6 that is Initially a contract is done between the owner and demolition contractor that is may be based on per square feet or may be based on No loss no gain. According to the per square feet basis, the owner has to pay a sum of money for per square feet of demolition that is INR 50/Square feet in Jaipur. Whereas according to No Loss No Gain, the owner does not have to pay any money to demolition contractor but the owner is not liable for the salvage material value. In this type of contract, the owner will get the clear site and does not care about the demolition, dumping and value of salvage material. There is no need to clean the stones waste that resulted significant saving in terms of cost on labour and material.

After visiting the demolition sites and observing the process of demolition in person, the characterization and composition of C&DW in Jaipur is found to be different from the composition of India as shown in **Figure 7**.

There is a lot of stone waste in the composition of C&DW in Jaipur, so there may be more chances of getting better quality of recycled aggregates.

After analysing the data collected through questionnaire and personal interviews, there is a scope of various opportunities and challenges in management and utilization of C&DW in Jaipur, some of these are listed under , that is,

- There are no municipal rules and regulations pertaining to utilization and management of C&DW as per the demolition contractors.
- Demolition contractors are not aware about the utilization of C&DW in concrete and other construction material.
- There is no accurate data available for the estimation of the generation of the C&DW.
- Illegal dumping is prevalent in Jaipur as per the observation that lead to the choking of the roads, rivers, canals and landfills.
- Environmental degradation due to illegal dumping of C&DW is the big concern.
- There is no separate landfill for the dumping of the C&DW in Jaipur.
- Demolition contractors don not know about the business in processing of C&DW.
- There is a lack of technological-know-how in processing the C&DW.
- There is lack of government Support and incentives for management of C&DW.
- Easy and cheap disposal of the C&DW.
- There is a lack of economic viability related to production of recycling of C&DW.
- There is no permission needed for the demolition of any kind of structure in Jaipur as per the demolition contractor.
- The quality and nature of C&DW depends on the age of the structure, availability of resources and the demolition process.
- Limited technical resources are available on the quality and quantity of the recycled aggregates use from C&DW as recently IS-383 recently allowed 30-40% replacement by recycled concrete aggregates.
- There are project related challenges that is economic and time constraints for the demolition contractors as they rely on the low cost option.
- The separation of the constituents from the debris is a time consuming and tedious job for the demolition contractors.

Only 5% demolition contractor knows about the recycling of the C&DW. All the demolition contractors dump the debris along the roads, nearby low-lying areas, vacant plots, along the canals and rivers. As per the observation, the demolition business seems to be very beneficial as there is market for the salvaged material.

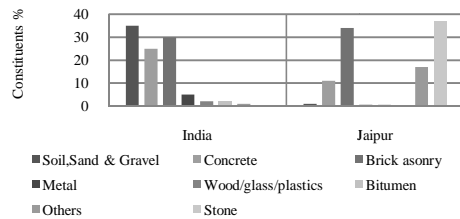


Figure 7 Comparison of composition of C&DW in India and Jaipur

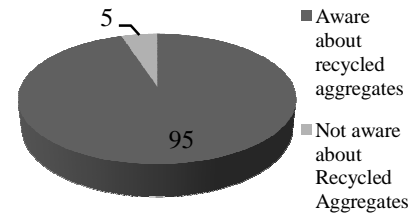


Figure 8 Awareness about recycled aggregates

CONCLUSION AND RECOMMENDATIONS

There are lot of challenges and opportunities in recycling of construction and demolition waste in Jaipur after analysis of the data collected through demolition site visit, personal interview and the surveys through questionnaire. Here are some of the challenges and opportunities, which are relevant in the field for better implementation of management plans.

- There is no local municipal rules and regulations pertaining to utilization and management of C&DW as per the demolition contractors.
- Demolition contractors are not aware about the utilization of C&DW in concrete and other construction material.
- There is no accurate data available for the estimation of the generation of the C&DW in Jaipur.
- Illegal dumping is prevalent in Jaipur as per the observation that lead to the choking of the roads, rivers, canals and landfills.
- Environmental degradation due to illegal dumping of C&DW is the big concern.
- There is no separate landfill for the dumping of the C&DW in Jaipur.
- Easy and cheap disposal of the C&DW.
- There is a lack of economic viability related to production of recycling of C&DW.
- There is no permission needed for the demolition of any kind of structure in Jaipur as per the demolition contractor.
- The quality and nature of C&DW depends on the age of the structure, availability of resources and the demolition process.
- The separation of the constituents from the debris is a time consuming & tedious job for the demolition contractors.

Based on the challenges and opportunities derived in this study, here are some recommendation for the management and utilization of the C&DW as a processed building material that is recycled aggregates.

- There is lack of supervision of the local municipal body, which lead to illegal dumping and inefficient management. Therefore, there should be separate cell for the management of C&DW.
- There should some strict or concrete laws for demolition of structure and disposal of C&DW.
- To encourage the utilization of the recycling of C&DW waste, recycling of the C&DW must be incentivised by the government agencies.
- The government agencies should carry out awareness drive for better implementation of recycling of C&DW through better advertisement by highlighting the quality for the acceptance.
- Segregation of the different constituents of the C&DW at source is the best way to get better quality of the recycled aggregates.
- The synchronization of different processes that is segregation, collection, reuse and recycling must initiate for better utilization and management of the C&DW.
- Maximise the use of processed C&DW in road construction as some countries are utilizing 90% of the C&DW by recycling it into recycled aggregates.



REFERENCE

1. TIFAC. Utilization of waste from Construction Industry, Technology, Information, Forecasting and Assessment Council, New Delhi India, 2001.
2. Centre for Science and Environment, Construction and demolition waste, New Delhi, 2014.
3. B. Darshan, K. Mangala, and R. K. Preethi, Study on use of recycled fine aggregates in masonry mortar. The International Reviewer, Volume 1, Number 2, pp 18-20, 2014
4. GIZ., Resource Efficiency in the Indian Construction Sector: Market Evaluation of the use of Secondary Raw Materials from Construction & Demolition Waste. New Delhi: Deutsche Gesellschaft fur Internationale Zusammenarbeit (GIZ) GmbH, 2015.
5. B. Huang, X. Wang, H. Kua, Y. Geng, and R. Bleischwitz, Resources, conservation and recycling construction and demolition waste management in China through the 3R principle, Resources, Conservation and Recycling. Elsevier, Volume 129 (October 2017), pp. 36–44. doi: 10.1016/j.resconrec.2017.09.029, 2018.
6. S. Lockrey, et al. Recycling the construction and demolition waste in Vietnam: opportunities and challenges in practice, Journal of Cleaner Production. doi: 10.1016/j.jclepro.2016.05.175, 2016.
7. C Medina, F J Alegre and E. Asensio. Assessment of Construction and Demolition Waste plant management in Spain : in pursuit of sustainability and eco-efficiency', Volume 90, pp. 16–24. doi: 10.1016/j.jclepro.2014.11.067, 2015.
8. M. R. Ponnada and P. Kameswari, Construction and Demolition Waste Management – A Review', Volume 84, 2015
9. S. Ulubeyli, A. Kazaz, and V. Arslan, Construction and Demolition Waste Recycling Plants Revisited : Management Construction and demolition waste recycling plants revisited : management issues, Procedia Engineering. The Author(s), Volume 172, pp. 1190–1197. doi: 10.1016/j.proeng.2017.02.139, February 2017.
10. P. Villoria, et al. 'Resources, conservation and recycling best practice measures assessment for construction and demolition waste management in building constructions, Resources, Conservation & Recycling'. Elsevier B.V., Volume 75, pp. 52-62. doi: 10.1016/j.resconrec.2013.03.009, 2013.
11. H. Yuan and P. D. Associate, Barriers and countermeasures for managing construction and demolition waste : A case of Shenzhen in China', Journal of Cleaner Production. Elsevier Ltd, 157, pp. 84–93. doi: 10.1016/j.jclepro.2017.04.137, 2017.
12. L. Zheng, et al. Characterizing the generation and flows of construction and demolition waste in China', Construction and Building Materials. Elsevier Ltd, 136, pp. 405-413. doi: 10.1016/j.conbuildmat.2017.01.055, 2017.



Flood Response to Catchment Characteristics in West Flowing Rivers of Kerala

T K Drissia^{*1}, V Jothiprakash¹, A B Anitha²

Indian Institute of Technology, Bombay, Powai, Maharashtra¹, drissia13@gmail.com^{*}

Centre for Water Resources Development and Management, Kozhikode, Kerala²

ABSTRACT

Many factors including morphology of drainage basins influence the hydrological processes and propagation of floods. A study was conducted to understand the morphometry of the catchment area of 43 gauging stations in Kerala, the southern State in India. The objective of the study is to group the similar catchment characteristics and to find the flood response of each parameter in the group. Another objective is to find the flood response of 4th, 5th, 6th and 7th order streams. This study used radar plots using sorted normalised values for grouping of the catchment characteristics and eventually three groups formed in 7th order watersheds and 2 groups in 5th order watersheds. The order of catchments in each parameter are different in the above radar plot. Another grouping of catchment characteristics by radar plots used same order of catchments, ultimately formed eleven groups. The area of the catchment, perimeter in group 1, total length of streams and total number of streams forms group 2. Main channel length and maximum basin length forms group 3. The fourth group includes stream frequency, length of overland flow, constant of channel maintenance and drainage density. Form factor and elongation ratio forms group 5 and Circulatory ratio and shape factor forms group 6. The other parameters were not clubbed with any other characteristics. The behaviour of the average peak discharge of 43 stations with above parameters are analysed using regression analysis. The regression coefficient of each parameter in a group was similar in the second grouping. The parameters that are highly correlated with the peak discharge are catchment area (A), perimeter (Pe), length of the basin (Lb), main channel length (Lc), shape factor (Sf), circulatory ratio (Cr), Stream order, total length of streams (Lu) and total number of streams (Nu). This study helps in understanding the hydrologic processes in the river basins.

KEYWORDS Morphometric analysis; Peak discharge; Catchment characteristics; Classification

INTRODUCTION

The discharge of a river is affected by the hydrological characteristics of the catchment. This can be described in terms of area, shape, relief, linear measurements and drainage pattern [1]. To define the catchment characteristics, many researchers defined morphometric parameters. Morphometric analysis refers to the quantitative evaluation of characteristics of the earth surface [2]. Horton started the formulation of morphometric parameters in 1945. Many other researches modified and added parameters [3,4]. Thereafter in many studies these parameters were applied to evaluate the characteristics of the catchment and its response to the discharge [5,6]. Geospatial techniques had been used for morphometric analysis in recent years [7]. In seventeen sub-watershed of Zidder watershed, in western Himalaya, morphometric analysis was carried to understand the hydrological behaviour [8].

Some of the catchment characteristics are described in this session. The stream length ratio has important relationship with surface flow, discharge and erosion stage of the stream [9]. Bifurcation ratio is considered to be an important parameter that articulates the degree of ramification of the drainage network. The relatively high bifurcation ratio indicates early hydrograph peak with a potential for flash flooding during the storm events in the areas in which these stream orders dominate. The closeness in bifurcation values of watersheds with in a basin indicates similarities in the geological features [10].

Stream frequency (Fs) is a vital morphometric indicator and provides additional information concerning the response of drainage basin to runoff process [11]. The circulatory ratio mainly concerned with the length and frequency of streams, geological structures, land use/land cover, climate, relief and slope of the basin [8]. Higher the circulatory ratio, higher is the flood hazard at a peak time at the outlet point. Form factor indicates the flow intensity of a basin of a defined watershed [9]. The value of R_f would always be less than 0.7854 (for a perfectly circular



basin).

Shape factor refers to a value that is affected by an object's shape but is independent of its dimensions. Shape factors are calculated from measured dimensions such as diameter, chord length, area, perimeter, centroid, moments, etc. The dimensions of the particles are usually measured from two-dimensional cross sections or projections, as in microscope field, but shape factors also apply three-dimensional objects. Shape factors are often normalized, that is, the value ranges from zero to one. A shape factor equal to one usually represents an ideal case or maximum symmetry, such as a circle, sphere, square or cube.

Length of overland flow (Lo) is one of the most vital self-governing variables affecting hydrologic and physiographic development of drainage basin [9,12]. It is inversely proportional to half of reciprocal of drainage density and is the length of water over the ground before it gets concentrated into definite stream channels [9].

In this study, an attempt was made to group the catchment characteristics in west flowing rivers in Kerala. The objective of the study is to compare catchment characteristics of 4th, 5th, 6th and 7th order rivers in Kerala. The relation between peak discharge and catchment characteristics were also analysed. This study gave an idea of the effect of parameters on discharge.

STUDY AREA AND DATA USED

Kerala is the southern state of India with Arabian Sea at the east and Western Ghats in West. The location of the State is between 8°15'N and 12° 50'N latitudes and between 74° 50'E and 77° 30'E longitudes. The rivers in this State are small and medium rivers with short length and steep slope. All rivers start from Western Ghats, but 41 Rivers reaches Arabian Sea and three rivers reaches Bay of Bengal.

The discharge data of 43 stream gauge were collected from Central Water Commission, Government of India and Water Resources Department, Government of Kerala. The annual maximum discharge data were extracted. Spatial data like boundary and drainage map of 43 watersheds were digitized from survey of India topographic maps (1: 50000) in ArcGIS.

METHODS

The topographic characteristics of the catchment area of gauging stations include area of the catchment (A), perimeter (Pe), maximum basin length (Lb), main channel length (Lc), slope (S), stream order (U), total number of streams (N), total length of streams (L), that has been worked out by direct measurements. Other parameters like bifurcation ratio (Rb), stream length ratio (Rsl), drainage density (Dd), stream frequency (SF), length of overland flow (Lo), constant of channel maintenance (Cc), circulatory ratio (Cr), shape factor (Fs), form factor (Ff), elongation ratio (Er) were estimated from the parameters directly measured. Apart from these distance from the river gauging station from the river mouth (Drg) and elevation (E) were also considered. Streams were assigned order as per the guidelines given by Strahler[3].

$$\text{Bifurcation ratio (R}_b\text{)} \quad R_b = N_u / N_{u+1} \quad (1)$$

$$\text{Mean stream length} \quad L_{sm} = \frac{L_u}{N_u} \quad (2)$$

$$\text{Stream length ratio (Rsl)} \quad R_L = L_{sm} / L_{sm-1} \quad (3)$$

Where N_u is the number of streams and L_u is the total stream length of given order u.

$$\text{Drainage density (D}_d\text{)} \quad D_d = L/A \quad (4)$$

$$\text{Stream frequency (F}_s\text{)} \quad F_s = N/A \quad (5)$$

$$\text{Circularity ratio (R}_c\text{)} \quad R_c = 4\pi A/P^2 \quad (6)$$

$$\text{Elongation ratio (R}_e\text{)} \quad R_e = (2\sqrt{(A/\pi)}) / L_b \quad (7)$$

$$\text{Form factor} \quad A/(L)^2 \quad (8)$$

$$\text{Shape factor} \quad P/(4 \times 3.14 \times A)^{1/2} \quad (9)$$

$$\text{Constant of channel maintenance} \quad Cc = \frac{1}{D_d} \quad (10)$$

RESULTS AND DISCUSSION

The catchment characteristics described in the above session are estimated. The catchment area of the 45 stream gauges are divided into 5 groups according to the stream order as 4th order, 5th order, 6th order, 7th order and 8th order watersheds. The similar catchment characteristics were grouped using radar plots. For each group regression



coefficient were estimated with peak discharge. Only one watershed belong to 8th order stream and 2 watersheds belong to 4th order stream and hence are not included in the analysis. An attempt was made to group the catchment characteristics for each order. The catchment characteristics are normalised dividing by maximum value of each group.

The radar plot from sorted normalised values of 7th order, 6th order and 5th order watersheds are given in **Figures 1, 2 and 3**. In 7th order streams, the radar plot showed three distinct groups as marked in dark line though at higher value all line merged. The inner circle forms a group consisting of area, elevation and relief ratio. The outer cluster forms drainage density, elongation ratio, bifurcation ratio, and Lb/Lc and shape factor. The 6th order watersheds were not exhibited any grouping in the radar plot (**Figure 2**). the fifth order watersheds formed two distinct groups. The outer group formed include Lb/ Lc, elongation ratio, circulatory ratio, constant of channel maintenance, drainage density, stream frequency and bifurcation ratio. The rest of the catchment characteristics forms the other group. In the above radar plots the order of watersheds are not same for all the catchment characteristics. This represents only how the catchment characteristics are varying with each other irrespective of the watersheds in a group.

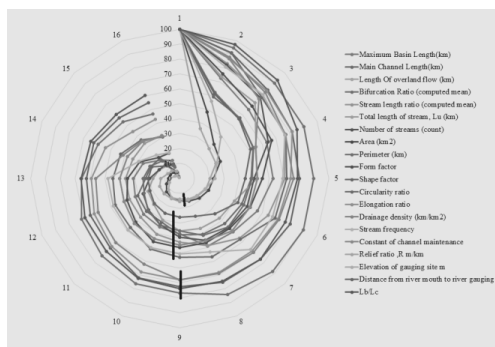


Figure 1 Radar plot of catchment characteristics for 7th order stream

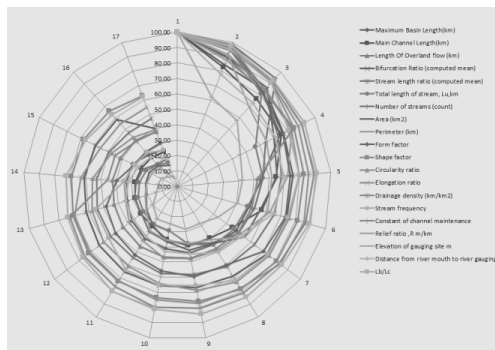


Figure 2 Radar plot of catchment characteristics for 6th order stream

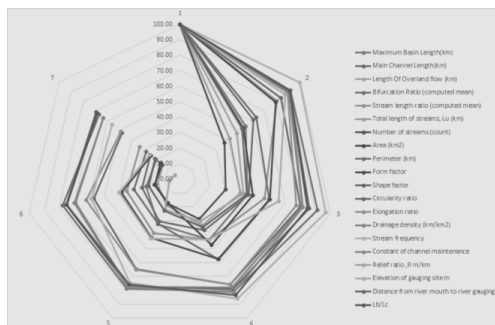


Figure 3 Radar plot of catchment characteristics for 5th order stream

Another grouping of catchment characteristics were carried out with the same order of characteristics. Eventually 11 groups were formed for 6th an 7th order watersheds. The radar plot of 6 groups of 7th order watersheds are shown



in **Figure 4**. Area and perimeter formed group 1, number of streams and total length of streams formed group 2, maximum basin length and main channel length formed group 3, stream frequency, constant of channel maintenance, length of overland flow and drainage density formed group 4, elongation ratio and formfactor formed group 5, circulatory ratio and shape factor formed group 6. The other parameters are single and hence not shown in the figure. In fifth order watersheds group 1, 2 and 3 are merged to one group and subsequently a total of 9 groups are formed.

The regression coefficient was estimated by plotting the catchment characteristics with peak discharge. The first three groups were found have good correlation with peak discharge in 6th and 7th order watersheds which is same as group 1 in 5th order watersheds. The parameters in these groups are directly measured from the maps. Group 6 also exhibit good correlation in all order watersheds. Shape factor and circulatory ratio are derived from area and perimeter.

Interestingly, in few parameters r value was increasing as the order of watershed reduces. This include area, total length of streams, number of streams, maximum basin length, form factor, elongation ratio, shape factor and circulatory ratio. All the parameters that fall in group 2, 5 and 6 shows this property. In group 1 and 3 each parameter is showing reverse nature. Area shows increasing R -value as order decreases whereas perimeter shows decreasing R -value. The characteristics in group 4 shows high correlation in 7th order watersheds but as the order reduces to 6th and 5th the correlation became weak.

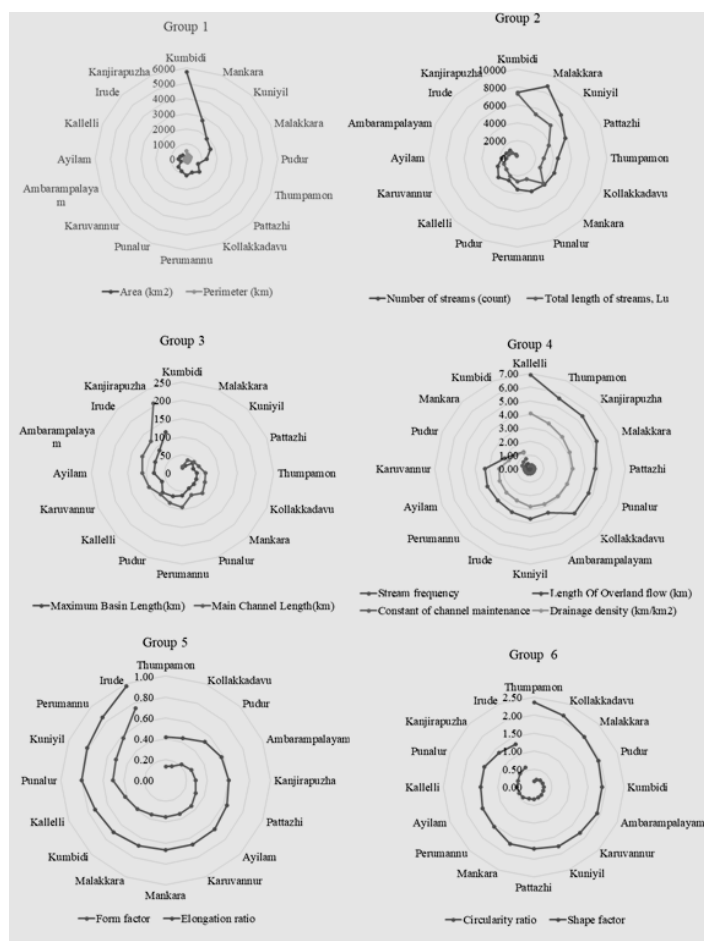


Figure 4 Radar plots of 7th order watersheds

Table 1 The groups of catchment characteristics and their r value



Catchment characteristics	Groups	7th r	6th r	Groups	5th
Area, km ²	Group 1	0.642	0.681	Group 1	0.724
Perimeter, km		0.935	0.682		0.707
length Lu	Group 2	0.550	0.539		0.660
Number of streams, count		0.481	0.510		0.644
Maximum basin length, km	Group 3	0.353	0.608		0.673
Main channel length, km		0.958	0.661		0.566
Stream frequency	Group 4	0.606	0.236	Group 2	0.035
Length of overland flow, km		0.677	0.259		0.043
Constant of channel maintenance		0.801	0.259		0.043
Drainage density, km/km ²		0.650	0.574		0.026
Form factor	Group 5	0.010	0.235	Group 3	0.278
Elongation ratio		0.049	0.257		0.316
Shape factor	Group 6	0.265	0.494	Group 4	0.580
Circularity ratio		0.353	0.423		0.533
Bifurcation ratio (computed mean)	Group 7	0.383	0.327	Group 5	0.109
Stream length ratio (computed mean)	Group 8	0.612	0.556	Group 6	0.430
Relief ratio, R m/km	Group 9	0.362	0.574	Group 7	0.135
Elevation of gauging site m	Group 10	0.246	0.071	Group 8	0.014
Distance from river mouth to river gauging	Group 11	0.312	0.020	Group 9	0.260

CONCLUSION

The catchment characteristics of 43 gauging stations were grouped using radar plot. The radar plot of normalised sorted characteristics showed varied grouping for each order. In 7th order 3 groups were formed, but in 6th order there is no district group that can be found from radar plot. Another grouping were formed based on the same order of watersheds when sorted. A, Pe, L, N, Lb Lc falls in first three groups and have good correlation with peak discharge in all stream order watersheds.

REFERENCE

1. V.M. Ponce, Engineering Hydrology Principles and Practices, Prentice Hall, New Jersey, 1989.
2. V. Gardiner and C. C. Park, Drainage basin morphometry, Prog. Phys. Geogr., Volume. 2, Number 1, pp. 1–35, 1978.
3. A.N Strahler, Quantitative geomorphology of drainage basins and channel networks section 4-2, Handbook of Applied Hydrology. Ed. Vent e Chow, McGraw-Hill, New York. Volume 4, Number 35, 1964.
4. A. A. Schumm, Evolution of drainage systems and slopes in Badlands at Perth Amboy, New Jersey, Bull. Geological Society of America, Volume 67, Number 50, pp. pp 597-646, 1956.
5. O. Christopher, A.O. Idowu, and A.S. Olugbenga, Hydrological analysis of onitsha north east drainage basin using geoinformatic techniques, World Applied Sciences Journal, Volume 11, Number 10, pp 1297-1302, 2010.
6. Q. A. Rasool, V. K. Singh, and U. C. Singh, The evaluation of morphometric characteristics of upper subarnarekha watershed drainage basin using geoinformatics as a tool , Ranchi , Jharkhand, Int. J. Environ. Sci., Volume 1, Number 7, pp. 1924–1930, 2011.
7. J. M. Nongkynrih and Z. Husain, Morphometric analysis of the Manas river basin using earth observation data and Geographical Information System, Int. J. Geomatics Geosci., Volume 2, Number 2, pp. 647–654, 2011.
8. F Altaf, G Meraj, and S. A. Romshoo, Morphometric Analysis to Infer Hydrological Behaviour of Lidder Watershed, Western Himalaya, India, Geogr. J., Volume 2013, pp. 1–14, 2013.
9. R. E. Horton, Erosional Development of streams and their drainage basins; hydrophysical approach to quantitative morphology, Geol. Soc. Am. Bull., Volume 56, Number 1, pp. 275–370, 1945.
10. [10]S. Shankar, Drainage morphometry of flood prone rangat watershed , Middle Andaman , India- A Geospatial Approach, Number 11, pp. 15–22, 2014.
11. W. B. Langbein and E. Al., Topographic characteristics of drainage basins, Geol. Surv. Water-Supply Pap. 968-C, Volume 968-C, pp. 125-155, 1947.
12. A. Javed, M.Y. Khanday and S. Rais, Watershed prioritization using morphometric and land use/land cover parameters: a remote sensing and GIS based approach, Journal Geological Society of India. Volume 78, pp 63-75, 2011.



Revisiting Indian Road Congress Code Guidelines for Conduction of Road Safety Audit at Detailed Design Stage

Shawon Aziz^{*1}, Pradeep Kumar Sarkar²

Intercontinental Consultants and Technocrats Pvt. Ltd., New Delhi, India¹, shawonaziz786@yahoo.in*

Asian Institute of Transportation Development, New Delhi²

ABSTRACT

The study is focussed on application of Indian Road Congress (IRC) code guidelines for conduction of road safety audit at design stage. The problem of road crashes is dynamic and complex in nature and requires a collaborative effort of engineering, management, enforcement, education and information technology measures. In the process of preparation of a detailed project report, several deficiencies with respect to safety of road users ought to occur in an engineering design. The entire detailed design needs to be scrutinized to identify the design deficiencies with respect to safety and suggest corresponding engineering solutions which can rectify the design faults. Unless the design deficiencies are rectified before the beginning of construction, the final structure and its alignment may have deficiencies with respect to safety, which may lead to road crashes and subsequently create accident black spots along the road stretch. The study highlights typical examples of deficiencies in engineering design which come across a Road safety engineer while audit of various design drawings. The study suggests appropriate engineering solutions applicable to all safety related issues as per the IRC code provisions so that any ambiguity in the road environment gets removed and positive guidance is provided to all road users.

KEYWORDS Safety, Audit, Design, Signs, Marking

INTRODUCTION

Road crashes are a major but neglected public health issue worldwide. People deal with it on a day-to-day basis. As per World Health Organization, road traffic crashes is the 8th leading cause of death and it is the main cause of death among those aged 15 to 29 years [1]. Road Injury Mortality rate in India is 18.9 per one lakh population which is higher than the Global average of 18 deaths per one lakh population [2]. As per Ministry of Road Transport and Highways (MoRTH), in India, the total no. of accidents that occurred in 2015 was 5,01,423. The accident statistics saw a dip by 4% in the year 2016 as the total number of accidents was confined to 4,80,652 [3]. The reason for concern from the MoRTH Statistics is that number of fatalities in road accidents increased by 3.2% from 1,46,133 in 2015 to 1,50,785 in 2016. The problem is dynamic and complex in nature and requires a collaborative effort of engineering, management, enforcement, and education and information technology measures. This paper deals with application of engineering measures as per code provisions of Indian Road Congress (IRC) for rectification of disorders and faults in the engineering design. The study checks for consistency of general standards and guidelines for road attributes such as road signs, pavement markings and other traffic calming measures.

LITERATURE REVIEW

Road Safety Audit (RSA) is a formal procedure for assessing accident potential and safety performance in the provision of new road schemes and schemes for the improvement and maintenance of existing roads. Road Safety Audit is based on the principle of an independent review. Road safety audit process reveals that three parties will be involved in this process - Client, Designer and Auditor. To be effective, the safety audit needs to be carried out by specialists, who are independent of the design process. In this way auditors will be taking a fresh look at the project without the distraction of having been involved in their design. Road safety audit involves one set of professionals checking the work of other professionals. [4]

Audits identify deficiencies and could be viewed as threat to road designers. It is critical that the focus be on the process and audit report not be viewed as criticism of the project design. A designer may have legitimate reasons for making decisions that consider factors other than safety in the proposed design and the compromise could be identified in the audit. Factors influencing a decision would be identified in a response to the safety audit. Since a structured safety audit can usefully identify potential problems and make recommendations for alleviating them, a safety audit, as such, should be regarded as an aid to design of safer roads. [5]

DETAILED DESIGN STAGE AUDIT



Road Safety Audit is carried out at following stages, namely, Feasibility Study Stage; Preliminary Design Stage; Detailed Design Stage; Pre-Opening Stage; Safety Assessment (existing road).

The present study discusses stage 3 audit after completion of detailed design. Stage 3 is recommended on completion of detailed design and before preparation of contract documents, to assess detailed junction layout, markings, signs, signals, lighting details, etc. Tender documents must not be issued to bidders until auditing at this stage has been completed and all agreed changes have been incorporated in the project documents [6]. The cost of road safety audit and the consequent cost of changing a design are significantly less than the cost of remedial treatments after works are constructed. It is easier to change the lines/alignment or so on a plan than to move concrete structures. With less remedial work included in a highway authority's works Programme, budgets can be kept down or the same money can be utilized more effectively. The vital road attributes that have been assessed in the present study are as follows : Horizontal Alignment, Vertical Alignment, Cross Section, Junctions, and Road Side Facilities. For each of these issues, the safety concerns have been narrated along with suitable recommendations.

HORIZONTAL ALIGNMENT

Reason for Concern :When sharp curves are introduced in the road alignment, speed reduction and delineation measures are required to reduce the speed of vehicles, so that they can negotiate the curve safely and avoid runoff accidents. An example of sharp curve has been shown in **Figure 1**, if the design drawing with sharp curve is deficient in terms of safety, a road safety auditor shall propose appropriate traffic calming measures as per IRC code provisions.

Recommendations :As per Section 9.2.7 of IRC:SP:73-2015 (for 2 lane road with paved shoulder) and Section 9.2.7 of IRC:SP:84-2014 (for 4 lane road), wherever the Project Highway alignment is on a curve, there shall be advance cautionary signs for sharp curves (depending on whether it is on left or right) and chevron signs (rectangular in shape with yellow background and black arrow) at the outer edge of the curve. Following guidance shall be adopted while installing curve signs [7] :

- W-beam crash barrier should be provided along all curves having radius up to 450m for complete length of the curves including transitions and 20m further before and after the curve;
- The curves with radii upto 450 m shall be provided with curves warning sign in advance of hazard and single Chevrons on outer edge of curve. Spacing of Chevron signs on the curve and before the curve shall be as per Table 15.3 of IRC: 67-2012;
- The curves with radii 451 m to 750 m shall be installed with single Chevrons on outer edge of curve at 75 m spacing;
- The curves with radii 751 m to 1200 m with deflection angle greater than 20 degree shall be provided with single Chevron signs. Spacing of Chevron signs on the curve and before the curve shall be as per Table 15.3 of IRC: 67-2012;
- For curves with radii 751 m to 1200 m with deflection angle less than 20 degree and also curves with radii from 1201 to 2000 m shall be provided with forgiving type delineator posts at 40 m spacing on outer edge of curves;
- Due to any reason if there is any curve with radius less than 450 m, the safe negotiating speed for the particular curve shall be placed along with curve warning sign at both approaches, that is, install Figure 15.01/15.02 of IRC:67-2012 for the curve sign along with speed limit sign Figure 14.37 in yellow backing plate at distance of 180-245m before start of affected length on both approaches .The permissible speed limit for a particular can be determined from Curve formula;
- Generally if the difference between the approach speed and permissible negotiating speed of any curve is more than 15 km/h, the curve warning and speed limit sign shall be placed on shoulder side and median side also.

The road signs shall be as per IRC:67-2012. The following provisions from the code are recommended:-

- Install Speed Limit Sign (Figure 14.37 of IRC:67-2012 for and Curve Warning Sign (Figure. 15.01 / 15.02 as applicable) mounted on a single post before the start of curve;
- Depending upon the sharpness of the curve, Single Chevron (Figure 15.72), Double Chevron sign (Figure 15.74) and Triple Chevron Sign Figure. 15.75) can be installed. If the Single Chevron signs are to be used for roads operating at or more than 100kmph, relatively bigger size single chevron (Figure 15.73) shall be used. [8] The Curve Delineation 4 lane roads shall be as per Figure V.7 of IRC:67-2012 as shown in **Figure 2**.

The road markings shall be as per IRC:35-2015. The following provisions from the code are recommended:-



- Provide Transverse Bar Marking (TM08) before the start and end of Transition curve. The number of TM08 Strips, its spacing and dimensions shall be as per Table A.2, Annexure: A of IRC:35-2015;
- The curve section along with its transition length must be treated as a No overtaking section and Pavement marking must be provided as per Table 4.3 (for Undivided Carriageways) and Table 4.4 (for Divided Roads) of IRC:35-2015;
- When the curve is on a undivided road, as per section 4.3.6 of IRC 35-2015, on horizontal curves where carriageway has been widened and radius of curve is below 60m, the placement of centerline shall be as per Table 4.3 and as presented in Figure 4.2 of IRC 35-2015. On such acute curves if the paved portion is more than extra widening required, the overtaking line can be splayed to form an central island and hatched as shown in Figure 4.3 of IRC-35-2015.

Other Recommendations with respect to safety and delineation are as follows:-

- Provide Road studs as per Table 9.1 Warrants for Road Studs of IRC:SP:73-2015 (for 2 lane road with paved shoulder) and IRC:SP:84-2014 (for 4 Lane road) as applicable;
- For both two lane and four lane roads, on horizontal curves with radius up to 300 m, width of pavement and roadway in each carriageway shall be increased as per Table 2.5 of IRC:SP:84-2014.



Figure 1 Example of a sharp curve in design drawing

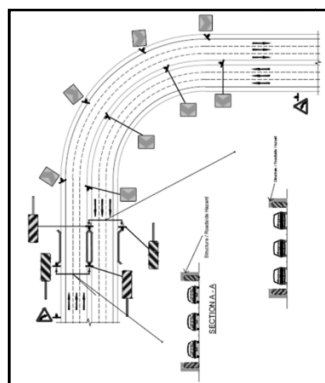


Figure 2 Curve delineation for divided carriageway as per Figure 5.7 of IRC:67-2012

VERTICAL ALIGNMENT

Broken Back Curves in Vertical Alignment

Reasons for Concern : As per Section 2.9.1 of IRC:SP:73-2015, curves in same direction separated by short Tangents, known as Broken Back curves should be avoided as far as possible. [9] At many locations, broken back curves have been introduced for vertical profile. It can be appreciated that such broken back curves have been given to reduce the (bill of quantity) of profile corrective course, as it is invariably attempted by the normal designer to follow the existing horizontal and vertical profile to the maximum extent possible. Since the Project road shall carry considerable multi-axle trucks with heavily loaded commodities, a slight jerk due to inconsistent vertical geometry may affect the center of gravity (with undue momentum in a direction across the highway) and can cause toppling accidents of heavily loaded trucks. An example of Broken Back curve in engineering design been shown Figure 3.

Recommendations: Avoid such broken back curves and provide single curve for each such case requiring some re-grading for vertical profile (by cutting or filling) or even by extra profile correction course thickness. As per Section 7.1 of IRC:SP:023 Vertical Curves for Highways, Grade changes shall not be too frequent as to cause kinks and visual discontinuities in the profile. Desirably there should be no change in grade within a distance of 150 m [10]. Thus it is advisable to revise the entire vertical profile of the project highway to comply with the IRC requirement to make minimum distance of 150 m for change of vertical grade as mandatory requirement.

Frequent Change of Vertical Grade

Reasons for Concern : The vertical grade has been changed at short distance as shown in **Figure 4**. Once again for the same reason of minimizing the profile correction of the existing vertical alignment. There are chances of toppling accidents when trucks are passing through highways where vertical grade is changed so frequently.

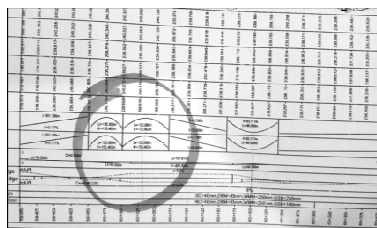


Figure 1 is a cross-sectional diagram of a road pavement structure. The diagram shows a 10m wide road with a 2.5m wide shoulder on each side. The pavement layers from top to bottom are: 1. Asphalt Concrete (AC) 100mm thick, 2. AC 80mm thick, 3. AC 60mm thick, 4. AC 40mm thick, 5. AC 20mm thick, 6. AC 10mm thick, 7. AC 5mm thick, 8. AC 2.5mm thick, 9. AC 1.25mm thick, 10. AC 0.625mm thick. The subgrade is 100mm thick. The diagram also shows the road surface profile, including a 10m wide road, a 2.5m wide shoulder, and a 10m wide road. The diagram is labeled with various dimensions and materials.

Diagram illustrating the cross-section of a road shoulder construction. The diagram shows the existing road surface (Scarifying existing Black top surface) and the proposed shoulder construction (Selected Earth). The shoulder width is 3.0 m. The existing road surface has a 2.5% slope. The proposed shoulder surface has a 3.0% slope. The area between the existing surface and the proposed shoulder is labeled 'Earth Work'.

Diagram illustrating the required distance between a W-beam crash barrier and the edge of the pavement. The diagram shows a cross-section of the road with the following dimensions and labels:

- 1000**: Distance from the crash barrier to the edge of the earth shoulder.
- EARTHEN SHOULDER**: The area between the crash barrier and the paved shoulder.
- 1500**: Distance from the edge of the earth shoulder to the edge of the paved shoulder.
- PAVED SHOULDER**: The paved area adjacent to the main road.
- W-BEAM CRASH BARRIER**: The safety barrier.
- SELECTED EARTH**: The material used for the shoulder.
- 3.5%**: Slope of the earth shoulder.
- 2.5%**: Slope of the paved shoulder.
- This distance should be minimum 600mm**: The required distance between the crash barrier and the edge of the pavement.

THERE MUST BE AT LEAST 1000 CLEARANCE BETWEEN THE BACK OF THE W-BEAM POST AND ANY SOLID OBJECT

600mm Minimum

750mm to 1000mm Minimum

OUTER EDGE OF BITUMINOUS SURFACE

W-BEAM ON SHOULDER / EMBANKMENT SIDE

33rd Indian Engineering Congress, Udaipur, 2018: Technical Volume



JUNCTIONS

T Junction

Reason for Concern : **Figure 9** shows an example of T Junction where there is no right turn protected arrangement for the right turning traffic from the project road to minor road as shown in the junction layout. The turning traffic needs a safe shelter before turning or else it may lead to rear end collision.

Recommendations : The proposed drawing for the T Junction with Shelter lane has been shown in **Figure 10**. The following recommendations are applicable to make movements safer on this 3 arm priority T Junction:-

- As per Figure 3.2 of IRC:SP:84-2014, 55.0 meters is the minimum storage length to be provided based on deceleration length. The storage length may be increased In order to cater peak hour turning traffic volume of 10th year [12];
- All Road Signs shall be as per Figure V.1 in Annexure V of IRC: 67-2012as shown in **Figure 11**;
- All Pavement markings shall be as per Figure 9.8 of IRC:35-2015 as shown in **Figure 12**;
- Provide Road studs as per Table 9.1 Warrants for Road Studs of IRC:SP:73-2015 (for 2 lane road with paved shoulder) and IRC:SP:84-2014 (for 4 Lane road) as applicable.

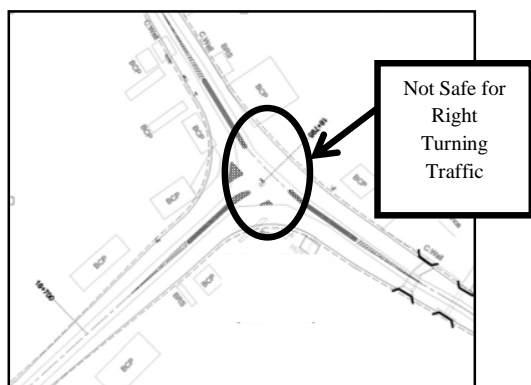


Figure 9 Example of a T Junction from Engineering design drawing

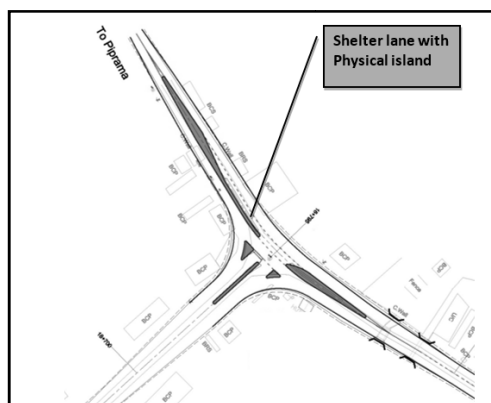


Figure 10 Improved junction proposal with shelter lane

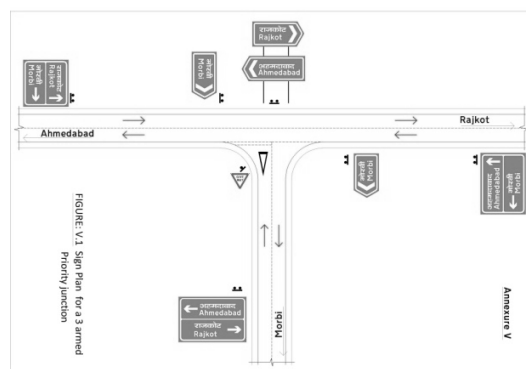


Figure 11 Signage plan for 3 arm priority junction as per Figure V.1 of IRC:67-2012



Figure 12 Pavement marking for 3 arm priority junction as per Figure 9.8 of IRC:35-2015

Skew Y Junction

Reason for Concern : As shown in **Figure 13**, a Skew Y Junction with angle of intersection less than 70° would create lot of confusion resulting in unsafe operations and accidents. It may lead to Head on Collisions which may turn out to be fatal.



Recommendation : As per Figure 3.2 of IRC:SP:84-2014, the angle of intersection between Project Highway and side road shall ideally be 90° and shall never be less than 70° . Thus a right turn protected junction with perpendicular angle of intersection as shown in the **Figure 14** shall be proposed. The layout is provided with triangular islands to enhance safety of turning traffic at the junction. All Road Signs shall be as per Figure V.1 in Annexure V of IRC: 67-2012 as shown in **Figure 11**. All Pavement markings shall be as per Figure 9.8 of IRC:35-2015 as shown in **Figure 12**. Road studs shall be provided as per Table 9.1 Warrants for Road Studs of IRC:SP:73-2015 (for 2 lane road with paved shoulder) and IRC:SP:84-2014 (for 4 Lane road) as applicable.

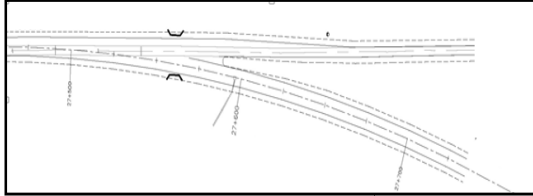


Figure 13 Example of Skew Y Junction from engineering design drawing

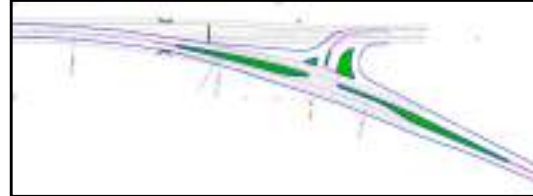


Figure 14 Improved junction with channelizing island and intersection angle of 90°

Major Four Legged Cross Junction

Reason for Concern : **Figure 15** shows a four armed cross road junction. If such a junction is without control by traffic signals, it generally turns highly unsafe in operation; and accident potential is high with higher level of risk and severity. Any collision which may occur shall be a right angle collision with high speed. There would be 32 conflict points for the cross road junction. Since all the approach roads are equally important, having considerable straight ahead and right turning movements, any conflict would be dangerous with high impact energy.

Recommendation : As shown in **Figure 16**, it will be better to provide a roundabout, which will have inherent property of round-the-clock traffic control by its design. A roundabout can be accommodated in the same land area as shown in the design provided in the four legged junction. The triangular islands shall be physical/raised islands with diagonal marking at the approach ends. Signages and markings shall be provided as recommended in IRC:67-2012. Any collision in roundabout is angular and that too at low operating speed, as speed of traffic will get reduced on approaching the roundabout. Speed of traffic in circulatory carriageway is very low; implying an accident in roundabout cannot be fatal. When a cross road is converted into a roundabout, the number of conflict points can be reduced from 32 to 8. [13] Since all approach roads are equally important, having considerable straight ahead and right turning movements, this traffic pattern perfectly match for a roundabout. The road signs on a roundabout shall be as per Figure V.3 of IRC:67-2012 as shown in **Figure 17**. The Pavement markings on the roundabout shall be as per Figure 9.15 of IRC:35-2015 as shown in **Figure 18**.



Figure 15 Example of 4 legged cross junction from engineering design drawing

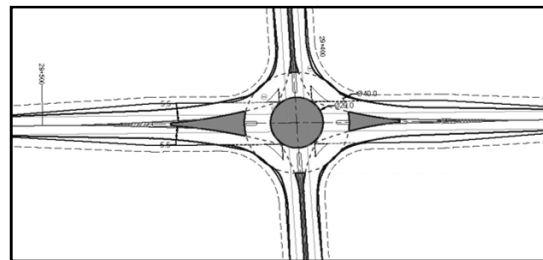


Figure 16 Recommendation of roundabout

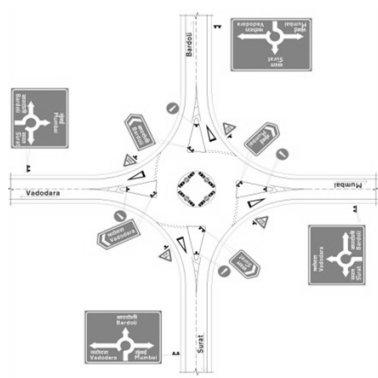


Figure 17 Road Signage Plan for Roundabout as per Figure V.3 of IRC:67-2012

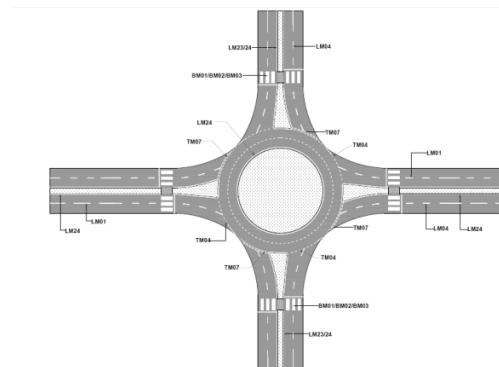


Figure 18 Pavement Marking for Roundabout as per Figure 9.15 of IRC:35-2015

ROADSIDE FACILITIES

Bus Bay

Reason for Concern : **Figure 19** shows an example of Bus Bay. The separating islands in bus bay drawings can be easily hit as it is narrow and is not provided with hazard markers. Advance direction signs of Bus bay and pavement markings are also missing in the design drawing as shown in **Figure 19**.

Recommendations : As shown in **Figure 20** provide hatch marking for separating islands at the approach and also provide hazard makers at the tip of the island. Also, provide bus bay facility informatory signs. The pavement markings on Bus Bay shall be as per Figure 12.3 of IRC:35-2015 as shown in **Figure 21**.

Truck Lay Bye

Reason for Concerns : **Figure 22** shows an example of Truck Lay Bye from Engineering Design Drawing. The separating islands in truck lay bye can be easily hit as it is not provided with hazard markers. The Pavement markings are not shown properly.

Recommendations : As shown in **Figure 23**, provide hatch marking for separating islands at the approach and also provide hazard makers at the tip of the island. Also, provide truck lay bye informatory signs. The pavement markings on a Truck Lay-By shall be as per Figure 12.4 of IRC:35-2015 as shown in **Figure 24**.

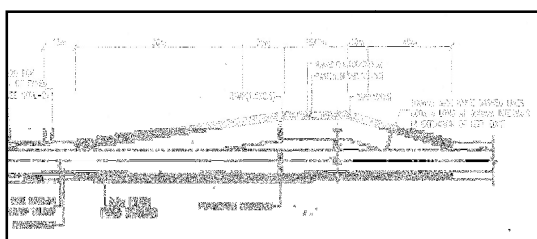


Figure 19 Example of bus bay from engineering design drawing

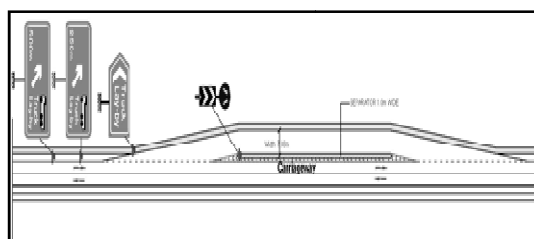


Figure 20 Typical layout of bus bay as per IRC:SP:73-2015

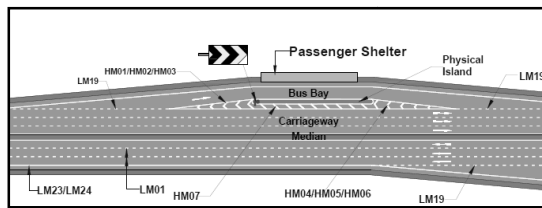


Figure 21 Pavement markings as per Figure 12.3 of IRC:35-2015

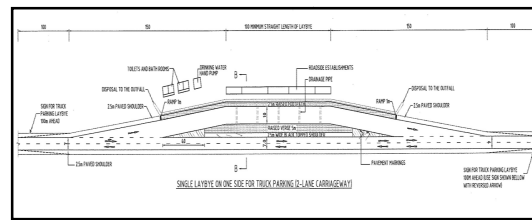


Figure 22 Example of truck lay bye in engineering design drawing

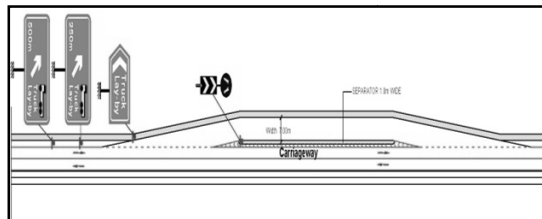


Figure 23 Typical Layout of Truck Lay Bye as given in IRC:SP:73-2015

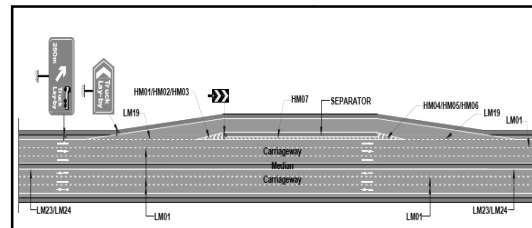


Figure 24 Pavement marking on truck lay bye as per Figure 12.3 of IRC:35-2015

CONCLUSION

The study highlights a few of major inconsistencies in design with respect to safety which come across a road safety auditor during design audit. The importance of design audit lies in the fact that, this audit is at pre construction stage, thus rectification of design drawings is much cheaper and easier than performing safety treatments after the road infrastructure physically comes into existence. With upgradation and development of road network, the riding quality improves tremendously which in-turn imposes serious threat to safety of road Users as well as to safety of People living in habitations along the road. Engineering Countermeasures for safety bring forth immediate effect on safety performance of the road while it takes a long period for the behavioral change among the road users through education and enforcement programs. Thus a design audit must be meticulously performed and the Auditor must ensure that the design adheres to all provisions of IRC Code so that any ambiguity in the road environment gets removed and positive guidance is provided to all road users.

REFERENCES

1. Global status Report on Road Safety 2015 by World Health Organization http://www.who.int/violence_injury_prevention/road_safety_status/2015/en/ Accessed August 5, 2017
2. Accidental Deaths & suicides in India 2015 Report by National Crime Records Bureau, Ministry of Home affairs, India <http://ncrb.gov.in/> Accessed August 5, 2017
3. Press Information Bureau, Government of India, Ministry of Road Transport & Highways <http://pib.nic.in/newsite/PrintRelease.aspx?relid=170577> Accessed December 5, 2017
4. Manual on Road Safety Audit, IRC:SP:88-2010, pp 4-7 (2010)
5. Manual on Road Safety Audit, IRC:SP:88-2010, pp 8-10 (2010)
6. Manual on Road Safety Audit, IRC:SP:88-2010, pp 21-22 (2010)
7. Manual of Specifications & Standards for Two Lanning of Highways with Paved Shoulders (First Revision), IRC:SP:73-2015, Section 9.2.7 pp 73 (2015)
8. Code of Practice for Road Signs, IRC:67-2012, Section 15.63, pp 45 (2012)
9. Manual of Specifications & Standards for Two Lanning of Highways with Paved Shoulders (First Revision), IRC:SP:73-2015, Section 2.9.1 pp 13 (2015)
10. Vertical Curves for Highways, IRC:SP:023-1993, Section 7.1, pp 25 (1993)
11. Manual of Specifications & Standards for Two Lanning of Highways with Paved Shoulders (First Revision), IRC:SP:73-2015, Section 9.7.1 pp 86 (2015)
12. Manual of Specifications & Standards for Four Laning of Highways through Public Private Partnership, IRC:SP:84-2014, Fig.3.2, pp 30 (2014)
13. Guidelines for Planning and Design of Roundabouts, IRC:65-2017, Section 1, pp 2 (2017)



Sedimentation: It's Impact and Management

Kumar Abhishek Kishore^{*1}, Prashant Kumar¹
Water Resources Department, Government of Bihar¹, kakaewrd@gmail.com*

ABSTRACT

Floods are the most common and widespread of all natural disasters. India is one of the highly flood prone country in the world. Further Bihar is one of the important states of India which falls under Ganga river basin. The entire North Bihar is crisscrossed by the major rivers such as Gandak, Bagmati, Kosi, Mahananda etc. which all, meet the mighty Ganga on its left bank. All these rivers originate in Nepal from the Himalayas which meet the river Ganges in the lower reach where flow velocity is considerably reduced. Development activities involving deforestation, mining, and agriculture in upper part of catchment causes soil erosion from upland area. The fast flowing rivers when surge down from hills and spread out in plains are generally prone to silting up. The silt causes the rise in river bed resulting to disturbing the natural longitudinal course of the river and river tries to flow towards lateral path (left to right). It results in change of river course which further leads to erosion of nearly land or breach of embankment. Flooding due to breaches of embankment are the more disastrous as river starts flowing through the villages and other developed areas. Kosi breach (2008) is still an example. A case study has been taken at upstream of Kahalgaon, Bihar in River Ganga where a lateral shift of around 10 Km is observed during last 30 years. Presently this reach is protected by embankment and river training structures but still vulnerable during monsoon period. Downstream of Kahalgaon Kosi joins the Ganga. Kosi carries a heavy silt load from its upland areas and River Ganga also carries a tremendous silt load collected from other rivers and by its own catchment. Velocity of flow in plain area also becomes considerably low due to flatter gradient. This cumulative effect leads to deposition of silt and consequently the adverse effects caused due to sedimentation. This paper highlights the issues related to sedimentation and its impact on river course with a case study of River Ganga in Bhagalpur, Bihar. It also briefly describes the practice for silt management.

KEYWORDS Erosion; Sedimentation; Silt management; Ganga

INTRODUCTION

Rivers are natural channels to drain water from highlands to lowlands/seas. Erosion and aggradations are geological processes by which large amounts of sediments being brought from the higher elevations to the plains (Water Notes, GoWA, 2000). As the river flows from high gradient to low gradient, momentum of the flow reduces which ultimately results in silt deposition en route. River or a stream channel can be considered to be relatively stable when its water flow and sediment flux are in balance over time (**Figure 1**).

If there is a change in either of these two factors, then the channel will adjust its slope, depth, width, meander pattern, bed composition and vegetation density accordingly. The extent and rate of these adjustments are dependent on the extent and rate of change in the water flow and sediment load. Sedimentation in river has significantly increased due to encroachment of flood plains by ever rising population. As of now there is also a notion that flood problems are on rise. Rising trend of flooding is generally due to reduced carrying capacity of rivers on account of silt deposition in river beds.

FACTORS INFLUENCING SEDIMENTATION

Erosion is a natural process where wind and water transport soil, sand and gravel slowly redefining the landscape over hundreds or thousands of years. However, there are some activities which significantly increase the natural erosion rates leading to massive changes in sedimentation over a relatively short period.

Agricultural Depletion

To cater the increasing food demand people have started expanding the farming activities. Farming activities degrades the top layer soil leading to increased erosion. To plant a field, farmer has to breaking up and loosening the top soil so that new plants can take root. Once the plants are harvested, the soil remains loose and wind or rain can easily erode it away.

Deforestation

Deforestation is another practice significantly increasing the rate of erosion. Plant life as long-lived trees and other species put down roots that literally help hold the soil together and checks the erosion rate. Due to deforestation such binding of soils looses and hence erodes away. If the operation plants new trees to replace the old ones, the younger plants require years to put down the kind of root system that once protected the soil.



Development and Expansion

Urban and suburban development can also exacerbate erosion, especially if the developers ignore the natural state of the land. Any development activities start with construction of infrastructure which begins by clearing the area of any plants or other natural defenses against soil erosion. In addition, some landscapers replace natural ground cover with plant species unsuited to the climate, and these plants may not be as effective at preventing erosion.

River Training Works

River training works like embankments, spurs etc are being adopted along the river course to avoid unfavorable wandering of the main currents. River training works undertaken in response to a pre-existing problem of river instability plays remarkable role in ensuring the safety of people from floods. But it may cause aggradation at one place and degradation at other place in floodplain, erosion of riverbed, decrease of low and even mean water levels, loss of flood water conveyance capacity etc.

Construction of Structures like Dams and Barrages

Structures like dam and barrages constructed on rivers alter the equilibrium of flow of water and sediment in alluvial channels. It reduces the velocity of water in upstream leading to aggradation and relatively silt free water released in downstream causes degradation and erosion. Construction of dams leads to decrease the magnitude of flood flows by moderating them but due to encroachment of downstream floodplains for development activities by local population due to reduced risk of flood exposes them to higher risks of siltation and erosion. Similar in case of construction of barrages due to reduced water velocity in upstream cause aggradation leading to siltation.

Sand Mining

Unscientific sand mining depletes the mines at rates at which the river system cannot replenish it. Excessive mining undermines the ability of riverbeds and riverbanks to support the infrastructure. Also, the continued collapse of such banks lead the river course to deviate towards developed lands and poses ever increasing threats to them.

IMPACTS OF SEDIMENTATION

Right from origin to the destination of the River Ganga its flow has been obstructed by a number of structures constructed across it. Even before Devprayag, Tehri dam has been constructed on River Bhagirathi whereas a number of dams have been constructed on River Alaknanda before its confluence at Devprayag. In West Bengal, Farakka Barrage too is on River Ganga. In addition of these, a hundreds of structures have been constructed in the entire path of the river. These structures along river path have broadly affected the characteristics flow of river as well as sediment load (bed as well as suspended) followed by its adverse impacts.

Reduced Discharge Carrying Capacity

Rapidly flowing rivers from the high lands carries silt which gets laterally deposited on the banks of the rivers. When the river is dammed, its flow velocity suddenly gets lessened leading to stagnant or semi-stagnant conditions. The buoyancy of the silt particles then gets lowered and they gradually settle on the river bed. Due to this sedimentation process river bed rises and discharge carrying capacity of river gets lowered.

Shifting of River Bank and Flooding

Siltation causes the level of river bed to rise resulting the natural longitudinal (straight) course of the river is disturbed. These high aggradations of river bed and sediment bed load offer enough resistance to the water, forcing the river to find alternate paths, resulting in lateral shift of the river course. Therefore the river searches for a lateral path (left or right) resulting to change in its course which further causes shifting of river banks (B. Kaur, DownToEarth, 2018). It may breaches the embankments on the new path it has created which ultimately results devastating flood tragedy.

Obstruction in Waterways

The waterways planned on various rivers are an important mean of cargo transportation. The Ganga, Gandak and Kosi are of specific strategic importance as these waterways are amongst the 37 waterways which have been prioritized for development by 2019. National Waterway-1, on Ganga –Bhagirathi and Hooghly river system and passes through the states of Uttar Pradesh, Bihar, Jharkhand and West Bengal. By the Governments of India and Nepal has declared that Kosi and Gandak would be developed as International Indo-Nepal waterways, to provide sea connectivity to Nepal. Developing these waterways to allow large barges to transport cargo requires creation of channels in these rivers with adequate depth and width to allow these vessels to move. Rivers in Bihar do not have this adequate depth naturally because of the heavy sediment load. The high sediment load in these rivers means that heavy costs will be incurred for dredging and disposal of dredged material for these waterways. Since flowing rivers



keep bringing silt into such navigation channels, dredging is required in an ongoing manner in most waterways (Verma et al 2018). Further these rivers keep shifting their channels and formation of shoals.

Altered Instream Vegetation and Dynamic Flow

Where sediment accumulates in shallow, slow flowing areas of a river, it provides a base for the colonisation of semi-aquatic plants which readily colonise new habitats as well, may prevail in these areas. The colonisation of plants will slow the flow across these areas and cause further sediment to settle out. These areas may become islands within the stream channel, causing flow to divert around them and altering channel shape. The accumulation of sediment may also raise the channel bed and thereby reduce channel capacity to carry high flows (Water Notes, GoWA, 2000).

Reduced Photosynthesis Affecting Aquatic Life

Sediment increases water turbidity making it difficult for light to penetrate the water. This causes problems for aquatic plants that need sunlight for photosynthesis. Water plants and algae require light for photosynthesis. Without it they cannot survive and if light is reduced their growth rate will decline. This effect may be particularly problematic in mid-order streams where turbidity is generally low and an open canopy permits light to reach the stream bed. In these areas water plants and algae form an important component of the food web and their absence or reduced growth will affect the microbes and animals that feed upon them. Macroinvertebrates, such as caddisflies, stoneflies and mayflies, which like to live in clean gravel beds, become less abundant. Worms and midge larvae, which prefer finer sediment, become more abundant.

Case Study of River Ganga in Bhagalpur, Bihar

Bhagalpur is the district in Bihar known as silk city of India (Tannen 1986). The Bhagalpur district has population more than 30 lakhs with density closer to 1200 people per square kilometers (Census, 2011). The river Ganga has been the lifeline of Bhagalpur (Bihar). This mighty river runs for 2525 Kilometers through Haridwar, Kanpur, Allahabad, Varanasi, Patna, Bhagalpur and Kolkata (Tiwari et al. 2014). Any alluvial river of such magnitude has problems of bank erosion attached with it, the Ganga is no exception.

Study Area

Vikramshila setu to Kahalgaon in Bhagalpur district, Bihar has been taken as study area (**Figure 2**). The study focuses on adverse impacts of siltation observed during the period. Study was conducted using historical satellite image of the area from year 1984 to 2016. The Vikramshila setu (Bhagalpur, Bihar) is located approximately 135 km downstream of Mokama Bridge and 190 km downstream of Mahatma Gandhi Setu, Patna. Further Kahalgaon is located around 28 Kilometers downstream of Vikramshila setu along the river Ganga.

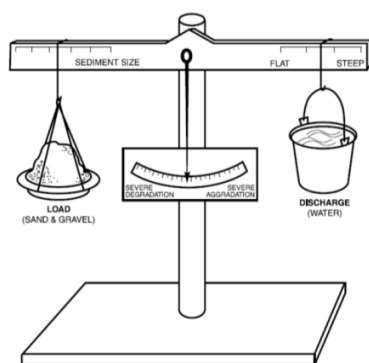


Figure 1 Stream balance scenario (Source-Water Notes, GoWA, 2000)

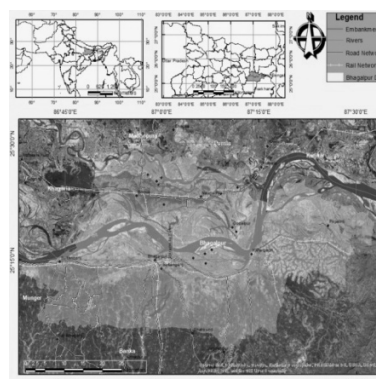


Figure 2 Study Area, River Ganga in Bhagalpur, Bihar

Methodology

The basic data used in this study are digital satellite images comprising of scenes for the years 1984 to 2016. The image taken with good visibility and being free of clouds. Results of interpretation and extracted layers from satellite images were transformed into GIS layers. Change of river segments was detected by superimposing data layers together. River was digitized by taking centre line of river channel with vector shape file. The regime of river Ganga is demarcated from each set of imagery. Change in regime of river Ganga during the period (1984 to 2016) is



estimated by GIS software tools through delineating the river regime. Shifting of the river Ganga over the period in downstream of Vikramshila Setu was confirmed using satellite images.

RESULTS AND DISCUSSION

At Vikramshila setu the river is confined to follow the fixed waterway by means of training structures and at Kahalgaon, no erosion takes place on right bank due to presence of rocky strata. Within these two points shifting of the river Ganga can be clearly observed. Interpretation of satellite image from year 1984 to 2016 shows a continuous shift of the river towards left and during the entire period a total shift of around 10 Kilometers (**Figure 3**) This shifting of river confirms the theory of finding alternate paths by a river resulting to lateral shift because of disturbance in natural longitudinal (straight) course due to sedimentation.

In the way to shifting the river, the settlements felled within this play zones has been completely destroyed and the villages have sacrificed their existence. A decade back in order to check further shift of river an embankment Ismailpur Bindtoli Tagging Bandh has been constructed on left bank which was further armoured with so many river training and embankment protection structures like spurs, launching apron, bed bars etc. The present status is still alarming. The embankment is under heavy pressure and regularly needs flood protection works over it. It is always under the heavy threat of breach and if so happens it will cause devastating flood (**Figure 4**).

Further in this stretch heavy siltation led sand bars are hindering vessel navigation in waterways. The river after changing its course now flowing in a northward loop along Naugachhia near Khagaria district. This has also led to reduced availability of water for ships passing through the southern side. The Inland Waterways Authority of India plans to dig a pilot channel in the river through dredging. However, IWAI's sub-office at Sahebganj in Jharkhand, said only 700 m of the seabed could be cleared after a month of dredging works while around 1,700 m of seabed needs to be dredged to provide water depth for bigger ships to sail under the Vikramshila bridge. The Bhagalpur stretch of the Ganga river is part of the area declared National Waterways No 1 – a Rs 5,000 crore project for which the World Bank has provided financial assistance. The work includes development of three multi-modal hubs at Varanasi in Uttar Pradesh, Haldia in West Bengal, and Sahebganj in Jharkhand (Scroll.in).

SEDIMENT MANAGEMENT

Once sediment has entered waterways it is difficult and expensive to remove, requiring engineering solutions and heavy equipment. So preventative measures aimed at reducing further sediment transport are the best approach. Recommended practices for effective sediment management are listed as follows.

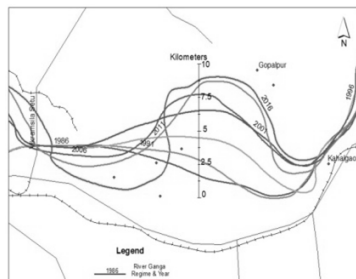


Figure 3 Lateral shift of River Ganga in Bhagalpur from year 1986 to 2016

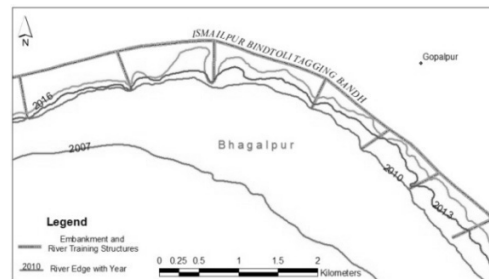


Figure 4 Status of Left bank of River Ganga in Bhagalpur, Bihar

Catchment Area Treatment

Catchment Area Treatment with good agricultural practices is necessary to reduce silt inflow into the river system. This is the best way to control sedimentation issue by minimizing it within the catchment itself before entering to river network. Main limitation in this practice are for rivers like Kosi, Gandak, Brahmaputra etc. major part of the catchment falls outside the country so there is least to no control over that part of catchment.

Storage Reservoirs

The reservoirs are primarily built to store water but incidentally, these also act good as settling tanks for the sediment and trap the sediment carried by the river. Therefore the sediment concentration of the water released from the reservoir gets effectively reduced.

Gravel and Sand Mining

Gravels and sand deposited in sand bed should be mined and used for construction purpose. It will reduce the major



port of sediment. However it must be scientifically done in controlled manner. The 'Sustainable Sand Mining Management Guidelines – 2016' of MoEF&CC and 'GSI Guidelines for riverbed gravel/ sand mining' should be followed.

River Training Works

River bank erosion significantly adds up the sediments in river. So river training works used to control the erosion of river banks reduces the sediments intake in river.

Ensuring Environmental Flow Requirements

Regular flushing of rivers is important for maintaining bed load transport at sustainable levels, and also to prevent sediment accumulation in streams. To ensure it environmental flows are considered in water allocation exercises. It is also necessary to maintain aquatic flora and fauna.

Desiltation / Dredging

Desilting is very effective in increasing the serviceability of a channel. However, mechanical desilting in large rivers may not be techno-economically feasible. However, there exists some locations such as congestion at confluence points and the likes which can be tackled by desilting after thorough examination. For navigation purpose also the river reaches in the waterway path can be dredged, to have minimum draft for plying vessels. Desilting also improves the hydraulic efficiency if done near outlets and intakes.

Lateral Connectivity for Sediment Management

Construction of embankment has resulted in breaking the lateral connectivity of river with its flood plain. Therefore, the silt carried by the river is being deposited in river bed only leaving the flood plains devoid of sediments. This has resulted in rising of river bed and causing bank erosion at high flood levels. In order to provide lateral connectivity to the river with its flood plains, sluice gates may be provided at appropriate places in the embankment to allow controlled flooding in flood plains. This will allow silt carried by the river to be deposited in its flood plains in thin layers distributed over vast areas and will ultimately result in reduction of silt loads in rivers and will make the agriculture fields in flood plains fertile.

CONCLUSION

Sediment transport, bank erosion and associated channel mobility represent key physical processes of rivers. Most alluvial rivers have experienced increased sedimentation or bed load deficit, both due to natural processes and series of human interventions in the river catchment or on river itself. Rapid urbanization in flood plains, encroachment of river beds, changes due to human activity and deforestation in catchment area of rivers are causing sedimentation in rivers. It results in loss of channel capacity reducing its benefits like navigational requirement and aquaculture and increasing the risk of flooding and shifting of river banks. So effective management of sediment in rivers is becoming increasingly important from an economic, social and environmental perspective. In order to minimize the sedimentation, a scientific approach to sediment management is desirable. It includes catchment area treatment up to possible extent, storage reservoirs as detention basins, controlled sand mining and river training works, maintaining environmental flow requirements and dredging when essentially required.

REFERENCES

- Verma, J. Sandbhor, S. Dharmadhikary, National Inland Waterways in Bihar: Viable or desirable ? *Manthan Adhyayan Kendra*, South Asia Network on Dams, Rivers and People, 2018.
- Kaur, Why does Kosi river cause devastating floods so often? answer lies in massive siltation: study, DownToEarth. (2018)
- H. Tiwari, N. Sharma, Bank Shifting of River Ganga in the Downstream of Bhagalpur Vikramshila Setu, *Journal of River Engineering*, Volume 2, Issue 4, 2014.
- International Sediment Initiative, Technical Documents in Hydrology, Sediment Issues and Sediment Management in Large River Basins Interim Case Study Synthesis Report, UNESCO Office in Beijing and IRTCES, 2011.
- Ministry of Water Resources, River Development and Ganga Rejuvenation, Draft Policy on Sediment Management, New Delhi, 2017.
- Office of the Registrar General & Census Commissioner, India, Ministry of Home Affairs, G.O.I., Census of India, <<http://censusindia.gov.in/>>, 2011.
- S. Bandyopadhyay, Natural floods and unnatural disasters in Bihar, *India Climate Dialogue*, 2017.
- D. Tannen, That's Not. What I Meant! How Conversational Style Makes or Breaks Relationships, New York: Ballantine, 1986.
- Water Notes for River Management, Sediment in Streams, Water and River Commission, Government of Western Australia, 2000.
- <https://scroll.in/latest/861186/ganga-river-abandons-original-course-in-bhagalpur-sand-bars-hinders-vessel-movement-says-report>.



Improved Cement Quality and Grindability by using Grinding Aids

Devendra Kumar Patel

J K Cement Ltd. Mangrol, Rajasthan, dkpatel1971@gmail.com

ABSTRACT

In this study, the effect of grinding aids (liquid additives) on the cement grinding were estimated on the lab as well as large scale. In dry fine grinding process the increase in the particle -particle interaction increases with the increase in the product fineness. These increase in the interaction lead to decrease in the grindability and other process control such as charge development on product particle, agglomeration of particle (lump formation), material coating on the grinding media. The absorption of grinding aid on the product particle is the common measure to control avoid such conditions, to ensure an effective grinding aid application, the impact of additive on the particle and bulk properties, which influence the micro process inside the mill need to be understood. The impact of grinding aids were analyzed on different level from laboratory to the actual ball mill. Its effects were evaluated by measuring the dry particle size distributions i.e. PSD and Blaine specific surface area and its effects on the grinding power consumptions, other effects were observed on particle specific surface energies, coating on grinding media, powder flowabilities. It has shown that grinding aids drastically effects the grinding efficiency. The bulk flow also determines the results of grinding aids as it change the powder flowabilities and stress mechanism inside the mill. Moreover the study shows the direct relationship between grinding aid and its influence on product.

KEYWORDS Ball Mill, Grinding Aids, PSD, Blaine

INTRODUCTION

Grinding in the cement industry is one the core process, Grinding operation is achieved by two major components by pulp flow and stress applications. Specifically these process includes transport of material to the grinding zone and subjecting the material into grinding action, leading possibilities to propagation and initiation of cracks followed by transport of material to the end outlet. Any parameter affects any mechanism it affects overall grinding process. while pulp flow process involves the transport of material inside the mill which depends on the pulp fluidity, which is influenced by the nature of interaction of the particle with grinding media and also among themselves, hence grinding aids act on the pulp flow process.

In cement industry from raw material input to final output all the done by size reduction, that is, limestone from mines comes in 1 m³ size. It goes to the crusher for crushing converted into 25 mm size, furthermore it goes to raw grinding in raw mill where it reduced to 90-212 μ m known as raw meal. After pyro processing clinker with addition of gypsum goes to finishing mill cement mills where it reduced to ultra-fine particles 3 to 30 μ m.

Thus grinding is one of the important industrial operation for size reduction, production of larger surface area, liberation of valuable minerals/contents from the matrix. However grinding operations is known as one of the least energy efficient unit operation (60 to 70% electrical energy consumed in grinding process only). Grinding aids helps grinding of material thus increase the grinding efficiency by small amount of addition in the ball mill. Grinding aids can leads to contamination in the final products but it can be minimized by using the selective grinding aids. Grinding aids are liquid compound formulated as water based organic liquid compound with high charge density such as alcohol based, ester of glycol based, alkanolamines and carboxylate alkanolamines. Grinding aids are usually entered in the mill entrance together with clinker, gypsum and other admixtures as fresh feed. Main function of grinding aids is to neutralize the charge developed during the formation of new product particle reduce the surface free energy of the newly formed particle, the effect is carried out by additive particle which absorbed over the newly formed particle by weak electrostatic force, developing the repulsive force and hindering the agglomeration of particle thus improve grinding efficiency. Furthermore it also avoid the material coating formation over the grinding media because of the charge neutralization.

Recently, the effect of grinding aids has been studied extensively. Many chemical species have been evaluated (amines, glycols, phenols, etc.), employing different parameters in the characterization of the performance of these products. The evaluation of the grinding aid performance of the additives is normally carried out by monitoring the evolution of fineness with the operation time. From the technical literature, it can be concluded that the more representative parameters are:

Specific Surface Area (SSA)

It is defined as total surface area in sq. meter of all cement particles in one kilogram of the cement, unit is m²/kg. It



is one of the basic property of the powder. Higher the total surface area of the cement of unit mass more finer will be the cement.

Breakage Rate (C)

It is defined as the slope of the evolution of fineness of product with its time.

Grindability Index (GI)

It is defined as the ratio between the fineness (determined by Blaine test of the sample) and the number of mill revolutions required to achieve that fineness.

Experiment

Grinding apparatus used in the experiment is a ball mill with having dimensions 70 cm in length and 55 cm in diameter, filled with 30 % by grinding media of different sizes ranging from 2 to 8 cm, around one third portion is filled with material (2 kg clinker + Gypsum + PI), this is for lab scale but for large scale we used closed circuit ball mill having diameter 4.2 m, length 13.75 m having rated TPH of 100, and other is combo circuit ball mill with high pressure roller press having ball mill diameter 4.1 m and 11 m length rated capacity of 240 TPH.

Chemical Composition of Clinker, wt. %									
SiO ₂	Al ₂ O ₃	Fe ₂ O ₃	Cao	MgO	SO ₃	Mineral phases			
						C ₃ S	C ₂ S	C ₃ A	C ₄ AF
21.5	4.5	5.2	65	0.95	1.2	53	25	4	15

In all the experiment raw material which include clinker, gypsum and performance improver are same and the grinding time and ball mill rotation speed is also remain constant. In order to reduce the amount of wear from the materials, the ball mill grinding chamber is equipped with the ceramic plates. The experiment was carried out in a batch and sample is taken out from the mill in the particular time interval to check the grinding time interval. Furthermore after the test is done after a specific interval of time i.e. 30 minutes. The Blaine specific surface areas of the samples were periodically determined using an air-permeability apparatus in accordance with ASTM standard. In this experiment we use Triethanolamine (TEA) as grinding aid with concentrations and take out its impact on the grinding of the material and its fineness. List of the different types of grinding aids are given below the exact action of grinding aids with cement paste is very complex, depending upon the type of cement used and concentration of grinding aids (% by weight of cement). For compressive strength measurements, fresh pastes of normal consistency were thoroughly mixed in a mixer for 5 minutes and then cast into $2 \times 2 \times 2$ cm³ cube. The cubes were stored at an atmosphere of more than 95 % relative humidity at 25°C for about first day and then it were cured in lime water at 25°C until the time of testing.

Amine Based Grinding Aids : Monoethanolamine (MEA), Diethanolamine (DEA), Triethanolamine (TEA), Triisopropanol amine (TIPA)

Alcohol Based Grinding Aids : Ethylene glycol (EG), Diethylene glycol (DEG)

Ether Based Grinding Aids : Poly Carboxylate Ether (PCE)

Additives	Density, kg/m ³	Chemical formula	Molecular mass, g/mole	Additive dosage , wt %
Triethanolamine (TEA)	1124.50	N(CH ₂ CH ₂ OH) ₃	149.19	0.05, 0.10, 0.15, 0.5

RESULTS AND DISCUSSIONS

Fineness is very important quality parameter of cement, that significantly influences the rate of hydration and hence the rate of gain of strength, especially at early ages, and also the rate of evolution of heat at the time of reaction. Cement manufacturers control this quality parameter by measuring both Blaine specific surface area and residue on sieve. Basic motive for the addition of the grinding aid is to improve the grinding efficiency of the clinker, but results of the experiment found that it also contribute to the mechanical property such as settling time, mortar



workability, surface area, compressive strength of finished product. It is clearly visible in the experiment results given below which are tested with grinding aid and without grinding aid (blank).

Figure 1 is showing the contribution of grinding aid in the strength of finished product.

Figure 2 is showing the effect of grinding aid on PPC grinding. It is clearly seen that fly ash consumption and strength increased with the addition of grinding aid. Further, there is a significant increase in the Blaine value of the products with respect to the blank. TEA increases the value by almost by 15 % in OPC 43 grade cement.

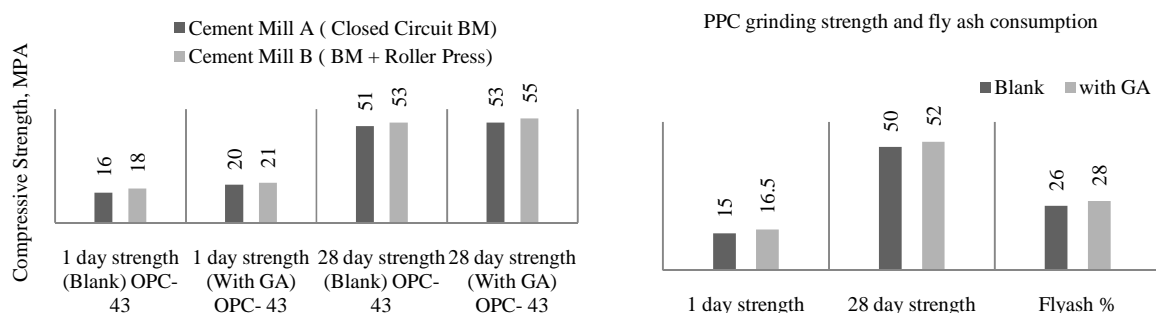


Figure 1 Contribution of grinding aid in the strength of finished product **Figure 2** Effect of grinding aid on the lab ball mill

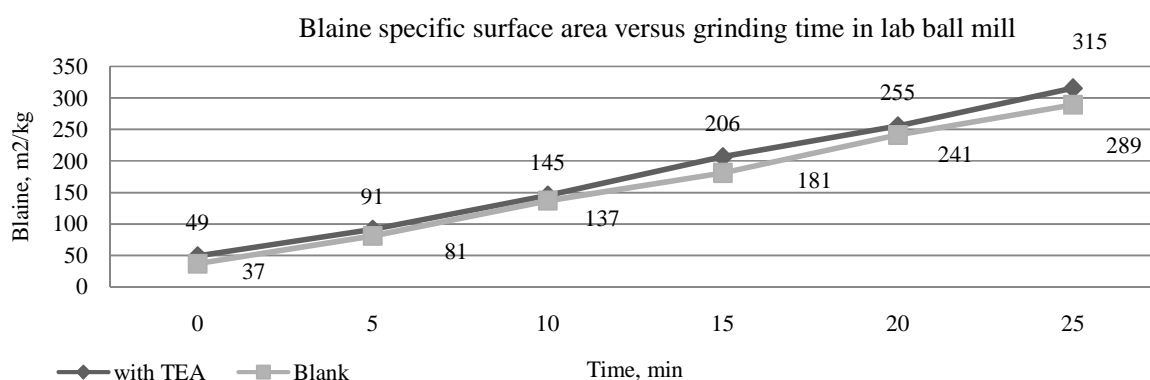


Figure 3 Increase in the mill output with the application of grinding aids

It has been observed that use of organic liquid TEA, the vapor of organic liquid reduces the force of adhesion between the particle that leads to reduction in agglomeration of particle and increased fluidity of particle, thus it increases the grinding efficiency and productivity. From the experiment we have developed the optimized dosage of grinding aids in the cement grinding, because as the percentage by weight of grinding aids increase, it increases the specific surface area SSA of the grind particle but as long as we keep on increasing the percentage of grinding aids by weight of material after certain value it shows negative effects, that is it decreases the surface area of particle this term is known as 'negative grinding' or re-agglomeration of the particle. From economic point of view TEA cost around Rs. 1.1 to 1.3 per ton of cement. It also contribute to the energy saving in terms of specific power per tons of cement (electrical energy consumption, kWh /ton of cement) reduced by Rs. 5 to 7 per ton of cement. The enhancement of mill output is shown in **Figure 4**, which also shows the increase in the productivity lead to reduction in the specific power consumption by the effect of grinding aid.

Effect of Grinding Aid (TEA) on The Engineering Properties of Cement

Settling time describe the stiffening behavior of the cement paste when mixed with water. The results were calculated by the measurement of product with and without grinding aid, TEA increases initial and final settling time of cement, product with higher blaine value has more reaction surface area. If TEA don't have any effect on hydration settling time would have reduced but it is increased but it effects the hydration rate, hence it acts as a



retarding agent when mixed with proper concentrations. It has concluded that at low concentration TEA acts as retarding agent (up to 0.5%), while at higher it acts as accelerator of hydration of cement.

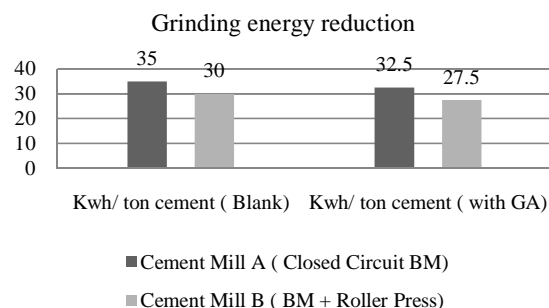
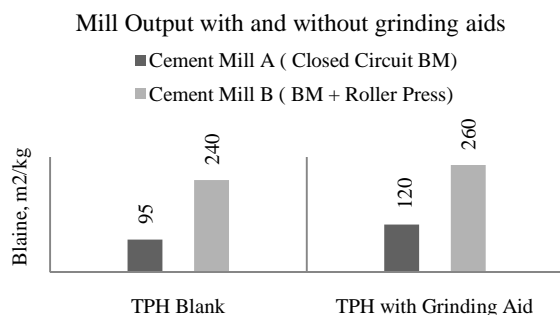


Figure 4 Increase in productivity leads to reduction in SPC

Figure 5 Effect of grinding aid

Grinding aid also effect on the water consistency. It is defined as the relative mobility of cement paste, or its ability to flow, at constant water ratio we have tested slump retention test to check the cement flowability, spread diameter of the particle the flowability is reduced. The spread diameter is the measure of the flowability of the paste, connected with the size and shape of the cement particles. Which are always agglomerated with the addition of water, at constant water ratio, this lead to increase in viscosity with increase in volume, part of water is trapped in the porosity of the particles and prevent contribution to the flowability.

CONCLUSION

From the above experiment done in lab scale as well as industrial scale, its effect are clearly seen form the graphs shown in the result section, thus we have concluded that the effect of grinding aid over cement propertyare:-

- Enhance setting time
- Surface area increased
- Increased compressive strength of cement
- Mortar workability improve.
- Grinding mill can be loaded with higher mass (TPH) by the use of grinding aid,
- Specific power consumption due to higher productivity drastically decreased, thus save energy.

REFERENCES

- Global Cement Review Magazine
- Industrial parameter by cement industry.
- Fosroc technical review about grinding aids.
- S. P. Deolalkar, Handbook for designing cement plants.
- S.N. Ghosh, Advances in cement technology: Critical review on quality control, optimization and use.
- Data from National counseling of Cement& Building Materials, Delhi



Linear Earthquake Analysis of Multi-storey Building on Raft Foundation including Soil Structure Interaction

S Mondal¹, K Bhattacharya*¹

Department of Civil engineering, NIT Durgapur, dr.k.bhattacharya@gmail.com*

ABSTRACT

During earthquakes the individual response of the superstructure, the foundation and the soil below influences each other and together forms a complete system and there comes the concept of soil structure interaction (SSI). An attempt has been made in this paper to study the seismic response of a frame building using the effect of soil-structure interaction. A G+27 storied building subjected to seismic forces is modelled and analyzed through the finite element software program LUSAS 15.2. Maximum considered earthquake (MCE) is considered in the study. Static (seismic coefficient method), Dynamic (Response spectra method during SSI by obtaining the response spectra using Deep Soil 6.1 for deconvolution and re-convolution of earthquake data for a deep soil assumed as 60 m thick from the raft), Pseudo-static method are used in the linear analysis of the structure. Comparison based on the shear and lateral force distribution of the structure is made between the above methods of analysis. The study reveals that soil flexibility has significant effect on the response of structure as the base shear increases from hard to medium to soft soil. There is also a decrease in natural frequency of structure vibration of frame building especially on soft soil.

KEYWORDS High rise building, Soil-structure interaction, linear analysis, Pseudo-static method, Deconvolution of earthquake.

INTRODUCTION

Designers have been trying hard for centuries to combat the effect of the catastrophic act of nature, the earthquakes and for constructing earthquake-resistant buildings with necessary strength and stiffness. One of the most common types of construction in buildings is a dual system comprising of set of shear walls and moment resisting frame which interacts with each other along the building height to resist the large lateral forces of the earthquake. The shear walls respond by bending as a cantilever and the frame deflects in a so called shear mode. Their combined action causes the frame to restrain the shear walls in upper stories and the shear walls to restrain the frame in the lower stories, hence reducing the lateral sway of the building, improving the overall stiffness and making an able earthquake resistant structure[1]. The successful performance of the structure against earthquake hazard also depends on the consideration of soil structure interaction. The first aspect of soil structure interaction comes from the kinematic interaction effects arising out of wave propagation. As the seismic waves propagate through the soil during earthquakes, 'disconnection' in the medium of wave's propagation at the soil and structure foundation interface causes diffraction, reflection, refraction of the seismic waves at the interface changing the ground motion which is much different from that which would have been seen in the absence of the structure and foundation. Moreover the seismic wave propagations take place due to deformations in the medium. Inertial interaction is the second aspect that arises due to the dynamic response induced by the vibrating structure and foundation [2]. Degree of influence of SSI on response of a structure depends on factors like stiffness of soil, dynamic characteristics of structure itself i.e. natural period and damping factor, stiffness and mass of structure. Chaithra and Manogna [3] evaluated the seismic performance of the fifteen storey, RC building with raft and piled raft foundation using linear time history analysis by SAP 2000 Ver 14.0. Results shows that the base shear, displacements and time period increases with incorporation of soil flexibility being maximum for soft soil. Kuladeepu[4] showed that the fundamental natural time period, lateral displacement and base shear values of RC moment resisting structure without infills over raft foundation considering interaction is more than that of non-interaction investigation as it increases with increase in soil flexibility and also with expansion in number of stories. Roopa, et al [5] carried out response spectra analysis of an G + 12 apartment on raft foundation at Mambakkam, Tamil Nadu .India using ETABS 9.7.4 for modeling and SAP2000 ver17 for SSI analysis showing that the base shear for flexible base condition is increased compared to fixed base condition. The natural time period in case of building with flexible base increase by 37.39% when compared to fixed base for first mode.



In the present study an investigation based on seismic responses is carried out on a G+27 storied frame structure with raft foundation with and without soil structure interaction. The seismic behaviour is evaluated using seismic coefficient method, response spectra method as specified earlier and pseudo-static method.

RESEARCH DESIGN

Objectives

1. A linear analysis of a G+27 storied frame building is carried out for :
 - (i) Building on raft foundation considered as fixed i.e. without SSL.
 - (ii) Building on raft foundation on different soils with SSL.
2. Seismic coefficient method, Response spectra method, Pseudo-static method are carried out for the above two cases and comparative studies are made based on the seismic responses.

Modeling

LUSAS 15.2 [6] is finite element software used in the modeling and analysis. While including soil-structure interaction in the response spectra analysis Deep Soil 6.1 is used for de-convolution-re-convolution of earthquake data to obtain the response spectra at the 60 m depth which is twice the least width of the building plan [7] to be applied to the model.

Geometric Modeling

The building frame with the plan view is documented in Taranath [1]. The main geometric and material properties are as follows:

- Beams = 1.07×0.5 m
- Haunch girders = 1.07×0.5 m for the exterior part of 8.5 m length, with a haunch in the interior tapering from a span depth of 0.5 m to 0.84 m.
- Skip joists = $0.15 \text{ m} \times 0.5 \text{ m}$
- Shear walls = $0.45 \text{ m} \times 5.96 \text{ m}$
- Columns = $0.965 \text{ m} \times 0.864 \text{ m}$.
- Slab = 0.15 m thick is provided in all the floors.
- Height of each floor is 3 m.
- Raft foundation = 1.5 m deep
- Soil extent = $80 \text{ m} \times 190 \text{ m}$
- Soil depth = 60 m (approximately 2 times the least lateral dimension).

Table 2 Material properties of concrete

<i>M30 grade of concrete used</i>		
Density, kg/m^3	Poisson's ratio	Elastic modulus, N/m^2
2548.420	0.20	2.74×10^{10}

Table 3 Details of the soil parameters [8,9]

Type of soil	Density, kg/m^3	Poisson's ratio	Elastic modulus N/m^2	Shear wave velocity, m/s
Hard	1600	0.30	1.4976×10^9	600
Medium	1600	0.35	80×10^6	300
Soft	1600	0.40	20×10^6	150

BOUNDARY CONDITIONS

Fixed Base

- Fixed support at the boundary below raft .
- To ensure complete moment transfer the joint between shear wall and beam is restrained in rotation in the Z direction



Building on Raft Resting on Soil

The soil underneath is actually infinite in extent. In a study [7] it is seen that the extent of soil in lateral direction if made nine times to the respective dimension of the structure and the depth of the soil strata is twice the least dimension than the effect of the soil left beyond the zone may be neglected. Later in another study [10] it was seen that the least lateral dimension may be six times to get approximately close results to that of nine times. But due to limitation of calculating capacity the least dimension is hereby considered as only three times with sides are kept restrained appropriately.

- The bottom of the soil is fixed in X, Y and Z direction (X, Z on plan, Y is the vertical axis).
- Along the face parallel to Z-axis the soil is fixed in X-direction.
- Along the face parallel to X-axis the soil is fixed in Z-direction.

Finite Element Modeling

- Beams and columns are modeled as 3D linear thick beam line elements (BM121).
- Shear wall and raft as thick shell with four node quadrilateral (QTS4) linear element.
- Slab is modeled with both triangular (TTS3) and quadrilateral (QTS4) thick shell elements.
- Soil is modeled using 8-noded 3D Solid continuum Element (HX8M).

The iso-metric view of the building frame with soil is shown in Figure 1.

Earthquake Analysis

The building is assumed to be located in seismic zone V [11] and MCE has been taken into analysis.

Seismic Coefficient Method

Based on the formulations given in code of practice IS 1893:2002 the following data has been calculated:

Approximate fundamental natural period of moment resisting frames without brick infill panels is found out =

$$T_a = 0.075h^{0.75} = 2.081s$$

The seismic base shear (V_B) along principal x-direction is shown in Table 3.

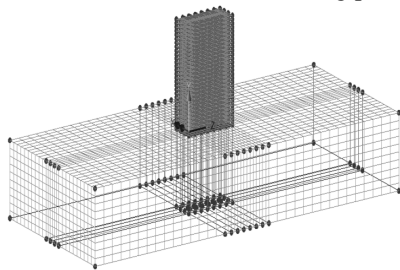


Figure 1 Building with raft foundation resting on soil

Table 4 A_h and V_B of building with fixed base and incorporating SSI

Type	$A_h = Z \frac{S_a}{g}$	$V_B = A_h W, \text{ kN}$
Fixed base	0.1729	83807.990
Hard soil	0.1729	83807.990
Medium soil	0.2353	114120.486
Soft	0.2889	140116.483

The base shear (V_B) computed are distributed along the height of the building as lateral force at i_{th} level $Q_i =$

$$V_B \frac{w_i h_i^2}{\sum_{j=1}^n w_j h_j^2}$$

RESPONSE SPECTRA METHOD

Characterization and Simulation of Earthquake Data

To account for the SSI effect de-convolution-re-convolution is carried out from the simulated data to reproduce the specific ground motion. Earthquake ground motions developed for seismic analyses in the codes are usually provided as outcrop motions. However seismic input must be applied at the base of the model rather than at the ground surface. Thus the appropriate input motion at depth can be computed through a 'de-convolution' analysis [12] using a 1-D wave propagation code such as the equivalent linear program Deep soil 6.1.



To determine the appropriate base input motion applied to the model:

- The target acceleration spectra compatible time histories (TARSCTHS) [13] code generates a synthetic time history of ground acceleration for design elastic response spectra (codal spectra)
- This synthetic time history response is given as an input to DEEP SOIL 6.1 [14] as an within motion and the output in the form of response spectra is obtained at the top of rock (60 m below)

Thus, the response spectra at ground surface for 5% damping according to IS 1893 (Part 1): 2002, converted to factored response spectra at the ground surface corresponding to MCE of Zone V undergoes deconvolution analysis to obtain response spectra at the top of the rock as shown in **Figure 2** which is the applied spectra at the base of soil-structure having 60 m soil strata below the structure.

For checking the correctness of the de-convoluted response spectra, the time history data obtained at the top of rock in DEEP Soil 6.1 is re-convoluted to obtain time-history data at the ground surface. This re-convoluted time history data at ground surface is converted to re-convoluted response spectra which are compared with the factored response spectra obtained from the ISCODE 1893:2002 (Part 1) at the ground surface. It is seen that the code specified and the re-convoluted response spectra at the ground surface are almost same as shown by **Figure 3** for soft soil. Thus the use of Deep soil 6.1 is justified in de-convolution analysis.

The factored MCE response spectra at ground surface corresponding to hard soil are used for the building with fixed base. The de-convoluted response spectra for hard, medium, soft soil as in **Figure 2** is used for response spectra analysis of the building on raft foundation resting on hard, medium, soft soil respectively.

Pseudo Static Method [15]

It is a combination of the static and dynamic method. The lateral forces obtained at each floor from the storey shear distribution of the building from the response spectra analysis are distributed along the height of the building and then linear analysis is performed.

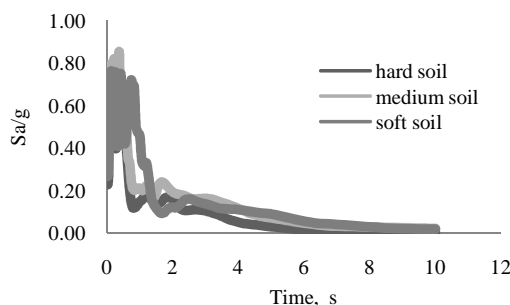


Figure 2 Deconvoluted response spectra at top of rock (at 60m depth) as per IS 1893 (Part 1) : 2002

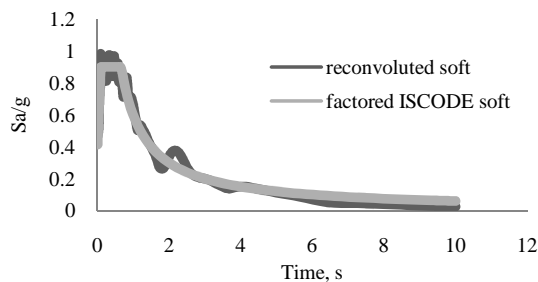


Figure 3 Response spectra at ground surface for soft soil

RESULTS AND DISCUSSIONS

VARIATION OF NATURAL FREQUENCY

From results of the response spectra analysis the importance of considering soil structure interaction is noticed as it affects the fundamental natural frequency of the structure and thus its time-period. It is observed that, the inclusion of soil flexibility in buildings decreases the value of natural frequency.

The decrease is maximum in case of soft soil and minimum in hard soil. The percentage variation in lateral natural frequency incorporating soil stiffness as compared to fixed base condition is tabulated in Table 4. The percentage variation in natural frequency is maximum for building on raft resting on soft soil which is about 38.87% when compared to building with fixed base.

Comparison of Shear Force and Lateral Force Distribution with Storey Level and Base Shear between Seismic Coefficient, Response Spectra and Pseudo-static Method

The seismic lateral vulnerability of structures is reflected by the seismic shear force and lateral force distribution of the structure and essentially of the determination of the base shear which is one of the main parameter in seismic design. The following section shows the comparison of the shear and lateral force distribution of the building with



fixed base and also incorporating soil structure interaction effects. It is observed that the Lateral Force (Q_i for the i^{th} floor) distribution curve obtained from the three methods overlaps each other irrespective of foundation and soil types. However, the Storey Shear Force (V_i acting at the i^{th} floor given by $V_i = \sum_{j=i}^n Q_j$) distribution curves overlaps each other in three methods in the lower stories after which they vary as the building height increases; the variation is maximum in soft soil. It is also seen that the base shear of the structure increases from hard to medium to soft soil. From the three methods it is seen that there is an average increase of base shear by 57.95% for building over raft on soft soil when compared to building with fixed base. The base shear values for fixed base and including SSI effect obtained by Seismic Coefficient Method are less than the values obtained by Response spectra and Pseudo-static methods. The storey shear and the lateral force distribution curve for building on hard and soft soil is shown in Figure 4 and Figure 5, respectively.

Table 4 Percentage variation in natural frequency

Building type	Soil type	Natural frequency, Hz		Variation, %
		Without SSI	With SSI	
Building with fixed base	-	0.4399	-	-
	Hard	-	0.4285	2.6
Building	Medium	-	0.3493	20.59
	Soft	-	0.2689	38.87

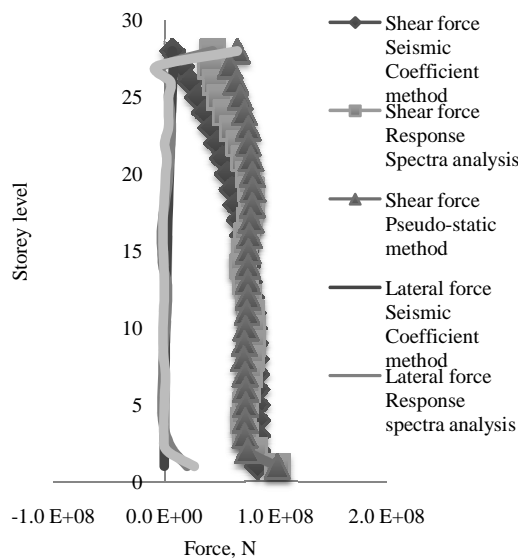


Figure 4 Shear and lateral force distribution of building resting on hard soil

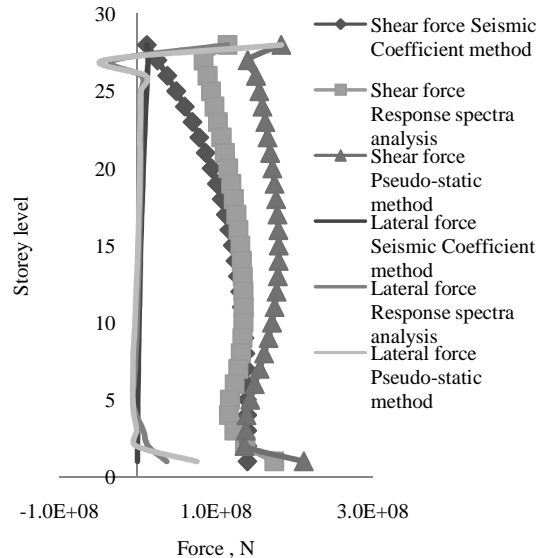


Figure 5 Shear and lateral force distribution of building resting on soft soil

CONCLUSIONS

- Frequency of vibration of structure decreases with soil flexibility by the incorporation of SSI effect when compared to fixed base model.
- The base shear of the building increases with soil flexibility from hard to medium to soft soil.
- The lateral force distribution curve obtained from the three methods (Seismic Coefficient, Spectral Analysis and Pseudo-Static) overlaps each other in case of building with fixed base and while including SSI effect.
- The storey shear curve overlaps each other for three methods in the lower stories while it gradually varies with upper stories, the variation being maximum in soft soil.
- The base shear values obtained by Seismic coefficient method are less than the values obtained by response spectra method and Pseudo-static method showing that the performance of the response spectra and the pseudo-static analysed structure is quite good in resisting the earthquake forces compared to the static analysed structure.



REFERENCES

1. Taranath, B.S. Structural Analysis and Design of Tall buildings. s.l. : McGraw-Hill book Company, (1988).
2. M., Agarwal. P., Shirkhande. Earthquake resistant Design of Structures. New Delhi, India : Printice- Hall of India Private Ltd., (2006).
3. Dynamic Soil Structure Interaction Analysis for Piled Raft Foundation. Chaithra T P, Manogna H N. 7, International Journal Of Engineering And Computer Science ISSN:2319-7242 , Vol. 4, pp. 13601-13605(2015).
4. Soil Structure Interaction Effect On Dynamic Behavior Of 3d Building Frames With Raft footing. —, Kuladeepu M N, Vol. 4, pp. 87-91(2015) .
5. Soil Structure Interaction Analysis on a RC Building with Raft foundation under Clayey Soil Condition. Roopa, Naikar, Prakash. 12, International Journal of Engineering Research & Technology (IJERT) ISSN: 2278-0181, Vol. 4(2015).
6. Modeller Reference Manual Version 15.2 LUSAS. Kingston upon Thames, Surrey, United Kingdom (2016).
7. Dynamic soil-structure interaction effects on the seismic response of assymetric buildings. A Shakib, A Fuladgar, ELSEVIER, Soil Dynamics and Earthquake Engineering, pp. 379-388(2014) .
8. Soil-Structure interaction effects on seismic response of a 16 storey RC framed building with shear wall. Chinmayi H.K., Jayalekshmi B.R. American Journal of Engineering Research (AJER) e-ISSN : 2320-0847 p-ISSN : 2320-0936, Vol. 2, pp. 52-58(2013)
9. APPC-Soil properties , SK Kong-Academia-edu. https://www.academia.edu/8149496/APPC-Soil_properties. [Online]
10. Chakraborty, Abhijit. Earthquake response of 3D Asymmetric building with infill wall under soil-structure interaction(2017).
11. IS: 1893 (Part – 1) – 2002 - Code of Practice for Criteria for Earthquake Resistant Design of Structures, Part 1: General Provisions and Buildings, Bureau of Indian Standards. .
12. Earthquake deconvolution for FLAC. L.H media, E.M Dawson,4TH International FLAC Symposium on Numerical Modelling in Geomechanics-2006-Hart and Verona (eds). pp. 4-10 (2006).
13. TARSCTH-User's Manual, Version 1.0 . Engineering Seismology Laboratory (ESL) in the State University of New Work at Buffalo.
14. Hashash, Y.M.A., Musgrove, M.I., Harmon, J.A., Groholski, D.R., Phillips, C.A., and Park, D. DEEPSOIL 6.1, User Manual. (2016).
15. Sarma, T.S. Design of R.C.C Buildings using STAAD PRO V8I with Indian examples, Static and Dynamic methods.



Assessment of Lattice Towers through Web Integrated Technologies

Srinivas Tanuku^{1}, Ganesh Kolli¹, Sayi Raghu Ram Achanta¹
RAMBOLL India Private Limited, Hyderabad, Telangana, India¹, srinit@ramboll.com**

ABSTRACT

In India, Telecom user base is growing exponentially which demands more number of towers. Nearly 4,50,000 towers were built, and tower population expected to grow further in coming years to cater the on-going demand. Department of Telecommunication, India (DOT) has encouraged operators to share the passive infrastructure in order to reduce capital cost and carbon foot print. Hence, A critical review on structural safety of existing tower plays major role to ensure controlled implementation of antenna equipment at elevated heights. Traditional approach on assessment of lattice tower may not be sufficient for highly time dependent domain, may result in loss of user base for untimely response. In this paper, an approach on Assessment of Lattice Towers through web integrated technologies are presented through back ground study, basic system requirements along with presentation of project case study followed by summary on integrated approach for assessment of telecom towers are presented. From the detailed analysis, it is concluded that Assessment of lattice tower through web technologies integrating project management and engineering analysis is best reliable solution for faster response, accurate results and handling of data analytics at larger numbers along with green initiation to ensure controlled implementation of additional loading.

KEYWORDS Telecom Lattice towers, Structural Assessment, Analysis, Tower database Management

INTRODUCTION

In India, nearly 4,50,000 Towers were built by operators / infrastructure providers in different phases from nearly two decades by using various tower structural designs. Some of tower designs are well documented-known design, some of them are not documented - unknown designs. In view of dynamically challenging business scenario, few of telecom infrastructure companies were merged to reduce the capex cost as well carbon foot print and aligned to sharing of passive telecom infrastructure between operators as per guidelines given by Department of Telecommunication, India (DOT). Therefore, an engineering activity shall be required to ensure controlled implementation of additional loading on existing towers. This activity basically consists – to group all existing towers in to known and unknown designs followed by tower feasibility study for existing and proposed loading on tower with or without strength enhancement techniques. Structural Engineering Integrated with software technology (including web based technologies) is best realistic solution on handling huge number of towers through uniform approach in the highly time dependant domain.

In this paper, an approach on Assessment of Lattice Towers through web integrated technologies are presented through back ground study, basic system requirements along with presentation of project case study followed by summary on integrated approach for assessment of telecom towers.

BACKGROUND

Number of Tower IP Companies are merging in order to reduce the capital investment. Detailed understanding on the conditional assessment of telecom structures and their adequacy is highly essential during merging of different entities in to single entity. In these scenario, engineering activity being taken up IP Companies from different locations for defined objective which can resulted in following deficiencies in this approach, that is,

- Non-Uniform approach due to level of different competencies
- Not setting end objective clearly
- Doubtful on overall qualitative conclusions
- Challenge on meeting quantitative demands from Operators due to coordination of different stake holders
- Handling of data logistics

Therefore, a systematic web based integrated approach on conditional assessment of structures is best reliable approach and is essential solution to handle dynamically challenging time dependent Telecom Sector. Following are basic advantages on web based integrated approach compared to traditional.

- Well defined uniform structured approach
- Easy Handling / retrieval of numerous data



- Faster response to the service request raising by operator
- Centralized data monitoring and controlling
- Effective stake holder management through well-defined communication channel.
- Reduces unnecessary tasks / duplicate efforts which leverages cost and time.
- Dedicated focus while refinement of technical processes and advancement of solutions
- Overall quality assurance through defined decision gates in process

BASIC REQUIREMENT FOR INTEGRATED APPROACH

Defining of basic requirements is very important milestone for sustainability of the system. The requirements are majorly depending on stake holder, that is, Operator, IP Companies, Structural Engineer, Filed Engineer, Project Manager, Statutory requirement etc. Typical requirement against each major stake holder are presented in **Table 3.1**.

Table 3.1 Typical basic requirements from each stake holder

Stake Holder	Basic Requirements
1 Operator	Faster Response to Service Request Adherence to Statutory Requirements Effective Stake Holder Management Easy Access to Milestone progress reports Data Management and Analytical Reports Controlling & Monitoring of Scope of Work, SLA Adherence etc.
2 Infrastructure Companies	Adherence to Statutory Requirements Access to site wise technical results Identification of Extremely critical sites, Action plan Easy to Draw Risk Mitigation Plan Forecast reports on Business potentiality based on Structural safety Planning based on Site Geographical location through digitalized Maps Provision for Uploading Survey Data Bulk Uploading of Site data (Report, Photos Etc.) Easy Graphical Interface for entering mandatory Fields Access to Project Progress reports along with Milestones
3 Structural Engineering	Basic Validation by System on Field Data Accuracy Efficient Communication Channel between stake holders. Integrated Tower Design Database - Access, Retrieval, Amendments Structural Analysis through web integrated technologies Auto Generated technical feasibility Reports Provision for Engineering Judgement at Each Decision Gates Online Report Submittals and Customer Acceptance Identification of Extremely Critical Sites

PROJECT CASE STUDY

The concept of web integrated approach has been initiated through critical review of basic requirements of each stake holder and web – integrated system is developed and deployed for successful execution of project. Following sections are outlined detailed project flow and system capabilities which are used during project execution along with highlighting benefits of integrated approach.

Project Process Flow

Project initiated with collection of basic requirements from customer after duly approval of design checking criteria being followed in rest of project. Decision gates were set at different stages – Pre-Processing, Survey (Partial / Full), Tower Design Classification, Engineering analysis followed by auto generated feasibility report through engineering judgement. Site which are not adequate during analysis were routed to development of solution and submission of relevant BOQ for implementation.

Integrated Tower Design Database

Unified Master design database module has been created in web tool which enabled features, that is, addition, modification and deletion of respective tower design along with unique code against each design. Unique code



generally contains – Tower Type, configuration, tower height, wind speed, consultant originally designed, this unique code is very much helpful on validation of tower feasibility results with original designed condition.

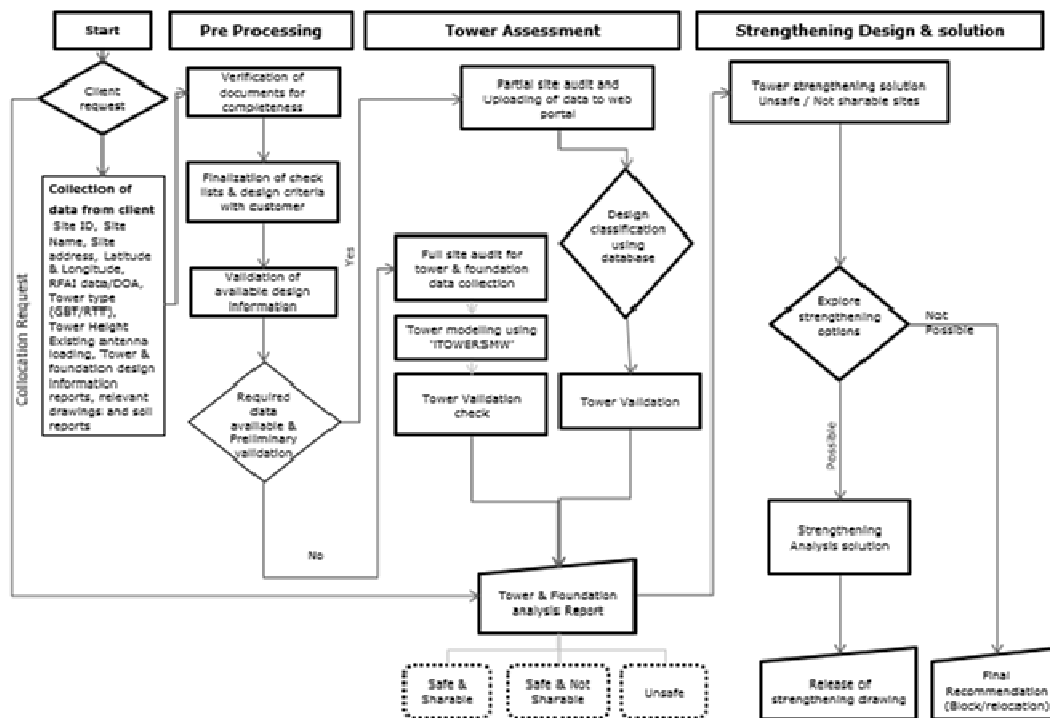


Figure 4.1 Project process flow

Software Tool Capabilities

Project management tool with integration of engineering software is used in web application for quick response on feasibility of each site.

Typical Project Management tool capabilities are listed below.

- Defining Base Lines, Milestones, durations
- Assign Responsibilities
- Handover between interfaces
- Reporting structure and Focus
- Undisputed data (one version – one original)
- Forecasting capabilities based on undisputed data
- Clearly identifiable bottlenecks through milestone.

Engineering software capabilities used in project listed below.

- 3D Modelling with secondary members
- Geometry creating using Predefined Template
- Auto Pattern library
- Auto reports and Drawings
- Easy to implement new amendments in standards
- Customized reports based on project requirement.





Figure 5.1 Typical progress report

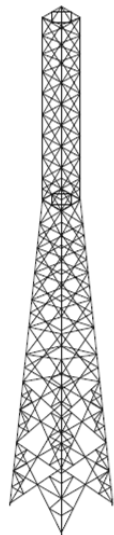


Figure 5.2 3D analysis model (Typical)

Project Highlights

An integration of project management and engineering software in web integrated technologies are resulted in smooth execution of project and nearly 50,000 towers were assessed over 5 years period with structured approach resulted in faster response on sharing request and optimum utilization of resources.

ONCLUSION

From the details discussion in previous sections, Assessment of lattice tower through web technologies integrating project management and engineering analysis is best reliable solution for faster response, accurate results and handling of data analytics at larger numbers along with green initiation.

REFERENCE

1. Emil Simiu, Robert H. Scanlan., Wind Effects on Structures, Fundamentals and Application to Design, Third Edition, John Wiley & Sons, Inc. 1996
2. <https://tarangsanchar.gov.in>
3. https://en.m.wikipedia.org/wiki/Web_API
4. <https://docs.microsoft.com/en-us/aspnet/web-api/overview/getting-started-with-aspnet-web-api/tutorial-your-first-web-api>
5. IS: 875 (Part 3) 1987 Wind Loads – Code of Practice for Design Loads (Other than Earthquake) for Buildings and structures.
6. IS: 802 (Part 1/Sec 2) 1995 Material, Loads and Permissible Stresses – Use of Structural Steel in Overhead Transmission line towers
7. IS: 806 1968 Use of Steel Tubes in General Building Construction.
8. IS: 1161 2014 Steel Tubes for Structural Purposes - Specifications
9. N. Subramanian, Design of Steel Structures, Oxford University Press, India, 2008
10. Ronald D. Ziemian (Editor), Guide to Stability Design Criteria for Metal Structures, Sixth Edition, John Wiley & Sons, Inc. 2010



Experimental Studies on the Performance of Hybrid Fiber (Areca nut + Plastic) Reinforced Concrete

M.N Sumukh^{*1}, Manjunath Itagi¹, B.P. Annapurna¹

Department of Civil Engineering, University Visvesvaraya College of Engineering, Bangalore University, Bangalore¹,
sumukhmn87@gmail.com*

ABSTRACT

This study presents the performance of Hybrid Fiber Reinforced Concrete (HFRC). Fibre Reinforced concrete (FRC) is a composite material consisting of mixture of cement based matrix with random distribution of fibers. The variation of two or more fibers is called as hybrid fiber reinforced concrete. In this study an attempt is been made to study the influence of hybrid fiber of Areca nut fiber (natural fiber) and Plastic fiber (industrial waste -wind mill waste). Fiber Reinforced Concrete acts as crack resistor and substantially improve its properties. The dispersion of fiber in concrete is been studied for two types of dispersion. (i) Dispersion in overall Concrete of the specimen (both in tension and compression zone). (ii) Dispersion in concrete of the Tension zone. The effect of fiber has been studied for different percentages of fiber 0.5% to 2.0% by weight of cement with variation of 0.5% i.e. 0.5%, 1.0%, 1.5%, 2.0%. The Grade of concrete is M20. The use of two or more types of fibers in a suitable combination potentially improve the overall properties of concrete and result in better performance of concrete. As a result of hybridization of fiber it has the ability to arrest cracks, increased extensibility and tensile strength, both at first crack and ultimate load, particularly under flexural loading.

KEYWORDS Areca nut fiber, Plastic fiber, Dispersion, Compression Zone, Tension Zone.

INTRODUCTION

Fiber Reinforced Concrete (FRC) is a concrete containing fibrous material which increases structural integrity. It is a short discrete fibers that are uniformly dispersed and randomly oriented. Fiber reinforced concrete with mono fiber system provides limited enhancement of properties. Therefore for better, improved performance. Combining two different fiber at suitable proportion in concrete can offer more attractive engineering properties because the presence of one fiber enables the more efficient utilization of potential properties of other fiber.

The variation of two or more fibers is called as hybrid fiber reinforced concrete. The function of short-cut fibers as a secondary reinforcement in concrete is mainly to inhibit the crack initiation and propagation. This research focuses on the hybrid fiber of natural and industrial fiber such as Areca nut fiber and plastic type of fiber (wind mill waste).

Need for the Present Work

The use of fibers in cement concrete mix has altered the behaviour of fiber-matrix composite after it has cracked, and caused in improvement in toughness. Due to improper curing, Cracks will develop. So Use of fibers arrest the crack and increases structural integrity. Hence Areca nut fiber and plastic fiber can be utilized as the reinforcing material in the concrete.

Objective

Aim of the study is to utilizing the natural fiber and industrial waste fiber such as Areca nut fiber and plastic fiber is utilize in useful manner and to reduce the problem of disposal.

Scope of the Work

- Firstly an experimental work is carried out to investigate the mechanical properties of M20 grade concrete with addition of Areca nut fiber by 0.5% to 2.0% by weight of cement with a variation of 0.5% (0.5%, 1.0%, 1.5% and 2.0%).
- With addition of equal proportions in Areca nut + plastic fiber by 0.5% to 2.0% by weight of cement with a variation of 0.5% (0.5%, 1.0%, 1.5% and 2.0%).
- Secondly an experimental work is carried out to study the flexural strength of slabs of size 600 × 600 × 60 mm of M20 grade concrete. (i) with addition of Areca nut fiber by 0.5% to 2.0% by weight of cement with a variation of 0.5% (0.5%, 1.0%, 1.5% and 2.0%). (ii) with addition of equal proportions in Areca nut + plastic fiber by 0.5% to 2.0% by weight of cement with a variation of 0.5% (0.5%, 1.0%, 1.5% and 2.0%). The flexural



strength of slab is studied for two types of dispersion of fibers, (i) Dispersion of fibers both in compression and tension zone (ii) Dispersion of fibers in critical tension zone. (Bottom depth of 30 mm) Description of concrete specimen is presented in **Table 1**.

EXPERIMENTAL INVESTIGATION

Materials

1. Cement-Ordinary Portland cement of 53 grade, specific gravity -3.15, initial setting time -55min and final setting time -550 min.
2. Fine aggregate - Locally available M- sand confirming to grading zone II of IS 383-1970, passing through IS 4.75 mm sieve and specific gravity - 2.65.
3. Coarse aggregate - Locally available crushed granite stones confirms to the specification of IS 383-1970 and it passing through 12.5mm sieve and retained on 4.75mm sieve.
4. Water - Ordinary portable water.
5. Arecanut fiber- The fiber is obtained from Arecanut Seeds, length -25 mm and dia -0.25 mm.
6. Plastic fiber- The plastic fiber is of windmill waste, length -25 mm and dia. - 0.3 mm.

Mix Design

Using the properties of materials listed above the mix design for M20 grade of concrete has been designed as per IS 10262-2009. The concrete mix ratio obtained is 1:2.12:2.15.

Experimental Programme

Firstly the experimental program is designed to evaluate the properties of M20 grade concrete with addition of fibers: (i) Arecanut fiber and (ii) Arecanut + plastic fiber. The standard cubical (100 mm × 100 mm × 100 mm), cylindrical (length 300 mm and dia -150 mm) and prismoidal (100 mm × 100 mm × 500 mm) specimens were casted with and without fibers. In the first series the specimen were casted with Arecanut fibers (CAF) of 0.5%, 1.0%, 1.5% and 2.0%. In the second series the specimens were casted with equal proportions in Arecanut + plastic fiber (CAPF) for varying percentage of fibers 0.5%, 1.0%, 1.5% and 2.0%.

Secondly the slab of size 600mm×600mm×60mm of M20 grade concrete with addition of fibers: (i) Arecanut fiber and (ii) Arecanut + plastic fiber. The slabs were casted for two types of dispersion of fibers: (i) Dispersion of fibers both in compression and tension zone (ii) Dispersion of fibers in critical tension zone.

Testing of Specimen

After curing the specimens for 28 days. Concrete cubes, prism and cylinders for various percentages of fibers were tested for compression, flexural and split tensile strength respectively according to IS specification.

The slabs of 600 mm × 600 mm × 60 mm size for different percentage of fibers were casted and cured for 28 days. After curing the slabs were tested for nine point loading, placing the slab simply supported on all four side as shown in **Figure 1**. The load and deflections were recorded.

RESULTS AND DISCUSSION

Compressive Strength of Cubes

Figure 2 presents the compressive strength of concrete with Arecanut fiber (CAF) and Arecanut+plastic fiber (CAPF) along with the conventional concrete (CC - 0% Fiber). From the figure it is observed that with the addition of fibers the compressive strength increases compared to conventional concrete.

For concrete with addition of arecanut fiber compare to conventional concrete of 0.5%, 1.0%, 1.5% and 2.0% the increase in strength is observed to be 5.5%, 9.7%, 10% and 9.3% respectively. With the addition of equal proportion of Arecanut + plastic fiber the strength enhances, compared to the concrete with only Arecanut fiber. For 0.5%, 1.0%, 1.5% and 2.0% of concrete with Arecanut + plastic fiber the increase in strength is 10%, 17.4%, 21.4% and 20% respectively compared to conventional concrete.

Flexural Strength of Prisms

Figure 3 presents the variation of flexural strength of concrete for different % of fibers with Arecanut fiber (CAF), Arecanut + plastic (CAPF) fiber and conventional concrete (CC -0% fiber). From the figure it is observed that with the addition of fibers the flexural strength of FRC increases compared to conventional concrete. The increase in flexural strength is higher than compressive strength.



Table 1 Description of concrete specimen

Description of concrete	Designation	Percentage of fiber	Number of specimen		
			cubes	prism	cylinder
Conventional Concrete	CC	0	3	3	3
FRC with Arecanut fiber for varying % of fiber (0.5% to 2.0%)	CAF	0.5	3	3	3
		1	3	3	3
		1.5	3	3	3
		2	3	3	3
		0.25+0.25	3	3	3
FRC with Arecanut + plastic fiber for varying % of fiber (0.5% to 2.0%)	CAPF	0.5+0.5	3	3	3
		0.75+0.75	3	3	3
		1+1	3	3	3
		0.5	1 slab		
FRC Slab with Arecanut fiber dispersed both in compression and tension zone for varying % of fiber (0.5% to 2.0%)	SCAF(CT)	1	1 slab		
		1.5	1 slab		
		2	1 slab		
		0.5	1 slab		
FRC Slab with Arecanut fiber dispersed in critical tension zone for varying % of fiber (0.5% to 2.0%)	SCAF(T)	1	1 slab		
		1.5	1 slab		
		2	1 slab		
		0.5	1 slab		
FRC Slab with Arecanut + plastic fiber dispersed both in compression and tension zone for varying % of fiber (0.5% to 2.0%)	SCAPF(CT)	1	1 slab		
		1.5	1 slab		
		2	1 slab		
		0.25+0.25	1 slab		
FRC Slab with Arecanut + plastic fiber dispersed in critical tension zone for varying % of fiber (0.5% to 2.0%)	SCAPF(T)	0.5+0.5	1 slab		
		0.75+0.75	1 slab		
		1+1	1 slab		
		0.5	1 slab		



Figure 1 Experimental set up of testing of slab

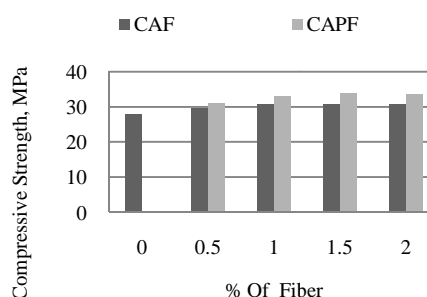


Figure 2 Comparison of compressive strength of concrete with different % of fiber

The fiber reinforced concrete with addition of Arecanut fiber (CAF) when compared to conventional concrete. For a fiber content of 0.5%, 1.0%, 1.5% and 2.0% the increase in strength is observed to be 11.7%, 14.3%, 18.9% and 9.6% respectively. For 0.5%, 1.0%, 1.5% and 2.0% of Arecanut + plastic fiber(CAPF) in FRC compare to conventional concrete the increase in strength is 28.4%, 31.5%, 33% and 30% respectively.

Split Tensile Strength of Cylinder

Figure 4 presents the split tensile strength of concrete with CAF and CAPF along with the conventional concrete. From the figure it is observed that the split tensile strength increases with the addition of fibers and the strength is maximum at 1.5% of CAPF.

For concrete with addition of CAF of 0.5%, 1.0%, 1.5% and 2.0% the increase in strength is observed to be 7.4%, 13%, 15% and 10.3% respectively when compared to conventional concrete. For 0.5%, 1.0%, 1.5% and 2.0% of



concrete with CAPF the increase in strength is 21.4%, 25.5%, 27.7% and 27.7% respectively compared to conventional concrete.

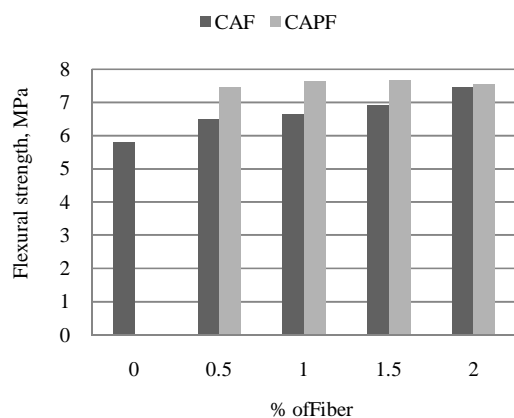


Figure 3 Comparison of flexural strength of concrete with different % of fiber

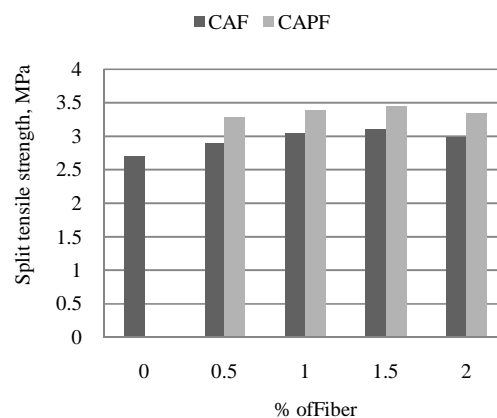


Figure 4 Comparison of split tensile strength of concrete with different % of fiber

Test on Slabs

First Crack Load

Figure 5 presents the first crack load of FRC slabs with Arecanut fiber (SCAF) and hybrid fiber of Arecanut + plastic (SCAPF) fiber for different % of fibers along with the conventional concrete.

Fiber reinforced concrete slab of Arecanut fiber dispersed in both tension and compression zone (SCAF(CT)) of 0.5%, 1.0%, 1.5% and 2.0% the increase in first crack load is observed to be 4.4%, 14.3%, 25% and 24% respectively when compared to conventional concrete. Concrete with addition of Arecanut fiber dispersed in critical tension zone (SCAF(T)) of 0.5%, 1.0%, 1.5% and 2.0% first crack load increases by 12.4%, 25.9%, 35% and 33% respectively compared to conventional concrete.

Concrete with equal proportion of Arecanut + plastic fiber dispersed in both tension and compression zone (SCAPF(CT)) the increase in first crack load for 0.5%, 1.0%, 1.5% and 2.0% fiber is 13%, 25.8%, 33% and 27% respectively compared to conventional concrete. Concrete with Arecanut + plastic fiber dispersed in critical tension zone (SCAPF(T)) the increase in first crack load is 19.5%, 35.7%, 38.4% and 36.6% for 0.5%, 1.0%, 1.5% and 2.0% fiber content respectively compared to conventional concrete.

Deflection at First Crack Load

Figure 6 presents the deflection at first crack load of FRC slabs with Arecanut fiber and hybrid of Arecanut + plastic fiber and the conventional concrete. From the figure it is observed that with the addition of fibers the deflection at first crack load increases compared to conventional concrete.

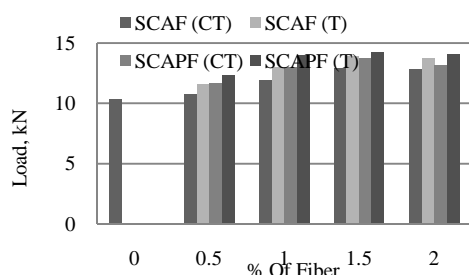


Figure 5 Comparison of first crack load of slab with different % of fiber

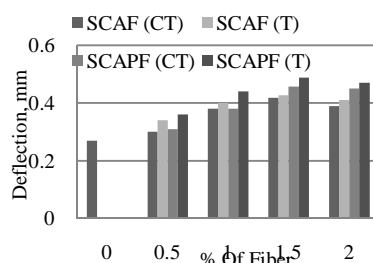


Figure 6 Comparison of deflection at first crack load of slab with different % of fiber



For FRC slab with SCAF(CT) compared to conventional concrete(SCC) the increase in deflection at first crack load for fiber 0.5%, 1.0%, 1.5% and 2.0% is observed to be 11%, 40.7%, 54% and 44% respectively. For FRC slab with SCAF (T) with addition of fiber of 0.5%, 1.0%, 1.5% and 2.0% the increase in deflection at first crack load is observed to be 25%, 48%, 58% and 51% respectively compared to conventional concrete.

For 0.5%, 1.0%, 1.5% and 2.0% addition of fiber of SCAPF(CT) compared to conventional concrete the increase in deflection at first crack load is 14.8%, 40.7%, 70% and 66% respectively, for SCAPF(T) the increase in deflection at first crack load is 33%, 62%, 77% and 74%, respectively.

Ultimate Load

Figure 7 presents the ultimate load of FRC slabs with Arecanut fiber, Arecanut + plastic fiber and Conventional concrete.

With addition of Arecanut fiber of 0.5%, 1.0%, 1.5% and 2.0% For SCAF(CT) compared to conventional Concrete the increase in ultimate load is observed to be 2.3%, 5.6%, 9.3% and 8.6% respectively, For SCAF(T) the increase in ultimate load is observed to be 4.7%, 8.5%, 11.8% and 9.7% respectively compared to conventional concrete.

For fiber content 0.5%, 1.0%, 1.5% and 2.0% of concrete in SCAPF(CT) the increase in ultimate load is 4.5%, 8.29%, 12.4% and 9.6% respectively compared to conventional concrete, for SCAPF(T) compare to SCC the increase in ultimate load is 6.2%, 10.72%, 14.9% and 10.2% respectively. However in FRC slab with the addition of fibers the increase in first crack load is considerably higher compared to increase in ultimate load.

Deflection at Ultimate Load

Figure 8 presents the deflection at ultimate load of FRC slabs with Arecanut fiber and Arecanut + plastic fiber along with the conventional concrete. From the figure, it is observed that FRC slab with the addition of fibers the corresponding deflection of FRC slab at ultimate load increases substantially compared to conventional concrete.

For SCAF(CT) compared to conventional concrete addition of fiber 0.5%, 1.0%, 1.5% and 2.0% the increase in deflection at ultimate load is 3.6%, 8.5%, 34.3% and 22%, respectively, for concrete SCAF(T) the increase in deflection at ultimate load is 6.7%, 18.4%, 43% and 39%, respectively.

For fiber content of 0.5%, 1.0%, 1.5% and 2.0% of SCAPF(CT) the increase in deflection at ultimate load compared to conventional concrete is 5.5%, 14%, 41% and 28% respectively, for SCAPF(T) the increase in deflection at ultimate load is 8.58%, 21.4%, 46.6% and 43% respectively compared to conventional concrete.

Cracks in Slabs

Figures 9,10 and 11 shows the cracks produced in the slabs SCC, SCAF, SCAPF for 1.5% fiber, from the figure, it is been observed that the number of cracks produced are very less in slabs SCAPF slabs compared to SCAF and SCC slabs. However in SCAPF (T) slabs the cracks are further reduced than the SCAPF (CT) slab.

Side and only on tension side, with 1.5% of Arecanut fiber.

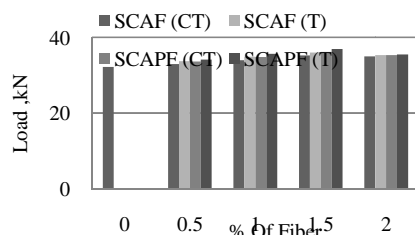


Figure 7 Comparison of ultimate load of slabs with different % of fiber

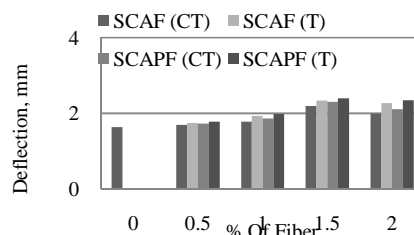


Figure 8 Comparison of deflection at ultimate load of slabs with different % of Fiber

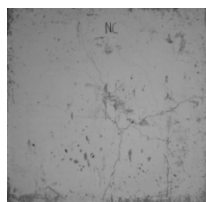
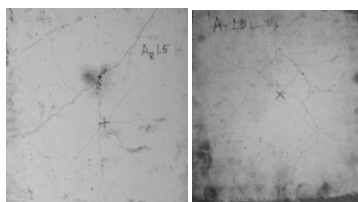
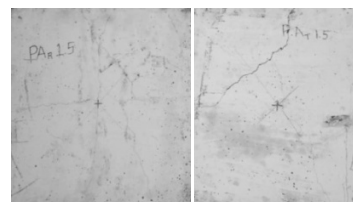


Figure 9 Crack pattern of conventional concrete slab



SCAF (CT)
Figure 10 Crack in FRC slab SCAF when concrete is dispersed on the compression and tension



SCAPF (CT) SCAPF (T)
Figure 11 Crack in FRC slab SCAPF when concrete is dispersed on the compression and tension

CONCLUSION

- The mechanical property of FRC and flexural strength of FRC slab increases with the addition of fiber up to 1.5%. Though there is decrease in strength for 2% but compared to conventional concrete the strength of FRC is higher. Thus the addition of Fiber to the concrete enhances its Strength.
- The concrete with equal proportion of Arecanut + Plastic fiber shows the maximum increase in compressive strength, split tensile strength and flexural strength compared to conventional concrete, for CAPF with 1.5% fiber the strength is found to be increased by 21.4%, 27.7% and 32.25% respectively.
- The FRC slabs with fiber dispersed on the tension side shows maximum increase in its strength, first crack load, ultimate load and their corresponding deflections.
- The addition of Fiber to the concrete shows maximum increase in the First crack load and its corresponding deflection compared to ultimate load.
- The first crack load and its corresponding deflection of FRC slabs of SCAPF (T) with 1.5% fiber compared to conventional concrete is found to be increased by 38.4% and 77% respectively.
- The ultimate load and its corresponding deflection of FRC slabs of SCAPF(T) with 1.5% fiber compared to conventional concrete is found to be increased by 14.9% and 46.6% respectively.
- The slab with Fiber dispersed on Tension side, SCAF (T) and SCAPF (T), shows more resistant to crack propagation. Number of cracks produced are considerably less compared to SCC, SCAF (CT) and SCAPF (CT).

REFERENCES

1. R.H.Mohankar, M.D.Pidurkar, P.VThakre, S.S.Pakhare, Hybrid Fibre Reinforced Concrete, International Journal of Science, Engineering and Technology Research (IJSETR), Volume 5, Issue 1, January 2016.
2. Jirobe Sudheer, S Brijbhushan, P D Maneeth, Experimental Investigation on Strength and Durability Properties of Hybrid Fiber Reinforced Concrete, International Research Journal of Engineering and Technology (IRJET) Volume 02 Issue 05 August 2015, pp. 891-896.
3. G. C. Mohan Kumar, A Study of Short Areca Fiber Reinforced PF Composites, Proceedings of the World Congress on Engineering 2008 Volume II WCE 2008, July 2 - 4, 2008, London, U.K.
4. Raghuveer H. Desai, L. Krishnamurthy, T. N. Shridhar, Effectiveness of Areca (Betel) Fiber as a Reinforcing Material in Eco-friendly Composites: A Review, Indian Journal of Advances in Chemical Science S1, pp.27-33, 2016.
5. N. Ramesh, Tasneem Abbasi, S. M. Tauseefand, S. A. Abbasi, Utilization of fiber-reinforced plastic (FRP) waste generated by a wind-turbine manufacturing company, International Journal of Engineering and Scientific Research Volume 6 Issue 2, February 2018, ISSN: 2347-6532, pp.103-129.
6. R. Kandasamy and R. Murugesan, Fibre reinforced concrete using domestic waste plastic as fibres, ARPN Journal of Engineering and Applied Science. Volume 6, Number 3, pp. 75-82, 2011.
7. C.V. Srinivasaa, A. Arifullab, N. Gouthamb, T. Santhoshb, H. J. Jaeethendrab, R. B. Ravikumarb, S. G. Anilb, D.G. SanthoshKumarb, J. Ashishb, Static bending and impact behaviour of areca fibers composites, Materials and Design 32, pp. 2469-2475, 2011.



Mix Design Methodology for Concrete Paving Blocks in India

B.C.Panda¹, P. K.Parhi^{*2}

Department of Civil Engineering, IGIT, Sarang, Dhenkalal, Odisha¹

Department of Civil Engineering, CET, Bhubaneswar, Odisha², pkparhi@cet.edu.in*

ABSTRACT

Concrete Paving Blocks (CPB) are of the size of bricks and are used in interlocking concrete block pavement (ICBP) systems, which consists of concrete blocks connected together with jointing sand, placed on bedding sand over a suitable sub-base. Immediate use after installation reuses of original blocks, ease of placing and removal, and aesthetic appeal makes it popular for use in urban areas. In recent years, there has been a heavy demand in India and for which a necessity in the principles of the mix design procedure for production of concrete paving blocks has been inspired. This research study will present the mix design procedure for concrete paving blocks as per specific requirements and as laid in relevant guidelines in Indian environment. Based on the developed procedure, cube as well as paving block specimens have been prepared and experimental results be provided for easy implementation of the process.

KEYWORDS ICBP, CPB, Mix design, Compressive strength.

INTRODUCTION

Interlocking Concrete Block Pavement (ICBP) consists of discrete blocks of brick-size units, which are laid on thin bed of coarse sand by using vibration between edge restraints. These blocks are glued together by spreading and inserting the fine sand (jointing sand) from top with help of a plate vibrator. Concrete Paving Blocks (CPB) along with bedding and jointing sand function the purpose of both wearing and base course and form a composite layer called as Equivalent Block Layer (EBL). The EBL is constructed over a sub base layer on sub-grade. The cross section of the whole pavement is shown in **Figure 1** [1]. Over past 75 years, ICBP has been used as an alternative to conventional concrete and asphalt pavement for special application in typical situations or specific problem areas. ICBP has been widely applied in many countries of world like Argentina, Australia, Canada, China, France, Germany, Israel, Italy, Japan, Netherlands, New Zealand, South Africa, UAE, UK, and USA. Since 35 years, the use of ICBP has started in India especially in footpaths, parking lots, garden, city roads, petrol pumps, industrial floors, ports and harbor areas, boarder roads, etc.

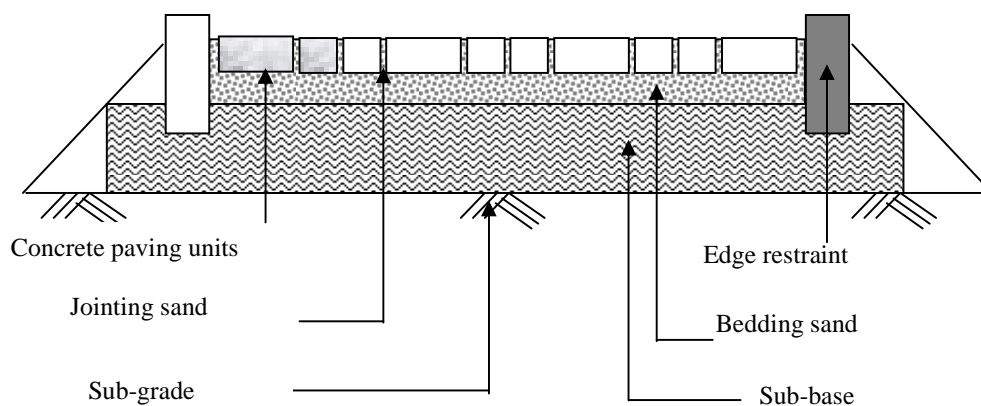


Figure 1 Components of a concrete block pavement [1]

CPBs are mass-produced from semi-dry concrete mixes [2]. To accomplish denseness, high compressive strength and durability of blocks, vibration or pressure or both of them are applied to the mix during the manufacture process [3]. There exists a huge demand for the paving blocks in the country and is increasing linearly year to year. Little investigations have been carried out in India for development of appropriate mix design procedure specific to manufacturing requirement for paving blocks. Therefore, there is a need to develop a local mix design method using available scientific guidelines (IS 10262-2009, IS 15658:2006, IRC: SP:63-2004, IS 456:2000) [2-6]. This paper will discuss various factors affecting the mix design of concrete and will present a simple mix design procedure for the use of engineers and manufacturers for mass production of paving blocks. As per the developed procedure, M30



grade concrete and CPBs of 80 mm, 100 mm and 120 mm will be prepared in the laboratory. Finally, the mechanical properties thereof will be determined at 7 and 28 days and corresponding results will be presented.

BACKGROUND

General Requirement

The fundamental aspect of mix design is to obtain adequate strength and quality in hardened state and sufficient workability and cohesiveness of the plastic concrete with as lean a mix as possible [3]. In general, the compressive strength and durability of concrete of given proportions increase with reduction in ratio of water to cement and at the same time, the workability decreases. The reverse is true with increase in the water/cement proportion. Thus, there is a need to establish the relationship between these properties and the characteristics of the mix, that governs the procedure for selecting the mix proportions. IS 10262: Indian standard concrete mix proportioning – guide lines provide the procedure for proportioning concrete mixes concrete making materials (IS 10262-2009)[4]. In general, it is applicable to standard concrete grades for use in a number of concrete structures like beam, slab, coulomb, pier, bridge, pavement, etc. However, there are specific quality requirements for CPBs for which the mix design procedure should be suitably modified as per guidelines meant for the same.

Dowson was the first researcher to propose separate mix design procedure for concrete paving blocks [3]. After that globally, several researchers have developed different mix design methods as per suitability for manufacture of concrete paving blocks. Cement Concrete Institute of South Africa has recommended basic principles of mix design to assist manufacturers for producing a durable and consistent quality of concrete blocks (SABS 1058:2002)[7]. Nanda et. al. have successfully replaced 50 % of fine aggregate by of crusher dust for making CPBs[8]. Natraj and Das have made concrete paving blocks by replacing 50 % of natural aggregate with recycled aggregate with mixed proportion of 1:1.5:3 with W/C of 0.5 [9]. Sachdeva et. al. [10] have developed different concrete mix starting from M30 to M50 by replacing cement up to 40% by fly ash. Santhos and Talluri have manufactured paving blocks by replacing cement with fly ash at varying percentage (i.e. 0, 10, 20, 30 and 40)[11]. Gawatre et. al. have tested paving blocks by replacing coarse aggregate with demolished concrete waste up to 13.25 % for M35 grade of concrete[12]. Sultan et. al. have performed experiments on concrete paving blocks by replacing natural aggregate with demolition concrete wastes for a target design strength of 33 MPa[13]. It is found that most of the studies have followed the mix design procedure laid in IS 10262:2009 without considering the guidelines specific to IS 15658:2006 and IRC: SP:63-2004 specially published for production of CPBs. Hence, there is a need to follow IS 10262:2009, IS 456:2000, IS 15658:2006 and IRC: SP:63-2004 simultaneously in the mix design for manufacturing concrete paving blocks in India[4-7].

Specific Requirements of Concrete Paving Blocks

As per IRC : SP : 63 guidelines for the use of interlocking concrete block pavements, for the manufacture of paving units a dry, low-slump concrete mix is required (IRC: SP:63-2004). Also, there are certain requirements as per IS 15658 : 2006 : Precast Concrete Blocks for Paving – Specification. The following desired specific characteristics are required for use of concrete paving blocks.

(i) Grade of Concrete Mix

Though the strength of paving blocks is not a vital factor to the satisfactory performance of ICBP, minimum compressive strength of 30 MPa is required to resist wearing and tearing of blocks, edge damage and to keep strict dimension tolerance. Based on traffic categories, application areas and thickness of blocks, concrete grade varying from M30 to M55 have been recommended as per IS 15658:2006.

(ii) Characteristics of Aggregates

The aggregates, both coarse and fine shall conform with the requirements of IS 383 (IS 383:1970)[14]. The size of coarse aggregate should lie between 6 mm and 12 mm (IRC SP 63:2004). However, IS 15658 specifies maximum size of coarse aggregate as 12 mm for production of paver blocks (IS 15658:2006). The aggregate/cement ratio shall be in a range of 3:1 to 6:1. The proportion of coarse aggregate in the mix is typically 40% and the fine aggregate (sand) 60% (IRC: SP: 63:2004).

(iii) Cement Content and Type

Ordinary portland cement (33 grade or 43 grade or 53 grade), Portland slag cement, Portland-pozzolana cement and rapid hardening cement shall only be used for production of CPBs (IS 15658:2006). The quantity of cement in the mix shall be in the range of 380 kg/m³ to 425 kg/m³. The water/cement ratio shall be within 0.34 to 0.38 (IRC SP 63:2004).

(iv) Water Quality and Content



The water to be used in production of paving blocks shall confirm to the requirements specified in IS 456 (IS 456:2000, IS 15658:2006). The water content in the mix shall be within 5 to 7% of total mix (IRC SP 63:2004).

(v) Addition of Pigment

Comparing to normal concrete, the peculiarity to paving blocks is that CPBs are produced in different desired colors for aesthetic purpose. In fact, appropriate type and amount of pigments are added during mixing in form of powder or slurry. Inorganic pigments, mostly metal oxides, are more durable and hence preferred for consistency and purity. Pigment volume shall be within 5 % to 9 % of cement content. Pigments shall be finer than cement (finer value between 2 to 15 μm / gram, IRC SP 63:2004, IS:15658:2006). For same slump, addition of pigment requires increase in mixing water, for which suitable adjustments in water content may become necessary to avoid a loss in strength.

(vi) Other Additives

Supper plasticizers around 0.4% of cement by weight may be added for high early strength. Admixtures of calcium stearate are used to reduce water absorption. Air entraining agents, blast furnace slag or fly ash may be added for reduction in needed amount of cement.

Factors Influencing Mix Proportion and Quality of Paving Blocks

The key factors which influence mix proportion and quality of CPBs are cement content, water content and aggregate characteristics. Also density, curing conditions, addition of pigments, and addition of other admixtures influences the output of mix design.

- Cement Content:** The production process of paving blocks requires low slump concrete. As a fact, the existing water in the mix is hardly enough to hydrate fully the cement. The notion that further addition of cement will increase the strength of concrete is wrong. Actually, addition of cement lowers workability and reduces the strength, as the cement acts as a filler [3].
- Water Content:** Increase in water content within the range from 5% to 7% of total mix will decrease the strength as well as durability. So, the addition of water may be carried out carefully.
- Characteristics of Aggregate:** The quality of concrete is mostly influenced by the cleanness, the shape, surface texture, and the grading of the aggregates. The fine aggregate shall not contain more than 25% acid soluble material on that fraction retained on the 600-micron sieve [3]. The grading shall be such that the packing of aggregates will yield maximum density.
- Effect of Density:** The materials shall be fully compacted to achieve maximum density. Lower the density, higher will be water absorption and lower in strength.
- Curing Condition:** Usually, paving blocks are cured in any of the three types viz: - i) natural air curing ii) water curing iii) accelerated curing. Higher 28 days' strength are obtained in water/humidity curing compared to natural air curing. In steam curing, 1-day strength is higher and the 28 days' strength may be 20% lower comparing to naturally cured blocks [3].
- Pigments Addition:** To have maximum intensity of colour there is an optimum dose of pigments. Different colors require different water content because of their particle shapes. The strength of paving blocks increases with increase in concentration of pigments at constant water/cement ratio.
- Effect of Admixture:** There are several materials like natural occurring pozzolanas and artificial pozzolanas, flyash, blast furnace slag and chemicals, which can be used as a partial replacement of cement. The admixtures shall be used depending upon their characteristics to achieve the strength and durability.

Proposed Mix Design Procedure

In 1919 Abrams developed a relationship between water cement ratios and compressive strength of concrete [15]. As per the hypothesis, the strength of concrete is inversely proportional to the water/cement ratio. This hypothesis has remained the basis for most of the mix design procedures even in the modern age. Now-a-days different cements, supplementary cementitious materials, aggregate of different maximum size, grading, surface texture, shape and other characteristics may produce concretes of different compressive strength for the same free water/cement ratio. Therefore, new relationship between strength and free water cement ratio should be determined for the materials actually to be used. However, for the mix of concrete paving units, already there has been established guidelines for selection of water/cement ratio and water content (IRC SP:63:2004, IS:15658:2006) and it is not required to carry out experiments for the same.

Proper estimation of water absorption by aggregates is essential in the development of concrete mix for paving blocks. Finally, water content shall be adjusted based on the absorption and the current moisture content to generate equivalent of saturated surface dry condition of the aggregate. It is an established fact that fresh and hardened properties of the concrete mix mostly depend on the packing of its coarse and fine aggregates. Proper packing of



different aggregates sizes is an essential step in the concrete mix design procedure (Andersen and Johassen 1993). However, aggregate cement ratio, maximum size of aggregate and the proportion of coarse aggregate and fine aggregate have been specified in IRC: SP:63:2004 for manufacture of concrete paving blocks.

The mix design procedure proposed for the development of concrete mix for paving blocks can be briefed in the subsequent steps:

Step 1: Specifications for proportioning: The required grade designation, type of cement to be used, maximum nominal size of aggregate, minimum cement content, maximum water cement ratio and workability shall be specified. Also, exposure condition, method of concrete placing, degree of supervision, type of aggregate, maximum cement content and chemical admixtures (if any) shall be detailed.

Step 2: Properties of raw materials: The physical and chemical characteristics of individual constituent materials are required in the calculation to work out the final mix proportion. Specific gravity of cement, coarse aggregate, and fine aggregate shall be found out for the use. Also, water absorption, free moisture content and sieve analysis of coarse and fine aggregate are required.

Step 3: Target strength : The target strength i.e. the minimum average 28 days' compressive strength shall be determined as per the following equation.

$f_{ck}^d = f_{ck} + K S$, where, f_{ck}^d is the target strength, f_{ck} is characteristic strength, $K = 1.65$ for normal concrete cubes (IS 10262:2009) and $S =$ standard deviation $= 5 \text{ N/mm}^2$ for normal concrete cubes (IS 10262:2009).

Step 4: Fixing water/cement ratio: As per IRC: SP: 63:2004 the water cement ratio shall be within 0.34 to 0.38. because CPB require dry, low-slump mixes as well as higher compressive strength in the range of 30 N/mm^2 to 55 N/mm^2 . For starting of mix design water/cement ratio of 0.38 may be adopted for compressive strength of 30 N/mm^2 and 0.34 for compressive strength of 55 N/mm^2 .

Step 5: Selection of water content : As already discussed, the machine is the governing factor in the choice of water content ("W" in kg/m^3), normally this lies between 5% to 7% of the total mix. The density of plane cement concrete is 2400 kg/m^3 (IS 456:2000). Thus total water content can be determined.

Step 6: Determination of cement content : Cement content ("c" in kg/m^3 of concrete) of mix is determined from the adopted water/cement ratio. Cement content "c" in $\text{kg} = w/(w/c)$ per cubic meter of concrete. The cement content shall be fixed in between 380 in kg/m^3 to 425 in kg/m^3 depending on the equipment being used for block making.

Step 7: Determination of coarse and fine aggregate: The amount of total aggregate can be determined using the absolute volume method. Total concrete volume $= 1 \text{ m}^3$, Assume air content $= 2\%$, Air $= 0.02 \text{ m}^3$, Actual concrete volume $= 0.98 \text{ m}^3$.

From Steps 5 and 6 the amount of water and cement used in the mixture is obtained. As assumed above cement content is 'C' in kg/m^3 and water content is 'W' in kg/m^3 .

Volume of paste (V_{paste}) $= (C/G_C + W/G_W)$, where G_C and G_W are the cement and water specific gravity respectively. Total volume of aggregate (V_{agg}) $= (0.98 - V_{\text{paste}}) \text{ m}^3$. In the combined aggregate grading for concrete paver blocks let the percentage of coarse aggregate (Ca) in the total aggregate content be X% and that of fine aggregate (Fa) content be Y%. Volume of coarse aggregate (V_{Ca}) $= X\% \times V_{\text{agg}} \text{ m}^3$. Volume of fine aggregate $= Y\% \times V_{\text{agg}} \text{ m}^3$, the weight of fine aggregate $= V_{Fa} \times G_{Fa}$, the weight of coarse aggregate $= V_{Ca} \times G_{Ca}$, where G_{Fa} is the specific gravity of sand and G_{Ca} is the specific gravity of coarse aggregate. However, total amount of aggregate calculated shall be checked so that the aggregate/cement ratio to be with in 3:1 to 6:1. Similarly the fraction of coarse aggregate and fine aggregate shall be checked to remain as 40:60.

Step 8: Determination of extra water required: When computing, the requirement of mixing water allowance shall be made for the free (surface) moisture contributed by the fine and coarse aggregates. On the other hand, if the aggregates are dry, the amount of mixing water should be increased by an amount equal to the moisture likely to be absorbed by the aggregates. The surface water and percent water absorption of aggregates shall be determined according to IS 2386.

Experimental Program

Materials and Proportions

OPC cement of 43 grade conforming to IS 8112(1989) with specific gravity of 3.14 is used. Sand collected from Brahmini river conforms to grading zone II as per IS 383-1970. Locally available crushed granite stone of 10 mm nominal size from Talcher area is used as coarse aggregate. This is less than the nominal maximum size of aggregate of 12 mm as specified in IRC: SP: 63:2004. The specific gravity of fine aggregate and coarse aggregate are 2.72 and 2.64 respectively. Portable water available in laboratory has been used for mixing and curing. M30



grade of concrete have been prepared in the laboratory for casting of cubes and paving blocks. W/C ratio of 0.38 and water content of 6.6 % of the total mix have been used for for a target strength of 38.25 N/mm^2 . Finally, the mix proportions of 1:2.68:1.78, has been arrived for M30 grade concrete as per IS 10262:2009 which has remained within prescribed limit as per guidelines of IRC: SP: 63:2004 and IS: 15658:2006.

Test Procedure

Six cubes of size $150 \text{ mm} \times 150 \text{ mm} \times 150 \text{ mm}$, six prisms of size $100 \text{ mm} \times 100 \text{ mm} \times 500 \text{ mm}$ and twenty four concrete paving blocks with size of 100 mm width, 200 mm length and in three different thickness of 80mm, 100 mm and 120 mm have been prepared. The cubes and prisms are tested for compressive and flexural strength respectively as per IS 516 – 1959. The CPBs are tested for compressive strength as per IS: 15658:2006: Annexure-D. Corresponding results have been reported for 7 days and 28 days.

TEST RESULTS AND DISCUSSIONS

Compressive Strength of Cubes and Flexural Strength of Prisms

The 7 days and 28 days mean compressive strength of concrete cubes and flexural strength of prisms have been presented in **Table 1**. Theoretical 28 days target mean strengths determined as per IS 456: 2000 are presented in the same table. From the experimental results, it is found that the 28 days mean compressive strength of concrete cubes are above the mean target strength. This validates the perfection of the mix proportions for M30 grade concrete calculated as per the proposed methodology.

Table 1 Compressive strength of concrete cubes and flexural strength of prisms (M30 Grade).

Days tested Test Type	7 days, N/mm^2	28 days, N/mm^2	Target mean strength as per IS 456: 2000, N/mm^2
Compressive strength of cubes (average of 3 specimens)	30.90	42.10	38.25
Flexural strength of prisms (average of 3 specimens)	4.43	5.17	4.51

Compressive Strength of Concrete Paving Blocks

The 7 days and 28 days mean compressive strength of concrete paving blocks have been presented in **Table 2**. The theoretical minimum average 28 days strengths (determined as per 15658:2006, Dowson 1980) are also presented in the same table. From the experimental results, it is found that the 28 days mean compressive strength of concrete paving blocks are above the minimum average strength calculated as per IS: 15658:2006. Hence, the concrete paving blocks produced using the mix proportions for M30 grade concrete calculated as per the proposed methodology meet the required strength as per guidelines.

Table 2 Compressive strength of concrete paving blocks (M30 Grade)

Days tested Thickness of blocks, mm	7 days average (4 specimens) strength, N/mm^2	28 days average (4 specimens) strength, N/mm^2	Minimum average strength as per IS: 15658:2006, N/mm^2
80	14.08	34.25	32.89
100	23.12	41.30	
120	25.64	46.14	

CONCLUSION

Based on the theoretical analysis and experimental results of the above study for mix design of concrete paving blocks, following conclusions may be drawn:

1. The proposed method is very simple and reliable for the proportioning of concrete mix to be used in the manufacture of concrete paving units.
2. Specific requirements for the mix design of concrete paving blocks have been discussed keeping in view the suggestions provided in different guidelines as per IS 10262:2009, IS 15658:2006 and IRC SP 63:2004.
3. The average 28 days compressive strength of concrete cubes and flexural strength of concrete prisms have remained above the mean target strength.
4. The 28 days average compressive strength of concrete paving blocks as obtained are above the minimum average strength.
5. Thus, the mix design procedure followed in this research study may be used by manufacturers for producing concrete paving blocks.



REFERENCE

1. B. C. Panda and A. K. Ghosh, Source of jointing sand for concrete block pavement, Journal of Materials in Civil Engineering, American Society of Civil Engineers, Volume 13, Number 3, pp 235 – 237.2, 2001.
2. IRC: SP: 63:2004, Guidelines for use of Interlocking Concrete Block Pavement, Indian Roads Congress, New Delhi, India.
3. A. J. Dowson, Mix design for concrete block paving, Proceedings of the First International Conference on Concrete Block Paving, Newcastle-upon-Tyne, U.K., pp 121-127, 1980.
4. IS 10262:2009 on Indian standard concrete mix proportioning – Guidelines (First revision), Bureau of India Standard, New Delhi, India.
5. IS: 15658:2006 on Precast Concrete Blocks for Paving – Specification, Bureau of Indian Standards, New Delhi, India.
6. IS 456:2000 on Indian standard plain and reinforced concrete code of practice (fourth revision), Bureau of India Standard, New Delhi, India.
7. SABS 1058:2002 on South African standard specification for concrete paving blocks, Johannesburg, S.A.
8. Radhikesh P. Nanda, K Amiya Das, and N C Moharana, Stone crusher dust as a fine aggregate in Concrete for paving blocks, International Journal of Civil and Structural Engineering, Volume 1, Number 3, pp 613 – 620, 2010.
9. M C Nataraja and Lelin Das, A study on the strength properties of paver blocks made from unconventional materials”, IOSR Journal of Mechanical and Civil Engineering, pp 01 – 05, 2012.
10. Som Nath Sachdeva, Vanita Aggarwal, and S M Gupta, High volume fly ash concrete for paver blocks, International Scholarly and Scientific Research and Innovation, Volume 8, Number 3, pp 242 – 248, 2014.
11. Joel Santhosh, and Ravikant Talluri, Manufacture of interlocking concrete paving blocks with fly ash and glass powder, International journal of civil engineering and technology, Volume 6, Issue 4, pp 55 – 64, 2015.
12. W. Gawatre, Dinesh, S. Chhajed, Rohit, B. Panpatil, Prashik, Desarda, S. Shubham, Chetan S. Waghchaure, and Nikhil S. Agrawal, Manufacture of paver block using partial replacement of construction and demolition concrete waste”, International Journal of Pure and Applied Research in Engineering and Technology, Volume 4, Issue 9, pp 11 – 18, 2016.
13. Suad Abdul-Aziz Sultan, Ban Sahib Abduljalel, and TalibQasim Talib, Evaluating the performance of sustainable interlocking concrete blocks manufactured from recycled Concrete aggregate, Journal of Engineering and Sustainable Development, pp 1 – 23, 2017.
14. IS: 383:1970 on, Indian standard specification for coarse and fine aggregate from natural sources for concrete (Second revision), Bureau of India Standard, New Delhi, India.
15. D. A. Abrams, Design of concrete mixtures, Structures Materials Research Laboratory, Lewis Institute Chicago, 1919.
16. IS 8112: Specification for 43 grade ordinary Portland cement : Bureau of Indian Standards.
17. IS 2386-1: Methods of Test for Aggregates for. Concrete, Part I: Particle Size and Shape, Bureau of India Standard, New Delhi, India, 1963.
18. IS 516: Method of Tests for Strength of Concrete, Bureau of India Standard, New Delhi, India.



Use of Emerging Technologies for Rural India

Amitabh Kumar Sinha

MACO Corporation (India) Pvt Ltd, Kolkata, amit1950@yahoo.co.in

ABSTRACT

Some of the most pressing and urgent question, which mankind faces today are the future availability and cost of the energy supplies. Are the available resources sufficient to meet the growing demand of energy? Will the decline in the conventional source of energy affect the quality of living in rural India?

Concern being expressed today for searching more and more renewable source of energy stems largely from the fact that the mankind today depends predominantly on fossil fuels such as coal, gas or petroleum products. Availability of these fuels is dwindling and may be consumed fully within a foreseeable future. Other concern about use of fossil fuels is its effect on environment and carbon foot prints. Solar energy is one convenient and clean source of energy and fully suitable for rural India even for the inaccessible areas. This implores us to find and ways to use this energy in rural areas, which is made possible due to availability of efficient and affordable solar photo voltaic cells and related equipments.

KEYWORDS Solar, Energy, Rural, India

INTRODUCTION

Rural India is starved of electricity. Many villages are yet to be electrified. Even those which are electrified received electricity only for limited hours in a day.

For Indians till now the crisis meant whether the millions will have enough food to cook and fuel to cook it. With declining world reserve of not so environmental friendly conventional fuel we had developed gobar gas plants as source of alternative energy and fertilizers, Now the emerging technologies such as solar / wind power or hybrid units enable us use of affordable source of un conventional and convenient source of power.

Use of solar power is steadily getting popular in rural area for domestic, community and street lighting, solar powered pumping units, solar powered heating and cold storage units.

AVAILABILITY ASPECT OF SOLAR ENERGY

The Earth receives enormous amount of energy in the form of sunlight. The amount of energy received can be estimated as follows:

As per solar power hand book [1] radiation received by an area of one square kilometer perpendicular to sunrays in India = 1.36×10^6 kW.

Projection of total area of the Earth normal to sunrays at any time = $\pi \times R^2$ where R= radius of earth (**Figure 1**).

Energy received annually = 1.5×10^{18} kWh

As far as India is concerned this will mean that radiation over just 200 square kilometer (just .006 % of land area of India) can supply total power requirement of the country.

Sun is the brightest object in the heaven, but for its light, heat and life would be impossible on earth. The light and heat from Sun is the ultimate source of nearly all the energy which maintains plant and animal life and also the prime cause of weather, climate and wind. Sun is also source of all energy resources mankind uses, namely, coal, gas, petroleum, hydroelectricity, tidal power, wind mill, fire wood, et al.

Use of Solar energy is needed for two reasons: (i) No other energy source is available at the location, for example, communication satellites, street lights and community TV in remote areas; and (ii) solar energy is cheap and hence can be used for heating of houses, swimming pools, water heaters or pre heaters for hotels etc.

It shall be interesting to scan through some of the recent news on use of Solar Power in India:

- Solar water pumps can help India surpass 100 GW target.-PTI| Jul 31, 2018,
- US agency signs MOU with Indian company for 41 MW power project in Andhra - PTI Jul 31, 2018
- The road to 100GW: lighting up India with solar power-3rd April 2018
- Farmers to pay only 10% cost of solar pumps under Budget scheme: Minister, IANS February 03, 2018

- Kochi airport becomes world's first to operate completely on solar power-First Post August 19-2015
- Guwahati, (Assam) [India] May 16 (ANI) Guwahati now has India's first railway station run by solar power.

Solar power can be put to use in two ways:

Solar Thermal System (Use of Solar Thermal Energy Directly)

In Solar Thermal System heat from sun rays are directly used through a collector or concentrator (**Figure 2**) to heat up, e.g. solar powered water heating system, solar powered cold storage, solar cookers or even power plant where water is heated and steam formed is used for power generation by using solar power concentrator. Solar powered water heating in its simplest form was in use even in 1900 when water tanks were painted black.

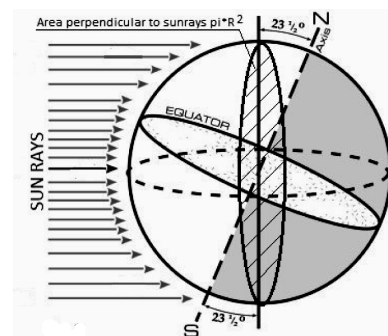


Figure 1 Projection of Earth's area normal to sunrays

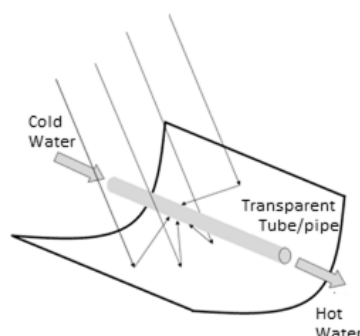


Figure 2 Parabolic solar concentrator

We are well aware of concentration of sun rays by using convex lens. In 1772 diamond was cut using this technique by Lavoisier. In experiments in France using large concave mirror built up with segments, temperature of 3500°C in 1946 and 5900°C – which is surface temperature of the Sun itself in 1968 were achieved.

This paper is aimed at elaborating use of Solar Thermal Systems for water heating systems and cold storages which are relevant to rural areas of India as well as use of Solar photo voltaic cells for production of electricity.

Let us discuss some of the use of Solar Thermal Systems.

Cooking is an important activity that is undertaken to prepare food for human survival. It is a well known fact that, most prominent cooking energy in most developing world is fire wood. One of the alternatives to fire-wood / fossil fuel energy is solar energy, but the major problem with the use of solar energy is that, it is very dilute and fluctuates with time and weather condition. Solar cooker was one of the first simple systems widely publicized and subsidized by Indian government. The system was simple with a mirror used as concentrator and a black painted or reflective insulated box with a glass cover as collector. A part from being economical, this type of cooker is smokeless and preserves nutrition value of the cooked food too. A box type solar cooker is shown in **Figure 3**.

Payback period for such cookers (without any subsidy) in India is $4000/40/0.67 = 149$ days; based on Annual sunshine at Delhi (**Table 1**) 2993 h out of total sunshine of 4422 h/year, that is, for 67% in an year and fire wood need to be used for 33% of the days. Assuming cost of box type solar cooker as ₹4000/- (₹1200/- after subsidy in Haryana) and consumption of 5 kg fire wood @ ₹ 8/- per kg for cooking one meal.

Table 1 Yearly solar radiation data in different parts of India as per Hand Book (1)

Place	Yearly hours of sunshine	Annual radiation, kWh/m ²
Delhi	2993	2026
Kolkata	2445	1805
Mumbai	2701	1972
Chennai	2737	2062

COLD STORAGE IN RURAL INDIA

Storage and preservation of food have been the concern of mankind since they wandered as food gatherers. Then it meant storing food at times in plenty and using them during periods of short supply. However, as man learnt the



values of various vegetables, fruits and meats he became interested in preserving them too. It was sheer luck that low temperature was found useful for food preservation.

Refrigeration in true sense was first employed by Harappans, Romans and Greeks who cooled water and wine by storing them in porous earthen pots.

However, the real breakthrough was achieved when ice was manufactured in early 19th century. Earliest patent for practical ice manufacturing was granted in 1834 to Jacob Perkins, an American who lived in London.

Present day refrigeration works on two principle vapor compression or vapor absorption.

Vapor compression is best suited where electricity is available to drive compressors or where large systems are required. The cycle is clear from **Figure 4** and elaboration is discussed subsequently.

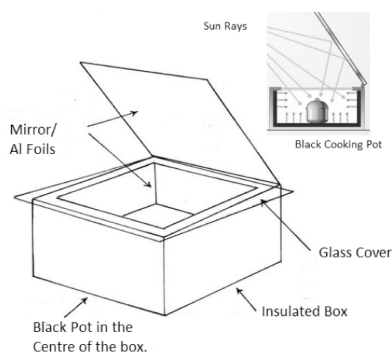


Figure 3 Box type solar cooker

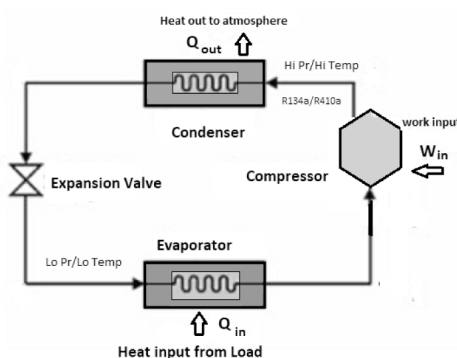


Figure 4 Vapor compression cycle

Compression

The refrigerant 'gas' at low pressure and low temperature enters the compressor. Here due to compression the temperature and refrigerant pressure rises. The refrigerant then leaves the compressor and enters to the condenser. An electric motor is used for compressor.

Condensation

The condenser is essentially a heat exchanger. Heat is transferred from the refrigerant to atmosphere through air or water. As the refrigerant flows through the condenser, it is in a constant pressure.

Expansion

The cooled refrigerant expands through a throttling valve, and pressure is released. Such expansion results fall in temperature and pressure.

Evaporation

At this stage refrigerant is at a lower temperature than its surroundings. Therefore, it evaporates and absorbs latent heat of vaporization. At this stage heat from the load is extracted. Refrigerant at low pressure and low temperature then enters the compressor and the cycle continues.

Vapor Absorption Cycle

This type of refrigeration cycle uses heat energy instead of mechanical energy to raise pressure and temperature of refrigerant, achieved in compressor of above described cycle. Due to this very reason this cycle can use alternative source of energy such as solar heater, wood fired heating etc.

Absorption cycle based on solar power is shown in **Figure 5**. The cycle is similar to compression cycle, but we have generator instead of compressor and absorber for absorption of vapor. The refrigerant used is Ammonia solution. The system does not need electricity and is a silent system. For the system to be suitable for alternative fuel source when the sun is not shining- the pumps between absorber and generator may be replaced by gravity flow where as air cooling may be adopted instead of water cooling shown above.

The system is quite suitable for use in rural India.



Solar Powered Cold Storage

In rural India storing vegetables and fruits such as potato or apple grown locally is of prime importance. Whereas mechanical systems are available for use in areas with availability of regular electrical power, in villages with no or irregular power supply it is essential to have a non mechanical system without moving part such as intermittent absorption system. Authors and designers Srivastava [2] and Abhichandani, et al [3] have suggested this method for use in solar powered cold storage / milk chilling units.

This type of system has following advantages:

- (a) Such cold storages can be established even in remote non electrified or areas starved of electricity.
- (b) Cold storages can be located near to production areas of potato or other perishable items.
- (c) Transportation cost to conventional cold storages located in urban areas may be saved and spoilages avoided or minimized.
- (d) Dependence of electricity is nil and alternative source of fuel to be used during rainy days are cheap and simple.
- (e) The system may attract state subsidies.
- (f) Energy required are more in summer, which matches with available solar energy.
- (g) The system has low noise.

Disadvantages of the system are:

- (a) Initial investment may be heavy.
- (b) System may not function in rainy days when alternative fuels may be needed.
- (c) Ice making cannot be resorted to.

Typical design calculation for solar cold storage system:

Basis of design of any cooling system is heat load that need to be pumped out. The heat load for the system comprises of:

- (a) Leakage heat load
 - (b) Product heat load
 - (c) Heat load due to air change
 - (d) Other heat loads due to solar radiation, light bulbs/lamps, humans etc.
- (i) Leakage heat load in (HL) is proportional to heat conductivity co-efficient ($K = 0.132$ for insulation thickness of 250 mm and conductivity of $0.033 \text{ kcal/h/m}^2/^{\circ}\text{C}$) of insulation, wall and roof, and proportional to wall/roof area ($A = 350 \text{ sq.m}$) and temperature difference between cold area ($t_2, 5^{\circ}\text{C}$) and the ambient ($t_1, 35^{\circ}\text{C}$). $HL = K.A.(t_1 - t_2)$. For 100T storage this is roughly 33,264 kcal / day.
 - (ii) Product heat load (HP) : For a storage capacity of say 100 T assuming 10% withdrawal and replenishment, that is, 10000 kg/day. If the product intake temperature is 35°C and cold product temperature is 5°C . Then with specific heat (S) of the product = 1, product heat load = $10000 \times 1 \times (35 - 5) = 3 \times 10^5 \text{ kcal / day}$.
 - (iii) Air change heat load: Air change due to door opening etc is (say) 2.7 per day. The volume (V) of storage of size $15 \times 10 \times 4 \text{ m} = 600 \text{ m}^3$, Heat gain due to air at 35°C at 60% RH = 40 kcal/m^3 . $600 \times 2.7 \times 40 = 64800 \text{ kcal/day}$.
 - (iv) Heat load due to solar radiation, burning lamps/ bulbs in the storage, and heat load due to humans inside are ignored at present.
 - (v) Total heat load per day = 398064 kcal. We consider that to maintain 5°C inside the storage, the refrigerant need to be kept at -9°C in evaporator. Thus the difference if temperature is 14°C . Similarly temperature difference between NH_3 in Generator (75°C) and after cooling in condenser (35°C) is 40°C . The coefficient of performance = $Q_2/Q_1 = 14/40 = 0.35$, For removing heat load of 64800 kcal/day, we need to input an energy of $398064/0.35 = 1137325.7 = 790 \text{ kcal/min}$. Solar radiation received is $1.36 \times 10^6 \text{ kw/sq km} = 19 \text{ kcal/min}$. Hence area of solar collector needed @60% efficiency = $790/.6/19 = 69 \text{ sq.m}$.

Photo Voltaic Cells

Second method of using solar energy is via photovoltaic (PV) cells, which directly convert solar energy to electrical energy. The electricity so generated is used directly or with storage batteries. This is most widely used method today and large solar farms are built up to feed entire locality or airport, such as 13.1 MW solar power plants for Cochin International airport.



During about 200 years of its existence photo voltaic cells have undergone lot of changes. As per Wikipedia Alexandre Edmond Becquerel discovered photo electric effect in 1839 by shining light on an electrode dipped in a conductive solution which produced an electric current.

Between 1873 to 1876 the photoconductivity of Selenium was discovered. It was found that Selenium became electrically conductive and that Selenium could produce electricity from light without heat or moving parts. This meant that solar power can be harvested for production of electricity. In 1883 first Selenium based solar cell was created and in 1956 first Silicon based more efficient and economical solar cells were commercially produced. Within 2 years in 1958 the solar cells were used as power source for satellites.

For about 100 years the photo voltaic cells remained very inefficient and were used only to measure intensity of light. Shortly after invention of transistor Russell Ohl invented a solar cell in 1941.

On March 11 this year during an International Solar Alliance Summit in Delhi, Our Hon. PM has set a target of achieving 100 Giga Watt (GW) by 2020, out of 175 GW India plans to produce through renewable sources. Country has already achieved 20 GW of solar power production by now.

While the invention of photo-voltaic cells found many usage for urban India and has been recently used for massive solar power plants to provide power for one airport or a railway station, rural usage are mainly for street or domestic lighting, water for irrigation and drinking, refrigeration and cooking. Recent developments in few areas also allows the residents of both urban and rural to offset their ever increasing electricity bills with reverse flow of energy using their roof top solar panels.

Solar energy is used from stand alone lanterns to cold storages. The solar panels generate DC electrical power only during sunlight hours. There is some usage which may use DC power directly and only during sunlight hours such usage are simple and without much complicated electrical controls. One of such use in rural areas are pumping units which pumps water from bore wells or from other water bodies to places where it shall be used for drinking or irrigation purpose. DC motors driven by solar cells directly are available in simplest forms. Between solar panels and the pump a controller and regulator are used. Solar panels are usually connected in series to have little higher DC voltage matching the voltage of the pump motor. Such circuit allows using the pump only during sun-light times. It matches with the farm requirement since you do not need water for irrigation during those times when cloud restricts the sun light. For domestic use it means storing drinking water instead of electrical energy. A regulator is used to regulate DC voltage in the same way stabilizer is used for AC voltage.

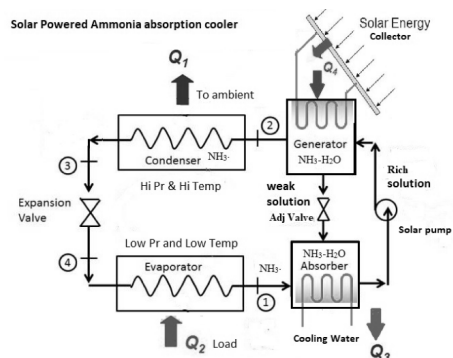


Figure 5 Vapor absorption refrigeration cycle

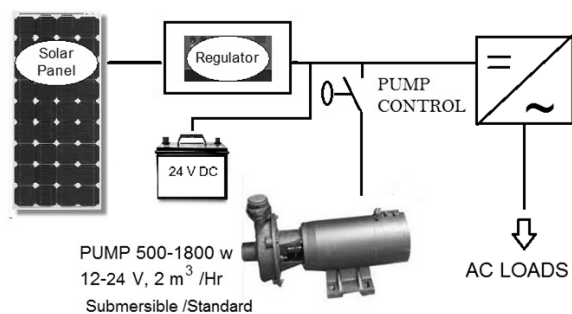


Figure 6 Basic solar system for DC, DC+Battery, AC loads

For those installations where continuous power is needed, notwithstanding whether sun shines or not the energy is stored in batteries usually of 12-24 V DC and the using it for DC pump and lights (connected directly to battery bank) or for AC loads fed through VFD/ Inverter. The AC loads are pumps, lights, AC or heating units, cold storages etc. Some of such loads are specific to rural areas. A schematic of the discussed system is shown in **Figure 6**.

Further for areas where electrical power is available and grid feedback is allowed solar powered system with grid feedback (**Figure 7**) may be used. The inverters in such cases work in parallel with utility power and inverter is duly synchronized with the utility. When the solar energy produced is more than the load requirement, the excess energy is fed back to the utility grid and the energy meter reverses and results in savings for such feedback.

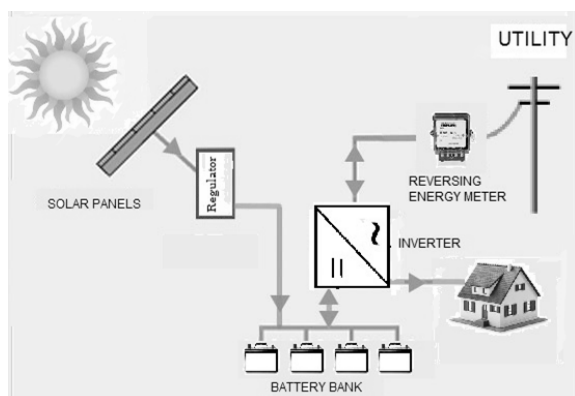


Figure 7 Solar system with battery and grid feed back

One such use in rural area is cold storage powered by solar power system having battery storage and inverter for DC-AC conversion, power from utility may also be used in parallel. For such cold storage no alternative source of energy is needed.

Payback Period

While cost of PV solar systems is coming down, cost of electrical power supply from utility is going up. Thus feasibility of solar system is getting better day by day. We can briefly analyze the feasibility as following:

5 kW 'On Grid Solar System' with battery and inverter for a small building = Rs 6.80 lakh, with 30% sale offer = Rs 4.75 lakh. Installation Cost Rs 0.75 lakh Total Cost = Rs 5.5 lakh (without Government subsidy but with grid feedback), cost of capitals per month = Rs 4583/- For 3000 kWh consumption and feedback to grid and a cost of Rs 7.30 per unit (as in Delhi) saving in electricity bills = Rs 21900-4583 = 17317/-. Payback period = $550000/16417 = 32$ month.

CONCLUSION

Need of the hour is use of renewable energy in place of fossil fuels which is likely to be exhausted in foreseeable future. Solar power is a very viable alternative today. In rural area the source and load are both are locally available and there is no need for transmission and distribution. Various types of usage have been discussed in this paper and use of solar power quite feasible. The need of hour is to promote Solar electrical units. Government of Jharkhand is likely to make roof top solar panel must for houses bigger than 3000 sq.ft. GOJ has even proposing 50% subsidy.

REFERENCES

1. Anna Mani. Handbook of Solar Radiation data for India.
2. SUN: Mankind's future source of Energy: Proceedings of The Solar International Energy Society Congress, New Delhi, January 1978.
3. Proceedings of fifth national symposium on refrigeration and air conditioning, IIT Madras



Performance Analysis of PV Panel under Dusty Condition

Abhishek Kumar Tripathi*¹, Mangalpady Aruna², Ch.S.N. Murthy²

Department of Mining Engineering, AKS University, Satna, India¹, abhintrkl12@gmail.com*

Department of Mining Engineering, NITK, Surathkal, Karnataka, India²

ABSTRACT

The accumulation of dust on the surface area of PV panel is the prime concern of its performance reduction in an outside regime. The accumulated airborne dust particulates of various sizes form thin layer on the surface of PV panels, which significantly affects the penetration of solar radiation in to the surface area of photovoltaic panel. In the present study the performance analysis of photovoltaic panel under the dusty zone was carried out. The study reveals that the reduction in short circuit current and maximum output power of a dusty panel when compared to a clean panel are respectively, 39.58% and 43.18%, after five days of its exposure to outside regime. Moreover, an abrupt reduction in the performance of PV panel was observed during the initial stage of dust deposition where as it slowdown in the later stages.

KEYWORDS Dust, short circuit current, Open circuit voltage, Maximum power output

INTRODUCTION

The production of electrical energy is based on non-renewable and renewable energy sources. In this, the renewable energy sources are considered as clean and environment friendly energy sources. There are many renewable energy sources, but among all the solar energy experienced a rapid growth and popularity in the last decade, because of its ease of operation and maintenance. Thus, the solar energy is becoming a vital source of electric power generation in present situation [1-4].

In solar energy system, sunlight is converted into electricity by the help of solar photovoltaic (PV) cell [5]. Whenever the sunlight falls on the photovoltaic cell surface, it excites the electrons of the valence band to move to conduction band and this generates hole in valence band. As a result of this, photo current starts flowing to the external circuit. In solar photovoltaic system, a photovoltaic module consists a group of PV cells and a PV panel consists a group of PV module. In general, the PV panel are operated in an open atmosphere, where it experiences a significant variation in atmospheric parameters, such as wind speed, temperature, solar irradiance, moisture content and dust pollutants [6]. These atmospheric parameters disturb the effective operation of solar PV panel in an open atmosphere and among them dust plays a vital role in reducing its performance.

The deposition of dust on PV panel surface creates a barrier between the PV panel surface and sunlight falling on its surface, which attenuates the part of the incoming sunlight. The attenuation of sunlight depends on the size of dust, density of dust and type of dust [7]. This attenuation of sunlight considerably reduces the performance of PV panel [8-9].

The exposure time of PV panel in real atmospheric environment is even important in the deposition of dust on its surface. In a study it was found that the reduction in spectral transmittance and overall glass transmittance of PV panel was respectively 35% and 20% due to 5g/m² of dust deposition on its surface with 45 days of exposure to real atmospheric environment [10]. One more study reported that there was power loss of 3% to 4% due to dust deposition on PV panel for 5 weeks of its exposure to the atmospheric condition [11]. Similarly, another study indicated that the reduction in glass transmittance of PV panel was from 90.7% to 87.6% after 33 days of its exposure to the outside environment [12].

An experiment was carried out to study the effect of dust deposition on electrical parameters of the panel shown that there was a drop of 28.6% and 30.6% in short circuit current (I_{sc}) and maximum power output (P_{max}), respectively after its exposure to the atmospheric condition for 12 days [13]. Similarly, one more study reported a reduction in the



P_{\max} of the panel was ranging from of 6.9% to 16.4% during one month of its exposure to an open desert environment[14].

This paper highlights an experimental study which was carried out in a surface mine in Chithradurga District of Karnataka to understand the influence of dust on the panel performance under highly dusty condition. The study helps to draw a scheme for systematic cleaning of panel surface in a dusty environment.

PERUSAL OF SELECTED SITE

The field study was carried out during the month of January in a surface mine in Chithradurga District of Karnataka, India. This mine is situated at the coordinates of 14° 8' 55.4928" N, 76° 40' 1.1424" E. The site endures good solar radiation profile. During a sunny day the peak solar radiation of 1182 W/m² was recorded. Due to high solar radiation, good atmospheric temperature (generally 25°C to 37°C) and good wind profile (peak value of 4m/s), this site could be a good choice for the installation of PV panel.

METHODOLOGY

To study the influence of dust accumulation on the panel performance, two identical 20 W polycrystalline panels were installed in a mine, side by side, which were directed towards the south. The average solar radiation received by these panels was recorded as 1120 W/m². Among these two panels, one panel was kept uncleaned (which was considered as a dusty panel) and other one was cleaned regularly (i.e. every day in the morning, so that it was considered as a clean panel). To measure the mass of dust deposition on the panel surface a filter paper (of known weight) of size equal to that of panel surface was kept beside the clean panel. This filter paper was kept flat and steady. Every day in the morning the filter paper was removed carefully and weighed to know the mass of the deposited dust. **Table 1** gives the value of the dust deposition on the panel surface for all five days.

The electrical output (i.e. output power, current and voltage) of both the panels were measured for five days using 320Ω rheostat and two digital multi-meters (one is used as an ammeter and the other one as a voltmeter of the circuit).

Table 1 Dust deposition on panel surface

Day	Day to day dust deposition, g	Total dust deposition, g
First Day	2.58	2.58
Second Day	2.54	5.12
Third Day	2.57	7.69
Fourth Day	2.57	10.26
Fifth Day	2.60	12.86

RESULTS AND DISCUSSION

The electrical responses of a clean and a dusty panel were recorded for five days. The obtained electrical parameters of both the panels were compared to analyze the performance of a panel under two different operating conditions (i.e. clean and dusty environment). **Table 2(a)** and **Table 2(b)** gives the measured electrical responses of both the panels for five days. Based on the readings as indicated in **Table 2**, the reduction in electrical responses of PV panel due to dust deposition were calculated and is presented in **Table 3(a)**.

The performance of a PV panel in a dusty environment can be defined by the term normalized power output [15]. The normalized power output of a PV panel indicates the performance of a dusty panel with respect to a clean panel, which was calculated using Eq. (1). The higher value of normalized power output represents the better operation of the panel in dusty environment. The normalized power output of panels was calculated for all the five days, which is also given in **Table 3(b)**.

$$P_N = \frac{P_d}{P_c} \times 100 \quad (1)$$



where, P_N = normalized power output, %; P_d = power output of dusty panel, W and P_c = power output of clean panel, W.

As observed from **Table 3(a)** and **Table 3(b)**, the reduction in I_{sc} and P_{max} of dusty panel are respectively, 39.58% and 43.18% compared to clean panel, after five days of exposure. Similarly, the reduction in open circuit voltage (V_{oc}) of dusty panel is up to 4.35% after five days of its exposure. This emphasizes that the reduction in V_{oc} due to dust deposition is meagre when compared to I_{sc} and P_{max} . **Figure 1** shows the comparison of I-V characteristics of clean and dusty panels for all the five days of its exposure for outdoor condition. Based on **Table 3(a)** and **Table 3(b)** the reduction in the P_{max} of a PV panel is plotted with respect to the number of exposure days, which is shown in **Figure 2**. As depicted in **Figure 2**, the P_{max} of a PV panel reduces with increase in exposure time, under dusty environment. The graphical representation of normalized power output with respect to number of days of exposure of the panel for the outside environment is presented in **Figure 3**.

Table 2(a) Measured electrical parameters of clean panel

Day	Clean Open circuit voltage, V	Short circuit current, A	Maximum power output, W
1	20.62	0.65	8.82
2	20.51	0.58	7.60
3	20.57	0.60	8.51
4	20.60	0.80	10.94
5	20.65	0.96	13.38

Table 2(b) Measured electrical parameters of dusty panel

Day	Dusty Open circuit voltage, V	Short circuit current, A	Maximum power output, V
	20.37	0.53	6.84
1	20.06	0.45	5.32
2	19.80	0.43	5.47
3	19.77	0.53	6.53
4	19.75	0.58	7.60

Table 3(a) Reduction in electrical responses of a dusty panel compared to a clean panel

Day	Reduction in open circuit voltage, %	Reduction in short circuit current, %	Reduction in maximum power output, %
1	1.21	18.46	22.41
2	2.10	22.41	30.00
3	3.74	28.33	35.71
4	4.02	33.75	40.28
5	4.35	39.58	43.18

Table 3(b) Reduction in electrical responses of a dusty panel compared to a clean panel

Day	Normalized power output, %	Reduction in normalized power output, %	Daily reduction in normalized power output, %
1	77.55	22.45	22.45
2	70.00	30.00	7.55
3	64.27	35.73	5.73
4	59.68	40.32	4.59
5	56.80	43.20	2.88

As shown in **Figure 3**, initially the reduction in the panel performance is predominant, whereas it reduces gradually with the exposure time. There is a sudden decrease in the panel performance on the first day (i.e. decrease in performance on first day was 22.45% which is quite high when compared to succeeding days), which is corroborated by the steep gradient of the curve. The gradient of the curve gradually reduces with time, which represents a slowdown in the reduction of panel performance. This is mainly due to the overlapping of dust particles rather than settling on the panel surface.

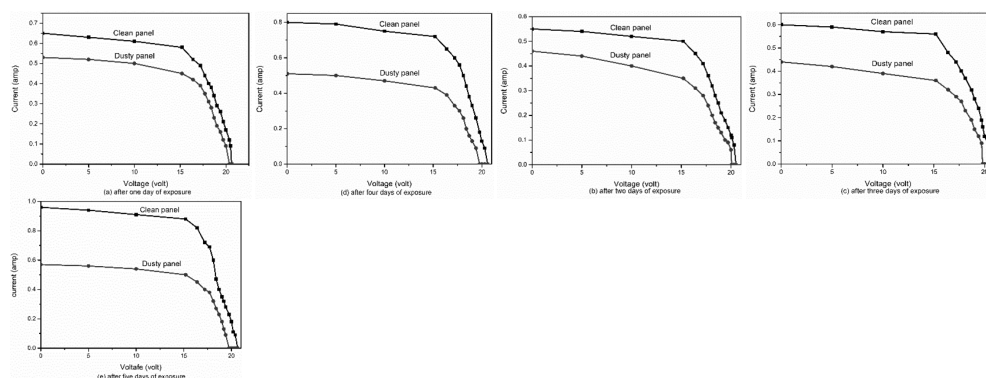


Figure 1 Comparison of I-V curves of clean and dusty panel in outdoor test condition

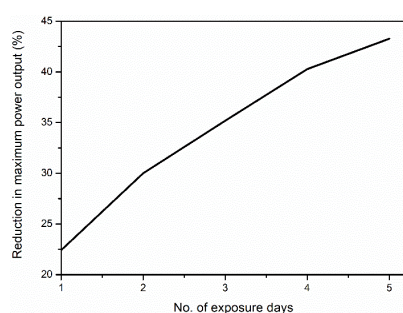


Figure 2 Reduction in maximum power output of PV panel with respect to number of days of exposure

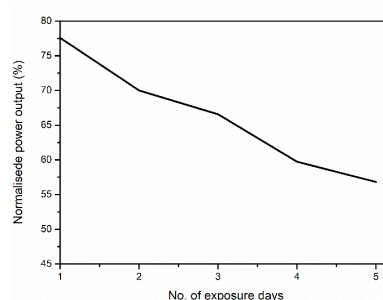


Figure 3 Normalized power output of PV panel with respect to number of days of exposure

CONCLUSIONS

The generation of the electric power via solar PV system is becoming more and more attractive as fossil fuels prices are increasing. The performance of solar PV system depends on the incoming sun light to the module surface. This incoming sun light reduces due to the deposition of dust pollutants on the panel surface. The deposition of dust mass reduces its I_{sc} and P_{max} more significantly when compared to its V_{oc} . The reduction in I_{sc} and P_{max} of a dusty panel when compared to a clean panel are respectively, 39.58% and 43.18%, after five days of its exposure to outside regime (in an iron ore mine). In five days 12.86 g of dust was deposited on the panel surface. However, the reduction in V_{oc} was 4.35%, which is quite low when compared to I_{sc} and P_{max} .

From the field study it was also observed that there is an abrupt reduction in the normalized power output (i.e. 22.45% on first day) during the initial stage of dust deposition where as it slowdown in the later stages (i.e. 7.55% on second day, 5.73% on third day, 4.59% on fourth day and 2.88% on fifth day). This study demonstrates that the performance of PV panel degrades predominantly in a highly dusty environment.

REFERENCES

1. S. Mekhilef, R. Saidur, A. Safari, A review on solar energy use in industries. Renewable and Sustainable Energy Reviews. Volume 15, Number 4, pp 1777-1790, 2011.
2. A. A. Bayod-Rújula, A. Ortego-Bielsa, A. Martínez-Gracia, Photovoltaics on flat roofs: energy considerations. Energy, Volume 36, Number 4, pp 1996-2010, 2011
3. M. Oliver, T. Jackson, Energy and economic evaluation of building-integrated photovoltaics. Energy, Volume 26, Number 4, pp 431-439, 2001.
4. F. J. Chueco-Fernández, A. A. Bayod-Rújula, Power supply for pumping systems in northern Chile: photovoltaics as alternative to grid extension and diesel engines. Energy, Volume 35, Number 7, pp 2909-2921, 2010.
5. A. Goetzberger, C. Hebling, H. W. Schock, Photovoltaic materials, history, status and outlook. Materials Science and Engineering: R: Reports, Volume 40, Number 1, pp 1-46, 2003.
6. H. Jiang, L. Lu, K. Sun, Experimental investigation of the impact of airborne dust deposition on the performance of solar photovoltaic (PV) modules. Atmospheric Environment, Volume 45, Number 25, pp 4299-4304, 2011



7. Z. A. Darwish, H. A. Kazem, K. Sopian, M. A. Al-Goul, H. Alawadhi, Effect of dust pollutant type on photovoltaic performance. *Renew. Sustain. Energy Rev.*, Volume 41, pp 735–744, 2015.
8. S. A. Sulaiman, A.K. Singh, M.M. Mokhtar, M.A. Bou-Rabee, Influence of dirt accumulation on performance of PV panels. *Energy Procedia*, Volume 50, pp 50–56, 2014.
9. S. Semaoui, A.H. Arab, E.K. Boudjelthia, S. Bacha, H. Zeraia, Dust effect on optical transmittance of photovoltaic module glazing in a desert region. *Energy Procedia*, Volume 74, pp 1347–1357, 2015.
10. S.A. Said, H.M. Walwil, Fundamental studies on dust fouling effects on PV module performance. *Sol. Energy*, Volume 107, pp 328–337, 2014.
11. R. Appels, B. Muthirayan, A. Beerten, R. Paesen, J. Driesen, J. Poortmans, The effect of dust deposition on photovoltaic modules. *Photovolt. Spec. Conf. PVSC 2012 38th IEEE*, 001886–001889, 2012.
12. J. Y.Hee, L.V. Kumar, A.J. Danner, H. Yang, C.S. Bhatia, The effect of dust on transmission and self-cleaning property of solar panels. *Energy Procedia*, Volume 15, pp 421–427, 2012.
13. M.S. El-Shobokshy, A. Mujahid, A.K. Zakzouk, Effects of dust on the performance of concentrator photovoltaic cells. *IEE Proceedings I-Solid-State and Electron Devices*, Volume 132, 1, pp 5–8, 1985.
14. M. Saidan, A.G. Albaali, E. Alasis, J. K.Kaldellis, Experimental study on the effect of dust deposition on solar photovoltaic panels in desert environment. *Renew. Energy*, Volume 92, pp 499–505, 2016.
15. O. A.Rosyid, Comparative performance testing of photovoltaic modules in tropical climates of Indonesia. *AIP Conf. Proc.*, AIP Publishing, 020004, 2016.



An Efficient Static Rotor: Resistance Control for the Motors of Preparatory Devices of a Sugar Factory

Vinay Kumar^{*1}, Sanjiv Kumar²

Sugar Engineering Division, National Sugar Institute Govt. of India, Kanpur, Uttar Pradesh¹, vinay_ind@yahoo.com*
Electrical Engineering Department, Harcourt Butler Technical University, Kanpur, Uttar Pradesh, India²

ABSTRACT

The prime mover of cane preparatory devices of a sugar factory is invariably a Slip ring induction motor (SRIM). These devices are equipped with huge rotating knives (chopper) and heavy rotating hammers (shredder). At the far end of the shaft of the preparatory devices, a flywheel is installed for providing load equalization. Additionally, a residual resistance (buffer/slip resistance) is left in-line throughout the operation to mitigate the large swing in the motor current. Conventionally, the value of this buffer/slip resistance is kept such so that a 15% slip is realized at full load. Conventionally, The value of this resistance remains constant throughout the operation during all the load conditions. The I^2R power loss in this buffer/slip resistance, therefore, remains a function of load torque and hence the rotor current (I) only. The system can be made more efficient by selecting the value of these resistances optimally and making the power loss a function of resistance (R) also thereby reducing the power loss. This paper presents a detailed study of the conventional system and analysis of the various waveforms i.e. stator current, rotor rpm, the torque developed and power loss in buffer/slip resistance as obtained from simulation on Simulink. The need of making the value of buffer/slip resistance also load dependent (dynamic) is also studied keeping in view the peculiar highly fluctuating load of these devices, to save power wasted in buffer/slip resistance. From the study carried out and analysis done, designing and simulation of an efficient method based on static rotor –resistance control technique on MATLAB/Simulink has been carried out so as to mitigating large swing in current in preparatory devices of cane sugar industry as well as reducing power loss.

KEYWORDS Slip Ring Induction Motor, Static Rotor-resistance Control, Ton Crush Per Hour, Buffer/Slip Resistance

INTRODUCTION

In a typical Sugar Industry, there are more than 400 electrical motors for different operations. Out of these only three (or sometimes four) motors are SRIMs which consumes around 25% of the total electrical power. These SRIMs are installed at preparatory devices which basically chop the cane with the help of huge rotating knives and then shred it with the help of heavy rotating hammers, for making the cane suitable for crushing and thereby extracting the juice efficiently. Owing to huge inertia of huge knives/heavy hammers and the flywheel (installed for load equalization), these SRIMs are started with the help of external resistances inserted in the rotor circuit. Here, the prime function of the external resistance is not to control the speed but to provide high starting torque during starting of the motor and to mitigate high swing in the current during load fluctuations while preparing the cane. For this, the full resistance is inserted in the rotor circuit during starting, and a buffer/slip resistance is left in-line throughout the operation in the rotor circuit of these SRIMs as shown in **Figure 1**. The value of buffer resistance is kept such that it offers a slip of 15% at full load to mitigate the huge swing in peaks in the current drawn as the load, typically, fluctuates heavily [1, 2].

In the present paper a detailed study is carried out and an efficient Static Rotor-Resistance Control method is proposed for the cane preparatory devices having huge rotating knives or hammers so as to make I^2R losses in rotor circuit a function of both I and R , where ' I ' is rotor current, and ' R ' is external buffer/slip resistance. Also, it is proposed that the value these resistances be reduced to near zero during steady-state operations to save the power further. Conventionally, ' R ' remains constant.

Characteristics of Load Current and Power Consumption in Cane Preparatory Devices having Rotating Knives

The typical current (RMS) waveforms as obtained from Distributed Control System (DCS) for the various preparatory devices (choppers and shredder) is shown in **Figure 2**. The large swing in the peaks of current as can be seen from the figure is reduced by buffer/slip resistances. On the one hand these resistances in the rotor circuit mitigates the effect of frequent and rather periodic fluctuating load, but on the other hand, a huge amount of power



is lost in the form of heat in these buffer/slip resistances as the value of these resistances remain constant throughout the operation.

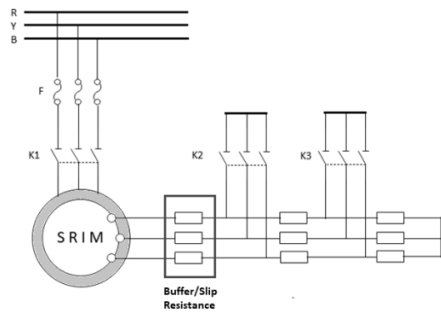


Figure 1 Buffer/slip resistance in SRIM of preparatory devices

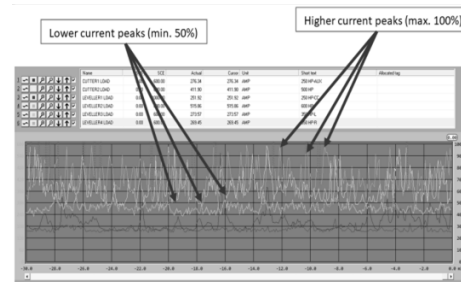


Figure 2 Snap shot of current (RMS) trends of the various preparatory devices from a sugar factory showing the huge swing in current drawn by the motors

The very nature of highly fluctuating load and buffer/slip resistance in the rotor circuit gives a scope of tapping the loss of power by making the variation of rotor resistance as a function of varying load. The loss of power in these buffer/slip resistances should be sacrificed judiciously for mitigating the adverse effects of the high swing in the load. Also, the loss of power in these resistances during steady state condition is undesirable and can be reduced to nearly zero by shorting the buffer/slip resistance. In such kinds of loads, static rotor resistance control method can be implemented to provide a smooth starting of the motor with high starting torque and retaining an optimum value of buffer resistance to mitigate the adverse effects of high swing in peaks of the current drawn by the motor and reducing of loss of power.

For both milling and diffusion, a greater breakage of the sugar-containing cells results in higher extraction and lower final bagasse moisture [3]. If the preparatory Index (PI) is increased from 68 to 87, then extraction in milling is increased by 3.2% from 91.3 to 94.5% [4].

The power required mainly depends on the design of knives, tip speed of the knives and tip clearance. Hugot (1986) reports values given by Farrei for power absorbed by knives running at 600 rpm as 1.8 kW/tch for 20 mm pitch knives and a 25 mm clearance, and 1.5 kW/tch for 38 to 50 mm pitch knives with a 150 to 200 mm clearance. Installed power should be 33% higher than these figures [5]. Peter Rein (2007) recommends the installed power vis-à-vis tip speed and tip clearance as shown in **Table 1**[3].

Table 1 Recommended cane knife installed power, speed and clearance

Knife location	Specific power, kW/tch	Tip speed, m/s	Tip clearance, mm
Leveler knives	0.90	50	1000
First knives	2.25	60	200
Second knives	4.35	60	50
Total	7.5		

A typical 5000 TCD (ton crush per day) sugar plant has around 6MW of installed power from which around 1.5MW of power is used for the preparatory devices for rotating knives/hammers. A buffer/slip resistance to provide 15% full load slip is left in the rotor circuit after the external rheostat is brought to minimum value during starting. These motors have huge inertia due to knives (along with a flywheel) and hammers as shown in **Figure 3**. The external resistance is reduced gradually to its minimum value once motor picks up the speed.

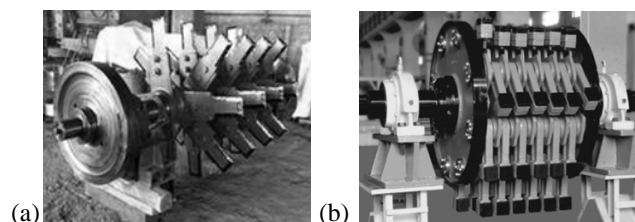


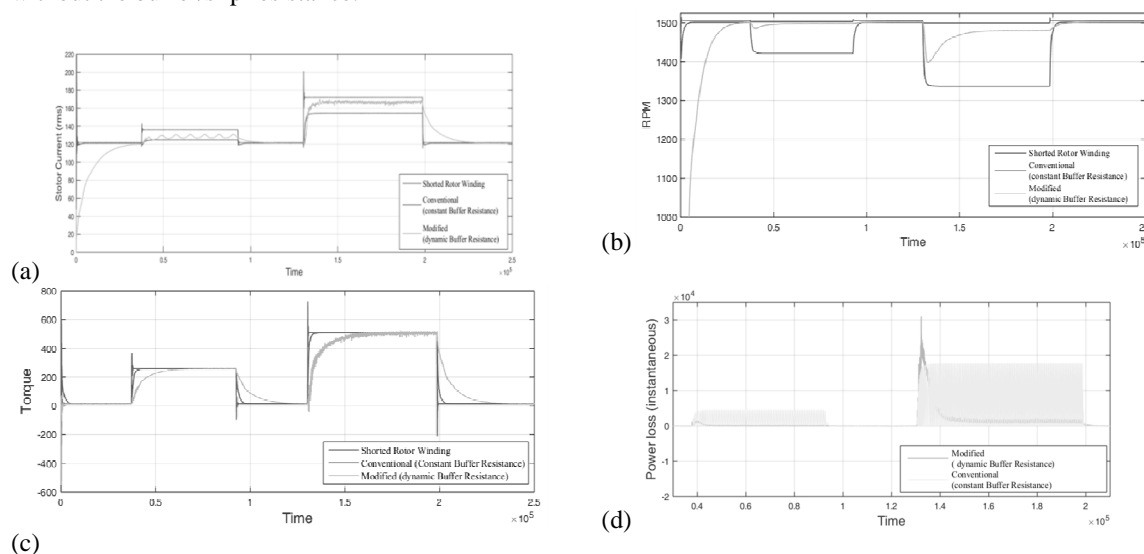
Figure 3 (a) Knives with a flywheel of cane chopping device (b) Hammers of cane shredding devices

However, at full load around 150 kW of power, collectively for all preparatory devices, is dissipated in these external resistances and rotor windings for a 5000 TCD factory.

Simulation of Conventional and Modified SRIM Drive for Chopping Action in Cane Preparation

Simulation for Squirrel Cage Induction Motor

SRIMs has been carried out for 1/4th, 1/2, 3/4th and full load on MATLAB/Simulink to assess the performance of buffer/slip resistance of 15% slip on full load. The various waveforms are shown in **Figure 4** (for 1/4th and 1/2 of full load condition) and **Figure 5** (for 3/4th and full load condition). It can be seen from the various waveforms that this resistance proves good during transients when there is sudden increase in the load by mitigating the overshoot current and torque pulsation and also smoothen the current and torque during sudden off-loading conditions. During steady state, the current drawn by the motor with buffer/slip resistance remains lower than that of the motor without the buffer/slip resistance.



(a) Stator current (b) RPM and (c) torque developed by motor for three cases, i.e. with the rotor winding shorted, with and without buffer resistance. (d) instantaneous power losses in buffer resistance.

Figure 4 Simulation results for 1/4th and 1/2 of full load

Similarly, the torque developed by the motor with buffer/slip resistance remains lower than that of the motor without the buffer/slip resistance. Also, the speed of the motor is reduced due to an increase in the slip. Further, the difference of current, torque and speed of the motor in the above two cases increases as the load is increased. The reduction in speed up to 15% slip at full load is highly undesirable as it results in non-uniform cane preparation which results in erroneous calculations on which subsequent sugar making process is run. Therefore, there is no need for these resistances during steady state condition. Else the values of the resistance should be dynamic and should be in proportion to the load. One such arrangement for varying the Buffer/slip resistance dynamically is shown in **Figure 5**. An uncontrolled bridge rectifier is connected in rotor circuit and the value of Buffer/slip resistance (R) is varied as per the firing angle 'δ' of the parallel power electronic switch (SW) the value of 'R' is varied from near zero during no or light loads to the value so as to offer a 15% slip at full load condition. In steady state at all the loads, the value is kept near to zero.

The effective value for the Buffer/slip resistance (R_{eq}) and the power dissipated (P_r) in it is given by

$$R_{eq} = R (1 - \delta)$$

$$P_r = I_d^2 R (1 - \delta)$$

(1)

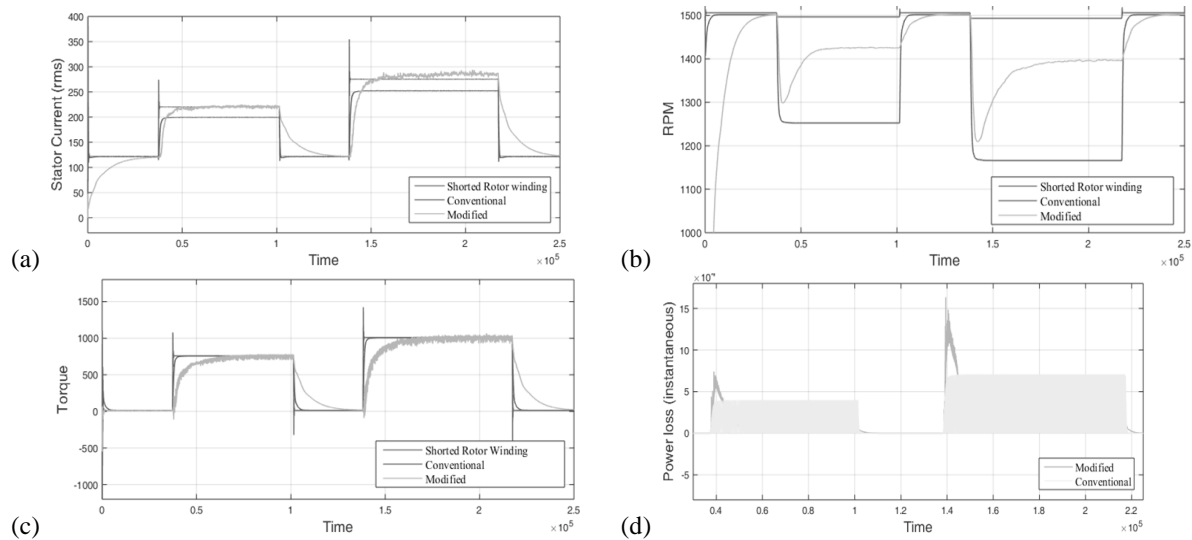
It can be seen from the waveforms that the constant value of buffer resistance results in over-damped condition especially during loads below the full load. These problems can be addressed by current-limit control by adequately modulating the firing of power electronic switch in static rotor-resistance control to realize critical damping to mitigate surging of current and reduce wastage of power during steady state condition [6].

It is observed that the periodicity of the variation of the load from a low peak to high peak is around 20 to 30 s. If transient condition in such particular case is assumed as 20 to 30% of the total cycle then, accordingly, it is estimated that about 70 to 80% of the power, which otherwise is wasted in these constant valued Buffer/slip resistance, is saved as well as the variation in speed is reduced thereby maintaining rather constant Preparatory



Index (PI) of the sugarcane. The various parameters for all the four load conditions are analyzed and summarized as in **Table 2**.

It can be deduced that the variation of stator current and rotor speed is marginal in case of the modified system whereas the variation increases with respect to a great extent in case of the conventional system with constant buffer resistance.



(a) Stator current (b) RPM and (c) torque developed by motor for three cases, i.e. with the rotor winding shorted, with and without buffer resistance (d) instantaneous power losses in buffer resistance.

Figure 5 Simulation results for 3/4th and full load

Table 2 Values of various parameters for different load conditions

State of rotor winding circuit	Steady-state current, A	Steady state speed	Loss in Buffer resistance (approx.), kW
(a) 1/4th of full load			
Shorted rotor winding	135	1495	-
Conventional (constant Buffer resistance)	125	1420	3
Modified (dynamic Buffer resistance)	130	1492	0.5
(b) 1/2 of full load			
Shorted rotor winding	175	1491	-
Conventional (constant Buffer resistance)	150	1340	12
Modified (dynamic Buffer resistance)	170	1485	3
(c) 3/4th of full load			
Shorted rotor winding	227	1488	-
Conventional (constant Buffer resistance)	200	1250	30
Modified (dynamic Buffer resistance)	225	1440	7
(d) full load			
Shorted rotor winding	275	1485	-
Conventional (constant Buffer resistance)	275	1200	50
Modified (dynamic Buffer resistance)	250	1400	12

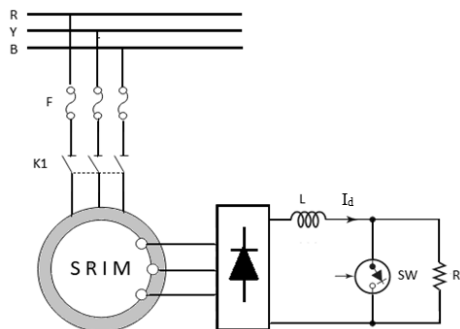


Figure 6 Static rotor resistance control with current limiter

CONCLUSION

Simulation for squirrel cage induction motor and SRIM with static rotor-resistance has been carried out for various load conditions on MATLAB/Simulink to assess the performance of the improved system. It is seen from the various waveforms that if the value of buffer resistance is inserted optimally as per the load conditions giving the critical damped condition for both current drawn by the motor and torque developed. The torque oscillations are also reduced. Also, buffer resistance is made near zero during steady state conditions thereby making power loss in these resistance negligible. Moreover, the speed of motor remains near to the rated speed in steady state condition. This ensures the uniform preparation of cane which is highly desired for estimating other related inputs during sugar manufacturing process.

REFERENCES

1. J.H. Nicklin, Power and Energy requirements for cane preparation, 34th conference of Queensland Society of Sugar Cane Technologist, 1967.
2. T.L. Boshoff, Shredder Drives, Proceedings of The South African Sugar Technologists' Association, June 1994.
3. Peter Rein, Cane Sugar Engineering, Verlas Dr. Albert Bartens KG, Berlin, pp. 94-96, 2007.
4. Peter Rein, Cane Preparation, Sugar Bulletin, Volume 80, Number 6, pp 9-11, 2002.
5. Hugot E, Handbook of Cane Sugar Engineering, Elsevier, Amsterdam, 3rd Edition, 1986
6. Gopal K Dubey, Power Semiconductor Controlled Drives, Prentice Hall, Englewood Cliffs, New Jersey, Ch-9



Evaluation of the Performances of Biomass Briquettes Produced with Sugarcane Bagasse and Cow Dung for Domestic and Small Scale Industries

Anupriya Gupta^{*1}, Deepak Sharma¹, N. L. Panwar¹

Department of Renewable Energy Engineering, CTAE, MPUAT, Udaipur¹, anayagupta18@gmail.com*

ABSTRACT

Sugarcane is one of the principle agriculture crops cultivated in all the tropical countries. The annual world production of sugarcane is ~ 1.60 billion tons, and it generates ~280 million metric tons (MMT) of biomass residues (bagasse and leaves). Agriculture waste management during processing is one of the most serious rural-urban environmental problems in India. In this study, binderless briquettes were produced from sugarcane bagasse and cow dung mixture using hand operated briquetting machine. Different Treatments of briquettes were produced with these raw materials in the ratio of 50: 50 (treatment 1), 55: 45 (treatment 2) and 60: 40 (treatment 3) sugarcane bagasse and cow dung respectively. The results of the performance evaluation showed that the moisture content of all the briquettes was in the range of 6 to 6.5%. The ash content of the briquettes was 5.3, 5.9, 6.2%; the fixed carbon content 19.7, 18.1, 14.8% and volatile matter was 75, 76, 8% of treatment 1, 2 and 3, respectively.

KEYWORDS Sugarcane, Sugarcane bagasse, Briquettes, Volatile matter, Ash content

INTRODUCTION

Majority (90%) of world's energy comes from non-renewable conventional energy sources such as coal, crude oil and natural gases which have limited availability. Oil is the leading source of the world's energy consumption, accounting for 32.9% [1]. Increasing demand by the world's growing population for households, industries and commercial buildings make non-renewable energy sources more scare and it will lead to exhaust these resources in the near future. International Energy Outlook (2013) predicted that the energy consumption of the world will grow by 56% between year 2010 and 2040 [2]. On the other hand, conventional energy sources are significant contributors of global warming, and other environmental issues this affect human health. Security of supply and heightened environmental concern of conventional energy resources bring the focus on the renewable energy sources in the world. Therefore, it has become essential to explore the available potential of renewable and environmental friendly alternative energy sources [3]. Recent estimates show that the total agro-residue availability in India is more than 500 million metric tons per annum. Around 20 to 25% of it is used to produce energy [4]. Agricultural wastes are non-product outputs of processing and production of agricultural products that may contain material that can benefit man but whose economic values are less than the cost of collection, transportation, and processing for beneficial use. Due to increased agricultural production, a large quantity of livestock waste, agro-industrial byproducts and agricultural crop residues are being generated. Hence there are chances that agricultural waste generation increases globally if developing countries continue to intensify farming systems. Agricultural waste generation is from a number of sources namely from cultivation, aquaculture and livestock. The energy recovery from residual biomass is one of the leading alternatives within renewable energy resources, without competing with the planted area of food crops and, at the same time giving an important value to these residues. The energy scenario in rural areas is complex, worse, mixed and biomass based.

Bagasse is the fibrous matter that remains after sugarcane is crushed to extract its juice. It is dry and pulpy waste material which is left, when the juice is extracted out of it. Bagasse is now days being used as a biofuel and also in the manufacturing of building materials and pulp industries. The chemical analysis of bagasse shows that it is composed of Cellulose 45 to 55%, Hemicellulose in the range of 20 to 25%, Ash content of 1 to 4%, Lignin in between 18 to 24% and the content of waxes is less than 1%. Bagasse is a heterogeneous material containing around 30 to 40% of 'pith' fiber, which is derived from the core of the plant. In many sugar mills they use bagasse as the basic fuel for power generation. When bagasse is combusted in large quantities, it provides sufficient heat energy which can be utilized to meet out the energy needs of the sugar mill. As sugarcane bagasse is quite rich in cellulose content, it is being repeatedly investigated for its capabilities for producing handsome amount of cellulosic ethanol. In many tropical and subtropical countries, sugarcane bagasse is commonly used for the substitution of the natural wood as it may lead to problems like deforestation. In many countries such as India, Iran, China, Colombia, Argentina, and Thailand bagasse is being used for the production of paper, pulp and board

Briquettes can be defined as a product formed from physic-mechanical conversion of loose and tiny particle size materials with or without binder in different shapes and sizes. Depending on the equipment used for briquetting,



volume could be reduced by 8 to 10 times and specific density of the biomass can be increased to about 1000 to 1200 kg/m³ compared to 30 to 150 kg/m³ of loose biomass [5]. Rajasthan is one of the leading producers of sugarcane and apparently it is left with large amounts of waste after its harvesting. Due to high calorific value of the biomass it is widely used as fuel for cooking in domestic areas and is often burnt on farm. The accumulation of huge quantities of sugarcane bagasse spoilage and disposal problems is caused year round. The use of sugarcane bagasse waste for production of briquette improves the net calorific value per unit volume and also helps to reduce deforestation by providing a substitute for fuel wood as well as conventional fuel. The technology of briquetting improves the biomass fuel characteristics. Briquetting of biomass improves the bulk density of raw material and proves very helpful in solving the problem of storage and management of waste. Therefore we can say that using various technologies such as gasification etc. we can generate electricity/thermal heat. In this study, potential of sugarcane bagasse as a feedstock for biomass briquetting is studied.

MATERIALS AND METHOD

Sugarcane bagasse was collected from the local markets and the street vendors of Udaipur, Rajasthan. Due to high moisture content it was allowed to dry in the sun for 2 to 5 days. Then they were chopped into small pieces using the crush machine. Pre-processed bagasse materials were thoroughly mixed with cow dung and water was used for agglomerating the mixture in the ratios of 50SB:50CD, 55SB:45CD and 60SB:40CD. Briquettes were produced from each mixture using hand operated briquetting machine. In this study various important energy properties like moisture content, fixed carbon content, volatile matter content and ash content are determined.

Proximate Analysis of Sugarcane Bagasse

Moisture Content

It can be defined as the amount of water per unit mass of the wet solid. It can be measured by heating the briquette in a hot oven, and then the %age of loss in weight gives moisture content %age. Moisture content is an important parameter which is responsible for production and combustion of a briquette.

The moisture content of sample is calculated by following formula, [6].

$$\text{Moisture content} = \frac{W_1 - W_2}{W_1}$$

Where, W_1 and W_2 = Weight of sample before and after drying.

Volatile Matter

It can be measured by heating the known amount of sample in a crucible at 550°C for 3 hours in a closed furnace. The loss in weight gives the volatile %age [6].

$$\text{Volatile matter, \%} = \frac{\text{Loss in weight due to reduction of volatile matter}}{\text{Weight of sample taken}} \times 100$$

Ash Content

For determination of ash content the residual samples obtained after volatile matter determination can be heated gradually in a muffle furnace to 700 ± 50°C for half an hour as per ASTM D-3174.

$$\text{Ash content, \%} = \frac{\text{Weight of ash left}}{\text{Weight of ash taken}} \times 100$$

FIXED CARBON

The fixed carbon content is found by applying the mass balance for the biomass sample.

percent of Fixed carbon = 100 - % of (moisture + volatile matter + ash)

RESULTS AND DISCUSSIONS

All those biomass briquettes which have moisture content greater than 15% are fragile and break easily [7]. All the types of the sugarcane bagasse and cow dung briquettes had a moisture content of the range of less than 10% which is unacceptable range. When determining volatile matter content, biomass generally has volatile matter content of around 70 to 86% of the weight of the dry biomass, the volatile matter in this range makes the fuel very reactive [8].



And all the three types of the sugarcane bagasse-cow dung briquettes had volatile matter content within the acceptable level of 70 to 86%. A low volatile content denotes that the fuel is of low quality which results in smoldering combustion. The non-combustible component of biomass is the ash content and its amount affects the fuel efficiency. Ash deposits on heat transfer surfaces of boilers affect the handling and accelerate corrosion thus reducing efficiency of the burning process. Treatment 3 types of briquettes had significantly high ash content of 6.3% than Treatment 2 and Treatment 1 briquette types as presented in **Figure 1**. All the three type of sugarcane bagasse and cow dung briquettes showed ash content below 10%. The fixed carbon is the carbon available for char combustion. All the three briquette types had fixed carbon content below 20%. Treatment 3 types of briquettes had significantly lower amount of fixed carbon (14.8%) as it had higher amount of volatile matter (80%).

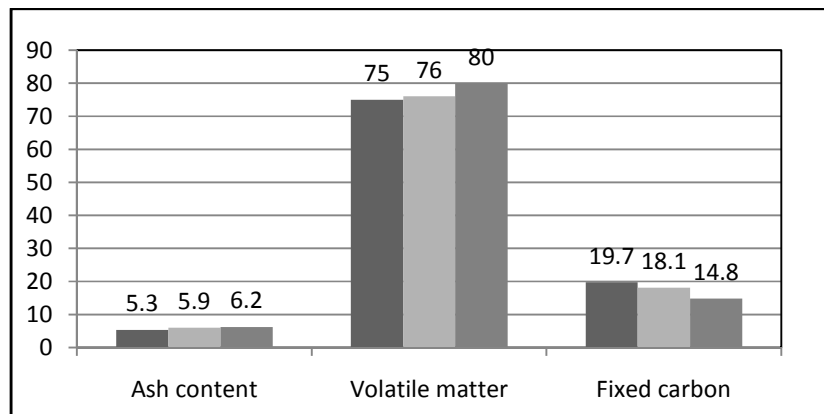


Figure 1 Proximate analysis of bagasse briquettes

CONCLUSION

The ash content, fixed carbon content, moisture content and volatile matter content of all the produced briquettes were in the desired range of values. Hence, the study proves that the biomass namely sugarcane bagasse has a good potential to be used a feedstock for briquetting purposes and could readily be used as a domestic fuel and also at industrial level in boilers and also for generating electricity.

REFERENCES

1. World Energy Council, World Energy Sources, 2016.
2. EIA U, International Energy Outlook. US Energy Information Administration, 2013.
3. P V Kamat, Meeting the clean energy demand. Nanostructure architectures for solar energy conversion. JphyChem Volume C111, Number 7, pp 2384-2860, 2007.
4. Channankaiah Murali, P. Goutham, I. Enamul. P. Hasan, Anbarasan, Performance study of briquettes from agricultural waste for wood stove. International Journal of ChemTech Resources. Volume 8, pp 30-36, 2015.
5. J. S. Tumuluru, C. T. Wright, J. R. Hess, K. L. Kenney, A review of biomass densification systems to develop uniform feedstock commodities for bioenergy application. Biofuels, Bioproducts and Biorefining. Volume 5, Number 6, pp 683-707, 2011.
6. S. H. Sengar, A. G. Mohod, Y. P. Khandetod, S. S. Patil, A. D. Chendake, Performance of briquetting machine for briquette fuel. International Journal of Energy Engineering. Volume 2, Number 1, pp 28-34, 2012.
7. N. Kaliyan, R V Morey, Factors affecting strength and durability of densified biomass products. Biomass and Bioenergy Volume 33, pp 337-359, 2009.
8. C Sheng, J LT Azevedo, Estimating higher heating values of biomass fuels from basic analysis data. Biomass and Bioenergy. Volume 28, pp 499-507, 2005.



Solar Net Metering: Perspective and Challenges

Shreya Karmakar^{*1}, Joy Chakraborty²
Ashrampara, Basirhat, West Bengal¹, shreya03karmakar@gmail.com*
WBREDA, Bikalpa Shakti Bhawan, Sector V, Salt Lake, Kolkata²

ABSTRACT

The depletion of fossil-fuel resources has necessitated an urgent search for substitute energy sources. For rapid change of weather conditions, seasonally and periodically, standalone Solar Photovoltaic (SPV) system and wind energy system are not sufficient to ensure continuous supply of energy. In such a context, grid connected energy systems are now being implemented, that combines Renewable energy (RE) including solar and utility grid. The energy meter which can move in both the direction is known as smart bi-directional meter or import-export meter or the net meter. It can record quantum of energy as taken from the utility grid (import) and quantum of energy as pushed to the utility grid (export). This energy (export) comes from the Rooftop PV Power Plant. Here, in the system of net metering, major focus is on optimum utilisation of the electricity as generated by the rooftop Solar PV Power Plant. The quantum of energy, which is surplus after self-consumption of the user, is sent to the utility grid for its utilisation. Through this process, the electricity bill of the consumers is reduced both in tariff slab and in quantum of energy used by the consumer from the utility/DISCOM grid. India has fixed a target to add 100 GW of Solar Energy by 2022. Out of this, 40 GW is Rooftop Solar PV, which is the area of potential coverage of net metering. Though India has already installed 24.6 GW of Solar Power till date: penetration of Rooftop with Net Metering is not up to the mark. This paper is aimed to develop a knowledge base on Net Metering System on Solar PV Projects. This article covers the Net Metering concept, a critical review of schemes available in India, role of Distribution Companies (DISCOMs), impact on electricity bills and revenue of DISCOMs, gross meter and a proposed intervention in the policy level. With the increasing penetration of Solar PV in India, a pragmatic and doable net metering policy is needful.

KEYWORDS SPV systems, Net metering, DISCOM, Proposed new electricity policies

INTRODUCTION

Grid Connected Rooftop Solar project offers various benefits. These include savings in Transmission and Distribution losses, environmental benefits like Green House Gas emission reduction, reduction in water consumption level associated with thermal power generation. Rooftop PV installation takes place with effectively no extra land requirement. The avoided capacity of the DISCOM during peak solar generation is again a great benefit. State regulatory framework allows DISCOMs to be eligible for deemed Solar RPO benefit. This is because the solar power is primarily consumed by the consumer when the solar power as generated from the rooftop system is either less than or equal to the energy need of the consumer. The extent of impact of grid connected rooftop solar system on DISCOMs may invite an uncertain future for its revenue and business model.

Globally Rooftop solar installations have been driven by incentives as offered through various schemes. These incentives are in the form of upfront capital subsidy, tax credits; net metering, solar specific Renewable Purchase Obligations etc. In India, governments, both at centre and state have launched different schemes to harness the available solar energy potential. The Government of India has recognized Renewable Energy (RE) as a technology to help the Indian Power System and reduce pollution. Till date, considerable efforts have been put in place to develop the rooftop Solar PV sector in India by the government, regulatory commissions and agencies concerned. Rooftop Solar PV assists DISCOMs also by reducing the peak demand during daytime and decreases T&D losses as the power is consumed at the point of generation. Success of Rooftop can be detrimental to the business of DISCOMs in the sense that they lose out mainly on prime and subsidized consumers that they were paying their charges with higher tariffs. In such a position, to make solar a success story in India and also to address DISCOM concerns, regulatory frame work needs to evolve continuously based on experiences, studies and challenges faced by all the stake holders.

CONCEPT OF NET METERING

Net metering is such a billing system where customers are allowed to sell excess electricity generated by Solar PV Plant to local or preferred electric utility (DISCOM). Here net energy between export of Solar PV generated energy and import of DISCOM energy for a billing month is recorded. It can record both the import and export energy values in compliance with parameters as notified by the Central Electricity Authority (CEA) metering regulations and DISCOM procedures in existence. DISCOM procedure is guided by the regulations of the State Electricity



Regulatory Commission. Net metering policies vary state to state. Rooftop solar users normally are entitled for adjustment of their electricity bill at the same rate at which they purchase the electricity from the grid of the DISCOM. This rate covers the variable cost of the power, fixed costs of the installations, required infrastructure which make the electric grid safe and stable. This includes the cost of infrastructure as needed by the DISCOM to accommodate solar systems into their grid. Through the credit or received payment, net-metered customers can effectively avoid cost payment for the grid.

Process of Approaching for NET Metering in West Bengal

- The consumer/user will fix up / select the vendor. There is no such restriction in regard to select a vendor like the vendor should have experience of this and that etc.
- The vendor will provide detailed technical specifications to the consumer/user.
- The consumer will approach to the nearby Divisional Manager or Regional Office of the WBSEDCL or the CESC and will place an application as per format of the WBSEDCL/CESC regarding the installation of the plant. Online application can also be placed.
- Then WBSEDCL will visit at the site and in case of their satisfaction, they will provide an agreement format, where in case of WBSEDCL, a No Objection (NOC) Letter is required from the State Nodal agency for Renewable Energy, which is WBREDA.
- A copy of application, as submitted to WBSEDCL, may also be placed to WBREDA with other technical documents. WBREDA will take fees from the consumer/user/applicant for physical inspection and evaluation towards issuance of the NOC. Then WBREDA will do an inspection. In case of the satisfaction of WBREDA, they (WBREDA), they will issue NOC.
- Then the agreement in between the consumer and WBSEDCL can be executed. After completion of this process, WBSEDCL will provide Net Meter to the consumer premises.

Necessary Documents for Obtaining NOC from the SNA

- Copy of the contract agreement, order to the implementing agency/vendor towards supply, installation, commissioning of the Solar Photovoltaic [SPV] Power Plant.
- Single Line Schematic Diagram of the Grid Interactive Solar PV System in triplicate.
- Certificates/Test reports complying IEEE Standard. IEC test certificate of 61000 of Grid-tied inverters is also required as per the 'CEA Technical Standards for Connectivity of the Distributed Generation Resources Regulations 2013' with complete manufacturer's specification of the Inverter.
- IEC test certificates of PV modules: IEC 61215, IEC 61730.
- Protection scheme at DC side and AC side including test result of the earthing system.
- Copy of current electricity bill of the Distribution Company like WBSEDCL, CESC.

Eligibility Criteria for Net Metering in West Bengal

- Areas where grid quality power supply is stable at least 1st half of the day.
- Consumer must have Three Phase Power Supply.
- Consumers, other than individual households are eligible for net metering system.

Advantages

- It will reduce electricity bill in two ways.
- Quantity of power consumption will reduce.
- Slab of electricity tariff will reduce.

Disadvantage

- If three phase power supply is not at the consumer premises, the consumer will not be eligible for net metering.
- In case of load shading for the FIRST HALF of the day, no solar power can be feed to grid.
- In the evening and at night, the Solar Power Plant fails to supply in the event of grid failure – implying the plant fails when it is needed most by the consumer. The Central Electricity Authority [CEA] (Installation, and Operation of Meters) The Amendment of CEA Regulations in 2014 has a provision to have battery with the Rooftop PV Power Plant for use by the consumer in case of load shedding or grid failure. In many occasions, this note is overlooked by concerned stake holders.
- The inverter of Solar Plant is stated not capable to support the reactive power requirement So, the Solar Plant in Net Metering mode is not capable of supplying dynamically varying reactive power support, required for the consumer appliances.



- In West Bengal minimum capacity of PV Net metering system is 5KWp. So, consumers cannot have a Net Metering arrangement with lower capacity PV
- A small consumer (10 kW or less size) is likely to spend about Rs. 40 to 50 thousand per kWp to get about 1200 to 1300 kWh of Solar Electricity per year per kWp. With average cost of capital @ 12 % p.a, annual depreciation @ 4 %, annual O & M @ 3 to 4 %, average annual expenses are of the order of Rs. 9000/- per kWp. The average per unit cost is Rs 6.50 per kWh or unit. This cost is competitive only for those consumers whose energy charges are more than Rs.6.50 per unit or so.

REVENUE OF DISCOM

It is said that the loss of revenue to DISCOM is limited. It is limited to the loss in 'cross-subsidy'. If these consumers who were paying more than the cost of supply, will install rooftop Solar PV system in net metering mode, it will be a loss to the DISCOM. DISCOMs will be benefitted, if subsidized category of consumers (those having tariffs below the cost of supply) adopt the rooftop solar systems. The extent of impact of grid connected rooftop solar system on DISCOMs may invite an uncertain future for its revenue and business model. Generally the retail tariff of electricity is designed in such a way that the fixed cost for the grid upkeep is not recovered by the fixed charges payable by the consumers. The fixed cost in the electricity business is more than 50% of the total cost, whereas the fixed charge payable by the consumer is just about 15% or less. A large portion of the fixed cost is recovered through the Energy Charges. Thus a Solar consumer may put some burden on non-solar consumer by not paying his/her fair share for grid upkeep.

CONCERNS OF DISCOM

- There should be a cap for the capacity of SPV sources by which may otherwise lead to issues relating to the uncomfortable power flow and upper recovery of revenue by the DISCOM. For example, in CESC area in Kolkata, the Netaji Subhash Chandra Bose International Airport authority has installed 15 MWp of PV plant there. This is because, in the regulation of the West Bengal Electricity Regulatory Commission (WBERC), there is no upper cap of PV installation in net metering mode. It may be kept in mind that on today's principle, Net Metering is intended primarily for partial offsetting the consumer's own requirement.
- SPV sources beyond a capacity (say 500 kWp) can be subjected to Availability Based Tariff (ABT) or Demand Side Management (DSM) so that DISCOMs are not burdened on account of fluctuations of generation from the large PV sources.
- The cumulative capacity of a SPV Sources against a Distribution Transformer (DT) varies widely from 20 to 80 % in India, which requires an upper cap. Primarily, the concern for limiting the cumulative capacity of SPV sources against one DT in case of DISCOM arise out of the Power Quality issues like Voltage Regulation and Harmonics.
- Net Metering is more beneficial for consumers who are paying at a higher rate as it is offsetting their high energy charges. Slab tariff exists almost everywhere. Consumer with high consumption under slab tariff is paying at a high rate for consumption beyond highest slab. Inverter is tested once by the DISCOM during testing visit at the time of Net Meter installation.
- Inverter is tested only once by DISCOM during initial testing at the time of installation of the Net Meter. Though the consumer is advised to submit yearly testing certificate, it is practically very difficult to monitor such activity over the time. There is a rare possibility of failure of inverter to disconnect the system in case of power failure.
- Smart Meter has different categories like Prepaid, Post Paid, Export-Import [Net Meter, **Figure 1**]. Higher Self Power Consumption is there for smart meters, 5 W against 0.7 W for the ordinary meters. It is a big challenge for DISCOMs regarding accommodation of this additional
- In the USA, in general, the consumer pays for the difference. In Germany, the consumer has to pay for the injected power.

NET METERING IMPACT ON CUSTOMER BILLS

Bills of electricity consumers are linked with the electric utility's [DISCOM] cost for providing electric services. This covers the cost of fuels as used to generate electricity. This includes the cost of transmission and distribution of the electricity for its supply at the consumer premise and the maintenance cost of the utility grid. There exists consumer assistance government programmes at different states for low-income group like people under below poverty level. Energy efficiency measures, environmental improvements etc are also covered within the cost of electricity. All electricity customers have electric meter. This meter records the quantum of electric power as delivered by the DISCOM. As electricity is used, the meter moves forward. Here the meter records energy use in kilowatt-hours (kWh). Customers are only billed for their 'net' energy use. So when rooftop solar users generate electricity, they avoid paying for the utility's power. This is justified as they do not use this electricity from



DISCOM. But, they also avoid the payment for all of the fixed costs of the grid required to deliver power when they need it.

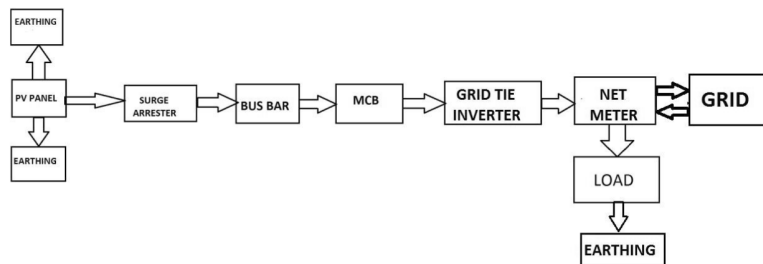


Figure 1 Block diagram of net metering system

Proposed Updation of Net Metering Policies

After the net-metering concept was introduced, costs of producing solar power have declined substantially. Financial benefits of net metering have not been adjusted to reflect this reduction of solar power installation cost. It was plan fully limited to a certain quantity of utility to incentivize the market. With that accomplished, many states are now meeting or exceeding their caps on net metering customers, even with some states are granting extensions to the upper caps of Solar Installation under net metering mode. State legislatures and state regulatory commissions across the country are taking initiatives to modify and re arrange the prevailing backdated net metering policies. It is to enforce their limiting caps and to eliminate the shift in costs from customers with rooftop solar systems to customers without the systems. Until this is applied, non-Solar net Metered customers will bear ever-increasing costs continuously. Presently Net Metering is necessarily associated with solar generation. So, other forms of Power Generation like electricity from Biogas, Biomass, aero-generator etc are not considered here. The future perspective of Net Metering is to be seen in this perspective.

CONCLUSION

The Government of India has decided that Solar rooftop is going to play a leading role in meeting India's fast growing energy demand. India has set its ambition target to be a global leader in solar power. The present study indicates that India provides multiple benefits to DISCOMs in terms of meeting the day time peak demand, curbing technical losses, reducing power purchase cost from generation companies etc. In some cases, it also affects utility business through reduction in sales volume, reducing demand etc. In the country, solar roof-top provides limited installed capacity using huge potential. Now this segment requires effective support from major stakeholders of the country like policy makers in the NitiAyog, State Planning Boards, Electricity Regulator Sand DISCOMs etc.

India has set an ambitious target to install 175 GW of Renewable Power by 2022. Out of this, 40 GW is targeted to be installed from the Roof Top Solar. To achieve India's ambitious target of 40 GW of rooftop capacity by 2022, there is a need to formulate a dedicated and modified mechanism to improve the capacity of DISCOMs. In this connection, the Ministry of New and Renewable Energy (MNRE) has taken initiative to introduce a programme to build capacity of DISCOMs in specific areas such as creating solar cell, developing interconnection framework, web portal for online processing etc. Any kind of initiative step in the way to bring utilities on board. It can help makers to formulate schemes for adoption of market driven models etc. Here DISCOMs have to play an active role so that issues associated with implementation of solar rooftops can be mitigated. Through such measures and steps, India can be able to reach at its desired targets and meet its objective to reduce carbon emissions. So there is a need to change popular perception on Net Metering in a significant manner on today. This change should be based on ground reality, government's target and pragmatism, so that higher and desired level of penetration can be achieved.

REFERENCES

1. Jagruti Thakura, Basab Chakraborty, Sustainable Net Metering Model For Diversified, India
2. Net Metering Using Solar VaibhavPandav 1, Rucha Hawaldar 2, Hrushikesh Nevase 3, Hrishikesh Deshmukh4, Sachin Sawant5
3. Field level inspection of PV Rooftop Net Metering
4. Supported by Shakti Sustainable Energy Foundation and carried out by Deloitte Touche Tohmatsu India LLP.
5. The CEA (Installation and Operation of Meters) amendment Regulations, 2014
6. Water and Energy International, September, 2018
7. Discussions with officials of WBREDA, WBSedCL, CESC, WBERC regarding Import-Export Energy Meter.



Transformation of Electrical System in Commercial Vehicles

Manas Kumar Mishra¹, Anuj Kapoor², Sushant Mishra³, Kumar Satyam⁴
TATA Motors Ltd^{1,2,4}, mkmishra@tatamotors.com,
TATA Technologies Ltd³

ABSTRACT

Truck illustrates the fascinating possibilities of connectivity; drive systems, future display, control technologies, telematics and self-sufficient power supply. These features are provided for drivers comfort, safety and for better fuel economy. The current Indian market for commercial vehicles are very focused for Emission control and feature for driver assistance. The electrical system further evolved to add more and more driver assistance rather manual intervention for driver's information for vehicle health status and safety. Transition in the additional sensors and actuators has taken place from BS I to BS IV and upcoming to BS VI. Engine did not have any sensor other than temperature transducer but now in BS IV vehicles have sensors and actuators, which provides digital signal to ECU.

KEYWORDS Vehicle electrical system, Functionality, Features, Current generation vehicles, Troubleshooting

REASONS FOR EVOLUTION ARE

To reduce emissions and make vehicles fuel-efficient. Transition in the additional sensors and actuators has taken place from BS I to BS IV. BS I did not require electronic control but now in BS IV vehicles, we have all digital signals from various sensors to Engine Management Systems (EMS). To make the vehicle safer during braking and turning (Anti-lock Braking System / Electronic Stability Control) has been made mandatory.

Faster response to road situations and for more efficiency E- power steering and electronically controlled air suspension has been introduced.

To give the vehicle driver, more information regarding the condition of vehicle, On Board Diagnosis, (OBD) Telematics and navigation system are the features, which reduces maintenance cost and time of the vehicle.

for improved comfort, full automatic temperature controller, auto light ON, auto-functioning of wiper, rear vision camera, part assist system, immobilizer remote keyless entry (RKE) are some example for vehicle ergonomics.

INTRODUCTION

The word 'Automobile' is derived from two ancient words: 'auto' means self and 'mobile' means movable. This means a vehicle that moves itself, rather than being pulled or pushed by any external sources such as animals. The automobile industry is continually replacing mechanical systems with electronic systems. Emerging technologies and applications frequently changes and the automobile industry is no exception. Automobile industry, the business of producing and selling self-powered vehicles, including passenger cars, trucks, farm equipment, and heavy commercial vehicles. Complaints about auto pollution, traffic congestion, and auto safety led to the passage of government regulations beginning in the 1970s, forcing auto manufacturers to improve fuel efficiency and safety. Auto companies are now experimenting with alternative energy sources as natural gas, electricity, hydrogen fuel cells, and solar power.

Today, automobiles have become a crucial part of our lives, an extension of the human body that provides us faster, cheaper and more convenient mobility every passing days. The history of automobile is very fascinating as it reflects an evolution of the automobile that took place worldwide.

IMPLEMENTATION

A truck is a vehicle designed for commercial transportation. These vehicles vary greatly in load carrying capacity and power of the engine. Commercial trucks size and length of chassis varies according to the tonnage of the vehicle. Trucks are also designed to mount special utility equipment, such as in the fire fighter, concrete mixers and cranes.

Current generation trucks are largely powered by diesel engines and diesel is the major contributor of source of energy. This diesel engines are further classified into their Emission Norms.

The current generation trucks are covered with 60 to 70 % to electrical and electronics system as more of sensors addition to meet the Emission norms. Engine system layout is shown in **Figure 1**.



Emission standards emission norms where allowable quantities of Nitrogen Oxide (NO_x), Particulate Matter (PM), Hydrocarbons (HC) and Carbon Monoxide (CO) are AUS32 to achieve control on emission. Nitrogen Oxide (NO_x) is the most harmful element, which contributes to acid rain.

Specific sources over specific timeframes. Emissions norms are designed to achieve air quality standards and to protect human life from toxics.

Bharat Stage (BS) Emission Stages

The basic difference of BS-I, BS-II and BS-III (Figure 2) engines is the presence of catalytic convertor.

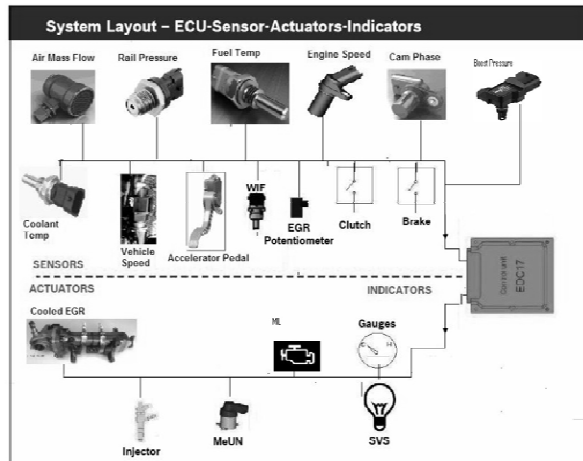


Figure 1 Engine system layout

Catalytic convertor is present in BS-III engine, which helps in reducing the formation of hydrocarbon and carbon monoxide. While in BS-I BS-II engine, no catalytic convertor is present.

Introduction of BSVI

Tightened Emission Limits:

Carbon Monoxide and Hydrocarbon + Nitrous Oxide ($\text{HC} + \text{NO}_x$) emission levels

BS III norms - 1.00 g/km

BS IV norms - 0.75 g/km

This means engines have to be changed in order to emit less pollutant from the exhaust.

Tata Motors Commercial Vehicles are BS-IV ready with Exhaust Gas Recirculation (EGR) with a new future leading Selective Catalytic Selective Catalytic Reduction (SCR), was introduced in 2010 for BS IV for commercial vehicles in Indian Market.

Tata Motors has developed EGR in-house and covers the entire range of Tata engines including the new generation 3 l and 5 l engines.

In 2014, Tata Motors Limited had created a new benchmark with SCR technology for M&HCV Truck and bus applications with Tata Cummins engines.

Selective Catalytic Reduction (SCR) is an advanced technology of after treatment to reduce NO_x ($\text{NO}_2 + \text{NO}$) outside the engine.

- Engines expels out many harmful /polluting gases and other by products of combustion through exhaust.
- NO_2 and NO is the most harmful element which contributes to acid rain.
- AUS 32 is injected upstream of a catalyst in the exhaust system using a very accurate dosing pump.

Bharat Regulation Table

Regulation	Year incorporated in Europe	Year incorporated in India	CO Carbon Monoxide	HC Hydrocarbon	NO _x Nitrogen Oxides	PM Particulate Matter
B S III	2002	2008 (select cities)	2.10	0.66	5.00	0.10
		2010 all cities	5.45	0.78	5.00	0.16
B S IV	2005	2010 (select cities)	1.50	0.46	3.50	0.02
		2013 all cities	4.00	0.55	3.50	0.03
B S V	2008		1.50	0.46	2.00	0.02
			4.00	0.55	2.00	0.03
B S VI	2013		1.50	0.13	0.40	0.01
			4.00	0.16	0.40	0.01

NO_x - Leads to Bronchial infections, cold, headaches and eye irritations.

CO - Reduces the ability of blood to carry oxygen.

HC - Drowsiness, eye irritants, cough and cause cancer.

PM - Respiratory infections, persistent cough and throat irritants.

Figure 2 BS Emission Stage



- The engine ECM controls the amount of AUS 32 injected by the pump.

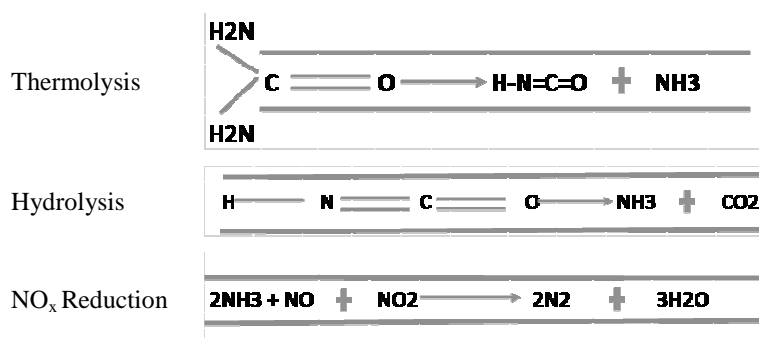
Exhaust Gas Recirculation (EGR), a method of returning part of the exhaust gases to an engine by means of a valve (EGR valve) in order to reduce the combustion temperature, which leads to a reduction in the formation of NO_x.

SCR Fundamentals

Thermolysis of AUS 32 to Iso-cyanic Acid and Ammonia (Decomp Reactor) requires heat and time.

Hydrolysis of Iso-Cyanic Acid to Ammonia and CO₂ (SCR Catalyst), water, heat and time is required with enhanced by catalyst.

Reduction of Nitrogen Oxides to Nitrogen Gas and H₂O (SCR Catalyst) heat and time is required with enhanced catalyst.



The above compound are shown to understand the chemical reaction which reduces the NO_x content from the exhaust system which is released in environment.

The reaction shows the steps of Thermolysis, Hydrolysis and NO_x reduction in sequence.

The process of SCR and comparison of SCR with EGR are depicted in **Figure 3**.

Sensor Types

Any devices that transforms physical quantities into digital/analog output signals which could also be used as input for control system is said to be a sensor. In automobiles multiple/various different sensors are used to transmit signals for controlling, monitoring or as an information device. These sensors are fit mainly in powertrain, Engine, cabin and chassis system.

In engine application, the sensors are not only used for controlling the mechanics preciously by also being used for diagnostic purpose.

Nowadays, Engines Control units have a user friendly behavior, through which it can control a wide range of parameters which helps to meet the emissions standards.

Few critical parameters which are controlled by ECU are fuel injection system, fuel injection amount, air flow, EGR, monitor the air intake temperature, real time engine temperature monitoring and logging the data, exhaust oxygen content, and exhaust temperature and so on. To control and monitors these features a wide range of sensors are being used.

Moreover, few sensors can be used strictly for diagnostics or strictly for control. There are also another type of concept which are not adequately captured in a conventional definition of sensors is the concept of virtual sensors.

Virtual sensors are not actually physical sensors. But these are software routines that are used as inputs, which comes from physical sensors, to estimate the measurable values that are either difficult to measure adequately.

There may be 12 to 30 sensors for engine operation, brakes, safety, and Emission Controls.

- Crankshaft Angle Sensor
- Camshaft Angle Sensor
- Mass Airflow Sensor



TELEMATICS

Global positioning system is a satellite based radio navigation, by which the object position can be known through the application. Total 4 satellites are used to visualize the position of the object (viz. X-axis, Y-Axis, Z-axis and time frame).

Telematics is electronics unit which not only gives the position of the vehicle but has several other uses too. The unit can also be used to interact with Engine ECU to fetch data like Engine Speed, Vehicle Speed, Fuel Efficiency and these data can be flashed along with the position to the customer for monitoring purpose.

This unit is very innovative which can transmit the data to the owner on real time basis. This unit is user friendly and avoids many irrelevant abuses to the vehicle which used to affect the owner commercially.

Practical Applications of Vehicle Telematics

Vehicle tracking, trailer tracking, container tracking, fleet management, telematics standard, satellite navigation, mobile data, wireless vehicle safety communications, emergency warning system for vehicles, intelligent vehicle technologies, car pooling, auto insurance/usage-based insurance.

TROUBLESHOOTING

Automotive maintenance and the troubleshooting of even basic problems can be incredibly complex.

Steps to understand the Problem Area

- Verify the Complaint / Problem

Note voice of customer. Check the drawings / manual whether it meets the functioning. Is the complaint continuous / intermittent?

If conditions are repeated, does the problem reoccur?

Vibrate parts / sensors /ECU slightly to simulate vibration related problems

- Determine the Problem Area

Determine which circuit / system is related.

Find clues to location of the problem. Based on the location of the problem, determine which part of circuit is involved.

How much of circuit is affected?

If entire circuit is inoperative then chances of-fuse blown or chance of positive/ground ineffective load or component is bad

If only one part of circuit does not work, then maybe the component is bad or wire is trapped / cut. Check the splice condition.

In case of systems like EMS, with help of diagnostic tester, the fault can be located faster.

Always check DTC code first. Clear code & start vehicle again to re verify the code. Locate the Pins / splices and components in the path of the circuit

- Analyze the Problem

Which components are affected?

Is the problem related to open circuit / short circuit / high resistance / feedback?

When does the problem occur?

Trace the current flow paths

- Isolate the Cause

Find probable areas. Determine where to begin checks – Components easy to access / historical problem areas. Make your inspection.

Any problem should have a structured Problem Solving Approach (SPS Approach). Before applying structured problem-solving, you need to identify if there is a standard operating procedure. If not, you need to prepare a standard. If there already exists an SOP check if the same was followed or not.

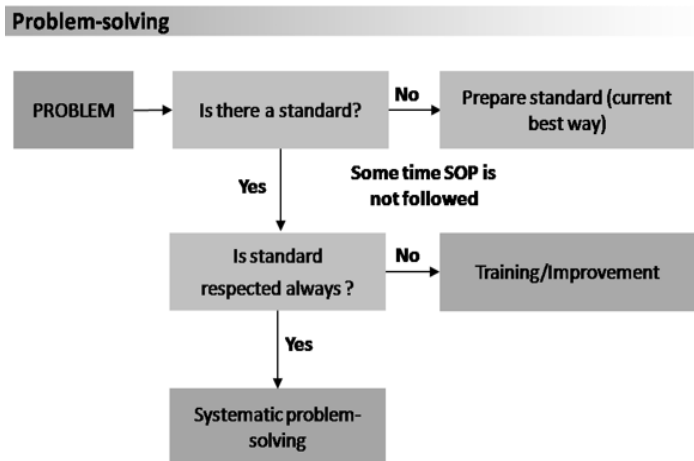


Figure 5 Problem solving approach

Structured Problem Solving as shown in **Figure 5** should always tend to resolve the problem by Correction, Corrective Actions and Preventive Actions.

Correction: If there is a headache, visit a doctor. Or, if there is a wound putting bandage is a correction. Correction includes repair, rework, or adjustment and relates to the disposition of an existing nonconformity. Correction is action taken on symptoms.

Corrective action: After putting a bandage to the wound going to the doctor for the examination of the wound is a corrective action. This means a solution meant to reduce or eliminate an identified problem. This means action taken on the cause.

Preventive action: It is a long terms action. Getting tetanus or an antibiotic injection can be a long term measure so that infection does not spread is a preventive action. The action was taken to remove or improve a process to prevent potential future occurrences of a nonconformance.

By resolving the problem and horizontally deploying to the other similar area, we can minimize the risk of failure and achieve First Short OK (FSOK) in the industry while transforming and introducing the emerging Electrical System in the Commercial vehicle.

CONCLUSION

The upcoming technologies for Heavy Commercial Vehicles are Electric Vehicle (EV) and Self-Driven Trucks.

Electric Vehicle (EV)

In Electric Vehicle System, popularly known as EV, uses one or more DC Electric Motor or Traction Motor for vehicle transmission. EV will cover the 90% of electrical and electronics in vehicle. The major requirement of EV is power source and its regeneration. Currently Tata Motors handed over 25 hybrid electric buses to the cities is planning authority MMRDA.

Self-Driven Trucks

Future advancement believes in driver less cars. Similarly, it is expected too in commercial vehicles. A driverless vehicle will be controlled through GPS and will cover the distance according to the given input. However, vehicles with Advance Emergency Braking System are introduced in Trucks (AEBS).



Integration of Solar Photovoltaic (SPV) Module with Direct Ethanol Fuel Cell (DEFC) Technology: A Review

R. G. Bodkhe^{*1}, R. L. Shrivastava², R. B. Chadge³, Vinodkumar Soni⁴

Department of Mechanical Engineering, Yeshwantrao Chavan College of Engineering, Nagpur 441110, M.S., India^{1,2,3},
rgbodkhe37@gmail.com*

Central Railway, Nagpur 440021, M.S., India⁴

ABSTRACT

Direct Ethanol Fuel Cell (DEFC) technology is modular, compact, lightweight cell, suitable for portable applications and simple to construct. This cell uses Ethanol as a fuel and generates electricity which can be used during non sunshine hours. This paper focuses on integration of solar photovoltaic module with water electrolyzer for Hydrogen generation and applications of Fuel Cell technology especially in remote areas for driving small electrical loads such as portable power devices. In this paper also discussed about the active and passive DEFC system. To reduce both ethanol and water crossover without sacrifice of performance is a challenge in passive DEFC system. It is a thrust area to develop a fuel cell system which has positive net energy. In this paper we reviewed that the technical status of hydrogen and direct ethanol fuel cell technologies, progress towards research in solar hydrogen.

KEYWORDS Renewable energy, Solar photovoltaic module, Hydrogen, Green house gas, Passive direct ethanol fuel cell, Proton exchange membrane, Methanol, Electricity

NOTATIONS

SPV	Solar photovoltaic
Si	Silicon
GaAs	Gallium Arsenide
DC	Direct current
AC	Alternating current
DLFC	Direct Liquid Fuel Cell
DEFC	Direct Ethanol Fuel Cell
DMFC	Direct Methanol Fuel Cell
EOR	Ethanol Oxidation Reaction
ORR	Oxygen Reduction Reaction
GHG	Green House Gas
PEM	Polymer Electrolyte Membrane
PEMFC	Polymer Electrolyte Membrane Fuel Cell
NaOH	Sodium hydroxide
C ₂ H ₅ OH	Ethanol

INTRODUCTION

A solar cell is made up of semiconductor materials like silicon (Si) or other semiconductor materials like GaAs. When sunlight (in the form of photons) falls on these semiconductor materials, electricity is generated. The amount of this generated electricity depends upon some factors like solar radiation intensity, size of the solar cell, type of semiconductor material and ambient temperature. From one solar cell, only a fraction of electricity is obtained which is provided in a considerable amount by connecting these solar cells in series and parallel combinations called photovoltaic (PV) modules. These modules are again fabricated in series-parallel combination to form photovoltaic arrays which are generally used to solar photovoltaic (SPV) plants to have enormous amount of power to supply it



for residential and industrial applications. Fuel cell is an electrochemical device which converts chemical energy into electrical energy directly.

ELECTROLYZER

The solar-generated electricity can be further used to drive electrolysis, which produces hydrogen. The electrolyzer uses electricity from solar PV module to break water into hydrogen and oxygen. This is photo electrolysis, which is conducted in an electrochemical cell. The electrochemical cell represents a compact device that combines the photovoltaic cell with an electrolyzer [1]. It can be operated with distilled water without caustic solutions or acids. This process can produce pure hydrogen without pollution when the electrical source is renewable energy. The operation of fuel cell is similar to that of electrolyzer. Except the reaction that occurs in the anode and cathode are reversed. In an electrolyzer, the hydrogen gas is produced at the cathode and in a fuel cell; the hydrogen gas is consumed at the anode. **Figure 2** shows the schematic of The PEM electrolyzer.

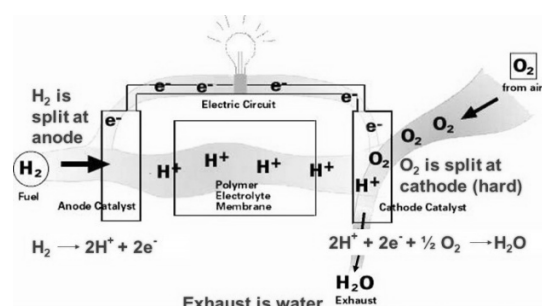


Figure 1 Working of fuel cell

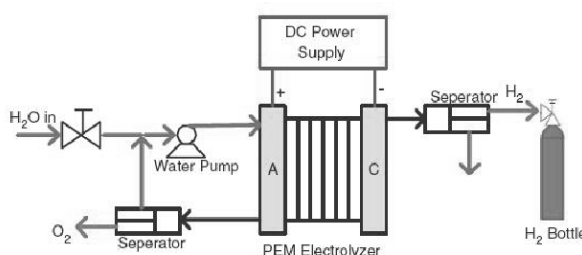


Figure 2 Operating principle of the PEM electrolyzer (Voutetakis et al., 2010)

After literature cited, it is revealed that, ethanol is sustainable, carbon-neutral transportation fuel than methanol. It has higher energy density and ease of transportation, storage and handling compared to hydrogen and methanol [2]. The ethanol fuel can be used instead of hydrogen in the direct ethanol fuel cell to generate electrical energy. Ethanol is a good fuel choice for overcoming the problems with methanol. Ethanol has higher energy density. It also can be produced from agricultural bioprocesses and is considered a renewable energy [3]. Additionally, ethanol has been proven by researchers to have a lower crossover rate and affects cathode performance less severely than methanol. PEMFC is suitable for powering portable devices due to its fast start up and use of a solid electrolyte [4].

DIRECT ETHANOL FUEL CELL

Different DEFC systems have been reviewed. Hydrogen production, transportation and distribution is a major concern for the fuel cell commercialization. Ethanol is an alternative fuel to hydrogen which can be used for fuel cell directly or indirectly. Direct ethanol fuel cells are the key technology for various applications such as transport, portable power systems, backup power and especially power for remote areas and large scale power generation. For indirect ethanol fuel cells, ethanol is externally reformed to produce a mixture of CO and H₂ with steam reforming followed by conversion of CO to CO₂ in a water gas shift reactor. The hydrogen thus produced can be used in most fuel cells. Although the efficiency of such system is less. Ethanol in diluted form can directly fed to the anode chamber of the fuel cell and oxidized at electrolyte offering substantially higher efficiency. Ethanol is a large molecule and need of 12 electrons in the electrochemical reaction for its direct oxidation. And the kinetics of its oxidation is more sluggish and many intermediate products are formed which leads to its incomplete of oxidation and poisoning of catalysts. The anode catalysts development is the key technology for DEFC in addition to the ethanol crossover and poisoning of the catalyst in PEM fuel cells [5]. Also fuel delivery system and carbon deposition on the anode side are the main challenges in these systems.

DEFC has potential as an alternative future power sources such as portable power systems. The membrane characteristics such as low ethanol crossover, high ionic conductivity, high mechanical, chemical and thermal stability. All these parameters are desirable for the high performance of DEFC [6]. Direct liquid fuel cells (DLFC)



are the main focus towards commercialization. DMFC seem to be the most commercialized type of DLFC followed by DEFC. Due to the high energy density and independent from an electrical power source for charging, DLFC is a promising candidate. Currently the development of DLFC towards electronic portable devices, vacuum cleaner, home gadgets such as lamps, fans, grass cutters, coffee machines, portable juice machine, to power health monitoring equipment, medical equipment such as blood pressure monitor machines and blood glucose test meters, which make those products difficult to use in a remote areas that lacks a constant electric supply. The main problem with the DLFC at present is higher cost of catalyst. This issue is important to find the catalyst for both the anode and the cathode at the cheaper cost and to improve the membrane electrolyte assembly fabrication and to promote better utilization of fuel cells [7].

The new sustainable hydrogen clean energy with zero emissions and potential to be more cost effective by using renewable energy represents in all regards a superior solution to the carbon fossil fuel systems [8]. Currently In this paper we reviewed that the technical status of hydrogen and direct ethanol fuel cell technologies, progress towards research in solar hydrogen, DEFC, focused on energy storage applications and comparisons between the hydrogen, methanol, ethanol for fuel cell with respect to theoretical specific energy, electrical energy density, boiling point, vapour pressure, availability, infrastructure facility, simplicity of handling, flammability, explosiveness and toxicity[11]. Because of use of fossil fuel, contribution of green house gas emission is a major concern in this world. The objective of this paper is to propose the new method of Integration of solar PV module with DEFC technology. Fuel cell is a promising candidate as a renewable energy source. This cell uses ethanol as a fuel and generates electricity which can be used during day and night hours.

Ethanol is considered as renewable fuel as it is prepared from biomass which is used as fuel for lighting, cooking and also as automotive fuel compared to the conventional fuel. Conventional method of production of hydrogen is very energy intensive.

Ethanol has higher energy density than methanol and hydrogen and also easy for transportation, handling and storage [10]. In DEFC, to avoid ethanol crossover through the membrane is a major concern reported by the many researchers. Ethanol should be transported through the proton exchange membrane without taking part in the electrochemical reaction. However, It is interestingly to know the effect of cell voltage, current density, and efficiency of the cell and its overall performance under the working condition. Researchers also revealed that the rate of crossover decreases the current through direct ethanol fuel cell, however it is not yet clear that the current density is reduced due to incomplete oxidation or ethanol crossover. This is remaining challenge for the researchers[9].

After literature cited, it is understood that the DEFC can be classified as the active and passive systems. Active system needs moving parts to feed oxygen and ethanol to the cell which require external source to operate. This type of system preferred for large power generation especially for transportations. Passive systems do not require external source to operate. Directly fuel and oxygen supply to the cell. Passive system uses natural convection to achieve the goal. It is more suitable for portable power, stationary application. Based on the study done by the researchers the main challenge is how to reduce the ethanol and water crossover [9].

Present study is covering two promising alternative energy sources, that is, solar energy and Ethanol as a fuel in fuel cell as a renewable source. Both are the trust area for study worldwide.

Wealth-from-waste, green and clean, abundant, inexhaustible and eco-friendly is the salient characteristics of such system. Development of such system is a reviving opportunity in urban and rural areas, creating new opportunities for small businesses, developing new products, spawning new research, creating more good-paying jobs and more income for families would re-invigorate the economy of nation. Based on the literature review the research gaps have been identified and a comprehensive research work is proposed to bridge the gaps as under –Conversion efficiency of individual and combined system would enable us to identify critical design and operating factors of fuel cell. Individual and combined efficiency of individual components viz. PV module, electrolysis, fuel cell etc. will be carried out. Apart from determining the efficiency, chemical and calorific analysis of fuel gas will also be carried out to check the quality and yield of the electrolyzer, Storage system for fuel gas should also be studied, so that its role in improvement of the overall efficiency of the system can be explored.



INTEGRATION OF TECHNOLOGIES

The present paper focuses on Integration of Solar Photovoltaic Module with water electrolyzer for Hydrogen and Direct Ethanol Fuel Cell system for driving small electrical loads like portable power applications and an alternative to batteries and diesel generators for backup power applications especially for supply of electricity for pumping sets in the villages especially in remote areas such as cellular phone towers without transmission lines. In India presently maximum electric power generation takes place through fossil fuels which are responsible to increase the environmental pollutions and green house gas (GHG) emissions. Now this is a right time to think about reduction of these emissions as fast as possible otherwise it will lead again the global warming effects, also these conventional source will not be available in the near future, because of its maximum consumption. As crude oil prices also increases because of its higher demand throughout the world.

Now in this modern era, it is reviewed that, many of the researchers are focusing and finding the ways of using renewable energy sources such as wind energy, solar energy which is pollution free and available in the nature free of cost etc. A government administration, industries, academic institutes also encourages us for the research and development in this field.

Hydrogen is receiving attention driven by growing concern about climate change, air quality issues, and integration of variable renewable into energy system. Recent energy and economic studies suggest that hydrogen and fuel cells could be important technologies for simultaneously addressing these challenges in future renewable intensive, low carbon energy system. Hydrogen is increasingly seen as a key energy carrier for a future low carbon energy system.

CONCLUSION

Conventional method of production of hydrogen is very energy intensive. If fuel cell and associated components are not designed properly, it may lead to negative net energy. Many of the researchers reported their work on this topic have covered various methods of electrolysis for hydrogen fuel production and conversion of the same into electricity. If fuel cell and associated components are not designed properly, it may lead to negative net energy. Use of renewable energy such as solar energy for the hydrogen generation through electrolyzer and its use in fuel cell technology is better alternative for the onsite electrical power generation without transmission line especially in remote areas, military applications and also helpful to reduce the green house gas emissions which is produced from automobile industry currently.

REFERENCES

1. Dincer, C. Zamfirescu, Sustainable Energy systems and Applications, springer science, DOI 10.1007/978-0-387-95861-3_13, 2011.
2. M.Z.F. Kamarudin, S.K. Kamarudin, et al, Review: Direct ethanol fuel cells, Int. J. Hydrogen Energy, Volume 38, pp 9438 – 9453, 2013.
3. S. Abdullah, S.K. Kamarudin, et al., Development of a conceptual design model of a direct ethanol fuel cell, int. J. of hydrogen energy, Volume 40, pp 11943 -11948, 2015.
4. L. An, T.S. Zhao, R. Chen, Q.X. Wu, A novel direct ethanol fuel cell with high power density, Journal of Power Sources Volume 196, pp 6219-6222, 2011.
5. S.P.S. Badwal, S. Giddey, A. Kulkarni, J. Goel, S. Basu, Direct ethanol fuel cells for transport and stationary applications – A comprehensive review, J. Of Applied Energy, Volume 145, pp 80 -103, 2015.
6. Z. Zakaria, S. K. Kamarudin, et al., Membranes for Direct Ethanol fuel Cells: An Overview, J. of Applied Energy, Volume 163, pp 334- 342, 2016.
7. [7] B.C. Ong, S.K. Kamarudin, S. Basri, Direct liquid fuel cells: A review, Int. J. Hydrogen Energy, Volume 42, pp 10142-10157, 2017.
8. Alvin G. Stern, A new sustainable hydrogen clean energy paradigm, Int J. Of Hydrogen Energy, Volume xxx, pp 1-12, 2018.
9. J.P. Pereira, D.S. Falcão, et al., Performance of a passive direct ethanol fuel cell, Journal of Power Sources Volume 256, pp14-19, 2014.
10. Barakat, A. M. Nasser, Mohammad, A. Abdelkareem, Hak Yong Kim. Ethanol electro-oxidation using cadmium-doped cobalt/carbon nanoparticles as novel non precious electrocatalyst, Applied Catalysis A General, 2013.
11. Helena Berg, Joakim Nyman, et al., Direct Ethanol Fuel Cells: Ethanol for our future fuel cells? Swedish Hybrid Vehicle Centre, ENERGIFORSK, ISBN 978-91-7673-137-6, 2015.
12. G. Tzamalís, E.I. Zoulias, et al., Techno-economic analysis of an autonomous power system integrating hydrogen technology as energy storage medium, Renewable Energy Volume 36, pp 118-124, 2011.



Advanced Distribution Management System: State-of-Art Integration of Technologies in Power Distribution

P. Devanand^{*1}, Tarun Batra¹, Md Shadab Ahmad¹, Tarun Bhardwaj¹
Tata Power - DDL, New Delhi¹, p.devanand@tatapower-ddl.com*

ABSTRACT

Advanced Distribution Management System (ADMS) is a masterwork integration of different information and operation technologies (IT-OT) which is implemented by Tata Power Delhi Distribution Limited (Tata Power-DDL) recently. ADMS is an integrated platform with one user interface for Supervisory Control and Data Acquisition (SCADA), Distribution Management System (DMS) and Outage Management System (OMS), which is integrated with different information technologies like Geographical Information System (GIS), Enterprise Resource Planning (ERP), Customer Relationship Management (CRM), Field Force Automation (FFA) and Meter Data Management System (MDMS), and equipped with advanced analysing and planning application. It is also capable to integrate with upcoming disruptive technologies like Distributed Energy Resources (DER), Automatic Demand Response (ADR) and Battery Energy Storage System (BESS). Hence, ADMS provides monitoring, control, analysis, training and planning application on a common machine. It is integrated with GIS for importing complete electrical network (from energy exchange point to consumer service point) and mapping of each and every consumer on these electrical network. It is also well integrated with sensors and relays installed at electrical sub-stations which send status of protective and isolating devices and other analog parameters and digital signals. It has interface with CRM for complete detail of consumer, fetching consumer outage complaints intantaneously when it get registered and updating power supply status of consumer when any tripping occurred in electrical network. All these outages detail are shared with FFA application which is used by field crew to manage and monitor outages. This article describe how integration of all these technologies come possible in ADMS and how it will help in improving reliability, quality and enhancing customer satisfaction by reducing outage duration, effective network management and timely communication with our consumer.

KEYWORD Advanced Distribution Management System (ADMS), Technology Integration, Information and Operation Technologies (IT-OT), System Reliability, Consumer Satisfaction.

ABBREVIATIONS

ADMS	Advanced Distribution Management System
ADR	Automatic Demand Response
AMI	Advanced Metering Infrastructure
AT&C	Aggregate Technical and Commercial
BESS	Battery Energy Storage System
CIM	Common Information Model
CIS	Customer Information Service
CRM	Customer Relationship Management
DA	Distribution Automation
DER	Distributed Energy Resource
DPF	Distribution Power Flow
DMS	Distribution Management System
EMS	Energy Management System
ERP	Enterprise Resource Planning
FFA	Field Force Automation
GIS	Geographical Information System
GSAS	Grid Sub-station Automation System
ICCP	Inter Control Centre Communication Protocol
OMS	Outage management System
PPM	Power Portfolio Management System
SAIDI	System Average Interruption Duration Indices
SAIFI	System Average Interruption Frequency Indices
SCADA	Supervisory Control and Data Acquisition
SLDC	State Load Dispatch Centre



INTRODUCTION

Tata Power Delhi Distribution Limited (Tata Power-DDL) is a joint venture between Tata Power and the Government of NCT of Delhi, distributes electricity in North & North West parts of Delhi with a registered consumer base of 1.64 million and a peak load of around 1947 MW (recorded in June 2018). It has been the frontrunner in adopting new and advanced technologies to improve power quality, enhance power reliability and enrich consumer delight in its licensee area. Due to continuous initiatives and innovations Aggregate Technical and Commercial Loss (AT&C) reduced from 53% to 8.40% in span of 15 years (**Figure 1**). There is incessant improvement in Reliability Indices (SAIDI, SAIFI) since its inception in 2002. SAIDI decreased from 8.6 h to 2.68 h whereas SAIFI decreased from 6.5 to 2.5 in last 10 years (**Figure 2**). These reaffirm position of Tata Power-DDL in the league of top global utility.

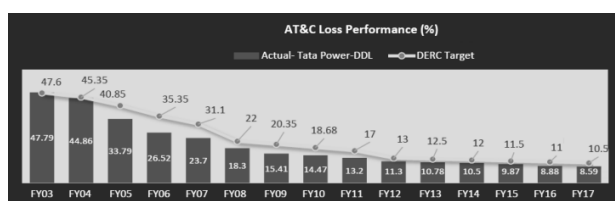


Figure 1 AT&C performance vs regulator target

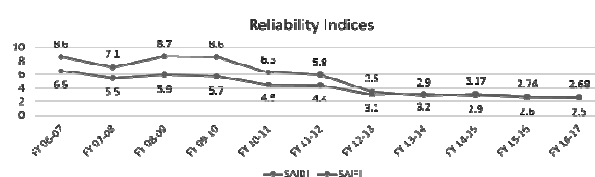


Figure 2 SAIDI and SAIFI trend

To achieve benchmark, Tata Power-DDL had implemented high-tech automated systems for managing customer outages, monitoring load and other electrical parameter and managing and mapping of assets.

- Supervisory Control and Data Acquisition (SCADA) along with Grid Sub-station Automation System (GSAS): to monitor and control Sub-transmission Network.
- Distribution Management System (DMS) along with Distribution Automation (DA): to supervise and control 11kV distribution network.
- Outage Management System (OMS): for complaint handling, outage management and crew management.
- Field Force Automation (FFA): used by field crew to manage and monitor outages effectively and efficiently.
- Geographical Information Service (GIS): for mapping of all electrical, communication and structural asset of organization.
- Enterprise Asset Management (SAP- EAM): for managing complete life cycle (from commissioning to retiring) of asset
- Customer Information Service (SAP-CIS): unified juncture for consumer interaction and convey necessary information.

Tata Power-DDL Challenge

- All these technologies were implemented at different times and operated in different environments. This lead to inefficiency and ineffectiveness sometime. For example:
 - Status information of device could flow from DMS to OMS through ICCC, but the reverse information flow i.e. from OMS to DMS was not happens. Consequently, the DMS dispatchers have no idea about the scope of consumer outages and OMS dispatchers have little idea about the cause of outages. This often results in delayed and to some extent, inaccurate information being conveyed to the customers.
 - In same way,sometimes, network mismatches are also observed at DMS and OMS end as both platform maintain their power network separately. Due to which the update at both the DMS and OMS level becomes unclear.
- Also, Tata Power-DDL strives to sustain its reliability parameters, but taking into consideration the growth of the disruptive technologies like Distributed Energy Resource (DER) and Electrical Vehicles, it is bound to meet the Regulatory and the customer requirements. To meet their further expectation Tata Power-DDL has stride toward Smart Grid technology like Smart Meters, Meter Data Management System (MDMS), Automatic



Demand Response (ADR), Battery Energy Storage System (BESS). All these technologies need to be integrated and should be controlled by single platform for safe operation and economical load dispatch.

- (iii) These evolving technologies increase volume of data to be managed and analysed. Existing Technology like SCADA, DMS and OMS can handle limited data and unable to respond on new and relevant data coming from both grid sensors and consumers smart meters effectively.
- (iv) As it is era of digitization, Big Data Analytics and Business Intelligence will play a vital role in the success of any organization in near future. So, integration of operation technologies with these application is demand of time now

Therefore, a requirement of more advanced application arises which can integrate existing technologies into single platform and which is capable to organize and analyse the massive volumes of real-time complex data for effective and efficient outage management and network management. So, Advance Distribution Management System (ADMS) has been implemented to overcome all aforementioned challenges. This system acts as an integrator between all information and operation technologies (IT-OT). Tata Power-DDL is the first utility in the world to implement ADMS and integrate it with other existing technologies in the utilities at such large extent.

End To End Integration

To ensure reliable power supply and to provide best in class to its customers, Tata Power-DDL has implemented several world class technologies such as ADMS which is designed to replace the conventional SCADA-DMS-OMS. ADMS is well integrated with existing GIS through Common Information Model (CIM) for importing power network from energy exchange point to consumer service points as shown in **Figure 3**. So, there will be single database for complete network model for all application in organization which reduces chances of error. Like SCADA, ADMS is also capable to communicate with telemetry device like sensor and relays installed at remote substations. Both analogue and digital signal can be acquiesced for supervision and control. So, on the basis of breaker status, ADMS define scope of outage.

It has also interface with CRM, through SOAP interface, which is a platform used by Consumer Care Centre (CCC) for lodging their complaints. So, ADMS get consumer outage complaints instantaneously when it get registered at CCC. Also ADMS update power supply status of consumer to CRM when it get any information of tripping through telemetric devices. All these outages detail are shared with FFA application, which is used by field crew to manage and monitor outages. All these integration help to reduce outage time by providing faster resolution of faults through more efficient and accurate results which result in improved reliability, operation safety and consumer satisfaction.

Apart from the operational technologies, ADMS is also integrated with Big Data Analytics for real time reports and progressive analysis for improving reliability, consumer satisfaction and defining business strategy and long term targets. It is also integrated with Power Portfolio Management (PPM) for real time power scheduling, load dispatching and day ahead load forecasting. It is also compatible for Inter Control Centre Communication Protocol (ICCP) for real time data exchange with other control centres like SLDC.

ADMS is also capable of integration with emergent technologies which is going to be implemented in Tata Power-DDL in near future like Smart Meter Data, Automated Demand Response, Battery Energy Storage System and Distributed Generation.

ADMS-GIS

Earlier DMS and OMS were different platforms that were integrated with each other but maintaining their own network at their end. Since these were different platforms, so sometimes mismatches in network were observed with respect to each other. Hence, the update at both the DMS and OMS level becomes ambiguous and unclear. But ADMS, as a single platform, serve the purpose of both DMS and OMS is well integrated with GIS through CIM for importing electrical network (**Figure 4**). It is also to underline that it is the first time that any utility has put in place, a platform, where ADMS-CIM-GIS is integrated together to provide top to bottom network solution. CIM is basically IEC Standard Model to exchange data between two separate systems. It converts GIS proprietary data file to CIM file (.gml and .xml format) which can be consume by any other technology. Geography Mark-up Language (.gml) file contain geographical information of asset and Extensible Mark-up Language (.xml) file contain different attributes of asset. These data files are consumable to ADMS. ADMS run a utility to convert both files to Patch file which is in Data Manipulation Language (.dml) format. Patch file contain forward and reverse difference of incremental changes done in GIS design.



Since, there is only one point of truth (i.e. GIS) for network in whole organization, so it should be accurate from all aspect i.e. network connectivity, geographical location, its various attribute. So, we have re-engineered our process to update network alteration in GIS in minimum timeline, so that chances of ambiguity has been subsided.

As network is updated in GIS the same will be updated in ADMS also. So, network will be updated along with consumers as per actual site condition. In this way supply status of actual consumer will be updated more accurately in case of any outage which improve consumer satisfaction. Hence, ADMS provides an efficient visual interactive work environment that integrates all relevant information on a common real time workspace which helps in accurate estimation of consumer affected and extend of interruption as all work is done on a common GIS based platform and hence maintaining integrity of network.

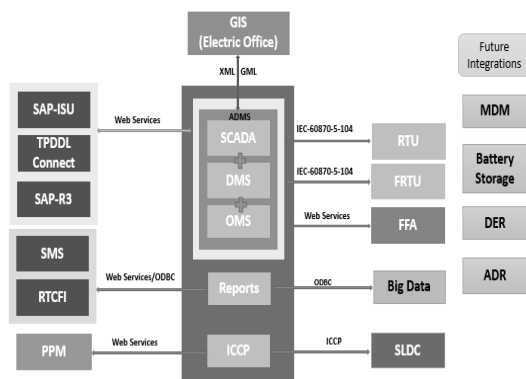


Figure 3 Block diagram: integration of ADMS with other technologies



Figure 4 GIS-CIM-ADMS interface

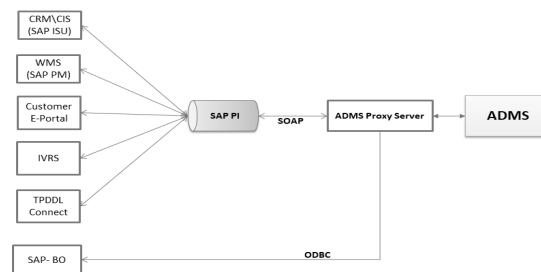


Figure 5 SAP-ADMS interface

ADMS-SAP

SAP is a market leader for enterprise application solutions which offer to simplify different business processes. Tata Power-DDL is also using different module and application of SAP to streamline their processes. **Figure 5** depicts this SAP-ADMS interface as described below.

SAP CRM: It contain database of consumer information, their complete billing cycle, service status and payment details.

SAP BCM: It is a communication solution in our Consumer Care Centre to interact with our consumer through multiple interface like IVRS, sms, voice call etc.

SAP PM: It is a functional module which handles all the maintenance process of electrical equipment (either preventive or predictive) performed in our organization.

SAP BO: It is a reporting and analytics Business Intelligence (BI) platform based on HANA database.

ADMS communicate data bidirectionally with different modules of SAP through Process Integrator (PI). Data is transferred in SOAP (Simple Object Access Protocol) data model. SAP-BO is one way integration through ODBC only.

ADMS-FFA

This interface provides the ability to connect to a third-party Field Force Automation System. It is also called Mobile Work-force Management System (MWM). It has direct bidirectional interface with ADMS through standard web-services. All the outages created or predicted in ADMS reflects in FFA application instantaneously. Through this application field crew manage and monitor outages and assigned crews effectively. After attending problem, crew complete the outage after filling fault report in FFA. The same will be reflected back in ADMS again to complete lifecycle of outage.



ADMS-MDMS

MDMS is a platform to manage and control smart meters and its data and signals. This interface allows the ADMS system to obtain meter data by interrogating the MDMS using the MultiSpeak protocol. The user can request readings from any meter and display the data on-demand in the ADMS network diagram. Users can also define schedules for the ADMS system to automatically interrogate the MDMS for specific meter data. The received data is stored in the analogue points. This data can also be used by other advanced ADMS applications such as Distribution Power Flow (DPF). This interface can also be used to activate demand response.

ADMS-PPM

Power Portfolio Management System (PPM) is responsible for short term and day- ahead load forecasting and real time power scheduling. All these processes require total power consumed by Tata Power DDL as whole and at all individual exchange points as input. So, this system is integrated with ADMS to exchange analog data of exchange points in Time Series Data Structure (TSDS). ADMS also share data of Delhi State Load Dispatch Centre (SLDC) which it get through ICCP for improving accuracy in forecast and power scheduling. In case of overdrawling (when draw power from grid more than permissible limit of schedule power), to stabilise power system if load shedding is required then PPM may request quantum of load to be shed to ADMS. ADMS will shed prescribed load through its Group Tele-Control Application (GTC) and return the quantum of actual load shedding to PPM.

CONCLUSION

To attain organization vision to be most trusted and admired provider of reliable power and to create benchmark to become global utility leader, only adoption of cutting edge technologies is not enough. To get the more fruitful result, technologies should work in cohesive and integrated manner, not in isolated environment. Along with integrated technology, business processes should also be re-engineered in aligned with new technologies to achieve key result targets. ADMS along with its integration with other technologies is a milestone to accomplish organization mission to become of Smart DISCOM. It will surely help in improving system reliability, increase operational safety and enhancing consumer satisfaction. Hence, ADMS is going to be the biggest technology integrator in the power utility sector which will lead us towards the era of digitalization.

REFERENCES

1. Power On Advantage – Advanced Distribution Management by GE Grid Solutions
2. Artur R. Avazov, Liubov A. Sobinova, Article on Advanced Distribution Management System, National Research Tomsk Polytechnic University
3. White paper on Advanced Distribution Management by Oracle Utilities
4. Advanced Distribution Management System (ADMS) - Smart Grid Solution for Electricity Distribution Networks by Schneider Electric



Integrated DC Micro Grid, Renewable Energy and AC Grid with Energy Efficient Hybrid Appliances Pilot Study at NLCIL, Neyveli, Tamilnadu, India

M. Coumarane^{*1}, V. Manoharan¹

Centre for Applied Research and Development (CARD), NLC India Ltd, Neyveli, Tamilnadu¹, couma_rane@yahoo.com^{*}

ABSTRACT

The primary purpose of that pilot work is to investigate the viability and energy-savings potential of using Direct Current (DC) generated by on-site renewable energy systems in its DC form, rather than converting it first to Alternating Current (AC) for distribution to the loads. Interest in direct-DC is motivated by a combination of factors: the very rapid increase in residential and commercial photovoltaic (PV) power systems in India, the rapid expansion in the current and expected future use of energy efficient products that utilize DC power internally. The demonstrated energy savings of direct-DC power use in DC micro Grid, energy efficient appliances and the current emergence of direct-DC power standards and products designed for grid-connected residential and commercial products. Residential PV use began with direct-DC in off-grid systems running DC appliances, instead of AC appliances.

KEYWORDS Micro grid, Renewable energy, Energy efficient, Hybrid appliances, Photo voltaic

INTRODUCTION

Direct current power distribution systems and micro grids have become the topic of substantial research due to their potential to reduce power conversion losses, improve power quality, increase system reliability, reduce system costs [1], and facilitate a transition to inherently more efficient DC-based devices in buildings. The resulting research has led to the recent adoption of DC distribution systems in data centers and commercial lighting installations, among others [2]. As these systems have been proven in niche applications, a discussion has emerged as to whether more buildings should be wired with DC circuits in addition to – or in place of – AC. Around 50% of the energy presently used in buildings is either consumed as DC in electronic loads or passes through a transient DC state as a means of motor control, resulting in significant losses when grid distributed AC is rectified using inefficient, distributed power supplies. When a source of DC generated electricity such as a solar PV array is available, dedicated DC circuits reduce the usual losses that occur both in the inversion from generated DC to grid AC, as well as the rectification back to DC at the end load. It is given that in a DC distribution system with DC source and appliances 47% energy can be saved [3] and 27% system efficiency can be improved [4].

Every major appliance in a modern home could be replaced by a more efficient device that can operate on DC. Most of these devices are currently intended for off-grid applications. For example, the motors currently found in home appliances are primarily a mix of AC induction motors for larger loads and universal motors for smaller loads. Brush-less DC (BLDC) permanent magnet motors are inherently more efficient than both types of motors, with savings estimated at 5 to 15% for constant speed applications. In variable speed configurations, BLDC motors operate even more efficiently and generate substantial savings when compared to AC motors. In air conditioner condensing unit applications, existing variable speed refrigerant compressors driven by BLDC motors achieve cooling efficiencies nearly twice the minimum requirement for energy star certification. The research study shown that overall 24% efficiency of the system improved by replacing AC motors with BLDC motors [3].

NLCIL – CASE STUDIES

NLCIL pilot works on roof top solar with hybrid appliances (cooling device, ceiling fan and LED lights) connected DC micro-grid and AC grid operation using with intelligent controller is a R&D initiative in the study of direct DC power and energy efficient appliances [5]. This system comprises the following:

- Power Source: (i) 10 kW –roof top solar PV (thin film); and (ii) AC Grid Source.
- Connected Loads: (i) 1300 W/1.5 tonne air conditioner (BLDC – compressor/condenser) – 06 number; (ii) 35 W – ceiling fan (Sweep – 1400 mm) / BLDC –Motor -15 number; and (iii) 40 W – LED panel lights – 12 numbers.
- Operation Modes: (i) Direct DC – power operation; and (ii) AC Grid operation

PV Panel and Hybrid Appliances – System Arrangement

Figure 1 shows that 10 kW PV panel is connected to Solar Hybrid Controller Unit and Hybrid appliances like BLDC – ceiling fans, 1.5 T hybrid air conditioners and LED panel lights. Appliances are operated through control panel and intelligent control mechanism. **Figure 2** shows that PV panel mounting arrangement. The PV panel specification is demonstrated in **Table 1**.

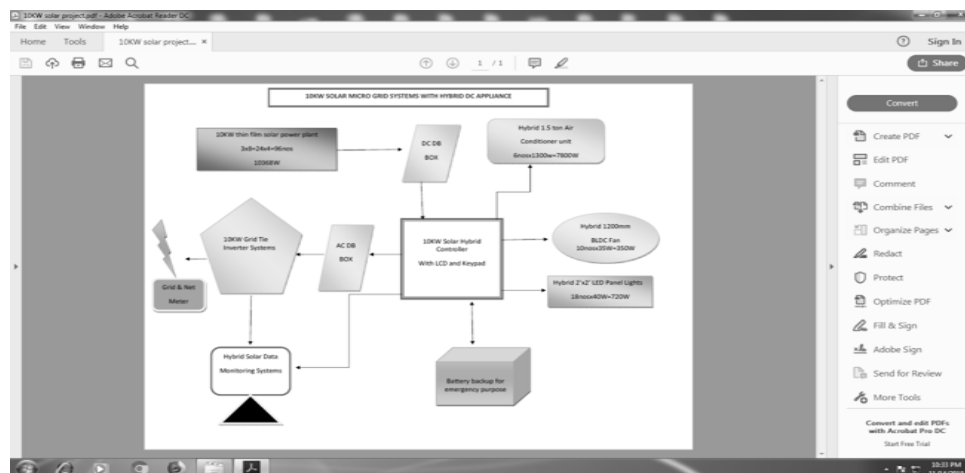


Figure 1 Schematic diagram of PV panel and Hybrid Appliances



Figure 2 PV panel mounting arrangement

Table 1 PV panel specification

Description	Value
Type	Thin film silicon photo voltaic
Power rating	103W @ 25 °C
Voc_inc	142.6 V
Isc_in	1.27 A
Vmpp_ini	110.9 V
Impp_ini	1.15 A
Ambient temperature	40 °C
Number of panels	96 numbers
Degree of production	IP 65
Frame	Anodized aluminium
Certification	IEC 61215/IEC61730



Mode of Operation

Solar Hybrid Controller Unit has the arrangement of DC/AC hybrid operation and intelligent control mechanism. It is designed for the following mode of operations:

(i) Direct DC – Power Operation

PV panel connected to hybrid controller has four sections, covering two sections to air conditioner load and another two sections cover lighting and BLDC ceiling fan loads. Selection of DC mode of operation by hybrid controller feather switch provided at panel surface. All loads can be operated through portable remote control switch. The selection of load based on the available PV power generation and weather condition.

(ii) AC Grid Operation

At the requirement of DC power to operate the hybrid load is sufficiently not enough, load change over to AC grid mode by means of hybrid controller selector switch. Appliances are designed to operate both in AC and DC accordingly each appliance designed for that with suitable driver unit.

(iii) Grid –Tie Mode Operation

At the time of power not required to operate the hybrid appliances, PV power diverted to EB grid through online Grid Inverter. Both inflow and out flow power for the system is recorded through Net meter. **Figure 3** shows that Solar Hybrid controller, Online Inverter and Net meter set up.

Hybrid Controller Unit

A set of power control mechanism are arranged suitably for operating the above three mode of operations. It distributes the power (DC/AC) to the loads based on the mode of operation. Mode selector feather switch is mounted on the top of the panel with light indication and display the status of the operation mode. **Figure 4** shows the hybrid controller and intelligent control mechanism.



Figure 3 Solar hybrid controller, online inverter and net meter –set up



Figure 4 Hybrid controller and intelligent control mechanism

Intelligent Controller

Intelligent controller was designed with IC PIC -16F series. It carries out all the three mode of operations. It is powerful (200 nanosecond instruction execution), yet easy-to-program. It has features like 256 bytes of EEPROM data memory, self programming facility, an ICD, two Comparators, eight channels of 10-bit Analog-to-Digital (A/D) converter, two capture/compare/PWM functions. With this feature, it is planned for further to program for automatic source, load balancing based on PV power generation and solar radiation.

HYBRID APPLIANCES

Hybrid 1.5T Air Conditioner

The use of BLDC motors for indoor and outdoor units reduces the noise level and energy consumption. The specification of 1.5T air conditioner is given in **Table 2**.



Table 2 Hybrid 1.5T air conditioner specifications

Description	Value
Input supply	320 V DC
Input power	1300 W
Ambient temperature	45 °C
Compressor	BLDC Motor
Refrigerant	R410 A
Liquid pipe dia	6 mm
Gas pipe dia	12 mm
Length of pipe with standard gas charge	4 m
Additional gas charge	30 g/m
Maximum distance between indoor and outdoor units	15 m
Maximum level between indoor and outdoor units	5 m
User interface	Through an IR remote

Hybrid 35W BLDC Ceiling Fan

Most of the appliances having rotary part use universal DC motors or AC single phase induction motors which have low efficiency because of carbon brush and mechanical commutation, bearing a major maintenance cost and mechanical losses. All such motors can be replaced with BLDC which has a high efficiency, low noise, low power consumption and a wide range of speed. The specifications for hybrid 35W BLDC ceiling fan and hybrid 40W LED panel light are demonstrated in **Tables 3** and **4**.

10kW Solar powered with Hybrid Appliances installed at NLCIL Auditorium for carry out pilot study on hybrid grid and energy studies. **Figure 5** shows the arrangement of hybrid appliances. It is a model pilot work for future Hybrid Grid integration and standardisation.

Table 3 Hybrid 35W BLDC ceiling fan specifications

Description	Value
Sweep	1400 mm
Rated voltage	320V DC
Motor	Brushless permanent magnet DC motor
Insulation	Class B
Motor enclosure	Totally enclosed air over type
Ambient temperature	45 °C
Free air delivery	210 m ³ /min
Input power	35 W
Speed control	By IR remote

Table 4 Hybrid 40W LED panel light specifications

Description	Value
Power	40 W
Rated voltage	320 V DC
Driver type	Constant current
Power factor	> = 0.9
High surge protection	2.5 kVA
Optics	Polycarbonate diffuser
Accessories	With driver
Ambient temperature	45 °C



Figure 5 Solar powered auditorium with hybrid appliances

CONCLUSION

The Integration of DC micro-grid, renewable energy and AC grid with energy efficient hybrid appliances pilot study at NLCIL has proven that better energy saving and effective operation of DC micro-grid. Energy saving was



effectively achieved through hybrid appliances and intelligent control mechanism. After completing this pilot study, the final report will be used in evaluating the system efficiency and total energy savings. The idea of wasting solar power is eliminated by operating both ON grid and isolated grid mode of operation with the above control mechanism.

ACKNOWLEDGEMENT

The authors would like to acknowledge NLC India Ltd management for granting permission to present this paper with a special mention of Director (Project & Planning) for his continuous support and encouragement.

REFERENCES

1. Brock Glasgo, Ines Lima Azevedo, Chris Hendrickson, How much electricity can we save by using direct current circuits in homes? Understanding the potential for electricity savings and assessing feasibility of a transition towards DC powered buildings, Paper published in the International Journal –Elsevier by 2016.
2. Muhammad kamran, Muhammad Bilal, Muhammad Mudassar, DC home Appliances for DC Distribution System, Mehran University Research Journal of Engineering and Technology, Volume 36, Number 4, October 2017.
3. Gholase, Fernandes B.G , Design of Efficient BLDC Motor for DC operated Mixer-Grinder, IEEE International Conference on Industrial Technology, Seville 2015.
4. Anand, Fernandes, Optimal Voltage Level for DC Micro Grid, IEEE 36th Annual conference on Industrial electronic Society, Glendale 2010.
5. Jimenez A. Improving the economics of photovoltaic power generation with innovative direct current applications: feasibility and example site evaluation, Palo Alto, CA:2005



Design and Control of Power Quality Improved 250 kW PV-based Grid-tied System with Low Voltage Ride Through

B Murali Krishna^{1}, Suhashini Shinde¹, Gireesha.B¹, BVVN Manikanta²*

*Department of Electrical Engineering, School of Engineering, Central University of Karnataka, Karnataka, India¹,
muralikrishna.cuk@gmail.com**

Near Ramalayam, Seethanagaram Mandal, Rajahmundry, East Godavari, Andhra Pradesh²

ABSTRACT

This paper presents the design and control of a PV-based 250 kW grid-tied system. The feature of the proposed system is capable to overcome one the power quality issue of the power blackout. As in view of power quality improvement schemes, Low Voltage Ride Through (LVRT) is one of the most leading grid connection requirements to be met by the power generation systems. In this work, an improved PV-based 250 kW grid connected system with Perturb and Observation (P&O) based Maximum Power Point Tracking (MPPT) unit has developed and the Battery Energy Storage System (BESS) is controlled in such a way that the power conversion unit (Inverter) remains connected to the grid even during fault conditions as long as satisfying modern grid codes/standards.

KEYWORDS Renewable energy (RE) systems, Photo voltaic (PV) systems, Distributed generation (DG) systems, LVRT, Fault ride through (FRT), BESS, Power quality.

INTRODUCTION

Since few decades' renewable energy based generation systems have been becoming popular in the electrical energy sector for so many reasons like, to reduce the unnecessary emission from the conventional generating stations and motto of utilization of locally available renewable energy sources to generate electric power. In the electric power generation sector, the conventional electric power generation stations like, fuel/coal based power generation systems releases unwanted emissions and threaten the future of the planet. Since few decades in the electric energy sector there are promising technologies that use Renewable Energy Sources (RES) have been tested and used worldwide for electric power generation. Such technologies can be easily installed locally with low investments thus saving cost related to transmission lines [1, 2]. The RES such as solar, wind, bio-mass and hydro are considered attractive in this venture both for grid-tied and off-grid systems. Among the RES based electric power generation systems, photo-voltaic (PV) systems are one of the reliable system because of its simple installation for both grid-tied and off-grid systems, noise-less operation, low Operation and Maintenance (O&M) cost, eco-friendly, easy and simple system, etc[2]. Distributed Generation (DG) systems, including grid-tied power generation systems installation by using locally available energy sources, shows a significant increase in the past few decades. The energy security levels to the next upcoming decades more electric energy is expected from the RE systems and those should be reliable, flexible, economical and eco-friendly with high power quality. Consequently, 'grid codes and standards' should be revised thoroughly for the best operation of grid-connected RE systems [1]. One of the improvement schemes of power quality for the grid-tied systems is the design of the system with capable of low voltage ride through (LVRT) during the fault conditions in the system by either at the source side and/or load side. Dynamic Voltage Supporting (DVS) and LVRT enabled grid-tied PV systems increasingly becoming important along with the increasing penetration of PV-systems. If a sudden disconnection of PV generation systems from an existing energy by means of any internal fault in the systems, then grid triggers serious problems such as voltage flickers and power outages. To improve the power quality, security, controllability level and stability of the grid during the sudden fault conditions, some important standards require large-capacity PV-systems to allow the LVRT under fault conditions [9, 10, 12]. The standards of LVRT for grid-tied systems being monitor by the Central Electricity Authority (CEA), India [1].

PV- System with MPPT

The Standard equivalent circuit, modelling and simplified calculations of PV-Array have reported in the literature [5-8]. In this work, 250 kW PV-system has been considered. The Various MPPT techniques for solar systems have been reported in literature. In this 250 kW system, Perturb and Observe (P&O) algorithm is adapted for obtain the MPPT because of various reasons, like easy in operation and fast in execution. The working of P&O algorithm compares the old and new power values and adjusts the duty cycle of dc-dc converter accordingly [2]. The working principle of P&O is given below by stepwise.



Step 1: Measure the Voltage (V(k)) and Current (I(k)) values.

Step 2: Calculate the Power (P(k)).

Step 3: If the calculated Power (P(k)) > (P(k-1)), then (Yes) go to Step A, otherwise (No) go to Step B.

Step A: If (P(k) > (P(k-1))), then (Yes) increase the Duty Cycle (D) value otherwise (No) decrease the Duty Cycle (D) value; Resultant value go to Step 4.

Step B: If (P(k) > (P(k-1))), then (Yes) decrease the Duty Cycle (D) value otherwise (No) increase the Duty Cycle (D) value; Resultant value go to Step 4.

Step 4: Return.

Controlling Principles of LVRT for 250 kW Grid-tied System

The proposed control block diagram of the proposed system to implement LVRT 250 kW PV-based system is shown in **Figure 1**. The control block implements the LVRT by using BESS and circuit breaker control.

In the proposed system, the controller tracks the MPPT and operates as a boost converter accordingly. It also senses the voltage across DC-link switches the bidirectional converter accordingly and finally switches the circuit breaker operation according to the specifications and grid voltage. The controller senses grid voltage and takes ratio of grid voltage to nominal voltage. If this ratio is within the specified limits mentioned by the CEA, then the system remains connected to the grid or else gets disconnected.

As shown in **Figure 1**, the inverter control scheme employs the synchronous reference frame control and the necessary formulas to implement the scheme is given by Eqs. (1) to (13) [11,13]. P and Q controllers are used to derive i_d reference and i_q reference. PI controller is employed for easy operation of the complex circuit.

Here in **Figure 1**, I_{d_ref} is obtained by feedback of V_{dc_error} value through PI controller. The $K_p = 7$, $K_i = 800$ and I_{q_ref} is taken reference as 0. Where, the value of V_{dq_ref} can be obtained by feedback of I_{dq_error} through PI controller. The values of $K_p = 0.3$, $K_i = 20$ and $V_{dc_ref} = 2750$ V.

$$V_{dc_error} = \frac{V_{dc_measured} - V_{dc_ref}}{V_{dc_nominal}} \quad (1)$$

$$K = \frac{2}{3} \begin{bmatrix} \sin(\omega t) & \sin\left(\omega t - \frac{2\pi}{3}\right) & \sin\left(\omega t + \frac{2\pi}{3}\right) \\ \cos(\omega t) & \cos\left(\omega t - \frac{2\pi}{3}\right) & \cos\left(\omega t + \frac{2\pi}{3}\right) \\ \frac{1}{2} & \frac{1}{2} & \frac{1}{2} \end{bmatrix} \quad (2)$$

$$V_{dq0_measured} = K \times V_{abc} \quad (3)$$

$$I_{dq0_measured} = K \times I_{abc} \quad (4)$$

$$I_{dq_error} = I_{dq_ref} - I_{dq_measured} \quad (5)$$

$$V_{d_conv} = V_{d_measured} + I_{d_ref} * R - I_{q_ref} * L + V_{d_ref} \quad (6)$$

$$V_{d_conv} = V_{d_measured} + I_{d_ref} * R - I_{q_ref} * L + V_{d_ref} \quad (7)$$

$$V_{q_conv} = V_{q_measured} + I_{d_ref} * L + I_{q_ref} * R + V_{q_ref} \quad (8)$$

$$\text{Modulation index } m = |V_{dq}| = \sqrt{V_d^2 + V_q^2} \quad (9)$$

$$\text{Phase A voltage } V_a = m \sin \theta \quad (10)$$

$$\text{Phase B voltage } V_b = m \sin\left(\theta - \frac{2\pi}{3}\right) \quad (11)$$

$$\text{Phase C voltage } V_c = m \sin\left(\theta + \frac{2\pi}{3}\right) \quad (12)$$

$$\text{Translational angle } \theta = \tan^{-1}\left(\frac{V_q}{V_d}\right) \quad (14)$$

RESULTS AND DISCUSSIONS

This section shows the results of MATLAB/Simulink based 250 kW PV system with LVRT capability. Total simulation time is 7 s and a fault is created between 3 to 4 s. The BESS plays a vital role in the proposed system to balance the grid during fault conditions. **Figures 2** and **3** shows the inverter real power (P) without and with BESS respectively during fault condition. **Figures 4** and **5** show the inverter's reactive power (Q) without and with BESS during fault condition of 3 to 4 s, respectively. This shows that the DG supports the grid by delivering reactive power. Table shows the Total Harmonic Analysis (THD) of the three phase voltages. From the table, it is clear from the **Table 1**, the THD values are within the range of 5% for all three phases during normal and faulty conditions.

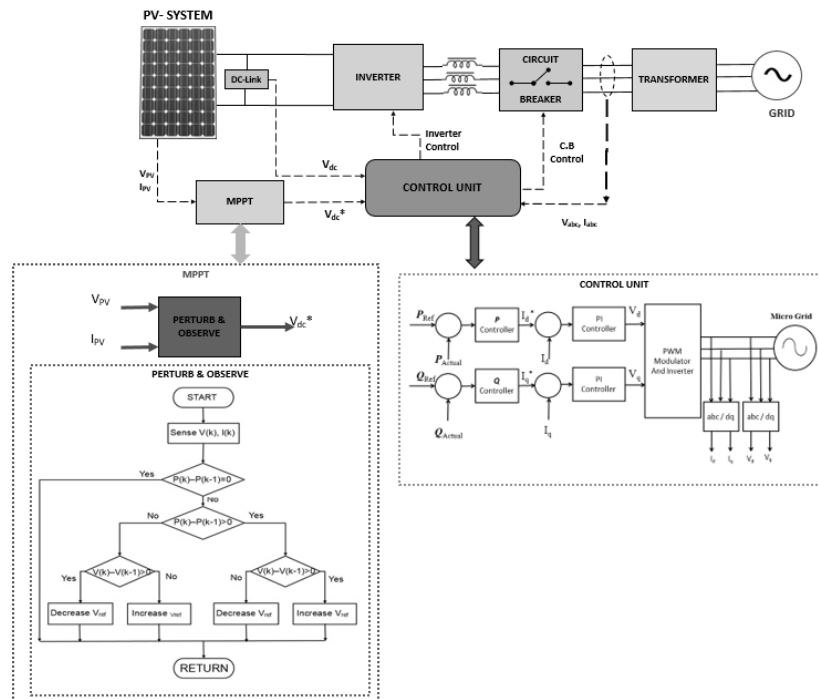


Figure 1 Complete control block diagram of proposed 250 kW PV- microgrid system with LVRT implementation

Table 1 THD analysis and percentage of power quality improvement of proposed PV Grid –tied system

Voltage (V)	Pre-fault	During fault	Post-fault
Voltage (V_{an})	0.78 %	1.85 %	0.54 %
Voltage (V_{bn})	0.78 %	1.85 %	0.54 %
Voltage (V_{cn})	0.78 %	1.85 %	0.54 %

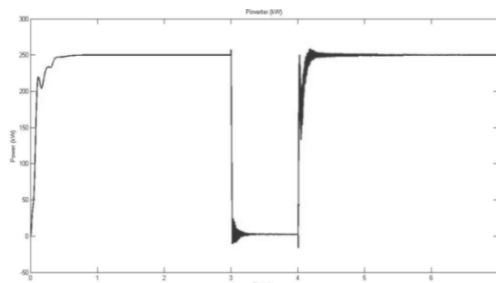


Figure 2 Inverter real power (P) in kW during fault condition without BESS

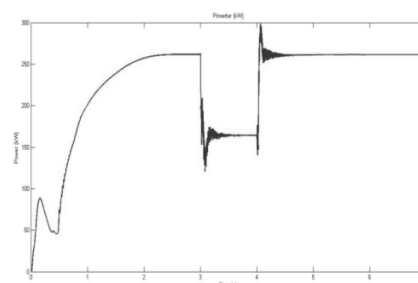


Figure 3 Inverter real power (P) in kW during fault condition with BESS

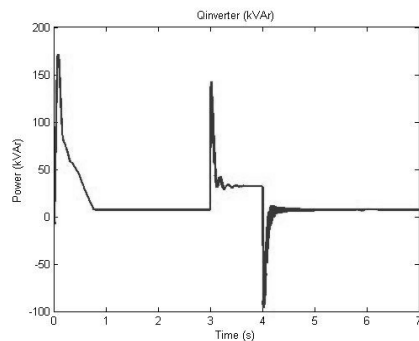


Figure 4 Inverter reactive power (Q) in kVAr during fault condition without BESS

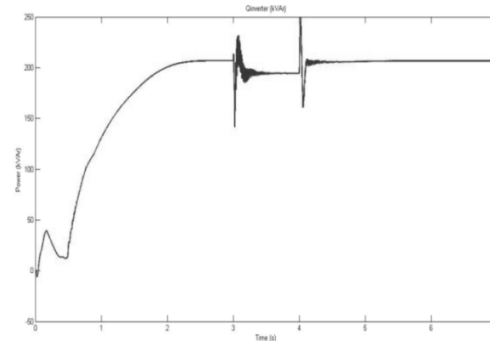


Figure 5 Inverter reactive power (Q) in kVAr during fault condition with BESS

CONCLUSION

A PV-based 250 kW grid-tied system with LVRT has developed in this paper. The smooth operation of LVRT is achieved by controlling voltage at DC-link capacitor. The voltage variations at the DC-link capacitor can be maintained within the desired limits by using bidirectional converter. The system dynamically supports the grid by delivering both active and reactive power during fault conditions without compromising the efficiency of PV-system. The circuit breaker disconnects the system from grid if the faulty condition values are beyond specified limits.

REFERENCES

1. Central Electricity Authority (CEA), Technical Standard for Connectivity to the Grid, Online available: [http://www.cea.nic.in/Regulations \(Part-3 Section-4\), 2013](http://www.cea.nic.in/Regulations%20(Part-3%20Section-4),2013),
2. Bala Murali Krishna. V, et al., Cost optimization by integrating pv-system and battery energy storage system into microgrid using particle swarm optimization. International Journal of Pure and Applied Mathematics, Volume 114, Number 8, pp 45-55, 2017.
3. Marcelo Gradella Villalva, Jonas Rafael Gazoli, Ernesto Ruppert Filho, Comprehensive Approach to Modeling and Simulation of Photovoltaic Arrays. IEEE Transactions on Power Electronics, Volume 24, Number 5, pp 1198-1208, 2009.
4. Deividi F. Zaions, Anderson J Balbino, Cassio L Baratieri, Adilson L. Stanakiewicz, Comparative analysis of buck and boost converters applied to different maximum power point tracking techniques for photovoltaic systems. 2017 Brazilian Power Electronics Conference (COBEP), 2017.
5. Parimita Mohanty, G. Bhuvaneswari B, R. Balasubramanian, Navdeep Kaur Dhaliwal, MATLAB based modeling to study the performance of different MPPT techniques used for solar PV system under various operating conditions. Renewable and Sustainable Energy Reviews Volume 38, pp 581–593, 2014.
6. Boualem Bendib, Hocine Belmili, Fateh Krim, A survey of the most used MPPT methods: Conventional and advanced algorithms applied for photovoltaic systems. Renewable and Sustainable Energy Reviews Volume 45, pp 637–648, 2015.
7. J. Prasanth Ram, T. Sudhakar Babu, N. Rajasekar, A comprehensive review on solar PV maximum power point tracking techniques. Renewable and Sustainable Energy Reviews Volume 67, pp 826–847, 2017.
8. Vijayan Sumathi, R. Jayapragash, Abhinav Bakshi, Praveen Kumar Akella, Solar tracking methods to maximize PV system output – A review of the methods adopted in recent decade. Renewable and Sustainable Energy Reviews Volume 74, pp 130–138, 2017.
9. Jun Yin, Renjie Xu, Photovoltaic Inverter with Control for Performing Low Voltage Ride through. US Patent No. US 8,687,328 B2, 2014.
10. Furong Xiao, Lei Dong, Shah Nawaz Farhan Khahro, Xiaoping Huang, Xiaozhong Liao, A Smooth LVRT Control Strategy for Single-Phase Two-Stage Grid-Connected PV Inverters. Journal of Power Electronics, Volume 15, Number 3, pp 806-818 2015.
11. Jon Are Suul, Kjell Ljokelsoy, Tarjei Midtstund Tore Undeland, Synchronous reference frame hysteresis current control for grid converter applications. Proceedings of 14th International Power Electronics and Motion Control Conference EPE-PEMC 2010
12. K Fujii, N Kanao, T Yamada, Y Okuma, Fault Ride Through Capability for Solar Inverters. European Power Electronics and Drives, September 2015.
13. F. Blaabjerg, R. Teodorescu, M. Liserre, A.V. Timbus, Overview of Control and Grid Synchronization for Distributed Power Generation Systems. IEEE Transactions on Industrial Electronics Volume 53, Number 5, pp 1398-1409, 2006.



An Investigative Study on Electric Generators for Isolated Operation

B Murali Krishna V^{1*}, V. Sandeep¹

Department of Electrical Engineering, School of Engineering, Central University of Karnataka, India¹,
muralikrishna.cuk@gmail.com*

ABSTRACT

This work presents an investigative study on electric generators in the off-grid /standalone/isolated mode of operation. Currently, following generators become popular due to their merits: self-excited induction generator (SEIG), permanent magnet synchronous generator (PMSG), brush-less synchronous generator (BLSG), switched reluctance generator (SRG) and synchronous reluctance generator (SynRG). Through the working phenomena and steady-state analysis of the electric generators, this study summaries the schematic working topologies of the generators for renewable energy applications. The paper illustrates on equivalent circuit models of electric generators in steady state condition. It also focuses on minimum excitation requirements to operate the electric generators in standalone mode of operation. The paper aims at critical review on various generators for further feasibility studies and needful.

KEYWORDS Renewable energy sources (RES), Self-excitation, Battery energy storage system (BESS), Power quality improvement

NOTATIONS

R_s, R_r, R_c	stator, rotor and core-loss resistances, respectively
$C_{ex}, C_{se}, C_{sh}, C_{min}$	excitation, series, shunt capacitors and minimum capacitance, respectively
X_{ls}, X_{lr}	per phase stator and rotor leakage reactance, respectively
X_m	magnetizing reactance
X_c	per phase capacitive reactance of the terminal capacitor
R_L	load resistance per phase
F, v	p.u. frequency and speed, respectively
I_s, I_r	per phase stator and rotor currents
I_L	load current per phase
V_t, V_g	terminal and air-gap voltage, respectively
P_{in}, P_{out}	input and output power, respectively

INTRODUCTION

To meet peak demand of energy and improve reliability in energy supply, the emerging economies are focusing on power generation using renewable energy sources (RES) in recent times, which maximizes the utilization of locally available energy resources like wind, hydro, solar, biomass, tidal, geo-thermal etc [1,2]. The share of renewable energy generation crosses 20 % in total installed capacity in India by 31st August 2018, which shows an impressive growth and sets a target of 175 GW by the year 2022[3]. Many advantages can be found out with RES based electric power generation systems (EPG) as compared to the conventional coal, oil and gas based systems, such as eco-friendly, non-polluted, high reliable, simple and safe operation and easy installation. The distributed generation is the main feature which directly involves the consumers and local utilities [4,5].

In the RES based systems, except the solar energy, the remaining major sources like, wind, hydro and bio-mass systems are electric generators based systems. In which electric generators generate the electric power by utilization of RES as a major input. Nowadays, distribution generation and isolated mode of operation systems are gaining popular with RES for many merits and few of the technical advantages like minimizing the transmission and distribution (T&D) losses, high installation cost, maintenance and its losses. For small scale applications, like domestic loads, offices and micro industries, the distribution generation systems are more attractive and promising technologies than grid-connected systems [2,5,6].

Various electric generators based EPG systems with RES are reported in the literature for the isolated mode of operation [1,2,4-8,12,14,16,18,19-27]. Much difference can be found for the same generators, while they are operating in grid-connected mode and isolated mode. When any EGs are operated in a grid-connected mode, their reactive power compensation is supplied by the grid but whereas the EGs are operated in the isolated mode of operation, with the lack of reactive power supply from grid, therefore we need to provide the same externally. Most of the EGs are not self-started machines and one more major disadvantage is the poor voltage regulation with low



efficiency of the system on direct unexpected load or dynamics in operation. Some certain requirements and operations make the machine as a self-started/self-excited generator with good voltage regulation, such as excitation capacitance and dedicated power electronic circuits. Sometimes, simple static converter systems (non-power electronic) may work for improvement of power quality if the nature of loading is not so critical and dynamic.

This paper deals with the popular generators for three-phase load supply, those are self-excited induction generator (SEIG), permanent magnet synchronous generator (PMSG), brush-less synchronous generator (BLSG), switched reluctance generator (SRG) and synchronous reluctance generator (SynRG) for RES based EPG systems. The basic physical phenomena, configurations, and minimum excitation requirement for isolated operation are briefly discussed. The study gives an idea, how to work with isolated generator for a particular RES.

Isolated EGs for RES

Phenomena, Configurations and Performance

In this study the basic phenomena, configurations of SEIG, PMSG, BLSG, SRG and SynRG have been described. The working principle is explained by the schematic diagram and performance analysis is given by the equivalent circuit for each EG separately.

Self- Excited Induction Generator (SEIG)

To run the induction generator as a self-started generator in a standalone mode of operation, a suitable rating of minimum capacitor has to be connected across the stator terminals of induction generator (IG) and this phenomenon in induction generator is called capacitor excitation phenomena and such a featured IG is called self-excited induction generator (SEIG). In SEIG, terminal voltage and frequency are not constant. At varying voltage and frequency, the air-gap flux varies and tends to operate at wider range of magnetic flux density in the saturated region and magnetizing reactance X_m assumes different values dependent on capacitor, speed and load [7,8].

As per the literature, IGs are more popular for small scale generation systems. Nowadays IGs are progressively becoming more popular than conventional synchronous generators. The advantageous things with the IGs are rugged construction, brushless arrangement, low cost, simplicity of operation, less maintenance, quick dynamic response, self-fault detection capability and able to generate electric power at varying input speeds. But the induction generator is not a stable candidate for wide speed range of operations and variable load conditions. One more drawback with SEIG is not a self-fault tolerance machine [2,5-9].

A basic experimental diagram of RES based SEIG is given in **Figure 1(a)** and the simplified electrical equivalent circuit is presented in **Figure 1(b)**, which is used for the steady state analysis of the machine [8]. As from the literature, the minimum capacitance value is chosen in such a way to make the induction machine as a SEIG and is given by the equation1 [8]. **Figure 1(b)** will be useful for finding the key parameters of the considered machine to work in isolated mode of operation. Single-phase operation is also possible with the three-phase induction generator and is reported in the literature[10].

$$C_{\min} = \frac{1}{\omega V^2 (X_{ls} + X_{S\max})} \quad (1)$$

$$C_{L\min} = KC_{\min} \quad (2)$$

Permanent Magnet Synchronous Generator (PMSG)

PMSG based small-scale and isolated generation systems are becoming popular because of many advantages, like no chance for loss of excitation, more efficient than SEIG and no need of slip-rings and brushes, but the major disadvantage with them is unregulated output voltage rating [2,14,16,18]. The PMSG can be able to possess a capability of inherent voltage compensation and which is desirable for maintaining a constant load voltage. The PMSG is a self-excited machine in isolated mode of operation and can be operated at high power factor (PF) [14,17,18]. According to the power electronic converter topologies and BESS control various blocks may be added but the general experimental layout diagram of RES based PMSG fed 3-phase load is given in **Figure 2(a)** and the simplified per-phase electrical equivalent circuit is given in **Figure 2(b)**, which is used for the performance analysis.

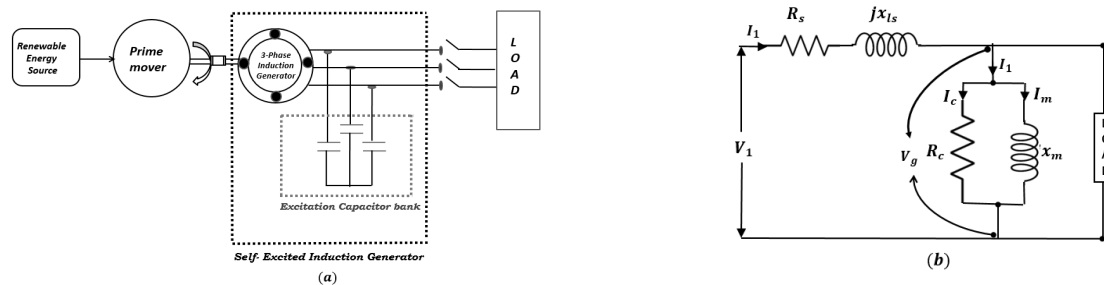


Figure 1(a) Basic experimental diagram of RES based standalone EPG with SEIG (b) simplified equivalent circuit of induction generator[8].

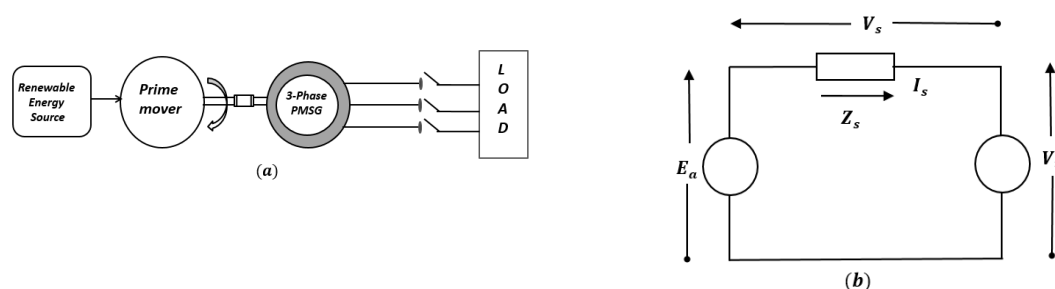


Figure 2 (a) Basic experimental diagram of RES based standalone EPG with PMSG (b) simplified equivalent circuit of PM synchronous machine[2].

Brush-less Synchronous Generator (BLSG)

Nowadays, for off-grid applications RE based EPG with BLSGs are becoming popular and in such a system RE potential drive the prime mover, which will further rotate the machine at the synchronous speed to generate the electric power (in terms of kVA or MVA) at the desired frequency. The output voltage will generate by the proper amount of excitation to the field winding of the machine [18,19]. Brushed and brush-less SGs are two types [17, 20], which are based on scheme of excitation. Small rating of BLSGs are much suitable for temporary/emergency power sources like, a very well-known example of diesel generator [2]. To make the error voltage zero in closed-loop operation of BLSG the exciter arrangement adjusts itself accordingly, so voltage across the load is regulated for all load conditions. Generally, the excitation elements are pre-charged capacitors of DC voltage source in BLSGs. DC excitation based BLSGs are well suited for variable speed operation. A general experimental layout diagram of RES based BLSG fed 3-phase load is given in **Figure 3(a)** and the simplified electrical equivalent circuit per phase is given in **Figure 3(b)**, which is used for the performance analysis.

Synchronous Reluctance Generator (SynRG)

Synchronous Reluctance Generator (SynRG) based EPG systems of RES represents an alternative solution in isolated systems instead of being used SEIG for many advantages than SEIG. As like the SEIG, the SynRG is having all the same benefits like, simple in design, robust nature, inexpensive operation, core loss is less, less noise in working condition, smooth starting torque because of no cogging torque and in addition to these advantages, can be avoided the rotor winding losses because of lack of rotor bars in its construction. Moreover, SynRGs are cheap in cost as compared to other brushless generators. The SynRG not a self-excited machine like SEIG in standalone operation it's also need the necessary excitation to build-up the terminal voltage. Even though existence of a minimum residual flux in the core of machine, which is not sufficient to get the self-excitation. Generally, the excitation elements are pre-charged capacitors and which are needed to be connected across the machines terminals; an example experimental set-up diagram is shown by **Figure 4(a)** and the simplified SynRG's per-phase equivalent circuit diagram is shown in **Figure 4(b)**, which is used for the performance analysis through dq-axis circuit analysis. The minimum capacitance value for a particular rating SynRG and availability of kinetic energy of RES is calculated by using the Eq. (3) [23-25].

$$C_{\min} = \frac{Q}{6\pi fV^2} \quad (3)$$

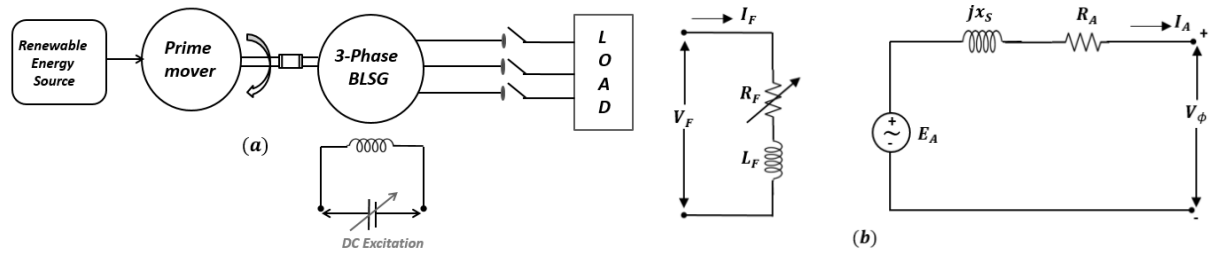


Figure 3 (a) Basic experimental diagram of RES based standalone EPG with BLSG (b) Simplified per-phase equivalent circuit of synchronous generator[19].

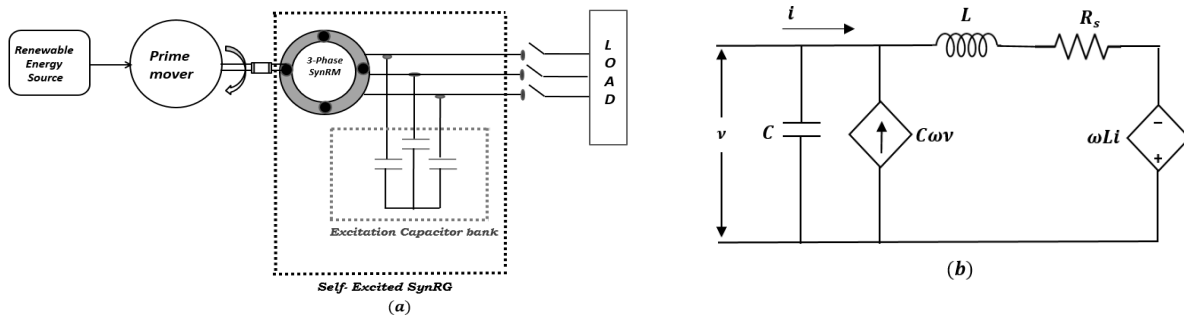


Figure 4 (a) Basic experimental diagram of RES based standalone EPG with SynRG (b) Simplified per-phase equivalent circuit of SynRG[23].

Switched Reluctance Generator (SRG)

In SR machines, during the generation mode, the proper synchronization of stator phase currents of SRG by means of an external DC source with its rotor position an e.m.f will induce [27]. The SRG produces negative torque and which is in opposite to the rotor rotation, hence extracts the energy from connected RES. Through an asymmetric half bridge converter, the phase winding will be energized. The turn-on/off triggering pulse angles of DC excitation unit are the variables. The common control methods association with SRGs are angle position control (APC), soft chopping current control (SCCC) and voltage chopping control (VCC) method. These methods are meant for controlling of phase voltage, currents and switching on/off. The SRGs are very simple in construction, rugged, cheap in cost, can be operate at higher speed, highly fault tolerant capability, no need of starting torque, high efficiency and can be suitable for high temperature environments also. As like PMGs, SRGs doesn't requires high torque to start & run and can be used in hard environmental conditions too. These are not recommended for low speed application because of its larger torque ripples. A schematic diagram of SRG is shown in **Figure 5(a)** and the simplified per-phase equivalent diagram is shown in **Figure 5(b)**, which is used for the performance analysis[28-30].

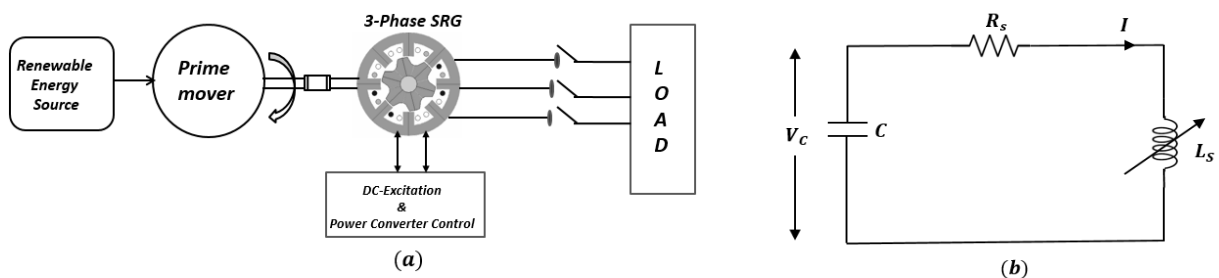


Figure 5 (a) Basic schematic diagram of RES based standalone EPG with SRG (b) Simplified Equivalent circuit of SRM[28].



Table 1 Comparative Table of Electric Generators

Aspect	SEIG	PMSG	BLSG	SynRG	SRG
Size and weight	Smallest and low weight simplest machine among Induction machines	Size and weight is higher than SEIG	Small size and reliable	Small in size and robust	Simple, robust and reliable
Cost	Lower cost than PMSG	High cost	Lower cost than PMSG	Low cost as compared to the all other brushless generators	Very low cost as compared to SEIG and PMSG
Self-excitation requirement	Yes required , preferably by means of out-side pre-charged capacitor banks	Not required	DC- excitation is needed for field winding	Yes required, preferably by means of out-side pre-charged capacitor banks	DC- excitation is needed for field winding
Control mechanism	Very simple control	Complex control mechanism	Simple control mechanism	Simple and sensor-less control mechanism	Flexible control
Efficiency	Lower Efficiency than PMSG at low and high speed operations	Higher Efficiency than SEIG at low and high speed operations	Moderate efficiency than induction machines	Higher efficiency than induction and Permanent magnet machines	Higher Efficiency than SEIG but Lower Efficiency than PMSG
Power factor (Name-plate)	Lower PF than PMSG	Higher PF than SEIG and almost operate at unity power factor	PF value is higher	Higher PF than IGs	Low PF value

CONCLUSION

The paper has presented an overview of various popular generators and their basic phenomena, experimental layout in standalone applications. The primary aspects of these generators are discussed and presented a comparative analysis. Simplified equivalent circuit models of the generators are highlighted for further steady state performance analysis. The primary objective of these standalone energy systems is to supply reliable and power quality improved supply to the consumers through distributed generation.

REFERENCES

- Puneet K. Goel, Bhim Singh, S. S. Murthy, Navin Kishore, Isolated Wind-Hydro Hybrid System Using Cage Generators and Battery Storage. *IEEE Transactions on Industrial Electronics*, Volume 58, Number 4, pp 1141-1153, 2011.
- Sreenivas S. Murthy, Renewable energy generators and control. Chapter. 12, *Electric Renewable Energy Systems*, pp 238-289, 2016.
- Online. Available: <http://www.cea.nic.in/reports>
- M. H. Nehrir, C. Wang, K. Strunz, H. Aki, R. Ramakumar, J. Bing, Z. Miao, Z. Salameh, A Review of Hybrid Renewable/Alternative Energy Systems for Electric Power Generation: Configurations, Control, and Applications. *IEEE Transactions on Sustainable Energy* Volume 2, Number 4, pp 392-403, 2011.
- R.C. Bansal, T. S. Bhatti, D. P. Kothari, Bibliography on the Application of Induction Generators in Nonconventional Energy Systems. *IEEE Transactions on Energy Conversion*, Volume 18, Number 3, pp 433-439, 2003.
- G. K Singh, Self-Excited Induction Generator for Renewable Applications. *Encyclopedia of Sustainable Technologies* Volume 4, pp 239-256, 2017.
- S.S. Murthy, O.P. Malik, A.K. Tandon, Analysis of self-excited Induction Generators. *IEE Proc*, Volume 129, Number 6, pp 260-265, 1982.
- N.H. Malik, S.E. Hague, Steady-State Analysis and Performance of an Isolated Induction Generator. *IEEE Transactions on Energy Conversion*, EC, Volume 1, Number 3, pp 134-140, 1986.
- B. Singh, S.S. Murthy, S. Gupta, Analysis and implementation of an electronic load controller for a self-excited induction generator. *IEE Proc.-Gener. Transm. Distrib.*, Volume 151, Number 1, pp 51-60, 2004.



23. Sandeep Vuddanti, S.S. Murthy, S.S. Murthy, Bhim Singh, An Optimum Solution for Field Deployment of Single-phase Power Generation using 3-Phase Self Excited Induction Generator. IEEE, 2016.
24. Paul C. Krause, Analysis of Electric Machinery, McGraw-Hill, New York, 1987.
25. T. F. Chan, Loi Lei Lai, Steady-State Analysis and Performance of a Stand-Alone Three-Phase Induction Generator with Asymmetrically Connected Load Impedances and Excitation Capacitances. IEEE Transactions on Energy Conversion, Volume 16, Number 4, 327-333, 2001.
26. Jamal A. Baroudi, Venkata Dinavahi, Andrew M. Knight, A review of power converter topologies for wind generators. Renewable Energy Volume 32, pp 2369-2385, 2007.
27. Sabha Raj Arya, Ashish Patel, Ashutosh Giri, Isolated Power Generation System Using Permanent Magnet Synchronous Generator with Improved Power Quality. J. Inst. Eng. India Ser. B, 2018
28. R. Krishnan, Permanent Magnet Synchronous and Brushless DC Motor Drives, CRC Press, Boca Raton, 2010
29. C. N. Bhende, S. Mishra, Siva Ganesh Malla, Permanent Magnet Synchronous Generator-Based Standalone Wind Energy Supply System. IEEE Transactions on Sustainable Energy, Volume 2, Number 4, pp 361-373, 2011.
30. T. J. E. Miller, Brushless Permanent-Magnet and Reluctance Motor Drives. Electronic Engineering No. 21, Oxford Science Publications, 1989.
31. Tze-Fun Chan, Weimin Wang, Loi-Lei Lai, Permanent-Magnet Synchronous Generator Supplying an Isolated Load. IEEE Transactions on Magnetics, Volume 46, Number 8, pp 3353-3356, 2010.
32. Tadashi Fukami, Takeshi Kondo, Toshio Miyamoto, Performance Analysis of a Self-Regulated, Self-Excited, Brushless Three-phase Synchronous Generator. IEEE, pp 89-91, 1999.
33. Sakutaro Nonaka and Katsumi Kesamaru, Analysis of Brushless Three-Phase Synchronous Generator Without Exciter. Electrical Engineering in Japan, Volume 113, Number 7, pp 135-144, 1993.
34. T. F. Chan, Steady State Analysis of Self-Excited Reluctance Generator. IEEE Transactions on Energy Conversion, Volume 7, pp 223-230, 1992.
35. Bhim Singh, Ram Niwas, Performance of synchronous generators for DG set based standalone supply system. Electric Power Systems Research Volume 113, pp 93-103, 2016.
36. S. S. Maroufian, P. Pillay, Self-Excitation Criteria of the Synchronous Reluctance Generator in Stand-Alone Mode of Operation. IEEE Transactions on Industry Applications Volume 54, Number 2, pp 1245-1253, 2018.
37. Maged Ibrahim, Pragasen Pillay, The Loss of Self-Excitation Capability in Stand Alone Synchronous Reluctance Generators. IEEE Transactions on Industry Applications, DOI: 10.1109/TIA.2018.2849407, 2018
38. Yawei Wang, Nicola Bianchi, Investigation of Self-Excited Synchronous Reluctance Generators. IEEE Transactions on Industry Applications, DOI 10.1109/TIA.2017.2781645, 2017
39. A.S.O. Ogunjuyigbe, T.R. Ayodele, B.B. Adetokun, Steady State Analysis of Wind-Driven Self-Excited Reluctance Generator for Isolated Applications. Renewable Energy, DOI: 10.1016/j.renene.2017.07.110, 2017
40. Nikolay Radimov, Natan Ben-Hail, Raul Rabinovici, Switched Reluctance Machines as Three-Phase AC Autonomous Generator. IEEE Transactions on Magnetics Volume 42, Number 11, pp 3760-3764, November 2006
41. Tarcio Andre dos Santos Barros, Pedro Jose dos Santos Neto, An Approach for Switched Reluctance Generator in Wind Generation System with Wide Range of Operation Speed. IEEE Transactions on Power Electronics, DOI: 10.1109/TPEL.2017.2697822
42. David A. Torrey, Switched Reluctance Generators and Their Control. IEEE Transactions on Industrial Electronics, Volume 49, Number 1, pp 3-13, 2002.
43. Siyang Yu, Fengge Zhang, Dong-Hee Lee, Jin-Woo Ahn. High Efficiency Operation of a Switched Reluctance Generator over a Wide Speed Range. Journal of Power Electronics Volume 15, Number 1, pp 123-130, 2015.



Rain Water Harvesting on Roads and Highways: An Innovative Approach to Conserve Water and to Prevent Waterlogging on Roads and Highways

Raghu Pillai

Daimler India Commercial Vehicles Pvt Ltd, Chennai, raghupillai2003@gmail.com

ABSTRACT

Rain Water Harvesting has been in practice for generations, mainly to meet the requirement of water for farming. More recently, roof top rain water harvesting has been mandated by the government on new buildings, to meet the ever increasing demand for water in cities.

A vast network of roads and highways are amides which are ideal locations for employing rain water harvesting. They are open to the skies and generally have bituminous hard surface; both of which are ideal from the point of view of rain water harvesting. If implemented, the dual objectives of conservation of water as well as prevention of flooding on roads and highways can be achieved.

KEYWORDS Rain, Water, Harvesting, Roads, Highways

INTRODUCTION

India is blessed with abundant rainfall to meet the needs of its population. However, poor water management is pushing our country towards very serious drought situation. The recent report brought out by NITI AAYOG predicts severe water scarcity of about 50% by 2030. Though many state governments have mandated roof-top rain water harvesting for new buildings, there is neither any mechanism available to ensure their implementation nor any data available on the quantity of water harvested.

On the other hand, many of the roads and highways face severe water logging, due to improper drainage system employed. Water accumulation can adversely affect the life of the road surface, and crores of rupees are spent, year after year, by state and central Govts on their repair.

If rain water harvesting is employed on the roads and highways, billions of litres of precious water can be saved from going waste, while at the same time find an effective solution for the effective and quick evacuation of rain water from the road surfaces.

PRESENT DESIGN OF ROADS AND HIGHWAYS

The cross-sectional view of a multi-lane road is provided in **Figure 1**.

The design of a multi-lane road provides a median or divider, running along the middle of the road, which separates the LHS traffic from the RHS traffic. On both sides of the road, storm-water drains are provided for evacuation of the rain water. A gentle lateral, downward slope is provided to the road surface from the median end (apex) towards the sides for the rain water to flow freely into the drains. The storm water drains are covered with slabs and are used as footpath for pedestrians. On city roads, the storm water drains are sometimes directly connected to the sewage system. The storm water drains run for km and hence the rain water has to take a torturous path to reach its final destination. As the drains are covered, cleaning and desilting of the drains happen only when there is a complete blockage. This design does not take into account the collection and storage of rain water, but only to get it drained completely and swiftly, to prevent flooding on the roads.

DISADVANTAGES OF THE PRESENT DESIGN

- This design does not consider conservation of rain water as an objective; instead it gives emphasis only on its evacuation through draining. Hence the entire water goes waste.
- As such, the drainage system should have the capacity to drain the entire rain water swiftly, before it starts flooding.
- The drains, however, due to improper maintenance get clogged frequently, and hence the rain water evacuation does not happen at the rate it is designed for. This leads to water logging.



- On city roads, the rain water gets mixed with the sewage, and when the drains get blocked, it flows back on to the roads, dirtying the surroundings.
- Accumulation of rain water adversely affects the life of the road surface, and also leads to disruption of traffic, damages to vehicles and accidents.

CHANGES PROPOSED TO THE PRESENT DESIGN

Cross-sectional view of a multi-lane highway as per the proposed design is provided in **Figure 2**.

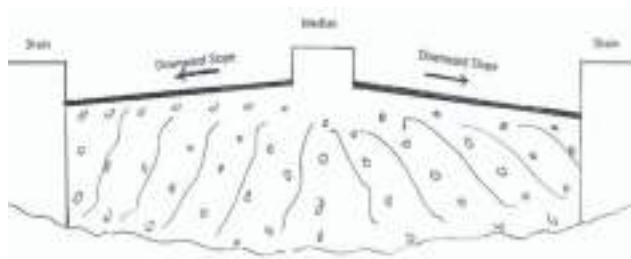


Figure 1 - Cross sectional view of a two lane road built as per the present design

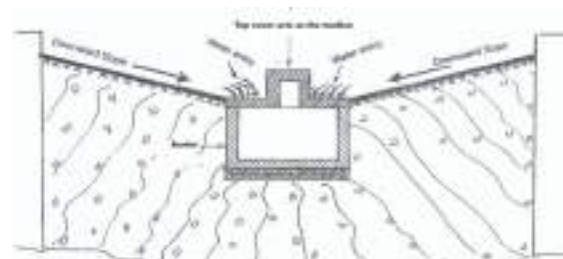


Figure 2 - Cross sectional view of a multi-lane highway as per the proposed design. The rain water falling on the road flows freely into the bunkers and get collected. As the bunkers are connected, overflow pipes are not required.

In this design, the roads are not only considered as a surface for vehicular movement, but also as a potential reservoir of precious water. If the design is adopted during the construction stage itself, then the cost and wastage can be brought down. The design is as explained below:

- A continuous trench is dug up in the location where the median is proposed. At the bottom of the trench, a thick layer of cement concrete is laid to have a level, load bearing surface. The dimensions of the trench is to be decided after considering the average rainfall that region experiences. The width may be kept the same, but the depth may be varied based on the rainfall.
- Pre-fabricated Reinforced Cement Concrete Bunkers of suitable dimensions are laid, in the trench, in-line, one after the other. The bunkers are connected end-to-end, in series, and together they act as reservoirs for the water collected. Pre-fabrication reduces the cost of manufacturing of the bunkers, assures uniform quality and significantly reduces the time for the road construction. The dimensions of the bunkers are decided based on the rainfall experienced in that area, and also on the convenience of its transportation and handling.
- While laying the bunkers in the trench, care should be taken to ensure that the overflow pipes of one bunker are concentric with the corresponding overflow pipes of the adjacent bunker. This is to ensure that the overflow can then happen to the bunker on the left or to the right. If height difference exists between the overflow pipes of adjacent bunkers, then the flow will be unidirectional; from the higher to the lower. The overflow pipes are connected using flexible and durable plastic pipes. This will take care of any issues arising due to the expansion of bunkers.
- The bunkers are provided with covers which are of concrete and having the cross-section of a hat. When placed over the bunker, the horizontal surfaces on both sides are at the road surface level. The raised portion at the middle projects upward and act as the median. The horizontal surfaces are provided with array of holes cast into them. Water enters the bunker through these holes.
- The lateral slope provided to the road surface in this design is just opposite to that in the present road design. The downward slope is provided from the sides of the road (apex) towards the median for the water to flow freely into the bunkers.

Working Principle

- The principle used here is to collect the maximum quantity of water at the source, and allow only the excess water to flow to the adjacent bunkers. This principle helps in quick evacuation of water as well as store the maximum quantity of rain water. As bunkers are connected in series, like the links of a chain, collection of the entire water without wastage is possible.
- The rain water falling on the road flows freely into the nearest bunker through the array of holes provided in the cover (termed 'Direct Flow'). It first fills the bunker up to the level of the overflow pipe. Any excess water

entering the bunker, flows outside through the overflow pipe into the adjacent bunker, to the left or to the right (termed 'Lateral Flow'). So every bunker may experience either direct flow, lateral flow or both.

- Since series of bunkers are connected, the excess water from one bunker flows into the next, then to the next and so on, until the entire water is captured and stored. By this way, the entire rain water falling in a particular area gets collected, thereby preventing water accumulation. Arrangement of bunkers are shown in **Figure 5**.

Bunker

Bunkers are rectangular tanks fabricated out of reinforced cement concrete (**Figure 3**). Pre-fabrication ensures their uniform quality and timely delivery. The dimensions are decided based on the convenience and ease of transportation and handling.

Suggested dimensions are 2 m width \times 10 m length, which may be kept constant. The depth may be varied between 1 m to 3 m based on the rainfall experienced; more the rainfall, more the depth. A bunker of size 2 m \times 10 m \times 1 m deep, can hold 20,000 l of water. Over a distance of 1 km, approximately, 95 such bunkers can be laid, which collectively has a capacity to store 1.9 million litres of water. By increasing the depth to 2 m or 3 m, the capacity can be doubled or tripled. This shows the potential of the design. It is also possible to mix bunkers of different depths, as long as the overflow pipes are at the same height and concentric with each other.

If the bunkers are properly dimensioned and quality maintained, then they can have a useful life of 50 years or more.

Cover

The bunkers are provided with covers which are of RCC and having the cross-section of a hat (**Figure 4**). When placed over the bunker, the horizontal surfaces on both sides are at the road surface level. The raised portion at the middle projects upward and act as the median. The horizontal surfaces are provided with array of holes cast into them. Water enters the bunkers through these holes.

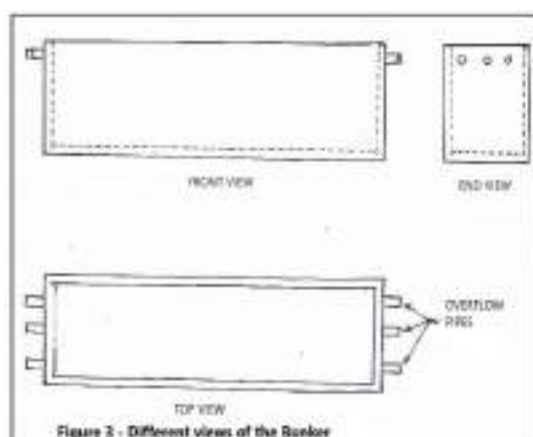


Figure 3 - Different views of the Bunker

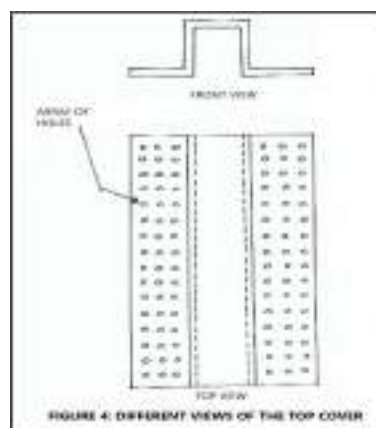


FIGURE 4: DIFFERENT VIEWS OF THE TOP COVER

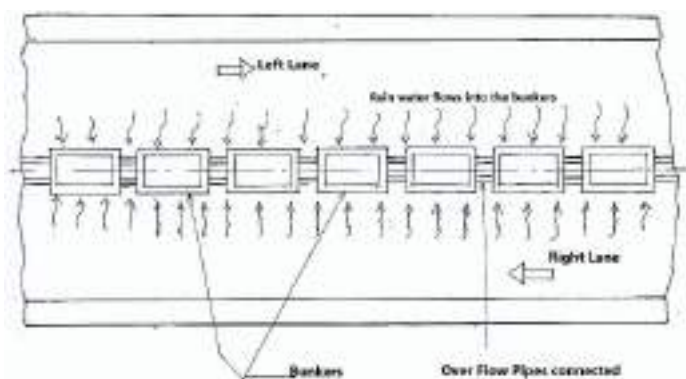


Figure 5 - Bunkers connected in series. Rain water from both lanes flows into the bunkers



ADVANTAGES OF THE PROPOSED DESIGN

- As explained above, the principle used here is to collect the entire rain water in underground bunkers and thereby prevent water logging. As such, no drains are required.
- As the water is stored in concrete bunkers, there is no loss due to seepage. The top cover prevents evaporation losses too.
- As thousands of km of roads are available where this concept can be applied, the roads can turn out to be huge reservoirs of water. Billions of litres of water can be stored in these bunkers.
- As the roads are the property of the Government, no acquisition of land is required or any environmental clearance is to be obtained to develop such huge reserves of water.
- The water thus stored shall be the property of the Government, and it has the exclusive right to decide on its usage. This water may be used to provide drinking water kiosks along the highway (after processing), or may be used for cultivating the fallow lands lying on both sides of highways.
- Huge quantity of water stored in a single location; like in a dam, is always risky, as any damage to the dam can inundate the nearby locality. Whereas in this case, the huge reserve is created along the roads and highways in multiple locations, so that the risk is practically zero. Even a natural calamity (like an earthquake) may damage only a few bunkers and the water gushing out of those bunkers do not create any alarming situation.
- The concrete bunkers, if properly designed and constructed, shall have a minimum life of 50 years or more. Which means that this system can provide unattended service for the next 50 years, year after year. It only needs occasional de-silting so that the bunker capacity does not get reduced.
- This does not need any external energy for its operation and functions on its own. So the system is self-sustaining and eco-friendly.
- The underground bunkers act like a retaining wall for the sub-soil, which gives added compaction to the sub-soil.
- By effectively preventing waterlogging on roads, the life of the roads improve, and the money spent year after year for repairing the roads and highways may be saved.
- The use of cement and steel for the construction of bunkers can trigger other economic activities and create additional jobs on a very large scale.
- On village roads, which may be mostly narrow roads without median, the bunkers may be provided along the middle of the road and lateral slopes may be provided from both sides towards the middle to direct the water towards the bunkers.
- This design may be introduced while constructing new roads, which can save on the construction cost. In the case of existing roads, this design may be implemented on those roads where waterlogging is severe.

CONCLUSION

- Rain Water Harvesting can be an effective tool for the evacuation of rain water from road surfaces.
- The present design is based on the evacuation of rain water through drains. The entire rain water gets wasted.
- The proposed design emphasises on evacuation by storage. The entire rain water gets stored in underground bunkers. Hence drains have no role to play here.
- Huge reserves of precious water can be created which may be used for productive purposes.

REFERENCES

1. Composite Water Management Index, June 2018, by NITI Aayog.
2. Two Laning of Highways through Public Private Partnership; Manual of Specifications and Standards, by Indian Road Congress.
3. Karnataka State Council for Science and Technology; Rain Water Harvesting from Roads.
4. Various newspaper articles on waterlogging on roads and highways citing poor drainage system.



Climate Change Impact on Indian Agriculture and Food Security

Parminder Singh Bhogal

Water Resources & Environment Department, Punjab, bhogal_ps@yahoo.co.in

ABSTRACT

Climate change is happening faster than expected one and its impacts are being noticed in the various regions of India by all of us. Climate change is affecting agriculture in a number of ways through changes in average temperatures, rainfall variation in space and time etc. There is reduction in crop yield over the time due to rise in temperature. Due to climate change unseasonal and insufficient rain fall has become quite common causing changes in cropping patterns. Crop yields have been declining in some parts of India because of high temperatures that many crops cannot tolerate. As per recent Economic Survey of India 2018, climate change will reduce agricultural growth by about 15% on average.

It is desired to reduce vulnerability to the impacts of climate change by building adaptive capacity and resilience. Farmers need to evolve new farming techniques to grow varieties of crops that maintain productivity in changing weather. Crop management strategies suiting a particular region as per local changing climate patterns are to be devised for limiting impact on agriculture growth. Adaptation measures aimed at protecting agriculture production, natural resources and human health are required. Adaptation measures appropriate to sustain agriculture production have been outlined in the paper. Adaptation measures required are at farm level and community level in addition to research and development of new crop varieties to sustain the agriculture production.

INTRODUCTION

Climate change is happening and it is a threat to mankind. Climate change and agriculture is an interrelated process as both take place on a regional and global scale. Future climate changes are likely to have more significant effect on crop production in India. Climate change will increase the risk of food insecurity for vulnerable groups. Climate change affects agriculture many ways through changes in average temperatures, rainfall variation in space and time, changes in atmospheric carbon dioxide, changes in the nutritional quality of some foods etc.

Since the end of the 19th century, the earth's average surface temperature has increased by 0.4 to 0.6°C, whereas over the last 40 years, the rise has been 0.2 to 0.3°C. The data of regular records available since 1860 clearly indicates that most of last 50 years have been the warmest since 1860. Temperature has risen by about 1°C since 1880 per available record. As per recent IPCC (Intergovernmental Panel on Climate Change) reports, global warming will be more serious and accelerating more than the present rate. As per experts, as per current phenomena, where temperature increase is already hovering just over 1°C compared to pre-industrial levels, the 1.5°C target may be breached by 2050.

CLIMATE OF INDIA

India exhibits a wide diversity of climate. Temperature varies from the freezing cold winter in the Himalayas to the scorching heat in the Thar Desert. The above two regions play a very significant role in controlling the weather of India.

The climate of India is dominated by the monsoon season from June to September which is the most important season of India, providing 80% of the annual rainfall. The monsoon of India is regarded as the most productive season in India. The monsoon severity has increased in the last few decades due to the process of global warming, leading to the severe floods in many parts of India. India depends heavily on monsoon for its agricultural productivity, failure of which result in the decreased crop productivity, leading to droughts. Of the total agricultural land in India, about 68% is prone to drought of which 33% is chronically drought prone, receiving rainfall of less than 550 mm per year. This is particularly in states of Maharashtra, Madhya Pradesh, Gujarat, Rajasthan, Karnataka, Andhra Pradesh and Orissa. The World Record of Drought was in 2000 in Rajasthan where people parched for water were ready to injure each other as they struggle to get water from a well in the drought affected areas.

IMPACT OF CLIMATE CHANGE IN INDIA

Climate change is happening and its impacts are being seen on our agriculture and weather patterns. A warmer climate changes rainfall and snowfall patterns, lead to increased droughts and floods, causes melting of glaciers and polar ice sheets and results in accelerated sea-level rise. Rising warmth will lead to an increase in the level of evaporation of surface water; the air will also expand and this increases its capacity to hold moisture.



Climate change affects food security through its impacts on all components of food production and food system stability. It also has an impact on human wealth, food production and distribution channels, as well as changing purchasing power. Its impacts will be both short term, resulting from more frequent and more intense extreme weather events, and long term, caused by changing temperatures and precipitation patterns. People who are already vulnerable and food insecure are likely to be the most affected.

There has been alarming effect of global warming on the climate of India. Many parts in India are already disaster prone; with the statistics of 27 out of 35 states are disaster prone, with most disasters being water related. An increase in the number of cyclones and hurricanes over the last few years has been attributed to changes in temperature. In recent years more occurrences of floods, draughts and cyclones has been witnessed in one or the other part of India. Nearly 8 million hectares area in India is affected by floods every year at one or the other place falling in the states UP, Bihar, Uttarkhand, West Bengal, Maharashtra, Madhya Pradesh, Odissa, Assam, Andhra Pradesh, Punjab, J&K. Recently severe floods occurred in Kerala. Also, more cyclones happened recently in India, for example, 2013 cyclone named Phailin, October 2014 cyclone named Hudhud on east coast of India, cyclone of November 2017 on coast of Tamil Nadu and Andhra Pradesh. Recent floods in Kerala State (August 2018) is another evidence of unprecedented rainfall due to climate change effects.

Water resources will be affected more than all other natural resources over the time. Significant segments of Earth's population are consuming groundwater quickly without knowing when it might run out. It is not exactly known how much is stored in each of these aquifers. In a water-scarce society, it can't be tolerated this level of uncertainty, especially since groundwater is disappearing so rapidly. The study notes that the dearth of groundwater is already leading to significant ecological damages and also declining water quality.

Impact on Crop Yield and Farm Income

Climate change has affected our crop production and yield. Many agricultural crops exposed to higher temperatures do have lower yields. The rain fed crop yield change is driven by both precipitation and temperature changes. In irrigated areas, crop yield impacts are from temperature changes alone where wheat and rice crops are hard hit.

As per recent economic survey of India 2017-18, farmer income will decline by 20 to 25 % in un-irrigated areas. Climate change can reduce agricultural growth by about 15% on average. At current level, farm income will have adverse impact of climate change and likely to result in reduction of income of more than Rs. 3600/- per year for medium farm house hold. Survey further adds that extreme temperature and rainfall events will lower crop yield up to 7.6 % and 14.7 % respectively as given in **Table 1**.

Table 1 shows the percentage decrease in production in response to temperature rise and rainfall decrease (significantly less than usual rainfall) in irrigated/un-irrigated areas in India – Economic Survey of India 2018.

There is reduction in crop yield over the time due to rise in temperature. Due to climate change unseasonal and insufficient rain fall has become quite common. This is causing the changes on cropping patterns. Crop yields have been declining in some parts of India because temperatures there are already high that many crops cannot tolerate. Additional warming will affect their marginal water balance also. As a result, wheat cultivation suffered in a big way. Cereal production has gone down causing food insecurity and loss of livelihood. Climate change is affecting agricultural yield directly because of alterations in temperature and rainfall, and indirectly through changes in soil quality, pests, and diseases. In particular, the yield of cereals is expected to decline in India. Extreme weather conditions such as high temperature, heavy rainfall, floods, droughts also affects crop production. Impact of change of temperature on variation in rice crop yield, as per a study, is as given in **Table 2**.

Table 1 Crop yield at different temperature

Crop	Extreme temperature	Extreme rainfall
Kharif average	-4%	-12.8%
Kharif irrigated	-2.7%	-6.2%
Kharif un-irrigated	-7%	- 14.7%
Rabi average	-4.7%	-6.7%
Rabi irrigated	-3%	-4.1%
Rabi un –irrigated	-7.6%	-8.6%

Table 2 Grain yield in several climatic condition

Climate scenarios	Temperature change	Crop duration	Grain yield
(% deviation over normal scenario)			
Extreme warm	+2.0°C	4	10
Greater warm	+1.5°C	3	8
Moderate warm	+1.0°C	2	3
Slight warm	+0.5°C	1	2



CHALLENGES TO SUSTAIN AGRICULTURE GROWTH

In India, projections indicate the possibility of loss of 4 to 5 million tons in wheat production with every rise of 1°C temperature throughout the growing period with current land use. In March 2004, temperatures were higher in the Indo-Gangetic plains by about 3°C, which is equivalent to almost 1°C per day over the whole crop season. As a result, wheat crop matured earlier by 10 to 20 days and wheat production dropped by more than 4 million tons in the country. Losses were also very significant in other crops, such as mustard, peas, tomatoes, onion, garlic, vegetable and fruit crops. Similarly, drought of 2002 led to reduced area coverage of more than 15 million hectares of the rainy-season crops and resulted in a loss of about 10% in food production.

In the near future the agriculture system will face the following challenges:

- An increase in crop water requirement to meet the increased evapo transpiration demands.
- Decrease in yield due to rise in temperature and variation in duration.
- A reduction in the amount of water available to plants in most place due to the predicted shortage in water supplies.
- Increase in extreme storms, drought, floods, high temperature winds etc.
- Food shortages which may further increases food prices and adversely impact the poor.

Threat to Food Security

Due to rise in the temperature, the sowing period is getting reduced and decomposition of organic matter in the soil has been speeded up leading to the deterioration in the quality of soil fertility. IPCC Report (2007) and a few other global studies indicate a probability of 10 to 40% loss in crop production in India with increase in temperature by 2050 – 2100. Thus it leads to food shortage and starvation. This likely to have effect on international food prices, trade and food security.

Studies carried out by the ICAR-Indian Agricultural Research Institute indicate the loss of 4-5 million tonnes in wheat production in future with every rise of 1°C temperature throughout the growing period. As the daily minimum temperature increases, or as nights get hotter, rice yields drop. It is because rice plants have to respire more during warm nights, so expending more energy, without being able to photosynthesize.

Increasing glacier melt in Himalayas is affecting availability of irrigation especially in Indo-Gangetic plains. Rise in temperature and insufficient rainfall and unseasonal rainfall could have significant effect on quality of cereals, fruits, aromatic and medicinal plants with resultant implications on their prices and trade. Pathogens and insect populations are increasing resulting in crop yield loss. Heat stress in dairy animals is badly affecting their production and reproductive performance.

World Bank 2016 report shows that climate change could push more than 100 million people into extreme poverty by 2030. In fact, in its new study released in June 2018, it claimed that South Asia alone would be warmer by 1.6°C to 2.2°C by 2050, far above the global average, sharply lowering living standards of over 800 million people.

Future projections by Indian Institute of Tropical Meteorology and various IPCC emission scenarios indicate following effects by the end of the year 2100.

- Global warming will be more serious and accelerating more.
- Number of rainy days may decrease by 20 to 30%.
- Extremes in temperature and rainfall also show increase in their frequency and intensity.
- Fall in India's water resources which when combined with the recession of Himalayan glacier would pose a threat to the food and water security.

Adaptation of Climate Change

Adaptation is relevant to sectors such as agriculture, water and natural resource management. Identifying options to adapt to climate change and evaluating them in terms of criteria such as availability, benefits, costs, effectiveness, efficiency and feasibility etc. Climate change adaptation is the adjustment in natural or human system in response to actual or expected climatic effects. Adaptive capacity to climate change is the ability of the system to adjust the climate change to moderate potential damages, to take advantage of opportunities, or to cope with the consequences. As communities are exposed to unexpected or unforeseen changes in weather patterns and increased risk, more robust adaptation plans are required to manage the additional risks.



The main objectives of the adaptation plans are:

- To reduce vulnerability to the impacts of climate change by building adaptive capacity and resilience;
- To facilitate the integration of climate change adaptation, in a coherent manner, into relevant new and existing policies, programmes and activities, in particular development planning processes and strategies, within all relevant sectors and at different levels, as appropriate.

Adaptation measures are very context specific and a blueprint approach is not advisable. However, some selected and general approaches are given below:

At farm level:

- Changes in crop management, for example, adjustment of planting dates, change of crop varieties or crop types as per changed climate system in a region.
- Livestock management, for example, feeding, animal health, livestock choice.
- Land use and land management (for example, laser leveling, fallowing, tree planting, water harvesting, erosion control etc.).

At community level:

- Soil conservation
- Water conservation
- Agro-biodiversity management
- Livelihood diversification
- Improved processing and marketing
- Supporting farmers' organization and associations

At research and public services level:

- Improved weather forecast
- Weather information systems installation and intimation to farmers directly
- Participation in land-use planning
- Plant breeding/seeds to be revised/modified
- Animal breeding systems to be revisited.

To achieve adaptation with success, funds are required at every level. Developing countries require international assistance to support adaptation. This includes funding, technology transfer and capacity building. Some funding for adaptation is provided through the various financial mechanisms which includes Green Climate Fund.

CONCLUSION

Climate change is happening rapidly posing new challenges to sustain our agricultural production to feed the nation. To meet this challenge, farmers will have to evolve new farming techniques to grow varieties of crops that maintain productivity in changing climatic conditions. In developing countries like India, climate change will cause yield declines for the most important crops. If the adequate action is not taking, climate change will rapidly alter the lands and waters we all depend upon for survival, leaving our future generations to difficult time.

Adaptation measures are required to sustain the agriculture production. Adaptation measures, if under taken immediately by all concerned, will help to sustain agriculture production to meet the future needs of increasing population. Adaptation measures at farm level, community level and agricultural universities level to research and develop new crop varieties suiting changed/changing climate patterns are required to sustain the agriculture production.

REFERENCES

1. IPCC Reports of 6 October 2018 and others.
2. Study Report of Indian Agriculture Research Institute.
3. World Bank Reports on Climate Change.
4. Study Reports of Indian Institute of Tropical Metrology.
5. Economic Survey of India 2018
6. Indian Journal of Agriculture Research. Global Climate Change and Indian Agriculture. Impact, Adaption, Mitigation – by P K Agarwal.
7. Book on Global Climate Change edited by W Shanthakumar.



Comparative Evaluation and Efficacy of using Different Heating Techniques for Effective Management of e-Waste

H. Mishra*, A. S. Pente, R. Mishra, S. K. Mishra, B. P. Patidar, G. K. Mallik, A. Sharma, C. P. Kaushik, A. P. Tiwari
Homi Bhabha National Institute, Bhabha Atomic Research Centre, Trombay, Mumbai, hmishra@barc.gov.in

ABSTRACT

One of the most accepted waste management strategy rely on making the strategy to achieve significant volume reduction and finding suitable methodologies for containment of every kind of waste followed by isolating it from the biosphere with an objective of protecting environment over an extended period of time. The relevance of the present work will be better appreciated when a background detail is discussed pertaining to the types of electronic waste, the nature of e-waste involved and quantum of annually expected e-waste out of the utilisation of electronic technology in the developing country like India[1,2]. In our country, environmental issues will be inevitably associated with large-scale production and deployment of advanced electronics and associated technology. Use of advanced technology is essential for the survival of human civilization and acts as a catalyst for the future growth of the nation. Therefore, the entire resources must be optimally developed and deployed to meet our short as well as long-term progress. Management of electronic waste is the major challenging task for present and the future digital world as well due to its increasing reliance with respect to public life as a whole. For example use of mobile phones, laptops, televisions and the other digital and electronic entertainment devices [3]. With respect to its demands, the issue need to be critically addressed for efficient recycle, reuse and proper disposal for better management of these types of wastes [4]. Present article gives the highlights of experimental work carried out for Thermal Characterisation such as DTA-TG-EGA of Printed Circuit Boards (PCBs) samples followed by comparative evaluation of different heating techniques such as resistance, induction and microwave to achieve maximum volume reduction for effective management and final disposal of e-waste residues using suitable technology.

KEYWORDS Electronic waste; Environment; Resistance; Induction and Microwave

PREAMBLE

Experimental studies have been carried out inside well-ventilated fume hood to evolve best and the most suitable treatment methodology for management of electronic waste. Different heating equipments such as resistance furnace, induction furnace and microwave heating chamber were suitably designed in-house and utilized for the study. In all these cases; rate of heating is different and faster heat gradient is expected to give better results in terms of e-waste volume reduction making it suitable for final disposal. The literature survey associated with e-waste management was extensively done and the inputs have been utilized during planning and execution of the experimental study pertaining to the heat treatment of representative e-waste sample with an objective to minimize the volume prior to its conditioning and disposal. Thermal characterization of representative PCB sample on milligram scale, heat treatment of the same samples on gram scale using different heating techniques and chemical analysis of water scrubber samples collected during above experiments are the major highlights of present work.

ISSUES WITH E-WASTE MANAGEMENT

In order to mitigate the pollution from the treatment of electronics-waste, efficient technology need to be formulated and required to be deployed on the larger scale. E-waste comprises of various metals, precious metals, chemicals, plastics, glass etc. It has aluminium, steel, iron, copper, gold, silver, palladium etc which can be recovered as a good commodities whereas mercury, cadmium, arsenic, cartridge inks, lead, beryllium fall under the hazardous category. Many of these substances are toxic and carcinogenic in nature. For example, Release of beryllium during recycle process of e-waste may certainly have adverse effects and lead to chronic beryllium disease and even the lung cancer. Inhalation or skin exposure to beryllium dust, fume, mist, or solutions may result in the beryllium sensitization. These materials seem to be complex in nature and have been found to be difficult to recycle in an environmentally sustainable manner leading to major health hazard. In the country like India; the impacts is found to be worse where general public is engaged in recycling of e-waste in an unorganised manner. People living in close proximity to dumps or landfills of un-treated e-waste and working without any protection or safe guards may have to face life-threatening difficulties. If recycling of e-waste is not done in a systematic manner; these hazardous materials get into waste stream resulting in the pollution of air, water and soil which can adversely affect the environment and biosphere. The open air burning of e-waste may possibly release hydrocarbons and their derivatives into the atmosphere. Processing of gold plated printed circuit boards (PCBs) and integrated circuit (ICs) using chemical stripping technique can leads to generation of brominated Dioxins, Furans and heavy metals.



Dumping of shells present in Cathode Ray Tubes (CRTs) generated from televisions and computer monitors could lead to leaching of hazardous elements like lead and barium into ground water. This can have serious health problems to local communities. Before we start thermal characterisation, basic constituents of e-waste sample need to be understood. The estimated composition of Printed Circuit Boards (PCB) residue, exposure limits of hazardous substance present in the e-waste and gases are shown in the following **Tables 1, 2 and 3** respectively.

Table 1 PCB Residue (250 gm e-Waste)

Components	Content, %
C	7.25
H	0.34
N	0.25
SiO ₂	28.56
Cu	28.57
CaO	10.9
Al ₂ O ₃	6.06
Br	2.33
Sn	4.98
Pb	2.81
Zn	3.42
Pt	0.0049
Mg	0.13
Fe	0.93
Ti	0.48
BaO	0.63
K	0.16
Ni	0.18
Sb	0.14
Mn	0.05
Hg	0
Cr	0.12
Ag	0.052
Au	0.022

Table 2 Hazardous Substance in e-Waste

Hazardous substance in E-waste	Exposure limit (OSHA Standard)
Lead	0.05 mg/m ³
Mercury	0.025 mg/m ³
Cadmium	0.005 mg/m ³
Chromium (VI)	0.005 mg/m ³
Halogenated substances (CFCs)	50 ppm
Polychlorinated biphenyls	1 mg/m ³
Poly-brominated di-phenyl ethers	0.02 µg / day

Table 3 Hazardous Gases

Components	Exposure limit (OSHA Standard)
H ₂	Less than 4 %
CH ₄	1000 ppm
CO	25 ppm
CO ₂	5000 ppm
CH ₃ Br	5 ppm
C ₂ H ₄	200 ppm
C ₂ H ₆	1000 ppm
C ₃ H ₈	1000 ppm
C ₂ H ₂	2.5% (25,000 ppm)
C ₂ H ₅ Br	200 ppm
C ₃ H ₆	500 ppm
C ₄ H ₈	<19.5 %

EXPERIMENTAL PROCEDURE

Thermal Analysis of e-Waste

Thermal characterization of PCB samples using advanced techniques like Differential Thermal Analysis (DTA) and Thermo Gravimetry (TG) have been carried out to have in-depth understanding about the temperature-based reactions and alterations during heating process and gaseous product generation during heat treatment of e-waste.

Thermogravimetry (TG) and Differential Thermal Analysis (DTA) of electronic waste were carried out using Setaram TG-DTA instrument. In the first step; the representative e-waste sample was crushed into very small pieces. About 20 mg of the representative sample was taken in a platinum crucible and heated in the temperature range of minimum 25 to maximum 1000°C at a heating rate of 10°C per minute under the flowing air atmosphere. The change in mass and the heat flux were recorded as a function of temperature during the above analysis. TG-DTA runs were repeated twice. **Figures 1 and 2** shown the TG-DTA plot of e-waste sample.

In both the cases a two step mass loss was observed in the temperature range of 260-350 and 350-550°C with a total loss of 16.6 and 18.85 %. The mass loss found to be 9.5 & 12.21 % in the first step and 7.1 & 6.64 % in the second step. Studies were further extended to understand the gaseous products generated during heating of e-waste upto 700°C under the flow of Argon gas using a TG-DTA-EGA instrument. **Figure 3** gives the TG-MS plot for the e-waste recorded under argon flow condition. The MS data recorded as a function of temperature showed the presence of 38 numbers of peaks in the mass ranging from 12-136. The intensity of these peaks has been plotted as a function of temperature in **Figure 3**. The mass corresponding to 40 which has the highest background is due to argon which is a carrier gas. The observed peak for the mass number 40 in the temperature range 290 to 430°C could be a



decomposition of Propane. The other intense peak such as 17, 18, 28, 44 could be due to H_2O , CO , CO_2 , respectively. These are the possible products from burning of hydrocarbons. It appears that most of the mass peaks could due to hydrocarbons and their decomposition products. The intensity of mass peaks due to the formation of highly toxic gases like Dioxin and Furan also need to be studied with EGA technique. Detailed study pertaining to this is in progress.

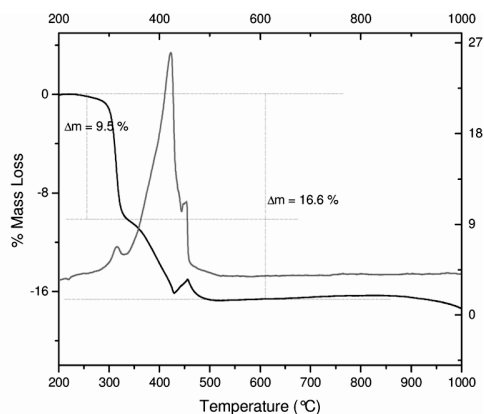


Figure 1 TG-DTA plot of e-waste sample A

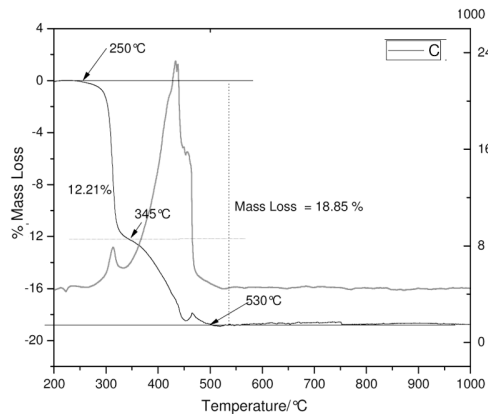


Figure 2 TG-DTA plot of e-waste sample-B

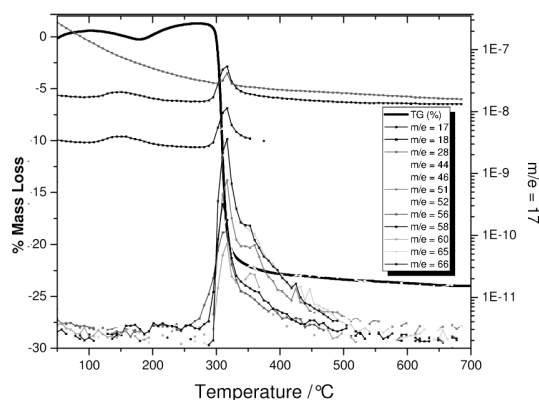


Figure 3 TG-MS plot for the e-waste

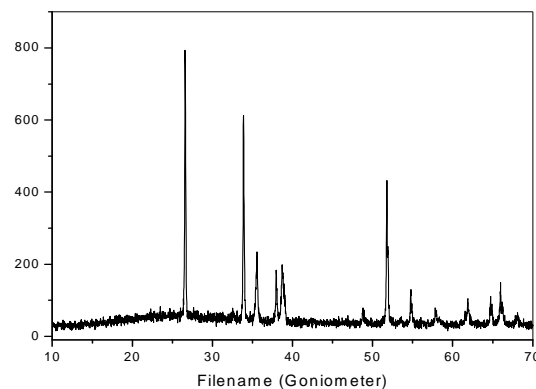


Figure 4 XRD plot of the e-waste residue

Table 4 Results of thermal analysis of e-waste

Sample	Step-I	Percentage of mass loss	Step-II	Percentage of mass loss	Total mass loss, %
	Temperature range, °C		Temperature range, °C		
e-waste	260-350 °C	09.50	350-550°C	7.10	16.60
e-waste (Repeat)	260-350 °C	12.21	350-550°C	6.64	18.85

The results of thermal analysis of e-waste are presented in **Table 4**. DTA, plots reveal that both mass loss steps are exothermic in nature, the second mass loss step being much more exothermic than first step.

Characterisation of e-Waste Residue

At the end of the thermal analysis; a black colour residue (reduced volume), which was insoluble in most of the aqueous or organic solvent was obtained. X-ray diffractometry of this residue was carried out to know the components present. **Figure 4** gives the XRD analysis plot of the residue, which indicates presence of SnO_2 , TiO_2 and Al_2O_3 phases. The volume of product formed is considerably less compared to the initial volume of e-waste. The products formed appear to be non-toxic oxides with major constituent oxides such as SnO_2 , TiO_2 and Al_2O_3 .

Safety Issues



Since this experimental study is planned with inactive samples of e-waste on 5 gram scale only,

radiological conditions will not get affected inside the fume hood and laboratory areas. Hence, manRem expenditure during the course of work is not at all expected.

- In view of toxic gaseous product expected to be generated, two numbers of scrubbers in series were used with small capacity vacuum pump, cleaned air ultimately releasing to fume hood exhaust as shown in **Figure 5**.
- Augmentation of adequate leak tightness of the furnaces used for experiments has been ensured to avoid spread of toxic gaseous product in the working area.
- The experimental study has been carried out with complete safety coverage, following industrial safety procedures.

Resistance Heating Furnace

Accurately weighed 5 gm of e-waste sample (PCB pieces) was taken in crucible kept inside furnace cavity lined with refractory bricks. Thermocouple was mounted inside the mass to monitor the temperature. Actual experimental setup used for this study is shown in **Figure 6**.

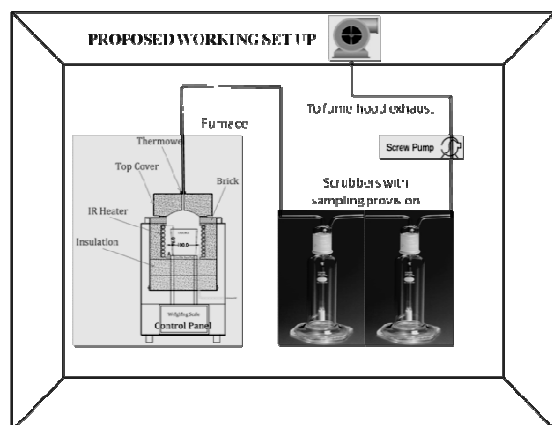


Figure 5 Working flow sheet for laboratory

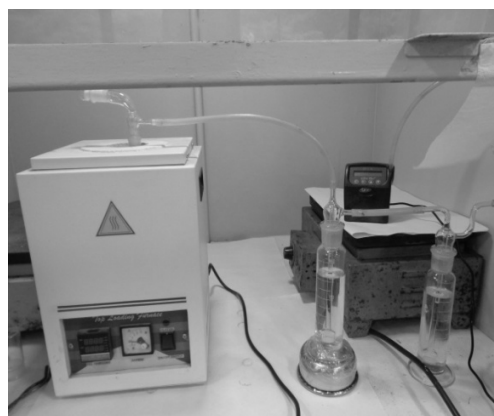


Figure 6 Resistance heating furnace with scrubbers

Heat treatment of the sample was performed in two steps with weight measurement and the experimental observations are presented in **Table 5**.

Induction Heating Furnace

Accurately weighed 5 gm of e-waste sample (PCB pieces) was taken in graphite crucible kept inside cavity made of heating coils. Pyrometer was mounted above the crucible to monitor the temperature. Actual experimental setup used for this study is shown in **Figure 7**. Heat treatment of the sample was performed in two similar steps with residue weight measurement and the experimental observations are presented in **Table 5**.

Microwave Heating Applicator

Accurately weighed 5 gm of e-waste sample (PCB pieces) was taken in silica crucible and placed inside a 2.45 GHz / 900 Watt Microwave Multi-mode Applicator and covered with a glass hood to adequately exhaust the evolving gases. Thermocouple was placed over the top of the mass to monitor the temperature. The experimental setup used for this study is shown in **Figure 8**. Heat treatment of the sample was performed in two similar quantity batches and the experimental observations are presented in **Table 5**.

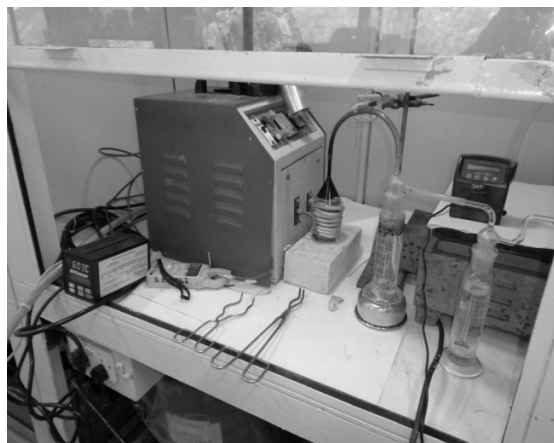


Figure 7 Induction heating furnace with scrubbers

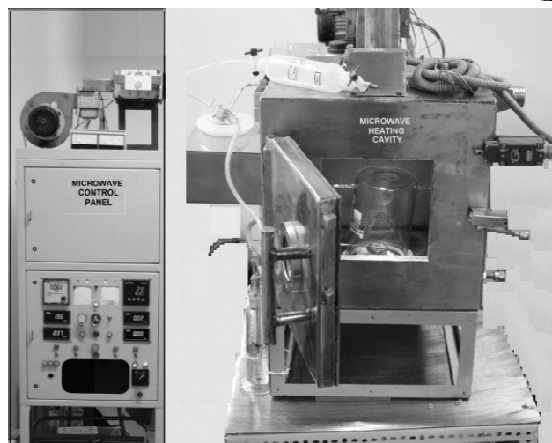


Figure 8 Microwave heating furnace with scrubbers and control panel

RESULTS AND DISCUSSIONS

Experimental parameters and outcome of the present studies carried out with different heating techniques are documented in the follows in **Table 5**. In resistive heating method good matching have been reported, thereafter the process is repeated in induction heating (kHz) wherein higher efficiency (23 to 29%) of mass reduction is recorded. The experiments were further extended by using 2.45 GHz / 900 Watt Microwave Multi-mode Applicator covered with a glass hood to adequately exhaust the evolving gases. Thermocouple was placed over the top of the e-waste mass to monitor the temperature. The experimental observations gathered during present study will provide input data for designing and optimization of microwave system for energy efficient remediation of e-Waste. E-waste heating results have been compared with in situ 20 mg process during DTA-TG analysis in the laboratory to 5 gm (250 times scaled up) e-waste material with respect to initial and final data on mass reduction within same temperature regime. Water scrubbers collected during each experiment were analyzed for elemental constituents and was found to contain Si and Ca as major elements whereas B, Cu and Zn were found in minor concentration ranges.

Table 5 Comparative parameters and outcome of the experimental studies

Technique		Value					
Parameters		Resistance		Induction		Microwave	
Scale		5 g		5 g		5 g	
Temperature, °C		415		415		350	
Weight loss, %		19.45		22.93		25.1	
Time, Minutes		25-35		25-35		5-6 min	
Temperature, °C		600		600		600	
Weight loss, %		3.40		6.50		1.2	
Time, Minutes		15-20		15-20		6-7 min	
Cumulated weight loss, %		22.8		29.43		26.30	
Elemental concentration in scrubber (200 ml each) mg/L		Scrubber		Scrubber		Scrubber	
Elements	Water	1	2	1	2	1	2
B	0.167	1.66	0.106	0.57	0.67	0.137	0.0968
Si	0.61	47.1	10.8	22.8	10.9	2.26	1.838
Cu	ND	0.048	0.021	0.04	0.05	11.7	7.73
Ca	ND	13.2	11.0	9.48	8.68	0.867	0.633
Zn	ND	1.14	0.321	0.32	0.03	0.021	0.01
Al	ND	BDL	BDL	BDL	BDL	BDL	BDL

Note: BDL value for Al is 0.034 mg/L and ND: Not detectable



CONCLUSION

Thermal analysis of e-waste samples indicates that the sample burns with evolution of significant amount of energy in the air. The volume of product formed is considerably less compared to the initial volume of e-waste. DTA, plots reveal that both mass loss steps are exothermic in nature, the second mass loss step being much more exothermic than first step. XRD analysis of the residue indicates presence of SnO_2 , TiO_2 and Al_2O_3 phases. Studies with different heating techniques and experimental results indicated that the microwave heating technique is promising methodology for e-waste management with respect to volume reduction and techno-economical viability. This has the potential to be scaled up after successful demonstration.

ACKNOWLEDGEMENT

Authors are grateful to Shri K. Agarwal, Director, NRG and Shri R. K. Rajawat, Associate Director, BTDG for their valuable guidance and support during the course of experimental work. Authors are also thankful to Smt. Savita Jain, Dy. Plant Supdt. (L), WMFT and Dr. Amar Kumar, Superintendent (Labs), WMFT for their valuable inputs and extending the resources for analysis of scrubbers.

REFERENCES

1. E-Waste Management: As a Challenge to Public Health in India; Monika and Jugal Kishore, Indian J Community Med. Volume 35, Number 3, pp 382–385, July 2010.
2. Ravindra Rajaraoa, Veena Sahajwallaa, Romina Cayumila, Miles Parkb, Rita Khannaa Novel Approach for Processing Hazardous Electronic Waste”, Procedia Environmental Sciences 21, pp 33–41, 2014
3. CPCB Guidelines for environmentally sound management of e-waste (as approved vide MoEF letter No. 23-23/2007-HSMD) Delhi: Ministry of Environment and Forests, Central Pollution Control Board, March 2008.
4. Jang YC, Townsend TG. Leaching of lead from computer printed wire boards and cathode ray tubes by municipal solid waste landfill leachates. Environmental Science and Technology. Volume 37, pp 4778–4, 2003.



Battery-run and Traditional Fuel Vehicle Mix: Perspectives of Road Traffic Environment and Operations

Sabyasachi Mondal¹, Pritam Saha^{*1}

Department of Civil Engineering, Indian Institute of Engineering Science and Technology, Shibpur, Howrah¹,
saha.pritam@gmail.com

ABSTRACT

Over the past few years, battery-run vehicles have become very popular in Indian transportation context. While, such vehicles are considered as environment friendly mode of transportation, they have an indirect effect on road environment and impact on operations of traffic as well. On the basis of a field study on sub-urban roads in the city of Kolkata, the paper has shown that lower speed potential of such vehicles results in frequent formation of platoons. Quite often, faster vehicles are entrapped inside those platoons and they are compelled to reduce their speed to the speed of such battery-run impeding vehicles. Eventually, lower speeds of faster vehicles increases consumption of fuel and emissions of pollutant gases. Empirical investigations on field data have shown that such emission is significantly higher on roads where battery-run vehicles are permitted compared to the ones where such modes are restricted.

KEYWORDS Road traffic, Environment, Operations, Suburban area, Battery-run vehicle

INTRODUCTION

Inadequate public transport facilities in sub-urban and rural areas have resulted in a tremendous growth of intermediate public transport (IPT). Until the last decade, three wheeled auto rickshaw was a very popular IPT in Indian transportation context. However, over the past few years, battery-run vehicles were observed to gain much attention and they have started replacing auto rickshaws. Such patronage shift is primarily due to the fact that battery-run vehicles are eco-friendly, comfortable and affordable for distance travel. Further, they provide employment opportunities for low-skilled workers; thereby, help in socio-economic development.

In view of the fact that limited natural resources of fossil fuel may lead to a global crisis of energy, battery run vehicles are considered as an alternative of traditional fuel vehicles in India since transport sector consumes about 17% of total energy [1]. Moreover, higher amount of fuel consumption increases vehicle emission and pollutes road environment. A fairly recent study reported that in metro cities every day about 3,000 MT of pollutants are produced in the form of CO₂, CO, NO_x, SO₂, unburnt HC etc. Notably, significant part of it is caused by vehicle emission; it was found to be 66% in Delhi, 52% in Mumbai and 33% in Kolkata respectively [2].

The fuel consumption and subsequent vehicle emission are, on the other hand, dependent on traffic mobility. At low speeds, usually consumption of fuel is large. Experiment shows that such consumption starts decreasing with the increase of speed. However, at excessively high speed it again increases to certain extent (**Figure 1**). There have been a number of researchers who calibrated the relationship for different vehicle types and fuels [3-5]. They suggested a speed range of 55 to 80 km/h against which fuel consumption could be optimum.

At many places particularly in sub-urban area, battery-run vehicles are found to share even more than half of the total traffic. Since speed potential of such vehicles is very low, typically about 20 km/h, they create impedance to the relatively faster vehicles [6]. As a result, faster vehicles start moving in following and platoons are formed. Length of such platoon increases with the increase of flow of traffic. Sometimes drivers of delayed vehicles take considerable risk and perform overtaking operations, thereby, affecting safety and mobility. At the same time, the petrol/ diesel-run vehicles that are entrapped inside platoons and moving at a speed of 20 km/h or lower are likely to affect the environment directly due to the low speed emissions. Accordingly, the current study indicates two major implications of such vehicles on roads: operations of traffic and road environment and perform systematic investigations aimed at understanding the extent of such impacts.

STUDY OBJECTIVES

The premise on which the current study is based considers mixed traffic composed of different vehicle types including battery-run vehicles. While, it is anticipated that the presence of such vehicles would reduce the air pollutants, their dynamics, however, indirectly increases the amount of those pollutants. It is, therefore, felt imperative to investigate the impact of battery-run and traditional fuel vehicle mix on road traffic environment and operations. Accordingly, the paper aimed at meeting the following objectives.

- Understanding the impact of battery-run and traditional fuel vehicle mix on traffic operations.



- Investigating the role of battery-run vehicles in increasing traditional fuel consumption and, thereby, affecting road environment.

METHODOLOGY

Frequency of platooning increases with proportion of slower vehicles. Operations of traffic are, thus, significantly affected when they are large in number. While, platoons are normally identified based on a headway threshold of 3 s [7], a recent study under mixed traffic has shown that under mixed traffic interaction between vehicles ceases beyond a headway threshold of 6 s [8]. Accordingly, the current study considered 6s as headway cut-off for the purpose of identifying platoons and length of which was expressed in terms of number of vehicles that are entrapped inside the platoon including the lead vehicle. Accordingly, impact of battery-run vehicles on traffic performance was studied based on two parameters; they are, traffic intensity and percent time-spent-following.

Traffic intensity (ρ) is defined as the ratio of average time spent by a vehicle next to a platoon leader while searching for an opportunity to overtake and average inter-arrival times at the back of the platoon [9, 10]. Eq. (1) demonstrates traffic intensity in terms of average numbers of headway inside platoon, Q_0 and the value should be less than 1.

$$\rho = 1 - \frac{1}{Q_0} \quad (1)$$

Percent time-spent-following (PTSF), on the other hand, is defined as the percentage of travel time that a vehicle spends in a platoon due to inability to pass [7]. The current study has used the method suggested by Polus and Cohen [9] for the purpose of determining PTSF [Eq.(2)].

$$\text{PTSF} = \frac{100Q}{Q_0 + N_0} \quad (2)$$

Where, Q = number of faster vehicles behind an impending slower vehicle; Q_0 = number of headways inside a platoon; N_0 = number of headways outside a platoon.

Following the experience that has been gathered from past research [4,5], the scheme of the current study was also to assess fuel consumption under the interference of slower vehicles to traffic in different proportions. The established emission factors were found useful in understanding the increase of pollutant gases like carbon dioxide (CO_2), carbon monoxide (CO), nitrogen oxides (NO_x) and sulfur dioxide (SO_2) at such traffic situation.

Data

Accordingly, field study was conducted on sub-urban road segments in the city of Kolkata. Two study sites (two-lane road) were selected in a way such that battery-run vehicle is permitted in one section whereas the other section does not permit such vehicles. Further, the road sections were free from the influence of intersection and curvature. Pavement condition was good and uniform throughout the study section.

Field study was conducted using video photographic survey. A trap of 10 m length was marked on the pavement and the camera was placed in a way such that it can cover the entire trap keeping some margin on its either side. Traffic data was videotaped during both peak and off peak hours on typical week days. Video files were played on a computer and vehicle type and entry-exit time were noted down.

Traffic composition was found to be quite similar at both the study sites (Figure 2); around 25% car, 20 to 30% two-wheeler, 5% bus and truck and 10% non-motorized vehicles (NMV). Three wheeler was found to share about 30% and Figure 2 indicates that introduction of battery-run vehicles has resulted a patronage shift from motorized three wheeler.

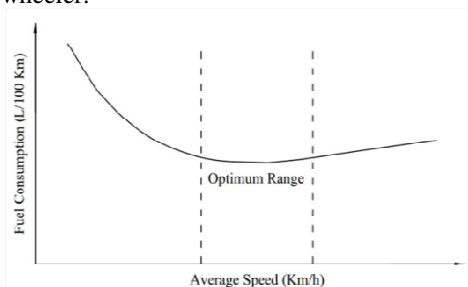


Figure 1 Rate of fuel consumption with speed variation

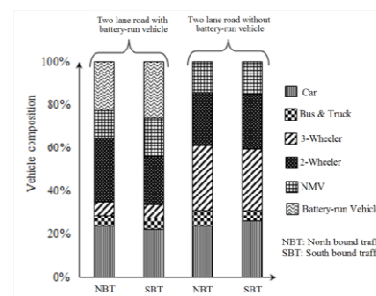


Figure 2 Traffic composition observed at study sites

RESULTS ANALYSIS

Traffic Operation

Field data were examined and travel speed, length of platoon and number of headways inside and outside platoons were accordingly measured. They were subsequently plotted against different proportion of three wheeled vehicles. Average length of platoon was found to increase with the increase of such vehicles (Fig. 3). Notably, such increment was found to be quite high in the event of battery-run vehicles. It was found that at 30 percent three wheeled vehicles, average length of platoon is about 8 in case battery-run whereas it reduces to about 3 in case of motorized ones. Further, average travel speed was observed to pass through insignificant change with the change in proportion of motorized three-wheelers in traffic which, however, is found to be significant in case of battery-run vehicles (Figure 3).

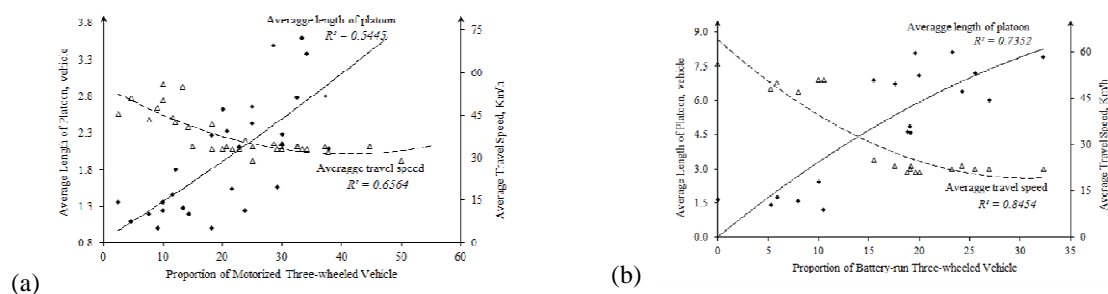


Figure 3 Variation of average platoon length and travel speed with respect to (a) motorized and (b) battery-run three-wheeled vehicles in traffic

Further attempt was made to investigate the impact of such frequent platooning on traffic performances. Two parameters, namely traffic intensity and percent time-spent-following were selected for such investigations. Traffic intensity was determined using Eq. (1) at different proportion of three wheeled vehicles. **Figure 4.a** indicates that for both the vehicle types, motorized and battery-run, traffic intensity increases initially (upto 20 percent of such vehicles) thereafter it was found to be insensitive to the presence of such vehicles. As anticipated, traffic intensity was quite high in case of battery-run vehicles.

By the same token, percent time-spent-following was determined using Eq. (2) and plotted against different proportion of three wheeled vehicles (**Figure 4.b**). It was found that the time, that a faster vehicle spends while following battery-run vehicle, is quite high compared to the situation when a motorised three wheeled vehicle is the impeding one; nearly double when they are more than 20% in traffic stream. Thus, it is evident that battery-run vehicles have significant impact on traffic operations.

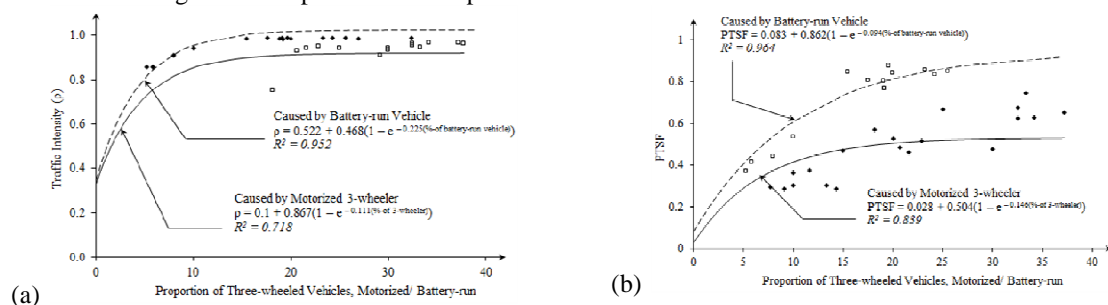


Figure 4 Comparison of traffic performance parameters: (a) traffic intensity and (b) percent time-spent-following Road Environment

While battery-run vehicles are considered as an environment friendly mode of transportation, their lower speed potential eventually reduces traffic speed to a considerable extent; the current study found about 30 percent speed reduction of motorized vehicles that are entrapped inside platoons. Since, at low speeds consumption of fuel and subsequent pollutant emission increases (**Figure 1**), battery-run vehicles start playing an important role in increasing such emission in an indirect way.

On the basis of established speed reliant fuel consumption models [4, 5], the current study estimated the fuel consumption at different proportion of three wheeled vehicles. **Figure 5** depicts the fuel consumption of a vehicle when it shares the same road space with respectively motorized and battery-run three wheeled vehicles. It



substantiates the fact that battery-run vehicles on roads results in higher amount of fuel consumption; in a way that it is around 30 percent more that that would have been caused by motorized ones.

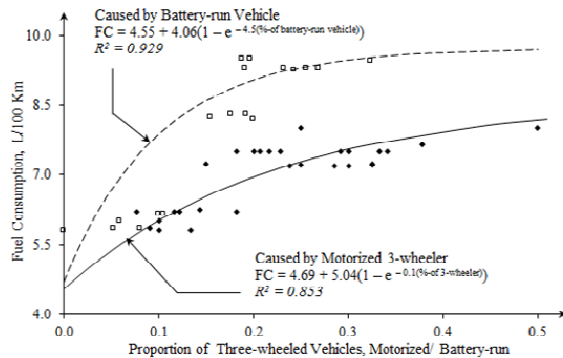


Figure 5 Consumption of traditional fuel at different proportion of slower vehicles

Further initiatives were taken to investigate the extent of pollutant gas rise, for instance: CO_2 , CO , NO_x and SO_2 with the increase of three wheeled vehicles in traffic. **Figure 6** indicates that battery-run vehicles in traffic results in higher amount (about 20%) of pollutant gases like CO_2 , CO , NO_x and SO_2 . Moreover, a battery-run vehicle consumes 10 kWh of electricity per charging and by which it can travel 150 km on average [11]. A study reported that 1.281 kg of CO_2 is emitted while producing one unit of electricity from coal thermal power stations [12]. The amount of CO_2 emission at the time of charging a battery-run vehicle was subsequently estimated to be 19.129 g/km [13].

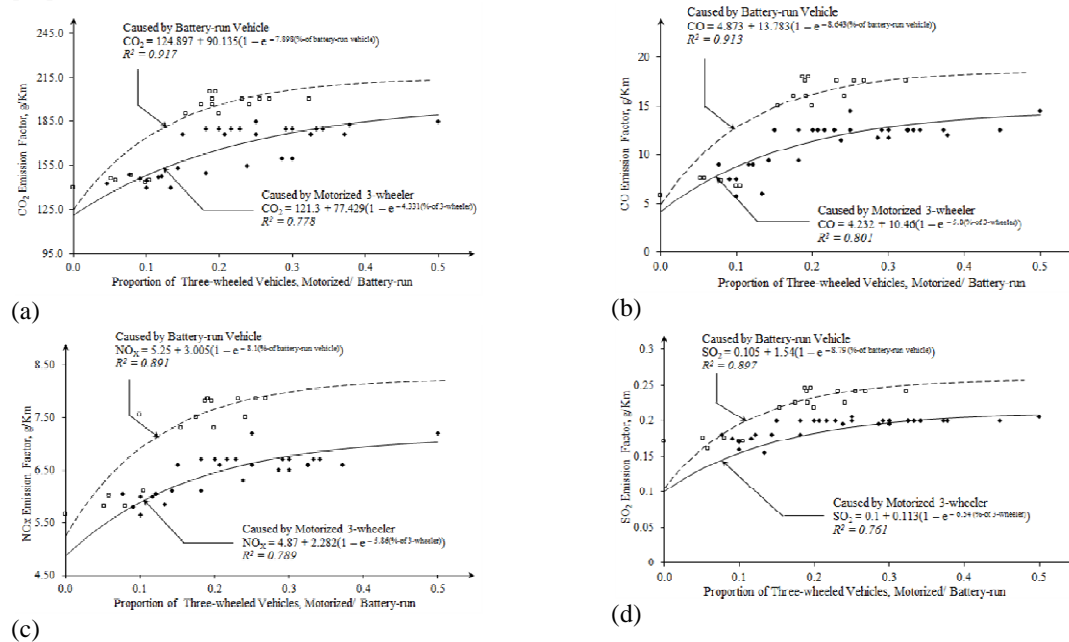


Figure 6 Emission of pollutant gases at different proportion of three wheeled traditional fuel/ battery-run vehicles: (a) CO_2 , (b) CO , (c) NO_x and (d) SO_2

CONCLUSIONS

Battery-run vehicles have become very popular in Indian transportation context especially over the past few years. However, traffic operations are observed to get affected due to low speed potential of such vehicles. Accordingly it increases congestion and subsequent delay. Moreover, such vehicles have been found to affect roads environment as well. Observations indicate that impeded faster vehicles move at very low speed and eventually they consume more fuel. Investigations indicate that amount of pollutant emissions are, therefore, considerably high on roads that permit battery-run vehicles.



REFERENCES

1. R. S. Dayal, J. Sandeep, S. Kawal, Growth of motorvehicles in India- Impact of demographic and economic development. *J. Eco. Soc. Stud.*, 1(2), 137-153 (2011).
2. R. K. Shrivastava, N. Saxena, G. Gautam, Air pollution due to road transportation in India: A review on assessment and reduction strategies. *J. Environ. Res. Develop.*, 8(1), 69-77 (2013).
3. Optimal Car Average Speed For Minimum Fuel Consumption. <https://www.myengineeringworld.net/2012/05/optimal-speed-for-minimum-fuel.html> (Accessed on 02.11.2018)
4. T. V. Mathew, Fuel Consumption and Emission Studies. Chapter 43, Transportation Systems Engineering, Chapter 43, National programme on technology enhanced learning.
5. D. C. Biggs, R. Akcelik, Models for Estimation of Car Fuel Consumption in Urban Traffic. *ITE Journal*, 56(7), 29-32 (1986).
6. S. Mondal, P. Saha, Rising Growth of E-rickshaws in Indian Traffic Context: A Challenge in Efficient Traffic Operations. In proc. 32nd Indian Engineering Congress. ISBN: 978-93-86724-29-8, 153-160 (2017).
7. Highway Capacity Manual, Transportation Research Board, 1650. 5th ed. 2010.
8. P. Saha, R. Roy, A. K. Sarkar, M. Pal, Preferred time headway of drivers on two-lane highways with heterogeneous traffic. *Transp. Lett.*, 1-8 (2017).
9. A. Polus, M. Cohen, Theoretical and empirical relationships for the quality of flow and for a new level of service on two-lane highways. *J. Transp. Eng.-ASCE*, 135(6), 380-385 (2009).
10. P. Saha, A. K. Sarkar, M. Pal, Evaluation of performance measures of two-lane highways under heterogeneous traffic. *Goal of Pertanika*, 23(2), 223-239 (2015).
11. M. A. Rahim, M. U. H. Joardder, S. M. Houque, M. M. Rahman, N. A. Sumon. Socio-economic and environmental impacts of battery driven auto rickshaw at Rajshahi city in Bangladesh. In International Conference on Mechanical, Industrial and Energy Engineering (2013).
12. T. Jash, *Renewable energy and environment. Geogr. Rev. India*, Volume 69, Number 1, 20-24 (2007).
13. D. Majumdar, T. Jash, Merits and Challenges of E-Rickshaw as An Alternative form of Public Road Transport System: A Case Study in the State of West Bengal in India. *Enrgy. Proced.*, 79, 307-314 (2015).



Exceptional Effects on Life and it's Remedies of Environmental Pollution in Earth

Samrin Sheikh^{*1}, Anil K Mathur¹

Department of Civil Engineering, Rajasthan Technical University, Kota, Rajasthan¹, samrin.sheikh1990@gmail.com*

ABSTRACT

Environmental pollution is a nuisance which is affecting each and every human being and is also adversely affects our health. This paper gives an impact of all types' environmental pollution which includes air, water, land and their associated hazards not only to living things but also to non living things, animals and plants. Accordingly, various types of bodies such as global institutions, NGO's, government have power to use advance resources to overcome environment pollution. As human being are more responsible for the contamination of environment. It varies from every age group. It is a worldwide problem which effects the human population more. The emphasis on human health in contrast with environment pollution is now a day's taken care in consideration.

KEYWORDS Environment pollution, Air pollution, Water pollution, Soil pollution, Land pollution

INTRODUCTION

The awareness of environmental factors is increasing day by day in relation with health and wellness of human population. In developed countries where urban industrial areas are located, the pollution level reaches at very serious level. In developing countries more than 80% contaminated water has been used for irrigation purpose. Industrial urban and semi urban areas are surrounded by densely populated, low income communities, they continue degrade the environment. Over the last three decades worldwide importance to the public health in relation with environmental pollution has been given. Environment pollution is caused by human activities and by naturally forces as well. The main reasons for the pollution in our environment are lack of awareness among public, natural disaster due to some selfish industries etc.

In current scenario, environmental auditing is optional in many industry sectors but due to this contamination in environment it would be mandatory. Many NGO's are involving worldwide conducting pollution control program. Environmental pollution level is increasing and it is affecting the life of human, animal plants, trees as well as forest also. There are many cities that come under the category of environmental pollution for example Indian cities are most polluted cities in world such as Mumbai, Delhi, Bangalore. They are seriously affected by pollution. These pollution level also effect soil and vegetation. Environmental pollution includes water pollution indoor and outdoor air pollution soil pollution that are subjected to health risk.

Environmental pollution involves in something unsustainable activities and that will result in sustainable health problem such as cancer, birth defects, asthma etc. There are many industries which have high level of pollution and have no environment auditing.

AIR POLLUTION

Air is important element in human's healthy life. Without air nobody can survive. Now a day's air we breathe is polluted and is common throughout the world especially in developed countries. Countries such as India, China, USA, are facing major issues related to air pollution. The term air pollution is basically an air that contains hazardous substances, pollutant, harmful gases that causes negative effects to the health. The major pollutants that exist in the air are lead, particulate matter, heavy metals, sulphur dioxide, nitrogen dioxide, carbon monoxide etc. Air pollutants at high level shorter the life of human being.

Accordingly, the major factors of air pollution are raising demands of motor vehicles, urban population, living standards of people, increasing industrialization, poor environmental rules, using old vehicles. Man made sources include cooking, heating, home cleaning agent, automobiles, tobacco smoke, insecticides, automobiles, congested roads, and age and poor maintenance of vehicles. The sources that are natural include incinerators and waste disposals, forest and agricultural fires.

WATER POLLUTION

Water that we drink is very essential for healthy life. The WHO states that one sixth of the world's population: approximately 1.1 billion people don't have access to safe water and 2.4 billion people lack basic sanitation. Water



that consists of sewage water, industrial discharge and household water discharge is termed as polluted water. Water pollution affects vegetation, quality of soil and also the health of human being. The consequence of water pollution are identify instantly or don't display up for months or year. Research shows that more than 50 countries of the world with an area of twenty million hectares area are treated with polluted or partially treated polluted water including parts of all continents and this poor quality water causes health hazards and death of human being, aquatic life and also disturbs the production of different crops. Water pollution results are put on to be the main source of death for humans.

It is the global concern that water pollution affects lakes, drinking water, rivers and oceans. As per the WHO's standard fluoride content of drinking water is from 0.6 to 1.7 mg/l but due to water pollution it ranges from 5.26 to 26.32 mg/l. In current situation due to industrialization and population increase, the effluents from the industries are carried out by drains and these drains discharge that polluted water into the canals and rivers. This type of untreated water cause many environmental hazards for aquatic life, drinking water, irrigation and human being. Polluted water when used for irrigation purpose, it will contaminate ground water and also food. Water pollution, air pollution, solid waste management all these environmental pollutions are facing by the urban areas of Indian cities while rural one are facing rapid deforestation, land degradation, crop failure.

LAND/SOLID WASTE POLLUTION

One of the principal sources of environmental pollution is inappropriate management of solid waste. Today one of the major problems that world is facing land pollution. Wastes produces by many heavy metals industries such as coal, uranium mines have not been taken special treatment before they are deposited into landfills. They generate serious pollution problem to the environment. They are disposed of into the open dumps without pretreatment. The main sources of solid wastes are chemical factories, open cast mines and aluminum industries.

Effects of Dying Environment on Human, Animals and Plants

The impact on Environment is harmful for all the living species on the planet. From time to time serious health issues have been identified among human and animals as well due to air, water pollution. Most of these disease are not curable such as cancer, asthma and premature deaths is also been increasing in recent surveys of environmental pollution. Another issue of air pollution is Acid rain which can directly affect humans and animals by polluting drinking water and it interferes the phenomena of aquatic life which kills sea creatures and flora and fauna which in results issues regarding vegetation, Typhoid in humans and other hormonal problem as well as kidney failures are major water born diseases that directly impacts humans. In recent years several studies have been conducted on environmental pollution and it has been found that the depletion of ozone layer , rise in sea level, climate change such as global warming are the major key factors that are responsible for affecting climate . Forests are kept on affecting due to these mentioned catastrophes which directly penetrates wild life in every similar way as for humans. If forests are affected in any manner our ecological balance has huge chances to be compromised.

The level of harmful chemicals is keep on increasing due to acid rain such as NaCl that is not good for animal consumption and it not only disturbs trees but also aquatic plants which are sunk beneath surface. Wastes from construction sites such as bits of wood, clay can affect plants and animals easily. The end results of all this impacts on plants disrupt photosynthesis hence resulting failure of ecosystem.

Another major problem is Soil pollution which affects children and diseases relate to it are cancer such as Leukemia and can cause development damage of brain and mercury in soil causes neuromuscular blockage that causes headaches, nervous system and skin rash. Soil pollution can alter mechanism of plants resulting less crop yields, killing essential micro organisms that are important during process of cultivation.

CONCLUSION

It is concluded that contaminated environment is a worldwide topic for concern. Now itself we have started facing worst results of polluted environment and it's just a start if necessary action will not be taken by now future generation will bear much more worst and divested impacts of polluted environment. Controlling pollution requires mass involvement of every individual not just the responsible organizations. A lack of research is still there in regions such as Asia. System has to make appropriate policies, make awareness program among people and set some standards of every country to minimize the impact of Environmental pollution which will give healthy life which in result are the main resource of successful business of any country.



REFERENCES

1. M. A. Ashraf, M. J. Maah, I. Yusoff, and K. Mehmood. Effects of Pollutant Water Irrigation on Environment and Health of People in Jamber, District Kasur, India International Journal Of Basic& Applied Sciences, Volume 10, Number 3, pp. 37-57, 2010.
2. O. Avdeev, and P. Korchagin, Organization and Implementation of Contaminated Waste Neutralization in the Ukraine National Report, Central. European Journal of Public Health, Volume 2 (suppl), pp. 51-52, 1994.
3. M. F. Blaxill. What's Going on? The Question of Time Trends in Autism. Public Health Reports. Volume 119, Number 6, pp. 536-551, 2004.
4. M. Brauer, G. Hoek, H. A. Smith, J. C. de jongste, J. Gerritsen, and D. S. Postma, Air Pollution and Development of Asthma, Allergy and Infection in a Birth Cohort, European Society For Clinical Respiratory Physiology, Volume 29, Number 5, pp. 879-888, 2007.
5. F.W. Carter, Pollution Problem in Post-War Czechoslovakia, Transactions of the Institute of British Geographers, Volume 10, Number 1, pp. 17-4, 1985.
6. T. M. Crips, E. D. Clegg, R. I. Cooper, W. P. Wood, D. G. Anderson, K. P. Baetcke, J. L. Hoffmann, M.S. Morrow, D. J. Rodier, J. E. Schaeffer, M. G. Zeeman, and Y. M. Patel, Environmental Endocrine Disruption: An Effects Assessment and Analysis, Environmental Health Perspectives, Volume 106, Number 1, pp. 11-56, 1998.
7. M. Cucu, M. I. Lupeanu, M. Nicorici, L. Lonescu, and S. Sandu, The Dangerous Wastes and Health Risks in Romania: National Report Central European Journal of Public Health, Volume 2(suppl), pp. 41-43, 1994.
8. G. D'Amato, G. Liccardi, M. D'Amato, and S. Holgate. Environmental Risk Factors and Allergic Bronchial Asthma, Clinical & Experimental Allergy, Volume 35, Number 9, pp. 1113-1124, 2005.
9. European Public Health Alliance. Air, Water Pollution and Health Effects. Retrieved From <http://www.epha.org/r/54>, 2009.
10. H. Fereidoun, M. S. Nourddin, N. A. Rreza, A. Mohsen, R. Ahmad, and H. Pouria. The Effect of Long-Term Exposure Particulate Pollution on the Lung Function of Teheranian and Zanjanian Students, India Journal Of Physiology, Volume 3, Number 2, pp. 1-5, 2007.
11. E. F. Fitzgerald, L. M. Schell, E. G. Marshall , D.O. Carpenter, W. A. Suk and J. E. Zejda, Environmental Pollution and Child Health in Central and Eastern Europe, Environmental Health Perspectives, Volume 106, Number 6, pp. 307-311, 1998.
12. Forestry Nepal (n.d) Pollution Effects on Plants and Trees, retrieved from <http://www.forestrynepal.org/notes/silviculture/locality-factors/16>
13. L. Gardiner. Air pollution Affects Plants, Animals, and Environmental. Windows to the Universe, 2006.
14. A. Gautam, M. Mahajan, and S. Garg. Impact of Air pollution On Human Health In Dehradun City, Retrieved, 2009



Network Biology Approach to Identify Key Components Triggered during Exposure to Fluoride for Therapeutics in Human

Shubham Pant¹, Rajesh Kumar Pathak¹, Mamta Baunthiyal^{*1}

Department of Biotechnology, Govind Ballabh Pant Institute of Engineering and Technology, Ghurdauri, Pauri (Garhwal), Uttarakhand¹, mamtabaunthiyal@yahoo.co.in*

ABSTRACT

Fluoride is one of the major environmental contaminant that is proved to have deleterious effects on humans. Its exposure forms various disorders in our body characterised by Dental fluorosis, Skeleton fluorosis, Stomach toxicity, Nephrotoxicity etc. Advances in genomics have generated a huge amount of data about fluoride-human interaction at molecular level. Therefore, there is a need of systems biology for integration of these data to identify hubs, that is, key gene(s)/protein(s) involved in disease progression after exposure to fluoride, which can be used as drug target for discovery of potent molecule(s). In the present computational study, 243 genes triggered during exposure of fluoride were retrieved from Expression 2 kinase (X2K) database and network was constructed to investigate the key transcription factor (TF), interacting proteins and kinases based on combined score obtained during analysis. Besides, the network was further imported to Cytoscape for topological analysis to identify putative molecular drug targets. Based on network analysis, five important nodes have been detected. Out of the five hubs, ESR1 (Estrogen Receptor Alpha) is the most significant one and therefore, can be consider for downstream validation. To the best of our knowledge, we are first to provide a network of fluoride associated genes and its components affecting its regulation. The obtained results from present study could help in future experimental studies for validation of these hubs in drug targeting against fluoride.

KEYWORDS Fluoride, Computational and system biology, Fluorosis, Expression 2 kinase, Cytoscape, ESR1.

INTRODUCTION

Humans are affected by several chemicals from their immediate environment. That exert either toxic or beneficial effects. Fluoride with the chemical formula (F^-) is an inorganic, monoatomic anionic form of fluorine (F) atom member of halogen family. Fluoride ions are generally found throughout the earth's crust. Fluoride is the simplest anion and the salts and minerals of it are important (Aigueperse, et al, 2005). Some examples of fluoride compounds are aluminium fluoride, sodium fluoride, calcium fluoride (fluorite) (Peckham, et al, 2014). Fluorosilicic acid (SiF_6^{2-}) and sodium fluorosilicate ($Na_2[SiF_6]$) are common compounds of fluoride used in water fluoridation (Chuah, et al, 2016).

The adequate intake of fluoride for men is 4.0 mg/day and 0.7 to 3.0 mg/day for adults and children as per the criteria of The U.S. Institute of Medicine (Whyte et al., 2005). To understand the toxicity of any chemical we have to understand pathway from which chemical is absorbed, used and released through our body. The low concentration of fluoride is used for making beneficial medicine to treat skin diseases (Flucytosine, an antifungal) and also in cancer treatment (Fluorouracil, an antimetabolite); trace amount of fluoride is added to toothpastes and drinking water for prevention of tooth decay (Griffin et al., 2007; Iheozor-Ejiofor et al., 2013; Fewell et al., 2006). But high level of exposure may harm our body and cause diseases like skeletal fluorosis, dental fluorosis, nephrotoxicity, stomach toxicity and cell apoptosis. Some studies also show the reproductive effect in human including lowering the fertility and testis and sperm damage is the result of higher exposure of fluoride (Sprando et al., 1997). Therefore, there is an urgent need of systems biology approach i.e. integrative and predictive for integration of genomic data available in public domain with respect to fluoride-human interaction for prediction of probable molecular drug target.

MATERIAL AND METHODS

243 genes of Human that were triggered via exposure to fluoride were retrieved from comparative toxic genomics database (CTD) (<http://ctdbase.org/>). Comparative toxic genomics database (CTD) contains data for study of environmental substances exposure and their effect upon humans. There are several data relationships available such as chemical-protein, chemical-gene interactions, disease-chemical and gene-disease relationships. The data is sorted by choosing name of organism. i.e. *Homo sapiens* (TAXON: 9606) and chemical i.e. fluoride in our study, (Devis et al., 2016). The YED graph editor tool is used to generate network. It forms a network of these three components with different colours which help in clear visualization of the network <http://www.yworks.com/yed>.



Further the analysis was performed by X2K. The top 10 TF, protein kinases and interacting protein were sorted based on combined score and p-value (Chaudhary et al., 2017). The generated network was further visualized by Cytoscape 3.6.1 (Shannon et al., 2001). Each protein of provided network is visualized as a hub, the interacting nodes are defined as edges. The degree shows the interaction of edges with any node. High degree nodes are considered as important hubs, which possess a key biological functions.

RESULTS AND DISCUSSION

Identification of Transcription Factors (TFs)

First step of present study was TFs enrichment analysis. Sets of differentially expressed genes were fed into transcription inference module of X2K software. ChEA database computes enrichment by comparing input list of genes and data stored in database using either the Fisher's exact test or combined score. There were STAT4, CLOCK, ESR1, EGR1, HNF4A, GFI1B, GATA2, GATA2, STAT3, TRP63, and TAL1 TFs. The related information regarding these TFs is described in **Table 1**.

Table 1 Top identified TFs triggered during exposure of fluoride

Transcription factor	Description	Localization in body/cell organelles
Signal transducer and activator of transcription 4 (STAT4)	Essential for development of TH1 cells from <u>CD4+ T cells</u> and <u>IFN-γ</u> production of response to <u>IL-12</u> .	<u>Myeloid cells</u> , <u>Thymus</u> and <u>Testis</u> .
Circadian locomotor output cycles kaput (CLOCK)	Helps in timing mechanism of the circadian clock	Cytoplasm, Nucleus
Estrogen receptor alpha (ESR1)	Performs physiological development and function of many organ system which includes the reproductive <u>system</u> , <u>central nervous system</u> , <u>skeletal</u> , and <u>cardiovascular systems</u> .	Reproductive organs and <u>Adipose Tissue</u> .
Early growth response protein 1 (EGR1)	It is known as tumour suppressor gene, it also regulates the expression of <u>VAMP2</u> which is a protein important for <u>synaptic exocytosis</u> process.	Brain, Neural Organelles
Hepatocyte nuclear factor 4 alpha (HNF4A)	Regulates the expression of many hepatic genes, role in development of body organ such as <u>liver</u> , <u>kidney</u> , and <u>intestines</u> , required for the <u>PXR</u> and <u>CAR</u> -mediated activation of <u>CYP3A4</u> .	Binds to DNA and high Cytoplasmic reliability
Growth factor independent 1B transcriptional repressor (GFI1B)	It encodes a zinc finger which contains transcriptional regulator which is primarily expressed in hematopoietic lineage cells.	Expression in Bone Marrow and Testis. It has high Periplasmic and extracellular reliability.
GATA binding protein 2 (GATA2)	Protein coded by this gene plays a wide role in functioning transcription of genes that are involved in endocrine cell lineages development and proliferation.	Appendix, Bone Marrow, Gall Bladder, Endometrium, Placenta, Prostate, Ovary, Skin, testis, urinary bladder, small Intestine, Salivary Gland and high Periplasmic reliability
Signal transducer and activator of transcription 3 (STAT3)	It plays a wide role in cellular processes comprises <u>cell growth</u> and <u>cell apoptosis</u> .	It has high cytoplasmic followed by nuclear reliability
Transformation-related protein 63 (TRP63)	It is involved skin development function and in adult stems cell regulation.	Head and Neck Squamous cell carcinomas, Prostate Gland and high Periplasmic and Cytoplasmic reliability
(T-cell acute lymphocytic leukemia protein 1) TAL1	It is an essential TF in normal and malignant hematopoiesis. It is required for selectivity of the blood program during its development process,	It has high Periplasmic and Cytoplasmic reliability



Identification of Interacting Protein Connecting TFs

The X2K have different 18 databases or datasets for Protein-Protein Interactions that interacts with TFs. These TFs was fed into the hub network module & X2K identified protein complexes further connected to the TF.

Identification of Protein Kinases

After identification of TFs centered complexes upstream of DEGs modules, using the G2N module of X2K, a sub network of the proteins was built to connect TFs. The network were utilized as an input list of proteins for Kinase Enrichment Analysis (KEA) module of X2K software (Lachmann et al.,2009). The related information regarding these Kinases is described in **Table 2**.

Table 2 Top identified protein Kinases triggered during exposure of fluoride

Kinases	Description	Sub cellular localization
<u>Mitogen-Activated Protein Kinase</u> (MAPK) 1	These are involved in functions like regulation of <u>meiosis</u> , <u>mitosis</u> , and <u>post mitotic</u> functions in human cells. Many different stimuli, which includes <u>growth factors</u> , <u>cytokines</u> , <u>virus</u> infection for G protein-coupled receptors, also activates the ERK pathway.	It has high Cytoplasmic reliability followed by Nuclear and Peroxisomal.
<u>Mitogen-Activated Protein Kinase</u> (MAPK) 3	It acts as a signalling cascade that regulates for different cellular processes which are <u>differentiation</u> , progression of cell cycle and <u>proliferation</u> , response to different extracellular signals.	It has high nuclear and Cytoplasmic reliability.
RAC-Alpha Serine/Threonine-Protein Kinase (ATK1)	These are activated by platelet derived growth factor it is catalytically inactive for serum-starved primary and immortalized <u>fibroblasts</u>	It has high Cytoplasmic reliability followed by Nuclear and ER.
Glycogen Synthase Kinase 3 Beta (GSK3B)	Involved in energy metabolism, neural cells development. Studies showed that it might be a therapeutic target for ischemic stroke.	It has high Nuclear and Mitochondrial reliability.
Conserved Helix Loop Helix Ubiquitous Kinase(CHUK)	It plays a major role for regulation of the <u>NF-κB</u> transcription factor, that functions independently for the NF- κ B pathway to regulate <u>epidermal differentiation</u> .	It has high Nuclear and Cytoplasmic reliability.
Casein Kinase II Subunit Alpha (CSNK2A1)	This <u>kinase</u> is exists in tetramer form and composed of α , α -prime, and two β subunits. α subunits contain the catalytic activity while the β subunits undergo <u>auto phosphorylation</u> .	It has high Cytoplasmic reliability followed by Nuclear and Mitochondrial.
Mitogen-Activated Protein Kinase 14(MAPK14)	Act as an point of various biochemical signals to integrate them, involve in cellular <u>differentiation</u> , <u>transcription</u> regulation, <u>proliferation</u> , and <u>development</u> .	It has high Cytoplasmic reliability
Cell Division Protein Kinase 4 (CDK 4)	Important for G1 phase cell cycle progression.	It has high Cytoplasmic reliability
Abelson Murine Leukemia Viral Oncogene Homolog 1 (ABL1)	This kinase encodes cytoplasmic and Nuclear protein <u>tyrosine kinase</u> that involve process of cell <u>division</u> , cell <u>adhesion</u> .	It has high Cytoplasmic, extracellular, Periplasmic reliability
Protein Kinase C Delta type (PRKCD)	The family members of PRKCD also serve as major receptors for esters like phorbol which is a class of <u>tumour</u> promoters, these are involved in <u>B cell</u> signalling and also regulates cell <u>growth</u> , cell <u>apoptosis</u> , and cell <u>differentiation</u> of a variety of cell types.	It has high Cytoplasmic reliability

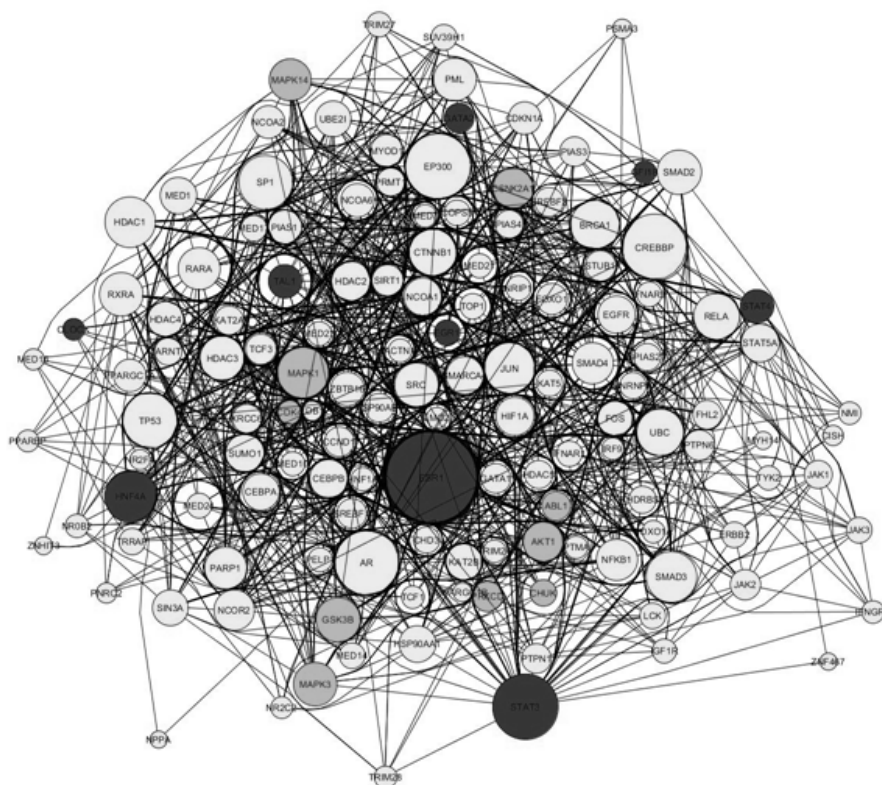


Figure 1 Network constructed through X2K showing TF, Kinases and associated protein triggered during exposure to fluoride

Prediction of Hubs involved in the Regulation of DEGs

The obtained network was analysed and visualized by cytoscape on the basis of topological parameter such as node number, edges, connected components, diameter of network, radius, betweenness, degree distribution shortest path length, etc. to map the node size and betweenness as the node colour in the parameter setting of the Network Analyzer (**Table 3**). The nodes ESR1, AR, EP300, TP53, CREBBP and CTNNB1 are found as hub nodes. After visualization of network in cytoscape the degree of main five hubs ESR1, AR, EP300, TP53, CREBBP, CTNNB1 were identified out of which ESR1 holds a maximum degree among all. Our study shows that ESR1 could be a hub that can be targeted for drug to prevent disease caused by fluoride exposure. ESR1 is ligand-activated TFs. It stands for Estrogen receptor alpha, which is activated by sex hormone Estrogen. The role of ESR1 is described earlier in (**Table 1**) since it plays a significant role in development and function of variety of human body organ system (Bondesson, et al, 2015) so it could be used to target many diseases related to fluoride exposure. Present study suggests that this component should be used as a drug target for future study. It will help to find the essential drug molecule by in silico studies such as molecular docking etc. followed by validation of cell line and clinical trials.

Table 3 Values of topological parameters

Node	137	CPL	1.935
Edge	1461	ND	3
CC	2	MENP	0
ANN	21.328	IN	1
SP	18360	NR	2

[CC, connected component; ANN, average number of neighbors; SP, shortest path; CPL, characteristic path length; ND, network diameter; MENP, multi-edge node pair; IN, isolated node; NR, network radius]

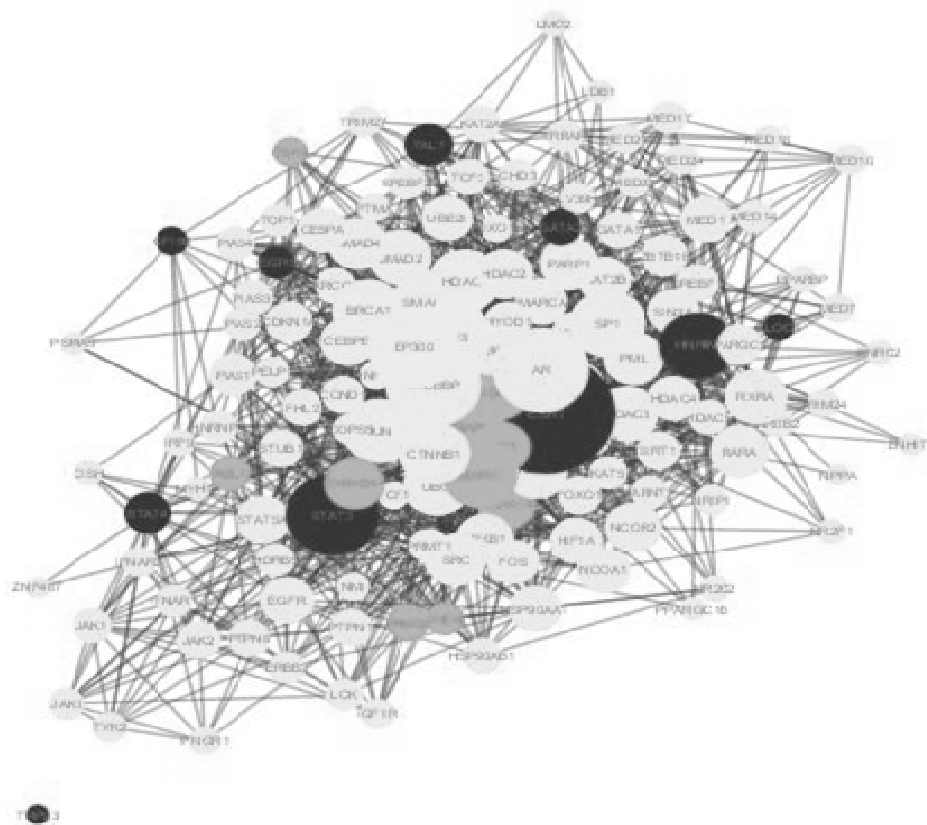


Figure 2 Representing of node in constructed network: visualization of whole network to map hub nodes.

CONCLUSION

Total 243 genes responsible for fluoride exposure were sorted according to gene having different family. A network was constructed using different protein for interaction. This study can help to target the cellular system toward a desired component by transcription factors, kinase using system biology approach. Our study suggested the interconnection of these components by forming a network using system biology approach. This shows the effect of fluoride exposure on function related to estrogen receptors. These disrupted functions can be up regulated by targeted a drug through estrogen receptor which will also effect proposed interconnected nodes. The application of X2K and cytoscape visualization presents an advancement study toward our ultimate goal of understanding mammalian cell signalling networks effected hubs from a global perspective at a molecular level of resolution.

REFERENCES

- J. Aigueperse, P. Mollard, D. Devilliers, M. Chemla, R. Faron, R. Romano, and J. P. Cuet. Fluorine compounds, inorganic. Ullmann's encyclopedia of industrial chemistry, 2005.
- M. Baitaluk. System biology of gene regulation. In Biomedical Informatics. Humana Press, Totowa, NJ, pp. 55-87, 2009.
- M. Bondesson, R. Hao, C. Y. Lin, C. Williams, and J. Å. Gustafsson. Estrogen receptor signaling during vertebrate development. Biochimica et Biophysica Acta (BBA)-Gene Regulatory Mechanisms, Volume 1849, Number 2, pp 142-151, 2015.
- J. K. Chaudhari, B. P. Sahariah, J. K. Choubey, et al. Netw Model Anal Health Inform Bioinforma, Volume 6, Number 7. <https://doi.org/10.1007/s13721-017-0148-7>, 2017
- C. J. Chuah, H. R. Lye, A. D. Ziegler, S. H. Wood, C. Kongpun, and S. Rajchagool. Fluoride: A naturally-occurring health hazard in drinking-water resources of Northern Thailand. Science of the Total Environment, Volume 545, pp 266-279, 2016.
- E. Y. Chen, H. Xu, S. Gordonov, M. P. Lim, M. H. Perkins, and A. Ma'ayan. Expression2Kinases: mRNA profiling linked to multiple upstream regulatory layers. Bioinformatics, Volume 28, Number 1, pp 105-111, 2011.
- A. P. Davis, C. J. Grondin, R. J. Johnson, D. Sciaky, B. L. King, R. McMorran, and C. J. Mattingly. The comparative toxicogenomics database: update 2017. Nucleic acids research, Volume 45(D1), D972-D978, 2016.



- F. Diella, S. Cameron, C. Gemünd, R. Linding, A. Via, B. Kuster, and T. J. Gibson. Phospho. ELM: a database of experimentally verified phosphorylation sites in eukaryotic proteins. *BMC bioinformatics*, Volume 5, Number 1, pp 79, 2004.
- J. K. Fawell. Fluoride in drinking-water. World Health Organization, 2006.
- S. O. Griffin, E. Regnier, P. M. Griffin, and V. Huntley. Effectiveness of fluoride in preventing caries in adults. *Journal of dental research*, Volume 86, Number 5, pp 410-415, 2007.
- P. V. Hornbeck, I. Chabra, J. M. Kornhauser, E. Skrzypek, and B. Zhang. PhosphoSite: A bioinformatics resource dedicated to physiological protein phosphorylation. *Proteomics*, Volume 4, Number 6, pp 1551-1561, 2004.
- D. W. Huang, B. T. Sherman, and R. A. Lempicki. Systematic and integrative analysis of large gene lists using DAVID bioinformatics resources. *Nature protocols*, Volume 4, Number 1, pp 44, 2008.
- Z. Iheozor-Ejiofor, L. A. O'Malley, A. M. Glenny, R. Macey, R. Alam, P. Tugwell, and H. V. Worthington. Water fluoridation for the prevention of dental caries. *Cochrane Database of Systematic Reviews*, Volume 12, 2013.
- M. Kanehisa, S. Goto, M. Furumichi, M. Tanabe, and M. Hirakawa. KEGG for representation and analysis of molecular networks involving diseases and drugs. *Nucleic acids research*, Volume 38 (suppl_1), pp D355-D360, 2009.
- T. S. Keshava Prasad, R. Goel, K. Kandasamy, S. Keerthikumar, S. Kumar, S. Mathivanan, and L. Balakrishnan. Human protein reference database—2009 update. *Nucleic acids research*, Volume 37 (suppl_1), pp D767-D772, 2008.
- A. Lachmann, and A. Ma'ayan. KEA: kinase enrichment analysis. *Bioinformatics*, Volume 25, Number 5, pp 684-686, 2009.
- R. Linding, L. J. Jensen, A. Pasculescu, M. Olhovsky, K. Colwill, P. Bork and T. Pawson. NetworKIN: a resource for exploring cellular phosphorylation networks. *Nucleic acids research*, Volume 36 (suppl_1), pp D695-D699, 2007.
- V. Matys, O. V. Kel-Margoulis, E. Fricke, I. Liebich, S. Land, A. Barre-Dirrie, and N. Voss. TRANSFAC® and its module TRANSCompel®: transcriptional gene regulation in eukaryotes. *Nucleic acids research*, Volume 34 (suppl_1), pp D108-D110, 2006.
- S. Peckham, and N. Awofeso. Water fluoridation: a critical review of the physiological effects of ingested fluoride as a public health intervention. *The Scientific World Journal*, 2014.
- Agency for Toxic Substances and Disease Registry (ATSDR) (2001). [Toxicological profile for Fluorides, Hydrogen Fluoride, and Fluorine](#). Atlanta, GA: U.S. Department of Health and Human Services, Public Health Service, 2014.
- E. Portales-Casamar, S. Thongjuea, A. T. Kwon, D. Arenillas, X. Zhao, E. Valen, and A. Sandelin. JASPAR 2010: the greatly expanded open-access database of transcription factor binding profiles. *Nucleic acids research*, Volume 38 (suppl_1), pp D105-D110, 2009.
- Z. Wang, M. Gerstein, and M. Snyder. RNA-Seq: a revolutionary tool for transcriptomics. *Nature reviews genetics*, Volume 10, Number 1, pp 57, 2009.
- P. Shannon, A. Markiel, O. Ozier, N. S. Baliga, J. T. Wang, D. Ramage, and T. Ideker. Cytoscape: a software environment for integrated models of biomolecular interaction networks. *Genome Research*, Volume 13, Number 11, pp 2498-2504, 2003.
- R. L. Sprando, T. F. X. Collins, T. N. Black, J. Rorie, M. J. Ames, and M. O'donnell. Testing the potential of sodium fluoride to affect spermatogenesis in the rat. *Food and Chemical Toxicology*, Volume 35, 9, pp 881-890, 1997.
- M. P. Whyte, K. Essmyer, F. H. Gannon, and W. R. Reinus. Skeletal fluorosis and instant tea. *The American journal of medicine*, Volume 118, Number 1, 78-82, 2005.
- C. S. Yu, Y. C. Chen, C. H. Lu, and J. K. Hwang. Prediction of protein subcellular localization. *Proteins: Structure, Function, and Bioinformatics*, Volume 64, Number 3, pp 643-651, 2006.



Feed-Forward Artificial Neural Network for Air Quality Index Prediction in Kota City

Shikha Saxena^{*1}, Anil K Mathur¹, A K Dwivedi¹

Department of Civil Engineering, Rajasthan Technical University, Kota¹, johrisaxena@gmail.com*

ABSTRACT

Air pollution problems in urban environment are a global problem over several decades. Since 1975, systematic monitoring of primary air pollutant was attempted. Many cities already crossed the tolerance limit of human exposure of individual pollutants. The major sources of such urban pollution are due to automobile exhaust and anthropogenic activities. Thus there is need for pollution alarming measures not only for local environmental protection but also for regulation of greenhouse gas emission. In This paper artificial neural network (ANN) is used to predict the air quality index (AQI) in one of the air quality monitoring stations of Kota city in Rajasthan state of India. Two years database (2012-2014) of criteria pollutants are used for this purpose and neural network model was constructed for prediction of air quality index. Concentrations of criteria pollutants, Respirable particulate matter (PM₁₀), Nitrogen dioxide (NO₂) and Sulfur-dioxide(SO₂) taken as predictor variables which are supposed to be the most significant parameters to predict Air quality index (AQI). The results proved that neural network can be applied successfully as tool used for making decisions in case of alarming situations and problem solving for better atmospheric management.

KEYWORDS Air Quality Index (AQI), Artificial Neural Network (ANN),

INTRODUCTION

Air pollution becomes a worldwide issue of concern throughout the world. The peaks of pollutants concentrations due to vehicular exhaust and industrial exhaust are the widespread outbreak for urban area. [1]. The adverse effects are clearly visible on human health, cultural heritage, monuments, vegetation etc. Ground level-ozone (O₃), carbon monoxide (CO), nitrogen dioxide (NO₂), Sulphur dioxide (SO₂), and particulate matter under 10 microns (PM₁₀) were used as API calculation. The prominent value out of the individual sub-index was taken as the API value [2,3]. The API values are used to make people aware of the real time conditions and act accordingly [4].

Some presumptive status of air quality needs to acquire for planning of controlling strategies. For health concerns, artificial neural network (ANN) had been used for prediction purposes, especially on air quality [5,6]. The performance of ANN can be evaluated on the basis of performance indices [7-11]. Also the credibility of its performance is better than other models [12]. ANN has capability to understand non linear patterns among variables which cannot be easily recognized by simple mathematical formulae [13]. The ANN performed well with new datasets after pattern recognition [14-16].

STUDY AREA

Kota city is well-known as education hub with over 16 lakhs habitants. It is situated on the bank of Chambal River in the southern part of Rajasthan. It is the third largest city after Jaipur and Jodhpur. The area of city is 527 sq.km and the cartographic coordinates are 25.18°N 75.83°E. It has semi arid climate with high temperature throughout the year. Maximum temperature reaches up to 48°C, which subsides in monsoon season. The average rainfall in Kota is 660.6 mm. Majority of region is rural in character. Kota is one of the three most polluted city as reported in Times of India. Here population is growing day by day due to coaching centers. It also comes under non attainment cities in terms of PM₁₀ as report published by RPCB 2012. The city situation is at the verge of explosion. This becomes the reason of closure of some of the industrial units in Kota. As Supreme Court and the Rajasthan Pollution Control Board (RPCB) claims that air quality level have been falling due to those anthropogenic activities. Industrial air pollution is prevalent in Kota due to coal/gas-based thermal power plants, calcium carbide (and) nitrogenous fertilizer (units), steam generating boilers, and cement factories Fast growth in vehicles resulting increase in pollutants levels the dynamics of RSPM (PM₁₀), SO₂ and NO₂ taken into account to study air quality levels.

MATERIALS AND METHODS

Air Quality Index

Air quality index is used to show the real time status of ambient air quality. The numerical value is calculated on the basis of various sub indices. Maximum Index value associated with prominent air pollutant is taken as air quality index of that region. It is then further divided into six categories which entitled as Good, Satisfactory,



Moderately polluted, Poor, Very Poor, and Severe depends on their impact on health. These are also termed as health breakpoints. Sub-indices are calculated for eight pollutants, that is, PM₁₀, PM_{2.5}, NO₂, SO₂, CO, O₃, NH₃, and Pb. **Table 1** depicts the breakpoints for the eight pollutants.

Artificial Neural Network

Artificial Neural Network (ANN) is a network of neurons which has the resemblance with the human brain neurological system [17]. It could process the information that had been fed into it and could generalize it for future predictions [18].

Feed-forward Artificial neural network is used for prediction purpose and to identify most significant parameters affecting API values. [19]

The structure of ANN model comprises of input layer, hidden layer and output layer [20]. Selection of significant inputs is done according to the nature of the problem and its influence over the predicting parameters. The numbers of hidden neurons are chosen on the basis of various error indices during analysis [21]. In this analysis 306 data sets were used. To develop ANN model, further datasets were divided into three sets, 70% data are used for training purpose, 15% for testing and remaining 15% as validation set. [22].

The network structure for the feed-forward ANN model was presented in **Figure 1**.

RESULTS AND DISCUSSION

Artificial neural network is widely used for prediction purpose according to literature survey. In this paper feed forward neural network employed to predict air quality index which is the indicator of quality of air.

Figures 2 and 3 show the performance plot during training state and regression plots during training state of feed-forward ANN models for forecasting API. Initially 70% (214) of the total samples used for training and 15% (46) of total samples for testing and 15% (46) for validation were kept aside. The values of R for training, testing and validation are 0.998, 0.999 and 0.999 respectively. Performance indices MSE (Mean square error), SAE (Sum absolute error), SSE (Sum square error) got in this analysis are $2.126291256151836e^{+04}$, $3.712387374757202e^{+04}$, $6.506451243824616e^{+06}$, respectively.

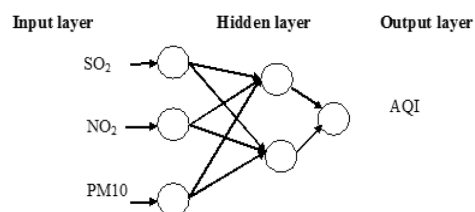


Figure 1 Feed-forward ANN model network

structure

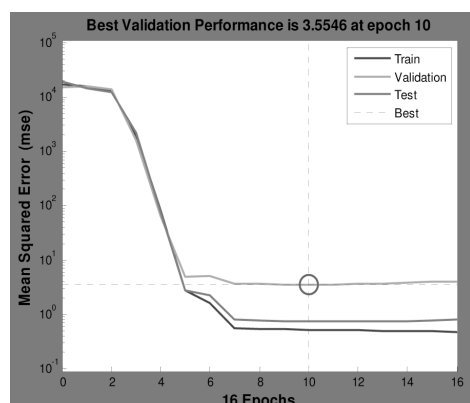


Figure 2 Performance plot during training state

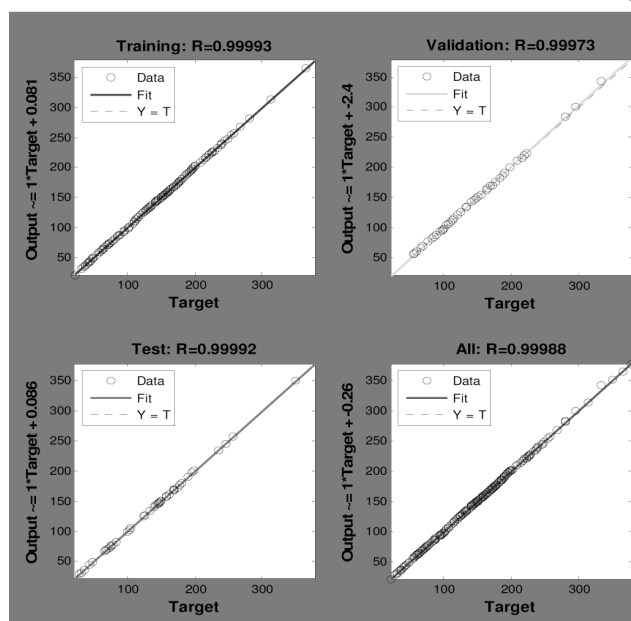


Figure 3 Regression plots during training state

Table 1 Characteristics of air quality index and respective concentration range of various pollutants

AQI Category	AQI	Concentration range*							
		PM10	PM2.5	NO ₂	O ₃	CO	SO ₂	NH ₃	Pb
Good	0- 50	0 - 50	0 - 30	0- 40	0 - 50	0 - 1.0	0 - 40	0 - 200	0 - 0.5
Satisfactory	51-100	51 - 100	31- 60	41 - 80	51 - 100	1.1 - 2.0	41 - 80	201-400	0.5 - 1.0
Moderately polluted	101- 200	101 -250	61- 90	81 -180	101 -168	2.1 - 10	81 - 380	401 -800	1.1 -2.0
Poor	201- 300	251 -350	91-120	181 -280	169 -208	10 - 17	381 -800	801 -1200	2.1 -3.0
Very poor	301 - 400	351 -430	12 -250	281 -400	209 -748*	17 - 34	801 - 1200	- 1800	- 3.1 -3.5
Severe	401 - 500	430 +	250+	400+	748+*	34+	1600+	1800+	3.5+

CO in mg/m³ and other pollutants in µg/m³; 2 h-hourly average values for PM10, PM2.5, NO₂, SO₂, NH₃, and Pb, and 8-hourly values for CO and O₃

CONCLUSIONS

In this study, feed forward artificial neural network is used to predict API. The concentrations of SO₂, NO₂ and PM10 are used as predictor variables in this study. It is clearly known through earlier studies and review of literature that one of the variables either PM10 or PM2.5 is needed to employ in the prediction or calculation of air quality index. Air quality index (AQI) is the prime value that describes air pollution level. Due to unavailability of data PM2.5 concentrations and various meteorological parameters are not taken into consideration although they play an important role in the pollution level prediction. This shows the need of continuous monitoring for correct and better prediction results.

REFERENCES

1. S.M.S. Nagendra and M. Khare, Modeling Urban Air Quality using Artificial Neural Network, Clean Technologies and Environmental Policy, Volume 7, Number 2, pp. 116-126, 2005.



2. M. B. Awang, A. B. Jaafar, A. M. Abdullah, M. B. Ismail, M. N. Hassan, R. Abdullah, S. Johan and H. Noor, Air Quality in Malaysia: Impacts, Management Issue and Future Challenges, *Respirology*, Volume 5, Number 2, 2000, pp.
3. D. Dominick, H. Juahir, M. T. Latif, S. M. Zain and A. Z. Aris, Spatial Assessment of Air Quality Patterns in Malaysia Using Multivariate Analysis, *Atmospheric Environment*, Volume 60, pp. 172-181.
4. M. M. Kamal, R. Jailani and R. L. A. Shauri, Prediction of Ambient Air Quality Based on Neural Network Technique, 4th Student Conference on Research and Development, Selangor, pp. 115-119, 27-28 June 2006.
<http://dx.doi.org/10.1109/SCORED.2006.4339321>
5. S. V. Barai, A. K. Dikshit and S. Sharma, Neural Net-work Models for Air Quality Prediction: A Comparative Study, In: A. Saad, et al. Eds., *Soft Computing in Industrial Application, Advance in Soft Computing*, Springer Verlag, Berlin, Volume 39, pp. 290-305, 2007, http://dx.doi.org/10.1007/978-3-540-70706-6_27
6. W. Wang, Z. Xu and J. W. Lu, Three Improved Neural Network Models for Air Quality Forecasting, *Engineering Computations*, Volume 20, Number 2, pp. 192-210, 2003, <http://dx.doi.org/10.1108/02644400310465317>
7. A. Mahboubbeh, A. Afsaneh and Z. Gholamreza, The Potential of Artificial Neural Network Technique in Daily and Monthly Ambient Air Temperature Prediction, *International Journal of Environmental Science and Development*, Volume 3, Number 1, pp. 33-38, 2012.
8. D. Silverman and J. A. Dracup, Artificial Neural Networks and Long-Range Precipitation in California, *Journal of Applied Meteorology*, Volume 31, Number 1, pp. 57-66, 2000. [http://dx.doi.org/10.1175/1520-0450\(2000\)039<0057:AN NALR>2.0.CO;2](http://dx.doi.org/10.1175/1520-0450(2000)039<0057:AN NALR>2.0.CO;2)
9. H. Hakimpoor, K. A. Arshad, H. H. Tat, N. Khani and M. Rahmandoust, Artificial Neural Networks' Application in Management, *World Applied Sciences Journal*, Volume 14, Number 7, pp. 1008-1019, 2011.
10. A. Chaloulakou, G. Grivas and N. Spyrellis, Neural Network and Multiple Regression Model for PM10 Prediction in Athens: A Comparative Assessment, *Journal of the Air and Waste Management Association*, Volume 53, Number 10, 2003, pp. 1183-1190. <http://dx.doi.org/10.1080/10473289.2003.10466276>
11. S. O. Haykin, *Neural Networks and Learning Machines*, Prentice Hall, Upper Saddle River, Volume 10, p. 936, 2009.
12. K. D. Karatzas and S. Kaltsatos, Air Pollution Modelling with the Aid of Computational Intelligence Methods in Thessaloniki, Greece, *Simulation Modelling Practice and Theory*, Volume 15, pp. 1310-1319, 2007, <http://dx.doi.org/10.1016/j.simpat.2007.09.005>
13. S. Palani, P. Tklich, Balasubramanian and J. Palanichamy, ANN Application for Prediction of Atmospheric Nitrogen Deposition to Aquatic Ecosystems, *Marine Pollution Bulletin*, Volume 62, pp. 1198-1206, 2011, <http://dx.doi.org/10.1016/j.marpolbul.2011.03.033>
14. S. H. Sohn, S. C. Oh and Y. K. Yeo, Prediction of Air Pollutants by Using an Artificial Neural Network, *Korean Journal of Chemical Engineering*, Volume 16, Number 3, pp. 382-387, 1999, <http://dx.doi.org/10.1007/BF02707129>
15. A. Kurt, B. Gulbagai, F. Karaca and O. Alagha, An Online Air Pollution Forecasting System Using Neural Networks, *Environment International*, Volume 34, Number 5, pp. 592-598, 2008, <http://dx.doi.org/10.1016/j.envint.2007.12.020>
16. A. Mahboubbeh, A. Afsaneh and Z. Gholamreza, The Potential of Artificial Neural Network Technique in Daily and Monthly Ambient Air Temperature Prediction, *International Journal of Environmental Science and Development*, Volume 3, Number 1, pp. 33-38, 2012.
17. D. Silverman and J. A. Dracup, Artificial Neural Networks and Long-Range Precipitation in California, *Journal of Applied Meteorology*, Volume 31, Number 1, pp. 57-66, 2000, [http://dx.doi.org/10.1175/1520-0450\(2000\)039<0057:AN NALR>2.0.CO;2](http://dx.doi.org/10.1175/1520-0450(2000)039<0057:AN NALR>2.0.CO;2)
18. H. Hakimpoor, K. A. Arshad, H. H. Tat, N. Khani and M. Rahmandoust, Artificial Neural Networks' Application in Management, *World Applied Sciences Journal*, Volume 14, Number 7, pp. 1008-1019, 2011.
19. A. Chaloulakou, G. Grivas and N. Spyrellis, Neural Network and Multiple Regression Model for PM10 Prediction in Athens: A Comparative Assessment, *Journal of the Air and Waste Management Association*, Volume 53, Number 10, pp. 1183-1190, 2003, <http://dx.doi.org/10.1080/10473289.2003.10466276>
20. S. O. Haykin, *Neural Networks and Learning Machines*, Prentice Hall, Upper Saddle River, Volume 10, pp. 936, 2009.
21. I. N. Daliakopoulos, P. Coulibaly and I. K. Tsanis, Groundwater Level Forecasting Using Artificial Neural Networks, *Journal of Hydrology*, Volume 309, pp. 229-240, 2005, <http://dx.doi.org/10.1016/j.jhydrol.2004.12.001>
22. J. M. Davis and P. Speckman, A Model for Predicting Maximum and 8 h Average Ozone in Atmospheric Environment, Volume 33, Number 16, pp. 2487-2500, 1999, [http://dx.doi.org/10.1016/S1352-2310\(98\)00320-3](http://dx.doi.org/10.1016/S1352-2310(98)00320-3)



Treatment Process Development for Iron Removal from Underground Water

Rajendrakumar V. Saraf

Viraj Envirozing India Pvt. Ltd. Pune sarafv@virajenvirozing.com

ABSTRACT

Iron is a vital mineral nutrient and main ingredient of human blood. According to IS 10500 for drinking water the permissible limit is 0.3 mg/l [1]. However, the natural and manmade factors, are responsible for increasing levels of iron in the water. The water with high iron content causes health problems, bad odor, unpleasant taste, red color of water and stains on laundry and plumbing fixtures. Number of technologies are available for removal of iron can be mainly divided into precipitation of iron, adsorption and absorption and biological removal. Ion exchange is also used to remove iron from water. In underground strata conditions usually favour the reduction of the natural ferric iron deposits to the ferrous state. As ferrous salts are highly soluble, ground water supplies frequently carry significant concentrations, and as this ferrous iron is in true solution, the water may be perfectly clear and colourless, with no visible evidence of the iron present. However, once ferrous iron is exposed to the atmosphere, oxygen from the air readily converts it to the ferric state. Ferric iron then reacts with the alkalinity in the water to form ferric hydroxide, the insoluble brown gelatinous matter which causes so much staining. Vegetables cooked in water containing excessive iron turn dark and look unappealing. Therefore, its presence in water to be used for food processing industry is not desirable. A food processing industry has been set up in Dalgaon located in Brahmaputra basin near Guwahati in Assam. Water table is just 2 to 3 m below the ground. Ground water is acidic and has high amount of soluble iron content. Underground water is the only source at the site. Treatment studies are carried out with underground water to develop the economical treatment process and design parameters to bring down iron content from 30 mg/l to 0.1 mg/l. A treatment plant of 0.5 MLD capacity consisting of Pre-chlorination, Aeration, pH adjustment, Alum dosing, Slow mixing, Sedimentation, Catalytic removal with Manganese dioxide, Sand filtration and Chlorination is installed and commissioned at site. Plant is working satisfactorily producing desired quality of water. The chemistry of iron and its impact on water quality, removal technologies and experience with working plant are discussed in this paper.

KEYWORDS Iron in ground water, Food processing industry, Treatability studies, Treatment process

INTRODUCTION

Groundwater is the water found underground in the cracks and spaces in soil, sand and rock. It is stored in and moves slowly through geologic formations of soil, sand and rocks called aquifers. It is often withdrawn for agricultural, municipal and industrial use by constructing and operating extraction wells. Rainwater, as it infiltrates the soil and underlying geologic formations dissolves the minerals, causing it to seep into aquifers that serve as sources of groundwater for wells.

Rains are the condensed water vapours and so in unpolluted area falling rainwater shall be without any solids. Therefore, rainwater is highly corrosive. It will have tendency to dissolve / leach solids from surrounding medium. When it precipitates from the clouds, gases & particulate matter both from natural and manmade emission become the parts of rainwater. Once it falls on the ground top layer of soil get fully saturated with water. Water in soil is in three forms, free, capillary and bound water. Depending on permeability of soil free water percolates downward. Part of water from soil also moves upward due to evaporation. During percolation it passes through different strata of soil and rocks. When it passes through soil it dissolves abundantly available chemicals like calcium, magnesium, and sodium etc. The water with dissolved solids then percolates further through the voids and fractures in the rocks. Leaching out from lower strata of soil and rock depends on solids in water percolated through the upper layer. There may be extraction and deposition when water percolates from one layer to other layer. The ground water quality is result of interaction of water with surrounding soil & rock medium and it remains unaltered for many centuries as result of natural equilibrium.

Soil and rock formation are different at different places. There is natural rate of percolation for groundwater recharging. The characteristics of soil and rocks determine the ground water quality. Hence, the geology of particular area has a greater influence on the occurrence and quality of water and its movement. Many times ground water carries a higher mineral content than the surface, when there is slow circulation and longer period of contact. Change in ground water quality with the passage of time has a hydrologic significance. The quality also varies due to a change in chemical composition of formations. The geochemistry of the aquifer is controlled by the surface topography of the underlying formations, the thickness and permeability of the alluvial deposits. The ground water

33rd Indian Engineering Congress, Udaipur, 2018: Technical Volume 339



chemistry is controlled by the composition of its recharge components as well as by geologic and hydrologic variations within the aquifer. The concentration of calcium and magnesium in ground water may be due to rock weathering and aquifer material [2]. High iron content in Assam and fluoride in Rajasthan are some of the examples of interaction between percolating water and soil.

GENESIS OF IRON IN WATER

Iron is one of the earth's most plentiful resources and is one of the most troublesome elements in water supplies. The main naturally occurring iron minerals are magnetite, hematite, goethite and siderite. Weathering processes release the elements into waters. Elementary iron dissolves in water under normal conditions. Many iron compounds share this characteristic. Naturally occurring iron oxide, iron hydroxide, iron carbide and iron penta carbonyl are water insoluble. The water solubility of some iron compounds increases at lower pH values. Other iron compounds may be more water soluble than the examples mentioned above. Iron carbonate has a water solubility of 60 mg/l, iron sulfide of 6 mg/l, and iron vitriol even of 295 g/l. Many iron chelation complexes are water soluble. Usually there is a difference between water soluble Fe^{2+} compounds and water insoluble Fe^{3+} compounds. The latter are only water soluble in strongly acidic solutions, but water solubility increases when these are reduced to Fe^{2+} under certain conditions. Iron in underground water is at stage of equilibrium with surrounding environment. If the conditions of environment are changed the chemical equilibrium is upset & leads to either solution of certain elements or their precipitation such as iron and manganese. The best example is pumping iron containing water from an underground aquifer, iron reacts with oxygen to form insoluble compounds. Therefore, in general oxygenated water (surface water and shallow groundwater) will always have low levels of iron. In surface water, iron and manganese are most likely to be trapped within suspended organic matter particles. Water that does not have regular contact with the atmosphere tends to be low in oxygen (oxygen poor). Iron carbonates in an oxygen poor environment are relatively soluble and can cause high levels of dissolved iron. However, if iron is associated with sulfur as iron sulfide rather than iron carbonate, dissolved iron remains low. Dissolved oxygen generally decreases with depth, so these types of conditions are more likely to occur in deep wells. Sometimes oxygen poor conditions can also occur in relatively shallow wells that have stagnant water with very slow turnover [3, 4].

Iron problems are most likely to occur in wells having water with high carbonate and low oxygen. The problem occurs when this type of water is pumped to the surface. The chemical equilibrium is changed due to exposure to the atmosphere. Oxidation of dissolved iron particles in water changes from white to yellow and finally to red-brown solid particles that settle out of water. A precipitated iron particle (colloidal) that does not settle down imparts red tint colour to water.

STUDY AREA

A food processing industry is located in Integrated Infrastructure Development (IID) Centre Dalgaoon. IID is located on NH 52 between Kharupatia and Dalgaoon. Dalgaoon is situated in Darrang (Mangaldai), Assam, India. Its geographical coordinates are 26°34'0" North, 92°12'0" East and its original name (with diacritics) is Dalgaoon. It comes under Brahmaputra Basin. Darrang consists of a narrow strip of plain lying between Himalayas and Brahmaputra River in the north-west part of Assam. The soil of this district is very fertile for cultivation and the main crops are paddy, oilseeds, sugarcane and jute.

At AIIDC around 2 decades before there was a pond at the site. It is filled with river sand to make the table land. The ground water table at site is just 1.5 m to 2 m below the ground. The area nearby is waterlogged. Due to soil characteristics and geological conditions and low water table, iron content in water is very high. Iron gets precipitated out within 15 to 30 min after pumping. Iron is also found in water from bore well dug up 30 m.

WATER REQUIREMENT AND WATER QUALITY

Variety of pickles, chutneys, continental sauces, jams and vinegar are the products manufactured at the Unit. Water is mainly required for fruit washing, vessel cleaning, syrup and brine preparations, steam generation etc. It requires filtered chlorinated water and soft water for steam generation. Desired water quality is as per IS 1050 for drinking water. As units manufacture food products value for iron shall not exceed in any case by 0.3 mg/l. The sole source of water is underground water. Two bore wells are dug and depth is 91 m. The yield test shows that bore well can give water @ 20000 l/h. Two water samples at the time interval of 6 months were collected from the site. The test results are given in **Table 1**.

**Table 1** Analysis report of underground water samples

Detail	Unit	Sample -1	Sample 2
Color		Yellowish	Yellowish
Turbidity	NTU	50	50
Total Solids	mg/l	108	189
pH		5.96	6.33
Total Alkalinity as CaCO ₃	mg/l	70	70
Total Hardness as CaCO ₃	mg/l	20	20
Alkaline Hardness as CaCO ₃	mg/l	20	20
Non-alkaline hardness as CaCO ₃	mg/l	0	0
Calcium as Ca	mg/l	8	12
Magnesium as Mg	mg/l	0	0
Chlorides as Cl	mg/l	25	24
Sulfate as SO ₄	mg/l	0	0
Nitrate as NO ₃	mg/l	0	0
Iron as Fe	mg/l	23	12

INTERPRETATION OF TEST RESULTS

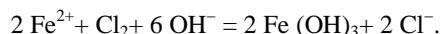
Turbidity is very high due to precipitated iron. When water is exposed to atmosphere iron precipitates out within 2 to 3 h. pH of both samples is acidic. Alkalinity reported is only methyl orange alkalinity indicating carbonate alkalinity. Therefore, hardness present is only alkaline hardness. Water is soft. Total hardness is only 20 mg/l. Calcium content is 8 mg and 12 mg/l in two samples. However, Magnesium content is found to be zero. Total dissolved solids are less than 200 mg/l. Iron in water is 23 and 12 mg/l.

TREATABILITY STUDIES

The objective of the treatability studies is to find out the low cost and easy to operate method to get desired quality of water. The samples are collected and treated with different alternatives. The findings are as follows:

Chlorination

The iron is oxidized by the chlorine. The oxidation/reduction reaction may be written as follows:



Sodium hypochlorite (10%) is used as source of chlorine. Sodium hypochlorite is alkaline and adds alkali to water to neutralize the pH. Measured amount of sodium hypochlorite is added in 500 ml of water. Chlorine is slowly mixed by magnetic stirrer for 15 s. It is observed that after addition of chlorine the oxidation process immediately starts with red color precipitation of iron. Alkali in Sodium Hypochlorite hastens the process by presence of hydroxyl ion and neutralized the acidity in water. 3.5 to 4 mg/l of chlorine is found to be the optimum dose to start the precipitation process.

Aeration

Iron is present in soluble form, it can only occur as protoxide, in combination with a soluble acid. As soon as water is exposed to atmosphere or aerated to encourage the absorption of oxygen the protoxide is transformed into an insoluble oxide.

Aeration is carried out by using air-stone (bubbler) and the air pump used for aquarium. Sample is aerated for 30 seconds, 1, 2, 5, 10, 15 and 30 min. It is observed that optimum reduction of iron by plain aeration of 30 min is 34%. Aeration also drives away dissolved carbon dioxide and accelerates the precipitation of iron.

Chlorination plus Aeration

Optimum dose of 4 mg/l of Chlorine is added and after 15 s of mixing aeration is started. The rate precipitation of iron increases. However, iron removal after 15 s of aeration is 70%.

Neutralization

The water after chlorination and aeration is acidic (pH 6.2 to 6.5). To neutralize pH, lime suspension is added. Addition of lime raises pH and also precipitate iron as its insoluble iron hydroxide.



Sample after chlorination and aeration is kept on the magnetic stirrer to mix the content. Measured quantity of lime suspension is slowly added to raise pH to 7.2. 10 mg of lime per liter is required to raise the pH. Red color of precipitate is formed. The mixing is required to complete the neutralization. It also enhances the iron removal may be due to the formation of iron hydroxide.

Sedimentation

Gravity sedimentation separates out the precipitated iron from water. The neutralize sample is kept to observe sedimentation of precipitated iron. The neutralized water with precipitated iron requires longer time (>2 hr) to settle down. Besides, settled water does not have the clarity.

Use of Flocculating Agent

Flocculants or flocculating agents are chemicals that promote flocculation by causing colloids and other suspended particles in liquids to aggregate, forming a floc. It also enhances the settling rate. Alum is the widely used flocculating agent in water treatment.

Jar test apparatus is used to find out optimum dose of alum. Chlorinated aerated and neutralize sample was taken for the test. Alum dosing for test is 2.5, 5, 7.5, 10, 12.5, 15, 17.5 and 20 mg/l. Once optimum flocculation is observed sample was allowed to settle down. It is observed that optimum alum dose is 15 mg/l to flocculate the suspended solids. Flocculated suspended solids settled down in 30 minutes. Around 80% iron removal is observed. The settled water has total Iron 1.0 mg/l.

Catalytic Removal of Iron

Manganese dioxide (MnO_2) is used for the purpose of softening hard water by the removal of iron and other soluble metals from water. An advantage in using MnO_2 filtration is that Fe and Mn that remain in solution become catalytically precipitated and then adsorb directly the MnO_2 present on the media. It is further oxidized to oxide.

A column of 25 mm diameter and 250 mm height is packed with Manganese Dioxide. Settled sample from above is passed through the column. Iron content in the filtered water is less than 0.3 mg/l.

Filtration

Filtrate from manganese dioxide filter is filtered again through the ordinary filter. Filtrate is crystal clear with iron content 0.1 mg/l. It is proposed to use the sand filter.

PLANT CAPACITY AND DESIGN PROCESS

Total water demand is $160 \text{ m}^3/\text{day}$. Assuming the future growth (25%) water demand may rise up to $205 \text{ m}^3/\text{day}$. The plant is designed for $20 \text{ m}^3/\text{h}$ capacity. It can give 400 m^3 fully treated water in 20 h of operation/day. On the basis of treatability studies treatment process is designed for Iron Removal Plant. Flow diagram is given in **Figure 1**.

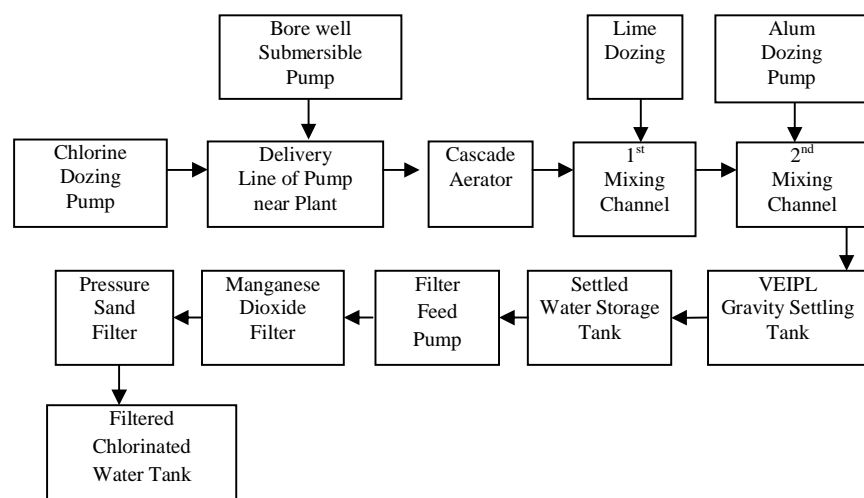


Figure 1 Process flow diagram



PLANT AND EQUIPMENT

Pre Chlorination

Sodium hypochlorite will be added in Chlorine dosing tank. It will be pumped by the electrically operated dosing pump into the inlet pipeline of the cascade aerator.

Cascade Aerator

Cascade aerator of circular shape is made in BBM work. The surfaces of the steps are embedded with pebbles from river Brahmaputra. Chlorine mixed well water will be aerated for removal of dissolved carbon dioxide and oxidation of iron in water. Water will fall on the steps. Embedded pebble on the wall and steps will activate oxidation of iron. Total area of Cascade aerator is 19.8 m^2 . Loading rate is $1.01 \text{ m}^3/\text{m}^2/\text{h}$.

Lime Dozing

Lime will be dozed from lime suspension tank by gravity into the inlet of mixing channel.

Mixing Channel

Purpose of mixing channel is to mix the chemicals created due to turbulence in the channels. Besides, it further aerates the water. There are total 5 channels each of 2.1 m length. The pebbles are embedded in the channel to create more turbulence. In the first channel lime is added for neutralization and provides enough alkalinity for flocculation by alum.

Alum Dozing Pump

Alum will be dissolved in water in Alum dosing tank. It will be pumped by the electrically operated Dosing pump into the second channel after lime addition. Alum will coagulate the turbidity in the water that will be further flocculated in the flocculation channel.

Gravity Settling Tank

It is hopper bottom square tank designed by VEIPL, for removal of suspended and flocculated iron oxides. Surface loading rate is $40 \text{ m}^3/\text{m}^2/\text{d}$. Settling area of the tank is 9 m^2 . It is provided with specially designed distribution channel, baffles for velocity reduction and overflow launder. Lime and alum mixed water enters into the distribution channel. Solids settle down to bottom and clear water overflow on the launder and finally gets collected in the settled water tank. Settled sludge is drawn from the sludge pipes of hopper provided in the tank.

Settled Water Tank

Water overflowing from the settling tank gets collected in settled water tank.

Settled Water Pump

The mono block pump transfers settled water from settled water tank to the filtration system.

Catalytic Iron Removal Filter

It is a pressure vessel made of MS having media coated with manganese dioxide and sand bed at the bottom. Dissolved iron is removed with the help of oxidizing agent manganese dioxide from settled water. The precipitated iron is trapped in the media and sand bed. Backwashing is required.

Multi Grade Pressure Sand Filter

Water is pumped to pressure sand filter for removal of suspended & flocculated fine solids from the Catalytic Iron filter. Water flows from top to bottom through the filtering media, suspended & flocculated solids are retained in the media. Only clear filtered water is collected through the collection system at bottom. Backwashing is required.

Chlorine Dosing Pump for Disinfection

Chlorine is a disinfecting agent. Sodium hypochlorite liquid chlorine will be used as disinfecting agent. Sodium hypo chlorite is added into the Chlorine dosing tank. Solution of chlorine is then pumped by the electrically operated Dosing pump into the delivery line of the filter

Treated Water Storage Tank

Chlorinated Filter water is stored in the filtered chlorinated water tank for required Chlorine contact time.

Backwashing



Backwash water pump is provided to pump fully treated water for backwashing of both filters. Backwash water is returned to inlet of mixing channel. Backwashing is done once in a shift or when the pressure difference is 0.8 kg/cm².

Sludge Drain from Settling Tank

After every 4 hours of operation under drain valve of settling tank is open to drain out the settled sludge.

Photographs of water Treatment Plant are given in **Figures 2 to 5**.



Figure 2 Cascade aerator embedded with pebbles



Figure 3 Mixing channel alum and lime dosing



Figure 4 Gravity settling tank



Figure 5 Catalytic iron removal filter and pressure sand filter

OBSERVATIONS AND FINDINGS

The Iron removal plant is commissioned in May 2006, since then it is working satisfactorily to produce 150 to 200 m³ of treated water for manufacturing various food products. The observation and findings during commissioning and operation are as reported here.

During first few days of commissioning the iron was not getting precipitated before sedimentation tank. It is observed that formation of coating of iron oxide on the pebbles of cascade aerator enhances the precipitation of iron.

The chlorine dose before cascade aerator needs adjustment. It is observed that around 3 ppm of residual chlorine in the inlet of cascade aerator shows better results. Lime addition is must to neutralize the water and precipitate out the iron likely in the form of hydroxide. Lime dose is finally adjusted to 10 mg/l.

In beginning it is observed that precipitated iron is not settling down in settling tank without alum addition. Alum dose of 10 mg/l improves the clarity of settled water overflowing from the settling tank. Sludge withdrawal after every 4 hours of operation is must otherwise the loss of sludge with overflow begins. Colour of sludge is red and suspended solids are around 5,000 mg/l.

On the basis of findings, standard code of operation and maintenance is prepared and given to the operator.

It is observed that after one year of operation there is sudden change in quality of water. The chlorinated water turns yellowish after 1 hour of exposure to atmosphere. Thorough investigation is carried out. It is found that increase in chlorine dose to 5 mg/l sorts out the problem. Residual chlorine in filter water is found to be 1 mg/l, therefore, the chlorine dosing for disinfection is discontinued. Since then no other operation problems are yet observed.



The media of sand filter and catalytic filter was changed in 2009. Then it was changed as and when required.

Catalytic filter needs regular backwashing otherwise the outlet of filter is found to turn yellowish colour. Due to the negligence of operators the catalytic filter is not backwashed. The filter is given an open backwash to get the clear water. Pressure Sand Filter needs regular backwash. Plant requires 1 days to get stabilized.

It is the biggest iron removal plant being operated in Assam. The Iron content in fully treated water remains always less than 0.1 mg/l. The plant is being operated by local skilled and unskilled operator. Only one person is operating the plant. Seasonal variation in treated water quality is not observed. It is proposed to dewater the sludge and use as pigment in paint manufacturing.

CONCLUSION

Design of Iron removal plant needs careful study and integration of chemical oxidation, aeration, neutralization, coagulation, sedimentation, catalytic filtration and sand filtration. A proper design can result in 99.9 % removal of iron from water.

REFERENCES

1. Bureau of Indian Standards, Drinking water, BIS-1050.
2. O'Connor, J. T. 1971. Iron and Manganese. In M. E. Flentje and R. J. Faust (ed.) pp. 380-396, Water quality and treatment - a handbook of public water supplies, 3rd Edition. Prepared by The American Water Works Association, Inc. McGraw-Hill Book Co., New York.
3. Hem, J. D. 1967. Equilibrium chemistry of Iron in groundwater. pp. 625-643, Principles and applications of water chemistry. S. D. Faust and J. V. Hunter (ed.) John Wiley and Sons, Inc., New York.
4. Machmeier, R. E. Reviewed 1990. Iron in drinking water, AG-FO-1318. Minnesota Extension Service, University of Minnesota, Agriculture.



IoT based Aqua Q Sense for Indian Railways

M. Gunasekaran

*Department of Electrical and Electronics Engineering, Annapoorana Engineering College, Salem, Tamil Nadu,
gunasekaranmadhu@gmail.com*

ABSTRACT

Most of us would have travelled through train at least once in our life as Indian railways are highly interconnected within the country. Amongst those who have travelled would also have used the washrooms while travelling and it would never be a surprise if we had ever come across a situation in which we found out that there was shortage of water in the washroom. This situation mainly arises due to poor information regarding shortage of water in the train and unpreparedness for water refilling while the train arrives a particular station. This embedded project aims to bring about a solution for this problem by implementing IoT and mesh network communication between the train coaches by sharing the water level information. It is implemented by using ESP-8266 Wi-Fi modules, Arduino Uno and ultrasonic sensors. This way station can be informed regarding which train coach has least water in it and the workers can be positioned accurately to ensure filling without any delay. In order to sense the level of water in train coaches, a sensor node installed within which detects the water level status and forwards it to the upcoming station database. From the station database the information is passed to workers to their mobile phones that notifies, which coach has low water level and the workers should fill that coach with water.

KEYWORDS Arduino uno, ESP- 8266 Wi-Fi module, Internet of things, Mesh network, Ultrasonic sensor.

INTRODUCTION

Water is a precious commodity for all living thing in earth and we humans are no different, in fact we can survive without food for days but not with water. We use it not only for drinking but also for cleanliness and refreshment. So water is important where ever we go. Travelling is something that we all humans mostly do, and in India travelling through train is the most common, cheapest and efficient mode of transportation. Journeys through train may take hours and at this instances lack of water to meet our basic needs becomes frustrating and agonizing. This is a regular scenario in Indian railway and the prime cause is not that there in unavailability of water but unmonitored refilling of water at the required train coaches.

It brings an important need in monitoring the quantity of water available for passenger usage and ensuring timely refilling at the allotted station without any delay. This project aims at solving the problem by providing better and effective notification mechanism directly to the worker who fills the water tank of the trains.

OBJECTIVE OF THE PROPOSED SYSTEM

The objective is to design smart water level detecting system for train using IoT. This will enable to monitor the Water level in each coach and transmit the data signal to a stations database so that it could be analyzed and assign workers to fill up the water tank when the train arrives.

Each coach has sensor and Wi-Fi node, and every node in the train are mesh connected so that no data is lost when connection is broken. All the data from each coaches send to main coordinator node that is located in the engine and from there it is send to station database .The workers can access the details of the water level in the coach using physical web in their mobile or other connectivity device.

WATER LEVEL DETECTION

Purpose

Day-by-day, there is more complaints on train water management system. People who are travelling in trains are facing problems due to lack of water. So in order to avoid that we came up with a solution named 'Aqua Q Sense' which detects the train water level status and sends it to upcoming station database. From that information workers will be allotted to fill the required tanks.

Operation

Firstly, the coaches are installed with a ultrasonic sensor node above 5 cm of the tank which will detect the water level. The sensor node installed will send ultrasonic waves of frequency ranging 20-22kHz. The waves sent by ultrasonic sensor are received back after they are reflected from the water surface. The received signal is collected

by the echo and the information is sent to a Wi-Fi node installed within the train coach. Each train coach is installed with different Wi-Fi modules and the modules are connected in a mesh network. The connected Wi-Fi nodes give information to the coordinator node that is to the main control unit and from the main control unit the data is sent to upcoming station database.

BLOCK DIAGRAM DESCRIPTION

Water Level Detector Unit (WLD)

Block Diagram (**Figure 1**) consists of two water level detector units which are connected to each other and they are connected to a main control unit. Water level detector consists of an ultrasonic sensor which is connected to a Wi-Fi node. The sensed data from water tanks with ultrasonic sensor is observed by Wi-Fi node and through that Wi-Fi node the data is sent to main control unit.

Main Control Unit

Main control unit consist of Arduino, LED indicators, LCD and Wi-Fi module. This is the part that is located in the engine of the train. Here the data from each connected coaches are received, which includes coach ID and water level present in the tank of that particular coach. These data are collected and transmitted to the database of the station

Station Control Unit

Station control unit receives the data coming from the upcoming train and stores it. The worker receives the data and coach number from this data base and thereby they can position themselves to fill the tank.

Hardware Description

Arduino

The Arduino Uno, as shown in **Figure 2**, is embedded with the ATmega328p microcontroller. It contains 20 input/output pins for interfacing to other extension boards and additional circuits of which 6 pins are Analog and other 14 pins are digital. In this 6 pins out of 14 digital pins can also be used as PWM output. This board is programmed b using type-B USB cable connected to the computer and the computer is installed with Arduino IDE. It has the clock speed of 16 MHz maintained by ceramic resonator, an In-circuit Serial programming header and inbuilt Reset button. The program is stored to the SRAM and it is done by flash, EEPROM, The operating voltage is 5 V and it can support input voltage of 7 to 20 V. It supports UART TTL serial communication through digital pin 0 as Receiver (RX) and pin 1 as Transmitter (TX).

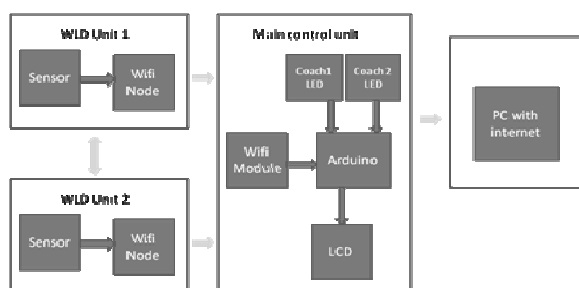


Figure 1 Block diagram

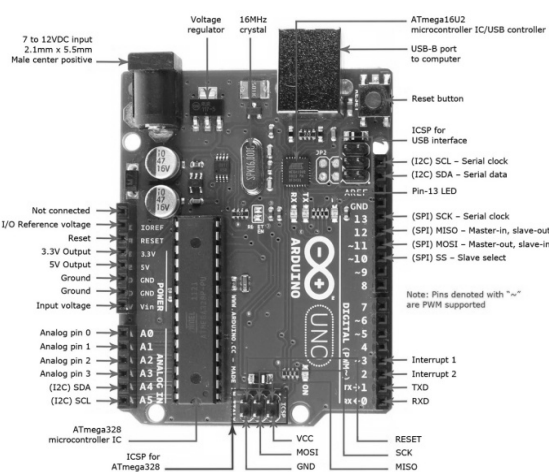
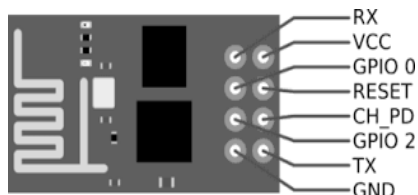


Figure 2 Arduino uno with pin details



Figure 3 ESP8266 Wi-Fi module with pin details

Input and Output

Each of the 14 digital pins on the Arduino uno can be used as an input or output, using `pinMode()`, `digitalWrite()`, and `digitalRead()` functions. They operate at 5 V. Each pin can provide or receive a maximum of 40 mA and has an internal pull-up resistor (disconnected by default) of 20 to 50 k Ω . In addition, some pins have specialized functions:

Serial: pins 0 (RX) and 1 (TX). Used to receive (RX) and transmit (TX) TTL serial data. These pins are connected to the corresponding pins of the ATmega8U2 USB-to-TTL Serial chip.

External Interrupts: pins 2 and 3. These pins can be configured to trigger an interrupt on a low value, a rising or falling edge, or a change in value. See the `attachInterrupt()` function for details.

PWM: 3, 5, 6, 9, 10, and 11. Provide 8-bit PWM output with the `analogWrite()` function.

SPI: Using the SPI library the SPI communication is done by four logic signals. The logic signals are Slave Select, Master In Slave Out, Master Out Slave In and Serial Clock.

LED: 13 There is a built-in LED connected to digital pin 13. When the pin is HIGH value, the LED is on, when the pin is LOW, it's off.

The Uno board has 6 analog inputs, labeled A0 through A5, each of which provide 10 bits of resolution (that is, 1024 different values). By default they measure from ground to 5 V, though is it possible to change the upper end of their range using the AREF pin and the `analogReference()` function. Additionally, some pins have specialized functionality:

TWI: Using the Wire library, the Two-Wire Interfacing communication is done by using bidirectional lines such as Serial Data and Serial Clock.

AREF: Reference voltage for the analog inputs. Used with `analogReference()`.

Reset: Reset button is added to shields which block the line LOW on the board and it will reset the microcontroller.

Wi-Fi Module

The ESP8266 Wi-Fi module as depicted in **Figure 3**, is a self contained SOC with integrated TCP/IP protocol stack that can give any microcontroller access to your Wi-Fi network. The ESP8266 is capable of either hosting an application or offloading all Wi-Fi networking functions from another application processor. Each ESP8266 module comes pre-programmed with an AT command set firmware, which means, you can simply hook this up to your Arduino device and get about as much Wi-Fi-ability as a Wi-Fi Shield offers (and that's just out of the box)! Because of inexpensive in nature ESP8266 module is widely used. This module has a powerful enough on-board processing and storage capability that allows it to be integrated with the sensors using GPIO pins. Its high degree of on-chip integration makes it small in size and less in need of external circuit.

The ESP8266 supports APSD for VoIP applications and Bluetooth co-existence interfaces; it contains a self-calibrated RF allowing it to work under all operating conditions, and it doesn't require any of the external RF circuit.

Note: The ESP8266 Module is not capable of 5 to 3V logic shifting and will require an external [Logic Level Converter](#). Please do not power it directly from 5V dev board. This new version of the ESP8266 Wi-Fi Module has increased the flash disk size from 512 kB to 1MB.

Features:

- 802.11 b/g/n,
- Wi-Fi Direct (P2P), soft-AP,
- Integrated TCP/IP protocol stack,
- Integrated TR switch, power amplifier and matching network,
- Integrated PLLs, regulators, DCXO and power management units,
- +19.5dBm output power in 802.11b mode,
- Low Power down leakage current (10uA),
- Flash Memory is about 1 MB,

- Application processor is a Integrated low power 32-bit CPU,
- Secure Digital card interface, synchronous and asynchronous serial communications,
- Fading channels during communication is by Space Time Block Coding technique,
- Within 2 ms it will come to Wake up state and packets get transmitted,
- Standby power consumption of < 1.0mW (DTIM3).

Ultrasonic Sensor

The ultrasonic sensor HC-SR04 is shown in **Figure 4**. It is widely used because of stability in performance, low cost and high accuracy level even for a longer distance of about 500 cm. It works with 5V DC supply and current of less than 2 mA. It has a resolution of 1 cm. The operating frequency of the sensor is about 40 kHz. The sequence chart for ultrasonic sensor is shown in **Figure 5**.

The ultrasonic sensor will transmit a short pulse and it will be reflected by an object then received back by the sensor and produces an electrical signal. After the echo is faded away the sensor will again send a pulse. The time taken for the process is called as cycle period and this will continue. This cycle period should be more than 50 ms. If the signal is not reflected back then output will give a high level signal of 38 ms. Otherwise the pulse width of echo gives the distance between object and sensor.



Figure 4 Ultrasonic sensor

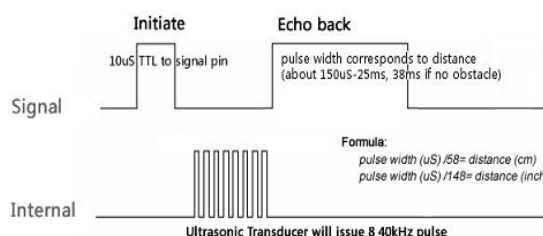


Figure 5 Sequence chart for ultrasonic sensor

Working Principle of Ultrasonic Level Sensor

This is a contact less level measuring sensor (**Figure 6**) unlike other sensors for example proximity sensor a contact type (i.e.) sensors have in contact with the water. As mentioned earlier the time travelled by pulse is measured because of the change in density of medium the transmitted signal is reflected back to receiver. Here the two mediums are air and liquid. In general air having low density than liquid. While going for real time implementation, the ultrasonic sensor having two major problems. Those problems are needed to be considered during design process. The first problem is we cannot receive signal in a small window where the transceiver is located. This can be avoided by placing the sensor at least 5 cm above the maximum level of water. The second problem is bouncing of signals by the tank walls. So the length and diameter of the tanks should be selected carefully. Length should be more than 5 cm and diameter should be more than 7.5 cm.

PROJECT IMPLEMENTATION

The project was started with inspiration and need to solve a problem that seems to be affecting lots of people who travel through Indian railway. Studies were done before the design of the system regarding its feasibility to be applied in the Indian railway. The concept of IoT was used in the system design which consist of several sensor node which communicate with each and the interconnection of these nodes are done through mesh network, Arduino is used for controlling and decision making of the system. It uses Wi-Fi communication to transmit data between the nodes. ESP nodes are used as Wi-Fi nodes which also have microcontroller capability so it provides better processing.

Mesh Network

A mesh network, as depicted in **Figure 7**, is a local network topology (i.e.) LAN, WLAN or VLAN. It has two ways of connections. One way is fully connected network where all the nodes are connected to each other. The second way is partially connected network where only few nodes are connected to all the nodes but all other nodes are connected to only selected nodes for exchanging data or information between them. When deploying IoT the mesh network will play a major role, because the single point of failure cannot affect the communication of others. All the nodes are connected to each other through wire will increase cost and it requires more space. In star topology networks, the router is needed for internet service. If it got damaged then the communication won't be possible. The



physical barriers and financial barriers of the wired connections in mesh network are eliminated because of the advancement to the wireless communications.

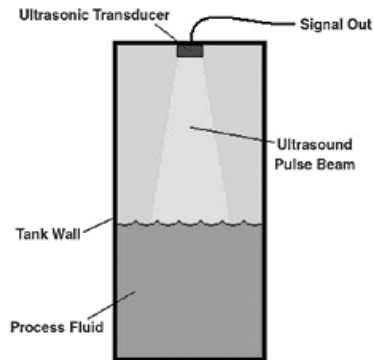


Figure 6 Level detection using ultrasonic sensor

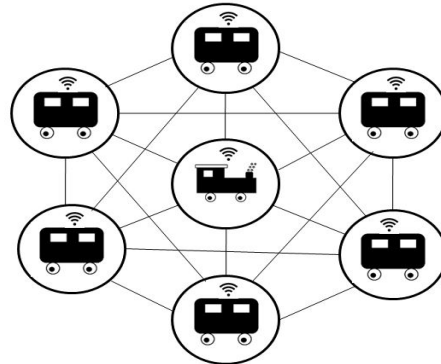


Figure 7 Mesh network between coaches

RESULTS

The concept and idea of the project was successfully implemented at various stages shown in **Figures 8 to 13**. Water level present in the tank was measured using ultrasonic sensor. The communication between nodes was established using mesh network topology in the ESP modules. The water level data was transmitted between the nodes with the use of Arduino uno board and the data was displayed on a website which the user can also access using a mobile device with internet connectivity and the same data is displayed in LCD located in engine.

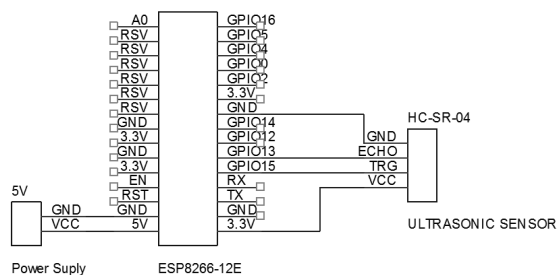


Figure 8 Circuit diagram of WLD unit in coaches

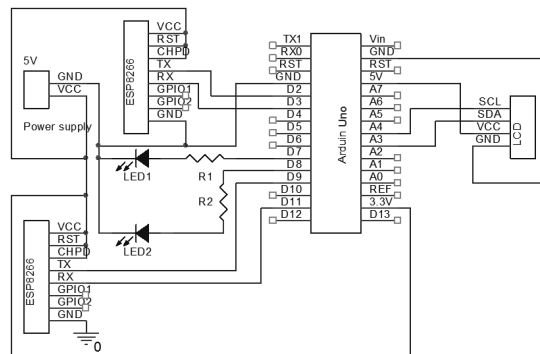


Figure 9 Circuit diagram of main control unit

```
*****RSV welcomes you*****
sensor value:73
Train ID:-12988
low water on coach2:
Sensor value:73
Train ID:-12988
low water on coach2:
Sensor value:63
Train ID:-12988
low water on coach2:
Sensor value:74
Train ID:-12988
low water on coach2:
74
*****Data send to esp*****
sensor value:74
Train ID:-12988
low water on coach2:
Sensor value:0
Train ID:0
Sensor value:61
Train ID:-12988
low water on coach2:
61
*****Data send to esp*****
Sensor value:72
Train ID:-12988
low water on coach2:
Sensor value:74
Train ID:-12988
low water on coach2:
Sensor value:73
Train ID:-12988
low water on coach2:
73
*****Data send to esp*****
Sensor value:73
Train ID:-12988
low water on coach2:
Sensor value:0
Train ID:0
6
```

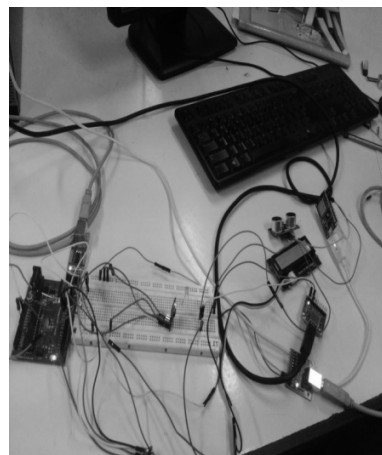




Figure 10 Serial port output in Arduino IDE



Figure 12 Prototype

Figure 11 Initial setup and Water status shown in LCD

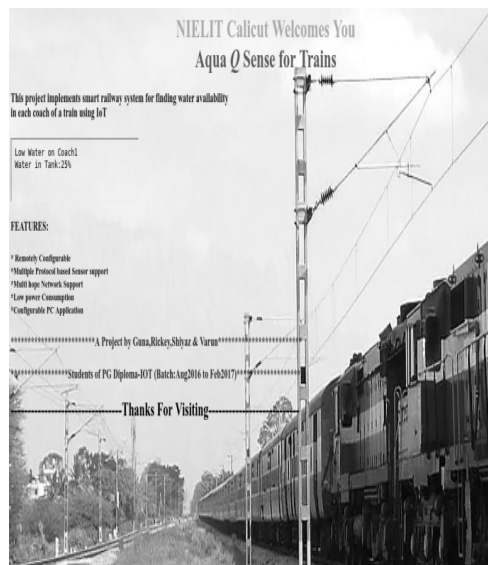


Figure 13 Web page

CONCLUSION

The concept and application of IoT and embedded system clearly resolves the problem with lack of water for basic necessities while travelling in train. It increases the efficiency of water management and comfort of travelling in a train by ensuring the proper refilling of water tank on train coaches. By introduction of IoT and wireless sensor network, the embedded system can able to make various smarter railway systems with reduced cost and efficiency.

FUTURE SCOPE

IoT based embedded systems are now becoming solution for many problems and its application is increasing tremendously. The idea of connecting devices to each other and communicating with each other makes problem detection fast and saves human time interacting with machines. This project also does the same, the ease with which the user can access data and take necessary actions to rectify the given situation. Also future application involves development of physical web where there won't be any need for particular app or software to be installed in the users mobile device but the user can access it through url of a particular database

ACKNOWLEDGMENT

The author would like to thank the faculties at NIELIT, Calicut for their valuable contributions and would also like to thank his friends for their efforts on the test-bed setup.



Hardware Programming to Improve Embedded System Performance

T. Harinath^{*1}, K. Lal Kishore²

Electronics Corporation of India Limited, Hyderabad¹, harinath.t@gmail.com*

Jawaharlal Nehru Technological University, Ananthpur, Andhra Pradesh²

ABSTRACT

Embedded systems are designed for realizing certain task(s) in specific applications. Embedded Systems are designed using either Hard Processor or Soft Processor. The Processors are used for operations like controlling, and coordinating operations, etc. Other logic functions are realized using ASICs. This paper deals with the design of embedded systems using hardware description languages without using any hard or soft processor. All the peripherals and logic circuits used are modelled with Hardware Description language only. As standard ASICs are not used and logic is totally realized with programmable hardware, there is a significant improvement in the performance of embedded system. The logic realized using this innovative technique can be integrated with any other logic on single or different chips to make this a part of a big system in an economical and reliable manner. This paper focuses mainly on Comparative Analysis of various parameters like Speed of processing, Clock requirements, Memory requirements and Power consumption. Finally, this paper stresses the advantages of Hardware Programming particularly in industrial applications with regard to design obsolescence, architecture dependence, design upgradeability, Design Cost and so on.

KEY WORDS Hardware, Software, Processor, FPGA, Programming

INTRODUCTION

An embedded system is an electronic system designed to execute certain specific functions. All these functions are pre-programmed and pre-planned. Design of embedded system revolves around the micro processor used. In addition to the micro processor and memory, embedded system consists of suitable peripheral devices which act as input, output or both input and output devices. The functioning of micro processor used in embedded system is governed by the firmware stored in Read Only Memory (ROM). Read, Write and other computational operations make use of Random Access Memory (RAM). Peripheral devices used can be individual Application Specific Integrated Circuits (ASICs) or can be part of an integral chip consisting of microprocessor and some I/O Devices. Block Diagram of Microprocessor based Man Machine Interface logic, which is nothing but an embedded system is given in **Figure 1**[1-3].

Present day design of embedded systems is facing the following five challenges.

Compactness: The logic components of the system should occupy as less space as possible. This can be achieved when component count is reduced to minimum [3].

Cost of design and development: Cost of the design and the development must be reasonable. Product cost should not go in waste for the unused resources in the logic. Programmable devices may be helpful to some extent for this purpose [4, 5] .

Low power consumption: Component count and silicon thickness will influence this parameter. Design can consume low power when it is made to shut down the logic not being used at any time [6].

Design up gradation / modification: Design needs to be modified or upgraded to meet the varying demands of the user / customer. Programmable devices will serve this purpose [7].

Design time: Design process must be completed within the shortest time possible. Problems that can occur must be forecasted well in advance and rectified without any change in the hardware. This is very much needed to reduce the wastage of time as well as money [8].

MICROPROCESSOR BASED EMBEDDED SYSTEM

Embedded Systems have been realized using a wide variety of micro processors, micro controllers, digital signal processors etc. The processors can be of different families like Intel, Motorola, Black fin, SHARC, Texas, Rabbit, Micro blaze, Pico blaze, NIOS, Power PC, ARM, etc. Peripherals being used can be either integral part of the processors used or separate individual ASICs. Programmable devices like FPGAs are explored to make system on chip design to gain advantage in Compactness, Power Consumption, Speed of operation and cost.

The following disadvantages have been found in the existing systems which need to be addressed to further improve the performance and capabilities of Embedded Systems:



- Functioning of a system depends on the architecture of the micro processor being used. If processor is changed total system needs to be changed.
- Embedded systems involve both hardware and software. Hence, persons with different skill set are required for efficient design.
- Large memory is required as software requires both ROM & RAM for storage of code as well as operands and results and also as Scratch Pad Memory.
- Additional resources like address decoding buffer/latches, multiplexing / demultiplexing, clock generation, etc are required.
- Microprocessor and Peripheral devices operate on different clock frequencies. Hence, multiple clock sources are required. Sometimes it is not possible with a single clock source to derive different clock frequencies as required for different peripherals.
- The ASICs being used are for multipurpose and hence include lot of functional modules. All of those functional modules need not be used for any single application. So, the power consumption is more and also the utilization of silicon is not proper.
- Component obsolescence is a threatening factor as the entire system must be redesigned in case of component obsolescence.
- There is very little scope for either upgrading or modifying the system.
- Speed of processing of the slowest devices in the system play a major role in the operation of the system and utilization of the processor capabilities.
- Software overheads will add to the data thereby reducing the effective data transfer rate.

Keeping in view all the above disadvantages of existing Embedded Systems, a Hardware programming is proposed which gives a suitable and conceptual solution for improving performance. [9- 11]

HARDWARE PROGRAMMING

Hardware programming is the innovative concept of realising embedded system without using a micro processor. All the controlling and coordinating activities of micro processor are realised using hardware description language. In this process all the peripherals as well as the activities to be done by the peripherals with respect to the system (in normal embedded system, software will do those activities) are modelled using hardware description language only. Block diagram of Hardware Programming based Man Machine Interface logic is given in **Figure 2**.

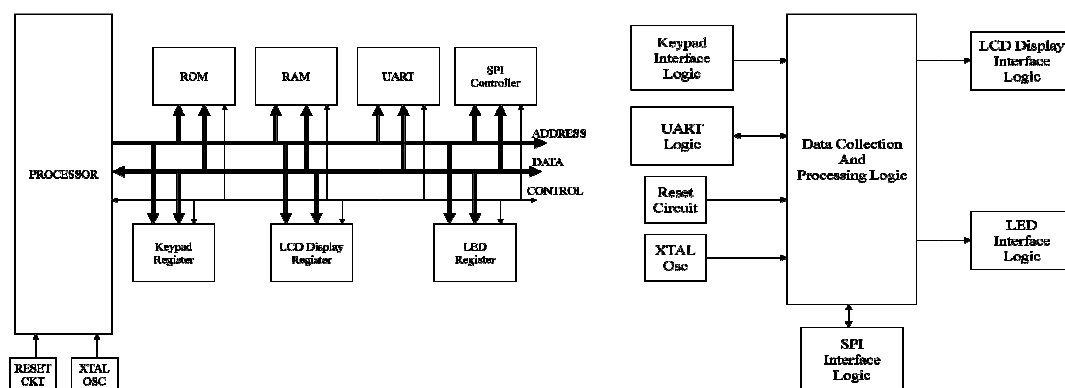


Figure 1 Block diagram of microprocessor based man machine interface logic

Figure 2 Block diagram of hardware programming based man machine interface logic

DESIGN APPROACH

For modelling Embedded System with hardware programming, the following things have been focused upon the Type of Interface, Timing of Signals, Protocol and Data Flow.

All the types of interfaces to the logic, through which data is being received or data is being transmitted, are analysed to arrive at a synchronization to ensure smooth and error free data transfer. The timing signals with respect to each interface are also generated to proper functioning of interface to avoid any data loss. Protocol in which data



is being transmitted or received is designed in such a fashion to ensure safe and error free data transfer without adding much to overheads. This allows the protocol used can be either standard or non-standard one.

Hardware programming concept focused on actual interface, the actual data transfer rate, the incorporation of actual data in a frame, extraction or insertion of the actual data in the frame being transmitted, and the mechanism of computation or storage.

This approach changed the focus from architecture of microprocessor / peripherals, scheduling of events, interrupt priorities, to actual data and its flow. Hence designer can do the data analysis in a much more reliable and economical manner.

All the interfaces of MMI are handled simultaneously by individual sub modules of MMI logic at the speeds of their signals. Data transfer rate and the size of the data word to be transmitted or received can be non-standard. The only limitation is they should fall in the range of parameters for the peripherals being used for the application [12].

DESIGN METHODOLOGY

Following is the design methodology adopted for Hardware programming.

- Identification of all the activities / functions to be performed by MMI.
- Dividing the logic into different functional sub modules, which can take up individual functions.
- Dividing each functional sub-module into events. Events are the activities done in a specific interval of time.
- Analysis of the protocols being used. In this process insertion of data into a frame and extraction of data from frame are addressed.
- Generation of timing signals for the individual events of all the functional sub-modules.
- Receiving data from respective interface.
- Processing of received data
- Storage of results computed
- Setting of different flags to enable data flow or to alert the process
- Transferring the data processed
- Enabling / Disabling the logic at appropriate intervals

BENEFITS OF HARDWARE PROGRAMMING

Following are the benefits observed when Embedded System is realised with hardware programming.

- Low power consumption
- Single source of clock input
- No requirement of additional resources
- Less memory requirement
- Optimized speed of processing
- No software overheads
- Effective utilization of silicon
- No architectural dependence
- Single skill set requirement
- Simplified design approach
- Reduced cost of development
- Easy design portability
- Good design flexibility
- Easy design upgradability
- No fear of component obsolescence [13-16].

PERFORMANCE EVALUATION

Performance of an embedded system is gauged with Performance Factor.

Performance Equation of a microprocessor based Embedded System is given below:

$$\text{❖ Performance Factor (Seconds/ Program)} = \text{Instruction Count} \times \text{Clocks per Instruction} \times \text{Clock Time} = (\text{Instructions / Program}) \times (\text{Seconds / Program}) \times (\text{Seconds / Clock})$$

Performance Equation of Hardware Programming based Embedded System is given below:



- ❖ Performance Factor of the system (Seconds / Program) = Maximum of (Performance Factor of Modules 1 to N in Seconds / Module)
- ❖ Performance Factor of a Module = Event Count \times Clocks per Event \times Clock Time = (Events / Module) \times (Clocks / Event) \times (Seconds / Clock)

SYSTEMS REALIZED WITH HARDWARE PROGRAMMING

Different modules are implemented using Hardware Programming. Details of some of the modules are given below.

All these modules are implemented without any processor even for data loading / unloading applications. Additional resources like Memory, Address Decoding, and Clock Generations Circuits etc., are not required. Block RAMs of FPGA are used for storing the data received or for data to be transmitted. Interfaces with non-standard values also could be realized. Hence the systems designed using hardware programming are suitable for highly confidential proprietary applications. Hardware programming ensured high data transfer rates due to simultaneous execution of events. Logic is realized using XC3S1600E FPGA of XILINX make and could be ported easily into other devices and also into other family devices with very minimal changes. Hence, component obsolescence will not be a problem to continue the embedded system designed using hardware programming [10-11, 13-16].

DEVELOPMENT OF ASYNCHRONOUS SERIAL INTERFACE ALONG WITH DATA COMMUNICATION

An Asynchronous Serial Interface is designed with the parameters: 22-bit data, Odd Parity, 2-Stop bits, and 1.024 Mbps Data Transfer Rate.

The resources utilized are 212 Slice Registers and 483 numbers of 4-input LUTs. One Block RAM of 16384×22 bit. These are very less compared to the resources that are required when designed using a microprocessor. Block Diagram of Asynchronous serial communication using hardware programming is shown in **Figure 3**.

DEVELOPMENT OF SYNCHRONOUS SERIAL INTERFACE ALONG WITH DATA COMMUNICATION

A Synchronous Serial Interface is designed with the parameters: 12-bit data, 1.024 Mbps Data Transfer Rate, and Single Chip Select for multiple slave devices.

The resources utilized for Master Logic are 184 Slice Registers and 374 numbers of 4-input LUTs. Two Block RAMs of 1024×12 bit each. And the Slave Logic consumed 154 Slice Registers and 322 numbers of 4-input LUTs. Two Block RAMs of 1024×12 bit each. These are very less compared to the resources that are required when designed using a microprocessor. Block Diagram of Synchronous Serial Communication using Hardware Programming is shown in **Figure 4**.

DEVELOPMENT OF SYSTEM BUS USING ASYNCHRONOUS SERIAL INTERFACE

An Asynchronous Serial Interface is designed as System Bus with the parameters: 12-bit data, 1.024 Mbps Data Transfer Rate, Odd Parity, and Two Stop Bits.

The resources utilized for Master Logic are 324 Slice Registers and 674 numbers of 4-input LUTs. Two Block RAMs of 4192×12 bit each. Slave Logic consumed 258 Slice Registers and 652 numbers of 4-input LUTs. Two Block RAMs of 4192×12 bit each.

Block Diagram of System Bus Transceiver using Asynchronous Serial Communication realized with Hardware Programming is shown in **Figure 5**.

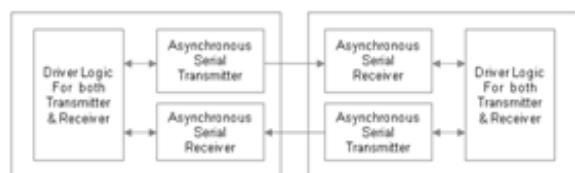


Figure 3 Asynchronous serial communication using hardware programming

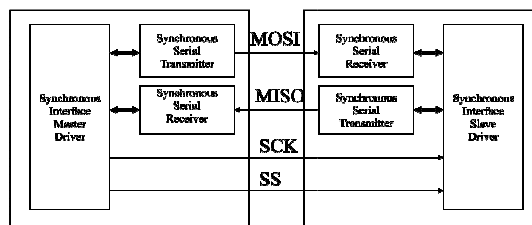


Figure 4 Synchronous Serial Communication using Hardware Programming



MENU DRIVEN OPERATIONS AND STATUS DISPLAY MECHANISM

Menu Driven Operations and Status Display Mechanism are designed with the following:

- 4 X 3 Keypad Interface,
- Two Row, 16 Characters per Row LCD Display Interface.

The resources utilized are 284 Slice Flip-Flops and 2254 numbers of 4-input LUTs. Block Diagram of Menu Driven Operations and Status Display Mechanism is shown in **Figure 6**. Timing Diagram of 12 bit Asynchronous Data Transfer is shown in **Figure 7**. Timing Diagram of 12-bit Synchronous Master Write Operation is given in **Figure 8**. Timing Diagram of 12-bit Synchronous Master Read Operation is given in **Figure 9**.

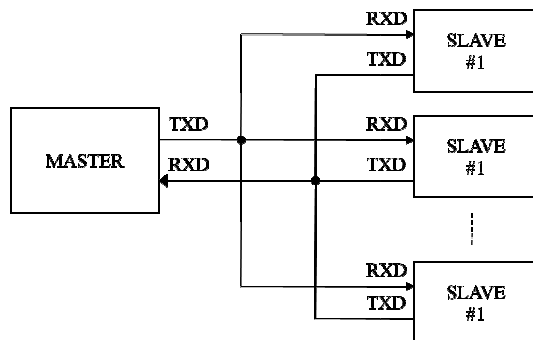


Figure 5 Asynchronous serial system bus transceiver using hardware programming

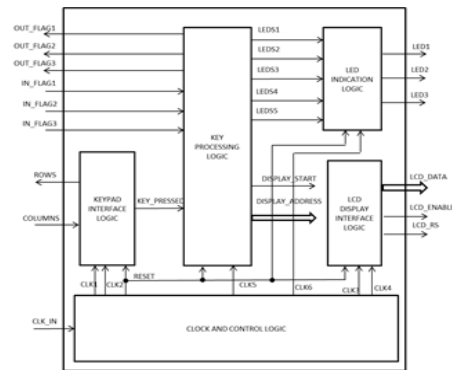


Figure 6 Menu driven operations and status display mechanism using hardware programming

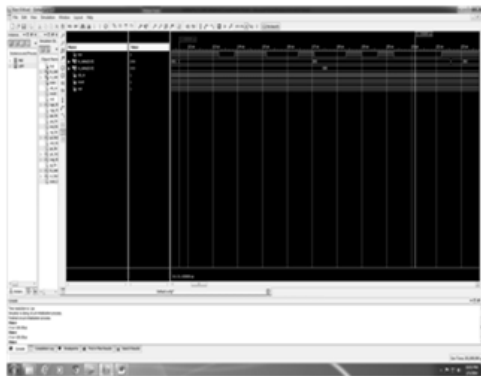


Figure 7 12 bit asynchronous data transfer

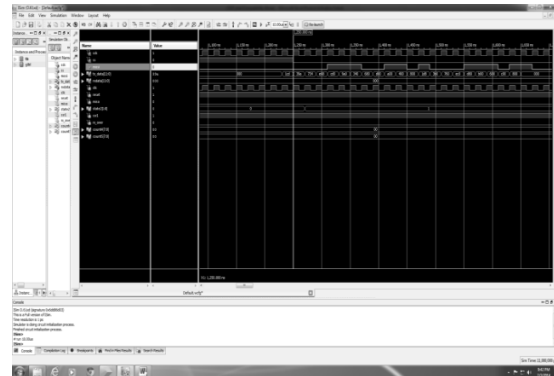


Figure 8 12-bit synchronous master write operation

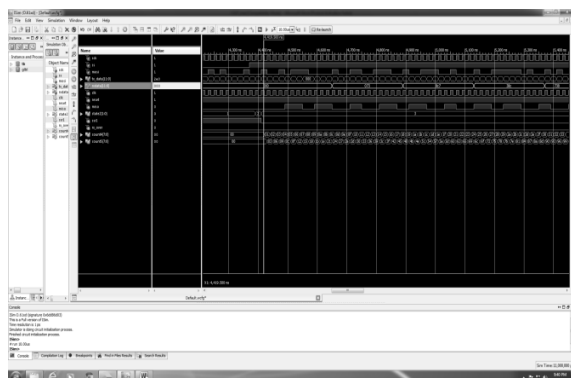


Figure 9 12-bit Synchronous Master Read Operation

Power consumption of microprocessor based system is of the order of a few hundreds of milli Watts. But Power consumption of Hardware programming based system is of the order of a few tens of milli Watts. An algorithm which required 100 operations consumed execution time of around 600 cycles of core clock of the microprocessor used. Whereas hardware programming based system consumed only 100 clock cycles and the clocks are of appropriate frequency, which in turn reduces the power consumption also. In microprocessor based system, different interfaces required different clock inputs. Hence, it is difficult to derive all the clock inputs from a single input clock source. But the Hardware Programming made the generation of clock inputs easy as different logics can be operated at different non-standard data transfer rates.

CONCLUSION

Concepts of Hardware Programming method of Embedded System design is best suited for the following cases:

- For the embedded system, in which peripherals operate at a wide variety of frequencies. This may lead to include a number of wait states or adopt DMA (Direct Memory Access) in case of Microprocessor based system. In Hardware programming such slow or fast operating modules are given appropriate clocks and flags are set at appropriate intervals. Rest of the related logic can be enabled or disabled to reduce the power consumption and smooth flow of data.
- For the embedded systems, wherein the peripherals or processor are of higher end and the resources of the processor / peripheral may be underutilized. With Hardware programming resource utilization can be very much optimized.
- Hardware programming is ideally suited for highly confidential proprietary applications.
- For embedded systems where all the activities are to be performed or completed at known time intervals, Hardware programming is recommended due to the fixed clock operations of Hardware involved.

Though approach of hardware programming technique is simplified, it requires thorough knowledge for an individual about the system including interfaces and protocols in addition to Hardware Design Concepts.

REFERENCES

1. Muhammad Ali Mazidi, Janice Gillispie Mazidi, The 8051 Microcontroller and Embedded Systems, Pearson Education, 2004.
2. Santanu Chattopadhyay, Embedded System Design, PHI Learning Private Limited, 2013
3. Fuming Sun, Xiaoying Li, Qin Wang, Chunlin Tang, FPGA Based Embedded System Design, Asia Pacific Conference on Circuits and Systems, DOI :10.1109/APCCAS, 4746128, pp 733-736, 2008.
4. Mahendra Vucha, Rajendra Patel, Arvind Rajawar, Dynamic Profiling Methodology for Rescue Optimization in Heterogeneous Computing System. Elsevier Science and Technology, DOI 10.1016/j.scs.2013.17, Volume 1, pp 41-46, 2013.
5. Koop Man, P, Embedded System Design Issues (the Rest of the Story), IEEE International Conference on Computer Design : VLSI in Computers and Processors, DOI : 10.1109/ICCD.1996.563572, pp 310-317, 1996
6. Paily Roy, Power-Delay Reduction in FPGA Implementations using Bypassing Technique, International Journal on Recent Trends in Engineering and Technology, DOI:10.1109/IJRTET.4.4.501, Volume 4, Issue 4, pp 111-115, 2010.
7. Ernst R, Codesign of Embedded Systems Status and Trends, Design and Test of Computers, DOI: 10.1109/54.679207, pp 45-54, 1998.



8. Sikun Li, Zhihui Xiong, Tiejun Li, Distributed Cooperative Design Method and Environment for Embedded System, Proceedings of the Ninth International Conference on Computer Supported Cooperative Work in Design, DOI :10.1109/CSCCWD.2005.194316, pp 956-960, 2005.
9. Wold W, Panel : Embedded Systems and Hardware-Software Co-Design: Panacea or Pandora's Box?, 30th Conference on Design Automation, DOI: 10.1109/DAC, 1993.203965, pp 308, 1993.
10. T.Harinath, K.Lal Kishore, Development of Customized Input Output Processor, International Journal of VLSI Design and Communication Systems, Volume 2, Issue 10, IJVDCS3313-197, pp 1069-1074, November 2014.
11. T.Harinath, K.Lal Kishore, Development of Versatile Multiplexer Logic, International Journal on VLSI Design and Communication Systems, IJVDCS7248-197, Volume 3, Issue 8, pp 1184-1191, October 2015.
12. T. Harnath, K.Lal Kishore, Hardware Programming as an alternative for Embedded System, International Journal on VLSI Design and Communication Systems, IJVDCS9724-70, Volume 04, Issue 5, pp 0357-0362, May 2016
13. T. Harnath, K. Lal Kishore, Development of Customized Interrupt Controller Logic, International Journal on VLSI Design and Communication Systems, IJVDCS7951-248, Volume 3, Issue 10, pp 1446-1449, December 2015
14. T. Harnath, K. Lal Kishore, Development of Customized Synchronous Serial Transceiver, International Journal of VLSI and Embedded Systems, ISSN: 2249-6556, Article 06364, Volume 5, pp 1054-1060, June 2014
15. T. Harnath, K. Lal Kishore, Development of Customized System Bus Transceiver, International Journal of VLSI and Embedded Systems, ISSN: 2249-6556, Article 06370, Volume 5, pp 1066-1073, June 2014.
16. T. Harnath, K. Lal Kishore, Development of Customized Asynchronous Serial Transceiver, Proceedings of 48th CST Infrastructure, Computer Society of India, pp 41-46, 13th – 15th December 2013.



Exploring Mechatronics System and Technical Investigation of Hydraulic and Pneumatic System Maneuver for Archetypal Engineering Applications

G.S. Mundada^{*1}, Rupesh C. Jaiswal¹, Zakee Ahmed¹

Department of Electronics & Telecommunication Engineering, Pune Institute of Computer Technology, Pune¹,
gsmundada@pict.edu*

ABSTRACT

Industry uses three methods for transmitting power mechanical transmission through gear, shaft, chain, and belts, while electrical transmission through wires, transformers and fluid power through liquid or gas in a confined space. Mechatronics is the synergetic integration of electronics engineering, mechanical engineering, computer engineering and electrical control engineering for design and development of electromechanical products. A rapid growth in Mechatronics observed in recent times is due to need of automation, Internet of Things (IoT), smart and intelligent devices. The hydraulic and pneumatic system are at the prime importance of mechatronics system. Hydraulic systems are complex fluid-operated systems that transfers energy to perform intended mechanical, measurement, control and operational work. These systems can serve many applications because of its small size-to-power ratios, ability to generate large torque for linear, rotational, oscillatory and reciprocative motion. The compact electro-hydraulic system further act as the limb to the physical system trading with the mechanical process and feasible deliverables. Hydrodynamic systems work with high flow rate and less pressure of fluid, whereas hydrostatic work with low flow rate and high pressure. Such systems work as a force multiplier that takes a smaller input force and transforms it into a bigger output force. Because of better power to weight ratio, these systems can deliver a noteworthy power to a load with a comparatively smaller mass. These characteristics allow them for aircraft applications where weight is most important. Life of equipment and components gets better because of self-lubrication phenomenon. These systems are rugged so as to operate in extreme temperature, environments and critical situation like reversal of motion. Pneumatics is derived from the greek term 'pneuma', which means breath or air. These system characterizes the behavior and application of compressed air. Pneumatic industrial systems work in a very analogous way to that of hydraulic industrial systems. The foremost dissimilarity is the high pressure air that is used instead of a fluid as it is more compressible and is much easier to store using reservoirs. Pneumatic systems are open systems, and exhausts the compressed air or any gas to atmosphere after its utilization, without causing any pollution. Hydraulic systems are closed systems and it re-circulates the oil or water after use. In manufacturing, pneumatics can turn out to be an effective alternative to electricity and may be a most prevalent and economical choice for implementing mechanical motion. This paper attempts to explore Mechatronics, present in general, the techniques used in Mechatronics engineering and in specific, to investigate hydraulic and pneumatic system maneuver for archetypal engineering applications.

KEYWORDS Mechatronics, Pneumatic systems, Hydraulic sytems, Design process, Force multiplier, Compression, Reservoirs

INTRODUCTION

Exploring Mechatronics System

The key elements of Mechatronics [1,3] systems can be classified as Information systems, Mechanical systems (connected with sensors and actuators components), Electrical systems (interfaced with ADC and DAC components), and Computer systems (includes controllers and display sections).

Figure 1 shows the key elements of Mechatronics System, which are:

- (a) Sensors [4] consisting Thermocouple, Strain gauge, Potentiometer, Switches, MEMS, Motion sensors etc.
- (b) Actuators [5,6] like Stepper motor, DC motor, Solenoids, Servomotor, Voice coils., Hydraulic actuators or Pneumatic actuators etc.
- (c) Electrical systems mainly consist of signal conditioning processes. Signal conditioning components used can be ADC, DAC, Amplifier, Filter, Rectifiers, Attenuators, Multiplexer and Demultiplexer, V to F and F to V converter, Isolation components, etc.
- (d) Digital controllers [7] like PLC (programmable logic controller), SBC, Logic circuits, Microcontroller, Communication controller, Arithmetic and Logic controller, Timing and Sequence controller etc.
- (e) Graphical displays used for visual feedback can be LCD, LED, CRT, TFT, Matrix displays.
- (f) Information systems [8] include the following important processes:

33rd Indian Engineering Congress, Udaipur, 2018: Technical Volume



- (1) System modeling process.
- (2) System analysis.
- (3) System design and development.
- (4) System testing.
- (g) Computer systems include hardware and software such as:
 - (1) Hardware (flip-flop, registers, counters, triggers, timers, microprocessors, ICs and other logic circuits).
 - (2) Software (low level and high level languages like C, assembly, FORTRAN, COBOL BASIC etc.).

Basically, mechatronics is the process of applying information system to physical systems (like mechanical, electrical and computer system). Sensors and actuators are used to transduce energy from mechanical side to electrical and computer side. Normally sensor output is electrical voltage.

Mechanical System [9] can include: (1) Fluid system, (2) Thermal system, (3) Acoustic system, (4) Pneumatic system, (5) Hydraulic system, (6) Chemical system, and (7) Other systems.

Most Mechatronics applications [10, 11] involve rigid-body systems and six fundamental laws are : (1) Newton's 1st law, (2) Newton's 2nd law, (3) Newton's 3rd law, (4) Newton's law of gravitation, (5) Parallelogram law for the addition of forces, and (6) Principle of transmissibility.

Recent Mechatronics systems can be classified into broad level as follows:

- Stand-alone system (CD player, auto-focus camera, washing machine etc.).
- System with high level of distributed relationships among.
 - Sensors.
 - Microcontrollers and
 - Actuators.
- Large factory system (also a distributed system) such as:
 - Automatic inspection stations etc.
 - Automated machining centers.
 - Multiple part handling robots.
- Artificial Intelligence [12, 13] based system or Intelligent control systems such as:
 - AI based smart home automation.
 - AI based security surveillance.
 - AI based warehousing system.
 - AI based fraud detection.
 - AI based automotive (cars, vehicles etc.).
 - AI based personal assistants.
 - AI based humanoid robot

MECHATRONICS DESIGN PROCESS

Mechatronics design [3, 16-21] process necessarily comprises of three phases as shown in **Figure 2**: (i) Modeling and simulation phase, (ii) Prototyping phase, and (iii) Deployment phase.

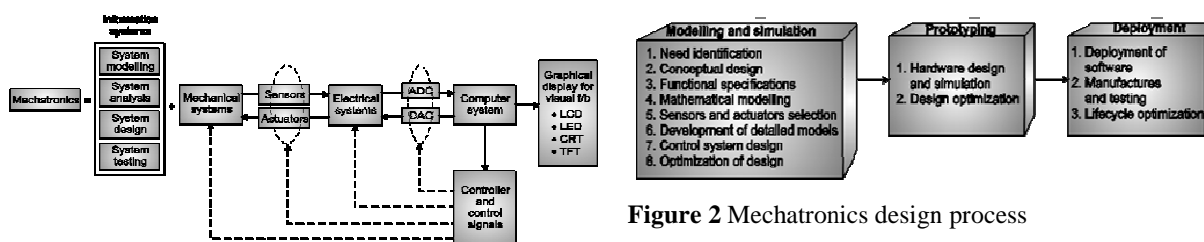


Figure 1 Key elements of mechatronics system

Figure 2 Mechatronics design process

Modeling and Simulation

Here, physical system (physical world problem) is represented by a suitable model so that it can represent the behavioral characteristics [14, 15] correctly.

Useful model explains all relevant aspects of a given situation [16, 17] and therefore used instead of experimentation to avoid cost of experimentation like labor, equipment and time etc. There are two broad categories of modeling techniques, like (a) Deterministic modeling and (b) Probabilistic modeling.

If outcomes or observations are always exactly the same if experiment is repeated under the same condition, then deterministic modeling is used (e.g. Kirchhoff's law: KVL and KCL). If outcomes vary when the experiment is



repeated under same condition, then probabilistic modeling is used. (communication and networks uses probabilistic modeling because of its uncertain and random behavior).

Computer simulation model [3, 18, 19] simulates or mimics the dynamics of a system. It is capable of representing system in greater detail than mathematical models but takes more computation time and hence they are slower than mathematical models. The representation of physical systems with mathematics also become highly complex and cannot be 100% accurate. Cost effectiveness and faster operations are the prime advantages of mathematical model.

Prototyping Phase: In this phase, non-computerized systems are replaced by actual hardware. Sensors and actuators are interfaced with input and output signal respectively. It is then connected with models, resulting in partial mathematical and real models. Mathematical model offers simulated [20, 21] response and real part delivers real time analysis in detail. These two parts are synchronized to optimize the design for further actual deployment.

Deployment Phase: This phase delivers final quality product. It also provides embedded software deployment [17] and lifecycle process with quality products [18] and proper maintenance. Some life cycle factors [16,19] are already explained in previous section like: (a) Maintainability, (b) Upgradability, (c) Delivery, (d) Disposability, (e) Reliability, and (f) Serviceability.

PHYSICAL COMPONENTS OF A HYDRAULIC SYSTEM

Hydraulic systems [17,18] are designed to move huge loads or extreme weight components by governing a high pressure fluid. This fluid is a part of reciprocating pistons and distribution lines and with system of different electromechanical valves.

A practical hydraulic system is shown in **Figure 3**. This system consists of a motorized pump to supply high pressure fluid. A pressure regular is used to limit or control the pressure in the given system. Control valves are used to control flow rates and pressures in this system. A distribution system shown here consists of various hoses of pipes and actuators. This actuator may be linear or rotary type.

Many hydraulic valve actuators [19,20] and related subsystems are powered by these types of arrangements.

Fluid is transferred from storage tank to cylinder and from cylinder to tank. It goes from tank to upper side of piston and then from lower side of piston to tank again. Pump converts a mechanical force into hydraulic power which is applied over upper portion of piston. Pressure regulator valve protects the system from high pressure. Also, excess fluid is also given back to the fluid tank. Cylinder uses moving fluid coming to upper part of piston to do the actual work. Cylinder movement is controlled by a control valve. Port 'M' is connected to pressure line and port 'N' to the tank for extending the cylinder. To reverse the motion, port 'N' is connected to the pressure line and port 'M' to the fluid tank. Speed control of the piston in cylinder is achieved by regulating the volume flow rates of the fluid to the cylinder.

The speed of piston in cylinder is given by :Velocity of piston (V_e) = $\frac{\text{Volume of fluid transferred in unit time}}{\text{Area of cylinder}} = \frac{V}{A}$

Also, the fluid in fluid tank must be very clean; hence a filter is necessary to remove dirt particles before the fluid passes from tank to pump which is operated by electric motor. A hydraulic pump [16, 17] is usually driven by an electric motor (e.g. a large A.C. induction motor) or an internal combination engine. The huge fluid pressure generated are used in heavy apparatus (e.g. construction equipment and large industrial machines) [17, 21] are in the range of 1000 psi (6.89 MPa) to 3000 psi (20.7 MPa).

The hydraulic fluid should have the following features:

- Decent lubrication to avoid wear and tear in continuously and fast moving components (e.g. between piston and cylinders).
- Corrosion resistance.
- Incompressibility to provide rapid response.

Most hydraulic pumps act by positive displacement, which means they deliver a fixed volume of fluid, with each cycle or rotation of the pump. The three main types of positive displacement pumps used in hydraulic related systems are vane pumps, piston pumps and gear pumps.

PHYSICAL COMPONENTS OF PNEUMATIC SYSTEM

Basic pneumatic system [17-19] depicted in **Figure 4**, comprises of the subsequent two parts: Production of compressed air, transportation system part and distribution system part and Consumption system of compressed air.



The detail modules of typical pneumatic systems are: Motor driven air compressor, Air receiver system, DCV (directional control valve), and Pneumatic cylinder.

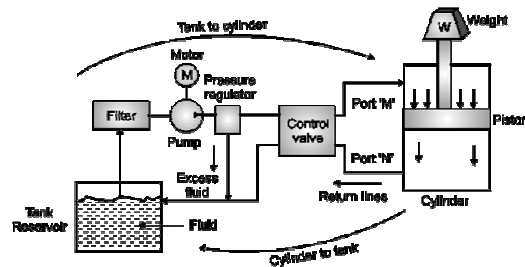


Figure 3 Typical hydraulic system

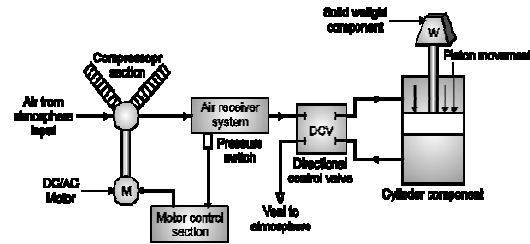


Figure 4 Pneumatic system in industry

Pneumatic system, as described in **Figure 5**, requires dry air which should be clean and free from dust and dirt. For this the filter system is used in the initial stages. Pneumatic system uses compressed air or compressed inert gas stored in a pressure vessel [19, 20] known as air receiver system. Filtered air is delivered to the air receiver by motor driven compressor.

Primary air treatment consists of air cooler and air separator. Air cooler [19] reduces the temperature of air after the process of air compression. Air separator removes water vapor from the compressed air. Air compressors are either diesel or electrically operated. Pressure increases because volume of compressed air is reduced in volume, effectively increases the pressure. It is basically used at a pressure of 6.5 kg/sq mm to 8.5 kg/sq mm. Maximum force up to 50 kN can be developed. The movement of the cylinder part is controlled by a DCV (Directional Control Valve) which directs the air into various parts of cylinder. Control valves [16, 17] are basically used to regulate the pressure, control the pressure and monitor the pressure. Also, the same is applicable for control of direction flow. The excess air from cylinder is removed and released to the atmosphere using DCV section.

SIGNAL FLOW IN PNEUMATIC SYSTEM

Energy sources used in pneumatic system uses following components as shown in **Figure 6**: (a) Air compressor, (b) Air pump, (c) Air receiver, (d) Air filter, and (e) Air regulator.

Input elements used in pneumatic system are: (a) Sensors, (b) Limit Switches, (c) Control Valves, and (d) Push Buttons.

Processing elements used in pneumatic system are: (a) Flow Control Valves (FCV), (b) Pressure Control Valves (PCV), and (c) Directional Control Valves (DCV).

Final control elements/actuating devices used are : (a) Linear Actuators and (b) Rotary Actuators.

The system transmission comparison between Pneumatic and Hydraulic system is given in **Table 1**.

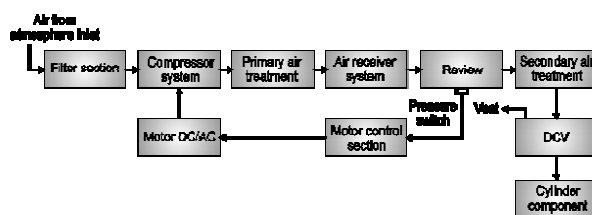


Figure 5 Components of pneumatic systems

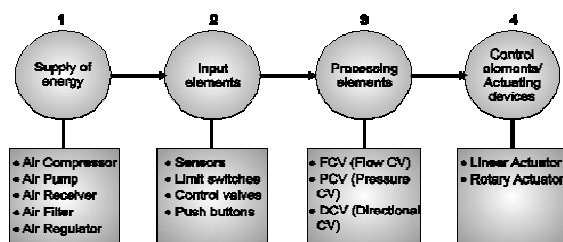


Figure 6 Pneumatic system signal flow

Table 1 System transmission comparison

Characteristics	Pneumatic	Hydraulic
Speed of operation	Fast speed	Slow speed
Position accuracy resulted	Good amount	Good amount
Efficiency delivered	Low efficiency	Low efficiency
Reliability achieved	Excellent reliability	Good reliability
Difficulty	Simple type	Medium type



Hardware Maintenance	Low	Medium
Utilities in systems	Compressor/power/ pipes	Pump/power/pipes
Control mechanism	Simple valves system	Simple valves system
Maintenance cost applicable	Low cost	High cost
Final Operating cost	Medium cost	High cost
Size of system	Low size/force	Very low size/force
Cost of purchase resulted	Low cost	High cost
Peak Power delivered	High amount	Very high amount

CONCLUSION

Mechatronics is the integration of electrical, mechanical and microprocessor control system. The traditional approach designs mechanical and electrical components separately and then connects together. The contemporary practice uses the integrated approach of Mechatronics engineering design. Different types of Mechatronics Systems are developed and used in different product manufacturing process like:

- (i) Control Systems:
 - Open loop control system.
 - Close loop control system.
 - ❖ Regulatory system,
 - ❖ Follow-up-system,
 - ❖ Servo mechanism system,
 - ❖ Continuous data F/B control system,
 - ❖ Sampled or discrete data control system.
- (ii) Automatic Control System Applications:
 - Furnace pressure control system,
 - Temperature control in a metal melting furnace,
 - Water level control system,
 - Temperature control in refrigerator,
 - Thrust and flight control system,
 - Photoelectric control system,
 - Shaft speed control system.
- (iii) Sequential Control System Applications:
 - Electric water heater system,
 - Electronic washing machine system.
- (iv) Microprocessor based Control System:
 - PLC based applications,
 - Automatic camera system,
 - Automatic camcorder system,
 - CD player system.

Thus hydraulics systems and pneumatics systems are simply a relatively small constituent of Mechatronics branch as a whole. Integration of electronics processes with hydraulics systems in Mechatronics applications are being widely used nowadays. Accordingly professionals should have basic as well as advance knowledge in the open loop control system and close loop control system with respect to Mechatronics. Thus entire success of design and related Mechatronics system functions requires different specialist from the areas like electronics engineering, mechanical engineering, computer engineering and control engineering.



FUTURE SCOPE

Mechatronics is one of the best brushwood if someone desires to be in the field like robotics, CNC, automation area and electro-mechanical production. Several internship programs, R&D projects are being offered internationally in the area of Mechatronics. Mechatronics engineering offers jobs to engineers in the area of R&D, production and service industry. It also offers jobs to service engineers to maintain equipments related to it. Mechatronics along with hydraulics and pneumatics gives efficient, quality concerned and safe manufactured product for end consumers at individual and industry level perspective. Emerging Mechatronics along with hydraulics and pneumatics products offers reliable computing to produce a simpler, more cost-effective and trustworthy system. In future, the Mechatronics system along with hydraulics and pneumatics products will provide accurate designing, systematic assembly, precise testing, and efficient evaluation of components and products.

ACKNOWLEDGMENT

Authors are grateful to HoD, Department of Electronics and Communication Engineering and Principal, Pune Institute of Computer Technology for providing resources to carry out the research and experiments and for their motivation and support.

REFERENCES

1. Y. Tang, Y. Li, Development of a laboratory HILs test bed system for small UAV helicopters, Proceedings of the IASTED International Conference on Robotics (Robo '11), Pittsburgh, Pa, USA, pp.428–436, November 2011.
2. Museum, Victoria, Albert. Catalogue of the mechanical engineering collection in the Science Division of the Victoria and Albert Museum, South Kensington, with descriptive and historical notes. Ulan Press. 2012.
3. G. Reinhart, M. Weissenberger, Multibody simulation of machine tools as mechatronic systems for optimization of motion dynamics in the design process, Proceedings of the IEEE/ASME International Conference on Advanced Intelligent Mechatronics (AIM '99), Atlanta, Ga, USA, pp. 605–610, September 1999.
4. D. K. Miu, Mechatronics, Springer, Berlin, Germany, 1993.
5. Brian S. Elliott, Compressed Air Operations Manual, McGraw Hill Book Company, 2006, ISBN 0-07-147526-5.
6. N. Wakami, H. Nomura, S. Araki, Fuzzy logic for home appliances, Fuzzy Logic and Neural Networks, C. H. Chen, Ed., McGraw-Hill, New York, NY, USA, pp. 21.1–21.23, 1996.
7. Heeresh Mistry, Fundamentals of Pneumatic Engineering, Create Space e-Publication, ISBN 1-49-372758-3, 2013.
8. H. S. Cho, Opto-Mechatronic Systems Handbook: Techniques and Applications, CRC Press, Boca Raton, Fla, USA, 2003.
9. D. A. Bradley, D. Dawson, N. C. Burd, and A. J. Loader, Mechatronics: Electronics in Products and Processes, Chapman and Hall, London, UK, 1991.
10. M. F. Zaeh, T. Oertli, and J. Milberg, Finite element modelling of ball screw feed drive systems, CIRP Annals, Volume 53, Number 1, pp. 289–293, 2004.
11. B. M. Cleery, N. Mathur, Right the first time, Mechanical Engineering, Volume 130, Number 6, pp. 30–34, 2008.
12. J. Lee, E-manufacturing-fundamental, tools, and transformation, Robotics and Computer-Integrated Manufacturing, Volume 19, Number 6, pp. 501–507, 2003.
13. Mendoza G A, Baumgartner B, Schreiber U, Krane M, Knoll A, Bauernschmitt R. Automebic: Fuzzy control development platform for a mobile heart-lung machine. Volume 25/7 of IFMBE Proceedings. pp 685–688, 2009.
14. Schreiber U, Eichhorn S, Mendoza A, Baumgartner B, Bauernschmitt R, Lange R, Knoll A, Krane M. A new fuzzy controlled extracorporeal circulation system. first results of an in-vitro investigation. CINC, Volume 36, pp 497–500, 2009.
15. Karnopp, Dean C., Donald L. Margolis, Ronald C. Rosenberg, System Dynamics: Modeling and Simulation of Mechatronic Systems, 4th Edition, Wiley, ISBN 0-471-70965-4 Bestselling system dynamics book using bond graph approach, 2006.
16. W. Boltan, Mechatronics: Electronic Control Systems in Mechanical and Electrical Engineering, 6th Edition, Pearson Education, 2016.
17. David Alciatore, Michael B. Hstand, Introduction to Mechatronics and Measurement Systems, 4th Edition, Tata McGraw Hill 2013.
18. K.P. Ramachandran, G.K. Vijayaraghavan, M.S. Balasundaram, Mechatronics-Integrated Mechanical Electronic Systems, Wiley Publication 2008.
19. Nitaigour P. Mahalik, Mechatronics-Principles, Concepts and Applications, Tata McGraw Hill, Eleventh reprint 2011.
20. Devdas Shetty, Richard A. Kolk, Mechatronics System Design, Thomson India Edition. HMT Limited, — Mechatronics, Tata McGraw-Hill Publishing House, 2007.



Circular Patch Partial and Slotted Ground with Rectangular CSRR Metamaterial Antenna for Wireless Application

Dheeraj Pandey^{*1}, Paras¹, Mitesh Upreti¹

Department of Electronics and Communication, College of Technology (COT), GBPUA&T Pantnagar¹,
d.pandey2711@gmail.com*

ABSTRACT

In this paper circular patch with Complementary Split Ring Resonator (CSRR) structure and partial ground antenna for Wireless Communication is presented. CSRR structure is used to reduce the antenna size and gain increment. Partial ground and slots are used to enhance the bandwidth of antenna. FR-4 epoxy substrate having permittivity of 4.4 and loss tangent of 0.02 with dimension of $35 \times 30 \text{ mm}^2$ and height of 1.6 mm is used to design the antenna. High Frequency Structure Simulator (HFSS 15.0) software is used to design and simulate the antenna. Proposed antenna resonates below -10dB return loss in the frequency band of 2.85-11.4 GHz and 16.35 to 19.5 GHz with the bandwidth of 8.55 and 3.15 GHz respectively. Simulated result shows antenna having peak gain of 9.57 dB at 16.6 GHz and maximum efficiency of 97.5% at 4.3GHz.

KEYWORDS Metamaterial, WLAN, WiMAX, Backward wave propagation, Miniaturization.

INTRODUCTION

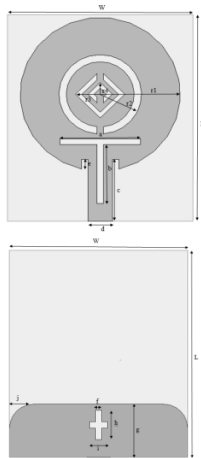
Wireless communication requires electromagnetic signals to propagate the information from one point to another. Antenna used as a transducer, is an eminent part of wireless communication [1]. As a result of technological advancement, the size of antennae has been greatly reduced and a single antenna should be capable of performing several distinct functions [2]. To incorporate a large variety of functions in a single antenna of small size, metamaterials have been used. Metamaterials do not occur naturally and have properties beyond normal materials[3]. Metamaterials are also known as double negative material (DNG), negative index material (NIM) or Left Hand (LH) materials and are manmade materials having negative permittivity and/or negative permeability [4]. Thin Wire (TW) and split ring resonator (SRR) structures are two of the most widely used metamaterial structures to get negative-permittivity and negative-permeability, respectively [5,6]. TW structure has high inductance which indirectly affects the effective permittivity of material [7] and SRR structure behaves like artificial dipole and is thus magnetic in nature [8]. Use of metamaterial structure changes the forward wave propagation into backward wave propagation by changing the sign of refractive index [9]. Refractive index plays an important role in propagation of light from one medium to another and is directly related to the permittivity and permeability [10]. Metamaterial allows for the propagation of electromagnetic waves by building a left-handed triad of electric field, magnetic field and phase constant in contrast to a right-handed triad in normal materials [11].

ANTENNA DESIGN

The proposed structure of the antenna is shown in **Figure 1** and its design parameters are illustrated in **Table 1**. Proposed antenna is printed on a $35 \text{ mm} \times 30 \text{ mm}$ FR-4 epoxy substrate having relative permittivity of 4.4 and loss tangent of 0.02 with 1.6 mm of thickness. The antenna is designed with a circular patch using transmission line model (TLM) for 3.2 GHz (used for radiolocation services). Inset feeding is used in the design to match the impedance of the transmission line with the antenna that slightly increases the antenna gain. The ground plane is used as a radiator and its dimensions control some of the antenna characteristics such as return loss [12]. Optimization is done to improve the S_{11} parameter. The reduction in the ground length using optimization and the best return loss characteristics are obtained when the ground length is approximately equal to the feed length. The comparison of return loss characteristics between full ground length and reduced ground length is shown in **Figure 2**. The reduced ground structure shows the improvement in bandwidth while maintaining a higher gain. The circular patch has been further modified by cutting a Rectangular CSRR with a circular slot. The CSRR structure with the circular slot is used to obtain metamaterial properties. The dimensions of CSRR unit cell are $18 \text{ mm} \times 18 \text{ mm}$ as shown in **Figure 3**. The permittivity and permeability values of CSRR unit cell, calculated using Nicolson-Ross-Weir (NRW) method [13] in MATLAB software are shown in **Figure 4**. NRW method requires real and imaginary parts of S_{11} and S_{21} to calculate real and imaginary parts of permittivity and permeability. Unit cell exhibits the negative values of permittivity at 2.5 GHz, 3.5 to 5.5 GHz and 6.5 to 7.2 GHz, 9.6 GHz while negative values of permeability at 6 to 6.8 GHz and 7.8 to 10 GHz. CSRR structure enhances the gain as well as bandwidth of antenna and shifts the resonating band towards lower frequency band as shown in **Figure 5**. Slots in the feed and ground plane are used to increase the effective current flow path which leads to an increase in the bandwidth of the antenna.



Optimization in the slot width and length is used to get better results. **Figure 6** shows that the bandwidth of antenna has been increased by etching the slots in the ground exactly opposite to the feed line.



(a) Patch view (b) Ground view

Table 1 Proposed antenna design parameters

Parameters	Length, mm	Parameters	Length, mm
r_1	13	E	1.65
r_2	6.7	F	1
r_3	4	G	9
r_4	2	H	5
a	13	I	3
b	10	J	4
c	10.5	L	35
d	4	W	30

Figure 1 Proposed antenna design configuration

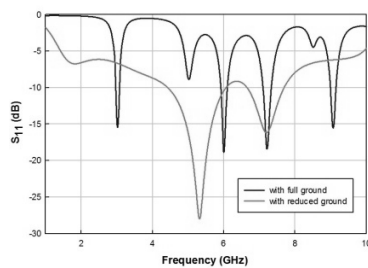


Figure 2 Comparison of simulated S_{11} with full ground and reduced plane

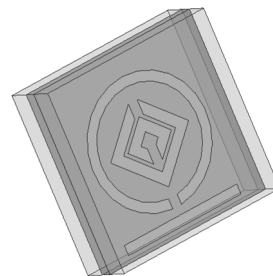


Figure 3 CSRR unit cell

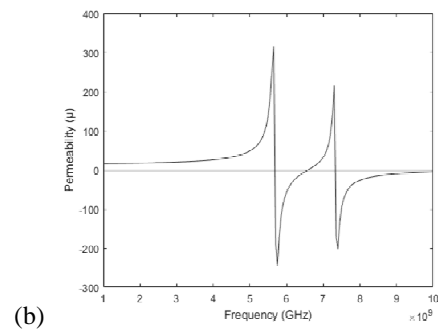
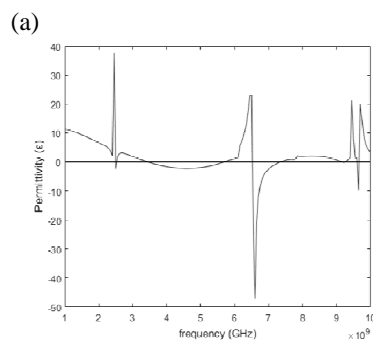


Figure 4 Permittivity and permeability of CSRR structure

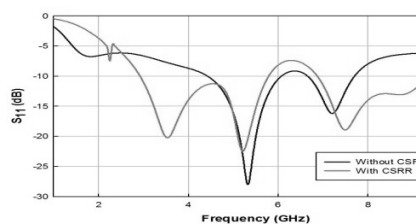


Figure 5 Comparison of simulated S_{11} with and without CSRR structure

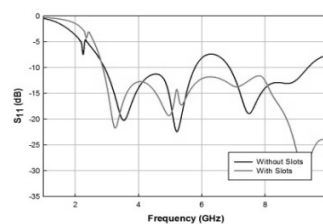


Figure 6 Comparison of simulated S_{11} with and without slots

RESULT AND DISCUSSION

HFSS designing software is used to simulate the proposed antenna at the set up frequency of 3.2 GHz. Simulated S_{11} in **Figure 7** shows that proposed antenna can propagate in the frequency range of 2.85 to 11.4 GHz and 19.35 to 19.5 GHz with the bandwidth of 8.55 GHz and 3.2 GHz, respectively. Major resonating peaks are at 3.2 GHz, 5 GHz, 9.2 GHz and 17 GHz with S_{11} value of -21.7 dB, -19.2 dB, -30.7 dB, -19.5 dB, respectively. **Figure 8** shows VSWR values between 1 to 2 in the range where $S_{11} \leq -10$ dB. **Figure 9** shows that the peak gain of proposed antenna is 2.73 dB at 3.2 GHz and it increases with the frequency and it reached upto 9.5 dB at 17 GHz. Simulated efficiency is above 70% in the entire resonating frequency region and reaches upto 97% at 3.2 GHz and 9.2 GHz as shown in **Figure 10**.

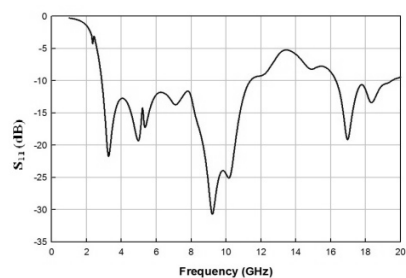


Figure 7 Simulated S_{11} of proposed antenna

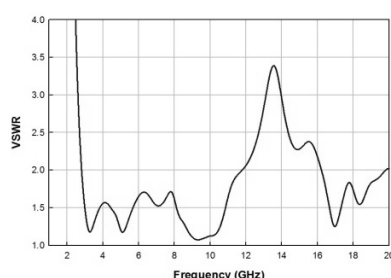


Figure 8 Simulated VSWR of proposed antenna

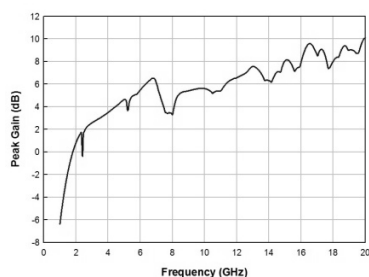


Figure 9 Simulated peak gain of proposed antenna

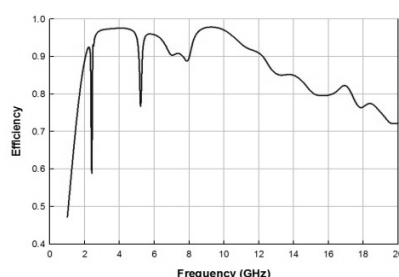


Figure 10 Simulated efficiency of proposed antenna

CONCLUSION

A circular patch antenna along with rectangular CSRR structure and partial ground has been illustrated in FR-4 epoxy substrate. Proposed antenna can be used for WLAN (3.6/4.9/5/5.9 GHz) and WiMAX (3.3/3.5/5.8 GHz), C band (4 to 8 GHz) and X band (8-12 GHz) applications. Proposed work shows that using partial ground and slots in patch and ground can be used to increase the impedance bandwidth of antenna. CSRR structure with negative values of permittivity and permeability can be used for antenna miniaturization and to gain improvement.

REFERENCES



1. C. A. Balanis Antenna Theory Analysis and Design, 2nd Edition, John Wiley & Sons, 1997.
2. A. M. Abbosh, Miniaturized Microstrip-Fed Tapered – Slot Antenna with Ultra Wide Band Performance, IEEE Antennas and Wireless Propagation Letters, Volume 8, pp. 690-692, 2009.
3. V. G. Veselago, The Electrodynamics of Substances with Simultaneously Negative Values of ϵ and μ , Sov. Phys. Uspekhi, Volume 10, Number 4, pp. 509–514, 1968.
4. Christophe Caloz, Tatsuo Itoh, Electromagnetic Metamaterial Transmission line theory and Microwave Application, John Wiley & Sons, 2006.
5. J. B. Pendry, A. J. Holden, D. J. Robbins, W.J. Stewart, Low frequency plasmons in thin-wire structures, J. Physics, Volume 10, pp. 4785–4809, 1998.
6. J. B. Pendry, A. J. Holden, D. J. Robbins, W.J. Stewart, Magnetism from conductors and enhanced nonlinear phenomena, IEEE Trans. Microw, Theory Tech., Volume 47, Number 11, pp. 2075–2084, 1999.
7. Q. Gang, J. F. Wang, M. B. Yan, W. Chen, H.Y. Chen, Y. F. Li, Lowering plasma frequency by enhancing the effective mass of electrons: A route to deep sub-wavelength metamaterial, Chinese Phys. B, Volume 22, Number 8, pp. 1–7, 2013.
8. D.R. Smith, W.J. Padilla, D. C. Vier, S. Schultz, Composite Medium with Simultaneously Negative Permeability and Permittivity, pp. 1–4, 2000.
9. A. Grbic, G.V. Eleftheriades, Experimental verification of backward-wave radiation from a negative refractive index metamaterial, journal of applied physics, Volume 92 10, pp. 5930-5935, 2002.
10. S. A. Ramakrishna, Physics of negative refractive index materials, Reports Prog. Phys., Volume 68, Number 2, pp. 449–521, 2005.
11. D. A. Kirzhnits et al., Experimental Verification of a Negative Index of Refraction, Volume 292, pp. 77–79, 2001.
12. M. Koohestani, M. N. Moghadasi, B. S. Virdee, Miniature microstrip-fed ultra-wide band printed monopole antenna with a partial ground plane structure, IET Microwave antenna propagation, Volume 5, Number 14, pp. 1683- 1689, 2011.
13. A. M. Nicolson. Measurement of intrinsic properties of material by time domain technique, IEEE Trans, On Inst. And Meas. Volume IM-19 Number 4, pp. 377-382, 1970.



A Metamaterial based Micro-strip Triangular Patch Antenna having Angular Steep with Triangular SRR and Defective Ground for Dual-Band Applications

Mitesh Upreti¹, Paras¹, Dheeraj Pandey¹

Department of Electronics and Communication, College of Technology, GBPUA&T, Pantnagar¹, miteshupreti@gmail.com*

ABSTRACT

This paper presents a metamaterial-based antenna having a triangular patch and Split Ring Resonator (SRR) structure with a defective ground antenna for Wireless Communication. Angular steeps have been etched along the three vertices of the patch for return loss improvement. The SRR structure is used to reduce the antenna size and to obtain increment in gain. Ground size has been reduced by optimization and a rectangular slot has been added to enhance the bandwidth. FR-4 epoxy substrate having permittivity of 4.4 and loss tangent of 0.02 with the dimensions of $32 \times 32 \text{ mm}^2$ and height of 1.6 mm is used to design the antenna. The antenna has been designed and simulated using High Frequency Structure Simulator (HFSS 13.0) software. Proposed antenna resonates at single frequency 4.5 to 7.4 GHz and 9.7 to 13.5 GHz having bandwidth of 2.8 and 3.8 GHz, respectively. Simulated result shows antenna peak gain of 9.57dB at 16.6 GHz and maximum efficiency of 97.5% at 4.3 GHz.

KEYWORDS Micro Strip patch antenna, Dualband, Angular steeps, SRR structure, Metamaterial, Defected Ground Structure (DGS)

INTRODUCTION

The designing of an efficient small size antenna for various applications is a major challenge. The Micro Strip patch antennae have found extensive applications owing to their advantages such as low profile, low fabrication cost and ease of integration with feed network [1-3]. The principal disadvantages of micro strip antennae are narrowband width, poor efficiency and size[4]. The miniaturization of antenna and improvement in bandwidth can be achieved by etching a slot in the ground and using metamaterial structures such as SRR and CSRR [5]. Metamaterial is a term given to defects which can be created either in the substrate, in the ground, or in other parts of the antennae. Such antennae with metamaterials have negative permeability and permittivity and thus are known as left handed (LH) materials. Metamaterial structure usage changes refractive index sign thereby changing the forward wave propagation into backward wave propagation [6]. Refractive index is directly related to the permittivity and permeability and plays an important role in the propagation of light from one medium to another [7]. Metamaterials help to build a left-handed triad of electric field, magnetic field and phase constant in contrast to normal materials which display a right-handed triad thus allowing for the propagation of electromagnetic waves [8]. It is better to have a dual band antenna than to have two different antennae to work at two different frequency ranges.

Split ring resonator (SRR) and Thin Wire (TW) structures are two of the most widely used metamaterial structures to get negative-permeability and negative-permittivity, respectively [5,6]. The effective permittivity of material is indirectly affected by the high inductance of TW structure [7] and SRR structure acts as an artificial dipole and is consequently magnetic [8]. Defected Ground Structure (DGS) is a kind of miniaturization technique which has been applied along with metamaterials in this antenna [9].

In this paper a triangular patch is designed at the center of the substrate and then angular steeps have been added along the three vertices of the triangular patch. The antenna is miniaturized by adding two triangular SRR structures along with thin wires below them[10]. Return loss characteristics have been improved by optimization of the ground structure. The later is reduced to 9 mm. DGS has been employed by creating a rectangular slot to improve the gain and bandwidth. The proposed antenna resonates at two frequency bands 4.5 to 7.4 GHz and 9.7 to 13.5 GHz which lie within the Wireless (4.9 GHz, 5GHz, 5.9 GHz), WiMAX (5.8 GHz), WIFI (5 GHz), C band (4 to 8 GHz) and X band (8 to 12 GHz).

ANTENNA DESIGN

The proposed antenna has been designed using FR-4 glass epoxy substrate with permittivity of 4.4, dielectric tangent loss of 0.02 and substrate thickness of 1.6 mm. The dimensions of the proposed antenna are 32 mm \times 32 mm. The geometry of the proposed antenna is shown in **Figure 1(a)**, which is the top view of the antenna and **Figure 1(b)** shows the bottom view. Further, its design parameters are illustrated in **Table 1**. The height of the substrate is taken to be 1.6 mm.

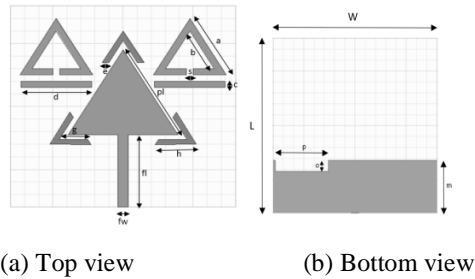


Figure 1 Proposed antenna

Table 1 Proposed antenna design parameters

Parameters	Length, mm	Parameters	Length, mm
a	10.392	h	1.65
b	6.928	fl	11.5
c	1	fw	1.6
d	10	m	9
e	1	o	2.4
s	1	p	10.4
pl	15.58	W	32
g	4.03	L	32

Design Configuration

The antenna was initially designed using transmission line model without the SRR structure. The initial dimensions thus were $40 \times 40 \text{ mm}^2$. After parametric study and miniaturization with the help of the SRR structure, the optimized dimensions of the proposed antenna were calculated to be $L = 32 \text{ mm}$, $W = 32 \text{ mm}$. The optimization of the size of the proposed antenna was carried out using Ansoft HFSS software. The ground was also optimized similarly and the best results were obtained at $m = 9 \text{ mm}$. **Figure 2** shows the comparison of return loss characteristics (S_{11}) between full ground and defected ground. The S_{11} parameters are inversely proportional to the reduction in the ground size until the optimum value of $m = 9 \text{ mm}$.

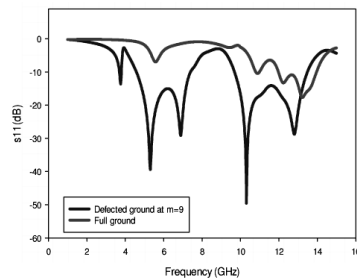


Figure 2 Comparison of simulated S_{11} between full ground and defected ground

SRR structure is incorporated in the antenna design with the use of a triangular ring along with a slot at the base of the ring and a thin wire is added just below the base of the triangular ring as shown in the **Figure 3(a)**. The symmetry of the structure has been maintained by adding two SRR structures at the top of the patch. The permittivity and permeability values of the SRR unit cell was calculated using Nicolson-Ross-Weir (NRW) method [11,12] in MATLAB Software 4 [**Figure 3(b)**, **Figure 3(c)**]. NRW method requires real and imaginary parts of S_{11} and S_{21} to calculate the real and imaginary parts of permittivity and permeability. Unit cell exhibits the negative values of permeability at 3.8 GHz, 6.8 to 7.3 GHz, 9.4 to 10.8 GHz while negative values of permittivity at 3.8 GHz, 7.8 GHz, 8.3 GHz as shown in **Figure 3(b)** and **Figure 3(c)**. The return loss comparison of proposed antenna with SRR and without SRR in **Figure 4(a)** shows that the SRR structure enhances the gain as well as bandwidth of the antenna and shifts the resonating band towards lower frequency band. The reduction in the ground also increases the peak gain of the proposed structure as shown in **Figure 4(b)**. Full ground structure displays lower peak gain than that displayed by defected ground structure.

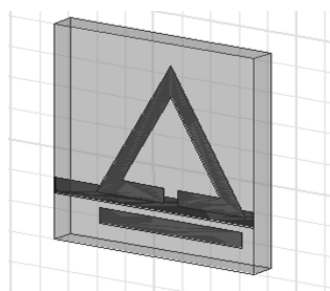


Figure 3(a) SRR unit cell

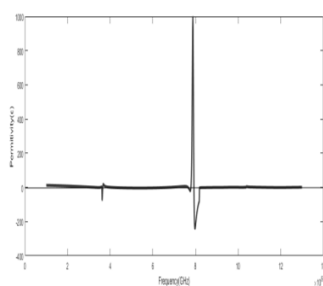


Figure 3(b) Permittivity of Unit Cell

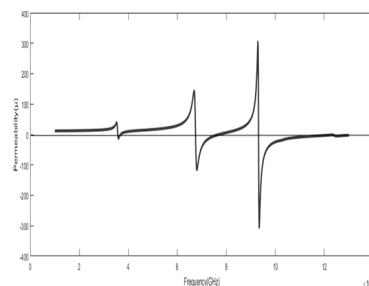


Figure 3(c) Permeability of unit cell

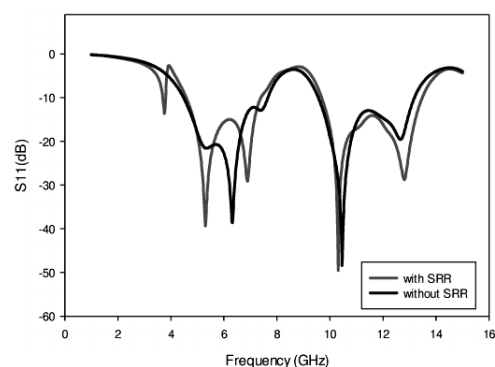


Figure 4(a) Comparison of Simulated S_{11} with SRR against without SRR

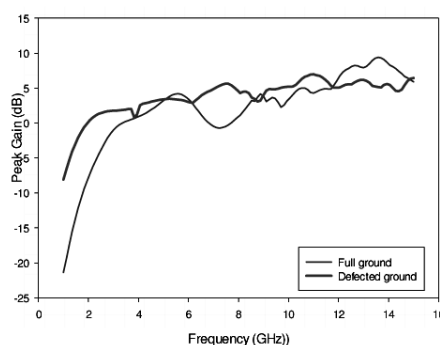


Figure 4(b) Comparison of peak gain with full ground and defected ground

RESULT AND DISCUSSION

Simulation was accomplished by utilizing Ansoft's high frequency structural simulator (HFSS). Metamaterial-based triangular patch antenna with angular steps and SRR structures resonates at 4.5-7.4 GHz and 9.7- 13.5 GHz with the bandwidth of 2.8 and 3.8 GHz, respectively. A comparison of S_{11} parameters is shown in **Figure 5(a)**. The defected ground structure at $m=9$ shows improvement in bandwidth and return loss characteristics as compared to reduced ground structure at $m=9$ with or without SRR structures. **Table 2** shows the comparative values. The frequency against peak gain curve of defected ground structure is also positive with gain always greater than 3 dB around the resonating frequencies as shown in **Figure 5(b)**. At the resonating frequencies 4.5 to 7.4 GHz and 9.7 to 13.5 GHz the peak gain is between 3.041 to 5.62 dB and 5.072 to 5.173 dB, respectively.

The polar plot of the proposed antenna at 5 GHz and 10 GHz is 3.4 dB and 5.58 dB (**Figure 6**).

Figure 7(a) shows that VSWR values fall in the range of 1 to 2 at all the points where $S_{11} \leq -10$ dB. Simulated efficiency is above 70% in the entire resonating frequency region and has reached upto 97% at 5.8 GHz and 10.5 GHz as shown in **Figure 7(b)**.

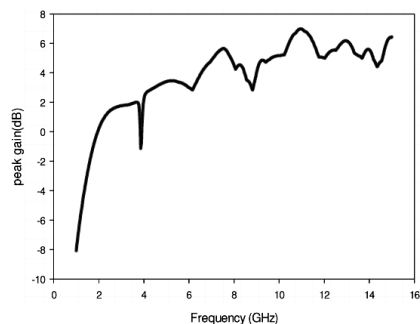


Figure 5(a) Comparison of return loss of characteristics

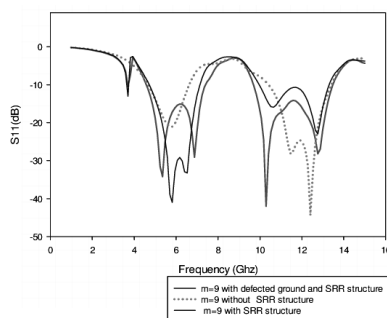
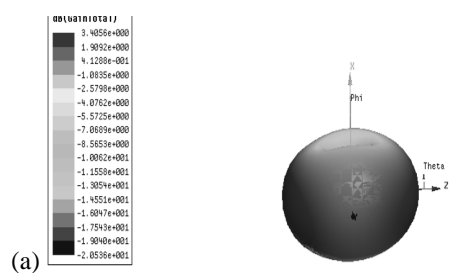
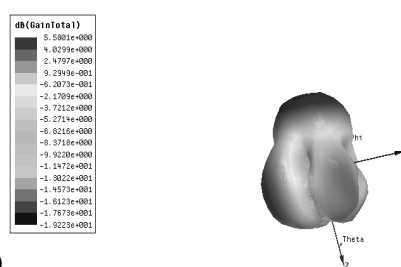


Figure 5(b) Simulated peak gain of proposed antenna



(a)



(b)

Figure 6 Polar plot of proposed antenna at (a) 5 GHz and (b) 10 GHz

Table 2 Comparative values for different kinds of the antennae

Details of the antenna	Resonant Frequency, GHz	Bandwidth, GHz
Reduced ground without SRR structure	4.6-6.6,10.4-13.4	2,2
Reduced ground with SRR structure	4.7-7.1,9.9-11.5,11.5-13.3	2.4,1.6,1.8
DGS with SRR structure (proposed)	4.5-7.4, 9.7- 13.5	2.8, 3.8

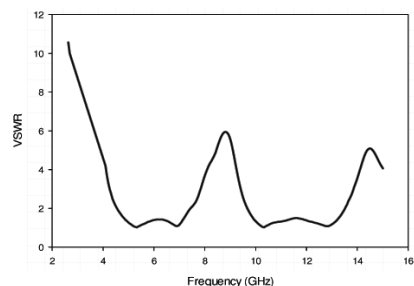


Figure 7(a) Simulated VSWR of proposed antenna

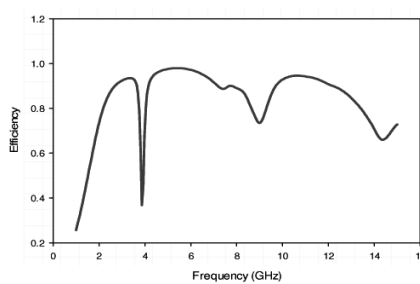


Figure 7(b) Simulated efficiency of proposed antenna

CONCLUSION



A compact metamaterial-based dual-band antenna having a triangular patch and Split Ring Resonator (SRR) structure with a defective ground structure has been designed for wireless communication applications covering Wireless (4.9 GHz, 5 GHz, 5.9 GHz); WiMAX (5.8 GHz); WIFI (5 GHz); C band (4 to 8 GHz) and X band (8 to 12 GHz). Essential parametric variations are carried out in order to find the optimum reduced ground length. The antenna resonates at 4.5 to 7.4 GHz and 9.7 to 13.5 GHz. The peak gain in the resonating frequencies is always between 3.041 to 5.62 dB and 5.072 to 5.173 dB, respectively. These bands are used for various communication systems. Micro strip feeding technique has been utilized. The antenna is simulated in HFSS.

REFERENCES

1. N. Herscovici, New considerations in the design of microstrip antennas, IEEE Trans. Antennas Propag., Volume 46, Number 6, pp. 807–812, 1998.
2. C. Science, Non-leaky Conduct or- baeke d Coplanar Waveguide-fe, September, pp. 94–99, 1997.
3. R. B. Waterhouse, S. D. Targonski, and D. M. Kokotoff, Design and performance of small printed antennas, IEEE Trans. Antennas Propag., Volume 46, Number 11, pp. 1629–1633, 1998.
4. O. T. Letters, J. Wiley, S. Dey, R. Mittra, and C. Engineermg, Compact microstrip patch antenna, Volume 13, Number 1, pp. 12–14, 1997.
5. J. B. Pendry, A. J. Holden, D. J. Robbins, W. J. Stewart, Low frequency plasmons in thin-wire structures, J. Physics, Volume 10, pp. 4785–4809, 1998.
6. J. B. Pendry, A. J. Holden, D. J. Robbins, Stewart. Magnetism from conductors and enhanced nonlinear phenomena, IEEE Trans. Microw, Theory Tech., Volume 47 Number 11, pp. 2075–2084, 1999.
7. Q. Gang, J. F. Wang, M. B. Yan, Chen W., H. Y. Chen, Y. F. Li. Lowering plasma frequency by enhancing the effective mass of electrons: A route to deep sub-wavelength metematerial, Chinese Phys. B, Volume 22, Number 8, pp. 1–7, 2013.
8. D. R. Smith, W. J. Padilla, D. C. Vier, S. Schultz. Composite Medium with Simultaneously Negative Permeability and Permittivity, pp. 1–4, 2000.
9. P. Dawar, A. De, Tunability of Triangular SRR and Wire Strip (TSRR-WS) Metamaterial at THz, Volume 2014, 2014.
10. A K Arya, A Pattnaik, Gain Enhancement of Micro-strip patch antenna using Dumbbell shaped Defected Ground Structure, December 2013.
11. A. B. Numan, M. S. Sharawi, Extraction of Material Parameters for Metamaterials Using a Full-Wave Simulator, Volume 55, Number 5, pp. 202–211, 2013.
12. A. M. Nicolson. Measurement of intrinsic properties of material by time domain technique, IEEE Trans, On Inst. And Meas. Volume IM-19, Number 4, pp. 377-382, 1970.



LPWAN Technology Enabling Industrial IoT Applications for Energy Intensive Industries

Surendra Kumar Dogra

National Aluminium Company Ltd. Angul, Odisha, surendradogra136@gmail.com*

ABSTRACT

In the present global scenario energy has been identified as one of the key driving factors for facilitating economic and social development of a country. As such the economic growth and [energy consumption](#) are interdependent functions and serves as an indicator to the standard of life in a country. Our country India is placed among the rapidly growing developing countries in the world which requires meeting of rapidly growing energy demand which otherwise results into imminent energy crisis and therefore requires immediate measures to be adopted to lessen the impact of such crisis. Under the situation analysis and reduction of energy consumption can be a deterministic factor to ensure overall energy economy. At present specific energy consumption of Indian manufacturing industries is on the higher side as compared to rest of the world. Hence, reduction of specific energy consumption in the Indian manufacturing industries is an imminent challenge. Data acquisition, analysis and controlling factors which influence the Energy Management in a particular industry are solution for improvements in the reduction of the specific energy consumption. There are identified five numbers of major energy intensive manufacturing industrial sectors in India. Aluminium, Iron and Steel, Cement, Fertilizer and Textile, of which Aluminium industry is the most energy intensive followed by [iron and steel industry](#) and together they consume more than 60% of the energy in this sector.

KEYWORDS EI, LPWAN, IoT, LoRa, Pot

INTRODUCTION

Consumption of energy per unit of the output produced is termed as specific energy consumption of a machine or system. However the total energy consumption in an industry depends upon various radical factors in addition to the direct energy consumed by the machines during the production process. Therefore, we shall use the common conceptual term 'Energy Intensity' which is also an indicator for evaluating the efficiency of the energy being utilized in an industry and economy by large. Energy Intensity (EI) is also defined as the energy consumed per unit output in the context of [industrial energy](#) practices. Also, it is a key factor to determine future energy projections against demand. Energy intensity is inversely related to [energy efficiency](#); lesser is the energy consumed for the production of a unit of output in terms of goods or services, the greater is the energy efficiency of the system.

India being a fast developing country, the issue of achieving the desired levels of energy efficiency in the energy intensive industrial sectors through lower levels of energy intensity needs special attention. This needs application of distinct technologies to meet such targets. Understanding of the factors which influence the trends in the energy intensity is a required step for [energy conservation](#) and basis for the projection of energy consumption needs in the future. In this context, various factors affecting the energy intensity and their usefulness as indicators in reducing the energy intensity are briefed below. The purpose of this paper is to identify and devise techniques for control of these factors having direct impact on energy intensive Indian manufacturing industries and their potential towards reduction in Energy Intensity in Cement, Iron and Steel, Textiles, Aluminium and Fertilizer Industries

Dependent Factors for Energy Intensity

Energy Intensity (EI) which is often used for the measure of energy efficiency. In the technical concept, energy efficiency increases when either energy inputs are reduced for a given level of output or there is increased or enhanced output for a given amount of energy inputs. As energy efficiency increases, the Energy Intensity is reduced. The various explanatory variables having impact on the Energy Intensity in the selected industrial sectors are explained as follows :

- Labor : This factor has positive impact towards EI of industry therefore larger labor force deployment will make an industry more labor intensive and therefore more Energy Intensive. This intensity can be somewhat reduced by application of Machine to Machine (M2M) and Internet of Things (IoT) applications under industry 4.0 standards.
- Repair and Maintenance : This has positive impact towards EI of industry therefore more repairs and maintenance expenditure of plant and machineries implies inefficient operation and hence lead to a larger value



of Energy Intensity. This can be reduced by real time monitoring of machine parameters through applicable condition monitoring class IoT Sensors.

- **Technology Development:** This has positive or negative impact towards EI of an industry. In our country due to lack of R&D activity technology development is one of the source of knowledge enrichment by an industry. The Technology Development is likely to affect the Energy Intensity (EI) in either ways depending upon its nature of application. However conversion to automated systems shall have a reduction effect on EI.
- **Raw Materials and Spares:** This has negative impact on EI of industry. Availability of raw materials and spares at competitive pricing shall bear inverse relation to Energy Intensity. More the availability of raw material and spares better will be the Energy Intensity.
- **Job outsourcing :** This has positive or negative impact towards EI of an industry. More the expenses on outsourcing in the industry better will be the Energy Intensity (EI) due to reduced volume of direct labor but only up to a threshold defined limit.
- **Software applications:** This has positive or negative impact on the EI of an industry. Software application is also directly related to Energy Intensity in either ways due to nature and complexities of the job involved. This can be improved with implementation of Artificial Intelligence applications under Industry 4.0 standards.
- **Plant and Machinery :** This has positive impact towards EI of an industry. Better is the Plant and Machinery efficiency better would be the energy efficiency. This can be improved with application of automated systems and M2M communications under Industry 4.0 standards.
- **Profit after Tax:** This has negative impact on the EI of an industry. An increase in the profit after taxes means that the industry has become efficient and therefore better is the Energy Intensity.

It can be concluded from above that reduction in the overall Energy Intensity can be achieved by concentrating on its dependent factors and adopting appropriate measures to optimize them. Any such optimization attempt shall need acquisition of real time data, its analysis and adoption of control measures derived thereof. In this context IoT based applications connected through Low Power Wide Area Network (LPWAN) as its backbone can play a crucial role towards wide area real time data connectivity.

A careful examination of the above factors that influence the energy intensity in an industry would reveal that various IoT application sensors (things) can be devised to fetch real time target data streams that can be manipulated into meaningful information for achieving optimization of that particular factor or factors. The sub systems below are indicative of various functional and data applicability:

- **Access Control:** Access control to specified areas and detection of people in non-authorized areas
- **Occupancy Detection:** Detect people engaged in different areas with their numbers
- **CCTV Surveillance:** Detect people and objects available in a specified area along with motion detection.
- **Remote Control:** Remote operation of equipment for energy saving purpose
- **Machine Health:** Monitoring of vibrations and conditions in plants and machinery for failure analysis
- **Water Leakages:** Detection of liquid leaking from storage tanks and pipe lines with pressure variations
- **Smart Lighting:** Intelligent control and weather adaptive lighting system installed in shop floors and interconnecting passages
- **Smart Grid System:** Energy consumption monitoring and management
- **Energy and Water Consumption:** Energy and water supply consumption monitoring system to save cost and resources
- **Solar Plant Installations:** Monitoring and performance optimization of solar energy plants
- **Moisture Sensing:** Moisture detection in data centers, warehouses and sensitive buildings to prevent break downs and corrosion of electronic equipments
- **Noise Level:** Noise level monitoring in shop floor areas and silence zones in real time
- **Traffic:** Monitoring of vehicles and pedestrian traffic to optimize driving and walking routes
- **Waste Management :** Detection of trash levels in dumps to optimize the garbage collection logistics



- Air Pollution : Toxic gas emissions level monitoring from factories and vehicles
- Potable Water Quality : Monitor the quality of drinking water and generate alerts beyond threshold levels.
- Radiation Levels: Distributed measurement of radiation levels due to presence of nuclear devices and generate alerts for leakage hazards
- Explosive and Hazardous Gases : Detection of hazardous gas levels and leakages in industrial environments
- Early Detection of Earthquake : Distributed control in specific places of seismic activity for alerts
- Effluent Leakage Detection : Detect leakages and wastes of factories in industrial discharge drains
- Tank Level : Monitoring of water, oil levels in storage tanks.
- Silos Stock : Measurement of level and weight of the material available in silo.
- Supply Chain Control: Monitoring of movement of goods along the supply chain and tracking
- Smart Product Management: Control of products availability in shelves and warehouses to automate restocking levels
- Quality of Shipment Conditions : Monitoring of vibrations, strokes, container openings or cold chain maintenance for insurance purposes.
- Item Location: Search of items in large yards or warehouses
- Storage Incompatibility Detection: Warning on storing inflammable goods enclosures which are close to others containing explosive material
- Fleet Tracking: Control of routes followed for transportation of goods and merchandises.
- Smart Parking: Monitoring of parking spaces availability and their utilization
- Payment Gateway Transactions : Monitoring of bills processed for party payments
- Meteorological Station Network: Study of weather conditions in a geographical location to forecast rain, snow or storm
- Non-intrusive Electrical Load Monitoring: This is a cost effective and convenient means of electrical load and status monitoring, since it requires fewer components therefore requires lesser space and faster installation.

We shall now discuss various means of wireless connectivity with above sensors in the field through the available wireless wide area network technologies.

Term Definitions

Industrial wireless sensor networks (IWSN) are a key technology facilitating industrial sensing, monitoring, and process automation; eliminating the need for special industrial cabling for harsh environments, guaranteed level of Quality of Service (QoS) with mesh networking and channel hopping features.

Machine-to-Machine, (M2M) term in general describes any technology that enables networked devices to exchange information among them and perform desired actions without any manual intervention.

The internet of things, or IoT, is a system of interrelated computing devices, sensors, machines, objects, animals or people that are assigned with unique identifiers (UIDs) and their ability to transfer data over a network without requiring human or computer interaction.

LPWAN Technology Overview

Low Power Wide Area Network (LPWAN) consists of various low power consuming WAN technologies available from different vendors in discrete configurations. LPWAN operates in licensed or unlicensed radio frequencies bands and works on proprietary or open standard platforms. The newly emerging LPWAN fills a unique niche of wireless connectivity that ensures long battery life over long range (typical 30 km). LPWAN technology can best serve M2M and IoT applications, automated metering, non-critical monitoring, alarm and security systems and other applications that do not require latency to be deterministic. In the long run, industrial connected wireless sensing, tracking, and control devices will rely upon LPWAN technology and will account for major share in the shop floor connectivity.

LPWAN technologies available from globally reputed vendors have been discussed in this article and comparative study of the features have been demonstrated in **Table 1**.



Table 1 LPWAN Technologies comparison table (<http://industrialgateways.eu>)

	 LoRa™	 sigfox	 3GPP	 QR®
Type	CDMA, open	UNB, closed	LTE	Short range, mesh, open
Standardization	Proprietary	Proprietary	Standardized	Proprietary
Availability	now	now	wide scale by 2020	now
Frequency	868MHz (Europe), 915MHz (North America) unlicensed spectrum	868MHz (Europe), 915MHz (North America) unlicensed spectrum	5 different bands- 5 different HW modules, 3 different European bands, licensed spectrums	868MHz (Europe), 915MHz (North America) unlicensed spectrum
Bandwidth	125KHz	100KHz	180KHz	100KHz
Uplink bandwidth	0.3-50kbps, 500x10 bytes/day	100bps, 140x12 bytes/day	250kbit/sec	20kbps
Downlink bandwidth	0.3-50kbps	4x8 bytes/day	20kbit/s	20kbps
Coverage (db)	157dB	149dB	164dB	120dB
Devices per AP	UL: >1 mil. DL: > 100k	<1M	<100k	239
Output power	75mW	25mW	25mW	12mW
Battery life	10y+	10y+	10y+	10y+
Bidirectional	Class dependent	No	Yes	bidirectional
Security	32bit, multilayer AES-128	16bit	3GPP(128-256bit)	multilayer, AES-128
Scalability	Medium	Low	High	Medium
Location support	Yes	No	Need GPS	-
Software	stack	on chip	on chip	OS+DPA+APP
Gateway	Many mfg	Proprietary	Expensive license cost 5G cellular networks	Few mfg
Nodes	Many mfg	Many mfg	Not widely available yet	Few mfg
Business Model	Private networks, Network operators	Own platform	Telcos as network operators	Own platform
Typical Urban range/Rural range	3Km / 15Km	3Km / 50Km	Cellular Network (15Km)	24Km/72Km
Typical application	Utilities, Smart cities, smart agriculture	Utilities, Smart cities, smart agriculture	Small business, B2C	building automation, telemetry, lighting control
Pros/Cons	Open standard and Lowest Cost/future interfering	Low cost/Proprietary	Best Coverage/Expensive	Mesh network/Proprietary

LoRa

The LoRa, specified and backed by the [LoRa Alliance](http://loralliance.org), transmits in several sub-gigahertz frequencies in the unlicensed band, making it less prone to interference. LoRa is short for ‘Long Range’ and requires end-devices that consume extremely low powers of the order of 10 to 25 mW. The physical (PHY) layer transmits data through FM Chirp Spread Spectrum (CSS) radio modulation technique with forward error correction (FEC) and a Media Access Control (MAC) layer with the LoRa wide-area-network (LoRaWAN) protocol (**Figure 1**). While the network can transmit and receive at many frequencies between 150 MHz and 1 GHz, LoRa technology operates in the 915-MHz band in the United States, the 868-MHz band in Europe, and the 433-MHz band in Asia. All are unlicensed industrial, scientific, and medical (ISM) bands. With a maximum throughput of 50 kbps with channel aggregation, LoRa transceivers from Semtech Corporation (for example, the SX1272) can operate with three programmable bandwidths: 125 kHz, 250 kHz, and 500 kHz.

Sigfox

The proprietary, unlicensed Sigfox is one of the most widely deployed LPWANs of today. Running over a public network in the 868 MHz or 902 MHz bands, the ultra-narrowband technology only allows a single operator per country. While it can deliver messages over distances of 30-50 km in rural areas, 3-10 km in urban settings and up to 1,000 km in line-of-site applications, its packet size is limited to 150 messages of 12 bytes per day. Downlink packets are smaller, limited to four messages of 8 bytes per day. Sending data back to endpoints can also be prone to interference.

NB-IoT

Narrowband Internet of Things (NB-IoT) operates on existing LTE and Global System for Mobile (GSM) infrastructure. It offers uplink and downlink rates of around 200 kbps, using only 200 kHz of available bandwidth.

NB-IoT and LTE-M are both 3rd Generation Partnership Project (3GPP) standards that operate on the licensed spectrum. While they have similar performance to other standards, they operate on existing cellular infrastructure, allowing service providers to quickly add cellular IoT connectivity to their service portfolios. In 3GPP LTE Release 13 and 14, NB-IoT was standardized for providing wide-area IoT connectivity for M2M communications and other enhanced features. Some vendors, including Orange and SK Telecom, are deploying both licensed and unlicensed technologies to capture both markets.



IQRF

IQRF is a technology for low power, low speed, low data volume, reliable and easy to use wireless connectivity in License free sub-GHz ISM bands, worldwide (434, 868, 916 MHz) for telemetry, automation in industry and buildings. With a RF output power up to 12.5 MW, programmable range 240 hops, up to 600 m/hop up to 240 hops with very low power consumption. It can be used whenever there is a need of wireless remote control, monitoring of remotely acquired data or connection of devices to a wireless network. IQRF is extremely easy to implement. IQRF is based on wireless RF Transceivers (TR). Operating System (OS) supporting networking which makes them powerful but unusually easy to apply.

LPWAN against Cellular, RF, Mesh

Bluetooth, [Zigbee](#) and Wi-Fi are more suitable technologies for WLAN and localized IoT connectivity. Many IoT applications particularly in industrial, city based and commercial deployments require LPWAN where large numbers of low power devices require connectivity in a wider area that can be supported in a cost effective manner.

Unlike earlier wireless technologies, LPWAN provides battery efficient, wide area connectivity, enabling more M2M and IoT applications that were previously prohibitive due to cost. However, a major trade-off is the amount of data that can be transmitted. Yet, according to estimates, 85% of all IoT devices use less than 3 MB of data per month, and 3 GPP estimates that 99.9% of LPWAN devices will use less than 150 kb of data per month.

Cellular networks often suffer from poor battery life and may have gaps in coverage. Cellular technologies are also subjected to frequent sunset. As many IoT devices are deployed for 10 years or longer, sun-setting cellular coverage is not a feasible option.

LPWAN Applications

With decreased power requirements, longer ranges and lower costs than traditional mobile networks, LPWANs enable a number of M2M and IoT applications, many of which were previously constrained by budgets and power requirement issues. Choosing an LPWAN depends on the specific application, namely the desired speed, data amounts and area covered (**Figure 2**). LPWANs are suitable for applications which do not require frequent uplinking of messages. Most LPWAN technologies also have downlink capabilities.

LPWANs are commonly used in applications including [smart metering](#), smart lighting, asset monitoring and tracking, [smart cities](#), precision agriculture, livestock monitoring, energy management, manufacturing, and [industrial IoT](#) deployments.

LPWAN Security

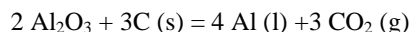
Different LPWAN technologies offer varying levels of security. Most include device or subscriber authentication, network authentication, identity protection, [Advanced Standard Encryption \(ASE\)](#), message confidentiality and key provisioning.

The Future of LPWAN

As newer technology, the LPWAN is constantly evolving and getting mature. With many technology developers it is not clear who will lead from the front, especially as the markets expand. Long term performance of each LPWAN technology is also uncertain, as many are still in their initial rollouts and real world testing are yet to be completed.

Typical Applications in the Aluminium Smelters

Aluminium is produced through Hall- Heroult process which is called Aluminium smelting process and is used industrially. Thus, liquid aluminium is produced by the electrolytic reduction of alumina (Al_2O_3) dissolved in an electrolyte (bath) mainly containing Cryolite (Na_3AlF_6). The overall chemical reaction can be written as:



During the electrolytic reduction process in the reduction pot lots of electrical energy is consumed in the form of DC Power which has specific norms at 13,500 kWh/ton of liquid metal produced. Further during the reduction process Carbon Anodes are consumed in the Pot Cells of Pot lines, which needs to be produced in Carbon Plant. A lot of energy is also needed to produce Carbon Anodes from Coke and Pitch in terms of electrical and fuel oil. Therefore being a potential Energy Intensive sector, applications that enables as detailed in the Energy Intensity analysis and by using real time data from LPWAN through can be used to determine instantaneous current and temperature distribution in the current carrying anode stems and cathode collector bars of electrolysis cell (Pot) can be deterministic in making operational changes and parameters for saving in DC power as well as improve current

efficiency and fugitive emissions of the process. Another application can be to monitor electrical power consumption by auxiliary equipment and plants for improvements in overall energy audit of Aluminium smelter and thereby improving its energy efficiency. This can be achieved through application of IoT sensors to all such energy consuming equipment such as electrical motors, furnaces, lighting etc.

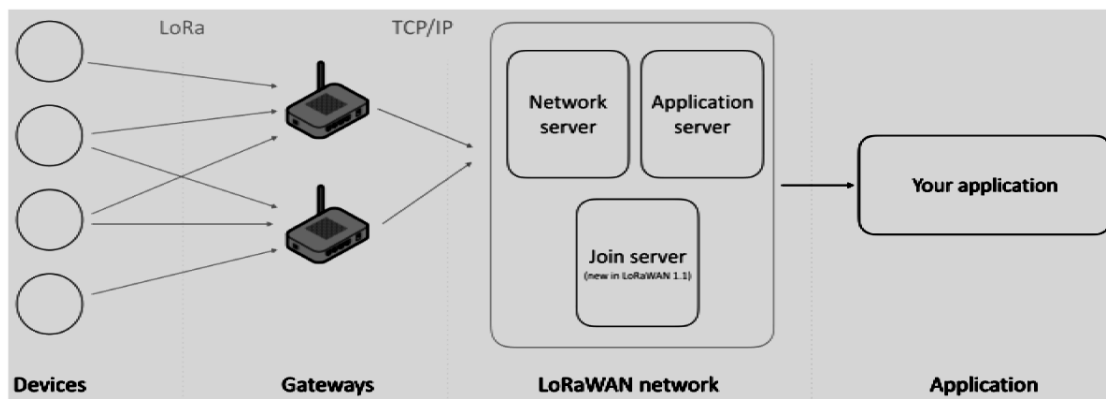


Figure 1 LoRa WAN logical connectivity (Source: <https://os.mbed.com/>)

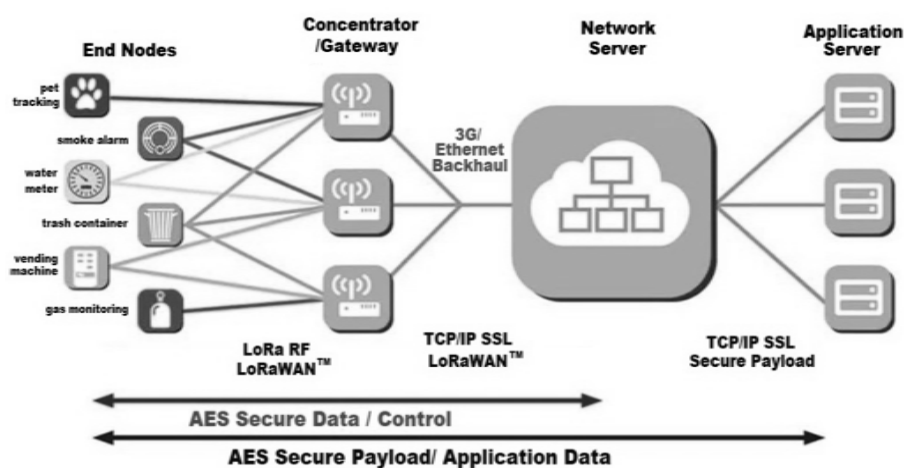


Figure 2 LPWAN architecture for IoT devices (Source: <https://biblio.ugent.be>)



Field based Observations of ECG Analysis in Night-Workmen using Time Series Analysis for Ascertaining of Circadian Rhythm

M. Srinagesh^{*1}, J. V. Anand¹

Department of Electronics and Communication Engineering, PACE Institute of Technology and Sciences, Andhra Pradesh¹,
srinagesh@pace.ac.in*

ABSTRACT

The impact of health constrains upon night workers is one of the pioneering area of research. This work focuses on circadian studies with heart rate. Circadian studies are mostly associated with melatonin secretion produced by pineal glands. Melatonin secretion has correlation with heart rate. The two signaling regularities taken pertaining to this work of heart rate taken are PR interval and QRS interval. Heart Beat Rhythm using Temporal and Frequency Components for Circadian Studies (HBRTFCs) has been proposed. In the clinical examination five patients were taken for sample study with age, duration of work, weight, blood pressure, body temperature and heart rate. Then the temporal components of PR interval and QRS interval are plotted against the respective voltages. Two samples are taken with heart rate from clinical values and the left ventricular and right ventricular are checked for permissible limits using Cardio-vascular Simulator. Statistical analysis is done with time series analysis using exponential smoothing for the impact of signaling interval and there corresponding voltage levels. The results reveal that there is a strong impact with circadian rhythm and heart rate. Hence, forecasting has been done with exponential smoothing were in lower and upper confident limits of amplitude is done for the PR interval. In addition, forecast is also done for predicting the lower and upper confident limits of QRS interval. Both the metrics predicts the lower and upper confident interval providing a feedback to the night workmen.

KEYWORDS Circadian clock, Heart rate, Time series analysis

INTRODUCTION

The biological aspect focusing on oscillators can be categorized into three divisions [1]. The first one denotes 'ultradian' which denotes a period less than twenty hours. The second which denotes 'infradian' with period greater than thirty hours. Finally, 'circadian' where the period lies between twenty and thirty hours.

International Classification of Sleep Disorder (ICSD) third version [2] build upon the prior version ICSD 2 states that sleep wake disorder can be categorized. The following were the main contributions of the disorder with regard to circadian rhythm, 'delayed sleep wake phase', 'advanced sleep wake phase', 'irregular sleep wake', 'Non continuous twenty four hour sleep wake process', 'shift work' and finally 'jet lag'.

The electrical activity of the brain and heart are the two important biomedical signals to be analyzed.

Electroencephalogram (EEG) analysis the brain, and Electrocardiogram (ECG) analysis the heart. This work focuses on shift work and its impact with field based study using Electrocardiogram (ECG).

The autonomic nervous system taxonomy for heart rate can be classified as 'parasympathetic' (decrease in heart rate) and 'sympathetic' (increase in heart rate). The mortality rate with cardio-vascular factor due to sleep disturbance has been examined [2] with heart rate and sleep disturbance. Partial sleep debt even has the tendency to evolve into a cardiovascular risk causing an increase in sympathetic activity [3]. The contribution to this research framework is the feedback provided to night workmen in time domain and frequency domain using an ECG with the activity pattern. Then the foremost contribution is impact of the dysfunction with forecast prediction using time series provides alternatives to change their patterns to circadian rhythm. The discussion of time series in [5] considered rather than considering the whole series subset of the series can be incorporated for analysis. Hence, the fold of work will design the subsets of electrical stability of cardiac with each time and frequency component and provides feedback.

LITERATURE SURVEY

Impact of Arrhythmia on Circadian

The ionic channel representation between the heart rate and the circadian rhythm produces sudden cardiac arrest [6]. The discussions showed the sudden cardiac arrest due to electrical instability.



Melatonin acts as a cardio protective agent preventing damage against myocardium [7]. Antioxidant effect due to melatonin leads to decrease in blood pressure and reduction in heart rate (myocardial ischemia) [8]. The impact of melatonin may also cause increased heart rate, which states that administrating the melatonin in a proper manner reduces heart rate [9]. If there is a mismatch in synchronization of the endogenous clock with external stimuli it leads to cardio vascular organ damage [10]. Cardiovascular diseases with peripheral clock of heart and its disorder were being discussed in molecular basis on circadian studies [11].

Circadian Studies Pertaining to Sleep

Molecular mechanisms with sleep still remain an enigma underpinning to its genetic activities [12]. The circadian variations pertaining to sleep fragmentation also affects cardio-vascular region affecting the sympathetic activity [13]. Sympathetic hyperactivity caused due to sleep debt can affect increasing the stress hormones, heart rate and blood pressure [14].

Two studies with circadian entrainment and circadian misalignment has been done in [15] with the impact of lighting conditions. The impact in the RQ signal interval states that there is no effect of energy expenditure. Then they proposed methods to counteract the circadian misalignment.

Problem Definition

The morphological feature of a signal of heart not only varies with chronobiology action. It also pertains to several aspects such as age, physical size, genetics behaviors and nature of work load. The discussions in [16] reveal that the hazards of shift workers in rotating shift had more impact with ischemic heart disease compared with regular day workers and regular night workers.

PROPOSED SYSTEM

Motivation

In order to ascertain the study the motivation behind this research frame is to analyze the autonomous nervous system with the time and frequency domains of night workmen and early diagnosis from cardiovascular risk.

Description of Algorithm

Heart Beat Rhythm using Temporal and Frequency Components for Circadian Studies (HBRTFCs) : Determine the electro cardiac heart sequence with the range S_N that value encompasses several instantaneous heart rates. The clinical values obtained are shown in **Table 1**.

Table 1 Sample characteristics of data taken

Age, years	Duration of work, h	Weight, kg	Blood pressure, mmHg	Body temperature	Heart rate
49	7	73	140/80	98.4	86
38	7	80	100/70	98.4	73
62	7	50	100/60	98.4	60
66	7	46	150/80	98.2	62
74	7	50	100/70	98.5	78

Several samples were collected. However, the first two samples were taken for consideration in this study. The low frequency noise occurs at the beginning of P-wave or at the end of T-wave caused by movement of electrode and skin. The low frequencies (0.04 Hz to 0.15 Hz) are due to sympathetic activity is associated with workload [17]. Higher frequency (0.15 Hz to 0.4 Hz) are associated with parasympathetic activity [17]. The temporal components are in **Table 2**.

The PR Interval should lie between 0.12 to 0.20 s. The QRS duration should be between 0.08 to 0.10 s. The QT interval should be between 0.4 to 0.43 s. The RR interval should be between 0.6 to 10 s. The frequency components as in **Table 3**. The speed taken for the ECG waveforms is 25 mm/s.



Table 2 Representation of ECG waveforms for time analysis

PR interval (S)	QRS interval (S)
0.123	0.088
0.153	0.094

Table 3 Representation of ECG waveforms for frequency analysis

PR interval, s	Amplitude of PR wave, mV	QRS interval, s	Amplitude of QRS wave, mV
0.123	0.10	0.088	1
0.153	0.11	0.094	0.9

RESULTS

The ECG interpretations can be obtained from several databases like Public Multi lead ECG database [18]. However, it is difficult to characterize with the gene type. Hence the work obtains clinical data and predicts their impact using time series analysis. Similarly, there exists several waveform based analysis of ECG platforms [19].

Implications

The cardiac restoration therapy [20] with twelve lead ECG waveforms states more attention should be given to QRS duration. The ischemic diseases prediction with heart rate variables from various major ECG databases states that it is mandatory to consider the ST duration [21]. The simulations were being done for the clinical data with cardio vascular simulator which is a computational model [22].

The heart rate obtained with clinical environment was given as input parameter shown in **Figure 1** for patient 1 and **Figure 3** for patient 2. The tested value of simulation for left ventricular pressure and right ventricular pressure is shown in **Figure 2** for patient 2 and **Figure 4** for patient 2.

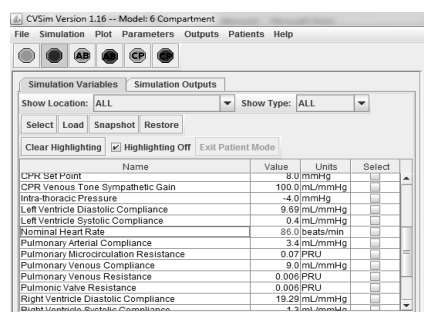


Figure 1 The value of heart rate given as input to the CVSim for patient 1

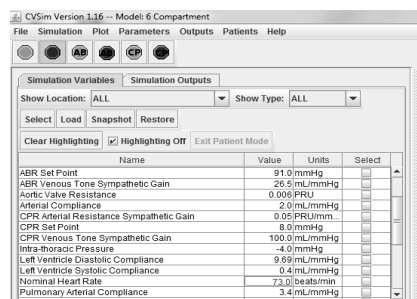


Figure 3 The value of heart rate given as input to the CVSim for patient 2

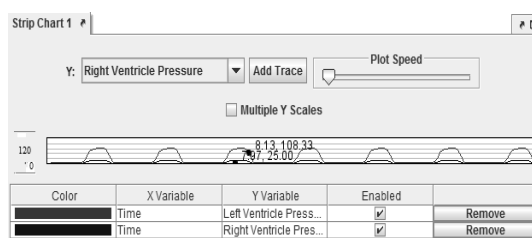


Figure 2 Left ventricular pressure versus right ventricular pressure for patient 1

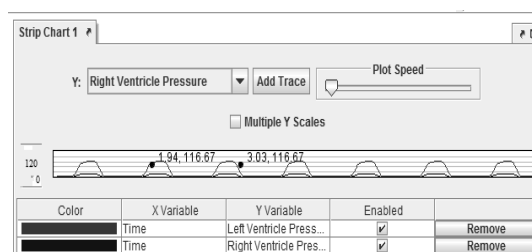


Figure 4 Left ventricular pressure versus right ventricular pressure for patient 2



Statistical Significance

The data set taken is very small. Hence, exponential time series is used. However, for large data sets applications time series has been used in different fields like wireless sensor networks using Auto regressive Integrated Moving Average (ARIMA) model [23]. To implement many forecasts, exponential smoothing is better compared with ARIMA model.

Formulation of Confident Interval

The motivation is an impact of signaling interval with the corresponding voltage levels (**Table 4**).

Table 4 Simple exponential smoothing for PR interval

PR interval, S	Amplitude of PR wave, mV	Lower confident level_ level_amplitude	Upper confident level_ amplitude
0.123	0.10	0.02	0.25
0.153	0.11	0.02	0.24

The data obtained with clinical examination are plotted with lower and upper confident limit of amplitude. PR interval is not predicted due to the value is known from ECG data obtained.

The data obtained with clinical examination are plotted with lower and upper confident limit of QRS interval (**Table 5**). The model fit statistics for PR and QRS intervals are given in **Tables 6** and **7**, respectively.

Table 5 Simple exponential smoothing for QRS interval

QRS interval, s	Amplitude of QRS wave, mV	Lower confident level_ QRS interval	Upper confident level_ QRS interval
0.088	1	0.026	0.158
0.094	0.9	0.025	0.157

Table 6 Model fit statistics for PR interval

Fit statistic	Mean	SE	Minimum	Maximum
Stationary R-squared
R-squared	-0.523	0.014	-0.533	-0.513
RMSE	0.017	0.012	0.009	0.026
MAPE	9.718	5.516	5.818	13.618
MaxAPE	12.590	7.618	7.204	17.977
MAE	0.012	0.009	0.006	0.018
MaxAE	0.015	0.011	0.007	0.022
Normalized BIC	-8.038	1.563	-9.143	-6.933

Table 7 Model fit statistics for QRS interval

Fit statistic	Mean	SE	Minimum	Maximum
Stationary R-squared
R-squared	-0.500	1.974E-13	-0.500	-0.500
RMSE	0.046	.058	0.005	0.087
MAPE	5.159	1.631	4.006	6.312
MaxAPE	5.949	1.592	4.824	7.075
MAE	0.032	0.040	0.004	0.060
MaxAE	0.037	0.047	0.004	0.071
Normalized BIC	-7.360	3.979	-10.173	-4.546

CONCLUSIONS

Belated diagnosis is reported to end in high mortality rate. Hence, this method of HBRTFCs for Circadian Studies forms a linear combination of ECG waveform and patient attributes. The examined sample characteristic shows that the HBRTFCs are appealing with ventricular depolarization. However, future work will deal with large samples of population to be examined with multiple days. In addition the impact of lighting conditions with tunable blue rich LED lightning which produces sun-like rays spectrum at night and associating it with melatonin secretion and work efficiency.

ACKNOWLEDGEMENTS

The authors acknowledge the contribution of Department of Science and Technology New Delhi for sponsoring the project "Adaptive Circadian Rhythm through Dynamic LED lighting - An approach for Non-medical treatment for



Sleeping disorders and improvised efficiency for Night-shift workmen” [Grant number: D.O. No. SR/CSRI/185/2016]

REFERENCES

1. U. Schibler. The daily rhythms of genes, cells and organs: biological clocks and circadian timing in cells. EMBO reports, Volume 6(S1), pp S9-S13, 2005.
2. M. J. Sateia. International classification of sleep disorders. Chest, Volume 146, Number 5, 1387-1394, 2014.
3. P. M. Nilsson, J. Å. Nilsson, B. Hedblad, G. Berglund. Sleep disturbance in association with elevated pulse rate for prediction of mortality—consequences of mental strain. Journal of internal medicine, Volume 250, Number 6, pp 521-529, 2001.
4. J. L. Dettoni, F. M. Consolim-Colombo, L. F. Drager, M. C. Rubira, S. B. P. Cavasin de Souza, M. C. Irigoyen, G. Lorenzi-Filho. Cardiovascular effects of partial sleep deprivation in healthy volunteers. Journal of applied physiology, Volume 113, Number 2, pp 232-236, 2012.
5. A. Bagnall, J. Lines, A. Bostrom, J. Large, E. Keogh. The great time series classification bake off: a review and experimental evaluation of recent algorithmic advances. Data Mining and Knowledge Discovery, Volume 31, Number 3, pp 606-660, 2017.
6. D. Jeyaraj, S. M. Haldar, X. Wan, M. D. McCauley, J. A. Ripperger, K. Hu, M. J. Cutler. Circadian rhythms govern cardiac repolarization and arrhythmogenesis. Nature, Volume 483, pp 7387, 2012.
7. R. J. Reiter, D. X. Tan, S. D. Paredes, L. Fuentes-Broto. Beneficial effects of melatonin in cardiovascular disease. Annals of medicine, Volume 42, Number 4, 276-285, 2010.
8. Y. Yang, Y. Sun, W. Yi, Y. Li, C. Fan, Z. Xin, D. Yi. A review of melatonin as a suitable antioxidant against myocardial ischemia–reperfusion injury and clinical heart diseases. Journal of pineal research, Volume 57, Number 4, pp 357-366, 2014.
9. F. Simko, T. Baka, L. Paulis, R. J. Reiter. Elevated heart rate and nondipping heart rate as potential targets for melatonin: a review. Journal of pineal research, Volume 61, Number 2, 127-137, 2016.
10. N. Takeda, K. Maemura. Circadian clock and cardiovascular disease. Journal of cardiology, Volume 57, Number 3, pp 249-256, 2011.
11. K. Maemura, N. Takeda, R. Nagai. Circadian rhythms in the CNS and peripheral clock disorders: role of the biological clock in cardiovascular diseases. Journal of pharmacological sciences, Volume 103, Number 2, pp 134-138, 2007.
12. A. Sehgal, E. Mignot. Genetics of sleep and sleep disorders. Cell, Volume 146, Number 2, pp 194-207, 2011.
13. J. Słomko, M. Zawadka-Kunikowska, J. J. Klawe, M. Tafil-Klawe, J. Newton, P. Zalewski. Cardiovascular regulation and body temperature: evidence from a nap vs. sleep deprivation randomized controlled trial. Physiological Research, 2018.
14. D. L. Kuetting, A. Feisst, A. M. Sprinkart, R. Homs, J. Luetkens, D. Thomas, D. Dabir. Effects of a 24hr- shiftrelated short-term sleep deprivation on cardiac function: A cardiac magnetic resonance based study. Journal of sleep research, e12665, 2018.
15. E. L. Melanson, H. K. Ritchie, T. B. Dear, V. Catenacci, K. Shea, E. Connick, K. P. Wright Jr., Daytime bright light exposure, metabolism, and individual differences in wake and sleep energy expenditure during circadian entrainment and misalignment. Neurobiology of sleep and circadian rhythms, Volume 4, pp 49-56, 2018.
16. Y. Fujino, H. Iso, A. Tamakoshi, Y. Inaba, A. Koizumi, T. Kubo, T. Yoshimura. A prospective cohort study of shift work and risk of ischemic heart disease in Japanese male workers. American Journal of Epidemiology, Volume 164, Number 2, pp 128-135, 2006.
17. G. Ernst. Heart rate variability. London: Springer, 2014.
18. R. K. Tripathy, S. Dandapat. Detection of cardiac abnormalities from multilead ECG using multiscale phase alternation features. Journal of medical systems, Volume 40, Number 6, pp143, 2016.
19. R. L. Winslow, S. Granite, C. Jurado. Waveform ECG: A Platform for Visualizing, Annotating, and Analyzing ECG Data. Computing in Science and Engineering, Volume 18, Number 5, pp 36-46, 2016.
20. M. Brignole, A. Auricchio, G. Baron-Esquivias, P. Bordachar, G. Boriani, P. M. Elliott. ESC Guidelines on cardiac pacing and cardiac resynchronization therapy: the Task Force on cardiac pacing and resynchronization therapy of the European Society of Cardiology (ESC). Developed in collaboration with the European Heart Rhythm Association (EHRA). European heart journal, Volume 34, Number 29, pp 2281-2329, 2013.
21. A. A. Samoilov, D. V. Telishev, I. V. Pyanov. Application of heart rate variability methods to the TT-intervals and ST-segments durations. In Young Researchers in Electrical and Electronic Engineering (EIConRus), IEEE Conference of Russian, IEEE, pp. 1928-1931, January 2018
22. T. Heldt, R. Mukkamala, G. B. Moody, R. G. Mark. Cvsim: An open-source cardiovascular simulator for teaching and research. The Open Pacing, Electrophysiology and Therapy Journal, Volume 3, pp 45, 2010.
23. J. V. Anand, S. Titus. Energy Efficiency Analysis of Effective Hydrocast for Underwater Communication. International Journal of Acoustics and Vibration, Volume 22, Number 1, pp 44-50, 2017



Design of Hybrid Style Full Adder for Low Power and High Speed Applications

Shivam Adhikari^{*1}, Vijay Joshi¹, Jyoti Kandpal¹, Abhishek Tomar¹

Department of Electronics and Communication Engineering, College of Technology, GBPUA&T Pantnagar, Uttarakhand¹, shiva.29.adi@gmail.com*

ABSTRACT

In this paper, a high speed and low power hybrid style CMOS full adder using 0.18 μm TSMC CMOS technology with the insertion of different modules is designed. The main aspiration of full adder design is to achieve good drivability, noise robustness, and low energy operation. In the designing of full adder, two stage design approaches is used. In first stage, XOR and XNOR logic generation circuit is implemented to ensure full swing and generation XOR and XNOR both signals simultaneously. In the next stage, sum and carry generation module are used with good drivability. To investigate the performance of designed adder, Cadence virtuoso simulation software is used. All the full adders are designed with 0.18 μm TSMC CMOS technology with 1.8 V supply voltage and 1 GHz signal frequency. The simulation results show that the proposed full adder having the delay of 66.4 ps with average power consumption of 27.66 μW with more 20% improvement in energy efficiency. Also, the total number of transistors used to design is 18 which are comparable to the previously proposed designs. The improvement achieved by improving the compatibility between I and II stage. The circuit can be used further in the high speed applications like digital image processing and ALU's.

KEYWORDS Full adder (FA), Hybrid logic, High speed, Level restoration, Low power

INTRODUCTION

Due to the large demand of battery-operated portable devices like cellular phones, Personal Digital Assistants (PDAs), and notebooks in daily life, the demand of VLSI circuits with improved power-delay-product characteristics is significantly increased. The power requirements can be reduced in the different level of design such as architectural, schematic circuit, and layout level for a given process technology [1, 2]. The complex logic in digital circuits are implemented using hierarchy approach. So, basic cell in the hierarchy become critical to improve the performance of circuit. Arithmetic operators are those critical cells in digital cells. So, these arithmetic operators are optimised for energy efficiency at schematic level.

As the computational speed of processor is increased, complexity of the critical arithmetic circuits increases and energy consumption became more important. Increase in the number and density of transistors on chip and faster clock makes the circuit more complex. In the complex arithmetic circuit, full adder performs the task like complex addition, multiplication, exponentiation, division etc. The design of full adder should be such that it must consume less power, no degradation in the output voltage and have the less delay[3]. The circuit must contain the same property even scale toward the deep sub-micrometre region. Good driving capability in different load condition without glitches makes the design more suitable for the application.

In this research paper, an energy efficient full adder with less delay is designed in hybrid logic style. The full adder schematic is divided in three modules [4-6]. Module I is XOR/XNOR logic, module II is sum logic and module III have carry block logic. The advantage of hybrid logic style is the freedom to choose the topology on the basis of parameters like switching capacitance, transition activity and short-circuit currents. The proposed full adder has incorporated the advantage of hybrid logic style as all the three blocks are designed using compatibility requirements of topology and then optimized as a single unit. In rest of the paper; section II reviews the literature; section III explains design approach of proposed full adder; section IV discusses the simulation results and finally gives the conclusion section V.

FULL ADDER REVIEW

Several logic styles have been already proposed in past to design the full adder. Every circuit have its advantages and disadvantages according to topology it uses. Standard static Complementary Metal-Oxide-Semiconductor (CMOS) full adder [8] is based on the pull-up and pull-down network. These circuits have series transistors at the output level which are weak drivers. So, additional buffers are required for providing the necessary driving power to



the next state. The advantage of this complementary CMOS style is its robustness against voltage scaling and transistor sizing. But the disadvantage is high input capacitance and requirement of buffer.

The Complementary Pass-transistors Logic (CPL) full adder with swing restoration is having dual rail structure[3]. The advantage is one pass-transistor network (either PMOS or NMOS) is sufficient to implement the logic function. But the pass transistor logic has an inherent threshold voltage problem. Therefore, output inverters are also used to ensure the drivability. CPL is not appropriate for low power application, because it have high switching activity of intermediate node, more transistor count, use of static inverters, and overloading of its input.

A Transmission Function Full Adder (TFA) [6] is made with the help of Transmission gate. A transmission gate is made by connecting a PMOS and NMOS parallel to each other, and it is controlled by complementary signals at the gate of each other. The PMOS and NMOS will provide path to both 1 and 0 simultaneously. The advantage is they have no voltage drop problem but the disadvantage is double the number of transistor for the same circuit.

Later the researchers focused on hybrid logic style approach which uses the advantages of previous proposed logic styles to enhance the performance of the circuit. Vesterbecka proposed 14-transistor hybrid style full adder [9] having more than one type of logic. Similarly, hybrid pass-logic with static CMOS output drive full adder (HPSC) was proposed by Zhang [10]. In this type of circuit, both XOR and XNOR are generated simultaneously. Although these hybrid logic style offers promising performance, most of these are suffered from poor driving capability issue.

PROPOSED FULL ADDER DESIGN

The design approach of the proposed the proposed full adder circuit is represented by three blocks as shown in **Figure 1** [11]. Module 1 is the module to provide the XOR and XNOR signals simultaneously. Module 2 is used to generate the sum signal using arrangement of transistor. Module 3 is used to generate the output carry signal (c_{out}). For the optimization in terms of power, delay, and power delay product, each module is generated individually. These modules are discussed next paragraph.

Functionality of XOR-XNOR Module

The module of XOR-XNOR is made with the help of cross coupled PMOS and NMOS transistors as shown in **Figure 2**. This circuit exhibit the phenomenon of cross coupling and level restoration. Previous proposed circuits having the cross coupled logic is having the full swing output at the output node. Two transistors are also used in the cross coupled circuit for level restoration. The advantage of these level restorer transistors is to provide full swing in all possible combination of input. The main key-feature of the circuit is the generation of XOR and XNOR module at the same time rather than using an inverter to generate one output from the other one. This design of XOR-XNOR provide full swing output and having small glitches, which reduces the overall power consumption of the circuit. The results are verified by performing the transient analysis of the circuit.

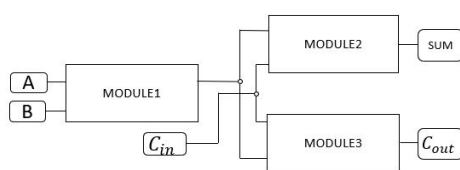


Figure 1 Schematic structure of proposed full adder

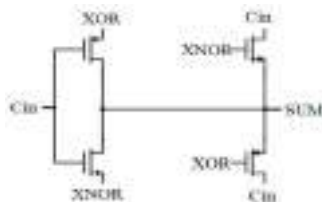


Figure 3 Schematic structure of sum generation module

Functionality of Sum Module

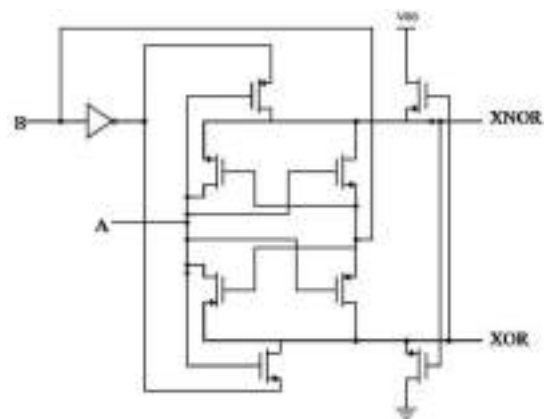


Figure 2 Schematic structure of XOR-XNOR module

The Sum module is shown having the 4 transistors in it as shown in **Figure 3**. Two PMOS and two NMOS are connecting in such a way that they are performing the action of SUM operation. The input for the sum module is directly taken from the XOR-XNOR module. The simultaneous generation of the signals from previous stage enhances the performance of sum stage and reduces the unwanted signals. The advantage of this circuit is less number of transistors during the propagation of sum signal. In some input combinations only 1 transistor and in other only 2 transistors connected parallel to each other effects the output SUM. Thus, this type of circuit provides less delay and less amount of power consumption for the generation of SUM signal.

Functionality of Carry Module

The carry module is actually the design of multiplexer cell as shown in **Figure 4**. Depending on the XOR and XNOR signals, the transistors are on or off. Here itself the carry module uses the output of the first stage which is generated at the same time instant. The circuit can be considered as 2 inverters connected to each other by their output node. The advantage of the circuit is the symmetrical structure, which provides less power consumption. By this type of structure, minimum number of transistors will provide less area and appropriate sizing of the transistors can reduce the delay and power consumption of the circuit to the minimum extant. Less transistor switching activity in this stage reduces the node capacitance and reduces the self loading effects of the circuit.

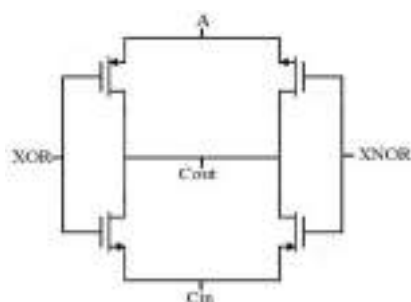


Figure 4 Schematic structure of carry generation module

RESULT AND DISCUSSION

The worst case delay, average power consumption and power delay product of the proposed circuit is compared with the previous circuits and shown in **Table 1**.

Table 1 Comparative values for different kinds of the full adder

Reference	Average power, μW	Delay, ps	PDP, fJ	Number of transistor
[8]	71.39	213.3	15.23	28
[3]	105.44	272.3	28.70	32
[6]	25.25	90.7	2.29	16
[4]	38.83	75.8	2.91	20
[9]	22.96	97.8	2.24	14
[2]	47.77	109.2	5.22	24
[11]	31.32	83.5	2.62	16
[present]	27.66	66.4	1.84	18

Compared to the power consumption of hybrid adder [2], 43% of total power is saved. Total power consumption of the proposed adder is found 27.66 μW .

Similarly, the worst case delay of the circuit is also calculated with the calculator in spectre tool, which is the delay to reach 90% of the steady state value. The proposed circuit shows worst case delay of 66.4 ps. The delay of other circuits is given in the table.

Power delay product of different adder cell is also compared. The proposed 18-T adder cell gives the best results in terms of power delay product as depicted in table. The proposed adder gives 1.84 fJ power delay product, which is comparatively less than others. **Figure 5** shows the comparison between power, delay and power delay product on the basis of the simulation results.



The circuit is also tested in a reference test bench in which the load of 10fF is connected in both outputs sum and carry. The input is also provided by using two inverters for the more realistic scenario. All the circuits are simulated in same test bench for the same input and same conditions. The input frequency during this analysis is taken as 200 MHz and the results of the proposed adder achieved better in comparison to other adders. This validates the performance of the adder in real time circuits. The transient analysis for the 200MHz signal is shown in **Figure 6**.

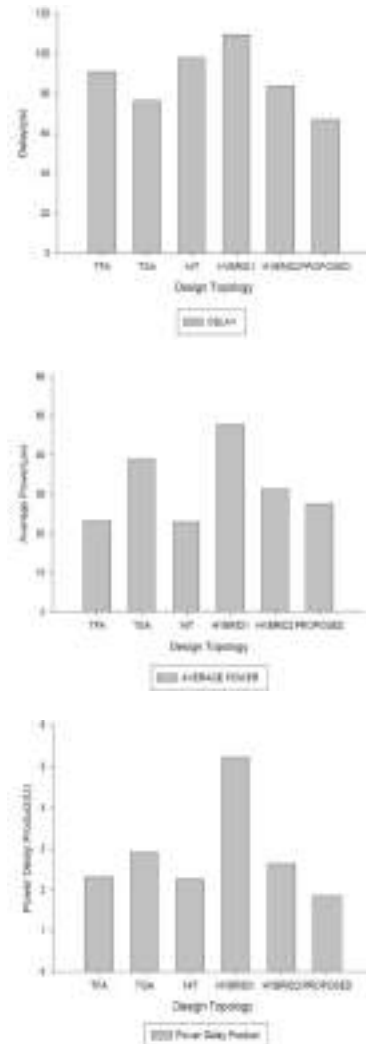


Figure 5 Comparison between power, delay and power delay product on the basis of the simulation results

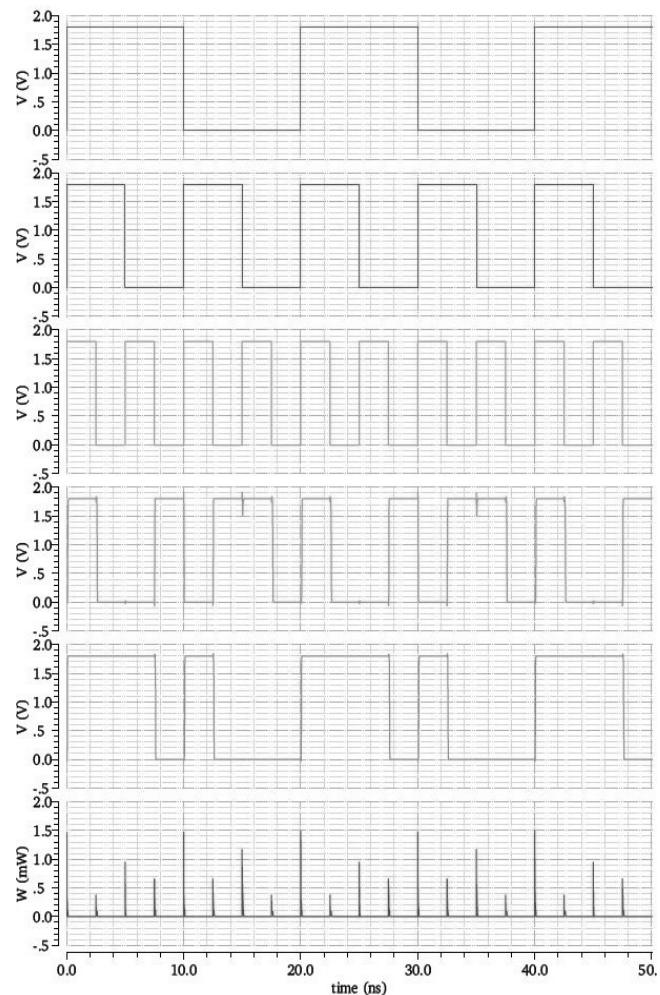


Figure 6 Transient response of the proposed full adder

CONCLUSION

This proposed work is an attempt to design a low power and high speed full adder custom cell using hybrid logic style in 0.18 μ m CMOS technology. In the proposed work, an 18 transistor (T) full adder cell has been proposed. The proposed circuit is a hybrid of CMOS, PTL logic style and involves the design of 10-T XOR-XNOR gate to implement the SUM and Cout circuit.

Total power dissipation through conventional, hybrid and proposed adder cell has been measured in the cadence spectra tool. The performance parameters such as power, delay and power delay product is measured by the tool and



compared. The results of the proposed adder are best in compare to others. So, the proposed adder provides advantages in terms of the performance.

This work analyzes the latest developments in hybrid logic implementation techniques and methods with an emphasis on speed improvement and power reduction. Transistor reduction methods like pass transistor logic and full swing technique like level restorer are analyzed.

The proposed work puts forth a hybrid circuit which is using standard CMOS and pass transistor logic techniques. The results shows are concluded as-

- Power dissipation of different logic styles is compared. Compare to the hybrid adder 2, the proposed adder shows the improvement of 12% in power consumption.
- The delay of the adder cells is compared and improvement is achieved in the proposed 18 T full adder. Compared to hybrid adder 2, proposed circuit shows 21% improvement in delay.

References

1. J. M. Rabey, A. Chandrakshan, and B. Nicolice, Digital Integrated Circuits: A Design Prospective, 2nd ed. Delhi, India: Pearson Education 2003.
2. S. Goel, A. Kumar, M. A. Bayoumi. Design of robust, energy-efficient full adders for deep-submicrometer design using hybrid-CMOS logic style, IEEE Trans. Very Large Scale Integr. (VLSI) Syst., Volume 14, Number 12, pp. 1309–1321, December 2006
3. R. Zimmermann, W. Fichtner. Low-Power logic styles: CMOS versus pass-transistor logic, IEEE Journal of Solid-State Circuits, Volume 32, Number 7, pp. 1079-1090, July 1997.
4. C. H. Chang, J. M. Gu, M. Zhang, A review of 0.18- μm full adder performances for tree structured arithmetic circuits, IEEE Trans. VeryLarge Scale Integr. (VLSI) Syst., Volume 13, Number 6, pp. 686–695, June 2005.
5. H. T. Bui, Y. Wang, Y. Jiang, Design and analysis of low-power 10-transistor full adders using novel XOR-XNOR gates, IEEE Trans. Circuits Syst. II, Analog Digit. Signal Process., Volume 49, Number 1, pp. 25–30, January 2002.
6. M. Alioto, G. Di Cataldo, G. Palumbo, Mixed full adder topologies for high-performance low-power arithmetic circuits, Microelectron. J., Volume 38, Number 1, pp. 130–139, January 2007.
7. O. A. Badry, M. A. Abdelghany, Low power 1-Bit Full Adder Using Full-Swing Gate Diffusion Input Technique, International Conference on Innovation Trends in Computer Engineering (ITCE 2018).
8. K. Navi, M. Maeen, V. Fororoutran, A novel low-power full adder cells for low voltage, VLSI J. Integr., Volume 42, Number 4, pp. 457-467, September 2009.
9. M. Vesterbacka, A 14-transistor CMOS full adder with full voltage-swing nodes, Proc. IEEE Workshop Signal Process. Syst. (SIPS), Taipei, Taiwan, pp. 317-320, October 1999.
10. M. Zhang, J. Gu, C.H. Chang, A novel hybrid pass logic with static CMOS output drive full-adder cell, Proceedings of the 2003 International Symposium on Circuits and Systems (ISCAS'03), Volume 5, May 2003.
11. P. Bhattacharya, B. Kundu, S. Ghosh, Performance Analysis of a Low-Power High-Speed Hybrid 1-bit Full Adder Circuit, IEEE Transactions on Very Large Scale Integration (VLSI) systems, Volume 23, Number 10, October 2015.



Integration Technology using Information and Communication Technology for Problem based Learning and Teaching Learning Process

Araddhana Deshmukh^{*1}, Girish Mundada², Aakanksha Girish Mundada³

Smt. Kashibai Navale College of Engineering, Pune, Maharashtra¹, aadeshmukhskn@gmail.com*

Pune Institute of Computer Technology, Pune, Maharashtra²

Larsen & Toubro Infotech, Mumbai³

ABSTRACT

The scene of instruction has profoundly changed in the course of the last decade: new advancements, new developments and new chances. Social orders the world over have seen the development of the cell phone, PCs, tablets, the web, Windows, Google and Facebook. The open door presently exists for innovation to disturb training in manners that can close the open door hole for a huge number of understudies the world over. Innovation has the ability to change how individuals learn using PBL & TLP. New innovation utilized in creative ways may hold the brilliant key to opening difficulties to instructive access and value. In the developed countries, 28% of classrooms don't use innovation and 69% of U.S. instructors keep on utilizing customary entire class guidance as their essential method of guidance. Just 50% of U.S. teachers believe that ICT innovations are compelling or exceptionally viable at diagnosing the requirements of understudies. We realize that we can manufacture and bridle the innovation expected to close these gaps. The exercise is certain that classroom advancement remains stale notwithstanding the fast change of computerized innovation.

We need to make another vision for instructive innovation in schools. This paper gives information and an investigation of ICT get to, addresses hindrances to execution and coordination in the training framework what's more, offers common sense answers for address these difficulties. It accentuates the requirement for instruction advancements in light of what we think about the way toward learning. It focuses on a vital way to deal with centered change and asks, what would we be able to do to get from where we are to where we should be?

On the off chance that our scholars are to exceed expectations in an advancing information society, we must saddle the innovation assets they have to work in a advanced age. It is not any more about furnishing each tyke with one PC. It is tied in with customizing learning and upgrading abilities that have not verifiably been in the instructor tool kit. For developments in instruction to be acknowledged, schools and educational systems must be updated in ways that cultivate understudy development by offering very customized learning ecologies.

With the help of PBL using TLP the preparation gave open doors for dynamic getting the hang of including demonstrating, peer instructing, co-educating, and co-improvement of exercises with the coach. In expansion, the preparation gave change compose exercises in a few different ways. Instructors got in the nick of time follow-up help and in-classroom showing bolster when problem coordinating workshop techniques into their classrooms. Review level groups met month to month to share and give an account of innovation incorporation exercises, and those exercises were made accessible to all educators through a common drive on the far reaching system. These were abridged every month in a network pamphlet.

KEYWORDS IT, ICT, PBL, TLP

INTRODUCTION

Need of PBL [Problem Based Learning] and TLP [Teaching Learning Process

The idea of Information and Communication Technologies (ICT) centers around correspondence, basic leadership and critical thinking aptitudes and is characterized as procedures, apparatuses and methods for : (i) assembling and distinguishing data; (ii) grouping and sorting out; (iii) condensing and orchestrating; (iv) breaking down and assessing; and (v) guessing and foreseeing.

In this specific circumstance, ICT can be characterized as an idea that assembles the data advances and correspondence advances related ideas under one idea and accentuates the relations between these innovations The previously mentioned definitions are for the most part clarified in three interrelated classifications in the writing.

The first classification imparting, asking, basic leadership and critical thinking incorporates abilities identified with the, getting to data through condemning, taking care of issues, speaking with the assets as per these targets, and overseeing and leading an examination. The abilities incorporated into the class anticipate that understudies will utilize their learning and aptitudes, all things considered, circumstances.



The second class fundamental tasks, information and ideas in innovation incorporates the idea of innovation and its belongings, moral utilization of the innovation, mass specialized devices in digitized setting, ergonomic and wellbeing issues, and essential PC, media transmission and multi-media activities.

The third class – forms for efficiency alludes to the capacity to utilize fundamental generation instruments and procedures to form writings, sort out information, make and control illustrations, sound and sight and sound, coordinate the media with showing forms, utilize electronic correspondence frameworks, coordinate electronically, share area and explore.

Learnersunderstudies can figure out how data is gotten to and sorted out in an extremely successful manner as they figure out how to utilize ICT, as it requires a functioning exploration. In this unique situation, ICT is imperative and essential for the changes anticipated from learning conditions, for it gives chances to changing customary instructor focused practices into understudy focused situations and furthermore conditions for sharing and collaboration . The nature of instruction on the coordination of instructive innovations with learning and educating rehearses in instructor training has been talked about often since training advances entered in classroom situations [1-3]. As indicated by the related writing, one of the viable apparatuses that empower the utilization of ICT as per an educational programs is ICT-helped venture based methodology.

Simpson (2010) gives the means of PBL, which incorporate venture begin, advancement, report, and appraisal. He clarifies that, "Beginning the venture includes choosing the point that is of intrigue and significance to understudies. The educator can make directing questions ... The task ought to test and spurring with the end goal that understudies can create and have the adaptability to work at their own level. At that point, Project advancement includes the examination, which is attempted by all gathering individuals either independently, in sets, or as a gathering. This ought to be chosen by the gathering before starting the task. Answering to the class includes showing and accepting criticism from different understudies. Ultimately, appraisal is the point at which the last item is assessed by an individual understudy, understudies as a gathering or an instructor." [4-6].

HYPOTHETICAL MODEL OF PBL [PROBLEM BASED LEARNING]

Existing Model

As shown in **Figure 1**, the conditions characterize the specific circumstance and help to characterize the objectives of learning at any given minute, and what the conditions for understanding these objectives are.

In the physical environment, the essential objective of learning can be the adjustment of spatial practices and the investigation of mental models, and in the meantime additionally the improvement of social aptitudes. The supremacy of the social condition brings social aptitudes into the point of convergence, and it is additionally associated with the production of mental models, with the material work on going about as an affecting variable out of sight. At the middle purpose of the social learning condition are standards, certainties and convictions associated to rehearses, ancient rarities, values and moral bases. Along these lines the sections of getting the hang of, delineating diverse conditions, give the foundation and characterize the space where learning ends up conceivable. Since the conditions are open, a more restricted idea of the space for learning is additionally required for the motivations behind innovative work, to all the more likely match the prerequisites of arranging.

The spaces for learning have been characterized as existing at first glance zones where the zones of learning meet. In the spatial-social space for learning [7], essential components are the practical and social connections to the topic, to the instruments and the co-actors, which shape the students' involvement. This raises questions with respect to the engineering of room, usefulness, and utilization of tactile data that spatial and social learning identified with work and polished methodology may require.

In the social-social space for learning[2], the most pivotal factor is figuring out how to handle diverse models of activity and thought, to work with various individuals and to tackle likewise morally difficult issues. The primary inquiry is, the thing that sort of reasoning, rationale, co-agent and critical thinking aptitudes are anticipated from an expert in the changing circumstances of their future working-life.

Proposed Model for PBL

As shown in **Figure 2**, considering the existing model, the proposed model is designed as follows :

- Organized and Sequenced Educational Modules: The obtaining of specialized, social and individual abilities needs to be organized and sequenced intelligently, with the goal that the understudies can grow very much expounded what's more, organized learning and aptitudes.



Adjusted multifaceted nature: The intricacy of the issue circumstance must be ideally coordinated to the understudies' level of mastery. Point by point arranging and association: The subjective time-on-errand ought to be kept high (except if specialized aptitudes have need). Point by point arranging and association of the learning exercises can bolster this. [8]

- Learning Resources : Proper learning assets with Adequate learning assets for the understudies' skill level and the multifaceted nature of the issue circumstance are given. Flexibilization of abilities need to enhance the adaptability of the procured aptitudes, there are different issues and application assignments in various settings at the understudies' transfer.
- Coaching : Singular instructing: The diverse learning forms activated by the issue circumstances are went with also, upheld as exclusively as could be expected under the circumstances (utilizing platform, and so forth.). The learning procedure is guided suitably to the understudies' level of skill. Separated input: Students get visit and separated criticism on the level of their abilities (specialized, social, individual abilities). The evaluation framework makes impetuses for understudies to participate in learning exercises exclusively and in addition in gatherings.[5]

In integration technology the fit between the intricacy of the learning condition and understudies' ability level has all the earmarks of being basic both from an intellectual and in addition from an inspirational brain science perspective. Educators can modify the multifaceted nature of a PBL learning condition specifically through the structure of the issue and by the level of bolster. By and by, the structure of an ideal multifaceted nature of the issue circumstance is a testing errand, particularly if the gathering of understudies has a heterogeneous level of fitness.

Moreover, the instructional help must be acclimated to the skill level of the understudies. PBL makes open learning situations, which permit understudies to pursue singular learning ways. For the benefit of the learning adequacy furthermore, effectiveness they should be limited with reasonable instructional and methodological measures and bolstered with proper instructional and authoritative measures. In the current discussion about constructivist guidance all advocates have featured the focal capacity of a fitting direction and altered help of the learning procedure.

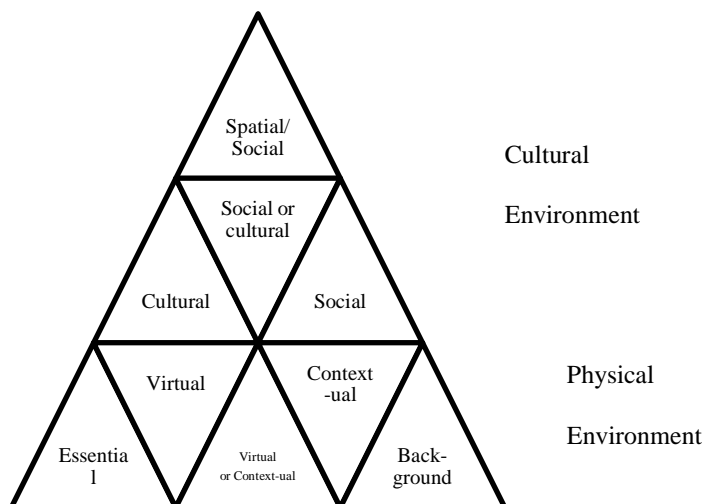


Figure 1 Hypothetical Model of PBL

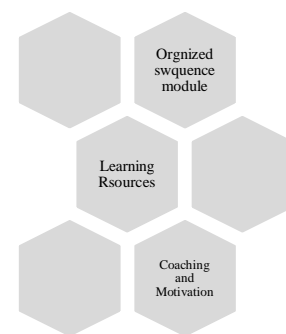


Figure 2 Proposed Model PBL

EXISTING MODEL OF TLP [TEACHING LEARNING PROCESS]

Web based life is a procedure, in which the performing artists develop regular implications. This occurs through substance, systems and web-advancements. In internet based life the clients are makers of the substance. At the equivalent time they are making systems. A channel for such system can be a blog, a wiki or another web webpage, which has been developed utilizing "web 2.0" innovation. Tim O'Reilly has been named as the maker of web 2.0 innovation. (O'Reilly, 2012). Web 2.0 innovation empowers the correspondences of the makers and the clients, in



the pilot think about unit case the connection between the understudies themselves and their coaches. The existing model of TLP is shown in **Figure 3**.

PBL has advanced from its start into various strands. In the pilot project we have concentrated on an open learning condition, which reformulates PBL to some degree in an unexpected way. Our model of PBL depended on two principle thoughts. As a matter of first importance, the form of PBL was concentrating on capability improvement. Also, virtual apparatuses were broadly used to help learning. Subsequently, we can reason that our PBL think about unit was either capability and issue based learning (CPBL) or because of the utilization of Social media, in particular blog and WIKI, an online-PBL or disseminated PBL[6,9].

PROPOSED MODEL FOR TLP

Singular understudies might be more qualified for learning especially, utilizing unmistakable modes for considering, relating and making. The thought of understudies, having specific learning styles, has suggestions for educating techniques. Since favoured methods of information and yield fluctuate starting with one individual then onto the next, it is important that instructors utilize a scope of instructing procedures to successfully address the issues of person students. This should prompt the students who are both inherently and outwardly persuaded to ask, gather, and decipher; to think brilliantly, basically and innovatively; and in the last examination to make utilization of the information and abilities they have picked up by getting to be powerful decision makers [10]. The proposed model of TLP is shown in **Figure 4**.

In integration technology various understudies will expect support to meet the destinations of the endorsed educational modules. This help might be as changes in instructing systems, methodologies or materials and may require the help of asset or potentially uncommon training educators. The Department's Special Education Policy Manual gives heading in addressing the necessities of understudies who require interchange or altered educational programs targets.

An understudy focused methodology which effectively connects with the youngster in the learning process is basic if aptitudes which result in solid practices are to be cultivated and created. A portion of the learning procedures that could be fused in a far reaching approach incorporate self-coordinated learning, co-agent learning, job playing, conduct practice, peer training and parent contribution. Thought ought to be given to enabling understudies to design some learning encounters. They could be given chances to distinguish points or zones for further examination, contribute data applicable to an issue for study as well as make proposals for development exercises[11]

In integration technology understudies ought to likewise be given the open door for self-evaluation and be energized to assess their propensities, states of mind, and practices as for individual wellbeing and prosperity. This can be proficient through genuine exercises or recreations in which understudies can wind up associated with a significant way. Exercises, for example, recording dietary patterns and planning an arrangement for smart dieting, taking a cohort's heartbeat, and examining ads for evident and concealed messages, enable youngsters to apply their comprehension of ideas to regular circumstances and events.



Figure 3 Existing TLP Model

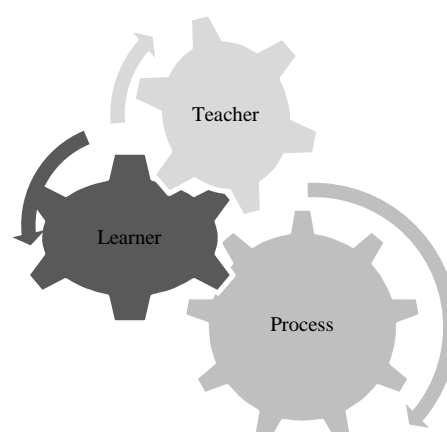


Figure 4 Proposed simple model of TLP



Teacher	Learner	Process
<ul style="list-style-type: none"> ✓ makes reference to previous experience, knowledge, and skills ✓ presents learning outcomes to be pursued (connects these with previous learning experiences, and places outcomes to be pursued in a context where students will focus on tasks or problems in search of new information) ✓ proposes relevant learning activities in order to develop interest and motivation ✓ facilitates the organization of the learning environment (human and material resources, space, time); gives instructions and suggests various methods of operation 	<ul style="list-style-type: none"> ✓ reflect on previous experience, knowledge, and skills ✓ make connections with previously acquired experience, knowledge, and skills and proposed outcomes ✓ determine that new skills and knowledge are required to achieve the outcomes ✓ define and clarify the tasks or questions to be solved in order to achieve the outcomes ✓ propose or choose motivating activities which will satisfy their need for new information ✓ organize themselves and interact with the learning environment (human and material resources, space, and time) 	<ul style="list-style-type: none"> ✓ students recall knowledge and skills previously acquired ✓ students make connections between present learning situation and previous learning experiences ✓ tasks or problems presented are understood and pertinent for all students (if not, teacher reformulates problem) ✓ students are inspired and motivated by the proposed learning activities ✓ students understand what is expected of them ✓ students design an effective workplace

CONCLUSION

The utilization of space as a supporting and directing learning resource is a very experiential thing from the perspective of the learner. Learning that takes place in a space can be observed using the experiential and reflective learning theory. Reflection is the core of learning and the key to directing the learner and understanding evaluation. Kolb (1984) states that reflection is the observation and analysis of experiences by the learner alone and together with other learners and with the instructor.

When learning is perceived as a process permeated by reflection, with the aim of producing experience and expertise, guidance is also required to be transparent and to support reflection in the students

In integration technology employing action pedagogy means making students into participants, co-operation between teachers in planning, and providing institutions of learning with the resources to create and continuously maintain spaces for learning. For example, by combining the advantages of problem-based pedagogy, which produces understanding, and those of project learning anchored in practice, the result can at best be a reflective and research-oriented learning process, which can be realized in learning spaces created in a varied and multidimensional manner, which will in turn produce the best professionals and experts.

REFERENCES

1. S. Clifford. Bringing History Alive in the Classroom. Social Studies Review, 32(3) pl2-16 Spring Cuban, L (1991). History of teaching in social studies. In J.P. Shaver (ed.), Handbook of research on social studies teaching and learning (197-209). New York: Macmillan, 1993.
2. E. Poikela (2012b) Knowledge, Learning and Competence – The Boundary Conditions of Simulation Pedagogy. In E. Poikela & P. Poikela (eds.) Towards Simulation Pedagogy. Developing Nursing Simulation in a European Network. Publication of Rovaniemi University of Applied Sciences. Serie A. No 2. Rovaniemi: ErwekoOy. 18-29.
3. E. Poikela (2012a) Learning, Work and Competence - Facing the challenges of expertise and entrepreneurship. In R. Pelli & S. Ruohonen (eds.) Learning and Competence Creating Ecosystem - LCCE. Publication of Kymenlaakso University of Applied Sciences. Serie A. No 32. Tampere: TammerprintOy. 24-33.
4. R.M. Concepts, constructs and insights: the essence of problem-based learning. In S.E. Chen, R.M. Cowdroy, A.J. Kingsland & M.J. Ostwald (eds.) Reflections on problem-based learning. Sydney: Australian PBL Network, 1994.
5. P. Westwood. What teachers need to know about Teaching methods. Camberwell, Vic, ACER Press, 2008
6. V Donche. Differential use of Learning Strategies in First-Year Higher Education: The impact of Personality, Academic Motivation, and Teaching Strategies". The British journal of Educational Psychology. Volume 83, Number 2, 2013.
7. R.G. Baker, S. Scott. The transfer of teaching skills into classroom practice: a follow up study of newly graduated teachers. Curtin University of Technology: Bentley, 1995
8. J. Mezirow, Critical theory of adult learning and education, Adult Education, Volume 32, pp 3-24, 1981
9. Gatto, John Taylor. A Different Kind of Teacher: Solving the Crisis of American Schooling. Berkeley Hills Books. ISBN 1-893163-21-0.
10. B. J. Fraser, K. Tobin, Combining qualitative and quantitative methods in classroom environment research. In B. J. Fraser & H. J. Walberg (Eds.), Educational environments: Evaluation, antecedents, and consequences. Oxford, UK: Pergamon Press. pp. 271–290, 1991
11. Powerful Learning: Studies Show Deep Understanding Derives from Collaborative Methods, By Brigid Barron, Linda Darling-Hammond, in Edutopia, October 8, 2008. Retrieved 2016-03-15



Reliability Evaluation of NBC Protection Shelter using the Fault Tree Analysis

Nitinkumar Pol^{*1}, Sushil Kumar Parida¹

Research and Development Establishment (Engineers), Pune¹, nitinkumar_pol@yahoo.co.in^{*}

ABSTRACT

The Reinforced Hardened Shelter (RHS) is an underground human occupancy shelter designed to provide Nuclear Biological and Chemical (NBC) protection to the occupants for a specified period during NBC threat. This paper describes the quantitative reliability assessment of RHS system using a Fault Tree Analysis (FTA) technique. The life critical systems of RHS viz., the structural, ventilation and water supply system are analysed in the present study. A top event as 'failure of RHS system' is considered in the analysis. A fault tree presenting graphical representation of logical relationships between the undesired event and the basic fault events have been developed considering the configuration and operational setup. The quantitative reliability analysis of RHS system is carried out for the mission time. The ventilation sub-system is found to be having highest failure probability in RHS system. The reliability of system has been improved by suggesting the replacing of critical components during the system operation. This will help in formulating the maintenance philosophy and the requirement of critical spares can be estimated from the presented study.

KEYWORDS FTA, Structural reliability, NBC Shelter

INTRODUCTION

The Reinforced Hardened Shelter (RHS) is designed to provide NBC collective protection to the 60 personnel for a period of seven days during NBC threat. The shelter is capable to withstand the blast, thermal and radiation effects due to nuclear detonation. Also, the shelter is able to cope up with any known Biological and Chemical (BC) threat. The vital electronic systems are safe against radiation and Nuclear Electro-Magnetic Pulse (NEMP) effects. The shelter houses communication equipment and life support equipment. The life support equipment ensures comfortable environment inside the shelter to the extent of survival. **Figure 1** shows the schematic diagram of RHS system. The failure of such strategic system may lead to catastrophic conditions for shelter occupants, and this makes it imperative to get the reliability of design and operating procedures evaluated.

Several tools are available for analyzing system safety and reliability [1,2]. These tools are used to determine the probability of system failure and the probability that a system will operate successfully. Fault tree analysis (FTA) is an applicable and useful analysis tool; it is an analytical technique used for identifying and classifying hazards, and calculating system reliability for both simple and complex engineering systems [3-5]. This paper describes the quantitative reliability assessment of RHS system using fault tree analysis technique. **Figure 1** shows the block diagram for RHS system. A fault tree model is developed for RHS system and reliability estimation is carried out for the mission time.

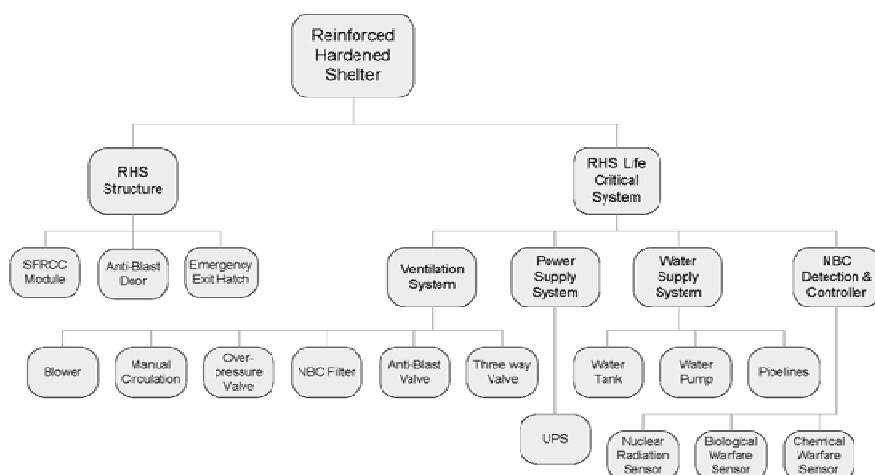


Figure 1 Block diagram for reinforced hardened shelter



A fault tree is a graphical representation of the logical relations between an undesired event (fire, explosion, etc.), called the 'top event' and the primary cause events. It is a deductive, failure-based approach. As a deductive approach, FTA starts with an undesired event, such as failure of a main engine, and then determines (deduces) its causes using a systematic, backward-stepping process. In determining the causes, a fault tree (FT) is constructed as a logical illustration of the events and their relationships that are necessary and sufficient to result in the undesired event, or top event. It is important to understand that a fault tree is not a model of all possible system failures or all possible causes for system failure. A fault tree is tailored to its top event that corresponds to some particular system failure mode, and the fault tree thus includes only those faults that contribute to this top event [6,7].

Fault Tree Model for RHS System

A fault tree model translates the physical system into structured logic diagram. **Table 1** shows the different types of symbols used in the fault tree model. **Figure 2** shows the fault tree model for RHS system. The fault tree for top event 'Failure of RHS' has been constructed based upon the technical specification and drawings of the RHS system. It has been developed using a deductive process and working backwards from effects to causes. The main elements of the fault tree model are event definition such as 'RHS Ventilation System Failure' or 'Anti-blast valve failure' and logic gates (AND and OR). These gates indicate the inter-relation between various failure events in the model. The OR-gate is used to show that the output event occurs only if one or more of the input events occur. The AND-gate is used to show that the output fault occurs only if all the input faults occur. The basic events of a fault tree are those events, which, for one reason or another, have not been further developed. These are the events for which probabilities have to be provided if the fault tree is to be used for computing the probability of the top event. As seen from **Figure 3**, the top event could occur if any of sub-system failure occurs in the model. This is shown by OR-gate linking the top event to the three sub-events. Each of this contributory causes are then further broken down into more basic causes, that is, basic events [8,9].

RELIABILITY EVALUATION METHODOLOGY

Mission time (t) for RHS

The reliability of RHS system is calculated for a specific mission time for which it is required to be operational. It is considered that one operational cycle of 7 days will be performed each year for the system. The design life for RHS system is 20 years. Hence the total time of operation for the system is calculated as 3360 h. This operational time of the systems is considered as the mission time and hence, reliability is predicted for the same.

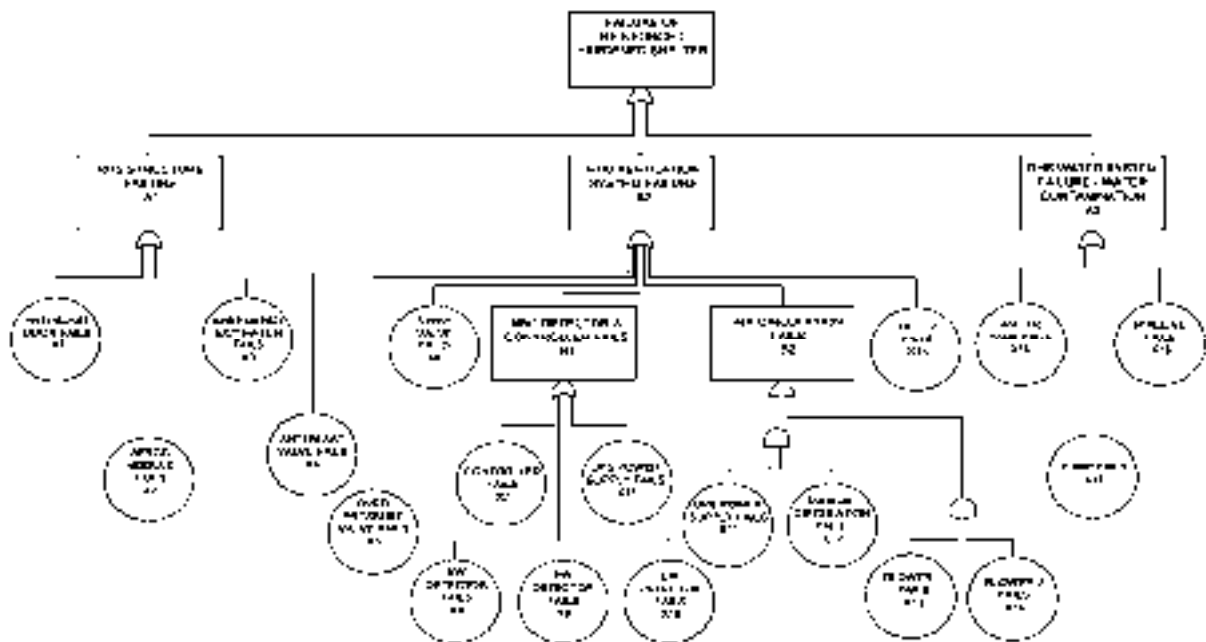


Figure 2 Fault tree model for RHS system

Table 1 Symbols used in fault tree model

Description	Symbol
Top event or intermediate event	
Basic Event	
OR-Gate	
AND-Gate	
Undeveloped event	

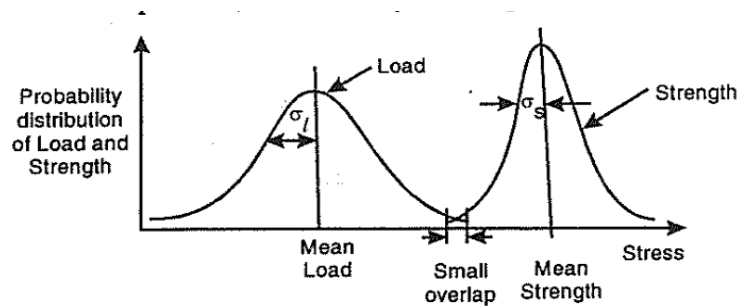


Figure 3 Strength-load interaction model

Failure Probability for Structure Items

The probability of failure for structural items of RHS is evaluated using the Strength-Load Interaction Safety Margin models. **Figure 3** shows the typical strength-load interaction. The reliability is calculated using the following relation and referring the normal statistical tables [10,11].

$$\text{Reliability} = 1 - \Phi \left[-\frac{\bar{S} - \bar{L}}{\sqrt{\sigma_L^2 + \sigma_S^2}} \right] \quad (1)$$

where, \bar{S} and σ_S are mean value and standard deviation of strength; and \bar{L} and σ_L are mean value and standard deviation of load.

The strength of anti-blast door, emergency exit door and SFRCC module are taken from the design document. It is considered that the strength is normally distributed with 5% variation.

The load (stress) acting on the structure of RHS is taken from the blast trail data conducted on the prototype RHS structures.

Failure Probability for Components at Basic Event Level

As seen from the constructed fault tree for RHS, the basic events are the failure of engineering components and items used in different sub-systems. The failure rate data for each components obtained from the OEM or from the published literatures, namely, Non-Electronic Part Reliability Data (NPRD) 2011, Reliability Handbook etc [12-14]. Based on obtained data, the probability of failure (P) for component having failure rate (λ) for mission time (t) is calculated by using the Eq.(2)[5].

$$P = 1 - e^{-\lambda t} \quad (2)$$

For components having higher failure rate and for which repair or replacement can be carried out, the Mean Time Between Failure (MTBF) is calculated using the Eq.(3). Also, the Mean Time To Repair (MTTR) for components are taken from maintenance aspect of the individual component in the system. In such cases, the component unavailability or probability of failure for repairable component is determined using the Eq.(4) [5].

$$\text{MTBF} = \frac{1}{\lambda} \quad (3)$$



$$MTBF = \frac{1}{\lambda} \quad (3)$$

$$P = \frac{\lambda}{\lambda + \mu} \left[1 - e^{-(\lambda + \mu)t} \right] \quad (4)$$

where, μ is repair rate (1/MTTR).

Probability Evaluation of Fault Tree Gates

The output event occurrence probability for OR and AND logic gates are determined to find the failure probability of intermediate and top events. It is calculated using Eqs. (5) and (6) for OR and AND gates, respectively, based upon probability of failure for the basic events or lower events.

For OR gate, the probability of occurrence of the output fault event A_o is given by [5],

$$P(A_o) = 1 - \prod_{i=1}^m \{1 - P(A_i)\} \quad (5)$$

Where, $P(A_i)$ is the probability of occurrence of input fault event A_i ; for $i = 1, 2, \dots, m$.

For AND gate, the probability of occurrence of the output fault event X_o is given by [5],

$$P(X_o) = \prod_{i=1}^k P(X_i) \quad (6)$$

Where, $P(X_i)$ is the probability of occurrence of input fault event X_i ; for $i = 1, 2, \dots$,

Table 2 shows the component reliability data used in the present study.

RESULTS AND DISCUSSION

The reliability evaluation using fault tree for RHS system is carried out according to above mentioned methodology. The failure probabilities for each basic event in the fault tree are calculated and presented in **Table 3**. The pump failure in RHS water system is having highest failure probability among the basic events for the constructed fault tree model. However, anti-blast valve was having the lowest MTBF among the components in RHS. This improvement in reliability for anti-blast valve failure basic event is attributed to possibility of replacing the failed component during the operation of the system. Similarly, for other basic components which are replaceable, the failure probability has been decreased accordingly. The sub-system failure probabilities for RHS are calculated using the basic event probabilities and logic gate output determination method describe above. The failure probabilities for sub-system of RHS are given in **Table 4**. As seen from **Table 4**, the ventilation system is having highest failure probability which can be attributed to presence of more no. of engineering components in ventilation system compared to other sub-systems. It is worth noting that, the reliability of ventilation system has been improved by considering the replacement of components. Also, the MTTR for replicable components is low which has further improved the reliability of ventilation sub-system. The probability of occurrence of top event in RHS fault tree is determined from the intermediate event probabilities. The top event probability is calculates as 0.1503. Hence, the reliability of RHS system is 0.8496.

Table 2 RHS component reliability data

Component	Ref.	MTBF, h	MTTR, h	Remark
Anti-blast valve	NPRD	124	4	Replaceable
Over pressure valve	NPRD	175438	-	
3 way valve	NPRD	114275	2	Replaceable
Controller	NPRD	79400	-	Replaceable
NW detector	OEM	1000	2	Replaceable
BW detector	OEM	28944	2	Replaceable
CW detector	OEM	1000	2	Replaceable
UPS	NPRD	21402	4	Replaceable
Blower 1 and 2	Handbook	819672	2	Replaceable
Filter	NPRD	73386	2	Replaceable
Water tank	NPRD	618811	-	
Water pump	NPRD	132625	-	



Table 3 Failure probabilities for basic events of RHS fault tree

Event ID	Event description	Failure probability
X1	Anti-blast door fails	0.0217
X2	SFRCC module fails	8.16×10^{-6}
X3	Emergency exit hatch fails	0.0183
X4	Anti-blast valve fails	0.03125
X5	Over pressure valve fails	0.0189
X6	3 way valve fails	1.75×10^{-5}
X7	Controller fails	0.0415
X8	NW detector fails	0.00199
X9	BW detector fails	6.9×10^{-5}
X10	CW detector fails	0.00199
X11	UPS power supply fails	0.00018
X12	Manual circulation fails	0.0500
X13	Blower 1 fails	2.44×10^{-6}
X14	Blower 2 fails	2.44×10^{-6}
X15	Filter fails	2.72×10^{-5}
X16	Water tank fails	0.00541
X17	Pump fails	0.0250
X18	Pipeline fails	0.02073

Table 4 Subsystem Failure Probabilities for RHS

Sub-system	Failure probability
RHS structure	0.0396
RHS ventilation system	0.0593
RHS water supply system	0.0511

CONCLUSION

Reliable design of Reinforced Hardened Shelter involves eliminating potential hazards by modifications to design, operation and maintenance procedures. The need for such changes is specifically brought out by the presented fault tree analysis when applied to RHS sub-systems. The application of fault tree analysis technique has highlighted the critical events which could lead to the occurrence of top event. The failure probability of top event in the fault tree model for RHS has found to be 0.1503. The ventilation sub-system has found to be having highest failure probability. The improvement in reliability as a result of preventive maintenance by replacing or repairing the components before its failure has also been quantitatively assessed through the presented study. This will help in formulating the maintenance philosophy and the requirement of critical spares can be estimated from the presented study.

ACKNOWLEDGEMENT

The authors are thankful to FD group for providing valuable inputs for carrying out the presented fault tree analysis. Authors also thank to Director R&DE(E) for his kind permission to publish this paper.

REFERENCES

1. M. Krasich, Use of Fault Tree Analysis for Evaluation of System - Reliability improvement in Design Phase. Proceeding Annual Reliability and Maintainability Symposium, pp 1-7, 2000
2. B.S. Dhillon, Design Reliability: Fundamentals and Application, CRC Press.
3. A.A. Baig, R. Ruzli, A. Buang, Reliability Analysis using Fault Tree Analysis: A Review. Int. J. Chemical Engg and Application. Volume 4, Number 3, pp 169-173, 2013.
4. A.Volkanovski, M. Cepin, B. Mavko, Application of the fault tree analysis for arrangement of power system reliability. Reliability Engg and System Safety. Volume 94, pp 116-1127, 2009.
5. NASA, Fault Tree Handbook with Aerospace Application. Volume 1.1, 2002.
6. W.S. Lee, D.L. Grosh, F.A. Tillman, C.H. Lie, Fault Tree Analysis, Methods, and Applications – A Review. IEEE Trans. Reliability. Volume 34, Number 3, pp 194-203, 1985
7. R.E. Barlow, F. Proschan, Importance of system components and fault tree events. Stochastic Process and their Application. Volume 3, pp 153-173, 1975.
8. C. Rajagopal, A.K. Jain, Hazard Assessment of a Nitration Plant using Fault Tree Analysis. Volume 44, Number 3, pp 323-330, 1994.
9. M. Cepin, B. Mavko, A Dynamic Fault Tree. Reliability Engg. and System Safety. Volume 75, pp 83-91, 2002
10. B. Dhillon, Stress-Strength Reliability Models. Microelectronics Reliability. Volume 20, pp 513-516, 1980
11. B. Bhadury, S.K. Basu, Terotechnology: Reliability Engg and Maintenance Management, Asian Books.
12. M.J. Rossi, Non Electronic Part Reliability Data. Reliability Analysis Center. Volume 3, 1985
13. NSWC, Handbook of Reliability Prediction Procedures for Mechanical Equipment. Volume 11, 2011
14. B. Dhillon, Mechanical Component Reliability under Environmental Stress. Microelectronics and Reliability. Volume 20, pp 153-160, 1980.



Improving the Fuel Efficiency of a Diesel Truck by Blending Online-Onboard Produced Hydrogen Gas with Diesel

Parth Jain¹, Sivarajan S^{*1}

School of Mechanical & Building Sciences, Vellore Institute of Technology, Chennai¹, sivarajan.s@vit.ac.in^{*}

ABSTRACT

Combustion of fossil fuels has caused serious complications to the environment and the geopolitical climate of the globe. In this work, diesel is blended with hydrogen and used as a fuel in truck. Tests were conducted to investigate efficiency and emissions. The experiments conducted shows that there is tremendous scope of improvement in efficiency and reduction of emission gases from CI and even SI engines. NO_x emission can be reduced but is higher at higher rpm. CO₂ emissions can be reduced but they are variable. Fuel efficiency is high on hill terrain and during acceleration. HC emissions are considerably reduced. There was a considerable reduction in engine noise and engine vibrations. The engine pickup has considerably improved. HHO cell can be integrated with gasoline engines in quite an impressive manner. The combustion efficiency has been improved.

KEYWORDS Hydrogen, diesel, emission

INTRODUCTION

Combustion of fossil fuels has caused serious problems to the environment and the geopolitical climate of the world. The main negative effects on the environment by fossil fuel combustion are emissions of NO_x, CO, CO₂, and unburned hydrocarbons. In this work, a hydrogen producing device has been constructed, it works on the principle of electrolysis. It generates hydrogen as required by the engine. The gas produced is called brown gas or simply HHO gas, it is made to flow through a silicon pipe and introduced into the engine near the intake manifold. The pressure is maintained via an air pump installed outside the truck. The test setup is connected to a gas analyzer that tests the gases for composition.

Electrical technology has been harnessed to quite a large potential and today zero emission vehicles are running on roads, this is huge improvement, we see NASA making use of fuel cells and clean technologies to eliminate pollution. This clearly indicates that organizations are inclined to working towards making a cleaner environment making earth a better place to live.

Another such technology is Hydrogen on demand technology (HHO) that utilizes a mixture of hydrogen and diesel for combustion in an IC engine, and is considerably successful in producing a considerable power. Therein lies a wonderful potential for future expansion and work on this noble technology.

Some new technologies could be mixture of hydrogen and CNG powered vehicles. Natural gas vehicles are an alternative to gasoline vehicles, in this prospect vehicles have been run on Hythane®, which is a mixture of 20% by volume of H₂ and CH₄ gas. Although energy output of these vehicles is low and is applicable to two and four-wheeler automobiles and not for heavy duty trucks. But here it is possible to increase the output by varying the hydrogen intake and also the air fuel ratio. The aim of this paper is to study how the emission gases can be reduced and how does brown gas addition affects it. The possibility to increase the mileage and performance of commercial vehicles to any extent is explored. The overhaul trucks are tested for HHO and results are given.

EXPERIMENTAL SET UP

The setup consists of six inline cylinder, 4 stroke engine connected to the battery and which in turn is connected to the cell. The test bed is provided with all the necessary tools for analyzing and testing purposes. The setup has its own fuel tank, air-box, fuel filter, fuel measuring unit, transmitters for air, fuel flow meters. The setup enables to study the variation of fuel and also analyses the gases emitted, variation with load and speed can be obtained in the form of graph. In case the engine backfires, the bubbler blocks the flame from passing through the pipe and igniting the gas produced in the cell. The bubbler is a very simple and very cheap device; it removes any traces of electrolyte fumes from gas before it is drawn into the engine. The second bubbler makes sure that HHO gas is washed out of electrolyte fumes.

Hydrogen has catalytic effect causes more efficient burn of existing fuel. To produce hydrogen on a vehicle and when the vehicle is in switch on condition, there has to be a connection between battery and the device. To make this happen a 5 cells have been constructed each cell consists of 6 plates and connected in series to the battery. Each

cell has been provided with a sensor so that it can be tapped and switch off when not needed. All recent engines have an ECU (Electric Control Unit) which controls the amount of fuel that is being sent to the engine. The ECU contains an oxygen sensor placed in the exhaust stream and when the much-improved exhaust gas that is produced with HHO system passes through it, it senses that there is a very lean mixture so it pumps more fuel. To counter this there is an electric sensor installed which controls this phenomenon.

The design of cell was done in Pro-E and Creo elements software. The plates were made of stainless steel and titanium. Material for screw was taken to be 316L-Stainless steel. The distance between the plates is 3 mm. Effective area is kept less than 36 in 2. Bubbler material was chosen to be HDPE. Acrylic sheets were used to close the cell and absorb the shocks and dissipate heat to atmosphere. Size of acrylic sheet was taken to be more than 64 in 2. Number of plates used is 6, each coupled with sensors that can be tapped every time variable HHO gas intake has to be taken working voltage was chosen to be 12V. Release rate is obtained around 2 to 3.1 l pm. Dissociation voltage at 25°C for water is 1.23V (EMF) and temperature co-efficient is - 0.85 MV/K, that is, at 100°C this voltage goes down to 1.17V. The screws can be between 24 to 30 cm long.

Engine performance is an indication of degree of efficiency of the engine i.e. the conversion of chemical energy stored in the fuel to mechanical work. These engine parameters were decided on the basis of engine used. Different engines require different emission parameters. The major emission parameters set in the test bed were NO_x, CO₂, HC, CO, smoke density, engine load, engine rpm, A/F ratio, power, specific fuel consumption.

RESULTS AND DISCUSSION

CO₂ emissions tend to be stable and lower and nearly same as that with gasoline as shown in **Figure 1(a)**. The reduction in CO₂ is mainly because of reduced carbon in the incoming fuel. Hydrogen is a carbon-less fuel and when mixed with diesel the formed mixture energy output is governed nearly by the amount of HHO gas that is being put inside the cylinder. As is the known relation that more is SFC less is the engine power. Clearly it can be seen in **Figure 1(b)**, here that when there is HHO substituted SFC becomes less and engine power is more.

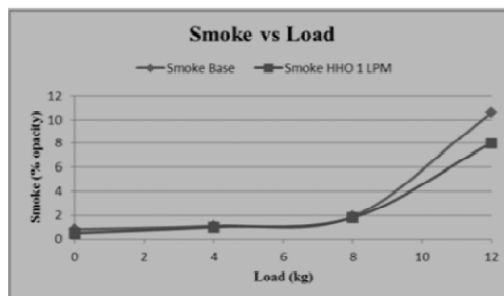
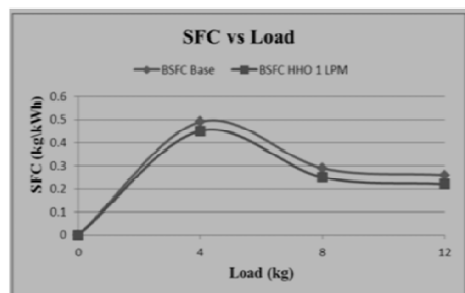
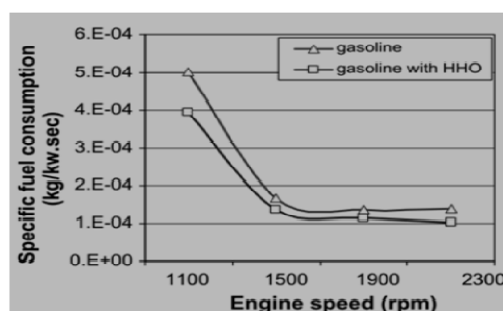
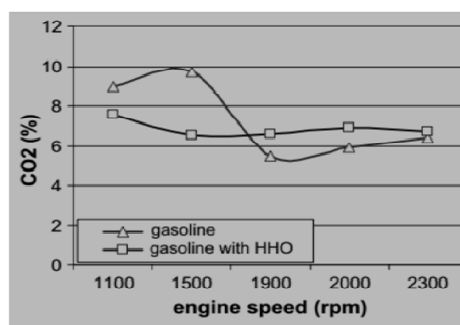


Figure 1 (a) CO₂ against engine speed (b) SFC against load

Figure 2 (a) SFC against engine speed (b) smoke against load

Smoke density is entirely related to how efficiently the atomization of fuel takes place. Since here along with diesel there is a gaseous fuel (hydrogen and oxygen gas) which to some extent reduced the smoke density in exhaust gas. The reduction in unburnt hydrocarbons is mainly due to better combustion, more flame speed and higher combustion temperatures. Moreover, since hydrogen is a carbon-less fuel carbon content becomes very less here. Even at high



loads and high rpm's unburnt hydrocarbon tend to be <500ppm. The formation of NO is due to peak combustion temperature, oxygen concentration in the combustion chamber and the residence time of high temperature gas in the cylinder. The enhanced combustion rate increases the cycle temperature, that leads to higher NO emissions in case of high engine loads. With HHO assisted combustion concentration of NO remains high but low as compared to pure gasoline combustion.

As is the case with CO₂ emissions same is with CO emissions. Zero carbon content in hydrogen takes in less carbon from the fuel and also carbon from inside the engine starts getting oxidized. Emission gas temperature tend to be higher when using HHO gas or brown gas this is because of the higher energy density of hydrogen gas. Same quantity of hydrogen gas releases more energy on combustion when compared to diesel fuel.

The above reading shows trial 1 variation when HHO is introduced and when run on pure gasoline. Note that the readings are for trial number 1 hence shows no significant changes, subsequent readings show remarkable changes.

The total plain highway run was of 120 km. Hill climb was 100 km. Acceleration test included test runs up to 90km. Acceleration test accelerates the truck from 0 to 40 km/h or 0 to 50 km/h and time wasn't taken into account. The hill top was with road being in spiral and slope increasing gradually. There's a potential drop of 2 V across every cell (fact) so with five cells it's going to be 10V and 2V can be spared for the battery.

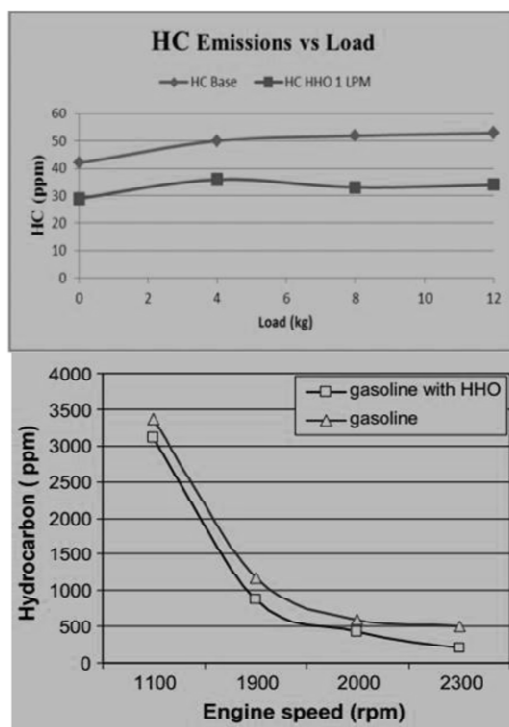


Figure 3 (a) HC emission against load (b) hydrocarbon against engine speed

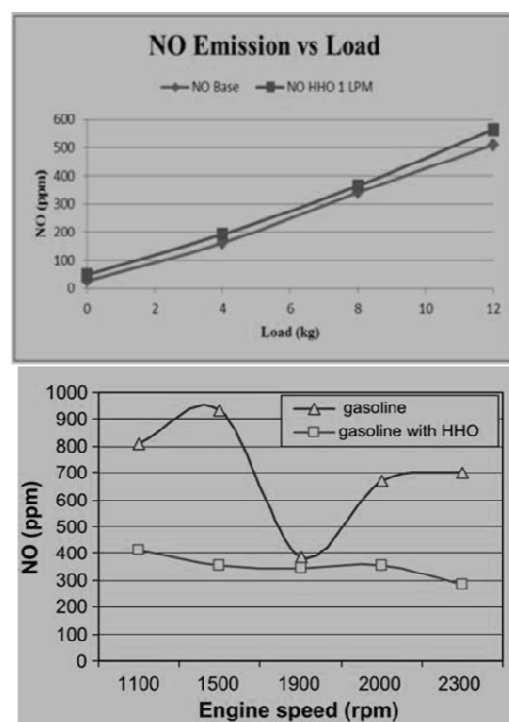


Figure 4 (a) NO emission against load (b) NO against engine speed

Table 1 Ignition status of HHO in different Terrain

Trial no	Fuel usage (without HHO unit), L	Fuel usage with HHO, L
1.Plain high way FE test	30	28.5
2.Plain high way acceleration test	30	28.4
3.Slanted hill terrain	25	21.7
4 Hill top	30	25.4



HHO system may not eradicate the world's problem with emissions and pollution, but it certainly can tackle and reduce them. The project conducted was utilizing low grade materials and engine used was appropriate for pure gasoline engine, if we tackle the engine design, there could be a design that is capable of any fuel that can be injected with diesel especially hydrogen. Hydrogen can be mixed with gasoline and generate more power leading to greater efficiencies. This could also open up developments in newer technologies like fuel cell. This cell experiment that was conducted here could also be extended to varying the hydrogen concentration, varying the fuel like ethanol or CNG or bio-diesel. At this juncture, most of materials used are low grade like instead of titanium, there could be platinum use possible. The use of hydrogen can reduce the prices of fossil by a large extent and save earth from pollution.

As a large project, there could be tweaking of engine design for allowing complete ignition of HHO (**Table 1**) or hydrogen gas and then mixing diesel. Also since there could be more heat generated anyway, so to utilize it there could be a redesigned cooling system that can sustain so much heat. There could be research on such materials that do not react with hydrogen at high temperatures, also research in metals or alloys that do not expand a great deal when large amount of heat is being dealt with.

CONCLUSION

The HHO gas experiment conducted is on an experimental level, but this shows that there is tremendous scope of improvement and reduction of emission gases from CI engines. NO_x emission can be reduced but is higher at higher rpm. CO_2 emissions can be reduced but they are variable. Fuel efficiency is high on hill terrain and during acceleration NO & CO emissions can be reduced to safe levels. HC emissions are considerably reduced. There was a considerable reduction in engine noise, engine vibrations. The engine pickup was considerably improved. In terms of fuel efficiency there was a considerable improvement up to 5% and nearly 18% when performed the test on increasing gradient and up to 13% when performed an acceleration test. HHO cell can be integrated with gasoline engines in quite an impressive manner. The combustion efficiency has been improved. When HHO gas is introduced in the system CO and HC have been reduced drastically. NO_x concentration is highly dependent on rpm.

REFERENCES

1. Light duty automotive technology and fuel economy trends through 1999. US Environmental Protection Agency Report, North Carolina, September, 1999.
2. J E Bennethum, J N Mattavi, Toepel RR. Diesel combustion chamber sampling-hardware, procedures and data interpretation. SAE Pap 1975:750849
3. A Tsolakis, J. Herneandez. Dual fuel engine operation using H_2 . Effect on particulate emissions. Energy & Fuel, pp 418-25, 2005.
4. US Patent NO: 5,452,688, Method and apparatus for enhancing combustion in internal combustion in internal combustion engines 1995.
5. Zhang H, Lin G, J. Chen Evaluation and calculation of a water electrolysis system for hydrogen production. Int. J Hydrogen Energy, Volume 35, pp 10851-8, 2010
6. N A Kelly, T L Gibson, D B Ouwerkerk. A solar-powered, high-efficiency hydrogen fueling system using high pressure electrolysis of water: design and initial results. Int J Hydrogen Energy, Volume 33, pp 2747-64, 2008.
7. Naber J. Hydrogen combustion under diesel engine conditions. Int. J hydrogen Energy, Volume 23, pp 363-71, 1998.
8. H Zhao, G Lowry, N Ladommatos. Time-resolved measurements and analysis of in-cylinder gases and particulates in compression ignition engines. SAE Pap, 961168, 1996.
9. N. Saravanan, G. Nagarajan, G. Sanjay, C. Dhanasekaran, K.M. Kalaiselvan, Experimental investigation of hydrogen port fuel injection in DI diesel engine, International Journal of Hydrogen Energy Volume 32, pp 4071-4080, 2007.
10. T Gatts, H Li, C Liew, S Liu, T Spencer, S Wayne, et al. An experimental investigation of H_2 emissions of a 2004 heavy duty diesel engine supplemented with H_2 . Int J Hydrogen Energy, Volume 35, pp 11349-56, 2010.
11. R. Stone. Introduction to internal combustion engines. 4th ed. New York: Palgrave Macmillan Limited, 2012.



Application of Technology Integration: Mechanical a Core Sector

Anurodh Prashant

Fellow, The Institution of Engineers (India), a.prashant@rediffmail.com

ABSTRACT

Technology integration is the use of technology tools in general content areas in practical field as well as in the education in order to allow students to apply computer and multi discipline combination i.e. say mechanical and electronics makes mechatronics, mechanical and hydraulics makes hydro mechanical, Geology and mining makes geo-technological skills to learning and problem-solving. In general a join of technology that is the integration of the technology is the prime most requirement of the present era. By using one process of production a competitive results with the best quality cannot be achieved. As we all know the uses of the multidiscipline of the engineering will only the way to survive now a day a general solution is readily available with everyone but to achieve some extra intermingling of different technology is must. This can be taught thoroughly during the classroom study by complex bonding to the students in such a way that when these are being taken to various fields for technical training they do the same exercise to get the required results. Technology integration develops more refined engineering fields and the study of the various engineering disciplines in combination with other disciplines of engineering to make a complex bonding engineering which develops the micro level knowledge of each discipline. The fundamentals of integration technology make an engineer more comfortable with the solutions and provides large domain to simplify the problems with greater area of approach.

KEYWORDS Multi discipline, Technological skills, Technology integration, Mechatronics, Complex bonding.

INTRODUCTION

Technology is a path to go ahead and without technology growth of any civilization is zero. Technology itself provide a sum or an integration of multiple diversification towards growth. A technology can be achieved by analysis of any trouble or a generated problem. Whenever a problem is analyzed something new comes up. This is an example of James Watt who invented steam engine. Newton who drives law of gravitation. The survival of the fittest also drives us to be the user of all the available technology in a proper way to get a suitable result. Thorough studies of all the related engineering fields with the related technology one cancocktail the various fields and get better results. On conceptual clearance of the fundamentals of engineering only can yield to the required field of results by using base line calculation on a particular turning point and that is the real logical approach to solve the complicated calculation. The critical problem solutions through most fundamental way of approach by most linear and comfortable to end users is the real emerging engineering paradigm.

In the present scenario of advanced development of multidisciplinary engineering atmosphere, one cannot be a part of fundamental one-dimensional engineering application user, one has to have integration of multiple engineering utilization of the area and by the using of integrated technological aspects only one can resolve the problems. Say if one engineer is a mechanical engineer wants to go for design a mechanical shed he has to go for design aspect of the shed which is quite related to the electronics CAD design system and he has to have consultation of software for safe and simulated load based construction, for this one has to go for computer engineering consultation and like this one mechanical engineer has to integrate the computer and electronics engineering which can provide us a refine construction of a safe shade with less time involvement and better and optimum design.

HUMAN BRAIN AND TECHNOLOGICAL INNOVATIONS

The human brain is the best and the safest computer in the world, the computers are also been innovated by these brains only and it is seen some times a computer makes mistakes on fast operational condition while a human mind do not. Sometimes we feel the operational speed our computer does not match with what we are operating and we have to wait for its operational completion, thus our technology integration feature is utmost necessary for the emerging engineering paradigm.

Figure 1 indicates that more than one idea must be in moving situation in a brain of an active man to resolve the hurdles of the path of different innovations.

A human mind is always more faster and more calculative than a computer, moreover, for an active man, there should be more utilization of human mind as much one can.



A simple, durable and new workable solution can attribute to any complicated problems but the classroom study practices cannot built the student versatile in all the situations and problem solving mere they can be educated theory of the problems and other theoretical studies but to achieve thorough exposure they will have to be posted for internship practices in various large and medium industries and they must be put forward commencing from grass root levels to make them understand each and every problem with their own and not to copy with the seniors or field staff. There are many examples where the integration of the technology has created remarkable changes in the field of education, practical fields and the field of day to day life related to human being individual. Technology is nothing but it is the requirement of human being. As we all know the necessity is mother of invention and in general all most all the inventions are the outcomes of necessity.

Any person who feels the requirement and use his brain to get rid of the requirement and if at that time he put his general and most fundamental knowledge he can make necessary changes in the present system and he innovate a new, economic, suitable and durable diagnose of the problem.

Whom so ever it is seen, the big businessmen, a successful man, a leading personality or a good knowledgeable person, almost all of them pass through the hurdles very closely and at that time most of them forget that moment and move forward. Most of these successful personalities faced the situation and they found a better way to get rid out of that and in that way achieved of their success through innovation or technology integration.

INNOVATION AND TECHNOLOGY INTEGRATION

For any innovation it is mandatory to use technology integration which is intermingling of various technologies which make a fine solution. Without integration of technology no solution of innovation is completed. It is just like that we have made one dynamic model and on movement of the model or during operational period only it gets break.

Thus using various technologies to innovate a good idea is mandatory. The integration of various technologies are shown in Figure 2.



Figure 1 Human brain : an interior image

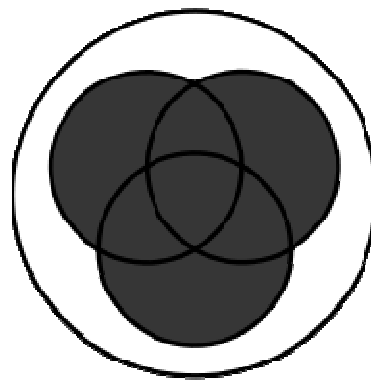


Figure 2 Technology integration

None of the innovation will go successes if any part of the study goes beyond the innermost part of the picture.

Innovation can't be achieved, if anything will be on the outer part of the circle. As the outer one moves more will be failure chances will be there.

The students can be taken for industrial visits to large and medium industries, they can be deputed for technical educative tours, and classroom industrial explanations be made from learned teaching faculties from different industries who has vast experiences in particular field provides a better environment of learning and they can be taught by working and non working models and presentations too.

A better technology is never the complicated technology but it should be a comprehensive, logical, and versatile and user friendly, the latest technology front is the fastest solution of each and every complicated problem. One must get the solution as he face any problem means there should be a simpler solution of each hurdle one can face. One engineer must think ahead to get solution before any hurdle comes forward. This is the concept of foresight seen what in general an ordinary man cannot even think before.



Example:

- (i) One EOT Crane beams designed to pre stressed so that they can with stand more rated load, by giving them opposite side bend.
- (ii) The fly over bridge beams are also being pre-stressed to undertake comparatively more load.
- (iii) The Railway overhang bridges to compensate load with less columns along the length of the bridges.
- (iv) Bearing pre stressed before fitment to undertake more torsion load.

Technology integration is the use of technology media i.e. computers, mobile devices like smart phones and tablets, digital cameras, social media platforms and networks, software applications, the Internet, etc. the matter of the integration is to combine various tools and make the learner to understand the usage of multimedia to achieve the end results in day to day requirements and the day to day studies [Table 1].

When the use of technology is:

- Routine and transparent,
- Accessible and readily available for the task at hand,
- Supporting the curricular goals, and helping the students to effectively reach their goals.

When the technology integration is in systematic use the learner cannot make the difference by how the teacher is making him understand and he feels it very normal and can understand in a better way.

Table 1 Technology integration and technology application

Using Technology	Technology Integration
It is used in random non directional	It is used planned in a designed manner
It is rare use in classroom study.	It is often used in classroom study as part of routine study.
It is used for sake of using technology	It is used for curricular goals and learning study.
It is used to instruct the students	It is used to engage the students.
Technology is used by instructor	Technology is mostly used by students.
Focus on technology	Focus to create and develop new paradigms
More time is spent to learn about technology	More time is utilized to implement the technology.
Technology is used to understand and to keep remember.	Technology is used to impart to develop and collaboration with others.
It is to use deliver information.	It is to construct and build knowledge.

Figure 3 indicates the curiosity of a man, when he goes to some new place. At later stage he tries to make all the curiosity solutions by making technology integration and by solving them at his own levels.

The asking various questions even those might be silly questions makes confident and these so called silly questions only one gets acquainted with the situations and can be known to others about the places and various conditions.

On repeatedly passing through the situations or attending the technology integration classes we can better know about their interest and importance of the theme.



Figure 3 Human curiosity and technology integration

A CASE STUDY OF HUSSON UNIVERSITY

Technology has transformed our world, and new innovations appear at dizzying speed. Since part of Husson University's mission is to prepare students for careers in current and emerging fields, delivering a degree program that enables students to thrive in the IT industry was a natural fit.



A Changing Name for a Changing Field

While the classic conception of IT might be solitary individuals working on hardware or software, the modern world of IT requires professionals who can work in a team, communicate effectively and manage projects well. The changing nature of IT requires a new kind of education and led Husson to reimagining its online Bachelor of Science in Software Development into the Bachelor of Science in Integrated Technology, with a Software Development concentration. This change more accurately represents the university's efforts to provide students with a complete curriculum designed to bridge technical knowledge with real-world applications.

Objective of Integrated Technology

The need of the integration of technology is to overcome the competition era available in the global market. By using single technology phenomenon one can compete in micro market while the requirement of present time is to compete the global market with utmost technology criteria. This can only be achieved by using the concept of a technology integration method by using different discipline of engineering with multi technology plan i.e. mechanical with electronics and electrical can get better opportunities to solve more conceptual problems and can provide better ideas related to auto functional mode of the machineries. A better choice and requirement of present scenario.

CONCLUSION

The study about the integrated technology defines the more refine knowledge about multidiscipline in engineering field and the integration provides strength in the engineering field. Use of integration of the technology provides strong and fundamental solutions of complex engineering problems which makes a significant difference in solving a problem in better way. It provides faster, smoother, safe, rigid technological solutions for all the engineering related problems and can simulate the results for better guide lines.

REFERENCES

- <https://online.husson.edu/integrated-technology-part-1/>
- wikipedia.org/wiki/Technology_integration
- AnurodhPrashant-M.Tech,MBA, PhD-Mechanicalengg. (Pursuing)- Paper No. MC/029/06
- Discipline: Mechanical Engineering.
- a.prashant@rediffmail.com



Feasibility Study of Solar Vapor Absorption Cogeneration Plant for Space Cooling or Heating and Electrification of Residential Buildings

Pereddy Nageswara Reddy

*Department of Mechanical Engineering, Gudlavalleru Engineering College, Gudlavalleru, Andhra Pradesh,
nageswara_pereddy@rediffmail.com*

ABSTRACT

In the present work, an attempt has been made to study the feasibility of solar operated vapor absorption cycle for cogeneration of electricity for domestic consumption and also to provide required cooling or heating for air-conditioning of residential buildings. The $\text{NH}_3\text{-H}_2\text{O}$ vapor absorption cycle is considered in the present study as it operates with positive pressures. The cycle of operation is split into two modes: (i) working on Kalina cycle, and (ii) working on absorption refrigeration cycle. The Thermic Fluids (TF) such as Xceltherm 600 (Paraffinic mineral oil) can be used as the heat transfer fluid in Parabolic Trough Solar Collector (PTSC) to capture solar energy at around 180°C and is used to distill ammonia vapor from the rich solution of $\text{NH}_3\text{-H}_2\text{O}$ in the generator and further to superheat it in the super heater. A simulation code is developed to study the potential of the plant in generating the required electrical energy and producing the cooling or heating for air-conditioning of residential buildings besides Domestic Hot Water (DHW). A case study is made for three major cities, viz. Bhopal, Jaipur, and Hyderabad with $100 \text{ sq.m PTSC area}$. Solar irradiation, electrical energy generated, refrigeration produced and heating capacity are plotted for different months from January to December. It is observed that the plant can produce electric energy of $12.0\text{-}36.0 \text{ kW-h/day}$ throughout the year besides producing refrigeration of 13.0 to 69.0 kW-h/day mainly for day-time cooling and heating of 50.0 to 140.0 kW-h/day for night heating as well as DHW depending on the geographical location and season. For night operation of the plant, the solar thermal energy can be stored in the Phase Change Material (PCM) A164, which changes phase at 164°C . The quantity of PCM required is estimated to be a maximum of 1800 kg with latent heat of fusion of 306 kJ/kg . The maximum cogeneration efficiency is found to vary from 27.5 to 29.5% depending on the geographical location. From the above, it is concluded that solar vapor absorption cogeneration plant is feasible for electrification as well as cooling or heating of residential buildings.

KEYWORDS Solar energy, Vapor absorption cycle, Kalina cycle, Cogeneration, Space cooling/heating, Electric energy

INTRODUCTION

The demand for electricity is forecasted to increase by 75% by 2040 [1]. As the temperature of earth's atmosphere is increasing because of global warming, the demand for air-conditioning and refrigeration is also increasing simultaneously. A considerable saving in electrical power is possible in cooling cogeneration plants due to generation of refrigeration and electric power simultaneously. It is not possible to operate a steam power plant at low temperature heat source. If the configurations of power and cooling are clubbed together, it is possible to generate power and cooling with low temperature heat source such as solar and geothermal.

The Kalina cycle is a reversed absorption cycle that normally uses $\text{NH}_3\text{-H}_2\text{O}$ binary mixture as the working fluid. Though ammonia is toxic and hazardous, it is more environmentally friendly than other working fluids and relatively cheap. The Rankine and absorption refrigeration combined cycles for electric power and refrigeration was proposed with binary ammonia-water mixture as the working fluid by Goswami, et.al. [2]. A new cooling cogeneration cycle was proposed by Shankar, et.al. [3] to generate more cooling with adequate power generation from single source of heat with two options in working fluids i.e. ammonia-water mixture and LiBr-water mixture. Wu, et.al. [4] reviewed the vapor absorption-cycle technologies, with particular emphasis on the cycle design and fluid selection.

Due to its abundant availability and the possibility of storage, solar thermal energy is garnering significant interest and investment worldwide. Solar energy is an ideal source for low temperature heating applications such as space and domestic hot water heating. The use of medium and low temperature solar collectors for combined cycle applications was investigated by Goswami and Xu [5]. Gershon G [6] compared the performance of single, double- and triple-effect absorption chillers used in solar air conditioning systems. A state-of-the-art review of the different

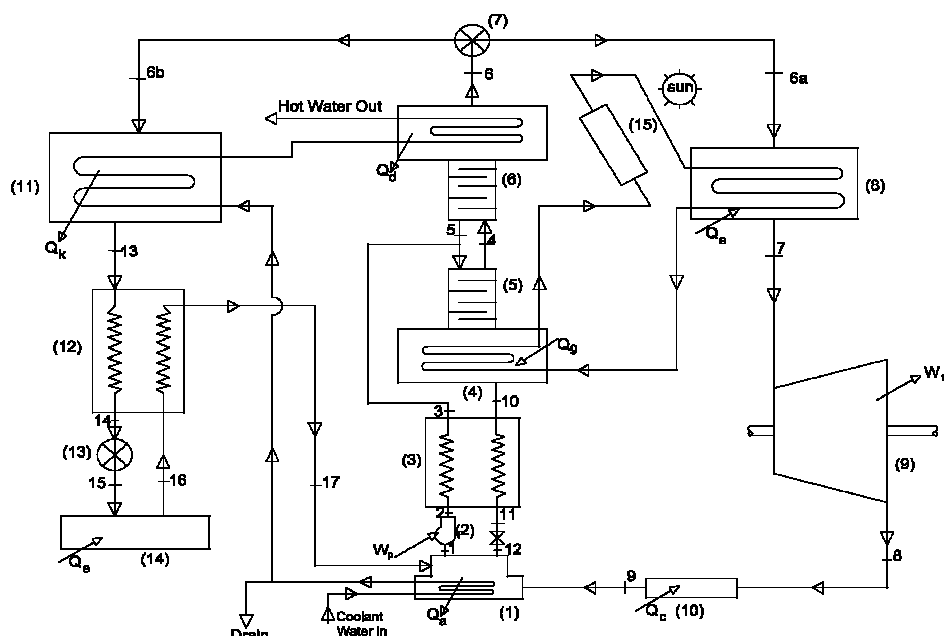
solar refrigeration technologies such as thermo-mechanical, absorption, adsorption and desiccant solutions was presented by Kim, et.al. [7].

Accurate estimation of thermodynamic properties of binary mixtures is a crucial task in analyzing vapor absorption systems. Methods of finding thermodynamic properties of ammonia-water mixture was presented in [8,9,10].

Solar electric generation systems currently in operation are based on parabolic trough solar collectors using synthetic oil heat transfer fluid in the collector loop to transfer thermal energy to a Rankine cycle turbine via a heat exchanger. Tian, et.al. [11] reviewed different types of solar collectors, both non-concentrating collectors (low temperature applications) and concentrating collectors (high temperature applications), and Various types of thermal energy storage systems. Different types of solar thermal collectors and their applications were presented by Soteris[12]. The efficiency of parabolic trough collectors was estimated with synthetic oil and water as the working fluids by Odeh, et.al. [13]. The characteristics of medium to medium-high temperature solar collectors and an overview of efficiency and cost of existing technologies was presented by Soteris[14]. The performance of a parabolic trough photovoltaic/thermal collector was studied by Joe [15]. The thermal efficiency around 58% and electrical efficiency around 15% was predicted under typical operating condition.

The benefits of a molten salt as heat transfer fluid were compared with other types of fluids by Kearney, et.al. [16]. Vignarooban[17] reviewed various types of heat transfer fluids such as air, water/steam, thermal oils, organic fluids, molten-salts and liquid metals for storing and transferring thermal energy in concentrating solar power systems in detail, particularly regarding the melting temperature, thermal stability limit and corrosion issues.

In the present work, a novel way of utilizing the solar energy effectively through vapor absorption cogeneration for electrification and cooling / heating of residential buildings and also for domestic hot water (DHW) based on the demand is proposed. The plant works on Kalina cycle for generating power and absorption refrigeration cycle for producing cooling. The flow of vapor through power and refrigeration cycles is adjusted by the control valve depending on the refrigeration loads of a residential building. A simulation code is developed to study the potential of the plant in generating the specified electrical energy and producing adequate cooling / heating for air-conditioning of residential buildings besides domestic hot water.



(1) absorber, (2) solution pump, (3) solution heat exchanger, (4) generator, (5) analyzer, (6) dephlegmator, (7) control valve, (8) super heater, (9) turbine, (10) cooler, (11) condenser, (12) liquid-vapor heat exchanger, (13) throttle valve, (14) evaporator, and (15) solar collector

Figure 1 Solar vapor absorption cogeneration plant

SOLAR VAPOR ABSORPTION COGENERATION PLANT

Working Principle



The schematic diagram of solar vapor absorption cogeneration plant is given in **Figure 1**. It consists of (1) absorber, (2) solution pump, (3) solution heat exchanger, (4) generator, (5) analyzer, (6) dephlegmator, (7) control valve, (8) super heater, (9) turbine, (10) cooler, (11) condenser, (12) liquid-vapor heat exchanger, (13) throttle valve, (14) evaporator, and (15) solar collector. The cycle of operation of $\text{NH}_3\text{-H}_2\text{O}$ vapor absorption plant is split into two modes: (i) working on Kalina cycle and (ii) working on absorption refrigeration cycle. The rich solution of $\text{NH}_3\text{-H}_2\text{O}$ is pumped from the absorber through solution heat exchanger into the generator. The Thermic Fluids (TF) such as Xceltherm600 (Paraffinic mineral oil) can be used as the heat transfer fluid in PTSC to capture solar energy at around 180°C and is used to distill ammonia vapor from the rich solution of $\text{NH}_3\text{-H}_2\text{O}$ in the generator. The enriched vapor from the generator-analyzer enters the dephlegmator wherein heat is removed from the vapor by the circulation of a cooling medium. The drip from the dephlegmator returns to the generator.

Nearly pure NH_3 vapor leaving the dephlegmator partly flows via super heater into the turbine where it is expanded to absorber pressure. The turbine is coupled to the alternator to generate electricity. The exhaust from the turbine flows into the absorber through the cooler wherein heat is added to the vapor from the air-conditioned space. The remaining ammonia vapor leaving the dephlegmator flows into the condenser wherein heat is removed from the vapor by the circulation of a cooling medium. Liquid ammonia from the condenser is sub-cooled in the liquid-vapor heat exchanger and then throttled to evaporator pressure. After throttling, liquid ammonia vaporizes in the evaporator by receiving heat from the air-conditioned space. Weak solution of $\text{NH}_3\text{-H}_2\text{O}$ returning from the generator enters the absorber via solution heat exchanger. In the absorber, the weak solution of $\text{NH}_3\text{-H}_2\text{O}$ absorbs the ammonia vapor exhausted from the turbine as well as the vapor formed in the evaporator to form the rich solution of $\text{NH}_3\text{-H}_2\text{O}$.

Cogeneration Plant Specifications

Table 1 presents the design data considered for simulation of solar vapor absorption cogeneration plant.

Table 1 Design data of vapor absorption cogeneration plant

Parameter name (Unit)	Value
Solar collector area, $A_{\text{collector}}$, m^2	100.0
Solar collector efficiency, $\eta_{\text{collector}}$	50%
Heat recovery efficiency, η_r	90%
Condenser pressure, p_k , bar	30.0
Evaporator pressure, p_0 , bar	2.0
Generator temperature, T_g , $^\circ\text{C}$	127
Absorber temperature, T_a , $^\circ\text{C}$	40
Temperature of vapor leaving the super heater, T_7 , $^\circ\text{C}$	137
Effectiveness of solution heat exchanger and liquid-vapor heat exchanger, ϵ	0.8
Turbine efficiency, η_t	90%
Solution pump efficiency, η_p	85%
Alternator efficiency, η_a	90%
Motor efficiency, η_m	90%
Energy input to drive miscellaneous units, W_{miss} , kW-h/day	2.0
Latent heat of fusion of PCM (A164, organic), L_{PCM} , kJ/kg	306.0

Thermodynamic Analysis

Based on **Figure 1**, the solar vapor absorption cogeneration plant is analyzed in detail. It is based on the following three equations which can be applied to any part of the system [18].

$$\text{Mass balance: } \sum m = 0 \quad (1)$$

$$\text{Material balance: } \sum m x = 0 \quad (2)$$

$$\text{Energy balance: } \sum Q + \sum m h = 0 \quad (3)$$

By energy balance around the generator,

$$m_3 h_3 + m_5 h_5 + q_g = m_4 h_4 + m_{10} h_{10} \quad (4)$$

where q_g is the heat energy supplied in the generator per kg NH_3 distilled.

By energy balance around the dephlegmator,

$$m_4 h_4 - q_d = m_5 h_5 + m_6 h_6 \quad (5)$$

where q_d is the heat energy removed in the dephlegmator per kg NH_3 distilled.



By energy balance around the super heater,

$$m_6 h_6 + q_s = m_7 h_7 \quad (6)$$

where q_s is the heat energy supplied in the super heater per kg NH_3 distilled.

By energy balance around the turbine,

$$m_7 h_7 - w_t = m_8 h_8 \quad (7)$$

where w_t is the work energy output from the turbine per kg NH_3 distilled.

By energy balance around the cooler,

$$m_8 h_8 + q_c = m_9 h_9 \quad (8)$$

where q_c is the cooling or refrigeration produced at the cooler per kg NH_3 distilled.

By energy balance around the absorber,

$$m_9 h_9 + m_{12} h_{12} + m_{17} h_{17} - q_a = m_1 h_1 \quad (9)$$

where q_a is the heat energy removed in the absorber per kg NH_3 distilled.

By energy balance around the solution pump,

$$m_1 h_1 + w_p = m_2 h_2 \quad (10)$$

where w_p is the work energy input to the solution pump per kg NH_3 distilled.

By energy balance around the condenser,

$$m_6 h_6 - q_k = m_{13} h_{13} \quad (11)$$

where q_k is the heat energy removed in the condenser per kg NH_3 distilled.

By energy balance around the evaporator,

$$m_{15} h_{15} + q_e = m_{16} h_{16} \quad (12)$$

where q_e is the cooling or refrigeration produced at the evaporator per kg NH_3 distilled.

Total mass of vapor distilled in the generator for the given solar collector area, $A_{\text{collector}}$ is calculated by making energy balance around the solar collector, generator and super heater as

$$M \times (q_g + q_s) / 3600 = Q_I \times A_{\text{collector}} \times \eta_{\text{collector}} \times \eta_r \quad (13)$$

where Q_I is the solar irradiation in $\text{kW-h/m}^2\text{-day}$, and M is the total mass of vapor distilled in the generator in kg/Day .

Electric power output of the plant is determined as

$$W_e = [f \times M \times w_t - M \times w_p / \eta_m - W_{\text{miss}}] / 3600 \quad (14)$$

where W_e is the net electric power output in kW-h/day , and f is the fraction of total vapor distilled that is expanded in the turbine.

Refrigeration capacity of the plant is determined as

$$Q_0 = [f \times M \times q_c + (1 - f) \times M \times q_e] / 3600 \quad (15)$$

where Q_0 is the refrigeration capacity in kW-h/day

Heating capacity of the plant is determined as

$$Q_h = [M \times q_d + (1 - f) \times M \times q_k] / 3600 \quad (16)$$

where Q_h is the heating capacity in kW-h/day

Mass of hot water produced by the plant is determined as

$$Q_h = M_w \times c_{pw} \times (T_{w2} - T_{w1}) / 3600 \quad (17)$$

where M_w is the mass of hot water produced in kg/Day , c_{pw} is specific heat of water in $\text{kJ/kg-}^\circ\text{C}$, and T_{w1} and T_{w2} are the inlet and outlet temperatures of water in $^\circ\text{C}$.

$$T_{w1} = \text{WBT} + \Delta T \quad (18)$$

where ΔT is the increase in temperature of water in the absorber, considered as 10°C , and WBT is the Wet Bulb Temperature.

Considering 50% of solar energy is utilized for night operation, the mass of PCM required is calculated as

$$Q_I \times A_{\text{collector}} \times \eta_{\text{collector}} \times 0.5 = M_{\text{PCM}} \times L_{\text{PCM}} / 3600 \quad (19)$$

where M_{PCM} is the mass of PCM in kg/Day , and L_{PCM} is the latent heat of fusion of PCM.

Solar collector area equivalent of heating capacity is given as

$$A_{h,\text{collector}} = Q_h / (Q_I \times \eta_{\text{collector}}) \quad (20)$$

Thermal efficiency of the plant is calculated as [2]

$$\eta_{\text{th}} = (W_e + Q_0 / \text{cop}) / (Q_I \times \eta_{\text{collector}} \times (A_{\text{collector}} - A_{h,\text{collector}})) \quad (21)$$

Cogeneration efficiency of the plant is calculated as

$$\eta_{\text{cogeneration}} = (W_e + Q_0 / \text{cop} + Q_h) / (Q_I \times \eta_{\text{collector}} \times A_{\text{collector}}) \quad (22)$$

where η_{th} is the thermal efficiency of the plant, and cop is the coefficient of performance of an air-conditioner, considered to be 2.8.



Thermodynamic Properties

Gibbs free energy equations of mixtures have been used for the evaluation of thermodynamic properties of $\text{NH}_3\text{-H}_2\text{O}$ at various state points and are compared with those presented in [8]. The concentration of NH_3 , enthalpy and mass flow at various state points are presented in **Table 2**.

Table 2 Concentration of NH_3 , enthalpy and mass flow at various state points

State point	Pressure (p), bar	Temperature (T), °C	NH_3 mass fraction(x), kg NH_3/kg mixture	Enthalpy (h), kJ/kg	Mass flow (m), kg/kg vapor distilled
1	2.0	40.0	0.530	-80.0	4.5840
2	30.0	40.0	0.530	-77.0	4.5840
3	30.0	96.0	0.530	180.1	4.5840
4	30.0	127.0	0.9432	1547.52	1.0
5	30.0	87.0	0.6763	205.8	0.1548
6	30.0	87.0	0.9921	1373.2	0.8452
6a	30.0	87.0	0.9921	1373.2	0.8452
7	30.0	137	0.9921	1529.7	0.8452
8	2.0	-16	0.9921	1148.9	0.8452
9	2.0	7.0	0.9921	1278.7	0.8452
10	30.0	127	0.4147	348.2	3.7388
11	30.0	57.4	0.4147	33.0	3.7388
12	2.0	57.4	0.4147	33.0	3.7388
6b	30.0	87.0	0.9921	1373.2	0.8452
13	30.0	65.7	0.9921	290.0	0.8452
14	30.0	35.7	0.9921	140.8	0.8452
15	2.0	-16.0	0.9921	140.8	0.8452
16	2.0	-10.0	0.9921	1200.2	0.8452
17	2.0	50.56	0.9921	1349.4	0.8452

RESULTS AND DISCUSSION

The fraction (\dot{f}) of vapor flowing through the turbine is adjusted depending on the refrigeration needs of the residential building to commensurate with DBT. Simulation results of solar vapor absorption cogeneration plant for utilization of solar energy for electrification and cooling/heating of residential buildings are plotted in **Figures 2(a)**, **3(a)** and **4(a)** for three locations, viz. Bhopal, Jaipur, and Hyderabad respectively. The maximum and minimum Dry Bulb Temperature (DBT) in °C, and solar irradiation for 100 m² solar collector area, Q_s , heating capacity, Q_h , electrical energy, W_e , and cooling capacity, Q_c (all are in kW-h/day) are plotted for the months from January to December. From these figures, it is observed that as the cooling capacity of the plant is increased from January to May with increase in DBT to provide adequate cooling in summer, the corresponding electrical energy output is decreased from 36 to 22 kW-h/day for Bhopal, 32 to 16 kW-h/day for Jaipur, and 29 to 19 kW-h/day. The maximum cooling capacity in the month of May varies from 64 to 75 kW-h/day depending on geographical location. Simultaneously the heating capacity will also increase from 58 to 141 kW-h/day for Bhopal, 51.5 to 146.5 kW-h/day for Jaipur, and 88 to 130 kW-h/day for Hyderabad as more vapor condenses in the condenser as the cooling load increases. The vapor flow rate through the turbine is ensured to generate a minimum of 12 units (kW-h) of electricity in all the months irrespective of solar irradiation. During the rainy days of June, July, August and September, there is a fall in solar irradiation and accordingly the electric power generated and cooling produced by the plant are proportionately reduced. However, except in the month of June, during the remaining three months, the cooling requirement of the building is also low because of low DBT and the refrigeration produced by the plant will be sufficient for air-conditioning of the building. During the winter months of October, November and December, the plant can produce required electricity and cooling/heating for air-conditioning as well as DHW.

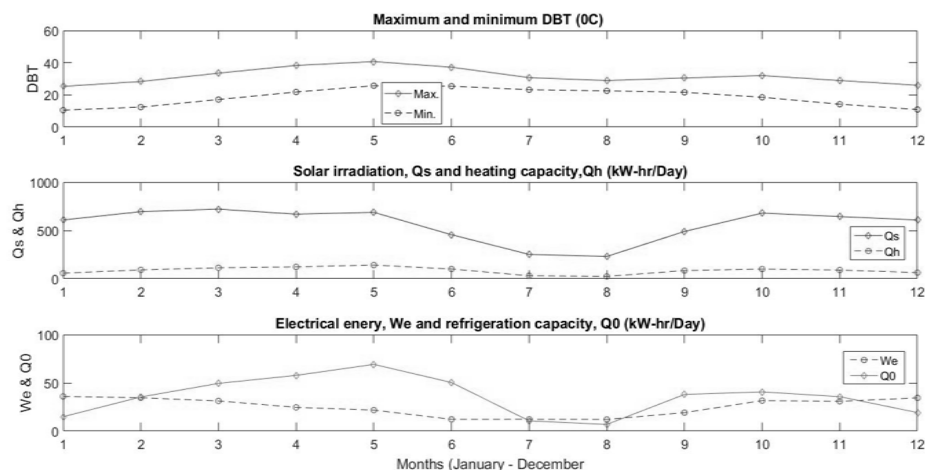


Figure 2(a) Utilization of solar energy for electrification and cooling/heating of residential buildings and DHW for Bhopal

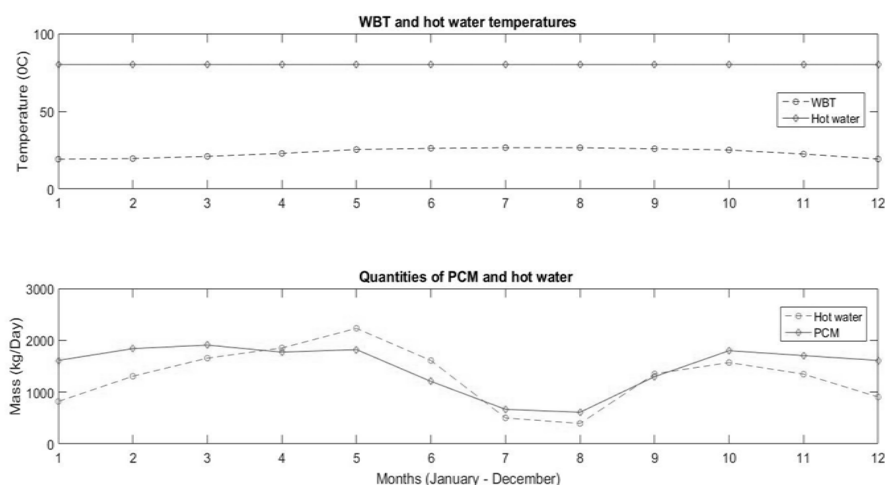


Figure 2(b) Quantities of hot water produced and PCM required for Bhopal

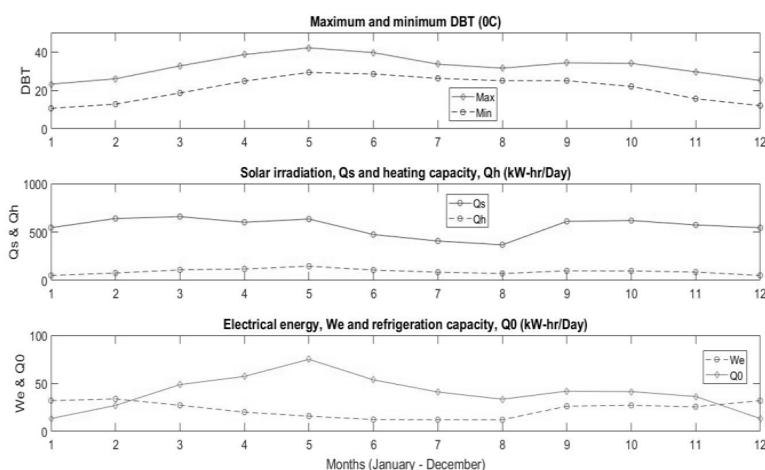


Figure 3(a) Utilization of solar energy for electrification and cooling/heating of residential buildings and DHW for Jaipur

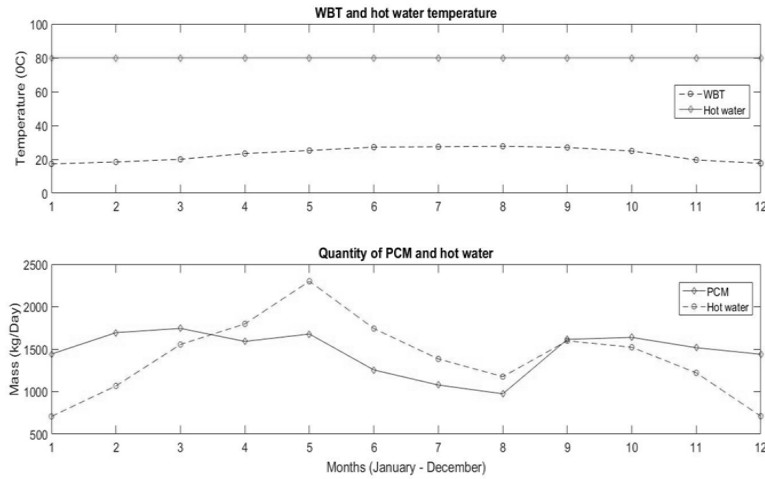


Figure 3(b) Quantities of hot water produced and PCM required for Jaipur

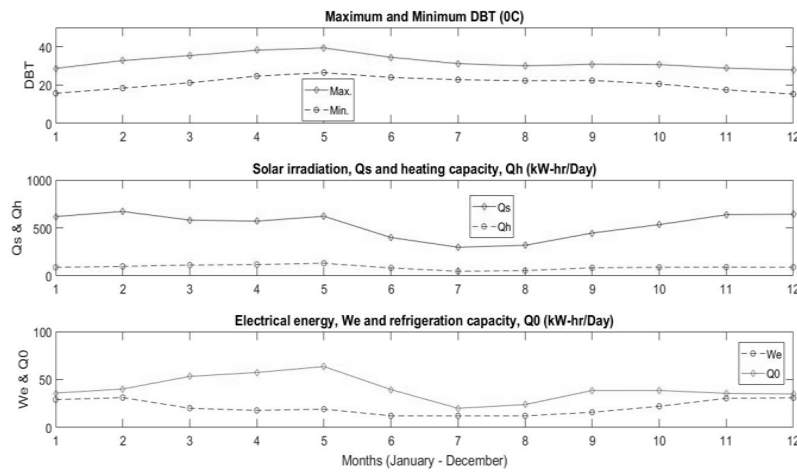


Figure 4(a) Utilization of solar energy for electrification and cooling/heating of residential buildings and DHW for Hyderabad

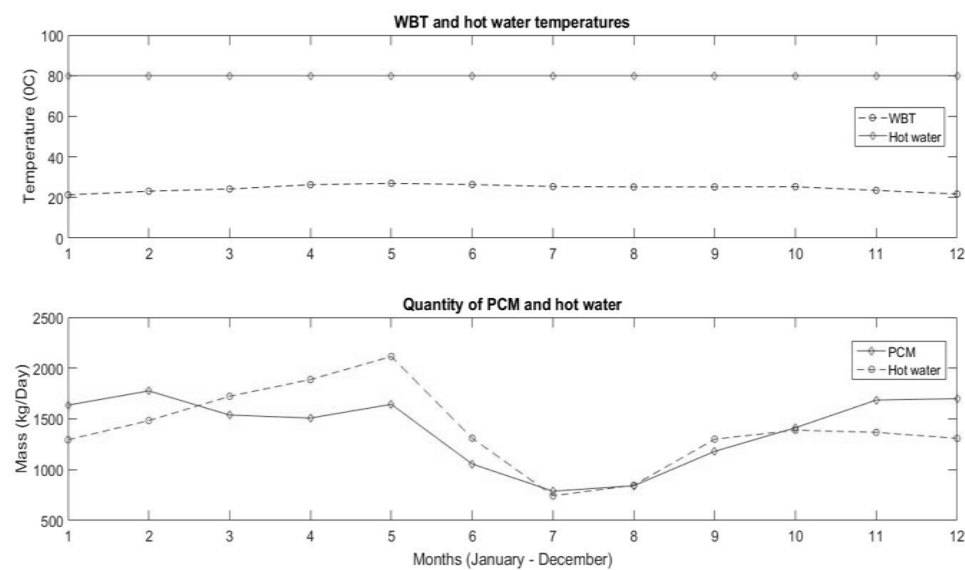


Figure 4(b) Quantities of hot water produced and PCM required for Hyderabad

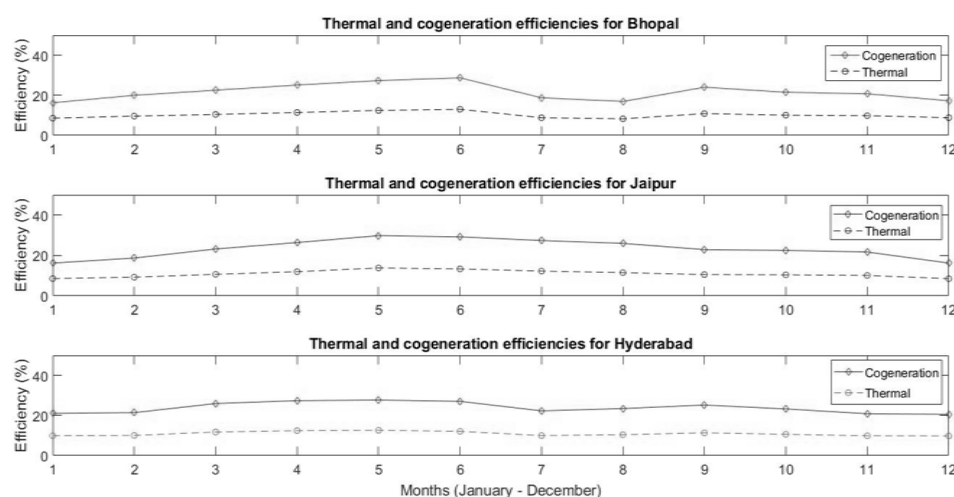


Figure 5 Thermal and cogeneration efficiencies of the plant for Bhopal, Jaipur and Hyderabad

The design WBT in °C, the quantity of hot water produced at 80°C for heating including Domestic Hot Water (DHW), and the quantity of PCM required to store solar thermal energy for night operation of the plant are plotted in **Figures 2(b), 3(b) and 4(b)** for three locations, viz. Bhopal, Jaipur, and Hyderabad respectively for the months from January to December. The quantity of PCM required is estimated to be a maximum of 1800 kg with latent heat of fusion of 306 kJ/kg. **Figure 5** shows the variation of thermal and cogeneration efficiencies of the plant from January to December for three locations viz. Bhopal, Jaipur, and Hyderabad respectively. It is observed that the cogeneration efficiency increases with increase in refrigeration load and corresponding decrease in electrical energy output as more heat is rejected at the condenser and vice versa. The maximum cogeneration efficiency varies from 27.5 to 29.5% depending on the geographical location.

Cost Analysis

The approximate cost of the entire unit of solar absorption cogeneration plant is presented in **Table 3**.

Table 3 Overall projected cost of the solar absorption cogeneration plant

S.No.	Name of the component	Capacity required	Cost per unit, Rs	Total cost, Rs
1	Parabolic trough collector	100 m ²	8000 per m ²	8,00,000
2	Vapor absorption chiller	3 TR	-	2,00,000
3	Turbine and alternator	2 kVA	-	2,50,000
4	Other items	-	-	1,50,000
Total projected cost				14,00,000

As the plant can produce an average of 25 units (kW-h) of electricity and 50 kW-h of refrigeration per day besides plenty of heating, the break even is expected to occur in 6 to 8 years.

CONCLUSION

Solar vapor absorption cogeneration plant is simulated for electrification, and cooling/heating of residential buildings. A case study is made for three different regions, viz. Bhopal, Jaipur, and Hyderabad. Simulation results and cost analysis show that the vapor absorption cogeneration plant is quite feasible for electrification, and cooling/heating of residential buildings in tropical countries like India.

REFERENCES

1. International Energy Agency, World Energy Outlook 2015 Factsheet. Paris, pp. 1–3, 2015.
2. Gunnar Tamm, et.al., Novel combined power and cooling thermodynamic cycle for Low Temperature Heat Sources, Part I: Theoretical Investigation, ASME, 125, pp. 218-222, 2003.
3. Shankar, et.al., Options in Kalina cycle systems, Elsevier, Energy Procedia, Volume 90, pp. 260-266, 2016.
4. Shenyi Wu, et.al., Innovations in vapour-absorption cycles, Elsevier, Applied Energy, Volume 66, pp. 251-266, 2000.
5. D. Y. Goswami, F Xu, Analysis of a new thermodynamic cycle for combined power and cooling using low and medium temperature solar collector, ASME J. Sol. Energy Eng., Volume 121, pp. 91–97, 1999.
6. GGershon, Solar-powered systems for cooling, dehumidification and air-conditioning, Solar Energy, Volume 72, Number 1, pp. 53-62, 2002.



7. D.S Kim, C.A. Infante F., Solar refrigeration options – A state-of-the-art review, *International Journal of Refrigeration*, Volume 31, pp. 3-15, 2008.
8. F. Xu, D. Y.Goswami, Thermodynamic properties of ammonia-water mixtures for power cycle applications, *Energy*, Volume 24, pp. 525–536, 1999.
9. Y. M.El-Sayed, M.Tribus, Thermodynamic Properties of Water-Ammonia Mixtures: Theoretical Implementation for use in Power Cycle Analysis, ASME, AES-Volume 1, 1985b.
10. A. I. Kalina, M.Tribus, Y. M.El-Sayed, A Theoretical Approach to the Thermophysical Properties of Two-Miscible-Component Mixtures for the Purpose of Power-Cycle Analysis, ASME Paper No. 86-WA/HT-54, 1986.
11. Y. Tian, C.Y. Zhao, A Review of solar collectors and thermal energy storage in solar thermal applications, *Applied Energy*, Volume 104, pp. 538-553, 2013.
12. A.K.Soteris, Solar thermal collectors and applications, Elsevier, *Progress in Energy and Combustion Science*, Volume 30, pp. 231-295, 2004.
13. S.D. Odeh, et.al., Modeling of parabolic trough direct steam generation solar collectors, *Solar Energy*, Volume 62, No. 6, pp. 395-406, 1998.
14. K.Soteris, The potential of solar industrial process heat applications, Elsevier, *Applied Energy*, Volume 76, pp. 337-361, 2003.
15. S. C.Joe, Performance of a concentrating photovoltaic /thermal solar collector, Elsevier, *Solar Energy*, Volume 78, pp. 211-222, 2005.
16. D. Kearney, et.al., Assessment of a molten salt heat transfer fluid in a parabolic trough solar field, ASME, *Journal of Solar Energy Engineering*, Volume 125, pp. 170-176, 2003.
17. K. Vignarooban, et.al., Heat transfer fluids for concentrating solar power systems – A review, Elsevier, *Applied Energy*, Volume 146, pp. 383-396, 2015.
18. C.P. Arora, Refrigeration and Air Conditioning, Tata McGraw-Hill, ISBN 0-07-463010-5, 2006.



Investigate the Effect of Multi-Stage and Single-Stage Forming on Sheet Metal Part, Brake Plate

Gajendra Kumar Nhaichaniya^{*1}, Chandra Pal Singh²

Brij Nagar Colony, Bharatpur, Rajasthan¹, singhgajendra0504@gmail.com^{*}

Samrat Ashok Technological Institute, Vidisha, Madhya Pradesh²

ABSTRACT

In this study manufacturing process, forming of brake plate was proposed by finite element method (FEM) and validated by experimentation. In traditional trial and error approach, huge number of trials have to be considered till meet the requirement. Using simulation modelling, number of trials reduced into very few, which helped to reduce tool development cost and time. Brake plate formed via single-stage and results are observed. Later on brake plate is formed via multiple stages, known as forming stage I and II, then results are compared with single-stage. Due to path dependent strain there is huge diversity in both results even for same contact and boundary conditions. Such diversity in results enhanced the interest to identify suitable way of forming to complex sheet metal part. However, deciding the parameters for earlier forming stages in such a way that requirement meet in subsequent forming stages, was quite challenging task and need many iterations. Which is quite time consuming and expensive task for experimentation. By use of CAE tool these iteration results can be found in shorter time. HyperForm simulation module from HyperWorks, taken as analysis tool to predict behavior of final formed component. The main objective of this paper is to investigate need of multi-stage forming process for manufacturing of complex sheet component in comparison with single stage.

KEYWORDS Multi-stage and single-stage forming of sheet metals, Finite Element Technique in sheet metal forming, Brake plate.

INTRODUCTION

In sheet metal forming processes force applied to a piece of metal (blank) to modify its size and shape, rather than remove any material. Developed stresses in the blank piece are beyond the yield limit of the blank material and permanent deformation take place, due to applied force. If applied forces are uncontrolled then material may get high thinning, tearing or wrinkling. However, the design of forming tool for complex component mainly depends on the engineers experience presently, if the design quality can't be ensured, its results too long time in trial and error to fulfill requirement [1]. CAE tool can be used for reduction in such trial time and cost of production based on virtual simulation results and plots. If need to change, can be easily modify and reanalyze. This way is much efficient compare to traditional approach.

Tool setup and number of stages in sheet metal work mainly depend upon thumb rule, height to diameter ratio (h/d) and complexity of component. As h/d ratio increases in deep drawing process, number of stages also increase and it need to go through multi-stage process. But for complicated sheet structure, where material flow is restricted in critical zones, to ensure quality of final component multi-stage forming is recommended even for lower h/d ratio. However, if possible multi-stage forming process generally avoided because of high tooling cost as well it decrease production rate. Needs of multi-stage process for manufacturing of brake plate and its comparison with single-stage are main observation point.

TOOL SETUP

To investigate the effect of single-stage and multi-stage forming, brake plate is assumed to be form by both process. All press tool standards and clearance are considered in design stage. To perform CAE analysis it need to import only Punch, Die, Binder, Support and Initial blank component in software. Once model is imported in software, blank is meshed via full integration 2D quad element and tool component (punch, binder, die) meshed via rigid element. Appropriate contacts are defined after mesh is done, as shown in **Table 1**.



TOOL SETUP FOR SINGLE-STAGE FORMING

The circular blank was first formed via single-stage. To do this blank directly placed on die face which partially holds by binder during forming operation. Necessary supports are provided to blank. For simplicity purpose in analysis external support are not considered. Tool setup for single-stage forming is shown is **Figure 1**.

Table 1 Contact conditions

Contact number	Comp 1	Comp 2	Coefficient of friction
01	Punch	Blank	0.125
02	Die	Blank	0.125
03	Binder	Blank	0.125

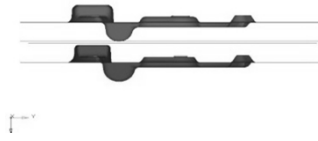


Figure 1 Single-stage tool setup

TOOL SETUP FOR MULTI-STAGE FORMING

Now the blank with same parameter formed in two stages. The tool setup for subsequent stages shown in **Figures 2** and **3**. To decrease overall tooling cost, open die is used in stage I. Output result of stage I (dome shape) used as input blank for stage II.



Figure 2 Multi-stage tool setup, stage I

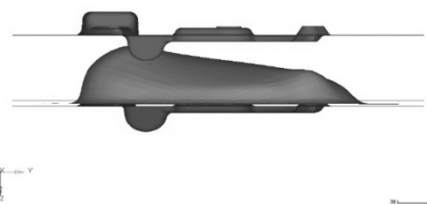


Figure 3 Multi-stage tool setup, stage II

Tool setup is mentioned in **Figures 1, 2** and **3** gives focus on forming stages only. To finalize the manufacturing of brake plate more number of stages required including trimming and piercing.

TOOL PARAMETERS

As shown in **Table 3**, tool parameters for both single-stage and multi-stage forming process are used to be same except punch travel height because of different blank shape and position. In multi-stage forming process to decide input of stage I, in such a manner that will give desire output in stage II, it need to iterate with different punch shape and travel height. For that, number of trial shape in stage I are proposed and investigate using CAE software as shown in **Table 2**. The punch travel height for stage I considered at least 40 mm, as per die shape of stage II.

Table 2 Trial setup for veyring punch height

Trial	Stage I punch height	Stage II punch height
1	40	45
2	42	47
3	44	49

Table 3 Tool setup parameters

Tool setup	Blank material	Blank thickness	Punch travel height	Punch speed	Blank holder force
Single-stage	CRDQ steel	2.5 mm	35 mm	2000 mm/s	40 kN
Multi-stage, stage I	CRDQ steel	2.5 mm	42 mm	2000 mm/s	40 kN
Multi-stage, stage II	CRDQ steel	Import from 1 st stage	47 mm	2000 mm/s	40 kN

SIMULATION RESULTS AND DISCUSSION

Thinning

Thinning is measurement of reduction in thickness of sheet. It is general practice in industry to use thinning as a failure criteria [2]. During forming operations if thinning reaches its critical value failure takes place, but it observed in different studies that thinning of the material before fracture is not a constant and is dependent on the strain path. Hence thinning cannot be used as failure criteria [2].

From simulation result, **Figure 5**, it is very clear that in single-stage forming due to high value of thinning, material get tear off from many regions. This lack of material is due to less ductility and strain rate. However, material is sufficient ductile to fulfill the requirement, but due to lack of flow of material at critical zones localize thinning and tearing appears. Bidirectional flow of material at critical zones is cause of stretching in sheet hence lack in material appears as shown in **Figure 4**.

In case I, by calculated amount of binder force, material flow can be control in such a manner that only acceptable amount of thinning and wrinkle will appear. Means by varying binder force, wrinkling and thinning can be control. But in case II for same binder force material have tendency to stretch instead of flow in die cavity. Due to excessive stretching of material there is of tearing of blank. If binder force decreased high wrinkles appears in blank.

Figure 5 shows maximum thinning as 93.931% and maximum wrinkle 174.668%. Such amount of thinning is actually tearing of the material and at nearby locations excessive amount of material stuck as wrinkle. However, to show tearing phenomena in software it need be consider fracture based material properties during modeling. That will increase the computation cost.

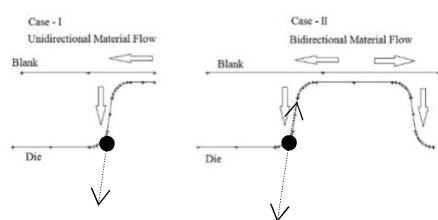


Figure 4 Flow of material

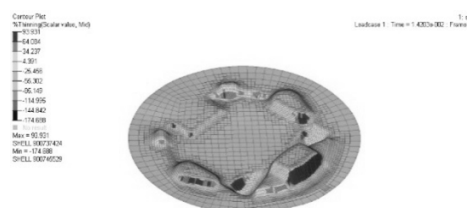


Figure 5 Thinning in blank for single-stage tool setup

To avoid lack of material at complicated regions, in multi-stage forming blank is first formed in pre calculated shape then reformed in second stage. In this way excessive stretching of material is avoided. Material flow point of view, both stages having unidirectional flow mostly so very few amount of stretching occurs. **Figures 6** and **7** shows stage I and stage II simulation results for trial 2. Maximum thinning occur in stage I is 9.87 % and maximum wrinkle is around 8%. Once simulation of stage I finished then formed shape with result data is imported as blank for stage II. The maximum thinning and wrinkling in stage II 17.53% and 23.43%, respectively. **Figure 8** shows thinning and wrinkling in final component at same scale as in single-stage.

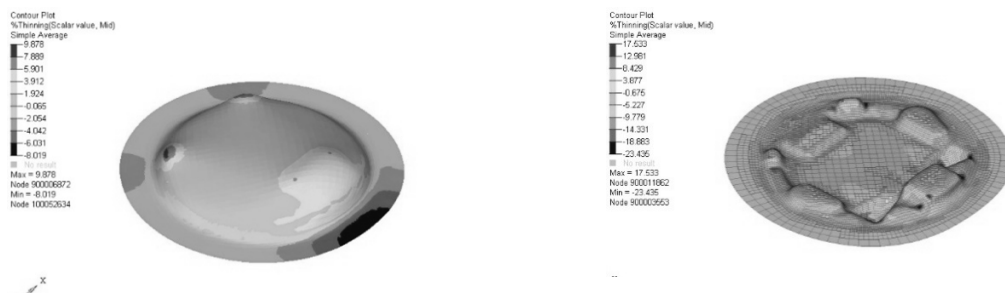




Figure 6 Thinning in blank for stage I of multi-stage tool setup (at original scale)

Figure 7 Thinning in blank for stage II of multi-stage tool setup (at original scale)

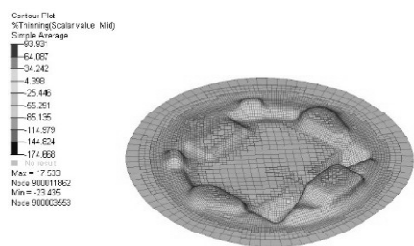


Figure 8 Thinning in blank for stage II of multi-stage tool setup (at same scale as **Figure 5**)

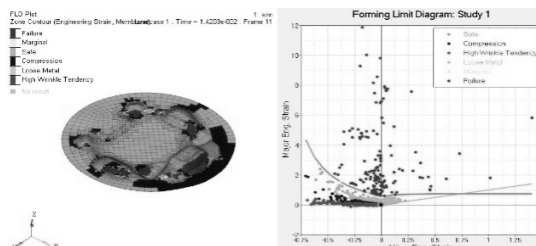


Figure 9 Forming limit diagram for single-stage tool setup

Forming Limit Diagram (FLD)

Due to extensive tensile deformation at localized area, necking and fracture are common in many sheet forming operations. At same time large compressive force is responsible for buckling in sheet. Such complex loading can't be analyze by simple uniaxial tensile test. Uniaxial tension test has limitation to use, when deal with formability in sheet metals. The state of stress during sheet metal forming is tri axial in nature, analyzing it with uniaxial tension test will mislead. Well known forming limit diagram (FLD) is used to analyze such complex loading conditions in sheet forming. In software FLD is plotted by measuring strain along two principal directions (principal strain) in circle grid for each element. Principal strain can calculated as the percentage change in length of the major and minor axes. The plot of the major strain versus minor strain gives the limiting strains corresponding to deformations. Combination of strains represented failure element above the forming limit curves (FLC) and safe deformations below the FLC. Strains measured near necking regions or fracture are the failure strains.

In **Figures 9** and **10** red curve is for FLC, yellow curve is marginal failure curve. It is observed that the slope of FLC decrease with increasing the strain hardening exponent, increasing the thickness of blank resultant increase in FLD.

For single-stage tool setup huge number of elements are above the FLC which shows failure element as in **Figure 9**. Such high strain occurs on localize elements due to excessive stretching of material. High wrinkling tendency element shown in pink color. Both high thinning and high wrinkling conditions are undesirable and it can be accepted up to certain limiting value only.

Trial 2 performed on multi-stage tool set up that gives favorable result due to change in strain path. In **Figure 10** there are all elements under safe forming or in acceptable range of wrinkling and thinning.

Experimentation

In order to validate simulation results of multi stage forming process, thinning of brake plate was measured at various section as shown in **Figure 11**. The high thinning region marked in simulation are main observation points. The manufactured component cut into pieces along line 1-3 then thickness measured on regions 1-3 by help of screw gauge. The percentage reduction in sheet thickness is ~20% by screw gauge and 17.5 % in simulation result. It means simulation and experimentation results having good agreement with 2.5 % error only.

Due to presence of high thinning and tearing in single-stage simulation result, it need not to validate even. There may chances of scratches in tool.



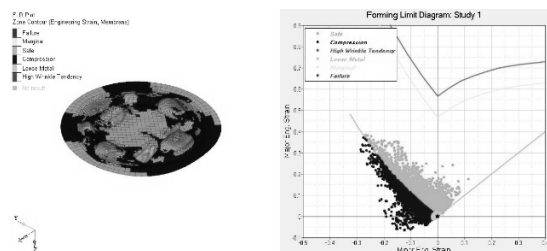


Figure 10 Forming limit diagram for multi-stage tool setup

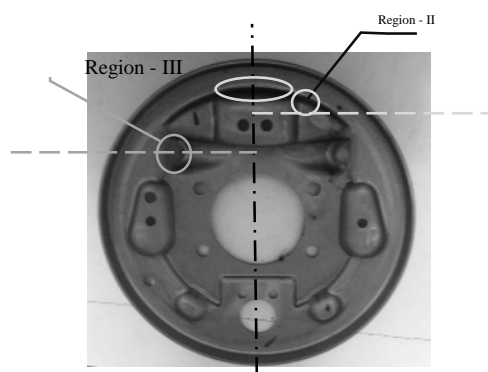


Figure 11 Manufactured brake plate

CONCLUSION

This study give a clear view that strain is path dependent and can be utilize for forming of complex sheet component. By changing path of strain, flow of material can be control in individual stages. However, decision of selecting number of stages in forming for complex structure still depends on the tool design experience.

In forming of brake plate where single-stage forming fail to give desired output, multi-stage forming is very suitable. Of course in multi-stage process also significant amount of thinning and wrinkles but within acceptable range. However, acceptable range of these parameters vary with application, quality and industrial standards. In multi-stage process the punch travel height of stage I considered at least 40 mm as per die shape and iterate for different values. The optimum results found at 42 mm of punch travel. Manufactured component by multi-stage process has approximate same thinning as shown by CAE result, within 2.5% of error.

For complex sheet structure it need to form in two or more stages but it is not always true. It may possible for some cases to achieve desire outputs via one stage by changing in tool assembly, provide additional supports and use of better lubrication. Such changes may increase tool complexity, hence cost will increase.

REFERENCES

1. W. Chen, Z.J. Liu, B. Hou, R.X. Du, Study on multi-stage sheet metal forming for automobile structure-pieces, *Journal of Materials Processing Technology*, 113–117 (2007).
2. B. Sarkar, B.K. Jha, D. Mukerjee, S. Jha, and K. Narasimhan, Thinning as a Failure Criterion During Sheet Metal Forming, *ASM International*, 63-64 (2002).
3. Surya Prakash, Dinesh Kumar, Investigation and analysis for the wrinkling behavior of deep drawn die sheet metal component by using fast form, *Proceedings of the National Conference on Trends and Advances in Mechanical Engineering*, YMCA University of Science & Technology, Faridabad, Haryana (2012).
4. Z. Marciniak, J.L. Duncan, S.J. Hu, *Mechanics of Sheet Metal Forming*, 2nd ed., Butterworth-Heinemann (2002)



Parametric Analysis and Optimization of Production of Karanja Methyl Ester using Taguchi Design of Experiment

Pramod Kumar^{*1}, Shailendra Sinha², Praveen Tyagi³

MMIT, Hathras, Technical Education Department, Government of Uttar Pradesh¹, *er.pramodtyagi@gmail.com**

Mechanical Engineering Department, Institute of Engineering and Technology Lucknow²

Department of Chemistry, St. John's College, Agra³

ABSTRACT

The optimum transesterification reaction conditions with the use of Taguchi Design of experiment for Karanja oil depends upon different optimization parameters like molar ratio, catalyst concentration, reaction time and temperature. Experiments are performed on the molar ratio 1:3, 1:6 and 1:9, temperature 50°C, 60°C and 70°C with 0.5%, 1% and 1.5% KOH at time interval of 45, 60 and 75 min for optimization of high quality of production of methyl ester. To remove fatty acids from Karanja oil to separate biodiesel and glycerol, the optimal parameter of Molar ratio 1:6, reaction temperature 60°, time 75 min. and catalyst concentration 1.5 wt % was obtained. The experiments performed under the optimization conditions gives a useful increased process performance for the production of Karanja biodiesel, using Taguchi L₉ orthogonal array of experiments with four parameters at three levels.

KEYWORDS Karanja oil, Transesterification, Optimization, Taguchi design of experiment, Orthogonal array

INTRODUCTION

Due to gradual depletion of the world petroleum reserve, rising petroleum prices, increasing warming attention has been diverted towards the search of cleaner, nonpolluting fuels that can effectively serve as an alternate to petro based energy. Biodiesel is an alternate fuel fulfills the increasing demand of petro diesel. Due to similarity of fuel properties in many non-edible oils, they can be used as alternate fuel for engine [1]. Jatropha, Karanja oils are mainly used for biodiesel production due to less consumption in domestic use[2]. Karanja oil (*Pongamia pinatta*) is non edible in nature is available abundantly in India [3]. Karanja is main dry land tree which provide a opportunity to produce biodiesel in rural area and fulfill the demand of engine fuel [4]. Environmental laws play an important role to divert the attention of many researchers towards low cost and pollution free biodiesel [5]. The methyl esters of non-edible oil are much cheaper than petroleum diesel [6]. A large number of vegetable oils can be used satisfactorily in CI engines by transesterification. There is an advantage with biodiesel, it is easily used in diesel engine without any alteration [7]. Vegetable oils are usually triglycerides with number of branched chains of different length. The polyunsaturated nature of the vegetable oils causes high viscosity [8]. Free fatty acids from vegetable oils are reduced by the process of transesterification in the presence of methanol and catalyst to convert the triglycerides in to methyl ester and glycerol. Almost all biodiesel is produced by using base catalyzed transesterification process, as it is the simple process and requiring only low temperature [9].

The main factors which affect the production of biodiesel are molar ratio, catalyst percentage, reaction time and temperature [10]. Production of high quality of biodiesel from rice bran oil is produced under the optimum condition, 9:1 0.75% (w/w), 1hour, 55°C molar ratio, catalyst concentration, reaction time reaction temperature respectively [11]. A high yield of Karanja biodiesel was opted on molar ratio 8:1 and catalyst percentage of NaOH, KOH and NaOCH₃ taken 0.8, 1.0 to 1.2% respectively by weight % and reaction temp between 59.5 to 60.5°C with time 45 to 60 min results 90 to 96% optimized yield production of biodiesel using mechanical stirrer [12]. For high production of biodiesel from Karanja oil, the optimum conditions were investigated with molar ratio 8-10, catalyst 1.5% w/w KOH, reaction time between 30 to 40 min and temperature between 68 to 70°C at 1 atm pressure [13]. Taguchi design of experiment having less number of experiments with optimum process parameters gave 96.7% yield percentage in case of production of biodiesel from rapeseed. [14].

The trees of Karanja can grow in any climatic conditions having production capacity of oil approximately 1350 billion tons. So we have chosen Karanja oil for production of biodiesel in our experimental study.

MATERIALS AND METHODS

The filtered Karanja oil was procured and purchased from Agrawal oil expeller Bichpuri, Agra (U.P.). Transesterification reactor is manufactured and purchased from J-SIL Scientific Industries, Nunhai Industrial Estate, Agra (U.P.). Chemicals related to the transesterification process like Methanol, KOH were purchased from Modern



Scientific Instruments Ltd, near St. John's College crossing, Agra. Mechanical stirrer is used for transesterification of raw Karanja oil.

TRANSESTERIFICATION PROCESS

In transesterification process (**Figure 1**) Fatty acids/triglyceride are mixed with methanol in presence of catalyst KOH/NaOH to form methyl esters and glycerol.

KARANJA OIL TRANSESTERIFICATION

In transesterification process, a known quantity of filtered oil is taken. The known quantity of KOH is dissolved in methanol in separate flask. The filtered oil and KOH dissolved in methanol is poured in to the biodiesel reactor. Mixture is stirred continuously using mechanical stirrer. The temperature of the mixture is nearly kept constant during reaction for definite time say 1 h. When reaction time is over then mixture is left over a night in a separate flask for settlement. Now two layers were observed. Upper layer is separated as methyl ester of Karanja oil and lower dark colour layer as glycerol.

Upper layer of methyl ester of Karanja oil was mixed with distilled water for washing and purification and then dried with silica for final utilization. The mechanical stirrer was used for transesterification which is shown in **Figure 2**.

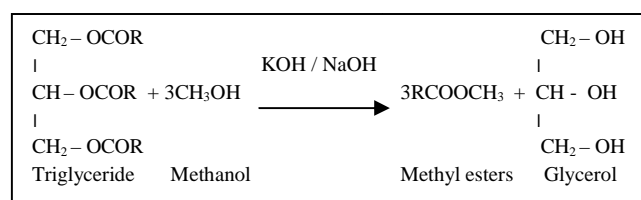


Figure 1 Transesterification process

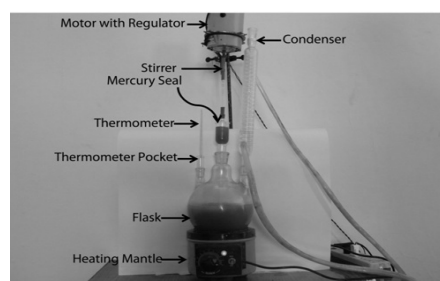


Figure 2 Experimental set up for transesterification reaction

EXPERIMENT ANALYSIS AND RESULTS

Taguchi Methods

Dr. Genichi Taguchi, "The Father of Quality Engineering," developed three types of process design i.e. system, parameter and tolerance design. For optimization, the parameter design is used to achieve the quality characteristics with low cost and less experiments [5].

Calculation for Degree of Freedom (D.O.F.)

Four factors are considered with three levels [16]; so all factors have

D.O.F = number of level - 1.

D.O.F. for each factor A, B, C and D is 2

Total (D.O.F_T) = 8

Orthogonal Array (O.A.)

The orthogonal array depends upon the following mathematical conditions:

O.A chosen \geq D.O.F. required

The total D.O.F for the four factors at three levels has 8 D.O.F. So we have chosen L₉ orthogonal array with 9 experiments with three level four factors.

Signal-to-Noise (S/N) Ratio

Signal to Noise ratio is the ratio of the Mean (Signal) to the standard deviation (noise). The S/N ratios have mainly three category i.e. larger the better, smaller the better and least the better [15]. The response variable considered in

this study, larger the better for high production of biodiesel from Karanja.
$$\text{S/N Ratio} = -10 \log_{10} \frac{1}{n} \sum_{i=1}^n \left(\frac{1}{y_i} \right)^2$$



where n is the number of repetitions of each experiment and y_i the yield of Karanja biodiesel. The S/N Ratio is shown in **Table 3** and the mean yield of Karanja biodiesel and S/N Ratio were 80.7% and 41.07 respectively.

OPTIMIZATION OF TRANSESTERIFICATION PROCESS FOR PRODUCTION OF KARANJA METHYL ESTER

Taguchi Design of Experiment for Optimization

The Taguchi method includes selection of parameters, utilizing an orthogonal array, conducting experimental runs, data analysis, determining the optimum combination and verification. The main operational parameters and levels are based on those previously reported studies by [4,8,14]. Process parameters and levels for production of biodiesel from karanja are listed in **Table 1**. For experiments the method of Taguchi is used for the 4 factors considered (Molar Ratio, Catalytic concentration, Reaction time, Reaction Temperature) at three levels. The basic Taguchi orthogonal array chosen is $L_9(3^4)$ for four selected parameters at three levels shown in **Table 1** [16].

Mean percentage of yield of Karanja biodiesel was found by nine sets of experiments and summarized in **Table 3**. From table it was found that experiment no. 6 which has a highest percentage of yield 93.7 % and experiment no. 4 has the lowest yield percentage of 64.5%.

Table 1 Process parameters and their levels

Process parameter	Process parameter	Levels		
		1	2	3
A	Molar ratio (oil/methanol)	1:3	1:6	1:9
B	Catalyst con., wt %	0.5	1.0	1.5
C	Reaction time, min	45	60	75
D	Reaction temp, °C	50	60	70

Table 2 The Basic Taguchi $L_9(3^4)$

Exp no.	Parameters and their levels Molar ratio (oil/methanol)	Catalyst con., wt %	Reaction time, min.	Reaction temp °C
1	1	1	1	1
2	1	2	2	2
3	1	3	3	3
4	2	1	2	3
5	2	2	3	1
6	2	3	1	2
7	3	1	3	2
8	3	2	1	3
9	3	3	2	1

Table 3 Mean % of Yield of Karanja methyl ester and S/N ratio

Exp no.	Yield of fatty acid methyl ester, %			S/N ratio, η , db
	Sample 1	Sample 2	Mean sample	
1	71.1	65.1	68.1	39.67
2	87.7	89.8	88.7	41.97
3	88.3	84.2	86.3	41.73
4	65.6	63.4	64.5	39.20
5	91.2	89.3	90.3	42.12
6	94.8	92.6	93.7	42.45
7	74.5	69.7	72.1	40.17
8	76.4	85.4	80.9	41.17
9	82.7	80.2	81.5	41.23
				Mean S/N ratio = 41.07



Analysis of Mean Effective Response for Raw Data

After analysis of mean effective response for raw data, the values are shown in **Table 4**. The term Delta (Δ) compare the result of the parameters, which shows the larger influence parameter for production of Karanja methyl ester.

Table 4 Mean Effective Response

Parameters	Level			Max-Min (Δ)	Rank	% Contribution
	1	2	3			
A molar ratio(oil/methanol)	81.0	82.8	78.2	4.6	4	12.8
B Catalyst concentration, wt %	68.2	86.6	87.2	19.0	1	52.9
C Reaction time, min	80.9	78.2	82.9	4.7	3	13.0
D Reaction temp, °C	79.9	84.8	77.2	7.6	2	21.1

From **Table 4** the value of Delta corresponding to the parameter (B) catalyst concentration gives the maximum influence on the production of biodiesel from Karanja oil followed by parameter (D) Reaction temp, parameter (C) Reaction time and parameter (A) molar ratio.

Analysis of Signal to Noise (S/N) Ratio

The mean S/N ratios were calculated from the effect of the parameter and their levels. Take parameter A and level 1, the mean S/N ratio (41.12 db) was calculated using values from experiment number 1, 2 and 3. On same parameter A select level 2, the average or mean S/N ratio (41.25 db) was calculated from experiment 4, 5 and 6 and On same parameter A select level 3, the average or mean S/N ratio (40.85 db) was calculated from experiment 7, 8 and 9. The mean S/N ratio and distribution for the four parameters are shown in **Table 5**. The highest value of S/N Ratio represents the optimal conditions at minimum deviation for selected parameters.

Table 5 Mean effective response for S/N ratio

Parameters	Level			Max-Min (Δ)	Rank	% Contribution
	1	2	3			
A Molar ratio	41.12	41.25	40.85	0.40	4	10.3
B Catalyst con., wt %	39.68	41.75	41.80	2.12	1	54.5
C Reaction time, min.	41.09	40.80	41.34	0.54	3	13.9
D Reaction temp., °C	41.0	41.53	40.70	0.83	2	21.3

CONFIRMATION OF EXPERIMENT

To validate the optimum Karanja methyl ester production from Karanja oil (A_2 , B_3 , C_3 , D_2) (molar ratio 1:6, catalytic concentration 1.5 wt %, reaction time 75 min, reaction temp 60°C) process parameter was obtained by the Taguchi design of experiments. Based on these parameters, the total two experiments were conducted for confirmation that were suggested by the experiment and yield of fatty acid methyl ester % have been calculated and is tabulated in **Table 6**.

Table 6 Percentage of Karanja methyl ester

Exp no.	Yield of fatty acid methyl ester %			S/N ratio, db
	Sample 1	Sample 2	Mean sample	
1.	92.6	94.8	93.7	42.45
2.	94.7	95.1	94.9	42.56

CALCULATION FOR ACTUAL RESULT

After conduction of confirmation of experiment, the results for the yield of the fatty acid methyl ester percentage found to be:

Total average of yield % = $(93.7 + 94.9) / 2 = 94.3 \%$

Mean S/N ratio = $(42.45 + 42.56) / 2 = 42.51 \text{ db}$



COMPARISON OF RESULTS

The results obtained from the confirmation of experiments are hereby compared by the prediction result of Taguchi Design experiment.

Actual Result

Total average of yield % = 94.3 %

Mean S/N ratio = 42.51 db

Predicted result (By Taguchi method)

Predicted mean of yield % = $A_2 + B_3 + C_3 + D_2 - 3Y = 82.8 + 87.2 + 82.9 + 84.8 - 3 \times 80.7 = 337.7 - 242.1 = 95.6 \%$

Predicted S/N Ratio = $\eta_{A2} + \eta_{B3} + \eta_{C3} + \eta_{D2} - 3\eta = 41.25 + 41.8 + 41.34 + 41.53 - 3 \times 41.07 = 165.92 - 123.21 = 42.71 \text{ db}$

CONCLUSION

Experiments performed on the basis of Taguchi Design of Experiment and results are analyzed. The optimum characteristics for the yield percentages of production of Karanja methyl ester are obtained and the experiments are conducted for the confirmation of data, then the results are collated. From the **Table 3.4** Average (Mean) Effective Response, the factor (B) catalyst concentration represents the largest influence on percentage yield of biodiesel production followed by factor (C) Reaction temperature, factor (D) Reaction time and finally factor (A) Molar ratio which is further verified with the Table 3.5 Mean Effective Response for S/N Ratio. The values of result from the confirmation experiments predicts that the Taguchi Design of Experiment Method is the best for biodiesel production variables i.e. 95.6% close to 94.3% (actual result). The actual result of S/N ratio 42.51 dB is nearby to the predicted result 42.71 dB. The paper has discussed an application of the Taguchi design of experiment for optimization of production of Karanja methyl ester with a relatively small number of experimental runs.

REFERENCES

1. A. Rehman, R.K. Pandey, S. Dixit, R.M Sarviya, Performance and emission evaluation of diesel engine fuelled with vegetable oil, International Journal of Environment res., Volume 3, Issue 3, pp. 463-470, 2009
2. B. B. Ghosh, S. K. Halder, A. Nag, , Synthesis of biodiesel from oils of jatropha, Karanja and putranjiva to utilize in ricardo engine and its performance and emission measurement. Proceedings of the 4th BSME-ASME International Conference on Thermal Engineering 2008, Dhaka, Bangladesh, pp.731-738, 27-29 December, 2008
3. R.K. Singh, S. Rath, Performance analysis of blends of Karanja methyl ester in a compression ignition engine, International Conference on Biomedical Engineering and Technology 2011, Singapore, IPCBEE Volume 11, pp. 187-192, 2011
4. L.C. Mehar, S.N.Naik, L.M.Das, Methanolysis of pongamia pinnata (karanja) oil for production of biodiesel, Journal of Scientific and Industrial Research, Volume 63, pp. 913-918, 2004
5. S.J.Ramchandra, E.R.Deore, S.P.Milind, S.D.Purushottam, Performance characteristics of single cylinder DI diesel engine fuelled with Karanja biodiesel. Proceedings of World Congress on Engineering, London U.K., Volume 3 July 6-8, 2011
6. M.V.Nagarhalli, V.M.Nandedkar, K.C.Mohite, Emission and performance characteristics of Karanja biodiesel and its blends in a CI engine and it's economics, ARPN Journal of Engineering and Applied Sciences, Volume 5, Issue 2, pp. 52-56, 2010
7. S.P.Kadu, R.H. Sarda, Use of vegetable oils by transesterification method as CI engines fuels: a technical review, Journal of Engineering Research and Studies, Volume 2, Issue 2, pp. 19-26, 2011
8. N.Prakash, A.A.Jose, M.G.Devanesan, T.Viruthagini, Optimization of karanja oil transesterification. Indian Journal of Chemical Technology, Volume 13, pp. 505-509, 2006
9. S.R.Kalbande, S.D.Vikhe, Jatropha and Karanja bio-fuel: an alternate fuel for diesel engine, ARPN Journal of Engineering and Applied Sciences, Volume 3, Issue 1, pp. 7-13, 2008
10. D.Y.C.Leung, W.Xuan, M.K.H.Leung, A review on biodiesel production using catalyzed transesterification, Journal of Applied Energy, Volume 87, pp. 1083-1095, 2010
11. S.Sinha, A.K.Agarwal, S.Garg, Biodiesel development from rice bran oil: Transesterification process optimization and fuel characterization. Journal of Energy Conversion and Management, Volume 49, pp. 1248-1257, 2008
12. Y.C.Sharma, B.Singh, J. Korstad, High yield and conversion of biodiesel from a nonedible feed stock (pongamia pinnata). Journal of Agric. Food Chem., Volume 58, pp. 242-247, 2010
13. Vivek Kumar A.K.Gupta, Biodiesel production from Karanja oil. Journal of Scientific and Industrial research, Volume 63, pp. 39-47, 2004
14. S.T.Kim, B.Yim, Y.Park, Application of Taguchi experimental design for the optimization of effective parameters on the rapeseed methyl ester production, Journal of Environment Engineering Research, Volume 15, Issue 3, pp. 129-134, 2010
15. S.M.Phadke, Quality Engineering Using Robust Design. New Jersey, Prentice Hill, 1989
16. P.J. Ross, Taguchi Techniques for Quality Engineering. New Delhi, Tata Mc Graw Hill, 2005



Material Selection in Product Design: An Extension of Pugh Chart

D. Das^{*1}, S. Bhattacharya², B. Sarkar³

Department of Mechanical Engineering, The Neotia University, Kolkata¹, debasis1004@gmail.com*

Department of Mechanical Engineering, Jadavpur University, Kolkata²

Department of Production Engineering, Jadavpur University, Kolkata³

ABSTRACT

To meet all the functional requirements, choosing an appropriate material takes the vital role in product design. In this paper, an extension is introduced in the traditional Pugh Chart which is a well-known method in the field of performance evaluation of the design alternatives. In traditional Pugh Chart, an alternative is evaluated as better (+), worse (2) or same in respect of a reference material. With the alternatives rated on every criterion, the ratings are summed up into average overall scores. In this situation, the average overall score may raise the best alternative, but a precise ranking throughout the alternatives may not possible. The proposed extension is a relative difference of scaled values assigned through 11-points scale to the alternatives and a datum material. The 11-points scale also acts as a normalizing process. Two stages spur gear reduction unit is considered as a case study. The analysis shows the preeminent gear material is Grade 80-55-06 (ductile cast iron).

KEYWORDS Product design; Material selection; Multi-attribute decision-making; Pugh chart

INTRODUCTION

The design process begins with a need which is based on customers' and markets' demands and ends with a finished product. A successful product enjoys good profits, good market share, and good customer satisfaction. Engineering design is the sequential decision-making process of compromising between shape, materials, and manufacturing [1]. Decision-making is the design activities that optimize the overall design objectives within the techno-socio-economic constraints in order to create an efficient product.

In most of the manufacturing unit, materials costs comprise 50% or more of the manufacturing cost. At the same time, material science has begot a wide range of new materials around the world like smart (intelligent), composite, and functionally graded materials and focused attention towards them besides the traditional materials like metals, ceramics, and polymers. Thus, a designer has a broad class of materials with the advancement of knowledge than ever before. These scenarios present the scope of implementing the innovation in design and to make the product competitive by utilizing the preeminent materials. The aim of this paper is to select the best material in design through the Pugh Chart by introducing the relative difference measurement.

MATERIAL SELECTION

Not all but most of the cases a product should be economically competitive with the fulfillment of required performance. A poorly chosen material not only affect the service performance but may have a negative impact on the entire product lifecycle. Material selection involves past experience along with decision-making aids. Like any other decision-making process, material selection can be characterized as the outcomes of alternatives generation followed by alternatives evaluation (**Figure 1**).

ALTERNATIVES GENERATION

In the design process (**Figure 2**), the customers' needs are generally translated into the function requirements (FRs) and mapping the FRs of the functional domain to the design parameters (DPs) of the physical domain to create a product of feasible embodiment that will fulfill the FRs [2]. It can be concluded that the functional requirements (FRs) are the function of design parameters (DPs). In typical mechanical design, the design DPs are the function of material (attributes) and shape (geometry) and can be represented as,

$$FR = f\{\text{material}(\text{attribute}), \text{shape}(\text{geometry})\}$$

In engineering design, material attributes and shape are interlinked and the good trade-off between material and shape generates the wide range of alternatives (in terms of material or in terms of geometry) to fulfill the required functional requirement.

ALTERNATIVES EVALUATION

Choosing between alternatives is a common feature of design activity. The goal of any materials selection endeavor is to choose the preeminent material for a given application that requires a finite set of alternatives, a set of well-



defined objectives (criteria or attributes) and performance ratings of i^{th} alternative with j^{th} criterion to form a decision matrix. Due to the importance of reliability in product design, the acceptability of the candidate materials is appraised against multiple criteria rather than considering a single criterion.

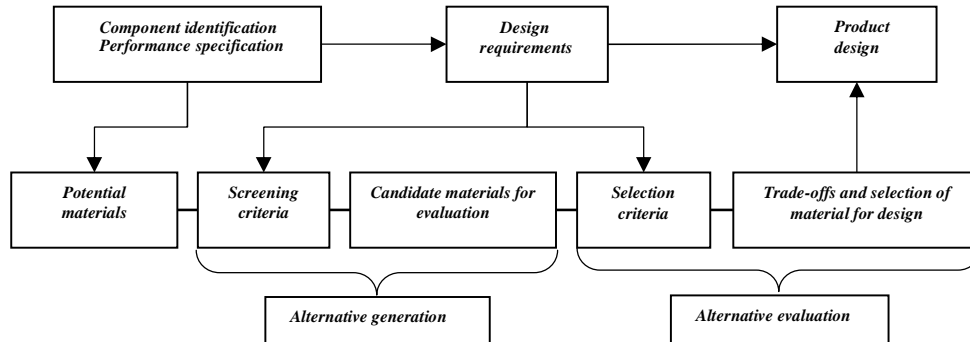


Figure 1 Material selection framework of a product design

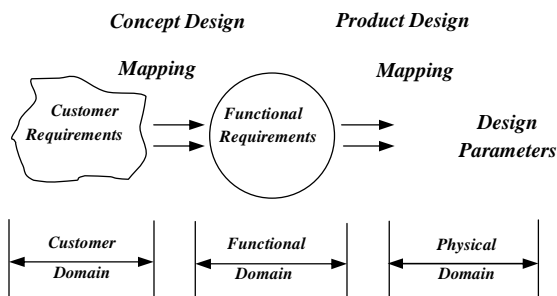


Figure 2 Alternative generation in the design process

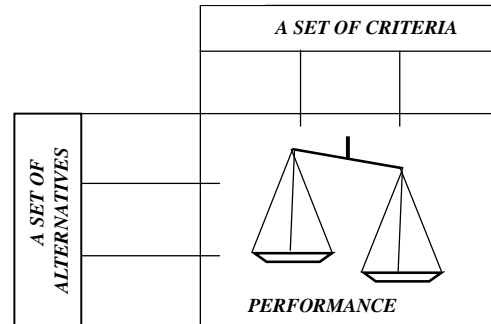


Figure 3 Multi-attribute decision-making framework

There are numerous decision matrix techniques have been developed based on multi-attributed decision-making framework (Figure 3) and are becoming very popular to select the most preminent material for advanced technology components employed in aeronautics, biomedical, and automotive industries shown in Table 1. Typically, in the domain of product design, Decision Matrix Method (Pugh Chart) and Weighted Objectives Method (Pahl and Beitz method) are widely pronounced to evaluate the performance of the alternatives [3,4]. Pahl and Beitz method is particularly well suited for configuration design, using a large number of criteria based on technical requirements, economic factors, and other general constraints. The performances of the alternatives against criteria are expressed by the points. Pahl and Beitz [4] suggested either 11-points scale or 5-points scale as shown in Table 3. Overall weighted value of an alternative is given by,

$$OWV(a_i) = \sum_j w_j \cdot v_{ij} \quad (1)$$

where w_j is weightage of j^{th} criterion and v_{ij} is the value on a relative scale of i^{th} alternative for j^{th} criterion. The preminent alternative is maximum of $OWV(a_i)$.

The Pugh Chart is a method with all criteria qualitatively evaluated with equal weight and each alternative is compared with datum or reference alternative in respect of each criterion and performance are rated better (+), worse (2), or the same (S). With the alternatives rated on every criterion, the ratings are combined into average overall scores to order the alternatives from best to worst and given by [3],

$$AOS(a_i) = \sum_j r_{ij}^+ + \sum_j r_{ij}^- \quad (2)$$

where r_{ij}^+ is a (+) score assigned to i^{th} alternative and r_{ij}^- is a (2) score assigned to i^{th} alternative.



Table 1 MADM methods applied in the material selection

Component	Preeminent material	MADM methods
Total knee replacement	Porous NiTi (SMA)	Comprehensive VIKOR [5]
Metallic bipolar plates	Austenitic stainless steel 316	VIKOR [6]
	Austenitic stainless steel 316	TOPSIS [7]
Flywheel	Kelver 49-epoxy FRP	VIKOR [8]
	Kelver 49-epoxy FRP	TOPSIS [9]
	Kelver 49-epoxy FRP	ELECTRE [8]
Gear	Carburised steel	Extended PROMETHEE II [10]
	Carburised steel	MULTIMOORA [11]
Cryogenic storage tank	Austenitic steel (SS 301- FH)	TOPSIS [12]
	Austenitic steel (SS 301- FH)	Fuzzy logic [13]

Pugh Chart is advantageous over Pahl and Beitz method because there is no need to assign the weightages to the criteria as the alternatives are compared with the known datum alternative which already exists. However, in simple average summation method for overall score, a (2) cancels a (+) which is not adequate. At the same time, one alternative may be (+++) better or (22) worse than the datum alternative, but there is some lack of precise overall ratings and thereby a precise ranking of the alternatives. The aim of this proposed paper is to overcome the above-mentioned discrepancy by assigning a discrete value through the relative measure in place of (+) and (2) while selecting a preeminent material. The specific objectives of this paper that will frame the aim and can be stated as:

- To select the preeminent material in design under uncertainty;
- To convert the performance ratings of the alternatives to a normalized value through a common scale;
- To compare the alternatives with datum alternative by the relative difference method and
- To rank the alternatives precisely.

Proposed Extension in Pugh Chart

Step 1: A set of alternatives (A) with performance ratings (D) in the form of attributes (E)

$$A = \{a_i | i = 1, 2, \dots, m\} \quad (3)$$

$$E = \{e_j | j = 1, 2, \dots, n\} \quad (4)$$

$$D = \{d_{ij} | i = 1, 2, \dots, m; j = 1, 2, \dots, n\} \quad (5)$$

Step 2: Identification of datum or reference material with performance ratings

$$a_k = \{a_i | i, k = 1, 2, \dots, m; i \neq k\} \quad (6)$$

$$d_{kj} = \{d_{ij} | i, k = 1, 2, \dots, m; j = 1, 2, \dots, n\} \quad (7)$$

Step 3: Transformation of performance ratings to a scaled value from common 11-points scale [4]

$$d_{ij} = \{v_{ij} | i = 1, 2, \dots, m; j = 1, 2, \dots, n\} \quad (8)$$

$$d_{kj} = \{v_{kj} | i, k = 1, 2, \dots, m; j = 1, 2, \dots, n\} \quad (9)$$

Step 4: Relative difference of a_i with respect to a_k

$$r_{ij} = \frac{v_{ij} - v_{kj}}{\max(v_{ij}, v_{kj})} \quad (10)$$

Step 5: Average overall score of a_i

$$AOS(a_i) = \sum_{j=1}^n r_{ij} \quad (11)$$

The higher score of $AOS(a_i)$ assures a preeminent material for the product design.

CASE STUDY: TWO-STAGE GEAR REDUCER UNIT

Gear reducers are used in all industries, they reduce speed and increase torque (**Figure 4**). An industrial gearbox can be delineated as a contrivance that transmits power with change in speed and torque used in automobile, aerospace, marine engineering etcetera. The gear elements are mainly classified according to axes lay out and tooth profile. For parallel axes lay out, spur gear is more preferred than helical gear due to ease of manufacturing. The case study basically based on the selection of spur gear materials. According to Lewis analysis in gear design, the gear tooth is subjected to bending causes bending stress due to the tangential load (F_{12} , F_{34}) through the pitch point (P_{12} , P_{34}). Besides the tangential load, the load along the line of action through the pitch point also causes the Hertzian contact stress [14]. To withstand against above-mentioned stresses, materials having good tensile strength and surface hardness are preferable. All mechanical properties are not indispensable during evaluation stage. To make a rational



decision we need to know the intent of the decision, the criteria of the decision, stakeholders and affected groups [15]. The set of criteria should be kept minimal for the ease of computation. The criteria are chosen as:

- Benefit criteria: Ultimate tensile strength, σ^{ut} (e_1) and Brinell hardness number, BHN (e_2).
 - Cost criteria: Density, ρ (e_3) and cost, c (e_4) to balance between customers' requirements and design requirements.
- Some of the featured candidate materials in the ferrous domain for spur gear with performance ratings under specific condition are shown in **Table 2** following the expression (3) to (5) [16]. Following the expression (6) to (7), the datum or reference material is AISI 4130 (a_1) as it is already well-known gear material and all the alternative will be compared with this reference material. According to Step 3, the material attributes are mapped in 11-points scale shown in **Table 3** and consecutive scaled values are putted in **Table 4**. Average overall score of the alternatives are tabulated in the **Table 4** following the expressions (8) to (11).

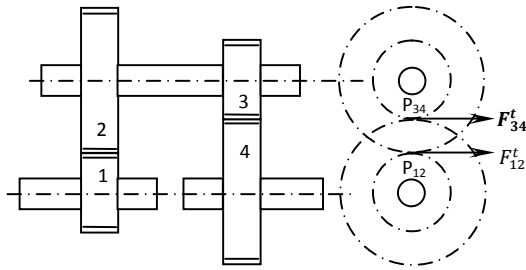


Figure 4 Two stage spur gear reduction

Table 2 Performance ratings of the spur gear materials [16]

Alternatives (a_i)	$\sigma^{ut}(e_1)$	BHN (e_2)	ρ (e_3)	$c(e_4)$
a_1 AISI 4130 (Datum)	560	156	7.85	2.00
a_2 AISI 1040	515	149	7.84	1.30
a_3 AISI 304	515	147	7.80	2.85
a_4 AISI 405	448	150	7.80	3.50
a_5 ASTM class 60	431	285	7.30	3.30
a_6 Grade 60-40-18	416	167	7.10	4.00
a_7 Grade 65-45-12	464	167	7.10	4.00
a_8 Grade 80-55-06	559	192	7.10	4.00

σ^{ut} – Ultimate tensile strength in MPa, BHN–Brinell hardness number, ρ – Density in g/cc, c – Cost in \$/kg

Table 3 Assessing value scale with the magnitude of gear material attributes [7]

Value scale (v_i)				Gear material attribute magnitude			
5-points scale		11-points scale		σ^{ut} MPa	BHN	ρ , g/cc	c \$/kg
Points	Meaning	Points	Meaning				
0	Unsatisfactory	0	Absolutely useless solution	370	100	8.00	5.00
		1	Very inadequate solution	390	120	7.90	4.60
1	Just tolerable	2	Weak solution	410	140	7.80	4.20
		3	Tolerable solution	430	160	7.70	3.80
2	Adequate	4	Adequate solution	450	180	7.60	3.40
		5	Satisfactory solution	470	200	7.50	3.00
3	Good	6	Good solution with few drawbacks	490	220	7.40	2.60
		7	Good solution	510	240	7.30	2.20
4	Very good (ideal)	8	Very good solution	530	260	7.20	1.80
		9	Solution exceed the requirements	550	280	7.10	1.40
		10	Ideal solution	570	300	7.00	1.00



Table 4 Pugh ratings of the gear materials

Alternatives (a_i)		$e_1(\sigma^{ut})$		$e_2(BHN)$		$e_3(\rho)$		$e_4(c)$		AOS(a_i)	Rank
		v_{i1}	r_{i1}	v_{i2}	r_{i2}	v_{i3}	r_{i3}	v_{i4}	r_{i4}		
a_1	AISI 4130 (Datum)	9	0.000	3	0.000	2	0.000	8	0.000	0.000	3
a_2	AISI 1040	7	20.222	2	20.333	2	0.000	9	+0.111	20.444	5
a_3	AISI 304	7	20.222	2	20.333	2	0.000	5	20.375	20.930	7
a_4	AISI 405	4	20.555	3	0.000	2	0.000	4	20.500	21.055	8
a_5	ASTM class 60	3	20.666	9	+0.666	7	+0.714	4	20.500	+0.214	2
a_6	Grade 60-40-18	2	20.777	3	0.000	9	+0.777	3	20.625	20.625	6
a_7	Grade 65-45-12	5	20.444	3	0.000	9	+0.777	3	20.625	20.292	4
a_8	Grade 80-55-06	9	0.000	5	+0.400	9	+0.777	3	20.625	+0.552	1

RESULTS AND DISCUSSION

The analysis shows the preeminent material is Grade 80-55-06 (ductile cast iron) which is consistent with result analyzed by Das et al. [16] using AHP-MAUT. Some methods predict the carburized steel as a spur gear material [10,17]. Carburized steel is also a popular gear material. At the same time, ductile cast iron is becoming favored as a gear material in automotive industries specially austempered ductile iron (ADI) due to its high strength to weight ratio, good damping quality and recyclability [18,19].

CONCLUSIONS

In product design, a designer selects the optimum configuration from a set of alternative solutions in respect of shape, materials, and manufacturing. Selection of a solution cannot be executed effectively without structured decision-making aids. In this paper, a simplified relative difference approach is implemented in the Pugh Chart to select the preeminent material by maintaining the originality of the Pugh concept. The Pugh Chart is advantageous due to the equal weightages to the criteria. In this approach, the attributes are converted into scaled values through common 11-points scale which is equivalent to normalizing process as compared with other MADM approaches. The whole concept is easy to understand and easy to compute.

REFERENCES

1. J.C. Albinana, C. Vila, A framework for concurrent material and process selection during conceptual design stages. *Mater. Des.* 41, 433-446 (2012)
2. N.P. Suh, *The Principles of Design*, Oxford University Press, New York, 1990
3. K. Otto, K. Wood, *Product Design: Techniques in Reverse Engineering and New Product Development*, 1st ed. Pearson Education, 2001
4. G. Pahl, W. Beitz, *Engineering Design*. London/Berlin: The Design Council/Springer-Verlag, 1998
5. M. Bahraminasab, A. Jahan, Material selection for femoral component of total knee replacement using comprehensive VIKOR, *Mater. Des.* 32, 4471-4477 (2011)
6. R.V. Rao, A decision making methodology for material selection using an improved compromise ranking method, *Mater. Des.* 29, 1949-1954 (2008)
7. A. Shaniyan, O. Savadogo, TOPSIS multiple -criteria decision support analysis for material selection of metallic bipolar plates for polymer electrolyte fuel cell, *J. Power. Sour.* 159, 1095-1104 (2006)
8. P. Chatterjee, V.M. Athawale, S. Chakraborty, Selection of materials using compromise ranking and outranking methods, *Mater. Des.* 30, 4043-4053 (2009)
9. D.H. Jee, K.J. Kang, A method for optimal material selection aided with decision making theory, *Mater. Des.* 21, 199-206 (2000)
10. P. Chatterjee, S. Chakraborty, Material selection using preferential ranking method, *Mater. Des.* 35, 384-393 (2012)
11. A. Hafezalkotob, A. Hafezalkotob, M.K. Sayadi, Extension of MULTIMOORA method with interval numbers: An application in materials selection, *Appl. Math. Model.* 40, 1372-1386 (2016)
12. A. Jahan, M. Bahraminasab, K.L. Edwards, A target-based normalization technique for material selection, *Mater. Des.* 35, 647-654 (2012)
13. R.S. Khabbaz, B.D. Manshadi, A. Abedian, R. Mahmudi, A simplified fuzzy logic approach for materials selection in mechanical engineering design, *Mater. Des.* 30, 687-697 (2009)
14. R.G. Budynas, J.K. Nisbett, *Shigley's Mechanical Engineering Design*. 8th ed. McGraw-Hill, New York, 2006
15. T.L. Satty, How to make decision: The Analytical Hierarchy Process. *Eur. J. Oper. Res.* 48, 9-26 (1990)
16. D. Das, S. Bhattacharya, B. Sarkar, Decision-based design-driven material selection: a normative-prescriptive approach for simultaneous selection of material and geometric variables in gear design, *Mater. Des.* 92, 787-793 (2016)
17. A.S. Milani, A. Shaniyan, R. Madoliat, J.A. Nemes, The effect of normalization norms in multiple attribute decision making methods: a case study in gear material selection. *Struct. Multidisc. Optim.* 29, 312-318 (2005)
18. W. Guessser, F. Koda, J. Martinez, C. da Silva, Austempered Ductile Iron for Gears, SAE Technical Paper 2012-36-0305 (2012)
19. J.R. Davis J, editor, *Gear Materials, Properties, and Manufacture*. ASM International, 2005.



From Logistic to Racing: Innovation in Trucks

Manas Mishra^{*1}, Rajesh Pandey¹, Naveen Mishra², Kunal Gaurav²

Tata Motors Ltd., Jamshedpur¹, mkmishra@tata motors.com*
Tata Technologies Ltd., Ranchi²

ABSTRACT

Truck racing is a form of motor racing, in which the modified versions of heavy truck compete with each other on racing circuits. Americans were the first to start this sport, but today it is equally popular in Europe and other parts. However, the game is unknown to most people in India. In India, truck-racing championship conducted under the aegis of Federation of International Automobile (FIA) and Federation of Motor Sports Clubs of India (FMSCI). The FIA is the governing body for world motor sport. Racing in India is also gaining its pace by the effort of Indian automobile industries. Integration of technologies and emergence of engineering in racing of heavy commercial vehicle (HCV) made possible to transform logistic trucks into racing trucks.

KEYWORDS 1000HP, Sub frame, Roll cage, Circuit barker, Jump starter

INTRODUCTION

Truck racing championship is the second most popular event after Formula 1 car racing. Many of us have perception that trucks are not meant to be fast. They are just big, strong and hard working. This perception have changed when a massive truck of huge weight roar along the racetrack faster than a formula racing car. Indian heavy commercial automobiles manufacturers brought truck racing in India. It is not a event only limited to manufacturers employees but worldwide participation can also be seen. On the racing track many trucks race against each other. Domestic as well as international drivers take part in this event. At the end of the race winners, get rewards. This rewards & recognition event not only rewards the winner but it upheld the dignity & feeling of pride to each individual drivers.

In India, drivers are the most marginalized and neglected section in the society. This racing event gives an opportunity to all drivers who want to show their driving potentials and their abilities. Driver selection process starts six months prior to the race. After the selection, they are provided with rigorous training on racing vehicles. The driving skill enhancement of regular truck drivers to a racing truck driver itself spreads a message of social responsibility of the corporate sector.

AIM OF DESIGN

- Introduction of special engine in Racing Truck of Power (BHP): 1000 HP.
- Reduction of gross average weight of Racing Vehicle: 5.5 t.
- Maximum Speed: 160 km/h.

TECHNICAL SPECIFICATION

1000 HP racing truck is designed as per FIA regulations to meet international racing standard. Vehicle gross weight 5.5 tonne. Weight distribution on front axle 3.2 tonne and on rear axle 2.3 tonne. Distance between front and rear axle centers, which also known as wheelbase is 3650 mm. The engine is powered by 12 liters turbo diesel engine, which picks acceleration from 0 to 100 km/h within 10 s. The ECG (ENGINE, CLUTCH & GEARBOX) assembly mounted in the center of chassis for equal weight distribution. The power from engine is managed by 16-speed gearbox with hydraulic assisted gear shifting, making it fastest race truck. Engine cooling is done via vertical intercooler and inclined radiator with two cooling fans positioned in a closed duct and nozzles provided for water spray on radiator and intercooler.

Suspension is modified to achieve racing truck specifications. Front spring is conventional leaf spring with two leaf mounted on frame. In front spring suspension mounting, pivot end mounted at front and shackle end mounted at rear whereas in rear spring suspension shackle end mounted at front and pivot end mounted at rear of rear springs. Caster angle for front axle is positive 20 degree. High caster angle improves stability during high speed cornering. Front and rear axle is fitted with disc brake. Alloy wheel rim and disc brake cooling is done with water flowing from inside to outside through nozzle. B-day extended cabin is fitted with roll cage. Cabin made lighter by removing BIW parts. Safety features such as, front under protected device (FUPD), rear under protected device (RUPD), side under



protected device (SUPD) and Roll cage are fitted on the vehicle. Following are the technical specifications of 1000 HP racing truck.

- Engine - 1000 HP, 12 l diesel engine with maximum torque -3500 Nm at 1600 to 2200 rpm, Maximum Speed- 160 km/h
- Gearbox-16 speed gearbox with hydraulic assisted gear shifting
- Enginecooling-Intercooler mounted vertically and inclined mounted radiator assisted by air and water.
- Chassis- Frame assisted by sub frame to enhance structural rigidity with two cross members only.
- Braking system-Front and Rear axle mounted with disc type brakes for higher braking efficiency.
- Brake disc cooling-Air pressurized waterfed to brake disc through sensor based nozzle jets. Primary cooling through continuous water flow and secondary cooling jet operated automatically on increases on brake disc temperature.
- Suspension-Two leaf springs along with pneumatic shock absorbers with displacement sensors.
- Steering wheel - Detachable type steering wheel with 20-degree caster angle for better steer-ability and self-centering at corner.
- Racing seat - Inclined sleeping mode type
- Cabin - B-day extended cab fitted with roll cage
- Roll cage - Cage like structure to protect driver during collapse of vehicle
- Fuel system - light-weight 80-l aluminum tank and fuel cooler.
- Tires and wheel rims - Racing specific slick type smooth tread tiers with aluminum alloy wheel rim. Less groove on tires provided more surface area in contact to road.
- Power cut off switch - Mounted at rear cross member operated manually in case of hazards.
- Electronics system- App based (WI-FI enabled) remotely controlled diagnosis.
- Driver information system - Provision of rear view camera, GPS and display unit with touch screen.
- Seat belt - Five point mounting, quick open seat belt for driver safety.

Innovation Involved

Sub frame

It is a box type caging like structure (**Figure 1**) which are made by welding of many hollow rectangular pipe links to appear as one rigid structure. During high speed-cornering, twist develops in frame of truck. At very high speed there is chances of frame failure. To avoid frame failure and to provide torsional rigidity sub frame is introduced along with main frame. For the ease of mounting of sub frame on main frame holes are provided on long member & bush welded in sub-frame link. The installation done with the help of nut and bolt.

Roll Cage

For the driver safety during collapse of racing vehicle a cage like structure provided in cabin (**Figure 2**). Seamless cold roll pipe linkages are welded together to make one unit. The pipe structure followed the curvature of cabin BIW (Body in White). Complete caging structure is mounted on four plates at each corners of the cabin floor with nut and bolt arrangement.

Fuel Tank

Fuel tank is mounted on the top of chassis with height and volume constrained as guided by FIA regulations. Fuel tank designed for 80-l capacity, aluminum material used to make it light for easy installation and fuel filling operation (**Figure 3**). Fuel tank mounting done on long member top by using rubber pad and nut-bolt arrangement. It is designed so that easy and quick dismantle can be done in case of any hazard.

Suspension

Front spring is conventional leaf spring with two leaf mounted on frame at pivot point at front & Shackle point as end. Rear spring is conventional leaf spring with two leaf mounted on frame at pivot end at rear & shackle end at front (**Figure 4**). Suspension is mounted with pneumatic shock absorbers with displacement sensors to measure shocker movement vertically.

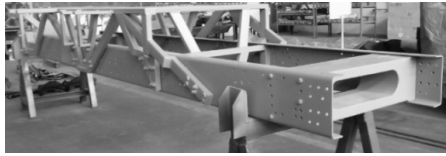


Figure 1 Sub frame



Figure 2 Roll cage

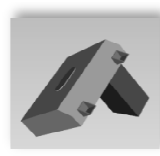


Figure 3 Fuel tank

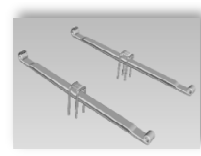


Figure 4 Suspension

Circuit Breaker

Truck racing event is risky event associated with fire hazard during operation. Mechanical and manual circuit breaker is provided to avoid such situation to arise. A circuit breaker is mounted on the rear cross member at the end of vehicle. It is easily accessible from out side. During any kind of fire hazards or wiring harness failure circuit breaker breaks the circuit and miss-happening can be avoid.

Jump Starter

Many time on racing track battery got damage or battery cable fails in that condition, battery unable to supply current. A jump starter is provided on racing truck to crank the engine without battery current supply.

Challenges and Design Constraints

There are many challenges during design and fabrication of racing truck. As 1000 HP racing truck has to meet global standard and regulations. Modern racing technologies and engineering has made this concept of racing into realities. Following critical challenges had to overcome during the entire process of vehicle building and operation.

Weight Reduction

Gross vehicle weight reduction is a major challenge. As per FIA regulations, vehicle weight should be minimum but not exceed 5.5 tonne. Trucks of same wheelbase has a minimum weight of 8 to 9 tonne. Approximately forty percent (40%) weight reduction is huge task. This weight reduction was achieved by following design modifications.

- Replacing heavy engine and gearbox mountings by lighter mounting brackets.
- Replacing conventional suspension with nine or more leaves to racing suitable two leaves suspension.
- Light spring mountings fitted instead heavy suspension mountings of high tonnage trucks
- Making cabin lighter by removing additional reinforcements in BIW (Body in White) parts
- Lighter FUPD, RUPD and SUPD mounting brackets fitted instead heavy commercial vehicle mounting brackets.
- Heavy cross members replaced by light rectangular box section cross members with 3 mm sheet thickness.
- Fuel tank designed for 80 l capacity and fabricated using aluminum alloy material.
- Aluminum alloy wheel rim used.
- Heavy fifth wheel coupling replaced by aluminum 3 mm sheet made coupling.
- Aluminum lightweight battery box fitted instead regular sheet metal battery box.

Engine Cooling

Due to high power, engine heat generation will also be high. Engine cooling requirement is achieved by providing double fan air-cooling with jet water assisted cooling. Continuous sprinkling of water through nozzle is provided on radiator. Inclined radiator mounting provided instead vertical mounting to access more air through first cross member cutout. Intercooler vertically mounted assisted by water-cooling through water jet sprinkling. Engine cooling is via vertically and inclined radiator with 2 cooling fans positioned in a closed duct while added nozzles for water spray are situated on radiator and intercooler.

Fuel cooler is also designed to cool return high temperature oil from engine. It is mounted behind engine on long member. The unburned oil inlet is connected through oil cooler. Here it loses heat & return to engine through oil cooler outlet.

Brake Disc Cooling

Disc brake heat dissipation is taken away by water sprinkling through nozzle. There are two phases of cooling primary & secondary. On primary nozzle sprinkles water continuously on brake disc. Secondary cooling starts



operation on higher temperature. It is assisted & operated on the feedback of sensor attached to it. Six water tank is mounted on vehicle with total capacity of 180 Liters of water.

Cost

Huge cost involve in building process of racing truck. Engine, Gearbox, Tires, Pneumatic valves, Ionized Nut-bolts, Water tanks, Air tanks, all are imported parts from outside India.

Outcomes of Project

- Truck Racing in India is first of its kind.
- Public participation and awareness in truck racing through large-scale organized event.
- Indian Driver skill development through extensive training and event participation.
- Driver selection and reward program for racing drivers.
- Heavy commercial vehicle racing concept implementation in India.
- Branding and Business enhancement globally through truck racing.
- Technological advancement in heavy commercial vehicle.
- CSR: Corporate social responsibility to uplift the life & dignity of marginalized drivers.
- World class racing driver participation.
- Introduces new ways of boosting driver engagement.
- Increase in market share of regular commercial vehicle
- Under social responsibility insurance policy for truck drivers and scholarship for their kids launched under this event.

CONCLUSION

Innovation in racing trucks enhances technical advancement in heavy commercial vehicle. The new ideas of racing can also be implemented in regular production vehicle where ever look feasible. Sub frame, ECG center mountings, engine cooling, light weight fuel tank etc. concept can be implemented in regular vehicles. The racing event not only entertain the masses but also led to increase business. The decision will also help the company focus its resources on strengthening the performance of its commercial vehicle business. Market share of commercial vehicle will also get a push through branding and advertisement via racing. Corporate social responsibility is well taken care through this organized event. The event also serves its key purpose of providing dignity to truck drivers. Insurance policy for drivers and scholarship for their kids will enhance better living standard.

REFERENCES

1. <http://tata-motors-officially-announces-t1-prima-truck-racing-championship-12134.htm>
2. <http://www.btra.org/>
3. British truck racing association website
4. http://www.wabco-auto.com/press_releases/wabco-india-to-sponsor-tata-motors-t1-prima-truck-racing-championship-as-official-braking-technology-partner/



Value Engineering and Value Analysis Methodology

*Manas Kr. Mishra^{*1}, Bhushan Vaidhya², Peeyush Anshu³, Rajeev Mishra³*

*Tata Motors Ltd., Jamshedpur¹, mkmishra@tatamotors.com**

Tata Motors Ltd, Pune²

Tata Technologies Ltd, Jamshedpur³

ABSTRACT

Value Analysis/Value engineering is a systematic and organized procedural decision-making process used in almost any kind of application. It helps people in creatively generating alternatives of process/product/design to secure essential functions at the greatest worth as opposed to costs. This is referred to as VALUE. Value Analysis, Value Management, and Value Planning being some of the synonyms of the Value Analysis/Value engineering. The major objective of VE is the functional approach to get desired VALUE. When technique is applied on an existing product or process is called Value Analysis. When technique is applied during design stage is called Value Engineering.

KEYWORDS VA-VE, Multidisciplinary, Structured, Functional Approach, Creativity

INTRODUCTION

The current business scenario is very demanding with a continuous demand from the market forces to reduce the product price. The pricing as demanded by the market, forces the businesses to reduce product development and manufacturing costs to remain competitive.

Manufacturing costs of a product can be broadly categorized in the following heads: • Raw material, • Labor, and • Process that is technology driven.

Product engineers are constantly faced with the following challenges: • Reduce production cost, and • Reduce the material cost.

TYPES OF VALUES

- (a) Use value - which is based on those properties of the product, which enable it to perform work or service.
- (b) Cost value - which is based on the minimum cost of achieving a useful function.
- (c) Esteem value - which is based on those properties of the product, which contribute to pride of ownership.
- (d) Exchange value – which is based on those properties which make a product valuable for exchange purposes.

VALUE ENGINEERING AND VALUE ANALYSIS METHODOLOGY

Value engineering is brainchild of General Electric Co. It was need of the hour during World War II. War caused paucity of skilled hands and basic raw materials required to run the businesses.. Lawrence Miles and Harry Ehrlicher at GE took the challenge and explored the substitute materials. They deduced from their study that these alternative options also decreased the product cost as well as increased the value. The Synopsis of the study resulted in the invention of a systematic process and they termed it as “Value Analysis”. Soon the process was accepted across industries and its name gradually became “Value Engineering”. VAVE is a system driven process used by cross functional teams, aimed at analyzing the functions of a design, system, process, product, project or service for the purpose of achieving the essential functions at the least product life cycle cost keeping required reliability, performance, quality, availability and safety consistent. VAVE is the process of cost reduction while the project is still in development phase. This process is performed by analyzing and assessing processes, materials and or products and suggesting best suited alternatives. The resultant of the process should be savings to the project owner / end user without diminishing the design intent, i.e. by maintaining or improving quality requirements and performance of the product. By acquiring the process, hitting the bull’s eye means, achieving the desired results without compromising on performance and quality of the product. If the VAVE process is adopted in the initial development or concept defining stages, it is more likely to be successful due to common understanding of the requirements, objectives and deliverables. At this point of project, major design and development sources have not been frozen and the way forward for the basic function of the project has not been established, so alternative ways can be identified and considered. Flexibility and creativity involved in the process, makes Value Engineering almost unlimited in its ability to identify areas of potential savings. An important characteristic of Value Engineering is



defined by its ability to respond with creativity, flexibility and timeliness,. It can be applied to running or future programs, all project phases, and for organizational processes. Value Engineering can be applied for improvement in quality, cost reduction, adhering necessary compliances, improving efficiency, teamwork and reduce risks.

Those projects which have a good potential to improve profits are generally under taken for this. A dedicated team comprising of engineers specializing in VAVE to achieve cost reductions of products.

A typical VAVE exercise have the potential to reduce the total cost of a product by 5 to 40%. The basic elements of a VAVE exercise are shown in **Figure 1**.

To catch hold of current state of the project constraints / requirements as Einstein stated if he had 6 min to solve a problem, on which his life depended, he would spend:

- 40 min on gathering information
- 15 min on Analysis
- 5 min on making the decision

VITAL POINTS TO NOTE

- Avoid guess work and generalization,
- Record actual figures from authentic sources,
- Verify the data, if necessary,
- Record data in neat, clean check sheets,
- Authentic data.

Functional Analysis

Understanding the project from a functional point of view; what project is intended to do, instead of how the current project is conceived. The function describes the basic working of a project and function analysis is the process involving team reviews of the project's functions to explore the upgradation possibilities. Function Analysis can be made more fruitful by the graphical mapping tool termed as the Function Analysis System Technique (FAST). FAST applies intended logic to test functions, create a common tool for a team, and test the authenticity of the functions in the project.

Functions are of two forms:

- Primary functions - Those that define the basic existence of the project, for example, plumbing in an infra structure project as a primary function.
- Secondary functions - Those that are additional of project without been core to the project. For example, a base project might have as a secondary function maintaining the view of the next building.

Functions are defined in verb/noun pairs, namely “supply water to all suites,” or “Maintain view of adjacent park.” For a project, the team should come up with 10 to 20 functions. You might be surprised how many secondary functions exist for most projects. It would be a great resource, but in their absence an appropriate level of creative thinking and analysis are important.

Creative

Generate a number of ideas related to alternate ways of performing the functions. This stage comprises of generation of improvement ideas. The team explores the other way out to perform the running/current ways that the project can perform. At this stage, the functions are considered individually and each one gets a list of alternative ways to perform the function. There should be no pre- judging between the importance of the various functions.

Evaluation

Reduce the number of generated totally to a shortlisted ideas with the strongest potential in improving the project and achieving the aim of Value Engineering study.

Development

Further analysis of the selected ideas and develop the elite ones, into value alternatives.



CLASSICAL VAVE METHODOLOGY

- The Value Methodology focuses on improving value for any given product, process, system, service, or facility by identifying the most cost efficient way to reliably accomplish various functions that meet the performance expectations of the customer or client.
- The Value Methodology never degrades those required functions which the 'Voice of the Customer' defines are necessary in order to meet his level of expectation for the product, process, or service to be provided.
- The Value Methodology will help to identify functions not absolutely required by the customer or client.

VAVE flowchart and for principal pillars of VAVE are shown in **Figures 2 and 3**, respectively.

PROCESS OF CLASSICAL VAVE

The following process are required for classical VAVE Workshop:-

- Random Function Analysis
- FAST-Function Analysis System Tanique
- Function Cost Analysis Matrix
- Function Based Idea Evaluation
- Business Case Study

Random Function Analysis

- A two word performance description using an
- Active verb and a measurable noun
- For maximum clarity and Simplicity
- A function describes what a product, process, project or service does.
- Functions enable us to focuses on required performance/need rather than on components.

FAST-Function Analysis System Technique:

It is a systematic flow diagram technique (**Figure 4 and 5**) that logically identifies and visually displays the important functions to accomplish a design purpose.

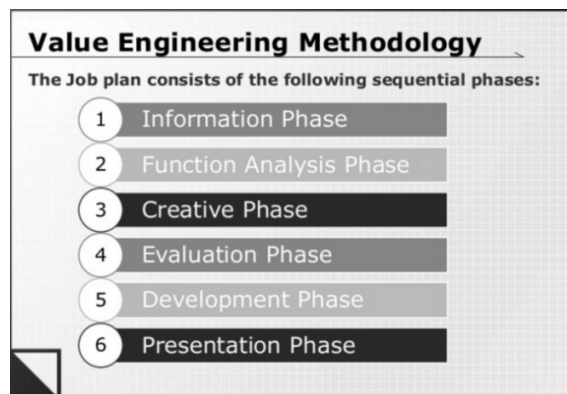


Figure 1 Value engineering methodology

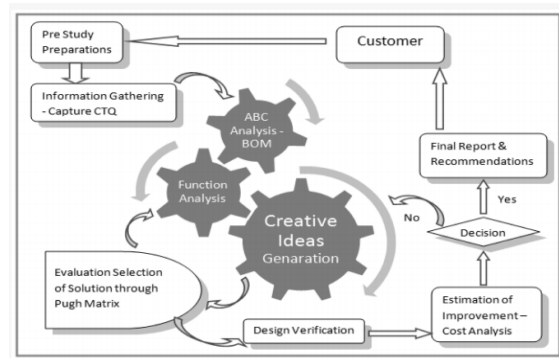


Figure 2 VAVE flowchart

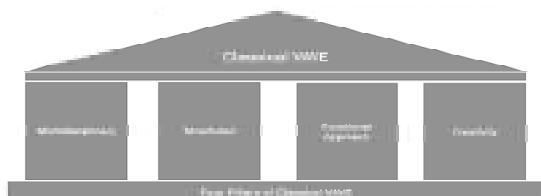


Figure 3 Four Pillars of Classical Value Engineering

Active Verbs			Measurable Nouns		
Verb-Noun Listing for MANUFACTURED PRODUCTS					
absorb	create	pivot	access	energy	motion
access	decrease	position	air	entry	noise
actuate	direct	prevent	appearance	environment	part
~allow	enclose	protect	bending	feature	path
Apply	enhance	~provide	circuit	flow	performance
Attach	extend	reduce	climate	fluid	pressure
Attract	generate	regulate	cold	force	stability
Circulate	guide	resist	comfort	form	style
Conduct	improve	rotate	component	friction	surface
Connect	increase	seal	convenience	heat	torque
contain	isolate	sense	corrosion	impact	travel
control	limit	support	current	mass	vibration
convert	maintain	transmit	deflection	material	weight
~Avoid these verbs (no real action)			drag	moisture	
Black words are <i>Work Functions</i>			Green words are <i>Sell Functions</i>		

Figure 4 Random Function Analysis

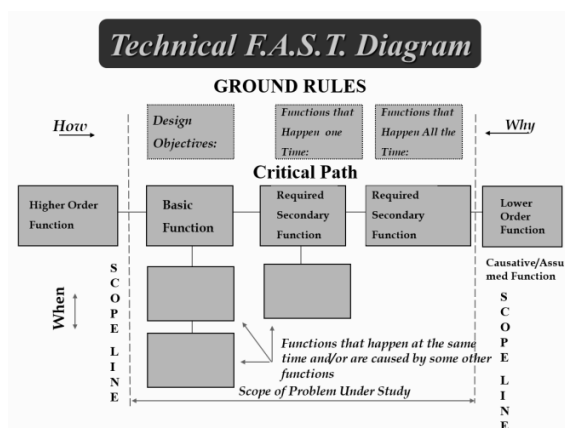


Figure 5 FAST Diagram of a PENCIL

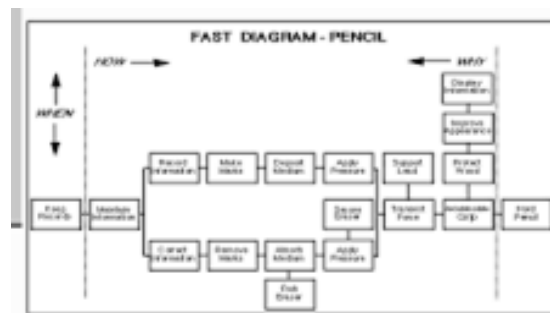


Figure 6 FAST model of pencil

How to Draw a Technical FAST

- Prepare a list of all functions,
- Use Verb & noun to define a function,
- Write each function on a small card,
- Select the card which appears the basic function,
- Apply logic questions 'How' & 'Why' to determine relations,
- Functions satisfying 'How-Why' logic are Required Secondary Functions,
- Draw scope line (Dotted) left side of the basic function,
- Higher order function on left of left side scope line,
- Lower order function (Causative/Assumed) Function on right of right side scope line,
- Simultaneous functions below each other,
- All time functions- Right Hand top corner, One time Functions at Centre top,
- Design objectives above basic function,
- Path indicated by Basic function and required secondary functions is critical path including HOF and LOF.

The flowchart to prepare a FAST is shown in **Figure 6**.

Application of FAST Diagram

- Basic function
- Critical Path Function How – Why Logic
- Required Secondary Function
- Simultaneous Function When Logic
- All time Functions
- One time function
- Higher Order Function
- Lower order /Causative Function
- Design Objective (Design Function)

Function Cost Analysis Matrix

- Cost Bill Of Material
- Process of Sample part
- Random function analysis list



FCA matrix is shown in **Figure 7**.

Function Phase Continue..

FUNCTION COST MATRIX

DATE: 28/04/14	TEAM: EBCS, Radolfzell, Germany
FACILITATOR: Jim Solon	PROJECT: Keypad Switch Team

PART or OPERATION	Cost	Check sum	MANTAIN CONTINUTY	TRANSMIT SIGNAL	SEND SIGNAL	MANTAIN INTEGRITY	TRANSFER FORCE	RESIST ENVIRONMENT	MINIMIZE RATTLE	ILLUMINATE DEVICE	MANTAIN APPEARANCE
KNOB MOLDING	8.8961	100%	0.014	15%		0.029	30%	10%	0.019	20%	0.301
PAINTING COST	8.3341	100%						0.033	10%		0.301
LASER ETCHING	8.1873	100%		0.011	10%					0.004	0.032
REFLECTOR MOLDING	8.8261	100%	0.001	0.001	5%	0.001	5%	0.003	10%	0.016	0.004
SUB-ASM. KNOB/REFL.	8.8448	100%	0.002	5%		0.002	0.009	0.002	5%	0.028	0.002
HOUSING MOLDING	8.8421	100%	0.004	10%		0.021	0.003	0.004	10%	0.004	0.001
GREASE HOUSING	8.8398	100%							0.040	100%	
PCB RAW FROM SUPPLIER	8.8534	100%	0.011	0.018	0.018		0.005	0.005	10%		
ELECTRONIC PARTS	8.1436	100%	0.016	20%	30%			0.016	10%		0.041
ACTION (COMPLAINT) PINS	8.8268	100%	0.004	20%	30%	0.004	0.002	0.004	10%		0.001
POPULATION & PCB ASM.	8.8122	100%	0.018	10%	10%	0.018	0.012	0.018	10%	0.018	0.001
RUBBER KEYPAD	8.8518	100%	0.006	10%	0.003	0.003	0.010	0.005	0.005	0.005	0.003
FINAL ASSEMBLY/TESTPACK	8.8144	100%	0.077	10%	10%		0.077	10%		0.103	0.103
FUNCTIONAL TOTAL	\$ 1.61		0.16	0.14	0.51	0.88	0.14	0.89	0.07	0.34	0.49
FUNCTIONAL RANKING:			3	4	5	7	4	6	7	2	1
			MANTAIN CONTINUTY	TRANSMIT SIGNAL	SEND SIGNAL	MANTAIN INTEGRITY	TRANSFER FORCE	RESIST ENVIRONMENT	MINIMIZE RATTLE	ILLUMINATE DEVICE	MANTAIN APPEARANCE

Figure 7 Function cost analysis

Function Based Idea Evaluation

Objectives of Function-Based approach

- To cultivate as many alternative ideas.
- Focus on root (most important) functions.
- Generate ideas without anticipating current situation/solution.

Rules of Function-Based approach

- It's always better to have good quantity of generated idea.
- Idea generation should be done without any assumptions are pre-decisions..
- The creative ideas should be appreciated. Imaginative ideas can open the road for new possibilities and opportunities.
- Create a chunk of Good ideas. It may be fused to create a single better idea.

Facilitator Hints

- Have faith and confidence in the process. Function-Based approach is a dependable and efficient approach to generate genuine ideas.
- Explain the rules of process.
- Identify the Basic/most important functions of the project and / or process. Start with the requirement or issues of the project or process in force.
- Select a function where most imaginative ideas are expected to be alternative ideas.
- Cultivate your own ideas if ideas are not flashing.
- Creative thinking against Top order Functions (Functions to the left side of the FAST diagram), are likely to produce original/creative ideas for the greatest change. Lower order Functions (Functions farther to the right of the FAST Diagram) will likely lead to less significant change.

Characteristics of Creative Thinkers

- They have an "absolute discontent" with the status quo.
- They seek alternative solutions to problems or opportunities.
- They have a "prepared mind", always alert to things that trigger NEW ideas.
- They think positively.
- They work hard on the ideas generated.



- A group of people using their collective thinking power to create ideas. This is more productive than a person thinking alone.
- The objective is to generate as long a list of ideas as possible.

Desired output of VA/VE process are

- Obtaining the most value for the budgeted program cost
- Emphasizing that team work is necessary to accomplish the effort
- Tailoring our work process to the need of the project
- Following rational steps to achieve the intended functions
- Continuing to meet state, local, and federal/agency codes
- Obtaining full participation from the VE team as well as others to achieve the greatest results

CONCLUSION

The benefits of using Value Analysis/Value Engineering include:

- A Return on Investment typically ranging from 20:1 to 100:1.
- Cost savings while achieving required functions.
- Improved understanding of the project and validation of costs.
- The value engineering process results in recommendations on how to provide the necessary functions of the project safely, reliably, efficiently, and at the lowest overall cost. The goal of the process is to improve the value and quality of the project, and hopefully reduce the time to complete the project.

REFERENCES

1. Value Analysis Benefits - Value Analysis Canada, www.valueanalysis.ca/vabenefits.php
2. Function Analysis system Technique (FAST) - Canadian Society of Value Analysis, www.valueanalysis.ca/fast.php
3. Value Chain Analysis | SMI - Strategic Management Insight, <https://www.strategicmanagementinsight.com > Strategy Tools>
4. Value Analysis and Function Analysis System Technique, www.npd-solutions.com/va.html
5. Function Analysis Phase - Canadian Society of Value Analysis, www.valueanalysis.ca/functionanalysis.php
6. Value Analysis & Value Engineering – Satyam Venture, <https://satyamventure.com/solutions/product.../value-analysis-value-engineering/>
7. Function-Based Brainstorming - Canadian Society of Value Analysis www.valueanalysis.ca/brainstorm.php



Remote Operation of Fuel Handling Systems of Prototype Fast Breeder Reactor

H.Nalini¹, S.Narasimhan¹

*IT and Instrumentation, Bharatiya Nabhikiya Vidyut Nigam Ltd, Department of Atomic Energy, Kalpakkam, Tamil Nadu¹,
nalini_bhavini@igcar.gov.in**

ABSTRACT

Fuel handling system (FHS) of any nuclear reactor is a crucial system as it is the backbone of whole reactor operation. Instrumentation and Control system of FHS always play a vital role in nuclear facilities. The I&C of Fuel Handling Systems play a major role in operating the machines remotely and ensuring availability. The delay in fuel handling, results in longer outage time and penalizes the company on daily revenue generation. This paper brings out the major I&C systems of FHS, which is an integration of micro precision instruments in industrial environment, real-time computer-based control system, a dedicated reliable network and Graphical user interface. The paper also explains the physical constraints and problem faced during the erection and commissioning of the I&C system of FHS with a limitation of remote/blind operation, use of proven technology and a huge number of logics/ interlocks for every operation, confined and crucial operations with difficulties in approach. The software-based control system follows all the programming guidelines specified by the Atomic Energy Regulatory Board (AERB).

KEYWORDS FHS I&C, Remote operation, Signal processing, DDCS

INTRODUCTION

The fast breeder reactor technology is the second stage of nuclear power program in India. Prototype Fast Breeder Reactor (PFBR) is a 500 MWe sodium cooled pool type plant being set up at Kalpakkam. Mixed oxide of uranium and plutonium is used as fuel and depleted uranium is used as the blanket. This reactor works on fast neutron spectrum and is capable of breeding its fuel from the blanket.

In PFBR, one-third of the core is replaced by fresh fuel subassemblies during every refueling phase. This is an offline operation i.e. the refueling is done only after the shutdown of the reactor. There are many machines and process systems involved in the refueling process of PFBR. These are operated from a remote control room in a separate building at a distance of around 200m.

FUEL HANDLING SYSTEM

The Fuel Handling System of PFBR (**Figure 1**) handles both the fresh fuel and the spent sub-assemblies. The various machines used to transfer the fuel into the reactor and vice versa are done from a separate control room away from these machines. The instrumentation in these systems hence plays an important role in the operation of these machines. The major machines which handle the fuel are Transfer Arm (TA), Rotatable Plugs (RP), Inclined Fuel Transfer Machine (IFTM) and Cell Transfer Machine (CTM). These are independent machines which operate in coordination with each other for handling fresh and spent fuel from the reactor core. These machine operations are blind as the machines are not approachable during operation, hence we depend completely upon the I&C system for the positioning, loading, and unloading subassemblies.

ROLE OF INSTRUMENTATION IN FUEL HANDLING SYSTEM

The I&C of fuel handling system is safety class 2 (Class IB) as per AERB SG D-1. The I&C of these systems play a major role because of the following reasons:

- ♦ The operator is dependent on the instruments to know the positions of the various drives and conditions of the machines.
- ♦ The machine operation may depend on other factors like the pressure and temperature in the machine's environment. It may also be dependent on the other machine's positions. Hence the control system integrates the other system's signals in the logics where ever required.
- ♦ In many places like, machine parts inside the reactor vessel, direct measurements are not possible hence a relative motion is converted to the value equivalent to the required measurement.
- ♦ The stringent requirements compel us to have highly accurate measurements, as dispositioning or dropping of the fuel sub-assembly in any situation will cause a serious accident.



Being a nuclear reactor, these machines are exposed to radiation and also they handle sodium drenched fuel. Hence, the instrumentation and control systems are expected to have robustness, higher availability and reliability by ensuring multiple levels of redundancy.

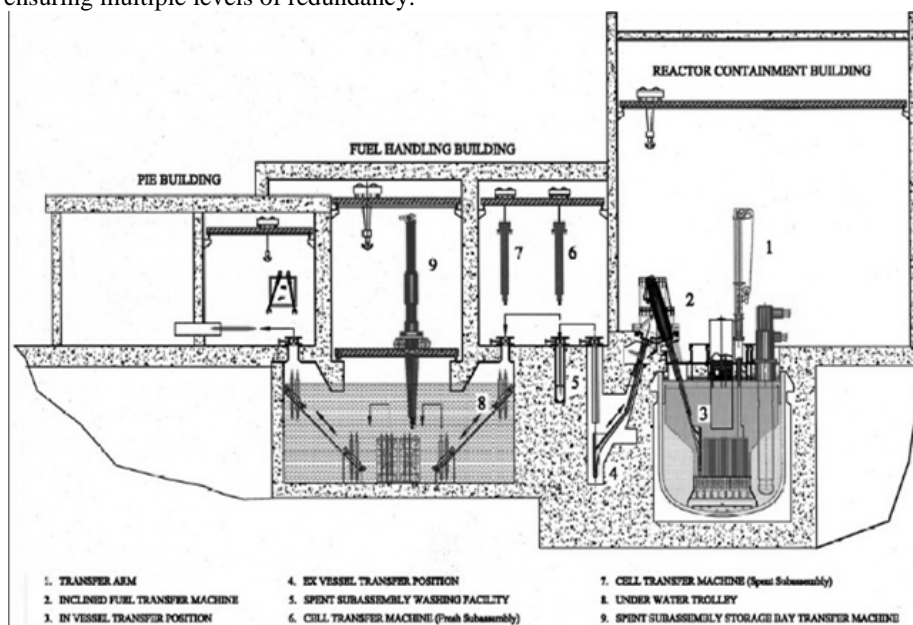


Figure1 Fuel handling systems of PFBR

FIELD INSTRUMENTS

The field level redundancy is ensured by redundant/diverse sensors. The major parameters that need to be measured on any machine are displacement, discrete position, load, pressure, flow, and temperature. These are qualified for the requirements like environmental tests including EMI/EMC, Seismic and radiation tests. Only qualified instruments are used in these machines. In the zone of high temperature and radiation, Mineral Insulated (MI) cables are used and in other areas Flame Retardant Low Smoke (FRLS) cables are used for instrumentation. Flexible silicon rubber cables are used in the cable drag chains. Draw wire potentiometers, LVDT, synchro and encoders are the major instruments used for displacement measurement while limit switches, reed switches, proximity switches etc. are used for discrete position sensing.

Redundant instruments are used in places where the positions or parameter has to be dually ensured. And diverse instruments are used to meet the single failure criteria.

The fuel handling systems being safety class-2 systems, the redundant and diverse instrument signals are taken through separate cables and the cabling from the field is ensured to take different routes to the extent possible. But being a machine with mobile/rotary portions, there is only a single drag chain system. In such cases, the distance between the cables of redundant signals is maintained as large as possible.

All the instruments once erected, are offered to Quality Assurance (QA) group for inspection. The analog instruments are tested by creating a known value, for example, the machine is moved to a known distance and then checked if the output from the instruments is equivalent to the distance to be measured. For all the analog inputs, 5 point calibration methodology is followed to ensure the performance of the instruments. All the digital instruments are actuated and tested, for example, the mechanical limit switches are physically actuated and seen if there is a contact change over.

SIGNAL PROCESSING CABINETS

In the next level, the various field instrument signals are connected to the in-house developed real-time embedded system which is a fault tolerant, hot standby redundant system. All the interlocks related to the remote operation of the machine for an intended command is programmed in these systems. The control commands are sent by these systems to field for operation of the machines.

The signal Processing cabinets (SPC) are positioned in the Local Control Centre (LCC) in the same building in which the machine is located. Every signal from the field is connected through an interface module (IFM) in the signal processing cabinet which multiplies the signals. The two signals are routed to two redundant SPCs. The software for the machines resides in EPROM in the CPU card of this system. Both the SPCs process the signals and



generate output. The system which boots up first becomes online while another system is a hot standby system. As and when the first system fails, the second system becomes online. All the signals in a particular building are connected to the LCC in the same building after which the signals are processed and taken as soft signals through fiber optic cable which reduces cable laying and enables viewing of the signals in multiple places. The data sharing between systems for satisfying interlocks becomes easier due to use of networks.

The outputs from both the systems are checked by a Switchover- logic system which decides which output to be routed to field. The output of the system which ever is online, shall be routed to field. If both the systems are unhealthy, all the outputs go to fail safe conditions that is de-energized condition.

The cabinet is powered by 240 V AC UPS power supply from two feeders which are from different divisions of power supply. Hence ensuring the availability of the control system even if one of the two feeder fail.

All the digital inputs routed to the system (**Figure 2**) are potential free contacts while all the analog signal in whatever form they be, are converted in 0.5 to 9.5V and then sent to the card. Other than the usual cards like analog input, digital input (**Figure 3**), analog output and digital output, there are special purpose cards, for instruments like the encoder and the synchro. All the analog outputs are 4 to 20 mA signals. The CPU card of the SPC system has two Ethernet connectivity too. One port is connected to LAN 1 while the other to LAN 2.

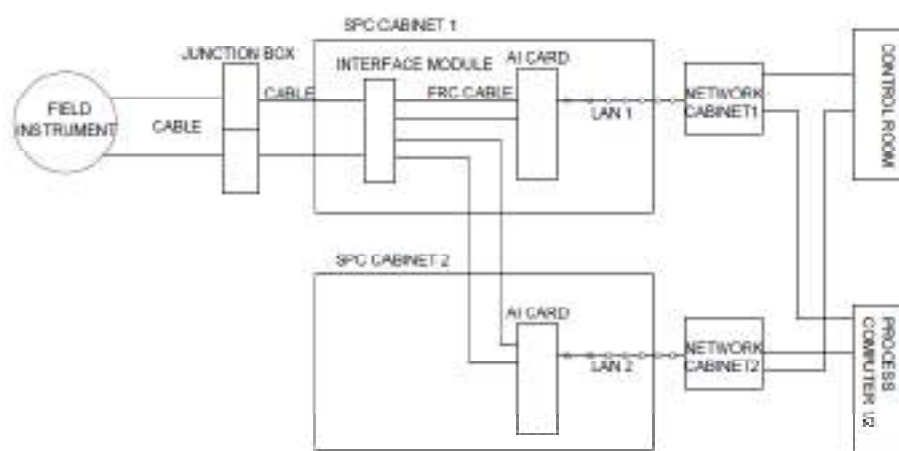


Figure 2 Routing of digital input signals

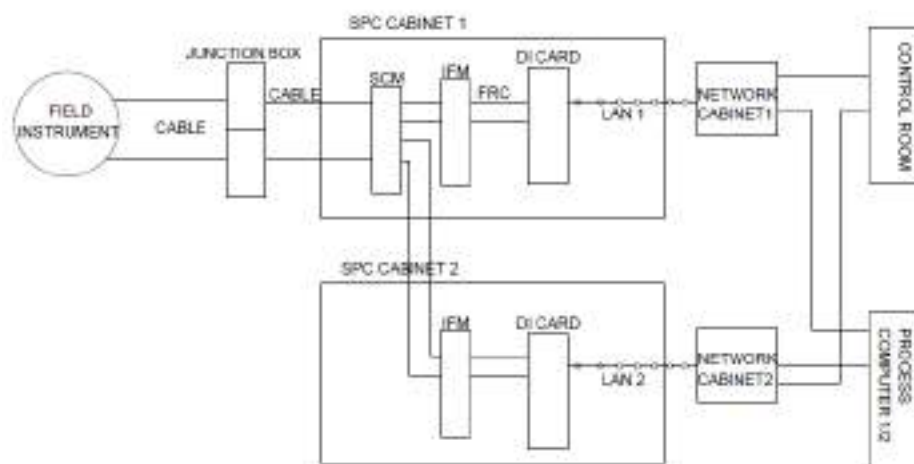


Figure 3 Routing of analog input signals

The outputs generated from these systems are mainly for operation of various drives of the machine. The motors that operate the machines, are with variable frequency drives for speed change over. The position in which speed changeover is to happen is also decided by the control system.

Distributed Digital Control System:



The machines related to fuel handling systems are distributed in different buildings of the reactor. The field signals are processed in the respective buildings. The Distributed Digital Control System (DDCS) forms the top layer to integrate and establish the link between different systems through switched-Ethernet connection, hence enabling the operation of the various machine from the control room, through the HMI in control desks.

The distributed digital control system (DDCS) comprises of the whole network which integrates all the reactors system for display and control from the control room. It works on TCP/IP protocol has a dual LAN connected to two independent process computers. Each SPC system is connected to both the LAN which ultimately connect to the process computer. These process computers communicate with each other and the all the other SPC systems. DDCS serves as the backbone of the whole I&C system by enabling sharing of data and flexibility to operate from multiple work stations.

Dry commissioning is one of the most important steps followed before starting the commissioning of the system. In this, the SPC cabinet is tested in integration with DDCS by simulating all the signals one by one from the field. All these steps are done in coordination with QA and a report is generated.

INTEGRATION OF TECHNOLOGY

The overall fuel handling operation is an integrated one and hence the interdependency is critical and important for operation. Precision positioning, real-time computer-based system, a dedicated reliable network, and Graphical user interface(GUI) are integrated together for the operation of these machines.

The integration of the machine with the control system call for a detailed understanding of the machine. For example, the position measurement through a rotary potentiometer calls for ascertaining the linear movement of the drive for every one full rotation of the sensor. This gain along with number of rotations are required to model a linearized equation with calculation of co-efficient. The amount of precision required is in the range of ± 1 mm for a total travel of 23 m. In some cases positional accuracies are to be obtained on all three co-ordinates for more than 200 work posts. Further the control system shall be tuned with the VFD to vary the speed as per the positional accuracy desired. This called for a mixture of analog signal processing, embedded RTC to linearise and perform interlocks, a high level process computer to provide graphic representation to the user as well as providing window for co-efficient entries and configuration. Even though every machine is independent in their operation, the position and state of each machine is interlocked for integrated operation for handling the sub-assemblies. Hence the process computer was to assimilate all data, synthesize and share it over the network for all the SPC systems to provide for required interlocks.

The instruments like synchro, potentiometer, encoders etc. give different types of signals as output. The control system accepts all these types of signals of different formats and gives the operator a single type of parameter. This control system is also programmed to identify the over-speeding of the machine. The data from subsequent scan cycle is compared and matched with the reference distance to be traveled every cycle. If the machine moves faster then, an automatic trip signal is generated to all the drives of that machine.

The machines being inside the reactor vessel or inside cell areas, the control system becomes the eyes of the operator. Additionally the software based GUI enables a user friendly yet a guided sequence which helps the operator with what is to be done next. If a logic is not satisfied, then system notifies the operator, about the conditions that are not fulfilled. Hence the troubleshooting time also reduces.

In addition to this, there are different levels of alarm that alert the operator about the machine, its electrical systems and its I&C systems. The alarm as per their importance are categorized as window alarm in control room panel, and alarm in operator console (soft alarm).

As a part of commissioning, all the signals are checked once again with the machines from the control room. And then one by one all logics are checked and output is generated.

As per the AERB safety guide D-25 the SC-2 computer based systems should follow a proper documentation procedure including a detailed validation at the site. This is done based on the Site Validation Procedure (SVP). An Independent verification and validation team is formed to verify the system development process and validate the system at the site in an integrated environment.

Constraints Faced During Erection and Commissioning of I&C Systems

The major requirements, while selecting the instrumentation for fuel handling system are as follows,



- The accuracy of alignment of the fuel subassemblies to any position shall be ± 1 mm. An instrument along with the electronics shall have this accuracy.
- As the alignment accuracy is in millimeter, instruments need to have high precision too.
- The response time of the control system used for operation of machines should be very less, so as to stop the machine correctly at the intended position.
- The network level integrity of the system is checked by implementation of cyclic redundancy check etc. This ensure data integrity between the Process Computer and the SPC cabinets.

The following are the major challenges encountered during the erection & testing of there mote operation of fuel handling system controls. .

- None of the instrument located on the machine are accessible. Hence the height/location of the machines is always critical.
- The initial testing phase experienced a commissioning failures in hardware and a lot of changes in software due to various site considerations like layout, mechanical tolerances, process system conditions and changes etc.
- The total time taken for a fuel subassembly is a as per design shall be achieved after all the differences/changes seen at the site.
- The implementation of new design changes according to the machine's mechanical behavior results into additional signals in I&C system.
- Also there are design changes in the system due to recommendations by the regulatory body which also need to be taken up even after the erection job at the site has been completed.
- The I&C system is tightly coupled to the related electrical and mechanical system. Hence individual testing of the I&C system and testing with the machines itself shows many changes.
- For machines which are in the cell area, it is still difficult as the cell itself is difficult to approach.
- The tuning of the instruments is the most difficult part of commissioning of these systems. In analog signals, the redundant signals need to be tuned to show the same value through-out the range of the machine. This become difficult to achieve when the instrument has a non-linear behavior. In digital signals, for example, if there is a limit switch and a reed switch then it has to be tuned in such a way that the both the signals actuate at the same time, so the permissive logic for the further command is satisfied.
- The instrument's performance depends on the machine too. As the fuel handling machines are mobile machines, many a times they seem to work fine mechanically. But when the same is measured by an instrument, it seems to be different.
- The control system of the machine has all the logic controls built into it. The major point behind every logic is that the output shall always be fail safe.
- The availability of the machine is as important as its reliability. The control system cannot afford to generate a wrong out, while its failure may delay the overall fuel handling time.
- The proven technology many a times is an outdated technology and hence availability of spares in market is difficult. Hence a large number of spares have to be procured.
- Re-installations/checking of instruments like temperature sensors for surface temperature measurement becomes very difficult as these mostly insulated and more over in in-accessible locations.
- The IV and V site validation, is a lengthy but useful process which also brings out the bugs in the software which come out only when it is tested as a whole integrated system. Hence many times, after any modification in the software, the whole system has to be re-tested.
- IV and V process checks all the positive and negative logics. Hence the machine is operated many times for this testing which consumes a considerable life of the mechanical components. So the stringent checking of the I&C system is done before coupling to the machine.

CONCLUSION

The I&C for fuel handling machines ensures the proper handling of the fuel within the stipulated time from remote (Control room) without compromising the reliability and robustness. The erection and commissioning of the fuel handling system is a good experience with a lot of day today issues which were solved and the mission of building the Fast breeder reactor with offline fueling is being perceived and taken ahead for commissioning.

REFERENCES

1. Atomic Energy Regulatory Board safety guide D-1 and D-25.



Integration of Various Active and Passive Cooling Techniques on MJT Solar Cell

Yogesh Nandurkar^{*1}, R.L.Shrivastava¹, Vinod Kumar Soni²

Department of Mechanical Engineering, Yeshwantrao Chavan College of Engineering, Nagpur¹, ynandurkar1@gmail.com*
Central Railway, Nagpur²

ABSTRACT

In Multi junction tandem MJT solar cell, amount of light that is not converted into electricity gets converted into heat. This waste heat is responsible for increasing the temperature of the cell. Operating temperature of cell plays vital role in the performance of CPV System as efficiency and power output depend linearly on operating temperature. Performance of the cell decline with increasing operating temperature. Maximum power, voltage, efficiency and long life can be achieved by operating the MJT under standard test condition. Passive and active cooling techniques are popularly used to cool the cell. In passive cooling methods, extended surfaces, heat pipe and micro fins are mostly used whereas, Peltier effect cooling, compressed air, water jet etc. are active cooling techniques. Integration of various active and passive cooling techniques reported by worldwide researchers are critically reviewed in this paper.

KEYWORDS Concentrated photovoltaic module, Multijunction solar cell, Temperature dependence performance, and ways of cooling.

NOMENCLATURE

A	Area, m ²
CPV	concentrated photovoltaic
CR	Concentration ratio (-)
G(λ)	Spectral DNI, W/m ² /nm
Ge	Germanium
InGaAs	Indium Gallium Arsenide
InGaP	Indium Gallium Phosphide
MJT	Multi Junction Tandem
P _{in}	Incident power, W
P _m	Maximum power output, W
q _{heat}	Heat power, W
V _{oc}	Open circuit voltage
λ	Wavelength, nm
η _{cell}	Cell efficiency
η _{opt}	Optical efficiency



INTRODUCTION

The increasing worldwide demand for power, growing crude oil prices and increasing anxiety about green house effect have prompted us to consider usage of geothermal power resources. Insolation is the most promising natural energy resource available on the planet. The mechanism for converting solar energy to electrical energy has made a lot of development, however, minimum conversion efficiency and high capital price are the major problem which come in the way of frequent use of these technologies. To increase the performance of solar power system various techniques have been attempted over the years consistently. Solar energy is the world's largest remaining source of untapped renewable energy. The major part of the global community are away from the electrical network and do not have proper ingress to the electricity. Laying out electric lines from power grid to remote areas is often not yet economically feasible and hence the decentralized power sources, such as the CPV module, are a favourable substitute. Multijunction cells consist of more than one pair of p-n junctions. It is designed in such a way that solar energy of different wavelengths can be converted into electricity through different layers of cell as shown in **Figure 1**. Typically layers are stacked on top of each other, with light incident on the largest-band gap layer, which transmits longer wavelengths to smaller-band gap layers underneath.

MJT's are categorized as Concentrated Photovoltaic (CPV) where, immense heat is generated through concentration. However efficiency of MJT is reported to be around 46% according to National Renewable Energy Laboratory. Solar cell can be economically feasible if sunlight is concentrated by a factor greater than 300x [1]. The amount of light not converted into electricity is converted into heat. This waste heat deteriorates both the performance and codal life of the cell.

The solar cell's efficiency is defined as the ratio of the maximum power output of the cell and the direct normal irradiance which is incident on the cell.

$$\eta_{\text{cell}} = \frac{P_{\text{out}}}{P_{\text{in}}} = \frac{P_{\text{in}}}{\int CR \cdot A \cdot \lambda \cdot G(\lambda) \cdot \eta_{\text{opt}}(\lambda) \cdot d\lambda} \quad (1)$$

Therefore the heat power produced on the cell is

$$q_{\text{heat}} = P_{\text{in}}(1 - \eta_{\text{cell}}) \quad (2)$$

Concentrated photovoltaic result in high heat flux on the solar cell's surface and a rapid increase in the cell's temperature. High temperature reduces open circuit voltage and the maximum power voltage [2]. It has been observed that under 500x concentration and without any cooling arrangements, the solar cell can exceed 1000°C [1]. This emphasizes the need of proper cooling methodology to maintain the temperature within secure operation limits as well as to avoid insignificant performance and probability of system deterioration [3].

LITERATURE REVIEW

Exhaustive endeavour are being made worldwide to reduce the operating temperature of CPV System to increase performance in terms of electrical efficiency, power output and codal life of the module. Numbers of researchers have worked on cooling the CPV/PV module with various active and passive cooling techniques. Some of these techniques are discussed in following section.

Peltier Effect (Active Cooling)

Figure 2 shows schematic of the combined PV-TEC system, aluminum sheet is sandwich between TEC module and PV cell in order to spread the cooling effect at the back surface of PV cell. Whenever solar radiation is incident on the top surface of PV cell, some amount of photon energy is converted into electric field and rest is wasted as heat through the top and bottom surface of PV cell. This small amount of generated energy is used to place TEC module in order to provide cooling effect for the PV cell.

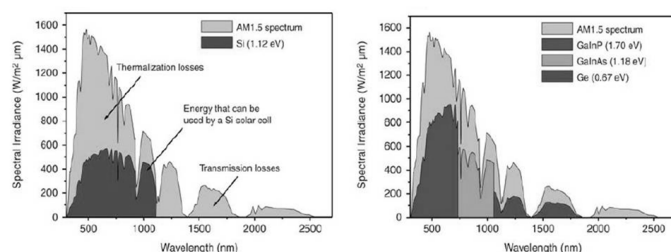


Figure 1 Spectrum utilization through conventional PV and MJT solar cell

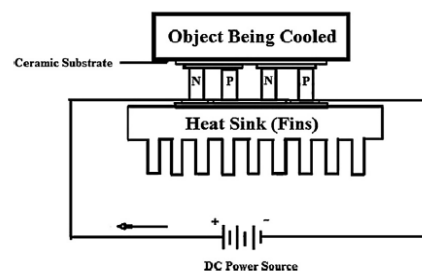


Figure 2 Schematic of the thermoelectric cooling system

It can be observed that high cell temperature can give minimum power output for fixed solar radiation. At 3200 W/m^2 heat flux, if we can operate a PV cell at the temperature of 25°C then it can generate 80% more power output than the cell operated at 87°C , with proper usage of cooling system especially at high solar radiation of concentrated photovoltaic system [4].

Forced Cooling (Active Cooling)

Forced cooling is another alternative way of cooling PV module. **Figure 3** shows schematic of pulsating cooling pipe arrangement on the rear side of PV panel. A direct current fan of 12 V is used to dissipate the heat from the heat pipe at the top shown in the **Figure 3**. The power output of water cooled concentrated photovoltaic module is 4.7 to 5.2 times greater than that of photovoltaic module (without concentration and cooling) [5].

Natural Cooling (Passive Cooling)

Micro-fins is another alternative solution for CPV cooling. It can improve the thermal performance and at the same time lowers the weight of the system. **Figure 4** shows cross-sectional view of the micro-finned silicon wafer and zooms on the fins. The CPV model is tested under-concentrator standard test conditions: 1000 W/m^2 heat flux, the cell efficiency is 42.5% and 2.20W of waste heat is produced. Worst case conditions: 1000 W/m^2 heat flux, the cell efficiency is 0% and 3.83W of waste heat is produced [6].

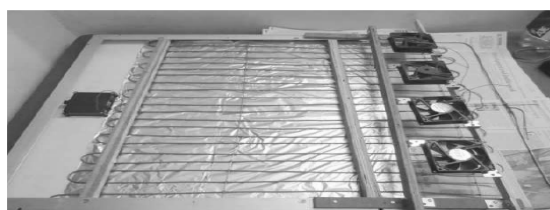


Figure 3 Pulsating cooling pipe arrangement on the rear side of PV panel



Figure 4 Schematic of micro-finned silicon wafer

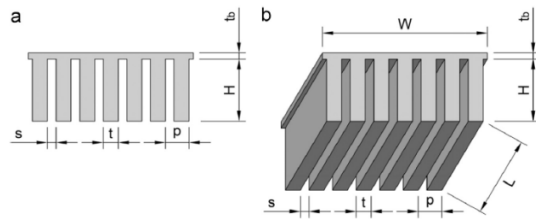


Figure 5 Schematics of a finned heat sink (a) front view and (b) 3D rendering

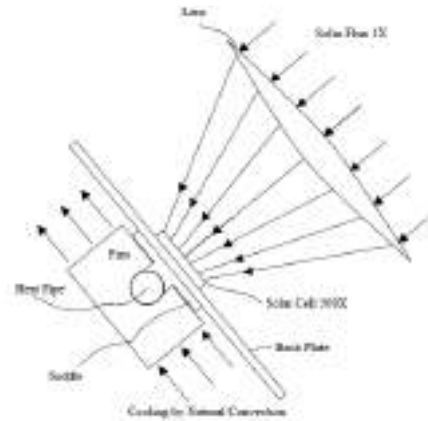


Figure 6 Passive cooling by using Heat Pipe, Fins and Fresnel lens

Extended Surface Cooling (Passive Cooling)

Extended surfaces are commonly used to extend transfer area to enhance conventional heat transfer passively. Fins are widely used in multiple fields where cooling is required from industrial to electronics applications. **Figure 5** shows schematic of finned heat sink is attached at the back side of CPV module and result shows that cell temperature goes up to 120°C without fins and cell temperature decreases up to 80°C with fins under standard testing condition [7].

Heat Pipe (Passive Cooling)

At high concentration ratio, single cell arrays is suitable for Heat pipe cooling, e.g. 1000 suns, and for low concentration ratio linear concentrator is suitable for Heat pipe cooling, e.g. 30 suns [8]. Heat pipe with fins is used to remove heat by natural convection. The temperature difference between the cell and the ambient air was roughly 30°C [9]. A comparative study between heat pipe and forced convection water cooling for single cell system was conducted and observed that the heat pipe cooling system was more efficient and effective [10]. Heat pipe is used to cool a linear concentrator with the help of copper thermosyphon using 20 incident suns on the solar cell. Refrigerant r-11 is used as a working fluid due to minimum operating temperature of 40°C. Passive cooling is used to remove heat to the atmosphere [11]. A concentrated photovoltaic module consist of heat pipe, back plate, saddle as shown in **Figure 6**. A MJT cell of 500x is mounted on a back plate. The heat flux (1X) is concentrated 500 times by using Fresnel lens. High concentrated heat flux strike the solar cell and produced electric power. The some amount of waste heat pass from the cell through the saddle and into the heat pipe rejected to the atmosphere by passive cooling having temperature difference of 43°C [12].

Integration of Cooling Techniques

Solar cell cooling is an integral part of CPV system. The operating temperature of CPV system has noticeable effect upon its overall performance is well documented. As it linearly deteriorates its performance in terms of power output, efficiency and codal life of cell. Therefore, decreasing the operating temperature of CPV module can boost the electrical efficiency. Integrating various active and passive cooling techniques will improve the performance of CPV module. Many researchers have studied the various active and passive cooling techniques, but these techniques were performed on various CPV/PV system material and configuration in diverse geographical condition. Therefore, it is too complicated to decide which one is more productive. As a result it's field of reference to perform a



research with integrating these various cooling methodology on one setup and to analyzed which techniques is more optimum out of them.

CONCLUSION

Solar cell performance is a function of cell operating temperature and lower temperature gives maximum efficiencies. Cell cooling is an exceptional factor when designing CPV module. When cell temperature goes on increasing, its performance deteriorates in terms of power output, efficiency and codal life of cell. Therefore, maintaining the operating temperature of CPV system within STC can boost the overall performance. In passive cooling extended surfaces are commonly used to augment the heat from back of CPV system. Heat pipe is the most popularly used medium for passive cooling of CPV system. Micro fins on the back side of CPV system, with certain time interval, decreases the CPV module temperature remarkably.

Active cooling requires more power for functioning. Introducing Peltier cooling device at back of CPV module and force cooling with the help of compressed air are further used for maintaining the operating temperature of the system. Integrating these techniques have remarkable effect on minimizing CPV module operating temperature which results in overall performance improvement in terms of power output, electrical efficiency and codal life of cell.

FUTURE SCOPE

Various researcher claim that codal life of cell is doubled for every ten-degree depletion in thermal jaunt. So integration of various active and passive cooling techniques on MJT Solar cell will give optimum result.

REFERENCES

1. Cotal. H., Frost. J. Heat transfer modeling of concentrator multijunction solar cell assemblies using finite difference techniques. 35th IEEE PVSC, Honolulu, HI, USA (2010).
2. Cotal. H., Sherif. R. Temperature dependence of the IV parameters from triple junction GaInP/InGaAs/Ge concentrator solar cell . In: 4th World Conference on photovoltaic Energy Conversion, IEEE, pp.845-848 (2006).
3. Theristis, M., Odonovan, T. Electrical-thermal analysis of III-V triple –junction solar cells under variable spectra and ambient temperatures. Solar Energy 118, 533-546 (2015).
4. Najafi, H., Woodbury, K. Optimization of a cooling system based on Peltier effect for photovoltaic cells. Solar Energy 91, 152-160 (2013).
5. Raj. A., Kumar. S., Manikandan, G., Titus. P. An Experimental Study on the Performance of Concentrated Photovoltaic System with Cooling System for Domestic Applications. International Journal of Engineering and Advanced Technology, ISSN:2249-8975(2014).
6. Micheli. L., Reddy. K., Mallick. T. Plate micro-fins in natural convection: an opportunity for passive concentrating photovoltaic cooling. Energy Procedia 82, 301-308 (2015).
7. Micheli. L., Fernandez. E., Almonacid. F., Mallick. T. Performance, limits and economics perspectives for passive cooling of High Concentrator Photovoltaics. Solar Energy Materials & Solar Cells 153, 164-178 (2016).
8. Royne, A., Dey, C., Mils, D. Cooling Photovoltaic cells under concentrated illumination : a critical review. Solar Energy Materials & Solar Cells 86 451-483, (2005).
9. Beach. T., White. M., Heat Pipe for Passive Cooling of Concentrator Solar Cells. IEEE@1981 Proceedings of the 15TH Photovoltaic Specialists Conference, pp.75-85 (1981).
10. Farahat. A, Improvement in the Thermal Electric Performance of a Photovoltaic Cells by Cooling and Concentration Techniques. IEEE@2004 ISBN: 1-86043-365-0, 39th international Universities Power engineering Conference, New York, pp. 623-628.
11. Akbarzadeh. A., Wadowski. T. Heat Piped-Based Cooling System for Photovoltaic Cells Under Concentrated Solar Radiation. Applied Thermal Engineering 16(1), pp 81-87 (1996).
12. Aderson, W., Tamanna, S., Sarrat, D., Dussinger, P. Heat Pipe Cooling of Concentrating Photovoltaic (CPV) Systems. American Institute of Aeronautics and Astronautics, Advanced Cooling Technologies, Inc., Lancaster PA, 17601, (2007).



Factors Affecting Mixing and Fabrication of Polymer-ceramics Granules

Prakhar Khemka^{*1}, Harpreet Singh¹, Tanuja Sheorey¹
Mechanical Engineering Department, IIITDM Jabalpur¹, prakhar.khemka14@gmail.com*

ABSTRACT

Coated polymer-ceramic granules with controlled porosity, granule size, and granule shape are the key concern during fabrication using extrusion-spheronization process. In this process, a thermoplastic polymer particle and ceramic particle size are combined together to produce the desired granules under appropriate processing conditions. In the present scenario, the global demand for high strength to weight ratio material is steadily increasing with the availability of natural resource is diminishing. This makes the development of the alternative materials even more important. This paper is primarily focused on various factors affecting the qualities of the polymer-ceramic granules during mixing and fabrication. It also highlights post-processing of fabricated granules to translate the entire work into the product in use and includes the demanding application.

KEYWORDS Polymer, ceramics, granules, fabrication, mechanical properties

INTRODUCTION

Granules are small, free flowing, spherical or semispherical units, preferably required for the moulding of polymer based components [1]. Granulation of selected materials gives many benefits such as (a) improve the compaction characteristic of the mix, (b) granules being denser than powder material, occupies less volume per unit weight, (c) better compatibility with the moulding methods like extrusion/injection moulding, (d) they are more convenient for storage and shipment [2]. Generally, polymer based granules in the size range of 0.5 to 5.0 mm are fabricated using extrusion-spheronization process. Proper size of the granule depends primarily on application and molding method. The extrusion-spheronization process was invented in Japan and was introduced into Europe and the United States in the early 1960s [3]. The process consists of the following stages: mixing, extrusion and spheronization (**Figure 1**).

Generally, the procedure utilized for blending cover and powder can impact the homogeneity of feedstock materials. Feedstock material can be delivered either in a batch procedure or continuously. Four types of machine are used: high-shear blenders, roll mills, screw extruders and shear rolls. The initial two are models of batch tasks while the last two are for continuous task. Final selection of the approach depends on the details of the application and the materials to be utilized for the feedstock. When utilizing fine particles tending to agglomerate, batch mixing in planetary or z-cutting edge blenders (**Figure 2**) is favored, despite the fact that the procedure can take several hours. However, the same mixer poses difficulty when used with the ceramics introduced polymer powder material. Therefore, planetary blenders have experienced some significant upgrades as of late in light of advancing procedure needs. Given the present seriously aggressive market, R&D chiefs and process engineers are putting more efforts in analyzing mixing process closely [5]. The basic reason is to focus on the planetary mixer due to its unique versatility and durability factor as compared to other available options. The mixer blade geometry the rectangular depend on radial powers and gravity to keep item inside the blending zone.

During extrusion process (**Figure 3**), the critical solid volume concentration (CPVC) is one of the most important factors that decide the ideal polymer-ceramic mixture [6]. The extrusion operation is an integral part of the overall spheronization process in which the wet powder mass is forced through a restricted cross-section. The dimensions of the restriction in terms of radius and length differ from system to system [7]. A diameter of less than 500 μm is not often used. Nevertheless, some researchers have used an extruder screen of 400 μm in diameter to obtain pellets of this size range. Extruders of different sizes can be used depending on the load they can handle. In light of the kind of feed component used to exchange the mass towards the die, extruders are separated in three class i.e. (a) screw feed extruder (pivotal or end plate, vault or spiral), (b) gravity feed extruder (round and hollow move, equip move, outspread), (c) cylinder feed extruder (for the most part used for exploratory advancement). The nature of the extrudate is depending on an appropriate value of the process variables namely, screen pressure, die hole diameter, extruder type, screw speed, and extrusion temperature.

Once the extrudates are prepared, they are quenched in water and then taken to spheronizer, where it is spheronized using rotating cutters/contact plate that breaks the rod shaped particles into smaller particles and adjusted them to frame circles. The measure of the spheroids is basically relying on the diameter of circular die that adjusts the width of barrel shaped rods created in extrusion stage. For instance, with the end goal to get circles with a breadth of 1

mm, a 1 mm screen is utilized on the extruder, despite the fact that circles with a slighter greater measurement will now and again be gotten. If required, length of granules can be varied by changing the center distance between cutters, the release valve of the chamber is opened and the granules are released by the centrifugal force. **Figure 4** shows the mechanism of spheronization process. The nature of granules is very affected by the procedure parameters related for the most part with the extrusion stage and is generally contemplated by different research researchers. At the point when examination investigations of spheroids created from ram extruder and cylindrical extruder with fillers of various molecule measures were assessed, it was presumed that distinctive extruder impacts last spheroidal size [8]. On the other hand, a few studies demonstrated that distinctions in size consistency of spheroids are related with the gap and speed of the cutters or contact plate [9-10].

However, no clear information is available to control the extrusion-spheronization process precisely. Moreover, the complexity of making a good combination of process parameters throughout is a challenging task. As we know, extrusion-spheronization process is of imperative significance to all plastics preparing. In this paper, various stages of the extrusion-spheronization process are illustrated with the aim to describe various factors affecting the quality of the outcome. The demand and application areas of the outcome 'feed stock' have also been highlighted.

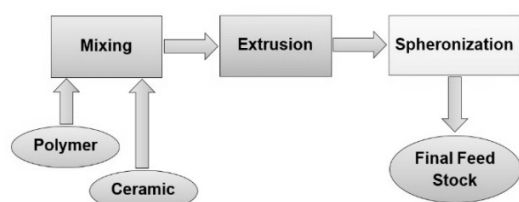


Figure 1 Stages of extrusion-spheronization process



Figure 2 Planetary mixer

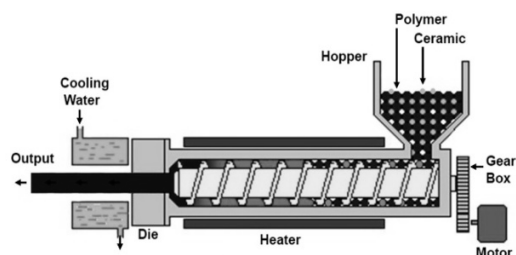


Figure 3 Schematic view of extrusion process

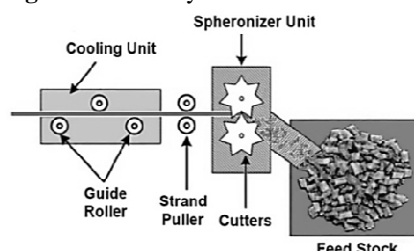


Figure 4 Mechanism of spheronization

FACTORES AND ITS EFFECTS

Material and Design

The objective of this segment is to acquaint the peruse with the significance of a reasonable material and design of various components of extrusion-spheronization process. Specially, die and extrusion barrel are highly important components; both can be varied in shape and complexity to meet the demands of the product being manufactured [11]. Materials mostly used for the major components of the extrusion-spheronization process are presented in **Table 1**. Generally, one basic shape of die i.e. circular is used to make regular rod before spheronization with the extrusion namely strand. Therefore, strand dies make simple geometric shapes, such as circles, squares, or triangles. The die openings in the screen or die plate might be of a few fundamental outlines. The state of opening fluctuates with the application. On the off chance that a denser item is required, a thicker plate or screen is utilized to withstand more prominent extrusion pressure utilized. **Figure 5** demonstrates some of the common die configurations. At the same time, compatibility of extruded material with component material should also be kept in mind to avoid excess moisture, temperature, corrosion, flow resistance, stickiness, etc.

For the better composition and structure of grains and uniformity, extrusion screw design is a major influencing parameter. Extrusion is performed using five main classes of extruders: screw, sieve, basket, roll, and ram extruders [9]. The type of features of all five classes are presented in **Table 2**. For plastic processing, screw extruders are extensively used in the present scenario due to its unique benefits such as better mixing, controlled heating and low



maintenance. Mainly it is used to build up the important strain to drive the material to course through uniform openings by the screw.

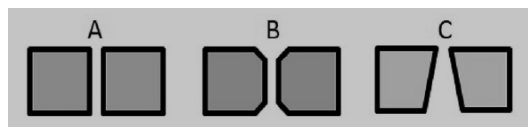


Figure 5 Substitute die designs: (A) cylindrical, (B) tapered inlet and/or outlet, (C) conical

Table 1 List of materials for major components

Mixer material	Barrel material	Screw material	Die material	Spheronization unit
Stainless Steel, Chrome Steel	Nitride Steel, Steel Alloy	Chrome Planting: Nitride, Tool Steel, Nickel Alloy	Carbon Steel, Die Steel, Stainless Steel, Titanium, Aluminium, Magnesium	Nickel Alloy, Stainless Steel, Steel Alloy

Table 2 Types of extruders and their features

S. No.	Types of Extruder	Features
1.	Screw Extruders	Consist of one or two screws feeding the plastic mass to an axial or radial extrusion screen
	Axial Type	Screen is placed at the end of the screw, perpendicularly with the axis of screw
	Radial Type	Die is placed around the screw, discharging the extrudates perpendicular to the axis of the screw
2.	Sieve Extruder	The granulate is fed by a screw into the extrusion chamber, where a rotating or oscillating device pushes the plastic mass through the screen. Here the screen is positioned at the bottom of the extrusion chamber
3.	Basket Extruder	Similar to sieve extruder, the difference being that the granulate is fed by gravity into the extrusion chamber and that the vertical walls of the chamber make up the extrusion screen
4.	Roll Extruder	
	With one perforated roll	Contains two contra-rotating wheels, of which one is perforated
	With two perforated roll	Both the contra-rotating wheels are perforated
	With the extrusion screen rotating around the rollers	Contains a perforated cylinder rotating around the rollers, which rotates around one or more rollers, discharging the material to the outside of the cylinder
5.	Ram Extruder	Based on a piston, which pushes the wet mass through the screen situated at the end of the barrel

Process Parameters

In the recent years, many studies have been reported to optimize the process parameters. Based on the collected data, details of process parameters and their typical range is given as: (a) barrel temperature range 130 to 200°C, (b) extruder speed 70 to 130 rpm, (c) extrusion pressure 40 to 80 MPa, (d) mold temperature 30 to 70°C, and (e) cutters speed 20 to 60 rpm [10, 12]. Details available on the processing of spheronization unit, especially for polymer-ceramic granules are scares. The size of the coated granules is dependent on the cutter speed, center distance and diameter of strands.

The quality of coated granules has a direct correlation to mixing and extrusion operating conditions. It had been reported that carbon-based reinforcement can likewise be inserted in a preceramic matrix in the state of fibers, to improve electrical and mechanical properties. Shibuya et al. [12] examined the impact of vapor-developed carbon filaments (VGCFs) on the electrical resistivity when the pyrolysis of a preceramic methyl silicon resin (MSR), utilized as an antecedent to a silicon oxycarbide clay (SiCO). An ideal mix of low density, high electrical conductivity and great mechanical properties was accomplished working with 10 wt% VGCFs and 50 wt% Poly(methyl methacrylate) (PMMA) microbeads concerning MSR [13]. The restricted between dispersion is a requirement additionally for the morphology of precious stones. All polymer-inferred mullite-based materials grew so far have, actually, equiaxed grains. A wonderful exemption is spoken to by as of late arranged covered filaments,

unmistakably displaying anisotropic gem development, as represented in **Figure 6(a)**. Such morphology is because of the presentation of little measures of borax (hydrated sodium borate, 3 wt% alluding to the heaviness of mullite) in silicone/ γ - Al_2O_3 blends. The Job of B_2O_3 in bringing down the mullitization temperatures and in advancing the anisotropic development of covered granules has been generally discussed in the literature [14]. The microscopic view of polymer-ceramic based extruder and ceramic dispersion arrangement is depicted in **Figures 6(b)** and **6(c)**, respectively.

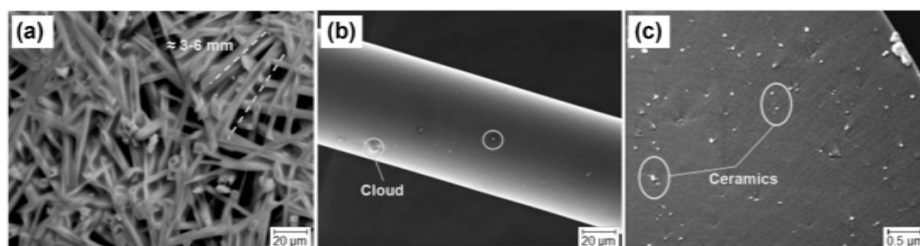


Figure 6 Microscopic view: (a) coated fiber, (b) polymer-ceramic extruders, (c) dispersed ceramic particles

APPLICATIONS

Polymer/polymer-ceramic material is used in a wide variety of applications for the production of various plastic parts ranging from simple to complex shapes, such as automotive bumpers, chemical tanks, cable insulation, gas cans, carpet fibers, gears, bushes, cams, bearings, weather proof coatings, automotive suspension bushings, cushions, electrical potting compounds, hard plastic parts. In every case, objectives of using polymer-ceramic based materials have been to reduce weight of product specially for planes. **Figure 7** shows pictorial view of the trending application areas. The industries acknowledge the financial and specialized favorable circumstances of polymer based gears, to be specific capacity to work without oil or oil grease, ease of creation, low thickness, high flexibility, and inner damping limit. Consequently, the utilization of plastic gears is consistently expanding. A few precedents of the field use of plastic gears incorporate the car industries, office machines and family unit utensils, and sustenance and material apparatus. Be that as it may, amid cross section of apparatus tooth, the warmth that is privately created stays focused and does not disperse. Therefore, there is a wide scope to extend the capabilities of plastic gears by introducing the best combination of polymer-ceramic composite material. The ceramic inclusion in plastic gear material, not just posture as a decent answer for dealing with the modern waste adequately however in a roundabout way decreasing the antagonistic impact on the environment.



Figure 7 A pictorial view of the trending application areas

CONCLUSION

The present paper explores detail of various components of extrusion-spheronization process and its applications for economical and ecofriendly polymer-ceramic based gear material manufacturing. Following conclusions can be drawn:

- Mixing has a direct correlation to the performance, strength and durability of specialty ceramics and composites.
- The piece and structure of grains and grain limit stages, and the dissemination of earthenware production, can be controlled to accomplish ideal item execution and unwavering quality.



- The quality of the extrudate is depending on an appropriate value of the process variables namely, screen pressure, die hole diameter, extruder type, screw speed, and extrusion temperature.
- Polymer-clay composites have ended up being adaptable and versatile designing material for some, applications, including aviation, air ship, car, development, marine, item, and sports.
- As regards the commercial situation, it can be stated that the market is still in a conflict phase, therefore much can still be done in order to explore more detail about the key components and their operating conditions.

REFERENCES

1. R. L.Junnila, Pelletization by extrusion and spheronization technique and evaluation of pellets-a literature review, Department of Pharmacy, University of Helsinki.
2. B. Gowthami, C. H. Sireesh, V. Jyothi, S. S. Manikiran, N. R. Rao, Advanced granulation technology, International Journal of Pharma and Chemical Research I, Volume 3, Number 3, 2017.
3. J. M. Newton, The preparation of pellets by extrusion-spheronization, Pharmaceutical Dosage Forms: Tablets, Informa, 2008.
4. G. G. Joamin, I. Duretek, C. Kukla, A. Poljsak, M. Bek, I. Emri, C. Holzer, Models to predict the viscosity of metal injection molding feedstock materials as function of their formulation, Metals, Volume 6, pp129; doi:10.3390/met6060129, 2016.
5. D.Drummer, S. Messingschlager, Material characterization of strontium ferrite powders for producing sintered magnets by ceramic injection molding, International Journal of Advanced Materials Science and Engineering, Article ID 651062, p 8, 2014.
6. K.P.Vimal, Effect of powder characteristics on compounding and green microstructure in the injection moulding process. International Journal of Am. Ceram. Soc., Volume 72, 1989
7. K. Le, Extrusion-spheronization process variables and characterization, updoc.tips.
8. S. Bhaskaran, P. K. Lakshmi, Extrusion spheronization - a review, International Journal of PhatmTech Res., Volume 2, Number 4, 2010
9. D.C. Hicks, H.L. Freese, Extrusion and spheronizing equipment, In: Ghebre-Sellassie I, editor. Pharmaceutical pelletization technology. NewYork: Marcel Dekker, pp 71–101, 1989.
10. Chaitanya S., Singh I., Sisal fiber-reinforced green composites: effect of ecofriendly fiber treatment, J International Journal of Polymer Composites, (2017) 1-12.
11. Chaitanya S., Singh A P., Singh I., Processing of lignocellulosic fiber-reinforced biodegradable composites, Natural Fiber-Reinforced Biodegradable and Bioresorbable Polymer Composites, 163 (2017). <http://doi.org/10.1016/B978-0-08-100656-6.00009-1>
12. Muley S., Nandgude T., Poddar S., Extrusion–spheronization a promising pelletization technique, Asian Journal of Pharmaceutical Sciences, 11 (2016) 684–699.
13. Shibuya M., Sakurai M, Takahashi T., Preparation and characteristics of a vapor-grown carbon fiber/ceramic composite using a methyl silicone precursor. Comp. Sci. Technol., 67 (2007) 3338–3344.
14. Colombo P., Bernardo E., Macro- and micro-cellular porous ceramics from preceramic polymers. Compos. Sci. Technol., 63 (2003) 2353–2359.
15. Bernardo E., Fiocco L., Parciannello G., Storti E., Colombo P., Advanced ceramics from preceramic polymers modified at the nano-scale: a review, Materials, 7, (2014) 1927-1956; doi:10.3390/ma7031927.



A Computational Fluid Dynamics Study on Various Methods for Enhancement of Bio-oil Recovery by using a Shell and Tube Condenser

B.L. Salvi^{*1}, T. Soni¹, S. Jindal¹, M.A. Saloda¹

Department of Mechanical Engineering, College of Technology and Engineering, Maharana Pratap University of Agriculture and Technology, Udaipur, Rajasthan¹, salvibl@yahoo.in^{*}

ABSTRACT

Increasing utilization of energy and exploitation of fossil fuel based natural resources of energy are resulting into environmental pollution and other problems to human beings including respiration, dazzling and smog. The sustainable development of civilization requires alternative renewable sources of energy. The bio-oil, as an alternative renewable source of energy to produce bio-diesel and thermal application in industries, can be produced from waste bio-mass. The present work is aimed for study on various methods for enhancement of bio-oil recovery by using shell and tube type condenser and its computational fluid dynamics analysis. In shell and tube type condenser, the water circulates through tubes and bio-oil vapour circulates in the shell. The hot vapour enters into condenser shell at temperature of 200 °C to 300 °C and is of acidic nature. Hence, selection of material for cooling water tubes, vapour retention period in condenser and cooling fluid circulation is of prime importance.

The Computational Fluid Dynamics (CFD) study was carried out for vapour and water flow and heat transfer in the shell and tubes made of stainless steel. The analysis was carried out for vapour condensation by varying the vapour flow rate, cooling water flow rate and its temperature. The volume rendering and stream lines for temperature has shown the internal flow pattern and cooling of vapour. The temperature reduction of vapour was increased with the use of baffle plates, which help in circulation of hot vapour in different zones more retention time for vapour.

The CFD analysis will help in better design of the condenser and its optimization. In all the bio-oil recovery will increase with the newly developed condenser with the baffle plates as compared to conventionally used shell and tube type heat exchanger.

KEYWORDS Condenser, Bio-oil, Computational fluid dynamic, Tar

INTRODUCTION

Ever-increasing utilization of energy and use of fossil fuel based natural resources of energy are resulting into environmental pollution and other problems to human beings such as respiration, dazzling, smog, etc. The increasing concern for the protection of the environment together with the rapid consumption of crude oils has led to the necessity of finding alternative renewable sources of energy. The biomass is extensively considered to be a prospective and renewable source of energy for the future [1]. The bio-oil, as an alternative renewable source of energy to produce bio-diesel and thermal application in industries, can be produced from waste bio-mass [2]. The bio-oil is biodegradable and renewable in nature. The heating value/energy density of bio-oils is much higher than that of the bio-mass, so it is convenient for transportation and utilization [3]. The bio-oil has got wide application including utilization in gas turbines [2] and combustion in a furnace or a boiler [1].

BIO-OIL PRODUCTION

Bio-oils are dark brown, free-flowing organic liquids that are comprised of highly oxygenated compounds. The bio-oil is also known by other names including pyrolysis oils, pyrolysis liquids, Bio-Crude Oil (BCO), wood liquids, wood oil, wood distillates, etc. [4]. The bio-oil is produced by thermal degradation of bio-mass, called pyrolysis. The pyrolysis processes may be slow or fast pyrolysis, depending on the operating conditions that are used. In pyrolysis process the wood decomposition begins at 200°C and reaches to maximum rate of mass loss at 350°C, and continued to 500°C [4].

The decomposed wood convert into bio-oil vapours, ash, tar, etc. The bio-oil vapour comes out from reactor at temperature of about 180°C to 250°C. The various design parameters/variables required for pyrolysis including



particle size, pre-treatment, reactor configuration, source of heat supply, heat transfer methods, heating rates, reaction temperature, vapour residence time, ash separation, vapour condenser, char separation, and liquid collection methods affect the yield of the bio-oil [5]. The highest yield of bio-oil from sugar cane trash was 31.95 wt% for N_2 as sweep gas at the flow rate of 160 cc.s^{-1} [6]. The slow pyrolysis produce bio-oil about 24 to 43% [7], whereas fast pyrolysis produce highest bio-oil yield of 56 wt% was obtained at 465°C from rice husk [1]. According to Bridgwater et al. [8], the bio-oil yield as high as 80% may be recovered in fast pyrolysis [7]. In both slow and fast pyrolysis, the effectiveness of bio-oil vapour condenser also play major role in the bio-oil yield.

BIO-OIL VAPOUR CONDENSER

The bio-oil vapour condenser is a type of heat exchanger, which is used to transfer heat between two process streams, i.e., hot and cold fluid. There are various types of heat exchangers including mixing type, and shell and tube condensers. A shell and tube condenser consists of a shell and a tube or series of tubes. The cold fluid may flow in tube or shell as per requirement. Usually, when vapour is to be cooled or condensed, the cold fluid flow inside the tube. The tubes may be made up of different types including plain, longitudinally finned, etc.

The selection of condenser used, i.e., type and size of condenser, can be based on suitability for a process depending on the type of fluid, its phase, temperature, density, viscosity, pressures, chemical composition and various other thermodynamic properties. The bio-oil is of acidic in nature, but its corrosiveness is very mild towards copper and stainless steel [3]. Therefore, condenser shell and tube material selected should be inert to the bio-oil vapour.

The bio-oil production efficiency was tested for various parameters including temperature, N_2 flow rate, feed-stock, particle size, and reaction time [9]; but detailed study of effectiveness of bio-oil vapour condenser is lacking. Proper Computational Fluid Dynamics (CFD) analysis of bio-oil condenser is also lacking. There is wide scope for CFD analysis of the bio-oil vapour condenser for production of bio-oil.

This work is aimed for study on various methods for condensation of bio-oil vapour for enhancement of bio-oil recovery by using shell and tube type condenser and its CFD analysis. The selection of material for cooling water tubes, vapour retention period in condenser and cooling fluid circulation is of prime importance.

MATERIALS AND METHODS

Experimental Set up for Pyrolysis

The experimental setup of fixed-bed type fast pyrolysis unit for feed rate of 20 kg/h, is available at DREE, College of Technology and Engineering, Udaipur, was used for fast pyrolysis [5]. The bio-oil vapour produced from pyrolysis was used as feed for vapour condenser. The shell and tube type counter flow condenser was use to cool the hot bio-oil vapour into bio-oil. The experiments were conducted on shell and tube condenser for counter flow and without baffle plates. The inlet vapour to condenser, i.e., bio-oil vapour and nitrogen as sweep gas, mass flow rate was maintained at 0.005 kg/s. The temperature variations were calculated from experiment for counter flow by varying the mass flow rate of cold fluid of 0.5 l/min to 2 l/min, which is controlled by rota meter and the temperature variations were noted by the K-type and J-type thermocouple sensors attached at the inlets and outlets of tube.

Development of Geometric Model

CFD technique which is a computer based analysis is used to simulate the condenser for vapour flow, cooling water flow and heat transfer. The condenser is shell and tube heat exchanger. The tube and shell is made of stainless steel as the hot vapour is quit acidic in nature and would corrode other materials. The water circulates through tubes and bio-oil vapour circulates in the shell around cold water tubes. The hot vapour enters into condenser shell at temperature of 150°C to 200°C .

Table 1 Main properties of bio-oil from cotton stalk [1]

Properties	Bio-oil from cotton stalk
H_2O , wt. %	24.4
pH	3.3
Density, kg/m^3	1160
Viscosity, mm^2/s	125
LHV, MJ/kg	17.77

Table 2 Geometric dimensions of condenser

Specification	Dimension
Length of condenser shell, L	1150 mm
Shell inner diameter, D_s	150 mm
Tube outer diameter, d_o	30 mm
Number of tubes, N_t	1
Baffle cut	55%
Baffle spacing	75 mm
Baffle thickness, t	04 mm
Number of baffle plates, N_b	7

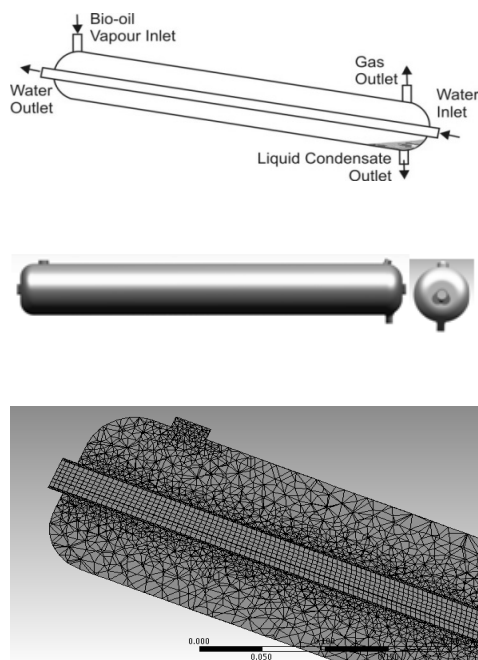


Figure 1 Schematic diagram, geometric model and mesh assembly of shell and tube condenser

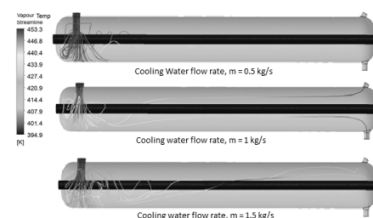


Figure 2 Effects of water flow rate on vapour temperature

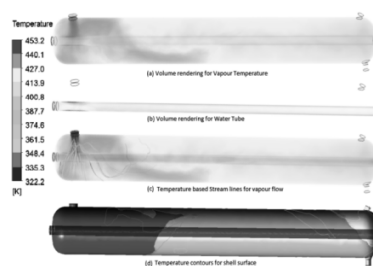


Figure 3 Volume rendering of (a) vapour temperature, (b) water tube, (c) streamlines for vapour flow and (d) contours for shell zone temperature

A geometric model as per dimensions given in **Table 2**, was prepared in CATIA V5 and imported into ANSYS 15.0 Fluent for numerical analysis [10]. The geometric model was meshed in medium-quality meshes in both element shape and smoothness. The number of nodes 76,837 and number of element 2,62,113 were generated. The high quality mesh would produce better results, but take more time for analysis. The mesh geometry of shell and tube condenser is shown in **Figure 1**.

Boundary Conditions

The condenser is a shell-and-tube heat exchanger; there are two inlets and three outlets. Different boundary conditions were applied for different zones. The vapour inlet was defined as mass flow rate of 0.005 kg/s, and gas outlet and liquid condensate were defined as pressure outlets at atmospheric conditions. The inlet mass flow rate of the cold water was kept constant, i.e., 0.5 kg/s. The outlet pressures were kept default, i.e., atmospheric pressure. The hot vapour temperature at inlet was 180°C and cold fluid cooling water inlet was 30°C. The shell was assigned wood-vapour as fluid and tube was assigned with steel material as available in the FLUENT database.

The transient heat transfer analysis was carried out using turbulence k- ϵ , realizable and scalable wall function model was used for accurate results from CFD. The solution method simple, least square cell based gradient was applied. Then, hybrid initialization was done and calculations were done for 200 iterations. Then, results were observed/processed by using the post processor FLUENT and simulated results were computed, i.e., temperature contours, pressure contours and velocity vectors.



Validation of Condenser Model

The simulated results were validated with the experimental values for fluid inlet and outlet conditions. The analysis shows that there is a difference between temperatures values computed from the experiment and the simulation by ANSYS 15.0. There was 10% to 20% error in the experimental and simulated numerical results for temperature. The simulated results are quite similar to the experimental results. Therefore, the numerical model is validated for the shell and tube condenser.

RESULTS AND DISCUSSION

The simulation study was carried out for analysis of bio-oil vapour flow in the shell and cooling water flow in the tube.

Effects of Cooling Water Flow Rate

It is found that for cooling water mass flow rate of 0.5 kg/s, there is no much effect on outlet temperature of the vapour. But, the vapour temperature decreased with increase in the cooling water flow rate.

The effect of cooling water flow rate on vapour temperature along the shell axis is shown in **Figure 2**, as temperature rendered streamlines. It can be observed from the **Figure 2** that vapour temperature is decreasing with increase in water flow rate as well as along the length of condenser shell.

Volume Rendering and Contours

Volume rendering of (a) vapour temperature, (b) water tube, (c) streamlines for vapour flow and (d) contours for shell zone temperature are shown in **Figure 3**. It can be seen that this volume rendering for temperature can provide the inside view of shell for cooling of bio-oil vapours and temperature of the cooling water tube. The temperature contours on shell shows the temperature condition of the surface of shell.

The temperature stream lines and particle tracking along the shell zone are shown in **Figure 4**. The stream line and particle movement can be tracked by CFD analysis. In order retain the vapour in shell for more time, the shell was provided with baffle plates. The volume rendering for vapour velocity and flow pattern in shell and tube condenser with baffles is shown in **Figure 5**. The internal flow pattern with different types of baffle plates can be analysed using CFD analysis.

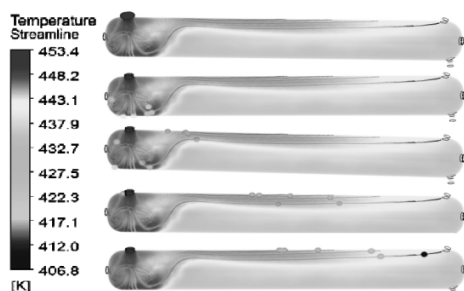


Figure 4 Temperature streamlines and particle tracking along the shell zone

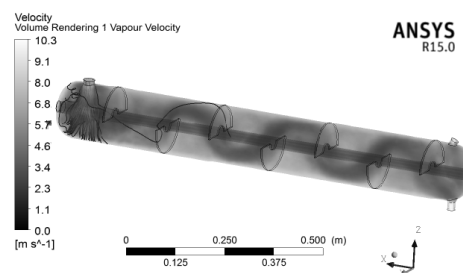


Figure 5 Volume rendering for vapour velocity and flow pattern in shell and tube condenser with baffles

This CFD analysis helps to design the condenser by changing the different variables very easily; otherwise it is very difficult if done practically. The CFD package ANSYS FLUENT provides the contours for temperature, pressure and velocity, and data which help to predict the performance of the condenser design and are effectively used. It has the ability to obtain optimal solutions before actual fabrication of the system, hence saving of time and resources.



CONCLUSIONS

In this study a geometric model of shell and tube condenser was developed and CFD analysis was carried out by using ANSYS Fluent R15.0. The condenser model was validated with the experimental results and then the parametric study was carried out for different inlet and outlet conditions of bio-oil vapour and cooling fluid in counter flow mode. The cooling water flow was varied from 0.5 kg/s to 1.5 kg/s and found that vapour temperature decreased with increase in cooling water flow rate, but flow rate is limited with tube diameter. The volume rendering and streamlines for vapour temperature has shown the internal flow pattern and cooling of vapour.

The heat transfers from vapour to cooling water and at higher temperature of bio-oil vapour the cooling water gets heated up rapidly and water vapour formation starts. This reduces the effectiveness of the condenser. It is suggested to use the binary circuit for cooling fluid. The temperature reduction of vapour was increased with the use of baffle plates, which help in circulation of hot vapour in different zones. This would increase the vapour condensation and more bio-oil recovery. The circular fins over water tubes would increase the heat transfer, but due to vapour flow in the condenser shell, there is flow separation, which reduces the heat transfer. This would result into no or very less effects on improvement in bio-oil recovery. Based on literature it is found that during condensation process some tar formation also takes place over the water tubes and reduces the condenser's effectiveness. The condenser tubes and shell can be cleaned periodically in order to increase the heat transfer and effectiveness of the condenser. It was found that CFD analysis can be effectively used for vapour and cooling fluid analysis in the shell and tube. Further study is required for variation in tube diameter, baffles in the shell and vapour flow rate. This CFD analysis will help in better design for more heat transfer and condensation of vapour to produce bio-oil.

ACKNOWLEDGEMENTS

The authors acknowledge the ICAR to financially support the project on Energy in Agriculture. The authors are also grateful to acknowledge Dr. NL Panwar, Department of Renewable Energy Engineering, College of Technology and Engineering, MPUAT, Udaipur, Rajasthan for providing necessary help in experimental work.

REFERENCES

1. Z. Ji-lu. Bio-oil from fast pyrolysis of rice husk: Yields and related properties and improvement of the pyrolysis system, J. Anal. Appl. Pyrolysis Volume 80, pp. 30–35, 2007.
2. M.E. Boucher, A. Chaala, C. Roy. Bio-oils obtained by vacuum pyrolysis of softwood bark as a liquid fuel for gas turbines. Part I: Properties of bio-oil and its blends with methanol and a pyrolytic aqueous phase, Biomass and Bioenergy Volume 19, pp. 337-350, 2000.
3. Z Ji-lu, Y. Wei-ming, W. Na-na. Bio-oil production from cotton stalk, Energy Conversion and Management Volume 49, pp. 1724–1730, 2008.
4. D. Mohan, Charles U. Pittman, Jr., and Philip H. Steele, Pyrolysis of Wood/Biomass for Bio-oil: A Critical Review, Energy & Fuels Volume 20, pp. 848-889, 2006.
5. P. M. Rajendra, Design and development of fixed-bed type fast pyrolysis unit, unpublished M.Tech. Thesis, College of Technology and Engineering, Udaipur, 2018.
6. W. Treedet, R. Suntivarakorn. Sugar Cane Trash Pyrolysis for Bio-oil Production in a Fluidized Bed Reactor, World Renewable Energy Congress, Linköping, Sweden, pp. 140-147, 2011.
7. Isahak WNRW, Hisham MWM, Yarmo MA, Hin TY, A review on bio-oil production from biomass by using pyrolysis method, Renewable and Sustainable Energy Reviews Volume 16, pp. 5910–5923, 2012.
8. A.V. Bridgwater, G.V.C. Peacocke. Fast pyrolysis processes for biomass. Renewable and Sustainable Energy Reviews 4, pp. 1–73, 2000.
9. F. Abnisa, Wan Daud WMA, JN Sahu. Optimization and characterization studies on bio-oil production from palm shell by pyrolysis using response surface methodology, Biomass and Bioenergy Volume 35, pp. 3604-3616, 2011.
10. ANSYS Fluent 15.0 User Guide, ANSYS Inc, 2013.



Integration of Analytical Software and 3D Platform in Plant Design and Engineering: A Paradigm Shift for the Upcoming and Revamped Process Plants

Anirban Datta^{*1}, Gautam Gangopadhyay¹

Richard Design Services India Private Limited (A fully owned Subsidiary of Richard Industrial Group, USA), Kolkata¹,
ani_dat@yahoo.co.in*

ABSTRACT

Industrial and process plant design engineering for greenfield as well as retrofitted/revamped projects are now heavily dependent on different design and analytical software, particularly in 3D environment. Over the last decade, this has become industry standard, by reducing time, cost and resource involvement in plant design, along with imparting accuracy in layout and quantity. Also, decreasing competency and knowledge in practising engineering personnel has also set the ground for reliance on engineering software.

KEYWORDS Plant, Software, Design, Analysis, 3D

INTRODUCTION

Since last decade, the design engineering for industrial plants – oil and gas, petrochemical, power (coal/gas based), fertilizer, steel and metallurgical, etc – has grossly being driven with the assistance and back up of modelling and analytical software. Manual drawing preparation and design calculations have now become almost extinct. The 90s had seen the emergence drafting software like AutoCAD (developed and marketed by Autodesk Inc.), replacing the drawing boards. The new millennium took design engineering to the next level – developing total plant layout in three-dimensional virtual environment, with a realistic view of plant in constructed condition. This had been integrated with computer aided engineering (CAE). Manual engineering calculations, be it for civil, structural, equipment, piping, electrical or automation, are now practically replaced with computerized analysis. This has not only reduced the time of design, but has also increased the accuracy. In an environment where the cost of design engineering is just 1% to 2% of the total project cost (and project proponents would like to get it reduced further), it is now practically impossible to complete the plant design without the aid of software platforms. In addition, there are two more driving forces behind this: (i) tight schedule of completion for engineering design to open the front for execution/construction, and (ii) shortage of competent engineering personnel in design engineering field.

PLANT LAYOUT

Overall plot plan or overall plant layout is a master plan, which shows the footprint of each unit/facility within the plot boundary for different process industries, namely, Refinery, Chemical/Agro-Chemical/Petro-Chemical/ Organic and Inorganic Chemical, Fertilizer, Pharmaceutical, Metallurgical and Power Generation.

Development of overall plant layout or plot plan requires certain pre-requisites in form of data/information, such as:

(i) Process Data

- Knowledge on the type of plant
- Size/capacity of the process unit
- Sequence of process flow
- Type of hazard
- Overall operating philosophy
- Raw material receipt and product dispatch philosophy
- Storage Philosophy

(ii) Meteorological Data

- Ambient Temperature throughout the year
- Rainfall – maximum, average, minimum
- Predominant wind direction and intensity (wind rose)
- Seismic zone
- Wet and Dry Bulb temperatures
- Flood level of the site



(iii) Civil

- Plane table survey map
- Contour survey map (at 10 m grid)
- Soil bearing capacity
- Nature of soil
- Rail/road access to site

(iv) Electrical

- Location of Electric Supply Point
- Supply voltage levels and fault levels and required voltage level(s) for the plant
- Power distribution/evacuation scheme

(v) Utilities

- Source and/or terminal point of raw water
- Quality of water available at terminal point
- Water consumption for process(s)
- Requirement of different types of utilities e.g. steam, air, nitrogen, demineralised water, etc.

(vi) Statutory Requirements

- Central/State Industrial Development Corporations
- Central/State Pollution Control Boards
- Factory Inspectorate
- State Electricity Boards
- Chief Controller of Explosives
- Static and Mobile Pressure Vessel Rules
- Tariff Advisory Committee (TAC)
- Aviation Laws
- Chief Inspector of Boilers
- Oil Industry Safety Directorate (for oil and gas installations)
- Food and Drug Administration (if applicable)
- Ministry of Environment and Forest

Until the beginning of this millennium, overall plant layout (**Figure 1**) meant to be a large drawing, preferably drawn on an A0 size paper; and perhaps it was the only design document for a project, which was subject to modification/revision until the commissioning of the plant. Further, the overall plant were sub-divided into unit specific plans, wherein the process equipment, piping, structural grids, electrical cable trays, HVAC ducts, etc. pertaining to that particular were to be shown. Construction and erection of these items were done with paper drawings, with adequate sectional views and isometrics in some cases.

However, with emergence of 3D software platforms, this entire process is now carried out with the aid of software, which not only enables placing all components of a process plant, but also the generation of construction drawings is now a matter of a click of computer mouse. Moreover, the clash/interference between pipes, equipment, structure, electrical cable tray, ducts can be checked and resolved in very effective and error-free manner; so that the construction/erection can be progressed with a fast pace, thus reducing the project completion time.

In addition, bill of materials for civil, structural, piping, electrical, instrumentation and automation items has become very easy and accurate, as those can be readily extracted from software platform itself.

ENGINEERING PROCESS FOR A TYPICAL EPC PROJECT IN 3D PLATFORM

Figure 2 represents 3D model generated for earthwork [1].

Once the design criteria for foundations of equipment and structure are established, design calculations for sizing of foundations are done in STAAD-PRO, RISA, or other software with international repute, and are modelled in 3D platform.

Figure 3 shows a snapshot of foundation model [1].



This enables the front for placing structural members over foundations; viz. mechanical equipment supporting structures, pipe rack structures, cable and duct supporting structure, etc.

Mechanical equipment/piping engineering teams proceed with design/selection calculations for equipment/piping, such as design of fabricated pressure vessels as well as static and dynamic stress analysis of interconnecting piping in compliance with international and project specific codes & standards. First of all the integrity/stability of the equipment/piping are ensured in form of stress compliance. Once these are frozen, the load data are transmitted to civil/structural engineering teams.

After capturing the structures in 3D model, equipment, piping, cable trays, ducts are placed in 3D. **Figure 4** shows an integrated 3D model of a process unit [2].

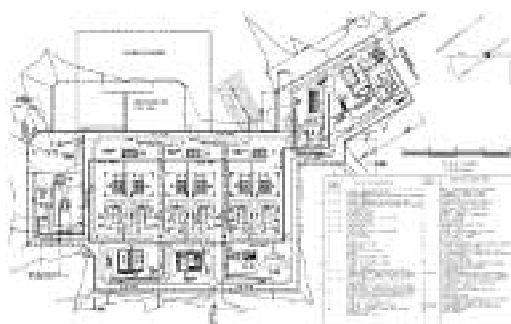


Figure 1 Typical overall plot plan for a process plant

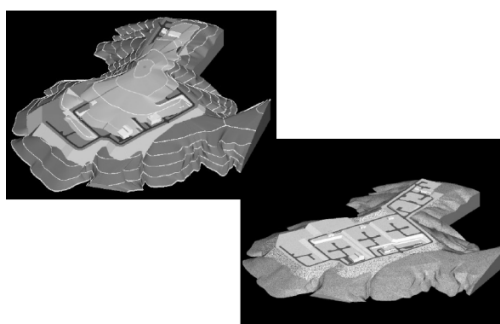


Figure 2 3D model for earthwork

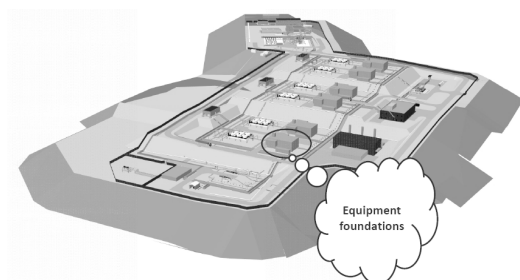


Figure 3 3D model for foundation

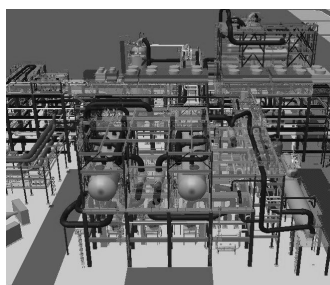


Figure 4 Integrated 3D model of a process unit

There are three stages of completion and review of plant 3D model, viz. 30%, 60% and 90%, involving concurrence by all stakeholders up to that stage. Each of these stages are to be defined at the start of design engineering so that every stakeholder are on same page of what is to be accomplished prior to and during the reviews, and the engineering team remain focused on the parameters to be established in model reviews. **Table 1** shows a sample model review matrix, indicating the check points [3].

Ground Rules

1. Inclusion of pipe size of 6" and above in 30% model is a judgment call. Some areas, racks for instance, may require that 2" and above be modeled at this stage.
2. All model review comments are to be addressed immediately following the model review session.
3. No changes to approved or frozen items are allowed without approval from Project Engineering Manager.
IFA – Issued for Approval
IFE – Issued for Engineering
IFC – Issued for Construction

It is worthwhile to mention that these 30%, 60% and 90% plant 3D model completion and review stages have been standardized over last 10 years and followed world-wide. Also, the 100% complete model means 'As-Built', i.e. after 60% review, civil and structural construction would commence, and after 90% review, mechanical, piping, electrical, instrumentation, HVAC erection would progress. Between 90% and 100%, the plant model may be required to be updated to address the issues raised by construction group. However, unless there are major changes, revised drawings are need not to be extracted at this stage.



Table 1 Model progress and review matrix

Required by Review Stage	30% Review	60% Review	90% Review
Process Design			
Process Studies	Complete	----	----
Process flow diagram and mass balance	IFE	IFC	----
Piping and instrumentation diagram	IFA	IFE	IFC
HAZOP	----	Complete	—
Line sizing	Critical lines complete	All lines complete	—
Line list	IFA	IFE	IFC
Piping specifications	Approved	----	—
Vendor Information			
Valves	Prelim. data for 6" and above	Approved data for 4" and above	Certified data for all sizes
Special Items	Prelim. data for 6" and above	Approved data for 4" and above	Certified data for all sizes
Equipment	Prelim.	Approved	Certified
Instruments	Prelim.	Approved	Certified
Mechanical and Piping Design			
Plot Plan	IFA	IFE	IFC
Equipment layout	Major equipment modelled to prelim. data	Equipment locations (coordinates) finalized modelled to approved data	Equipment modelled to certified data
Piping stress analysis	6" and above critical lines stress checked; other lines under review	All critical lines stress checked; other lines under review	Stress analysis complete
Piping modelling	6" and above lines modelled	4" and above lines modelled	All lines including drains and vents modelled
Pipe supports	All major pipe supports modelled	All pipe supports modelled	----
Utility stations/eye wash/Safety showers	Not started	Preliminary locations modelled	Final locations modelled
Civil/Structural Design			
Foundations	Major foundations modelled	All foundations modelled	----
Concrete / steel structures	Beams / columns / major members modelled	Minor members modelled	----
Design for Constructability / Operability / Maintainability / Safety / Environment			
Constructability	Road access; crane movement and reach	Field erected equipment/piping/skid	Filed mounted hydro-test drains and vents located
Operability	Platforms, ladders and stairs, access-way	Ergonomic aspects; e.g. valve access	----
Maintainability	Davits, monorails and cranes, access between equipment, width and height requirements under pipe and cable racks	Removal clearance, e.g., heat exchanger tube bundle removals, O/H cranes above rotating equipment	----
Safety and environment	Escape routes, roads, paved areas and drainage.	—	----
Design for Future Expansion			
Land	To be identified	----	----
Facilities	Future pipe rack requirements, e.g., widths, number of levels	----	----



Clash/Interference Check and Resolving

Automated clash checking is run on integrated plant model. This is a periodic activity, done by respective engineering discipline lead engineers.

The six types of clash checks to be run are: Piping to Piping, Piping to Equipment, Piping to Steel, Piping to Electrical, Piping to Building, and Equipment to Steel. **Figure 5** shows some typical interferences found in clash run of plant 3D model.

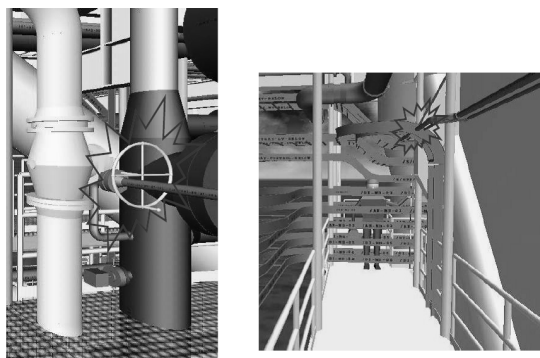


Figure 5 Clash / Interferences

After the clash run, the lead engineer(s) are required to document the clash test report (to be extracted from software itself) and initiate action resolve.

Model Closure and Handing Over

Normally, after commissioning of the plant, the engineering company is supposed to hand over the 3D model (both native models and integrated model) to client. However, among all the project deliverables, the 3D models are often least understood and least discussed at initial stage of engineering, and later become the most controversial. Unless those are not specifically mentioned in the engineering contract as a deliverable, the engineering company may not be willing to hand them over to client, although clients assume that they have paid for the models. Even when those are listed in the contracts or the engineering company is willing to hand them over, they may still be unwilling to hand over the customizations/configurations/set-ups that they have incorporated to the software. Due to this, the models often tend to be almost unusable for future expansion/modification work by another engineering company.

In order to resolve this fiasco, there are some ground rules to be set at the time of award of design engineering contract [3] –

- (a) For those on the engineering company side of the fence:
 - (i) The software platform which would be used needs to be clearly informed to the client and agreed upon
 - (ii) Software version/release;
 - (iii) Exclusions in the model (but can be available at an additional pre-agreed cost).
- (b) For those on the client side of the fence:
 - (i) It is to be understood that the models and databases are having many intricacies;
 - (ii) The software, version of software, client's requirements and expectations in terms of usability are needed to be documented and agreed upon with engineering company;
 - (iii) If there is lack of the in-house expertise, an outside independent consultant/agency should be engaged to assist client to define the parameters of the 3D model.

MAJOR ADVANTAGES OF 3D PLANT DESIGN OVER 2D DESIGN

- (i) Equipment, piping, foundations, structures, cable trays, ducts can be placed at accurate coordinates.
- (ii) Possibilities of clash/interference between facilities are minimised.
- (iii) Visualisation of the entire unit/plant would have more clarity.
- (iv) Database built-up by engineering company are repetitive, i.e. those can be used for future projects.
- (v) Lack of availability of skilled design manpower can be overcome.



- (vi) Engineering completion schedule and man-hour used for design engineering would be much less.
- (vii) Real-time navigation over the model is possible, which help the construction group

INTEGRATION OF 3D MODELLING SOFTWARE WITH ANALYTICAL SOFTWARE

Followings are some of the widely used 3D plant modelling software platforms, which are now used worldwide:

- (i) Plant Design System (PDS), developed by Intergraph;
- (ii) Plant Design and Management System (PDMS), developed by AVEVA;
- (iii) Smart Plant 3D (SP3D), developed by Intergraph;
- (iv) CADWorx, developed by Intergraph;
- (v) AutoPlant, developed by Bentley;
- (vi) AutoCAD Plant 3D, developed by Autodesk.

Above software, platforms are used in tandem with design review software platforms such as:

- (i) SmartPlant Review (SPR), developed by Intergraph;
- (ii) Navisworks, developed by Autodesk.

On the other hand, there are analytical software, which have now become industry standards:

- (a) CAESAR II, developed by Intergraph, used for pipe stress analysis,
- (b) PV-ELITE, developed by Intergraph, used for pressure vessel design,
- (c) PRG Suite, developed by Paulin Research Group, used for finite element analysis,
- (d) AutoPIPE, developed by Bentley, used for pipe stress analysis,
- (e) STAAD-PRO, developed by Bentley, used for civil and structural design.

These software have been developed based on code compliance requirements stipulated in international codes and standards, viz. ASME Boiler and Pressure Vessels Code, ASME Pressure Piping Code, etc.

These analytical software have linkage with 3D modelling software (but not both ways in some cases), i.e. equipment, piping or structures modelled in 3D platform can be imported in the respective analytical platform, and after carrying out precision design, the same can be exported back to 3D platform.

The major advantage of using these analytical software is ease of performing repetitive calculations, and obtaining error-free, code-complied results. As an example, the scope of the pipe stress analysis has increased exponentially in the past 30 years. This is due to the stringent regulatory requirements for the modern process plants. For example, in the 1960 s, the pipe stress analysis and support design effort level required for a typical petrochemical plant was about 4000 man-hours. Same was the case for a nuclear power plant as well. Nowadays, the pipe stress and support effort level required for a petrochemical plant has increased by ten folds to about 50,000 man-hours. The effort required by a nuclear power plant has grown thousand folds to reach as high as 2 million man-hours. This shows an exponential growth in the design engineering man-hours involved, which also increases the probability of getting sub-standard/erroneous output from some of the engineering personnel. An efficient pipe stress analysis computer program does not only play the role of a time-saving tool by significantly reducing the cost of designing a plant, but also greatly improves the quality of the plant by ensuring compliance with code [4].

NEW HORIZON – LASER SCANNING, 4D AND 5D SIMULATION

If first decade of new millennium experienced the emergence and establishment of plant design engineering in 3D, second decade thrust upon emergence of laser scanning as well as 4D and 5D simulation. Laser scanning has emerged as an effective tool to generate 3D navigable view of existing industrial plants which would undergo retrofitting/revamping. This is particularly important for age-old plants, of which the 'As-Built' drawings are not available, or even if available, not legible. But without having the information of existing facilities, it is practically impossible to design and install new ones. In such cases, laser scanning has been proved to be an effective tool, through which image of the existing facilities are first captured, and then those images are processed to obtain a 3D model of the plant with maximum accuracy. Next step is to use this model as background, and modelling the new facilities over this, which enables the designer to visualize the entire facility, minimising deployment of personnel at project site for survey and information gathering.

At present, the thrust is upon 4D and 5D simulations. In 4D simulation, the fourth dimension is time. Plant 3D model can be integrated with project construction schedule and construction/erection sequence, which would



simulate the step-by-step execution of the project in computer. This has been proved to be a very effective project planning and monitoring tool.

In 5D simulation, cost is the fifth dimension, which can be integrated with 3D model and execution sequence, so that the project authority can have a clear picture of cash flow at any point of execution.

CONCLUSION

The design engineering for industrial plants are relying more on software tools, and this would see an upturn in next decade, not only due to advancement in software development, but also attributable to shortage of competent engineering manpower. It is not the intent of the software to play a complementary role to replace basic engineering skill and concept, but it would definitely act as a supplement to the designing, drafting, checking and compliance process. New-age engineers would not only have to possess the engineering knowledge and skill, they would also be required to be conversant with software tools. Also, there would be requirement of continuous updation and upgradation of the competency.

REFERENCES

1. Herve Baron, Oil & Gas Engineering Training Suite, Volume 190, 199, pp - 181, 186, 522, 528,
2. Herve Baron, The Oil & Gas Engineering Guide – Plant Layout – Audiobook, pp – 33
3. Richard G. Beale, Paul Bowers, Peter Smith, Process Piping Design Handbook, Volume Three: Planning Guide to Piping Design, Gulf Publishing Company, pp – 73-75
4. Liang-Chuan (L.C.) Peng, Tsen-Loong (Alvin) Peng, Pipe Stress Engineering, ASME Press, pp – 2



Development of Glass Reinforced Metal Matrix Composite and Study of its Properties

Ajay Biswas^{*1}, Moutoshi Singha Roy¹, Akshar S. Vasekar²

Mechanical Engineering Department, National Institute of Technology Agartala¹, ajaybiswas6719@gmail.com^{*}
QA Engineer Metalmam Auto Pvt. Ltd. Aurangabad²

ABSTRACT

The use of Metal Matrix Composite (MMC) is very attractive because it has higher specific strength and stiffness than monolithic metal. Due to addition of reinforcement, properties like wear resistance, thermal resistance and electrical conductivity changes remarkably. Mechanical properties of Metal Matrix Composite is mostly dependent on the manufacturing method, selection of material and selection of reinforcement, reinforcement size and weight ratio. Manufacturing of aluminum based metal matrix composite by stir casting method is most prominent route for producing MMC. One of industrial barrier for using MMC is main stream material's cost, which increases with type of reinforcement and manufacturing method. Already lot of work has been done with carbide reinforcement such as silicon carbide, boron carbide, alumina oxide etc., but very less work has been reported on glass powder as reinforcement. The present work is attempted to confirm the compatibility of glass reinforcement in 6063 aluminum alloy. The experiment has been conducted to determine the effect of reinforcement size, reinforcement weight ratio and stirring speed on the mechanical properties of MMC. Design of experiment is incorporated as per Taguchi's L9 orthogonal array in order to reduce the number of experimental runs. The experimental result shows the increase of hardness of the MMC developed by glass reinforcement in 6063 aluminium alloy.

KEYWORD Glass reinforcement, 6063 aluminium alloy, Taguchi's design of experiment, Stir Casting Method.

INTRODUCTION

The focus of this paper is to manufacture the metal matrix composite at least possible cost for commercial use. Recent use of aluminum based metal matrix composite is common in automotive and aerospace application like aluminum engine blocks, suspension components, body panels, and frame members. Properties can be improved in wear resistant, light weight, high thermal and electrical conductivity, high strength and high stiffness [1]. Hashim et al. [2] stated that the main problem in implantation of MMC on industrial level is the cost of manufacturing. To overcome this problem uniform distribution of reinforcement particles in base metal is necessary. The parameters affecting the uniform distribution are rheological behavior of the matrix melt, the particle incorporation method etc. Ravi et al. [3], studied the parameters which affect the production of metal matrix composite with water model with graphite added to water. It is found that optimum stirring speed is 260 rpm. Stirrer should be inserted $2/3^{\text{rd}}$ of molten metal, good distribution is obtained when blade is 30 degree with stirring axis and it is rotated in clockwise direction. Among the variety of processing techniques, stir casting is one of the methods accepted for commercial practice. It is attractive because of simplicity, flexibility and most economical for large sized component fabrication.

MATERIAL SELECTION AND PREPARATION

Aluminum alloy (Al6063) is selected as matrix material because it has good corrosion property compared to other aluminum alloy. Borosilicate glass is selected as reinforcement for this experiment because the density of glass (2.3 g/cc) is less than the density of base aluminum alloy (2.7g/cc), due to which overall weight of the composite decreases. Vandana et al. [4] prepared composites having composition ranging from 3 to 7 wt % glass reinforcement produced by low cost, stir cast route by using commercially pure Aluminum as matrix material. Hardness increases from 24 to 72 BHN and tensile value increased from 80 to 136 N/mm², the ductility values observed are in the range of 25-30 % by varying the wt% of glass particles. Glass powder is prepared by crushing scrap borosilicate beaker collected from chemistry lab. A suitable fixture is fabricated for crushing to avoid any injury to the operator. Size wise grits are then sorted by using standard numbered sieves according to the requirement. Glass powder is



separated in the size range order of 38 to 63, 64 to 90, 91 to 125 and 126 to 212 μm with the help of sieves of sizes 38, 63, 90, 125 and 212 μm . Extreme care has been taken to avoid mixing of any impurities with the glass powder.

LITERATURE REVIEW

Anilkumar, et al [5] use industrial waste fly ash as reinforcement for producing aluminum based composite, different particle size and weight fraction of fly ash is mixed with aluminum alloy with the help of stir casting process, uniform distribution of reinforcement is produce in matrix, tensile strength, compression strength and hardness increases with weight fraction and decreases with increasing particle size. Mohan K Manoharan [6] concluded that after addition of small amount of reinforcement into wrought aluminum its tensile strength can be increased. Reddy [7] experimented different weight fraction of Al_2O_3 with Al6061, Al6063 and Al7075. Result showed that alloy 6061 gives large value of yield strength, ultimate tensile strength and ductility but low value of hardness compared to Al-6063 and Al-7075. Kulkarni [8] fabricated hybrid composite with base metal Al-2024 and reinforcements are E-glass particles and fly ash, with 5% fly ash and 6% E-glass possesses maximum tensile strength, with 7% fly ash and 6% E-glass possesses maximum compression strength. Naher et al. [9] conducted a study on stir casting process in which visual experiment has been performed with the simulation of actual stir casting of aluminum and SiC particles. A minimum stirring speed of 100 rpm for water and 200 rpm for glycerol/water–SiC mixtures is required for uniform dispersion to occur. Ghazi [10] experimented with Al alloy and SiC reinforcement and concluded that the hardness, ultimate tensile strength and yield strength of composites increased with increased addition of reinforcements in the composites up to 20 weight percentage.

EXPERIMENTATION

Permanent mould is prepared for casting to accommodate tensile and hardness specimen. Taguchi's L9 orthogonal array has been adopted to restrict the number of experimental runs. Three variables in three levels are selected carefully after considerable numbers of trial run. The stir casting set-up and stirring of molten metal are shown in **Figures 1(a)** and **1(b)**, respectively.

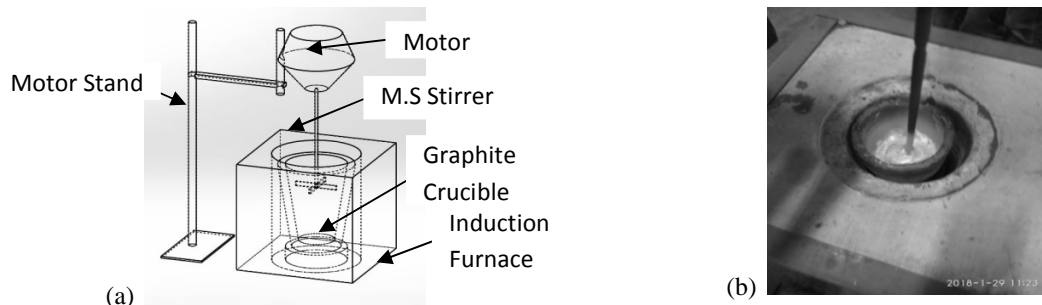


Figure 1(a) Stir casting setup outline made in a SOLIDWORKS. **(b)** Stirring of molten metal (real image)

Taguchi Method

Taguchi is a problem solving tool which can improve the performance of system, design, and product. Taguchi design aim at minimizing the variance while keeping mean on target. All experimental runs are carried out at each level of the signal factor and response is measured. Three variables in three levels are selected carefully for the present investigation.

Identifying main function and its effect on desirable property

- Main function : Manufacturing of metal matrix composite by stir-casting route
- Side effect : Variation on mechanical properties

Table 1 gives the list of processing parameters which can affect on mechanical properties of composite.

Table1 List of control factor and noise factor

Control Factor	Noise factor
Stirring Speed	Particle clustering
Particle size	Cracks generation
Wt% of Particle	Segregation

Composite Preparation

The intersection between casting parameters may also play constructive role in deciding hardness of composite. Aluminum alloy blocks of weight 500g placed in graphite crucible and heated for 15 min with induction furnace at 650°C. Reinforcement is added and stirred well so as to uniform distribution of the reinforcement. The metal is poured in the mould. The temperature of molten metal was measured using infrared gun. The dross removed from molten metal was finally gravity poured into preheated mould. Composite bar is injected from mould after complete solidification and cooled to room temperature. Hardness testing specimens are prepared from composite bar. The cast composite bars are shown in **Figure 2**.

Test Conducted

Mechanical property, namely, hardness, was thoroughly investigated because literature survey reveal very little information on development of aluminum alloy 6063 by addition of glass powder as a reinforcement using simple foundry conventional casting.

Hardness Measurement

The glass powder addition helps in increasing the hardness of aluminum alloy. Aluminum alloy is soft and glass particles are hard in nature, contribute positively in hardness of the composite. For hardness value measurement specimens are cut out from bottom and top of the bar and average of five readings from each specimen is taken. At higher stirring speed glass particles are distributed equally hence hardness value obtained are near equal. Hardness is measured on Brinell hardness testing machine with 5 mm diameter of ball indenter and 500 kgf load and by measuring diameter of indentation, BHN is calculated. The hardness of the specimens as measured are shown in **Figure 3**.



Figure 2 Composite bar as casted

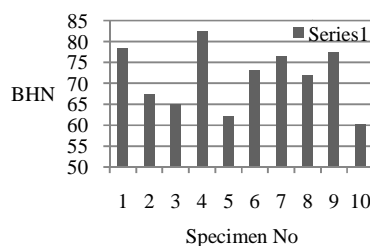


Figure 3 Hardness of each specimen (specimen 1-9 are from experiment and specimen 10 is from parent metal)



CONCLUSION

From the present investigation through the experimental results and subsequent analysis the following conclusions are established within the present experimental domain:

- There is a general tendency of increasing hardness of Al6063 due to the formation of MMC by using Borosilicate glass powders in different weight ratio.
- Hardness is influenced by the powder particle sizes.
- Addition of Borosilicate glass particles in aluminum matrix can lead to value added disposal of Borosilicate glass scrap from laboratories which may lead production of economic composites with improved hardness.

REFERENCES

1. Rohatgi, Anthony Macke BF Schultz Pradeep. Metal Matrix Composites Offer the Automotive Industry an Opportunity to Reduce Vehicle Weight. Improve Performance, pp 19-23, 2012.
2. J. Hashim, , L. Looney, and M. S. J. Hashmi. Particle distribution in cast metal matrix composites—Part I. Journal of Materials Processing Technology Volume 123, Number 2, pp 251-257, 2002.
3. K. R. Ravi, et al. Optimization of mixing parameters through a water model for metal matrix composites synthesis. Materials & Design 28.3, pp 871-881, 2007.
4. Vandana J. Rao, Anil Parmar. Use of Glass Particles for Development of Low Cost Aluminium Matrix Material.
5. Anilkumar, H. C., H. S. Hebbar, K. S. Ravishankar. Mechanical properties of fly ash reinforced aluminium alloy (Al6061) composites. International journal of mechanical and materials engineering 6.1, 41-45, 2011.
6. Mohan, T., and N. Manoharan. Experimental investigation of tensile and impact behaviour of aluminium metal matrix composite for turbocharger. ARPJ Journal of Engineering and Applied Sciences 10.13, 5672-5674, 2015.
7. Reddy, A. Chennakesava. Evaluation of mechanical behavior of Al-alloy/Al₂O₃ metal matrix composites with respect to their constituents using Taguchi. International Journal of Emerging Technologies and Applications in Engineering Technology and Sciences 4.2, 26-30, 2011.
8. Kulkarni, Preetam. Evaluation of Mechanical Properties of AL 2024 Based Hybrid Metal Composites. IOSR-JMCE Volume 12, Issue Sept-Oct 2015.
9. Naher, Sumsun, Dermot Brabazon, and Lisa Looney. Simulation of the stir casting process. Journal of Materials Processing Technology 143, 567-571, 2003.
10. Ghazi, J. H. "Production and properties of silicon carbide particles reinforced aluminium alloy composites." International Journal of Mining, Metallurgy & Mechanical Engineering 1.3, pp 191-194, 2013.



Blending of Lignite: Impacts and Challenges

S. Raghuthaman

Power Station Engineering, NLC India Limited, Neyveli, raghuthaman.s@nlcindia.com

ABSTRACT

Coal or lignite is a naturally available mineral whose properties vary significantly from one mine to another. While designing the boiler for thermal plants, most available common range of coal/lignite is considered. Designing of furnace will be very much challenging if the properties of coal/lignite vary significantly. When the furnace is designed for design coal and operated with worst coal/lignite, flue gas flow would increase substantially resulting in higher gas velocity which will lead to erosion of water wall tubes and reduce availability of the plant for generation of electricity. On the other hand, if the furnace is designed for worst coal/lignite, the size of the furnace would be very large and during operation with design coal/lignite, the operation would be very uneconomical. The furnace design problem due to wide variation in the calorific value, ash content and sulphur content can be very well solved by blending of different grades of fuel before firing. Generally, blending is done by using any one of three methods namely, (a) Blending in coal stock yard (b) Use of dedicated mill for Firing different grade coal and adjust mill parameter, and (c) Blending in the right proportion using belt weigh feeder. The focus is on the blending method adopted for the Barsingsar Thermal Power Station Extension (BTPSE)(1X250 MW) using silos and belt weigh feeders.

KEYWORDS CHP, Furnace, Higher Heating Value, Blending, Belt Weigh feeder

INTRODUCTION

India is the third largest electricity producer in the world as of July 2018 with installed capacity of 222.66 GW of which 66% comes from fossil fuel based thermal plant despite the current debate on renewable energy and CO₂ reduction. Sources of coal for a thermal power plant may vary which may be indigenous coal or imported coal. The indigenous coal may be further classified as run off mine coal or washed coal. In India, boilers are designed for firing indigenous and imported coal blended in the ratio 70:30 as per the guidelines of Central Electricity Authority. The quality of coal (GCV, HGI, moisture content, ash content) influence much on design of furnace and also the coal handling plant (CHP).

IMPACTS ON FURNACE DESIGN

Coal or lignite is a naturally available mineral whose properties vary significantly from one mine to another. While designing the boiler most available common range of coal/lignite is considered. Hence, three cases namely design coal, performance coal and worst coal are to be considered while designing the furnace of power plant.

Designing of furnace will be very much challenging if the properties of coal/lignite vary significantly. When the furnace is designed for design coal and operated with worst coal, flue gas flow would increase substantially resulting in higher gas velocity which will lead to erosion of water wall tubes and reduce availability. On the other hand, if the furnace is designed for worst coal, the size of the furnace would be very large and during operation with design coal, the operation would be very uneconomical.

RECOMMENDED CRITERIA FOR BLENDING

Blending shall be based on the following guidelines

- (a) The Hard Groove Grindability Index shall be narrow in range so that there will not be any pulverising problems
- (b) The ash chemistry of the component coals must be compatible so that slagging and fouling problems can be avoided. The percentage of CaO and Na₂ O in ash of the constituent coals/lignite in the blend shall be less than 10% and 1%, respectively.
- (c) The size coal to be blended shall be the same
- (d) As it is necessary to ensure uniform blending, it is desirable to have blending in Coal/Lignite handling plant.

BLENDING METHODS

Blending In Coal/Lignite Stock Yard

In coal/Lignite stock yard different grades of coal are received at different locations in different layers one above the other using a stacker. Then the stacked coal is reclaimed and fed to the conveyor to feed boiler bunkers. In this



method homogeneity cannot be ensured as mixing takes place only at transfer points. Further, in this method, operation hours of stock yard machinery is more and tedious also. The proportion of mixing of two grades cannot be precisely controlled. The method is less costly and can be done in coal handling plant with available machinery and layout.

Using Dedicated Mill for Firing Different Grade

Coal/Lignite of a particular grade is filled in one or two bunkers of the boiler. In the remaining bunkers another grade of coal/lignite is filled and all mills will be taken in to service. Actually the blending takes place in the furnace. Though this method is simple and easy, it has serious disadvantages such as slagging of furnace, high unburnt carbon in bottom ash and furnace temperature control problems.

Blending in the Right Proportion using Belt Weigh Feeders and Silos

A typical case with Hadla mine lignite for the Barsingsar Thermal Power Station Extension (BTPSE)(1X250 MW) will clearly explain the difficult situation faced in furnace design. In BTPSE two grades of lignite one from Hadla mines of inferior in quality (with reference to GCV, ash content and sulphur content) and Barsingsar mine with superior quality are required to be considered after blending in the ratio 79:21 by weight for design of boiler. Hadla mine lignite which constitute greater proportion is kept as performance lignite and guarantees will be based on Hadla mine lignite only.

The characteristics of Hadla lignite is furnished in **Table 1**.

Table 1 Characteristics of Lignite

Constituent / characteristic	Value for design lignite	Value for worst lignite
Moisture, %	41.75	50
Ash, %	25.73	30
Sulphur, %	1.56	2.0
Gross calorific value (GCV), kCal/kg	1947	1600

With the above values, the consumption / generation data work out as **Table 2**.

Table 2 Lignite properties

Description	With design lignite	With worst lignite
Hourly lignite consumption, tph	341.71	415.82
Annual lignite consumption @ 80% PLF, MT	2.4	2.91
Hourly ash generation, tph	88.47	124.75
Annual ash generation @ 80% PLF, MT	0.62	0.87
Hourly sulphur fired in the boiler, tph	5.33	8.31
Hourly sulphur di oxide generated, tph	10.66	16.63
Hourly limestone consumption, tph	33.32	51.98
Hourly gypsum formed, tph	45.31	70.69
Hourly (ash + gypsum) formed, tph	133.23	195.43

If the boiler is designed for design lignite and operated with worst lignite there will be wide variation in the lignite consumed and also the ash generated for the rated load. To obviate these difficulties blending of fuel in the right proportion and feeding to boiler is the only solution. The characteristics of Barsingsar lignite is furnished in **Table 3**.

Table 3 Characteristics of Barsingsar lignite

Constituent / characteristic	Value for design lignite	Value for worst lignite
Moisture, %	42.75	50
Ash, %	14.79	20
Sulphur, %	0.35	0.75
Gross Calorific Value (GCV), kCal/kg	2759	2200

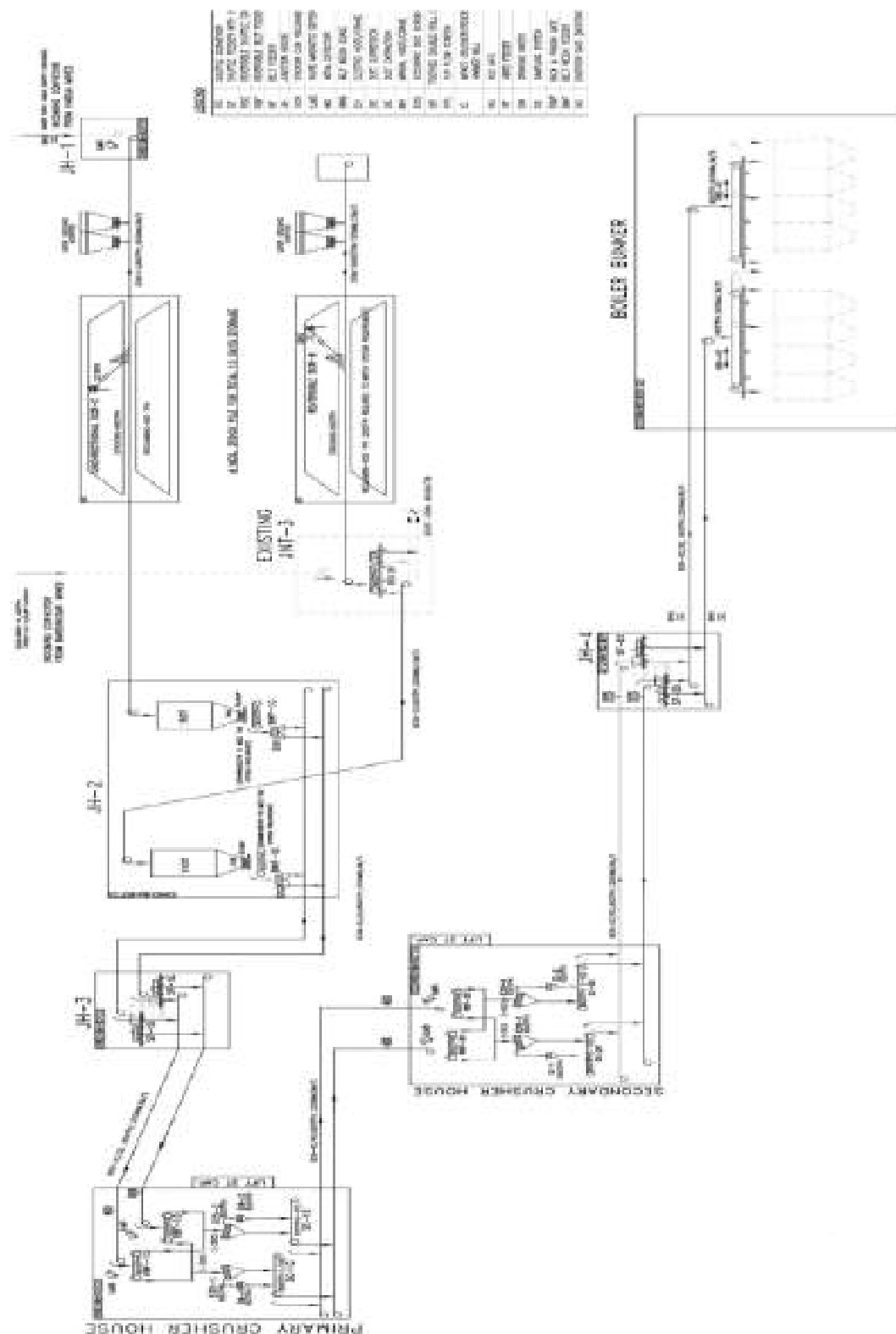


Figure 1 Blending scheme



The average GCV of Barsingsar Mine Lignite is 2760 k.cal/kg and the average GCV of Hadla Mine lignite is 2037 k.Cal/kg. While conceiving the project, it was proposed to blend the Hadla and Barsingsar lignite in the ratio 79:21 by weight so that the average GCV of blended lignite will be 2191 kCal/kg.

Comparison table for ash chemistry and HGI of Hadla Mine lignite and Barsingsar Mine lignite is shown in **Table 4**.

Table 4 Comparison table for ash chemistry and HGI of Hadla Mine lignite and Barsingsar Mine lignite

Parameter/Constituents	Hadla mines lignite	Barsingsar mine lignite
HGI (Average)	96	143
CaO %	4.07	8.29
Na ₂ O	0.39	1.46

The blending of two grades of lignite from Hadla Mines and Barsingsar Mines are achievable for the following reasons.

- Hard Groove Grindability Index of the lignite from two different mines are comparable and are in narrow range.
- In order to reduce slagging, the % of CaO and Na₂O in ash of the constituent lignite in the blend shall be less than 10% and 1%, respectively. The % of CaO in ash of the constituent lignite individually are within the prescribed value. However, there is a slight increase in Na₂O value.

Blending at Lignite Stock Yard

The blending scheme is furnished in **Figure 1**. In this case, Silo and belt weigh feeder method is employed. Lignite from Hadla mines is stored in a silo of capacity 150 tonne. Lignite from Barsingsar mines is stored in another silo of 150 tonne capacity. Each silo is provided with a belt weigh feeder underneath. The belt weigh feeder will load the lignite to the upstream conveyor with a specified quantity drawn from the storage silo. By varying the speed, we can vary the quantity of lignite drawn from the silo for which a variable frequency drive is provided to the feeder. Each silo is connected to the common conveyor leading to crusher house for crushing the lignite and to be sent to boiler bunkers.

Lignite will be fed on the conveyor in layers one above the other and thoroughly mixed in the process of travelling from silo to bunker bay. Since the lignite is sent through various transfer points before reaching the bunker bay it thoroughly gets mixed to achieve homogeneity. As per design of the boiler 79% by weight of Hadla mine lignite shall be blended with 21% by weight of Barsingsar mine lignite to achieve the desired level of combustion.

The belt weigh feeder precisely control the quantity of lignite admitted into the conveyor and hence the blending ratio can be very well maintained.

In the event of providing a online lignite analyser for determining the calorific value of the blended lignite, a feedback can be obtained for fine tuning of blending of two different types of lignite.

This scheme is conceived at the initial stage of the project and hence stockyard equipments are optimised to achieve blending.

CONCLUSION

As the fossil fuel is getting depleted and there is anecessity for importing coal for thermal power plants, it si prudent to employ effective methods of blending by applying blending criteria and also to select stockyard equipmetnts for succesful blending.

REFERENCES

CEA report on Blending of imported coal with domestic coal April 2012



Formulation of Optimisation Methodology for Prevention of any Emergency Scenario while Permitting Cost-effective Design Safety Margin

Rajesh Kumar Mishra^{*1}, Vinay Karanam¹

Homi Bhabha National Institute and Reactor Safety Division, Bhabha Atomic Research Centre, Mumbai¹, rmishra@barc.gov.in*

ABSTRACT

The limit on design value has always been a million dollar question. For many applications where operational uncertainties are high, in absence of any specific codal guidelines addressing the specific scenario, a designer is required to choose his safety margins and struggle to justify the same. In such scenario, choosing high design safety margin could be detrimental from the economy point of view and a way less could put the integrity of the component under jeopardy. Hence, it is very important that a designer chose design margins prudently. An attempt is made in this study to formulate an optimisation methodology using tools of operations research to decide on the limiting design values. The developed formulation is applied to creep phenomena of a nuclear grade silicon alloyed aluminium based alloy used inside a nuclear reactor. For this case, there could be several parameters which may form the basis for deciding design safety margins. The potential candidates include a secondary creep strain value, transition from secondary to tertiary region and rupture strain. Merits of each parameter of choice are discussed and a novel optimisation methodology is proposed based on which, condition of operation and choice of parameter is recommended.

KEYWORDS Optimisation, Operations research, Design limit, Creep.

INTRODUCTION

Every engineering design targets to keep safety margins to prevent arousal of any emergency scenario out of extreme operational phenomena. This requires appropriate addressing of two conflicting requirements. On one hand, keeping a very high safety margin value in design could be detrimental from economic point of view and on other hand, keeping very low safety margin will put the integrity of the component under jeopardy which in turn, may lead to emergency scenario affecting the plant, people and environment. Hence, it is very important that a designer chose design margins prudently. Hence, an attempt has been made to formulate an optimisation methodology using tools of operations research to decide on the limiting design values. The developed formulation is applied to creep phenomena of a nuclear-grade aluminium-silicon alloy used inside a nuclear reactor. For this case, there could be several parameters which may form the basis for deciding design safety margins. The potential candidates include a secondary creep strain value, transition from secondary to tertiary region and rupture strain. Merits of each parameter of choice are discussed and the applicability of a novel optimisation methodology is proposed with which, condition of operation and choice of parameter is recommended. The developed formulation is applied to a nuclear grade silicon alloyed aluminium based alloy used inside a nuclear reactor. The material is very close to commercial 4032 aluminium grade but however, it is attuned to the nuclear industry. The material is designed to work under a very high homologous temperature and very high homologous stress [1]. From the nuclear safety point of view it is very important to have an adequate margin on its safety [2]. However, having very high margin could actually turn out to be a bad design and thus, may hamper economically-viable functionality. A close margin could call for extensive research and intense experiments to validate the margins [2]. As a trade-off best of both ends are met through a scientific approach using a smart methodology.

DESCRIPTION OF PROBLEM DEFINITION

The fundamental principle of operation in the atomic energy industry is having sufficient safety margin to prevent emergence of any emergency scenario. To maintain high design safety margins, costing of the product, economical-operation and revenue are adversely affected. To meet the energy deficit, rise in number of nuclear reactors across the world is quite imminent. With the emergence of the number of reactors and their technologies, the design is getting competitive both in terms of material costing and in the time frame. The atomic energy today is facing a challenge in catering to superior performance, reliability in safe operation and lower cost of design.

The nuclear industry today is looking at non-engineering factors such as the cost of optimal design. To keep up with competition, cheaper, faster, better principle needs to be in place while keeping safety margins checked under all conditions. When there are conflicting requirements one needs to address it through optimisation. That raised the



question regarding opportunity and what minimum is acceptable. Often it is seen that lower the material volume ideally it is considered the optimal, however, it may not hold true for many applications. The definition of optimal design is synonymous to designing for maximum value. Value is a subjective term as decided by a designer (which may be based on environmental impact, cost, revenue, etc.). Allowing subjectivity in any design should always be avoided. To avoid subjectivity, an effort has been made to scientifically develop an optimisation methodology based on operation research, applicability of which has been demonstrated in this paper.

FORMULATION OF METHODOLOGY

A typical plot of creep of the material is shown. The creep plot typically consists of the primary region, secondary region, secondary to tertiary transition region and tertiary region. O-A marked in the **Figure 1** is called primary region. A-B is secondary, B-C is transition region from secondary to tertiary. C-D is tertiary region. D is the rupture point.

Choosing point A, B, C or D and under what conditions these choices may be beneficial has been attempted to address in this paper. Qualitatively choosing A would give a structural engineer a great comfort but from the nuclear physicist point of view it would be over design and the huge material thickness would be detrimental to the functioning of the nuclear reactor. On the other hand choosing point D would make a margin on safety zero.

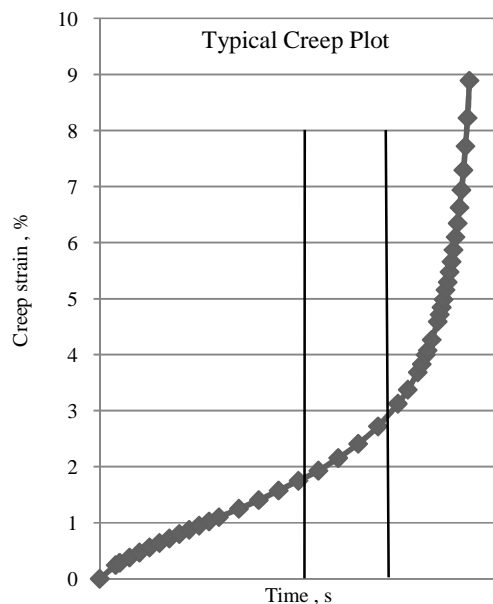


Figure 1 Comparative plot of the model and experimental data for case-1

Case 1: Choosing 'A' as a design limit

If the beginning of secondary creep strain is taken as the design limit. The thickness of a fuel clad tube would be very high and functionally it might be unacceptable.

Case 2: Choosing 'B' as a design limit

If the end of secondary creep strain is taken as the design limit. The thickness of a fuel clad tube would be adequate but however, the additional material would never be consumed for maintaining the integrity.

Case 3: Choosing 'C' as a design limit

If the beginning of tertiary creep strain is taken as design limit. The thickness of a fuel clad tube would be optimal. Most of the material will participate in various operating conditions and structure also maintains its integrity. The rest of the region unused shall accommodate for uncertainties.

Case 4: Choosing 'D' as a design limit



If the rupture is taken as the design limit. The margin on safety or uncertainties is zero. The structure may not maintain its integrity under all operational conditions.

Hence, the point of optimisation lies somewhere between C and D.

The sequential quadratic programming (SQP) algorithm shall be used in simultaneous optimisation as multi-parameters are involved and the nature of the problem is highly non-linear.

Find global minima of function $P(x)$ with constraints $f_i(x) \geq 0$, where $i = 1, 2, 3 \dots n$

the vector 'x' contains 'm' design parameters. The function $P(x)$ is called the objective function. The problem matrix $P(x)$ contains the second-order variations of the objective function with respect to each design variable and is given by the $m \times m$ matrix $A(x)$.

$$\text{Laplacian } \{ P(x) \} = A(x) = \begin{pmatrix} \frac{\partial^2 P}{\partial x_1^2} & \dots & \frac{\partial^2 P}{\partial x_1 \partial x_m} \\ \vdots & \ddots & \vdots \\ \frac{\partial^2 P}{\partial x_1 \partial x_m} & \dots & \frac{\partial^2 P}{\partial x_m^2} \end{pmatrix}$$

A quadratic programming problem is solved in the design space to determine the parameter for optimisation. A line balancing heuristics is then used to balance linearly for each parameter in the next iteration.

It is important that ill-conditioning and bad scaling of the parameters are avoided as it could lead to non-convergence of the problem matrix due to small eigenvalues.

$$E(A) = \frac{\lambda_{\max}(A)}{\lambda_{\min}(A)} \geq 1$$

where $\lambda_{\max}(A)$ and $\lambda_{\min}(A)$ are max. and min. eigenvalues of A respectively. ' A ' is a symmetric matrix. If the $E(A) \sim 1$ it is called well-conditioned and it is ill-conditioned if $E(A)$ is very large.

RESULTS AND DISCUSSION

This novel methodology was used to check on various thickness of the fuel clad tubes satisfying various stages of the creep as limit values. Further, the values associated with each scenario and other design constraints were considered. This resulted in the simultaneous minimisation of parameters.

The thickness decreased by 15%, the damage parameter is chosen as 0.59 as the optimised point at which it is no longer safe to its structural integrity and the time of rupture chosen as 72% of the rupture time experimentally determined.

Results presented here is for a simple material thickness or volume based costing method. Calculating nuclear in-core component cost as the linear behaviour of thickness is a simplified approximation. The overall optimisation point must be so chosen that the frequency of emergency scenario is captured and quantified.

CONCLUSION

A simultaneous optimisation of multi-parameter design component is detailed. By this methodology, the various scenarios arising due to various point of limit value is discussed. By apt trade-offs, the design limit could be fixed based on the operating condition with aim to avoid occurrence of any emergency situation while allowing cost-effective design.

ACKNOWLEDGEMENT

Authors would like to thank Director BARC for all the support extended.

REFERENCES

1. Gill P. E., Murray W., Wright M. H., Practical Optimization, Academic Press, London, pp. 346–354. 1981
2. Vinay K., Mishra R., Modelling tertiary creep of in-core pure aluminium using hyperbolic function, International Journal of Modern Manufacturing Technologies, ISSN 2067–3604, Volume 9 Number 2, n print. 2018



Elimination of Gear Grinding Operation of Gears by Finish Hobbing Manufacturing of Gears

Arup Mukherjee*¹, Sanjiv Ranjan², Abhijit Kar²
Tata-Hitachi (THCM), Kharagpur¹, arup.mukherjee@tatahitachi.co.in*
Tata-Hitachi (THCM), Jamshedpur²

ABSTRACT

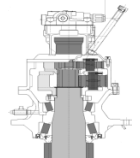
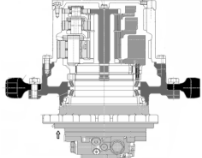
Tata-Hitachi Construction Machinery Company Private Ltd. (THCM) has been manufacturing Transmission Reduction devices for many years. We had been following the conventional method of manufacturing of gears to achieve the desired accuracy level. Our Final Product requirement was DIN9 standard. Since our Production volume started increasing, we were facing constraints in gear manufacturing to meet the high demand of production with existing methods. At this point, we thought that to follow conventional methods, we have to incorporate huge investment in terms of separate hobbing Machines and Grinding Machines. Further, man power cost would have to be born to meet the demand. From Our company, considering various advancements in technology we wanted to augment the gear manufacturing process with best resources available and best economical option. The team came out with the idea of 'FINISH HOBGING OF GEARS'.

KEYWORDS THCM, DIN, TD, PG, SD.

INTRODUCTION

We mainly manufacture gears which includes Sun Gear (SG) and Planetary Gear (PG) for the Swing Device (SD) and Travel Device (TD). In general, a single SD requires (Total qty of gears - 8 No's) and Total Quantity of Gears (TD-11 No's). As the production demand increased, we were unable to meet the production demand by manufacturing gears from the conventional route of gears. When we discussed within the THCM, visited our existing suppliers and approach machine manufacturers for the various process options. We had option of trying shaving but, it again required one extra process added. Thus, our lead time reduction for the part manufacturing could not be met and thus production demand could not be met easily. Then as an idea of finishing the gears at the hobbing stage itself was itself unique and the same time difficult to achieve. Since, we needed this kind of innovation and uniqueness, we decided to proceed with the idea.



	
Swing Device *Qty-1 per Machine	Travel Device Qty -2 per Machine

METHODOLOGY

First, we studied the drawings and our requirements. We analyzed our requirements.

As shown in **Figure 1**, our conventional route was grinding route, where grinding of gear flanks was the last operation to reach the drawing specification of DIN 9. The cycle time in this grinding was as high as 25 min. Further, our Finish Hobbing route was the route where we wanted to eliminate the grinding operation. As shown in the **Figure 2**, we not only need to develop the hobbing process but also needed to confirm the Parameters at three stages. First stage, being the Raw Material Stage, which includes forging and normalizing (Heat Treatment). Second stage is being the turning and hobbing stage. Third stage is being the Carburizing (Heat Treatment). Since, the major concern was to make the gears in the accuracy range of DIN7. As shown in **Figure 2** we restricted the incoming stage drawing of the part to the parallelism of 30 µm and perpendicularity to 15µm. In terms of Machine, we aimed to meet the production demand with smaller cycle time for the part and at the same time sustaining/reliability of the manufactured parts.



By integrating with Japanese Technology, we could come up with the Machine which could meet Indian Conditions (high temp. up to 50°C) and fixtures designs which could retain the accuracy for longer time. Although, Machine could run at higher parameters we required cutting tools to sustain higher parameters. With access to latest Japanese manufacturing, we procured special hobs (Cermet /Carbide). Since the price of the tools was very high, we come up with the idea of combined hob methodology as shown in **Figure 3**. We used HSS Hob for roughing and carbide hob only for finishing operation. In this way, we could lower the tooling cost. After various iterations, we established the Class of the Hobs meeting our requirement. For roughing hob, we used A Class Hobs and for Finishing operations AA/AAA class of gears meeting our requirement.

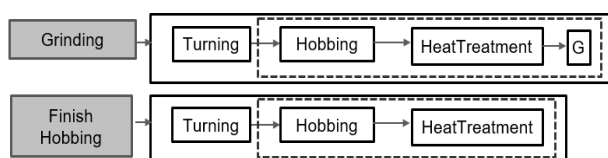


Figure 1



※Class AAA hobs: they hob DIN 7 quality gears.
 ※Class AA hobs: they hob DIN 8 quality gears.
 ※ Class A hobs: they hob DIN 9 quality gears.

Figure 3

Specifications		With Grinding Route	Required	Solutions
Semi-finished	Parallelism	0.12	0.03	Controlling semi-finish turning of gear blanks
	Perpendicularity	0.12	0.015	
	Bore Toll.	0.05	0.025	
Machine Specification	RP/M	400	1200	Mitsubishi Dry hobbing M/C
Jigs/Fixtures		Mechanical	Pneumatic	Developed along with MHI
Tooling Requirement		Normal HSS A grade	Ceramic material (AAA grade)	MHI Mach 7 material, carbide and cermet
Heat Treatment Furnace Spec.		Distortion allowed	Controlled distortion	VFD & Hot oil quenching
Tooling Regrinding & Coating		Manual	CNC hob grinding	Develop inhouse

Figure 2

Using the Technology was one thing but Tool Grinding was a challenge for the team. The team searched within India and various cutting tool suppliers for the regrinding process but it was a challenge to develop this and cost of regrinding the tool was a big task at the supplier end. We were having one Machine at our end and with little customization and consulting the grinding wheel suppliers we came up with the idea of regrinding at our end. After various iterations, we could retain the class of gears even after grinding stage.

Then came up the most difficult part of the whole project i.e. Carburizing (Heat Treatment). Initially we did the trials of the parts with only Heat Treatment but we were unable to sustain the gear accuracy errors within DIN9 range. We were unable to clear where to control the parameters and correlated the various factors for the Heat Treatment. It included the following parameters.

- Normalizing Temperature.
- Carburizing Temperature.
- Quenching Temperature.
- Position of the Gears.
- Oil Agitation Speed during Quenching.

Figures 4 and 5 contains the conditions of the Heat Treatment Trial conditions which we tried and based on the above mentioned 5 parameters, observed the data for the analysis. Based on the data, we applied the multiple regression analysis.

Based on the regression analysis, we could establish that the effect of various of parameters. The major change in Heat Treatment areas are in



- (i) Defining proper normalizing temp. so as to prevent any distortion during carburizing (Normalising Temp. to be maintained +20 C above Carburising Temp).
- (ii) Carburising Temp. and carbon potential was optimized to reduce cementite formation thus reducing residual stress during quenching.
- (iii) Fixtures were modified in order to improve the flow rate of quenching oil to reduce localized distortion and charging pattern was standardized.
- (iv) Introduction of quenching at elevated temperature so as to reduce the distortion. In fact, we introduced special grade oil with high kinematic viscosity and higher cooling rate to reduce the vapor phase during quenching assisted by moderate quenching rate.

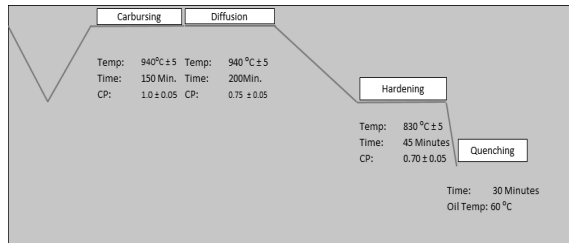


Figure 4

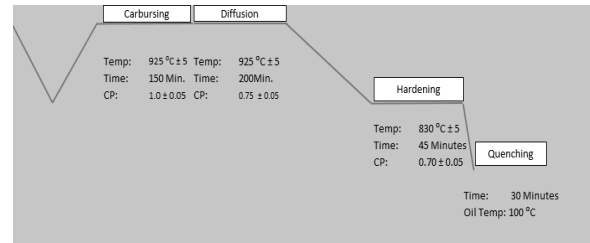


Figure 5

The observation result is shown in **Table 1**.

Table 1

Parameters \ Process Stage	Before Heat Treatment (Target DIN7)		After Heat Treatment (Target DIN9)	
	Actual	Tolerance	Actual	Tolerance
Profile error	8.4µm	19µm	25.8µm	37µm
Lead error	7.5µm	19µm	18µm	24µm
PCD Error	26.5µm	55µm	55µm	80µm

RESULTS

We could establish finish hobbing of gears and achieve the final gear parameters in the range of DIN8-DIN9 range. We were successfully in establishing the customized tools and fixtures for the hobbing process.

- We eliminated the used of cutting oil in hobbing and achieved the first of its own kind dry hobbing machine in Tata-Hitachi (Go Green: use of Coolant Eliminated).
- Lead time reduction of the manufacturing process by eliminating the grinding process.
- We could reduce the carbon footprint by 20 to 40% by lower energy consumption /eliminating coolant usage.
- We did the endurance test of the gears and have found the life of gears has improved as compared to grinding.
- Annual Savings of 5 millions achieved due to elimination of process

CONCLUSION

Our Technical know-how in the gear manufacutring got improved .This is the first time and till now probably the first in India to use Finish Hobbing Technology. We could create a process which was innovative and at the best economical option at the same time (integration with the latest Japanese Technology)

FUTURE SCOPE

In future, we would like to apply the similar approach in manufacturing methods and utilise the best use of technological advancements.

- (i) We want to study the effect of Gear Module and the Hob life.
- (ii) Tool life improvement at Finish Hobbing Stage by improvement in the fixutre design/tool design.

REFERENCES

1. <https://www.microingranaggi.it/en/gear-accuracy-grades-comparing-of-standards/>
2. <https://www.mhi-machinetool.com>



3. John O. Rawlings, Sastry G. Pantula, David A. Dickey Applied Regression Analysis: A Research Tool, Second Edition.
4. P. Shanmugasundaram, Statistical Analysis of Heat Treatment, Load and velocity of dry sliding wear behavior of Aluminum Alloy November 10, 2014.
5. Case-Hardening of Steel , Howard E Boyer , ASM Publication
6. Physical Metallurgy for Engineers , Clark and Varney , EWP publication
7. Testing of Metallic Materials by A V K Suryanarayana
8. Analysis of Metallurgical Failures by Colangelo and Heiser, Wiley Publication



Investigation of Thermofluid Properties of Open Cell Copper Metal Foam for Cooling of Power Electronics Devices

Kishor Borakhade¹, Ashish Mahalle²

Sant Gadge Baba Amravati University, Amravati¹, krborakhade@gmail.com*

Department of Mechanical Engineering, Government College of Engineering, Amravati²

ABSTRACT

Increasing industrial automation requires the use of mechatronics systems with high power electronics devices. Higher surrounding air temperature and self-heat generation through electronic circuits create a challenge for a design engineer to ensure proper working of power electronic devices. In this direction detailed experimentation carried out with 40 PPI, 50PPI, 60 PPI open cell copper metal foam in forced convection for heat dissipation application. Metal foam samples tested at various heater surface temperatures and input air velocities to understand thermofluid characteristics of open cell copper metal foam. Different parameters such as Reynold number, Nusselt no and their effect on solid to fluid convective heat transfer coefficient studied in details. It was observed that in forced convection various properties of metal foam such PPI, diameter of the pore, diameter of fiber has a predominant effect on permeability and convective heat dissipation. Experimental results confirmed that open cell Cu metal foams are an excellent choice for the heat dissipation in many high power electronics devices.

KEYWORDS Metalfoam, PPI, Reynold number, Nusselt number, Convective heat transfer coefficient, Diameter of the pore, Diameter of fiber

NOTATIONS

a_{sf}	Specific interfacial surface area of porous layer, m^{-1}
A_i	Surface area, m^2
C_p	specific heat at constant pressure, J/kg K
D_a	Darcy number, K/R^2
d_f	fiber diameter, m
d_p	mean pore diameter, m
h	convective heat transfer coefficient, $W/m^2 K$
h_{sf}	solid to fluid heat transfer coefficient, $W/m^2 K$
H	Height (m)
k	Thermal conductivity (W/m K)
k_d	Dispersion conductivity (W/m K)
k_{fe}	Fluid effective thermal conductivity (W/mK)
k_{se}	Solid effective thermal conductivity of the (W/mK)
K	Permeability of the metal foam (m^2)
L	Length (m)
Nu	Nusselt number, hR/k_f
Nu_{sf}	Interfacial Nusselt number,
$(Nu_{sf})d_f$	Interfacial Nusselt number related to the metal foam fiber diameter
P	Pressure (N/m^2)
PPI	Pore density (pores/inch)
q''	Heat flux (W/m^2)
R	Height of channel (m)
Re	Reynolds number, $u_0 R/\nu$
Re_{df}	Reynolds number based on the fiber diameter,
T	Temperature (K)
V	velocity vector (m/s)
W	width (m)
Greek symbols	
ε	porosity of the porous metal foam
λ_{eff}	total effective thermal conductivity



μ	dynamic viscosity (kg/m s)
ν	kinematic viscosity (m^2/s)
ρ	density (kg/m^3)
e_{ff}	effective
f_e	effective value for the fluid

INTRODUCTION

Metal foam is a cellular structure consisting of a porous medium with a large number of cell fibers connected with each other. Metal foams classified into two groups close cell metal foam and open cell metal foam. In the open cell type, filaments inside the metal foam are interconnected, which creates the passage for the gas or fluid. The fluid molecules passing through the metal foam structure interface with the solid surface of cell fiber. Open cell metal foam is isotropic with a polyhedron type structure and has superior stability. Metal foam layer application in the heat exchanger increases the heat transfer area which enhances heat dissipation. The metal foam represented by its configuration and has a very high surface area per unit volume. The metal foam porous structure is made of interconnected cells fibers as shown in **Figure 1**. Many researchers had studied metal foams to investigate physical properties of metal foams and various parameters affecting heat dissipation rate.

Nield, [1] studied the flow of incompressible fluid and its hydrodynamic stability characteristics through a plane and circular duct arrangement filled with metal foam. In this study, Brinkman equation is considered for analysis which accurately describes the flow of fluid through porous media. Rahimian and Pourshaghagh, [2] described in details numerical methods for analysis of fluid flow in porous region. With this method desired region of porous media generated by the random distribution of solid rods. Khayargoli et al.[3] studied the effect of the microstructure of metal foams on the flow parameters. Samples from various manufacturers, with different geometrical forms were used. Results showed that as the pore density increases, the surface area also increases with more resistance to fluid flow.

Bhattacharya and Mahajan [4] described results of experiments conducted with aluminum metal foams of 90% porosity and pore density of 5 PPI, 20 PPI. The porous fins tested for forced convection heat dissipation with of one, two, four and six fins arrangement. The experimental results showed that with use of porous fins significant heat enhancement was achieved. Calmidi et.al [5] analyzed thermal dispersion and thermal no equilibrium effects in porous media by experimental and numerical methods. Results indicated that for foam-air combinations, the thermal dispersion was extremely low, but for liquid foam combinations the thermal dispersion was very high.

Zumbrunnen et al. [6] studied experimentally various porous metal foams with different geometrical properties. Experimental results showed that when the temperature difference across the porous solid is high, radiation is significant and the overall thermal conductance increased. Kadle and Sparrow, [7] investigate both numerically experimentally heat transfer from an array of parallel longitudinal fins to turbulent air flow. Experimental results showed that the convective heat transfer at particular point vary with the porous fin surface and base plate surface. Sunar, et al, [8] reported the results of a numerical investigation of convection heat dissipation in a horizontal surface channel and inclined surface channel. The channel was uniformly heated from below and resulting heat transfer enhancement affected by the Grash of number, Reynolds number, and channel inclination angle. Phanikumar and Mahajan [9] analyzed numerically and experimentally fluid flow in high porosity metal foam by considering the thermal equilibrium assumption. Alkam and Al-Nimr, [10] introduced the method of enhancement of heat dissipation of a conventional collector by using porous layer at the inner side of the collector tube.

The porous layer improved the convective heat dissipation between the fluid and tube surface which raised the thermal efficiency of collector. Avenall [11] analyzed experimentally various parameters in copper and nickel metal foam [12]. Studied two energy equation and Brinkman – Forchheimer Darcy model for metal foam. Experimentation conducted with aluminum metal foams 10 PPI, 20 PPI and 40 PPI with varying porosity and found that metal foam substrate enhanced the heat transfer rate. Dukhan [13] presented experimental results of aluminium metal foam cylinder with 20 PPI pore density and constant heat input to walls of the cylinder. Results showed that the Nusselt number varies with the axial direction of fluid flow. Moon and Kim [14] described numerical and experimental results of the heat exchanger with 40 PPI metal foam insertions. The Metal foam used was filled filament type and hollow filament type. Experimental results showed that heat dissipation was more in filled filament type metal foam. Chen, et al [15] Studied heat dissipation of multiple heat source in the horizontal channel. Experimental results showed that at the same velocity when higher heat dissipation from porous metal foam to fluid achieved, the



temperature difference between porous metal foam surface and fluid was low. At this stage porous metal foam attained thermal equilibrium state.

From the review, it is clear that more efforts are required to investigate open cell copper metal foams for heat dissipation properties. This experimentation aims to investigate the effect of input variables such as heater surface temperatures and input air velocities on different parameters Reynold number, Nusselt number. In this experimentation effect of geometric properties such as pore diameter, fiber diameter on permeability and heat dissipation rate are studied in details. Pressure drop, friction factor calculated for all the samples. Experimental results validated with numerical solution by CFD analysis.

EXPERIMENTAL METHODOLOGY

The experiment conducted with open cell copper metal foam samples of pore densities 40 PPI, 50 PPI, and 60 PPI. Properties of metal foam samples given in **Table 1**. Copper metal foam samples of size 100 mm x 100 mm x 10 mm are tested in a square duct arrangement of 100 mm x 100 mm size as shown in **Figure 2**. The duct section and entry of duct bell mouth designed as per ASME standards MFC-26-2011 and length of duct calculated for fully developed flow. The heat input is given by heater attached to the base of the metal foam. The heat input controlled by the PID controller and temperature readings of the heater surface and metal foam surface is measured with calibrated RTDS. Input velocity of air measured with calibrated velocity transmitter and pressure drop measured with calibrated differential pressure transmitter. The datalogger used to record the different values of temperature, velocity and pressure drop during experimentation.

Table 1 Properties of open cell copper metal foam

Property	Sample 1	Sample 2	Sample 3
Size, mm	100×100×10	100 ×100×10	100 ×100×10
PPI	40	50	60
ε	0.96	0.94	0.95
d_p , m	0.000565	0.000533	0.000495
K , m^2	1.340E-09	1.306E-09	1.0012E-09
a_{sf} , m^{-1}	11446.31	13902.74	15137.3

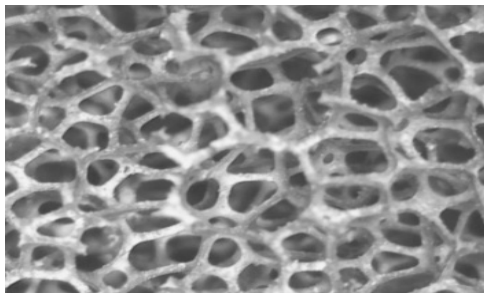


Figure 1 Open Cell Copper Metal Foam Structure [11]



Figure 2 Experimental Setup with sensors and Data Logger (ASME Standards MFC-26-2011)

Mathematical Equations

The effective thermal conductivity of metal foam is calculated by

$$k_{eff} = k_{fe} + k_{se} = \varepsilon k_f + B(1 - \varepsilon)^{0.763} k_s \quad (1)$$

Dispersion conductivity is expressed by

$$k_d = \gamma \rho (C_p \sqrt{K} |\vec{V}|) \quad (2)$$

Interfacial solid to fluid area of metal foam cell



$$a_{sf} = \frac{3\pi d_f}{(0.59d_p)^2} \left[1 - e^{-(1-\varepsilon)/0.04} \right] \quad (3)$$

Nusselt number based on diameter of fiber

$$(Nu_{sf})_{df} = \frac{h_{sf} d_f}{k_f} \quad (4)$$

Reynold Number based on fiber diameter

$$\text{Where } Re_{df} = \frac{|\vec{v}|_{df}}{v} \quad (5)$$

Effect of Pore density on permeability

The pore density of Cu Metal foam depends on the pore diameter of the cell. Higher the pore density lower is the permeability as shown in **Figure 3**. In 60 PPI copper metal foam the pore density is higher than 40 PPI and 50 PPI metal foam. 60 PPI metal foam with reduced pore size increases contact of air molecules with surface of cell fiber. Low permeability also leads to higher pressure drop across the metal foam.

Effect of Velocity on Nusselt no based on a_{sf}

Reynold number increases with an increase in input air velocity. At high Reynold number, fluid turbulence is considerably large and the dynamic forces are more predominant. Higher turbulence increases the interface of fluid with metal foam fiber surface which enhances the convective heat transfer coefficient. In 60 PPI metal foam the Nusselt number is higher even at low velocity as compared to 40 PPI and 50 PPI metal foam as shown in **Figure 4**.

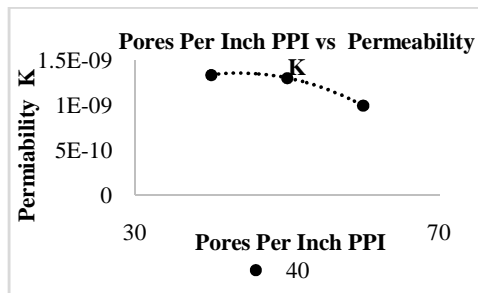


Figure 3 Effect of pore density on Permeability

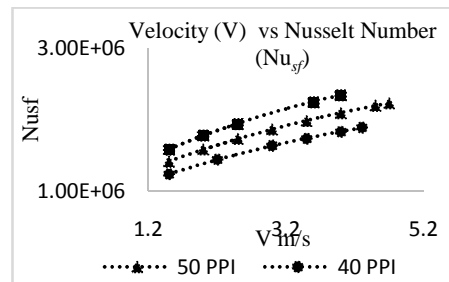


Figure 4 Effect of velocity on Nusselt number (Nu_{sf})

Effect of Heater Temp on Metal foam Heat Flux at $V=1.6$ m/s

Experimental results showed that at constant air velocity of 1.6 m/s and for various heater surface temperature the heat flux was high in 60 PPI metal foam sample as shown in **Figure 5**. The convective heat transfer from the metal surface per unit area was higher in 60 PPI metal foam due large interfacial surface area available.

EXPERIMENTAL RESULTS VALIDATION

CFD analysis has been carried out using fluent 16.0. For analysis, the flow is considered steady, incompressible in nature and two-dimensional. The buoyancy effects and radiation effects neglected. The properties of the air and the metal foam material assumed to be constant. Local thermal non-equilibrium (LTNE) condition considered for metal foam and air at the constant velocity of the fluid. The experimental values of the metal foam mean surface temperature related to various input heater surface temperature validated with numerical solution values. CFD results of the temperature gradient in 60 PPI metal foam at velocity 1.5 m/s and heater surface temp 336K shown in **Figure 6**.

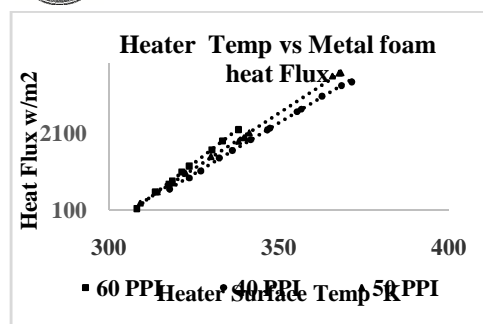


Figure 5 Effect of heater temp on metal foam heat flux at air velocity 1.6 m/s

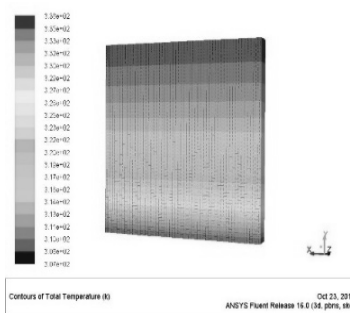


Figure 6 CFD results of Cu Metal Foam 60 PPI at velocity 1.5 m/s and heater surface temp 336 K

CONCLUSION

Experimental results show the thermal properties of open cell Copper metal foam mainly depends upon geometric properties and the thermal conductivity of the base metal. Geometric properties such as fiber diameter and pore diameter affect the permeability of metal foam. With the graphical trends of different parameters, the following conclusion can be made focusing mainly on the heat dissipation of Cu metal foam. Cu metal foam with higher pore density has more numbers of pores per inch which results in the higher specific solid-fluid interfacial surface area (a_{sf}). With this available heat transfer area, higher convective heat dissipation is achieved.

Results also confirm that 60 PPI Cu metal foam have low permeability due to reduced pore size. Low permeability is also responsible for higher pressure drop. At low velocity 1.2 m/s, the Nusselt number is higher in case of 60 PPI metal foam due to the high specific solid-fluid interfacial surface area (a_{sf}). It observed that in copper metal foam higher heat transfer coefficient achieved with the increase in air velocity.

All the copper metal foam samples 40 PPI, 50 PPI, 60 PPI are tested from 313 K to 370 K input heater surface temperature and air velocity ranging from 1.2 m/s to 4.5 m/s. The result showed that even at low velocity open cell copper metal foam heat dissipation rate was high which satisfies the low noise requirements of many power electronic devices. From this experimentation it is confirmed that open cell copper metal foams are the best choice for heat dissipation application in power electronics devices.

REFERENCES

1. D. A. Nield, The stability of flow in a channel or duct occupied by a porous medium. International Journal of Heat and Mass transfer. Vol. 46, pp 4351-4354. 2003.
2. M. H. Rahimian A. Pourshaghagh, Direct simulation of forced convection flow in a parallel plate channel filled with porous media. Int. comm. of heat and mass transfer, Vol. 29, No. 6, pp 867-878, 2002.
3. Khayargoli, P., Loya, V. Lefebvre, L.P., Medraj M., The Impact of Microstructure on the Permeability of Metal Foams, CSME 2004 Forum. 2004.
4. Bhattacharya, R. L. Mahajan, Finned Metal Foam Heat Sinks for Electronics Cooling in Forced Convection, ASME Vol. 124 PP155-163 September 2002.
5. Calmidi, V.V. and Mahajan, R. L. Weber, T., Forced Convection in High Porosity Metal Foams, Journal of Heat Transfer. Vol. 122, pp. 557 – 565. (2000) Nuremberg Cauerstr. 4, D- 91058 Erlangen, Germany. 1999
6. Zumbrennen, D.A., Viskanta, R. Incropera F.P., Heat Transfer through Porous Solids with Internal Geometries, International Journal of Heat and Mass Transfer. Vol. 29, pp. 275- 284. 1986
7. D. S. Kadle, E.M. Sparrow, Numerical and Experimental study of Turbulent Heat Transfer and Fluid flow in longitudinal fin arrays Journal of heat transfer" Vol. 108, pp. 16-23. 1985.
8. A OZ Sunar, S. Baskaya, M. Sivrioglu, Numerical Analysis of Grash of number, Reynolds Number and Inclination Effects on mixed convection heat Transfer in Rectangular Channels. International Journal of Heat and Mass Transfer, Vol. 28 P.P. 985 – 994. 2001.
9. Phanikumar, M.S., Mahajan, R.L. Non-Darcy Natural Convection in High Porosity, Metal Foams, Int. Journal of Heat and Mass Transfer, vol. 45, pp. 3781-3793. 2002.
10. M. K. Alkam, Solar collector with tubes partially filled with M. A. Al-Nimr porous substrates. ASME Journal of heat transfer, pp 20-23, Vol. 121, Feb, 1999.



11. Ryan Jeffrey Avenall, Thesis on “use of metallic foams for heat transfer enhancement in the cooling jacket of a rocket propulsion element, pp 23, 2004.
12. S. Boulahrouz, Y. Avenas, A. Chehhat, CFD Simulation of Heat Transfer and Fluid Flow within Metallic Foam in Forced Convection Environment, vol. 21, no. 3, pp. 611–635, 2017.
13. N. Dukhan, Experimental Fully-Developed Thermal Convection for Non-Darcy Water Flow in Metal Foam, J. Therm. Eng., vol. 2, no. 2, pp. 677–682, 2016.
14. C. Moon and K. C. Kim, Flow and Heat Transfer Characteristics in High Porosity Metal Foams, Proc. World Congr. Mech. Chem. Mater. Eng. MCM 2015 Barcelona, Spain–July, no. 333, pp. 20–21, 2015
15. C. C. Chen, P. C. Huang, and H. Y. Hwang, “Enhanced forced convective cooling of heat sources by metal-foam porous layers, Int. J. Heat Mass Transf., vol. 58, no. 1–2, pp. 356–373, 2013.



Trends in Brake System for Mass Rapid Transport System in Metro Cars

Gautam Dua^{*1}, M. Sudhrashan¹, Sunil Kumar¹, Manjunath S¹
BEML Ltd, Bengaluru¹, gautam.dua@td.beml.co.in^{*}

ABSTRACT

Mass rapid transport system is the lifeline for urban commuters as it is the most efficient mode in terms of comfort, safety and faster way to reach destinations. Typically in a metro train, the operating parameters are very demanding, viz different track alignment/tighter curves, underground/elevated rail lines, heavy passenger loading/unloading cycles, Short distance between stations. To meet all these requirements, design of brake system and pneumatic suspension becomes very vital, as it demands high accuracy, safety and efficient brake application. Design and development of various metro projects in which brake system was designed considering various safety and other vital parameters has been discussed in this paper. The paper aims to present the approach adopted, capturing different scenarios of braking considering variable passenger loads and available adhesion, installation of various brake aggregate within the critical envelop (SOD) below under frame and interface with train control / management system. This article will give the concept of electro pneumatic brake system, basic brake calculation and manufacturing/installation approach.

KEYWORDS EP brake, ED brake, Brake response time, Pneumatic suspension, Levelling valve.

INTRODUCTION

Brake system designed for Mass Rapid Transport is Electro pneumatic (EP) brake system in combination with Electro dynamic (ED) and regeneration. Main purpose of the brake system is to stop the car at designed deceleration to meet the stopping distance. It also reduces the force on coupler by absorbing significant amount of the dynamic force during stopping. Different mode of brake are applied as per the requirement. They are service brake, emergency brake, towing and shunting brake, parking brake. All these different mode have specific braking characteristic.

Load signal required for braking is sent through secondary suspension (pneumatic suspension). Depending on the load the required brake pressure is derived and supplied to brake cylinder. Fitting of various brake item below under frame is a challenging job since the space availability is a constraint. Hence, the brake items were arranged in module and the modules were installed below under frame. Various controlling pressure switches were put together in valve box to keep them away from dust and water and to provide easy access for maintenance and pressure setting.

Mechanical design tools have been extensively used during design of brake system, interface check and finalisation of layout. This has given confidence for installation of aggregates during vehicle build up, in-turn reducing the design / development time by good margin.

Brake Mode

Brake system adopted in MRTS can be single pipe and twin pipe brake system. Selection of piping system depends on the operator requirement. Various brake mode are service brake, emergency brake and parking brake. In addition back up brake (brake through distributor valve) which is purely pneumatic actuation is available with twin pipe brake system.

Service Brake Mode

This mode is primarily used during regular service. Blending of Electro dynamic and Pneumatic braking happens in this mode (**Figure 1**). Electro dynamic brake remains in priority and remaining force is compensated through pneumatic brake. Combination of Electro dynamic and pneumatic pressure is called blending. Proper care is taken to avoid any jerk during the blending process.

ED Brake is controlled by traction control unit. This force avoid wearing of moving parts and increase the life of frictional part (Brake Disk, Brake Pad) thus save energy. During ED application regeneration happens which is picked by trailing car in DC supply, can be sent back to grid in AC supply.

Brake Electronics continuously monitored the ED force applied by traction and calculate the missing force. Through digital control loop brake electronic commands the brake control unit to apply the remaining required force.

ED force depends on speed of the car and remain maximum at certain speed. ED brake force fade at lower speed. Train finally stopped with Pneumatic force and holding brake is applied. Holding brake force is lesser then applied service brake force and remain active until traction have enough torque to move the train forward. This avoid roll back at gradient. This is shown in **Figure 2**.

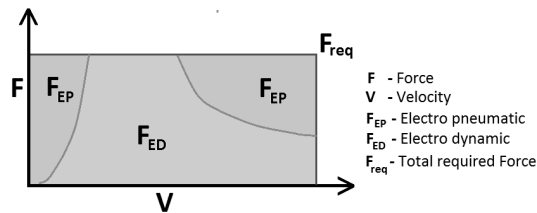


Figure 1 Blending principle

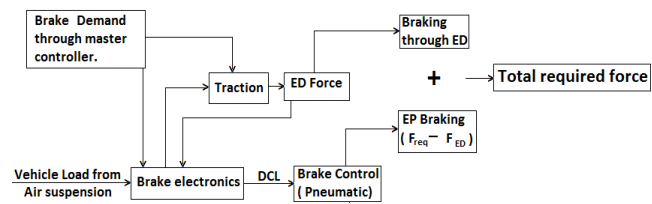


Figure 2 Service brake

Brake application can be car control or bogie control. Single pneumatic brake control and electronic unit will be for car control system. Whereas two brake control and electronic unit will be present in car for each bogie control brake system.

Emergency Brake

Emergency brake is pure pneumatic brake applied through emergency brake magnetic valve. Emergency brake loop remain charged and avoid the application of emergency brake. For emergency brake application the EB loop line needs to be de-energised. Any number of safety equipment can be added in the loop. Hence malfunctioning of safety item will cause EB application. The emergency brake actuation is represented in **Figure 3**.

Parking Brake

Application of parking brake is to stop the train from rolling as long as required without any pneumatic supply. The parking brake is spring actuated. In normal condition, the brake pad and disc remains isolated. The diaphragm present in parking brake chamber compresses the spring in the presence of pneumatic air. Once pneumatic force reduces the spring start to regain its position. During this process the brake pad come in contact with brake disc. Full application of parking brake happen when the air is fully drained out of parking brake chamber. A parking brake actuator is shown in **Figure 4**.

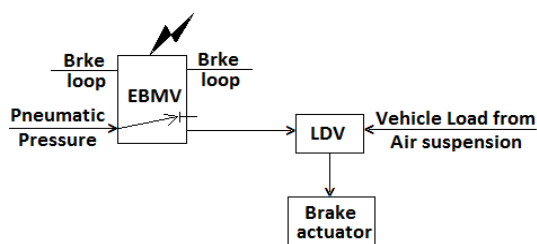


Figure 3 Emergency brake actuation

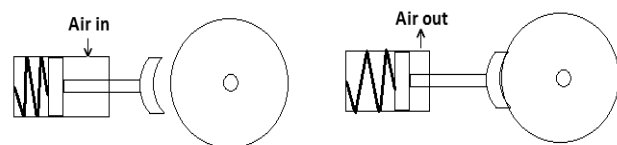


Figure 4 Parking brake actuator

Parking brake magnetic valve is used to apply or release the parking brake through train operator. Magnetic valve release the air from parking brake cylinder to apply the brake and charge the cylinder to release the parking brake. Parking brake force is calculated to make the car remain in standstill at defined gradient. Provision of manual release also present to release the parking brake and care to be taken that train is not at gradient or manual release was done purposefully. Reapplication of parking brake will happen only in the presence of pneumatic pressure. Train set left idle will automatically apply the parking brake when the total pressure drain out.



Brake through Distributer Valve

This is also known as backup brake. This type of brake requires twin pipe system. BP (Brake pressure), MRP (Main reservoir pipe) are maintained in two different pressure. Distributer valve is used to apply the brake through driver brake valve. Distributer valve keeps the BP and MRP in equilibrium position. Reduction in BP pressure will disturb the equilibrium and MR pressure rushes to the brake cylinder via load dependent valve and thus brake is applied. A driver brake valve present in the driver cabin is used to charge and vent the BP line. Charging of BP line happens through MR. BP pressure is maintained lesser than MRP.

Brake Calculation

The brake calculation is the basis of brake design, is an estimation on average values within tolerance. Various values such as deceleration, stopping distance are determined for different brake mode through various calculation at different speed and assumed adhesion. The calculation is done on various load condition such as tare load, half loaded and fully loaded car. Method of calculation is according to EN14531-1 at level track.

Parameter required for calculation of stopping distance:

t_{10} = delay time (from brake demand to 10% force built up)

t_{90} = brake build up time (from 10% to 90% force built up)

t_{eq} = equivalent response time ($t_{10} + t_{90}/2$) equivalent response time for emergency braking is lesser than service braking

$$\text{Total required brake force: } F_{\text{brake}} = M_{\text{rot}} \times a_e \quad (1)$$

Where M_{rot} is the total dynamic mass (T car load + 5% or T car, M car load + 10% of M car); and a_e is the equivalent acceleration.

Required brake cylinder pressure is calculated from total required brake force (F_{brake}) by considering parameter such as piston area, compression ratio, rigging ratio, rigging efficiency, wheel diameter, brake pad friction and other losses.

$$\text{Stopping distance: } S = v \times t_e + v^2 / (2 \times a_e) \quad (2)$$

$$\text{Average deceleration: } a_{av} = v^2 / (2 \times s) \quad (3)$$

Illustration:

Assuming 3 car unit consist of two motor car and one trailer car, temperature remain constant. The various calculations for brake at different speed in shown in **Table 1**. The brake performance characteristic is represented in **Table 2**.

Table 1 brake calc for different speed

		M	T	M	
M, tonne	Tare load	30	30	30	
	Half load	46.25	46.25	46.25	
	full load	62.5	62.5	62.5	
M_{rot} , tonne	Tare load	33	31.5	33	97.5
	Half load	50.8	48.5	50.8	150.3
	full load	68.7	65.6	68.7	203.1
a_e , m/s ²	1.45 m/s ²		t_{eq} s	0.85	
F_{brake}	Tare load	141	kN		
	Half load	218	kN		
	full load	295	kN		
V, kmph	10	50	80	120	160
S, m	5.0	78.3	189.1	411.4	719
a_{av} , m/s ²	0.76	1.23	1.30	1.35	1.37

Table 2 Brake performance characteristic

	Deceleration	Brake application time
Service brake	0.9-1 m/s ²	>2.5 s
Emergency brake	1.3 m/s ²	>2 s

Air Supply System

Air supply system provides the pneumatic air required for application of brake and operation of auxiliary equipment such as horn, operation of auto coupler, operation of pantograph/ current collector, secondary suspension extra.

Basic circuit of air driver consist of electrically operated air compressor, oil separator (for oil compressor), air dryer, air filter, Main reservoir. All other system was feed through main reservoir. Air consumption calculation for round trip was done for designing main reservoir.

Pressure sensor, were installed to start and stop compressor through train management system. Pressure governor a hardwired switch also can be used start and stop the compressor at set pressure value. Generally both are used to add redundancy to the system.

Wheel Slide Protection

This protect the wheel from sliding if the axle gets locked during braking thus protecting the wheel wear. The basic principle of wheel slide protection is that it contentiously monitor the rotation of all axle present in a car. When there is variation in wheel rpm during braking it activate dump valve (aka antiskid valve) to release the brake cylinder pressure thus allow the wheel to rotate. It again re apply the brake once the wheel rpm matches with other rotating wheel. The working of a WSP is shown in **Figure 5**. WSP detection is axle wise, application can be bogie or axle wise.

Secondary suspension: Nowadays, air spring are used as secondary suspension instead of helical coil spring. The main purpose is to provide quality riding to the passenger, actual load required for powering and braking, to maintain constant floor height for any given load condition. The working of a secondary suspension is shown in **Figure 6**.

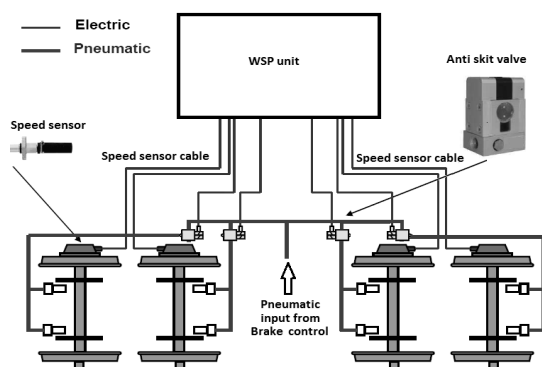


Figure 5 Wheel slide protection logic

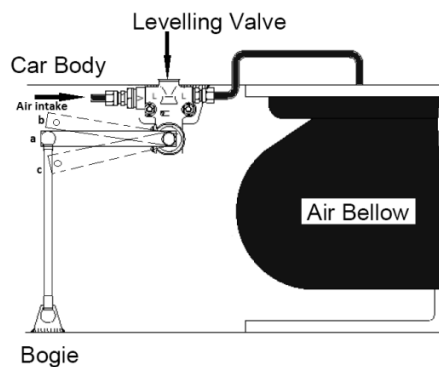


Figure 6 Secondary suspension

Any dynamic changes in air spring is taken care by levelling valve which charges or discharges the air as per requirement. When the load reduces the below raises up which move the levelling valve handle to position 'c'. In this position levelling valve releases the air from below to bring the handle position to 'a'. Similarly, when the car load increases the handle position move to b due to the compression in air spring. In this position air intake happens in the air spring till the handle position moves to 'a'. Thus at any load condition the car body floor height is maintained.

Brake Actuator

Brake actuator device can be tread brake unit, disc brake unit. Tread brake unit apply force on the tread of the wheel where as disc brake apply force on the disc through calliper. The disc can be axle or wheel mounted as per the requirement.

Brake Installation

Various components are installed in different steel frames as per requirement. frames installed with brake item also called as frame module (**Figure 7**) are mounted below the under frame with proper fasteners. This provide easy access for maintenance, occupy lesser space and keeps to be within the Schedule of dimension (SOD). The component, put together in frame module also help in determining weight which in turn help in weight distribution. Anti vibration mounting is used for compressor module to isolate vibration to the under frame. Various safety valves



at different pressure are installed to protect the overcharging of the pneumatic line. Test points are installed for regular checking of various pressure in the system. Pressures switches / governor are installed together in valve box for easy access, pipe routing and maintenance. 3D piping software were used to route the piping. Coordinate for pipe bending were derived from software. This reduced the installation time, interference issues during modelling.

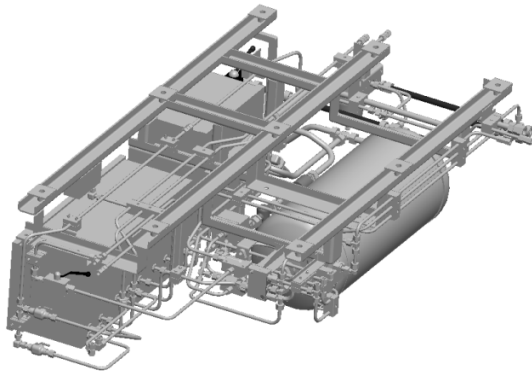


Figure 7 Frame module

Testing

The protocol under go extensive type test and various parameter were checked. Test include static and dynamic test. IEC 61133 is followed for brake testing.

Static test is to check the electrical interface between brake electronic and train management system. Pneumatic static test were done to see the actuation of brake actuator, various pressure etc. Only after gaining the confidence on static test dynamic test is done. Dynamic test starts with lower speed and gradually the speed is increased. The stopping distance, deceleration are recorded on event recorder. Various sensor such as thermal sensor, pressure sensor were fitted and reading are recorded to check the actual pressure, heat generated on brake friction area during running. Fine tuning of brake is done if required.

CONCLUSION

Methodical brake calculation, air consumption calculation, installation drawing reduces the error during manufacturing and required brake performance is achieved. Brake and air consumption calculation will be the basis for designing reservoir capacity, selection of brake actuator. Very close correlation was noticed between brake calculation and physical testing.



Sixty Years of Hot Metal Production in SAIL

Bishnu Kumar Das^{*1}, Ajay Arora¹, Anand Kumar²

Research & Development Centre for Iron & Steel, SAIL, Ranchi¹, bishnu@sail-rdcis.com*

Operations Directorate, Corporate Office, SAIL, New Delhi²

Abstract

The blast furnace process has remained efficient and competitive owing to several innovative developments that have taken place over the years. Hot metal production rate of around 12000 to 15000 ton/day, fuel rate of around 400-450 kg/thm, productivity levels of 2.5-3.5 ton/m³/day, campaign life of more than 25 years, low silicon hot metal etc. are the results of stability of operations, improved process control, better understanding of the BF process. As a result, amongst all iron making process, the blast furnace, which has been in the existence for the long period, still remains dominant. From a one million ton capacity at the time of independence, to being the 3rd largest producer of crude steel in the world since 2015, the journey of the Indian steel industry has been an eventful one. There is significant potential for growth as the low per capita steel consumption of 65 kg in India, as compared to world average of 215 kg in 2017. As per National Steel Policy 2017 of Government of India (GOI), India is going to produce about 300 million ton of crude steel by 2030. Existing steel producers in India both in Public & Private sector have been in the process of substantial expansion by installing bigger size blast furnace (> 4000m³). Though first industrial growth was through centralized planning and mobilization of national resources by GOI, the second turnaround was disintegration of centralized administered economy in 90's. Many new plants involving huge investments are being announced on a regular basis. Large blast furnaces are the key features of Iron Making in India since last few years and are true examples of Make in India Campaign. Advances in the field of blast furnace iron making have been remarkable in SAIL. The steel plants at Burnpur and Durgapur were built with British assistance, that in Rourkela with German Consultants and those in Bhilai and Bokaro with Soviet collaboration. Major improvements have been brought not only in design and engineering but also in the metallurgy of the process. SAIL made serious efforts to improve productivity and capacity utilization of Coke Ovens, Sinter Plants, Blast Furnaces etc. Apart from major modernization of their steel plants, SAIL upgraded their technologies by implementing bell less top (BLT) charging, cast house slag granulation, coal dust injection, oxygen enrichment, better raw material handling facilities, increase in usage of imported coal etc helped in overall improvement of blast furnaces as a whole. As blast furnace size increased, most of the world's new technologies like high pressure process equipment, stove cooler systems, large capacity stoves, hydraulic mud gun etc have been introduced. Energy saving technologies like top gas pressure recovery turbine, waste heat recovery systems from modern sinter machines & stoves, coke dry quenching are being adopted. SAIL has taken a target of 23.5 million ton of hot metal after current modernization. SAIL is celebrating the 60 years of Hot Metal Production in 2018. The paper presents the development of Iron making in SAIL in last six decades.

INTRODUCTION

KEYWORDS Blast Furnace, Hot Metal, Iron Making, SAIL, India

Although the history of Iron-making in India dates back thousand of years ago, the first commercial- scale attempt to produce hot metal was started in 1857 at Kulti, West Bengal. Blast Furnace is the dominant reactor for iron making throughout the world. From 1880 to about 1950 most of the developments were in the field of furnace design and engineering. There were no significant changes in process technology because of lack of knowledge of physicochemical and metallurgical aspects of blast furnace reactions. Only some information on input and output was known. The first breakthrough occurred in the 1950's, when a running blast furnace in Japan was chilled by blowing cold nitrogen through its tuyeres. Most of hot metal in SAIL is produced by BF's at five integrated steel plants namely, BSP, DSP, RSP, BSL and ISP located at Bhilai, Durgapur, Rourkela, Bokaro and Burnpur respectively. Journey of SAIL in the field of iron making in the last six decades have been eventful. The performance of blast furnace is judged by indices like productivity, coke rate, injectant rate, total energy consumption, quality of hot metal, campaign life etc. Today SAIL is producing 50000 to 55000 ton of hot metal per day from 18 operating blast furnaces after interventions of new technologies in almost all areas like mining, coal & coke making, raw material handling, sintering, large size blast furnaces etc. SAIL have taken a target of producing 23.5 million ton of hot metal after current modernization and is in process of making detailed modernization programme to produce 52.5 million ton of hot metal by 2030 keeping country target of 300 million of steel as per latest National Steel Policy of Government of India.



JOURNEY OF IRON MAKING

Since 1950 [1], advances in the field of blast furnace iron making have been remarkable. Much of this is because of better understanding of the underlying science and inner working of the blast furnace following research and development studies. Consequently, major improvements have been brought not only in design and engineering but also in the metallurgy of the process. Some of the important developments are as follows:

- Iron ore beneficiation
- Use of prepared burden in the form of sinter and pellets
- Sized and better quality coke
- Various methods of injection of liquid, gaseous and pulverised solid hydrocarbons mainly coal through tuyeres
- Larger Furnace Volume
- Higher Blast Temperature
- Higher percentage of Oxygen enrichment of the air blast
- High Top Pressure Operation
- Better Burden Distribution
- Better quality of refractory and cooling systems
- Computer based process control etc.

Year wise developments [2] in blast furnace technologies are shown in **Figure 1**. During 1950-60 [3], capacity expansion of existing BF's, reinforcement of raw material technologies (sinter machines, coke ovens, installation of raw materials processing, conveyors etc), importance of ore sizing, blast furnace process improvement through various burden material stabilization such as use of high grade ore, self fluxed sinter etc. were adopted.

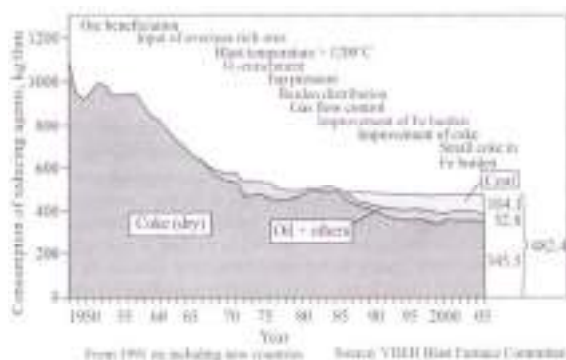


Figure 1 Year wise development (up to 2005) in Blast Furnace Technologies

During 1960-70's, improvements were done in the field of large scale production like construction of integrated steel works, improvement in coke quality, advances in blowing technologies like moisture control blast, dehumidified blast, oxygen enrichment, use of pellets as BF burden, heavy oil and coke oven gas injection and introduction of operational control systems.

In the 1970's, large blast furnaces were built. As blast furnace size increased, most of the world's new technologies like high pressure process equipment, stove cooler systems, MTA & BLT charging system, large capacity stoves, hydraulic mud gun etc. were introduced in this century. Detailed Dissection studies on blast furnaces were done in this century. Post oil crisis (which happened world over during post 1973 and 1981), energy saving technologies like top gas pressure recovery turbine (TRT), waste heat recovery systems from sinter machines and stoves, coke dry quenching (CDQ), introduction of pulverized coal injection etc. were adopted. Low fuel rate operation, low silicon operation, multiple fuel injection etc. in blast furnaces got importance during this period.

Recycling technologies including waste plastics injection in BF and Coke oven, dust and scrap recycling were focused area after Kyoto Protocol (after 1990'). Blast furnace service life was also extended through the development of carbon blocks, introduction of copper staves, hearth protection by using ilmenite bearing material and through other measures.

Development of various blast furnace process control models took place in the beginning of this century. The blast furnace process has remained efficient and competitive owing to several innovative developments that have taken place over the years. Hot metal production rate of around 12000 to 15000 ton/day, fuel rate of around 400 to 450



kg/thm, productivity levels of 2.5 to 3.5, furnace availability of around 97 to 98%, campaign life of more than 25 years, low silicon hot metal are the results of stability of operations, improved process control, better understanding of the BF process. As a result, amongst all iron making process, the blast furnace, which has been in the existence for the long period, still remains dominant.

Performance of SAIL Blast Furnaces

The blast furnaces of SAIL differ in their design and technical features. Their performance indices also differ from plant to plant. Most of the blast furnaces in SAIL were commissioned in late 50's and early 60's with the state-of-the-art-technologies. In the early yearly years of operations, most of the blast furnaces achieved the rated capacity. This trend more or less continued till mid 70's. In the initial period, raw materials including coal available to steel plants were of acceptable quality. From mid 70's to mid 80's, there had been a declining trend in performance. This was largely attributed to deterioration and inconsistency in the quality of raw materials and technological obsolescence [4]. Some of the important factors contributing to adverse performance parameters are: high ratio of alumina to silica in iron ores (2 to 3), high ash content of coke (25 to 29%), poor coke strength (M_{10} : 10-18%), high alkalis in flux materials, low percentage of prepared burden (0 to 70%), low blast temperature (600 to 1000°C) etc. This was further aggravated by poor control of size range of input materials, inadequate facilities for burden preparation, lack of facilities for high top pressure operation in most of the furnaces and inadequate instrumentation and control systems [5]. Some of the important design parameters of SAIL blast furnaces before 1980's are presented in **Table 1**.

During 70's and 80's, productivity of SAIL blast furnaces varies in the range of 0.8 to 1.2 t/m³/d, coke rate varied from 650 to 1150, slag rate varied from 500 to 700 kg/thm, alumina in slag varied from 21 to 25%, silicon content in hot metal varied in the range of 1.2 to 2.5%. Because of the process constraints and technological obsolescence, SAIL blast furnace performance has more or less stagnated. In spite of all unfavourable factors SAIL Blast furnaces at one time or other, have achieved or exceeded their rated capacity. The various factors responsible for unsatisfactory performance in those years have been summarised in **Table 2**.

Table 1 Design parameters of SAIL blast furnaces before 1980's

Steel plants	Number of BF	Hearth dia, m	Useful volume, m ³	Production capacity, t/d
Burnpur	2 (1-2)	5.1	500	600
	2 (3-4)	7.62	1170	1200
Bhilai	3 (1-3)	7.2	1033	1135
	3 (4-6)	9.1	1719	1735
	1(7)	9.75	2000	2640
Rourkela	3(1-3)	7.4	1139	1000
	1(4)	9.0	1658	1500
Durgapur	3(1-3)	8.23	1323	1250
	1(4)	8.84	1754	1500
Bokaro	5(1-5)	9.75	2000	2640

Table 2 Some important parameters of SAIL BF's during 70's envisaged at commissioning stage (DPR)

Parameters	BSP	BSL	RSP	DSP	Burnpur
Ash in coal blend, %	17-18	17	17	15.4-17.2	19
VM in coal blend, %	26	27.9	26	26.5	26.5
Ash in coke, %	23	22.5	24	23.5	-
Coke M10, %	11	8	10	11	12
Sinter in BF burden, %	48	75	53	40	Nil
Coke rate, kg/thm	890	714	900	859	-
BF productivity, t/m ³ /d(UV)	1.0-1.1	1.32	-	0.81-0.91	-

From 1985-86 the performance of the blast furnaces in SAIL has shown a distinct improvement trend. This has been achieved through a number of specific steps which can be broadly categorised as follows:

- Improvement in quality of input materials,
- Improvement in technological facilities,
- Optimization of process parameters.

The improvement in quality of coke has been achieved through use of imported coal in the blend, improved performance of coke ovens and reduction in oversize (+80 mm) in BF coke. Consistency in quality of iron bearing materials, higher percentage of screened sinter, improved quality of sinter and use of low alkali flux etc. have been achieved by proper selection of input materials and improved performance of sinter plants.



There has been continuous effort to bring consistency in operation by maintaining technological discipline. Increased efforts have been put towards improvement in blowing parameters such as raceway adiabatic flame temperature (RAFT) optimisation and automatic control of RAFT with higher blast temperature and blast humidification, optimisation of kinetic energy of blast with change in tuyere parameters, oxygen enrichment of blast, optimisation of slag regime (Basicity and MgO), Alkali management, better thermal control, improved drainage practice, use of better quality ramming mass, and anhydrous mud gun clay etc.

The improvement in technological facilities has been possible through installation of better burden distribution facilities (MTA & BLT in place of two bell), twin tap hole in number of furnaces, screening facilities in stock house, skip charging, coal dust injection system, better mud gun drilling machines, cast house modifications, slag granulation facilities, better instrumentations and computer based process control systems etc. These facilities have been added through various modernization schemes of SAIL during 1990's.

But in the last decades or so, concerned efforts have been made in SAIL toward a better understanding of the phenomena involved in the blast furnace process and to find solutions to age-old problems in the field of Iron Making in SAIL. Development of various blast furnace process control models took place in the beginning of this century. Adoption of Large blast furnaces of size more than 4060m³ are the key features of SAIL. Since last few years and are true examples of Make in India Campaign of Government of India. As blast furnace size increased, most of the world's new technologies like high pressure process equipment, stove cooler systems, BLT charging system, large capacity stoves, hydraulic mud gun etc have been introduced. Energy saving technologies like top gas pressure recovery turbine (TRT), waste heat recovery systems from sinter machines & stoves, coke dry quenching (CDQ) have been adopted. Old Blast Furnaces with old technologies have been closed & many blast furnaces have been upgraded with latest technologies. **Table 3** shows current status of Blast Furnaces in SAIL. Today most of SAIL blast furnaces have injection facilities to reduce coke rate and cut down dependency on imported coal, coke oven batteries have been upgraded, large sinter machines have been installed, new technologies have been retrofitted in almost all fields of iron making.

Due to high Al₂O₃ and SiO₂ content of iron ores and high ash content of coke, sinter composition varies over a wide range of basicity (1.5-2.5), Al₂O₃ (1.5-3.5%), FeO (5-11%), MgO (2-4%) in different plants in SAIL. Sinter percentage in BF burden varies from 55-80 % depending upon quality and availability of sinter. No pellet plant is in operation in SAIL at present. But trials have been taken in different blast furnace in SAIL by purchasing pellet. As per corporate plan, BF burden will have 10-15 % pellets in near future by installing new pellet plants.

Close control of raw material sizing, its improved physical and chemical properties, higher percentage of prepared burden in the charge and effect on burden distribution have led to improved bed permeability and better gas flow. Higher level of instrumentation has enabled operators to understand better the furnace behaviour and take remedial action in advance. However, compared to international level operation, level of instrumentation and control in SAIL old blast furnaces are short of the requirement and variation in quality of input materials and operating parameters being high, the smooth operation of our blast furnaces depends largely on experience and expertise of operation.

Table 3 Current status of blast furnaces in SAIL

Plant	BF number	Hearth dia, m	Working volume, m ³	Modernization of furnaces
BSL	1,3,4,5	9.75	1758	BFs # 2, 3, 4 & 5 :CDI, BF # 1: CTI, SGP : BF# 2, 3, 4 & 5, BF#2 has been modernized with latest facilities
	2	10.2	2250	
BSP	1-3	7.2	886	[BFs # 1, 5, 6 & 7 :CDI], [BF # 2 ,3 & 4: CTI], [SGP : BF# 4, 5, 6 & 7],
	4-6	9.1	1491	BF # 8 modernised with latest facilities
	7	9.75	2105	
	8	13.4	3455	
DSP	2-3	8.60	1204	BF # 1: Phased out, [CDI: BFs 2, 3 & 4], [SGP : BF# 3 & 4]
	4	9.40	1539	
ISP	5	13.6	3551	[BF # 1,2,3,4: Phased out] New BF # 5 with All modern facilities
RSP	1	8.4	1491	BF #1 added with latest facilities after phasing out BF # 1 & 2 together,
	3	7.4	1139	[BFs # 1,4, 5: CDI], [SGP : BF# 1, 4, 5], New BF # 5 added with latest
	4	9.0	1448	facilities
	5	13.2	3470	
VISL	1	5.4	530	SGP facility is available



RAW MATERIALS FOR IRON MAKING

Iron ore, sinter and coke are the major raw materials for SAIL blast furnace iron making. These materials need to be carefully prepared to achieve appropriate physico-chemical properties to ensure consistency in quality especially directed towards a reduction in thermo-chemical requirements during smelting in blast furnace.

Iron Ore

SAIL iron ore Fe content varying from 60-65 %, often associated with soft ores and naturally occurring fines to the extent of 20 %. The major problem in SAIL iron ore is their high alumina content and higher alumina/silica ratio. SAIL has the second largest mining outfit in the country after Coal India Ltd. Spread over the mineral rich states of Jharkhand, Orissa and Chhatisgarh, the mines of SAIL started their operations as captive sources of raw materials of its integrated steel plants. By virtue of their locations and also having developed under the different steel plants for more than five decades, they present a picture of fascinating diversity, not only in the nature of their reserves/deposits but in their legacies as well, with each one of them being remarkably distinct from the other.

In 1989, SAIL formed Raw Materials Division (RMD) as a separate unit and by June 1990 had brought all its mines that were captive to its steel plants in the eastern sector – RSP, DSP, BSL and ISP under its umbrella. The mines attached to Bhilai Steel Plant are Dalli, Rajhara, Rowghat. Presently, RMD, with its headquarters at Kolkata, has seven iron ore mines at Meghahatuburu, Kiriburu, Bolani, Barsua, Kalta, Gua and Manoharpur and three operating flux mines at Kuteshwar, Bhawanathpur and Tulsidamar. Various capacity expansion projects have been taken up at the RMD mines so as to cope up with the enhanced requirement of iron ore and lime stone of desired quality.

Coal and Coke

Steel plants need good metallurgical coal for conversion to hard coke, which is required as a fuel and reductant in blast furnaces. In this process of conversion, the volatile matter in the coal is expelled which forms the coke oven gas, which is used as fuel in steel plants. All over the world, coke from coking coals with ash level of less than 10% are used in the blast furnaces. Unfortunately, a large part of Indian coking coals have a very high ash content of nearly 25%. Such coals cannot be used in the steel plants. These have to be washed to a level of around 15 to 17% ash. The reserves of coking coal in India are also limited and are located mostly in Jharkhand and Bengal coal fields. The availability of these coals is not keeping pace with the increasing requirements of the steel industry. The high ash content of coke reduces the availability of carbon at the combustion front and increases the gangue input. Consequently flux rate and slag rate goes up, increasing the thermal load of the furnace. It is well known that about 75 % of coke burns at tuyere level, releasing ash which has to be fluxed at this level. Another unfavourable feature of Indian coal is their low caking index resulting lower coke strength (M_{10} , M_{40} , CSR, CRI, size etc.). This results in considerable generation of fines in the furnace which affects permeability and furnace productivity. Fluctuation in moisture content of coke is high affecting carbon input at the top and hence disturbs heat balance and reduction process inside blast furnace. Increased usage of imported coal has helped to tackle above problems. SAIL have taken various steps like installation of long batteries, CDCP, PBCC etc to improve coke quality.

In order to optimise the productivity of SAIL blast furnaces and also to make good coke and to meet the shortfalls in the availability of coking coal, it was necessary to import low ash coking coal. The low ash, high strength coking coal has resulted in higher productivity of BF and lower coke rate. In addition to the above, SAIL has envisaged reduction of specific consumption of coking coal through technological innovation in the area of raw materials other than coal. In order to be self sufficient in coking coal, SAIL has decided to acquire and exploit virgin blocks of Prime and Medium Coking Coal. SAIL is looking for large areas where integrated mining and processing can be undertaken.

Flux and Sinter

Sintering is the process of agglomeration of fines in to porous mass by incipient fusion caused by heat available from the fuel contained in the charge. The lumpy porous mass thus available is known as “Sinter” and comprises an effective blast furnace feed. For sinter to be good quality, the physico chemical properties of input raw materials to the sinter plant viz. iron ore fines, limestone, dolomite, coke breeze, etc. should be good. Regarding iron ore fines,



improved washing techniques to reduce gangue content have to be resorted to. Regarding the fluxes, both limestone and dolomite are used in the sintering plant. As our metallurgical coal is high in ash content, and iron ores contribute high alumina, slag volume in blast furnaces is high resulting in lower productivity of the blast furnaces. Therefore, to increase productivity of the blast furnace and the quality of hot metal, control should invariably be aimed at reducing the coke rate. SAIL have upgraded their sinter plants, various process control measures have been taken to improve sinter quality. Presently SAIL is charging 65-80 % of Sinter in their blast furnaces.

MODERN TECHNOLOGICAL DEVELOPMENTS IN SAIL IN IRON MAKING

Some of the modern technological developments implemented at SAIL plants are follows:

- (i) Beneficiation : To upgrade the quality of Iron ore, special emphasis is for preferential removal of alumina and silica from the gangue.
- (ii) Bedding, Blending, Sizing and Screening of Burden : Physical and chemical characteristic of iron ore, coal and limestone vary from deposit to deposit and also from one mine to another. For trouble-free operation of blast furnaces, it is essential to ensure supply of raw materials of consistent and uniform quality. The bedding and blending of the incoming raw is adopted before processing them.
- (iii) Use of 70 to 80% Prepared Burden (sinter / pellet) : It has been proved that with the use of sinter/pellet in the burden, the productivity of Blast Furnace increases.
- (iv) Skip and Conveyor Charging : Old system of charging from scale car has been removed. All burden materials are delivered to the furnace top by conveyor/skip. This is economical for bigger blast furnaces. Most of the bigger blast furnaces at SAIL have this provision. All new upcoming blast furnaces of larger size will have this charging system.
- (v) Bell-less Top : In place of conventional two bell charging system, two charging hoppers with rotating chute are installed. The rotating chute distributes the material in the desired manner. The system is easy to maintain. The system has been adopted in BF-4, 5, 6, 7, 8 of BSP, BF-1, 3, 4, 5 of RSP, BF-3 of DSP, BF-5 of ISP and all the Blast Furnaces of BSL. This system is being incorporated in upcoming/new blast furnaces of SAIL.
- (vi) Furnace Probes : Probes are fitted above the stock level/ below the stock level in order to monitor temperature distribution and collect samples of burden material and gas.
- (vii) Cast House Slag Granulation : In this design the liquid slag from cast house runner is led to the granulating unit located very near to the cast house. This would eliminate the need for maintenance of large fleet of slag ladles, reduce the cost of production, avoid delays and increase the yield of granulated slag. BF No. 4, 5, 6, 7, 8 of BSP is having cast house slag granulation. This facility is installed in BF - 2, 3, 4, 5 of BSL. This facility also exists in BF- 1, 4 and 5 of RSP, BF-5 of ISP and BF-3 and 4 of DSP.
- (viii) Coal Dust Injection : Non-coking coal in injected through tuyere using nitroten as carrier. This reduces the coke rate and thus saves the valuable coking coal, which is also not abundantly available in India. Coal dust injection is normally associated with high blast temperature and oxygen enrichment, BF - 2, 3, 4, 5 of BSL , BF - 2, 3, 4 of DSP, BF-1, 5, 6, 7, 8 of BSP and BF -1,4,5 of RSP have been provided with a coal dust injection system.
- (ix) Higher Hot Blast Temperature and Increased Oxygen Enrichment : Most of the stoves have been upgraded to achieve higher hot blast temperature (1000 to 1100°C). Bigger size BF's in SAIL is operating with (1150 to 1200°C). New oxygen plant have been installed and commissioned to get higher oxygen enrichment (5 to 6%) for process intensification. Higher HBT and oxygen enrichment further helps in increasing CDI rate.
- (x) External Desulphurisation of Hot Metal: With the introduction of continuous casting technology and increased demand for high quality steel, requirement of low sulphur (less than 0.025%) hot metal has increased. For this purpose hot metal from BF is desulphurised by injecting desulphurising agents such as calcium carbide, lime soda ash, magnesium in the hot metal ladle. One desulphurising unit has been installed each at ISP,RSP and BSP. This facility is being installed at BSL.
- (xi) Cast House Desiliconisation : Silicon from hot metal is partially removed by adding mill-scale, iron ore, along with lime in the hot metal runner. Such trials have taken place earlier in SAIL.
- (xii) Dephosphorisation of Hot Metal : Dephosphorising agents like soda ash and lime based flux are added in hot metal in transport vessel to reduce phosphorous content of hot metal. This facility was there in DSP.
- (xiii) Automation and Computer Control : In case of fully automatic operation, the computer receives signals from various sensors which determine the optimum point values and commands the equipments to operate automatically. Automatic control of charging, stoves, blast furnace and other auxiliary units are provided in



most of the blast furnaces in SAIL.

SAIL INTEGRATED STEEL PLANTS

Brief journey of SAIL steel plants have been enumerated below.

Bhilai Steel Plant

An agreement was signed in New Delhi on 2nd February 1955 between the Government of India and Soviet Union to set up an integrated steel plant at Bhilai with a capacity of 1 MT of ingot steel. The plant began its operation on 31 January 1959 when Coke Oven Battery No-1 was commissioned. Production of Pig Iron at Bhilai began on 4 February 1959 when Blast Furnace No-1 was commissioned. Situated in Chhattisgarh, this was one of the three 1 MT capacity (BF - 1, 2 and 3 commissioned) crude steel plants set up in the Public Sector in the late fifties [6]. Subsequently it was expanded to 2.5 MT ingot capacity (BF 4, 5 and 6 commissioned), further to 4.0 (BF 7 added) and enhanced to 4.7 MT (BF 7 upgraded). Recently New BF # 8 have been commissioned and finally BSP have 7.5 million ton hot metal capacity.

Rourkela Steel Plant

RSP is the first integrated steel plant set up in the public sector in the country in 1959. With an initial capacity of 1MTPA, RSP had three identical blast furnaces (BF 1, 2, 3). Fourth blast furnace of 1658 m³ useful volume was installed under 1.8 MTPA in 1967. The hot metal capacity of the plant was further upgraded to 2.0 MTPA in late 80's [7]. RSP have installed to new blast furnaces (BF # 1 after phasing out 1 and 2 and new bigger BF#5) expanding hot metal capacity to 4.5MT.

Bokaro Steel Plant

The plant was conceived as the country's first 'Swadeshi' steel plant, to be built with maximum indigenisation going into the equipments, materials and know-how. Thus, this marked a radical shift from the earlier dependence on foreign sources for know- how and consultancy, design and equipment, engineering, supervision and erection to almost a full measure of self-reliance and confidence.

Bokaro Steels first phase of 1.7 MT commenced on 2nd October, 1972 with the commissioning of 1st Blast Furnace and completed on 26th February 1978 with the commissioning of 3rd Blast Furnace. After upgradation of BF # 2 in 2007 and current modernisation, BSL's hot metal capacity will be 5.8 MT.

Durgapur Steel Plant

Set-up with an initial annual capacity of 1 million tonnes of ingot steel (BF # 1,2 & 3), DSP was later expanded to 1.6 million tones (BF # 4) and further expanded to 1.876 MT by reconstruction during 1994 (BF # 2& 4) and 2002 (BF # 3) [8]. After current modernization hot metal capacity of DSP will be 2.5 MTPA.

IISCO Steel Plant

The erstwhile Indian Iron and Steel Company (IISCO), one of the oldest steel plants of the country has been amalgamated with Steel Authority of India Limited (SAIL) with effect from 16th February 2006. Following merger, IISCO has now been renamed as IISCO Steel Plant (ISP), the fifth integrated steel plant of SAIL. The plant is all set to achieve new milestones implementing its growth plan in tune with SAIL's Corporate Plan. Post modernisation and technological upgradation of the IISCO Steel Plant and its collieries ISP's annual hot metal production capacity is envisaged to go up to 2.9 MT (MT).

ISP, one of the oldest integrated steel plants, started production of iron way back in 1870 in its Kulti Works of Bengal Iron Works Company. ISP's Burnpur Works was incorporated on 11th March 1918, started iron making in 1922 and steel making in 1939. In the late 1950's, it expanded further to become a million tonnes steel plant. ISP has got an integrated steel plant at Burnpur, captive collieries at Chasnalla, Jitpur and Ramnagore.



Table 4 Performance of SAIL BF's during 2017-18

Parameters	Units	BSL	BSP	DSP	ISP	RSP
		BFPS Jan'18	BFPI Aug'17	BFIS Mar'18	BFPS Feb'18	BFPS Feb'18
Productivity	t/m ³ d	2.02	2.30	2.06	1.84	2.33
Coke rate	kg/thm	489	468	449	378	372
Hot coke rate	kg/thm	34	22	21	21	38
CDI rate	kg/thm	42	63	70	119	146
Fuel rate	kg/thm	636	554	539	519	506
Slag rate	kg/thm	368	363	317	380	306
Sinter	%	65.1	70.1	67.2	78.6	75.9
Blast Temp	°C	1036	935	993	1197	1190
Oxygen enrich	%	1.5	2.1	3.7	2.1	5.0
Blast Pressure	kg/cm ²	2.24	1.54	1.86	3.90	3.98
Top Pressure	kg/cm ²	1.10	0.44	0.80	2.40	2.47
Al ₂ O ₃ in Slag	%	19.1	16.9	21.5	19.2	17.1
Hot Metal Si	%	0.78	0.77	0.83	0.78	0.64

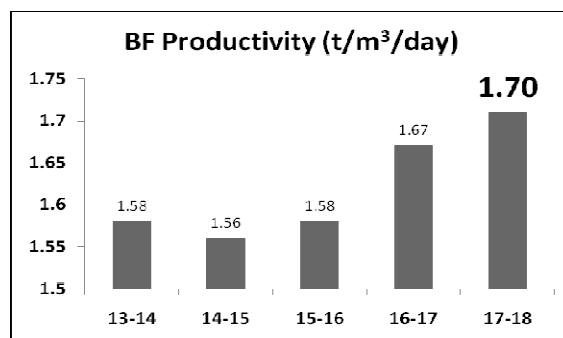


Figure 2 SAIL blast furnace productivity

SAIL BLAST FURNACE PERFORMANCE IN LAST FEW YEARS

Performances of blast furnaces of SAIL in last year have been shown in **Table 4**.

With concentrated efforts at mines, coke ovens, sinter plants, raw material handling area, better selection of technologies (new and upgraded blast furnaces with state-of-the-art technologies), better selection of raw materials and fluxes and various process interventions in coke making, sintering, blast furnace, utilization of in-plant waste, SAIL performance with respect to techno economic parameters is improving (**Figures 2, 3 and 4**). BF productivity of SAIL blast furnaces is varying between 1.55 to 2.35 t/m³/d, coke rate is in the range of 350 to 480 kg/thm and coal dust are being injected at the rate of 60 to 160 kg/thm depending upon available resources and technologies.

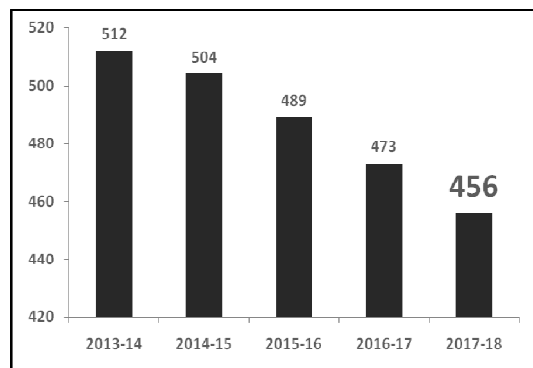


Figure 3 SAIL blast furnaces coke rate

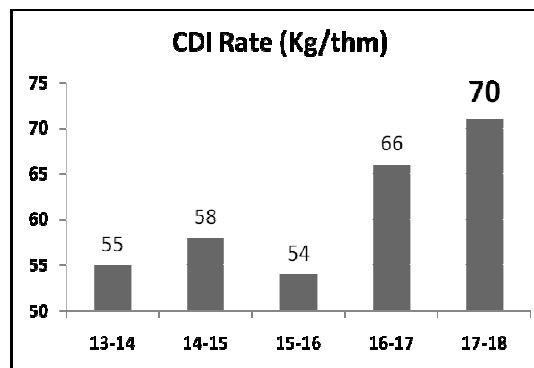


Figure 4 SAIL blast furnace coal dust injection rate

CONCLUSION

SAIL, as one of the largest Iron and Steel producer in the country, has played a leading role in industrial development of the country in the last sixty years. It is among the top 25 steel producers of the world. Challenging targets have been there for SAIL Blast Furnaces. After the introduction of new technologies, the productivity, quality and specific energy consumption have improved significantly. Besides achievement of set goals, endeavour in future should be to earn reasonable profits and establish excellence in most of the technological areas.

REFERENCES



1. A. Ghosh, A. Chatterjee, Book on Iron Making and Steelmaking – Theory and Practice, pp 10-11, 24-25
2. Hans Bodo Lungen et al, Iron Making in Western Europe – Status quo and future trends, METEC 2015, Dusseldorf – Germany, 15-19 June 2015
3. Ironmaking Technology for the last 100 years: Deployment to Advanced Technologies from Introduction of Technological Know-how, and Evolution to Next-generation Process – Masaaki NAITO, Kanji TAKEDA, Yoshiyuki MATSUI , ISIJ International, Volume 55, Number 1, pp 7-35, 2015
4. Technology Awareness Programme on Blast Furnace Technology by TDC, RDCIS, SAIL, Ranchi, Feb 4-6, 1998.
5. S K Gupta, V I Litvinenko, E F Vegmann, Book on Iron Ore Processing and Blast Furnace Iron Making, pp 208-209
6. Book on Blast Furnace : Iron Production Technology, Bhilai Steel Plant, pp 4-7
7. National Seminar on ‘Recent trends in iron making’, pp 4-1 to 4-8, 12 December 1997
8. Operational Statistics 2009-10, Durgapur Steel Plant



Effect of Operational Logistics on Steel Ladle Life in a Steel Plant

Rakesh Kumar Singh^{*1}, Rajeev Kumar Singh¹
RDCIS, SAIL, Ranchi¹, rksingh@sail-rdcis.com*

ABSTRACT

Steel ladle cycle, from steelmaking to casting, invariably includes secondary treatment of steel at different stations like ladle furnace and/or vacuum degassing units. It is generally considered that performance of steel ladle depends upon operational parameters and the refractory properties. However, operational logistics have significant effect on the ladle performance in terms of its reliability to hold the liquid steel without causing any damage to vessel, as well as, remain inert to reaction with liquid steel. Life of refractory lining depends both on duration of metal contact and duration of empty state. These durations have two major components; operational requirement and logistic. Better logistic cuts down on the idle time thereby improving ladle circulation. This reduces thermal shock to refractory lining which is detrimental for its health and conserves heat energy. Ladle movement from steelmaking units after tapping to secondary treatment stations and lastly to casting is dependent on availability of transfer cars, overhead cranes and vacancy at next station. Unavailability of any of these resources leads to waiting of ladle with molten metal inside, causing erosion of refractory lining. Similarly, after casting is over, the return of ladle to cleaning and preparation stations again depends on availability of ladle cars and overhead cranes. Delay in this return route causes thermal shock to lining leading to erosion because of structural spalling of refractory lining and also loss of heat energy. Improved and efficient logistics increase the number of heats taken in a ladle per day, which means better ladle circulation. This increases ladle availability and reduces thermal loss. Ladle fleet management is generally done manually based on experience and shop layout. An automatic ladle fleet management system has been developed using high temperature RFID tags for ladle identification throughout the shop. Application of this automatic ladle fleet management system in a steel plant has increased ladle utilisation from 4.5 heats/ladle/day to 5 heats/ladle/day.

KEYWORDS Steel, Ladle, Refractory, Logistics

INTRODUCTION

Steel ladle is a refractory lined bucket shaped vessel as shown in **Figure 1**, used for carrying molten steel from steelmaking unit to the casting or teeming platform. During steel production, the ladle receives liquid steel from converter, and then at the rinsing station the liquid steel is stirred with argon flow inserted into the vessel from bottom to remove some impurities and improve the steel quality.

The ladle is then sent to Ladle Furnace (LF) station where the liquid steel is further treated with argon and heated for producing high quality steel. Then, the ladle moves with liquid steel to casting station for making different steel products. After casting is over, the ladle is then returned to slag dumping area where slag remaining in ladle after casting is poured out. This empty ladle is then brought to hot maintenance station for cleaning, checking, component changing (if required) and making it ready for receiving the next batch (tapping) of steel from converter. This process and time from one tapping to another is called a ladle cycle. A ladle circulates a number of times in this cycle before it goes to cold repair station, where the eroded refractory lining is dismantled and a new lining is placed for a new campaign. Ladle is also taken out of circulation once or twice for interim repair, where it is cooled and functional refractory components like well block and seating blocks as well as slag zone of refractory lining are changed. After new lining or repair at cold repair station, ladle is pre-heated to a temperature of ~1000°C at pre-heating station which is a vertical stand with cover fitted with burner. Total preheating time is 12 to 15 h. This pre-heated ladle is ready for taking molten steel from converter.

It is generally considered that performance of steel ladle depends upon operational parameters and the refractory properties. However, operational logistics have significant effect on the ladle performance in terms of its reliability to hold the liquid steel without causing any damage to vessel, as well as, remain inert to reaction with liquid steel. Life of refractory lining depends both on duration of metal contact and duration of empty state. Another factor which affects refractory lining life is pre-heating of ladle, which depends on duration of empty state or frequency of cold interim repair.



Heat Cycle

In a ladle, time between one tapping from converter to next tapping is called one heat cycle. Each heat cycle has two parts; with liquid metal and empty. Duration of these two parts have two major components; operational requirement and logistic. Operational requirements, like LF treatment time, is dependent on steel quality to be produced and may vary from 10 to 30 min. However, the treatment time will increase if tapped steel's temperature is lower as the output steel temperature from LF is fixed for a shop. This output liquid steel temperature has 15 to 25°C superheat, which means the liquid steel temperature is 15 to 25°C above liquidus temperature of steel for casting. The casting duration depends on shape and size of steel product being cast like slab, bloom, billet etc. and can vary from 40 to 70 min. Similarly, during empty/return cycle, slag dumping time, hot maintenance time etc are operational requirement. Besides operational time, remaining time of a cycle is determined by logistic management e.g. availability of ladle for taking heat, availability of crane and ladle car for transportation of filled or empty ladle, vacancy at next station etc. Generally, a heat cycle varies from 180 to 240 min, depending upon shop facilities and layout. It has been observed that around 20% of total cycle time is logistic time. Optimisation of this logistic time reduces the total cycle time, which makes ladle move faster. After tapping of steel from converter to ladle, ladle car on which ladle is placed comes out and ladle is lifted by overhead crane for carrying it to LF station. Availability of crane at that instant of time comes under logistic management. Delay in lifting of ladle increases the time of metal contact with ladle refractory lining causing more erosion. It also leads to heat and productivity loss. Delay in lifting ladle from LF station to caster turret also has similar impact. During return cycle, after casting, delay in moving ladle from turret for dumping of left over slag by overhead crane results in cooling of slag and this viscous slag deposits over purging plug and inside teeming nozzles. During hot maintenance of ladle this deposited slag is cleaned with oxygen lancing. This process causes extra erosion of porous plug and teeming nozzle, thus reducing its life. Moreover, lancing also extends ladle preparation time. This can be avoided or reduced by early dumping of slag after casting over, as hot slag is quite fluid and can be completely dumped in slag pot.

Optimal Ladle Fleet Size

An optimal production of 3.84 Mt/y is reached with 10 steel ladles and using additional ladles do not add significantly to the annual production [1]. When more steel ladles are used, the number of emptied ladles that first go to the preheating station before being refilled again at the converter also increases. The utilisation of the crane that handles the empty steel ladles also increases, together with the number of steel ladles since more movements are required. It has been observed that average preheating time for a steel ladle increases from 13 min for 8 ladles, to 15 min for 10 ladles, to 25 min for 12 ladles. Using too many ladles would therefore result in an unnecessary high usage of the preheating facility, which would lead to an increase in energy consumption. It also increases refractory consumption as extra preheating causes decarburisation of refractory lining surface leading to its erosion. Using the right amount of steel ladles leads to cost-efficient plant practice

Energy Optimization

The steel production process (from manufacturing crude steel in a converter to complex treatment in secondary metallurgy to casting the steel in continuous casting machines) is very energy-intensive. Starting from the target temperature required at the continuous casting machine, production processes usually incorporate energy buffers for every upstream facility to compensate for the temperature losses occurring between tapping and treatment, including waiting time, and to cover unforeseen production interruptions [2]. If logistic delays in process flow lead to higher waiting times and thereby in temperature losses, heat becomes too cold for casting and needs to be reheated in the ladle furnace with high energy expenditure, or even recharge in the primary facility if significant temperature drop happens after LF which prevents further casting. The situation offers significant potential for energy cost reduction through optimised logistic management. Increase in travel and waiting time after tapping from converter causes temperature drop of liquid steel in ladle. In ladle furnace this temperature drop is compensated through electrical heating using arcing. Higher temperature drop requires more arcing time, which increases power consumption. Further, longer arcing time makes slag more fluid at slag metal interface leading to extra corrosion of slag zone refractories affecting overall ladle lining life. After casting, during empty cycle of ladle, logistic delay causes temperature drop of ladle leading to reduction in total heat content of ladle. This reduced heat content results in drop in liquid steel temperature during tapping from converter. To overcome this, tapping temperature is increased. Higher tapping temperature increases phosphorous reversal in steel and affects the quality of steel. It also has significant effect on refractory lining performance of converter. Prolonged cooling of ladle during heat cycle subjects refractory lining to thermal shock, which induces structural spalling of the surface resulting preferential



erosion of the lining. Thus, an efficient logistic management of steel ladle saves thermal energy and also increases refractory performance leading to reduction in refractory consumption.

Ladle Management System

Since, ladle fleet is managed manually and based on experience human judgement, there is always a chance of inconsistency in logistic management. In order to overcome this, an automatic ladle management system has been developed. It provides complete information about ladle like the ladle heat information, exact ladle position, ladle idle time, ladle life, metal holding time, ladle empty time causes of delay and maintenance requirement. The system detects exact arrival and departure time for each ladle to the processing stations along with its idle time. From the information supplied by the automation system, the management system maps the heat information, exact processing time for each ladle. The Automatic Ladle Management System captures all the information related to maintenance activities performed on a particular ladle and gives a clear understanding of the ladle availability for future heats. The system also maintains history of each ladle which helps supervisor to analyze the ladle's performance profile. Ladle profile includes ladle life, heat-wise history, temperature profile, aging etc. This system monitors real time ladle movement automatically and seamlessly. A snapshot of the Automatic Ladle Management system realtime view is shown in **Figure 2**.

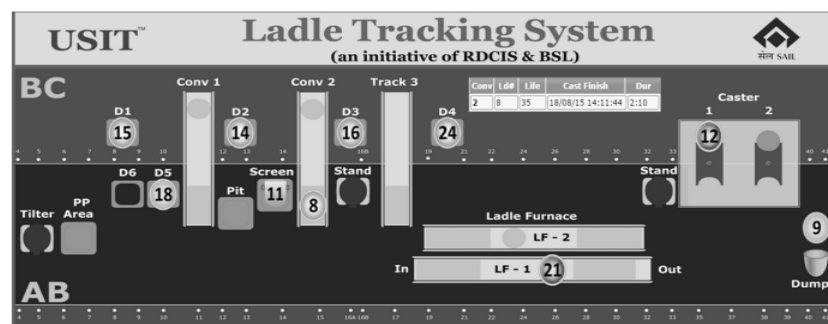


Figure 1 Steel ladle

Figure 2 Realtime display of in service ladles in Steel Melt Shop

The philosophy and operating principle behind this Automatic Ladle Management System is the use of RFID based system to track all the in-service ladles in the ladle fleet always for its entire life cycle. This tracking is done without any human intervention. Human intervention is required only to push a ladle out of service for repairs or bring back ladles in operation after repair. For this, ladles are tracked at all locations such as preheaters, converter tapping, ladle furnace, caster turrets, slag dumping and ladle preparation bay to monitor the process, transport and idle times for all ladle at each station. The ladle tracking system is designed with the following basic principles [3-5]:

- **Identification:** Precise identification of any number of ladles in circuit through the steel melt shop via RFID tags fitted on each ladle.
- **Process Adherence:** Limits on input parameters and timing sequences that triggers alarms.
- **Documentation:** Collect data for each process step in database with upload and download capacity to network computer to defined reports.
- **Process Monitor:** Shift wise/ Daily/ Weekly/ Monthly reports for ladle movement time along the process route for each cycle.
- **Process Improvement:** Establish production Key Performance Indicators.
- **Process Traceability:** Monitor the movement of all ladles during the process route and identify any process deviations such as missing of slag dumping, porous plug cleaning bay etc.
- **Real Time Monitoring:** Monitor the status of each ladle in real time.
- **Remote Display:** Ability to display the status of ladle through HMI screen on remote desktops on the network.
- **Robustness of Hardware:** Protection of RFID tags against continuous exposure to high temperature, steel splashes and accidental collisions with other equipment or structure.



Use of this system helps in time planning of transport equipment and maintenance of ladle components, reducing the logistic time inside the steel shop.

CONCLUSION

Ladle management system based on RFID sensors has been successfully developed and implemented in an integrated steel plant. This system monitors real time ladle movement automatically and seamlessly. Process parameters of each heat cycle also get associated with the respective ladle, which helps in analysis of thermal status of ladle and its refractory lining performance. Documentation of the ladle movement cycle has helped in improving logistics and bringing down incidents of aberrations such as missing slag dumping, delayed slag dumping, missing of porous plug cleaning. Strict and timely adherence to process route has helped in improving process indices and the plant has achieved almost 99.98% porous plug opening. Ladle utilization has been optimized and its usage increased from 4.5 heats/ladle/day to 5 heats/ladle/day leading to substantial savings.

REFERENCES

1. F. Schrama, D. Merkestein, M. Jansen, W. Vortrefflich and B. v. d. Berg, Steel plant model for optimisation of steel plant logistics, Millennium Steel India, pp. 43-47, 2014.
2. H.-J. Ponten and B. Kleimt, Temperature-controlled planning for energy optimisation in steel plants, STAHL- Opportunities and Prospects, 2009.
3. F. J. Ahualli, J. G. Sagasti, S. Meyer and F. Memoli, Physical Ladle Tracking, AIS Tech Conference Proceedings, 2014.
4. C. Liu, M. Zhang, C. You and C. Xu, Development of a Novel Ladle Monitoring System Based on Internet of Things Technologies, Journal of Convergence Information Technology(JCIT), Volume 8, Number 10, May 2013.
5. S. Yin, M. Yang, C. Wang and R. Lou, The research and realization of a new iron ladle tracking system, International Conference on Applied Science and Engineering Innovation. ASEI, 2015.



Thermo-Mechanical Processing of High Strength Low Carbon Microalloyed Steel for Automotive Sector at Bokaro Steel Plant

Santosh Kumar^{*1}, N Mondal¹, B Sunita Minz², R Dodrea², B Mishra¹, D Kumar¹, S Kumar¹

R&D Centre for Iron and Steel, Steel Authority of India Limited, Ranchi, Jharkhand¹, santosh@sail-rdcis.com*

Bokaro Steel Plant, Steel Authority of India Limited, Bokaro Steel City, Jharkhand²

ABSTRACT

For better fuel economy and to reduce greenhouse gas emissions, the requirement to decrease the weight of automobiles has become more stringent in recent years. In order to meet these demands, the traditional focus of material development has been mainly in the areas of high-strength and highly formable steels. Bokaro Steel Plant developed steel like HSFQ450 grade for application in automotive segment. HSFQ450 is known to have UTS in the range from 520 MPa to 550 MPa with high formability. Effect of micro-alloying elements like Ti, Nb, V etc. and thermo-mechanical controlled process are studied with respect to change on microstructure and properties during development of new steel products for specific application.

KEYWORD HSLA Steel, Ferritic Microstructure, Nano-precipitate, Micro-alloying, Formability, Automotive steel.

INTRODUCTION

Development of new steel to achieve reduced weight, improved formability, surface finish and crash performance of vehicles are one of the prime focus point in automotive industry. Steel manufacturers are focusing to develop an improved formable grade steel with high strength in thinner gauge so that weight can be further reduced. HSFQ450 is one of such HSLA category steel.

HSFQ 450 grade have been developed by optimizing processing parameters through BOF-LF-CC route at Bokaro Steel Plant, SAIL. Designing of alloy chemistry with high level of cleanliness with respect to inclusion and gas content and optimizing hot rolling parameters with respect to thickness tolerance, finishing temperature and coiling temperature are critical issues during development work. These high strength formable grade steel have better substitute for IS 2062 and BSK46 grade steel. YS/UTS less than 0.85 steel become more formable, so manufacturer can applied these grades in press forming. High hole expansion ratio, low YS/UTS ratio and higher elongation are characteristics of high formability of the steel. However solid solution strengthening and precipitate particles formation during thermo-mechanical processing enhances the strength and toughness of the material. These steel is used as a load bearing component like dummy axle, chassis etc. in automobile (**Figure 1**).

STEELS USED IN AUTOMOBILES

In automobile sector, conventional category steels to ultra-high strength grade steels are applied. Depending of application, the steel strength varies from 140 MPa to more than 2000 MPa strength steel. For making higher-performance steels, different techniques like solid-solution strengthening (by alloying element), grain refinement, precipitation hardening (by carbide, nitride or carbo-nitride forming element), work hardening, and heat treatment are applied during manufacturing.

Basically, formability of steel is a change of shape of a steel sheet before fracture or crack initiation and can be assessed by % elongation by tensile test, hole-expansion test, cup drawing test and formability limit diagram. Formable grade steel is subject to different forming process like stamping, bending and flanging. Stamping is a process with uniform deformation over the thickness such as stretching and deep drawing. And second one are, processes with a strong gradient over thickness such as bending and flanging.

Application of particular steel grade is primarily dependant on the strength required and formability. For safety-critical parts, especially for B-Pillar and front cross member, Ultra High Strength Steels is applied. Chassis and frame require High Strength Steels having a good balance of strength, formability, energy absorption and durability. Steels with excellent formability are used for sheet metal works like roofs and side panel. Blanks are cut from coil, and subsequently formed. Whereas, outer panels are generally made of conventional mild steels or interstitial free (IF) steels. Structural parts are more often made from high strength steel, the group of ferrite or ferrite + Pearlite phase steel which are stronger due to precipitation hardening and solid solution hardening. The increased strength comes at the expense of elongation, with a repercussion on formability; albeit mostly in stamping.

For higher strength, multiphase steels known as advanced high strength steels are used. The usage of steels based on their tensile strength and percentage elongation is provided in **Figure 2**.



Figure 1 HSFQ450 steel used in long chassis members of vehicle

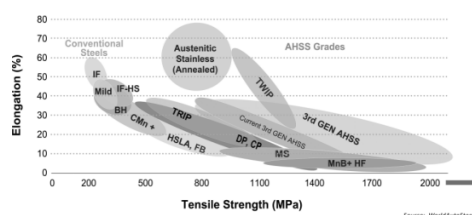


Figure 2 Illustration of automotive sheet steel grades based on strength and ductility [1].

THERMO-MECHANICAL PROCESSING

Development of the High Strength Low Alloy steel with superior properties and performance are both an opportunity and challenge for steel manufacturers. Understanding of the microstructure-property relationship with respect to composition (alloy design) and processing is foremost important for new development. The alloy composition and reduction rate during rolling influences three critical temperatures of austenite. These temperatures are: the grain coarsening temperature (T_{GC}), non-recrystallization temperature (T_{nr}); and transformation temperature (T_{Ar3}).

Each of the alloying elements has different solubility capability in austenite. And formation of precipitate of these elements' affect the parameters like roll finish temperature and coiling temperature during the thermo-mechanical processing of HSLA steels. VC is substantially more soluble in austenite than other carbide, consequently it can form on cooling a higher volume fraction of precipitate, and result in more precipitation hardening. On, the other hand, TiN having lowest solubility, so once formed, likely to remain out of solution at higher temperature, thus is more effective in grain growth. Therefore, during reheating of slab, TiN control the grain coarsening, whereas, NbC and Nb(C,N) are used to control the temperature of non-recrystallization (T_{nr}) and the transformation temperature T_{Ar3} . At the cooling stage of coil, VC and VN are precipitated and strengthen the ferrite matrix during the austenite to ferrite transformation.

The temperature of non-recrystallization T_{nr} is one of the most important parameters in thermo-mechanical processing of microalloyed steel. For microstructure uniformity, the control of temperature at every steps like reheating temperature of slab, roughing finish temperature, temperature at transfer bar and final finish temperature (i.e T_{nr} and T_{Ar3}) are foremost important to achieve desired properties. During deformation process, a large number of inter-crystalline defects like deformed grain boundaries, deformation bands, and annealing twin boundaries can be produced in austenite. These defects act as a nucleation sites for ferrite [2]. There are several equations available in published literature to calculate the T_{nr} and T_{Ar3} of steels. One of the most popular equations is the one proposed by Borato, et al [2].

$$T_{nr} = 887 + 464[C] + \left(6445[Nb] - 644\sqrt{Nb}\right) + \left(732[V] - 230\sqrt{V}\right) + 890[Ti] + 363[Al] - 357[Si] \quad (1)$$

$$T_{Ar3}(^{\circ}C) = 910 - 310C - 80Mn - 20Cu - 55Ni - 15Cr - 80Mo + 35[(Cu) - 8] \quad (2)$$

where, [X] is in wt.% and the T in $^{\circ}C$.

The final stage to the microstructural refinement of microalloyed steel is controlled by finishing rolling temperature and the coiling temperature. The proper selection of these two temperatures decide the final as-hot rolled microstructure and hence the mechanical properties.

EXPERIMENTAL PROCEDURE

For the present study, heat was made at 300 t capacity BOF converter with combined blowing technology at Bokaro Steel Plant. The chemical composition of the product is given in **Table 1**.



The heat was casted into 225 mm thick slab and hot rolled into 6 mm thick hot rolled coil at Hot rolling mill at Bokaro steel plant. The concast slabs were reheated up to 1250°C and then hot rolled into desired thickness. Finish rolling and coiling temperatures were kept in the ranges of $880 \pm 10^\circ\text{C}$ and $615 \pm 15^\circ\text{C}$ (**Figure 3**) and minimum draft of 85% in the finishing zone.

Table 1 Chemical composition of the high strength formable grades steel (wt %)

Grade	C	Mn	P	S	Si	Al	Nb	V	Ti
HSFQ450	0.06-0.08	1.20-1.40	0.018 max	0.010 max	0.20-0.25	0.020-0.050	0.040 max	0.040 max	0.01 min

Hot rolled coil was characterized for validation of process designed. For microstructure evaluation, sample was prepared as per ASTM E3-2001 standard. 2% nital was used as etchant. It was carried out by Leica Reihert Microscope as per ASTM E45-2005 standard.

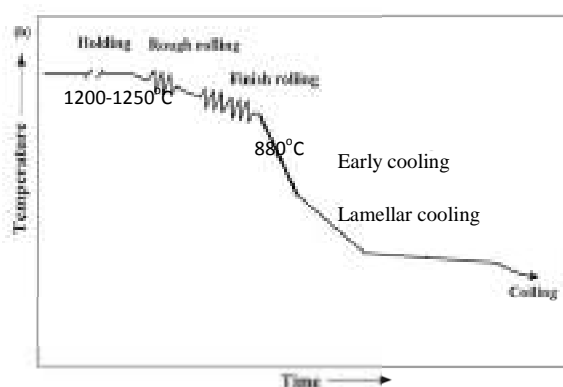


Figure 3 Thermo-mechanical treatment at Hot strip mill

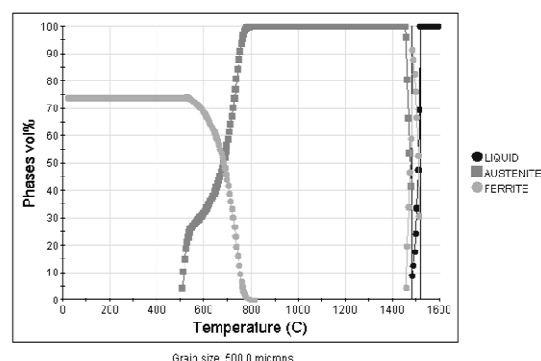


Figure 4 phase volume of cast product at different temperature

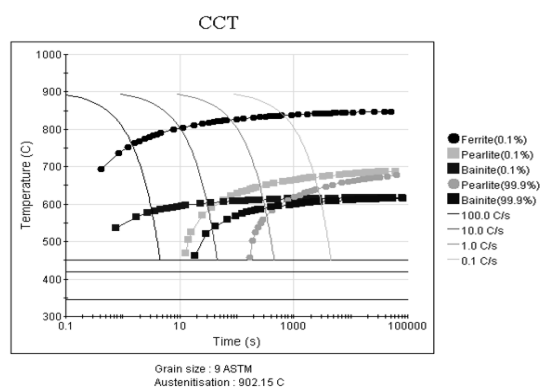


Figure 5 CCT Diagram of HSFQ450 grade steel

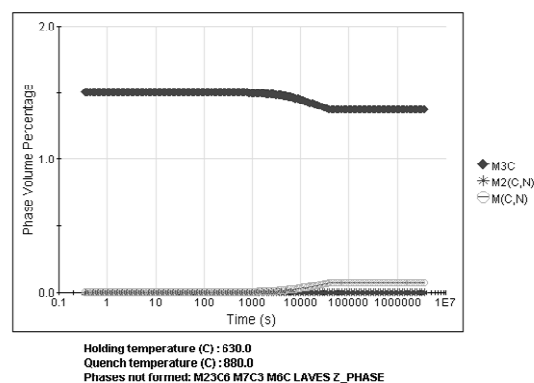


Figure 6 Precipitate particle volume of rolled product with respect to time

RESULTS AND DISCUSSIONS

Several laboratory trail test, simulation have been carried out to study the effect of alloying & micro-alloying elements before commercial production. Investigations were also carried out to study the effect of rolling and cooling parameters. Continuous-Cooling Transformation (CCT) and phase volume of cast product was characterized by using simulation software JMatPro 7 (Figures 4 and 5). The austenization temperature of this grade is around 800°C and around 73% ferrite structure obtained in room temperature.

During controlled rolling, as the temperature drops down to 630°C, precipitation takes place in austenite of carbides and carbonitrides of Niobium, Vanadium and Titanium on the grain boundaries [1].

The resulting overall effect is to control the processes of recovery and recrystallization, and to inhibit grain growth of the austenite. Many researcher have found that carbo-nitride precipitation influences microstructural evolution during the hot rolling of microalloyed steels [3, 4].

Simulation software (JMatpro 7) also shows the formation of M₃C, M₂(C,N) and M(C,N) precipitate particles (M= Nb, V, Ti) with 10 to 20 nm size (Figures 6 and 7).

The steel with lower Nb (0.04%) and higher Si (0.25 %) contents has superior formability properties in terms of higher elongation (32%) and hole expansion ratio (145 %) coupled with lower YS/UTS value (0.84) [5]. The mechanical properties of these grade is illustrated in **Table 2**.

Table 2 Mechanical properties

T × W	YS, MPa	UTS, MPa	% El	YS/ UTS
mm × mm				
6 × 1250	480- 520	580- 650	28- 35	0.80-0.85

The mechanical properties achieved are very encouraging with respect to lower YS/UTS ratio (0.84) and close bend which are very much suitable for forming operations. **Figure 8** shows the typical ferrite pearlite microstructure in the hot rolled coil. The grain size was found to be 7.0 to 8.0 microns and these fine grains are very much suitable for forming applications.

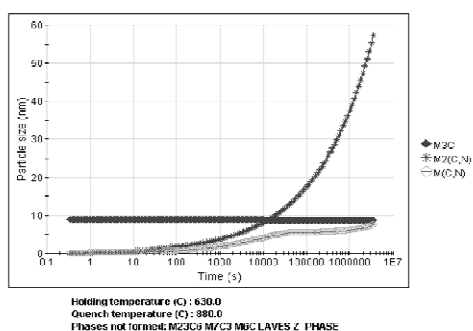


Figure 7 Precipitate particle size with respect to time

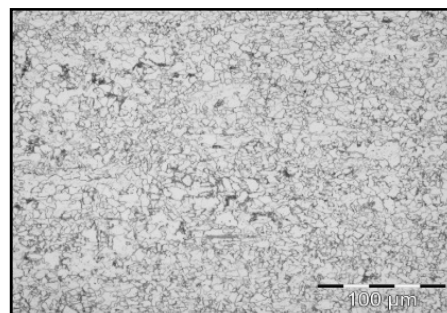


Figure 8 Microstructure of HSFQ 450 Grade HR Coil

CONCLUSION

HSFQ450 possess an attractive combination of strength and formability which is quantified as high elongation and hole expansion ratio coupled with lower YS/UTS ratio (0.80-0.85). This has been possible as a result of innovative alloy design and synergistic effect of micro-alloy during controlled processing. Enhanced precipitation of carbonitrides resulting into formation of fine ferrite and pearlite grains. The grain size was found 7 to 8 microns equivalent to ASTM No. 11-12 and these fine grains are very much suitable for forming applications like long and cross members of auto chassis etc.

REFERENCES

1. R Rana, S B Singh, Automotive Steels : Design, Metallurgy, Processing and Applications, Woodhead Publishing, pp 20, 2017
2. F. Borato, R. Barbosa, S. Yue, J.J. Jonas, Thermo-mechanical processing of steels and other materials, Proceedings Thermec'88, Iron and Steel Inst., Tokyo, p. 383, 1988.
3. John J Jonas, The Hot Strip Mill as an Experimental Tool, ISIJ International, 2000, Volume 40, Number 8, pp 731-738.
4. E. V. Pereloma, Crawford and Hodgson, Strain-induced precipitation behaviour in hot rolled strip steel, Material Science and Engineering, A299, pp. 27, 2001.
5. A K Bhakat , P K Maini , M K Pradhan , C Muthuswamy, Development of High Strength Hot Rolled Coils with Enhanced Formability Property, International Journal of Metallurgical Engineering, 2013, Volume 2, Number 3, pp 249-253.



Slow Strain Rate Testing Behavior of Tailor Welded Blank (TWB) of Al 5052 H32-6061 T6 Alloy

Arpit R Patil^{1*}, S T Vagge^{*1}

Department of Metallurgy and Materials Science, College of Engineering Pune¹, arpitpatil@gmail.com*

ABSTRACT

The reduced heavy weight and high strength to weight ratio of Al and its alloys make them good alternatives to ferrous materials in particular industrial applications. Thus with the aim of reducing weight of the vehicle aluminium alloys are increasingly employed in the automotive industry. Thus when any component is welded in such a fashion it will be under continuous loading. This loading may strain the weld at a very low strain rate. Most of the previous researcher concentrated on study of parent metal for slow strain rate testing. Again some researchers had studied the welded joint for slow rate testing but they had used only those tensile specimens for the slow strain rate tests, which were prepared with the tensile direction perpendicular to the welding direction. Thus there is scarcity of research in the area of SSC of welded aluminium alloy. Therefore it is need to analyze the behaviour of such a joints under application of very small strain rate. In the present study, the slow strain rate testing behavior of Tungsten Inert Gas Welded (TIG) Al 5052 H32-6061 T6 is studied. The rectangular shape tensile specimens were used for the slow strain rate tests, which were prepared such a that each specimen is with the tensile direction perpendicular to the welding direction, another specimen parallel to the welding direction such a that the 6 mm width of specimen contain 3 mm Al 5052 H32 with 3 mm weld, and another tensile specimen consisting of 3 mm weld with Al 6061 T6 alloy, another specimen with the 6mm width of weld alone, and the parent alloy of weld i.e. Al 5052 H32 and Al 6061 T6. This type of specimen testing will cover the overall direction study of slow strain rate testing on the Tailor Welded Blank (TWB). The in-situ slow strain rate tests were performed in air environment with strain rate of 0.0017 mm/min (i.e. 2.8×10^{-8} m/s) on a slow strain rate testing machine. Each data represents the average of at least three test results. In the present conference we will try to present the work related to comparison of results obtained during testing in air environment. The Al 6061 T6 (Yield strength of 338 N/mm²) has shown higher strength over Al 5052 H32 (Yield strength of 223 N/mm²). The specimen with weld zone transverse to loading direction has shown lowest strength while those specimens having weld zone parallel to loading direction had shown intermediate values of strength. The specimen with welding direction parallel to loading direction has shown brittle nature for weld while that for parent blank it has shown ductile failure. This work can be further extended to study the welded joint for other environments for varying strain rates.

KEYWORDS Aluminium alloys, Tailor welded blank, Slow strain rate testing, Optical microscopy.

INTRODUCTION

In today's manufacturing scenario, much research is carried out to reduce the weight of automotive vehicles. Tailor Welded Blanks (TWBs) became popular since late 90s to achieve such reduction in weight of the vehicles. Lot of issues have been discussed by many researchers regarding the forming of tailor welded blanks.

The main problem which may usually occur during forming of TWBs is "formability deterioration". Most of the researchers have suggested many options to overcome such type of problem. Initially many researchers have concentrated on TWBs made from steel and its high strength alloys. Laser welding became popular to manufacture TWBs from high strength steels. However, recently the use of Aluminium alloys has attracted automotive field and hence in last decade more research work is going on to study the forming behaviour of Aluminium alloys. As material is changed, its joining methods are changed and joining methods like Tungsten Inert Gas TIG welding and Friction Stir Welding (FSW) came into focus to prepare TWBs from different Aluminium alloys. Different grades of Aluminium, whose weld-ability is good, have proven themselves suitable for many applications in Ship building, Aerospace industries and Automobile industries[1,2]. The welding of Aluminium and its alloys is difficult due high thermal conductivity, high hydrogen solubility, high oxygen reactivity.

EXPERIMENTAL METHODS

Table 1 shows the standard properties of the parent material and **Table 2** shows the composition of the parent material used for TWB.



TIG Welding

Figure 1 shows the TIG welding setup. The blank of Al5052 H32 and 6061 T6 are tighten by using clamping. The aluminium AA4045 rod is used as a fillet material.

Table 1 Blank material (mechanical properties)

Property	AA5052-H32	AA6061-T6
Tensile strength, MPa	240	368
Yield strength, MPa	193	279
Total Elongation, %	10.4	10

Table 2 Chemical compositions (%) of blank material

Element	Si	Fe	Cu	Mn	Mg	Cr	Zn	Ti
AA5052-H32	0.120	0.300	0.005	0.095	2.463	0.191	0.001	0.015
AA6061-T6	0.64	0.34	0.25	1.038	1.03	0.193	0.004	0.023

SLOW STRAIN RATE TEST

Slow Strain Rate Test (SSRT) is a test carried out on special purpose test machine and it is similar to a normal tensile test carried out on general purpose Universal Testing Machine (UTM) machine. The only difference is the strain rate. In slow strain rate test machine the value of strain rate can be kept to very low value i.e. up to 0.0017 mm/min (2.8×10^{-8} m/s). SSRT is usually carried out to see the effect of environmental corrosive action on a component which is always undergo a very small amount of loading. Hence, this test is carried out in different environment such as different solution environments like sea water, different chemicals or in simple air environment. Any component used in automotive part, especially TWBs, will also be under continuous loading. This loading may strain the weld at a very low strain rate. SSRT gives the information about how material responds to very small amount of straining. Most of the previous researcher concentrated on study of parent metal for slow strain rate testing. Some researchers had studied the welded joint for slow rate testing but they had used only those tensile specimens for SSRT, which were prepared with the tensile direction perpendicular to the welding direction. Thus there is scarcity of research in the area of SSRT of welded aluminium alloy. Therefore it is required to analyze the behaviour of such joints under application of very small strain rate. In the present study, the slow strain rate testing behavior of (TIG) Welded AA5052-H32 and AA6061-T6 is studied. The dumbbell shape tensile specimens, as per ASTM E8 [3] standards (sub-size specimen), were prepared by wire cut process for the slow strain rate tests as shown in Figure 2.

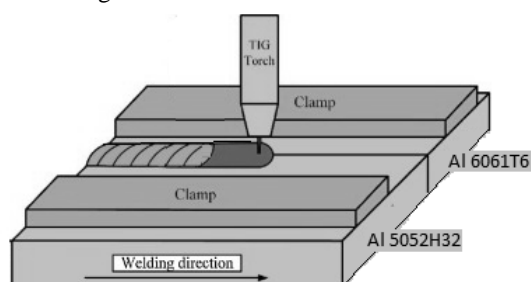


Figure 1 TIG welding setup

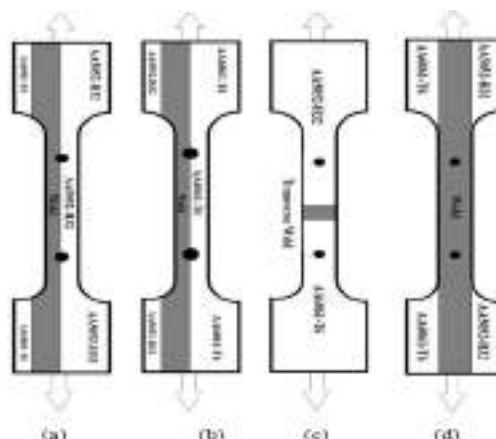


Figure 2 Tensile specimens of TWBs for SSRTs



These specimens were prepared such a way that, in specimen (a) and (b) loading direction of tensile load is kept parallel to the welding such a that the 6 mm width of specimen contains 3 mm AA5052-H32 with 3 mm weld, and another tensile specimen consisting of 3 mm weld with AA6061-T6 alloy. Specimen (c) is of transverse loading i.e. the tensile direction is kept perpendicular to the welding. Specimen (d) is of longitudinal loading with the 6 mm width of weld alone. The parent materials i.e. AA5052-H32 and AA6061-T6 are also wire cut in the above shape. This type of specimen testing will cover the overall direction study of slow strain rate testing on the TWBs. The in-situ slow strain rate tests were performed in air environment with strain rate of 0.0017 mm/min (i.e. 2.8×10^{-8} m/s) on a slow strain rate testing machine (the lowest possible strain rate). The results of the same are discussed in following section of this paper.

Results of Slow Strain Rate Tests (SSRTs) The blanks (TWBs) obtained after TIG welding operation are cleaned. Then the dumbbell shape tensile specimens (sub-size specimens), as per ASTM E8[3] standards, were prepared by wire cut process for the slow strain rate tests as shown in **Figure 2**. The slow strain rate testing is performed according to standard ASTM G129 [4] on “United SSTM- 20KN” machine. The results in terms of stress-strain

Very slow strain rate tests, such as $1 \times 10^{-8} \text{ s}^{-1}$, lasting for longer period of time, have been used where, concern over long crack initiation periods (perhaps related to chemistry and/ or potential changes experienced in service) or a low Crack Growth Rate (CGR) justified it, or it was desired to avoid significant plastic deformation and get failures below or slightly above the yield stress[5]. It can be clearly seen from **Figure 3** that, the stress-strain curve of parent materials (without welding) have shown ductile failure and their Yield Tensile Strength (YTS) is noted up to 223 MPa for AA5052-H32 and 338 MPa for AA6061-T6. However, for all TWBs (both transverse and parallel loading), the stress-strain curves are showing brittle failure and their respective YTS values are mentioned in Table 3 below. **Table 3** shows that, when weld undergoes transverse loading, it exhibits good strength than that of when it is loaded in parallel directions. It means that, if material is getting stretched perpendicular to weld direction then it will have good strength. But, if material is getting stretched parallel to weld direction, then it may fail early because of less strength of the weld in parallel loading. In case of TIG welding, very high temperature increases the peak temperature of the molten weld pool causing slow cooling rate, intern causes relatively wider dendritic spacing in the fusion zone as observed from the **Figure 3** [6]. Previous researcher also quoted the same reason for failure of TIG welded Al 6 series [7,8]. The porosity also plays an important role in deciding the strength of the weld produced by TIG welding operation. Porosity occurring in aluminum alloy fusion welds was mainly due to the removal of hydrogen during weld solidification, and excessive porosity in the fusion zone reduced the static strength of weld [9].

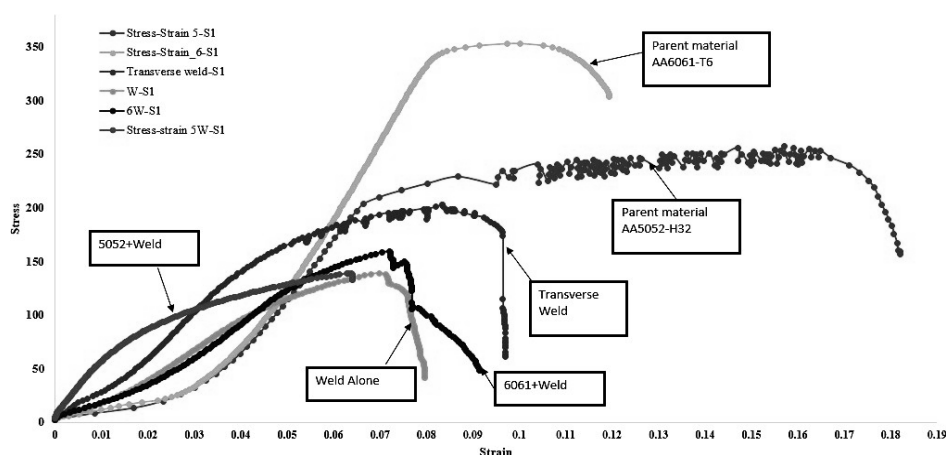


Figure 3 Stress-strain diagrams of TWBs obtained from SSRTs

Table 3 YTS of TWBs obtained from SSRT

Type of loading	Specimen (as per Figure 4)	YTS, MPa	When compared with YTS of AA5052-H32	When compared with YTS of AA6061-T6
Transverse	c	203	91.03%	60.06%
	a	140	62.78%	41.42%
Parallel	b	160	71.75%	47.34%
	d	138	61.88%	40.83%

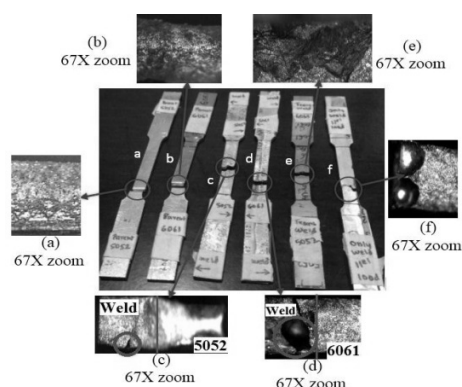


Figure 4 Failed tensile samples of SSRTs and their respective microstructure

Hence further, the portions, where all specimens are failed, are observed under Rapid- I Vision Measuring System with 67X zooming capacity. The microstructure at this level is sufficient to conclude whether the nature of failure is “tensile” or “brittle”. **Figure 3** shows the SSRT failed samples and their respective microstructures. It can be clearly seen from the microstructures of weld samples (c), (d), (e) and (f) that, the failure occurs due to porosity of the weld. The weld portion responds like brittle material and parent material shows ductile failure (please see red marked circle in **Figure 4** (c) and (d)). Hence, there is further scope of more microstructure study to find out the affecting element which is contributing in the brittle fracture of the weld. The silica content in AA6061-T6 (i.e. 0.64%) may be causing brittle type of failure in weld as the literature[10] suggest that the Si content above 0.1% causes crack formation. The TIG welded zone has shown lower strength of 138 MPa with brittle failure and the parallel welds have shown lower strength than transverse weld this may be due to the porosity and the crack generation due to Si present in the weld material [11]. If conical shapes are formed, material gets elongated in radial direction and if we try to form TWBs then weld portion of TWBs gets elongated similarly, which means weld is getting stretched in parallel direction and as the strength of weld in parallel direction is weak, it fails [12,13]. Brittle nature of the weld portion may be the reason behind this weak strength. But it is not getting clear idea from stress-strain curve that really the weld portion exhibits brittle failure or not [14, 15].

CONCLUSION

- Samples having Transverse weld i.e weld direction perpendicular to loading has shown greater strength 203 MPa than the samples having weld parallel to loading axis.
- The TIG welded zone has shown lower strength of 138 MPa with brittle failure.
- The fractography of failed samples with welds parallel to loading direction has shown ductile failure of the parent metal while brittle nature for weld zone.

REFERENCES

1. K.S. Arora, S. Pandey, M. Schaper, R. Kumar, Journals of Advanced Manufacturing Technology, Volume 50, pp 941–952, 2010.
2. J Altenkirch., A Steuwer, M Peel, D.G. Richards, P.J. Withers, Materials Science and Engineering A, Volume 488, pp 16–24, 2008.
3. ASTM E 8M, Standard Test Methods for Tension Testing of Metallic Materials



4. ASTM G129, Standard Practice for Slow Strain Rate Testing to Evaluate the Susceptibility of Metallic Materials to Environmentally Assisted Cracking, Volume 3, Number 2, 2013.
5. M. Henthorne, The Slow Strain Rate Stress Corrosion Cracking Test — a 50 Year Retrospective, *Corrosion*, Volume 72, Number 12, pp 1488-1518, December 2016.
6. W. Xunhong, W. Kuaishe, S. Yang, H. Kai, *Journal of University of Science and Technology Beijing, Mineral, Metallurgy, Material*, Volume 15, pp 280-284, 2008.
7. M. M. Sharma, J. D. Tomedi, T. J. Weigley. Slow strain rate testing and stress corrosion cracking of ultra-fine grained and conventional Al-Mg alloy. *Materials Science and Engineering: A*, Volume 619, pp 35–46, 2014.
8. G. Singh, A. S. Kang, K. Singh, J. Singh. Experimental comparison of friction stir welding process and TIG welding process for 6082-T6 Aluminium alloy. *Materials Today: Proceedings*, Volume 4, Number 2, pp 3590–3600, 2017.
9. X. Wang, K. Wang, Y. Shen, K. Hu. Comparison of fatigue property between friction stir and TIG welds. *Journal of University of Science and Technology Beijing, Mineral, Metallurgy, Material*, Volume 15, Number 3, pp 280–284, 2008.
10. Leong Huat Hardware. Effect of Mn, P, S, Si & V on the Mechanical Properties of Steel. <https://www.leonghuat.com/articles/elements.htm>.
11. S. P. Lynch "Mechanistic and fractographic aspects of stress-corrosion cracking (SCC)", *Stress corrosion cracking*, Woodhead Publishing Limited, 2011, 1-87.
12. W. Dietzel and P. Bala Srinivasan, Testing and evaluation methods for stress corrosion cracking (SCC) in metals, *Stress corrosion cracking*, Chapter 3, Woodhead Publishing Limited, pp 1-34, 2011.
13. Seong-Jong Kim, Jae-Yong Ko and Min-Su Han, Evaluation of the characteristics using slow strain rate tests of 5456 Al-Mg alloy for ship construction, *Korean J. Chem. Eng.*, Volume 23, Number 6, pp 1028-1033, 2006.
14. A. Atrens, *Stress corrosion cracking (SCC) of magnesium alloys*, *Stress corrosion cracking*, Chapter 3, Woodhead Publishing Limited, pp 1-40, 2011.
15. T. Shoji, Z. Lu and Q. Peng, Factors affecting stress corrosion cracking (SCC) and fundamental mechanistic understanding of stainless steels, *Stress corrosion cracking*, Chapter 6, Woodhead Publishing Limited, pp 1-28, 2011.



Material Selection for Wear Control in Industries

Pradip Sahana^{*1}, K K Singh¹

Engineering Metallurgy and Tribology Group, RDCIS, SAIL, Ranchi¹, pradipsahana@sail-rdcis.com*

ABSTRACT

Material loss due to wear is one of the important factors that affects the longevity of costly machine components in the industries. Identification of suitable material is the appropriate choice to secure them for longer time. Alloyed white cast irons, tool steels, martensitic stainless steel, high manganese austenitic steel are well known for wear resistance for different applications. The extraordinary performance of the above materials is due to the presence of large amounts of carbides in microstructure which exhibit high hardness. Shape, size and type of the carbides control the wear resistance and toughness. The wear can be extensively improved by varying the composition or by imparting specific heat treatment. Besides metals and alloys, ceramics and polymers are also extensively used for wear resistance application. The present paper presents an overview on wear and identification of different types of materials commonly used for life improvement of costly machine components exposed to wear.

KEYWORDS Wear, White cast irons, Tool steels, Stainless steels, Ceramics, Polymers

INTRODUCTION

Wear is the gradual loss of materials from one body when subjected to contact and relative motion with another body and consider as one of the influencing factors limiting the effective life and performance of engineering component. There are several types of wear takes place in industrial components amongst abrasive wear is considered as the prominent mode of wear. Roughly three-fourths of failure in components or machine parts are due to wear [1] and more than half of the total wear related failure of industrial components is due to abrasive wear [2]. The cost of abrasive wear is very high and has been evaluated as 1 to 4 pct of a gross national product of an industrialized nation [3]. The volume of wear debris produce (Archard wear equation) is proportional to contact load, sliding distance, wear coefficient and inversely proportional to the hardness of the material exposed to abrasive wear. Decreasing contact load, reducing sliding distance and reducing the coefficient of friction can reduce the abrasive wear loss. However, variations of these parameters are repeatedly impossible in operation if the function of a machine is to be maintained. Then, increasing hardness by means of material selection with imparting proper heat treatment and or surface engineering will be the most practical and comparatively easy way to resolve an abrasive wear problem.

IMPORTANT FACTORS AFFECTING WEAR

There are several factors which influence the wear and it depends on normal load, sliding speed, surface roughness of the contact surfaces, type of material, temperature, relative humidity. Among these factors type of material, sliding speed and normal load are the major factors that play a significant role for the alteration of wear rate. It has been observed from Archard wear equation, that the hardness is inversely proportional to wear of the material. The hardness of the material gives an indication of the wear resistance of a material; however, studies have indicated that the introduction of certain alloying elements increases the wear resistance but not the hardness. The rate of wear increases with increasing the load and speed exerted on the system. Kumar [4] showed that the effect of load shows greater influence on wear as compared to sliding speed which can result in degradation of material at a faster rate than normal condition. The surface roughness of the contact surfaces has a major role on the wear rate. With a decrease in surface roughness wear rate decreases. Generally, an increase in temperature of the contact surfaces tends to produce an increase in wear rate, because with the increase in temperature the material associated with become softer.

IDENTIFICATIONS OF THE CAUSES OF WEAR AND THE WEAR SITUATION

It is important for the material technologist to identify the nature of wear taking place in a given situation because the selected materials to reduce wear will depend on the nature of the wear process. However, it may be important to consider the cause of wear in a much more general sense, because the most common causes of excessive wear are not related to the selection of superior wear resistance materials. Different causes of wear problem may include the supply of incorrect material, wrong heat treatment, faulty manufacture and changes in the operating parameters/conditions. If neither the operating parameters nor the materials fault leads to a solution to the wear problem, it becomes necessary to reconsider the selection of superior materials.



In order to make the best selection of material to resist wear for a given situation, it is mandatory to identify the type of wear mechanism which is taking place. The various wear mechanism takes place in the system, it may include sliding wear, three body abrasion, low stress abrasion, gauging wear, fretting, erosion and corrosion wear. A great deal of information may be obtained from the examination of the worn surface about the wear mechanism taking place in the tribo-system.

WEAR RESISTANCE MATERIALS

For any tribo-system, hardness and toughness of the materials are key parameters for selection of material for wear resistance application. The chemical composition or microstructure of the material is one of the attributes that make it more resistant to wear. Heat treatment is another factor that helps in forming secondary carbide in the materials to improve the wear resistance by forming different phases which give the material to the required high hardness and toughness. Through variations in composition and heat treatment, hardness and toughness can be adjusted to meet the needs of particular wear applications. For the selection of suitable wear resistance material following points i.e. cost of replacement, a cost to life ratio, ease of fabrication, ease of replacement, access for maintenance and amount of production loss should also be considered. Several types of materials i.e. Iron base alloy, Steel base alloy, Ceramic base and Polymer base can be used to increase the wear resistance. Most common types of wear resistance materials used in industrials applications are discussed below.

Alloyed White Cast Irons are the most wear resistant iron base alloys. Their wear resistance is mainly due to the formation of hard carbides during solidification. The alloyed white irons are included high-chromium, chrome-molybdenum, nickel-chrome. The compositions of typical alloyed white cast irons are given in **Table 1**.

Table 1 Composition (wt %) and hardness of wear resistant white irons as per ASTM A532-87 (1992)

Class/ type	Designation	Composition, wt%	Mn	Si	Ni	Cr	Mo	Cu	P	S
I A	Ni-Cr-HC	2.8-3.6	2.0	0.8	3.3-5	1.4-4.0	1.0	-	0.3	0.15
I B	Ni-Cr-LC	2.4-3.0	2.0	0.8	3.3-5	1.4-4.0	1.0	-	0.3	0.15
I C	Ni-Cr-GB	2.5-3.7	2.0	0.8	4.0	1.0-2.5	1.0	-	0.3	0.15
I D	Ni-HiCr	2.5-3.6	2.0	2.0	4.5-7	7.0-11	1.5	-	0.10	0.15
II A	12%Cr	2.0-3.3	2.0	1.5	2.5	11.0-14	3.0	1.2	0.10	0.06
II B	15%Cr-Mo	2.0-3.3	2.0	1.5	2.5	14.0-18	3.0	1.2	0.10	0.06
II D	20%Cr-Mo	2.0-3.3	2.0	1-2.2	2.5	18.0-23	3.0	1.2	0.10	0.06
III A	25%Cr	2.0-3.3	2.0	1.5	2.5	23.0-30	3.0	1.2	0.10	0.06

HC: High
Carbon,
LC: Low
Carbon,
GB:
Graphite
bearing

High Chromium White Irons: High chromium white cast iron is one of the wear resistant materials used in different applications where stability in a hostile environmental is a main requirement. These alloyed white irons are acknowledged as contributing the best combination of wear resistance and toughness obtainable among the white cast irons. Their outstanding wear resistance is largely because of their solidification microstructures. During solidification, high levels of chromium present in material lead to the formation of a high-volume fraction of eutectic M₇C₃-carbides. Heat treatments of these alloys are necessary to change their microstructure and to improve wear resistance to suit the individual application. These applications include in coal-grinding mills/ pulverizing mill



roll, slurry pumps, brick molds, shot-blasting equipment, rolling mills rolls, and components for quarrying, hard-rock mining and milling.

Chromium-Molybdenum White Cast Irons: It provides the highest level of wear resistance and toughness. It complies with ASTM A532 Class II, Type B and D chemical requirements. Molybdenum increases the strength and hardness of cast irons by lowering the pearlitic phase transformation temperature. It also increases high temperature strength and creep resistance. High chromium irons with 2 to 3 wt % molybdenum show prominently greater impact toughness than Mo-free grades and are suitable for severe wear conditions like those encountered in crushing, mining, milling etc.

Nickel-Chromium White Irons (Ni-Hard Iron): In Nickel-Chromium white irons, nickel (3 to 5%) is the primary alloying element. Chromium (1.4 to 4%) ensures that the formation of irons carbides and to retard the graphitizing effect of nickel. The optimal composition of a nickel-chromium white iron alloy depends on the properties required for the operation conditions and the weight and dimensions of the casting. These alloys are suitable for applications includes in ash pipes, slurry pumps, roll heads, augers and coke crusher segments.

Steel Base Alloy: Among the steel base wear resistance materials; tools steels, martensitic stainless steels and high manganese stainless steels are the most commonly used.

Tool Steel: It contains a variety of carbon and other alloy elements such as Cr, Mo, V and W. The presence of carbides in their matrix plays the important role in the qualities of these steel. Among the tool steels; high-carbon high-chromium cold-work tool steels (D2), chromium hot-work tool steels (H13) and molybdenum high-speed tool steel (M2) are considered as well known materials for wear resistance applications. Nominal compositions and typical heat treatment cycle of the above mention tools steels are present in **Table 2** [5].

Table 2 Nominal composition and heat treatment cycle of different tool steel.

AISI	Alloying elements (wt.%)								
	C	Mn	Si	Cr	Ni	Mo	W	V	
D2	1.40-1.60	0.60 max	0.60 max	11.0-13.0	0.30 max	0.70-1.20	-	1.10 max	
H13	0.32-0.45	0.20-0.50	0.80-1.2	4.75-5.50	0.30 max	1.10-1.75	-	0.80-1.20	
M2	0.78-0.88	0.15-0.40	0.20-0.45	3.75-4.50	0.30 max	4.50-5.50	5.5-6.75	1.75-2.20	
Heat treatment cycle (in °C) and the surface hardness in as quenched cond (HRC)									
	Hardening	Tempering	HRC						
	D2	1000-1040	500-540	61-64					
	H13	1040-1050	630-650	51-54					
	M2	1150-1250	600-620	64-66					

High Carbon, High-Chromium Cold-Work Tool Steels (D2): The high carbon, high-chromium tool steels is the most highly alloyed cold-work steels. Chromium is the main alloying element, but nickel, molybdenum, vanadium; manganese may be added in significant amounts in D2 steels. These steels are deep hardened by heat treatment and hardness can be achieved HRC 61-64. Due to high carbon and high chromium content, the wear resistance of D2 tool steel is approximately eight times that of plain carbon steels. Not only is tempered high-carbon martensite an important component of the microstructure, but large volume fractions of alloy carbides also play an important role in attaining high wear resistance. Typical applications are roller shell for coke crusher, tools for intensive sinter mixer in sinter plant, shear blades, forming rolls, forming dies, punches, knives, scrap choppers etc.



Chromium Hot-Work Tool Steels (H13): Chromium hot-work tool steels for hot-work applications have the important properties to resist softening during long or repeated exposures to high temperatures and used for hot work applications. It contains nominally 5 wt % Cr and significant amounts of other elements including molybdenum, silicon and vanadium. The carbon (0.32- 0.45 wt %) promotes toughness by limiting the carbon concentration of the martensite and by controlling the size of alloy carbide particles. **Typical applications** are hot forging and pressing dies, extrusion dies, mandrels and punches, hot chisels, hot heading tools, pressure pads, blanking and bending tools, extrusion stems and rams, backer blocks.

Molybdenum High-Speed Tool Steel (M2): Molybdenum high-speed tool steel is well known for a balanced combination of wear resistance, toughness and good red hardness. Due to its comparatively low carbon content, it has an excellent combination of toughness properties and wear resistance when properly hardened and tempered. This steel has the ability to maintain high hardness at elevated temperatures (typically, 52 HRC at 540°C). It is used for steel mills rolls, crushing and hammering tools, reamers, broaching tools, milling tools, metal saws knife, punch and die applications.

Martensitic Stainless Steel: Martensitic stainless has better wear resistance than any other stainless steel, because of its high hardness that can be achieved through proper heat treatment. The size and volume fraction of the carbide particles present and the amount of retained austenite play a vital role in determining the hardness, strength, toughness and wear resistance of the steel. Tempered martensitic steel gives an excellent combination of high hardness and toughness, used largely for shear blades, coal handling and in mining equipment. Typical grades of martensitic stainless steel are AISI 410, AISI 420, AISI 440C etc and are listed in **Table 3** [6].

Table 3 Typical chemical composition and hardness of martensitic stainless steel.

AISI	Alloying elements, wt.%							
	C	Mn	Si	Cr	Mo	Ni	S	P
410	0.15	1.00	1.00	11.50-13.50	-	0.50	0.03	0.04
420	0.15-0.40	1.00	1.00	12.00-14.00	-	0.50	0.03	0.04
440C	0.95-1.20	1.00	1.00	16.00-18.00	0.75	1.00	0.03	0.04
Hardness (HRC)	AISI 410: 38-45 HRC	AISI 420: 53-57 HRC	AISI 440C: 58-60 HRC					

High-Manganese Austenitic Steel: It contains about 1 to 1.4% C and 11 to 19% Mn is used as materials for resistant to wear under high dynamic loads. Carbon and manganese content plays an important role in improved properties of high manganese steel. High manganese steel has a high capacity for work-hardening upon impact. In gouging abrasion, high manganese austenitic steel performs better than wrought alloy steels, cast alloy steels, stainless steels, tool steels or high-chromium steel and white cast irons [7]. Due to its unique service properties, it has been used widely in a number of applications like jaw crushers and a number of high impacts hammer, liners of coke crusher rollers, earth moving equipment, rail tracks, dredge buckets etc.

Ceramics are widely used in the process industries and manufacturing industries because of its high hardness, wear resistance, low density, high melting point, thermal and corrosion resistance. The finer the grain size is important for the higher strength and toughness of ceramics. Among the ceramics; alumina and silicon carbide are widely used for wear resistant application and their properties are given in **Table 4** [8].

Alumina Oxide is the most commonly used ceramics, because of its wide acceptance; alumina has a high hardness of all materials except diamond, excellent wear and corrosion resistance. It is also fairly economical to manufacture, involving low-cost of alumina powders. Depending upon the requirements for toughness, zirconia toughened alumina can be used. The sintered alumina tiles may be formed with rubber/ polymer or steel backing plates where it is required to resist severe abrasion and impact due to abrasive medium. Alumina ceramics, typically having alumina contents from 85 to 99% Al_2O_3 . Depending upon on service requirement, the purity of alumina can be varied. For most of the abrasion resistance components application, purity of alumina in order of 92 to 96% is sufficient. Alumina ceramic tiles and linings are frequently used in applications like chutes, hoppers, pipes, conveyor belts, and production systems where there is moving object sliding across surfaces.



Silicon Carbide has found many applications in advanced ceramics. There are actually two families of silicon carbide, one known as direct-sintered SiC (SSiC), and the other known as reaction-bonded SiC (also referred to as siliconized SiC) (RBSiC or SISiC). Silicon carbide has a high hardness (second only to diamond), low density—approximately the same as aluminum and excellent thermal shock resistance. The properties of the two families of SiC are shown in **Table 4**. Both materials have very high hardness and high strengths (> 460 MPa). However, the fracture toughness of both materials is generally low (3 to 4 MPa m^{1/2}). The major differences are found in wear resistance. Direct-sintered SiC has a greater ability to withstand severely abrasive environments. Silicon carbide steel shell lined with products, due to its good wear resistance and corrosion resistance, is acceptable for conveying powder, slurry, widely used in power plants, mining, mineral processing and other industries.

Table 4 Properties of alumina and silicon carbide ceramics.

Material	Bulk density, gm/CC	Flexure strength, MPa	Hardness, GPa	Fracture toughness, MPa m ^{1/2}
85 to 99.9 % alumina	3.41 -3.96	317-552	9-15	3-4
Sintered SiC	3.10	550	29	4
Reaction bonded SiC	3.10	462	29	3-4

Polymer: Polymers are used extensively for many applications because of their wide variety of properties (that is, strength, lightness, good wear resistance, environmental resistance and low cost) and relative ease of tailoring them. Among the polymer, Ultra High Molecular Weight Polyethylene and Polyurethane are widely used for abrasion resistant application and their properties are given in **Table 5** [9].

Ultra High Molecular Weight (UHMW) polyethylene is the world's toughest polymer and can be used up to 80°C. It has excellent wear resistance as well as high impact strength, excellent chemical resistance, extremely low moisture absorption and a very low coefficient of friction. Because of the above mentioned properties, UHMW is highly effective in a variety of applications. Its natural lubricity leads to extensive use for lining chutes, bin, silos, stacker/reclaimer bucket liners and hoppers to protect metal surfaces and to keep solid materials like iron ore, sinter and coal moving smoothly.

Polyurethane is an elastomeric material of exceptional properties including toughness, resistance to wear, high load bearing capacity and flexibility. The excellent wear resistance of polyurethane is a result of their high resilience and tendency to elastic deformation that allows the absorption of impact energy of erodant particles with minimum damage. Polyurethane unites the toughness of metal with the elasticity of rubber. Applications include chute, hopper liners, slurry transfer pipe, seals, gears, wheels, bearings, and solvent lines.

Table 5 Properties of UHMWPE and polyurethane

	UHMWPE	Polyurethane
Rockwell Hardness (R, shore D scale)	62 Shore D	R119
Izod impact strength (Joules/m)	No break	320
Tabor Abrasion (mg loss/1000 cycles)	30	<45
Maximum service temp, °C	82	82

CONCLUSIONS

- Wear is one of the important causes of premature failure of the components of industries equipment. It can be controlled by selecting a suitable material for a particular tribo-system.
- Selection of suitable wear resistant materials for a particular system is based on the composition, microstructure, hardness, fracture toughness etc.
- Hardness and toughness of the materials are *key parameters* for the determination of *wear resistance* of the materials. Presence of carbides present in the matrix plays an important role to improve wear resistance.
- Alloyed white cast irons i.e. high chromium white iron, chrome-molybdenum white iron and nickel-chromium white iron are the most wear resistant iron base alloyed with limited impact resistance compared to steels.



- (e) Tool steels, particularly high carbon-high chromium cold work tool steel, Molybdenum high speed steel, chromium hot work tool steel with varying Carbon (0.5-1.5%), Chromium (3.75-13.0%), Ni-Mo-V with proper heat treatment are most suitable for wear resistance applications.
- (f) High manganese austenitic steels are recommended for wear resistance under high dynamic loading condition.
- (g) Martensitic stainless steels provide better wear resistance than any other stainless steel with proper heat treatment condition.
- (h) Ceramics materials are the best choice for wear resistance applications where the components are exposed to low impact, high temperature and thermal shock.
- (i) Polymer materials are used for abrasion resistance applications where material requires high load bearing capacity with low weight and effective under high impact conditions because much of the impact energy can be dissipated through elastic deformation.

ACKNOWLEDGMENT

The authors acknowledge the constant support and guidance provided by GM (RT) RDCIS, SAIL and for granting permission to prepare and submit the paper. The help provided by DGM & HOG, RDCIS, SAIL is duly acknowledged.

REFERENCES

1. Mohd Shadab Khan, Zahir Hasan, Syed Mohd Farhan, Effect of Orientation and Applied Load on Abrasive Wear Property of Brass 60:40, Journal of Minerals and Materials Characterization and Engineering, 2, 49-53, (2014).
2. M. Adamiak, J. Gorka, T. Kik. (2009), Comparison of abrasion resistance of selected constructional materials, Journal of Achievements in Materials and Manufacturing Engineering, Volume 37, Issue 2, 375-380, (2009).
3. Ann Sundstrom, Jose Rendon, Mikael Olsson, Wear behaviour of some low alloyed steels under combined impact/abrasion contact conditions, Wear, Volume 250, Issue 1-12, 744-754, (2001).
4. S Kumar, V K Pathak, Effect of static load on Wear behaviour of 0.58% carbon steel, IJAMSE Vol.5, No.1, pp 21-27, (2016).
5. Tool steel, Vol 5, allaboutmetallurgy.com/wp/wp-content/uploads/2016/12/Tool-Steels.pdf.
6. Falgun Suthar, Uday Puntambekar, Mandar Joshi, Rojaleena Daspujari: Comparative evaluation of abrasive wear resistance of various stainless steel grades, GE-International Journal of Engineering Research, volume -3, issue-7, pp 21-35, (2015).
7. Sedmak, A. (2010), Austenitic Manganese Steels, <http://www.Keytometals.com/art69.htm>, (2013).
8. Structural Ceramics, AMS Hand book vol 2.
9. www.stug.com.au/materials/engineering-plastics-properties/index.php



Creep Studies of Nuclear-Grade Aluminium-Silicon Alloy

Vinay Karanam^{*1}, Rajesh Kumar Mishra¹

Homi Bhabha National Institute and Reactor Engineering Division, Bhabha Atomic Research Centre, Mumbai¹,

flvinay@gmail.com^{*}

ABSTRACT

Creep studies have been carried out on nuclear grade aluminium silicon alloy. The material is a popular candidate for nuclear in-core applications owing to its low cross section for neutron absorption and good thermal properties. The homologous temperature of operation which this material experiences is very high. The creep behaviour needs to be understood so as to estimate its creep strain rate and rupture time for ascertaining its structural integrity under all reactor operational conditions. An analytical model has been developed which estimates secondary region, the transition from secondary to the tertiary region, tertiary regions and rupture. The model is attuned to aluminium-silicon alloy under study and experiments carried out at various stress and temperature levels. Comparative plots of estimation made by the model developed in this study and experimental data are presented. The error in the model is within experimental uncertainties and is in good agreement.

KEYWORDS Creep; Aluminium Silicon alloy; Nuclear grade; model; tertiary region.

INTRODUCTION

In-core materials in nuclear reactors are expected to have low neutronic absorption cross section and good structural strength. Aluminium and its alloys are a good candidate material for many in-core components. The material behaviour such as high-temperature deformation under creep is an important parameter for the design of these in-core components. The high temperature creep deformation of a material is often characterized by steady-state secondary creep, initiation of tertiary creep and rupture time. Many researchers [1, 2] have extensively studied aluminium and their alloys. Many analytical models have been developed which can predict secondary region [3]. However, to study tertiary region and rupture, one needs to model at damage scale. The damage scale modelling often invokes many material constants. To determine these material constants numerous experiments needs to be carried out and tuned. The models are often computationally expensive, cumbersome and time intensive. To overcome these problems an attempt has been made to develop a damage based mathematical expression which would estimate creep behaviour of the material under study. The expression aims at predicting creep behaviour at various operating conditions which could prove to be user-friendly and handy designer's tool.

DESCRIPTION OF EXPERIMENTAL CONDITIONS

The aluminium alloy is silicon-based 4-series (4032) material popularly called Silumin. The material is in as-fabricated condition on which the experiments have been carried out. The composition of the material is Silicon 11 to 13%, Nickel 1 to 2%, rest being Aluminium. All other impurities individually shall be less than <0.1%.

Experiments have been carried out on cylindrical specimens with 4mm Dia., the gauge length of 30 mm and held with M8 × 10 thread on both ends.

The experimental conditions are listed in the **Table 1**.

DESCRIPTION OF THE ANALYTICAL MODEL

Mathematical modelling at damage scale has been developed which potentially can predict secondary region, tertiary region and rupture owing to the growth of damage parameter. This expression is modified Garafalo[4] and Kachanov [1] equations with the innovation of introducing hyperbolic expression by the authors in the study of creep behaviour using hyperbolic function [5].

$$\frac{d\varepsilon}{dt} = A \sinh\left(\frac{\sigma}{G}\right)^n e^{\left(\frac{-Q}{RT}\right)} \sinh\left(\frac{1}{(1-\omega)}\right)$$

$$\frac{d\omega}{dt} = B \left(\frac{\sigma}{G}\right)^n \sinh\left(\frac{1}{(1-\omega)}\right)$$

Where, ε – strain; A, B, n – material constants; σ – stress, MPa; G – shear modulus, MPa; Q – activation energy; R – ideal gas constant; T – temperature in K; t – time; ω – damage parameter.



In the expression developed by Kachanov [1], the damage parameter is power law-driven and is non-zero from the beginning of the creep curve. Ideally, the damage parameter is expected to be zero till the on-set of the tertiary region. This damage parameter grows and accelerates the creep behaviour. Theoretically, when the damage parameter, ω becomes one, the material fails.

RESULTS AND DISCUSSIONS

Experimental data and creep behaviour as predicted by the model developed in this study have been plotted. The creep strain is expressed in % and time is expressed in seconds. The creep strain initially grows at a rapid rate known as a primary region and then saturates into a steady state creep known as a secondary region. The secondary region starts accelerating and leads to rupture known as a tertiary region. The plots of creep strain against time are made and presented in **Figures 1, 2 and 3**.

Table 1 Details of experimental conditions

Case-1	Case-2	Case-3
T=400°C,	T=450°C,	T=500°C
$\sigma=14\text{MPa}$	$\sigma=7\text{MPa}$	$\sigma=3\text{MPa}$
T/T _m =0.72	T/T _m =0.78	T/T _m =0.84
$\sigma/\sigma_y=0.78$	$\sigma/\sigma_y=0.64$	$\sigma/\sigma_y=0.50$

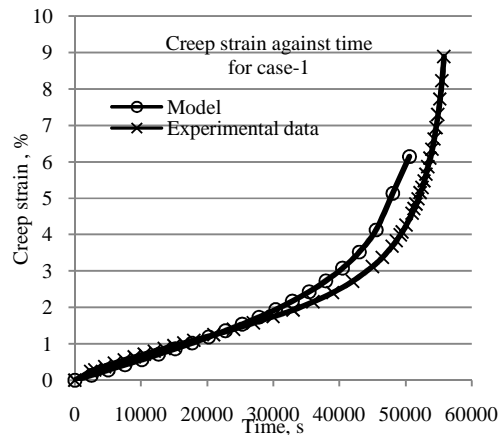


Figure 1 Comparative plot of the model and experimental data for case-1

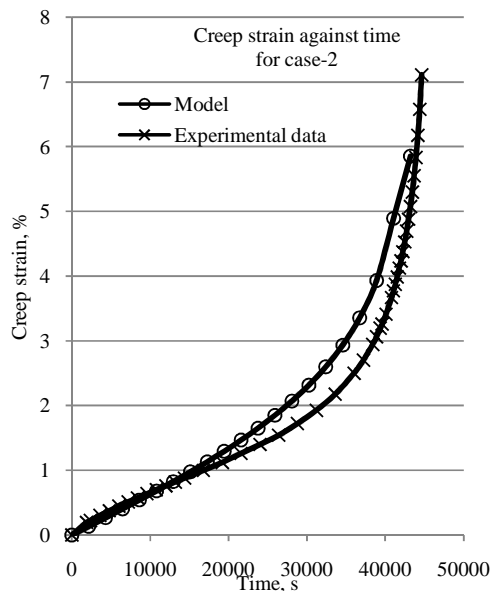


Figure 2 Comparative plot of the model and experimental data for case-2

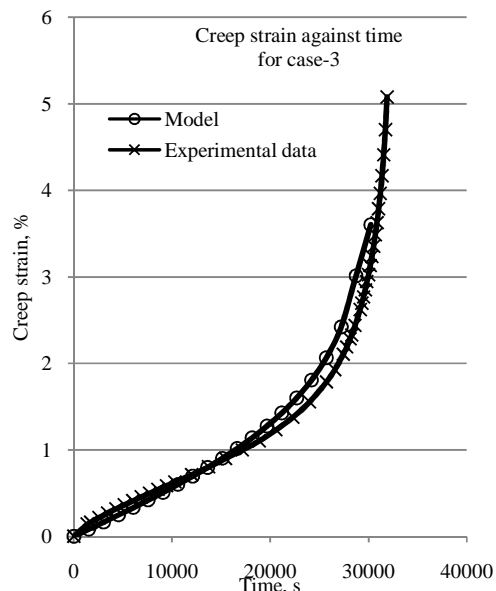


Figure 3 Comparative plot of the model and experimental data for case-3



From the above plots, it is seen that the experimental data and creep behaviour as predicted by the model developed in this study are in good agreement. The model is able to capture steady state secondary region, damage-inducing transition from secondary to the tertiary region, tertiary region and rupture. The error in model prediction is within 8% maximum which is within experimental uncertainties. The creep strain at rupture predicted by the model is lesser compared to experiments. This is due to the reason that the damage rate grows at a much rapid rate and reaches unity. At unity, the problem of singularity comes as hyperbolic sine tends to infinity. To avoid the singularity problem the expression is truncated at a value much before unity. This numerical assumption leads to under-estimation of creep strain at rupture.

CONCLUSION

An analytical model has been developed at the damage scale which predicts all the regions of creep. The model prediction is compared with experimental data for an aluminium silicon alloy which is used for in-core application of a nuclear reactor. There is good agreement with experimental data and model prediction for various temperature and stress conditions.

ACKNOWLEDGEMENT

Authors would like to thank Shri S. K. Sinha, Head VLS, RED for constant encouragement and opportunity to study. Also, would like to thank Head RED for all the technical suggestions made and permission to pursue this study. Thanks are also due to AD RD&DG and Director BARC for all intangible helps extended.

REFERENCES

3. Kachanov LM, Rupture time under creep conditions. Int. Journal of Fracture, 97:11–18 (1999)
4. Rabotnov Y.N. Creep rupture. In: Hetényi M., Vincenti W.G. (eds) Applied Mechanics. International Union of Theoretical and Applied Mechanics. Springer, Berlin, Heidelberg (1969).
5. F. H. Norton, The creep of Steels at High Temperatures, Mc-Graw-Hill, New York(1929).
6. Garofalo F., Fundamentals of Creep and Creep-Rupture in Metals, McMillan. Series in Materials Science, McMillan, New York (1965).
7. Vinay K., Time dependent simplistic model for tertiary creep deformation of reactor grade aluminium using modified garofalo-robinson equation, International Journal for Scientific and Engineering Research, 9(2), 1118-1123 (2018).



Sustainable use of Natural Resources: Integrating Technologies for Iron Making from Low Grade Ores

A. Ghosh^{*1}, B. Sensarma²

*Department of Mechanical and Material Handling, M.N. Dastur and Company (P) Ltd, Aneet.G@dastur.com**

Department of Mining and Mineral Beneficiation, M.N. Dastur and Company (P) Ltd²

ABSTRACT

Conventional process of iron making through Blast Furnace has predominance of using iron ore sinter as the primary Fe burden. Indian steel industry has been traditionally enjoying a strategic advantage of domestic availability of good quality of iron ore. Apart from such high grade iron ore, India is also endowed with large reserves of low grade iron ore. Over the years, with substantial mining of high grade reserves, shifts has been realized towards enrichment of beneficiation of low grade iron ore or even slimes through the route of pelletization which is of course is a positive step towards resource conservation and also helps to mitigate the environmental issues. Thus iron ore pelletization has become a focus technological process in ore to metal conversion chain for iron making in recent times. Iron ore pelletizing is of course preceded by development of appropriate technologies by adopting suitable beneficiation techniques for the utilization of low grade iron ore / slimes. This process of beneficiation is carried out in a wet state in the form of slurry. The beneficiated slurry, thus extracted as the product of beneficiation, is converted to an iron ore concentrate through suitable dewatering process and filtration. The concentrate thus produced is used as the primary Fe bearing raw material in the iron ore pelletizing process. BF grade pellets are prepared adding flux and binder and converting the mix into green pellets (balls) and then allowing the green pellets (balls) to pass through a process of induration to finally produce iron ore pellets fit to be fed to BF as a substitute of high grade lump ore and / or iron ore sinter to certain extent. In recent times, there is a tendency to maximize the use of iron ore pellets in BF process of iron making in order to effectively use the low grade ores / slimes. The integration of beneficiation technology and pelletizing technology could become an interesting area to explore, since it not only involves integration of multiple technologies, but also high skill system integration techniques in order to effectively develop a workflow aligned to present day endeavour of 'Make in India' movement.

INTRODUCTION

Indian steel industry has been traditionally enjoying a strategic advantage of domestic availability of good quality hematite ore. However, with the prevailing practice of mining, such deposits are depleting fast and getting exhausted. Apart from such high grade iron ore, India is also endowed with large reserves of low grade iron ore such as Banded Hematite Quartzite (BHQ), Banded Hematite Jasper (BHJ), Banded Magnetite Quartzite (BMQ) and Magnetite.

The abundance of low grade iron ores and ore fines has become a challenge in iron making process, particularly with a depleted availability of high grade lump ores. Hence, utilization of such ores and ore fines in order to effectively extract metal is in focus in the present day scenario. The intent to reduce lump ore and sinter in the burden charge to blast furnace is more and more growing across the globe, with US and Sweden leading the race for iron making with substantial pellet utilization. Traditionally, German & Russian technologies are more tending towards sinter and lump ore usage in blast furnace, still a tendency could be noticed even there also to shift to pellet route to substitute both for sinter and lump ore. Accordingly, the process of enrichment of iron ore through removal of impurities by adopting suitable beneficiation techniques recovers substantial iron values. The utilization of abundant low grade ores and ore fines has obvious advantage related to environment friendliness as well. An attempt has been made to briefly outline the iron ore beneficiation and pelletization technologies and integration of the same to effectively deliver saleable product from the available ores.

IRON ORE BENEFICIATION

The iron ore, which is mined, is crushed and screened at the mine head to produce various grades of products to be used in the downstream iron making process. The lump ore which can be directly used in the burden charge in a blast furnace is only a part of the entire volume of ore mined. The coarser fines could be utilised in sintering, while ultra fines remain unutilised in the conventional iron making process and subsequent use in blast furnace. Apart from the above, low grade ores are also needed to be enriched by adopting suitable beneficiation technologies due to presence of high alumina. The abundance of availability of fines and also such low grade ores in India, demands adopting a full scale beneficiation process to effectively utilise the reserve in the entire chain of ore to metal conversion by



adopting the pellet route. According to an estimate (vide IBM Year Book 2017), of the total mined ores, 64.18 million ton is lump (33%), 126.73 million ton is fines (66%) and balance is concentrate. According to Table – 1 : reserves/resources of Iron Ore (Haematite) as on 1.4.2015 (by grades/states), the All India proved reserve (STD111) is about 4 billion ton, out of which only 1.2 billion ton is high grade lump ores.

Iron ore beneficiation is a process through which low grade/lean ore is upgraded to desired quality to recover the substantial iron values by adopting suitable beneficiation process. Since, we are in discussion regarding iron ore, the specific ore mined from the identified deposit, undergoes micronisation by means of crushing and grinding to reach the particulate size in order to liberate the impurities concerned, mainly alumina and silica. In this process the gangue gets separated by the process of classification followed by upgradation in gravity concentrator or magnetic separator. This process route is determined through a pilot test to be carried out reputed laboratories. Complex analysis of mineralogy of the ore needs to be carried out in order to arrive at the liberation size.

The ground ore wetted with water in a slurry form is then exposed to various stages of physical separation in specialized equipments like spirals, screw classifiers, magnetic separators, etc in order to recover the iron bearing particles. The iron rich slurry is then exposed to magnetic separation (high and low intensity depending on the case specific) for further enrichment. This stage of critical recovery of iron rich particles is determined in the pilot lab test which is unique for a specific ore type. Hence, the stages of physical separation including the magnetic separation are unique and a common process flow not likely to apply across various ore characteristics. The enriched slurry is then processed in a dewatering circuit in order to extract the enriched concentrate to be fed to the pelletization process.

In the full scale beneficiation technique, the process of grinding, classification, magnetic separation are not linear steps and may need to be iterated to include regrinding, fine grinding, subsequent stage of high intensity magnetic separation and so on. The complexity associated with the process flow is primarily determined during the pilot lab test with specific defined samples of the ores. The sampling and sample collection is also critical and demands technological expertise to arrive at a representative sample. The process flow is largely arrived at during the test work and hence the same has a critical role in defining the process flow. The major stages of beneficiation process are: Crushing and Grinding, Classification, Magnetic Separation, Regrinding, Follow up Classification / Magnetic Separation, and Dewatering.

Among the above, grinding and magnetic separation (high intensity) are power intensive processes and determines the major part of cost for conversion.

IRON ORE PELLETIZING

The pelletizing process was adopted in history primarily to treat ultra-fine mineral dressed products as a part of mine up-gradation because of the concern felt in those days that the availability of high grade ore appeared to be inadequate for development of steel industry. Subsequently, in order to improve blast furnace performance, there has been an increased demand of burden material rich in iron.

Thus the pelletizing process has been developed in its own rights to produce iron rich products to suit the burden permeability in blast furnace. A schematic is shown in **Figure 1**. Initially, fluxed pellets were not produced because it would require limestone to be transported to mine and returning it within pellet balls which are expensive to manufacture and lowering the iron content as well. However, as per the demand of the iron making process in blast furnace, fluxed pellets (basic pellets) have been subsequently incorporated in the process of pellet production. Accordingly, the ultra-fine ore concentrate is mixed with ground flux additives like limestone and dolomite, anthracite coal as solid fuel and the binder element, bentonite. This mixing takes place in a drum type mixer or a high intensity mixer as is often used in large pelletizing plants built in recent times. The ultra-fine particulates are supposed to have necessary specific surface area (cm^2/gm) in order to facilitate the balling effect achieved in a disc or drum pelletiser. In case the particulate specific surface area is low after beneficiating the ore, the extracted concentrate after dewatering circuit is processed in a Roller Press to improve the same. The mixing action is critical because it brings in the homogeneity of the constituent mix in the desired proportion. The mixed material is then fed to individual disc or drum pelletiser for green balling. The green balling phenomena is achieved through capillary action. Deep study has been carried out in history to develop the green balling technology. The green ball generation and its stability are of immense significance in the pelletizing process, since the productivity of the plant is actually achieved in this stage. The strength of the balls is low and tendency to degenerate remains during transportation. Hence, the transportation methodology has to handle the sensitivity associated with degeneration of green balls



which adversely affects the productivity of the plant at large. The green balls thus formed are screened to recycle the undersize rejects along with degenerated balls so that no incoming iron bearing particle is lost.

The charge of green balls is then led to a process of induration, wherein the balls are dried, pre-heated and fired at 1250°C to 1350°C under oxidized condition. As a result, oxide bridging, grain growth and some slag bonding occurs and the pellet strength is developed. The fired pellets are then cooled down to ambient temperature through forced air cooling. Since the process of induration is carried out in an oxidized environment, energy recuperation is adopted to optimise the energy needed for the conversion process. The thermal energy need is generally correspond to the ore characteristics and a typical estimate is furnished in **Figure 2**.

The pelletizing process is power intensive primarily because of the preceding grinding and filtration processes in order to produce the concentrate input. A typical estimate of electrical energy required for the entire process is given in **Figure 3**.

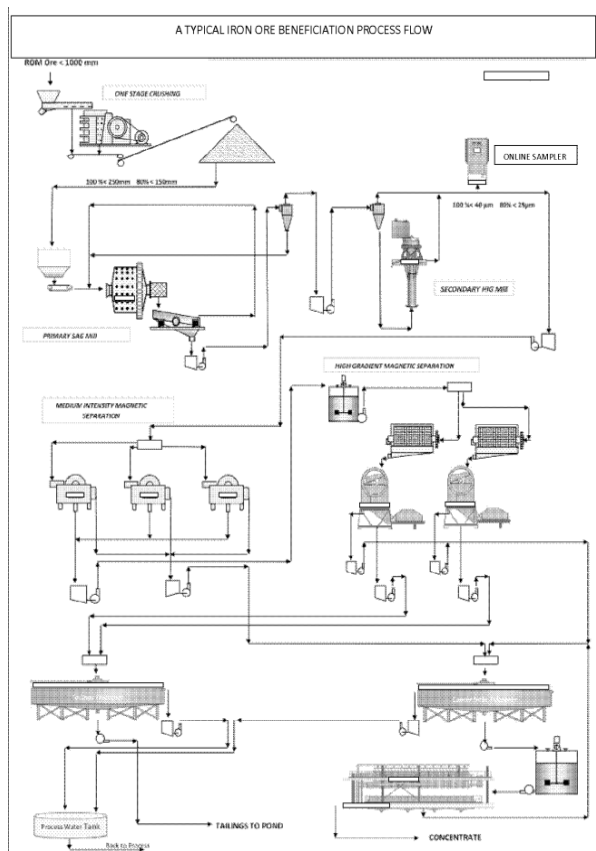


Figure 1 Typical iron ore beneficiation process flow to produce concentrate for pelletization

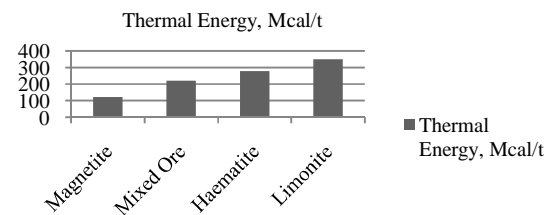


Figure 2 An approximate estimate of thermal energy requirement for pelletizing process for various ores

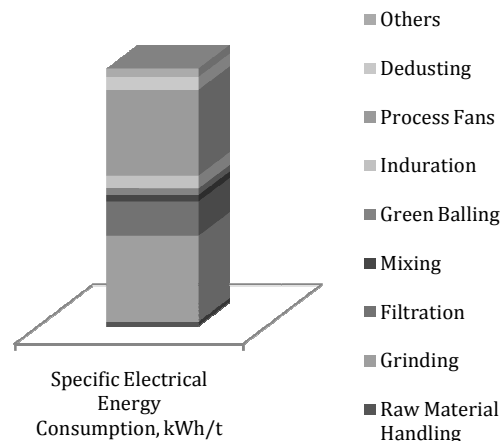


Figure 3 Graphical comparative of specific electrical energy consumption for pelletizing sub processes

Typical consumption range may be as indicated : Grinding-Filtration Unit = 25-30 kWh/t and Mixing-Green Balling-Induration-Process Fans-Dedusting-Others= 30-35 kWh/t.

Grinding and dewatering are part of beneficiation process. However, when the ore quality does not need a full scale beneficiation, only grinding and dewatering stages are needed to produce the concentrate for further pelletization. Hence, energy consumption for pelletizing includes the same.

The product pellet characteristics are measured in terms of the size, resistance to tumbling and abrasion, compressive strength, reducibility and other features. The advantage of pellet is that it has sufficient strength to be transported from mine to steel plant without the fear of getting degenerated, as opposed to sinter, which is fragile



and not suitable for long transportation. The pellets also provide a substitute for high grade lump ores which has its limitation as regard to availability.

Typical major pellet properties are as follows:

Pellet Properties	Value
Size	9 – 16 mm (ISO 4701)
Compressive Strength	250 kg/pellet (ISO 4700)
Tumbler Index	Min. 94% (ISO 3271)
Abrasion Index	Max 6% (ISO 3271)

The process of induration is carried out in either of the two technologies, namely: Travelling Grate Technology and Grate-Kiln Technology.

While, both the technologies are having its own advantages and disadvantages, generally for hematite ores, Travelling Grate is more established and the capacity of plants with such TG based technologies can be as high as 7 to 8 MTPa corresponding to a grate area 768 m² to 816 m².

Travelling grate technology involves individual pallet cars being transported through pushing action over a defined reaction area. The pellet burden stays static within the pallet cars and so there is no chance of degeneration of pellet balls due to internal friction or impact. The pallet cars are moved through drying and pre-heating zones and then through the firing & after firing zones, where fuel burners are arranged along the two side walls of the top hood to provide required thermal energy. The under grate is provided with wind boxes to vent out the process gas either to be released or to be recuperated into the process. The last section of the reaction area after firing and after-firing constitutes the cooling section. Ambient air is forced in through the under grate wind boxes in the cooling section, which picks up heat while cooling the pellets and circulates within the system to carry out the entire process of induration. The cooled pellet is screened further to separate out the undersize and the hearth layer. A typical travelling grate pelletizing plant process flow and Plant Layout are shown in **Figures 4** and **5**, respectively.

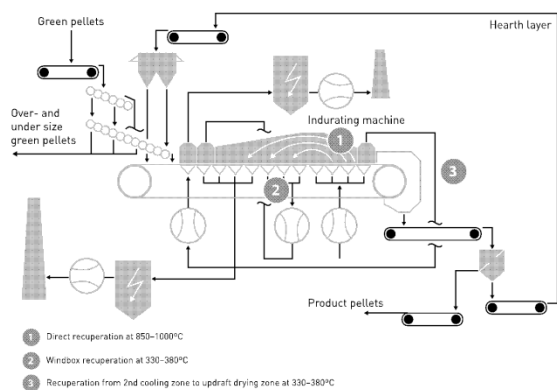


Figure 4 A typical travelling grate pelletizing process flow

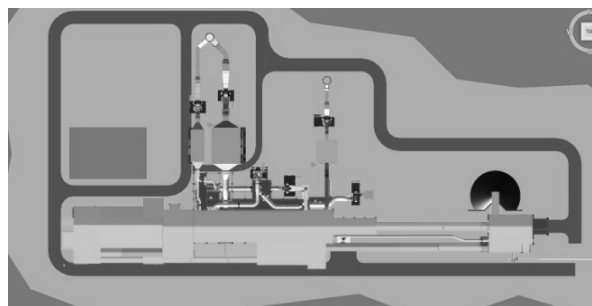


Figure 5 A typical travelling grate pelletizing plant layout

The Grate-Kiln has a chain grate in the drying and pre-heating zone and then the pre-heated pellets are fed into a Rotary Kiln provided with a single ignition burner. The firing process is achieved inside the Rotary Kiln. Since the rotary action causes fall of pellets, there is a chance of degeneration unless the inherent strength achieved by individual pellet particles till then is enough to withstand the impact of fall. Generally, haematite ores are not



suitable since the reaction process favours magnetite ores only to get hardened. The subsequent cooling is carried out in a separate cooler.

PLANT DESIGN

The integrated plant design translates the process into an installed base. The operation of the plant is highly automated through new generation Distributed Control System working in conjunction with sophisticated field devices to achieve the accuracy of the process parameters and also ensuring safety. Typically, space requirement of various plant sizes are as follows:

- 1-1.2 MTpa Plant:
 - Grinding-Dewatering: 100 m × 50 m
 - Full Scale Beneficiation: 250 m × 100 m
 - Pelletizing: 250 m × 150 m
- 4-6 Mtpa Plant:
 - Grinding-Dewatering: 150 m × 150 m
 - Full Scale Beneficiation: 300 m × 200 m
 - Pelletizing: 400 m × 200 m

CONCLUSION

The objective of this work is not only to highlight the importance of the integrated beneficiation and pelletizing technologies, but also to point out the fact that there should be an endeavour to maximize the sourcing of such technological equipments within the country in line with the present day “Make in India” movement. These equipments are manufactured out of high quality / high strength steel & alloy steel and other metallic & non-metallic materials. It needs precision manufacturing technology and organised quality control. Further, it also needs an integration of the entire chain from the technological process itself till the manufactured components. Hence, an integrated effort needs to be in place with capabilities and understanding of the entire chain and this will call for collaboration between multiple agencies, ably led by the larger stakeholders. The strategic initiative taken by Government of India may be utilised as an opportunity to create a platform in order to facilitate technological developments within the Nation in an ore to metal conversion process. This will not only elevate the capability levels within the country, but also would reduce high dependence on overseas countries in matters related to the same.

REFERENCES

- Indian Minerals Yearbook. Ministry of Mines, Government of India, 2017
- D F Ball, J Dartnell, J Davison, A Grieve, R Wild. Agglomeration of Iron Ores, Heinemann Educational Books Ltd, London
- F Cappel, History & Development of Iron Ore Sintering. Lurgi GmbH
- Mineral Processing Technology. ISBN 0750644508
- <https://www.outotec.com/products/sintering-and-pelletizing/traveling-grate-pelletizing-plant>



USE OF GOETHITIC ORE FINES IN SINTERING AND MEASURES TO IMPROVE SINTER PLANT PERFORMANCE

MAHADEO ROY^{*1}, S. DHARA¹, M. K. SINGH¹, SUDIP ACHARYYA¹, S.A. BALAJI¹, S.K. PAN¹
R & D Centre for Iron and Steel, SAIL, Ranchi¹

*mahadeo@sail-rcis.com**

ABSTRACT

Production of strong and quality sinter for the blast furnace is the main purpose of iron ore sintering. This is achieved by partially melting a sinter raw material mix at high temperature and then allowing the melt to solidify into a bonding phase within particles of mix. The melt formation and subsequent solidification processes are highly dependent on the composition of the blended mix. Main source of iron ore for Durgapur (DSP) and IISCO (ISP) sinter plants are Bolani and Gua Mines. Ore fines from these sources are mostly goethitic in nature which has chemically bonded water about 5 to 6%. This water gets evolved out during sintering process at temperature from 250°C to 450°C and increases moisture level of sinter charge mix and thereby the micro-pellets get disintegrated resulting in decrease in Vertical Sintering Speed (VSS) and productivity. From a fundamental evaluation of the sintering process, it is clear that productivity can be an issue with goethitic ores because of their low bulk density and high porosity. The effect of goethitic ores on coke consumption rate is also a matter of general concern. The properties of melt have been shown to be particularly important in determining yield from a sinter machine and it is evident that the easy melting properties of goethitic ores will also have an impact on this area. To overcome the above problem, laboratory pot sintering study has been carried out using goethitic ore fines. Number of experiments carried out with varying amount of coke and mill scale as well as process parameters optimized to retain the strength and productivity. Also, few set of experiments have been conducted with permeability bar.

After achieving encouraging result with permeability bar, it has been decided to introduce this at SP-2, DSP. To improve permeability of mix on the pallet, “permeability rod” system has been developed and fitted in sinter plant. Sinter mix is charged on the fixed permeability rod over the machine and due to continuous movement of machine, voids are created inside material and thus permeability of mix on the pallet improves. This paper describes the effect of goethitic ore fines in sintering and recommends measures to overcome losses in productivity & strength.

KEYWORDS Iron ore sintering, Goethitic ores, Permeability, Productivity, Yield, Sinter quality

INTRODUCTION

Sintering process begins with the preparation of raw mix from iron ores, fluxes, in-plant dust and spillage fines, solid fuel and return fines. These materials are mixed and granulated in one or more stages. Water is added in order to assist the raw mix in obtaining optimum permeability. The mix is charged onto the sinter machine and then ignited from the top, air being sucked through the ignited layer and sintering proceeds in the vertical direction in the sinter strand's material bed. Subsequently, the sinter is cooled, usually in a separate sinter cooler, located at the sinter machine's discharge outlet. The cooled sinter is crushed to a pre-determined maximum particle size. Undersized sinter, that is not suitable for the blast furnace, is recycled to the return fines bin. The product sinter obtained from the process is a blast furnace feed of superior quality.

It is clear from the literature that since the early 1980s, Japanese Steel Mills (JSM) have given considerable attention to the development of appropriate sintering technology for high goethitic ore blends. From around 1990, there have been many noteworthy publications in this area — for example, melt properties[1,2], behaviour of ore blends containing significant goethitic ores [3-5], bed structure [6,7], green and sintering bed permeability [8].

From a fundamental evaluation of the sintering process, it is clear that productivity can be an issue with goethitic ores because of their low bulk density and high porosity. The effect of goethitic ores on coke rate is also a matter of general concern. The properties of melts have been shown to be particularly important in determining yield from a sinter machine and it is evident that the easy melting properties of goethitic ores will also have an impact on this area. The decline in productivity was also observed in laboratory pot tests and plant trials in Australia [9].



When pisolitic ore is blended at a high ratio, the fluidity of melt decreases, and pore development and agglomeration are delayed, which can be considered to result in a decrease in the strength of the sinter. The addition of mill scale improves fluidity and thus reducing the delay in pore development and agglomeration. In high pisolitic ore operation, experiments with a commercial sintering machine confirmed that it is possible to improve yield by adding mill scale, and that permeability can be improved by inserting plates at the bottom of the bed in the ore feed section [10].

DSP and ISP sinter plants are using iron ore fines mainly from Bolani and Gua Mines. Ore fines from these sources are mostly goethitic in nature. The water gets evolved out during sintering process at temperature from 250°C to 450°C and increases moisture level of sinter charge mix in the bottom layer and thus the micro pellets gets crumbled resulting in decrease in VSS and productivity.

To investigate the above problem, number of experiments were carried out using goethitic ore with varying amount of coke, mill scale as well as process parameters optimized to retain the strength and productivity. Introduction of permeability rod in preparation of bed has also been tried.

After getting encouraging result with permeability rod, it has been decided to introduce this at SP-2, DSP. To improve permeability of mix on the pallet, permeability rod system has been developed and implemented. Sinter mix is fed on the fixed permeability rod over the machine and due to continuous movement of machine, voids are created inside material and thus permeability of mix on the pallet improves.

EXPERIMENTAL

Description of the laboratory sintering unit

The unit consists of a replaceable sinter pot of internal diameter 310 mm and the pot is installed on a vacuum chamber. Necessary suction for this unit is provided by an exhaustor and it can be controlled by means of a butterfly valve. The waste gas is cleaned in a scrubber where water is continuously sprayed as cooling and de-dusting agent. The under grate suction is measured with the help of a digital pressure meter. All fixed parameters of the experimental set up are shown in **Table 1**.

RAW MATERIALS

Iron ore fines (Bolani, Gua, BSP mines), lime stone fines, dolomite fines, coke breeze, mill scale, lime dust etc. were used as raw material. All raw materials were brought from ISP and BSP. Chemical analysis was carried out and the results are shown in **Table 2**. Physical analyses were conducted through screening and the results are presented in **Table 3**.

Table 1 Fixed parameters of the experimental set up

Parameters	Value
Bed height	700 mm
Hearth layer	2 kg
Ignition time	2 min 30 s
Suction during ignition	200 mmwc
Suction during sintering	1250 mmwc

Table 2 Chemical analysis of raw materials

Raw materials	Fe (T), %	SiO ₂ , %	Al ₂ O ₃ , %	CaO, %	MgO, %	LOI, %
BSP ore-1	61.2	5.4	4.7	-	-	1.8
BSP ore-2	60.6	4.7	5.1	-	-	2.9
Gua iron ore	60.0	3.8	3.4	.04	.04	6.5
Bolani iron ore	61.7	3.2	6.2	.06	.04	4.9
Lime stone	2.2	3.4	1.01	49.9	2.3	40.6
Dolomite	0.07	0.6	0.02	31.6	21.2	45.8
Coke breeze (ash)	22.4	39.9	19.8	3.1	1.1	74.8
Mill scale	67.8	1.08	0.3	0.3	0.1	-



Table 3 Physical analysis of raw materials

Raw materials	+10 mm, %	+5 mm,%	+3 mm,%	+1 mm,%	-1 mm,%
BSP ore-1	5.0	27.1	12.3	23.9	31.7
BSP ore-2	6.1	21.0	8.5	28.5	35.9
Gua iron ore	1.7	16.2	7.6	25.1	49.4
Lime stone	—	2.0	12.0	36.0	50.0
Dolomite	-	2.0	5.0	33.0	60.0
Coke breeze (ash)	-	5.0	10.0	32.5	52.5
Lime dust	-	-	-	-	-
Mill scale	-	5.0	2.5	17.5	75.0
RMP waste	-	2.5	10.0	30.0	57.5

EXPERIMENTS WITH VARIOUS PROPORTIONS OF GUA FINES⁹[11]

Laboratory experiments using different ratios of BSP ore 1, 2 and Gua iron ore fines have been carried out. Sintering time, Temperature & Suction were recorded during experiments. Before carrying out the experiments, a charge calculation was done through software and the design of experiments was also made. Various parameters obtained during experiments are presented in **Table 4**.

Table 4 Various parameters obtained through experiments

Ore 1: Ore 2: Gua, %	VSS, mm/min	Yield,% (+5 mm)	TI, %	Productivity, t/m ² /h	Balling index
60-40-0	20.34	78.05	68.33	1.53	1.96
54-36-10	17.95	76.7	67.72	1.364	1.7
48-32-20	17.95	73.35	68.35	1.285	1.7
42-28-30	20	74.7	68.33	1.45	1.85
36-24-40	21.2	76.05	67.35	1.525	2.0
30-20-50	19.23	73.86	65.33	1.365	1.6
54-36-10 (with 35kg MS)	21.05	77.3	67	1.566	1.8
48-32-20 (with 35kg MS)	20	78.76	67	1.50	1.78

PRODUCTIVITY

From **Table 4**, it can be seen that productivity varied from 1.285 to 1.53 t/m²/h with an use 25 kg of mill scale (Exp.1 to 6) per ton of sinter. However, at Ore-1: Ore-2: Gua :: 36 : 24: 40, the maximum productivity of 1.525 t/m²/hr is achieved. The maximum yield of 78.76 % was achieved when 20% Gua ore fines and 35 kg of mill scale (in place of 25 kg of mill scale) use in the blend. The maximum drum Tumbler Index was 68.35% when 20% Gua ore fines and 25 kg mill scale were used. From **Table 4**, it is clear that balling index is less at 10% and 20% Gua ore fines use that resulted in low VSS and hence productivity.

The variation of productivity as a function of Gua ore fines is plotted in **Figure 1**. This figure shows that the productivity decreases as the amount of Gua ore fines in the blend increases up to 20%. The Figure also indicates that productivity increases as the amount of Gua ore fines increases from 20 to 40%. Again this value decreases as amount of Gua ore fines goes up more than 40%. With increase of Gua ore fines beyond 20%, the balling index improves and hence the VSS. The detrimental effect of goethitic ore is thus partially eliminated with improvement in balling index.

The effect of mill scale with Gua ore fines is presented in **Figure 2**. This Figure shows that productivity increases with the addition of higher amount of mill scale by keeping the amount of Gua ore fines constant.

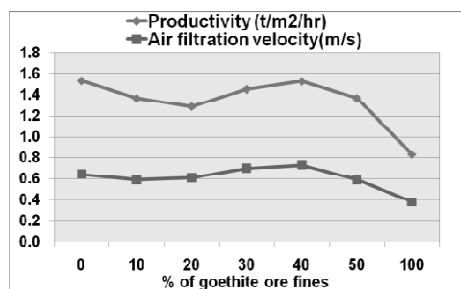


Figure 1 Variation of productivity with addition of Gua ore fines

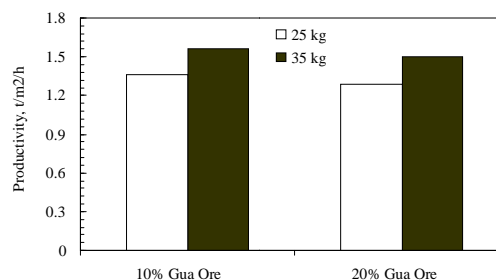


Figure 2 Effect of mill scale with Gua Ore fines

YIELD AND DTI

The variation of yield and DTI with percentage of Gua ore fines is plotted in **Figure 3**. This Figure indicates that yield value decreases with the addition of Gua ore fines up to 20%. Thereafter, the yield value increases with more than 20 % Gua ore fines addition and it reaches to 76% at 40% Gua ore addition. The value gets decreased with higher than 40% Gua ore addition.

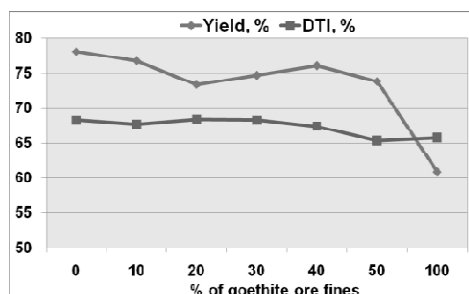


Figure 3 Variation of Yield & DTI with addition of Gua ore fines

Goethitic ores are inherently more porous and cause deterioration in granulation efficiency, which can be recovered by the addition of more water during granulation. Goethitic ores have lower bulk densities and will reduce sinter plant productivity if machine speed and/or yield are not increased. Iron ores have different assimilation properties under realistic sintering heating profiles because of differences in ore porosity. Initial melts are extremely mobile and porous ores have very high reaction surface areas, resulting in the formation of increased melt volume during sintering[12].

From these studies it is very clear that with the introduction of porous ores, maintaining granulation efficiency is extremely important if productivity losses are to be avoided. It is well known fact that granulation efficiency is very important in sintering process. Other than ore porosity, particle size distribution is important. Fine particles in the sinter mix (< 0.5 mm) adhere onto the surfaces of nucleus particles (~2.0 mm) while the intermediate sized particles (greater than 0.5 mm and less than 2.0 mm) tend to remain unchanged. As intermediate particles will only be captured through embedment in the formed adhering fines layer they have a detrimental influence on bed permeability, particularly at low mix moisture.

In Gua ore fines, the < 1 mm size fraction is around 50%. When Gua's contribution increases above 20% in the entire sinter mix, then the total amount of finer particles increases and subsequent percentage of intermediate sized particles decreases. This may result in stronger granules formation and better balling index. More work is to be done to confirm if this is true in every situation.



POT TEST OF ISP RAW MATERIALS

ISP sinter plant is using mainly Gua and Bolani ore fines. Iron ore fines from these sources are goethitic in nature. Laboratory pot sintering tests have been carried out keeping ISP's sinter plant in operating conditions. Gua and Bolani ore was used in the ratio of 2:3 ratios. Coke breeze and mill scale were varied as shown in **Table 5**. Coke breeze and mill scale quantity were optimized to get the best result in sintering of goethitic ore. Variation of DTI, Yield, +10 mm sinter, VSS and productivity with change in Coke breeze and mill scale quantity is shown in **Figure 4**. Best results in terms of yield, productivity and DTI are obtained with 4.4% coke breeze, mill scale 0.8% to 3.9%. Also, experiments were carried out with permeability bar and without permeability bar. Result obtained corresponding to each change is also shown in **Table 5**. Permeability bar reduces lower bed resistance of mix. Pot test data clearly shows that in case of sintering with high LOI ore, that is, goethitic ore, use of permeability rod intensify VSS, yield, productivity as well as DTI.

Table 5 Result of pot test of ISP raw materials

Variable	VSS, mm/min	Yield (+5 mm)%	Productivity, T/m ² /h	DTI, %	+10 mm sinter %
base with 3.85%CB	19.7	66.5	1.21	60.8	50.9
CB-3.85%, MS-.8%	21.7	55.3	1.09	55.0	37.0
CB-3.85%, MS 1.3%	19.7	65.1	1.22	60.3	48.7
CB-3.85%, MS-3.85%	23.2	63.8	1.28	60.4	48.1
CB-3.85%, MS-3.9%	21.3	64.8	1.23	61.3	49.2
base with CB 4.4%	20.3	69.5	1.31	63.0	52.8
CB-4.4%, MS-.5%	22.7	73.1	1.48	65.0	55.8
CB-4.4%, MS-.8%	22.8	75.3	1.55	64.8	59.4
CB-4.4%, MS-1%	22.4	74.6	1.38	63.8	57.1
CB-4.4%, MS-3.85%	21.3	70.8	1.38	68.7	51.6
CB-4.4%, MS-3.9%	22.0	77.2	1.51	66.0	62.9
CB-4.3%, MS-.8%	23.2	67.9	1.43	65.0	52.9
CB-4.2%, MS-.8%	18.8	69.4	1.17	66.0	55.1
With permeability bar, MS-0	22.7	64.2	1.26	62.9	
Without permeability bar, MS-0	19.7	54.2	0.93	60.8	

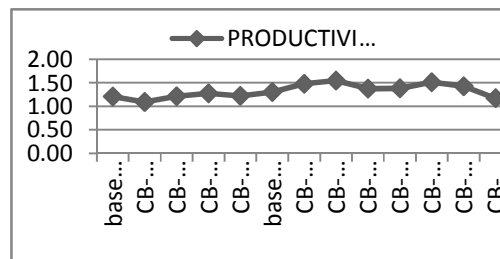
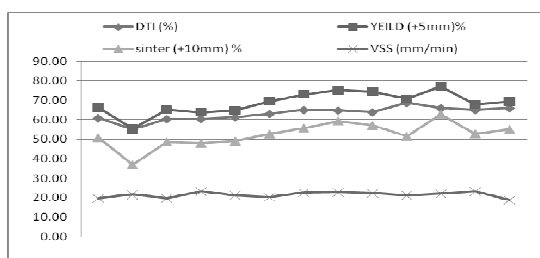


Figure 4 Variation of DTI, Yield, +10mm sinter, VSS and productivity with change in coke breeze and mill scale quantity

INDUSTRIAL TRIALS WITH PERMEABILITY ROD

Wear resistant permeability rod assembly for sinter machine consisting of rods along with necessary fixing hardware and support system have been installed at SP-2, DSP. One row containing 10 numbers of permeability rods were installed as shown in **Figure 5**. Strips attached with the bars were hard faced at the site.



Figure 5 Permeability rod installed at SP-2, DSP

After installation of permeability rods over sinter machine, industrial trials have been carried out. Results of trials are shown in **Figures 6 and 7** which clearly indicates improvement in air filtration velocity through sinter bed and productivity. Life of the permeability rods has also been increased by more than 5 times (earlier 4 months). Also PLC based technological controls at SP2 enhanced automatic feed rate control and comprehensive monitoring of sintering process.

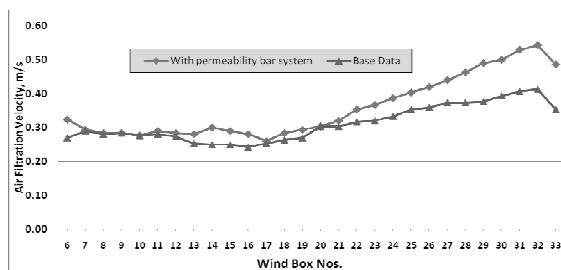


Figure-6 Air filtration velocity with and without permeability rod at SP-2, DSP

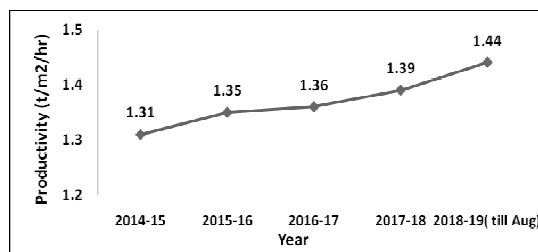


Figure-7 Specific productivity of SP-2, DSP

CONCLUSIONS

From these observations the following conclusions were drawn:

1. A productivity of 1.53 t/m²/h can be achieved at 40% Gua ore fines and 25 kg mill scale in the blend mix.
2. Productivity increases with the addition of higher amount of mill scale by keeping the amount of Gua ore fines (high LOI) constant.
3. Permeability bar reduces lower bed resistance of mix. In case of sintering with high LOI ore i.e. goethitic ore, use of permeability rod intensify VSS, yield, productivity as well as DTI.
4. Green bed and sintering bed permeability (as determined by pre- and post ignition air flow rates) are strongly dependent on each other. This explains the importance of maintaining green bed permeability in sintering operations. Monitoring green bed permeability on a sinter strand is very important when introducing goethitic ores.

REFERENCES

1. E. Kasai, Y. Sakano, T. Kawaguchi and T. Nakamura: ISIJ Int., Volume 40, p 857, 2000.
2. E. Kasai, S. Wu and Y. Omori: ISIJ Int., Volume 31, p 17, 1991.
3. L. X. Yang, D. Witchard and Z. N. Yu: ISIJ Int., Volume 40, p 647, 2000.
4. L. X. Yang and L. Davis: ISIJ Int., Volume 39, p 239, 1999.
5. L. X. Yang and D. Witchard: ISIJ Int., Volume 38, p. 1069, 1998.
6. M. V. Ramos, E. Kasai, J. Kano and T. Nakamura: ISIJ Int., Volume 40, p 448, 2000.
7. T. Otomo, N. Taguchi and E. Kasai: ISIJ Int., Volume 36, 1338, 1996.
8. E. Kasai, W. J. Rankin and J. F. Gannon: ISIJ Int., Volume 29, p 33, 1989.
9. C. E. Loo: Trans. Inst. Min. Metall. C, 100, C127, 1991.
10. Kouichi Nushiro et.al.: Kawasaki Steel Technical Report No. 38, pp. 17-23, April 1998.
11. Mahadeo Roy et.al.: Steel India, Volume 37 Number 2, pp 74-79.
12. C. E. Loo: ISIJ Int., Volume 45, Number 4, pp. 436-448, 2005.



A Critical Study of Environmental Impact of Responsible Mining Practice for Kotah Stone within Framework of Initiative Responsible Mining Assurance (IRMA) Standards-16

S. C. Agarwal

Former President, A.S.I.(Kotah) Lt India, scagarwal42@yahoo.com

ABSTRACT

Mining is a complex and intensive process that can have major environmental and social impacts. In even the best-managed mines some degree of disturbance is inevitable. In some cases the potential for harm may mean that a decision not to mine may be the best option. However, in most cases the most negative safety and environmental impacts can be avoided if companies operate according to best practice standards. The Initiative for Responsible Mining Assurance (IRMA) has released the second revised draft Standards for Responsible Mining, as a first ever global certification programme for industrial-scale mine sites, planned to begin in late 2016. IRMA-16 has elaborated the requirements of standards in the field of environmental responsibility, water quality and quantity, mine waste management, air and noise quality, greenhouse gas emissions, protected areas, biodiversity outside officially protected areas, reclamation and closure, delivering benefits, environmental and safety impact assessment (EIA) beside working conditions, occupational health and safety, human rights due diligence and compliance, mining and conflict-affected or high-risk areas, HIV/AIDS, tuberculosis (TB) and malaria 57, obtaining community support and cultural heritage and resettlement.

The author had taken initiative in 1992 to develop responsible practice of mining of dimensional limestone, commercially known as Kotah Stone. Comparison has been drawn between what has been achieved on environmental performance after adopting best mining practice in mining Kotah Stone visa-vis IRMA Standards. On evaluation, the performance on improvement in environmental safety standards after adopting responsible mining with best mining practice, found to be compatible with IRMA Standards.

KEYWORDS Responsible mining, Kotah stone, IRMA standards, Environmental impact.

INTRODUCTION

Nearly everything manufactured or constructed – from buildings to roads to computers and trains – contains material mined from the Earth. Mining is a complex and intensive process that can have major environmental and social impacts. In even the best-managed mines some degree of disturbance is inevitable. In some cases the potential for harm may mean that a decision not to mine may be the best option. However in most cases the most negative social and environmental impacts can be avoided if companies operate according to best practice standards.

The Initiative for Responsible Mining Assurance (IRMA) has recently released the second revised draft Standards for Responsible Mining, as a first ever global certification programme for industrial-scale mine sites, planned to begin in late 2016. The author had taken initiative as early as in 1992 to develop best practice of mining dimensional limestone, commercially known as Kotah Stone. Kotah stone has been used world over as an excellent flooring stone **Figure 1**.

In this paper an effort has been made to analyse the environmental performance of the best mining practice and score it on the scale of requirements of IRMA Standards.



Figure 1 Flooring with Kotahstone



RESPONSIBLE MINING AS DEFINED BY IRMA STANDARDS

The goal should be to maximise the contribution to the Social well-being of the current generation in a way that ensures an equitable distribution of its costs and benefits, without reducing the potential for future generations to meet their need own.

OBJECTIVE AS DEFINED BY IRMA

The overall objective for Responsible Mining is that industrial mining should provide safe, healthy and respectful workplaces, avoid or minimise harm to the environment; leave positive legacies beside respectively the human rights and aspirations of affected communities. It is said to be aimed at to support the achievement of this overall objective by defining best practice in relation to the environmental and social aspects of mining within its defined scope.

MINING FOR KOTAH STONE

Kotah Stone is naturally splittable flaggy limestone. The rocks containing Kotah Stone belong to Semri series of Lower Vindhyan. It occurs over an area of +55 sq.km in Kota district (India) **Figure 2a**. Active mining for Kotah Stone has been going on in this area since 1945. In recent years a large area of Kotah Stone has also been discovered in adjoining district Jhalawar where active mining has been going on for 7 to 10 years. The deposit of Kotah Stone is confined to 15 m thick zone which is overlaid with OB containing non-splittable and inconsistent layers of low grade limestone beside soil and subsoil **Figure 2b**. The deposit gently slopes from 7 to 12 degree. The OB zone has since then increased from 4 m at out crop (1945) to as much as + 60 m as of now.

CONVENTIONAL MINING FOR KOTAH STONE

Mining for Kotah Stone has started as early as in 1945 but all manual employing a large workforce. Mineable zone (15 m) of Kotah Stone is first exposed by removing overlying burden. Initially it was all done manually **Figure 3**. But with increasing thickness, in 1986 HEMM were deployed to excavate and transport waste to dumps, however the extraction of Kotah Stone continued to be all manual. Explosive has been used to fragment the OB rocks. It started first by peeling the layers, one by one, using hammers and crowbars. The layers get separated from natural bondage but in non-dimensional shape and size. These non-dimensional sized blocks layers were then splitted along cleavage plane by knocking all along cleavage plane to yield a single solid slabs/ tile with smooth surface. Each layer consist of 2 to 4 splits in varying thickness. In early days splits only in thickness of +12 mm – 75 mm had been mined and rest thrown as waste as it was difficult to carry and use thicker slabs.

ENVIRONMENTAL IMPACT OF CONVENTIONAL MINING

In past Kotah Stone mining was all manual and it was more of a handicraft. Though it provided large employment to both males and females, even to those who migrated from adjoining states, but it was very wasteful both on human effort as well on natural resources. Productivity was very low, resulting in low earning despite both husband and wife working. To supplement income at times even children were engaged. Each family had to borrow money for discharging social responsibilities. Non-payment of advances/ loan lead to many criminal activities and even lead to bonding.

Education among children was very low, poor living conditions were poor and one could hardly see a pucca dwelling for mine workers. Poor health standards, poor health care facilities, bad drinking habits resulted in lungs diseases. Lack of appropriate mining technology has been major cause of poor safety standards, occurrence of large number of accidents including fatal and serious body injury as well as excessive human suffering. Major part of human efforts has been wasted in non-productive jobs causing excessive fatigue and mental stress, inflicting excessive injuries to eye, leg, foot, arm, fingers and spinal cord. Mineral recovery was hardly exceeding 45% and rest was thrown as waste, as can be seen in **Figure 4**.

It lead to fast depletion of natural resources of Kotah Stone. Even fast degradation of precious soil and vegetation reduced agriculture proceeds, grazing fields, fast run-off of rain water resulted in scarcity of drinking water. After every rainy season, quarry has to be bottomed up by de watering the rain water for resuming mining of Kotah Stone. This caused serious scarcity of ground water.

BEST PRACTICE AND RESPONSIBLE MINING FOR KOTAH STONE

IRMA Standards Requirement for Responsible Mining

The standards, as defined by IRMA, should consist of a set of auditable requirements that reflects a process on the most effective way to achieve the various objectives given the current state of knowledge. To address economic and

environmental issues arising from manual mining, an innovative mining technique was evolved. The concept was to first cut the layers in-situ to size required before separating them from natural bondage, **Figure 5**.

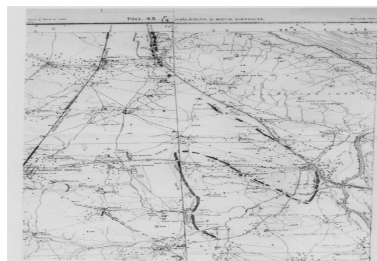


Figure 2a Occurrence of Kotah stone

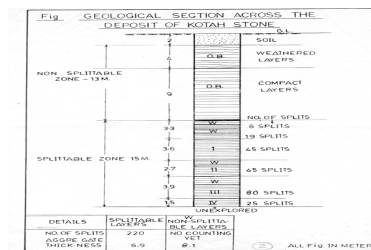


Figure 2b Section across deposit of Kotah stone

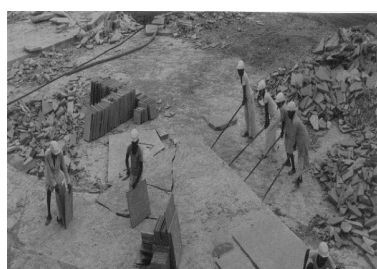


Figure 3 Manual quarrying of Kotah stone



Figure 4 Generation of huge waste in manual mining

All sides cut blocks were then splitted by same techniques to yield all sides cut slabs/ tiles. To do so portable diamond cutter were designed fitted with steel blades tipped with diamond cutting bits. Various size of blade, cutting tool rotating at varying speed were tried and optimised. The cutter is electrically operated on portable track. The m/c cuts both ways, up and down. Water is used at pressure to cool the cutting tool and also flush out the cutting slurry. Blades of 36" dia, tipped with 64 to 56 diamond bits ($24 \times 7 \times 5\text{mm}$) electrically rotating at 760 rpm were found to give the optimum performance. Cut to a depth of 30cm were given in two passes, up and down.

IMPACT OF BEST PRACTICE OF MINING KOTAH STONE ON ENVIRONMENTAL RESPONSIBILITY

Waste Management

Solid quarry waste has been biggest polluter in Kotah Stone mining, partly as production waste at quarry floor and major chunk comes as OB waste. With best practice of mining, the waste has been managed in three options:

Reduce : production waste has been reduced to 1/6th after adoption of best mining practice. However, OB waste continue to generate more progressively by 8%.

Recycle : Through extensive R/D work technology has been established to enrich low grade limestone quarry waste and utilise it to manufacture normal Portland cement of 45 grade. This will generate employment even after Kota Stone mineral get exhausted. It will also reclaim degraded land to original level for original use. The practices adopted for waste management are depicted in **Figure 6**.

RECLAMATION AND MINE CLOSURE

It is observed that lessees of Kota Stone have abandoned the worked out quarries and waste dumps without any reclamation owing to ignorance about compliance of provisions of mine closure plan. Man made mountains of quarry dry waste dumps could be seen in the entire +55 sq.km lease area.

This has damaged the aesthetic value of the region and regional environment. Laws have been framed but compliance is very less. Reclamation of worked out land is a legal provision in EC granted by MoEF, but did not materialise in this sector. Most of lessee being unorganised groups managed an escape route from legal compliance of reclamation.



However, one lessee made sincere effort of back-filling the worked area **Figure 7** and raised excellent crop on reclaimed land **Figure 8**.



Figure 5 Innovative mining for Kotah stone

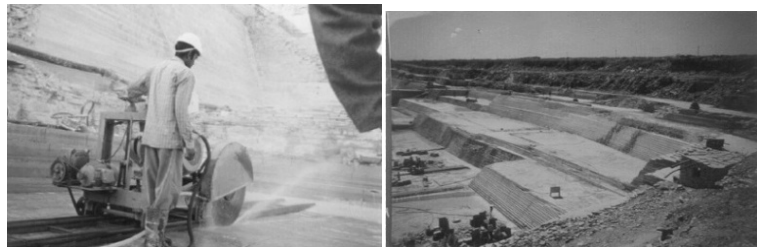


Figure 6 Best practice of mining for Kotah stone



Figure 7 Quarry waste land after reclamation to ground level



Figure 8 Standing crop on reclaimed waste land

Another lessee made sincere effort to rehabilitate the waste dump by dense plantation after soil capping **Figure 9** and developing picnic spot **Figures 10** and **11**. But most of other lessee did not follow the suit.

GREENHOUSE GAS EMISSIONS

For poor quality and quantity of grid power supply, in the beginning of implementation of Best Practice, DG sets were installed as source of electric supply to portable diamond cutters. One DG of 165kVA for an annual production of 36L sqft and consuming annually 30,000 l of HSD, emitting 80T of CO₂. For current year, over 110 DG sets of this capacity are in operation emitting +9,000 T of CO₂ besides other noxious gasses. This is 1/3rd of total emission while the balance 2/3rd is emitted from HEMM deployed for OB excavation and other vehicular traffic operated on HSD. One the biggest lessee in corporate sector producing 1/3rd of total production and introducing Best Mining Practice did not multiply.

WATER QUANTITY

The Kota Stone quarries gets filled up with rain water **Figure 2**. This water on test found to be potable and safe for drinking. However, for the purpose of drinking, the abandoned pits are fenced and secured from animals to avoid of water pollution. Active mining pits get polluted from cutting slurry and water is used for cooling cutting tools. This Best Practice in Kotah Stone mining has brought some relief to availability of water by deferring the de-watering of quarries from earlier 3 months to now 9 months. Water from quarries is now available even in peak summer for washing, agriculture, bathing and cleaning.



Figure 9 Dence plantation around Hanuman Temple on



Figure 10 Temple of Lord Shiva on waste dump with plantation around

waste dump



Figure 11 Picnic spot on waste dump



Figure 12 Kotah stone quarry filled with rain water

AIR QUALITY

Wet drilling or drilling with dust collector are adopted religiously to contain dust pollution. Actual extraction of Kota Stone slabs and tiles is wet process, hence results in least dust pollution. However, due to heavy vehicular traffic dust pollution was unavoidable. Regular water spray on haul roads and dump area was the only solution.

NOISE

Processing process generate noise of varying level and nature. The development of innovated mechanised process and use of mechanical equipment have increased the noise problem both during extraction as well as in processing. For last few decades, human concern about protection environment against noise has grown rapidly as it has been recognised that the rise in noise beyond certain level can't be allowed indefinitely. Prolonged exposure of human beyond acceptable limits leads to hearing loss and other adverse changes in physiological, psychological and behavioral consequences.

- Average level of noise level at and in surrounding of a pit with 6 diamond cutter = 76.2dB (A)
- Average level of noise at drilling site varies from 92.4dB to 79.5dB (A) as per different activities.
- Average level of noise at loading level by 35T dumpers and hydraulic excavator varies between 90.1 to 93.4dB (A)
- Average level of noise during operation of hydraulic excavator. Varies between 72.7 to 90.6dB (A) as per different activities.
- Average level of noise during dozer operation is of the order of 101dB (A)
- Average level of noise during operation of generator varied from 97.9dB in side and 78.4dB outside of generator room.
- At the processing level, average noise level varied from 92.7 to 107.9dB(A).

NOISE CONTROL MEASURES

Provision and use of earplugs and ear head sets by workman was made mandatory at workplace both at mine and processing plant level. Regular checkup of bearings and other maintenance of machinery was made a regular feature.

CONCLUSION

Environmental degradation is inevitable in mining. Degree of disturbance depends on extraction technique. However, in most cases the most negative safety and environmental impacts can be avoided through responsible mining adopting best mining practice. The technology innovated for mining Kotah Stone met all standards of Responsible mining as defined by IRMA-2016 and maximized contribution to all stake holders especially the social well-being of locals living in the vicinity, without reducing the potential for future generations to meet their own.

REFERENCE

IRMA Standards-2016



An Overview of Modified Foreign Technology for Indian Mining Conditions

P.Venkatesan

NLC India Ltd, Neyveli, venkat_0531@rediffmail.com

ABSTRACT

Advancement and adoption of technology has been the trend of sustainable development of any industry in particular mining industry. NLCIL has been forefront in adopting the technology of Specialized Mining Equipments in 1960s itself and since then has strived to achieve a predominant position in the Indian mining industry. This paper presents an overview of continuous mining technology using Specialized Mining Equipments and Belt conveyors in Neyveli mines, the past history, challenges faced in adopting the technology, successful implementation, indigenization and assessment of using SME has been made.

KEYWORDS Specialized Mining Equipments, Belt Conveyors.

OPEN PIT MINING

The winning of minerals throughout the world is increasingly executed by open pit mining. The advantages of open cast mining lie in considerably reduced losses during the excavating process compared with underground mining. In addition, surface mining techniques result in higher productivity through extensive mechanisation and automation. Effectiveness of selective extraction technique depends on the continuous physio mechanical properties of the strata, the type of excavation, technological parameters of the mining and other factors.

The Continuous Excavating Technique Bucket Wheel Excavators for excavation/mining, Conveyors for handling and Spreaders for Dumping/Spreading are required to achieve continuous production that too with very good rate of production.

These Specialized Mining Equipments (SMEs) are to be supported by other equipments like blast hole drills, dumpers, loaders, dozers and other auxiliary units to handle the hard and semi-hard rock formations usually found in the overburden strata. The mineral deposits which cannot be effectively mined out using SMEs are also to be mined out using these equipments. Bucket wheel excavators are having an edge over other mining equipments due to the ability of removing the material continuously and consistently for the entire bench height (Crest to Toe). The excavated overburden/mineral is handled by the belt conveyors and finally dumped/stacked by Spreader/Stacker.

SIZE OF OPEN PIT MINES

The size of an open pit mine depends on one hand, on the quantity of ore to be dug and on the other hand, on the reserves available. The best measure of mine efficiency is the specific output per man shift. The strong demand for lignite, which lies under variable thicknesses of easily excavated unconsolidated soil, provides the incentive for developing continuous, fully mechanised and automated mining systems. This is the cradle and proving ground of the 'German mining technique' which has secured an outstanding place in opencast mining technology throughout the world.

BENCHES IN OPEN PIT MINES

Optimum open pit mining operations are characterized by the minimisation of the number of benches upon which material is transported. When giant BWEs are employed at depths of 250m to 300m, excavation can be carried out on three levels. The combination of a giant BWE and a separate loading station connected to each other by an intermediate conveying bridge, (Bridge boon BWE) permits positioning of the excavator one or two benches above or below the conveying level. The face length of open pit mines depends on the size and shape of the mine or the subdivisions being excavated.

The amount of rainfall greatly influences the availability factor of an open cast mine. The greatest danger is presented by large quantities of rain falling over short periods, during cyclones and in the monsoon seasons.

DEVELOPMENT OF NEYVELI MINES



Neyveli lignite is of sedimentary type formation. The type of soil beneath and over lignite seam is weak and is not suitable for underground mining. Lignite is found mainly in single seam and with a gradient of 1 in 100. The ratio of overburden to lignite is around 1: 5.5 to 7.0.

For winning these lignite deposits by open cast mining method, surface mining method of continuous type is used. Bucket Wheel Excavators with very high production capacity are used for removal of overburden and mining of lignite. Belt conveyor system is used for handling the waste/mineral. Waste material i.e. overburden is dumped in the de-coaled area by deploying Spreaders and lignite is stacked in the Stockyard/Bunker using Stackers.

NLCIL started its mines with BWEs having 350 Lit capacity and in due course it added higher capacity BWEs - 700 lit & 1400 lit. NLCIL mines are facing the challenge of adverse hydrological conditions which requires continuous pumping of water. This is due to the artesian aquifer water occurs beneath the entire lignite seam. The upward pressure ranges from, 5 to 8 Kg/cm² and it is required to pump the water and to reduce the pressure. By drilling bore wells in a suitable pattern and pumping water to the optimum level, the upward pressure is lowered. Thermal power stations and nearby villages are the main consumers of this pumped out water.

The technology designed to handle comparatively soft overburden and lignite in German lignite mines was imported and adopted in Neyveli lignite mines in early 60's. Four lignite mines-three at Neyveli, Tamil Nadu and one at Barsingsar, Rajasthan, is now being operated by NLCIL. The total capacity of Neyveli Mines is 28.5 Million Tonnes per Annum and Barsingsar Mine is having the capacity of 2.1 Million tonnes per Annum.

Bucket Wheel Excavators (BWEs) are recommended to deploy in Neyveli Mines since the conditions are similar to German and Australian lignite mines. NLCIL's first lignite mine was started 60 years back initially with CME equipments and in due course SMEs were deployed.

ADOPTING CONTINUOUS TECHNOLOGY IN NEYVELI LIGNITE MINES

- * Strata conditions were more or less similar to Australian and German lignite mines which were operating with BWE and Conveyor technology in those days.
- * Lignite seam in Neyveli mines is occurring as a single seam with fairly flat deposit without major geological disturbances such as faults and folds which was ideal for bucket wheel excavator technology.
- * Since this BWE technology adopted runs 100% on electricity, there was very little necessity for diesel or petrol consumption which eliminated all the pollution hazards.
- * Stripping ratio of 1:6 in opencast mines in early 1956-57 was more economical with this BWE-Conveyor mining technology.
- * Developments in belt conveyors being mounted on sleeper frames to which rails attached to enable the whole assembly to be moved laterally without dismantling.
- * Considering the Hydro-geological conditions and location of Neyveli at cyclonic prone coastal area, the adoption of BWE technology with the reverse cut keeping the track and conveyors at higher elevations proved safer for continuous mining even in rainy days.

Lignite mining in Neyveli mines has remarkably advanced with the advancement of technology and by deploying higher capacity BWEs. Initially smaller capacity 350litres BWEs with 1000mm fabric belt conveyors were deployed and they had been upgraded to 1400 litres BWEs and 2400mm steel cord conveyors to augment the lignite production from 3.5 MTPA to 28.5 MTPA.

Lignite mining using BWEs was a remarkable event, and it made the company to grow. Successful mining using BWEs after suitable/necessary structural changes and modifications in parts like buckets, teeth etc is being carried out for facing the hard overburden strata consisting of sandstone which is hard compared to the strata of German mines.

SME TECHNOLOGY

In SME technology, NLC has acquired considerable experience, expertise besides indigenization of various parts and spares in India. SME technology is very much suitable for soft strata like sand, alluvium etc. However, at Neyveli, the strata are bit harder resulting in reduced efficiency of SME operation with low productivity. To improve the productivity after analyzing the experience gained during the operation of SME over 5 decades, the imported technology was modified periodically to suit the indigenous conditions prevailing at Neyveli mines. This made the SME technology a perfect match for the geo-mining condition at Neyveli where lignite is associated with unconsolidated sandstones and clays when compared with the sand stone, silt stone and shale in coal deposits.



At Neyveli mines, for deploying the CME, the shovel dumper combination was not technically feasible in the strata having more water content. Formation of haul road and its maintenance to meet the requirement of high capacity dumpers is difficult. Further, high stripping ratio demands more fleet which endangers safety. Added to this, the Neyveli region is subject to more rainfall/cyclones hindering the operation of dumpers.

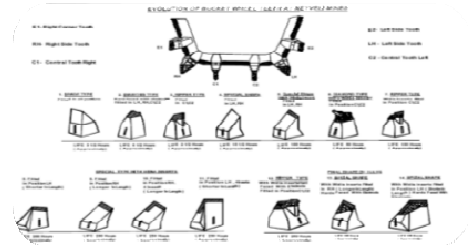
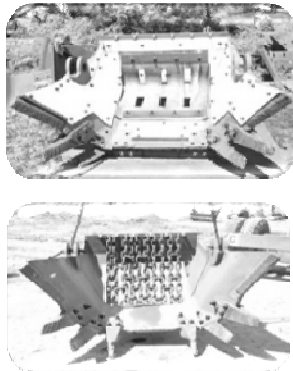
For production of overburden of about 159 Mm³ per annum at the Mines at Neyveli, within the available range of CME equipments, the capital cost involved and operating cost including carpeting the working benches for CME technology balances with the capital intensive SME technology.

During the first deployment of BWEs, NLCIL Mines faced many stumbling blocks. All those stumbling blocks were crossed over by making the necessary changes/alterations in the design of parts of BWEs.

UPGRADATIONS IN CONTINUOUS MINING TO SUIT NEYVELI MINES

Modification in the Bucket

The overburden soil in the top most bench, due to its sticky nature got stuck up with the bucket and thereby reduced the bucket volume and hence reduced the production rate. This problem was overcome by fixing chain mate on the backside of all the buckets.



MODIFICATION IN THE BUCKET TEETH

Bucket Wheel Excavators are severely strained due to the hard nature of the sandstone, resulting in reduced teeth life, damages to differential and other gears, the slewing mechanism and the structures with consequent reduction in efficiency of operation. Yet another factor is the reduction in the hourly output of production which varies inversely as the square of the hardness of the strata.

A large scale experimenting on teeth design and finally providing Tungsten Carbide tips with hard-faced sides on the teeth and modifications on the structural side of the bucket wheel excavators reduced, the strain on the machine to certain extent.

Other modifications done in BWEs

- * Bucket wheel is modified with thick wear plates and hoppers were provided with synthetic material lining to avoid accumulation of soil and wear.
- * Cyclo gears in Slew Mechanism and Rotary plate drives are modified into planetary gears.
- * Bucket wheel boom head were modified with solid plate construction and all booms made either with plate construction or with built up sections instead of lattice construction.
- * Slewing counter weights were modified in the old BWEs and totally eliminated in the new ones.
- * BWEs which were designed with three conveyor belts were modified to have two conveyor belts.
- * In 700 litres BWEs, the position of the slew centre bearing changed and centre pivot bearing was strengthened.
- * In Bucket Wheel Gear Box, to avoid frequent failure in differential system, single step down gearbox without speed variation was introduced.

Safety devices in SMEs



- * CCTV surveillance in SMEs and other strategic locations.
- * Sequence operation in Conveyors and SMEs.
- * Position limit switches in Conveyors and SMEs.
- * Over speed protection devices
- * Slip and Zero Speed supervision devices.
- * Roller Protection switches.
- * Ground gradient monitors, Collision protection devices.
- * Safety fuses and Circuit breakers, Fusible plugs, Magnetic clutches etc.
- * Automatic Sirens, Belt Sway identifiers.
- * Pressure, Wind speed, Brake Wear monitors etc.

BLASTING

Even after these modifications to improve the productivity, it is thought of loosening the hard strata akin to the looseness of OB in the German mines. Blasting of the overburden to loosen the strata for efficient handling by bucket wheel excavators has made a remarkable improvement in production. Loosening the hard strata has become beneficial to the bucket wheel excavator by reducing strain on it and thereby increasing the rate of output.

In the past, Cartridge Explosives were the main type of explosives used in NLCIL. Presently around 70% is Site Mixed Emulsion (SME) type explosives and the balance 30% is met out with Cartridge explosives due to

- (a) Superior bore hole coupling result in better utilization of explosive energy.
- (b) Highly safe as it is non explosive until it is mixed at site.
- (c) Eliminates the manual loading, unloading and threat of pilferage.
- (d) Operation Cost of manpower and explosive van is lowered.

Latest systems available in the market like Electronic Detonators and Gas bags are being regularly used in the sensitive areas.

IMPLEMENTATION OF VVVF DRIVES

This improvisation is helpful in optimizing power consumption.

- ❖ Individual motors are replaced with VVVF (Variable Voltage and Variable Frequency) drives which are more quality controlled and also speed control is achieved.
- ❖ Increased power factor can be achieved in case of VVVF drives which in turn saves energy.
- ❖ VVVF drives provide smooth starting and so the time lost is also less.
- ❖ Conveyor drives also replaced with VVVF drives.

PLC BASED AUTOMATION SYSTEM FOR LIGNITE BUNKER

Uninterrupted supply of lignite to the connected Thermal Power Stations was a long felt need at NLCIL mines. To accomplish this, PLC based automation control including retrofitting of relay logic with PLC, control by unifies control system, using both way paging and CCTV systems were established even before a decade.

The latest generation SMEs in NLCIL mines are procured with the above technical advancements to have more working hours and lesser down time.

Wireless Based Centralized Monitoring Operation and Control System

In one of the NLCIL mines, one system comprising of one BWE, one Mobile Transfer Conveyor, one Spreader and Belt conveyors for a total length of around 5 km is made automated to enable centralized control & monitoring. Wireless communication technology is used for this. This has resulted in reduced stoppages and effective maintenance of equipments.

Maintenance Management based on Systems, Applications and Products in Data processing Software

To reduce the out of orders, to plan the routine maintenance activities and to cut down the inventory, a system for Maintenance Management of Mining equipments was introduced. In this system computerization of the details of SMEs, their preventive maintenance work details, crew details and replacement parts was done. Work permits with all relevant details will be produced for the any type of repair and maintenance works.

Condition Monitoring for SME Equipment



Condition monitoring is being accepted as an effective method to assess the requirements of maintenance and to increase the operating life of installed plant and machines. Many parameters can be monitored for an effective health condition of the equipment. Condition monitoring of SMEs are carried out using the technique of “Vibration Analysis and Diagnostic Studies” in which vibration analysis is being applied to pinpoint the health condition of the SME equipment.

WATER MANAGEMENT

NLCIL mines require meticulous management of ground water as well storm water.

Ground Water

Observation wells at strategic locations are established to monitor the ground water level and quality regularly. In addition, regional water level and quality monitoring is being done in and around Neyveli area as a part of the ground water management. Using the experience gained for the past periods, pumping of ground water was reduced considerably by drilling of wells at appropriate locations. Water pumped out from mines is gainfully utilized in captive Thermal Power stations.

Storm Water

In Mine-I rain water from catchment area of mines and water oozing out from overburden was collected in reservoirs formed during mining operation. To save water, clear water from these reservoirs is treated in Treatment plant (8000 GPM) and used in residential areas.

In case of Mine II the water collected in reservoirs are treated and used in the connected Power plants of capacity 1470 MW and 500 MW. By utilizing the storm water for drinking/industrial use, ground water pumping is reduced resulting in conserving valuable ground water.

In addition to these, the water collected in mines is pumped to the nearby areas for irrigation activities, which helps in raising crops three times in a year. This, in a great way helps in conserving the ground water in the region.

Eco friendly mining through SME technology

- * Mining by electrically operated Specialized Mining equipments, the pollutant gases released which one can experience by doing mining by CME has been reduced considerably.
- * Since the Neyveli mines is big in all three dimensions, sufficient natural movement of air is developed. Due to this the pollutant gases emitted were thinned by mixing with air.
- * By raising around 22 million trees in NLCIL's region, the mean temperature of the region was reduced by 2°C, attenuated the noise generated by mines and TPSs and reducing the levels of SO₂ in air.
- * The sharp teeth fitted in the buckets of BWEs produce very little dust and thereby dust pollution is reduced.
- * Water spraying with pressure at the cutting face while excavating lignite by BWEs controls the production of lignite dust which harmful to human health.
- * Haul roads, Inspection roads adjacent to conveyors and the approach roads to all areas of mines are water sprayed at regular intervals by sprinklers and fixed water jet nozzles/guns.
- * Every drilling machines used for making holes for blasting are fitted with dust pullers. In case of wells for pumping ground water, wet drilling is in practice.
- * The peripheral approach road connecting all working areas is formed with blue metal. The haul roads are usually laid with gravel /laterite topping.
- * Ground Water Pumping was optimized by drilling wells closer to the lignite excavation to get the draw down effect.
- * Rain water harvesting and artificial recharging are being done regularly.
- * Concurrent refilling of mined out areas, reclamation and restoring is being followed in NLCIL mines.
- * To control land degradation, NLCIL takes necessary measures by afforestation, top soil conservation, bio-reclamation and integrated farming system in reclaimed areas.

CONCLUSION

In pursuance of NLCILs high level of success in adopting SME technology, it is suggested that consideration of this technology in large opencast mines on the basis of environment friendliness and high production grounds. Profit of NLCIL over the decades substantiates this. In fine, SME technology is continued to be the preferable mining methodology in Neyveli Mines due to its wide applicability in large format continuous mining system with back to back reclamation and its significant contribution towards energy conservation and environment friendliness.



Challenges in the Restoration of Inland Waterways for Navigation: A Case Study of Parvathy Puthanar in Kerala

*N.M. Sabitha*¹, B G Sreedevi¹*

*National Transportation Planning and Research Centre, Thiruvananthapuram, Kerala¹, sabithanm@gmail.com**

ABSTRACT

Water transport was the main mode of transport of public and goods for many centuries in Kerala. With the introduction of faster modes of transport, these waterways remained neglected. The Govt. of Kerala has taken initiative to re-introduce water transport in the state by restoring the canals from Kovalam to Kasaragod of about 610 km. This paper presents the various measures adopted for cleaning and preventing the pollution of Parvathy Puthanar passing through Thiruvananthapuram City, Kerala, which is a manmade canal with length of 16.5 km and make it operational. A detailed study was conducted by NATPAC at the instance of KWIL, to approach the problem in a holistic manner, since the cleaning, deepening as well as disposal of the waste are major challenges as the canal passes through thickly populated areas. The task has been divided in to two phases namely, cleaning and desilting. As a part of the program, the first stage is to clean the aquatic weeds and other waste which has dumped into the canal. An Aquatic weed shredder was used to remove the aquatic weeds while an amphibious Truxor was used to remove the waste.

In the second stage of cleaning, silt pusher equipment is planned to use to clean the silt accumulated in the canal and to provide a water depth of 1.5 m, so as to make the canal navigable. Measures for solid and liquid waste management, beautification of the canal, construction of jetties and other tourism related infrastructure are also included in the implementation plan to sustain the canal system offer restoration.

KEYWORDS Inland waterway, Parvathy Puthanar, Restoration, Thiruvananthapuram

INTRODUCTION

In Kerala, Inland Water Transportation (IWT) holds enormous potential for improving the mobility, increasing accessibility and supporting redevelopment objectives. Kerala is one of the fastest urbanising states in India. According to Census 2011, nearly half of its population (48%) lives in urban areas as against 31 per cent at the national level.

Kerala is having a very good network of road, rail and waterways. The total length of the waterways in the state is 1895kms. This includes rivers, backwaters and man-made canals. The main waterway in the state is the West Coast Canal (WCC), which connects Kasargod in the North and Kovalam in the South having a length of about 610 km. A portion of the West coast canal, i.e. from Kottappuram to Kollam, has been declared as National waterway-III in 1993.

The Government of Kerala has accorded top priority for the development of Kovalam-Kasaragod stretch of West Coast Canal. As part of this, the development of the portion of Parvathy Puthanar between Kovalam and Akkulam, which connects two major tourist locations of the area, is in progress. This is being executed by Kerala Waterways and Infrastructures Ltd (KWIL), an SPV formed for the purpose of developing waterways by Govt of Kerala and CIAL.

SCOPE AND OBJECTIVES

The scope of the study is limited to the Kovalam-Akkulam section of Parvathy Puthanar, a manmade canal. The major objective of the study is to develop the waterway between Kovalam and Akkulam to ensure sustainable inland water transport. The study includes preparation of detailed drawings, obstruction analysis, recommendations on various parameters like boat services, critical vessels, landing facilities, safety and management aspects, environmental aspects, tourism aspects, technical, economic and financial feasibility and propose the implementation strategy to sustain the canal system after restoration.



STUDY AREA

The study stretch extending from Kovalam to Akkulam is 16.50 km and runs almost parallel to Sea and NH bypass. The waterway passes through Panathura, Edayar island, Poonthura, Vallakadavu, Trivandrum airport and ends at Akkulam lake. The study area map is shown in **Figure 1**.

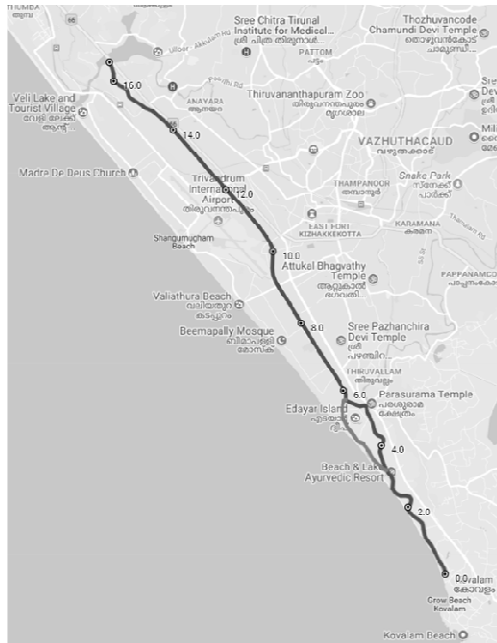


Figure 1 Study area map

METHODOLOGY

The methodology adopted includes secondary data collection, canal inventory, details of households/encroachments and its location. The collected data were analysed to find out the existing problems and to assess the development strategy and future development potential of the canal.

Detailed Surveys

Detailed inventory was conducted to assess the present condition of the canal. Other bottlenecks such as missing links, insufficient width/depth, points of sewage discharge, dumping of solid waste etc were located. The present condition of the waterway were collected including vertical and horizontal clearances, type, connectivity and condition of cross structures and bank protection.

The topographic survey was conducted along the canal stretches for preparing the base map of the study area using advanced survey equipments like Differential Global Positioning System (DGPS) and Total Station. Hydrographic survey was conducted using echo sounder wherever possible. The existing bed profile of the canal and water level were collected at 100 m interval. The estimation of dredging quantity was done.

Socio-economic Survey was done through a questionnaire survey to collect details of demography, type of buildings, built up area, drainage facilities, sanitary facilities, sources of water, availability of water, water demand, disposal of waste water and solid waste and usage of canal by the households.

Environmental Status

Water samples were collected from locations where there is change in the characteristics and were tested in the laboratory for parameters like pH, temperature, turbidity, conductivity, total dissolved solids, hardness, chloride, sulphate, nitrate, iron, calcium, magnesium, Chemical Oxygen Demand, total suspended solids and E-coli.

DESIGN OF CANAL

Since many different sizes of vessels will use the waterway depending upon the cargo, user etc., a typical vessel with limiting dimensions for the channel has to be arrived at. This is termed as the "Design Vessel". The major constraints that come under consideration for design vessel are the SM lock and the Railway bridges at Chakka for



which changing the vertical clearances are very difficult. In order to make the SM lock operational, which is a bottleneck, lock gates are to be provided and this will reduce the horizontal clearance of SM lock further to around 4.5 m from the existing 5m. So the critical canal dimensions to be considered in the existing condition with minimum modification are HC = 4.5 m, VC = 3.2 m and length of lock 27.5 m.

The dimension for the design vessel that can navigate safely in the above stretch will have length = 20 m, Moulded breadth = 4 m and air draft = 3 m with loaded draught of 1.3 m (if depth of 1.5 m can be maintained initially). Another bottle neck in the Kollam Kovalam section is the tunnels at Varkala and Sivagiri. So after considering the dimensions of SM lock and tunnels, the dimension for the design vessel that can navigate safely in the above stretch will have length = 20 m, Moulded breadth = 2.5 m and 2.1m overall height with loaded draught of 1.2 m. The recommended clearances for cross structures includes, 20.0 m of clear span under bridges and 6.0 m clear height above HFL under bridges for new bridges. For existing bridges, clear span under bridges will be 5.0 m and clear height above HFL under bridges will be 3.20 m.

IMPROVEMENT PROPOSALS

In order to develop the canals to a sustainable waterway, for tourism and passenger transport, certain improvement proposals which are to be implemented are charted out as given in the following sections.

Cleaning of Canal

The canal is polluted with both solid and liquid waste. In many places drains are joining the canal which pollutes the canal. Bushes and branches of trees which are obstructing the waterway are to be cleared. The water weeds are to be cleaned and plastic waste are to be removed.

Dredging

The canal is to be dredged to maintain the flow of water and to achieve the minimum required depth of water for boat movement. In the initial phase no land acquisition is proposed and so the narrower section with less than 20m width is proposed to be dredged with the existing width as width of canal. For wider sections, a rectangular section is proposed with canal of width 20 m and water depth of 1.5m.

New Canal Cutting

Cutting is needed at Panathura, where new canal is to be constructed at the location where the road is crossing the canal near Panathura Temple and the nearby area for a length of 160m where canal does not currently exist. The cutting quantities estimated for developing the stretch is 541.6 m².

Bank Protection

Permanent bank protection should be provided to give sufficient structural strength to banks. In the Akkulam Moonnattumukku section, the banks were protected with pile and slab and a sloping stone pitching was provided from the top of the pile slab construction to the ground level. The stone pitching was damaged in many places which is to be repaired and new stone pitching is to be provided wherever needed.

Jetty and Landings

Jetties are the one of the major infrastructure facilities needed for inland navigation. Total number of 5 jetties is proposed for the canal at Kovalam, Thiruvalla, Chakka, Akkulam and Vallakkadavu.

Navigational Aids

Navigational aids are provided to assist in safe navigation along the prescribed channel thereby guaranteeing the safety of the travel. Fixed shore structures are to be erected at bridge sites and places where branch canal join. Channel markers, information, warning and direction signboards are proposed in the study stretch. It is estimated that the total number of 54 units of lights are proposed to mount on the structures. 52 sign boards are to be installed in the waterway. Traffic signals are to be provided at SM lock and Chakka Bridge, where the canal is narrow, to regulate traffic.

Cross Structures

As per the study, there are 28 structures existing in the canal. Among this, two structures are rail bridges and the rest comprises of 11 road bridges and 10 Foot over bridges (FOB), three pipelines one lock and an aqueduct. Among the existing structures, three bridges are to be reconstructed.



Tourism Prospects

As part of developing tourism, it is proposed to undertake canal beautification by providing foot path, hand rails and concrete benches along the stretch between Venpalavattom and Akkulam on both sides and connecting it with a rainbow bridge. The jetty at Kovalam has to be developed along with a facilitation centre. Amenities like children's park, restaurant, kiosks etc are proposed. As canal is comparatively wider, water sports facilities can be provided.

Jogging track and Butterfly Park are to be developed on banks so that it could be developed as a leisure place during early morning and evening hours. At Vallakkadavu, along with the Eco Bio park, a light and sound show can be organised. A boat tour and island tourism facility can be developed around the Edayar island connecting the pozhi and nearby island area.

WASTE MANAGEMENT

Sewage System in Thiruvananthapuram City

In Thiruvananthapuram Corporation only, 30% area is covered by the underground sewerage system. The households in the remaining areas depend on various on-site systems namely, septic tanks, borehole latrine and community toilets whereas 8% of the population do not have access to safe sanitation. The sewage is disposed at the Muttathara Sewage Treatment Plant, which handles 32 million litres per day.

The present system of disposal of sewage is functioning based on the obsolete technology of fodder farming, which is unable to treat the increasing sewage load reaching the farm area. Hence the entire sewerage system is practically defunct, with raw sewage finding its way through punctured manholes and leaky sewer lines, ultimately dumping into open yards or surface water bodies. A complete unhygienic condition prevails in and around the sewage farm area. All these factors are the constraints for the waste water treatment of the city.

A household survey was conducted to assess the socio-economic characteristics of the dwellers along the canal bank. The survey questions were designed to capture information on ownership of the property, family particulars, type of building, location of building, age of building, built up area, details of the existing sanitation facilities and other relevant details were also collected.

The details were collected from 980 households. The location of all buildings was marked with the help of a handheld GPS. From the collected data, it was observed that , a total number of 4585 people are occupying the 980 households surveyed. About 94% of the buildings on the banks of the canal are residential buildings. Only 4% of the buildings are commercial buildings. The details of existing drainage and sanitation facilities were also collected from the households. More than 98% of the buildings have toilet facilities, while about 77% of the buildings do not have septic tank. The buildings that are not equipped with septic tank currently discharge the waste into the canal, making the canal polluted.

Sanitation facilities like latrine, drainage, etc are not offered to the people settled on the canal banks. It causes serious environmental and health hazards to the people also it affects the nature of canal by discharging of the human excreta. So community toilets at every 1km interval have to be constructed. Nine community toilets between Moonattumukku and Vempalavattom has to be constructed and the cost of one community toilet is 12.5 lakhs and the total cost for constructing the community toilets is 112.5 lakhs.

Bio gas plants are proposed for bio degradable waste which is to be installed at 4 locations and the total cost will be Rs. 200 lakhs. The total cost of providing septic tank and related facilities for 506 families will be Rs. 129.26 lakhs.

Management of Solid Waste

Other major environmental issue in this area is solid waste disposal. The generation of solid waste include decayed vegetables and fruits, leaves, kitchen wastes, paper pieces, cloth pieces etc. At present the settlers are directly disposing the solid waste into the canal, which is becoming a huge barrier for flow in canal.

Basically there are four types of disposal techniques in solid waste management : Sanitary land fill, Incineration, Bio-gasification and Composting.

Based on the characteristics of solid wastes the appropriate disposal method is listed out in **Table 1**.

Involvement of Trivandrum Corporation Development Authority and Local NGO's are required for effective waste management of the area.

Cost Estimate

The cost estimation for improvement of canal with 20.5 m fairway has been done and the results are shown in **Table 2**.

Table 1 Solid waste disposal method

Chainage, km	Location	Disposal method
3.2	Near Beach and Lake resort	Composting
5.3	Edayar Island	Composting/land filling
8.5	Muttathara	Composting/land filling
14.9	World Vegetable Market	Composting

Table 2 Summary of cost estimation

Item	Total Rs. in lakhs
Cleaning	55.0
Dredging	582.61
Cutting	1.84
Bank protection	2613.04
Sanitation facilities	112.5
Biogas plant & solid waste management	200
Septic tank	129.26
Jetties	705.4
Navigational aids	17.02
Canal Beautification	70
Boat	90.0
	4576.67

IMPLEMENTATION OF THE WORK

The cleaning works were implemented by KWIL and NATPAC was the supervision consultant during the cleaning of the canal.

Cleaning of the Canal

One of the equipments used for cleaning was Truxor equipment which is an amphibious machine capable of operating in slushy conditions with low or nil water depth. It can cut through submerged vegetation and rake out cut and floating vegetation. Attachments like Milling and Clamshell can uproot the plants. Aquatic weed shredder was used to shred the weeds and a Pontoon crane was used to remove the shreaded weeds from the canal. The cleaned materials/rubbish/ weeds etc., were stored temporarily on the immediate banks of the canal for drying and it was loaded and transported to the identified disposal sites by means of trucks and finally disposed it off at designated locations on the banks of canals at suitable locations by burying under a soil cover. Figure 2 shows the equipments used and Figure 3 shows the view of canal before and after cleaning.

Cutting of Trees

The trees and bushes obstructing the waterway were cleared and the old logs fallen into the canal were removed to make the canal navigable.

Desilting

Desilting is proposed to be done using silt pusher instrument.



Figure 2 Equipments used for cleaning



Figure 3 Canal before and after cleaning



RESULTS AND DISCUSSION

The study was carried out to make the Kovalam-Akkulam section of the waterway navigable. Detailed surveys were conducted and improvement proposals were proposed. A detailed plan for tourism development and waste management was also proposed to have a sustainable development model for the waterway.

The total cost of improvement for the project will be Rs. 45.77 crores. The available land can be developed by constructing walkways and other tourism facilities, thus increasing the potential of the waterway and also as an alternative source of income. Private participation may be involved for tourism development, vessel operation and maintenance of the waterway. The cleaning and desiltation activities are in progress by KWIL and it is expected that the waterway will be navigable by 2020.

ACKNOWLEDGEMENT

The authors express their sincere gratitude to the Kerala Waterways and Infrastructures Ltd (KWIL) for providing necessary financial assistance for the study.

REFERENCES

1. L. R. Kadiyali, Updating Road User Cost Data in India, Final Report, Ministry of Surface Transport and the Asian Development Bank, L. R. Kadiyali and Associates, New Delhi, 1991
2. IRC:SP-30, Special Publication 30, Manual for Economic Evaluation of Highway projects in India, The Indian Roads Congress, New Delhi, 1993
3. C. A. Nash, Economic and Environmental Appraisal of Transport Improvement Projects, Chapter-14, Transport Planning and Traffic Engineering, Edited by C. A. O'Flaherty, John Wiley & Sons, 1997
4. S. Sriraman, Inland Water Transport in India: Issues and Prospects, Asian Transport Journal, Asian Institute of Transport Development, New Delhi, June 1998.
5. N. Rangaraj, and G. Raghuram. Viability of Inland Water Transport in India". ADB India Resident Mission: INRM Policy Brief No-13: 13, 2007



Preparing Organizations for Digital Manufacturing

K V Santhosh

Operations & TPM Facilitation, Essae Digitronics Private Limited, Bangalore, k.v.santhosh@mails.essae.in

INTRODUCTION

The significant growth of Information technology enabled the global business in a big way and the customer requirements are exceeding the expectations since last one decade. Today the products are developed and delivered at the shortest cycles and organizations are using online commercial platforms to sell their product globally. The global digital selling platforms are created a tough competition for the organizations in terms of Profit, Over heads and Speed of new product launches.

Our daily life is running more and more on digital information and technology. One click from your mobile phone is enough for you to get the daily needs to your door step. Our personnel data, bank transaction, personnel transportation and communication network across the globe is run by digital technology. Since it is integrated to our daily life, the practice and behavioural changes happened without any external pressure or compulsion.

Even though technology is improving very fast and when it comes to application in a typical Indian industry, we are facing many challenges due to inertia effect of our existing practices and the way the organizations are designed and run for many decades. There are many practices running in a highly ineffective manner due to human interference. It is hampering organization growth and many organizations realized it very late.

Today, great challenge are being faced to re-engineering the business processes and it is becoming a major hurdle to build competency inside the organization. Human competency to understand and implement the current technological changes are very much essential.

In the above context the article is relevant to contemporary organization in India and those who are trying to upgrade the business practices also.

MAJOR STEPS FOR DIGITAL TRANSFORMATION

- Digital transformation strategy and customer focus
- Mapping of Current process
- Identification of **Major** gaps
- Design of the revised business process
- Identification of '**right**' technology to address the improvement in the process
- Human resource development
- Technology partner development
- Design of MIS & Decision making
- Design of Knowledge bank.

STRATEGY AND ROAD MAP FOR DIGITAL TRANSFORMATION

Every business opportunity start from the customer need identification it is nothing but 'information'. The accuracy of the information only will help us to realize the product or service to satisfy the customer requirements. The challenge in a traditional manufacturing organization the data is completely depend on manual transactions and the information will not completely reach to all connected in the supply chain (**Figure 1**).

Organization strategy should address the enhancement of value of services and products offerings by transforming to a digital manufacturing environment.

TheMicrosoft's survey, of 615 manufacturing firms in 15 economies across Asia Pacific, identifies managing costs as the biggest business concern among CEOs in the region. And, it is through that lens that they view digitalization largely as a way reducing expenditures. In its analysis, agreed that while rising costs represent a real worry, it is a backward way of looking at the power of digital transformation. The expected results from digital transformation are shown in **Figure 2** and **Figure 3**.



Figure 1 Digital transformation overviewed



Figure 3 Impact to long-term performance

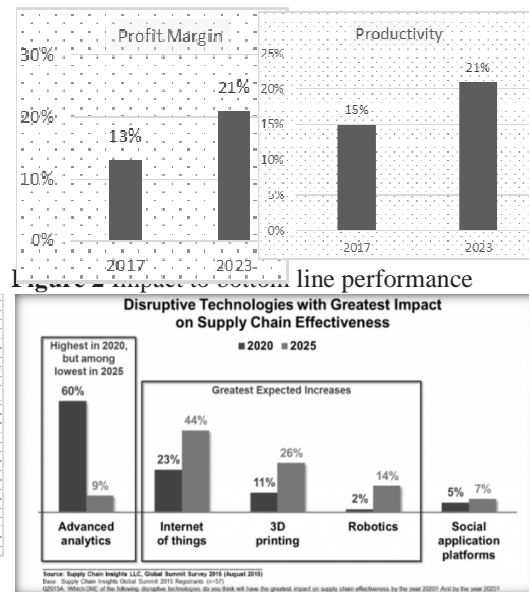


Figure 4 Future supply chain effectiveness by Year 2025

ENABLERS FOR IDENTIFYING GAPS IN PRESENT BUSINESS

In the present condition we are not aware of many inefficiencies existing in the systems and practices.

It is recommended that use of systematic tools or applications will help us to draw or map the current stage of process in our operations. There are many enablers to improve manufacturing efficiencies like Total Productive Maintenance (TPM) Lean manufacturing, Six sigma etc. All the above said tools will help to reduce variations, waste in operations, losses in machines, major manpower losses and losses from tools, jigs and dies etc. This will help us to map the current practices in the organization since the tools are designed in logical manner to improve the process. The losses and variations are attributed by a poorly designed process or a practice and thereby it is affecting the expected rate of performance.

The enabling tools are opened up various opportunities for identifying the problems and future opportunities. Even though the inefficiencies are exposed, the data related to them needs to be collected, analysed and used it in proper manner to improve the current process efficiency of organization

IDENTIFICATION OF THE RIGHT TECHNOLOGY

The digital manufacturing science will play a major role to handle data effectively and enable organization to overcome the problems related cost, quality and other business challenges like over heads increase, slow speed to market, customer satisfaction and declining profit.

It is the foundation on which various modern advanced manufacturing systems become a reality, and the realization of any modern manufacturing system must be constructed on the basis of a digital manufacturing system. Thus it is necessary to clarify the operation mode of the digital manufacturing system and the demands of its architecture before studying the digital manufacturing system and constructing its integral model system. The basic platform to be prepared for going for the implementation of Digital Manufacturing.

The following are process design initiatives will drive the digital transformation towards its goal: (i) Standardization of products (modular design / design for manufacturability) (ii) Design of supply chain (iii) Standardization of process (iv) Application of quality management systems (v) Manufacturing management and data acquisition (vi) Network and grid technology (vii) Engineering database (viii) Virtual stimulation technology (ix) Metadata.

STANDARDIZATION OF PRODUCTS/ DESIGN PROCESS

Standardization applicable not only to the hardware used in product but also require a standardized process. There are many case studies in my organization and other organizations known to me about failure in the design process



leads to customer dissatisfaction and loss of business opportunities and thereby it emphasizes on the requirement of a standardized design process.

The customer expectations are changing and product life cycle is getting shortened day by day and we require a systematic process with highly predictable results. The digitized platform only can give the repeatability of the process. Product design can have a basic platform to handle modularity is preferable today. It is possible to handle in design software like “solid works” by creating a customized library. Concurrent engineering practices in digitized platform will improve the consistency in the design process and human elements are removed from it. Example Product Dozier an APQP application uses concurrent engineering in digital platform.

Virtual and simulation tools to be selected for design validation and verification to reduce the development time and cost.

DESIGN FOR MANUFACTURABILITY AND IoT FEATURES IN PRODUCT

Design for manufacturability was a basic requirement and that is why it was going in hand to hand with manufacturing. But in today's scenario many products required serviceability based on information and integrating to other equipments are becoming important to sell or buy in global market.

We have to build necessary intelligence to products and equipments to handle information receiving and communicating to other equipments or accessories.

STANDARDIZATION OF PROCESS AND QUALITY MANAGEMENT SYSTEMS

As stated in introduction, the inertia effect of human practices are affecting our system practices and it is not giving the desired result. Human elements can affect the logical flow and only IT platform can eliminate it. Selection of the technology driven intelligence also important in a digital platform.

For example, if you are in manufacturing company dealing with dynamic customer requirements and Short LCC products then you should be using CAD CAM/3D printing and other simulation tools to reduce the product development time. In the case of Project Management organization you may be using Project monitoring resource monitoring platforms.

The Selection of right technology to bring artificial intelligence into your process is very much essential. We are having thousands of technology solutions but right selection is important.

PRODUCT CODES AND PROCESS CODES ENABLING SUPPLY CHAIN DESIGN

Codification of process and products is very much essential to manage the transactions in platforms like ERP /SAP. The digital manufacturing play a major important role in our supply chain. The supply chain design should consider many of the aspects for handling information through a digital platform.

The success of any organization mainly depend on the supply chain network in the company integrating suppliers and customers .The goods and information flow in parallel and information is equally important as goods today .

Various techniques like Electronic Data Inter Change (EDI) Barcoding, Point of Sale (POS) information integrated to a MRP will help the management of demand and supply effectively.

MANUFACTURING MANAGEMENT AND DATA ACQUISITION

The manufacturing is undergoing rapid changes and we are going to a platform of industry 4.0.

At present many manufacturing shops are facing various challenges in term of data and information management. This is due to various reasons like,

- Present manufacturing systems and practices.
- Limited capability of existing resources
- Partial automation and poor integration of equipments and process
- Limitations in supply chain design
- Knowledge gap of Human resources

Digital transformation in manufacturing is all about how you prepare yourself. We need a clear road map for transformation since the complexity in manufacturing environment is higher when compared to other operational area.

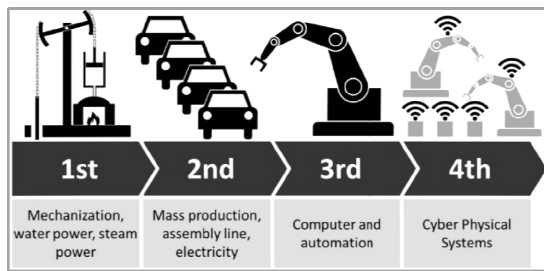


Figure 5 Industrial revolution stagewise

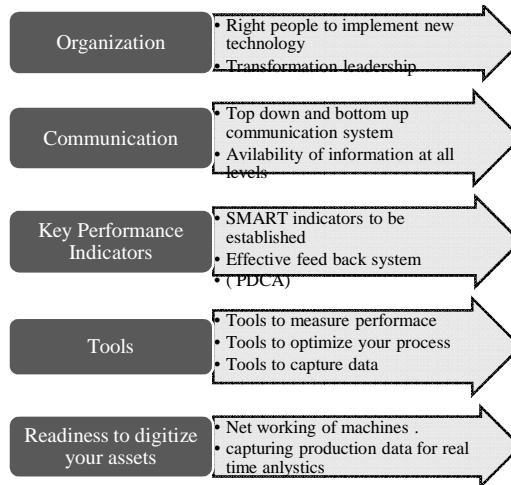


Figure 6

The intelligence is built into the equipments for digitizing to manage sequencing operations, material handling and quality control .There are many modules developed throughout the world to manage the digitization.

The main components are Processors, Transceivers like Ethernet, Wi-Fi, miniature power supply, Sensors and activators are the eyes and ears of IoT, actuators transform electrical data into energy. Gateways and routers will help to integrate the equipments through networking.

The digitised equipments will perform the actual works, either through a PLC controlled or through a remote controlled system which integrate the equipments (Machines, Robots and other Material handling systems)

Predictive Maintenance Systems are embedded in the integrated software and it will give real time information about the performance of parts and timely attention for the maintenance team will enhance the reliability of the equipments.

Manufacturing data acquisition features will enable the storage, processing and application of manufacturing knowledge. It will help for creating and effective MIS and supporting the decision making.

Virtual simulation technology is making decision making process simple when we are dealing with complex manufacturing systems. Further, Rob CAD is a popular software used in digital manufacturing. Models of automated machinery and production lines can be created and simulated in real time.



Figure 7 Rob CAD model

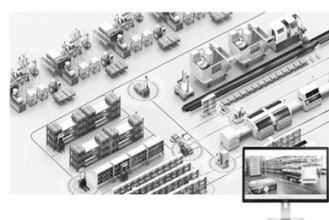


Figure 8 Digital manufacturing cell



Figure 9 Equipment performance monitoring in an integrated manufacturing

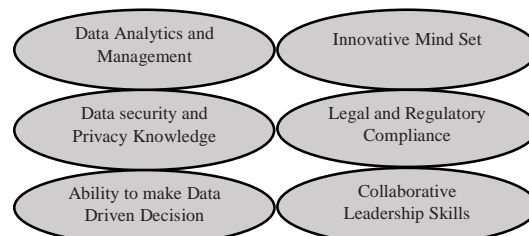


Figure 10 Factors to build up on integrated HR



HUMAN RESOURCE DEVELOPMENT IN DIGITAL TRANSFORMATION

Human resource is the most important elements in any organization. The HR personnel across the globe is bringing new dimensions in HR capabilities to manage the changing needs of digital age. Accordingly, major capabilities to build in HR is shown in **Figure 10**.

Organizational structures are changing from the traditional set up and Information and Technology managers are finding places in Organizational Hierarchy.

Managing information and data is very significant as we handle funds. The future industrial atmosphere is going to change and the information and data will transfer along all supply chain as the materials and services.

Creation of the talent pool for the next generation of industry is the bigger challenge in our nation to meet this requirement.

Our educational and training systems require a complete transformation to meet the future challenges.

Computer literacy in our nation is improved significantly in the last two decades but today we require 'right' computer knowledge. We have to create more analytical & application talents to take care of the changing needs of industry.

Technology Partners

Today many technology solution providers are coming up across the globe. Major players are HCL, SIEMENS, BOSCH, Microsoft and SAP Lab etc. The selection of the modules will be industry specific.

Considering Indian conditions there are many small players coming up through start up and Machine learning, Artificial intelligence is in very nascent stage and every case to be handled on a research based projects.

Today in my organization we are having partial digitised areas but in total integration is a big failure. For example, these are enough customer complaint data from various sites from nationwide. The data is used only for calculating satisfaction index of installation and only to find out the number of complaints from regions. Further analytics is required and the tool can be machine learning and can progress to AI to connect to customer and other internal functions.

There will be similar challenges every Indian Company as well. As it has explained earlier that the strategy of organization playing an important role for the selection of Objectives and targets to achieve through digitization. The right partners can be selected only after preparing the road map.

CASE STUDY

The Company X is in automotive components and sub assembly business from year 1996. The current challenges are:

- Pressure of profits shrinking from Year to Year.
- Competition is bringing the cost down of components.
- Threat of Chinese supply.
- Costings are made on traditional approach.
- New products are not taking up because of cost not meeting the customer price.
- Not enough data about actual performance of assets.
- People competency is the challenge.
- Existing SAP platform is inapt and the decision making is arduous like Operation Process is not properly mapped which throws inaccurate inventory
- Partial automation not giving desired results.
- Forecasting errors leads in high or low inventory.
- Customer Quality and Delivery ratings are not satisfactory.

The weakness identified:

- Not able to justify the non-acceptance of orders due to price.
- Cost structure is traditional.
- New product development and proving cycle time is more.
- Not having real time data from manufacturing to address the actual costing and using norms based on past history.
- No clear road map for manufacturing.



- Not utilizing SAP effectively. The analytical parts not utilized and only focussing on Transaction part.

SOME OF IDENTIFIED SOLUTION

Processing cost is area where company is beaten down by competitors. TPM tracker with IoT to get the real time data for actual machine hours and asset efficiency. The bias in the costing decision will be eliminated.

New product proto development and actual machining simulation can be done on offline without disturbing the actual machines. Fancu simulation tools can be used. The will integrate concurrent engineering practices and machining conditions. Also we can estimate the costing to an extent of 90% accuracy.

TPM tracker can give the major losses where company can focus and it will help us to take action by using technology. The above are some of the solutions identified for the business challenges.

DECISION AND MIS

The most important function in organization is the right decision making. Data analytics will give many predictive out puts and later we can convert to prescriptive.

Decisions: There are plenty of decision making tools available in the business management .The question is why we emphasis on digital data.

The digital data is free from bias because it is generated form an integrated system and where every elements are interacting without human interference.

MANAGEMENT INFORMATION SYSTEMS

MIS is the final outcome of analytics and information generated from an integrated systems. Digital dash boards are used in organizations, from security to board room. The visual management is becoming more popular and it is the sign of a 'Connected Factory'. Dynamics of business runs only on the faster business decisions.



Figure 11 Changing organisational structure

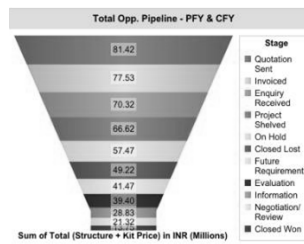


Figure 12 Dash board used in SFDC (sales force dotcom)

The major benefits from digital manufacturing are as follows

- More integrated management and decision making system.
- Transparent market analysis and evaluation system.
- Product collaborative manufacture and control system of manufacturing process.
- Product quality management system.
- Product marketing system.
- Customer service system.
- Effective supply chain management.
- Improved Quality of life of Employee
- Efficient knowledge bank for future of organization.

CONCLUSION

The digital manufacturing is going to be future of manufacturing across globe and especially India is the right direction now .Our Prime minister is taking more and more initiatives to make India as DIGITAL INDIA, let us support our country to become a great manufacturing hub in near future.



Simultaneous Engineering for New Product Implementation

Manas Kr. Mishra¹, Arnab Dasgupta², Bivas Bhattacharyya², Ankit Mehta^{*2}
Tata Motors Ltd., Jamshedpur, India¹
Tata Technologies Ltd, Jamshedpur, India², ankit.mehta@tatatechnologies.com*

ABSTRACT

Simultaneous Engineering (SE) is method of performing tasks simultaneously to reduce lead-time, production cost and reduced rework for New Product Implementation. It replaces conventional method of product release with an integrated approach involving Design Release (DR) gateways to reduce product development time. In order to provide seamless manufacturing of product “Simultaneous Engineering” caters to the Quality/Feasibility Issue at an early phase. Process of validation supported by system-based approach using “My SE Portal”, which ensures smooth validation process. Design and Bill of Materials (BOM) validation enables reduction of Product Launch Lead Time.

KEYWORDS SE, DR Gateways, Digital design validation, MySE portal, BOM

INTRODUCTION

Globalization has led to increased competition in terms of Launch Time and Quality of New Products, which not only caters to the demands of customers but also provides quality service. In order to gain market share organization needs to reduce lead-time of New Product Launch to stay ahead of their adversaries. To achieve these objectives one needs to work towards reducing idle and rework time during New Product Building phase before mass production.

Simultaneous Engineering (SE), also known as Concurrent Engineering [1], has been answer to achieve all the aforementioned objectives. SE is an integrated systematic approach [2] to perform simultaneous tasks to improve quality and reduction of product development time.

Requirement to develop new method of Design Release is due to mentioned below reasons - :

- (a) Increase in variety of products and complexity results long lead time for new product development
- (b) Increase in number of competitors in this emerging market has led to demand of reducing product development time.
- (c) Needs and demands of customers have also led to increased pressure for faster development of product which may otherwise result in loss of market share and customer trust.
- (d) Large number of departments working to support various functionalities of organization need a common platform for interaction. With increased division of work, system based mechanism is required for interaction between various departments.
- (e) Government standards also require product development to be robust to adapt required changes in short time.
- (f) With world becoming more technology driven, prolonged product development time may render it outdated or demands of customer may change during that period.

SIMULTANEOUS ENGINEERING VS CONVENTIONAL PROCESS

Conventional approach involves (**Figure 1**), design phases as mentioned below:-

1. Project Initiation Phase –
 - Market Analysis/Research – current requirement and demands of customers
 - Competitor Product Assessment – assessing products of competitors already present in market.
 - Product Planning Strategy – forecast of production cost and targets for the product.
2. Concept Selection Phase –
 - Idea generation for product with features which meet needs of customer
 - Benchmarking and Reverse Engineering of competitor product[3]
 - Internal & External Styling themes of product
 - Probable packaging/manufacturing feasibility requirement
 - Cost estimates for manufacturing and assembly of vehicle
3. Concept Development Phase –
 - Styling and technical specification freezing of product



- Design aggregates with respect to technical specifications released of product
 - Computer Aided Design Failure Analysis of developed designs
 - Integration of aggregates and Vehicle Building feasibility
 - Finalization of probable suppliers and required machineries and plant layout for production
4. Design Release Phase –
- Freezing designs and drawings of aggregates
 - Plant Layout and resource finalization for production
 - Resource Planning and Line Balancing for assembly of product
 - Supplier finalization for bought out parts
5. Proto Building –
- Post “Design Release Phase” prototype of Product is developed to test design & process
 - Provide feedback for improvements in design and process for volume production
 - Ensuring readiness of plant for mass production of product, also availability of bought out parts and equipment for same
6. Launch of Product –
- Considering improvement in design and process and resolution of all issues faced during proto building
 - Volume production of Product is initiated

SE process (**Figure 2**) is a ZERO-defect approach, which focuses on reducing the overloading activities at PROTO/LAUNCH phase by Digital Validation/Simulation using e-Tools to foresee/rectify potential Design/Mfg./Tooling issues at preponed stage to minimize later on rework & costing. “MySE Portal”, system based approach, is being used to enable SE process and monitoring/tracking of projects.

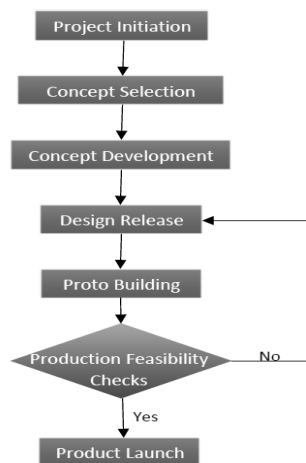


Figure 1 Conventional approach of product building

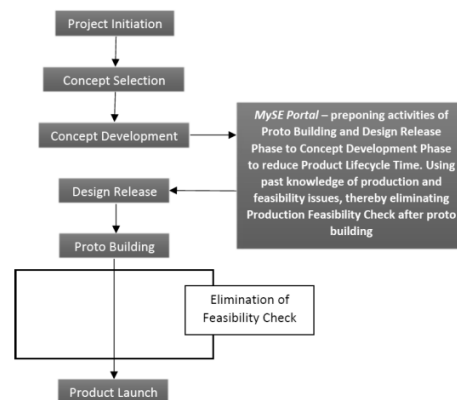


Figure 2 Simultaneous engineering approach of product building

Essential four pillars of “Digital Design Validation” are as follows[1]:

1. Digital Vehicle Building–Product validation in digital environment before the commencement of physical production on assembly line. Validation of product in line with current assembly line facility and processes, providing feedback for improvements in design that result in cost reduction and time required for implementing new changes. Involved process helps ensuring minimal changes in existing tools/process, which reduces time



required for installation of new equipment. Prediction of possible line stoppage issues due to ergonomically difficult fitments with knowledge of available production practices. Provide proposals for alternate solution to improvements in design to accommodate smooth development of product with respect to current production practices.

2. E-BOM Compliance : Part complexity reduction/commonization by providing Design BOM Compliance that includes developed parts suggestion and restrict the introduction of any new part unless specifically required resulting in elimination of time required for development and procurement of new parts. Alternate part suggestion without affecting functionalities of parts in Vehicle. Also suggestion of alternate assembly sequencing with respect current plant layout and resource availability.
3. Digital VLO (Vehicle Layout) : Vehicle roll out & quality audit process is facilitated by digital VLO to reduce vehicle booking/clearance time by validating potential layout issues & implementation of correct process in Assembly floor. Ensuring layout of vehicle as standard guidelines to reduce rework proto build phase. Identifying potential functional issues in terms of layout and providing alternate solutions for it. Adherence of Vehicle Layout with AISC (Automotive Industry Standards Committee) Standards.
4. Cross Functional Team (CFT) Approach : Communicating design issues and possible solutions to integrated Design & Production teams for immediate resolution of issues. Also, put forward relevant concerns of respective cross-functional department (Design, Planning, Production, Quality, Service etc.) to provide alternative and suggestions for productivity improvements. Documentation of concerns raised during discussions for future reference.

SIMULTANEOUS ENGINEERING - MYSE PORTAL WORKFLOW

Implementation of Simultaneous Engineering process is supported by system based approach through MySEPortal. Portal supports database maintenance through Digital library creation of brackets/clamps, VLO Guideline, fasteners and bulk items for reference during Design review and Design BOM compliance. The processes involved in a project via MySE Portal (**Figure 3**) are as follows:

1. Request initiation by Designer, with details of project under scope of review. Designer proceeds for project submission once 'Design Concept' is frozen and design of aggregates is final.
2. Cross check of vehicle major aggregates with respect to major functional/assembly issues. Reverting the request back to designer in case of major discrepancy as to release of aggregates with in contradiction with technical specification of vehicle. Assignment of project to team member after crosscheck of data provided.
3. Preparation and compilation of E- BOM of the vehicle for the analysis. Identification of new parts and suggestion of alternate parts without affecting the functionality. Reference database for alternate parts and bulk fastener, i.e., being use in production, against new released parts. Validation of drawings and design for checking functionality/layout issues. Design validation for tool and ergonomic accessibility in terms current line practice and process validation for building of product. Addressing past concerns raised by various department (Production, Supplier, Service, Assembly Line etc.) to reduce rework on physical product. Referring issues raised by customers and checking of design for those issues. Preparation proposals with alternate solution for concerns identified.
4. Report compilation with new parts report and alternate suggestion against those new parts for complexity reduction and manufacturing cost reduction. Compilation of issues with alternate solution for design and fitment issues capture during review and by acknowledging past concerns.
5. Discussion on compiled report in presence of CFT – Design, Production, Service, Quality etc. Departments for acceptance and brainstorming on other more frugal and acceptable solution of issues identified. Addressing present concerns being face on development of product resulting in quick solutions at design phase.
6. CFT team agrees upon issue resolution reached during discussion phase and required changes are communicated to designers before design release.
7. Design is released after the agreed changes are incorporated into the design and product development is smooth as simulated in digital environment.
8. In addition associateship to above-mentioned workflow, this is close with Proto Building Team to identify bottleneck areas of proto building. Issues being faced in assembly line, part procurement and quality audits of vehicle. Vehicle testing issues, which may be functional or aesthetic, are documented for further reference along with resolution reached on physical vehicle. Reference of design release document also unable team for alternate part fitment against parts, which are unavailable during vehicle building (**Figure 4**).

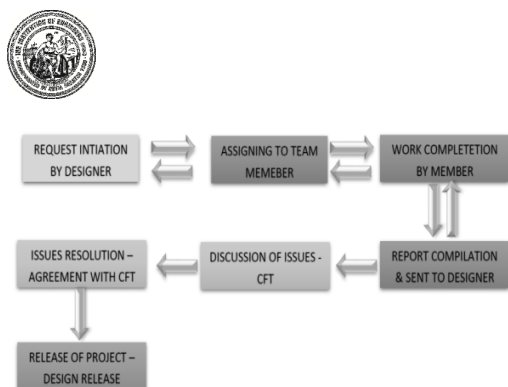


Figure 3 Brief workflow of MySE portal

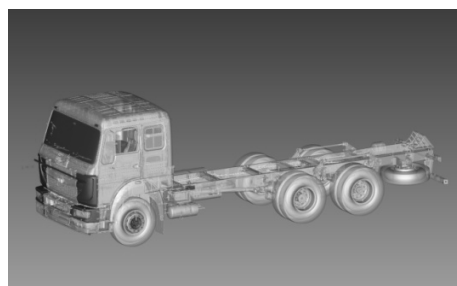


Figure 4 Vehicle building in digital environment

ADVANTAGES OF SE SYSTEM – MYSE PORTAL

From, **Figure 5**, it is clearly visible that there is vast time reduction for New Product Launch using our defined SE portal based approach. In addition to this use of Simultaneous Engineering has provided organization with mentioned below benefits :-

1. Reduction in rework in Design after Proto Building results in less time consumption for Product Development.
2. Provides a common platform for various department to raise their concerns in Design Phase, which enables zero defect design release.
3. Commonisation /alternate suggestion of parts enables reduction in manufacturing cost and time required for new part development.
4. Provides an insight to designer to come up with design release which adheres to current line facility and process with minimal changes.
5. Quality of Vehicle Build increases as major functional and layout issues are resolved at Design Phase.
6. Common database for future references to use past learning and solution to tackle possible issues.

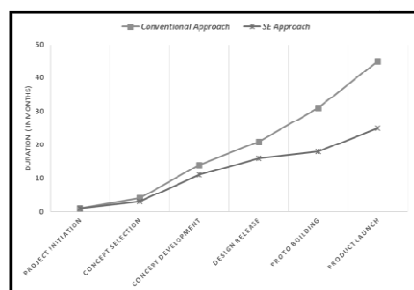


Figure 5 Graph of conventional against simultaneous engineering method

CONCLUSION

In order to be market ready to changing technology and demands of customer it has become an increasingly important to come up with Design Process which provides feedback system at every step. Simultaneous Engineering – MySEPortal has provided to all the requirements of product development by enabling design phase with real time feedback of assembly process and function issues.

REFERENCES

- Andrew Kusiak. Concurrent Engineering: Automation, Tools and Techniques
- The Principles of Integrated Product Development. NPD Solutions. DRM Associates. 2016. Retrieved 7 May 2017.
- Tim Cooper. The Significance of Product Longevity. Longer Lasting Products: Alternatives to the Throwaway Society. Farnham, UK.: Gower. ISBN 9780566088087, 2010.
- Bill of Materials. Inventory Interface. Gerald Drouillard. 2001-12-28. Retrieved 2011-06-07.

Integrated Casting of Steel and Cast Iron by Full Mold Process

Sunil Sahu^{*1} A. N. Dutta²

Tool and Die Engineering Division, Maruti Suzuki India Limited, Gurgaon Plant, Haryana¹, sunil.sahu@maruti.co.in^{*1}
BSL Castings (P) Ltd., Faridabad, Haryana²

ABSTRACT

Stamping dies for A-class sheet metal components are made of castings. Existing practice of die manufacturing has a working part made of steel and a body of grey cast iron. The casting process used for manufacturing the casted parts is full mold casting process.

Full Mold casting is an evaporative-pattern casting process which is a combination of sand casting and lost foam casting. It uses an expanded polystyrene foam (commonly known as Thermocole) pattern which is then surrounded by sand, much like sand casting. The metal is then poured directly into the mold, which vaporizes the foam upon contact and gets filled into the space.

Both the parts (working part - Steel and body - grey cast iron) are machined and assembled to form a stamping die. High lead time and cost is incurred in machining and assembling these parts.

This presentation relates to the development of integrated casting, in which the working part (made of steel) and body (cast iron) is integrated through a joining band, resulting in weight reduction of the casted parts. This also involves special design of mold box and separate runner/feed layout for both material grades.

KEYWORDS Integrated casting, Lead time, Cost, Stamping die, Weight reduction.

DIE AND MOLD DESIGN DETAILS

Old/Existing

In the manufacture process of stamping dies for sheet metal working, existing practice was to produce a tool body made of grey cast iron. The tool body is produced by full mold casting process and heat treated to relieve the stresses. The tool body is then machined so that required parts like working part, guide bars, sensors, etc. can be assembled and it itself can be fixed/assembled in the press machine.

Working part (made of steel), which carries out the working like forming, cutting, re-strikes operation, was also produced by full mold casting process. The working part used to be machined at top and sides to perform the required operation and at bottom side to assemble on the tool body. Assembly of working part with the tool body was done with the help of bolts and location ensured by Tenon keys. The working part is heat treated (flame hardening) so that required operations (like forming, cutting, etc.) can be carried out. Heat treatment is followed by finish machining/grinding, etc. Schematic diagram is shown in **Figure 1**.

Die development in above explained method is extremely time consuming and expensive. This process also involves heavy machining and energy consumption.

The mold box design for developing the tool body and working part was traditional one and having the standard components like mold box, molding sand, pouring sprue, runner and gating system, etc. and schematic diagram is shown in **Figure 2**.

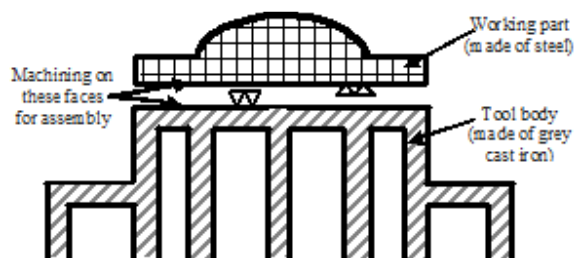


Figure 1 Traditional design of a stamping die (schematic diagram)

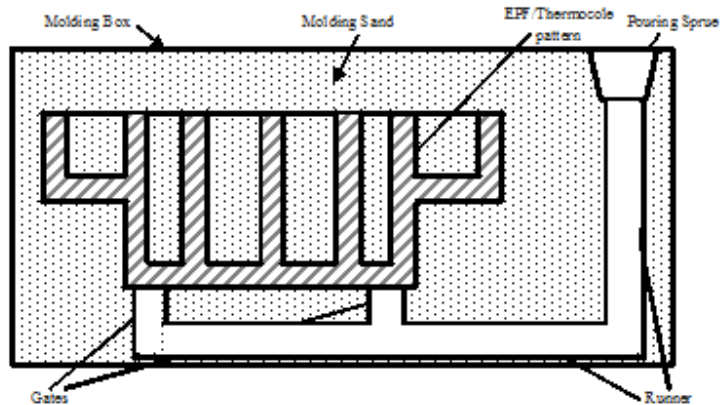


Figure 2 Molding box of full mold casting process (schematic diagram)

Design and Development of Integrated Casting

This presentation explains the method to develop integrated casting and method of its manufacture, where the casting has different material composition in different areas.

Integrated casting in stamping die is intended to join the working part (made of steel) and the tool body (made of grey cast iron). By joining these parts, the design of the die gets simplified and results in reduction of casting weight. Schematic diagram is shown in **Figure 3**.

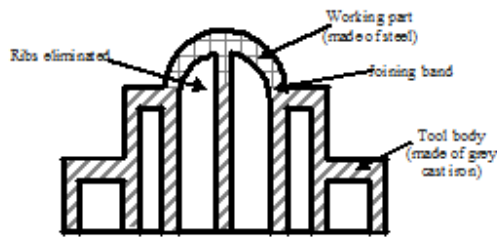


Figure 3 Die design of a stamping die having integrated casting (schematic diagram)

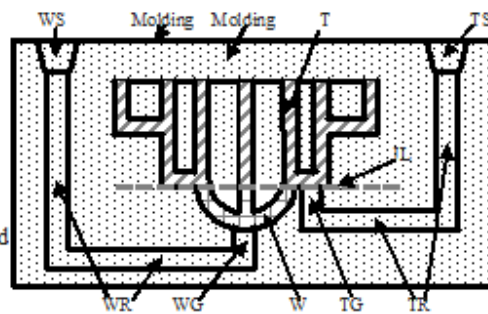


Figure 4 Molding box for integrated casting (full mold casting process) (schematic diagram)

The molding box design for integrated casting has two separate systems of pouring sprue, runner and gating system, in one molding box. The placement of gates is done accordingly in order to get the desired joining line or interconnected band.

The pouring sequence is designed according to the density of the material. Denser material, that is, steel (having density 7.8 g/cm^3) is poured first and followed by the pouring of lighter material, that is, cast iron (having density 7.2 g/cm^3).

The preparation and timing calculation of the molten material should be precise in order to get the desired joining line or interconnection band.

DETAILED DESCRIPTION OF MOLDING BOX OF INTEGRATED CASTING

Molding box (fabricated as per requirement) is planned and made to withstand EPF/thermocole pattern along with sand. It contains dedicated sprues, runner and gates for pouring of each type of material, a typical labeled mold box is shown in **Figure 4**, and details of abbreviations are as below:



W relates to the section of the mold intended for development of working part (made of steel) and represented in square hatches. This part is designed for operations like cutting, hole making, bending, shaping operation, etc. WS- Sprue for pouring of working part (Steel); WR- Runner for pouring of working part (Steel); WG- Gate for pouring of working part (Steel)

T relates to the section of the mold intended for development of tool body (made of grey cast iron) and represented in angular hatches. This part is the structural part. TS- Sprue for pouring of body part (Grey cast iron); TR- Runner for pouring of body part (Grey cast iron); TG- Gate for pouring of body part (Grey cast iron); JL is the desired line at which interconnection band is intended.

WORKING PRINCIPLE

Steel (having density 7.8g/cm^3) is poured first and cast iron material (having density 7.2g/cm^3) is poured on it. Since, grey cast iron is lighter in weight, it does not get mixed up with the steel material completely and joining band is formed. Joining band is mix up of steel and cast iron and has the thickness of around 2.5 to 3 mm only. The mechanical properties (tensile strength, hardness, etc.) of the joining band are superior to grey cast iron but inferior to steel.

Working

Both the materials (i.e. steel and grey cast iron) are prepared in two different furnaces and transported to the molding station in the heat resistant ladles. One ladle has molten steel material and the other has molten grey cast iron material.

The pouring hole of ladle carrying molten steel material is opened first and metal flowed through pouring sprue (WS), runner (WR) and gates (WG) to fill the section W of the molding box.

As soon as the steel material of the ladle gets finished, the pouring hole of the ladle carrying the grey cast iron material is opened and molten grey cast iron material is flowed through pouring sprue (TS), runner (TR) and gates (TG) to fill the section T of the molding box.

The time lag between the pouring finish of steel material and pouring start of grey cast iron material is kept minimum possible in order to avoid the joining defects.

Testing

To ensure homogeneity of material and correct formation of joining band, it was need of the hour to perform rigorous tests before actually putting the trials into production dies. Various tests to check mechanical properties of the test bars produced from the integrated casting were done. The mechanical properties like tensile strength, hardness, etc. of the Joining band is found superior to grey cast iron but inferior to steel.

Ultrasonic Testing and Magnetic Particle Impregnation testing of the working part are done and found as per standard.

RESULTS

- (i) The integrated casting reduces the scope for machining and assembly in manufacturing of a stamping die, by integrated two parts which were traditionally made different and then joined.
- (ii) Integrated casting also eliminates the use of fasteners like bolts, dowels, Tenon keys for assembling of two parts.
- (iii) Reduction in carbon footprints by reduction in casting weight and machining scope.
- (iv) Reduction in part manufacturing lead time
- (v) Integrated casting reduces the cost incurred in die manufacturing on account of above points.

The actual values of the results achieved from the development die are: machining time reduced by 5%, fitting time reduced by 3%, casting weight reduced by 5%, and oie cost reduced by 6%.

REFERENCES

- Archives of Material Science and Engineering, Volume 48, Issue 2, April-2011
- Bimetallic layered castings: alloy steel – grey cast iron



Calibration of Core Temperature Measurement Channels of Prototype Fast Breeder Reactor

R. Pandiarajamani^{*1}, S. Narasimhan¹

IT & Instrumentation Section, Bharatiya Nabhikiya Vidyut Nigam Limited¹, rajamani_bhavini@igcar.gov.in^{*}

ABSTRACT

Prototype Fast Breeder Reactor is a Mixed Oxide fuelled, sodium cooled, 500MWe, pool type fast breeder reactor under commissioning at Kalpakkam. The reactor core consists of hexagon shaped fuel subassemblies wherein fuel pins are stacked and assembled together vertically. The coolant enters at the bottom of the fuel subassemblies and transfers the nuclear heat generated from the core to non-active sodium loops and finally to feed water for power generation. The power density of fast breeder reactor is very high. Continuous monitoring of coolant temperature is necessary to maintain the reactor in safe operating condition.

KEYWORDS Real Time Computer, CTMS

INTRODUCTION

Reactor inlet and fuel subassembly outlet temperatures are continuously monitored to ensure the adequacy of core cooling and to protect the reactor in case of any abnormal temperature rise inside the core. These temperature signals are used for detection of core anomalies such as plugging of fuel subassemblies during start up, error in core loading and fuel enrichment error.

The main function of Core Temperature Monitoring System (CTMS) is (a) to monitor the inlet and outlet temperatures (b) to find the variation of coolant temperature of individual subassemblies (c) to find the core anomalies like plugging of fuel subassemblies (d) to find the error in core loading, fuel enrichment error and fuel orifice error.

This system processes the temperature signals and derives the mean core outlet temperature, calculates temperature rise across the core, difference between inlet and outlet temperatures, and deviation in the individual subassembly over the expected value. It generates SCRAM (Safety and Control Rod actuation mechanism) signal when the reactor inlet temperature, central subassembly outlet temperature, mean temperature across the core and the deviation in the individual subassembly from the expected value crosses the safety set points. Further, it sends the SCRAM signals to the safety logic system to safely shutdown the reactor. This system is classified as Safety critical (Safety Class 1) system.

CORE TEMPERATURE MONITORING SYSTEM

This system consists of three systems

1. Reactor Inlet Temperature Monitoring System;
2. Central Subassembly Temperature Monitoring System;
3. Subassembly Outlet Temperature Monitoring System.

REACTOR INLET TEMPERATURE MONITORING SYSTEM

Two Primary sodium pumps located inside the reactor circulates the coolant to the fuel subassemblies. Reactor inlet temperature is measured at the suction side of the primary sodium pumps. Three guide tubes with the thermowell are provided in each pump. Two thermocouples are provided in each thermowell. Out of six, three thermocouples are processed by three independent hardwired systems. Other three thermocouples are processed by three independent Real Time Computer (RTC) based core temperature monitoring system.

CENTRAL SUBASSEMBLY TEMPERATURE MONITORING SYSTEM

Central subassembly temperature is measured at the outlet of central fuel subassembly. Twelve thermocouples are fixed on the central canal plug which is in direct contact with sodium. No thermowell is provided. It directly measures the sodium jet temperature coming out from the central subassembly. Among the twelve thermocouples, three thermocouples are processed by three independent hardwired systems. Other three thermocouples are



processed by three independent RTC based core temperature monitoring system. Remaining six thermocouples are in-situ spares and are wired up to control building.

SUBASSEMBLY OUTLET TEMPERATURE MONITORING SYSTEM

Core outlet temperature is measured at the outlets of 180 fuel subassemblies and at 30 blanket subassemblies of the first blanket ring (210 subassemblies). Thermocouple probe with two thermocouples are provided at the outlets of each subassembly. These thermocouples are installed in thermowell which are part of the control plug. The bottom ends of these thermowells are at a distance of 100 mm from the top of the subassembly during normal reactor operation. Sodium enters at the bottom of the subassembly and takes the nuclear heat generated from the fuel and comes out from the subassembly as a jet and hits the tip of the thermowell. Two thermocouple signals of each subassembly are multiplied into three signals and the triplicated signals are processed by triplicated Real Time Computer based systems.

FIELD SENSOR

Mineral insulated, stainless steel sheathed, ungrounded junction, k-type Chromel-Alumel thermocouples (TC) with the overall diameter of 1 mm with an accuracy of $\pm 2.3^{\circ}\text{C}$ (at a nominal operating temperature of 570°C) are used for core temperature monitoring. **Figure 1** shows core thermocouples.

RTC BASED CORE TEMPERATURE MONITORING SYSTEM- SYSTEM CONFIGURATION

Core outlet A and B thermocouples together emerging from the reactor are independently routed to the signal processing cabinets located at two different local control centres in the reactor building. Thermocouple millivoltage signals are converted into current signals (4 to 20 mA) by the signal conditioning modules (SCM). The current signals are transmitted to the multiplier unit. Each current signal is multiplied into three voltage signals. Further, the voltage signal is amplified by the isolation amplifiers.

A thermocouple signal is multiplied into A1, A2, and A3. Similarly, B thermocouple signal is multiplied into B1, B2, and B3. These triplicated signals are connected to triplicated RTCs (A1B1 to RTC1, A2B2 to RTC2, and A3B3 to RTC3) as shown in **Figure 2**. Similarly, three reactor inlet thermocouples from each pump and three central subassembly thermocouples are also connected with this RTC system for calculating the temperature rise across the central subassembly and mean temperature rise across the core. Real time computer system is a bus based system with microprocessor based CPU card and Analog and Digital Input / Output cards. Analog / Digital input cards acquires the field signals, processes them and sends the data to CPU card. CPU card receives the input signals and checks the logic or interlocks, generates the outputs through analog and digital output cards.

ARCHITECTURE

This RTC acquires reactor inlet temperatures, central subassembly outlet temperatures and subassembly outlet temperatures. It validates the temperature signals, calculates mean core outlet temperature (θ_M), mean temperature rise across the core ($\Delta\theta_M$), temperature rise across central subassembly ($\Delta\theta_{CSA}$), and perform plugging detection (check for deviations in individual subassembly outlet temperatures against the expected values) (δ_{θ}). It generates alarms or SCRAM signals when the computed values cross the respective alarm thresholds or SCRAM thresholds. It sends the acquired and computed data to the dual redundant Safety Class I data highway of Distributed Digital Control System.

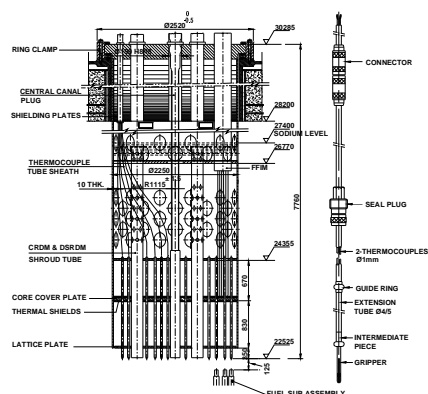


Figure 1 Core thermocouples

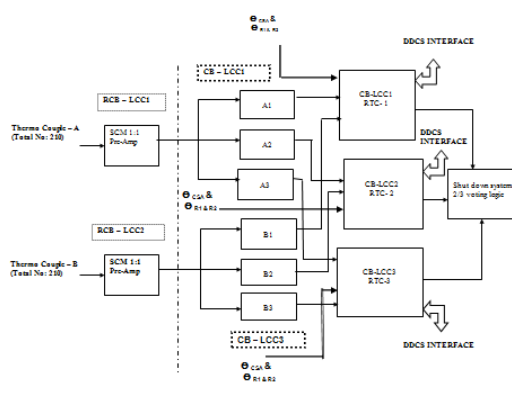


Figure 2 Core temperature monitoring system



NEED FOR CALIBRATION

The acceptable accuracy limit for each temperature measurement channel specified is $\pm 2.78^\circ\text{C}$.

- (a) Thermocouples were procured from standard manufacturer. The millivoltage to current convertor SCM is a commercially off the shelf available items. The multiplier unit has the resistor network connected in series wherein the current was allowed to pass through to get three equal voltages at the output. The isolation amplifiers are again a commercially off the shelf available items with the analog input voltage. CPU card and analog input cards were manufactured separately. Each component is specified with the accuracy limit for the various operating conditions. All the items were procured / manufactured from various agencies and are calibrated separately at factory and at site. After installing all these items at site, the complete chain is to be checked for achieving the required accuracy. If required, slight tuning of SCMs and Isolator modules are required to achieve the required accuracy.
- (b) Thermocouples are installed at field, SCMs are placed in Signal processing cabinets in reactor containment building, Isolator modules & RTC modules are located in the signal processing cabinets of control building. Sensors and processing units are located across various buildings and are interconnected through extension and instrumentation cables. Hence, each channel from field along with all interconnections and components are to be calibrated for the required accuracy limits.
- (c) Each RTC receives both A and B (A1B1, A2B2, A3B3) thermocouple data and it generates Alarm / SCRAM signals if it crosses the Alarm set point / SCRAM set point and sends the same to safety logic system. Safety logic system performs 2/3 voting logic and finally routes the SCRAM signal to shut down the reactor. The alarm and SCRAM thresholds are 5°C and 10°C . If the thermocouple signal error is more, it may spuriously generate alarm / SCRAM which will affect the safety / availability of the reactor. Since CTMS is a critical system, the each and every channel is to be calibrated for the required accuracy before starting the reactor.

CHALLENGES IN CALIBRATION

After erection, the standard method is to simulate the signals with the handheld millivoltage source from the field isolating the field instruments and the outputs from each channel is to be checked at Main Control room. If required, the SCMs and isolation modules are to be adjusted to bring down the error within the acceptable limits. At site, the following challenges were faced on performing the calibration with the standard methods as follows.

- (a) A&B signals are to be simulated together. Either temperature or millivoltage shall be simulated for carrying out calibration. Since the cold junction compensation (CJC) is done by SCMs, the CJC temperature at SCM to be measured and to be subtracted from the corresponding temperature to be simulated. The SCMs are installed at two different LCC rooms in Reactor Containment building in air-conditioned environment. Room temperature at both the locations cannot be maintained at the same value.
- (b) CJC temperature values are different for A and B channels. Two different temperature / millivoltages are to be fed at the field for simulating the same temperature for A and B.
- (c) CJC temperature was measured at the input terminal blocks of SCMs and was subtracted and fed as an input from the field. The output observed at the control room was with more error. It was found that the temperature measured at the input terminal of the SCM was different than the CJC actually it takes for compensation. Another method was tried by shorting the input terminals at the SCM input and the corresponding temperature reading measured at the control room which was exactly matching with the CJC temperature what it compensates for. Every time, the field cables are to be disconnected, input terminals are to be shorted, get the CJC value from MCR, connect the field cables at SCM and subtract the same from input millivoltage, fed it from the field. By the time, cables were connected / disconnected, the CJC temperature was continuously changing based on the room temperature. This was adding more error in the simulation.
- (d) c) SCM has the Isothermal terminal block, the CJC temperature is to be exactly measured at the internal part of isothermal terminal block. Different temperatures were found on the SCM surface, at the terminal blocks and by shorting the input terminals. It is not possible to measure the cold junction temperature exactly without disturbing the connections.
- (e) The extension cable from the field is directly connected to the SCM. No terminal blocks for terminating the field cables. During calibration, many times the field cables have to be connected / disconnected. Often



connecting and disconnecting the cables in the screw terminals may damage the terminals which in turn damage the SCM. This may end up in loose connection which will give erroneous reading during reactor operation.

- (f) As per the datasheet of SCM, the accuracy limit specified for Cold junction compensation upto 45°C. During calibration, If the ventilation system fails then the CJC compensation will introduce more error in the calibration process.
- (g) Two sensors (either RTD or Thermocouple) with the measuring instruments are required for measuring the cold junction temperature. Two millivoltage sources for feeding the signals at the field, two temperature measuring instrument with an indicator are required to be used for calibrating two channels. Multiple measuring instruments are to be used for calibration. Each instrument will have its own errors and it is very difficult to exactly simulate both the temperature without any difference.
- (h) Since the thermocouple is with the mating connector and further routing of the signals are through disconnectable connectors, the calibrator cannot be connected with the filed cable directly. Since the mating cable is with the connector, a separate cable with the connector is to be fabricated for connecting the millivoltage calibrators which will add one more junction in the measurement path.

It is not possible to calibrate 420 measurement channels with the conventional method from field. So many trials were carried out at site and finally a separate method was devised to calibrate all the 420 temperature measurement channels. The test setup should have the provision to simulate both A and B temperature at the same value.

NEW TEST SET-UP PROPOSED

- (a) It was decided to simulate the actual temperature itself instead of sourcing the millivoltage. So that CJC temperature measurement can be avoided. Since two temperatures are to be simulated at a time, potable temperature bath with the actual thermocouple probe (spare) similar to the one which was installed at site was selected. This will simulate the exact plant condition (actual temperature itself).
- (b) Even though the range of K type thermocouple is -100°C to 1350°C, the normal operating temperature of the reactor is 547°C and the minimum temperature to be maintained is greater than 98°C. Hence, the calibration range was chosen in such a way that the maximum accuracy is achieved in the operating temperature range. Range of calibration finalized was from 50°C to 600°C.
- (c) Standard reference temperature sensor is required for calibration. Since the range of calibration was (50 to 600)°C, a standard reference Resistance Temperature Detector (RTD) was selected as a reference sensor.
- (d) Spare thermocouple probe and the reference RTD were inserted inside the temperature bath. The field extension cable (cable end connector mating part) was disconnected from the actual thermocouple probe and connected with the spare thermocouple probe as per the test set up in shown **Figure 3**.

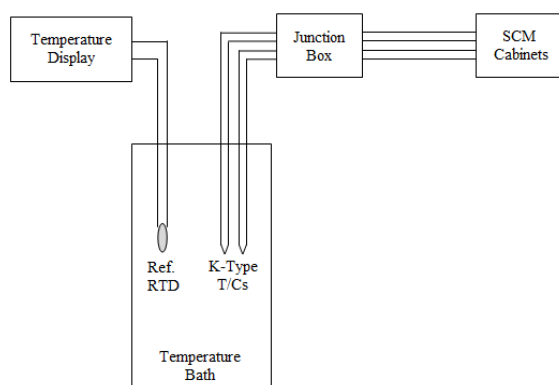


Figure 3 Test Set-up

CALIBRATION METHODOLOGY

The test set-up was placed at site close to thermocouple outlet from the reactor. The field 2P extension cable of each thermocouple probe was connected with the spare thermocouple probe and the readings were checked at Main



Control Room, verified A&B channels of the thermocouple probe read the room temperature in the specified location as per the identified tag number.

Hot tip of the thermocouple probe and reference RTD were inserted inside the temperature bath. The bath temperature was adjusted till the RTD reads 50°C. The median of A1, A2, A3 temperature readings was taken for adjusting the offset of the Signal conditioning modules. The offset of SCMs was adjusted to bring the readings close to RTD temperature. After SCM adjustment, if there is a difference among A1, A2, A3 temperature readings then the offset of the corresponding isolator modules in control building was adjusted to bring the readings close to the RTD temperature value. Similarly, B1, B2, B3 readings are adjusted to get the temperature close to RTD temperature value.

Bath temperature was further increased till the RTD reads 600°C. The median of A1, A2, A3 temperature readings was taken for adjusting the gain of the Signal conditioning modules. The gain of the SCMs was adjusted to bring the readings close to RTD temperature. After SCM adjustment, if there is a difference among A1, A2, A3 temperature readings then the gain of the corresponding isolator modules in control building was adjusted to bring the readings close to the RTD temperature value. Similarly, B1, B2, B3 readings are adjusted to get the temperature close to RTD temperature value.

Again a bath temperature was lowered so that RTD reads 50°C and checked that the calibrated values are not changing. Bath temperature was adjusted to RTD temperature values as 150°C, 300°C, 450°C, and 600°C. A1, A2, A3, B1, B2, B3 readings in each point was recorded from Main control Room.

The above procedure was repeated for all 420 (210*2) thermocouple probes, reactor inlet thermocouples and central subassembly thermocouples connected to CTMS and the corresponding values were recorded from the Main Control Room SC1 display station.

CALIBRATION

Calibration of all 420 thermocouples was completed and the final error was within the acceptable limits of $\pm 2.78^\circ\text{C}$ at all five points.

Figure 4 and **5** shows three sets of A&B thermocouple readings at 50°C and 600°C plotted before and after calibration.

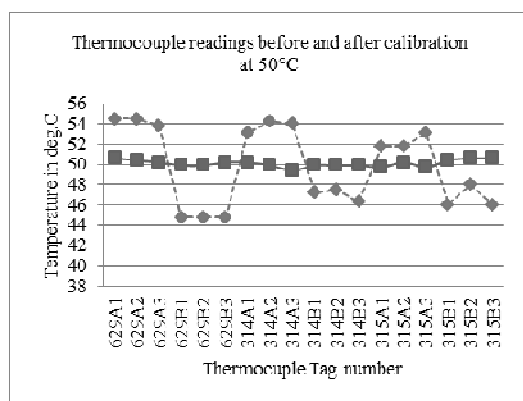


Figure 4 Thermocouple readings before and after calibration at 50°C

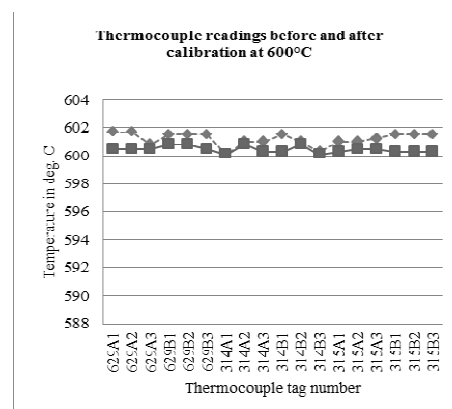


Figure 5 Thermocouple readings before and after calibration at 600°C

CONCLUSION

Since Core temperature Monitoring System is a safety critical system and generates many SCRAM parameters, the accuracy of the temperature signals plays crucial role on the safety and availability of the reactor. With this method, 5 point calibration was carried out for all the temperature measurement channels of core outlet thermocouples, reactor inlet thermocouples and central subassembly thermocouples connected with the real time computer system successfully. The error was within the acceptable limit of $\pm 2.78^\circ\text{C}$.

REFERENCES

- AERB Safety Guide SG-D1 and SG -D25



Technology Integration: the Mantra for Progress

Satheeschandra.P¹, Shaji Jose¹

NLC India Limited, Tamilnadu, satperooly@gmail.com

ABSTRACT

Latest trend in the energy market has imposed changes in conventional power plants. More economical way of operating any process control system without compromising on efficiency and an ever growing demand for operation of machines / manufacturing of equipments and products for foods / pharmaceuticals / agriculture / medical diagnostics / transportation in a highly demanding market has become the need of hour. This element has imposed new ways to operate more flexibly power plants / factories/ process control based production lines/ hospitals / civil constructions / image processing / logistics / communication/ weather forecasting and almost anything we can imagine or lay our hands upon. This has called for the design / implementation of equipments /controllers for various needs and requirements with more number of parameters and variables with stringent guidelines and quality control which were quite unthinkable and has called for changes in strategies which were impossible to implement or was only able to imagine sometime back. But with the advent of Electronics hardware and software based programmable controllers, micro/ super computers, hydraulic systems, power trains, CNC machines, transducers with extraordinary sensing capabilities lot of these things have become a reality. Thus electronics, mechanics, fluidics, architecture ,strength of materials, material science, metallurgy, machine design combined with our basic sciences like chemistry, physics, mathematics and biology along with engineering , medicine , agriculture and space sciences has become a reality. Thus the integration of technologies has become the mantra for progress or a trump card for modernization and development.

KEYWORDS Efficiency, Flexibility, Market demand, Manufacturing process, Development

Agriculture

One can see the usage satellite mapping technology/ super computers for weather prediction, to advanced methods of chromatograph in judging the soil conditions to selecting of the suitable crop for cultivation to deep freezing technology based refrigerators for preservation of the harvest to its final marketing with the help of a well spread communications system, we can see how technological integration has come to harvest a bumper crop in agriculture. Bio-sensors which can sense ripe/ good quality of apples/oranges/peaches by their colour and smell to help the farmers to sort them out for their sales in the market and also for the making of better quality of value added food products. This is in addition to helping them pluck from the trees using machine hands without the need of humans thus avoiding crude methods which were time consuming and prone to damaging them thereby reducing their shelf life period. The development of tissue culture based saplings, drip irrigation coupled with essential nutrients distribution to the individual plants, organic pesticides to bio-controls have all been due to contributions from physical and chemical sciences. The tractor, the harvester, the combine and many other machines and devices gave farmers the mechanical advantage they had longed for, to ease the burdens / hardship and to make the lands and the effort they put up truly profitable.

Mechanization enormously increased farm efficiency and productivity and when combined with other engineering developments such as processing equipments and higher quantity transportation and fast distribution systems, it has provided the world with vast agriculture resources at the lowest cost of production which in reality should help us to fight against famine and hunger in this millennium. Climate prediction has become so reliable and handy even for a common man that it has grown from being an unknown entity to a commonly accessible necessity. The ability to transport and store fresh foods and other perishables simplified shopping and has widened our choices for marketing and production.

ARCHITECTURE

From the chemical formulation of a wonder mixture called cement which has the flexibility to be moulded to any desired size and shape and with the inner skeleton of TMT-steel, the strength it can derive from the combination has helped the mankind to build simple living domes to multi storied sky scrapers. Development of materials with good bonding properties (Chemical Engineering/Material Science), design of beams and structures (Structural Engineering), finding out the optimum design with the least cost to the aesthetically designed halls/houses/buildings with the help of computer aided design software, technology has come a long way in helping the Civil/Architecture



Engineering to reach its present heights. Nowadays from house building to town planning, bridges to multi layered flyovers, ordinary flats to multi storied shopping malls, all the constructions are done this way.

Well aided by the simulation method utilizing computer models to the actual field analysis based on the crystallographic study of the surface, (material science) scanning done by solid state X-ray equipments helping us to study the wear and tear pattern of the structure / material surface, situated in a critical location and to assess their fatigue before it suffers a real failure.

FOOD INDUSTRY

The preservation of milk and dairy products were a problem till the discovery of refrigerator. The tetra packed UHT milk can be kept at room temperature for up to 120 days without the need of refrigeration. Indeed this is a result of combining Biology and Mechanical engineering. Similar is the case of other dairy products like cheese, butter and milk powder. Likewise breads, biscuits and cake of good quality which were once available only to people of urban locality is now easily available to the common man residing in villages, thanks to the development in the field of automation and process control in the baking industry .

But for the mechanization of the process of preservation, storage at ambient conditions and automatic bottling, the brewery/wine industry would not have been able to give spirits to the sagging markets. From the harvesting to crushing to storage under desired conditions of humidity and temperature to transferring them to bottles of desired colour to transporting them to the needy consumer, everywhere it is hand in hand combination of technologies.

So is the case meat (poultry/beef/pig) industry where meat of high quality in different grades made in hygienic conditions (untouched by human hands) has been made available and is within the reach of common man. Likewise has been the growth of its marketing and improved shelf life. To have a taste of Sausages, Hamburgers, Hotdogs one does not have to necessarily go to costly eateries but they can be made just at our homes thanks to technology.

HOUSEHOLD LIFESTYLE

The range of food processing equipments that is available to the homemaker is really astonishing. Baking ovens/ Cooking ranges and also those with all 3 facilities of Oven/Toaster/Grill (OTG), microwave oven, electric rice cooker, sandwich toaster, electric mixer etc are only some of them. Now the automatic dosamaker which can make Dosas with more than 25 different toppings/ types with desirable thinness/ thickness and that too @ 30 numbers per hour have reached the market as a help to the tasty hotel industry, so also the automatic bread maker which serves the bread on a platter just at the click of a button on our dining table – aided by a micro computer to the smart house wife, thanks to advances in the field process control automation

MEDICAL SCIENCES

Another major beneficiary is the medical sciences. Almost all the steps in forward direction were courtesy to the advancement in science and technology. From the simple Stethoscope to X-ray to CAT-scan to NMR imaging it has been a concoction of Physical sciences, Material science, Electronics and Computer engineering. Bio-Medical instrumentation has played a major role in the evolvement of Life supporting systems used in Intensive Care Units (ICUs). Usage of radio isotopes for cancer treatment to the usage of highly sophisticated invasive and non-invasive systems for the early detection to the diagnosis of diseases, highly advanced computerized blood component analyzers to the usage of laser scalpels for medical surgery all have made the job of a qualified medical doctor more precise and easier. Nowadays with the facility of operation theatres in almost all the hospitals to have their surgery being watched / recorded by CCTV for guidance /comments from the experts to the ironing out of the possible errors that can happen, credit should be given to technological innovations in fields other than Medical sciences.

The advancement in the field of artificial insemination to the preservation of the fertilized embryo, to the pregnancy by a third party, the medical field has come a long way. The recently opened branch of DNA mapping or Genome has been made possible not just by biological sciences but also is well assisted by other branches like Physics, Statistics and Computer Engineering.

PETROCHEMICAL INDUSTRY

It is a matter of wishful thinking that mankind would not have been today, but for the discovery of petroleum products and its synthesis and the advancement of the refining process for the separation of its various ingredients , notable among them being diesel and petrol and a host of other organic chemical constituents. Since 1913 when this technology was first introduced, when our production levels were just a few million barrels per year, we have reached a level where we presently produce 82 million barrels per day. Major advances in the fields of thermal and catalytic cracking in the refining process (Chemical Engineering and Process Control) enabled a huge



transformation in the field of Petroleum refining and production. This has also given us a host of plastics ranging from synthetic fabrics like rayons, terene, styrene to pesticides, fertilizers and cosmetics all of which are of use in our daily life and also other valuable organic by products for industries like benzene, toluene, phenol and tar etc.

PHARMACY

Pharmaceutical industry is yet another major branch which has benefitted by the cross-linking of various branches in engineering with Botanical Sciences and Chemical Engineering. Synthesis of various chemical elements and combining them with an assortment of bulk drugs through complicated manufacturing processes of in a highly hygienic, dust-free/moisture-free/bacteria-free environment and exacting conditions (Process Control Engineering.) to finding out the exact formulations and further developing of them through long term R&D (courtesy Computerized Electron microscope and Organic/ Inorganic Chemistry). Progress in the making of medicines from the simple Aspirin tablets to the creation of bulk drugs which form the base for the manufacture of several other individual and combination drugs to the development of Radio isotopes for the treatment of tumors and cancerous growths, pharmacology has advanced a lot thanks to contribution from Physical sciences and Chemical engineering.

It is not just the manufacture of medicines essentially needed for the treatment of various diseases / infections but also provide formulations for the upkeep of health to improving body vigor by means of Tonics, beverages which are nutrient sources, to the Vitamin enriched tablets/ capsules which are meant to improve the immunity of the willing buyer, Pharmacology has made permanent entry to the highest percentage of consumers in the world.

SUPER CONDUCTIVITY

The ability of certain materials to conduct electricity with zero resistance is the contribution by Material Science, Electrical Engineering and Chemical Engineering. Though this phenomenon was discovered only a few years back it has made giant strides in the scientific world. The areas of research now are the elevation of the transition temperature when the electrical resistance becomes zero thus enabling a very high current flow and formulating a chemical combination whereby the ductility and mechanical strength of the conductor is enhanced. Maglev trains, NMR machines, Tokamak fusion atomic reactors, low loss conductors and super magnets are some of the applications.

TRANSPORTATION

Covering of distances physically was a big challenge for mankind and not to speak about the transportation of materials. From the invention of wheel to the present day automobile car that was invented by Daimler in 1886, we have travelled a long way to reach to the production of around 4 million cars in India and over 70 million in the world now. Since the First Airplane Kitty Hawk was invented by Wright Brothers in 1903 and flew for just 12 seconds presently there are over 5000 flights in air USA alone and it works to be more than 100,000 flights per day in the world. Today flights have become easier/ faster than a/c trains. So is the design and manufacture of multi axle Trucks to Ships covering thousands of kilometers with agricultural goods/ industrial products of several tons, to the Bulk carriers transporting millions of tons of petroleum products from oil fields to various countries over large distances, thanks to mechanical engineering, automobile technology and naval architecture.

RECENT DEVELOPMENTS IN THE FIELD OF MECHANICAL ENGINEERING CAD/CAM

While CAD uses software to design, control machine tools and related ones in the manufacturing of work pieces, CAM is the use of a computer to assist in all operations of a manufacture, including planning, design, analysis/ evaluation management, transportation and storage. CAM is a subsequent computer-aided process after computer-aided design (CAD) and engineering, which then controls the machine tool for the manufacture of end pieces.

With the help 3D modeling and Auto cad software it is not only the linear movements in the x, y, z axis but the angular rotations in those three axis are taken into consideration. For problems related to any specific function like stress/strain, heat transfer, static/dynamic stability and rigidity of a given structure, the solution can be designed, modeled and manufactured within the desired tolerance for any precise and challenging needs.

CAD/CAM is widely used not just in automobile design, ship building, aircraft manufacture but also in the preparation of environment impact reports and for the proposal of building/ structural design to counter natural calamities.



CNC MACHINES

Probably one of the greatest developments in this field, CNC machines have caught the imagination of manufacturing and production industry. This can be said as an ultimate amalgamation of Computer Technology and Mechanical Engineering. CNC machine is an ideal blending of precise lathes, milling machines, shapers, cutters and grinders all rolled into one and all the more it can do these functions one by one in a predefined sequence, in a systematic way without the need of human intervention.

And that too with an exactness or accuracy that can match any demanding applications and combined with its ability to work on a host of materials like wood, plastics, metals ranging from aluminum, brass, mild steel to steel and with tools ranging from Tungsten carbide tipped ones to high precision laser beams. Almost any complicated designs can be replicated to the same size or scaled up/ down versions. And for this reason it has captured the world by storm and has become the heart of CAD / CAM application.

It has entered many engineering areas like Gear production, Automobile design and fabrication and manufacture of Critical components and spares, Aerospace, Satellite design and assembling, Turbine blade profile design and manufacturing and a host of military applications. By the latest 3D printing technology developed, one can create virtually any forms / contours/ shapes for our utility/ purpose. With this application at hand, the range of products that can be developed for the scientific community are simply mind blowing.

HYDRAULIC POWER DEVICES

Fluids such as oil, water etc have the noteworthy ability to perform amazing constructive work. Hydraulics, the branch of science that studies the mechanical properties of fluids, has helped people to conceive many applications founded on the simple Pascal's law which states that a pressure applied to a liquid in a confined space, gets transmitted equally to all other points in it. And the beauty is that this force so generated can be multiplied by the area on which it is acting.

Based on this, many equipments have been devised which have remarkable and wonderful applications. From the simple hydraulic car lifts seen in car workshops to hydraulically operated hoists which can lift mammoth weights and place them on to the assigned work spot that too in a confined space with the required settings or hydraulic power cylinders which operate with remarkable precision and ease as in airplanes or against a huge workload have become a reality. Power brakes which can bring to a halt a high speed automobile with anti skid technology or Backhoes/JCBs which can carry out herculean civil works day in and day out thus saving time and cost have all been the joint contributions by Science and Engineering.

ROBOTICS

From 1948 when Norbert Wiener formulated the principles of cybernetics, the basis of practical robotics to the first digitally operated and programmable robot, the Unimate, in 1961 to lift hot pieces of metal from a die casting machine and stack them, this branch which includes Mechanical Engineering, Electronics Engineering, IT and Computer Science has driven the scientific temperament to utopian worlds due to the practically attainable limit it is capable of achieving.

Robots which can work in deep seas or carry out formidable tasks in extremely harsh and cold extraterrestrial areas as in deep space / zero gravity endeavors in space shuttles, cavernous mines, which are inaccessible or fearsome to humans or carry out highly skilled work as in the manufacturing and assembly of automobiles/ airplanes/ military hardware /computer chips /SMDs have become the order of the day. Executing the jobs in a highly constricted and hazardous working environments have become a normal subroutine for a phenomenal machine called robot. They find jobs in cleaning up contaminated materials or toxic nuclear wastes and also as agricultural robot for planting and related jobs, hospital robot as couriers of medicines, domestic robot to clean / mop up floors and as industrial robot in complicated welding applications and systematic assembling of automobile parts.

CONCLUSION

It is the interaction / integration of various branches of sciences among themselves and also with engineering technology that has made the present world advanced and comfortable to live in as it is seen today.



A Study on High Efficiency Particulate Air (HEPA) Filtration Process

E Dey¹, U Choudhary¹, R Bhattacharyya¹, S K Ghosh^{*1}

Department of Jute and Fibre Technology, University of Calcutta, Kolkata¹, ijtskg40@gmail.com*

ABSTRACT

Nonwovens have distinct advantages for dry filtration applications due to their unique characteristics like random orientation and three-dimensional arrangement of fibres, bulkiness of the fabric, higher fluid flow rate, etc. As a result, high collection efficiencies of dust particles can be obtained without increasing the pressure drop. Nonwoven filter media, in their simplest, form are used to separate one or more phases from a moving fluid such as liquid, gas or super critical fluid passing through the filter media where the fluid can only pass. This paper outlines an industrial review on the efficacy of HEPA filtration process which offers removal of high percentage of biological and particulate material from the air at lower energy consumption, longer filter life, high filtration capacity and easier maintenance which are elaborated from manufacturing point of view.

KEYWORDS Air filtration, Filter media, Nonwoven, Particulate matters, Particle size

HISTORY

HEPA is an acronym for High Efficiency Particulate Air Filter, which was used in U.S. military specifications beginning around World War II. HEPA filters are used mainly for isolation and immune compromise units, operation theatres, removal of allergens from the air and other applications where maximum reduction or removal of submicron particulate matter from air is required. HEPA filter is usually designed to remove 99.97% of airborne particles measuring 0.3 microns or greater in diameter passing through it and they are generally available in two standard depths of nominally 150 mm and 300 mm.

INTRODUCTION

Filtration is the method which is used to separate the solid particles from a liquid or gas where they were arrested and contaminated through a barrier which is the filter medium. Whether the main aim is cleaner air to breathe, water to drink or a more efficient fuel system, nonwoven is becoming the substrate of better choice because of the random entangled fibre structure. Thus, due to their structure, they have high filtration efficiencies, that is, 25 to 99.9%. The usage of the filter fabrics varies according to their end-use. This depends on the properties the filters have which ultimately depends on the characteristics of the raw material used for the manufacturing of the filter fabric. Nonwoven filter media are randomly oriented fibre structures that are employed to separate one or more phases from a moving fluid passing through the filter media, where filtration is generally observed as the removal of particulate phases from the moving fluid by entrapping the particulate matter in the tortuous structure of the filter medium [1]. In their gross structures, these media have the form of nonwoven fabrics, wet-laid papers, or air-laid glass fibre mats spun from continuous fibres or blown from molten glass. Some membranes and open-cell foams also have fibrous structures. The solid content of these media is low, with the fibre volume typically less than 10 % of the volume of the media. These media range in thickness from a fraction of a millimetre to several centimetres. The production processes of nonwoven fabrics provide a lot of scope for obtaining a wide of fabric properties to suit specific filtration requirements at competitive cost. Generally manufacturers of nonwoven fabrics supply filtration media having mean flow ratings ranging from 1 to 500 micron. Micron ratings depend significantly on the test procedure by which the manufacturer rates the media. Fabrics having micron ratings below 10-15 micron must be calendared, in order to achieve the finer micron ratings[2]. With the micron pore rating, dirt holding capacity, flow rates and differential pressure data are also considered. Presently, the nonwoven fabrics market size for filtration media on a worldwide basis is approximately \$2 billion[3]. Needle-punched nonwoven filter media allows higher filtration efficiency at relatively lower pressure drop combining the possibility of greater flexibility and versatility in construction [4]. Fine glass fibres are traditional in air filtration from Heating, Ventilation and Air-Conditioning (HVAC) to HEPA filters. Resin bonded glass fibre liquid filter cartridges also provide many excellent properties like their use in medical devices such as dialysis systems [5]. More and more nanofibre-based products are finding applications either as standalone filter media or in combination with conventional nonwovens. The direct web processes produce fine and sometimes continuous filaments and in case of spun bond, a strong and non-shedding web which cannot be achieved by any other means for a comparable cost. No single media can or will ever satisfy every filtration requirement. But nonwoven fabrics, suffer from certain disadvantages too, like clogging of filter media, less flow rate, early cake formation on layer of the filter fabric and difficulty in cleaning the filter fabric [6]. The structural and dimensional properties of the fabrics are not easily achieved for nonwoven fabrics, because of the nature of the manufacturing processes and resultant constructions [7]. So, gradually a dire need to design and



engineer a sophisticated and precise medium which will be able to purify the air to the maximum possible level of purity evoked the emergence of HEPA filtration process [8]. This type of air filter can remove least 99.97% of dust, pollen, mold, bacteria and any airborne particles with a size of 0.3 micrometres (μm) [9]. Particulate air filtration for Collective Protection Systems (CPS) proves very much effective particularly against chemical-biological-radiation (CBR) agents by means of fulltime CBR filtration, total protection zone with a collective protection system that provides a toxic free environment by filtering air and maintaining an overpressure in the zone to prevent contaminants from leaking into it [10]. CPS contains both a High Efficiency Particulate Air (HEPA) filter and a Gas Absorber Filter. The CBR HEPA filter is a two stage, pleated-medium filter for removing solid and aerosol CBR contaminants and has a rated flow capacity of 200 cubic feet per minute (CFM). The gas absorber filter consists of activated charcoal for removing chemical warfare agents.

CONSTRUCTION OF HEPA FILTRATION MEDIUM AND ITS TYPES

HEPA filters consist of a rigid frame into which a filter wool, constructed by folding a continuous sheet of media into closely spaced pleats, is sealed. The pleats are separated by serrated aluminium baffles or stitched fabric ribbons, which direct airflow through the filter. Because of the density of the media, air flow is restricted and the pleating is used to increase the amount of media (surface area) allowing for a greater ratio of media to air flow [11]. The different types of fibres which are commonly used for HEPA filtration media are described in **Table 1** [12] and the various types of HEPA filters are detailed in **Table 2**.

Table 1 Fibres used for filtration with their properties

Uses field	Dry filtration		Liquid filtration	Hot gas filtration			
Fibre/ properties	Polyester	Polyamide	Polypropylene	Nomex	Sulphur	Ceramic	Glass
Density, g/cc	1.38	1.14	0.91	1.38	1.34	2.7	2.54
Withstanding temperature, °F	2700	2000	2000	4000	3750	2100	500
Resistance to acids	Fair	Poor	Excellent	Fair	No effect	No effect	No effect
Resistance to alkalis	No effect	Good	Excellent	No effect	Excellent	Good	Good
Biological resistance	No effect	No effect	Excellent	No effect	No effect	No effect	No effect
Moisture regain, %	0.4	7-8	0	4	0.06	0	0

Table 2 Types of HEPA filters

Types	Application	Performance
A	Industrial, noncritical	99.97 % @ 0.3 μm
B	Nuclear containment	99.97 % @ 0.3 μm (certified by DOE*)
C	Laminar flow	99.99 % @ 0.3 μm
D	Ultra-low penetration air (ULPA)	99.9995 % @ 0.12 μm
E	Stopping toxic, nuclear, chemical and biological threats	99.999 % efficiency

*DOE = Department of Energy, Washington D.C., USA

HEPA FILTRATION MECHANISM

Nonwoven HEPA filter mechanism involves sieve effect, inertial impaction, interception, Brownian diffusion, and static charge effect [13]. The simplest kind of filter is the sieve which are holes that are big enough to trap some particles and small enough to let others through. For the type of filter discussed here, this would include all particles above 5 μm in size and larger [14]. The particle, due to its inertia, impacts a fibre and is captured. **Figure 1** shows how this works.

This effect is dominant from around the 0.5 μm region up to around 5 μm . The next effect is interception. Interception occurs when a particle is so large that it is unable to quickly adopt the abrupt alterations in streamline direction near a filter fibre and the former, due to its inertia, will continue to traverse along its original path and strike the filter fibre. This type of filtration mechanism is most predominant when larger particles have higher mass and are harder to turn than smaller particles due to inertia. Once the particle comes in contact with the fibre, it becomes attached and is filtered from the air stream [15]. This effect is visible in the range of 0.1 μm to about 1 μm . **Figure 2** shows the working principle of interception.

Brownian diffusion is the most difficult air filtration mechanism to imagine [16]. Very fine particles in the air stream come in contact with fibres due to diffusive effects. The particles collide with air molecules and are pushed around



as shown in **Figure 3**. Because of Brownian motion, small particles do not precisely follow the airstream, but instead vibrate and move erratically. This effect is dominant for all particles smaller than $0.1\ \mu\text{m}$ [17].

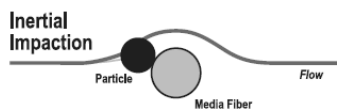


Figure 1 Diagram explaining inertial impaction mechanism

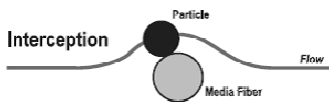


Figure 2 Schematic showing interception



Figure 3 Diagram explaining Brownian diffusion

The last effect is electrostatic effect by electrostatic precipitator (ESP). This effect is a function of the type of media used, the environment in which it is used, and the geometry of the fibres. Different materials will hold different levels of static charge [18]. A glass rod when rubbed with fur will build quite a static charge. It will also build a charge if placed in an air stream. In filters, as air passes over the fibre, a charge will build up much the same way, a very small charge certainly but a charge none the less [19]. The shape, size and orientation of fibre material influence the deposition of quantity of localized electrostatic charge on its surface. Plastic generally holds large quantity of static charges [20]. Humidity in the air also determines the quantity of static charge getting deposited on the fibre surface, along with the moisture vapour transmission rate (MVTR) through the media [21]. Fibre geometry and its orientation along with the media thickness greatly influence the efficiency of a filter medium. The smaller the fibre is, greater will be its capacity in holding the small particle and smaller the fibre spacing, the greater is its filter efficiency [22]. On the other hand, the larger the fibre cross section, the greater is the holding capacity [23]. Some air purifier manufacturers have combined the electrostatic and mechanical filtration effectively to produce air purification systems that can achieve better results than either technology alone. Blue air united advanced filter media and particle-charging where an ion particle charging chamber applies a negative charge to the incoming particles, thus ensuring that they stick to the advanced filtration media. This exclusive HEPASilent™ technology, is fairly noiseless and simple to maintain, and effectively removes airborne particles down to $0.1\ \mu\text{m}$ with a definite minimum effectiveness of 99.97%.

ADVANTAGES AND DISADVANTAGES OF HEPA FILTERS

Air purifiers have HEPA filters that aid in cleaning the air around that is circulated and able to remove 99.97 percent of any particle bigger than $0.3\ \mu\text{m}$. They help to get rid of contaminants and impurities from the air. HEPA filters can clear the air of dust, pollen, pet dander, smoke and almost all pollutants present in the air. But inspite of enjoying such advantages HEPA filtration has some disadvantages too. The HEPA filters however cannot trap the other pollutants such as gases, fumes, chemicals and odours. The HEPA filter is extremely delicate and needs to be handled in a very expensive, state of the art system and proves to be very costly when replacing filters [24].

CONCLUSIONS

HEPA filters are designed to prevent the spread of airborne bacterial and viral pathogens. HEPA filters are used in a regular basis in modern amenities and infrastructures to control the spread of air intoxicants [25]. These filters find their use in surgical operating rooms, and other critical medical air filtration applications. HEPA filters are there to provide the maximum possible protection for products, people and the medical laboratory environment. HEPA filter safeguards the life and health of both patients and medical staff. The wide arena of applications of HEPA filters are surgical smoke evacuation, surgical respirator systems, negative pressure isolation rooms, microderm abrasion, industrial vacuum cleaners, etc. [26].

REFERENCES

1. M. Hutten, Introduction to nonwoven filter media in Burlington, Handbook of Nonwoven Filter, Elsevier Ltd., 1st Ed., USA, pp.1-2, 2007
2. P. P. Sakpal, S. M. Landage, A. I. Wasif, Application of nonwovens for water filtration, Int. J. of Advanced Res. in Management and Social Scis. Volume 2, Number 2, pp 28-47, 2013
3. The Global Market Forecast from 2010 to 2024, Nanotubes future market, 2nd Ed., pp.74-77, 2014
4. E.C.Gregor, Primer on Nonwoven Fabric Filtration Media, Edward C. Gregor & Associates, LLC Charlotte, pp. 1-6
5. E. Vaughn, G. Ramcharan, Fibreglass vs. air filtration media, Int. Nonwovens J. Volume 11, Number 3, pp 41-53, 2002.
6. D. Das, A. K. Pradhan, R. Chattopadhyay, S.N. Singh, Composite nonwovens, Textile Progress, Volume 44, Number 1, pp 1-84, 2011



7. K. M. Raghvendra and L. Sravanthi, Fabrication techniques of micro/nano fibres based nonwoven composites: A Review, OMICS, Int. Modern Chem. & Applications, Volume 5, Number 1, pp 1-11, 2017.
8. H. Ma, H. Shen, T. Shui, Q. Li, L. Zhou, Experimental study on ultrafine particle removal performance of portable air cleaners with different filters in an office room, Int. J. of Environmental Res. and Public Health, Volume 13, Number 102, 1-15, 2016.
9. NIOSH, Guidance for filtration and air-cleaning systems to protect building environments from airborne chemical, biological, or radiological attacks, Department of Health and Human Services Centers for Disease Control and Prevention National Institute for Occupational Safety and Health, Cincinnati, pp. 3-15, 2003.
10. H.G. Brauch, Concepts of security threats, global environmental change, disasters and security, hexagon series on human 61 and environmental security and peace 5, Springer-Verlag Berlin Heidelberg, pp.2, 61-70, 2011
11. P. Linder, Air filters for use at nuclear facilities, International Atomic Energy Agency by IAEA Technical Reports Series Number 122, Austria, pp.12-16, 1970
12. V. K. Kothari, A. Das, S. Singh, Filtration behavior of woven and nonwoven fabrics, Indian J. of Fibre & Textile Res. Volume 32, Number 2, pp 214-220, 2007.
13. J. Larzelere, New and novel technologies in particulate filtration, Naval Surface Warfare Center, Dahlgren Division, Dahlgren, VA, pp. 1-9, 2006.
14. N. P. Cheremisinoff, Pollution control handbook for oil and gas engineering, Scrivener Publishing, Wiley, USA, pp. 647, 2016
15. S.T. Cox and D.T. Healey, Melt blown composite HEPA filter media and vacuum bag, US Patent 6,524,360 B2, Volume 25 February 2003.
16. Fibrous absorbent material and methods of making the same, fibrous absorbent material and methods of making the same, US 20030220039 A1, pp.1-5, 2003.
17. Particulate Matter, Air Quality Guidelines, WHO Regional Office for Europe, 2nd Ed., Copenhagen, pp.10-15, 2000.
18. B. K. Wiberd, The role of electrostatic effects in organic chemistry, J. of Chemical Education Volume 73, Number 11, pp 1089, 1996.
19. D. F. Shriver, M.A. Drezdson, The manipulation of air sensitive compounds, John Wiley and Sons, 2nd Ed., USA, pp.118-128, 1986.
20. P. Walker, W.H. Tarn, Handbook of Metal Etchants, CRC Press, USA, pp. 306, 2007.
21. A. Joubert, J. C. Laborde, L. Bouilloux, S. Callé-Chazelet, D. Thomas, Influence of humidity on clogging of flat and pleated HEPA filters, Aerosol Sci and Technology, Volume 44, pp 1065-1076, 2010.
22. B. J. Mullins, I. E. Agranovski, R.D. Braddock, Particle bounce during filtration of particles on wet and dry filters, Aerosol Sci. and Technology, Volume 37, pp 587-600, 2003
23. L. Boguslavsky, High efficiency particulate air (HEPA) filters from polyester and polypropylene fibre nonwovens, CSIR Materials Science and Manufacturing, Polymers & Composites Competence, J. of Applied Poly Sci., Volume 10, pp 1-15, 2010.
24. E. Deborah, L. Casey, Biosafety in microbiological and biomedical laboratories, National Institutes of Health, U.S. Department of Health and Human Services Public Health Service Centers for Disease Control and Prevention, 5th Ed., USA, pp. 104-107, 2009.
25. N. Bhuiyan, A framework for successful new product development, J. of Ind. Engg. and Management, Volume 4, Number 4, pp 746-770, 2011.
26. H. Leibold, I. Doeffert, T. Leiber, J.G. Wilhelm, The application of HEPA filter units in gas stream in high dust concentrations, Int. Atomic Energy Agency, Volume 25, Number 5, pp 540-553, 1993.



Automatic Electronic Fibre Bundle Strength Tester for Multiple Fibres

G Roy^{*1}, S C Saha¹, G Sardar¹, A Sarkar¹

ICAR- National Institute of Research on Jute and Allied Fibre Technology, Kolkata¹, gautamroy1234@yahoo.com*

ABSTRACT

The quality parameters of jute and allied fibres are key factors in its utilization and fixing the prices [1]. During the marketing, price is usually fixed on the basis of rough subjective judgment of the fibre quality. One of the parameter is bundle strength. For measuring bundle strength of jute and allied fibres, manual Bundle Strength Testing Instrument [2-4] is used, which has been developed by ICAR-National Institute of Research on Jute and Allied Fibre Technology (ICAR-NIRJAFT) and accepted by Bureau of Indian Standards [5]. It is essentially a balance of two unequal arms, the shorter arm holds a suspended clamp holder, holding the fibre bundle at one end and the other end is mounted on a fixed clamp holder rested below. Tension on the bundle is then gradually increased by driving a weight load, which slides over the long arm. The weight load automatically stops its movement when the bundle breaks. The movement is controlled by hand. Thus human error is involved in the measurement process and it varies from operator to operator. To eliminate the human error totally a new electronic automated instrument has been developed with the aim to replace the manual system. The electronic fibre bundle strength tester for multiple fibres is equipped with microcontroller based control unit along with motor set and load cell as the active transducer. This instrument automatically breaks the sample and measures corrected tenacity in gm/tex of the multiple fibres at the point of break, breaking load in kg and elongation in percentage (%) for the test sample. Provision is there to store the results in the built in memory unit of the instrument, which can be downloaded in a computer at later stage in Excel format using USB interface. This instrument is easy to operate and gives reliable results comparable to those obtained from the existing manual model.

KEYWORDS Jute, Allied fibres, Bundle strength, Micro-controller, Automatic

INTRODUCTION

Agricultural products play a major role in Indian Economy. India, being very rich in natural resources and diversities, about 75% of the Indians are still dependent on agriculture for their livelihood. But, in most of the places, the farmers of India suffer a lot. One of the reason for this is the different varieties of agricultural produce, including natural fibres, are not graded properly and all qualities of produce are sold in one common lot. Thus farmers producing better qualities are not assured of a better price. Besides, the chain of middle man in agricultural market is so large that the share of the farmers is reduced substantially.

In order to prevent such type of deprivation it was a crying need for the researchers to develop a set of instruments especially for jute, ramie, sisal, sunnhemp and flax fibres growers to find the correct grade of the fibre, as the price of the products depends upon the grades of the fibre.

Farmers' are not aware about the fibre quality; as a result, a cultivator was unable to find out the quality of his produce. 'Hand and Eye Method' is generally used in the market for on the spot assessment of the quality and grading of fibres. This method is subjective and assessment may vary from grader to grader.

Important contributions have been made by NIRJAFT, ICAR in the domain of instrumentation in relation with grading for jute, ramie, sisal, sunnhemp and flax fibres. One of the contribution includes the development of Electronic Fibre Bundle Strength Tester, which is now being used for accurate measurement of the strength. This is the most important parameter for quality assessment of the fibre and thereby preventing deprivation of the farmers from getting their proper dues.

THEORY OF OPERATION

The ability of the fibres to resist strain to the limit of rupture is called the strength of the fibre. The strength is measured as the breaking load of the fibre sample under test divided by the linear density of the unstrained fibre and is called tenacity.

The principle is same both in the manual and in the microcontroller based electronic fibre bundle strength tester. In the existing bundle strength tester there is a balance with two unequal arms resting on a fulcrum on the top of a pillar, the shorter arm holds a suspended clamp holder, holding the fibre bundle at one end and the other one is mounted on a fixed clamp holder rested there. The distance between the jaws of the clamp (gauge length) is 50 mm.



Tension on the bundle is then gradually increased by driving a weight load by sliding on the long arm. The weight load stops movement when the bundle breaks. The result of breaking load in terms of kg is read manually from the scale and then it is converted to tenacity mathematically. **Figure 1** shows the photograph of manual bundle strength tester.

In microcontroller based instrument the manual weight imparting the system on the arm has been replaced by a permanent magnet dc motor which is fed from a ramp type voltage generator circuit, which produces a linearly increasing current with respect to time and having a constant slope. A load cell is used to sense the breaking load and an encoder is used to measure the percentage of elongation of the fibre bundle under test at the time of break.

The new instrument has been developed with an aim to test the bundle strength of the other natural fibres including jute in a single instrument. **Figure 2** and **Figure 3** show the photograph of an automated fibre bundle strength tester and the schematic diagram of the instrument respectively. Here a selection switch SEL has been introduced to select the type of fibre before the experiment starts. The fibre sample is prepared as per standard method having length of 125 mm from the middle portion of the fibre reed. After testing numerous number of different fibre samples the recommended bundle weight for jute is 250 mg to 300 mg, for sunnhemp 200 mg to 300 mg, for sisal 200 mg to 250 mg, for flax 250 mg to 350 mg and for ramie 200 mg to 300 mg. Two high speed DC gear motor are used to operate the jaws. Thus the testing time is much less compared to the manual instrument. The grip of the jaws has been designed in such a fashion that the instrument can test others fibre also. The distance between the jaws of the clamp that is gauge length is 50 mm and total test length is 125 mm. Another high speed DC gear motor has been used to move the right jaw in a constant velocity of motion. A sensitive active transducer is attached with left jaw in such a manner that when the motor pulls the right jaw, the applied load directly comes to the transducer. Depending upon the load the transducer gives the breaking load in kg. Basically a ramp type dc voltage is applied to the gear motor so that it can produce a linear value of torque in the shaft of the gear motor. It pulls the fibre sample under test at linear and constant velocity through specially designed slot. The breaking point is observed from the rate of change of current (di) with respect to time (dt), that is, di/dt value of the current intake of that motor. At the point of break of the fibre bundle, the rate of change of current with respect to time will be a negative maximum. At this point of time the voltage obtained from sensitive transducer indicates the breaking strength of the fibre at different scale. The signal is passed to the control unit through differential amplifier to remove the spurious noise signal. A magnetic proximity sensor connected just parallel to motor pulls the right jaw and it gives pulses with the movement of the motor. By this proximity sensor and suitable encoder the instrument can measure elongation percentage of the fibre bundle under test at the time of break.

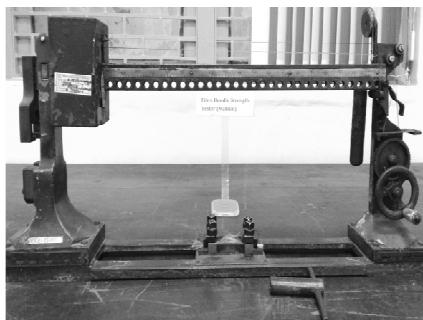


Figure 1 Mechanical fibre bundle strength tester



Figure 2 Multiple fibre bundle strength tester

SAMPLE PREPARATION: (a) clean the test sample and cut 150 mm of sample from middle portion of the fibre reed, (b) clean the fibre by hand and cut the sample into 125 mm in length and weight the sample as per requirement given in the theory of operation.

OPERATIONAL STEPS

1. Power ON the instrument and wait for 10-15 seconds for initial set-up.
2. Select the fibre by SEL switch
3. Weight the test sample and set the bundle weight in mg by SETBW knob on the control unit
4. Place the weighted fibre sample between the jaws

5. Press TEST switch and automatically operated fibre grips will now be closed and the sample is now under test after breaking the bundle the test result will be displayed in the display unit in terms of breaking load in kg, elongation in percentage and tenacity in gm/tex directly.

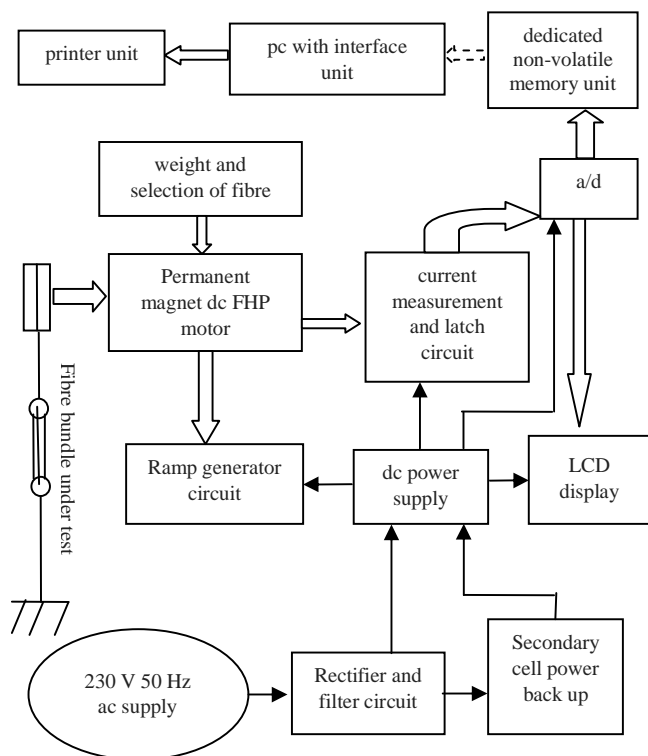


Figure 3 Schematic diagram of automatic electronic fibre bundle strength tester for multiple fibre

The recommended bundle weight for different fibre samples: Jute: 200 to 400 mg, Flax: 250 to 350 mg, Sunnhemp: 250 to 300 mg, Ramie: 200 to 300 mg, and Sisal: 200 to 250 mg.

Major Advantages

- Provides digital display of results of test samples.
- No expertise is required to operate the instrument.
- Operates automatically and reduces human error completely.
- Experimental results stored in the memory and can be downloaded in Excel format.

RESULTS AND DISCUSSION

Comparison of results in electronic instrument and conventional instrument has been conducted. Twenty five tests for each of the four fibres has been conducted using the same fibre samples in both conventional manual system and electronic instrument. The results are shown in **Table 1**.

Table 1 it shows that better tenacity, CV% and high correlation coefficient in case of electronic instrument. This is due to reduction in human error during testing and the inclusion of accurate constant rate of loading by using gear motor set and also for accurate display of the results by digital form. The display of time to break helps to eliminate the erroneous results.

Repeatability of New Instrument

Table 2 shows the results of 75 tests of ramie, sisal, sunnhemp and flax fibre samples. The average tenacity, breaking extension and time to break of 3 sets of 25 samples of each fibre sample were conducted. Statistical significance tests show that the difference between the results of 3 set of samples is insignificant in the 95% confidence limit. Hence, the results of the instrument for each fibre sample are repetitive in nature.



Table 1 Comparison of results of the instrument with conventional machine

Name of fibre	Average tenacity, g/tex	Tenacity, cv%	Standard deviation	Elongation at break, %	Time to break, s
Ramie					
Conventional manual machine	19.6	13.7	2.7	-	18
Multiple fibre testing instrument	19.9	14.8	2.9	2.2	17
Sisal					
Conventional manual machine	23.4	15.2	3.6	-	19
Multiple fibre testing instrument	25.2	12.5	3.2	1.7	18
Sunnhemp					
Conventional manual machine	18.3	24.0	4.4	-	17
Multiple Fibre testing instrument	18.4	23.3	4.3	0.8	18
Flax					
Conventional manual machine	20.4	17.7	3.6	-	18
Multiple fibre testing instrument	19.8	18.0	3.6	2.6	17

Table 2 Repeatability test

Name of fibre	Tenacity, g/tex	Elongation at break, %	Standard deviation	Time to break, s
Ramie				
1 st set	19.9	2.2	3.0	17
2 nd set	20.3	1.8	2.8	18
3 rd set	21.3	2.0	2.4	17
Sisal				
1 st set	25.2	1.7	3.2	19
2 nd set	23.7	1.8	4.8	18
3 rd set	24.0	1.7	4.2	18
Sunnhemp				
1 st set	18.3	0.8	4.3	17
2 nd set	18.6	1.0	3.4	16
3 rd set	20.1	0.9	4.5	18
Flax				
1 st set	19.8	2.6	3.4	17
2 nd set	18.7	2.6	2.8	18
3 rd set	20.6	2.8	3.1	18

CONCLUSION

An electronic multiple fibre bundle strength tester on constant rate of loading principle has been designed and developed which is very simple, easy to operate and maintains high order of repeatability. It also shows average tenacity value, breaking elongation in percentage and time to break automatically.

ACKNOWLEDGEMENT

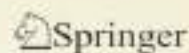
The authors are thankful to Director, ICAR-NIRJAFT for his constant encouragement to do the job successfully and for granting permission to publish the paper.

REFERENCES

1. G Roy, S C Saha, A Sarkar, G Sardar, Journal of Scientific and Industrial Research, Volume 76, pp. 515, 2017.
2. S B Bandyopadhyay and S K Mukhopadhyay, Jute Bulletin, Volume 27, Number 8, pp. 193, 1964.
3. S B Bandyopadhyay, Jute Bulletin, Volume 27, Number 11, pp. 278, 1965.
4. S B Bandyopadhyay, Textile Research Journal, Volume 38, Number 2, pp. 135, 1968.
5. Bureau of Indian Standard (BIS) IS No. 7032, Part-7, 1986.



IEI – Springer Journal Series



online paper submission :
www.editorialmanager.com/ieia
ISSN Print: 2250-2148
ISSN Online: 2250-2167



online paper submission :
www.editorialmanager.com/ieib
ISSN Print: 2250-2190
ISSN Online: 2250-2174



online paper submission :
www.editorialmanager.com/ieic
ISSN Print: 2250-2245
ISSN Online: 2250-2265



Online paper submission :
www.editorialmanager.com/ieid
ISSN Print: 2250-2122
ISSN Online: 2250-2133



Online paper submission :
www.editorialmanager.com/ieie
ISSN Print: 2250-2483
ISSN Online: 2250-2491



The Institution of Engineers (India) has tied up with Springer, a reputed publisher in the World to increase the visibility, greater acceptability, impact factor and SCOPUS indexing of the Institution Journals. This tie up added a greater value to the publish research works and results in quantum jump in the circulation of the Journals to a wide spectrum of learned community.

The details of scheduled publications by Springer and the subscription rates are given hereunder :-

Series of Journals of IEI	Number of issues per year	Month of publication	I Institutional subscription, INR	II Institutional subscription, US\$	III Individual subscription (Non-member, IEI), INR	IV Individual subscription (Non-member, IEI), US\$	V Individual subscription (Member, IEI), INR	VI Individual subscription (Member, IEI), US\$
Series 'A' (SCOPUS Indexed) (Civil, Architectural, Environmental and Agricultural Engineering)	4	March, June, September & December	₹ 15725/-	US\$ 480/-	₹ 2080/-	US\$ 115/-	₹ 1783/-	US\$ 113/-
Series 'B' (SCOPUS Indexed) (Electrical, Electronics & Telecommunication and Computer Engineering)	4	February, April, June, August, October & December	₹ 17320/-	US\$ 440/-	₹ 2080/-	US\$ 115/-	₹ 1783/-	US\$ 113/-
Series 'C' (SCOPUS Indexed) (Mechanical, Aerospace, Production and Marine Engineering)	4	February, April, June, August, October & December	₹ 15725/-	US\$ 480/-	₹ 2080/-	US\$ 115/-	₹ 1783/-	US\$ 113/-
Series 'D' (SCOPUS Indexed) (Metallurgical & Materials and Mining Engineering)	2	June & December	₹ 2890/-	US\$ 230/-	₹ 1080/-	US\$ 85/-	₹ 1285/-	US\$ 91/-
Series 'E' (SCOPUS Indexed) (Chemical and Textile Engineering)	2	June & December	₹ 2890/-	US\$ 230/-	₹ 1080/-	US\$ 85/-	₹ 1285/-	US\$ 91/-

I Institutional subscription means subscriptions sold throughout the world to academic institutions, corporate sectors and libraries.

II Individual subscription means subscriptions sold throughout the world to an individual person who is not the Member of The Institution of Engineers (India).

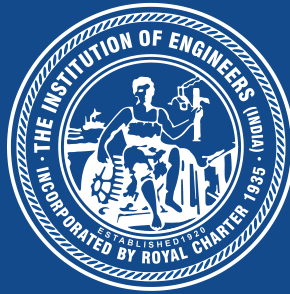
III Individual subscription means subscriptions sold throughout the world to Members of The Institution of Engineers (India). The Members of The Institution of Engineers (India) will continue to have free e-access to the Journals based on request received through: technical@ieindia.org

For any query regarding subscription for IEI Journals (Series A to E) and details of payment, please contact :-

Mr Arvind K Mehta
Assistant Manager, Subscriptions
Springer India Pvt. Ltd., 7th Floor, Vijaya Building, 17, Rameshwara Road, New Delhi - 110028
Ph: 91-11-43594077 (Direct), 91-11-43758888 (Extn.017); Fax: 91-11-43758888
Email: Arvind.Mehta@springer.com / indianjournals@springer.com

ISBN NO:978-81-938404-9-8

Technical Volume
33rd Indian Engineering Congress
Udaipur, December 21-23, 2018



The Institution of Engineers (India)

8 Gokhale Road, Kolkata 700020

Ph : +91(033) 2223-8311/14/15/16; +91 (033) 2223-8333/34; +91 (033) 4010-6299

Fax : +91 (033) 2223-8345

e-mail : technical@ieindia.org; iei.technical@gmail.com

web site : [http : //www.ieindia.org](http://www.ieindia.org)